VOLUME 27 / NUMBER 2
JANUARY 23, 1989
ACC. NOS. N89-10830 TO N89-11688

STAR
AN ABSTRACT JOURNAL

Scientific and Technical Aerospace Reports

PRODUCED BY THE
SCIENTIFIC AND TECHNICAL
INFORMATION
DIVISION

NASA

NATIONAL AERONAUTICS AND SPACE ADMINISTRATION

WHAT YOU CAN DO FOR *STAR*

All users of this abstract service are urged to forward reports to be considered for announcement in *STAR*. This will aid NASA in its efforts to provide the fullest possible coverage of all scientific and technical publications that might support aeronautics and space research and development. If you have prepared relevant reports (other than those that you will transmit to NASA, DoD, or DOE through the usual contract- or grant-reporting channels), please send them for consideration to the NASA Scientific and Technical Information Facility, P.O. Box 8757, BWI Airport, Maryland 21240.

Reprints of journal articles, book chapters, and conference papers are also welcome. These will be considered for announcement in *STAR's* companion journal, *International Aerospace Abstracts*.

You may specify a particular source to be included in a report announcement if you wish; otherwise the report will be placed on public sale at the National Technical Information Service. Copyrighted publications will be announced but not distributed or sold.

PURCHASE OF *STAR*

The semimonthly issues are available to registered users on annual subscription for $99.00 from the NASA Scientific and Technical Information Facility, ATTN: Registration Services, P.O. Box 8757, BWI Airport, MD 21240. *STAR* is publically available on annual subscription for $99.00 from the Superintendent of Documents, U.S. Government Printing Office, Washington, DC 20402.

PUBLISHED BY:

UNITED STATES GOVERNMENT
NATIONAL AERONAUTICS AND SPACE ADMINISTRATION
SCIENTIFIC AND TECHNICAL INFORMATION DIVISION
Scientific and Technical Aerospace Reports, Volume 27, is prepared by the NASA Scientific and Technical Information Facility operated for the National Aeronautics and Space Administration by RMS Associates.

The Administrator of the National Aeronautics and Space Administration has determined that the publication of this periodical is necessary in the transaction of the public business required by law of this Agency. Use of funds for printing this periodical has been approved by the Director of the Office of Management and Budget through March 22, 1989.

US ISSN 0036-8741

INTRODUCTION

Scientific and Technical Aerospace Reports (STAR) is a major component of a comprehensive National Aeronautics and Space Administration information system covering aeronautics, space, and supporting disciplines. *STAR* is issued on the 8th and 23rd of each month and announces current publications of the following types:

- NASA, NASA contractor, and NASA grantee reports
- Reports issued by other U.S. Government Agencies, domestic and foreign institutions, universities, and private firms
- Translations in report form
- NASA-owned patents and patent applications
- Other U.S. Government Agency and foreign patents and patent applications
- Domestic and foreign dissertations and theses

Journal, book, and conference literature, cover-to-cover journal translations, and certain foreign dissertations are announced in a companion journal, *International Aerospace Abstracts (IAA),* available on subscription from the American Institute of Aeronautics and Astronautics, Technical Information Service, 555 West 57th Street, 12th Floor, New York, New York 10019.

SUBJECT SCOPE

Subject scope of *STAR,* and *IAA* includes all aspects of aeronautics and space research and development, supporting basic and applied research, and applications. Aerospace aspects of earth resources, energy development, conservation, oceanography, environmental protection, urban transportation, and other topics of high national priority are also covered.

OTHER NASA PUBLICATIONS

Other NASA publications and information services are described in the publication, *The NASA Scientific and Technical Information System ... and How to Use It,* available without charge from the NASA Scientific and Technical Information Facility, P.O. Box 8757, BWI Airport, Maryland 21240.

HOW TO USE *STAR* SUBJECT CATEGORIES

STAR is categorized by 10 major subject divisions divided into 76 specific subject categories and one general category/division. The major subject divisions are listed in the Table of Contents, together with a note for each that defines its scope and provides any cross-references. For example:

AERONAUTICS

Includes aeronautics (general); aerodynamics; air transportation and safety; aircraft communications and navigation; aircraft design, testing and performance; aircraft instrumentation; aircraft propulsion and power; aircraft stability and control; and research and support facilities (air).

For related information see also *Astronautics.*

Each major division is further divided into as many as nine specific categories, which are identified by category numbers.

Abstracts in *STAR* are grouped by specific category, the categories appearing in sequential order. Category breaks in the abstract section are identified by the category number and title, and a scope note. Cross-references to other categories are provided as appropriate. For example:

02 AERODYNAMICS

Includes aerodynamics of bodies, combinations, wings, rotors, and control surfaces; and internal flow in ducts and turbomachinery.

For related information see also *34 Fluid Mechanics and Heat Transfer.*

CROSS-REFERENCES

Individual *STAR* abstracts are not ordinarily cross-referenced, except for certain conference reports or book translations that have had separate abstracts written for their component papers or chapters. Citations and abstracts of the components follow immediately after those of the parent document. When the subject content of a component differs sufficiently from the general content of the parent, a cross-reference citation also is printed at the end of the category to which it normally would have been assigned if it were independent.

DOCUMENTS ON MICROFICHE

Documents on microfiche(1) are designated by a pound sign (#) following the accession number. The pound sign is used without regard to the source or quality of the microfiche.

AVAILABILITIES

One or more sources from which a document announced in *STAR* is available to the public is given in each citation. The most commonly indicated sources and their acronyms or abbreviations are listed below. If the publication is available from a source other than those listed, the publisher and his address will be displayed on the availability line or in combination with the corporate source line.

Avail: NTIS. Sold by the National Technical Information Service. Prices for hard copy (HC) and microfiche (MF) are indicated by a price code following the letters HC or MF in the *STAR* citation. Current values for the price codes are given in the tables on page vii.

Initially distributed microfiche under the NTIS SRIM (Selected Research in Microfiche) is available at greatly reduced unit prices. For this service and for information concerning subscription to NASA printed reports, consult the NTIS Subscription Section, Springfield, Va. 22161.

NOTE ON ORDERING DOCUMENTS: When ordering NASA publications (those followed by the * symbol), use the N accession number. NASA patent applications (only the specifications are offered) should be ordered by the US-Patent-Appl-SN number. Non-NASA publications (no asterisk) should be ordered by the AD, PB, or other *report number* shown on the last line of the citation, not by the N accession number. It is also advisable to cite the title and other bibliographic identification.

Avail: SOD (or GPO). Sold by the Superintendent of Documents, U.S. Government Printing Office, in hard copy. The current price and order number are given following the availability line. (NTIS will fill microfiche requests, as indicated above, for those documents identified by a # symbol.)

(1) A microfiche is a transparent sheet of film, 105 by 148 mm in size, containing as many as 60 to 98 pages of information reduced to micro images (not to exceed 26:1 reduction).

Avail: BLL (formerly NLL): British Library Lending Division, Boston Spa, Wetherby, Yorkshire, England. Photocopies available from this organization at the price shown. (If none is given, inquiry should be addressed to the BLL.)

Avail: DOE Depository Libraries. Organizations in U.S. cities and abroad that maintain collections of Department of Energy reports, usually in microfiche form, are listed in *Energy Research Abstracts*. Services available from the DOE and its depositories are described in a booklet, *DOE Technical Information Center - Its Functions and Services* (TID-4660), which may be obtained without charge from the DOE Technical Information Center.

Avail: ESDU. Pricing information on specific data, computer programs, and details on ESDU topic categories can be obtained from ESDU International Ltd. Requesters in North America should use the Virginia address while all other requesters should use the London address, both of which are on page vi.

Avail: Fachinformationszentrum, Karlsruhe. Sold by the Fachinformationszentrum Energie, Physik, Mathematik GMBH, Eggenstein Leopoldshafen, Federal Republic of Germany, at the price shown in deutschmarks (DM).

Avail: HMSO. Publications of Her Majesty's Stationery Office are sold in the U.S. by Pendragon House, Inc. (PHI), Redwood City, California. The U.S. price (including a service and mailing charge) is given, or a conversion table may be obtained from PHI.

Avail: NASA Public Document Rooms. Documents so indicated may be examined at or purchased from the National Aeronautics and Space Administration, Public Documents Room (Room 126), 600 Independence Ave., S.W., Washington, D.C. 20546, or public document rooms located at each of the NASA research centers, the NASA Space Technology Laboratories, and the NASA Pasadena Office at the Jet Propulsion Laboratory.

Avail: Univ. Microfilms. Documents so indicated are dissertations selected from *Dissertation Abstracts* and are sold by University Microfilms as xerographic copy (HC) and microfilm. All requests should cite the author and the Order Number as they appear in the citation.

Avail: US Patent and Trademark Office. Sold by Commissioner of Patents and Trademarks, U.S. Patent and Trademark Office, at the standard price of $1.50 each, postage free. (See discussion of NASA patents and patent applications below.)

Avail: (US Sales Only). These foreign documents are available to users within the United States from the National Technical Information Service (NTIS). They are available to users outside the United States through the International Nuclear Information Service (INIS) representative in their country, or by applying directly to the issuing organization.

Avail: USGS. Originals of many reports from the U.S. Geological Survey, which may contain color illustrations, or otherwise may not have the quality of illustrations preserved in the microfiche or facsimile reproduction, may be examined by the public at the libraries of the USGS field offices whose addresses are listed in this Introduction. The libraries may be queried concerning the availability of specific documents and the possible utilization of local copying services, such as color reproduction.

Avail: Issuing Activity, or Corporate Author, or no indication of availability. Inquiries as to the availability of these documents should be addressed to the organization shown in the citation as the corporate author of the document.

NASA PATENTS AND PATENT APPLICATIONS

Patents and patent applications owned by NASA are announced in *STAR* under appropriate subject categories and are referenced in the *STAR* indexes. In the Report/Accession Number Index, patents are indexed by the NASA Case Number (which appears in lieu of the report number in other indexes), the U.S. Patent Number, the U.S. Patent Application Serial Number, and the U.S. Patent Class. Patent applications for which patents have not yet been issued are indexed by the NASA Case Number and the U.S. Patent Application Serial Number.

NASA *patent application specifications* are sold in paper copy by the National Technical Information Service at price code A02. Microfiche are sold at price code A01. The US-Patent-Appl-SN- number should be used in ordering either paper copy or microfiche from NTIS. Printed copies of *patents* (which are not microfiched) are available for purchase at $1.50 per copy from:

Commissioner of Patents and Trademarks
U.S. Patent and Trademark Office
Washington, D.C. 20231

When ordering patents, the U.S. Patent Number should be used, and payment must be remitted in advance, preferably by money order or check payable to the Commissioner of Patents and Trademarks. Prepaid purchase coupons for ordering are also available from the Patent and Trademark Office. The patents and patent applications announced in *STAR* are owned by NASA and are available for royalty-free licensing. Requests for licensing terms and further information should be addressed to:

Associate General Counsel for Intellectual Property/Code GP
National Aeronautics and Space Administration
Washington, D.C. 20546

ELIGIBILITY AND REGISTRATION FOR NASA INFORMATION PRODUCTS AND SERVICES

A variety of services is available to organizations of the following types that have registered with NASA to receive specific services or products:

1. NASA offices, research centers, contractors, subcontractors, grantees, and consultants;
2. Other U.S. Government agencies and their contractors;
3. Libraries in the United States that have arrangements with NASA to maintain collections of NASA documents for public reference;
4. Other organizations in the United States having a need for NASA documents in work related to aeronautics and space research;
5. Organizations abroad that have established reciprocal document exchange arrangements with NASA.

Only the central service points or central points of document acquisition and control within qualified organizations are eligible to register for NASA products and services. Domestic organizations that may be eligible to receive various classes of NASA publications and services should address their requests for registration or for further information to:

NASA Scientific and Technical Information Facility
ATTN: Registration Services
Post Office Box 8757
BWI Airport, Maryland 21240

Organizations abroad should direct requests to Manager, International STI Activities, NTT, NASA Headquarters, Washington, D.C. 20546.

AVAILABILITY OF *STAR* ABSTRACTS ON MICROFICHE

Microfiche of the abstract sections of this issue and other issues of *STAR* are available on annual subscription from NTIS as PB89-911300, Attn: Subscriptions, 5285 Port Royal Road, Springfield, Virginia 22161. Annual subscription rates are $70.00 North America; $140.00 foreign. Abstract sections for previous years retroactive to 1964 are available at the current rates. Microfiche for individual *STAR* issue abstract sections are not available.

PUBLIC COLLECTIONS OF NASA DOCUMENTS

DOMESTIC: NASA and NASA-sponsored documents and a large number of aerospace publications are available to the public for reference purposes at the library maintained by the American Institute of Aeronautics and Astronautics, Technical Information Service, 555 West 57th Street, 12th Floor, New York, New York 10019

EUROPEAN: An extensive collection of NASA and NASA-sponsored publications is maintained by the British Library Lending Division, Boston Spa, Wetherby, Yorkshire, England for public access. The British Library Lending Division also has available many of the non-NASA publications cited in *STAR*. European requesters may purchase facsimile copy or microfiche of NASA and NASA-sponsored documents, those identified by both the symbols # and * from ESA - Information Retrieval Service European Space Agency, 8-10 rue Mario-Nikis, 75738 Paris CEDEX 15, France.

FEDERAL DEPOSITORY LIBRARY PROGRAM

In order to provide the general public with greater access to U.S. Government publications, Congress established the Federal Depository Library Program under the Government Printing Office (GPO), with 50 regional depositories responsible for permanent retention of material, inter-library loan, and reference services. At least one copy of nearly every NASA and NASA-sponsored publication, either in printed or microfiche format, is received and retained by the 50 regional depositories. A list of the regional GPO libraries, arranged alphabetically by state, appears on the inside back cover. These libraries are *not* sales outlets. A local library can contact a Regional Depository to help locate specific reports, or direct contact may be made by an individual.

ADDRESSES OF ORGANIZATIONS

American Institute of Aeronautics and Astronautics
Technical Information Service
555 West 57th Street, 12th Floor
New York, New York 10019

British Library Lending Division,
Boston Spa, Wetherby, Yorkshire,
England

Commissioner of Patents and Trademarks
U.S. Patent and Trademark Office
Washington, D.C. 20231

Department of Energy
Technical Information Center
P.O. Box 62
Oak Ridge, Tennessee 37830

ESA-Information Retrieval Service
ESRIN
Via Galileo Galilei
00044 Frascati (Rome) Italy

ESDU International
P.O. Box 1633
Manassas, Virginia 22110

ESDU International, Ltd.
251-259 Regent Street
London, W1R 7AD, England

Fachinformationszentrum Energie, Physik, Mathematik GMBH
7514 Eggenstein Leopoldshafen
Federal Republic of Germany

Her Majesty's Stationery Office
P.O. Box 569, S.E. 1
London, England

NASA Scientific and Technical Information Facility
P.O. Box 8757
B.W.I. Airport, Maryland 21240

National Aeronautics and Space Administration
Scientific and Technical Information Division (NTT)
Washington, D.C. 20546

National Technical Information Service
5285 Port Royal Road
Springfield, Virginia 22161

Pendragon House, Inc.
899 Broadway Avenue
Redwood City, California 94063

Superintendent of Documents
U.S. Government Printing Office
Washington, D.C. 20402

University Microfilms
A Xerox Company
300 North Zeeb Road
Ann Arbor, Michigan 48106

University Microfilms, Ltd.
Tylers Green
London, England

U.S. Geological Survey Library
National Center - MS 950
12201 Sunrise Valley Drive
Reston, Virginia 22092

U.S. Geological Survey Library
2255 North Gemini Drive
Flagstaff, Arizona 86001

U.S. Geological Survey
345 Middlefield Road
Menlo Park, California 94025

U.S. Geological Survey Library
Box 25046
Denver Federal Center, MS914
Denver, Colorado 80225

NTIS PRICE SCHEDULES

(Effective January 1, 1989)

Schedule A
STANDARD PRICE DOCUMENTS AND MICROFICHE

PRICE CODE	NORTH AMERICAN PRICE	FOREIGN PRICE
A01	$ 6.95	$13.90
A02	10.95	21.90
A03	13.95	27.90
A04-A05	15.95	31.90
A06-A09	21.95	43.90
A10-A13	28.95	57.90
A14-A17	36.95	73.90
A18-A21	42.95	85.90
A22-A25	49.95	99.90
A99	*	*
NO1	55.00	70.00
NO2	55.00	80.00

Schedule E
EXCEPTION PRICE DOCUMENTS AND MICROFICHE

PRICE CODE	NORTH AMERICAN PRICE	FOREIGN PRICE
E01	$ 9.00	18.00
E02	11.50	23.00
E03	13.00	26.00
E04	15.50	31.00
E05	17.50	35.00
E06	20.50	41.00
E07	23.00	46.00
E08	25.50	51.00
E09	28.00	56.00
E10	31.00	62.00
E11	33.50	67.00
E12	36.50	73.00
E13	39.00	78.00
E14	42.50	85.00
E15	46.00	92.00
E16	50.50	101.00
E17	54.50	109.00
E18	59.00	118.00
E19	65.50	131.00
E20	76.00	152.00
E99	*	*

*Contact NTIS for price quote.

IMPORTANT NOTICE

NTIS Shipping and Handling Charges

U.S., Canada, Mexico — ADD $3.00 per TOTAL ORDER

All Other Countries — ADD $4.00 per TOTAL ORDER

Exceptions — Does NOT apply to:

ORDERS REQUESTING NTIS RUSH HANDLING
ORDERS FOR SUBSCRIPTION OR STANDING ORDER PRODUCTS *ONLY*

NOTE: Each additional delivery address on an order requires a separate shipping and handling charge.

VOLUME 27 NUMBER 2 / JANUARY 23, 1989

TABLE OF CONTENTS

AERONAUTICS

Includes aeronautics (general); aerodynamics; air transportation and safety; aircraft communications and navigation; aircraft design, testing and performance; aircraft instrumentation; aircraft propulsion and power; aircraft stability and control; and research and support facilities (air).

For related information see also *Astronautics.*

01 AERONAUTICS (GENERAL) 143

02 AERODYNAMICS 145

Includes aerodynamics of bodies, combinations, wings, rotors, and control surfaces; and internal flow in ducts and turbomachinery.

For related information see also *34 Fluid Mechanics and Heat Transfer*

03 AIR TRANSPORTATION AND SAFETY 149

Includes passenger and cargo air transport operations; and aircraft accidents.

For related information see also *16 Space Transportation* and *85 Urban Technology and Transportation.*

04 AIRCRAFT COMMUNICATIONS AND NAVIGATION 150

Includes digital and voice communication with aircraft; air navigation systems (satellite and ground based); and air traffic control.

For related information see also *17 Space Communications, Spacecraft Communications, Command and Tracking* and *32 Communications and Radar.*

05 AIRCRAFT DESIGN, TESTING AND PERFORMANCE 152

Includes aircraft simulation technology.

For related information see also *18 Spacecraft Design, Testing and Performance* and *39 Structural Mechanics.* For land transportation vehicles see *85 Urban Technology and Transportation.*

06 AIRCRAFT INSTRUMENTATION N.A.

Includes cockpit and cabin display devices; and flight instruments.

For related information see also *19 Spacecraft Instrumentation* and *35 Instrumentation and Photography.*

07 AIRCRAFT PROPULSION AND POWER 153

Includes prime propulsion systems and systems components, e.g., gas turbine engines and compressors; and onboard auxiliary power plants for aircraft.

For related information see also *20 Spacecraft Propulsion and Power, 28 Propellants and Fuels,* and *44 Energy Production and Conversion.*

08 AIRCRAFT STABILITY AND CONTROL 154

Includes aircraft handling qualities; piloting; flight controls; and autopilots.

For related information see also *05 Aircraft Design, Testing and Performance.*

09 RESEARCH AND SUPPORT FACILITIES (AIR) 154

Includes airports, hangars and runways; aircraft repair and overhaul facilities; wind tunnels; shock tubes; and aircraft engine test stands.

For related information see also *14 Ground Support Systems and Facilities (Space).*

ASTRONAUTICS

Includes astronautics (general); astrodynamics; ground support systems and facilities (space); launch vehicles and space vehicles; space transportation; space communications, spacecraft communications, command and tracking; spacecraft design, testing and performance; spacecraft instrumentation; and spacecraft propulsion and power.

For related information see also *Aeronautics*

12 ASTRONAUTICS (GENERAL) 155

For extraterrestrial exploration see *91 Lunar and Planetary Exploration.*

13 ASTRODYNAMICS 158

Includes powered and free-flight trajectories; and orbital and launching dynamics.

14 GROUND SUPPORT SYSTEMS AND FACILITIES (SPACE) 158

Includes launch complexes, research and production facilities; ground support equipment, e.g., mobile transporters; and simulators.

For related information see also *09 Research and Support Facilities (Air).*

15 LAUNCH VEHICLES AND SPACE VEHICLES 159

Includes boosters; operating problems of launch/space vehicle systems; and reusable vehicles.

For related information see also *20 Spacecraft Propulsion and Power.*

16 SPACE TRANSPORTATION 159

Includes passenger and cargo space transportation, e.g., shuttle operations; and space rescue techniques.

For related information see also *03 Air Transportation and Safety* and *18 Spacecraft Design, Testing and Performance.* For space suits see *54 Man/System Technology and Life Support.*

17 SPACE COMMUNICATIONS, SPACECRAFT COMMUNICATIONS, COMMAND AND TRACKING 159

Includes telemetry; space communications networks; astronavigation and guidance; and radio blackout.

For related information see also *04 Aircraft Communications and Navigation* and *32 Communications and Radar.*

18 SPACECRAFT DESIGN, TESTING AND PERFORMANCE 160

Includes satellites; space platforms; space stations; spacecraft systems and components such as thermal and environmental controls; and attitude controls.

For life support systems see *54 Man/System Technology and Life Support.* For related information see also *05 Aircraft Design, Testing and Performance, 39 Structural Mechanics,* and *16 Space Transportation.*

19 SPACECRAFT INSTRUMENTATION N.A.

For related information see also *06 Aircraft Instrumentation* and *35 Instrumentation and Photography.*

20 SPACECRAFT PROPULSION AND POWER 162

Includes main propulsion systems and components, e.g. rocket engines; and spacecraft auxiliary power sources.

For related information see also *07 Aircraft Propulsion and Power, 28 Propellants and Fuels, 44 Energy Production and Conversion,* and *15 Launch Vehicles and Space Vehicles.*

CHEMISTRY AND MATERIALS

Includes chemistry and materials (general); composite materials; inorganic and physical chemistry; metallic materials; nonmetallic materials; propellants and fuels; and materials processing.

23 CHEMISTRY AND MATERIALS (GENERAL) N.A.

24 COMPOSITE MATERIALS 162

Includes physical, chemical, and mechanical properties of laminates and other composite materials.

For ceramic materials see *27 Nonmetallic Materials.*

25 INORGANIC AND PHYSICAL CHEMISTRY 165

Includes chemical analysis, e.g., chromatography; combustion theory; electrochemistry; and photochemistry.

For related information see also *77 Thermodynamics and Statistical Physics.*

26 METALLIC MATERIALS 170

Includes physical, chemical, and mechanical properties of metals, e.g., corrosion; and metallurgy.

27 NONMETALLIC MATERIALS 176

Includes physical, chemical, and mechanical properties of plastics, elastomers, lubricants, polymers, textiles, adhesives, and ceramic materials.

For composite materials see *24 Composite Materials.*

28 PROPELLANTS AND FUELS 179

Includes rocket propellants, igniters and oxidizers; their storage and handling procedures; and aircraft fuels.

For related information see also *07 Aircraft Propulsion and Power, 20 Spacecraft Propulsion and Power,* and *44 Energy Production and Conversion.*

29 MATERIALS PROCESSING 181

Includes space-based development of products and processes for commercial application.

For biological materials see *55 Space Biology.*

ENGINEERING

Includes engineering (general); communications and radar; electronics and electrical engineering; fluid mechanics and heat transfer; instrumentation and photography; lasers and masers; mechanical engineering; quality assurance and reliability; and structural mechanics.

For related information see also *Physics.*

31 ENGINEERING (GENERAL) 181

Includes vacuum technology; control engineering; display engineering; cryogenics; and fire prevention.

32 COMMUNICATIONS AND RADAR 183

Includes radar; land and global communications; communications theory; and optical communications.

For related information see also *04 Aircraft Communications and Navigation* and *17 Space Communications, Spacecraft Communications, Command and Tracking.* For search and rescue see *03 Air Transportation and Safety,* and *16 Space Transportation.*

33 ELECTRONICS AND ELECTRICAL ENGINEERING 190

Includes test equipment and maintainability; components, e.g., tunnel diodes and transistors; microminiaturization; and integrated circuitry.

For related information see also *60 Computer Operations and Hardware* and *76 Solid-State Physics.*

34 FLUID MECHANICS AND HEAT TRANSFER 193

Includes boundary layers; hydrodynamics; fluidics; mass transfer and ablation cooling.

For related information see also *02 Aerodynamics* and *77 Thermodynamics and Statistical Physics.*

35 INSTRUMENTATION AND PHOTOGRAPHY 202

Includes remote sensors; measuring instruments and gages; detectors; cameras and photographic supplies; and holography.

For aerial photography see *43 Earth Resources and Remote Sensing.* For related information see also *06 Aircraft Instrumentation* and *19 Spacecraft Instrumentation.*

36 LASERS AND MASERS 203

Includes parametric amplifiers.

For related information see also *76 Solid-State Physics.*

37 MECHANICAL ENGINEERING 207

Includes auxiliary systems (nonpower); machine elements and processes; and mechanical equipment.

38 QUALITY ASSURANCE AND RELIABILITY 211

Includes product sampling procedures and techniques; and quality control.

39 STRUCTURAL MECHANICS 211

Includes structural element design and weight analysis; fatigue; and thermal stress.

For applications see *05 Aircraft Design, Testing and Performance* and *18 Spacecraft Design, Testing and Performance.*

GEOSCIENCES

Includes geosciences (general); earth resources and remote sensing; energy production and conversion; environment pollution; geophysics; meteorology and climatology; and oceanography.

For related information see also *Space Sciences.*

42 GEOSCIENCES (GENERAL) N.A.

43 EARTH RESOURCES AND REMOTE SENSING 217

Includes remote sensing of earth resources by aircraft and spacecraft; photogrammetry; and aerial photography.

For instrumentation see *35 Instrumentation and Photography.*

44 ENERGY PRODUCTION AND CONVERSION 219

Includes specific energy conversion systems, e.g., fuel cells; global sources of energy; geophysical conversion; and windpower.

For related information see also *07 Aircraft Propulsion and Power, 20 Spacecraft Propulsion and Power,* and *28 Propellants and Fuels.*

45 ENVIRONMENT POLLUTION 222

Includes atmospheric, noise, thermal, and water pollution.

46 GEOPHYSICS 224

Includes aeronomy; upper and lower atmosphere studies; ionospheric and magnetospheric physics; and geomagnetism.

For space radiation see *93 Space Radiation.*

47 METEOROLOGY AND CLIMATOLOGY 228

Includes weather forecasting and modification.

48 OCEANOGRAPHY 233

Includes biological, dynamic, and physical oceanography; and marine resources.

For related information see also *43 Earth Resources and Remote Sensing.*

LIFE SCIENCES

Includes life sciences (general); aerospace medicine; behavioral sciences; man/system technology and life support; and space biology.

51 LIFE SCIENCES (GENERAL) 233

52 AEROSPACE MEDICINE 234

Includes physiological factors; biological effects of radiation; and effects of weightlessness on man and animals.

53 BEHAVIORAL SCIENCES 234

Includes psychological factors; individual and group behavior; crew training and evaluation; and psychiatric research.

54 MAN/SYSTEM TECHNOLOGY AND LIFE SUPPORT 234

Includes human engineering; biotechnology; and space suits and protective clothing.

For related information see also *16 Space Transportation.*

55 SPACE BIOLOGY 235

Includes exobiology; planetary biology; and extraterrestrial life.

MATHEMATICAL AND COMPUTER SCIENCES

Includes mathematical and computer sciences (general); computer operations and hardware; computer programming and software; computer systems; cybernetics; numerical analysis; statistics and probability; systems analysis; and theoretical mathematics.

59 MATHEMATICAL AND COMPUTER SCIENCES (GENERAL) N.A.

60 COMPUTER OPERATIONS AND HARDWARE 235

Includes hardware for computer graphics, firmware, and data processing.

For components see *33 Electronics and Electrical Engineering.*

61 COMPUTER PROGRAMMING AND SOFTWARE 238

Includes computer programs, routines, algorithms, and specific applications, e.g., CAD/CAM.

62 COMPUTER SYSTEMS 242

Includes computer networks and special application computer systems.

63 CYBERNETICS 243

Includes feedback and control theory, artificial intelligence, robotics and expert systems.

For related information see also *54 Man/System Technology and Life Support.*

64 NUMERICAL ANALYSIS 245

Includes iteration, difference equations, and numerical approximation.

65 STATISTICS AND PROBABILITY 248

Includes data sampling and smoothing; Monte Carlo method; and stochastic processes.

66 SYSTEMS ANALYSIS 250

Includes mathematical modeling; network analysis; and operations research.

67 THEORETICAL MATHEMATICS 250

Includes topology and number theory.

PHYSICS

Includes physics (general); acoustics; atomic and molecular physics; nuclear and high-energy physics; optics; plasma physics; solid-state physics; and thermodynamics and statistical physics.

For related information see also *Engineering.*

70 PHYSICS (GENERAL) 250

For precision time and time interval (PTTI) see *35 Instrumentation and Photography;* for geophysics, astrophysics or solar physics see *46 Geophysics, 90 Astrophysics,* or *92 Solar Physics.*

71 ACOUSTICS 251
Includes sound generation, transmission, and attenuation.
For noise pollution see *45 Environment Pollution.*

72 ATOMIC AND MOLECULAR PHYSICS 251
Includes atomic structure, electron properties, and molecular spectra.

73 NUCLEAR AND HIGH-ENERGY PHYSICS 253
Includes elementary and nuclear particles; and reactor theory.
For space radiation see *93 Space Radiation.*

74 OPTICS 254
Includes light phenomena and optical devices.
For lasers see *36 Lasers and Masers.*

75 PLASMA PHYSICS 255
Includes magnetohydrodynamics and plasma fusion.
For ionospheric plasmas see *46 Geophysics.* For space plasmas see *90 Astrophysics.*

76 SOLID-STATE PHYSICS 260
Includes superconductivity.
For related information see also *33 Electronics and Electrical Engineering* and *36 Lasers and Masers.*

77 THERMODYNAMICS AND STATISTICAL PHYSICS 269
Includes quantum mechanics; theoretical physics; and Bose and Fermi statistics.
For related information see also *25 Inorganic and Physical Chemistry* and *34 Fluid Mechanics and Heat Transfer.*

SOCIAL SCIENCES

Includes social sciences (general); administration and management; documentation and information science; economics and cost analysis; law, political science, and space policy; and urban technology and transportation.

80 SOCIAL SCIENCES (GENERAL) N.A.
Includes educational matters.

81 ADMINISTRATION AND MANAGEMENT N.A.
Includes management planning and research.

82 DOCUMENTATION AND INFORMATION SCIENCE 270
Includes information management; information storage and retrieval technology; technical writing; graphic arts; and micrography.
For computer documentation see *61 Computer Programming and Software.*

83 ECONOMICS AND COST ANALYSIS N.A.
Includes cost effectiveness studies.

84 LAW, POLITICAL SCIENCE AND SPACE POLICY N.A.
Includes NASA appropriation hearings; aviation law; space law and policy; international law; international cooperation; and patent policy.

85 URBAN TECHNOLOGY AND TRANSPORTATION 273
Includes applications of space technology to urban problems; technology transfer; technology assessment; and surface and mass transportation.
For related information see *03 Air Transportation and Safety, 16 Space Transportation,* and *44 Energy Production and Conversion.*

SPACE SCIENCES

Includes space sciences (general); astronomy; astrophysics; lunar and planetary exploration; solar physics; and space radiation.
For related information see also *Geosciences.*

88 SPACE SCIENCES (GENERAL) 274

89 ASTRONOMY 276
Includes radio, gamma-ray, and infrared astronomy; and astrometry.

90 ASTROPHYSICS 278
Includes cosmology; celestial mechanics; space plasmas; and interstellar and interplanetary gases and dust.
For related information see also *75 Plasma Physics.*

91 LUNAR AND PLANETARY EXPLORATION 280
Includes planetology; and manned and unmanned flights.
For spacecraft design or space stations see *18 Spacecraft Design, Testing and Performance.*

92 SOLAR PHYSICS 281
Includes solar activity, solar flares, solar radiation and sunspots.
For related information see *93 Space Radiation.*

93 SPACE RADIATION 281
Includes cosmic radiation; and inner and outer earth's radiation belts.
For biological effects of radiation see *52 Aerospace Medicine.* For theory see *73 Nuclear and High-Energy Physics.*

GENERAL

Includes aeronautical, astronautical, and space science related histories, biographies, and pertinent reports too broad for categorization; histories or broad overviews of NASA programs.

99 GENERAL 281

Note: N.A. means that no abstracts were assigned to this category for this issue.

SUBJECT INDEX I-1
PERSONAL AUTHOR INDEX I-51
CORPORATE SOURCE INDEX I-59
CONTRACT NUMBER INDEX I-71
REPORT/ACCESSION NUMBER INDEX I-73

TYPICAL CITATION AND ABSTRACT

NASA SPONSORED
ON MICROFICHE
ACCESSION NUMBER
N89-10248* # National Aeronautics and Space Administration, Washington, D.C.
CORPORATE SOURCE
TITLE
RESONANT EXCITATION OF SPATIAL PERTURBATIONS IN A BOUNDARY LAYER IN THE PRESENCE OF A PRESSURE GRADIENT
AUTHOR
I. Maslennikova Aug. 1988 13 p Transl. into ENGLISH of Russian report (Novosibirsk, USSR, Academy of Sciences), 1987 p 46-52 Transl. by Scientific Translation Service, Santa Barbara, Calif.
PUBLICATION DATE
CONTRACT OR GRANT
(Contract NASw-4307)
AVAILABILITY SOURCE
REPORT NUMBER
(NASA-TT-20305; NAS 1.77:20305) Avail: NTIS HC A03/MF A01 CSCL 20D
PRICE CODE
COSATI CODE
The calculation results presented indicate that resonant interaction in triads in the presence of a pressure gradient is qualitatively similar to the case of nongradient flow. The amplitude of the plane wave is the primary factor determining mode discrimination and the evolution of the triplet. If the amplitude of the plane wave is greater than some sufficiently low threshold level, a broad spectrum of three-dimensional subharmonic perturbations will be excited in all the flows considered. In slower flows the amplitudes of the primary wave and subharmonic are equalized in a narrower range of Reynolds numbers and the rates of increase of both components are much higher. The above makes it possible to infer that a positive pressure gradient has a destabilizing effect on resonant interaction in triads, which makes the role of gradients decisive in subharmonic transitions on actual streamline bodies. Author

VOLUME 27 NUMBER 2 / JANUARY 23, 1989

Scientific and Technical Aerospace Reports

A Semimonthly Publication of the National Aeronautics and Space Administration

01 AERONAUTICS (GENERAL)

N89-10830# Politecnico di Torino (Italy). Dipartimento di Ingegneria Aeronautica e Spaziale.
[ORIGIN, OBJECTIVES AND ACTIVITIES OF THE DEPARTMENT OF AEROSPACE ENGINEERING] Annual Report, 1985
Nov. 1986 38 p
Avail: NTIS HC A03/MF A01

The research activities of the Department of Engineering of the Turin Polytechnic are reported. Department activities are concerned with both teaching and research. The research is broadly based and covers all traditional disciplines of aeronautical and aerospatial engineering. Allied research themes are also developed, such as industrial aerodynamics, material science, biofluidynamics, laser matter interaction and other topics where one can find new application fields for the methodologies and the knowledge of aerospace disciplines. Brief summaries are given of research activities for 1985. E.R.

N89-10831# Advisory Group for Aerospace Research and Development, Neuilly-Sur-Seine (France). Guidance and Control Panel.
COMPUTING SYSTEMS CONFIGURATION FOR HIGHLY INTEGRATED GUIDANCE AND CONTROL SYSTEMS
Jun. 1988 164 p Lectures held in Bourges, France, 20-21 Jun. 1988, in Neubiberg, West Germany, 23-24 Jun. 1988, and in Seattle, Wash., 6-7 Jul. 1988
(AGARD-LS-158; ISBN-92-835-0464-X) Copyright Avail: NTIS HC A08/MF A01

Modern military air vehicles have to comply with sophisticated performance requirements. As a result, full advantage must be taken of the rapid advances in computer hardware/software and future micro-electronics technologies. New design and development strategies must be implemented in order to obtain the overall performance benefits offered by advanced integrated systems for guidance and control, avionics, weapon delivery and tactical performance management. In a two-day program this Lecture Series addresses issues which have demonstrated notable and outstanding advances in the field of computing system design, design tools and techniques, computers, data buses, and architectures. In particular, the second day's program will show how technological advances have enabled the design of a modern computing system architecture. Future trends and new directions will be subjects for round table discussions. For individual titles, see N89-10832 through N89-10837.

N89-10832# Messerschmitt-Boelkow-Blohm G.m.b.H., Munich (West Germany). Aircraft Div.
COMPUTING SYSTEM CONFIGURATION FOR FIGHTER AIRCRAFT FLIGHT CONTROL SYSTEMS **c08**
H. J. Kaul, H. Lueers, and J. Rauch *In* AGARD, Computing Systems Configuration for Highly Integrated Guidance Control Systems Jun. 1988 32 p (For primary document see N89-10831 02-01)
Copyright Avail: NTIS HC A08/MF A01

Flight Control Systems (FCS) for present and future Fighter Aircraft developments are based on three basic technologies, CCV-ACT-digital signal processing. These technologies have opened a new degree of freedom for optimizing overall weapon system performance by extending the requirements to be implemented by the FCS. The computing subsystem of the FCS is the key element of the FCS by which this performance optimization can be achieved. Digital FCS for fighter aircraft in service or under development exhibit a basically common architecture (static parallel redundancy, centralized heavily burdened computing subsystem) which has continuously evolved since the early days of CCV and ACT activities. The objectives of the paper are to relate this classical architecture to the advancing requirements and the new emerging technologies and to analyze its potentials for future developments. Author

N89-10833# Electronique Serge Dassault, St. Cloud (France).
A HIGHLY RELIABLE COMPUTER FOR AIRBORNE APPLICATIONS **c60**
Michel Muenier *In* AGARD, Computing Systems Configuration for Highly Integrated Guidance and Control Systems Jun. 1988 17 p (For primary document see N89-10831 02-01)
Copyright Avail: NTIS HC A08/MF A01

The reliability features of the CMF (French Military Computer) AIR embedded computer supporting its operational software are described. This computer was designed to meet the requirements of the ACE (European Combat Aircraft)/RAFALE D aircraft. Therefore, it has to be highly dependable to satisfy severe physical requirements (size, weight, power consumption, etc.) and to support real-time software execution (this software being written in high-level languages such as Ada and LTR3, a French Pascal-like real-time language). The general structure of the computer is first presented, emphasis being placed on the technological choices (for example, the use of ASICs: Application Specific Integrated Circuits). The various protective mechanisms provided at the level of the machine (hardware and microcode) are then presented: data access control and code execution control. Finally, a short presentation of the software production environment is given. In conclusion, the compromise made between operational dependability and performance characteristics are summarized. Author

N89-10834# Air Force Wright Aeronautical Labs., Wright-Patterson AFB, Ohio. Avionics Lab.
ADVANCED AVIONICS ARCHITECTURE PAVE PILLAR **c06**
John C. Ostgaard *In* AGARD, Computing Systems Configuration for Highly Integrated Guidance and Control Systems Jun. 1988 8 p (For primary document see N89-10831 02-01)
Copyright Avail: NTIS HC A08/MF A01

The increased use of advanced electronics has given modern combat aircraft phenomenal levels of performance, but at a stiff price in initial cost, maintenance workload and aircraft availability. Hence, aircraft design is shifting to give equal emphasis on performance, affordability, maintainability, and reliability in the development of avionic systems. The paper discusses the challenges and benefits of an avionics architecture concept which integrates avionic functions at the system level thereby improving the system's accuracy, increasing its immunity to failure, and decreasing its reliance on multiple redundant sensors. This design philosophy, which permits resources to be shared across subsystems, requires a highly coupled system-wide management and control program (operating system) supported by a wide-band

distribution network, high-speed data and signal processors, and extensive mass memory. The implementation strategy for this avionics architecture is the system-wide utilization of common modular building blocks using advanced microelectronics such as VHSIC, standard 3/4 ATR modules and integrated racks, all interconnected by fiber optic networks. The generic integration approach and architecture produced by the PAVE PILLAR program is the foundation for avionics development in the next generation aircraft for the U.S. DOD and include such aircraft as the USAF Advanced Tactical Fighter (ATF). Author

N89-10835# Air Force Wright Aeronautical Labs., Wright-Patterson AFB, Ohio. Data and Signal Processing Group.
DATA AND SIGNAL PROCESSING ARCHITECTURES FOR FUTURE AVIONICS **c06**
Mark T. Michael *In* AGARD, Computing Systems Configuration for Highly Integrated Guidance and Control Systems Jun. 1988 12 p (For primary document see N89-10831 02-01)
Copyright Avail: NTIS HC A08/MF A01

Pave Pillar architecture incorporates a Common Signal Processor (CSP) concept as a key building block of a USAF advanced avionics suite. This concept embodies the use of standard internal interfaces, a family of modules, use of the programming language Ada to express application program for the data processors within CSP, and the use of a Graph Notation to represent signal processing functions for the signal processing components of the CSP. The modularity permits upgrading any hardware or software component with minimal disruption to the rest of the design. CSP is an open architecture in that the interfaces and module specifications are non-proprietary and can be built by other vendors. The paper will address the system concept, hardware architecture, and software philosophy comprising the CSP system. It will describe in general terms how the CSP hardware works and its expandability. Existing modules will be listed and potential future modules identified. A brief description of the Graph Notation and its advantages will be provided. The CSP Local Operating System capabilities and use will be summarized. Application studies to determine the suitability of the CSP concept for different avionic applications such as radar, electronic warfare, communications, and electro-optical sensors will be briefly summarized. The role of the MIL-STD-1750A processors in CSP and their limitations will be touched on, and future upgrades to 32-bit machines discussed. Author

N89-10836# Harris Corp., Melbourne, Fla. Government Aerospace Systems Div.
FIBER OPTIC BUSES AND NETWORKS FOR ADVANCED AVIONICS ARCHITECTURES **c06**
R. W. Uhlhorn *In* AGARD, Computing Systems Configuration for Highly Integrated Guidance and Control Systems Jun. 1988 15 p (For primary document see N89-10831 02-01)
Copyright Avail: NTIS HC A08/MF A01

An avionics architecture exploiting high-speed, high density VLSI and VHSIC technology by repartitioning the traditional avionics suite requires subsystem interconnection via backbone and backplane buses and networks operating at data rates far exceeding those used for avionics in the past. In fact, the rates are high enough that fiber optics is the only interconnect technology that does not impose substantial size, weight, and life cycle cost penalties on the overall system. In the Pave Pillar architecture the fiber optic multiplex bus for command and control, block transfer, and flight control functions, based on a variation of the IEEE 802.4 and 802.2 token-passing bus protocol for the physical and data link layers, operates at 50 Mbps. A number of specific implementations have emerged. The parallel internal bus protocol ties users (data processors) together in the backplane and through a bus interface unit to the multiplex bus. Other kinds of networks are used to serve subsystems connecting video terminals, sensors, signal processors, etc. An overview of the multiplexed high-speed data bus and parallel backplane bus designs and their interface is presented. The implementation details and options for the fiber optic network which supports the interconnection of avionics bus interface modules in different physical locations are discussed. Passive and active star-coupled networks are compared and conclusions drawn. The state of the art in packaging of the avionics bus interface and related line replaceable modules is illustrated. Author

N89-10837# Air Force Wright Aeronautical Labs., Wright-Patterson AFB, Ohio. Avionics Lab.
HIGH SPEED PARALLEL PROCESSING NETWORKS FOR ADVANCED ARCHITECTURES **c60**
D. Reed Morgan *In* AGARD, Computing Systems Configuration for Highly Integrated Guidance and Control Systems Jun. 1988 17 p (For primary document see N89-10831 02-01)
Copyright Avail: NTIS HC A08/MF A01

Many force multiplier improvements in vehicle control, situation awareness and crew decision aiding will be made possible if affordable, flyable supercomputers and associated software can be developed for next-generation military aircraft. New functional architectures will emerge because dramatic improvements in processing speed can be implemented through tightly coupled networks. Unconstrained system architectures can be developed where the system designer will have the capability to fuse together needed logical functions irrespective of previous boundaries. In addition, increased local processing (e.g., smart sensors) will be made possible to improve threat and target classification. Robust use of real-time artificial intelligence at both local, functional and system levels will be achievable, along with inprovements in fault tolerance and system diagnostics. Author

N89-10838*# Joint Inst. for Advancement of Flight Sciences, Washington, D. C.
PROGRAM OF RESEARCH IN STRUCTURES AND DYNAMICS
Final Report
Sep. 1988 35 p
(Grant NGR-09-010-078)
(NASA-CR-183191; NAS 1.26:183191) Avail: NTIS HC A03/MF A01 CSCL 01B

The Structures and Dynamics Program was first initiated in 1972 with the following two major objectives: to provide a basic understanding and working knowledge of some key areas pertinent to structures, solid mechanics, and dynamics technology including computer aided design; and to provide a comprehensive educational and research program at the NASA Langley Research Center leading to advanced degrees in the structures and dynamics areas. During the operation of the program the research work was done in support of the activities of both the Structures and Dynamics Division and the Loads and Aeroelasticity Division. During the period of 1972 to 1986 the Program provided support for two full-time faculty members, one part-time faculty member, three postdoctoral fellows, one research engineer, eight programmers, and 28 graduate research assistants. The faculty and staff of the program have published 144 papers and reports, and made 70 presentations at national and international meetings, describing their research findings. In addition, they organized and helped in the organization of 10 workshops and national symposia in the structures and dynamics areas. The graduate research assistants and the students enrolled in the program have written 20 masters theses and 2 doctoral dissertations. The overall progress is summarized. Author

N89-10839# Centre National d'Etudes Spatiales, Toulouse (France).
FLIGHT MECHANICS AND AEROTHERMODYNAMIC SOFTWARE
J. C. Agnese, P. SaintPe, and T. Voiron 6 Mar. 1988 35 p In FRENCH; ENGLISH summary
(CNES-CT/DTI/MS/MN/069; CNES-DLA/SDT/ED/SA; ETN-88-93094) Avail: NTIS HC A03/MF A01

Aerothermodynamics software for heat flow computation on an axisymmetric structure, plane sheet, arrow cylinder; wall heating with or without ablation; thrust nozzle free jet computation and its interaction with a wall (plane or truncated segment); and flight mechanics software for Ariane takeoff and booster separation is described. ESA

02 AERODYNAMICS

Includes aerodynamics of bodies, combinations, wings, rotors, and control surfaces; and internal flow in ducts and turbomachinery.

For related information see also *34 Fluid Mechanics and Heat Transfer.*

N89-10840# Sandia National Labs., Albuquerque, N. Mex.
AN APPROXIMATE, MAXIMUM TERMINAL VELOCITY DESCENT TO A POINT
G. Richard Eisler and David G. Hull (Texas Univ., Austin.) 1987 15 p Presented at the Guidance, Navigation and Control Conference, Minneapolis, Minn., 15 Aug. 1988
(Contract DE-AC04-76DP-00789)
(DE88-000349; SAND-87-3011C; CONF-880818-2) Avail: NTIS HC A03/MF A01

No closed form control solution exists for maximizing the terminal velocity of a hypersonic glider at an arbitrary point. As an alternative, this study uses neighboring extremal theory to provide a sampled data feedback law to guide the vehicle to a constrained ground range and altitude. The guidance algorithm is divided into two parts: (1) computation of a nominal, approximate, maximum terminal velocity trajectory to a constrained final altitude and computation of the resulting unconstrained groundrange, and (2) computation of the neighboring extremal control perturbation at the sample value of flight path angle to compensate for changes in the approximate physical model and enable the vehicle to reach the on-board computed groundrange. The trajectories are characterized by glide and dive flight to the target to minimize the time spent in the denser parts of the atmosphere. The proposed on-line scheme successfully brings the final altitude and range constraints together, as well as compensates for differences in flight model, atmosphere, and aerodynamics at the expense of guidance update computation time. Comparison with an independent, parameter optimization solution for the terminal velocity is excellent. DOE

N89-10841# Sandia National Labs., Albuquerque, N. Mex.
AERODYNAMIC DESIGN CONSIDERATIONS FOR A FREE-FLYING DUCTED PROPELLER
Robert J. Weir Jan. 1988 32 p Presented at the AIAA Atmospheric Flight Mechanics Conference, Minneapolis, Minn., 15 Aug. 1988
(Contract DE-AC04-76DP-00789)
(DE88-006867; SAND-88-0021C; CONF-880836-1) Avail: NTIS HC A03/MF A01

The design philosophy for a free-flying vehicle powered by a ducted propeller is presented from an aerodynamic viewpoint. Airframe design concentrates on duct inlet lip curvature, diffuser angle, and methods of vehicle control. Wind tunnel test results are given to evaluate two inlet designs, two exit designs, and the effect of external appendages such as a camera pod or a forebody. Finally, a simple, analytic method of ducted propeller blade design is presented and the results compared with an existing ducted propeller blade. DOE

N89-10842*# National Aeronautics and Space Administration. Langley Research Center, Hampton, Va.
EXPERIMENTAL RESULTS FOR THE EPPLER 387 AIRFOIL AT LOW REYNOLDS NUMBERS IN THE LANGLEY LOW-TURBULENCE PRESSURE TUNNEL
Robert J. McGhee, Betty S. Walker, and Betty F. Millard Oct. 1988 232 p
(NASA-TM-4062; L-16430; NAS 1.15:4062) Avail: NTIS HC A11/MF A01 CSCL 01A

Experimental results were obtained for an Eppler 387 airfoil in the Langley Low Turbulence Pressure Tunnel. The tests were conducted over a Mach number range from 0.03 to 0.13 and a chord Reynolds number range for 60,000 to 460,000. Lift and pitching moment data were obtained from airfoil surface pressure measurements and drag data for wake surveys. Oil flow visualization was used to determine laminar separation and turbulent reattachment locations. Comparisons of these results with data on the Eppler 387 airfoil from two other facilities as well as the Eppler airfoil code are included. Author

N89-10843*# Pennsylvania State Univ., University Park. Dept. of Aerospace Engineering.
REYNOLDS STRESS CLOSURE IN JET FLOWS USING WAVE MODELS Semiannual Progress Report
P. J. Morris 29 Sep. 1988 11 p
(Grant NAG1-657)
(NASA-CR-180226; NAS 1.26:180226) Avail: NTIS HC A03/MF A01 CSCL 01A

Ways of implementing the turbulence closure scheme based on modeling the large scale coherent structures as instability waves were sought. The computational tools necessary to apply this scheme to jets of arbitrary geometry were developed. The model, developed earlier, was extended to the shock structure of supersonic jets of arbitrary geometry and multiple jets. It was found that though the qualititate features of the unsteady flow field could be predicted there were always difficulties with some of the quantitative features. This led to the new formation of the closure scheme. The schemes for computations tools which were developed are efficient and represent the application of the very powerful mathematical tools to the problems of practical significance. B.G.

N89-10844*# National Aeronautics and Space Administration. Lewis Research Center, Cleveland, Ohio.
THREE COMPONENT LASER ANEMOMETER MEASUREMENTS IN AN ANNULAR CASCADE OF CORE TURBINE VANES WITH CONTOURED END WALL
Louis J. Goldman and Richard G. Seasholtz Nov. 1988 44 p
(NASA-TP-2846; E-4183; NAS 1.60:2846) Avail: NTIS HC A03/MF A01 CSCL 20D

The three mean velocity components were measured in a full-scale annular turbine stator cascade with contoured hub end wall using a newly developed laser anemometer system. The anemometer consists of a standard fringe configuration using fluorescent seed particles to measure the axial and tangential components. The radial component is measured with a scanning confocal Fabry-Perot interferometer. These two configurations are combined in a single optical system that can operate simultaneously in a backscatter mode through a single optical access port. Experimental measurements were obtained both within and downstream of the stator vane row and compared with calculations from a three-dimensional inviscid computer program. In addition, detailed calibration procedures are described that were used, prior to the experiment, to accurately determine the laser beam probe volume location relative to the cascade hardware. Author

N89-10845# National Aerospace Lab., Tokyo (Japan). Computational Sciences Div.
HIGH RESOLUTION SCHEMES FOR THREE-DIMENSIONAL EULER EQUATIONS. 1: ESTIMATION OF RECENT TVD SCHEMES
Tomiko Ishiguro, Satoru Ogawa, and Yoko Takakura (Fujitsu Ltd., Tokyo, Japan) Oct. 1987 23 p
(PB88-214416; NAL/TR-950T) Avail: NTIS HC A03/MF A01 CSCL 01A

Numerical estimations of TVD (Total Variation Diminishing) schemes (Yee-Harten's TVD and Chakravarthy-Osher's TVD) in 3-D general coordiante systems are performed by solving the Euler equations around the ONERA M6 wing. It is known that their TVD schemes do not give good solutions in curvilinear coordinate schemes, and several modifications with regard to treatment of metrics are carried out. Compared with the solution of the Beam-Warming scheme, the authors modified TVD schemes yield excellent solutions with very few numerical oscillations for strong shock waves; and they have a high ability to capture the leading edge expansion. GRA

N89-10846 Loughborough Univ. of Technology (England). Dept. of Transport Technology.
FULL SCALE WIND TUNNEL TESTS ON A FORD ESCORT Mk 3
M. A. Passmore and E. G. Jenkins Feb. 1988 46 p
(TT-8802; ISBN-0-90-4947-07-6) Copyright Avail: Issuing Activity

Any investigation into the resistance to motion of a vehicle on the road depends on an understanding of the main contributions to that resistance. One such contribution is the drag caused by the vehicle aerodynamics. This report describes tests conducted in a full-scale wind tunnel to measure the aerodynamic forces and moments on a test vehicle, with and without extra instrumentation installed on-board to measure ambient wind conditions, and torque at the driven wheels. An increase in the drag coefficient at zero yaw angle of approximately 4 percent was recorded when the instrumentation was installed. The basic shape of the three force coefficient against yaw angle curves are unchanged with the addition of the instrumentation. The on-board anemometry was significantly affected by the pressure field in front of the vehicle, correction factors were determined from the test data to correct the yaw angle and airspeed measurements. A model of the drag distributions associated with the vehicle aerodynamics is developed from the literature and using the data obtained in the wind tunnel. A simplified version of this model is proposed for use in analyzing data obtained at the test track.
Author

N89-10847# National Aeronautical Lab., Bangalore (India). Aerodynamics Div.
TESTS ON 3 NACA 0012 AIRFOIL MODELS OF DFVLR IN THE NAL 0.3 TUNNEL: AN ASSESSMENT OF 2-D WALL INTERFERENCE
R. Gopinath, Santha Kumari, and R. Sridharan Dec. 1987 117 p
(TM-AE-8705) Avail: NTIS HC A06/MF A01

Tests were conducted on three NASA 0012 airfoil models. A range of Mach numbers from 0.6 to 0.9 and incidence of the model from 0 degrees to 7 degrees with both free and fixed transition on the airfoil model, was covered. Flow visualization studies were also carried out at a few Mach numbers and incidence. Interference corrections were computed from wall pressures measured along the slat on the top and bottom liners of the modified test section and the corrected data compared with those from other tunnels. An analysis of the data on the three models of chord lengths 100mm, 150mm and 200mm respectively, from the standpoint of interference due to tunnel walls, is presented.
Author

N89-10848 Virginia Polytechnic Inst. and State Univ., Blacksburg.
ACCURACY ANALYSIS OF THE SEMI-ANALYTICAL METHOD FOR SHAPE SENSITIVITY ANALYSIS Ph.D. Thesis
Bruno Barthelemy 1987 77 p
Avail: Univ. Microfilms Order No. DA8804393

The semi-analytical method, widely used for calculating derivatives of static response with respect to design variables for structures modeled by finite elements, is studied. The research shows that the method can have serious accuracy problems for shape design variables in structures modeled by beam, plate, truss, frame, and solid elements. Local and global indices are developed to test the accuracy of the semi-analytical method. The local indices provide insight into the problem of large errors for the semi-analytical method. Local error magnification indices are developed for beam and plane truss structures, and several examples showing the severity of the problem are presented. The global index provides us with a general method for checking the accuracy of the semi-analytical method for any type of model. It characterizes the difference in errors between a general finite-difference method and the semi-analytical method. Moreover, a method improving the accuracy of the semi-analytical method (when possible) is provided. Examples are presented showing the use of the global index. Dissert. Abstr.

N89-10849*# National Aeronautics and Space Administration. Ames Research Center, Moffett Field, Calif.
THE 1987 GROUND VORTEX WORKSHOP
Richard J. Margason, ed. Feb. 1988 216 p Workshop held at Moffett Field, Calif., 22-23 Apr. 1987
(NASA-CP-10008; A-88008; NAS 1.55:10008) Avail: NTIS HC A10/MF A01 CSCL 01A

The purpose of this workshop was to discuss the current understanding of the ground vortex phenomena and their effects on aircraft, and to establish directions for further research on advanced, high-performance aircraft designs, particularly those concepts utilizing powered-lift systems; e.g., V/STOL. ASTOVL, and STOL aircraft. For individual titles, see N89-10850 through N89-10857.

N89-10850*# National Aeronautics and Space Administration. Ames Research Center, Moffett Field, Calif.
THE CHARACTERISTICS OF THE GROUND VORTEX AND ITS EFFECT ON THE AERODYNAMICS OF THE STOL CONFIGURATION
Vearle R. Stewart *In its* The 1987 Ground Vortex Workshop Feb. 1988 p 1-38 (For primary document see N89-10849 02-02)
Avail: NTIS HC A10/MF A01 CSCL 01A

The interaction of the free stream velocity on the wall jet formed by the impingement of deflected engine thrust results in a rolled up vortex which exerts sizable forces on a short takeoff (STOL) airplane configuration. Some data suggest that the boundary layer under the free stream ahead of the configuration may be important in determining the extent of the travel of the wall jet into the oncoming stream. Here, early studies of the ground vortex are examined, and those results are compared to some later data obtained with moving a model over a fixed ground board. The effect of the ground vortex on the aerodynamic characteristics are discussed.
Author

N89-10851*# Pennsylvania State Univ., State College. Applied Research Lab.
SUMMARY OF AN EXPERIMENTAL INVESTIGATION ON THE GROUND VORTEX
Michael L. Billet and John M. Cimbala *In* NASA, Ames Research Center, The 1987 Ground Vortex Workshop Feb. 1988 p 39-60 (For primary document see N89-10849 02-02)
Avail: NTIS HC A10/MF A01 CSCL 01A

The results of an experimental investigation into the position and characteristics of the ground vortex are summarized. A 48-inch wind tunnel was modified to create a testing environment suitable for the ground vortex study. Flow visualization was used to document the jet-crossflow interaction and a two-component Laser Doppler Velocimeter (LDV) was used to survey the flowfield in detail. Measurements of the ground vortex characteristics and location as a function of freestream-to-jet velocity ratio, jet height, pressure gradient and upstream boundary layer thickness were obtained.
Author

N89-10852*# National Aeronautics and Space Administration. Ames Research Center, Moffett Field, Calif.
GROUND VORTEX FLOW FIELD INVESTIGATION
Richard E. Kuhn, John H. DelFrate, and James E. Eshleman (Lockheed-California Co., Burbank.) *In its* The 1987 Ground Vortex Workshop Feb. 1988 p 61-90 (For primary document see N89-10849 02-02)
Avail: NTIS HC A10/MF A01 CSCL 01A

Flow field investigations were conducted at the NASA Ames-Dryden Flow Visualization Facility (water tunnel) to investigate the ground effect produced by the impingement of jets from aircraft nozzles on a ground board in a STOL operation. Effects on the overall flow field with both a stationary and a moving ground board were photographed and compared with similar data found in other references. Nozzle jet impingement angles, nozzle and inlet interaction, side-by-side nozzles, nozzles in tandem, and nozzles and inlets mounted on a flat plate model were investigated. Results show that the wall jet that generates the

ground effect is unsteady and the boundary between the ground vortex flow field and the free-stream flow is unsteady. Additionally, the forward projection of the ground vortex flow field with a moving ground board is one-third less than that measured over a fixed ground board. Results also showed that inlets did not alter the ground vortex flow field. Author

N89-10853*# Air Force Wright Aeronautical Labs., Wright-Patterson AFB, Ohio.
F-15 SMTD LOW SPEED JET EFFECTS WIND TUNNEL TEST RESULTS
William B. Blake *In* NASA, Ames Research Center, The 1987 Ground Vortex Workshop Feb. 1988 p 91-119 (For primary document see N89-10849 02-02)
Avail: NTIS HC A10/MF A01 CSCL 01A

Key results from low speed wind tunnel testing of the F-15 STOL and Maneuver Technology Demonstrator (SMDT) with thrust reversers are presented. Longitudinally, the largest induced increments in the stability and control occur at landing gear height. These generally reflect an induced lift loss and a nose-up pitching moment, and vary with sideslip. Directional stability is reduced at landing gear height with full reverse thrust. Nonlinearities in the horizontal tail effectiveness are found in free air and at landing gear height. Author

N89-10854*# National Aeronautics and Space Administration. Langley Research Center, Hampton, Va.
AN ASSESSMENT OF GROUND EFFECTS DETERMINED BY STATIC AND DYNAMIC TESTING TECHNIQUES
John W. Paulson, Jr. and Guy T. Kemmerly *In* NASA, Ames Research Center, The 1987 Ground Vortex Workshop Feb. 1988 p 121-146 (For primary document see N89-10849 02-02)
Avail: NTIS HC A10/MF A01 CSCL 01A

A new testing technique was developed wherein the rate of descent can be included as a parameter in ground effects investigations. This technique simulates the rate of descent by horizontal motion of a model over an inclined ground board in the Langley Vortex Research Facility (VRF) During initial evaluations of the technique, dynamic ground effects data were obtained over the inclined ground board, steady state ground effects data were obtained over a flat portion of the ground board, and the results were compared to conventional static wind tunnel ground effect data both with and without a moving belt ground plane simulation. Initial testing and analysis led to the following conclusions: the moving belt ground plane had little effect on static ground effects for the configurations tested unless thrust reversers were employed; in general, rate-of-descent reduced ground effects to the point that for reversed thrust cases an expected loss of lift due to ground effects was eliminated at approach conditions; and, in general, the steady state results from the VRF matched static results obtained from the wind tunnel once the flow field stabilized over the flat portion of the ground board. Author

N89-10855*# Florida State Univ., Tallahassee. Fluid Mechanics Research Lab.
EFFECTS OF A GROUND VORTEX ON THE AERODYNAMICS OF AN AIRFOIL
A. Krothapalli and D. Leopold (Stanford Univ., Calif.) *In* NASA, Ames Research Center, The 1987 Ground Vortex Workshop Feb. 1988 p 147-166 (For primary document see N89-10849 02-02)
(Grants NAG2-111; NAG2-198)
Avail: NTIS HC A10/MF A01 CSCL 01A

An experimental investigation was carried out to study the aerodynamics of an airfoil with a rectangular jet exiting from its lower surface at fifty percent of the chord. The airfoil was tested with and without the influence of a ground plane. Surface static pressures were measured on the airfoil at jet to free stream velocity ratios ranging from 0 to 9. From these pressures, the variation of C sub L with velocity ratio was easily determined. The measurements indicated significant positive and negative pressure regions on the lower surface of the airfoil ahead of and after the nozzle exit respectively. The presence of a ground plane enhanced these pressure regions at low velocity ratios, but at a particular ratio for each plane location, a recirculation zone or vortex formed ahead of the jet resulting in decreased pressures and a drop in C sub L. Author

N89-10856*# National Aeronautics and Space Administration. Ames Research Center, Moffett Field, Calif.
NOISE OF THE HARRIER IN VERTICAL LANDING AND TAKEOFF **c71**
Paul T. Soderman and John D. Foster *In its* The 1987 Ground Vortex Workshop Feb. 1988 p 167-190 (For primary document see N89-10849 02-02)
Avail: NTIS HC A10/MF A01 CSCL 01A

The noise of the Harrier AV8C aircraft in vertical takeoff and landing was measured 100 feet to the side of the aircraft where jet noise dominates. The noise levels were quite high - up to 125 dB overall sound level at 100 feet. The increased noise due to jet impingement on the ground is presented as a function of jet height to diameter ratio. The impingement noise with the aircraft close to the ground was 14 to 17 dB greater than noise from a free jet. Results are compared with small-scale jet impingement data acquired elsewhere. The agreement between small-scale and full-scale noise increase in ground effect is fairly good except with the jet close to the ground. It is proposed that differences in the jet Reynolds numbers and the resultant character of the jets may be partially responsible for the disparity in the full-scale and small-scale jet impingement noise. The difference between single-jet impingement and multiple-jet impingement may also have been responsible for the small-scale and full-scale disagreement. Author

N89-10857*# National Aeronautics and Space Administration. Ames Research Center, Moffett Field, Calif.
NUMERICAL INVESTIGATION OF A JET IN GROUND EFFECT USING THE FORTIFIED NAVIER-STOKES SCHEME
William R. VanDalsem and Joseph L. Steger *In its* The 1987 Ground Vortex Workshop Feb. 1988 p 191-206 (For primary document see N89-10849 02-02)
Avail: NTIS HC A10/MF A01 CSCL 01A

One of the flows inherent in VSTOL operations, the jet in ground effect with a crossflow, is studied using the Fortified Navier-Stokes (FNS) scheme. Through comparison of the simulation results and the experimental data, and through the variation of the flow parameters (in the simulation) a number of interesting characteristics of the flow have been observed. For example, it appears that the forward penetration of the ground vortex is a strong inverse function of the level of mixing in the ground vortex. Also, an effort has been made to isolate issues which require additional work in order to improve the numerical simulation of the jet in ground effect flow. The FNS approach simplifies the simulation of a single jet in ground effect, but it will be even more effective in applications to more complex topologies. Author

N89-10858*# National Aeronautics and Space Administration. Lewis Research Center, Cleveland, Ohio.
EXPERIMENTAL INVESTIGATION OF THE PERFORMANCE OF A SUPERSONIC COMPRESSOR CASCADE
D. L. Tweedt, H. A. Schreiber, and H. Starken (Deutsche Forschungs- und Versuchsanstalt fuer Luft- und Raumfahrt, Cologne, West Germany) Jun. 1988 30 p Presented at the 33rd International Gas Turbine and Aeroengine Congress and Exposition, Amsterdam, The Netherlands, 5-9 Jun. 1988; sponsored by ASME
(NASA-TM-100879; E-4113; NAS 1.15:100879) Avail: NTIS HC A03/MF A01 CSCL 01A

Results are presented from an experimental investigation of a linear, supersonic, compressor cascade tested in the supersonic cascade wind tunnel facility at the DFVLR in Cologne, Federal Republic of Germany. The cascade design was derived from the near-tip section of a high-through-flow axial flow compressor rotor with a design relative inlet Mach number of 1.61. Test data were

obtained over a range of inlet Mach numbers from 1.23 to 1.71, and a range of static pressure ratios and axial-velocity-density ratios (AVDR) at the design inlet condition. Flow velocity measurements showing the wave pattern in the cascade entrance region were obtained using a laser transit anemometer. From these measurements, some unique-incidence conditions were determined, thus relating the supersonic inlet Mach number to the inlet flow direction. The influence of static pressure ratio and AVDR on the blade passage flow and the blade-element performance is described, and an empirical correlation is used to show the influence of these two (independent) parameters on the exit flow angle and total-pressure loss for the design inlet condition.
Author

N89-10859# Centre d'Etudes et de Recherches, Toulouse (France). Dept. d'Etudes et de Recherches en Aerothermodynamique.
INVESTIGATION ON OF THE FLOW AROUND A BACKWARD FACING STEP WITH SPANWISE BLOWING Final Report [ETUDE DE L'ECOULEMENT AUTOUR D'UNE MARCHE DESCENDANTE AVEC SOUFFLAGE TANGENTIEL]
X. deSaint-Victor and W. Hajlbrahim Jan. 1988 71 p In FRENCH
(Contract Aerospatiale-21-003395)
(CERT-RF-OA-68/2259-AYD; DERAT-52/5004-23; ETN-88-93105)
Avail: NTIS HC A04/MF A01

Spanwise blowing of the boundary layer to eliminate recirculation zones downstream of helicopter motor fairings/rotor heads was analyzed numerically. Flow around a backward facing step with a slit at riser level for the blowing was studied. Two slit/step height ratios were chosen and several ratios of blowing velocity to infinite upstream velocity were considered. Results show that the calculation method can predict flows with strong separation, and that spanwise blowing can eliminate recirculation downstream of an obstacle.
ESA

N89-10860# Office National d'Etudes et de Recherches Aerospatiales, Paris (France). Direction de l'Aerodynamique.
FLOW AROUND A DELTA WING WITH OR WITHOUT A CANARD (Phi BA = 60 DEG). PART 2: HYDRODYNAMIC VISUALIZATIONS IN UNSTEADY FLOW (PITCHING OSCILLATIONS) [ECOULEMENT AUTOUR D'UNE AILE DELTA SANS OU AVEC PLAN CANARD (PHI BA = 60 DEG), DEUXIEME PARTIE: VISUALISATIONS HYDRODYNAMIQUES EN INSTATIONNAIRE (OSCILLATIONS EN TANGAGE)]
H. Werle Feb. 1988 43 p In FRENCH
(ONERA-RT-11/2891-AN-Pt-2; ETN-88-93111) Avail: NTIS HC A03/MF A01

Turbulence phenomena around a thin delta wing were visualized and measured in a hydrodynamic test facility with a model in unsteady flow. The model was subjected to harmonic pitching oscillations of amplitude + or - 10 deg, around an average incidence of 15 and 20 deg. Vortices at a wing with a canard configuration were studied at Reynolds numbers between 20,000 and 100,000 and at frequency K between 0.18 and 0.46. Results show the effectiveness of the canard is greatly reducing bursting. Curves showing the alternating displacement of the vortex axis and vortex bursting point, and their evolution as a function of flow parameters are obtained.
ESA

N89-10861# Centre d'Etudes et de Recherches, Toulouse (France). Dept. d'Etudes et de Recherches en Aerothermodynamique.
EXPERIMENTAL INVESTIGATION OF FLOW NEAR A CORNER, PART 2 [ETUDE EXPERIMENTALE D'UN ECOULEMENT AU VOISINAGE D'UN COIN (DEUXIEME PARTIE)]
Guy Pailhas Jan. 1988 159 p In FRENCH
(Contract STPA-85-95-004)
(CERT-RT-OA-24/5025-AYD; DERAT-24/5025-14; ETN-88-93113)
Avail: NTIS HC A08/MF A01

Flow in the angle of intersection of two walls was studied using a wind tunnel model to simulate the joint of a highly swept (arrow) wing and a fuselage, the wing being at incidence. A hot-wire anemometer was used to obtain the average flow field and turbulence field in different flow planes. Results show that the combination of sweep and incidence does not contribute to the creation of a pressure gradient strong enough to allow an important deformation of the flow lines downstream. Geometric parameters (sweep, profile incidence) appear to be essential in determining flow tropism in corners.
ESA

N89-10862# Deutsche Forschungs- und Versuchsanstalt fuer Luft- und Raumfahrt, Brunswick (West Germany). Inst. fuer Flugmechanik.
INVESTIGATION OF WAKE VORTICES OF LANDING AIRCRAFT AT FRANKFURT AIRPORT (FEDERAL REPUBLIC OF GERMANY)
Rolf Ulken May 1988 70 p In GERMAN; ENGLISH summary
(DFVLR-Mitt-88-15; ISSN-0176-7739; ETN-88-93183) Avail: NTIS HC A04/MF A01; DFVLR, VB-PL-DO, 90 60 58, 5000 Cologne, Federal Republic of Germany, 24.50 deutsche marks

Wake vortices were investigated to see whether and under which meteorological conditions landing aircraft could be endangered by wake vortices generated by leading large transport aircraft on a parallel glide path. The crosswind shows an evident influence on the horizontal motion of a vortex. But its velocity during 56 pct of the time of the main air traffic is so slow that a vortex cannot reach the parallel glide path with dangerous intensity due to its limited life-span. Within the remaining time the danger to a following aircraft depends very strongly on the meteorological conditions of the vicinity.
ESA

N89-10863*# Sverdrup Technology, Inc., Cleveland, Ohio.
A DIAGONALLY INVERTED LU IMPLICIT MULTIGRID SCHEME FOR THE 3-D NAVIER-STOKES EQUATIONS AND A TWO EQUATION MODEL OF TURBULENCE Final Report
Jeffrey W. Yokota Oct. 1988 13 p Prepared for presentation at the 27th Aerospace Sciences Meeting, Reno, Nev., 9-12 Jan. 1989; sponsored in part by AIAA
(Contract NAS3-25266)
(NASA-CR-182209; E-4412; AIAA-88-0467; NAS 1.26:182209)
Avail: NTIS HC A03/MF A01 CSCL 01A

An LU implicit multigrid algorithm is developed to calculate 3-D compressible viscous flows. This scheme solves the full 3-D Reynolds-Averaged Navier-Stokes equation with a two-equation kappa-epsilon model of turbulence. The flow equations are integrated by an efficient, diagonally inverted, LU implicit multigrid scheme while the kappa-epsilon equations are solved, uncoupled from the flow equations, by a block LU implicit algorithm. The flow equations are solved within the framework of the multigrid method using a four-grid level W-cycle, while the kappa-epsilon equations are iterated only on the finest grid. This treatment of the Reynolds-Averaged Navier-Stokes equations proves to be an efficient method for calculating 3-D compressible viscous flows.
Author

N89-10864# Centre d'Etudes et de Recherches, Toulouse (France). Dept. d'Etudes et de Recherches en Aerothermodynamique.
THREE DIMENSIONAL SHEAR FLOW. ANALYSIS OF THE FLOW IN A DELTA ARROW WING WITH INCIDENCE ANGLE [ECOULEMENTS CISAILLES TRIDIMENSIONNELS. ANALYSE DE L'ECOULEMENT A L'INTRADOS D'UNE AILE EN FLECHE ET EN INCIDENCE]
Guy Pailhas Mar. 1987 27 p In FRENCH
(Contract STPA-85-95-004)
(CERT-RTS-OA-25/5025-AYD; DERAT-25/5025-14;
ETN-88-93319) Avail: NTIS HC A03/MF A01

Wind tunnel tests were performed on a delta wing to evaluate the average velocities and the turbulent fields. A four wire anemometer was used. The model was placed at large incidence angles and simulated a delta winged aircraft body. The analysis of the turbulence shows that the corner flow is the result of a conflict between the fluid coming out of the boundary layer below

the wing, which could be receptive to the turbulence order imposed by the systems geometry, and the external fluid which forces the flow to retake the initial direction. ESA

N89-10865*# National Aeronautics and Space Administration. Lewis Research Center, Cleveland, Ohio.
EXPERIMENTAL AERODYNAMIC PERFORMANCE OF ADVANCED 40 DEG-SWEPT 10-BLADE PROPELLER MODEL AT MACH 0.6 TO 0.85
Glenn A. Mitchell Sep. 1988 43 p
(NASA-TM-88969; E-3437; NAS 1.15:88969) Avail: NTIS HC A03/MF A01 CSCL 01A

A propeller designated as SR-6, designed with 40 deg of sweep and 10 blades to cruise at Mach 0.8 at an altitude of 10.7 km (35,000 ft), was tested in the NASA Lewis Research Center's 8- by 6-Foot Wind Tunnel. This propeller was one of a series of advanced single rotation propeller models designed and tested as part of the NASA Advanced Turboprop Project. Design-point net efficiency was almost constant to Mach 0.75 but fell above this speed more rapidly than that of any previously tested advanced propeller. Alternative spinners that further reduced the near-hub interblade Mach numbers and relieved the observed hub choking improved performance above Mach 0.75. One spinner attained estimated SR-6 Design-point net deficiencies of 80.6 percent at Mach 0.75 and 79.2 percent at Mach 0.8, higher than the measured performance of any previously tested advanced single-rotation propeller at these speeds. Author

N89-10866# Aeronautical Research Labs., Melbourne (Australia).
NON-LINEAR AERODYNAMIC CHARACTERISTICS OBTAINED FROM THE ANALYSIS OF FLIGHT-DATA
R. A. Feik Nov. 1987 35 p
(AR-004-571; ARL-AERO-TM-390) Copyright Avail: NTIS HC A03/MF A01

A least squares regression analysis program has been documented and its advantages and shortcomings when used for analyzing flight data have been summarized. It has been shown that the shortcomings can be largely overcome by pre-processing flight measurements via compatibility checking. A particular advantage of the least squares approach is the ability to partition data into angle of attack subsets. Application to flight data from a delta wing aircraft at Mach 0.65 has been successful in extracting nonlinear features, including a sharp drop in pitch damping at around 4 degrees angle of attack, possibly associated with the development of the leading edge vortex. Comparison with previous results, internal consistency, and small scatter all confirm the effectiveness of this approach even with moderate quality instrumentation. The methodology described has considerable potential for application to highly nonlinear flight regimes. Author

N89-10867# General Dynamics/Fort Worth, Tex.
UNSTEADY LOW-SPEED WINDTUNNEL TEST OF A STRAKED DELTA WING, OSCILLATING IN PITCH. PART 1: GENERAL DESCRIPTION AND DISCUSSION OF RESULTS Final Report, Jun. 1985 - Aug. 1987
A. M. Cunningham, Jr., R. G. DenBoer, C. S. Dogger, E. G. Guerts, and A. J. Persoon Apr. 1988 140 p
(Contract F33615-85-C-3013)
(AD-A196456; AFWAL-TR-87-3098-Pt-1) Avail: NTIS HC A07/MF A01 CSCL 01A

Results of a wind tunnel test of an oscillating straked wing indicate unsteady airloads and pressure distributions for a range of incidences (-8 to 50 deg) and amplitudes (1 to 16 deg). The wind speed was 80 meters/second, which provided reduced frequencies up to 0.50 based on root chord. The zeroth and first harmonic as well as the continuous time history of the pressure and overall loads were measured. Flow visualization was performed for flow of 30 meters/second using a pulsating laser light sheet. This part presents the description of this wind tunnel test and preliminary discussions of results obtained from the test. Details are provided on the model, instrumentation and support system as well as test program condition/run member cross-reference tables for use with the data base presented in parts 2 through 6 of this report. Model geometry and force data processing procedures are presented in the appendices. Also presented in the appendices are updated values of force data obtained from the steady tests of the model suspended by a wire balance. GRA

N89-11067# Joint Publications Research Service, Arlington, Va.
NUMERICAL SIMULATION OF TRANSONIC FLOW AROUND ASUKA
Susumu Takanashi *In its* JPRS Report: Science and Technology: Japan 4 Jun. 1987 p 24-25 Transl. into ENGLISH from Kogiken Nyusu (Toyko, Japan), Sep. 1986 p 2 (For primary document see N89-11061 02-31)
Avail: NTIS HC A05/MF A01

N89-11069# Joint Publications Research Service, Arlington, Va.
CAD WIND TUNNEL TEST FOR HALF-CUT MODEL OF ASUKA
In its JPRS Report: Science and Technology: Japan 4 Jun. 1987 p 29-32 Transl. into ENGLISH from Kogiken Nyusu (Toyko, Japan), Sep. 1986 p 5-6 (For primary document see N89-11061 02-31)
Avail: NTIS HC A05/MF A01

03 AIR TRANSPORTATION AND SAFETY

Includes passenger and cargo air transport operations; and aircraft accidents.

For related information see also *16 Space Transportation* and *85 Urban Technology and Transportation.*

N89-10868# National Transportation Safety Board, Washington, D. C. Bureau of Accident Investigation.
AIRCRAFT ACCIDENT/INCIDENT SUMMARY REPORT, COPPERHILL, TENNESSEE, FEBRUARY 22, 1986
30 Mar. 1988 9 p
(PB88-910407; NTSB/AAR-88/02-Summ) Avail: NTIS HC A02/MF A01; also available on subscription, North American continent HC $70.00/year; all others write for quote CSCL 01C

This report is a summary of an aircraft accident investigated by the National Transportation Safety Board. The accident location and date is Copperhill, Tennessee, February 22, 1986. GRA

N89-10869# Systems Control Technology, Inc., Arlington, Va.
AERONAUTICAL DECISION MAKING FOR AIR AMBULANCE HELICOPTER PILOTS: SITUATIONAL AWARENESS EXERCISES Final Report
R. J. Adams and J. L. Thompson Jul. 1988 45 p
(Contract DTFA01-87-C-00014)
(DOT/FAA/DS-88/6) Avail: NTIS HC A03/MF A01

The following materials are based upon actual helicopter air ambulance accidents, which cover four broad accident types most recently associated with aeromedical accidents: night flying, weather, obstacle strikes, and mechanical failures. Three types of information are included for each accident type. These are: introductory/background material to provide the historical importance and frequency of each accident type; training knowledge that should be learned in order to avoid mistakes of the past; and decision making exercises. Author

N89-10870# Aviation Safety Commission, Washington, D.C.
AERONAUTICAL DECISION MAKING FOR COMMERCIAL PILOTS
Richard S. Jensen and Janeen Adrion Jul. 1988 68 p Prepared for Systems Control Technology, Inc., Arlington, Va.
(Contract DTFA01-80-C-10080)
(DOT/FAA/PM-86/42) Avail: NTIS HC A04/MF A01

Aviation accident data indicate that the majority of aircraft mishaps are due to judgement error. This training manual is part of a project to develop materials and techniques to help improve pilot decision making. Training programs using prototype versions of these materials have demonstrated substantial reductions in

pilot error rates. The result of such tests were statistically significant and ranged from approximately 10 to 50 percent fewer mistakes. This manual is designed to explain the risks associated with commercial flying activities, the underlying behavioral causes of typical accidents, and the effects of stress on pilot decision making. It provides a means for the individual pilot to develop an attitude profile through a self-assessment inventory and provides detailed explanations of pre-flight and in-flight stress management techniques. The assumption is that pilots receiving this training will develop a positive attitude toward safety and the ability to effectively manage stress while recognizing and avoiding unnecessary risks. Author

N89-10871# National Transportation Safety Board, Washington, D. C. Bureau of Field Operations.
AIRCRAFT ACCIDENT REPORTS, BRIEF FORMAT, US CIVIL AND FOREIGN AVIATION, ISSUE NUMBER 2 OF 1987 ACCIDENTS
5 Feb. 1988 399 p
(PB88-916906; NTSB/AAB-88/06) Avail: NTIS HC A17/MF A01; also available on subscription, North American continent HC $185.00/year; all others write for quote CSCL 01C

The publication contains selected aircraft accident reports in Brief Format occurring in U.S. civil and foreign aviation operations during Calendar Year 1987. Approximately 200 General Aviation and Air Carrier accidents contained in the publication represent a random selection. The publication is issued irregularly, normally eighteen times each year. The Brief Format represents the facts, conditions, circumstances and probable cause(s) for each accident. GRA

N89-10872*# National Aeronautics and Space Administration. Ames Research Center, Moffett Field, Calif.
AVIATION TECHNOLOGY APPLICABLE TO DEVELOPING REGIONS
John Zuk and Larry R. Alton Sep. 1988 94 p
(NASA-TM-89425; A-87093; NAS 1.15:89425) Avail: NTIS HC A05/MF A01 CSCL 01C

This paper is an analysis of aviation technologies useful for formulation of development plans to the year 2000 for emerging nations. The Caribbean Basin was used as a specific application. This development promises to be so explosive over the next 15 years as to be virtually unpredictable. Author

N89-10873# National Transportation Safety Board, Washington, D. C.
AIRCRAFT ACCIDENT REPORT: EXECUTIVE AIR CHARTER, INC., dba AMERICAN EAGLE, FLIGHT 5452, CASA C-212, N432CA, MAYAGUEZ, PUERTO RICO, MAY 8, 1987
2 Aug. 1988 51 p
(PB88-910409; NTSB/AAR-88/07) Avail: NTIS HC A04/MF A01 CSCL 01C

On May 8, 1987, at 0650 local time, flight 5452 of Executive Air Charter, Inc., doing business as Americam Eagle, crashed short of runway 9 while on a visual approach to the airport at Mayaguez, Puerto Rico, in visual meteorological conditions. The safety issues examined in the accident investigation were pilot performance, air carrier maintenance procedures and practices, bilateral type certification of the airplane, and FAA surveillance of the air carrier. Author

04 AIRCRAFT COMMUNICATIONS AND NAVIGATION

Includes digital and voice communication with aircraft; air navigation systems (satellite and ground based); and air traffic control.

For related information see also *17 Space Communications, Spacecraft Communications, Command and Tracking* and *Communications and Radar.*

N89-10874# Advisory Group for Aerospace Research and Development, Neuilly-Sur-Seine (France). Avionics Panel.
THE NAVSTAR GPS SYSTEM
Sep. 1988 141 p Lecture series held in Wessling, West Germany, 19-20 Sep. 1988, in Athens, Greece, 22-23 Sep. 1988, in Ankara, Turkey, 26-27 Sep. 1988, and in Lisbon, Portugal, 29-30 Sep. 1988
(AGARD-LS-161; ISBN-92-835-0477-1) Copyright Avail: NTIS HC A07/MF A01

A comprehensive and up-to-date lecture series on the NAVSTAR GPS System is presented. Among the subjects covered are the system concept, navigation principles, system design, user applications, and techniques involved. The lectures are a balanced presentation of theory, application, and measured performance. For individual titles, see N89-10875 through N89-10884.

N89-10875# Aerospace Corp., El Segundo, Calif.
THE GPS OVERVIEW AND NAVIGATION SYSTEM CONCEPT
Edward Lassiter and Mohan Ananda *In* AGARD, The NAVSTAR GPS System Sep. 1988 13 p (For primary document see N89-10874 02-04)
Copyright Avail: NTIS HC A07/MF A01

The Global Positioning System (GPS) objective for both military and civil applications and the historical evolutions of the SPS are presented. The GPS concept validation phase, full-scale engineering developments, system test phase and operational system phase are described. The fundamental principles of the GPS concept are briefly reviewed. The GPS radiometric measurements of pseudo-range and accumulated delta range and how these measurements are used in forming the navigation equations to solve for the user position parameters are described. The current program status and future plans for system enhancements are outlined. Author

N89-10876# Aerospace Corp., El Segundo, Calif.
THE GLOBAL POSITIONING SYSTEM (GPS) CONSTELLATION AND COVERAGE
Mohan Ananda *In* AGARD, The NAVSTAR GPS System Sep. 1988 17 p (For primary document see N89-10874 02-04)
Copyright Avail: NTIS HC A07/MF A01

The NAVSTAR Global Positioning System (GPS) is a space-based system that will be operational in 1990 and will enable a user to determine position, velocity, and time with greater accuracy on a worldwide basis that it had ever achieved. The GPS is currently undergoing full-scale engineering development and testing. The test constellation and available coverage for testing the various system segments are reviewed. Also discussed is the 18-, 21-, and 24-satellite operational constellations. The current baseline constellation consists of 18 satellites with three active spare satellites. The concept of constellation value and various dilution-of-precision parameters due to geometry are discussed, such as geometrical dilution of precision (GDOP) and position dilution of precision (PDOP). The constellation design issues related to minimizing the reduced accuracy regions due to geometry problems are also reviewed. Coverage maps over the globe are presented for the test constellation, as well as for the operational constellations. Author

N89-10877# Aerospace Corp., El Segundo, Calif.
THE GLOBAL POSITIONING SYSTEM (GPS) ACCURACY, SYSTEM ERROR BUDGET, SPACE AND CONTROL SEGMENT OVERVIEW

Mohan Ananda *In* AGARD, The NAVSTAR GPS System Sep. 1988 17 p (For primary document see N89-10874 02-04)
Copyright Avail: NTIS HC A07/MF A01

The NAVSTAR Global Positioning System is a space-based navigation system that will provide continuous, all weather, global navigation capability to properly equipped users with high accuracy. The position, velocity, and time accuracy that can be achieved by a user of the GPS are discussed. The system accuracy will be examined in light of the Geometric Dilution of Precision parameter and measurement error. Also reviewed is the system error budget for the three subsystem segments: space, control, and user. A discussion of the user range error (URE) and its relationship to three-dimensional position error expressed in spherical error probable (SEP) and horizontal position error expressed in circular error probable (CEP) is presented. The role of the World Geodetic System reference frame in the GPS is discussed. A brief overview of space and control systems is also presented. Author

N89-10878# Naval Materiel Command, Haakonsvern (Norway).
GPS SIGNAL STRUCTURE
Per W. Nieuwejaar *In* AGARD, The NAVSTAR GPS System Sep. 1988 6 p (For primary document see N89-10874 02-04)
Copyright Avail: NTIS HC A07/MF A01

The characteristics of the Global Positioning System (GPS) signal structure, frequencies, codes, and navigation-message are described. The content of the navigation-message and the user algorithms associated with the navigation-message are described in some detail. Author

N89-10879# Air Force Space Div., Los Angeles, Calif. GPS Joint Program Office.
USER EQUIPMENT OVERVIEW
Elio Bottari *In* AGARD, The NAVSTAR GPS System Sep. 1988 11 p (For primary document see N89-10874 02-04)
Copyright Avail: NTIS HC A07/MF A01

The Global Positioning System (GPS) includes all the hardware and software needed to determine the user's position, velocity, time data, and other derived parameters, as required. Additionally, the GPS User System can be integrated with other navigation systems to provide accurate navigation under severe dynamics and hostile environmental conditions. During the development phase, various classes of users were defined based on user requirements and characteristics such as desired accuracy, user maneuvering, antijamming capability, and cost. The application of GPS user equipment (UE) in various types of host vehicles, used under a wide variety of operational conditions, has led to the development of three types of UE sets: LD = Low Dynamic (one channel); MD = Medium Dynamic (two channels); and HD = High Dynamic (four or more channels). A brief description of GPS signals is given to better describe the functions and operating concept of user equipment. Author

N89-10880# TAU Corp., Los Gatos, Calif.
GPS/INTERIAL NAVIGATION SYSTEM INTEGRATION FOR ENHANCED NAVIGATION PERFORMANCE AND ROBUSTNESS
Robert P. Denaro and G. Jeffrey Geier *In* AGARD, The NAVSTAR GPS System Sep. 1988 12 p (For primary document see N89-10874 02-04)
Copyright Avail: NTIS HC A07/MF A01

The emergence of the Global Positioning System (GPS) from the laboratory and the test range into the operational environment, with affordable, high-performance receivers now available, has heralded a widespread study of the integration of GPS with the current standard in precise positioning, inertial navigation systems. Once considered by some to be a potential competitor of inertial navigation, GPS is now recognized by most navigation system developers as having tremendous potential for system performance improvement over either system in isolation by integrating with inertial systems. So powerful is this synergism that deep integration of the two systems often dictates potential major design modifications in the inertial measurement unit (IMU) as well as the GPS receiver. These design modifications are necessary to exploit the performance potential to the maximum, particularly in the military environment, and at the same time to realize substantial cost savings in the system as an additional benefit. Author

N89-10881# Naval Materiel Command, Haakonsvern (Norway).
AIDING AND INTEGRATION OF A GPS RECEIVER
Per W. Nieuwejaar *In* AGARD, The NAVSTAR GPS System Sep. 1988 10 p (For primary document see N89-10874 02-04)
Copyright Avail: NTIS HC A07/MF A01

The need for receiver aiding due to contingencies such as satellite outages, jamming, and terrain masking is described. Alternative aiding methods are also described, such as: integration of GPS/INS or Attitude Heading Reference System (AHRS); integration of GPS and baro-altimeter; integration of GPS and atomic clock; use of altitude hold or mean sea level information; and integration of GPS/Transit/LORAN-C and/or Omega. Author

N89-10882# Air Force Space Div., Los Angeles, Calif.
CIVIL AND MILITARY APPLICATIONS OF GPS
Hans J. Kunze *In* AGARD, The NAVSTAR GPS System Sep. 1988 19 p (For primary document see N89-10874 02-04)
Copyright Avail: NTIS HC A07/MF A01

The objectives are to give an overview of military and civil applications of the NAVSTAR Global Positioning System (GPS), to discuss the resulting benefits for the users, and to present a planned system development that will provide the user community with the GPS information, such as overall system status or satellite data, required for their mission. Author

N89-10883# TAU Corp., Los Gatos, Calif.
DIFFERENTIAL OPERATION OF NAVSTAR GPS FOR ENHANCED ACCURACY
Robert P. Denaro and Rudolph M. Kalafus *In* AGARD, The NAVSTAR GPS System Sep. 1988 18 p (For primary document see N89-10874 02-04)
Copyright Avail: NTIS HC A07/MF A01

The NAVSTAR Global Positioning System has demonstrated impressive absolute accuracy in tests and operational use. Most applications will benefit from the increased accuracy afforded by GPS over conventional systems. However, many applications require even better accuracy than GPS can provide in the stand-alone mode. Differential GPS is a practical solution in many situations. The subject of differential GPS is fundamentally a simple concept, but implementation details can be more complex, and handling of all cases takes special care to achieve continuously reliable results. The concept and objective of differential GPS is covered, and a methodology for implementation presented. Example test results are presented which validate the potential of differential GPS. Author

N89-10884# TAU Corp., Los Gatos, Calif.
GPS NAVIGATION PROCESSING AND KALMAN FILTERING
Robert P. Denaro and Peter V. W. Loomis *In* AGARD, The NAVSTAR GPS System Sep. 1988 9 p (For primary document see N89-10874 02-04)
Copyright Avail: NTIS HC A07/MF A01

The processing of Global Positioning System (GPS) signals is a complex process of dealing with two observables, the range and the Doppler of the signal. This provides opportunities for substantial sophistication in processing techniques in the tracking loops, and later in the navigation processing of the Kalman filter or other filter. In total, the combination of techniques is a closely interrelated set of algorithms that provide near-optimum performance. Author

N89-10885# Arinc Research Corp., Annapolis, Md.
IN-SERVICE EVALUATION OF THE TRAFFIC ALERT AND COLLISION AVOIDANCE SYSTEM (TCAS) INDUSTRY PROTOTYPE
Daniel H. Tillotson, Loren D. Bolstridge, and Gary P. Gambarani May 1988 306 p

(Contract DTFA01-80-C-10093)
(DOT/FAA/SA-88/2; Rept-3011-01-03-4675) Avail: NTIS HC A14/MF A01

An operational evaluation of the Traffic Alert and Collision Avoidance System (TCAS 2) Industry Prototype was conducted to assess the utility of the TCAS to flight crews, to assess the impacts of TCAS on flight crew workload, to assess the impacts of TCAS on the air traffic control (ATC) system, and to obtain flight crew comments on TCAS design parameters and cockpit displays. The evaluation was conducted on one Boeing 727 aircraft operating in airline revenue service with Piedmont Airlines. Quantitative data on TCAS performance were collected to characterize the location and frequency of TCAS advisories. Quantitative data were collected from flight crews and cockpit observers to assess the utility of TCAS and to assess the impacts of TCAS on ATC and the flight crews. Minor operational anomalies were identified and changes to operational procedures or TCAS logic were recommended.
Author

N89-10886# Army Engineer Topographic Labs., Fort Belvoir, Va.
CONTINUOUS DEFORMATION MONITORING WITH GPS
Stephen R. DeLoach 12 Apr. 1988 39 p Presented at the ASCE Specialty Conference, Nashville, Tenn., 11-14 May 1988
(AD-A196447; ETL-R-138) Avail: NTIS HC A03/MF A01
CSCL 13B

The U.S. Army Corps of Engineers makes extensive use of modern instrumentation for measuring the behavior of large structures. One of these instrumentation programs is high precision geodetic surveying which provides a reliable measure of displacement as a function of time. Typically, accuracies of 5 to 10 mm can be achieved. Final accuracy of the displacement is a function of many factors, including: network geometry, field procedures, survey crew experience, and equipment. Unfortunately, the high precision geodetic survey is labor intensive, time consuming and rather expensive. For this reason, surveys are made infrequently, or sometimes not at all unless there is a suspicion of structural distress. The NAVSTAR Global Positioning System has the potential to be used in an automatic mode to continuously monitor structural deformations. During the next few months, a system will be developed to operate such a system. It will then be installed at the USACE Corps of Engineers Dworshak Dam in Idaho for demonstration. Testing of presently owned government GPS equipment indicates the system will detect movements of about 6 mm in three dimensions if reference points and object points are within a few kilometers of each other.
GRA

05 AIRCRAFT DESIGN, TESTING AND PERFORMANCE

Includes aircraft simulation technology.

For related information see also *18 Spacecraft Design, Testing and Performance* and *39 Structural Mechanics*.For land transportation vehicles see *85 Urban Technology and Transportation*.

N89-10887 California Univ., Los Angeles.
AEROELASTICITY AND STRUCTURAL OPTIMIZATION OF HELICOPTER ROTOR BLADES WITH SWEPT TIPS Ph.D. Thesis
Roberto Celi 1987 507 p
Avail: Univ. Microfilms Order No. DA8800601

Structural optimization techniques are used to minimize the oscillatory vertical hub shears for a helicopter in forward flight, subject to aeroelastic stability constraints, blade natural frequency placement constraints, and autorotation constraints. A special technique is used to build a sequence of approximate, inexpensive to solve approximate optimization problems, the solutions of which converge to the solution of the exact, expensive to solve optimization problem. Blade configurations with both straight and swept tips, and single- and double-cell cross sections are analyzed. The results show that the approach used is very efficient, and produces improved designs with a very small number of blade aeroelastic analyses. A special finite element for the modeling of a swept tip rotor blade is derived. A methodology for the formulation of the aeroelastic stability and response for helicopter rotor blades is proposed, which reduces considerably the implementation effort, and is applicable to both straight and swept tip blades. The methodology is combined with a finite element model of the blade, and a quasilinear solution technique. As a preliminary to the analysis of swept tip blades, a study was conducted of the aeroelastic behavior of rotor blades with noncoincident elastic axis, aerodynamic centers, and centers of mass. Dissert. Abstr.

N89-10888# Tokyo Univ. (Japan). Inst. of Space and Astronautical Science.
A FREE-FLIGHT EXPERIMENT OF VEHICLES RANGING FROM HIGH SUBSONIC TO HIGH SUPERSONIC SPEEDS
H. Oguchi, K. Funabiki, S. Sato, and M. Hatakeyama (Musashi Inst. of Tech., Tokyo, Japan) Apr. 1987 10 p
(ISAS-RN-362) Avail: NTIS HC A02/MF A01

Reported is a preliminary experiment on the free-flight range which is contrived to be driven by means of a sort of fast-acting valve. The remarkable characteristics of this range is operational feasibility and the wide coverage of flight speed from high subsonic to high supersonic speeds. Both sphere and vehicle models are tested with shadowgraph observations and flight speed measurements are made at several locations. Author

N89-10889 Southampton Univ. (England).
THE USE OF THE COMPLEX SUMMATION METHOD FOR FORMULATING ALGORITHMS FOR DECOUPLING VERTICAL/HORIZONTAL MOTIONS OF ROLLING AIRCRAFT Ph.D. Thesis
E. M. Belo 1987 249 p
Avail: Univ. Microfilms Order No. BRD-80844

Algorithms produced for rolling Aircraft Flight Control Systems to decouple vertical from horizontal motions are assessed. The aim is to study the use of the Complex Summation Method as a technique to assist the designer in the selection of algorithms choosen to achieve this objective. The benefit of this method for decoupling objective is that the presence of coupling is easily seen by the existence of imaginery coefficients in the complex system equations. A numerical example is presented and results in terms of time responses are obtained from the application of an algorithms which transforms it into a Similar and Antisymmetrically Coupled (SAC) system with outputs being the acceleration decoupled in Inertial Axes. Dissert. Abstr.

N89-10890*# Massachusetts Inst. of Tech., Cambridge. Dept. of Aeronautics and Astronautics.
FLIGHT TEST RESULTS FOR THE DAEDALUS AND LIGHT EAGLE HUMAN POWERED AIRCRAFT
R. Bryan Sullivan and Siegfried H. Zerweckh 7 Jun. 1988 138 p
(Grant NAG1-836)
(NASA-CR-183305; NAS 1.26:183305) Avail: NTIS HC A07/MF A01 CSCL 01C

The results of the flight test program of the Daedalus and Light Eagle human powered aircraft in the winter of 1987/88 are given. The results from experiments exploring the Light Eagle's rigid body and structural dynamics are presented. The interactions of these dynamics with the autopilot design are investigated. Estimates of the power required to fly the Daedalus aircraft are detailed. The system of sensors, signal conditioning boards, and data acquisition equipment used to record the flight data is also described. In order to investigate the dynamics of the aircraft, flight test maneuvers were developed to yield maximum data quality from the point of view of estimating lateral and longitudinal stability derivatives. From this data, structural flexibility and unsteady aerodynamics have been modeled in an ad hoc manner and are used to augment the equations of motion with flexibility effects. Results of maneuvers that were flown are compared with the predictions from the flexibility model. To extend the ad hoc flexibility

model, a fully flexible aeroelastic model has been developed. The model is unusual in the approximate equality of many structural natural frequencies and the importance of unsteady aerodynamic effects. the Gossamer Albatross. It is hypothesized that this inverse ground effect is caused by turbulence in the Earth's boundary layer. The diameters of the largest boundary layer eddies (which represent most of the turbulent kinetic energy) are proportional to altitude; thus, closer to the ground, the energy in the boundary layer becomes concentrated in eddies of smaller and smaller diameter. Eventually the eddies become sufficiently small (approximately 0.5 cm) that they trip the laminar boundary layer on the wing. As a result, a greater percentage of the wing area is covered with turbulent flow. Consequently the aircraft's drag and the pow er required both increase as the aircraft flies closer to the ground. The results of the flight test program are examined critically, especially with respect to future applications. Maneuvers that allow the observation of stability derivatives for flexible aircraft are detailed. Considerations for the design of autopilots for future human power aircraft and high-altitude RPV's are discussed. Techniques useful in estimating the power required to fly aircraft of very high lift to drag ratio are described.

N89-10891# Department of Defence, Canberra (Australia). Central Studies Branch.
SOME STATISTICAL ASPECTS OF ATTRITION STUDIES
B. K. McMillan May 1988 27 p
(AD-A196665; CSB-MEMO-3; DODA-AR-005-257) Avail: NTIS HC A03/MF A01 CSCL 12C

A methodology for analysing aircraft attrition data and establishing the reliability of the results is given. Underlying assumptions include exponentially distributed times between attritions, and a mean that increases with operating experience. Principal techniques used are Maximum Likelihood Estimation and Jackknifing. An example is given drawn from F/A-18 data. GRA

06 AIRCRAFT INSTRUMENTATION

Includes cockpit and cabin display devices; and flight instruments.

For related information see also *19 Spacecraft Instrumentation* and *35 Instrumentation and Photography.*

N89-10834# Air Force Wright Aeronautical Labs., Wright-Patterson AFB, Ohio. Avionics Lab.
ADVANCED AVIONICS ARCHITECTURE PAVE PILLAR
John C. Ostgaard *In* AGARD, Computing Systems Configuration for Highly Integrated Guidance and Control Systems Jun. 1988 8 p (For primary document see N89-10831 02-01)
Copyright Avail: NTIS HC A08/MF A01

N89-10835# Air Force Wright Aeronautical Labs., Wright-Patterson AFB, Ohio. Data and Signal Processing Group.
DATA AND SIGNAL PROCESSING ARCHITECTURES FOR FUTURE AVIONICS
Mark T. Michael *In* AGARD, Computing Systems Configuration for Highly Integrated Guidance and Control Systems Jun. 1988 12 p (For primary document see N89-10831 02-01)
Copyright Avail: NTIS HC A08/MF A01

N89-10836# Harris Corp., Melbourne, Fla. Government Aerospace Systems Div.
FIBER OPTIC BUSES AND NETWORKS FOR ADVANCED AVIONICS ARCHITECTURES
R. W. Uhlhorn *In* AGARD, Computing Systems Configuration for Highly Integrated Guidance and Control Systems Jun. 1988 15 p (For primary document see N89-10831 02-01)
Copyright Avail: NTIS HC A08/MF A01

07 AIRCRAFT PROPULSION AND POWER

Includes prime propulsion systems and systems components, e.g., gas turbine engines and compressors; and onboard auxilliary power plants for aircraft.

For related information see also *20 Spacecraft Propulsion and Power, 28 Propellants and Fuels,* and *44 Energy Production and Conversion.*

N89-10892# Naval Air Propulsion Test Center, Trenton, N.J.
STATISTICS ON AIRCRAFT GAS TURBINE ENGINE ROTOR FAILURES THAT OCCURRED IN US COMMERCIAL AVIATION DURING 1982 Final Report
R. A. DeLucia and J. T. Salvino Jul. 1988 24 p
(Contract DOT-FA71NA-AP-98)
(DOT/FAA/CT-88/23) Avail: NTIS HC A03/MF A01

Statistics are presented relating to gas turbine engine rotor failures which occurred during 1982 in U.S. commercial aviation service use. One-hundred and sixty-one rotor failures occurred in 1982. Rotor fragments were generated in 88 of the failures and, of these, 16 were uncontained. The predominant failure involved blade fragments. Seven disk failures occurred and all were uncontained. Seventy percent of the 161 failures occurred during the takeoff and climb stages of flight. This service data analysis is prepared on a calendar year basis and published yearly. The data support flight safety analysis, proposed regulatory actions, certification standards, and cost benefit analyses. Author

N89-10893# Naval Air Propulsion Test Center, Trenton, N.J.
EXPERIMENTAL GUIDELINES FOR THE DESIGN OF TURBINE ROTOR FRAGMENT CONTAINMENT RINGS Final Report, 21 Mar. 1979 - 29 Nov. 1985
James T. Salvino, Robert A. DeLucia, and Tracy Russo Jul. 1988 36 p
(Contract DOT-FA71NA-AP-98)
(DOT/FAA/CT-88/21; NAPC-PE-144) Avail: NTIS HC A03/MF A01

Results of experimentation to determine design guidelines for turbine rotor fragment containment rings are presented in this report. The project consisted of two tasks. Task 1 was an investigation of the containment characteristics of cloth rings. Task 2 determined the engine casing thickness required for single and triple blade containment. This effort was conducted as part of the overall Rotor Fragment Protection Program. Author

N89-10894# Rohr Industries, Inc., Chula Vista, Calif.
DE-ICING OF AIRCRAFT TURBINE ENGINE INLETS Final Report
H. A. Rosenthal, D. O. Nelepovitz, and H. M. Rockholt Jun. 1988 68 p
(Contract DTFA03-86-C-0050)
(DOT/FAA/CT-87/37) Avail: NTIS HC A04/MF A01

The results of an FAA investigation to determine the effects of using de-icing, as opposed to anti-icing, in aircraft turbine engine inlets are given. A literature search was conducted. Ice protection equipment technology was assessed. The icing/de-icing process, de-ice system operation and performance, ice detector characteristics, and a method for determining the effects of the de-icing process on the turbine engine and its associated induction system are discussed. Author

N89-11063# Joint Publications Research Service, Arlington, Va.
RESEARCH ON CATALYST COMBUSTION FOR GAS TURBINE
Shigeru Hayashi *In its* JPRS Report: Science and Technology: Japan 4 Jun. 1987 p 12-14 Transl. into ENGLISH from Kogiken Nyusu (Toyko, Japan), Aug. 1986 p 3-4 (For primary document see N89-11061 02-31)
Avail: NTIS HC A05/MF A01

08 AIRCRAFT STABILITY AND CONTROL

Includes aircraft handling qualities; piloting; flight controls; and autopilots.

For related information see also *05 Aircraft Design, Testing and Performance.*

N89-10895*# Princeton Univ., N. J. Dept. of Mechanical and Aerospace Engineering.
A STUDY OF HELICOPTER STABILITY AND CONTROL INCLUDING BLADE DYNAMICS Final Report, Jul. 1983 - Sep. 1987
Xin Zhao and H. C. Curtiss, Jr. Oct. 1988 169 p
(Grant NAG2-244)
(NASA-CR-183245; NAS 1.26:183245) Avail: NTIS HC A08/MF A01 CSCL 01C

A linearized model of rotorcraft dynamics has been developed through the use of symbolic automatic equation generating techniques. The dynamic model has been formulated in a unique way such that it can be used to analyze a variety of rotor/body coupling problems including a rotor mounted on a flexible shaft with a number of modes as well as free-flight stability and control characteristics. Direct comparison of the time response to longitudinal, lateral and directional control inputs at various trim conditions shows that the linear model yields good to very good correlation with flight test. In particular it is shown that a dynamic inflow model is essential to obtain good time response correlation, especially for the hover trim condition. It also is shown that the main rotor wake interaction with the tail rotor and fixed tail surfaces is a significant contributor to the response at translational flight trim conditions. A relatively simple model for the downwash and sidewash at the tail surfaces based on flat vortex wake theory is shown to produce good agreement. Then, the influence of rotor flap and lag dynamics on automatic control systems feedback gain limitations is investigated with the model. It is shown that the blade dynamics, especially lagging dynamics, can severly limit the useable values of the feedback gain for simple feedback control and that multivariable optimal control theory is a powerful tool to design high gain augmentation control system. The frequency-shaped optimal control design can offer much better flight dynamic characteristics and a stable margin for the feedback system without need to model the lagging dynamics. Author

N89-10896# George Washington Univ., Washington, D.C. Graduate School of Engineering and Applied Science.
INVESTIGATION OF THE TUMBLING PHENOMENON USING COMPUTER SIMULATION M.S. Thesis
Scott Powell Fears Sep. 1985 138 p
Avail: NTIS HC A07/MF A01

A single degree-of-freedom free-to-pitch simulation of the X-29A was developed and used to investigate the tumble susceptibility of the X-29A with its controls fixed. Validation of the ability of the aerodynamic models used in this simulation to accurately describe tumbling was accomplished by comparing the simulation results to dynamic wind-tunnel test results. The wind-tunnel and simulation results showed a strong tendency to tumble in the nose-down direction for the controls-fixed X-29A. A three degree-of-freedom piloted simulation of the X-29A using similar aerodynamic models was developed and used to test the tumble susceptibility of the X-29A with its controls active. These tests showed that high initial pitch rates are required for tumble entry from trimmed flight. Finally, a parametric study of the aerodynamic characteristics that affect tumble susceptibility was conducted using the single degree-of-freedom simulation and generic aerodynamic data representing the X-29A configuration and a conventional configuration at various static margins. It was shown that an ordinate direction shift in the static pitching-moment data, differences in the pitching-moment magnitudes or alpha ranges of the positive and negative regions of the static pitching-moment data, reduced static margins, reduced stable pitch damping magnitudes, and regions of unstable pitch damping will contribute to the tumble susceptibility of a given configuration. Author

N89-10832# Messerschmitt-Boelkow-Blohm G.m.b.H., Munich (West Germany). Aircraft Div.
COMPUTING SYSTEM CONFIGURATION FOR FIGHTER AIRCRAFT FLIGHT CONTROL SYSTEMS
H. J. Kaul, H. Lueers, and J. Rauch *In* AGARD, Computing Systems Configuration for Highly Integrated Guidance Control Systems Jun. 1988 32 p (For primary document see N89-10831 02-01)
Copyright Avail: NTIS HC A08/MF A01

09 RESEARCH AND SUPPORT FACILITIES (AIR)

Includes airports, hangars and runways; aircraft repair and overhaul facilities; wind tunnels; shock tubes; and aircraft engine test stands.

For related information see also *14 Ground Support Systems and Facilities (Space).*

N89-10897*# National Academy of Sciences - National Research Council, Washington, D. C.
REVIEW OF AERONAUTICAL WIND TUNNEL FACILITIES
27 Jul. 1988 64 p
(Contract NASw-4003)
(NASA-CR-183057; NAS 1.26:183057) Avail: NTIS HC A04/MF A01 CSCL 14B

The nation's aeronautical wind tunnel facilities constitute a valuable technological resource and make a significant contribution to the global supremacy of U.S. aircraft, both civil and military. At the request of NASA, the National Research Council's Aeronautics and Space Engineering Board organized a commitee to review the state of repair, adequacy, and future needs of major aeronautical wind tunnel facilities in meeting national goals. The comittee identified three main areas where actions are needed to sustain the capability of NASA's aeronautical wind tunnel facilities to support the national aeronautical research and development activities: tunnel maintenance and upgrading, productivity enhancement, and accommodation of new requirements (particularly in hypersonics). Each of these areas are addressed and the committee recommendations for appropriate actions presented. Author

N89-10898# Sandia National Labs., Albuquerque, N. Mex.
SANDIA NATIONAL LABORATORIES FLIGHT SIMULATION FACILITIES
T. M. Criel and F. V. Wyatt May 1988 14 p
(Contract DE-AC04-76DP-00789)
(DE88-012108; SAND-87-2034) Avail: NTIS HC A03/MF A01

Flight simulation computer facilities and motion simulator facilities at Sandia National Laboratories include an AD-100 (both real-time digital simulation computers), two AD-5s (analog computers), a VAX 11/780 (a digital mainframe), a PDP 11/60 (a digital computer), and a Carco S-450R-3/R three-axis motion simulator. This report describes the current equipment. DOE

N89-10899# Sandia National Labs., Albuquerque, N. Mex. Photometrics and Optical Development Div.
SCHLIEREN MEASUREMENTS AT THE 10,000-FOOT SLED TRACK
R. A. Hill, R. L. Hughes, and A. A. Sehmer Jul. 1988 19 p
(Contract DE-AC04-76DP-00789)
(DE88-012748; SAND-88-0497) Avail: NTIS HC A03/MF A01

A schlieren technique has been used at the 10,000-foot sled track to record the interaction of the horizontal bow shock produced by a supersonic sled with the track structure. Under the conditions of these tests, the bow shock reflected from the west retaining wall is observed to interact with the aft portion of the sled; the bow shock reflected from the east rail passes to the rear of the sled. DOE

N89-10900*# California Univ., Davis. Dept. of Mechanical Engineering.
DESIGN AND EVALUATION OF A COCKPIT DISPLAY FOR HOVERING FLIGHT
Ronald A. Hess and Peter James Gorder 2 Oct. 1988 39 p (Contract NCC2-383)
(NASA-CR-183247; NAS 1.26:183247) Avail: NTIS HC A03/MF A01 CSCL 14B

A simulator evaluation of a cockpit display format for hovering flight is described. The display format is based on the position-velocity-acceleration representation (PVA) similar to that used in the Pilot Night Vision System in the Army AH-64 helicopter. By only varying the nature of the display law driving the primary indicator in the PVA format, i.e., the acceleration symbol, three candidate displays are created and evaluated. These range from a Status display in which the primary indicator provides true acceleration information to a Command display, in which the primary indicator provides flight director information. Simulation results indicate that two of the three displays offer performance and handling qualities which make them excellent candidates for future helicopter cockpit display systems. Author

N89-10901# Oak Ridge National Lab., Tenn.
PROTOTYPE DATA ACQUISITION AND ANALYSIS SYSTEM FOR NAVY OPERATIONAL FLIGHT SIMULATORS
R. C. Muller, G. O. Allgood, and B. VanHoy 1988 6 p Presented at the American Institute of Aeronautics and Astronautics Simulation Technology Conference, Atlanta, Ga., 7 Sep. 1988
(Contract DE-AC05-84OR-21400)
(DE88-014557; CONF-8809108-1) Avail: NTIS HC A02

A problem of flight simulators has been the discomfort experienced by some pilots to the point of nausea. Likely explanations are a significant lack of synchronization between sight and movement as well as motion in the critical frequency magnitude region. A program to examine this problem has been undertaken at Oak Ridge National Laboratory, and the selection of appropriate computer hardware and software for analyzing motion and visual systems in real time is described. While requirements such as high data acquisition rate and high rates of arithmetic operations have driven the sections, rapid advances in computer technology have guided system development toward easy upgrade at modest cost. Results from use and demonstration have been positive, especially in the areas of reliability and ease of use. DOE

12 ASTRONAUTICS (GENERAL)

For extraterrestrial exploration see *91 Lunar and Planetary Exploration.*

N89-10902*# National Aeronautics and Space Administration. Goddard Space Flight Center, Greenbelt, Md.
THE 1988 GET AWAY SPECIAL EXPERIMENTER'S SYMPOSIUM
Lawrence R. Thomas, ed. and Frances L. Mosier, ed. (RMS Technologies, Inc., Landover, Md.) Sep. 1988 127 p Symposium held in Cocoa Beach, Fla., 27-30 Sep. 1988 Sponsored by NASA, Washington
(NASA-CP-3008; Rept-88-158; NAS 1.55:3008) Avail: NTIS HC A07/MF A01 CSCL 22A

The Get Away Special (GAS) Experimenter's Symposium was held to provide a formal opportunity for GAS experimenters to share the results of their projects. The focus of this symposium is on payloads that have been flown on shuttle missions and on GAS payloads that will be flown in the future. Experiment design and payload integration issues are also examined. For individual titles, see N89-10903 through N89-10920.

N89-10903*# Jet Propulsion Lab., California Inst. of Tech., Pasadena.
THE FIRST CHINESE STUDENT SPACE SHUTTLE GETAWAY SPECIAL PROGRAM
Mark C. Lee, Xun-Shu Jin, Shou-Quan Ke, and Bing-Chen Fu (Chinese Society of Astronautics, Beijing.) *In* NASA, Goddard Space Flight Center, The 1988 Get Away Special Experimenter's Symposium Sep. 1988 p 1-8 (For primary document see N89-10902 02-12)
Avail: NTIS HC A07/MF A01 CSCL 22A

The first Chinese Getaway Special program is described. Program organization, the student proposal evaluation procedure, and the objectives of some of the finalist's experiments are covered. The two experiments selected for eventual flight on the space shuttle are described in detail. These include: (1) the control of debris in the cabin of the space shuttle; and (2) the solidification of two immiscible liquids in space. Author

N89-10904*# Fujitsu Ltd., Kawasaki (Japan).
DEVELOPMENT OF BIO-GAS SYSTEMS
M. Takayanagi, S. Kitamura, H. Nemoto, T. Kimura, Y. Zaiki, T. Kitakohji, S. Fujita, M. Kameda, M. Noda, and Y. Kawasaki (Mitsubishi-Kasei Inst. of Life Sciences, Tokyo, Japan) *In* NASA, Goddard Space Flight Center, The 1988 Get Away Special Experimenter's Symposium Sep. 1988 p 9-16 (For primary document see N89-10902 02-12)
Avail: NTIS HC A07/MF A01 CSCL 22A

Four experiment systems which have fundamental significance in the field of biotechnology are developed for the Get Away Special (GAS). Unique considerations were necessary to develop the systems which carry out biotechnological experiments under GAS's restricted conditions: delicate thermal control, fluid handling and protection from contamination. All experimental processes are controlled by internal sequencers and results of the experiments are recorded as images and numerical data within the systems. The systems are standardized in order to enable repeated use with a variety of experiments by replacement of the experiment modules and modification of experiment sequencing programs. Author

N89-10905*# Technische Univ., Berlin (West Germany). Dept. of Satellite Design and Technology.
TUBSAT-1, SATELLITE TECHNOLOGY FOR EDUCATIONAL PURPOSES
A. Ginati *In* NASA, Goddard Space Flight Center, The 1988 Get Away Special Experimenter's Symposium Sep. 1988 p 17-24 (For primary document see N89-10902 02-12)
Avail: NTIS HC A07/MF A01 CSCL 22A

TUBSAT-1 (Technical University of Berlin Satellite) is an experimental low-cost satellite within the NASA Get Away Special (GAS) program. This project is being financed by the German BMFT (Federal Ministry for Research and Technology), mainly for student education. The dimensions and weight are determined by GAS requirements and the satellite will be ejected from the space shuttle into an approximately 300-km circular orbit. It is a sun/star oriented satellite with an additional spin stabilization mode. The first planned payload is to be used for observing flight paths of migratory birds from northern Europe to southern Africa and back. Author

N89-10906*# Deutsche Forschungs- und Versuchsanstalt fuer Luft- und Raumfahrt, Cologne (West Germany).
FUTURE MAUS PAYLOAD AND THE TWIN-MAUS CONFIGURATION
S. Staniek, G. Otto, and J. Deopkens (Messerschmitt-Boelkow-Blohm/Entwicklungsring Nord, Bremen, West Germany) *In* NASA, Goddard Space Flight Center, The 1988 Get Away Special Experimenter's Symposium Sep. 1988 p 25-32 (For primary document see N89-10902 02-12)
Avail: NTIS HC A07/MF A01 CSCL 22A

The German MAUS project (materials science autonomous experiments in weightlessness) was initiated in 1979 for optimum utilization of NASA's Get Away Special (GAS) program. The standard MAUS system was developed to meet GAS requirements and can accomodate a wide variety of GAS-type experiments. The system offers a range of services to experimenters within the framework of standardized interfaces. Four MAUS payloads being prepared for future space shuttle flight opportunities are described.

The experiments include critical Marangoni convection, oscillatory Marangoni convection, pool boiling, and gas bubbles in glass melts. Scientific objectives as well as equipment hardware are presented together with recent improvements to the MAUS standard system, e.g., a new experiment control and data management unit and a semiconductor memory. A promising means of increasing resources in the field of GAS experiments is the interconnection of GAS containers. This important feature has been studied to meet the challenge of future advanced payloads. In the TWIN-MAUS configuration, electrical power and data will be transferred between two containers mounted adjacent to each other. Author

N89-10907*# Nippon Electric Co. Ltd., Yokohama (Japan).
DEVELOPMENT OF EXPERIMENTAL SYSTEMS FOR MATERIAL SCIENCES UNDER MICROGRAVITY
Jun Tanii, Shinzo Obi, Yotsuo Kamimiyata, and Akio Ajimine (Society of Japanese Aerospace Co., Inc., Tokyo.) *In* NASA, Goddard Space Flight Center, The 1988 Get Away Special Experimenter's Symposium Sep. 1988 p 33-40 (For primary document see N89-10902 02-12)
Avail: NTIS HC A07/MF A01 CSCL 22A

As part of the Space Experiment Program of the Society of Japanese Aerospace Companies, three experimental systems (G452, G453, G454) have been developed for materials science studies under microgravity by the NEC Corporation. These systems are to be flown as Get Away Special payloads for studying the feasibility of producing new materials. Together with the experimental modules carrying the hardware specific to the experiment, the three systems all comprise standard subsystems consisting of a power supply, sequence controller, temperature controller, data recorder, and video recorder. Author

N89-10908*# Max-Planck-Inst. fuer Extraterrestrische Physik, Garching (West Germany).
HIEN-LO: AN EXPERIMENT FOR CHARGE DETERMINATION OF COSMIC RAYS OF INTERPLANETARY AND SOLAR ORIGIN
B. Klecker, D. Hovestadt, G. M. Mason, J. B. Blake, and J. Nicholas (Air Force Technical Applications Center, Patrick AFB, Fla.) *In* NASA, Goddard Space Flight Center, The 1988 Get Away Special Experimenter's Symposium Sep. 1988 p 41-48 (For primary document see N89-10902 02-12)
Avail: NTIS HC A07/MF A01 CSCL 22A

The experiment is designed to measure the heavy ion environment at low altitude (HIEN-LO) in the energy range 0.3 to 100 MeV/nucleon. In order to cover this wide energy range a complement of three sensors is used. A large area ion drift chamber and a time-of-flight telescope are used to determine the mass and energy of the incoming cosmic rays. A third omnidirectional counter serves as a proton monitor. The analysis of mass, energy and incoming direction in combination with the directional geomagnetic cut-off allows the determination of the ionic charge of the cosmic rays. The ionic charge in this energy range is of particular interest because it provides clues to the origin of these particles and to the plasma conditions at the acceleration site. The experiment is expected to be flown in 1988/1989. Author

N89-10909*# National Aeronautics and Space Administration. Goddard Space Flight Center, Greenbelt, Md.
CSCP: A NEW GET AWAY SPECIAL (GAS) PROJECT
Jack J. Gottlieb *In its* The 1988 Get Away Special Experimenter's Symposium Sep. 1988 p 49-52 (For primary document see N89-10902 02-12)
Avail: NTIS HC A07/MF A01 CSCL 22A

The Get Away Special (GAS) program has instituted a new project called Complex Self Contained Payloads (CSCP) designed to support GAS type payloads that are beyond the scope of the GAS program. These payloads may be supported by GAS personnel and hardware and will fly as primary or secondary shuttle payloads. The definition, requirements and basic support package for CSCP's are discussed. Author

N89-10910*# National Aeronautics and Space Administration. Goddard Space Flight Center, Greenbelt, Md.
STS SAFETY APPROVAL PROCESS FOR SMALL SELF-CONTAINED PAYLOADS
Mary A. Gum *In its* The 1988 Get Away Special Experimenter's Symposium Sep. 1988 p 53-59 (For primary document see N89-10902 02-12)
Avail: NTIS HC A07/MF A01 CSCL 22A

The safety approval process established by the National Aeronautics and Space Administration for Get Away Special (GAS) payloads is described. Although the designing organization is ultimately responsible for the safe operation of its payload, the Get Away Special team at the Goddard Space Flight Center will act as advisors while iterative safety analyses are performed and the Safety Data Package inputs are submitted. This four phase communications process will ultimately give NASA confidence that the GAS payload is safe, and successful completion of the Phase 3 package and review will clear the way for flight aboard the Space Transportation System orbiter. Author

N89-10911*# National Aeronautics and Space Administration. Goddard Space Flight Center, Greenbelt, Md.
SYSTEMS REPORT FOR PAYLOAD G-652: PROJECT ORIGINS
J. Bellina, M. C. Muckerheide, J. Clark, M. Petry, D. Seeley, R. Sportiello, R. Sprecher, and M. Theiler *In its* The 1988 Get Away Special Experimenter's Symposium Sep. 1988 p 61-64 (For primary document see N89-10902 02-12)
Avail: NTIS HC A07/MF A01 CSCL 22A

Experiments conducted to investigate possible hardware configurations and methodologies for a Get Away Special payload designated G-652 are discussed. Test data collected from the operation of a free electron laser wiggler using simulated ram glow phenomenon are described. Results of an experiment to synthesize organic compounds within a primordial atmosphere using a laser induced plasma are discussed. An experiment is described which utilized neutron bombardment to assess the risk of genetic alterations in embyros in space. Author

N89-10912*# Delta-t, Lebanon, Pa.
GAS-611 FIREFLY IN ZERO GRAVITY **c29**
Tony Williams *In* NASA, Goddard Space Flight Center, The 1988 Get Away Special Experimenter's Symposium Sep. 1988 p 65-72 (For primary document see N89-10902 02-12)
Avail: NTIS HC A07/MF A01 CSCL 22A

The Get Away Special 611 (GAS-611) project will carry a small, self-contained biological experiment into a microgravity environment for a period of 120 hours. The payload will be a colony of Lampyridae (fireflies). The ability of this beetle to produce light with an efficiency of 98 pct will be evaluated in the micro-G environment. The chemical process that occurs could be assisted by the earth's gravitational pull and the very complex tracheae system found within this species of beetle. The effects of microgravity on mating and beetle larvae will also be studied. Author

N89-10913*# Instrumentation Technology Associates, Inc., Malvern, Pa.
ACCELERATION GROUND TEST PROGRAM TO VERIFY GAS PAYLOAD NO. 559 STRUCTURE/SUPPORT AVIONICS AND EXPERIMENT STRUCTURAL INTEGRITY
John M. Cassanto and Valerie A. Cassanto *In* NASA, Goddard Space Flight Center, The 1988 Get Away Special Experimenter's Symposium Sep. 1988 p 73-80 (For primary document see N89-10902 02-12)
Avail: NTIS HC A07/MF A01 CSCL 22A

Acceleration ground tests were conducted on the Get Away Special (GAS) payload 559 to verify the structural integrity of the structure/support avionics and two of the planned three flight experiments. The ITA (Integrated Test Area) Standardized Experiment Module (ISEM) structure was modified to accommodate the experiments for payload 559. The ISEM avionics consisted of a heavy duty sliver zinc power supply, three orthogonal-mounted low range microgravity accelerometers, a tri-axis high range

accelerometer, a solid state recorder/programmer sequencer, and pressure and temperature sensors. The tests were conducted using the Gravitational Plant Physiology Laboratory Centrifuge of the University City Science Center in Philadelphia, PA. The launch-powered flight steady state acceleration profile of the shuttle was simulated from lift-off through jettison of the External Tank (3.0 g's). Additional tests were conducted at twice the nominal powered flight acceleration levels (6 g's) and an over-test condition of four times the powered flight loads to 12.6 g's. The present test program has demonstrated the value of conducting ground tests to verify GAS payload experiment integrity and operation before flying on the shuttle. Author

N89-10914*# National Aeronautics and Space Administration. Goddard Space Flight Center, Greenbelt, Md.
UTILIZATION OF SPRAY ON FOAM INSULATION FOR MANNED AND UNMANNED SPACECRAFT AND STRUCTURES c18
Thomas M. Hancock, III *In its* The 1988 Get Away Special Experimenter's Symposium Sep. 1988 p 81 (For primary document see N89-10902 02-12)
Avail: NTIS HC A07/MF A01 CSCL 22B

The idea of using spray-on foam insulation as a passive thermal and micrometeorite protection system is explored. The benefits of applying an exterior coating of foam insulation can be: (1) the foam can provide a thermally stable shield that can assist in reducing the strain on traditional space radiator systems and can also act as a passive thermal guard, allowing a greater fault tolerance if the standard system should fail; (2) the foam can act as an ablative shell diminishing the effects of natural and manmade debris striking the structure; (3) the foam is lightweight - about 1/2 ounce per sq ft; (4) the foam is low cost and easy to maintain; and (5) the foam is a stable material that does not react when exposed to earth or lunar environments. Author

N89-10915*# Villanova Univ., Pa. Space Shuttle Experiments Program.
COMPUTERIZED MONITORING AND CONTROL OF EXPERIMENTS IN SPACE
Thomas V. Janisch *In* NASA, Goddard Space Flight Center, The 1988 Get Away Special Experimenter's Symposium Sep. 1988 p 83-88 (For primary document see N89-10902 02-12)
Avail: NTIS HC A07/MF A01 CSCL 22A

The computer subsystem of the Villanova University GAS (Get Away Special) experiment apparatus is discussed. The function of the computer subsystem is to provide data acquisition and control system support to the experiments. The computer subsystem will provide high availability, low power consumption and highly reliable data retention. The general layout of the subsystem provides for redundant processing units, control modules, and multiple data acquisition modules. Each of the two redundant processing units will be composed of a microprocessor, control logic, PROM, RAM, non-volitile memory, timers, self-check logic and data ports to the data acquisition and control modules. One unit will control the experiment while the other shadows the primary unit operation. The data acquisition module gathers data from the experiment. The data is transfered to the processing unit in digital form. The control module validates the data, decodes it and executes the command. Author

N89-10916*# California Polytechnic State Univ., San Luis Obispo. Space Systems Space Welding Project.
THE POTENTIAL OF A GAS CAN WITH PAYLOAD G-169
David Tamir *In* NASA, Goddard Space Flight Center, The 1988 Get Away Special Experimenter's Symposium Sep. 1988 p 89-96 (For primary document see N89-10902 02-12)
Avail: NTIS HC A07/MF A01 CSCL 22A

The feasibility of using welding for the construction, expansion and emergency repair of space based structures is discussed and the advantages of gas tungsten arc welding (GTAW) over other welding techniques are briefly examined. The objective and design concept for the G-169 Get Away Special payload are described. The G-169 experiment will allow the comparison of a space GTA welded joint with a terrestrial GTA welded joint with all parameters held constant except for gravitational forces. Specifically, a bead-on-plate weld around the perimeter of a 2 inch diameter stainless steel pipe section will be performed. The use of Learjet microgravity simulation for the G-169 and other Get Away Special experiments is also addressed. M.G.

N89-10917*# National Aeronautics and Space Administration. Goddard Space Flight Center, Greenbelt, Md.
HITCHHIKER CAPABILITIES
Theodore C. Goldsmith *In its* The 1988 Get Away Special Experimenter's Symposium Sep. 1988 p 97-107 (For primary document see N89-10902 02-12)
Avail: NTIS HC A07/MF A01 CSCL 22A

A carrier system has been developed for economical and quick response flight of small attached payloads on the space shuttle. Hitchhiker can accommodate up to 750 lb of customer payloads in canisters or mounted to an exposed side-mount plate, or up to 1200 lb mounted on a cross-bay structure. The carrier connects to the orbiter's electrical systems and provides up to six customers with standard electrical services including power, real time telemetry and commands. A transparent data and command system concept is employed to allow the customer to easily use his own ground support equipment and personnel to control his payload during integration and flight operations. A general description of the Hitchhiker program and the Shuttle Payload of Opportunity Carrier (SPOC) is given and future enhancements are outlined. M.G.

N89-10918*# Purdue Univ., West Lafayette, Ind.
THE PURDUE UNIVERSITY GET AWAY SPECIAL II (PUGAS II)
Christopher Olenski, Alan R. Crocker, Beth Stubbings, Laurie McCormick, and Paul K. Andersen *In* NASA, Goddard Space Flight Center, The 1988 Get Away Special Experimenter's Symposium Sep. 1988 p 109-111 (For primary document see N89-10902 02-12)
Avail: NTIS HC A07/MF A01 CSCL 22A

The Purdue University Get Away Special Project (PUGAS) is a student-run organization dedicated to preparing payloads for flight on NASA's space shuttle. The first such payload (PUGAS I) flew on Challenger in 1983. The second payload (PUGAS II) should be ready by the end of 1988 and will include three experiments. The first experiment will involve the production of tin metal foam under microgravity conditions. The second experiment will focus on the desorption of water from carbon-epoxy composite materials. The third experiment will use a solid polymeric material to detect radiation in space. Author

N89-10919*# National Aeronautics and Space Administration. Goddard Space Flight Center, Greenbelt, Md.
THE TRANSPORTATION OF FINE ARTS MATERIALS ABOARD THE SPACE SHUTTLE COLUMBIA. GAS PAYLOAD NO. 481: VERTICAL HORIZONS
Ellery Kurtz and Howard Wishnow *In its* The 1988 Get Away Special Experimenter's Symposium Sep. 1988 p 113-119 (For primary document see N89-10902 02-12)
Avail: NTIS HC A07/MF A01 CSCL 22A

The Vertical Horizons experiment represents an initial investigation into the transportation of fine arts materials aboard a space shuttle. Within the confines of a GAS canister, artist quality fine arts materials were packaged and exposed to the rigors of space flight in an attempt to identify adverse effects. Author

N89-10920*# Louisiana Tech Univ., Ruston. Dept. of Mechanical Engineering.
INORGANIC CHEMICAL PRECIPITATE FORMATION PAYLOAD DESIGN
Craig Friedrich *In* NASA, Goddard Space Flight Center, The 1988 Get Away Special Experimenter's Symposium Sep. 1988 p 121-127 (For primary document see N89-10902 02-12)
Avail: NTIS HC A07/MF A01 CSCL 22A

The Get Away Special payload to investigate the formation of inorganic precipitates (G-405) utilizes six transparent chemical reaction chambers to actively mix a dry powder with a liquid solution.

At predetermined intervals the progress of the precipitate formation is photographed and stored as data. The precipitate particles will also be subject to post-flight analysis. The various tasks performed during the 14 hour duration of the experiment are initiated and monitored by a custom-built digital controller. The payload is currently scheduled as a backup payload for STS-29 with a possible launch date of January, 1989. Author

N89-10921*# Jet Propulsion Lab., California Inst. of Tech., Pasadena.
OUTWARD TO THE BEGINNING: THE CRAF AND CASSINI MISSIONS OF THE MARINER MARK 2 PROGRAM
Jun. 1988 17 p Original document contains color illustrations
(NASA-CR-183133; NAS 1.26:183133; JPL-400/341) Avail: NTIS HC A03/MF A01 CSCL 22A

Two successive journeys will soon offer a perspective on the origin of the solar system and perhaps provide clues on the origin of life as well. The missions, the Comet Rendezvous Asteroid Flyby (CRAF) and Cassini (the Saturn orbiter/Titan probe), combine to form the first initiative of the Mariner Mark 2 program, a series of planetary missions whose common objective is to explore primitive bodies and the outer solar system, toward the ultimate goal of understanding the nature of our origins. Cassini and CRAF are exciting planetary missions. The objectives that they share, the region of the solar system in which comets, asteroids, and the Saturnian system have evolved and now reside, and the spacecraft that will carry both sets of experiments to their targets in the outer solar system are described. Author

N89-10922*# Alabama Univ., Huntsville. Center for Microgravity and Materials Research.
PROCESS MODELLING FOR SPACE STATION EXPERIMENTS Annual Report No. 1, 1 Oct. 1987 - 30 Sep. 1988
Franz Rosenberger and J. Iwan D. Alexander 24 Oct. 1988 51 p
(Grant NAG8-684)
(NASA-CR-183274; NAS 1.26:183274) Avail: NTIS HC A04/MF A01 CSCL 22A

The work performed during the first year 1 Oct. 1987 to 30 Sept. 1988 involved analyses of crystal growth from the melt and from solution. The particular melt growth technique under investigation is directional solidification by the Bridgman-Stockbarger method. Two types of solution growth systems are also being studied. One involves growth from solution in a closed container, the other concerns growth of protein crystals by the hanging drop method. Following discussions with Dr. R. J. Naumann of the Low Gravity Science Division at MSFC it was decided to tackle the analysis of crystal growth from the melt earlier than originally proposed. Rapid progress was made in this area. Work is on schedule and full calculations were underway for some time. Progress was also made in the formulation of the two solution growth models. Author

N89-10923*# Eagle Engineering, Inc., Webster, Tex.
RISK ANALYSIS OF EARTH RETURN OPTIONS FOR THE MARS ROVER/SAMPLE RETURN MISSION
13 Jul. 1988 141 p
(Contract NAS9-17878)
(NASA-CR-172081; NAS 1.26:172081; EE-88-183) Avail: NTIS HC A07/MF A01 CSCL 22A

Four options for return of a Mars surface sample to Earth were studied to estimate the risk of mission failure and the risk of a sample container breach that might result in the release of Martian life forms, should such exist, in the Earth's biosphere. The probabilities calculated refer only to the time period from the last midcourse correction burn to possession of the sample on Earth. Two extreme views characterize this subject. In one view, there is no life on Mars, therefore there is no significant risk and no serious effort is required to deal with back contamination. In the other view, public safety overrides any desire to return Martian samples, and any risk of damaging contamination greater than zero is unacceptable. Zero risk requires great expense to achieve and may prevent the mission as currently envisioned from taking place. The major conclusion is that risk of sample container breach can be reduced to a very low number within the framework of the mission as now envisioned, but significant expense and effort, above that currently planned is needed. There are benefits to the public that warrant some risk. Martian life, if it exists, will be a major discovery. If it does not, there is no risk. Author

13 ASTRODYNAMICS

Includes powered and free-flight trajectories; and orbital and launching dynamics.

N89-10924# Centre National d'Etudes Spatiales, Toulouse (France).
ELABORATION OF SPECIFICATIONS FOR AN EXPERT SYSTEM TO AID THE CHOICE OF ANALYTICAL METHODS OF ORBIT EXTRAPOLATION FOR SATELLITE LOCALIZATION
F. Laporte 13 Jun. 1986 140 p In FRENCH; ENGLISH summary
(CNES-CT/DTI/MS/MN/160; ETN-88-93096) Avail: NTIS HC A07/MF A01

Orbit extrapolation methods are reviewed and the difficulty in selecting a method for a given problem is pointed out. Specifications for an expert system to aid this choice are suggested. ESA

N89-10925# Air Force Inst. of Tech., Wright-Patterson AFB, Ohio.
THE UTILITY OF PARTICLE PRECIPITATION DATA AS AN INPUT TO THERMOSPHERIC DENSITY MODELS FOR SATELLITE ORBITAL ANALYSIS M.S. Thesis
Kelly J. Hand 1988 86 p
(AD-A196870; AFIT/CI/NR-88-69) Avail: NTIS HC A05/MF A01 CSCL 22B

The purpose of this thesis is to determine the relative (compared to the Ap index) utility of global hemispheric power (PPE), as measured by the NOAA/TIROS satellite Total Energy Detector (TED) system, in describing magnetospherically induced upper thermospheric density perturbations. This was accomplished using satellite accelerometer, satellite orbital, Goettingen Ap, and PPE data from the geomagnetically active period of March 20th to April 10th, 1979. The first part of the study used Air Force Geophysics Laboratory (AFGL) satellite accelerometer thermospheric density data to determine the correlation between it and the PPE. This was then compared to the density data correlation with the Goettingen Ap. the data was scaled to optimize the meaning and linearity of the correlation coefficients and to emphasize any density fluctuations due to geomagnetic variations. The time series cross-correlation produced about a 6-hour lagged response in obtaining maximum correlation. GRA

14 GROUND SUPPORT SYSTEMS AND FACILITIES (SPACE)

Includes launch complexes, research and production facilities; ground support equipment, e.g., mobile transporters; and simulators.

For related information see also *09 Research and Support Facilities (Air).*

N89-10926# Sandia National Labs., Albuquerque, N. Mex. Applied Mechanics Dept.
DETAILED ANALYSIS OF THE STRUCTURAL CONSEQUENCES OF RAILGUN AUGMENTATION
G. W. Wellman and K. W. Schuler Jun. 1988 66 p
(Contract DE-AC04-76DP-00789)
(DE88-013800; SAND-88-0617) Avail: NTIS HC A04/MF A01

The advantage of augmenting a plasma railgun is to provide the same driving force on the projectile as in an unaugmented railgun at a lower plasma arc current, thus producing less erosion and barrel damage. However, there are structural consequences to railgun augmentation which must be overcome before the

advantages of lower plasma arc currents can be realized. To investigate these consequences, a bolted V-block supporting structure is considered with two cores; unaugmented (a single pair of conducting rails), and augmented (conducting rails augmented by a second tandem set of conductors). For each core, a two-dimensional dynamic finite element structural analysis is performed. The loadings, applied sequentially, consist of the static bolt preload, the plasma pressure behind the projectile, and the magnetic pressure induced by currents flowing in the rails or augmenting conductors. The magnetic pressure induced by currents flowing in the rails or augmenting conductors. A maximum rail current is found for which the unaugmented railgun can be fired without permanent deformation of the gun bore, thus allowing repeated firings. For the augmented railgun, at the same projectile acceleration, large permanent deformations are shown. DOE

15 LAUNCH VEHICLES AND SPACE VEHICLES

Includes boosters; operating problems of launch/space vehicle systems; and reusable vehicles.

For related information see also *20 Spacecraft Propulsion and Power.*

N89-10927# Sandia National Labs., Albuquerque, N. Mex. Applied Mechanics Div.

SHED: A PROGRAM FOR THREE-DIMENSIONAL, RIGID BODY, SHROUD EJECTION DYNAMICS

Daniel J. Segalman Mar. 1988 43 p

(Contract DE-AC04-76DP-00789)

(DE88-012410; SAND-87-1432) Avail: NTIS HC A03/MF A01

The computer program SHED (for SHroud Ejection Dynamics) which calculates the exoatmospheric trajectory of a missile shroud is described. This rigid body dynamics program follows the motion of the shroud as its motors accelerate it ahead and away form the missile. Of particular interest is the ability of SHED to accommodate the forces produced by the motors which are fixed to the body in the sense that they both translate and rotate along with the body. The resulting program can accommodate an arbitrary number of motors, arranged in an arbitrary manner on the shroud, and each imposing an arbitrary schedule of thrust. The shroud may have any arbitrary shape. Guides can be accommodated which protect the payload by preventing shroud rotation or lateral motion until the shroud has passed over the guide. Limitations are that all bodies are assumed to be rigid and aerodynamic loads are not included. SHED has proven itself sufficiently robust and versatile to permit a critical comparison of a large range of shroud separation strategies in selecting a separation strategy for the Strategic TARgeting System (STARS) funded by the Army SDI Office. DOE

16 SPACE TRANSPORTATION

Includes passenger and cargo space transportation, e.g., shuttle operations; and space rescue techniques.

For related information see also *03 Air Transportation and Safety* and *18 Spacecraft Design, Testing and Performance.* For space suits see *54 Man/System Technology and Life Support.*

N89-10928# Lawrence Livermore National Lab., Calif. Nuclear Systems Safety Program.

REVIEW OF THE SPACE SHUTTLE PROPULSION PRESSURIZATION SYSTEM PROBABILISTIC RISK ASSESSMENT

James E. Wells and Gary L. Johnson 24 Jun. 1988 36 p

(Contract W-7405-eng-48)

(DE88-013163; UCID-21443) Avail: NTIS HC A03/MF A01

Lockheed Missiles and Space Company, Inc. has performed a probabilistic risk assessment of the space shuttle main propulsion pressurization system for NASA. A draft report of the assessment was completed in mid September 1987. We at the Lawerence Livermore National Laboratory (LLNL) were asked by NASA to perform an independent peer review of that risk assessment. This review assessed whether the analysis was done consistent with currently used methods for doing such analyses, pointed out deficiencies found in the analysis, and evaluated how these deficiencies affected the final result. DOE

N89-10929*# National Aeronautics and Space Administration. Langley Research Center, Hampton, Va.

PERFORMANCE OF A CIRCULAR BODY EARTH-TO-ORBIT WINGED TRANSPORT WITH VARIOUS STRAP-ON BOOSTERS

Ian O. MacConochie, J. Chris Naftel, and Frederick W. Widman Oct. 1988 33 p

(NASA-TM-100603; NAS 1.15:100603) Avail: NTIS HC A03/MF A01 CSCL 22B

Various types of twin strap-on boosters were evaluated by applying them to a core vehicle. The core vehicle has a clipped delta wing and a simple circular body, and is equipped with five Space Shuttle main engines. The only propellants in the core vehicle are liquid oxygen and liquid hydrogen. The strap-on boosters investigated include the current Shuttle solid rocket motors with steel cases and advanced solids with graphite composite filament-wound cases. Also, two types of liquid-oxygen/hydrocarbon boosters were investigated - one pair without crossfeed to the core vehicle and one with. The payloads obtained were tabulated for various assumptions, such as power levels on the core vehicle engines, number of engines, and maximum allowable flight dynamic pressures. The payload for the core vehicle with two filament-wound Shuttle solid rocket strap-on boosters was 83,000 lb and the payload for two liquid strap-ons with crossfeed was 84,000 lb. The core vehicle with Shuttle solid rocket strap-on boosters is regarded as a near term technology system. Author

17 SPACE COMM., SPACECRAFT COMM., COMMAND & TRACKING

Includes telemetry; space communications networks; astronavigation and guidance; and radio blackout.

For related information see also *04 Aircraft Communications and Navigation* and *32 Communications and Radar.*

N89-10930# Centre National d'Etudes Spatiales, Toulouse (France).

STUDY OF THE MULTIPLEXING OF IMAGE TELEMETRY DATA FROM SPOT 4 HRVIR AND VEGETATION SENSORS [ETUDE DU MULTIPLEXAGE DES TELEMESURES IMAGE HRVIR ET VEGETATION DE SPOT 4]

M. Grondin 16 Oct. 1987 35 p In FRENCH; ENGLISH summary

(CNES-87/229/CT/DRT/TIT/TR; ETN-88-93091) Avail: NTIS HC A03/MF A01

Multiplexing of HRVIR and Vegetation sensor data from SPOT 4 so as to use only 1 transmit antenna (8200 to 8310 MHz) and so as to maintain compatibility with existing SPOT ground stations is discussed. Degradations introduced by the presence onboard of an OMUX frequency multiplexer are considered. Results of software simulations of the telemetry link in terms of bit error rate degradations and carrier to interference ratios are presented. The simulations show that with the OMUX, acceptable multiplexing is achieved. For HRVIR predetection stations the present filter should be replaced by a three pole Butterworth filter. ESA

18 SPACECRAFT DESIGN, TESTING AND PERFORMANCE

Includes satellites; space platforms; space stations; spacecraft systems and components such as thermal and environmental controls; and attitude controls.

For life support systems see *54 Man/System Technology and Life Support.* For related information see also *05 Aircraft Design, Testing and Performance, 39 Structural Mechanics,* and *16 Space Transportation.*

N89-10931*# Jet Propulsion Lab., California Inst. of Tech., Pasadena.
SPACE SCIENCE/SPACE STATION ATTACHED PAYLOAD POINTING ACCOMMODATION STUDY: TECHNOLOGY ASSESSMENT WHITE PAPER
Richard Y. Lin, Kenneth E. Mann, Robert A. Laskin, and Samuel W. Sirlin 15 Dec. 1987 82 p
(Contract NAS7-918)
(NASA-CR-182735; NAS 1.26:182735; JPL-Publ-87-43) Avail: NTIS HC A05/MF A01 CSCL 22B

Technology assessment is performed for pointing systems that accommodate payloads of large mass and large dimensions. Related technology areas are also examined. These related areas include active thermal lines or power cables across gimbals, new materials for increased passive damping, tethered pointing, and inertially reacting pointing systems. Conclusions, issues and concerns, and recommendations regarding the status and development of large pointing systems for space applications are made based on the performed assessments. Author

N89-10932# Los Alamos National Lab., N. Mex.
LABORATORY INVESTIGATIONS OF LOW EARTH ORBIT ENVIRONMENTAL EFFECTS ON SPACECRAFT
Jon B. Cross 1988 16 p Presented at the Uranium and Electricity: the Complete Nuclear Fuel Cycle, Saskatoon, Saskatchewan, 18 Sep. 1988
(Contract W-7405-eng-36)
(DE88-009135; LA-UR-88-1229; CONF-880943-2) Avail: NTIS HC A03/MF A01

Operations in low earth orbit (100 to 500 km) must take into consideration the highly oxidative character of the environment. Partial pressures in the range of 10 to the 6th - 10 to the 7th torr of atomic oxygen are present which produces extensive oxidation of materials facing the direction of travel (ram direction). The ram oxidation is most severe not only because of the high flux (10 to the 15th O-atoms/s-sq cm) caused by the orbital velocity of the spacecraft but also because of the high collision energy of oxygen atoms with the ram surfaces (translational energy equivalent to approximately 60,000 K). Ground based simulation of these conditions has been accomplished using a CW laser sustained discharge source for the production of 1 to 5 eV beam of O-atoms with a flux of up to 10 to the 17th O-atoms/s-sq cm. The reactions of atomic oxygen with kapton, Teflon, silver, and various coatings have been studied. The oxidation of kapton has an activation energy of 2.3 Kcal/mole over the temperature range of 25 C to 100 C at a beam energy of 1.5 eV and produces low molecular weight gas phase reaction products (H_2O, NO, CO_2). Teflon reacts with approximately 0.1 to 0.2 efficiency to that of kapton at 25 C and both surfaces show a rug like texture after exposure to the O-atom beam. Angular scattering distribution measurements of O-atoms show a near cosine distribution from reactive surfaces indicating complete accommodation of the translational energy with the surface while a nonreactive surface (nickel oxide) shows specular like scattering with little accommodation (50 percent) of the translational energy with the surface. A technique for simple on orbit chemical experiments using resistance measurements coated silver strips is described. DOE

N89-10933# Oak Ridge National Lab., Tenn.
PHASE CHANGE PROBLEM RELATED TO THERMAL ENERGY STORAGE IN THE MANNED SPACE STATION
D. G. Wilson, J. B. Drake, and R. E. Flanery 1988 3 p Presented at the Institute for Mathematics and Its Applications Seminar, Minneapolis, Minn., 23 Feb. 1988
(Contract DE-AC05-84OR-21400)
(DE88-011390; CONF-880282-1) Avail: NTIS HC A02/MF A01

The system discussed consists of a solar collector lined with small metal canisters filled with a high temperature phase change material (PCM), lithium fluoride salt. The canisters are small enough to fit comfortably in the palm of one's hand and there are a hundred or more of them. A heat transfer fluid, an inert gas such as helium or neon, circulates through the pipes that pass through the metal canisters and carries heat away to turbines, generators, etc. The continual melting and refreezing of the PCM smears out the delivery of the solar energy to the transfer fluid, and hence, to the heat engines beyond. The motivation for using a PCM based thermal energy storage system is that a properly sized such system can store and deliver energy over a narrow temperature range near the melting point of the PCM, thus avoiding extreme temperature variations. DOE

N89-10934*# Control Dynamics Co., Huntsville, Ala.
TETHER APPLICATIONS Interim Report
Nov. 1986 94 p
(Contract NAS8-35835)
(NASA-CR-179392; NAS 1.26:179392) Avail: NTIS HC A05/MF A01 CSCL 22B

For a range of tether lengths, end masses, and orbits, tether deployment concepts were defined and/or analyzed from the Orbiter for steady state/dynamic and up/down deployments and from circular/elliptical orbits. Orbits were defined and/or analyzed for end mass releasing concepts with steady state and dynamic releases taking into account tether and end mass motion before and after release. For a range of tether lengths, end masses, and orbits, tether retrieving or disposing concepts were defined and/or analyzed for both reusable and disposable tethers. Tether programs were installed or updated on the MSFC VAX 11/780 computer. Author

N89-10935# Aerospace Corp., El Segundo, Calif. Space Sciences Lab.
VERIFICATION OF SINGLE EVENT UPSET RATE ESTIMATION METHODS WITH ON-ORBIT OBSERVATIONS
M. Shoga, P. Adams, D. L. Chenette, R. Kioga, and E. C. Smith (TRW, Inc., Redondo Beach, Calif.) 20 Jun. 1988 27 p Previously announced in IAA as A88-25385
(Contract F04701-85-C-0086)
(AD-A196226; TR-0086A(2940-05)-7; SD-TR-88-68) Avail: NTIS HC A03/MF A01 CSCL 20C

In an experiment aboard three Leasat vehicles at geosynchronous orbit, single event upsets (SEU) have been continuously monitored in a memory consisting of 93L422 RAMs. Using simultaneous measurements of the high energy galactic cosmic ray and solar flare particle environment from the experiments aboard the IMP-8 satellite, together with at Leasat mass distribution model and ground test measurements of the SEU susceptibility for the 93L422, accurate estimates of the SEU rate are calculated based on several improvements to the standard methods. These results are discussed and compared to the Leasat flight observations. GRA

N89-10936*# General Dynamics Corp., San Diego, Calif. Space Systems Div.
DEVELOPMENT OF A VERIFICATION PROGRAM FOR DEPLOYABLE TRUSS ADVANCED TECHNOLOGY Final Report
Jack E. Dyer Sep. 1988 161 p
(Contract NAS1-18274)
(NASA-CR-181703; NAS 1.26:181703) Avail: NTIS HC A08/MF A01 CSCL 22B

Use of large deployable space structures to satisfy the growth demands of space systems is contingent upon reducing the associated risks that pervade many related technical disciplines. The overall objectives of this program was to develop a detailed plan to verify deployable truss advanced technology applicable to

future large space structures and to develop a preliminary design of a deployable truss reflector/beam structure for use a a technology demonstration test article. The planning is based on a Shuttle flight experiment program using deployable 5 and 15 meter aperture tetrahedral truss reflections and a 20 m long deployable truss beam structure. The plan addresses validation of analytical methods, the degree to which ground testing adequately simulates flight and in-space testing requirements for large precision antenna designs. Based on an assessment of future NASA and DOD space system requirements, the program was developed to verify four critical technology areas: deployment, shape accuracy and control, pointing and alignment, and articulation and maneuvers. The flight experiment technology verification objectives can be met using two shuttle flights with the total experiment integrated on a single Shuttle Test Experiment Platform (STEP) and a Mission Peculiar Experiment Support Structure (MPESS). First flight of the experiment can be achieved 60 months after go-ahead with a total program duration of 90 months. Author

N89-10937# Physical Sciences, Inc., Andover, Mass.
THE DETERMINATION OF THE SPACECRAFT CONTAMINATION ENVIRONMENT Final Report, 12 Sep. 1983 - 28 Feb. 1987
B. D. Green, W. T. Rawlins, G. E. Caledonia, W. J. Marinelli, and C. White Oct. 1987 384 p
(Contract F19628-83-C-0139)
(AD-A196435; PSI-9139/TR-728; AFGL-TR-87-0303) Avail: NTIS HC A17/MF A01 CSCL 03B

This report details our efforts in the determination of the on-orbit environment surrounding spacecraft. The research was performed for the Spacecraft Interactions Branch of the Space Physics Division of the Air Force Geophysics Laboratory. This report includes contributions from our subcontractors EKTRON Applied Imaging and Miranda Laboratories. The multilayer project consisted of three major tasks: a literature survey, preparation for the data of the Particle Analysis Cameras for Shuttle (PACS), and the analysis of the data to create a model of the orbital particulate environment. During the literature search we discovered that many observations were presented with little or no insight provided. Physical Sciences Inc. (PSI) therefore undertook a critical review of the data in an attempt to reconcile seemingly contractory observations and provide needed understanding of the variety of unexpected processes occurring above spacecraft surfaces in low-earth orbit. We were able to make contributions to the understanding of the neutral molecular contamination cloud; the modifications of the ionic environment; the optical contamination glow; and the earlier observations of particulates. GRA

N89-10938# Panametrics, Inc., Waltham, Mass.
FABRICATE, CALIBRATE AND TEST A DOSIMETER FOR INTEGRATION INTO THE CRRES (COMBINED RELEASE AND RADIATION EFFECTS SATELLITE) SATELLITE
Paul R. Morel, Frederick A. Hanser, Bach Sellers, Ram Cohen, and Brian D. Kane Mar. 1988 37 p
(Contracts F19628-82-C-0090; F19628-78-C-0247; F19628-79-C-0175)
(AD-A196496; AFGL-TR-88-0066; SR-5) Avail: NTIS HC A03/MF A01 CSCL 22B

A Space Radiation Dosimeter has been fabricated, calibrated, tested, and has undergone successful integration testing in the CRRES spacecraft. This Dosimeter is essentially identical to that previously designed, fabricated, calibrated, tested and integrated into the DMSP F7 satellite. These dosimeters are primarily designed to measure the dose from electrons of greater than 1 MeV to greater than 10 MeV in four channels. Each channel has a different thickness aluminum dome. GRA

N89-10939# Naval Postgraduate School, Monterey, Calif.
ION GUN OPERATIONS AT HIGH ALTITUDES M.S. Thesis
Paul W. Werner Jun. 1988 98 p
(AD-A196965) Avail: NTIS HC A05/MF A01 CSCL 22A

Experiments in charge control were conducted on the P78-2 (SCATHA) satellite as part of a program on spacecraft charging at high altitudes. Experiments with the SCATHA ion gun were monitored by charged particle detectors and the electric field experiment, which was found to enable measurement of satellite potential during ion beam emission in sunlight and eclipse. Unneutralized ion beam emission in high energy (1 to 2 KeV) and high current (1 to 2 mA) modes resulted in the satellite momentarily charging to a negative potential near the magnitude of the beam voltage and then rising to some less negative value, typically -500 to -800 v. The net emitted current was apparently limited by the formation of a virtual anode. Low current (20 to 30 microamp), high voltage (1 kV) resulted in -10 to -50 V satellite potentials. Trickle mode (20 to 80 microamp, no accel voltage) operations resulted in satellite potentials near zero volts. In sunlight the spacecraft potential exhibited a spin modulation, attributed to variations in the neutralization of the beam as it passed through the photoelectron cloud. Rapid fluctuations of the spacecraft potential occurred which may be explained qualitatively by space charge instabilities. GRA

N89-10940# Naval Postgraduate School, Monterey, Calif.
IONS GENERATED ON OR NEAR SATELLITE SURFACES M.S. Thesis
Christopher W. Norwood Jun. 1988 131 p
(AD-A196966) Avail: NTIS HC A07/MF A01 CSCL 22A

Observations of positively charged particles that are generated on or near satellite surfaces have been made on several spacecraft. This thesis postulates sputtering of the satellite surface due to ambient ion impact as the generating mechanism. Calculations are made using the Sigmund-Thompson sputtering theory to determine the response at the satellite particle detectors. These calculations indicate that surface sputtering creates a sufficient flux to account for the observed phenomena. The NASA Charging Analyzer program was run to determine the trajectories for measured particles. The calculated trajectories were determined to lead to the spacecraft surface, again indicating that surface emission was the source. The sputtering flux as calculated was insufficient to cause any significant short-term damage to the spacecraft, beyond thin coating erosion. GRA

N89-10914*# National Aeronautics and Space Administration. Goddard Space Flight Center, Greenbelt, Md.
UTILIZATION OF SPRAY ON FOAM INSULATION FOR MANNED AND UNMANNED SPACECRAFT AND STRUCTURES
Thomas M. Hancock, III *In its* The 1988 Get Away Special Experimenter's Symposium Sep. 1988 p 81 (For primary document see N89-10902 02-12)
Avail: NTIS HC A07/MF A01 CSCL 22B

N89-11066# Joint Publications Research Service, Arlington, Va.
PAYLOAD BOOMERANG TECHNOLOGY DESCRIBED
Akira Onchi *In its* JPRS Report: Science and Technology: Japan 4 Jun. 1987 p 21-23 Transl. into ENGLISH from Kogiken Nyusu (Toyko, Japan), Sep. 1986 p 1-2 (For primary document see N89-11061 02-31)
Avail: NTIS HC A05/MF A01

19 SPACECRAFT INSTRUMENTATION

For related information see also *06 Aircraft Instrumentation* and *35 Instrumentation and Photography.*

No abstracts in this category.

20 SPACECRAFT PROPULSION AND POWER

Includes main propulsion systems and components, e.g., rocket engines; and spacecraft auxilliary power sources.

For related information see also *07 Aircraft Propulsion and Power, 28 Propellants and Fuels, 44 Energy Production and Conversion,* and *15 Launch Vehicles and Space Vehicles.*

N89-10941*# Jet Propulsion Lab., California Inst. of Tech., Pasadena.
THE STATE-OF-THE-ART OF dc POWER DISTRIBUTION SYSTEMS/COMPONENTS FOR SPACE APPLICATIONS
S. Krauthamer Jul. 1988 92 p
(Contract NAS7-918)
(NASA-CR-182743; NAS 1.26:182743; JPL-Publ-88-26) Avail: NTIS HC A05/MF A01 CSCL 10B

This report is a survey of the state of the art of high voltage dc systems and components. This information can be used for consideration of an alternative secondary distribution (120 Vdc) system for the Space Station. All HVdc components have been prototyped or developed for terrestrial, aircraft, and spacecraft applications, and are applicable for general space application with appropriate modification and qualification. HVdc systems offer a safe, reliable, low mass, high efficiency and low EMI alternative for Space Station secondary distribution. Author

N89-10942# Air Force Engineering and Services Center, Tyndall AFB, Fla. Environics Div.
HCl MEASUREMENTS IN SPACE VEHICLE EXHAUST CLOUDS
M. D. Smith, T. McRae, R. Kennedy, D. Garvis, T. Kulp, L. S. Berstein, F. Bien, W. Cheng, R. P. Domingue, and S. C. Richtmeier (Spectral Sciences, Inc., Burlington, Mass.) 1988 11 p Presented at the JANNAF Safety and Environmental Protection Subcommittee Meeting, Monterey, Calif., 23 May 1988
(Contract W-7405-eng-48)
(DE88-013815; UCRL-98893; CONF-8805173-1) Avail: NTIS HC A03/MF A01

The United States Space Program requires the use of large launch vehicles like the space shuttle, Titan 34D, Titan IV, and the proposed heavy-lift vehicle. These large launch systems utilize solid rocket motors to place heavy payloads into orbit. However, most solid rocket motors utilize ammonium perchlorate as an oxidizer and release an exhaust cloud, which is a dynamic mixture of water, hydrogen chloride, aluminum oxide, and aluminum chloride. Described in this presentation are two infrared monitors which are designed for HCl field measurements. One monitor, developed by Lawrence Livermore National Laboratory (LLNL), measures gaseous HCl and accounts for the presence of water and methane that absorb at the HCl wavelength. A detection limit of 0.2 ppM has been demonstrated. The second monitor, developed by Spectral Sciences, Inc., uses a unique HCl lamp which is free of interferences associated with conventional black body radiation sources. By combining the lamp with simple optics, a detection limit of 0.1 ppM has been obtained. Since much of the HCl in the ground cloud is entrained in small water droplets and the infrared technique measures only gaseous HCl, a method was required to account for aqueous HCl. The Spectral Sciences monitor features a preheater which vaporizes aerosols in the input gas stream so that total HCl can be measured. For both monitors, instrument design and operation are described in detail. DOE

N89-10943*# Page (R. J.) Co., Santa Ana, Calif.
PRELIMINARY DESIGN STUDY OF HYDROGEN AND AMMONIA RESISTOJETS FOR PRIME AND AUXILIARY THRUSTERS Final Report
Russell J. Page, Willis A. Stoner, and Larry Barker Oct. 1988 49 p
(Contract NAS3-23337)
(NASA-CR-182176; NAS 1.26:182176) Avail: NTIS HC A03/MF A01 CSCL 21H

Designs of high performance resistojets for primary and auxiliary propulsion are described.Thruster power for the primary propulsion application was in the 2 to 3 kW range while auxiliary propulsion power per thruster was 0.15 to 0.25 kW. Propellants considered were hydrogen and ammonia. The report described design techniques used to forecast the temperature and energy flux distributions using mathematical modeling by personal microcomputer. BASIC language is used throughout to give the designer rapid interaction and control. Both designs integrate compact first stage coils with concentric tubular heaters. The hybrid heater design allows better thruster power matching with the spacecraft power bus. Projected specific impulse levels were 760 to 830 s for hydrogen and 380 to 410 s for ammonia. Author

N89-10944*# National Aeronautics and Space Administration. Lewis Research Center, Cleveland, Ohio.
NUCLEAR PROPULSION: A VITAL TECHNOLOGY FOR THE EXPLORATION OF MARS AND THE PLANETS BEYOND
Stanley K. Borowski 1988 47 p Presented in the Case for Mars 3, Boulder, Colo., 18-22 Jul. 1987; sponsored in part by American Astronautical Society, JPL, Los Alamos Lab., NASA Ames Research Center, NASA Johnson Space Center, NASA Marshall Space Flight Center, and Planetary Socie
(NASA-TM-101354; E-4369; NAS 1.15:101354) Avail: NTIS HC A03/MF A01 CSCL 21F

The physics and technology issues and performance potential of various direct thrust fission and fusion propulsion concepts are examined. Next to chemical propulsion the solid core fission thermal rocket (SCR) is the olny other concept to be experimentally tested at the power (approx 1.5 to 5.0 GW) and thrust levels (approx 0.33 to 1.11 MN) required for manned Mars missions. With a specific impulse of approx 850 s, the SCR can perform various near-Earth, cislunar and interplanetary missions with lower mass and cost requirements than its chemical counterpart. The gas core fission thermal rocket, with a specific power and impulse of approx 50 kW/kg and 5000 s offers the potential for quick courier trips to Mars (of about 80 days) or longer duration exploration cargo missions (lasting about 280 days) with starting masses of about 1000 m tons. Convenient transportation to the outer Solar System will require the development of magnetic and inertial fusion rockets (IFRs). Possessing specific powers and impulses of approx 100 kW/kg and 200-300 kilosecs, IFRs will usher in the era of the true Solar System class speceship. Even Pluto will be accessible with roundtrip times of less than 2 years and starting masses of about 1500 m tons. Author

23 CHEMISTRY AND MATERIALS (GENERAL)

No abstracts in this category.

24 COMPOSITE MATERIALS

Includes physical, chemical, and mechanical properties of laminates and other composite materials.

For ceramic materials see *27 Nonmetallic Materials.*

N89-10945*# National Aeronautics and Space Administration. Langley Research Center, Hampton, Va.
A MIXED-MODE BENDING APPARATUS FOR DELAMINATION TESTING
John H. Crews, Jr. and James R. Reeder Aug. 1988 40 p
(NASA-TM-100662; NAS 1.15:100662) Avail: NTIS HC A03/MF A01 CSCL 11D

A mixed-mode delamination test procedure was developed combining double cantilever beam mode I loading and end notch flexure mode II loading on a split unidirectional laminate. By loading

the specimen with a lever, a single applied load simultaneously produces mode I and II bending loads on the specimen. This mixed mode bending (MMB) test was analyzed using both finite element procedures and beam theory to calculate the mode I and II components of strain energy release rate, G sub I and G sub II, respectively. The analyses showed that a wide range of G sub I/G sub II ratios could be produced by varying the applied load position on the loading lever. As the delamination extended, the G sub I/G sub II ratios varied by less than 5 percent. The simple beam theory equations were modified to account for the elastic interaction between the two arms of the specimen and to account for shear deformations. The resulting equations agreed closely with the finite element results and provide a basis for selection of G sub I/G sub II test ratios and a basis for computing the mode I and II components of measured delamination toughness. The MMB specimen analysis and test procedures were demonstrated using unidirectional laminates. Author

N89-10946*# Rensselaer Polytechnic Inst., Troy, N.Y.
COMPOSITE STRUCTURAL MATERIALS Annual Progress Report No. 51, 1 May 1987 - 30 Apr. 1988
Robert G. Loewy and Stephen E. Wiberley Aug. 1988 97 p Sponsored in part by AF
(Grant NGL-33-018-003)
(NASA-CR-180224; NAS 1.26:180224) Avail: NTIS HC A05/MF A01 CSCL 11D

A decade long program to develop critical advanced composite technology in the areas of physical properties, structural concept and analysis, manufacturing, reliability, and life predictions is reviewed. Specific goals are discussed. The status of the chemical vapor deposition effects on carbon fiber properties; inelastic deformation of metal matrix laminates; fatigue damage in fibrous MMC laminates; delamination fracture toughness in thermoplastic matrix composites; and numerical analysis of composite micromechanical behavior are presented. B.G.

N89-10947# Auburn Univ., Ala.
PLASMA EXPOSURE TESTS OF A CARBON FIBER/EPOXY COMPOSITE
R. Popple, C. Bush, R. F. Gandy, M. A. Henderson, T. Schneider, and J. Rome (Oak Ridge National Lab., Tenn.) Jul. 1988 6 p
(Contracts DE-FG05-85ER-53192; DE-AC05-84OR-21400)
(DE88-014724; DOE/ER-53192/T3) Avail: NTIS HC A02/MF A01

An experiment was conducted to test the exposure of a vacuum chamber made of a carbon fiber/epoxy composite to a plasma environment. In previous tests this material (CE 339, made by Ferro Corp.) has shown good vacuum properties and has also demonstrated the capability to withstand high energy electron beams in tests at the Naval Research Laboratory. Based on these promising results, the Torsatron Group at Auburn University conducted plasma exposure tests on a section of carbon fiber/epoxy composite pipe furnished by Oak Ridge National Laboratory. DOE

N89-10948# Sandia National Labs., Albuquerque, N. Mex.
ELECTRICALLY CONDUCTIVE RETICULATED CARBON COMPOSITES
A. P. Sylwester and R. L. Clough 1988 8 p Presented at the International Conference on Science and Technology of Synthetic Metals, Santa Fe, N., Mex., 26 Jun. 1988
(Contract DE-AC04-76DP-00789)
(DE88-012856; SAND-88-1784C; CONF-880669-4) Avail: NTIS HC A02/MF A01

This paper reports a new type of electrically conductive composite which offers advantageous properties and controlled processing. These new composites consist of a conductive open-celled, low-density, microcellular, carbonized foam filled with a nonconductive polymer or resin. The open-celled nature of the carbon foam provides a porous three-dimensional reticulated carbon structure. The large continuous-void volume can be readily filled with an insulating polymer or resin resulting in a three-dimensional conductive composite material. DOE

N89-10949# Lawrence Livermore National Lab., Calif.
A NOVEL APPROACH TO ABRASION RESISTANCE
W. A. Steele, P. B. Mohr, H. R. Leider, and T. B. Hirschfeld Mar. 1988 12 p Presented at IECEC '88, Denver, Colo., 1 Aug. 1988
(Contract W-7405-eng-48)
(DE88-014180; UCRL-98343; CONF-880885-2) Avail: NTIS HC A03/MF A01

The high abrasion and impact loads characteristic of many technologies require frequent maintenance or special materials. Conventional approaches to protection have used either extremely hard coatings or complaint elastomeric coatings. The former are typically ceramic or ceramic-like surfaces produced by direct deposition or by in situ formation by oxidation, carburization or nitriding. Ceramic coatings are very good against abrasion, but are vulnerable to impact damage. Elastomeric coatings have excellent impact resistance and are capable of withstanding deformation; however, they are limited in thermal range and chemical resistance. It is possible to combine the desirable properties of both types by using hair, a structure in which an extremely hard material can be simultaneously elastic and compliant by virture of a very high L/D ratio. We have demonstrated the good performance of carbon fiber hair in resisting damage from impacting particles and have identified a probable failure mechanism. DOE

N89-10950# Sandia National Labs., Albuquerque, N. Mex.
CARBON FILMS DERIVED FROM POLY(ACRYLONITRILE): OXIDATION, ELECTRICAL PROPERTIES, AND PROCESSING
C. L. Renschler and L. V. Salgado 1988 8 p Presented at the 196th American Chemical Society National Meeting, Los Angeles, Calif. 25 Sep. 1988
(Contract DE-AC04-76DP-00789)
(DE88-010352; SAND-88-1347C; CONF-880912-4) Avail: NTIS HC A02/MF A01

Carbon films made by pyrolytic decomposition of PAN poly(acrylontrile) can be made with controlled electrical conductivity by varying the final temperature of pyrolysis. Further, the conductivity is a function of precursor structure, with lower PAN content yielding lower conductivity. The gas phase oxidation proceeds through an intermediate surface oxidation, with an activation energy of ca. 33 kcal/mol. Films made in this way can be patterned using photolithography and oxygen etching; transfer of films from one substrate to another is accomplished with either dry or wet transfer techniques. DOE

N89-10951*# National Aeronautics and Space Administration. Langley Research Center, Hampton, Va.
TENSION FATIGUE ANALYSIS AND LIFE PREDICTION FOR COMPOSITE LAMINATES
T. K. OBrien, M. Rigamonti, and C. Zanotti (Costruzioni Aeronautiche Giovanni Agusta S.p.A., Gallarate, Italy) Oct. 1988 55 p
(NASA-TM-100549; NAS 1.15:100549; AVSCOM-TM-88-B-015)
Avail: NTIS HC A04/MF A01 CSCL 11D

A tension fatigue life prediction methodology for composite laminates is presented. Tension fatigue tests were conducted on quasi-isotropic and orthotropic glass epoxy, graphite epoxy, and glass/graphite epoxy hybrid laminates. Edge delamination onset data were used to generate plots of strain energy release rate as a function of cycles to delamination onset. These plots were then used along with strain energy release rate analyses of delaminations initiating at matrix cracks to predict local delamination onset. Stiffness loss was measured experimentally to account for the accumulation of matrix cracks and for delamination growth. Fatigue failure was predicted by comparing the increase in global strain resulting from stiffness loss to the decrease in laminate failure strain resulting from delaminations forming at matrix cracks through the laminate thickness. Good agreement between measured and predicted lives indicated that the through-thickness damage accumulation model can accurately describe fatigue failure for laminates where the delamination onset behavior in fatigue is

well characterized, and stiffness loss can be monitored in real time to account for damage growth. Author

N89-10952*# National Aeronautics and Space Administration. Lewis Research Center, Cleveland, Ohio.
LAMINATE BEHAVIOR FOR SiC FIBER-REINFORCED REACTION-BONDED SILICON NITRIDE MATRIX COMPOSITES
R. T. Rhatt and R. E. Phillips (Sverdrup Technology, Inc., Cleveland, Ohio.) Oct. 1988 40 p
(NASA-TM-101350; E-4377; NAS 1.15:101350; AVSCOM-TR-88-C-30) Avail: NTIS HC A03/MF A01 CSCL 11D

The room temperature mechanical properties of SiC fiber reinforced reaction-bonded silicon nitride matrix composite laminates (SiC/RBSN) have been measured. The laminates contained approx 30 volume fraction of aligned 142-micron diameter SiC fiber in a porous RBSN matrix. Three types of laminate studied were unidirectional: (1) (0) sub 8, (2) (10) sub 8, and (3) (45) sub 8, and (90) sub 8; cross plied laminates (0 sub 2/90 sub 2); and angle plied laminates: (+45 sub 2/-45 sub 2). Each laminate contained eight fiber plies. Results of the unidirectionally reinforced composites tested at various angles to the reinforcement direction indicate large anisotropy in in-plane properties. In addition, strength properties of these composites along the fiber direction were independent of specimen gage length and were unaffected by notches normal to the fiber direction. Splitting parallel to the fiber at the notch tip appears to be the dominant crack blunting mechanism responsible for notch insensitive behavior of these composites. In-plane properties of the composites can be improved by 2-D laminate construction. Mechanical property results for (0 sub 2/90 sub 2)sub s and (+45/-45 sub 2) sub s laminates showed that their matrix failure strains were similar to that for (0) sub 8 laminates, but their primary elastic moduli, matrix cracking strengths, and ultimate composite strengths were lower. The elastic properties of unidirectional, cross-ply, and angle-ply composites can be predicted from modified constitutive equations and laminate theory. Further improvements in laminate properties may be achieved by reducing the matrix porosity and by optimizing the bond strength between the SiC fiber and RBSN matrix. Author

N89-10953# Office National d'Etudes et de Recherches Aerospatiales, Paris (France). Direction Scientifique de la Resistance des Structures.
INVESTIGATIONS IN THE NONLINEAR DOMAIN OF COMPOSITE LAMINATE PLATES SUBJECT TO COMPRESSION LOADS Final Report [ETUDES, DANS LE DOMAINE NON LINEAIRE, DES PLAQUES COMPOSITES STRATIFIEES SOUMISES A UN CHARGEMENT DE COMPRESSION]
R. Girard and D. Louis Dec. 1987 40 p In FRENCH
(Contract DRET-87-34-001)
(ONERA-RT-17/3542-RY-070-R; ETN-88-93098) Avail: NTIS HC A03/MF A01

A flat finite element was developed and tested on multilayer panels subject to large displacements. The element was developed in the framework of a macroelement formulation for modeling composite stiffened panels, to study buckling and postbuckling problems of structures under compression loads. A program to calculate internal forces and tangential rigidity matrices was derived. It is needed to solve the nonlinear problem numerically by a Newton type iterative method. Tests show the usefulness of the element in inserting data into finite element grids, but it cannot be used to model shells because of excessive rigidity. ESA

N89-10954# Office National d'Etudes et de Recherches Aerospatiales, Paris (France). Division Scientifique de la Resistance des Structures.
NONLINEAR THEORIES OF COMPOSITE LAMINATES UNDER COMPRESSION WITH DELAMINATION Final Report [THEORIES NON LINEAIRES DES STRATIFIES COMPOSITES EN COMPRESSION AVEC DELAMINAGE]
D. GilettadeSaintJoseph Jan. 1988 35 p In FRENCH
(Contract DRET-84-34-001)
(CERT-RT-18/3542-RY-071-R; ETN-88-93099) Avail: NTIS HC A03/MF A01

Propagation of delamination through local buckling in a multilayer composite plate subject to compression was studied. The search for delamination propagation criteria is based on the notion of energy release rate. The methodology for calculating this quantity was included in a finite element method. The calculation can be carried out in the nonlinear domain (geometrical or physical) of material behavior. Test results show the accuracy of the method. ESA

N89-10955# Societe Nationale des Poudres et Explosifs, Vert-Le-Petit (France).
POLYSTYRYLPYRIDINE (PSP) RESIN-BASED SHORT-FIBER COMPOSITES (INJECTABLE COMPOUNDS) [ETUDE DE COMPOSITES A FIBRES COURTES (COMPOUNDS INJECTABLES) A BASE DE PSP]
Jean-Gabriel Maquart and Dominique Baroncini 9 Dec. 1987 59 p In FRENCH
(Contracts DRET-84-34-302; BC-85-302-21)
(Rept-NT-195/87/CRB/GTR.C/NP; ETN-88-93102) Avail: NTIS HC A04/MF A01

Compounds composed of short carbon fibers and PSP resin for thermostable injectable pieces were developed. After regulation of fiber ratio and viscosity, mold time is reduced to 6 to 10 min at 350 C. Thermomechanical performance is high. Results at 300 C in plasma torch and smoke density tests are superior to those of phenol based compounds. ESA

N89-10956# Deutsche Forschungs- und Versuchsanstalt fuer Luft- und Raumfahrt, Brunswick (West Germany). Abteilung Strukturberechnung.
PRIMEL: A PREPROCESSOR FOR THE ANALYSIS OF LAMINATED COMPOSITES. INTRODUCTION AND USER'S GUIDE (OPERATION SYSTEM OS/VS2 (MVS))
Bodo Geier and Ursula Renken Mar. 1988 47 p In GERMAN; ENGLISH summary
(DFVLR-Mitt-88-14; ISSN-0176-7739; ETN-88-93182) Avail: NTIS HC A03/MF A01; DFVLR, VB-PL-DO, 90 60 58, 5000 Cologne, Federal Republic of Germany, 17.50 deutsche marks

A dialog-oriented computer program providing the relevant data required for mechanical and/or thermomechanical analysis of laminated composite structures is presented. Its scope and how to use the program are explained. The formulas evaluated are presented. ESA

N89-10957# Societe Nationale Industrielle Aerospatiale, Suresnes (France). Direction Centrale de la Qualite.
INFLUENCE OF SPECIMEN DIMENSION ON DAMAGE AND BREAKING OF COMPOSITE MATERIALS [INFLUENCE DES DIMENSIONS D'EPROUVETTES SUR L'ENDOMMAGEMENT ET LA RUPTURE DES MATERIAUX COMPOSITES]
D. Lang 29 Mar. 1988 84 p In FRENCH
(Contract STPA-86-96-015-00-471-75-86)
(Rept-49-062/F; ETN-88-93317) Avail: NTIS HC A05/MF A01

The influence of the length of carbon fiber/epoxy resin specimens (25 to 100 mm) on tensile strength and the damage threshold is investigated. Different types of assemblies, with and without holes were studied. No influence of the specimen length on strength or damage threshold is observed. On the other hand, the initiation of transversal cracks and delamination vary strongly with the type of assembly and type of material employed. ESA

N89-10958# Texas Univ., Austin. Dept. of Chemistry.
NOVEL COMPOSITE MATERIALS: ALLOYS FROM IMMISCIBLE COMPONENTS Final Report, 1 Apr. 1987 - 31 Mar. 1988
Josef Michl 17 Jun. 1988 7 p
(Contract DAAL03-87-K-0055)
(AD-A197040; ARO-24449.4-CH) Avail: NTIS HC A02/MF A01 CSCL 11D

The ultrahigh-vacuum deposition chamber permits deposition of solid matrices under clean conditions onto a plate held at 20 K. As hoped for, the use of a clean environment and of very low deposition temperatures permitted the investigator to accomplish the primary objective of the research, single molecule isolation of dopants in an alkali halide matrix. Previously, it was only possible to obtain alkali halide matrices containing aggregated dopants. This breakthrough opens new vistas in matrix isolation spectroscopy, photochemistry, and chemistry. GRA

N89-11003# Joint Publications Research Service, Arlington, Va.
METHODOLOGY OF FLEXURAL FATIGUE TESTING COMPOSITE MATERIALS PRODUCED BY ELECTRON-BEAM EVAPORATION Abstract Only
Yu. F. Lugovskiy *In its* JPRS Report: Science and Technology. USSR: Materials Science 4 Apr. 1988 p 1 Transl. into ENGLISH from Problemy Spetsialnoy Elektrometallurgii (Kiev, USSR), no. 4, Oct. - Dec. 1987 p 61-65 (For primary document see N89-11002 02-26)
Avail: NTIS HC A03/MF A01

25 INORGANIC AND PHYSICAL CHEMISTRY

Includes chemical analysis, e.g., chromatography; combustion theory; electrochemistry; and photochemistry.

For related information see also *77 Thermodynamics and Statistical Physics.*.

N89-10959# Minnesota Univ., Minneapolis. Dept. of Chemistry.
VARIATIONAL TRANSITION STATE THEORY Progress Report
Donald G. Truhlar 1 Mar. 1988 4 p
(Contract DE-FG02-86ER-13579)
(DE88-013756; DOE/ER-13579/20) Avail: NTIS HC A02/MF A01

This project is concerned with the development and applications of generalized transition state theory and multidimensional tunneling approximations to chemical reaction rates. We have developed and implemented several practical versions of variational transition state theory (VTST), namely, canonical variational theory (CVT), improved canonical variational theory (ICVT), and microcanonical variational theory (MCVT). We have also developed and implemented several accurate multidimensional semiclassical tunneling approximations, the most accurate of which are the small-curvature semiclassical adiabatic (SCSA), large-curvature version 3 (LC3), and least-action (LA) approximations. We have applied the methods to thermal rate constants, using transmission coefficients based on ground state tunneling and we have also presented and applied adiabatic and diabatic extensions to calculate rate constants for vibrationally excited reactants. Our general goal is to develop accurate methods for calculating chemical reaction rate constants that remain practical even for reasonably complicated molecules. The approximations mentioned above yield rate constants for systems whose potential energy surface is known or assumed. DOE

N89-10960# California Univ., Berkeley. Lawrence Berkeley Lab. Applied Sciences Div.
REACTION RATES IN PREMIXED TURBULENT FLAMES AND THEIR RELEVANCE TO THE TURBULENT BURNING SPEED
R. K. Cheng, I. G. Shepherd, and L. Talbot Dec. 1987 21 p Presented at the 22nd International Symposium on Combustion, Seattle, Wash., 14 Aug. 1988
(Contract DE-AC03-76SF-00098)
(DE88-012021; LBL-25230; CONF-880802-8) Avail: NTIS HC A03/MF A01

An experimental procedure to measure the local reaction rate, bar w, in premixed turbulent flames is presented. It utilizes the flame crossing frequency sub-model for the reaction rate formulated by Bray-Champion-Libby (BCL) for turbulent flames with unstrained or equally strained flamelets. The experiments involve measuring the flame crossing frequencies and the conditioned mean velocity of two components using respectively Mie scattering and two color LDA techniques. A method of analysis has also been developed to deduce the turbulent burning speed from bar w. The turbulent/laminar burning speed ratio is obtained by integrating the reaction rates measured along 2D mean Lagrangian flowlines through the flame brush. The flowlines are traced automatically using feedback control for positioning the LDA probe. The method has been applied to study five v-flames and four large Bunsen type conical flames. The distributions of bar w are well predicted by the BCL model. The turbulent flame speed results based on bar w are in excellent agreement with those obtained by the conventional flame orientation method. The main advantage of using this method to determine the turbulent burning speed is that the uncertainties are lowered. Furthermore, it can be applied successfully to flames with complex geometries such as the flame tip region of a conical flame. DOE

N89-10961# Oak Ridge National Lab., Tenn.
RESEARCH NEEDS IN HIGH TEMPERATURE CHEMISTRY
Robert E. Mesmer 1987 4 p Presented at the Temperature Aqueous Solutions, Provo, Utah, 25 Aug. 1987
(Contract DE-AC05-84OR-21400)
(DE88-012929; CONF-8708178-3) Avail: NTIS HC A02/MF A01

Remarkable progress has been made in the last decade or so in the development of a data base on the thermodynamics and chemical properties of aqueous systems at high temperatures and pressures. Many of the conventional physical chemical methods have been adapted for use at high temperatures and pressures and recently some of the more significant ones of those have been the flow methods. A review of basic research needs in aqueous chemistry at high temperatures is presented. DOE

N89-10962# Sandia National Labs., Albuquerque, N. Mex.
MICRORHEOLOGICAL OBSERVATIONS OF THE ONSET OF NON-NEWTONIAN BEHAVIOR IN SUSPENSIONS
L. A. Mondy, A. L. Graham, and M. Gottlieb 1988 5 p Presented at the 10th International Congress on Rheology, Sydney, Australia, 14 Aug. 1988 Prepared in cooperation with Los Alamos National Lab., N. Mex.
(Contracts DE-AC04-76DP-00789; W-7405-eng-36)
(DE88-006198; SAND-87-2054C; CONF-880827-3; LA-UR-88-582)
Avail: NTIS HC A02/MF A01

As the column fraction of solids increases above about 0.30, suspensions of non-Brownian, uniform spheres in Newtonian liquids begin to exhibit shear-thinning, normal stresses, and other non-Newtonian behavior. Here, we report on observations obtained from falling-ball and capillary rheometry at these high volume fractions. Specifically, we find that measured viscosity values are dependent on the size-scale of the viscometer (cylinder diameter, D, and falling- ball diameter, d) relative to the diameter of the suspended spheres d(sub s). We report the dependence of the measured viscosity on the ratios d(d sub s), D(d), and D(d sub s), as well as critical values of these ratios above which the apparent viscosity is constant. DOE

N89-10963*# National Aeronautics and Space Administration, Washington, D.C.
OXIDATION REDUCTION POTENTIAL OF THE Cu(3)/Cu(2) SYSTEM IN ALKALINE SOLUTIONS
G. I. Rozovskiy and A. K. Misyavichios Aug. 1988 18 p Transl. into ENGLISH from Lietuvos TSR Mokslu Akad Darbai, Ser. B (USSR), v. 2, 1965 p 73-82 Transl. by Scientific Translation Service, Santa Barbara, Calif.
(Contract NASw-4307)
(NASA-TT-20309; NAS 1.77:20309) Avail: NTIS HC A03/MF A01 CSCL 07D

Potentials of barium and sodium cuprate coatings, obtained by an electrochemical method on platinum, and in isolated cases, on copper, were measured. It was shown that the stationary potentials were in the case of both cuprates. In 17-0.1 N NaOH solutions, the following dependencies were established: at 5 C, E = 0.77 to 0.52 lgaOH-, at 25 C E = 0.74 to 0.060 lgaOH-. In 10 to the -1

to 10 to the -3 N NaOH solutions, the slope slope coefficient for a linear dependence of the potential on pH is equal to (3/2) X (2.303RT/F). Upon addition of cuprite, the measured stationary potential complies with the dependence E = E1 - (2.303RT/F)lga (c* sub Cu(II) +C sub Cu(II) - (2.303RT/F)lgaOH-, where c sub Cu(II) is the concentration of the added divalent copper, and c* sub Cu(II) is the concentration of the species formed upon reduction of trivalent copper. Possible variations of potential determining reactions were discussed. Author

N89-10964# National Aeronautical Lab., Bangalore (India). Fluid Mechanics Div.
EXPERIMENTS ON LIQUID-VAPOUR PHASE CHANGE BETWEEN PLANE LIQUID SURFACES. PART 1: EXPERIMENTS WITH WATER, FREON AND MERCURY
P. N. Shankar and M. D. Deshpande Apr. 1988 48 p
(TM-FM-8804-Pt-1) Avail: NTIS HC A03/MF A01

An experimental setup was designed and constructued to measure temperature distributions in the vapor between an evaporating liquid surface and a cooler condensing surface. The vapor was contained in transparent chambers of a diameter of 105 mm with metal end-plates to heat and cool the liquid surfaces. Temperature distributions were measured using Chromel-Alumel thermocouples. This report described the theoretical background for the experiments, the equipment used and the preliminary results obtained with water, Freon 113 and mercury. The results obtained generally qualitatively conform with the theoretical predictions for vapors contaminated with inert gas. The results suggest that much higher levels of purity will have to be achieved if the anomalous temperature distribution is to be observed, assuming that it exists in nature. Author

N89-10965# Aerospace Corp., El Segundo, Calif. Chemistry and Physics Lab.
ELECTROCHEMICAL REACTIONS OF MIXED COBALT/NICKEL OXIDE HYDROXIDES IN ALKALINE ELECTROLYTE
A. H. Zimmerman and V. E. Johnson 15 Jul. 1987 35 p
(ATR-86(9561)-4) Avail: NTIS HC A03/MF A01 CSCL 07D

Thin films of mixed cobalt/nickel oxyhydroxides were electrodeposited on platinum substrates. The electrochemical reactions of these materials were characterized as a function of composition and potential in alkaline electrolytes. The materials formed by electrochemical reaction were also characterized structurally from X-ray diffraction powder data. Evidence is presented for several types of materials that are formed as the cobalt levels are increased in the oxyhydroxide. These materials range from solid-solution beta-nickel oxyhydroxide phases when the cobalt content is less than about 10 percent, to several mixed nickel/cobalt phases formed at intermediate cobalt concentrations, and finally above 90 percent cobalt to the doped cobalt oxyhydroxides. Materials formed at intermediate cobalt levels adopt nickel-rich structures below 50 percent cobalt and cobalt-rich structures above 50 percent cobalt. The nickel-rich and the cobalt-rich materials posses the electrochemical activity of nickel oxyhydroxides, although the cobalt-rich structure appears to have a charge storage capacity reduced approximately by a factor of 2. Author

N89-10966# Fermi National Accelerator Lab., Batavia, Ill.
THERMOPHYSICAL PROPERTIES OF ARGON. ADDENDUM
Al Jaques May 1988 10 p
(Contract DE-AC02-76CH-03000)
(DE88-012722; FNAL-TM-1517-A-Add) Avail: NTIS HC A02

The data presented in these tables were gathered with the use of the FORTRAN program FLUIDS which was provided by the National Bureau of Standards. Fluid properties at transitional boundaries and points are those obtained with the best fit equation or formula for that particular fluid. Consequently, at such divergent points as the triple and critical points, the accuracy of the properties given by FLUIDS can be off up to 10 percent in some cases. In listing the critical and triple point conditions within, values were taken from the National Bureau of Standards' publication, Thermodynamic Properties of Argon, not from FLUIDS. Outside of these two points, however, the error in FLUIDS is minimal, thus all other data in these tables were obtained through FLUIDS. The Temperature-Entropy Chart for Argon is also taken from NBS' Thermodynamic Properties of Argon. DOE

N89-10967 California Univ., Santa Barbara.
A STUDY OF THE EFFECT OF THERMAL RADIATION ON LAMINAR FLAME PROPAGATION AND IGNITION, 1981-1987 Ph.D. Thesis
Sheng-hua Zhu 1987 91 p
Avail: Univ. Microfilms Order No. DA8803884

The effect of radiative heat transfer on the ignition and propagation of the laminar diffusion flame is considered analytically. The energy equation is generated based on a set of assumptions similar to those utilized by Spalding in his analysis of one-dimensional unsteady-state laminar flame propagation. The radiative absorption and emission terms are formulated in integral form based on the exact solution to the one-dimensional radiative transfer equation. The differential-integral equation is solved approximately based on the integral method. Since the radiative heat transfer to and from the combustion zone and the hot and cold boundaries of a physical system, flame propagation in a radiative participating medium is intrinsically unsteady except in the optically thick and thin limits. From the numerical results, the initial optical thickness of the burnt and unburnt mixture are shown to have important effects on the flame propagation and ignition characters immediately after the two mixtures are brought into contact. Dissert. Abstr.

N89-10968# Pennsylvania State Univ., University Park. Dept. of Chemistry.
TRANSITION METAL MEDIATED TRANSFORMATIONS OF UNSATURATED MOLECULES Progress Report
Ayusman Sen 1 Jul. 1988 5 p
(Contract DE-FG02-84ER-13295)
(DE88-013482; DOE/ER-13295/2) Avail: NTIS HC A02/MF A01

The catalysis of organic transformations by soluble transition metal compounds has gained widespread attention because of the high efficiency, high specificity and low energy demands often associated with such systems. Research goals in this area are: (1) to achieve a fundamental mechanistic understanding of the important homogeneous catalytic systems, and (2) to use this knowledge to develop new and useful catalytic processes. We have focused on four broad areas of transition metal catalyzed/mediated transformations of organic molecules: (1) the selective functionalization of alkanes and arenas by electrophilic metal compounds, (2) the coupling of organic mono- and dihalides by low-valent, anionic, metal complexes, (3) transition metal mediated/catalyzed reactions of carbon monoxide, and (4) the oxidation chemistry of high-valent organometallic oxo complexes. Results are briefly summarized. DOE

N89-10969# California Univ., Berkeley. Lawrence Berkeley Lab.
NEAR-CRITICAL NaCl-H2O: AN EQUATION OF STATE AND DISCUSSION OF ANOMALOUS PROPERTIES
K. S. Pitzer and J. C. Tanger, IV May 1988 35 p Presented at the 10th Symposium on Thermophysical Properties, Gaithersburg, Md., 20 Jun. 1988
(Contract DE-AC03-76SF-00098)
(DE88-012029; LBL-25330; CONF-880606-2) Avail: NTIS HC A03/MF A01

The system NaCl-H sub 2 O near the critical point of pure water shows not only the remarkable properties of any two-component system near the critical point of one component but also an anomalous curvature of the T-x and P-x projections of the critical line in the range below mole fraction 0.0005. An equation of state is presented which is based on the Haar-Gallagher-Kell equation for pure water with a few terms involving the mole fraction of NaCl together with the temperature and density. Parameters in this equation were selected which yield

a good representation of the entire vapor-liquid coexistence surface from 250 to 600°C and from the three-phase pressure to the critical pressure (or to the vapor pressure of pure water below its T sub c). Derivatives of this equation yield densities, enthalpies, and heat capacities which are compared with experimental data. Also, the properties calculated for the vapor near the three-phase line are compared with those predicted by the successive hydration model previously developed for NaCl in steam in equilibrium with solid NaCl. Other related topics are discussed, including the anomalous features noted above. DOE

N89-10970# Argonne National Lab., Ill.
THEORETICAL STUDIES OF CHEMICAL REACTIONS: DYNAMICS
A. F. Wagner, M. J. Davis, G. C. Schatz, R. J. Duchovic, and R. Steckler 1988 5 p Presented at the Basic Energy Sciences Combustion Contractor's Meeting, Lake Geneva, Wisc., 31 May 1988
(Contract W-31-109-eng-38)
(DE88-011994; CONF-880543-1) Avail: NTIS HC A02/MF A01

Theoretical studies have been performed on the dynamics of interesting chemical reactions. The systems studied included the recombination reaction of methyl radicals to form ethylene, the addition of hydrogen atoms to carbon monoxide and the thermal dissociation of the formyl radical, the reaction of two hydroxyl radicals to form water and atomic hydrogen, the reaction of atomic chlorine with hydrogen chloride, and the intramolecular dynamics of highly excited OCS. DOE

N89-10971# National Aeronautical Lab., Bangalore (India). Fluid Mechanics Div.
LIQUID-VAPOUR PHASE CHANGE BETWEEN PLANE LIQUID SURFACES: A CONTINUUM ANALYSIS TO DETERMINE REAL GAS EFFECTS
P. N. Shankar Mar. 1988 38 p
(TM-FM-8803) Avail: NTIS HC A03/MF A01

A continuum analysis is given of the problem of steady evaporation and condensation between plane liquid surfaces of infinite extent. Following Marble (1966) the continuum equations are solved in the bulk of the gas with the appropriate boundary conditions coming from an analysis of the Knudsen laters near the liquid surface. The present analysis includes the diffusion effects caused by the presence of an inert gas on the phase change process. A valuable by-product of the present approach is that the real gas effects can be estimated. Formulae are given for the mass flux and temperature distribution which exhibits, under certain circumstances, the now familiar anomalous inversion. The real gas and diffusion effects turn out to be strikingly large. It is shown that the temperature jump in the case of polyatomic molecules is always smaller than the corresponding jump for a monatomic gas. The effect of contamination is always harmful. Contamination rapidly decreases the mass flux and the temperature jumps at the liquid surfaces. Some sample calculations are included of possibly experimentally relizable situations. The calculations clearly indicate the direction that experimental investigations ought to take.
Author

N89-10972# Institute of Gas Technology, Chicago, Ill.
WORLDWIDE SURVEY OF ABSORPTION FLUIDS DATA
Robert A. Macriss and Thomas A. Zawacki 1988 7 p Presented at the 2nd DOE/ORNL Heat Pump Conference: Research and Development on the Heat Pump for Space Conditioning Applications, Washington, D.C., 17 Apr. 1988
(Contract DE-AC05-84OR-21400)
(DE88-013204; CONF-8804100-10) Avail: NTIS HC A02

The overall objective of this study is to develop improved data for the thermodynamic, transport and physical properties of absorption fluids. A specific objective of this phase of the study is to compile, catalog and coarse-screen the available worldwide data of known absorption fluid systems and publish it as a reference document to be distributed to manufacturers, researchers and others active in absorption heat pump activities. DOE

N89-10973# National Aeronautical Lab., Bangalore (India). Fluid Mechanics Div.
EXPERIMENTS ON LIQUID-VAPOR PHASE CHANGE BETWEEN PLANE LIQUID SURFACES. PART 2: OBSERVATIONS OF LARGE TEMPERATURE JUMPS NEAR THE INTERFACES
P. N. Shankar and M. D. Deshpande May 1988 18 p
(TM-FM-8805-Pt-2) Avail: NTIS HC A03/MF A01

Experiments were carried out to measure the temperature distribution in mercury vapor confined between its liquid evaporating surface and a condensing plane surface. The data presented here clearly exhibit the large temperature jumps at the interface boundaries predicted by theory; jumps as large as almost 50 percent of the applied temperature difference have so far been observed. These results, therefore, settle one of the most controversial issues in this area. Author

N89-10974# Academy of Sciences of the Ukrainian SSR, Kharkov.
PECULIARITIES OF HEAT TRANSFER AT HELIUM BOILING IN CENTRIFUGAL FORCE FIELD
Yu. A. Kirichenko and K. V. Rusanov 1987 23 p In RUSSIAN; ENGLISH summary
(DE88-702809; INIS-SU-21) Avail: NTIS (US Sales Only) HC A03/MF A01

A new interpretation is given to some new effects observed at helium boiling in an intensive centrifugal force field. Formulas taking into account the influence of these effects on the heat transfer characteristics are proposed. A method is developed for evaluating the first critical density of the thermal flux during liquid boiling at differently oriented flat surfaces. DOE

N89-10975# Oak Ridge National Lab., Tenn. Chemistry Div.
PHOTOACOUSTIC SPECTROSCOPY AND THE IN SITU CHARACTERIZATION OF THE ELECTROCHEMICAL INTERFACE
Catherine E. Vallet 1988 26 p Presented at the Spectroscopic and Diffraction Techniques in Interfacial Electrochemistry, Puerto de la Cruz, Spain, 3 Jul. 1988
(Contract DE-AC05-84OR-21400)
(DE88-013848; CONF-880732-1) Avail: NTIS HC A03/MF A01

Photoacoustics is a new spectroscopic method which has been used for in situ characterization of the electrochemical interface during the past ten years. The basic principles of the photoacoustic effect and the principal results of the Rosencwaig-Gersho theory are discussed in light of the usefulness of the method in electrochemical studies. Different experimental arrangements suitable for in situ electrode studies are presented. A review of the use to date of photoacoustics in electrochemistry includes studies of electrochromic systems, semiconductor electrodes, passivation layers, and of electrocatalytic mixed oxides. These works demonstrated that, with relatively simple apparatus, it was possible to detect and to characterize very thin layers formed on electrodes. It is still not clear whether in most cases photoacoustic spectroscopy has an overwhelming advantage over well-established optical methods for adsorption measurements; however, all the potentialities of the method have yet to be explored. DOE

N89-10976# International Centre for Theoretical Physics, Trieste (Italy).
TEMPERATURE DEPENDENCE OF ENTROPIES AND SPECIFIC HEATS OF LIQUID Na AND K
R. N. Joarder and S. M. Mujibur Rahman Nov. 1987 22 p
(DE88-702986; IC-87/365) Avail: NTIS (US Sales Only) HC A03/MF A01

We have investigated the temperature variation of the entropies and specific heats of liquid Na and K. The systems are primarily modelled with a hard sphere (hs) description, but contributions arising from the soft forces and electronic part are also included with the basic hs model. The hard sphere ingredients at various temperatures are determined through the consideration that the difference between the relevant pair potential and its minimum

value is just equal to the kinetic energy of a free particle. The basic ingredients thus obtained are employed to calculate the entropies and specific heats of the systems at various temperatures. The calculated values are found to be in good agreement with experiments. DOE

N89-10977# Sandia National Labs., Livermore, Calif.
COMBUSTION OF ENERGETIC MATERIALS Semiannual Progress Report, Apr. - Sep. 1987
1988 45 p
(Contract DE-AC04-76DP-00789)
(DE88-011286; SAND-88-8001) Avail: NTIS HC A03/MF A01

Fundamental research is emphasized and directed towards understanding the combustion, chemistry and physics of energetic solids and liquids. The following are considered: (1) solid propellant thermal decomposition and deflagration studies, and (2) liquid monopropellant ignition and combustion studies. A gas-flame experiment designed to model the two-stage flame characteristics of solid propellant deflagration has been established and both conventional and laser diagnostics have been incorporated into it. Thermal decomposition (using laser heating) of solid propellants is being studied using a modulated molecular beam mass spectrometer that will be complemented by laser-induced fluorescence diagnostics. Gas-phase flame models used previously for hydrocarbon flame analysis are being extended to study gas-phase reactions in nitramine propellants. Quantum chemistry calculations are being performed to investigate the molecular decomposition mechanisms of energetic materials. Solid propellant deflagration is being modeled analytically and through the use of 2-D thermochemical codes developed earlier. Droplet combustion models developed for hydrocarbon fuels are extended for liquid monopropellant applications. DOE

N89-10978# California Univ., Berkeley. Lawrence Berkeley Lab. Applied Science Div.
THE IMPORTANCE OF THERMODYNAMICS TO THE MODELING OF NITROGEN COMBUSTION CHEMISTRY
Richard J. Martin and Nancy Brown Jul. 1988 32 p Presented at the 22nd International Symposium on Combustion, Seattle, Wash., 14 Aug. 1988
(Contract DE-AC03-76SF-00098)
(DE88-014656; LBL-24687; CONF-880802-9) Avail: NTIS HC A03/MF A01

Modeling calculations have been performed to illustrate the effect of using five commonly accepted data bases of thermochemical properties on predictions of temporal species profiles. The thermochemical properties are those used for the determination of equilibrium constants employed in the calculation of reverse rate coefficients for a chemical mechanism where forward rate coefficients are specified. The modeling study was performed for hydrogen/oxygen/argon/nitrogen compound mixtures where the nitrogen compound was either NO or NH3. The mixtures reacted isothermally at 1600 K and isobarically at 1 atmosphere, and a single kinetic mechanism for which forward rate coefficients were specified was used throughout. Mixtures of equivalence ratios of 0.625, 1.0 and 1.6 were considered. Modifications in sources of thermodynamic data have been substantial since 1971 for some species. Among the data bases, thermochemical properties varied greatly for the species NH, NH2, NNH, and HO2, and those for other species important in the mechanism had variations of less than 10 percent. The thermochemical property variations among the data bases in NH, NH2 and NNH have substantial effects upon the temporal species profiles for nitrogenous species. While this result is not surprising, unfortunately, it is often overlooked when modeling results are compared. This effect is most pronounced for rich combustion, and varies directly with equivalence ratio. Use of different data bases had little effect on the H/O species profiles. Radical species profiles (with the exception of HO2) tend to be influenced strongly by their own thermochemical properties. Computed profiles also were shown to be independent of algorithm (HCT or CHEMKIN) and thermodynamic property fitting procedure between 1000 and 2000 K. DOE

N89-10979# Sandia National Labs., Albuquerque, N. Mex.
A DIFFERENTIAL ABSORPTION SPECTROMETER FOR DETERMINING FLASH X-RAY SPECTRA FROM 10 TO 2000 KeV
G. A. Carlson and L. J. Lorence 1988 19 p Presented at the 25th Annual Conference on Nuclear and Space Radiation Effects, Portland, Oreg., 12 Jul. 1988
(Contract DE-AC04-76DP-00789)
(DE88-014844; SAND-88-0230C; CONF-880730-8) Avail: NTIS HC A03/MF A01

A differential absorption spectrometer has been developed and fielded on various bremsstrahlung sources (Pelletron, Saturn, and SPEED) with endpoint energies from 150 to 2000 keV. Spectral data were unfolded using response functions generated by TIGER and CEPXS/ONETRAN. Unfolded spectra are qualitatively in agreement with predicted spectra for steady-state bremsstrahlung sources from 150 keV to 900 keV. Applications and limitations of the diagnostic are discussed, and modifications and simplifications suggested. DOE

N89-10980# Syracuse Univ., N. Y. Dept. of Chemical Engineering and Materials Science.
MECHANISMS OF GAS PERMEATION THROUGH POLYMER MEMBRANES Progress Report, 16 Mar. 1987 - 15 Jan. 1988
S. A. Stern, S. Zhou, and R. Vaidyanathan Jan. 1988 9 p
(Contract DE-FG02-87ER-13649)
(DE88-007761; DOE/ER-13649/1) Avail: NTIS HC A02

Solution and diffusion coefficients are being determined for several gases in poly(n-butyl methacrylate) (PnBMA) and poly(n-propyl methacrylate) (PnPMA). It is concluded that the solubility and diffusivity of light gases in some polymers do not necessarily exhibit dual-mode sorption behavior below the glass transition temperature T sub g; e.g., no dual-mode sorption behavior was observed in PnBMA and PnPMA until the temperature was reduced at least 30 C below T sub g. This behavior depends on the excess free volume in the glassy polymer state and on the relative sizes of the penetrant gas molecules and of the mean free volume in the polymer. DOE

N89-10981# Lawrence Livermore National Lab., Calif.
FLUID MECHANICAL PROPERTIES OF FLAMES IN ENCLOSURES
D. A. Rotman, M. Z. Pindera, and A. K. Oppenheim (California Univ., Berkeley.) Jul. 1988 17 p Presented at the 11th International Colloquium on Dynamics of Explosions and Reactive Systems, Warsaw, Poland, 2 Aug. 1988
(Contracts W-7405-eng-48; DE-AC03-76SF-00098)
(DE88-014142; UCRL-99056; CONF-880889-1) Avail: NTIS HC A03/MF A01

In an enclosure where the reacting medium is initially at rest, the flame first generates a flowfield that then gets stretched, i.e., its front is pulled along the surface by the flowfield in which it then finds itself residing. A methodology developed for numerical modeling of such fields is described. Of key significance in this respect is the zero Mach number model - a reasonable idealization in view of the relatively high temperature, and hence sound speed, that exists, concomitantly with a comparatively low particle velocity, in the confinement of a combustion chamber. According to this model, the density gradient in the field is nullified, while across the flame front it approaches infinity. One has thus two regimes: one of the unburned medium and the other of the burned gas, each of spatially uniform density, separated by a flame front interface. The latter is endowed with four properties, of which the first two are purely kinematic and the others dynamic in nature, namely: (1) it is advected at the local velocity of flow; (2) it self-advances at the normal burning speed, the eigenvalue of the system; (3) it acts as the velocity source due to the exothermicity of the combustion process; and (4) it acts as the vorticity source due to the baroclinic effect generated by the pressure gradient along its surface and the density gradient across it. A solution obtained for a flame propagating in an oblong rectangular enclosure demonstrates that the latter has a significant influence upon the formation of the well known tulip shape. DOE

N89-10982# Oak Ridge National Lab., Tenn. Metals and Ceramics Div.
THE THERMAL RESISTANCE OF FINE POWDERS AT ATMOSPHERIC PRESSURE AND UNDER VACUUM
D. L. McElroy, F. J. Weaver, D. W. Yarbrough, and R. S. Graves 1987 29 p Presented at the Conference on Insulation Materials, Testing and Applications, Bal Harbour, Fla., 6 Dec. 1987
(Contract DE-AC05-84OR-21400)
(DE88-014556; CONF-871203-5) Avail: NTIS HC A03/MF A01

Heat transport measurements are reported on candidate insulation systems with relatively high thermal resistances for use in appliances. The thermal resistances of small diameter silica powders at atmospheric pressure and under vacuum were measured from 295 to 340 K using unguarded radial heat flow techniques. The thermal resistances of rectangular panels containing perlite or silica powder at reduced pressure were determined using an unguarded linear heat flow technique. Values of 1.2 sq m/(K/W) for 0.0254 m (R-7 per inch) were obtained at atmospheric pressure for powders of pure, fumed, amorphous 0.01 micron dia silica particles compacted to about 10 percent of theoretical density. Values of 0.7 sq m/(K/W) for 0.0254 m (R-4 per inch) were obtained at atmospheric pressure for powders of impure, amorphous (0.3 micron dia) silica particles. Under vacuum these particle systems yielded thermal resistances as high as 6 sq m/(K/W) for 0.0254 m (R-34 per inch), and mixtures with the pure silica particles yielded over 9 sq m/(K/W) for 0.0254 m (R-50 per inch). Evacuated panels of pure silica particles yielded thermal resistance values over 3 sq m/(K/W) for 0.0254 m (R-17 per inch) and decreased about 5 product in resistance in 39 months. Evacuated panels of a perlite powder yielded similar values. DOE

N89-10983# Sandia National Labs., Albuquerque, N. Mex.
COEFFICIENTS OF THERMAL EXPANSION OF COMMON ENCAPSULANTS
Douglas B. Adolf and Carolyn Childress Jul. 1988 39 p
(Contract DE-AC04-76DP-00789)
(DE88-015026; SAND-88-0777) Avail: NTIS HC A03/MF A01

The coefficient of thermal expansion (CTE) of common electronic encapsulating polymers were measured over the temperature range of minus 50 degree C to approximately 120 degree C. CTE's are presented for these systems as continuous functions of temperature in contrast to previous measurements. Comparison between the historical property chart CTE's and those obtained in this study are made when possible. The procedures used in this study are presented in detail so that, unlike the property chart, users will fully understand the accuracy and limitations of these values. DOE

N89-10984*# Michigan Univ., Ann Arbor.
TECHNIQUE FOR MEASURING THE DIELECTRIC CONSTANT OF THIN MATERIALS
K. Sarabandi and F. T. Ulaby 1988 25 p
(Grant NAG5-480)
(NASA-CR-183325; NAS 1.26:183325) Avail: NTIS HC A03/MF A01 CSCL 07D

A practical technique for measuring the dielectric constant of vegetation leaves and similarly thin materials is presented. A rectangular section of the leaf is placed in the tranverse plane in a rectangular waveguide and the magnitude and phase of the reflection coefficient are measured over the desired frequency band using a vector network analyzer. By treating the leaf as an infinitesimally thin resistive sheet, an explicit expression for its dielectric constant is obtained in terms of the reflection coefficient. Because of the thin-sheet approximation, however, this approach is valid only at frequencies below 1.5 GHz. To extend the technique to higher frequencies, higher order approximations are derived and their accuracies are compared to the exact dielectric-slab solution. For a material whose thickness is 0.5 mm or less, the proposed technique was found to provide accurate values of its dielectric constant up to frequencies of 12 GHz or higher. The technique was used to measure the 8 to 12 GHz dielectric spectrum for vegetation leaves, teflon and rock samples. Author

N89-10985# Leeds Univ. (England).
KINETICS OF BORON HYDRIDE INTERCONVERSION REACTIONS Periodic Report Nos. 1-5, May 1986 - May 1988
N. N. Greenwood May 1988 28 p
(Contract DAJA45-86-C-0019)
(AD-A196824) Avail: NTIS HC A03/MF A01 CSCL 20K

The mechanisms by which gaseous boron hydrides so readily interconvert and build up into larger clusters has excited considerable academic and industrial interest for several decades. This paper describes recent progress that has been made in unravelling this complex series of interconversion reactions. Initial reaction rates have been studied mass spectrometrically to obtain rate equations, orders of reaction and energies of activation. Detailed and continuous product analysis for H2 and all the volatile boranes formed, coupled with a study of cothermolysis reactions of selected pairs of boranes gives further insight into the processes occurring. Crucial aspects of the thermolysis of B2H6, B4H10, B5H11, and B6H10 are discussed, as are the effects of added H2 and the cothermolysis of B6H10 with alkenes. The final section presents data on the UV absorption spectra and photolytic stability of eight volatile boranes and the reaction kinetics of B6H10 photolysis. GRA

N89-10986# State Univ. Coll. of New York, Buffalo. Dept. of Chemistry.
THE COEFFICIENT OF FIRST VISCOSITY VIA THREE-PHONON PROCESSES IN BULK LIQUID HELIUM
C. I. Um, C. W. Jun, W. H. Kahng (Korea Univ., Seoul.), and Thomas F. George Jun. 1988 21 p Submitted for publication
(Contract N00014-86-K-0043)
(AD-A196902; UBUFFALO/DC/88/TR-71) Avail: NTIS HC A03/MF A01 CSCL 20J

The contribution of three-phonon processes to the coefficient of first viscosity in bulk liquid helium is evaluated explicitly as a function of temperature, which is shown to have a 1/T dependence. GRA

N89-10987# Georgia Tech Research Inst., Atlanta.
DEVELOPMENT OF AN EXPERIMENTAL MODEL OF SELF-PROPAGATING HIGH TEMPERATURE OXIDATION-REDUCTION REACTIONS Final Report, 15 Apr. 1985 - 14 Apr. 1988
K. V. Logan, E. W. Price, J. T. Sparrow, W. J. McLemore, and G. R. Villalobos 14 Apr. 1988 46 p
(Contract DAAG29-85-K-0125)
(AD-A196978; ARO-22530.3-MS) Avail: NTIS HC A03/MF A01 CSCL 19A

The goal of this program is to understand the particle-particle interactions of the aluminum thermite reaction in which titanium boride is produced. By understanding the interactions, the thermite reaction behavior can be predicted, and the reaction can be controlled to yield a desired product configuration. This final report summarizes the most important results of a three-year program to develop an experimental model of particle-particle interactions in an oxidation-reduction self-propagating high temperature reaction. The first year identified reaction parameter strategies necessary to characterize particle-particle interactions leading to ignition. The second year identified reaction parameter strategies just before and after ignition occurred. GRA

N89-10988# Aquanautics Corp., Emeryville, Calif.
OXYGEN CHEMISTRY Technical Report, 1 Jan. - 31 Aug. 1987
N. Ross Buckenham 31 Aug. 1987 9 p
(Contract N00014-87-C-0334; ARPA Order 4696)
(AD-A196989; AFIT/CI/NR-88-111) Avail: NTIS HC A02/MF A01 CSCL 13A

The Project objective was to demonstrate the technology of oxygen extraction from seawater by designing a submarine powered by a fuel cell and oxygen supplied by Aquanautics system. A new cell design concept has been introduced where the carrier fluid flows through the felt in a direction perpendicular to membrane separator. This allows much lower pressure head and therefore

lowers pumping costs since the fluid velocity and path length are small. The fluid also passes through all the electric potentials of the electrodes. GRA

N89-11163*# Pennsylvania State Univ., University Park. Dept. of Mechanical Engineering.
MODELING OF COMBUSTION PROCESSES OF STICK PROPELLANTS VIA COMBINED EULERIAN-LAGRANGIAN APPROACH
K. K. Kuo, K. C. Hsieh, and M. M. Athavale *In* NASA, Marshall Space Flight Center, Mixing and Demixing Processes in Multiphase Flows with Application to Propulsion Systems Jul. 1988 p 181-193 (For primary document see N89-11153 02-34)
(Contract DAAG29-83-K-0081)
Avail: NTIS HC A09/MF A01 CSCL 21B

26 METALLIC MATERIALS

Includes physical, chemical, and mechanical properties of metals, e.g., corrosion; and metallurgy.

N89-10989# Illinois Univ., Urbana. Dept. of Chemical Engineering.
EXPERIMENTAL AND THEORETICAL STUDY OF INCLUSIONS DURING INITIATION OF CREVICE CORROSION Ph.D. Thesis
Stephen Elder Lott 1987 179 p
(Contract DE-AC02-76ER-01198)
(DE88-014635; DOE/ER-01198/T21) Avail: NTIS HC A09/MF A01

The purpose of this investigation was to determine the initiation mechanism of crevice corrosion on stainless steel in a neutral nickel electrolyte. Kinetic experiments were run on MnS electrodes to understand the depassivation effect of the MnS inclusion on the stainless steel oxide film. The depassivation effect of the species produced at the MnS inclusions in conjunction with the nickel electrolyte led to a proposed mechanism to explain the initiation of breakdown. A mathematical model based on the proposed mechanism was written and incorporated the geometry of the crevice, the MnS surface inclusion density, and the electrochemical potential at the edge of the crevice. The range of validity of the model was tested by comparing the results from the model with stainless steel crevice corrosion experiments. DOE

N89-10990# Sandia National Labs., Albuquerque, N. Mex.
MICROSCOPY AND MICROANALYSIS OF SHOCK-PROCESSED MATERIALS
M. J. Carr and R. A. Graham 1988 14 p Presented at the MAS/EMSA Microbeam Analysis Conference, Milwaukee, Wis., 7 Aug. 1988
(Contract DE-AC04-76DP-00789)
(DE88-008471; SAND-88-0956C; CONF-880841-7) Avail: NTIS HC A03

The passage of a shock compressive pulse through a material consists of a brief excursion to high pressure and temperature, concurrent with high strain rate deformation, followed promptly by a return to nominal conditions. The short duration of the shock pulse and the rapid quench combine to produce complex chemical and microstructural changes on a very fine scale. The analytical electron microscope and electron microprobe have been successfully employed to analyze a variety of materials systems exposed to shock loading. Case studies of rutile, Al-Ni reacting powder mixtures, and zinc oxide-hematite reactions are used to illustrate the applicability of these methods to the characterization and analysis of shock processed materials. DOE

N89-10991# Oak Ridge National Lab., Tenn.
A PRELIMINARY STUDY ON THE USE OF MAGNETOHYDRODYNAMIC FORCES TO REMOVE IMPURITIES FROM MOLTEN METALS
D. O. Hobson Jun. 1988 19 p
(Contract DE-AC05-84OR-21400)
(DE88-013508; ORNL/TM-10747) Avail: NTIS HC A03/MF A01

Experimental and modeling work on the use of magnetohydrodynamic forces for separating particulate impurities from molten metals is described. Several experimental systems are described, which use ac or dc electromagnets and, thereby, either induced or direct currents to produce the required forces. Recommendations are made for further optimization of the separators. DOE

N89-10992# Instituto de Pesquisas Energeticas e Nucleares, Sao Paulo (Brazil).
SPECTROGRAPHY ANALYSIS OF STAINLESS STEEL BY THE POINT TO POINT TECHNIQUE M.S. Thesis
A. Bona 1986 99 p In PORTUGUESE; ENGLISH summary
(DE88-702302; INIS-BR-1038) Avail: NTIS HC A05/MF A01

A method for the determination of the elements Ni, Cr, Mn, Si, Mo, Nb, Cu, Co, and V in stainless steel by emission spectrographic analysis using high voltage spark sources is presented. The point-to-point technique is employed. The experimental parameters were optimized taking into account a compromise between the detection sensitivity and the precision of the measurement. The parameters investigated were the high voltage capacitance, the inductance, the analytical and auxillary gaps, the period of preburn spark and the time of exposure. The edge shape of the counter electrodes and the type of polishing and diameter variation of the stainless steel electrodes were evaluated in preliminary assays. In addition the degradation of the chemical power of the developer was also investigated. Counter electrodes of graphite, copper, aluminium, and iron were employed and the counter electrode itself was used as an internal standard. The relative errors were the criteria for evaluation of these experiments. The National Bureau of Standards-Certified reference stainless steel standards and the Electrometal Acos Finos S.A. samples (certified by the supplier) were employed for drawing in the calibration systems and analytical curves. The best results were obtained using the conventional graphite counter electrodes. The inaccuracy and the imprecision of the proposed method varied from 2 to 15 percent and from 1 and 9 respectively. This present technique was compared to others instrumental techniques such as inductively coupled plasma. X-ray fluorescence and neutron activation analysis. The advantages and disadvantages for each case were discussed. DOE

N89-10993 Direction des Recherches Etudes et Techniques, Paris (France). Centre de Documentation de l'Armement.
ATOMIC PROBE STUDY OF ORDERING AND PRECIPITATION IN NICKEL-BASED ALLOYS Final Report
1987 33 p In FRENCH
Avail: NTIS HC E04/MF E04; copy not available from STI Facility CSCL 11F

The ordering of a Ni3 Fe0.76 Al0.24 alloy was studied using an atomic probe. Analysis of the superstructural planes of the single phased alloy showed pure Ni planes alternating with mixed planes (50 percent Ni, 50 percent Al, Fe). A break in the stacking of these planes was observed and attributed to the existence of an antiphase wall between ordered domains. A study of the precipitation kinetics of the gamma (1) phase in NA4D alloys showed the evolution of the systems' microstructural parameters with age hardening. Results were qualitatively similar to those seen in hardening precipitate studies: the Al concentration, Ti in the particles, increases in proportion to the isothermic annealing time as the system approaches equilibrium. Author

N89-10994# Argonne National Lab., Ill. Chemistry Div.
EXPERIMENTAL STUDIES OF THE CHEMISTRY OF METAL CLUSTERS
E. K. Parks and S. J. Riley 1988 37 p Presented at the Enrico Fermi School of Physics on Nonlinear Topics in Ocean Physics Conference, Varenna, Italy, 26 Jun. 1988
(Contract W-31-109-eng-38)

(DE88-012034; CONF-8806161-1) Avail: NTIS HC A03/MF A01

The procedures for studying chemical reactions of metal clusters in a continuous-flow reactor are described, and examples of such studies are given. Experiments to be discussed include kinetics and thermodynamics measurements, and determination of the composition of clusters saturated with various adsorbate reagents. Specific systems to be covered include the reaction of iron clusters with ammonia and with hydrogen, the reaction of nickel clusters with hydrogen and with ammonia, and the reaction of platinum clusters with ethylene. The last two reactions are characterized by complex, multi-step processes that lead to adsorbate decomposition and hydrogen desorption from the clusters. Methods for probing these processes will be discussed. DOE

N89-10995# Los Alamos National Lab., N. Mex.
STRAIN HARDENING AT LARGE STRAINS
A. D. Rollett, U. F. Kocks, J. D. Embury, M. G. Stout, and R. D. Doherty (Drexel Univ., Philadelphia, Pa.) 1988 7 p Presented at the 8th International Conference on Strength of Metals and Alloys, Tampere, Finland, 22 Aug. 1988
(Contract W-7405-eng-36)
(DE88-007909; LA-UR-88-674; CONF-880844-1) Avail: NTIS HC A02/MF A01

The strain hardening properties of various fcc metals have been investigated at large strains by means of torsion tests of short thin-walled cylinders. The results show that Stage 4 occurs in all cases provided that a low enough test temperature is used; it is a nearly constant hardening rate of 2.10(sup -4) G in terms of resolved flow stress. Stage 4 strain hardening has been modeled by considering the effects of accumulation of dislocation debris, such as dipoles and loops, in the saturation stress. The saturation stress that can be obtained by extrapolation of Stage 3 is now a limiting flow stress that slowly increases with the accumulation of debris. The model reproduces the sharp transition from Stage 3 to Stage 4 that occurs experimentally at low temperatures and, for a reasonable choice of parameters, the rate of hardening in Stage 4. DOE

N89-10996*# National Aeronautics and Space Administration. Lewis Research Center, Cleveland, Ohio.
INDENTATION PLASTICITY AND FRACTURE IN SILICON
George C. Rybicki and P. Pirouz (Case Western Reserve Univ., Cleveland, Ohio.) Nov. 1988 30 p
(NASA-TP-2863; E-4184; NAS 1.60:2863) Avail: NTIS HC A03/MF A01 CSCL 11B

Measurements of the ductile-brittle transition temperature of heavily doped silicon were carried out using indentation techniques. Diamond pyramid hardness tests were performed on the (100) face of heavily doped N-type and P-type and intrinsic silicon single crystals. Tests were performed over the range 200 C to 850 C and loads of 100 to 500 g were used. Samples were subsequently etched to reveal dislocation rosettes produced by indentation. Intrinsic silicon underwent a ductile-brittle transition at 660 C, P-type at 645 C and N-type at 625 C. Hardness values varied from 1.1 GPa at 700 C to 11.7 GPa at 200 C. Significant effects of hardness on doping were present only at the highest temperatures. Lower loads generally produced higher hardness but load did not affect the Ductile-Brittle Transition Temperature (DBTT). Fracture toughness values ranged from 0.9 MPa m(1/2) at 200 C to 2.75 MPa m(1/2) near the DBTT. Doping did not affect the fracture toughness of silicon. P-type doping increased the size of dislocation rosettes observed after indentation, but N-type did not, in contradiction of the expected results. Results are discussed in terms of the effect of doping on the dislocation mobility in silicon. Author

N89-10997 United Kingdom Atomic Energy Authority, Risley (England). Dept. of Applied Chemistry.
THE EFFECT OF THERMAL AGEING ON THE STRESS CORROSION CRACKING OF 9Cr1Mo STEEL IN AQUEOUS CAUSTIC ENVIRONMENTS
P. Banks and P. Hurst May 1988 28 p
(NRL-R-1003(R)) Copyright Avail: Issuing Activity

Work has been carried out to gain a basic understanding of the effects of thermal aging on the stress corrosion behavior of 9Cr1Mo steel w/o NaOH solutions at 116 C and 300 C. This has involved slow strain rate and constant load stress corrosion tests, together with grain boundary and other microstructural studies. The results showed that 9Cr1Mo steel, although almost immune to stress corrosion attack under constant load conditions, was susceptible over a range of electrochemical potentials in slow strain rate tests. Thermal aging can enhance the susceptibility, and this has been correlated with microstructural changes which affect the distribution of segregated elements at the grain boundaries. Author

N89-10998# Kernforschungszentrum, Karlsruhe (West Germany). Projekt Wiederaufarbeitung und Abfallbehandlung.
STUDIES OF THE TRANSPASSIVE NITRIC ACID CORROSION OF VARIOUS AUSTENITIC CrNi STEELS IN THE PROLONGED HUEY TEST (65 PERCENT HNO3, 120 C, 720 h)
R. Kraft, S. Leistikow, and E. Pott 13 May 1988 100 p
(Contract DE-AC09-76SR-00001)
(DE88-010494; DP-tr-108) Avail: NTIS HC A05/MF A01

The aim of these experiments was to test the quality and the ability to withstand longtime service conditions of various austenitic stainless steels of type 18 10 CrNi and 25 20 CrNi by ASTM Standard Huey-Test, prolongated up to 15 periods of 48 h each. By gravimetry the rate of metal loss, by metallography the maximum depth of local dissolution, by microscopy the overall appearance of the corroded surface was checked and evaluated. Results show differences in metal dissolution rate as function of basic alloy composition (in Fe,Cr,Ni), content of minor elements (in C,Si,Mo,S), and bulk structure (grain size, distribution of inclusions, precipitation of carbides etc.) as resulting of industrial production and laboratory heat treatments. The best corrosion behavior was shown by the low carbon 25 20 CrNi stainless steels in the fine-grain, highly pure, solution annealed condition, not showing any trend to accelerate corrosion when sensitizing heat treatment or long-time exposure were applied. The prolonged Huey-Test proved to be a sensitive method to evaluate the corrosion behavior of steels for engineering purposes, especially the effects caused by the main alloy components, small impurity concentrations, and differences in homogeneity of the bulk structure. DOE

N89-10999# Oak Ridge National Lab., Tenn. Metals and Ceramics Div.
MICROSTRUCTURAL DEVELOPMENT OF TITANIUM-MODIFIED AUSTENITIC STAINLESS STEEL UNDER NEUTRON IRRADIATION IN HFIR UP TO 57 dpa
M. Suzuki, S. Hamada, P. J. Maziasz (Japan Atomic Energy Research Inst., Ibaraki.), M. P. Tanaka, and A. Hishinuma 1988 28 p Presented at the 14th International Symposium on Effects of Radiation on Materials, Andover, Mass., 27 Jun. 1988
(Contract DE-AC05-84OR-21400)
(DE88-013248; CONF-880613-15) Avail: NTIS HC A03

The Japanese prime candidate alloy (JPCA), a titanium modified austenitic stainless steel, has shown good performance after irradiation in High Flux Isotope Reactors up to 34 dpa at 300 C to 600 C, but considerable void swelling develops in solution annealed (SA) JPCA after irradiation 57 dpa at 500 C. However, cold worked (CW) or cold worked and aged (CW+A) JPCA still demonstrates good performance after similar irradiation. Swelling resistance appears to strongly depend on the behavior of fine titanium-rich MC precipitates. This paper describes the microstructural evolution process observed in the JPCA steel during HFIR irradiation. The onset of rapid void swelling was related to MC precipitate dissolution, and the instability of the MC was interpreted in terms of a model involving the build of and effects of a solute segregation zone in the matrix surrounding the precipitate particle. DOE

N89-11000 Illinois Univ., Urbana-Champaign.
MECHANICS OF HYDROGEN EMBRITTLEMENT Ph.D. Thesis

Petros Sofronis 1987 336 p
Avail: Univ. Microfilms Order No. DA8803207

Finite element analysis is used to model the mechanics of hydrogen embrittlement at a crack tip. In the case of non-hydride forming systems, hydrogen diffuses to the vicinity of the crack tip and affects the elastic-plastic behavior of the materials. In addition, the state of stressing modifies the diffusion paths. Large deformation elastic-plastic analysis at a blunting crack tip coupled with hydrogen diffusion in the material has been carried out to study the mechanics of the phenomenon. The results show that hydrogen can accumulate at microstructural defects-traps at much larger concentrations than at normal interstitial lattice sites. In this context the mechanics of hydrogen related fractures is assessed. In the case of hydride forming systems, combined mechanical effects and hydrogen diffusion cause hydride precipitation at the crack tip. The hydrogen transport along with the stress-induced hydride formation has been modeled in an elastically deforming two-phase composite material. The size, shape, amd density of the hydride zone was predicted. The result is used to explain the substantial reduction of fracture resistance in those materials.
Dissert. Abstr.

N89-11001# Argonne National Lab., Ill.
METHODOLOGIES FOR PREDICTION OF METAL OXIDATION-VAPORIZATION-EROSION
Y. Y. Liu and K. Natesan Dec. 1987 113 p
(Contract W-31-109-eng-38)
(DE88-013623; ANL/FE-88-2) Avail: NTIS HC A06/MF A01

High-temperature oxidation (or more generally, corrosion) and solid-particle erosion both involve the action of the environment on the near-surface region of materials. The interaction in oxidation/corrosion is primarily chemical and physical; that of erosion, which involves the transfer of kinetic energy of the erodent particles to the target materials, is principally mechanical. Sustained oxidation and erosion, acting alone or in combination, can cause serious damage to materials and are the major modes of degradation for components used in a variety of fossil energy systems. Numerous studies have been conducted in the past on oxidation, as well as on solid-particle erosion, of metals and alloys. However, very few studies have examined the fundamental aspects of oxidation-erosion, especially in regimes where the two modes act synergistically. This report documents recently developed models for the synergistic interaction of oxidation and erosion of metals and alloys. The models consider three competing processes: oxide scale thickening via growth, thinning via vaporization, and erosion. It has been demonstrated that not only do the models numerically reproduce the general features of oxidation-erosion observed in the few reported experiments on pure metals and alloys, but they also provide considerable insight into the conditions under which one mode (oxidation or erosion) can become dominant over the other. The approach enables the identification of oxidation- or erosion-dominant regimes for future experiments, and aids in the prediction of metal consumption as a function of exposure conditions.
DOE

N89-11002# Joint Publications Research Service, Arlington, Va.
JPRS REPORT: SCIENCE AND TECHNOLOGY. USSR: MATERIALS SCIENCE
4 Apr. 1988 37 p Transl. into ENGLISH from various Russian articles
(JPRS-UMS-88-007) Avail: NTIS HC A03/MF A01

Materials science topics are discussed. Fatigue testing of composite materials, protective coatings, corrosion resistance, heat treatment of metals, and welding are among the topics covered. For individual titles, see N89-11003 through N89-11006.

N89-11003# Joint Publications Research Service, Arlington, Va.
METHODOLOGY OF FLEXURAL FATIGUE TESTING COMPOSITE MATERIALS PRODUCED BY ELECTRON-BEAM EVAPORATION Abstract Only **c24**
Yu. F. Lugovskiy *In its* JPRS Report: Science and Technology. USSR: Materials Science 4 Apr. 1988 p 1 Transl. into ENGLISH from Problemy Spetsialnoy Elektrometallurgii (Kiev, USSR), no. 4, Oct. - Dec. 1987 p 61-65 (For primary document see N89-11002 02-26)
Avail: NTIS HC A03/MF A01

In order to determine the dependence of the endurance limit of dispersion-reinforced composite condensate materials for coatings produced by electron-beam vacuum evaporation on the volume fraction of the reinforcing phase, it has been necessary to develop a special methodology of flexural fatigue testing. Since standard specimens with variable cross-section cannot be produced on account of the very small coating thickness, coating specimens are mounted in cantilever fashion in an elastic vibrator beam-clamp of known stiffness. The test procedure involves high-frequency resonance loading, an appreciable acceleration of life tests being feasible with loading at frequencies of 300 to 20,000 Hz. Testing in the second vibration mode allows use of shorter coating specimens than for testing in the third mode, with the clamp preferably vibrating in a mode close to the first one. The methodology, theoretically validated experimentally in approximate but reliable determination of sigma sub minus 1 equals f (percent V) and sigma equals f(N) curves for a series of condensate composites consisting of a Cu matrix with disperse MeX reinforcing particles.
Author

N89-11004# Joint Publications Research Service, Arlington, Va.
CHARACTERISTICS OF LASER BEAM FOCUSING WITH SINGLE SPHERICAL MIRRORS DURING LASER TREATMENT Abstract Only **c36**
A. G. Borkin, S. V. Drobyazko, G. A. Kosheleva, Yu. V. Pavlovich, Yu. M. Senatorov, V. A. Fromm, and I. V. Kurchatov *In its* JPRS Report: Science and Technology. USSR: Materials Science 4 Apr. 1988 p 8 Transl. into ENGLISH from Avtomaticheskaya Svarka (Kiev, USSR), no. 11, Nov. 1987 p 55-57 (For primary document see N89-11002 02-26)
Avail: NTIS HC A03/MF A01

Focusing of a laser beam with a single spherical mirror is analyzed, such a mirror being combined with a rotatable annular plane mirror in a coaxial configuration. Its focal length must be sufficiently large to ensure adequately high power density and to avoid shielding. When the distance from mirror to laser cavity is too large, then the laser beam may degenerate into a nonannular one and its focusing without loss may become unattainable. Tilting the spherical mirror will make this possible, even when the laser beam is not annular, if astigmatism as well as spherical aberration are minimized. Such a focusing mirror made of metal is theoretically shown to be much more effective than a focusing lens made of KC1 crystal; this has been confirmed experimentally in a CO sub 2 laser facility for perforation of tubular seperator meshes.
Author

N89-11005# Joint Publications Research Service, Arlington, Va.
EFFECT OF PROTECTIVE COATINGS ON LIFE OF HEAT-RESISTANT NICKEL STEEL UNDER CYCLIC HEAT LOAD Abstract Only **c27**
G. N. Tretyachenko, G. R. Semanov, K. Yu. Yakovchuk, R. I. Kuriat, I. S. Malashenko, A. A. Rabinovich, and N. P. Vashchilo *In its* JPRS Report: Science and Technology. USSR: Materials Science 4 Apr. 1988 p 15 Transl. into ENGLISH from Problemy Prochnosti (Kiev, USSR), no. 12, Dec. 1987 p 3-7 (For primary document see N89-11002 02-26)
Avail: NTIS HC A03/MF A01

An experimental study of fireproof coatings on heat-resistant high-chromium nickel steel for gas-turbine blades was made, its purpose being to evaluate their effect on the fatigue resistance of this steel under cyclic heat load in an atmosphere containing products of diesel fuel combustion with up to 0.25 percent sulfur. Two multimetal coating materials Co-Cr-Al-Y and Ni-Co-Cr-Al-Y as well as a double-layer composite material Co-Cr-Al-Y-ZrO sub 2 Y sub 2 O sub 3 (25 to 70 micrometers thick layer of tetragonal + monoclinic Zr sub 2 stabilized by addition of Y sub 2 O sub 3) were tested, having been deposited on prismatic wedges of that steel by the electron-beam vaporization and vacuum condensation process. For comparison, bare wedges were also tested in the

same manner. Thermal cycling was done in three separate tests, with the maximum temperature 980 C, 1000 C, 1020 C (pressure 500 MPa) respectively. The life wedges were found to be extended by the coatings in tests with lower maximum temperature. Microstructural examination under MIM-7 and Neophot-2 optical microscopes, X-ray spectral phase analysis in a Cameca microanalyzer, and microhardness measurements with a PMT-3 tester under a 50 g load have revealed that the ceramic layer provides high erosion resistance only, while the metal layer provides the fatigue resistance and is where cracks originate at high temperature. Author

N89-11006# Joint Publications Research Service, Arlington, Va.
ALLOYING OF METALS BY TEATMENT WITH NANOSECOND LASER PULSES Abstract Only
A. M. Markeyev, V. N. Nevolin, and V. Yu. Fominskiy *In its* JPRS Report: Science and Technology. USSR: Materials Science 4 Apr. 1988 p 22 Transl. into ENGLISH from Fizika i Khimiya Obrabotki Materialov (Moscow, USSR), no. 5, Sep. - Oct. 1987 p 14-23 (For primary document see N89-11002 02-26)
Avail: NTIS HC A03/MF A01

Surface alloying of metals and steels by treatment with nanosecond laser pulses, resulting in formation of new metastable alloys in the surface layer, is evaluated on the basis of experimental studies of five binary systems. These are implantation of Sn film in Mo, Cr and 20Cr13 steel matrices, implantation of Fe film in Cu matrix, and implentation of Au film in Ni matrix. While Sn is thermophysically very different from Mo, Cr, and 20Cr13 steel, Fe is thermophysically similar to Cu and Au is not only thermophysically but also thermodynamically similar to Ni. Laser radiation of lambda equals 1.06 microns wavelength was used for implantation and the surface layers were then analyzed by the method of Mossbauer electron spectroscopy. The results indicate the feasibility of producing metastable alloys even when the components differ thermophysically and thermodynamically, the mechanism involving vaporization and plasma formation with subsequent diffusive or convective interaction of ionized hot implant vapor and the matrix surface layer. Irradiation through a transparent coating was found to raise the efficiency of this process. Author

N89-11007# Utah Univ., Salt Lake City.
LIGAND INTERMEDIATES IN METAL CATALYZED REACTIONS Technical Report: Third Budget Year
J. A. Gladysz 1 Apr. 1988 18 p
(Contract DE-FG02-85ER-13411)
(DE88-012123; DOE/ER-13411/3) Avail: NTIS HC A03/MF A01

A progress report is presented in which a new method for the activation of metal-bound methyl groups and the oxidative disproportionation of coordinated ethylene and methane are discussed. Also considered in the report is the divergent kinetic and thermodynamic acidity in organotransition metal hydride complexes and the synthesis, structure, and reactions of chiral rhenium vinylidene complexes. DOE

N89-11008# Argonne National Lab., Ill. Materials Science Div.
LASER RAMAN SPECTROSCOPY OF ANODIC CORROSION AND INHIBITOR FILMS ON IRON AND NICKEL
C. A. Melendres, T. Tipton, and N. Camillone, III 1988 3 p Presented at the 11th International Conference on Raman Spectroscopy, London, United Kingdom, 5 Sep. 1988
(Contract W-31-109-eng-38)
(DE88-009958; CONF-880950-1) Avail: NTIS HC A02/MF A01

Recent results are reported from studies of corrosion films formed on iron in phosphate and chromate solutions as well as inhibitor films formed on nickel in an acidic chloride environment. The surface films were prepared by constant potential electrolysis in 0.1 M solutions of the appropriate salt, then examined in-situ and ex-situ. The spectrometer consisted of a SPEX model 1403 double monochromator fitted with a photomultiplier tube detector. Excitation was by the use of a Coherent Radiation model CR6 Ar(+) laser using the 514.5 nm line at power levels between 50 and 150 mW. DOE

N89-11009# Comision Nacional de Energia Atomica, Buenos Aires (Argentina).
INFLUENCE OF MARTENSITIC PHASE IN ABRASION BEHAVIOUR OF STAINLESS STEEL 304 L [INFLUENCIA DE LA FASIA MARTENSITICA EN EL COMPORTOMIENTO EL DESGASE ACERO INOXIDABLE 304 L]
J. Ruzzante, P. Alvarez, A. Hey, G. D. Gestido, J. H. Vosen, and H. A. Fernandez 1986 19 p In SPANISH Presented at the 41st Annual Congress of the Brazilian Association of Metals, Sao Paulo, Brazil, 9 Nov. 1986
(DE88-702770; INIS-BR-1072; CONF-8611238) Avail: NTIS HC A03/MF A01

Abrasion behavior is studied in commercial stainless steels of different standardized class composition. The work achieved is guided by the structural analysis of the surface coating formed and its relation with abrasion variables, load and velocity, The abrasion is made at high velocity with abrasion and temperature variation registered on the piece being tested. The abrasion zone is studied under scanning electron microscope. The deformed surface area is studied relating its microstructure profile to its microhardness. DOE

N89-11010# Los Alamos National Lab., N. Mex. Center for Materials Science.
CALORIMETRY STUDY OF THE SYNTHESIS OF AMORPHOUS NI-TI ALLOYS BY MECHANICAL ALLOYING
R. B. Schwarz and R. R. Petrich 1988 32 p Presented at the International Conference on Solid State Amorphizing Transformations, Los Alamos, N. Mex., 10 Aug. 1988
(Contract W-7405-eng-36)
(DE88-006468; LA-UR-88-427; CONF-880837-1) Avail: NTIS HC A03/MF A01

We synthesized amorphous Ni33Ti67 alloy powder by ball milling: (1) a mixture of elemental nickel and titanium powders, and (2) powders of the crystalline intermetallic NiTi2. We characterized the reaction products as a function of ball-milling time by differential scanning calorimetry and X-ray diffraction. The measurements suggest that in process (1) the amorphous alloy forms by a solid-state interdiffusion reaction at the clean Ni/Ti interfaces generated by the mechanical attrition. In process (2), the crystalline alloy powder stores energy in the form of chemical disorder and lattice and point defects. The crystal-to-amorphous transformation occurs when the stored energy reaches a critical value. The achievement of the critical stored energy competes with the dynamic recovery of the lattice. DOE

N89-11011# Pennsylvania Univ., Philadelphia. Dept. of Materials Science and Engineering.
ATOMISTIC STUDIES OF GRAIN BOUNDARIES IN ALLOYS AND COMPOUNDS Progress Report, Jul. 1987 - Jun. 1988
V. Vitek Feb. 1988 7 p
(Contract DE-FG02-87ER-45295)
(DE88-011939; DOE/ER-45295/1) Avail: NTIS HC A02/MF A01

In this research project we investigate the atomic structure and atomic level processes which occur at grain boundaries in binary alloys, both disordered and ordered. Atomistic, computer simulation studies of grain boundaries are carried out with the aim to elucidate the differences in structure, cohesion and, in general, physical and mechanical properties of boundaries in alloys when compared with those in pure materials. Until now most atomistic computer simulations utilized empirically constructed pair-potentials to describe interatomic forces. This is adequate when studying those structural aspects which are general, common to boundaries in various metals and alloys, and do not involve electronic, chemical and cohesive properties. An example is the investigation of those differences between boundaries in pure f.c.c. metals and L1 sub 2 compounds that are related to the ordering tendency, which have been made as a part of this project. However, development of the studies of grain boundaries beyond purely structural considerations requires a more fundamental description of atomic interactions. For this reason we have concentrated at this stage upon the development of physically justified and

adequate descriptions of atomic interactions. Two different approaches have been followed. First, empirical many-body potentials are being constructed for binary alloys and, secondly, a quantum mechanically based tight binding method for treating extended lattice defects such as grain boundaries is being developed. DOE

N89-11012# Los Alamos National Lab., N. Mex.
MICROSTRUCTURE AND PROPERTIES OF RAPIDLY SOLIDIFIED BERYLLIUM-TRANSITION METAL ALLOYS
Loren A. Jacobson and Sherri Richardson 1988 11 p Presented at the 2nd International SAMPE Metals and Metals Processing Conference, Dayton, Ohio, 2 Aug. 1988
(Contract W-7405-eng-36)
(DE88-010937; LA-UR-88-1586; CONF-880855-2) Avail: NTIS HC A03/MF A01

Alloys of beryllium with small amounts of Ti, Zr and Y (1 to 3 wt percent) were rapidly solidified using an arc hammer splat technique. Each of these elements forms a dilute eutectic with beryllium, and has very low solid solubility in the alpha phase. In the case of Ti, the Be-rich compound is TiBe sub 12, and for Zr and Y, the compound is MBe sub 13. The objective of the work was to achieve a fine, uniform dispersion of particles of the intermetallic compound. Since these compounds have very high melting points, it was expected that rapidly solidified microstructures would be relatively stable at elevated temperatures. This microstructural stability should result in improved high temperature properties for the alloys. Microstructures have been characterized using optical, scanning and transmission electron microscopy. Microhardness measurements have been made in order to determine the effects of rapid solidification and to evaluate the effects of high temperature exposure on microstructural stability and property retention. The results will be presented in light of the potential of these alloys for intermediate temperature application. DOE

N89-11013# Sandia National Labs., Albuquerque, N. Mex. Surface Science Div.
THE CATALYTIC, STRUCTURAL, AND ELECTRONIC PROPERTIES OF STRAINED-METAL OVERLAYERS
D. W. Goodman 1988 7 p Presented at the Symposium on Preparation and Characterization of Catalysts, Los Angeles, Calif., 25 Sep. 1988
(Contract DE-AC04-76DP-00789)
(DE88-007932; SAND-88-0750C; CONF-880939-1) Avail: NTIS HC A02/MF A01

The present studies are part of a continuing effort to identify those properties of bimetallic systems which can be related to their superior catalytic properties. A pivotal question to be addressed of bimetallic systems (and of surface impurities in general) is the relative importance of ensemble (steric or local) versus electronic (nonlocal or extended) effects in the modification of catalytic properties. A complete understanding of surface impurity effects (including alloying) in catalysis will likely include components of both electronic and ensemble effects, the relative importance of each to be assessed for a given reaction and reaction conditions. An emphasis of our research has been to address the importance of these two effects regarding the influence of alloying and surface additives on surface reactions. Systems discussed are Cu/Ru and Ni/W. DOE

N89-11014# Lawrence Livermore National Lab., Calif.
DEVELOPMENTS AND TRENDS IN ELECTRODEPOSITION
J. W. Dini 30 Mar. 1988 10 p Presented at the 2nd International SAMPE Metals and Metals Processing Conference, Dayton, Ohio, 2 Aug. 1988
(Contract W-7405-eng-48)
(DE88-009822; UCRL-97328; CONF-880855-1) Avail: NTIS HC A02/MF A01

Electrodeposition is a very important technology. Covering inexpensive and widely available base materials with a thin (typically 0.1 to 10 mm) coating with specific properties extends their use to applications which otherwise would have been prohibitively expensive. Furthermore, the ability to provide property control in coatings as thick as 10 mm adds further value to this important technique of surface modification. In recent years a number of advances in areas such as composite plating, pulse plating and high speed plating have added further credence to the use of electrodeposition as a viable coating technology. This paper will review these branches of the industry and discuss future trends. DOE

N89-11015# California Univ., Berkeley. Lawrence Berkeley Lab.
WELDABILITY OF 2090 Al-Cu-Li ALLOY
A. J. Sunwoo and J. W. Morris, Jr. Apr. 1988 24 p Presented at the American Welding Society Meeting, New Orleans, La., 18 Apr. 1988
(Contract DE-AC03-76SF-00098)
(DE88-011963; LBL-25022; CONF-8804142-2) Avail: NTIS HC A03/MF A01

The weldability of 2090 was studied along with the metallurgical changes associated with welding and aging. Autogenous bead-on-plate welds are produced using two different base metal tempers, as-received condition (T3) and peak-aged condition (T8) and two different welding processes, gas tungsten arc welding (GTAW) and electron beam welding (EBW). The optimum aging condition is determined for the EB and GTA weldments. The results of weldability and aging studies indicate that the best aging temperature for the base metal and EB weldments is 160 C, which results in a 75 percent joint efficiency and for the GTA weldment is 190 C, which produces a 55 percent joint efficiency. Aging at 230 C leads to a serious deterioration in the properties. The distribution of precipitates in the fusion zone appears to be the primary factor in controlling the weldment strength and elongation. DOE

N89-11016# Argonne National Lab., Ill.
BRILLOUIN SCATTERING: ITS APPLICATION TO THE STUDY OF DAMAGE AND AMORPHIZATION
M. Grimsditch, R. Bhadra, K. Gray, R. T. Kampwirth, P. Okamoto, J. Pearson, and L. Rehn Feb. 1988 11 p Presented at the 8th General Conference of the Condensed Matter Division, European Physical Society, Budapest, Hungary, 6 Apr. 1988
(Contract W-31-109-eng-38)
(DE88-012053; CONF-880432-1) Avail: NTIS HC A03/MF A01

A brief review of Brillouin scattering is made emphasizing its advantages and disadvantages over conventional ultrasonic techniques. One of its advantages is that the elastic properties of very thin films (approx. 1 micron) can be investigated. The authors have used this technique to study changes in shear elastic constants of materials irradiated with high energy ions. These particles only penetrate approx. 1 micron into the material but produce very high defect concentrations which, in certain cases, can lead to amorphization. In Nb3Ir and Zr3Al very large changes are observed before the onset of amorphization, while in Si the changes occur concomitantly with amorphization. The significance of the hardening observed in Zr3Al when it becomes amorphous will be discussed. DOE

N89-11017# Sandia National Labs., Albuquerque, N. Mex.
NITRIDE LAYER GROWTH IN IRON AND TITANIUM ALLOYS: STUDIES BY ELECTRON PROBE MICROANALYSIS
A. D. Romig, Jr., R. E. Semarge, E. Metin, and O. T. Inal (New Mexico Inst. of Mining and Technology, Socorro.) 1988 21 p Presented at the MAS/EMSA Microbeam Analysis Conference, Milwaukee, Wis., 7 Aug. 1988
(Contract DE-AC04-76DP-00789)
(DE88-007207; SAND-88-0662C; CONF-880841-4) Avail: NTIS HC A03/MF A01

The present study addresses the surface hardening of Fe and Ti by plasma nitriding. The work describes quantitative electron probe microanalysis of the nitride layers and composition gradients which form during the nitriding process in iron (600 C) and titanium (800 to 1080 C). Such measurements are the key to developing quantitative diffusion models for the nitriding reaction which are

necessary to optimize the nitriding process (e.g., prediction of microstructural evolution as a function of time and temperature). It is the objective of the present work to develop the quantitative electron probe microanalysis (EPMA) techniques to determine the compositions of Fe and Ti nitrides and to measure concentration gradients of N in metallic phases of Fe and Ti. DOE

N89-11018# Michigan Univ., Ann Arbor. Dept. of Nuclear Engineering.
THE ROLE OF GRAIN BOUNDARY CHARACTER IN THE ENVIRONMENTALLY-ASSISTED INTERGRANULAR CRACKING MECHANISM OF NICKEL-BASE ALLOYS Progress Report, 1 Aug. 1987 - 31 Jul. 1988
G. S. Was Jul. 1988 28 p
(Contract DE-FG02-85ER-45184)
(DE88-014130; DOE/ER-45184/4) Avail: NTIS HC A03/MF A01

Grain boundary chemistry and structure of high-purity Inconel 690- type alloys (carbon doped) were studied. Heat treatments were carried out to assess the modified (for alloy 690) DEPLETE code. Chromium depletion profiles were measured. Grain boundary orientation will be measured using electron channeling. Constant elongation note tests were conducted to evaluate the dependence of IGSCC susceptibility on grain boundary chemistry. Effects of hydrogen on grain boundary fracture was studied as a function of grain boundary structure, temperature and alloy composition (Ni, alloy 600, alloy 690). DOE

N89-11019# Pacific Northwest Labs., Richland, Wash. Materials Science Dept.
NEAR SURFACE CHEMISTRY AND CORROSION BEHAVIOR OF EXCIMER LASER SURFACE-MELTED AISI TYPE 304 STAINLESS STEEL
D. R. Baer, D. J. Frydrych, and T. R. Jervis (Los Alamos National Lab., N. Mex.) May 1988 13 p Presented at the Symposium on Environmental Degradation of Ion and Laser Beam Treated Surfaces, Chicago, Ill., 25 Sep. 1988
(Contracts W-7405-eng-36; DE-AC06-76RL-01830)
(DE88-014440; LA-UR-88-1960; CONF-8809107-1) Avail: NTIS HC A03/MF A01

The effects of excimer laser surface melting on the near-surface chemistry, and corrosion behavior of AISI 304 stainless steel have been examined as a function of total energy deposited on the specimen. The surface chemistry resulting from the laser treatments has been examined using Auger electron spectroscopy. Electrochemical methods were used to monitor the corrosion behavior of the specimens in deaerated 0.1 M NaCl. Electron microscopy was used to characterize the extent of local corrosion of the specimens. Laser treatment was observed to increase the chromium concentration of the surface oxide and to reduce the number of pits. Two types of pits were observed on untreated material, but only one type of pit occurred after laser treatment. DOE

N89-11020# Centre d'Essais Aeronautique Toulouse (France). Section des Essais Mecaniques.
CREEP TESTS FOR SLOW AND FAST FATIGUE CONDITIONS ON ALUMINUM ALLOY SPECIMENS [ESSAIS DE FLUAGE DE FATIGUE LENTE ET RAPIDE SUR DES EPROUVETTES EN ALLIAGES D'ALUMINIUM]
27 Feb. 1987 69 p In FRENCH
(Contract STPA-437103/79)
(Rept-M0-535200; ETN-88-93321; Rept-437103/79) Avail: NTIS HC A04/MF A01

Tests were performed to evaluate the performance of aluminum alloys used in supersonic aircraft construction, as well as riveted joints assemblied with titanium alloy rivets. The creep tests were carried out at temperatures from 80 to 120 C. Results show acceptable values in the case of fatigue and fast fatigue tests, while the behavior of creep normal specimens is anomalous. The test conditions are discussed. ESA

N89-11021# Air Force Inst. of Tech., Wright-Patterson AFB, Ohio.
CHARACTERIZATION OF METALLIC COATINGS AND THIN FILMS PRODUCED BY RAILGUN DEPOSITION M.S. Thesis
Russell J. DeLuca 1988 95 p
(AD-A196382; AFIT/CI/NR-88-77) Avail: NTIS HC A05/MF A01 CSCL 11C

This project was an investigative and exploratory study into the use of a railgun material accelerator as a deposition tool. The railgun system was powered by new technology quick pulse capacitance discharge banks. These banks were capable of discharging up to 35 kJ of energy in less than 100 microseconds. Given such an energetic process, the goal was to produce unique depositions, and novel materials or coatings not readily produced by other commercial techniques. The study included over 150 discharges of the open bore railgun employing some 15 different metallic material systems. In addition, the machine hardware was modified for improvement throughout the entire investigation. In the systems final configuration, it was capable of producing two distinct types of depositions, relatively thick deposits with a graded structure, and very thin metallic films with a uniform structure. The latter, production of thin films by railgun deposition, is a new evolutionary technique. GRA

N89-11022# Army Belvoir Research and Development Center, Fort Belvoir, Va.
CONTROL OF ENVIRONMENT ASSISTED CRACKING OF Al 7075 USING INHIBITORS Final Report, Apr. 1983 - Jan. 1985
Donovan Harris and Dario A. Emeric May 1988 43 p
(AD-A196387; BRDEC-2464) Avail: NTIS HC A03/MF A01 CSCL 11F

This report is the second of three and summarizes the program of the Chemistry Research Division to formulate an inhibitor for high strength aluminum alloys against environment assisted cracking. Presented are the effects on the electrochemical and fatigue properties by various acid rain analogs, surface pretreatment, wetting agents, and different inhibitor formulas. The program was able to produce 6 candidate formulas for use against environment assisted cracking, and 12 formulas for use as general corrosion inhibitors. GRA

N89-11023# Defense Logistics Agency, Alexandria, Va.
STATE-OF-THE-ART-DEHUMIDIFICATION COST-EFFECTIVE CORROSION PREVENTION
Craig S. Laurent Jun. 1988 55 p
(AD-A196503) Avail: NTIS HC A04/MF A01 CSCL 11F

Moisture-induced corrosion significantly degrades spare parts and material readiness. It increases life cycle and maintenance support costs. Corrosion can be in the form of rust, water stains, mold, mildew or other types of organic and inorganic degradation. Corrosion reduces productivity - of people and of resources. The cost of corrosion to the U.S. economy is tremendous. It is estimated that some $2 to 4 billion in corrosion damage occurs annually in each of the individual U.S. Military Services. Protective coatings are widely used to protect against moisture-induced corrosion. Properly used, protective coatings such as paint or other topical coatings can be moderately effective in reducing corrosion and protecting against its impacts. GRA

N89-11024# Aeronautical Research Labs., Melbourne (Australia).
A TEST METHODOLOGY FOR AN INVESTIGATION INTO HEATING AND COOLING PHENOMENA IN GROSSLY DEFORMED TENSILE METALLIC BARS
L. Molent and S. Dunn Dec. 1987 39 p
(AD-A197047; ARL-Struc-TM-482; DODA-AR-004-595) Avail: NTIS HC A03/MF A01 CSCL 11F

The coupling between mechanical deformation and thermal energy in an elastic material, known as the thermoelastic effect, was first documented by Gough in 1805, who observed that the material experienced a change in temperature during elongation. More recently, investigation of the phenomenon of energy exchange in metals has been extended into the plastic regime, where a

material experiences heating after the elastic limit has been exceeded, i.e., the thermoplastic effect. It is proposed to measure the local temperature, strain and cross-sectional area of various specimens undergoing adiabatic elastoplastic deformation, and to deduce the local stress. These parameters are necessary if the relationship between the measured temperature and the dissipated and available energies is to be determined. Of the available devices for minute temperature measurements, namely thermistors and infra-red detectors, the latter were chosen for this work. GRA

27 NONMETALLIC MATERIALS

Includes physical, chemical, and mechanical properties of plastics, elastomers, lubricants, polymers, textiles, adhesives, and ceramic materials.

For composite materials see *24 Composite Materials.*

N89-11025# Georgia Inst. of Tech., Atlanta.
THE EFFECT OF CARBON AND BORON NITRIDE ADDITIONS ON THE FRACTURE TOUGHNESS OF SI3N4
A. H. Gorin May 1988 17 p
(Contract DE-AC05-84OS-21400)
(DE88-013249; Y/DV-724) Avail: NTIS HC A03/MF A01

Silicon nitride has long been an attractive high-temperature material, and its consideration for implementation in engine construction has placed a premium on the development of improved mechanical properties. The experiments performed here have a dual objective: (1) to observe the effect of low-level carbon (less than 2 percent) and boron nitride (less than 10 percent) additions on the fracture toughness of silicon nitride, and (2) to provide a foundation for possible microwave study of the material. All specimens were prepared by hot-pressing the heat-treated powders, using graphite dies and rams with conditions of approximately 1800 C, approximately 30 to 50 min., and pressure of approximately 2500 psi (approximately 17.2 MPa). Boron nitride, or grafoil, was used as a die release agent. Sections of each specimen were analyzed by X-ray diffraction, examined by scanning electron microscopy (SEM), evaluated for density, and mounted and polished for further study. To determine the toughness and hardness of each mounted-and-polished sample, a method incorporating the Vickers' indent size to crack length relationship provided by Oak Ridge National Laboratory was utilized. Results are presented and discussed. DOE

N89-11026# Oak Ridge National Lab., Tenn. Metals and Ceramics Div.
CRYSTALLIZATION OF Zr-Ni METALLIC GLASSES
C. G. McKamey, D. M. Kroeger, D. S. Easton, and J. A. Horton 1988 3 p Presented at the MAS/EMSA Microbeam Analysis Conference, Milwaukee, Wis., 7 Aug. 1988
(Contract DE-AC05-84OR-21400)
(DE88-007481; CONF-880841-5) Avail: NTIS HC A02/MF A01

The results of our study of the crystallization processes of Zr-Ni metallic glasses between 55 and 70 percent Zr, combined with the results of low-temperature specific heat measurements, indicate that the glass structures of these alloys are characterized by short range orderings (SROs) which are similar to, or which promote the formation of, the crystalline phases to which they transform. Glasses of 60 and 66.7 percent Zr transform rapidly to the metastable and Zr sub 2 Ni phases, respectively, as evidenced by a single sharp differential scanning calorimetry (DSC) exotherm. This indicates that their SROs are similar to the metastable and Zr sub 2 Ni phases, respectively, and that little diffusion in the glass is necessary for crystallization to proceed. However, as-quenched glasses between these compositions (around the eutectic) possess SROs characteristic of both phases. Individual areas of similar SRO, produced by phase separation during the quench from the liquid, must grow together (requiring diffusion of atoms) in order for crystallization to proceed. Evidence for the presence of a metastable phase centered at a composition of 60 percent Zr, plus the presence of an equilibrium phase at 66.7 percent Zr (Zr sub 2 Ni), both within 3.5 percent of the eutectic at approximately 63.5 percent Zr, lends feasibility to this hypothesis. DOE

N89-11027# Pennsylvania Univ., Philadelphia. Dept. of Materials Science and Engineering.
LOW STRESS BRITTLE FRACTURES IN POLYMERS Progress Report, 1 Aug. 1987 - 1 Aug. 1988
Norman Brown 1988 8 p
(Contract DE-FG02-84ER-45161)
(DE88-014236; DOE/ER-45161/T1) Avail: NTIS HC A02/MF A01

The results of the effect of molecular parameters show: (1) that crack resistance varies as (M sub w - M sub o) for PE where M sub w is weight average molecular weight and M sub o - 20,000; (2) butyl branches are more effective than ethyl; (3) crack resistance increases with branch density; and (4) there is an unknown factor that increases crack resistance even if molecular weight and branch density is the same. Fundamental parameters such as the stress distribution on the boundary of the process zone can now be measured. The activation energy of slow crack growth for different types of polyethylene range from 83 to 115 KJ/mol. The basic research data is being applied toward the prediction of the life-time of the 200,000 miles of polyethylene gas pipe that is now in service in the United States. DOE

N89-11028# Arizona State Univ., Tempe. Dept. of Physics.
SURFACE STRUCTURES AND REACTIONS OF CERAMICS AND METALS Progress Report, 1 Dec. 1985 - 30 Nov. 1988
J. M. Cowley Jun. 1988 22 p
(Contract DE-FG02-86ER-45228)
(DE88-013752; DOE/ER-45228/37) Avail: NTIS HC A03/MF A01

Several novel techniques using electron microscopy instruments, as well as standard techniques, have been applied to the study of the surfaces of ceramic oxides and the interaction of thin films and small particles of metals with the oxide surfaces. Reactions of thin metal films with cleavage surfaces of MgO have shown a strong dependence on the preparation of the surface, the temperature of deposition and the amount of electron irradiation by the incident beam. Small metal particles of oxide supports such as occur in supported catalyst systems, have been shown by use of microdiffraction to be epitaxed on the crystallites of the oxide support. Some show unusual crystalline forms, as in the case of the faulted body-centered-cubic crystals of Ru in Ru-Au bimetallic catalysts, or else a variety of states of oxidation. Electronic excitations of supported metal particles are strongly influenced by the form and composition of the support. In reflection diffraction and electron energy loss analysis from extended crystal surfaces, particular diffraction conditions give rise to surface channelling phenomena so that the observations are dependent on the structure and composition of the surface layers of atoms, providing the basis for new surface analysis techniques which may be correlated with high resolution. DOE

N89-11029# Argonne National Lab., Ill. Materials and Components Technology Div.
CHARACTERIZATION OF CERAMIC FILMS AND INTERFACES BY ELECTRON MICROSCOPIC AND SPECTROSCOPIC TECHNIQUES
A. Erdemir and C. C. Cheng 1988 31 p Presented at the Electron Microscopy of Surfaces and Interfaces, Oak Brook, Ill., 16 May 1988
(Contract W-31-109-eng-38)
(DE88-011957; CONF-8805152-1) Avail: NTIS HC A03

In this study, Auger Electron Spectroscopy (AES) in combination with inert gas ion milling and cross-sectional transmission electron microscopy (XTEM) were employed to investigate the chemical and microstructural characteristics of a TiN film on a M50 steel and the film-substrate interfaces formed during ion plating at 100 C and 500 C deposition temperatures. The results of both analytical techniques indicated that the coating produced at 100 C was composed of a thin Ti layer (approximately 1000 A) and a thick

TiN layer. Upon vacuum annealing at 500 C for 45 minutes, it was found that the Ti rich interlayer was transformed into a TiC phase. The coating produced at 500 C consisted of a thin TiC and a relatively thick TiN layer. Ion plating as well as post vacuum annealing at 500 C resulted in grain growth and reduced defect density. DOE

N89-11030# Mound Lab., Miamisburg, Ohio.
GLASS-CERAMIC FUSION WITH A CO2 LASER
Lauri Jean DeVore and Jonathan H. Mohler 1988 7 p Presented at the Medical and Material Processing Applications of Various Types of Lasers, Cincinnati, Ohio, 21 Apr. 1988
(Contract DE-AC04-76DP-00053)
(DE88-012871; MLM-3497(OP); CONF-8804159-1) Avail: NTIS HC A02/MF A01

Glass-to-ceramic sealing is possible with a carbon dioxide laser. Wetting of the ceramic by the glass is an important factor. It is necessary to either pre-coat the substrate with the sealing glass, or allow the substrate to remain hot in the sealing region for sufficient time for good wetting. Glass composition, substrate thickness, laser beam power density and scan rate all must be controlled to optimize sealing. Equal heating of the two glass-ceramic interfaces is also critical to uniform seal formation. DOE

N89-11031# Lawrence Livermore National Lab., Calif.
SURVIVABILITY OF COATINGS: PROGRAM REVIEW
J. A. Rathkopf, ed. 11 Mar. 1988 120 p Presented at the Passive Survivability Review Meeting, Livermore, Calif., 8 Dec. 1987
(Contract W-7405-eng-48)
(DE88-009863; UCID-21384; CONF-871298) Avail: NTIS HC A06

This report is a compilation of slightly edited transcripts of remarks presented at the Passive Survivability Review Meeting held December 8, 1987 at Lawrence Livermore National Laboratory (LLNL) by members of LLNL's Survivability of Coatings Program. Topics include: survivability of coatings program; computing X-ray effects in optics; X-ray effects in optics; film deposition and status; damage characterization; and quantitative damage measurements. DOE

N89-11032# Sandia National Labs., Albuquerque, N. Mex.
ELECTRONIC PROPERTIES OF SIGMA-CONJUGATED POLYSILANES
R. G. Kepler 1988 9 p Presented at the International Conference on Science and Technology of Synthetic Metals, Santa Fe, N. Mex., 26 Jun. 1988
(Contract DE-AC04-76DP-00789)
(DE88-012699; SAND-88-0270C; CONF-880669-5) Avail: NTIS HC A02/MF A01

Recent experimental results on charge carrier transport, charge carrier generation and exciton-exciton annihilation in sigma-conjugated polysilanes show that these materials have many interesting properties. The principal conclusions from these studies are: (1) only holes are mobile and in poly(phenyl methyl silane) the transport is non-dispersive with a mobility of 0.0001 sq cm/Vs; (2) charge carrier generation does not occur by band-to-band transitions but by injection from the surface when excitons contact the surface; and (3) singlet excitons are highly mobile in polysilanes and exciton-exciton annihilation is an important process at incident light intensities as low as 100 W/cu cm, if the light is strongly absorbed. DOE

N89-11033# Enerscope, Inc., Glendale, Ariz.
ADVANCED DESICCANT MATERIALS ASSESSMENT, PHASE 2 Final Report, Nov. 1986 - Jan. 1988
R. K. Collier Jan. 1988 73 p
(Contract GRI-5084-243-1089)
(PB88-217054; GRI-88/0125) Avail: NTIS HC A04/MF A01 CSCL 11C

The objective of the research was to quantify the relationships between desiccant matrix heat capacity, heat and mass transfer resistance, desiccant heat of absorption, and desiccant isotherm shape. The approach to the problem was to perform computer simulations of cooling system performance and to maximize that performance with respect to cycle time and regeneration fraction. Regeneration temperature was varied and results were compared to silica gel as a reference. In addition, various computer models were investigated with respect to numerical stability, convergence, ease of use and time of execution. Investigations of computer models resulted in a model with a combination of features found in two other models. One was the program originally developed by SERI and the other was the MOSHMX program developed by Ian McClaine-Cross in Australia. All of the system results were obtained using this model. The superiority of the Type 1M desiccant material over more conventional desiccants was demonstrated. It showed less sensitivity to matrix heat capacity and heat of absorption associated with practically-obtainable materials yielded near-maximum performance. It was also found that heat and mass transfer resistance affects all desiccant materials nearly equally and is not considered to be an important problem limiting system performance. GRA

N89-11034# Oak Ridge National Lab., Tenn.
MULTISTRESS AGING OF POLYMER FILMS
C. R. Brinkman and H. E. McCoy 1988 4 p Presented at the Institute of Electrical and Electronics Engineers Symposium on Electrical Insulation, Boston, Mass., 5 Jun. 1988
(Contract DE-AC05-84OR-21400)
(DE88-008094; CONF-880625-1) Avail: NTIS HC A02/MF A01

An experimental facility has been developed in which polymer film specimens can be simultaneously exposed to mechanical, electrical, and thermal stresses. The test environment is transformer oil at 90 C. The mechanical stress can be varied over a wide range, and the potential is regulated at about one-half the breakdown voltage. The facility can accommodate eight specimens run at the same time at various mechanical stresses, with or without an applied potential. The temperature of all eight specimens must be the same, and the applied potential must either be zero or the same value. DOE

N89-11035# Illinois Univ., Urbana.
INVESTIGATION OF A SELF-LUBRICATING ALUMINA COATING FORMED BY ANODIC SPARK DEPOSITION Ph.D. Thesis
Kent Allen Koshkarian 1988 148 p
(Contract DE-AC02-76ER-01198)
(DE88-014947; DOE/ER-01198/T25) Avail: NTIS HC A08/MF A01

Self-lubricating Al2O3 coatings were deposited with an incorporated second phase of MoS2. The Al2O3 was predominantly alpha phase with small, varying amounts of gamma and beta forms. Amount of gamma-Al2O3 was maximized in coatings deposited at 500 V. The coatings were porous and had variable adherence. The microstructure consisted of intersecting, highly stressed, elongated sets of similarly oriented grains with microcracks at the grain boundaries. Modulation was noted. The microstructure did not change with process parameters. The MoS2 particles were more prevalent in porous, cracked regions. The largest amount of incorporation, found in coatings deposited in 5.0 g/l MoS2 electrolyte, was on the order of 20 to 25 wt percent. The coatings formed in 5.0 g/l MoS2 electrolyte exhibited an approximately 50 percent lower wear rate. Only small amounts of MoO3 were detected. As the first investigation into the process of producing self-lubricating Al2O3 coatings by anodic spark deposition, this study showed promise and also raised several areas for future work. DOE

N89-11036# Sandia National Labs., Albuquerque, N. Mex.
MICROPOROUS POLYMER FOAMS FOR BIOMATERIALS
J. Aubert, A. Sylwester, and P. Rand 1988 9 p Presented at the 196th American Chemical Society National Meeting, Los Angeles, Calif., 25 Sep. 1988
(Contract DE-AC04-76DP-00789)

(DE88-010578; SAND-88-1121C; CONF-880912-5) Avail: NTIS HC A02/MF A01

A variety of microcellular foams were prepared for use in the fabrication of targets for inertial confinement fusion and pulsed driven X-ray lasers. The process consists of three steps. First a polymer and solvent are heated above their critical temperature to achieve a homogenous polymer solution. Next, the solution is quenched in a controlled fashion, usually within a mold. Quenching results in the formation of bi-continuous phases: a polymer-rich phase and a solvent-rich phase. Once phase separation has occurred, the solution can be frozen or alternatively with certain polymers the solution may form a stable gel. In the final step, the solvent is removed by sublimation of the frozen solvent or by liquid extraction of a resulting gel leaving behind a microcellular polymer foam. By controlling the phase separation during the quench, the foam morphology and pore size can be varied. DOE

N89-11037# Tennessee Univ., Knoxville.
CONDUCTIVITY OF ORGANIC POLYMERS: A NONLINEAR APPROACH
M. D. Narten and A. H. Narten (Oak Ridge National Lab., Tenn.) 1988 10 p Presented at the International Conference on Science and Technology of Synthetic Metals, Santa Fe, N. Mex., 26 Jun. 1988
(Contract DE-AC05-84OR-21400)
(DE88-013837; CONF-880669-7) Avail: NTIS HC A02/MF A01

Organic polymers are usually insulators or semiconductors; only after 7 to 30 percent of dopant is added do the materials become conducting. The dopant is not regularly distributed: existing spatial inhomogenuities in the solids become centers of attraction for the dopant, which is then concentrated in conducting areas or zones. A mathematical model is presented in which the conducting regions are considered as conducting zones of various sizes and shapes. These regions are irregularly distributed and imbedded in insulated or semiconducting media, and connected in a nonlinear way. Nonlinear integral equations are derived to describe the conductivity in such materials. Predicted results are in agreement with experimentally measured electric field relaxation curves. DOE

N89-11038*# National Aeronautics and Space Administration. Lewis Research Center, Cleveland, Ohio.
PHASE TRANSFORMATIONS IN XEROGELS OF MULLITE COMPOSITION
Mark J. Hyatt and Narottam P. Bansal (Case Western Reserve Univ., Cleveland, Ohio.) 1988 19 p
(NASA-TM-101349; E-4332; NAS 1.15:101349) Avail: NTIS HC A03/MF A01 CSCL 11C

Monophasic and diphasic xerogels have been prepared as precursors for mullite ($3Al_2O_3$-$2SiO_2$). Monophasic xerogel was synthesized from tetraethyl orthosilicate and aluminum nitrate nanohydrate and the diphasic xerogel from colloidal suspension of silica and boehmite. The chemical and structural evolutions, as a function of thermal treatment, in these two types of sol-gel derived mullite precursor powders have been characterized by DTA, TGA, X-ray diffraction, SEM and infrared spectroscopy. Monophasic xerogel transforms to an Al-Si spinel from an amorphous structure at approximately 980 C. The spinel then changes into mullite on further heating. Diphasic xerogel forms mullite at approximately 1360 C. The components of the diphasic powder react independently up to the point of mullite formation. The transformation in the monophasic powder occurs rapidly and yields strongly crystalline mullite with no other phases present. The diphasic powder, however, transforms rather slowly and contains remnants of the starting materials (alpha-Al_2O_3, cristobalite) even after heating at high temperatures for long times (1600 C, 6 hr). The diphasic powder could be sintered to high density but not the monophasic powder in spite of its molecular level homogeneity. Author

N89-11039# Naval Academy, Annapolis, Md. Dept. of Physics.
LOW FREQUENCY DIELECTRIC PROPERTIES OF POLYETHER ELECTROLYTES Interim Report, 1 Oct. 1987 - 30 Sep. 1988
John J. Fontanella and Mary C. Wintersgill Jun. 1988 34 p
(AD-A196494; TR-33) Avail: NTIS HC A03/MF A01 CSCL 07D

Beyond their interest as fundamental properties of a material, the dielectric constant and loss are of particular significance for ion conducting polymers. For example, the dielectric constant plays a fundamental role in the ability of a polymer to dissolve salts. The reason is that the dielectric constant is a measure of the reduction of Coulomb interactions and thus high dielectric constant fluids greatly reduce ion-ion interactions, inhibiting crystal formation. The dielectric loss is interesting as it probes a wide variety of phenomena including the electrical conductivity along with any relaxations which may be present in the material including that associated with the glass transition. Consequently, it is worth reviewing some of what is known concerning the dielectric properties of these materials. The discussion will be limited to poly(ethylene oxide) (PEO) and poly(propylene oxide) (PPO). GRA

N89-11040# Massachusetts Inst. of Tech., Cambridge. Dept. of Materials Science and Engineering.
NEW NON-LINEAR OPTICAL POLYMERS Final Report, 1 Sep. 1985 - 31 Dec. 1987
Gary E. Wnek Jun. 1988 112 p
(Contract F49620-85-C-0151)
(AD-A196859; AFOSR-88-0688TR) Avail: NTIS HC A06/MF A01 CSCL 20F

The synthesis of a new monomer, N,N-diaminoethyl-4-nitroamiline (DANA), which will be condensed with various diacyl halides to yield polyamides with interesting optical properties was achieved. Several compounds containing potentially electrically leaky atoms between donor (amino) and acceptor (nitro) moieties was prepared. The key finding is that the sulfide is extremely NLO-active. GRA

N89-11041# Aerojet Solid Propulsion Co., Sacramento, Calif. Chemical Research and Development Dept.
ENERGETIC THERMOPLASTIC ELASTOMER SYNTHESIS Quarterly Report No. 3, 1 Nov. 1987 - 31 Jan. 1988
G. E. Manser and R. W. Fletcher 25 Apr. 1988 12 p
(Contract N00014-87-C-0098)
(AD-A196885) Avail: NTIS HC A03/MF A01 CSCL 07F

The objective of our research is to synthesize energetic polyether binders with the ability to undergo reversible physical crosslinking at temperatures compatible with high energy propellant ingredients. Commercially available thermoplastic elastomers fail to meet our criteria because of excessively high processing temperatures and melt viscosity, high modulus and low stress/strain capability. It was proposed to synthesize ABA type block polymers with the A blocks being polymers able to form crystalline structure (as opposed to glasses) having a sharp melting point of 85 to 95 C. GRA

N89-11042# Aerojet Solid Propulsion Co., Sacramento, Calif. Chemical Research and Development Dept.
SYNTHESIS OF ENERGETIC BINDERS Quarterly Report No. 5, 1 Jan. - 31 Mar. 1988
G. E. Manser 25 Apr. 1988 2 p
(Contract N00014-86-C-0164)
(AD-A196886) Avail: NTIS HC A02/MF A01 CSCL 07F

During this reporting period we have optimized the synthesis of the carborane/oxetane monomer reported in our last Annual Report. We studied the effect of using various solvents, temperatures, and leaving groups on the carborane, and different metal salts of 3-hydroxymethyl-3-methyloxstane. Fine tuning of the reaction conditions and improving the isolation method will soon enable large scale synthesis of the monomer. A large lot of the starting carborane is expected soon. We have shown that the

Grignard reagent can be formed from bromopropylcarborane and reacts with the model alkylbromide butylbromide. GRA

N89-11043# Howard Univ., Washington, D. C. Dept. of Chemistry.
IR REFLECTANCE AND RAMAN SCATTERING OF DIAMOND FILMS Annual Technical Report No. 1, 1 Mar. 1987 - 28 Feb. 1988
George E. Walrafen 28 Feb. 1988 35 p
(Contract N00014-87-K-0109)
(AD-A196899) Avail: NTIS HC A03/MF A01 CSCL 07B

A significant amount of the first years work on this contract (ca. 50 percent) involved service work to characterize and evaluate diamond films supplied by other SDIO/IST contractors. The investigative work has involved analysis and interpretation of the features seen from the diamond films supplied by various workers mentioned. GRA

N89-11044# Alabama Univ., Birmingham. Lab. of Molecular Biophysics.
DEVELOPMENT OF ELASTOMERIC POLYPEPTIDE BIOMATERIALS Annual Report, 1 Jun. 1987 - 31 May 1988
Dan W. Urry, Eric Hunter, K. U. Prasad, and Marianna M. Long 25 May 1988 234 p
(Contract N00014-86-K-0402; Proj. RR0-4106)
(AD-A196900) Avail: NTIS HC A11/MF A01 CSCL 07F

The most significant accomplishment of the last year was the first demonstration of mechanochemical coupling (chemo-mechanical transduction) in synthetic polypeptides. The demonstration was achieved, not by copy of a known contractile protein but rather by a design based on a new principle of contraction which was derived independently of a known contractile protein. The new principle, described as chemical modulation of an inverse temperature transition, was derived from studies of the polypentapeptide of elastin, poly(VPGVG), and analogs. The goals of this project are to design, prepare and characterize novel elastomeric polymers comprised of repeating peptide sequences, primarily the elastin pentamer and analogs of it alone and combined with repeating related hexapeptides and/or tetrapeptides. The purpose is to develop polymers with different elastic moduli and increased extension limits, polymers with different temperature ranges for their inverse temperature transitions over which elastomeric force dramatically changes, polymers in which different heat changes effect the large changes in elastomeric force, polymers with different intensities and frequencies of their dielectric dielectric relaxations and polymers with wider temperature ranges over which they function as nearly ideal elastomers. In the elastomer design, the dominant repeat units will be pentamers and tetramers. Hexamers and alanine-rich, lysine-containing cross-linking sequences will be used to fine-tune properties. GRA

N89-11045# Florida State Univ., Tallahassee. Dept. of Chemistry.
THE MELTING AND CRYSTALLIZATION KINETICS OF HYDROGENATED POLYBUTADIENE
L. Mandelkern and R. G. Alamo 1988 3 p
(Contract N00014-07-G-0185)
(AD-A196988) Avail: NTIS HC A02/MF A01 CSCL 07C

The overall isothermal crystallization kinetics of a series of hydrogenated polybutadienes having narrow molecular weight and composition distributions have been studied using calorimetric and dilatometric techniques. In addition to the general inquiry into the crystallization kinetics and mechanisms of such well-constituted and characterized samples, the study was also promoted by the unusual melting temperatures and levels of crystallinity that are observed with molecular weight. The hydrogenated polybutadienes can be considered as copolymers with a random copolymer because of the narrow molecular weight and composition distribution. Special attention has been given to the influence of molecular weight and co-unit content on the crystallization process and to the long-time crystallization rate. GRA

N89-11005# Joint Publications Research Service, Arlington, Va.
EFFECT OF PROTECTIVE COATINGS ON LIFE OF HEAT-RESISTANT NICKEL STEEL UNDER CYCLIC HEAT LOAD Abstract Only
G. N. Tretyachenko, G. R. Semanov, K. Yu. Yakovchuk, R. I. Kuriat, I. S. Malashenko, A. A. Rabinovich, and N. P. Vashchilo *In its* JPRS Report: Science and Technology. USSR: Materials Science 4 Apr. 1988 p 15 Transl. into ENGLISH from Problemy Prochnosti (Kiev, USSR), no. 12, Dec. 1987 p 3-7 (For primary document see N89-11002 02-26)
Avail: NTIS HC A03/MF A01

N89-11062# Joint Publications Research Service, Arlington, Va.
DEVELOPMENT OF TRANSPARENT ZIRCONIA CERAMICS DISCUSSED
In its JPRS Report: Science and Technology: Japan 4 Jun. 1987 p 1-10 Transl. into ENGLISH from Kino Zairyo (Tokyo, Japan), Oct. 1986 p 31-37 (For primary document see N89-11061 02-31)
Avail: NTIS HC A05/MF A01

28 PROPELLANTS AND FUELS

Includes rocket propellants, igniters, and oxidizers; their storage and handling procedures; and aircraft fuels.

For related information see also *07 Aircraft Propulsion and Power, 20 Spacecraft Propulsion and Power,* and *44 Energy Production and Conversion.*

N89-11046# Argonne National Lab., Ill.
EXPERIMENTAL AND ANALYTICAL STUDY OF VAPOR EXPLOSIONS IN STRATIFIED GEOMETRIES
R. Anderson, D. Armstrong, D. Cho, and A. Kras 1988 9 p Presented at the 25th ASME/American Inst. of Chemical Engineers/American Nuclear Society National Heat Transfer Conference, Houston, Tex., 24 Jul. 1988
(Contract W-31-109-eng-38)
(DE88-011964; CONF-880724-20) Avail: NTIS HC A02/MF A01

Vapor explosions in stratified geometries were experimentally studied. The unpredictable stability of stratified systems in a horizontal orientation made them poor experimental subjects. Stratified explosions were successfully generated in a vertical, transparent, fully confined pressure vessel. The explosion propagated with a sharp front and a narrow reaction zone where the two liquids mixed and the cold liquid boiled. Behind the explosion wave the system was in local equilibrium. If two liquid layers of the same thickness mixed and came to 100 percent equilibrium they would need a total mixture depth of 6 mm to explain the measured equilibrium pressure. Less efficient reactions would require greater mixing depths. A comprehensive model of stratified explosions must include the strong two-dimensional effects. DOE

N89-11047# Lawrence Livermore National Lab., Calif.
THE INITIATION AND DETONATION OF EXPLOSIVES: AN ALTERNATIVE CONCEPT
F. E. Walker 11 Jan. 1988 29 p
(Contract W-7405-eng-48)
(DE88-014199; UCRL-53860) Avail: NTIS HC A03/MF A01

An observed phenomenon designated as low-velocity detonation is not described properly by the ZND theory of detonation, nor is the deflagration-to-detonation transition, in which a rapidly burning explosive suddenly detonates with no external initiating shock. The alternative concept discussed can provide useful explanations of these phenomena. It also is a microscopic or atomic-scale model that is consistent with modern molecular dynamics and quantum-mechanical descriptions of shock waves in explosive materials. DOE

N89-11048# Commission of the European Communities (Luxembourg). Bureau d'Etudes Industrielles.
EXPLOITATION AND UTILIZATION OF HYDROCARBONS Final Report
J. P. Jonchere, J. Seguret, F. Vachez, and B. Faucher 1988 263 p In ENGLISH and FRENCH Prepared in cooperation with Institut Francais du Petrole, Rueil-Malmaison
(DE88-012626; EUR-11360) Avail: NTIS (US Sales Only) HC A14

In order to better define the most urgent research needs in the large field of exploitation, production and utilization of hydrocarbons, the Commission of the European Communities instigated a study by the Bureau d'Etudes Industrielles et de Cooperation del l'Institut Francais du Petrole (BEICIP). In this they established the views of governmental bodies, research organizations, petroleum, gas and chemical producers and the transport industry. The principal lines of research suggested by these bodies are described in this report. This study might be used as a guideline for the preparation of a research and development programme in the area of the optimization of the production and utilization of hydrocarbons. DOE

N89-11049# Lawrence Livermore National Lab., Calif.
ROLE OF DEFLAGRATION IN EXPLOSIVE RESPONSE
E. L. Lee and A. M. Weston (Maxwell Labs., Inc., San Diego, Calif.) 20 Jun. 1988 28 p Presented at the 19th International ICT Conference on Combustion and Detonation, Karlsruhe, Fed. Republic of Germany, 28 Jun. 1988
(Contract W-7405-eng-48)
(DE88-014139; UCRL-97861; CONF-880693-4) Avail: NTIS HC A03/MF A01

Measurements on materials of varying burn rates, particularly at high pressure, show a strong correlation with the violence of the response of these materials to a range of hazard stimuli. We have analyzed the response using somewhat idealized model for deflagrating materials. The results can be compared with various tests for hazard reponse. We have studied confinement effects and chosen a particular confinement to quantify the explosive response. The effects of porosity, ignition behavior, and laminar burn rate are clearly revealed by the results of the model. Possibilities for formulating less vulnerable materials are discussed. DOE

N89-11050*# Roberts Research Lab., Torrance, Calif.
BASELINE CONFIGURATION DATA SET: NASA STANDARD INITIATOR-2 (NSI-2)
15 Jun. 1988 19 p
(Contract NAS9-17249)
(NASA-CR-172071; NAS 1.26:172071) Avail: NTIS HC A03/MF A01 CSCL 19A

The deposition bridge configuration for a titanium bridge is illustrated. Specifications for the design are presented. B.G.

N89-11051# Mound Lab., Miamisburg, Ohio.
FRICTION AND IMPACT SENSITIVITIES OF EXPLOSIVES: A COMPARATIVE STUDY
Pu Sen Wang and Genola F. Hall 1988 7 p Presented at the American Defense Preparedness Association Compatibility Symposium, New Orleans, La., 18 Apr. 1988
(Contract DE-AC04-76DP-00053)
(DE88-012864; MLM-3504(OP); CONF-880473-8) Avail: NTIS HC A02/MF A01

Impact and friction sensitivities of explosives were tested by the one-shot method. The Bruceton statistical method was used to derive 50 percent initiation levels. The materials tested include: PETN, HMX, CP, barium styphnate, TATB, RX26BB, RX26BH, PYX, BTF and various types of plastic bonded explosives (PBX). Some samples were investigated for aging effects, physical variables, and the effect of manufacturing parameters on these sensitivities. The results proved to have comparative values. CP and barium styphnate were found to be the most sensitive among the samples tested, while TATB was found to be relatively insensitive. DOE

N89-11052# Los Alamos National Lab., N. Mex.
SHOCK INITIATION OF EXPLOSIVES WITH A SENSITIVE RATE AND RELATED TOPICS Final Report
D. S. Stewart 1988 13 p Prepared in cooperation with Illinois Univ., Urbana.
(Contract W-7405-eng-36)
(DE88-008483; LA-SUB-651-2C-1) Avail: NTIS HC A03/MF A01

The aim of the research has been to provide a complete, rational, theoretical description of the process of detonation initiation, either by a shock or due to the growth of embedded hot spots (reaction centers) in a preconditioned explosive which has a sensitive, state-dependent reaction rate. A representative experiment modelled by these studies is that of piston driven shock initiation. In order to study the process in detail, a systematic asymptotic analysis of the reactive Euler equations with Arrhenius reaction-rate kinetics has been carried out. Through a combination of large activation energy asymptotics and numerics on sets of reduced equations, these studies have given a precise description of the distinct stages of the initiation event prior to the emergence of a full-fledged detonation: induction, localized thermal runaway, thermal explosion at the runaway site, and the birth of a supersonic reaction wave (a constant-volume detonation) propagating through an inertially confined medium. DOE

N89-11053# Lawrence Livermore National Lab., Calif.
A DETAILED CHEMICAL KINETIC REACTION MECHANISM FOR THE OXIDATION OF ISO-OCTANE AND n-HEPTANE OVER AN EXTENDED TEMPERATURE RANGE AND ITS APPLICATION TO ANALYSIS OF ENGINE KNOCK
Charles K. Westbrook, Juergen Warnatz, and William J. Pitz 11 Jan. 1988 21 p Presented at the 22nd International Symposium on Combustion, Seattle, Wash., 14 Aug. 1988
(Contract W-7405-eng-48)
(DE88-005370; UCRL-98040; CONF-880802-2) Avail: NTIS HC A03/MF A01

A detailed chemical kinetic reaction is developed to describe the oxidation of n-heptane, iso-octane, and their mixtures over a wide range of operating conditions. In addition to a high temperature submechanism, reaction paths are included to describe the lower temperature regimes in which the rate and intermediate products of oxidation are controlled by addition of molecular oxygen to alkyl and isomerized alkylperoxy radicals, internal H atom abstractions, and reactions involving O-heterocyclic species. The mechanism is then used to study the influence of fuel composition on knocking in internal combustion engines. Autoignition of mixtures of iso-octane and n-heptane is examined. The computations reproduce the variations of autoignition delay time with octane number and these variations are interpreted in terms of detailed differences in the structure of the two primary reference fuels. Sensitivity analyses of the computations are also presented. DOE

N89-11054# Air Force Inst. of Tech., Wright-Patterson AFB, Ohio.
A METHOD FOR OBTAINING EMPIRICAL CORRELATIONS FOR PREDICTING CRACK PROPAGATION IN A BURNING SOLID PROPELLANT GRAIN M.S. Thesis
Jeffrey A. Nimis 1988 70 p
(AD-A196689; AFIT/CI/NR-88-85) Avail: NTIS HC A04/MF A01 CSCL 21I

The importance of crack propagation in solid rocket motors is widely recognized. However, the processes of crack propagation and branching in burning solid propellants are not as yet well understood. These processes could be instrumental in creating large specific surface areas for burning causing rocket motor failure. Key factors influencing the crack combustion, propagation and branching process considered in the dimensional analysis include chamber pressurization rate, initial crack length, initial temperature, sample geometry, and mechanical and thermal properties of the solid propellant. GRA

29 MATERIALS PROCESSING

Includes space-based development of products and processes for commercial applications.
For biological materials see *55 Space Biology*.

N89-11055*# Stanford Univ., Calif. Center for Materials Research.
PROTEIN CRYSTAL GROWTH IN LOW GRAVITY Final Technical Report, 1 Jan. 1987 - 30 Jun. 1988
Robert S. Feigelson 21 Sep. 1988 53 p
(Grant NAG8-489)
(NASA-CR-183183; NAS 1.26:183183; CMR-88-9; SU-SPO-1018) Avail: NTIS HC A04/MF A01 CSCL 22A

The solubility and growth of the protein canavalin, and the application of the schlieren technique to study fluid flow in protein crystal growth systems were investigated. These studies have resulted in the proposal of a model to describe protein crystal growth and the preliminary plans for a long-term space flight experiment. Canavalin, which may be crystallized from a basic solution by the addition of hydrogen (H+) ions, was shown to have normal solubility characteristics over the range of temperatures (5 to 25 C) and pH (5 to 7.5) studies. The solubility data combined with growth rate data gathered from the seeded growth of canavalin crystals indicated that the growth rate limiting step is a screw dislocation mechanism. A schlieren apparatus was constructed and flow patterns were observed in Rochelle salt (sodium potassium tartrate), lysozyme, and canavalin. The critical parameters were identified as the change in density with concentration (dp/dc) and the change in index of refraction with concentration (dn/dc). Some of these values were measured for the materials listed. The data for lyrozyme showed non-linearities in plots of optical properties and density vs. concentration. In conjunction with with W. A. Tiller, a model based on colloid stability theory was proposed to describe protein crystallization. The model was used to explain observations made by ourselves and others. The results of this research has lead to the development for a preliminary design for a long-term, low-g experiment. The proposed apparatus is univeral and capable of operation under microprocessor control. Author

N89-11056*# Virginia Univ., Charlottesville. Dept. of Chemical Engineering.
MICROGRAVITY NUCLEATION AND PARTICLE COAGULATION EXPERIMENTS SUPPORT Status Report No. 3, 1 Dec. 1987 - 31 Aug. 1988
L. U. Lilleleht, F. T. Ferguson, and J. R. Stephens (Matrix Corp., Santa Fe, N. Mex.) Oct. 1988 12 p
(Grant NAG5-865)
(NASA-CR-183282; NAS 1.26:183282; UVA/528260/CHE89/103) Avail: NTIS HC A03/MF A01 CSCL 22A

Researchers at NASA Goddard Space Flight Center have embarked on a program to study the formation and growth of cosmic grains. This includes experiments on the homogeneous nucleation of refractory vapors of materials such as magnesium, lead, tin, and silicon oxides. As part of this program, the Chemical Engineering Department of the University of Virginia has undertaken to develop a math model for these experiments, to assist in the design and construction of the apparatus, and to analyze the data once the experiments have begun. Status Reports 1 and 2 addressed the design of the apparatus and the development of math models for temperature and concentration fields. The bulk of this report discusses the continued refinement of these models, and the assembly and testing of the nucleation chamber along with its ancillary equipment, which began in the spring of 1988. Author

N89-11057*# Physical Sciences, Inc., Andover, Mass.
MULTICOLOR PYROMETER FOR MATERIALS PROCESSING IN SPACE Quarterly Report No. 4, 1 Mar. - 31 May 1988
Michael Frish, Jonathan Frank, and Henry Beerman Aug. 1988 19 p Prepared in cooperation with Jet Propulsion Lab., California Inst. of Tech., Pasadena
(Contract NAS7-1002)
(NASA-CR-183189; NAS 1.26:183189; PSI-1038/TR-862) Avail: NTIS HC A03/MF A01 CSCL 22A

The program goals are to design, construct, and program a prototype imaging pyrometer capable of measuring the temperature distribution across the surface of a moving object suspended in space. The approach is to utilize an optical system which operates at short wavelengths compared to the peak of the blackbody spectrum for the temperature range of interest, thus minimizing errors associated with a lack of knowledge about heated sample emissivity. An analysis of the system's temperature measurement capability based on the camera's responsivity was performed and bound to be satisfactory. Details for the evolving optical design and the progress towards construction of a working model are discussed. Details of the algorithm developed for selecting the optimum colors to be used by the pyrometer are reported. Though final selection of the colors will have to await a final design of the optical system, results using a preliminary optical design are presented. Author

N89-11058# National Aerospace Lab., Amsterdam (Netherlands).
FLUID SCIENCE INVESTIGATIONS IN MICROGRAVITY
J. P. B. Vreeburg 1987 34 p Presented at the SRON Symposium on Microgravity Research, Utrecht, Netherlands, 2-3 Apr. 1987
(PB88-209754; NLR-MP-87023-U) Avail: NTIS HC A03/MF A01 CSCL 22A

An overview is given of fluid science investigations in microgravity. Emphasis is placed on results obtained by European scientists. In order to assess the merits of experiments, particular aspects of the microgravity environment are discussed. The fluid science subjects with microgravity relevance are ordered in four groups, as follows: (1) molecular physics; (2) thermodynamic properties and transport coefficients; (3) classical heat and mass transfer; and (4) fluid dynamics. Representative samples of different experiment classes from each group are outlined. Experimental equipment and some design aspects are discussed, and the National Aerospace Laboratory (NLR) activities and experience are introduced to illustrate various points. A recommendation is formulated for a well-conditioned experiment configuration to supply data to more than one investigator. GRA

N89-10912*# Delta-t, Lebanon, Pa.
GAS-611 FIREFLY IN ZERO GRAVITY
Tony Williams *In* NASA, Goddard Space Flight Center, The 1988 Get Away Special Experimenter's Symposium Sep. 1988 p 65-72 (For primary document see N89-10902 02-12)
Avail: NTIS HC A07/MF A01 CSCL 22A

31 ENGINEERING (GENERAL)

Includes vacuum technology; control engineering; display engineering; cryogenics; and fire prevention.

N89-11059# Lawrence Livermore National Lab., Calif.
ENGINEERING RESEARCH AND DEVELOPMENT: THRUST AREA REPORT, FY87
Apr. 1988 308 p
(Contract W-7405-eng-48)
(DE88-013792; UCRL-53868-87) Avail: NTIS HC A14/MF A01

This annual report describes the accomplishments of the Engineering Research Program for fiscal year 1987. Fifty-eight research and development projects are covered. For each project, goal(s), technical description, and an overview of future work are provided. DOE

N89-11060*# National Aeronautics and Space Administration. Lyndon B. Johnson Space Center, Houston, Tex.
LUNAR CONCRETE FOR CONSTRUCTION
Hatice S. Cullingford and M. Dean Keller (Los Alamos National Lab., N. Mex.) 1988 16 p Presented at the NASA Symposium

on Lunar Bases and Space Activities of the 21st Century, Houston, Tex., 5 Apr. 1988; sponsored by NASA, AIAA, Lunar and Planetary Inst., American Geophysical Union, American Nuclear Society and others
(Contract W-7405-eng-36)
(NASA-TM-89672; NAS 1.15:89672; DE88-014391; LA-UR-88-2405; CONF-8804104-3; LBS-88-7271) Avail: NTIS HC A03/MF A01

Feasibility of using concrete for lunar-base construction has been discussed recently without relevant data for the effects of vacuum on concrete. Experimental studies performed earlier at Los Alamos have shown that concrete is stable in vacuum with no deterioration of its quality as measured by the compressive strength. Various considerations of using concrete successfully on the moon are provided in this paper along with specific conclusions from the existing data base. DOE

N89-11061# Joint Publications Research Service, Arlington, Va.
JPRS REPORT: SCIENCE AND TECHNOLOGY: JAPAN
4 Jun. 1987 100 p Transl. into ENGLISH from various Japanese articles
(JPRS-JST-87-018) Avail: NTIS HC A05/MF A01

Translations are made of Japanese scientific articles from different periodicals. The subject areas covered are: Advanced materials; Aerospace, Civil aviation; Defense industries; Energy; Lasers, sensors, optics; Nuclear developments; and Transportation. For individual titles, see N89-11062 through N89-11069.

N89-11062# Joint Publications Research Service, Arlington, Va.
DEVELOPMENT OF TRANSPARENT ZIRCONIA CERAMICS DISCUSSED **c27**
In its JPRS Report: Science and Technology: Japan 4 Jun. 1987 p 1-10 Transl. into ENGLISH from Kino Zairyo (Tokyo, Japan), Oct. 1986 p 31-37 (For primary document see N89-11061 02-31)
Avail: NTIS HC A05/MF A01

The fabrication of highly transparent zirconia ceramics was difficult up to now; however, its fabrication became possible by adopting the new fabrication method which performs doping of titania. Since this transparent ceramic is easy to fabricate and possesses characteristics such as superior heat resisting property, infrared transmitting property, and a high refractive index, applications for use as optical parts are considered in the future. Explanations will be made briefly on the fabrication method and properties of transparent zirconia ceramics. Author

N89-11063# Joint Publications Research Service, Arlington, Va.
RESEARCH ON CATALYST COMBUSTION FOR GAS TURBINE **c07**
Shigeru Hayashi *In its* JPRS Report: Science and Technology: Japan 4 Jun. 1987 p 12-14 Transl. into ENGLISH from Kogiken Nyusu (Toyko, Japan), Aug. 1986 p 3-4 (For primary document see N89-11061 02-31)
Avail: NTIS HC A05/MF A01

In Japan the range of uses of the gas turbine has expanded to other fields besides aircraft such as large capacity composite electricity generation and dual purpose electricity and steam generation, and thus demands for the purification of gas turbine exhaust are expected to increase. The gas turbine is referred to as a clean motor, but because of its high temperature high pressure combustion, its discharge of nitrogen oxides (NOx), which have a close connection with photochemical smog and acid rain, is several times higher that in the boiler now controlled by regulations. Furthermore, the effort to raise temperature and pressure for improving the fuel consumption results in an increase of nitrogen oxides so far as the present combustion system is adopted. Experiments were conducted on the reaction characteristics of catalysts under the atmospheric pressure and also atmospheric pressure experiments of preburner system catalyst combustor. It was proven that the NOx concentration in the exhaust is more than 2 digits lower than in the flame combustion at 0.1 ppm or below and that a specific combustion intensity of the same level as the industrial gas turbine combustor can be obtained. Author

N89-11064# Joint Publications Research Service, Arlington, Va.
GOOD PERFORMANCE OF LE-7 LIQUID OXYGEN TURBOPUMP CONFIRMED **c37**
Kenjiro Kamijo *In its* JPRS Report: Science and Technology: Japan 4 Jun. 1987 p 15-17 Transl. into ENGLISH from Kogiken Nyusu (Tokyo, Japan), Aug. 1986 p 5-6 (For primary document see N89-11061 02-31)
Avail: NTIS HC A05/MF A01

A liquid oxygen turbopump for the first stage main engine of the H-11 rocket is tested. The first phase prototype liquid oxygen turbopump and its test equipment were completed. Cold running tests using liquid nitrogen for the pump fluid and cold hydrogen gas for the turbine driving gas were conducted, with the result that the design number of revolutions was attained and the fluid performance and the quality of structural design have become considerably clearer. A part of the results is introduced. Author

N89-11065# Joint Publications Research Service, Arlington, Va.
CASCADE FLOW ANALYSIS BY NAVIER-STOKES EQUATION **c34**
Osamu Nozaki *In its* JPRS Report: Science and Technology: Japan 4 Jun. 1987 p 18-20 Transl. into ENGLISH from Kogiken Nyusu (Tokyo, Japan), Aug. 1986 p 7-10 (For primary document see N89-11061 02-31)
Avail: NTIS HC A05/MF A01

As the performance of the large electronic computer has improved, numerical simulation of the flow around the blade of the aircraft, for instance, is being actively conducted. In the compressor and turbine cascades of aircraft engine, multiple blades are put side by side closely, and the pressure gradient in the flow direction is large. Thus they have more complicated properties than the independent blade. At present, therefore, it is the mainstream to use potential, Euler's equation, etc., as the basic equation but, for knowing the phenomenon caused by the viscosity like the interference of shock waves and boundary layers, it is necessary to solve the Navier-Stokes (N-S) equation. A two-dimensional cascade analysis program was developed by the N-S equation by expanding the two-dimensional high Reynolds number transonic profile analysis code NSFOIL and the lattice formation program AFMESH for the independent blade, which were already developed so as to fit the cascade flow. Author

N89-11066# Joint Publications Research Service, Arlington, Va.
PAYLOAD BOOMERANG TECHNOLOGY DESCRIBED **c18**
Akira Onchi *In its* JPRS Report: Science and Technology: Japan 4 Jun. 1987 p 21-23 Transl. into ENGLISH from Kogiken Nyusu (Toyko, Japan), Sep. 1986 p 1-2 (For primary document see N89-11061 02-31)
Avail: NTIS HC A05/MF A01

Payload boomerang technology means that after an experimental PS (payload satellite) is launched from the SS (space station) into space and experiments are performed while flying the experimental PS in space, the experimental PS will be recovered by the SS. Such an experimental PS can be regarded as a kind of free flier, and compared with free fliers which are usually considered. It is necessary to collect basic data on space experiments, and it can be considered that this payload boomerang technology is extremely useful because experiments can be performed readily and repeatedly. Author

N89-11067# Joint Publications Research Service, Arlington, Va.
NUMERICAL SIMULATION OF TRANSONIC FLOW AROUND ASUKA **c02**
Susumu Takanashi *In its* JPRS Report: Science and Technology: Japan 4 Jun. 1987 p 24-25 Transl. into ENGLISH from Kogiken Nyusu (Toyko, Japan), Sep. 1986 p 2 (For primary document see N89-11061 02-31)
Avail: NTIS HC A05/MF A01

Research is being conducted on the numerical simulation of transonic flow around a low noise short takeoff and landing (STOL)

experimental aircraft, Asuka. The purposes of this research are to evaluate the high speed aerodynamic characteristics of the Asuka, to evaluate the aerodynamic interference between the elements and airframe according to the parametric study, and to construct a numeric data base. Author

N89-11068# Joint Publications Research Service, Arlington, Va.
NEW TRIAL OF VIBRATION TESTING METHOD c39
Tetsuhiko Ueda *In its* JPRS Report: Science and Technology: Japan 4 Jun. 1987 p 26-28 Transl. into ENGLISH from Kogiken Nyusu (Toyko, Japan), Sep. 1986 p 3-4 (For primary document see N89-11061 02-31)
Avail: NTIS HC A05/MF A01

A trial of a vibration testing method which will be used in the time domain is discussed. The vibration test is indispensable for obtaining dynamically elastic characteristics of a structure. In particular, it is necessary to anticipate the flutter phenomenon which will cause structural destruction on the wings of aircraft, fins of rockets, turbine blades of engines, etc. Therefore, the identification of structural characteristics according to vibration tests plays an important role in this anticipation. The sine dwell method and transfer function method can be cited as methods being used widely and presently in such vibration tests. The sine dwell method is used to search for resonance points, and the transfer function method is used to process data mathematically in the frequency domain by using an fast Fourier transformation analyzer. The VATREM (vibration analysis in the time domain by the real eigenvalue method) is introduced. It is a new trial different from both of the above methods and can be regarded as a kind of time domain method. Author

N89-11069# Joint Publications Research Service, Arlington, Va.
CAD WIND TUNNEL TEST FOR HALF-CUT MODEL OF ASUKA c02
In its JPRS Report: Science and Technology: Japan 4 Jun. 1987 p 29-32 Transl. into ENGLISH from Kogiken Nyusu (Toyko, Japan), Sep. 1986 p 5-6 (For primary document see N89-11061 02-31)
Avail: NTIS HC A05/MF A01

A low noise STOL experimental aircraft, Asuka, is presently being researched and developed at a full scale flight experimental stage. The main wing itself of the C-1 transport, which is the mother aircraft of the Asuka, was not changed because the main purpose of this research was to establish a upper surface blowing which will realize a revolutionary STOL performance. Research has also been conducted on the possibility of a rise in aerodynamic performance of the optimum shape of main wings as part of the research on the practical use of future STOL aircraft. Tests were conducted in the above research by using a half-cut model with a main wing shape designed with a computer aided design system and are called low speed wind tunnel test. Author

N89-11070# Los Alamos National Lab., N. Mex.
SAFETY ASPECTS OF LARGE-SCALE HANDLING OF HYDROGEN
F. J. Edeskuty and W. F. Stewart 1988 14 p Presented at the Hydrogen Today, Moscow (USSR), 25 Sep. 1988
(Contract W-7405-eng-36)
(DE88-014422; LA-UR-88-2045; CONF-880925-1) Avail: NTIS HC A03/MF A01

Since the decade of the 1950s, there has been a large increase in the quantity of hydrogen, especially liquid hydrogen, that has been produced, transported, and used. The technology of hydrogen, as it relates to safety, has also developed at the same time. The possible sources of hazards that can arise in the large-scale handling of hydrogen are recognized, and for the most part, sufficiently understood. These hazard sources are briefly discussed. DOE

N89-11071# Naval Postgraduate School, Monterey, Calif.
THERMODYNAMIC IMPROVEMENTS FOR THE SPACE THERMOACOUSTIC REFRIGERATOR (STAR) M.S. Thesis
Michael P. Susalla Jun. 1988 172 p
(AD-A196958) Avail: NTIS HC A08/MF A01 CSCL 20M

The objective of the STAR project is to test and space-qualify a new continuous cycle cryogenic refrigeration system for cooling of sensors and electronics which is based on the newly discovered thermoacoustic heat pumping effect. The new refrigerator has no sliding seals, a cycle frequency of about 300 Hz, and uses acoustic resonance to enhance the overall power density and efficiency. This thesis is concerned specifically with the design and testing of the thermodynamic element (or stack), which is responsible for the thermo-acoustic power conversion, and the testing of binary inert gas mixtures as working fluids. Using the refrigerator's coefficient of performance relative to the ideal Carnot coefficient of performance as a measure of efficiency, a 93 percent improvement over previous designs has been achieved. GRA

32 COMMUNICATIONS AND RADAR

Includes radar; land and global communications; communications theory; and optical communications.

For related information see also *04 Aircraft Communications and Navigation* and *17 Space Communications, Spacecraft Communications, Command and Tracking.* For search and rescue see *03 Air Transportation and Safety,* and *16 Space Transportation.*

N89-11072# Lawrence Livermore National Lab., Calif.
THROUGH-THE-EARTH COMMUNICATION: EXPERIMENT RESULTS FROM BILLIE MINE AND MISSISSIPPI CHEMICAL MINE
H. M. Buettner, E. M. Didwall, and D. C. Bukofzer Jun. 1988 42 p
(Contract W-7405-eng-48)
(DE88-013162; UCID-21436) Avail: NTIS HC A03/MF A01

As part of the Lawrence Livermore National Laboratory (LLNL) effort to evaluate Through-the-Earth Communication (TEC) as an option for military communication systems, experiments were conducted involving transmission, reception, and performance monitoring of digital electromagnetic communication signals propagating through the earth. The two experiments reported on here not only demonstrated that TEC is useful for transmissions at digital rates above a few bits per second, but also provided data on performance parameters with which to evaluate TEC in various military applications. The most important aspect of these experiments is that the bit error rate (BER) is measured rather than just estimated from purely analytic developments. By measuring this important parameter, not only has more credibility been lent to the proof of concept goals of the experiment, but also a means for judging the effects of assumptions in BER theoretical models has been provided. DOE

N89-11073 British Broadcasting Corp., Kingswood (England). Research Dept.
POLARISATION CONVERTERS FOR A DBS FLAT-PLATE ANTENNA
M. C. D. Maddocks and D. H. Boardman Jul. 1988 14 p
(BBC-RD-1988/7) Copyright Avail: BBC, Kingswood Warren, Tadworth, Surrey, United Kingdom

The introduction of direct broadcast by satellite service requires suitable receiving antennas to be available. A polarization converter and an array of linearly-polarized elements have been found to be the most suitable way of receiving the circularly-polarized radiation that would be transmitted by a DBS satellite. In this Report the performance of various types of polarization converters is considered. It was found that a meander-line polarizer gave a cross-polar discrimination of better than 25 dB and an insertion loss of less than 1 dB over the required band. It should be possible to build the polarizer using relatively low-cost materials thus making it suitable for use in this application. Author

N89-11074*# Jet Propulsion Lab., California Inst. of Tech., Pasadena.
PROCEEDINGS OF THE TWELFTH NASA PROPAGATION EXPERIMENTERS MEETING (NAPEX 12)
Faramaz Davarian, ed. Aug. 1988 186 p Meeting held in Syracuse, N.Y., 9-10 Jun. 1988
(Contract NAS7-918)
(NASA-CR-182796; JPL-Publ-88-22; NAS 1.26:182796) Avail: NTIS HC A09/MF A01 CSCL 20N

The NASA Propagation Experimenters Meeting was convened on June 9 and 10, 1988. Pilot Field Experiments propagation studies, mobile communication systems, signal fading, communication satellites rain gauge network measurements, atmospheric attenuation studies, optical communication through the atmosphere, and digital beacon receivers were among the topics discussed. For individual titles, see N89-11075 through N89-11094.

N89-11075*# Jet Propulsion Lab., California Inst. of Tech., Pasadena.
PiFEx PROPAGATION EXPERIMENTS
Richard F. Emerson, Jeff B. Berner, and Loretta L. G. Ho *In its* Proceedings of the 12th NASA Propagation Experimenters Meeting (NAPEX 12) Aug. 1988 p 5-10 (For primary document see N89-11074 02-32)
Avail: NTIS HC A09/MF A01 CSCL 20N

An overview is presented of the Pilot Field Experiments (PiFEx) performed under the Mobile Satellite Experiment Program (MSAT-X) on the performance of MSAT-X equipment and subsystems. A brief history of PiFEx and plans for future experiments are given. Some results from the satellite experiment held last August are discussed. Author

N89-11076*# Jet Propulsion Lab., California Inst. of Tech., Pasadena.
PiFEx DATA AND ARCHIVAL FORMATS
Jeff B. Berner *In its* Proceedings of the 12th NASA Propagation Experimenters Meeting (NAPEX 12) Aug. 1988 p 11-17 (For primary document see N89-11074 02-32)
Avail: NTIS HC A09/MF A01 CSCL 20N

A standard archival format is presented for the Jet Propulsion Laboratory Mobile Satellite Experiment (MSAT-X) Pilot Field Experiments (PiFEx), which will overcome the deficiencies of the current set-up. This format allows ease of data processing, flexibility for future experiments, and controllable data dissemination to other researchers. Author

N89-11077*# Johns Hopkins Univ., Laurel, Md. Applied Physics Lab.
RESULTS OF 1987 MSS HELICOPTER PROPAGATION EXPERIMENT AT UHF AND L BAND IN CENTRAL MARYLAND
Julius Goldhirsh and Wolfhard J. Vogel (Texas Univ., Austin.) *In* JPL, Proceedings of the 12th NASA Propagation Experimenters Meeting (NAPEX 12) Aug. 1988 p 18-26 (For primary document see N89-11074 02-32)
Avail: NTIS HC A09/MF A01 CSCL 20N

This effort emphasizes several important results pertaining to a mobile satellite system propagation experiment performed in Central Maryland during June 1987. Fade distributions due to multipath and roadside trees at L Band (1.5 GHz) during a period in which the deciduous trees were in full bloom are examined. The multipath statistics for roadside trees are compared with previous multipath measurements made in canyon terrain in North Central Colorado. Also examined is the repeatability of previous UHF measurements made in Central Maryland and the attenuation effects of foliage on trees at UHF. Fade duration for the multipath mode for fade levels of 5 dB and 10 dB is also presented.
Author

N89-11078*# Virginia Polytechnic Inst. and State Univ., Blacksburg. Satellite Communications Group.
LMSS PROPAGATION MODELING AT VIRGINIA TECH
Warren L. Stutzman, R. Michael Barts, and Charles W. Bostian *In* JPL, Proceedings of the 12th NASA Propagation Experimenters Meeting (NAPEX 12) Aug. 1988 p 27-35 (For primary document see N89-11074 02-32)
Avail: NTIS HC A09/MF A01 CSCL 20N

Recent efforts in the modeling of land mobile satellite systems are reported. These include descriptions of a simple model for prediction of fading statistics, a propagation simulator, and results from studies using the simulator. Predictions are compared to available measured data. Author

N89-11079*# Texas Univ., Austin. Electrical Engineering Research Lab.
PRELIMINARY RESULTS OF MARECS-A MEASUREMENTS IN CENTRAL MARYLAND AND PLANS FOR 1988 MSS EXPERIMENT IN AUSTRALIA
Wolfhard J. Vogel and Julius Goldhirsh (Johns Hopkins Univ., Laurel, Md.) *In* JPL, Proceedings of the 12th NASA Propagation Experimenters Meeting (NAPEX 12) Aug. 1988 p 36-46 (For primary document see N89-11074 02-32)
Avail: NTIS HC A09/MF A01 CSCL 20N

Past and future efforts are described, using L Band (1.5 GHz) satellite signals for mobile satellite system (MSS) propagation measurements. Preliminary results from the December 1987 campaign in Central Maryland with the Atlantic Ocean MARECS satellite are given. The fade level statistics from this 22 degree elevation source are consistent with helicopter measurements made along the same roads. The day to day repeatability of the fade probabilities is shown to be usually better than about 20 percent. An experiment plan is presented for measurements using the Experimental Test Satellite-V's (ETS-V's) southern beam. These measurements will be made in Australia in collaboration with Australia's National Satellite System (AUSSAT) during the July/August 1988 time-frame. Author

N89-11080*# Ministry of Posts and Telecommunications, Kashima (Japan). Communications Research Lab.
ETS-V PROPAGATION EXPERIMENTS IN JAPAN
Shingo Ohmori *In* JPL, Proceedings of the 12th NASA Propagation Experimenters Meeting (NAPEX 12) Aug. 1988 p 47-54 (For primary document see N89-11074 02-32)
Avail: NTIS HC A09/MF A01 CSCL 20N

Propagation experiments on ship, aircraft, and land mobile earth stations were carried out using the Engineering Test Satellite-V (ETS-V), which was launched in August 1987. The propagation experiments are one of the missions of the Experimental Mobile Satellite System (EMSS). Initial experimental results of ETS-V/EMSS on propagation using ship, aircraft, and land mobiles with ETS-V are given. Author

N89-11081*# Virginia Polytechnic Inst. and State Univ., Blacksburg. Satellite Communications Group.
MOBILE SATELLITE PROPAGATION MEASUREMENTS AND MODELING: A REVIEW OF RESULTS FOR SYSTEMS ENGINEERS
W. L. Stutzman, ed., R. M. Barts, C. W. Bostian, J. S. Butterworth, R. Campbell, J. Goldhirsh, and W. J. Vogel (Texas Univ., Austin.) *In* JPL, Proceedings of the 12th NASA Propagation Experimenters Meeting (NAPEX 12) Aug. 1988 p 55-69 Previously announced as N88-25696 (For primary document see N89-11074 02-32)
Avail: NTIS HC A09/MF A01 CSCL 20N

An overview of Mobile Satellite System (MSS) propagation measurements and modeling is given, including a summary of results. The simple models presented should be of some use to systems engineers. A complete summary of propagation experiments with literature references is included. Author

N89-11082*# Westinghouse Defense and Electronic Systems Center, Baltimore, Md. Electronics Systems Center.
PROPAGATION HANDBOOK, FREQUENCIES ABOVE 10 GHz
Louis J. Ippolito *In* JPL, Proceedings of the 12th NASA Propagation Experimenters Meeting (NAPEX 12) Aug. 1988 p 70-80 (For primary document see N89-11074 02-32)
Avail: NTIS HC A09/MF A01 CSCL 20N

The progress and accomplishments in the developmet of the Fourth Edition of the NASA Propagation Effects Handbook for Satellite Systems Design, for frequencies 10 to 100 GHz, NASA Reference Publication 1082(04), dated May 1988, prepared by Westighouse Electric Corporation for the Jet Propulsion Laboratory are discussed. Author

N89-11083*# Johns Hopkins Univ., Laurel, Md. Applied Physics Lab.

RESULTS OF APL RAIN GAUGE NETWORK MEASUREMENTS IN MID-ATLANTIC COAST REGION AND COMPARISONS OF DISTRIBUTIONS WITH CCIR MODELS

Julius Goldhirsh, Norman Gebo, and John Rowland *In* JPL, Proceedings of the 12th NASA Propagation Experimenters Meeting (NAPEX 12) Aug. 1988 p 81-90 (For primary document see N89-11074 02-32)

Avail: NTIS HC A09/MF A01 CSCL 20N

In this effort are described cumulative rain rate distributions for a network of nine tipping bucket rain gauge systems located in the mid-Atlantic coast region in the vicinity of the NASA Wallops Flight Facility, Wallops Island, Virginia. The rain gauges are situated within a gridded region of dimensions of 47 km east-west by 70 km north-south. Distributions are presented for the individual site measurements and the network average for the year period June 1, 1986 through May 31, 1987. A previous six year average distribution derived from measurements at one of the site locations is also presented. Comparisons are given of the network average, the CCIR (International Radio Consultative Committee) climatic zone, and the CCIR functional model distributions, the latter of which approximates a log normal at the lower rain rate and a gamma function at the higher rates. Author

N89-11084*# Dartmouth Coll., Hanover, N.H. School of Engineering.

INTERFERENCE BY RAIN SCATTER

Robert K. Crane *In* JPL, Proceedings of the 12th NASA Propagation Experimenters Meeting (NAPEX 12) Aug. 1988 p 91-102 (For primary document see N89-11074 02-32)

Avail: NTIS HC A09/MF A01 CSCL 20N

The data from Japan and the U.S. (the Virginia Precipitation Scatter Experiment) show excellent agreement between the two-component rain scatter model predictions and bistatic scatter measurements. In employing the model, all the scattering geometries should be classified as backscattering as defined by Crane (1974). The forward scatter model should only be used for great circle paths with both antennas pointed at the horizon and at each other in a typical troposcatter communication system geometry. The forward scatter model can also be used for main-lobe, side-lobe coupling when one antenna is pointed toward the other along the great circle path. The forward scatter observations made over the Prospect Hill - Mt Tug path show that the two-component model is incomplete. Much stronger signals were observed at Ku-band than expected based on simultaneous C-band measurements. The discrepancies may be due to: (1) scattering by ice/snow at height (posssible in April) at the 1 km height of the scattering volume), (2) the coherent effects of turbulent fluctuations in the hydrometeor number densities and (3) errors in the modeling of the statistical relationship between attenuation along the path and scattering in the common volume. Author

N89-11085*# National Telecommunications and Information Administration, Boulder, Colo. Inst. for Telecommunication Sciences.

MILLIMETER-WAVE STUDIES

Kenneth C. Allen *In* JPL, Proceedings of the 12th NASA Propagation Experimenters Meeting (NAPEX 12) Aug. 1988 p 103-113 (For primary document see N89-11074 02-32)

Avail: NTIS HC A09/MF A01 CSCL 20N

Progress on millimeter-wave propagation experiments in Hawaii is reported. A short path for measuring attenuation in rain at 9.6, 28.8, 57.6, and 96.1 GHz is in operation. A slant path from Hilo to the top of Mauna Kea is scheduled. On this path, scattering from rain and clouds that may cause interference for satellites closely spaced in geosynchronous orbit will be measured at the same frequencies at 28.8 and 96.1 GHz. In addition the full transmission matrix will be measured at the same frequencies on the slant path. The technique and equipment used to measure the transmission matrix are described. Author

N89-11086*# National Oceanic and Atmospheric Administration, Boulder, Colo. Wave Propagation Lab.

GROUND-BASED RADIOMETRIC OBSERVATIONS OF EMISSION AND ATTENUATION AT 20.6, 31.65, AND 90.0 GHz

Ed R. Westwater, Jack B. Snider, and Michael J. Falls *In* JPL, Proceedings of the 12th NASA Propagation Experimenters Meeting (NAPEX 12) Aug. 1988 p 114-125 (For primary document see N89-11074 02-32)

Avail: NTIS HC A09/MF A01 CSCL 20N

During 1987, ground-based zenith-viewing observations of atmospheric thermal emission were made at frequencies of 20.6, 31.65, and 90.0 GHz. At the locations of the experiments, San Nicolas Island, California, and Denver, Colorado, radiosonde observations of temperature and humidity were also available. The data, after conversion to attenuation using the mean radiating temperature approximation, are processed to derive attenuation statistics. In addition, both clear and cloudy attenuation characteristics are examined and compared with the most recent theories. Finally, the predictability and interdependence of the three separate channels are examined. Author

N89-11087*# Jet Propulsion Lab., California Inst. of Tech., Pasadena.

LASER COMMUNICATIONS THROUGH THE ATMOSPHERE

Kamran Shaik and J. H. Churnside (National Oceanic and Atmospheric Administration, Boulder, Colo.) *In its* Proceedings of the 12th NASA Propagation Experimenters Meeting (NAPEX 12) Aug. 1988 p 126-131 (For primary document see N89-11074 02-32)

Avail: NTIS HC A09/MF A01 CSCL 20N

Atmospheric properties affecting laser propagation with reference to optical communications are reviewed. Some of the optical space network configurations and various diversity techniques that may need to be utilized to develop robust bi-directional space-earth laser communication links are explored. Author

N89-11088*# Ministry of Posts and Telecommunications, Kashima (Japan). Communications Research Lab.

PLAN OF PROPAGATION AND COMMUNICATION EXPERIMENTS USING ETS-VI

Shingo Ohmori *In* JPL, Proceedings of the 12th NASA Propagation Experimenters Meeting (NAPEX 12) Aug. 1988 p 132-137 (For primary document see N89-11074 02-32)

Avail: NTIS HC A09/MF A01 CSCL 20N

In 1992, an Engineering Test Satellite VI is scheduled to be launched by an H-II rocket. The missions of ETS-VI are to establish basic technologies of inter-satellite communications using millimeter waves and optical beams and fix satellite communications using multibeam antenna on board the satellite. Several kinds of frequency bands will be used for the communications missions. However, these frequencies can be used for propagation experiments. Author

N89-11089*# Ministry of Posts and Telecommunications, Tokyo (Japan). Space Communications Div.

PLAN OF ADVANCED SATELLITE COMMUNICATIONS EXPERIMENT USING ETS-VI

Tadashi Shiomi *In* JPL, Proceedings of the 12th NASA Propagation Experimenters Meeting (NAPEX 12) Aug. 1988 p 138-139 (For primary document see N89-11074 02-32)

Avail: NTIS HC A09/MF A01 CSCL 20N

Communications Research Laboratory (CRL, Ministry of Posts and Telecommunications, Japan) has been engaged in development of three advanced satellite communication payloads aiming at experiments by Japan's 2-ton class Engineering Test

Satellite VI (ETS-VI) which is to be launched in H-II rocket by NASDA in August 1992. CRL's three experimental systems are: (1) S-band inter-satellite communications; (2) millimeter-wave inter-satellite and personal-satellite communications; and (3) optical inter-satellite communications. CRL develops experimental optical communication system with telescope of 75 mm diameter which has gimbal mirror beam pointing/tracking mechanism. The onboard system has fundamental optical communication functions with laser diode transmitter of wavelength 0.83 micron, laser beam point-ahead mechanism, receiver of wavelength 0.51 micron, modulation/demodulation subsystem, and so on. Author

N89-11090*# European Space Agency. European Space Research and Technology Center, ESTEC, Noordwijk (Netherlands).
OPEX: (OLYMPUS PROPAGATION EXPERIMENT)
Gert Brussaard *In* JPL, Proceedings of the 12th NASA Propagation Experimenters Meeting (NAPEX 12) Aug. 1988 p 140-145 (For primary document see N89-11074 02-32)
Avail: NTIS HC A09/MF A01 CSCL 20N

The Olympus-1 satellite carries four distinct payloads for experimental utilization and research in the field of satellite communications: (1) the Direct Broadcasting Service (DBS) payload; (2) the Specialized Services Payload; (3) the 20/30 GHz Advanced Communications Payload; and (4) the Propagation Payload. Experimental utilization of the first three payloads involves ground transmissions to the satellite and hence sharing of available satellite time among experimenters. This is coordinated through the Olympus Utilization Program. Author

N89-11091*# Virginia Polytechnic Inst. and State Univ., Blacksburg. Satellite Communications Group.
ACTS AND OLYMPUS PROPAGATION EXPERIMENTS
Charles W. Bostian and Kenneth R. Baker *In* JPL, Proceedings of the 12th NASA Propagation Experimenters Meeting (NAPEX 12) Aug. 1988 p 146-156 (For primary document see N89-11074 02-32)
Avail: NTIS HC A09/MF A01 CSCL 20N

The OLYMPUS and ACTS satellites both provide opportunities for 10 to 30 GHz propagation measurements. The spacecraft are sufficiently alike that OLYMPUS can be used to test some prototype ACTS equipment and experiments. Data are particularly needed on short term signal behavior and in support of uplink power control and adaptive forward error correction (FEC) techniques. The Virginia Tech Satellite Communications Group has proposed a set of OLYMPUS experiments including attenuation and fade rate measurements, data communications, uplink power control, rain scatter interference, and small-scale site diversity operation. A digital signal processing receiver for the OLYMPUS and ACTS beacon signals is being developed. Author

N89-11092*# Signal Processors Ltd., Cambridge (England).
A DIGITAL BEACON RECEIVER
Peter D. Ransome *In* JPL, Proceedings of the 12th NASA Propagation Experimenters Meeting (NAPEX 12) Aug. 1988 p 157-163 (For primary document see N89-11074 02-32)
Avail: NTIS HC A09/MF A01 CSCL 20N

A digital satellite beacon receiver is described which provides measurement information down to a carrier/noise density ratio approximately 15 dB below that required by a conventional (phase locked loop) design. When the beacon signal fades, accuracy degrades gracefully, and is restored immediately (without hysteresis) on signal recovery, even if the signal has faded into the noise. Benefits of the digital processing approach used include the minimization of operator adjustments, stability of the phase measuring circuits with time, repeatability between units, and compatibility with equipment not specifically designed for propagation measuring. The receiver has been developed for the European Olympus satellite which has continuous wave (CW) beacons at 12.5 and 29.7 GHz, and a switched polarization beacon at 19.8 GHz approximately, but the system can be reconfigured for CW and polarization-switched beacons at other frequencies. Author

N89-11093*# Danish Research Center for Applied Electronics, Hoersholm.
OLYMPUS BEACON RECEIVER
Jens Ostergaard *In* JPL, Proceedings of the 12th NASA Propagation Experimenters Meeting (NAPEX 12) Aug. 1988 p 164-168 (For primary document see N89-11074 02-32)
Avail: NTIS HC A09/MF A01 CSCL 20N

A medium-size Beacon Receiving System for reception and processing of the B1 (20 GHz) and B2 (30 GHz) beacons from Olympus has been developed. Integration of B1 and B2 receiving equipment into one system using one antenna and a common computer for control and data processing provides the advantages of a compact configuration and synchronization of the two receiver chains. Range for co-polar signal attenuation meaurement is about 30 dB for both beacons, increasing to 40 dB for B2 if the receivers are synchronized to B1. The accuracy is better than 0.5 dB. Cross-polarization discriminations of the order of 10 to 30 dB may be determined with an accuracy of 1 to 2 dB. A number of radiometers for complementary measurements of atmospheric attenuation of 13 to 30 GHz has also been constructed. A small multi-frequency system for operation around 22 GHz and 31 GHz is presently under development. Author

N89-11094*# Colorado Univ., Boulder. Dept. of Electrical and Computer Engineering.
THE PROPAGATION INFORMATION CENTER AT THE UNIVERSITY OF COLORADO
Ernest K. Smith and Warren L. Flock *In* JPL, Proceedings of the 12th NASA Propagation Experimenters Meeting (NAPEX 12) Aug. 1988 p 169-172 (For primary document see N89-11074 02-32)
Avail: NTIS HC A09/MF A01 CSCL 20N

A Propagation Information Center is in the process of being established at the University of Colorado with connections to NAPEX and to the NASA program at Colodado University (CU) for Interdisciplinary Research in Telecommunications Policy and Technology Issues. The Propagation Information Center was conceived as a response to several items in the Science Review of the NASA Propagation Program carried out in September of 1986 by a distinguished panel of experts. The program for the Center is conceived as including archival aspects: a memory of past work by NAPEX members; accounts of relevant research activities around the world; papers published in pertinent areas of propagation; and pertinent propagation data files. Duties of the Center should include: exchanging information on future plans with research organizations around the world; scanning the literature for possible contributions; carrying out quick response studies requested by program management; conducting customer surveys of users; preparing a quarterly newsletter to help maintain communication amongst program participants; and assisting students and faculty who are working on policy issues for NASA in the propagation field. Author

N89-11095 Michigan State Univ., East Lansing.
INTERACTION OF ELECTROMAGNETIC WAVES WITH HETEROGENEOUS BODIES OF ARBITRARY SHAPE AND PARAMETERS Ph.D. Thesis
Huei Wang 1987 227 p
Avail: Univ. Microfilms Order No. DA8801885

The quantification of interaction of electromagnetic fields with finite heterogeneous bodies is examined, and an application of electromagnetic waves for detecting movements of a biological body behind a barrier is presented. Dissert. Abstr.

N89-11096 British Broadcasting Corp., Kingswood (England). Research Dept.
A FLAT-PLATE ANTENNA FOR DBS RECEPTION
M. C. D. Maddocks Jul. 1988 18 p
(BBC-RD-1988/6) Copyright Avail: BBC, Kingswood Warren, Tadworth, Surrey, United Kingdom

A flat-plate antenna for the reception of DBS transmissions using low-cost materials has been designed, built and tested. The antenna is essentially a multilayer printed structure consisting of a

polarization converter, an array of elements and a beamforming network. The antenna can be mounted flat on the most suitable wall of an arbitrarily-oriented house and aligned to receive signals from the satellite. Author

N89-11097 British Broadcasting Corp., Kingswood (England).
TELEVISION ANIMATION STORE: CONTROL SYSTEM OPERATION AND IMPLEMENTATION
D. G. Kirby May 1988 23 p
(BBC-RD-1988/4) Copyright Avail: BBC, Kingswood Warren, Tadworth, Surrey, United Kingdom

Described is the computer control system of the electronic rostrum camera animation system developed to enable picture sequences to be generated directly as television signals, instead of using cine film. The ergonomics of the control system are described, together with some of the more demanding aspects of its implementation, which allow complex animated sequences to be generated and replayed in real time. Author

N89-11098# Argonne National Lab., Ill.
WORKSHOPS AND PROBLEMS FOR BENCHMARKING EDDY CURRENT CODES
L. R. Turner, K. Davey, N. Ida, D. Rodger, A. Kameari, A. Bossavit, and C. R. I. Emson Feb. 1988 12 p Presented at the International Symposium on Fusion Nuclear Technology (ISFNT), Tokyo, Japan, 10 Jun. 1988 Prepared in cooperation with Georgia Inst. of Tech., Atlanta, Akron Univ., Ohio, Mitsubishi Atomic Power Industries, Inc., Tokyo, Japan, Electricite de France, Clamart and Science Research Council, Chilton, United Kingdom
(Contract W-31-109-eng-38)
(DE88-009996; CONF-8806121-1) Avail: NTIS HC A03/MF A01

A series of six workshops was held to compare eddy current codes, using six benchmark problems. The problems include transient and steady-state ac magnetic fields, close and far boundary conditions, magnetic and non-magnetic materials. All the problems are based either on experiments or on geometries that can be solved analytically. The workshops and solutions to the problems are described. Results show that many different methods and formulations give staisfactory solutions, and that in many cases reduced dimensionality or coarse discretization can give acceptable results while reducing the computer time required. DOE

N89-11099 Defence Research Establishment Valcartier (Quebec).
VERIFICATION OF EOSAEL (ELECTRO-OPTICAL SYSTEMS ATMOSPHERIC EFFECTS LIBRARY) SNOW TRANSMITTANCE PREDICTIONS
D. Hutt and R. C. Shirkey Mar. 1987 36 p Prepared in cooperation with Army Lab. Command, White Sands Missile Range, N. Mex.
(DREV-R-4423/87) Avail: NTIS HC E03/MF E01; copy not available from STI Facility

Measurements of atmospheric transmission during periods of snow fall were made in the visible and infrared. The measurements are compared to transmission predicted by the XSCALE module of the EOSAEL. The XSCALE predictions correspond well with measured transmittances in the visible but predictions in the IR are considerably less than the measured values. This suggests that the snow transmittance algorithm used in XSCALE is more accurate for transmissometers whose receiver diameters are much larger than the beam diameter. Author

N89-11100# Lawrence Livermore National Lab., Calif.
STATISTICAL EFFECTS IN HIGH-POWER MICROWAVE BEAM PROPAGATION
R. A. Alvarez, P. R. Bolton, and G. E. Sieger Jun. 1988 9 p Presented at the 4th National High Power Microwave Conference, Monterey, Calif., 9 May 1988
(Contract W-7405-eng-48)
(DE88-012440; UCRL-97832; CONF-8805132-11) Avail: NTIS HC A02/MF A01

At very high power levels pulsed microwave beams can generate air-breakdown plasmas which may limit the fluence that the beam can transport through the atmosphere. Conventional air breakdown is an avalanche process wherein free electrons, driven by the microwave fields, produce ionization through collisions with air molecules. Propagation of a beam is affected when the plasma electron density approaches the critical density for the particular microwave frequency. The rate of growth of the plasma depends on the competition between the ionization probability and electron loss processes such as attachment and diffusion. The physics of the avalanche process is reasonably well understood, and fluence limits can be fairly accurately predicted, so long as there are free seed electrons to initiate the breakdown. At sea level and low altitudes, seed electrons are, in fact, expected to be fairly rare, and air breakdown, and the consequences for beam propagation, must be treated as a statistical problem; the effective fluence limit may be much greater than would be predicted on the basis of conventional breakdown thresholds. The statistical effects are currently being investigated. DOE

N89-11101 British Broadcasting Corp., Kingswood (England). Research Dept.
BANDWIDTH COMPRESSION FOR HDTV BROADCASTING: INVESTIGATION OF SOME ADAPTIVE SUBSAMPLING STRATEGIES
M. J. Knee and N. D. Wells Jul. 1988 17 p
(BBC-RD-1988/9) Copyright Avail: BBC, Kingswood Warren, Tadworth, Surrey, United Kingdom

Two possible adaptive subsampling strategies for bandwidth compression of an HDTV signal are described and the results of computer-based investigations of their performance are given. The strategies, known as slope coding and BASS (Block Adaptive Sub-Sampling) coding, are examples of revolutionary or noncompatible versions of DATV (Digitally Assisted TeleVision). The results indicate that either of the strategies could be used to achieve a fourfold compression in bandwidth, enabling the transmission of an HDTV signal within a single WARC 77 DBS channel, but that BASS coding is the more promising of the two in terms of output picture quality, particularly when it is used in conjunction with motion compensation. Some practical considerations relating to hardware design are also discussed. Author

N89-11102*# Applied Research Corp., Landover, Md.
A NEW RADAR TECHNIQUE FOR SATELLITE RAINFALL ALGORITHM DEVELOPMENT
Arthur R. Jameson Sep. 1987 15 p
(Contract NAS5-30041)
(NASA-CR-183471; NAS 1.26:183471; ARC-R87-157) Avail: NTIS HC A03/MF A01 CSCL 17I

A potential new radar parameter was investigated for measuring rainfall, namely the summation of the phase shifts at horizontal and vertical polarizations due to propagation through precipitation. The proposed radar technique has several potential advantages over other approaches because it is insensitive to the drop size distribution and to the shapes of the raindrops. Such a parameter could greatly assist the development of satellite rainfall estimation algorithms by providing comparative measurements near the ground. It could also provide hydrologically useful information for such practical applications as urban hydrology. Results of the investigation showed that the parameters can not be measured by radar. However, a closely related radar parameter, propagation differential phase shift, can be readily measured using a polarization diversity radar. It is recommended that propagation differential phase shift be further investigated and developed for radar monitoring of rainfall using a polarization agile radar. It is also recommended that a prototype multiple frequency microwave link be constructed for attenuation measurements not possible by existing radar systems. Author

N89-11103 British Broadcasting Corp., Kingswood (England). Research Dept.
ARRAY ELEMENTS FOR A DBS FLAT-PLATE ANTENNA

M. C. D. Maddocks Jul. 1988 14 p
(BBC-RD-1988/8) Copyright Avail: BBC, Kingswood Warren, Tadworth, Surrey, United Kingdom

The introduction of a direct broadcast by satellite (DBS) television service requires suitable receiving antennas to be available. An alternative to the parabolic dish antenna is a flat-plate antenna. The overall design of a circularly-polarized flat-plate antenna which can be mounted flat on the wall of a building has been considered in a companion Report. In this Report various types of elements are investigated and their advantages and disadvantages discussed. The most suitable element for use in a flat-plate array is identified as a linearly-polarized folded-dipole element; its performance is reported here. Linearly-polarized elements are found to perform better than circularly-polarized elements and could be used with a polarization converter to receive the circularly-polarized radiation that would be transmitted by DBS. Author

N89-11104# Helsinki Univ. of Technology, Espoo (Finland). Electromagnetics Lab.
POLARIZABILITY AND EFFECTIVE PERMITTIVITY OF LAYERED AND CONTINUOUSLY INHOMOGENEOUS DIELECTRIC SPHERES
Ari Sihvola and Ismo V. Lindell Apr. 1988 31 p
(PB88-210091; ISBN-951-754-449-9; Rept-26) Avail: NTIS HC A03/MF A01 CSCL 20N

The polarizability and dipole moment of different types of small inhomogeneous scatterers are solved. After knowing the dipole moment, the effective permittivity of a dielectric mixture that contains these kinds of scatterers can be solved. Two ways to approach the exact solution are presented: the external and internal field solution. For cases where a scatterer does not possess sharp boundaries, a variational approach appears most efficient. A stationary functional for the polarizability is derived which can be used to calculate accurate estimates for the dipole moment with simple trial functions. Results are shown for multilayer scatterers, and inhomogeneous scatterers with linear, parabolic, and Gaussian permittivity profiles. Author

N89-11105# European Space Agency, Paris (France).
DETERMINATION OF CHARACTERISTIC RADIATION PROPERTIES OF A TORUS ANTENNA
Manfred Zink (Deutsche Forschungs- und Versuchsanstalt fuer Luft- und Raumfahrt, Oberpfaffenhofen, West Germany) Aug. 1988 104 p Transl. into ENGLISH of Bestimmung Charakteristischer Strahlungseigenschaften einer Torusantenne, DFVLR, Oberpfaffenhofen, Federal Republic of Germany Original language document was announced as N88-23049
(ESA-TT-1106; DFVLR-FB-87-46; ETN-88-93323) Avail: NTIS HC A06/MF A01; original German version available from DFVLR, VB-PL-DO, 90 60 58, 5000 Cologne, Federal Republic of Germany 30.50 deutsche marks

The integral equation method is used to investigate characteristic radiation properties of a torus antenna. The solution of the integral equation gives the surface-current distribution. Knowing the current distribution, the antenna input impedance and the radiation pattern can be computed. These characteristic parameters are determined for a dipole in free space, a monopole over a circular ground plane, and a torus antenna. Approximations are necessary to put the integral equation method into practice. Despite these assumptions, the results in the far field region are in good agreement with measured data. For the prediction of the input impedance no satisfactory results can be obtained. ESA

N89-11106*# Massachusetts Inst. of Tech., Cambridge. Dept. of Electrical Engineering and Computer Science.
POLARIMETRIC CLUTTER MODELING: THEORY AND APPLICATION
J. A. Kong, F. C. Lin, M. Borgeaud, H. A. Yueh, A. A. Swartz, H. H. Lim, R. T. Shim, and L. M. Novak (Massachusetts Inst. of Tech., Lexington.) 1988 18 p
(Grant NAG5-270)
(NASA-CR-183348; NAS 1.26:183348) Avail: NTIS HC A03/MF A01 CSCL 20N

The two-layer anisotropic random medium model is used to investigate fully polarimetric scattering properties of earth terrain media. The polarization covariance matrices for the untilted and tilted uniaxial random medium are evaluated using the strong fluctuation theory and distorted Born approximation. In order to account for the azimuthal randomness in the growth direction of leaves in tree and grass fields, an averaging scheme over the azimuthal direction is also applied. It is found that characteristics of terrain clutter can be identified through the analysis of each element of the covariance matrix. Theoretical results are illustrated by the comparison with experimental data provided by MIT Lincoln Laboratory for tree and grass fields. Author

N89-11107# Air Force Inst. of Tech., Wright-Patterson AFB, Ohio.
EFFECTS OF NOISE AND TASK LOADING ON A COMMUNICATION TASK LOADING ON A COMMUNICATION TASK M.S. Thesis
Dean H. Orrell, II 1988 111 p
(AD-A196378; AFIT/CI/NR-88-50) Avail: NTIS HC A06/MF A01 CSCL 25D

Previous research had shown the effect of noise on a single communication task. This research has been criticized as not being representative of a real world situation since subjects allocated all of their attention to only one task. In the present study, the effect of adding a loading task to a standard noise-communication paradigm was investigated. Subjects performed both a communication task (Modified Rhyme Test; House et al. 1965) and a short term memory task (Sternberg, 1969) in simulated levels of aircraft noise (95, 105 and 115 dB overall sound pressure level (OASPL)). Task loading was varied with Sternberg's task by requiring subjects to memorize one, four, or six alphanumeric characters. Simulated aircraft noise was varied between levels of 95, 105 and 115 dB OASPL using a pink noise source. Results show that the addition of Sternberg's task and little effect on the intelligibility of the communication task while response time for the communication task increased. GRA

N89-11108# Air Force Inst. of Tech., Wright-Patterson AFB, Ohio.
BIT-TO-BIT ERROR DEPENDENCE IN DIRECT-SEQUENCE SPREAD-SPECTRUM MULTIPLE-ACCESS PACKET RADIO SYSTEMS Ph.D. Thesis
Robert K. Morrow, Jr. May 1988 122 p
(AD-A196384; AFIT/CI/NR-88-160) Avail: NTIS HC A06/MF A01 CSCL 25E

Slotted direct-sequence spread-spectrum multiple-access (DS/SSMA) packet broadcasting systems with random signature sequences are analyzed within the framework of the lower three layers of the International Standards Organization Reference Model of Open Systems Interconnection. At the physical layer, we show that a widely-used Gaussian approximation (which we call the Standard Gaussian Approximation) for the probability of data bit error in a chip and phase asynchronous system is accurate only when there are a large number of simultaneous users on the channel; otherwise, this approximation can be optimistic by several orders of magnitude. For interfering signals with fixed delays and phases relative to the desired signal, however, the Standard Gaussian Approximation is quite accurate for any number of simultaneous users. To obtain a closer approximation to the probability of data bit error for an asynchronous system, we introduce the Improved Gaussian Approximation, which involves finding the distribution of the multiple-access interference variance over all possible delay and phase values and then taking a Gaussian approximation over the support of the distribution and averaging the results. To accurately analyze packet performance at the data link layer, we first use the theory of moment spaces to gain insight on the effect of bit-to-bit error dependence caused by the constant relative delays and (possibly) phases of the interfering signals over the duration of a desired packet. GRA

N89-11109# Air Force Inst. of Tech., Wright-Patterson AFB, Ohio.
A BROAD-BAND ARRAY OF APERTURE-COUPLED CAVITY-BACKED SLOT ELEMENTS M.S. Thesis
Joseph M. Burns 1988 91 p
(AD-A196400; AFIT/CI/NR-88-110) Avail: NTIS HC A05/MF A01 CSCL 09A

A broad-band array of aperture-coupled cavity-backed slot (CBS) elements was designed, constructed and tested. The antenna array design incorporated two major departures from previous CBS arrays; aperture coupling, and half-width cavities. Experimental results demonstrated these departures enhance the potential for larger operating bandwidths using less physical space than previous arrays of CBS elements. Computer simulation and test results also indicated that the antenna array was not hindered by the presence of a large structural stopband such as was observed in all previous CBS arrays. Consequently, modulation of the antenna feedline impedance was not required for satisfactory performance. Antenna patterns for the array were similar over the frequency range 1.75 to 3.5 GHz. GRA

N89-11110# Air Force Inst. of Tech., Wright-Patterson AFB, Ohio.
SYNTHESIS OF RESISTIVE TAPERS TO CONTROL SCATTERING PATTERNS OF STRIPS Ph.D. Thesis
Randy L. Haupt 1988 162 p
(AD-A196402; AFIT/CI/NR-88-131) Avail: NTIS HC A08/MF A01 CSCL 20C

Scattering occurs when an electromagnetic wave impinges on an object and creates currents in that object which reradiate other electromagnetic waves. Three primary methods exist to reduce microwave scattering from an object: covering it with absorber, changing its shape, and detuning it through impedance loading. Absorbers convert unwanted electromagnetic energy into heat. An example is lining an anechoic chamber with absorbers. Changing its shape channels energy from one direction to another, changes dominant scattering centers, or causes returns from one direction to another, changes dominant scattering centers, or causes returns from various parts to coherently add and cancel the total return. Impedance loading alters the resonant frequency of an object. Absorbers have the most attractive features. They have a broad bandwidth, attenuate the return in many directions, and may be used to reduce scattering from an object after the object is designed. Before trying to control scattering from complex shapes, such as an antenna or airplane, one should try to develop methods to control scattering from simple objects. A very simple object is two dimensional strip. It is infinitely thin, has a finite width, and an infinite length. The scattering pattern of the strip depends upon its width and material composition. Varying these two factors provides a means for controlling the radar cross-section (RCS) of the strip. The goal of this thesis is to synthesize resistive tapers for the strip that produce desired bistatic scattering and backscattering patterns. GRA

N89-11111# Air Force Inst. of Tech., Wright-Patterson AFB, Ohio.
DIGITAL SIGNAL DESIGN FOR METEOR-SCATTER COMMUNICATIONS M.S. Thesis
Jay M. Jacobsmeyer 1988 132 p
(AD-A196685; AFIT/CI/NR-88-56) Avail: NTIS HC A07/MF A01 CSCL 20N

The efficient design of digital modulation and error-control schemes for point-to-point meteor-scatter communication systems is discussed. The methods introduced exploit the unique properties of the meteor-scatter channel. A channel model is derived, which includes expressions for meteor arrival rate, burst duration, and received power. Meteor arrivals are modeled as a Poisson random process and the properties of the Poisson process are used extensively. Channel noise is modeled as additive, white, and Gaussian distributed. The multipath structure of the channel is evaluated only to the extent that it affects channel bandwidth, new expressions for long run average bit rate and mean message waiting time. Bounds on the improvement in mean waiting time over the fixed-rate modem are derived. M-ary modulation methods are investigated to find the optimal modulation for the fixed-rate modem and adaptive-symbol-rate modem. It is shown that the adaptive-symbol-rate modem is not optimal on a bandwidth-limited channel. An alternative scheme, called adaptive quadrature amplitude is evaluated and shown to outperform adaptive-symbol-rate modulation on a bandwidth-limited channel. GRA

N89-11112# Dayton Univ., Ohio.
DIELECTRIC MILLIMETER WAVEGUIDES. VOLUME 1 Final Technical Report, Mar. 1986 - Feb. 1987
Cavour Yeh Mar. 1988 16 p Prepared in cooperation with California Univ., Los Angeles
(Contract F30602-81-C-0206)
(AD-A196844; RADC-TR-88-32-Vol-1) Avail: NTIS HC A03/MF A01 CSCL 09A

This report summarizes the result of the research carried out for the Postdoctoral Task E-6-7108 administered by the University of Dayton under contract F30602-81-C-0206 with RADC. The primary objectives of this research program were to learn whether there exists a dielectric waveguide configuration which offers a lower loss figure than a circular dielectric rod and to establish an experimental technique to measure the guiding characteristics of waves on dielectric structures. These objectives were met. Future research areas are also described in this report. GRA

N89-11113# Naval Research Lab., Washington, D.C.
ON THE GENERATION OF WAVEFORMS HAVING COMB-SHAPED SPECTRA Final Report, Jun. - Aug. 1985
Bruce A. Black 6 May 1988 40 p
(AD-A196927; NRL-MR-6190) Avail: NTIS HC A03/MF A01 CSCL 17D

Two techniques, direct sequence and spread spectrum and frequency hopping are widely used to provide an antijam capability for communications systems. To test the effectiveness of such systems, suitable jammers must be devised. A frequency hopping system can be jammed by wideband noise, by a following frequency hopped carrier (if the hopper is slow enough), or by a multitone jamming signal. Multitone jamming signals are considered advantageous in that jamming power is not wasted on frequencies never visited by the frequency hopper, as is the case when wideband noise is used. This report considers several classes of waveforms having power spectra that are approximately comb-shaped. The report relates the properties of the comb spectrum to the time-domain properties of the waveforms. These are the repeated pseudorandom sequence, used to modulate a carrier, and the frequency-swept sinusoid. A good quality comb spectrum should have uniformly strong teeth over its passband, and the spectrum should fall away rapidly at the band edges. To minimize the distortion caused by saturating power amplifiers, it is helpful is the time-domain function has a constant envelope. It is shown that a pseudorandom sequence that is low-pass filtered prior to modulation can produce a very uniform comb with sharp band edges, provided that the required width of the comb is not excessive. A swept-frequency sinusoid can produce a comb of very wide bandwidth, also with sharp band edges. GRA

N89-11114# TRW Space Technology Labs., Redondo Beach, Calif. Fluid Mechanics Dept.
MODULATION OF RADAR BACKSCATTER FROM THE OCEAN BY A VARIABLE SURFACE CURRENT Final Report, 1 Jan. 1986 - 27 Jun. 1988
E. A. Caponi, D. R. Crawford, H. C. Yuen, and P. G. Saffman 27 Jun. 1988 68 p
(Contract N00014-86-C-0111)
(AD-A196952; Rept-4761-6002-UT-00) Avail: NTIS HC A04/MF A01 CSCL 17I

Calculations of surface wave and radar cross section modulation induced by a spatially varying surface current have been compared with field measurements made with SAR (X- and L-bands), real aperture radar (X-band), laser slope gauge, and CCD video camera during the Joint Canada/U.S. Ocean Wave Investigation Project

(JOWIP) which took place in August 1983. The comparison reveals that: (1) many existing wind-relaxation models underpredict the hydrodynamic effect of the current, (2) simple Bragg scattering model underpredicts radar backscatter modulation for higher frequency radars (e.g., X-band) but appears acceptable at lower radar frequencies (e.g., L-band), and (3) the discrepancy between measurements and calculations at high radar frequency is reduced, but not eliminated, when the effects of long surface waves have been accounted for. GRA

N89-11115# Harry Diamond Labs., Adelphi, Md.
THE PROPAGATION OF ELECTROMAGNETIC WAVES IN THIN DIELECTRIC SLABS Final Report, Jul. - Nov. 1987
Michael R. Stead May 1988 44 p
(AD-A196995; HDL-TR-2145) Avail: NTIS HC A03/MF A01 CSCL 20N

This report presents the solutions of Maxwell's equations for the TE and TM modes of propagation along a thin dielectric slab. From these, the propagation constants are determined and the electric and magnetic field patterns are plotted. These calculations are done with the use of the dielectric coefficients of LiNO3 and GaAs. The wavelengths used are 0.82 micrometers (diode laser), 1.064 micrometers (Nd:YAG laser), and 1.55 micrometers (diode laser). The thickness of the slabs range from 0.1 to 1.0 micrometers. GRA

33 ELECTRONICS AND ELECTRICAL ENGINEERING

Includes test equipment and maintainability; components, e.g., tunnel diodes and transistors; microminiaturization; and integrated circuitry.

For related information see also *60 Computer Operations and Hardware* and *76 Solid-State Physics.*

N89-11116# Sandia National Labs., Albuquerque, N. Mex. Exploratory Batteries Div.
COMPATIBILITY AND PERFORMANCE OF SEPARATORS IN LI/SOCI(SUB 2) CELLS
Wendy R. Cieslak 1988 7 p Presented at the 33d International Power Source Symposium, Cherry Hill, N.J., 13 Jun. 1988
(Contract DE-AC04-76DP-00789)
(DE88-011090; SAND-87-2396C; CONF-880665-1) Avail: NTIS HC A02/MF A01

Degradation of many common separator materials, such as polyethylene, excludes their uses in SOCl2 electrolytes. Degradation of the binder in an otherwise chemically-resistant separator may also eliminate it for use in this aggressive environment. We are interested in a separator that does not degrade during more than 10-year storage in either active or reserve cells. Even in reserve configurations, degradation may occur by reaction with Li. Additionally, the separator must be flexible and strong enough for a spiral-wound cell, and it must have the proper thickness and porosity for optimum performance. The properties of three categories of separator materials have been investigated: polymers, glasses and ceramics. We have performed compatibility tests in LiAlCl4/SOCl2 electrolyte and in contact with Li (no electrolyte), and we have assessed electrochemical performance in laboratory cells. The purpose of these tests was to screen a wide variety of materials to identify several candidate separators so that a specific product might readily be chosen on the basis of application requirements. DOE

N89-11117# Oak Ridge National Lab., Tenn. Atomic, Molecular and High Voltage Physics Group.
ELECTRON ATTACHMENT PROPERTIES OF EXCITED DIELECTRIC-GAS MOLECULES AND THEIR POSSIBLE USE FOR PULSE POWER SWITCHING
L. G. Christophorou, S. R. Hunter, L. A. Pinnaduwage, P. G. Datskos, and J. G. Carter 1988 4 p Presented at the 9th International Conference on Gas Discharges and their Applications, Venice, Italy, 19 Sep. 1988
(Contract DE-AC05-84OR-21400)
(DE88-009705; CONF-880948-1) Avail: NTIS HC A02/MF A01

Recent findings on the delicate and often large dependence of the electron attachment (and detachment) processes on the internal (vibrational) energy of dielectric-gas molecules are presented with specific reference to SO2F2 and several perfluorocarbons. Such effects are strongly dependent on the molecule and the mode (dissociative or nondissociative) of electron attachment and can be used---in a number of novel ways---to enhance the current switching efficiency, stability and recovery characteristics of high current spark gap closing and diffuse discharge opening and closing switches for pulsed power applications. Also, recent findings on the optically modified electron attachment properties of gases via laser-induced electronic excitation are reported with reference to thiophenol (C6H5SH) and TMAE (tetrakis-dimethyl amino ethylene). The large enhancement (up to 10 ^{6}) in the electron attachment coefficient we have observed in some molecules after irradiation of the gas with UV excimer laser (from low to high), thereby providing a means for actively and repeatedly extinguishing the gas discharge (i.e., opening the switch). DOE

N89-11118# Central Research Inst. of Electric Power Industry, Tokyo (Japan).
EVALUATION OF Li/MoS2 SECONDARY BATTERY FOR LOAD-CONDITIONER. DEEP-CYCLE PERFORMANCE OF AA-SIZE CELLS
Nobuyuki Terada, Kazuma Kumai, and Kaoru Ishihara Sep. 1987 26 p In JAPANESE; ENGLISH summary
(DE88-753437; CRIE-T-86088) Avail: NTIS (US Sales Only) HC A03/MF A01

The load-conditioner (LC) requires the battery which could deliver reliably high energy for a long period. For this, the lithium/molybdenum disulfide cell, technological development of which is most advanced among new type batteries, is a strong candidate even from the viewpoint of cost. In this report, the basic performance of AA-size Li/MoS2 cells which are now test-manufactured and available in the market, was investigated and the following items were examined: (1) Does it have performance superior to a Ni/Cd cell as a substitute for lead battery. --Its initial performance, which shows light discharge efficiency of 90 percent or more and energy density of 40 to 55Wh/kg, demonstrates the prospect of the battery as a new battery of light-weight and high power output. However, it requires a constant voltage circuit for the use as LC and its duration is shorter than that of Ni/Cd cell. (2) Is it made in a large scale which is necessary for LC. --Making it in a large scale is possible by inter alia making electrode material, etc. into thin film, making the electrode area large and making current density small. (3) What kind of technological development is necessary for the use as LC. -- For achieving its long durable life, such technological developments as improvement of electrolyte, etc., are needed. DOE

N89-11119# Sandia National Labs., Albuquerque, N. Mex.
MULTIPLE PULSE PHOTOCONDUCTIVE SEMICONDUCTOR SWITCHING
F. J. Zutavern, B. B. McKenzie, G. M. Loubriel, M. W. OMalley, R. A. Hamil, and L. P. Schanwald 1988 18 p Presented at the 18th Power Modulator Symposium, Hilton Head, S.C., 20 Jun. 1988
(Contract DE-AC04-76DP-00789)
(DE88-011792; SAND-88-0334C; CONF-880699-7) Avail: NTIS HC A03/MF A01

Photoconductive semiconductor switches (PCSS) with short carrier recombination lifetimes (1 to 100 ns) have exhibited comparable opening times in high power (57 kV, 1.0 kA) circuits. Such extremely fast recovery times are not available with the switches generally used for high power (greater than 10 kW) switching, e.g., spark gaps, thyratrons, and silicon controlled rectifiers. Furthermore, since these switches were made with relatively small pieces of semiconductor, and since PCSS scales

linearly in two dimensions to higher voltages and currents, much higher power switches may be developed. New high power switches which have the ability to open and close in a 1 to 10 ns time scale provide the tools to switch high power radiofrequency (RF) circuits above 10 MHz actively. This paper presents three methods to create RF bursts with PCSS. The feasibility of each method is explored, and experiments being performed to test these techniques are described. DOE

N89-11120 Bath Univ. (England).
HIGH FREQUENCY INVERTER-CYCLOCONVERTER SYSTEM FOR dc TO ac CONVERSION Ph.D. Thesis
M. R. D. Al-Mothafar 1987 315 p
Avail: Univ. Microfilms Order No. BRDX80114

A high frequency inverter-cycloconverter system for dc to ac conversion was studied. The primary stage produces a high frequency square wave (500 Hz) which is reduced to a lower frequency (50 Hz) by a cycloconverter which applies a sinusoidally weighted phase controlled technique to produce a pwm-like output. The modulation strategy is presented and harmonic analysis of the positive, negative group voltage waveforms and the resultant output voltage of the square wave cycloconverter is undertaken. The quality of output voltage waveform of conventional sinusoidal cycloconverter and sinusoidal pwm inverter is compared with that of the new cycloconverter for a range of switching frequencies from 500 Hz to 20 kHz. The effect of overlap on the output voltage spectra of the square wave cycloconverter is studied over the same range of frequencies. A prototype inverter-cycloconverter system was developed and tested. Some of the design critera are established and a range of experimental results are presented. These illustrate current and voltage waveforms throughout the system to demonstrate how it operates. Results for efficiency and regulation under open loop conditions are also presented.
Dissert. Abstr.

N89-11121# Instituto de Pesquisas Espaciais, Sao Jose dos Campos (Brazil).
MAGNETIC MOMENT TEST REPORT FOR THE MODEL SAR 8108 BATTERY
G. O. Ludwig, E. DelBosco, and A. Montes May 1988 12 p
(INPE-4574-NTE/280) Avail: NTIS HC A03/MF A01

The procedures are described for determining the magnetic moment of the Eagle-Picher Model SAR 8108 Battery. The results of a test performed with this battery is presented. The experimental method used was to map the flux density field around the battery. The value of the magnetic moment was evaluated from the experimental data by a numerical procedure based on a spherical harmonic analysis and was found to be 0.050 + or - 0.005 A sq m. Author

N89-11122# Sandia National Labs., Albuquerque, N. Mex.
SWITCHABLE AUTO GAIN AMPLIFIER
G. S. Phipps and J. P. Schaefer May 1988 15 p
(Contract DE-AC04-76DP-00789)
(DE88-012114; SAND-88-0079) Avail: NTIS HC A03/MF A01

An electronic amplifier capable of automatically reducing its gain to avoid output saturation is described. Design goals, electrical schematic, and samples of output waveforms are included. DOE

N89-11123# Centre National de la Recherche Scientifique, Toulouse (France). Lab. d'Automatique et d'Analyse des Systemes.
STUDY AND FABRICATION OF AlGaAs/GaAs DOUBLE HETEROJUNCTION BIPOLAR TRANSISTORS FOR INTEGRATED INJECTION LOGIC CIRCUITS Ph.D. Thesis - Toulouse Univ.
Jamal Jamai 1988 159 p In FRENCH; ENGLISH summary
(LAAS-88-138; ETN-88-93077) Avail: NTIS HC A08/MF A01

The operating conditions of integrated injection logic are recalled and the advantages resulting from the use of AlGaAs/GaAs double heterojunction bipolar transistors are summarized. The realization of samples by molecular beam epitaxy and ionic implantation is described, emphasizing the realization conditions used to meet the structure requirements. Electric characterization identified the physical mechanisms accounting for operation limitations. The correlation observed between the behavior of the direct and reverse operations confirms the importance of conduction and that of parasitic charge storage in the collector-base diode. The best performances obtained, highlighting maximum current gains of 500 in forward operation and 100 in reverse operation and an offset voltage as low as 3 mW, show that the properties of the realized epitaxial structures should match the operation of the projected test integrated circuits. ESA

N89-11124# Centre National de la Recherche Scientifique, Toulouse (France). Lab. d'Automatique et d'Analyse des Systemes.
A STUDY OF THE TURN-OFF BEHAVIOR OF HIGH POWER GATE TURN OFF THYRISTORS (GTO): COMPUTER-AID TO DESIGN AND UTILIZATION Ph.D. Thesis - Inst. National des Sciences Appliquees de Toulouse
Zoubir Khatir 1988 126 p In FRENCH; ENGLISH summary
(LAAS-88-164; ETN-88-93078) Avail: NTIS HC A07/MF A01

The turn-off process in high power gate turn off (GTO) thyristors was analyzed in order to improve their switching characteristics, especially in order to minimize their switching losses. A numerical model of the GTO turn-off process was derived, and successfully compared with experiment. Simple rules to evaluate the storage time as a function of the anode load conditions and the external gate drive are proposed. The influence on turn-off of the structural parameters of the device is highlighted. Off switching performances of asymmetrical diffused structures, and the gate assisted turn-off mode were also analyzed. ESA

N89-11125# Centre National de la Recherche Scientifique, Besancon (France). Lab. de Physique et Metrologie des Oscillateurs.
INTEGRATED QUARTZ OSCILLATOR FOR AEROSPACE APPLICATIONS Final Report [OSCILLATEUR A QUARTZ INTEGRE POUR APPLICATIONS AEROSPATIALES]
G. Marianneau and R. Brendel 27 Apr. 1988 53 p In FRENCH
(Contract DRET-86-044)
(ETN-88-93100) Avail: NTIS HC A04/MF A01

A thermostated quartz oscillator was realized using a miniature resonator. Tests on the packaged device show stability over 10 sec of 2.1 times 10 to the minus 11th power; at startup temperature = 20 C, 10 to the minus 7th power in 30 sec, 10 to the minus 8th power in 1 min; for minus 30 C, 10 to the minus 7th power in 30 sec, 10 to the minus 8th power in 3 min. The relative frequency variation between minus 20 and plus 20 C is 2 times 10 to the minus 8th power; between minus 30 and plus 55 C it is 10 to the minus 7th power. Ion impurities in the quartz were characterized by relaxation in a high electric field in order to reduce oscillator sensitivity to radiation. ESA

N89-11126# Instituto de Pesquisas Espaciais, Sao Jose dos Campos (Brazil).
ANALYSIS OF NONLINEAR CIRCUITS AT RF AND MICROWAVE FREQUENCIES BY THE HARMONIC BALANCE METHOD M.S. Thesis [ANALISE DE CIRCUITOS NAO-LINEARES EM RF E MICROONDAS PELO METODO DO BALANCO HARMONICO]
Edson Gusella, Jr. Sep. 1988 92 p In PORTUGUESE; ENGLISH summary
(INPE-4693-TDL/342) Avail: NTIS HC A05/MF A01

This work presents the analysis of nonlinear circuits at RF and microwave frequencies, driven by multiple tones, by the harmonic balance method. The main contributions are the following: (1) the method for analysis of linear networks, using S parameters, was generalized in order to allow greater flexibility in the interconnection of elements; and (2) the algorithm which determines the harmonic balance, using the modified Newton method, starts from an initial guess of the inverse of the Jacobian and updates this approximation at each iteration, decreasing the time needed for its evaluation.
Author

N89-11127*# National Aeronautics and Space Administration. Marshall Space Flight Center, Huntsville, Ala.

POWER QUALITY LOAD MANAGEMENT FOR LARGE SPACECRAFT ELECTRICAL POWER SYSTEMS

Louis F. Lollar Sep. 1988 23 p

(NASA-TM-100342; NAS 1.15:100342) Avail: NTIS HC A03/MF A01 CSCL 09C

In December, 1986, a Center Director's Discretionary Fund (CDDF) proposal was granted to study power system control techniques in large space electrical power systems. Presented are the accomplishments in the area of power system control by power quality load management. In addition, information concerning the distortion problems in a 20 kHz ac power system is presented. Author

N89-11128*# National Aeronautics and Space Administration. Lewis Research Center, Cleveland, Ohio.

STUDY OF OPTICAL OUTPUT COUPLERS FOR SUBMILLIMETER WAVELENGTH BACKWARD-WAVE OSCILLATORS (BWO's)

Jerry D. Cook, Norbert Stankiewicz, and Mark Podany (Analex Corp., Cleveland, Ohio.) 1988 19 p Prepared for presentation at the 13th International Conference on Infrared and Millimeter Waves, Honolulu, Hawaii, 5-9 Dec. 1988; sponsored in part by Society of Photo-Optical and Instrumentation Engineers

(NASA-TM-101360; E-4335; NAS 1.15:101360) Avail: NTIS HC A03/MF A01 CSCL 09C

The machining of slow wave structures for high frequency backward-wave oscillators (BWO) is extremely difficult beyond 1 THz. Recently a microfabrication technique using photolithography and ion-beam assisted etching has been used to construct a prototype BWO operating at 200 to 265 GHz. The output coupler for such tubes remains a problem. Waveguides do not exist or are very lossy at the frequencies of interest (300 to 2000 GHz). This paper discusses several scaled experiments of optical output couplers for submillimeter BWOs. Various designs of planar antennas (Vivaldi horns) and lens-feed systems (Hyperhemispherical lens) were constructed and tested between 20 and 100 GHz using a spectrum analyzer. The lens system was also tested at 337 GHz using a CO2 pumped FIR laser. Author

N89-11129*# National Aeronautics and Space Administration. Lewis Research Center, Cleveland, Ohio.

DEPOSITION AND CHARACTERIZATION OF ZnS/Si HETEROJUNCTIONS PRODUCED BY VACUUM EVAPORATION

Geoffrey A. Landis, Joseph J. Loferski, and Roland Beaulieu (Brown Univ., Providence, R. I.) 1988 18 p Presented at the 5th North Coast American Vacuum Society Symposium, Cleveland, Ohio, 2 Jun. 1988

(NASA-TM-101359; E-4389; NAS 1.15:101359) Avail: NTIS HC A03/MF A01 CSCL 09C

Isotype heterojunctions of ZnS (lattice constant 5.41 A) were grown on silicon (lattice constant 5.43 A) p-n junctions to form a minority-carrier mirror. The deposition process was vacuum evaporation from a ZnS powder source onto a heated (450 C) substrate. Both planar (100) and textured (111) surfaces were used. A reduction of the minority-carrier recombination at the surface was seen from increased short-wavelength quantum response and increased illuminated open-circuit voltage. The minority-carrier diffusion length was not degraded by the process. Author

N89-11130# Massachusetts Inst. of Tech., Cambridge. Microsystems Research Center.

A COHERENT VLSI DESIGN ENVIRONMENT Final Letter Report, for Period Ending 30 Sep. 1987

Paul Penfield, Jr. 5 May 1988 8 p

(Contract N00014-80-C-0622)

(AD-A196428) Avail: NTIS HC A02/MF A01 CSCL 09A

The CAD effort is centered on timing analysis and circuit simulation. Advances have been made in tightening the bounds of timing analysis. The superiority of the Gauss-Jacobi technique for matrix solution, over the Gauss-Seidel method, has been proven when the algorithms are implemented on massively parallel machines. In the circuits area, one result of importance is a new technique for calculating the highest frequency of operation of transistors with parasitic elements present. Work on a synthesis technique is under way. In the architecture area, many new results have been derived for parallel algorithms and complexity. One of the most astonishing is that a hypercube with a large number of faulty nodes can be used, with high probability, as another perfectly functioning hypercube of half the size, by using reconfiguration algorithms that are simple, fast, and require only local information. Also, the design of the message-driven processor is continuing, with several advances in architecture, software, communications, and ALU design. Many of these are being implemented in VLSI circuits. The theory work has as a central theme that the cost of communication should be included in complexity analyses. This has led to advances in models for computation, including volume-universal networks, routing, network flow, fault avoidance, queue management, and network simulation. GRA

N89-11131# Air Force Inst. of Tech., Wright-Patterson AFB, Ohio.

OPTIMIZATION OF MICROWAVE MAGNETOELASTIC DELAY LINES M.S. Thesis

Bruce F. Feldman May 1988 129 p

(AD-A196866; AFIT/CI/NR-88-62) Avail: NTIS HC A07/MF A01 CSCL 09A

A new ray tracing computer program which optimizes the design of linearly dispersive, two-port magnetoelastic delay lines operating at microwave frequencies has been developed. The simulation shows that delay line line bandwidth and dynamic range can be separately optimized for the value of a wave focussing parameter within a limited range. Whereas previous work had demonstrated that there are a potentially infinite number of synthesized magnetic fields which produce the desired linear delay function, choice of magnetic field can now be made to obtain a desired value of the wave focussing parameter and thereby optimize delay line performance. The computer simulation is correlated with experimental magnetoelastic delay line results. Previously, linearly dispersive two-port magnetoelastic delay lines with synthesized magnetic fields had been built in both a Strauss type configuration and with a novel, buried-antenna design where the antennas were wires inserted through separate holes drilled by laser in a YAG rod. The validity of the ray tracing is confirmed by the experimental data and, additionally, the simulation elucidates the causes of the differences in bandwidth performance between the design types. GRA

N89-11132# Illinois Univ., Urbana. Dept. of Aeronautical and Astronautical Engineering.

TEMPORAL VARIATIONS IN A CW HF MOPA (OSCILLATOR/AMPLIFIER) Final Report, 1 Apr. 1985 - 30 Sep. 1987

L. H. Sentman May 1988 41 p

(Contract N00014-85-K-0326)

(AD-A196915; AAE-88-5; UILU-ENG-88-0505) Avail: NTIS HC A03/MF A01 CSCL 09C

The experimental and theoretical studies directed toward characterizing the output of a CW HF oscillator/amplifier (MOPA) configuration are summarized. Scale effects when the size of a cw HF chemical laser was reduced by a factor of two were studied experimentally and theoretically. When the saturated gains of the single channel CL I laser and the two channel CL II laser were the same, the CL I power was 70 to 80 percent of the CL II power. This suggests that for only a 25 percent performance penalty, the size, weight and gas requirements of a laser can be reduced by a factor of two. The power spectral distributions of the CL I and CL II lasers when the saturated gains were the same, they were nearly identical. When the two lasers had the same cavity losses, the CL I power was an average of 45 percent of the CL II power. The Blaze II and MNOR03SR laser computer simulations gave good agreement with data as a function of mass flow rate, cavity losses, pressure and size of the laser.

Time-dependent oscillations on lines whose saturated gain did not fill the unstable resonator had a period of 47 ns. These oscillations did not occur for Fresnel numbers less than 3.2 and their amplitudes increased as the fraction of the resonator filled by the saturated gain of the oscillating line degreased. A 7 ns oscillation, which was superimposed on top of the 47 ns oscillation, was probably a mode beat of the laser. GRA

N89-11133# Texas Instruments, Inc., Dallas. Defense Systems and Electronics Group.
DESIGN DEFINITION FOR A DIGITAL BEAMFORMING PROCESSOR Final Report, Jan. - Nov. 1987
J. L. Langston, Shashikant Sanzgiri, Karl Hinman, Kevin Keisner, and Domingo Garcia Apr. 1988 133 p
(Contract F19628-87-C-0016)
(AD-A196983; RADC-TR-88-86) Avail: NTIS HC A07/MF A01 CSCL 12F

Very large scale integrated circuit technology now makes large bandwidth digital beamforming array antennas practical. Algorithms and architectures were investigated for the implementation of a processor capable of producing large bandwidth multiple output beams for both near and far-term applications. Algorithms in element space and beam space were investigated. Structures for dedicated algorithm execution with highly pipelined, systolic hardware were examined. Arithmetic execution alternatives were considered. The impact of channel errors were investigated and methods of calibrating the beamformer to compensate for these errors were developed. The effects of quantization errors were investigated and processor dynamic range requirements were assessed. The capabilities of Si and GaAs technologies were assessed. The implementation of a processor chip set using Application Specific Integrated Circuits (ASIC) was investigated. A recommended brassboard demonstration system design was derived. GRA

N89-11134# Minnesota Univ., Minneapolis. Corrosion Research Center.
CORROSION PHENOMENA DURING OVERCHARGE IN POLYMER ELECTROLYTE CELLS Technical Report No. 19, 15 Jul. 1985 - 30 May 1988
M. Z. Munchi, R. Gopaliengar, and B. B. Owens 19 May 1988 26 p
(Contract N00014-85-1588)
(AD-A196997) Avail: NTIS HC A03/MF A01 CSCL 10C

The corrosion behavior of the polymer electrolyte cell has been investigated using various surface analytical techiques. The results indicate that under normal cycling conditions, the cell components are perfectly intact with no evidence of any corrosion. However, cells placed on overcharge for prolonged periods showed and inability to discharge. GRA

N89-11135# Minnesota Univ., Minneapolis. Corrosion Research Center.
LITHIUM SECONDARY BATTERIES: ROLE OF POLYMER CATHODE MORPHOLOGY Technical Report No. 20, 15 Jul. 1985 - 30 May 1988
Katsuhiko Naoi, Tetsuya Osaka, and Boone B. Owens Jun. 1988 2 p
(Contract N00014-85-1588)
(AD-A196998) Avail: NTIS HC A02/MF A01 CSCL 07F

Electrically conducting polymers have been utilized both as the cathode and as the electrolyte element of Li secondary cells. Polymer cathodes were limited in their suitability for batteries because of the low energy content associated with low levels of doping and the inclusion of complex ionic species in the cathode. Recent studies have indicated that doping levels up to 100 percent can be achieved in polyanilene. High doping levels in combination with controlled morphologies have been found to improve the energy and rate capabilities of polymer cathodes. A morphology-modifying technique was utilized to enhance the charge/discharge characteristics of Li/liquid electrolyte polypyrrole cells. The polymer is electropolymerized in a preferred orientation morphology when the substrate is first precoated with an insulating film of nitrile butadiene rubber (NBR). Modification of the kinetic behavior of the electrode results from variations in the chemical composition of the NBR. GRA

34 FLUID MECHANICS AND HEAT TRANSFER

Includes boundary layers; hydrodynamics; fluidics; mass transfer; and ablation cooling.

For related information see also *02 Aerodynamics* and *77 Thermodynamics and Statistical Physics.*

N89-11136# Lockheed Missiles and Space Co., Palo Alto, Calif. Research Lab.
NUMERICAL SIMULATION OF AXISYMMETRIC BASE FLOW ON TACTICAL MISSILES WITH PROPULSIVE JET Final Technical Report, Jul. 1982 - Aug. 1983
P. D. Thomas, R. P. Reklis, R. R. Roloff, and R. J. Conti Nov. 1987 44 p Previously announced in IAA as A84-39307
(Contract DAAH01-82-C-0519)
(AD-A196169; AD-E951147; LMSC/D878344; AMSMI-RD-CR-85-9) Avail: NTIS HC A03/MF A01 CSCL 16D

The axisymmetric Lockheed Viscous Implicit Solver (LVIS) Navier-Stokes computer code is modified to incorporate the capability for computing the flow in the base region of a tactical missile with propulsive jet. Modifications include generalization of the computational space to accommodate the geometry of the base and implementation of two turbulence models of the two-equation type (kappa-epsilon and k-W). Computer runs are made with both turbulence models. The results of these computations are similar, but some differences are observed in the recirculating near-wake flow and in the shear layers that separate it from the high-speed streams of the propulsive jet and of the external flow. These differences are attributed to the greater eddy viscosity predicted by the kappa-epsilon model.
Author (GRA)

N89-11137# Argonne National Lab., Ill.
LASER/FLUORESCENT DYE FLOW VISUALIZATION TECHNIQUE DEVELOPED FOR SYSTEM COMPONENT THERMAL HYDRAULIC STUDIES
J. J. Oras and K. E. Kasza 1988 9 p Presented at the 3rd International Symposium on Refined Flow Modelling and Turbulence Measurements, Tokyo, Japan, 26 Jul. 1988
(Contract W-31-109-eng-38)
(DE88-012008; CONF-880772-1) Avail: NTIS HC A02/MF A01

A novel laser flow visualization technique is presented together with examples of its use in visualizing complex flow patterns and plans for its further development. This technique has been successfully used to study: (1) the flow in a horizontal pipe subject to temperature transients, to view the formation and breakup of thermally stratified flow and to determine instantaneous velocity distributions in the same flow at various axial locations; (2) the discharge of a stratified pipe flow into a plenum exhibiting a periodic vortex pattern; and (3) the thermal-buoyancy-induced flow channeling on the shell side of a heat exchanger with glass tubes and shell. This application of the technique to heat exchangers is unique. The flow patterns deep within a large tube bundle can be studied under steady or transient conditions. This laser flow visualization technique constitutes a very powerful tool for studying single or multiphase flows in complex thermal system components. DOE

N89-11138# Argonne National Lab., Ill. Materials and Components Technology Div.
FRICTION REDUCTION AND HEAT TRANSFER ENHANCEMENT IN TURBULENT PIPE FLOW OF NON-NEWTONIAN LIQUID-SOLID MIXTURES
U. S. Choi and K. V. Liu Feb. 1988 13 p Presented at the International Symposium on Heat Transfer Enhancement and

Energy Conservation (ISHTEEC), Guangzhou, People's Republic of China, 2 Aug. 1988
(Contract W-31-109-eng-38)
(DE88-010018; CONF-880858-1) Avail: NTIS HC A03/MF A01

Argonne National Laboratory (ANL) has identified two concepts for developing advanced energy transmission fluids for thermal systems, in particular district heating and cooling systems. A test series was conducted at ANL to prove these concepts. This paper presents experimental results and discusses the degradation behavior of linear polymer additives and the flow and heat transfer characteristics of non-melting slurry flows. The test results furnished strong evidence that the use of friction reducing additives and slurries can yield improved thermal-hydraulic performance of thermal systems. DOE

N89-11139# Sandia National Labs., Albuquerque, N. Mex.
A GENERAL ANALYSIS FOR OBTAINING THE VISCOSITY FUNCTION FROM VISCOMETRIC MEASUREMENTS: A CASE STUDY FOR THE HELICAL SCREW RHEOMETER
Andrew M. Kraynik and Louis A. Romero 1988 3 p Presented at the 10th International Congress on Rheology, Sydney, Australia, 14 Aug. 1988
(Contract DE-AC04-76DP-00789)
(DE88-006271; SAND-87-2052C; CONF-880827-2) Avail: NTIS HC A02/MF A01

The concept of viscometric flow is a cornerstone of rheology. The deformation history of a fluid element in such flows is essentially equivalent to steady simple shearing flow. Three material functions that depend upon shear rate, first derivative of gamma, -- the shear stress tau, first normal stress difference N (sub 1) and second normal stress difference N (sub 2) -- completely determine the extra stress and velocity fields for this special class of fluid motions. It is central to rheometry that material functions for fluids with quite general flow behavior can be measured only in a viscometric flow. In the following, we restrict our discussions to the most widely recognized and most easily measured flow property, the viscosity function, which is given by Mu (first derivative of gamma) = tau (first derivative of gamma)/first derivative of gamma. DOE

N89-11140# International Centre for Theoretical Physics, Trieste (Italy).
UNSTEADY HYDROMAGNETIC FREE-CONVECTION FLOW WITH RADIATIVE HEAT TRANSFER IN A ROTATING FLUID. 1: INCOMPRESSIBLE OPTICALLY THIN FLUID
A. R. Bestman and S. K. Adjepong Nov. 1987 14 p Previously announced in IAA as A88-51836
(DE88-702998; IC-87/384-Pt-1) Avail: NTIS (US Sales Only) HC A03/MF A01

We study the unsteady free convection flow near a moving infinite flat plate in a rotating medium by imposing a time dependent perturbation on a constant plate temperature. The temperatures involved are assumed to be very large so that radiative heat transfer is significant, which renders the problem very nonlinear even on the assumption of a differential approximation for the radiative flux. When the perturbation is small, the transient flow is tackled by the Laplace transform technique. Complete first order solutions are deduced for an impulsive motion. DOE

N89-11141# Lawrence Livermore National Lab., Calif.
GODUNOV METHODS AND ADAPTIVE ALGORITHMS FOR UNSTEADY FLUID DYNAMICS
J. Bell, P. Colella, J. Trangenstein, and M. Welcome Jun. 1988 6 p Presented at the 11th International Conference on Numerical Methods in Fluid Dynamics, Williamsburg, Va., 27 Jun. 1988
(Contract W-7405-eng-48)
(DE88-013094; UCRL-98976; CONF-8806125-3) Avail: NTIS HC A02/MF A01

Higher-order versions of Godunov's method have proven highly successful for high-Mach-number compressible flow. One goal of the research being described in this paper is to extend the range of applicability of these methods to more general systems of hyperbolic conversion laws such as magnetohydrodynamics, flow in porous media and finite deformations of elastic-plastics solids. A second goal is to apply Godunov methods to problems involving more complex physical and solution geometries than can be treated on a simple rectangular grid. This requires the introduction of various adaptive methodologies: global moving and body-fitted meshes, local adaptive mesh refinement, and front tracking. DOE

N89-11142# National Aeronautical Lab., Bangalore (India). Fluid Mechanics Div.
STUDY OF FLOW PAST A CIRCULAR CYLINDER USING A HIGHER ORDER SCHEME FOR NAVIER-STOKES EQUATION
T. K. Sengupta and S. Selvarajan Jun. 1988 13 p
(TM-FM-8806) Avail: NTIS HC A03/MF A01

The unsteady viscous incompressible flow around a circular cylinder is studied numerically for moderate to higher Reynolds number range by solving the 2-D Navier-Stokes equation in stream function/vorticity formulation. The stream function equation is solved by an ADI technique while the vorticity transport equation is solved by a third order upwinding scheme. The initial development in the near wake of a circular cylinder is computed and compared with experimental results. Author

N89-11143# Joint Inst. for Nuclear Research, Dubna (USSR). Dept. of New Acceleration Methods.
HYDRODYNAMICAL CHARACTERISTICS OF HELIUM TWO-PHASE FLOWS AT RELATIVELY HIGH MASS RATES
Zun Gan Son, S. Yu. Selyunin, and Yu. P. Filippov 1987 12 p In RUSSIAN; ENGLISH summary
(DE88-702936; JINR-R-8-87-446) Avail: NTIS (US Sales Only) HC A03/MF A01

A theoretical model is proposed for the pressure drop of channels through which the two-phase flow of helium with relatively high mass flow rates moves. With the help of this model the region of hydraulic crisis is predicted. Experimental results which are consistent with the theoretical model predictions are presented. It is shown that under certain conditions the hydrodynamical characteristics of helium two-phase flows and of steam-water ones are analogous and that the existence of some distinctions are caused by the difference in thermophysical properties of helium and water. The data obtained are compared with the results available in literature. DOE

N89-11144# Sandia National Labs., Albuquerque, N. Mex. Ground Motion and Seismic Div.
EXPLOSION AIRBLAST PREDICTIONS ON A PERSONAL COMPUTER AND APPLICATION TO THE HENDERSON, NEVADA INCIDENT
Jack W. Reed 1988 13 p Presented at the 23rd DOD Explosives Safety Seminar, Atlanta, Ga., 9 Aug. 1988
(Contract DE-AC04-76DP-00789)
(DE88-014991; SAND-88-0681C; CONF-880891-2) Avail: NTIS HC A03/MF A01

An airblast prediction program for explosions, called BLASTO, has been written for use with IBM-PC (or compatible) computers, to produce overpressure-distance curves for a variety of interactive input conditions. Several common units are allowed for each input, but calculation and output are in SAI metric units. Explosion yield (chemical or nuclear) and ambient atmospheric pressure are used to generate a referenced Standard overpressure-distance curve. Explosives may be point charges at any height, above ground or depth below the earth surface. Buried charges may also be distributed in a sheet, or HEST configuration. If upper air weather data or forecasts are available, they can be used to generate directed (wind effects) sound velocity versus height structures which are interpreted to give attenuated or enhanced overpressure-distance curves. These are calculated for directions around the compass or toward specified targets or communities. Evaluation of the recent accidental explosion at an ammonium perchlorate (A-P) plant in Henderson, Nevada, made use of BLASTO. Damage inspection gave some estimates for incident overpressure at various ranges. These showed considerable scatter, but they generally surrounded an overpressure versus

distance curve calculated for 1-kt NE free-air burst. Weather data and directed sound velocity calculations showed that some of the closest residential damages were in directions of minimal weather dependent blast distortion, allowing the conclusion that the largest explosion could be simulated by a 250-ton HE surface burst. Video-camera recordings, newspaper eye-witness accounts, post-accident aerial photographs, seismic recordings, and a report of the A-P storage pattern have been reviewed to show that this largest blast probably occurred in a 1500-ton A-P collection. This leads to 1:6 TNT airblast equivalence for A-P. DOE

N89-11145 California Univ., San Diego.
TURBULENT BOUNDARY LAYER DRAG REDUCTION ON AN AXISYMMETRIC BODY USING CIRCULAR RING MANIPULATORS Ph.D. Thesis
Kamal Poddar 1987 177 p
Avail: Univ. Microfilms Order No. DA8804748

Modification of the turbulent boundary layer on an axisymmetric body using circular ring manipulators, aimed at skin friction drag reduction, is investigated. Measurements of the mean and fluctuating components of the wall shear stress show that the presence of circular ring manipulators in the turbulent boundary layer reduces the wall shear stress. An optimum manipulator configuration, for both single and tandem manipulators, exists in the turbulent boundary layer for which reduction in local stress is maximum. The tandem manipulator configuration appears to be more effective in reducing the local shear stress and the skin friction drag. Measurements of various tubulence quantities including flow visualization have led to the identification of some of the mechanisms involved in the skin friction reduction. Author

N89-11146# Oak Ridge National Lab., Tenn.
AN OVERVIEW OF THE STIRLING ENGINE HEAT PUMP PROGRAM
F. C. Chen 1988 11 p Presented at the 2nd DOE/ORNL Heat Pump Conference: Research and Development on the Heat Pump for Space Conditioning Applications, Washington, D.C., 17 Apr. 1988
(Contract DE-AC05-84OR-21400)
(DE88-013833; CONF-8804100-21) Avail: NTIS HC A03

The paper summarizes the recent developments in the Stirling engine-driven heat pump program activities sponsored by the Department of Energy (DOE) through Oak Ridge National Laboratory (ORNL). This technology has displayed its ability to meet the thermal performance objectives. Enhanced technology options guided by value engineering principles are being pursued toward the development of an economically viable household engine-driven heat pump. DOE

N89-11147# Sandia National Labs., Albuquerque, N. Mex.
NUMERICAL DESCRIPTION OF CAVITATION ON AXISYMMETRIC BODIES
C. E. Hickox, C. E. Hailey, W. P. Wolfe, H. A. Watts, R. J. Gross, and M. S. Ingber (Iowa State Univ. of Science and Technology, Ames.) 1988 20 p Presented at the Cavitation and Multiphase Forum, Cincinnati, Ohio, 24 Jul. 1988
(Contract DE-AC04-76DP-00789)
(DE88-006826; SAND-88-0184C; CONF-880740-1) Avail: NTIS HC A03/MF A01

This paper reports on ongoing studies which are directed toward the development of predictive techniques for the modeling of steady cavitation on axisymmetric bodies. The primary goal of the modeling effort is the prediction of cavity shape and pressure distribution from which forces and moments can be calculated. Here we present an overview of the modeling techniques developed and compare predictions with experimental data obtained from water tunnel tests for both limited and supercavitation. DOE

N89-11148# Massachusetts Inst. of Tech., Cambridge.
RHEOLOGY OF HIGH CONCENTRATION POLYMODAL MULTIPHASE FLOW Quarterly Report
R. F. Probstein Jul. 1988 5 p
(Contract DE-FG22-86PC-90960)
(DE88-014541; DOE/PC-90960/8) Avail: NTIS HC A02/MF A01

Based on the MIT bimodal concept, it has been shown that the shear-dependent viscosity of coal-water mixtures is soley influenced by the presence of micron size colloidal particles and that the effect of the coarse particles which behave independently of the applied shear rates, is to increase the shear rate on the colloidal fraction to a higher effective value. In the last quarterly report, an expression was obtained that relates the effectively shear rate to the coarse particle volume fraction, phi (sub c). The expression was based on the hydrodynamic concepts, because of the non-colloidal behavior of the coarse particles, and it employed two empirical parameters: a matching constant of order unity and the maximum volume fraction at which the suspension can be sheared, phi (sub m). During this last quarterly period, this expression has been applied to the viscosity experiments runs at MIT on bimodal coal slurries. The shear-independent contribution, eta (sub cr), of the coarse particles to the net relative viscosity is thus calculated for different coarse volume fractions, phi (sub c), and the results are shown in Fig. 1. As a cross-check on the procedure, we plot in the same figure the previously obtained relative viscosity results of suspensions of coarse particles in glycerin at different loadings. The agreement between the results of the two independent experiments, we believe, strongly supports the ideas behind the MIT bimodal theory. An expression was next obtained on theoretical grounds to relate the shear-independent coarse relative viscosity, eta (sub c), to phi (sub c), and its derivation is summarized. DOE

N89-11149# Carnegie-Mellon Univ., Pittsburgh, Pa. Dept. of Mechanical Engineering.
EXPERIMENTAL AND THEORETICAL STUDIES OF VERTICAL ANNULAR LIQUID JETS Technical Report No. 2
Norman Chigier, J. I. Ramos, and K. D. Kihm May 1988 21 p
(Contract DE-FG02-86ER-13597)
(DE88-012971; DOE/ER-13597/T1) Avail: NTIS HC A03/MF A01

The objectives of this study are to determine the stability, dynamics, and convergence of vertical annular liquid jets as a function of the initial radius, sheet thickness, and velocity. The influence of variation of Froude, Reynolds, and Weber numbers and geometry on convergence and stability are examined. An implicit finite-difference scheme is developed for solution of the steady-state and time-dependent axisymmetric Navier-Stokes equations. In collaboration with Westinghouse, a cylindrical film chemical reactor will be designed for control of reactions such as reduction of zirconium. Annular liquid curtains have been formed with an initial curtain radius of 50 mm and initial sheet thicknesses of 0.5 and 1.0 mm. Three Froude numbers have been studied: 1.27, 4.27, and 8.87 with variation of the liquid flow rate. Pressure within the curtains has been varied progressively from 0 to 3 Pa. Several flow regimes were found: (1) non-pressurized, (2) pressurized, (3) oscillating, and (4) punctured. Curtain shape and convergence length were determined for each condition by photography. Axial mean velocity in the liquid curtain was measured by Laser Doppler Anemometry along the length of the curtain. The variation of liquid film thickness with axial distance was determined. DOE

N89-11150# Argonne National Lab., Ill. Materials and Components Technology Div.
MEASUREMENTS OF PRESSURE DROP AND HEAT TRANSFER IN TURBULENT PIPE FLOWS OF PARTICULATE SLURRIES
K. V. Liu, U. S. Choi, and K. E. Kasza May 1988 102 p
(Contract W-31-109-eng-38)
(DE88-013622; ANL-88-15) Avail: NTIS HC A06/MF A01

Argonne National Laboratory (ANL), under sponsorhip of DOE, Office of Buildings and Community Systems, has been conducting a comprehensive, long-range program to develop high-performance advanced energy transmission fluids for use in district heating and cooling (DHC) systems. The current study focuses on the

development of phase-change slurries as advanced energy transmission fluids. The objectives are: (1) to establish proof-of-concept of enhanced heat transfer by a slurry, with and without phase change, relative to heat transfer in a pure carrier liquid; (2) to investigate the effect of particle volumetric loading, size, and flow rate on the slurry pressure drip and heat transfer behavior with and without friction-reducing additives; and (3) to generate pressure drop and heat transfer data needed for the development and design of improved DHC systems. Two types of phase-change materials were used in the experiments: ice slush for cooling, and cross-linked, high- density polyethylene (X-HDPE) particles with diameters of 1/8 and 1/20 in. (3.2 and 1.3 mm) for heating. The friction-reducing additive used in the tests was Separan AP-272 at 65 wppm. This report describes the test facility, discusses the experimental procedures, and presents significant experimental results on flow and heat transfer characteristics of the non-melting slurry flows. DOE

N89-11151# Essen Univ. (West Germany). Inst. fuer Angewandtle Thermodynamik und Klimatechnik.
FURTHER INVESTIGATIONS ON NEW FLUID WORKING SYSTEMS FOR ABSORPTION HEAT PUMPS
A. Bothe, U. Nowaczyk, and E. L. Schmidt 1987 196 p In GERMAN; ENGLISH summary
(DE88-012622; EUR-11328) Avail: NTIS (US Sales Only) HC A09

This project comprises two parts: in part 1 work on new working fluid systems was continued and extended; in part 2 first steps in testing new working fluid pairs in real heat pump cycles was undertaken. The new working fluid systems are of the low pressure type and have been investigated as to their applicability for heat pumps and heat transformers. Special concern is given to molecular theoretical considerations leading to suitable fluid combinations with high mutual solubility. The donor-acceptor-properties of the functional groups are important. Solubility depends on the existence of H-bridges, in which the donator's potential is characterized by its acidity and the acceptor's potential by its basicity. Trifluoroethanol (TFE), hexafluoroisopropanol (HFIP) and perfluoropropionic acid (PFPA) have been selected for further investigations. Suitable absorbents could be found in the cyclic derivates of the N-alcyled urea, lactams, oxazolidinones, morpholines, carbonates and sulfones. Results are presented. DOE

N89-11152# Toronto Univ. (Ontario). Inst. for Aerospace Studies.
AN EXPERIMENTAL STUDY OF A LAMINAR WALL-JET IN THE PRESENCE OF A UNIFORM EXTERNAL FLOW Thesis
Allan Bradley Paige Mar. 1988 97 p Sponsored by the Natural Sciences and Engineering Research Council of Canada
(UTIAS-268; ISSN-0082-5263) Copyright Avail: NTIS HC A05/MF A01

An experimental investigation was carried out with 2-dimensional, initially laminar wall jets, both statistically and in a uniform flow. Transition was quantified in the augmented flow (free stream plus jet), and the effects of uniform flow and slot height on transition was measured. A suitable definition for transition of the static wall jet was desired. The experimental static wall jet mean velocity profiles were found to be in good agreement with previously developed theories and experiments for both the laminar and turbulent regimes. Experiments with the augmented flow revealed a delay in jet transition relative to the static wall jet. Author

N89-11153*# National Aeronautics and Space Administration. Marshall Space Flight Center, Huntsville, Ala.
MIXING AND DEMIXING PROCESSES IN MULTIPHASE FLOWS WITH APPLICATION TO PROPULSION SYSTEMS
Rand Decker, ed. and Charles F. Schafer, ed. Jul. 1988 191 p Workshop was held in Huntsville, Ala., 25-26 Feb. 1988; sponsored by NASA, Marshall Space Flight Center, Huntsville, Ala. and USRA, Huntsville, Ala. Sponsored by NASA, Washington, D.C.
(NASA-CP-3006; M-591; NAS 1.55:3006) Avail: NTIS HC A09/MF A01 CSCL 20D

A workshop on transport processes in multiphase flow was held at the Marshall Space Flight Center on February 25 and 26, 1988. The program, abstracts and text of the presentations at this workshop are presented. The objective of the workshop was to enhance our understanding of mass, momentum, and energy transport processes in laminar and turbulent multiphase shear flows in combustion and propulsion environments. For individual titles, see N89-11154 through N89-11163.

N89-11154*# National Aeronautics and Space Administration. Marshall Space Flight Center, Huntsville, Ala.
THE APPLICATION OF SINGLE PARTICLE HYDRODYNAMICS IN CONTINUUM MODELS OF MULTIPHASE FLOW
Rand Decker *In its* Mixing and Demixing Processes in Multiphase Flows With Application to Propulsion Systems Jul. 1988 p 3-13 (For primary document see N89-11153 02-34)
Avail: NTIS HC A09/MF A01 CSCL 20D

A review of the application of single particle hydrodynamics in models for the exchange of interphase momentum in continuum models of multiphase flow is presented. Considered are the equations of motion for a laminar, mechanical two phase flow. Inherent to this theory is a model for the interphase exchange of momentum due to drag between the dispersed particulate and continuous fluid phases. In addition, applications of two phase flow theory to de-mixing flows require the modeling of interphase momentum exchange due to lift forces. The applications of single particle analysis in deriving models for drag and lift are examined. Author

N89-11155*# Sandia National Labs., Albuquerque, N. Mex. Fluid and Thermal Sciences Dept.
CONTINUUM THEORIES FOR FLUID-PARTICLE FLOWS: SOME ASPECTS OF LIFT FORCES AND TURBULENCE
David F. McTigue, Richard C. Givler, and Jace W. Nunziato *In* NASA, Marshall Space Flight Center, Mixing and Demixing Processes in Multiphase Flows with Application to Propulsion Systems Jul. 1988 p 15-31 Previously announced as N88-24898 (For primary document see N89-11153 02-34)
(Contract DE-AC04-76DP-00789)
Avail: NTIS HC A09/MF A01 CSCL 20D

A general framework is outlined for the modeling of fluid particle flows. The momentum exchange between the constituents embodies both lift and drag forces, constitutive equations for which can be made explicit with reference to known single particle analysis. Relevant results for lift are reviewed, and invariant representations are posed. The fluid and particle velocities and the particle volume fraction are then decomposed into mean and fluctuating parts to characterize turbulent motions, and the equations of motion are averaged. In addition to the Reynolds stresses, further correlations between concentration and velocity fluctuations appear. These can be identified with turbulent transport processes such as eddy diffusion of the particles. When the drag force is dominant, the classical convection dispersion model for turbulent transport of particles is recovered. When other interaction forces enter, particle segregation effects can arise. This is illustrated qualitatively by consideration of turbulent channel flow with lift effects included. Author

N89-11156*# Alabama Univ., Huntsville. Dept. of Mechanical Engineering.
TURBULENCE MODELING OF GAS-SOLID SUSPENSION FLOWS
C. P. Chen *In* NASA, Marshall Space Flight Center, Mixing and Demixing Processes in Multiphase Flows with Application to Propulsion Systems Jul. 1988 p 33-53 (For primary document see N89-11153 02-34)
(Contract NAS8-36718)
Avail: NTIS HC A09/MF A01 CSCL 20D

The purpose here is to discuss and review advances in two-phase turbulent modeling techniques and their applications in

various gas-solid suspension flow situations. In addition to the turbulence closures, heat transfer effect, particle dispersion and wall effects are partially covered. Author

N89-11157*# National Aeronautics and Space Administration. Marshall Space Flight Center, Huntsville, Ala.
CONFINED TURBULENT FLUID-PARTICLE FLOW MODELING USING MULTIPLE-REALIZATION PARTICLE TRAJECTORY SCHEMES
A. A. Adeniji-Fashola *In its* Mixing and Demixing Processes in Multiphase Flows With Application to Propulsion Systems Jul. 1988 p 55-85 Sponsored in part by National Academy of Sciences - National Research Council, Washington, D.C. (For primary document see N89-11153 02-34)
Avail: NTIS HC A09/MF A01 CSCL 20D

A multiple-realization particle trajectory scheme has been developed and applied to the numerical prediction of confined turbulent fluid-particle flows. The example flows investigated include the vertical pipe upflow experimental data of Tsuji et al. and the experimental data of Leavitt for a coaxial jet flow, comprising a particle-laden central jet and a clean annular jet, into a large recirculation chamber. The results obtained from the numerical scheme agree well with the experimental data, lending confidence to the modeling approach. The multiple-realization particle trajectory turbulent flow modeling scheme is believed to be a more elegant and accurate approach to the extension of single-particle hydrodynamics to dilute multi-particle systems than the more commonly employed two-fluid modeling approach. It is also better able to incorporate additional force items such as lift, virtual mass and Bassett history terms directly into the particle equation of motion as appropriate. This makes it a suitable candidate for particle migration studies and an extension to situations involving liquid particulate phases with possible propulsion applications, such as in spray combustion, follows naturally. Author

N89-11158*# Washington State Univ., Pullman. Dept. of Mechanical and Materials Engineering.
PARTICLE DISPERSION MODELS AND DRAG COEFFICIENTS FOR PARTICLES IN TURBULENT FLOWS
C. T. Crowe, J. N. Chung, and T. R. Troutt *In* NASA, Marshall Space Flight Center, Mixing and Demixing Processes in Multiphase Flows with Application to Propulsion Systems Jul. 1988 p 87-107 (For primary document see N89-11153 02-34)
(Contract DE-F60686-ER-13567)
Avail: NTIS HC A09/MF A01 CSCL 20D

Some of the concepts underlying particle dispersion due to turbulence are reviewed. The traditional approaches to particle dispersion in homogeneous, stationary turbulent fields are addressed, and recent work on particle dispersion in large scale turbulent structures is reviewed. The state of knowledge of particle drag coefficients in turbulent gas-particle flows is also reviewed. Author

N89-11159*# Notre Dame Univ., Ind.
MIGRATION ARISING FROM GRADIENTS IN SHEAR STRESS: PARTICLE DISTRIBUTIONS IN POISEUILLE FLOW
D. T. Leighton, Jr. *In* NASA, Marshall Space Flight Center, Mixing and Demixing Processes in Multiphase Flows with Application to Propulsion Systems Jul. 1988 p 109-124 Sponsored in part by NSF, Washington, D.C. (For primary document see N89-11153 02-34)
Avail: NTIS HC A09/MF A01 CSCL 20D

Experimental evidence for the existence of shear induced migration processes is reviewed and the mechanism by Leighton and Acrivos (1987b) is described in detail. The proposed mechanism is shown to lead to the existence of an additional shear induced migration in the presence of gradients in shear stress such as would be found in Poiseuille flow, and which may be used to predict the amplitude of the observed short-term viscosity increase. The concentration and velocity profiles which result from such a migration are discussed in detail and are compared to the experimental observations of Karnis, Goldsmith and Mason (1966). Author

N89-11160*# Pennsylvania State Univ., University Park. Dept. of Mechanical Engineering.
OBSERVATIONS OF BREAKUP PROCESSES OF LIQUID JETS USING REAL-TIME X-RAY RADIOGRAPHY
J. M. Char, K. K. Kuo, and K. C. Hsieh *In* NASA, Marshall Space Flight Center, Mixing and Demixing Processes in Multiphase Flows with Application to Propulsion Systems Jul. 1988 p 125-133 Previously announced in IAA as A87-45426 (For primary document see N89-11153 02-34)
Avail: NTIS HC A09/MF A01 CSCL 20D

To unravel the liquid-jet breakup process in the nondilute region, a newly developed system of real-time X-ray radiography, an advanced digital image processor, and a high-speed video camera were used. Based upon recorded X-ray images, the inner structure of a liquid jet during breakup was observed. The jet divergence angle, jet breakup length, and fraction distributions along the axial and transverse directions of the liquid jets were determined in the near-injector region. Both wall- and free-jet tests were conducted to study the effect of wall friction on the jet breakup process. Author

N89-11161*# California Univ., San Diego.
NONGRADIENT DIFFUSION IN PREMIXED TURBULENT FLAMES
Paul A. Libby *In* NASA, Marshall Space Flight Center, Mixing and Demixing Processes in Multiphase Flows with Application to Propulsion Systems Jul. 1988 p 137-159 (For primary document see N89-11153 02-34)
(Contract DE-FG03-86ER-13527)
Avail: NTIS HC A09/MF A01 CSCL 20D

Recent theoretical and experimental results demonstrating the interaction between force fields and density inhomogeneities as they arise in premixed turbulent flames are discussed. In such flames, the density fluctuates between two levels, the high density in reactants rho sub r and the low density in products rho sub p, with the ratio rho sub r/rho sub p on the order of five to ten in flows of applied interest. The force fields in such flames arise from the mean pressure drop across the flame or from the Reynolds shear stresses in tangential flames with constrained streamlines. The consequence of the interaction is nongradient turbulent transport, countergradient in the direction normal to the flame and nongradient in the tangential direction. The theoretical basis for these results, the presently available experimental support therefore and the implications for other variable density turbulent flows are discussed. Author

N89-11162*# Los Alamos National Lab., N. Mex.
THE TURBULENT HEAT FLUX IN LOW MACH NUMBER FLOWS WITH LARGE DENSITY VARIATIONS
Peter J. ORourke and Lance R. Collins *In* NASA, Marshall Space Flight Center, Mixing and Demixing Processes in Multiphase Flow with Application to Propulsion Systems Jul. 1988 p 161-179 Previously announced as N88-21419 (For primary document see N89-11153 02-34)
(Contract W-7405-eng-36)
Avail: NTIS HC A09/MF A01 CSCL 20D

A transport equation has been derived which is the difference between the volume- and mass-averaged velocities and is simply related to the turbulent heat flux phi sup h. Using this equation and an assumption analogous to the drift flux approximation of two-phase flow modeling, an algebraic closure relation for phi sup h that exibits fluxes due to directed transport proportional to -del anti p and due to gradient transport proportional to -del tau has been obtained. Author

N89-11163*# Pennsylvania State Univ., University Park. Dept. of Mechanical Engineering.
MODELING OF COMBUSTION PROCESSES OF STICK PROPELLANTS VIA COMBINED EULERIAN-LAGRANGIAN APPROACH **c25**
K. K. Kuo, K. C. Hsieh, and M. M. Athavale *In* NASA, Marshall Space Flight Center, Mixing and Demixing Processes in Multiphase Flows with Application to Propulsion Systems Jul. 1988

p 181-193 (For primary document see N89-11153 02-34)
(Contract DAAG29-83-K-0081)
Avail: NTIS HC A09/MF A01 CSCL 21B

This research is motivated by the improved ballistic performance of large-caliber guns using stick propellant charges. A comprehensive theoretical model for predicting the flame spreading, combustion, and grain deformation phenomena of long, unslotted stick propellants is presented. The formulation is based upon a combined Eulerian-Lagrangian approach to simulate special characteristics of the two phase combustion process in a cartridge loaded with a bundle of sticks. The model considers five separate regions consisting of the internal perforation, the solid phase, the external interstitial gas phase, and two lumped parameter regions at either end of the stick bundle. For the external gas phase region, a set of transient one-dimensional fluid-dynamic equations using the Eulerian approach is obtained; governing equations for the stick propellants are formulated using the Lagrangian approach. The motion of a representative stick is derived by considering the forces acting on the entire propellant stick. The instantaneous temperature and stress fields in the stick propellant are modeled by considering the transient axisymmetric heat conduction equation and dynamic structural analysis. Author

N89-11164 Missouri Univ., Rolla.
MEASUREMENTS AND PREDICTIONS OF MIXED CONVECTION IN LAMINAR AND TURBULENT BOUNDARY LAYER FLOWS Ph.D. Thesis
N. Ramachandran 1987 164 p
Avail: Univ. Microfilms Order No. DA8802918

Measurements and predictions of laminar mixed convection adjacent to an isothermal surface are presented both in the thermal buoyancy assisting and opposing regions. Simple and accurate correlations are presented for the local and average Nusselt numbers, and the laminar mixed convection regime is established. A correlation is also developed for the onset of transistion from laminar to turbulent flow in terms of the critical Grashof number (Gr sub x,c) and the critical Reynolds number (Re sub x,c). Turbulent mixed convection along isothermal vertical and horizontal surfaces is numerically simulated using a modified k-epsilon turbulence closure model, and the different flow regimes (laminar, transistion and turbulent) are established. The numerical predictions are compared with available experimental data and good agreement is found between the two. For the vertical geometry, the assisting buoyancy forces tend to delay the transistion from laminar to turbulent flow and hence reduce the local heat transfer in this region. For the horizontal surface configuration, the presence of streamwise longitudinal vortex rolls make the flow field three-dimensional in the trasitional phase, and the two-dimensional equations are inadequate to characterize the flow in this region. Dissert. Abstr.

N89-11165# Oak Ridge National Lab., Tenn.
ENGINE DRIVEN HEAT PUMP PROGRAM OVERVIEW
George T. Privon and A. T. Braun (Tectonics Research, Inc., Minneapolis, Minn.) 1988 8 p Presented at the 2nd DOE/ORNL Heat Pump Conference: Research and Development on the Heat Pump for Space Conditioning Applications, Washington, D.C., 17 Apr. 1988
(Contract DE-AC05-84OR-21400)
(DE88-013240; CONF-8804100-6) Avail: NTIS HC A02

This overview presentation is a brief summary of the efforts that have taken place in the small commercial-sized internal combustion engine-driven heat pump project being carried out by the Oak Ridge National Laboratory for the Department of Energy. Aspects of the project discussed are: objectives and effort scope, the engine- compressor-seal concept, early results, recent developments, current status, and future plans. DOE

N89-11166# Lawrence Livermore National Lab., Calif.
APPLICATION OF A SECOND-ORDER PROJECTION METHOD TO THE STUDY OF SHEAR LAYERS
John B. Bell, Harland M. Glaz, Jay M. Solomon, and William G. Szymczak (Naval Surface Warfare Center, Silver Spring, Md.) Jun. 1988 7 p Presented at the 11th International Conference on Numerical Methods in Fluid Dynamics, Williamsburg, Va., 27 Jun. 1988
(Contract W-7405-eng-48)
(DE88-013095; UCRL-98977; CONF-8806125-2) Avail: NTIS HC A02/MF A01

In this paper we apply a second-order projection method for the time-dependent, incompressible Navier-Stokes equations to the study of shear layers. The algorithm represents a higher-order extension of Chorin's projection algorithm. In Chorin's algorithm one first solves the Navier-Stokes equations ignoring the pressure term and then projects the resulting velocity field onto discretely divergence-free vector fields. Our method introduces more coupling between the diffusion-convection step and the projection to obtain second-order temporal accuracy. Furthermore, the algorithm incorporates a second-order Godunov method that provides a robust treatment of the nonlinear terms at high Reynolds number. These features combine to give a method that is second-order accurate for smooth flows and remains stable for singular initial data such as cortex sheets, even in the limit of vanishing viscosity. DOE

N89-11167# International Centre for Theoretical Physics, Trieste (Italy).
UNSTEADY HYDROMAGNETIC FREE-CONVECTION FLOW WITH RADIATIVE HEAT TRANSFER IN A ROTATING FLUID OF ARBITRARY OPTICAL THICKNESS
A. R. Bestman and S. K. Adjepong Nov. 1987 11 p Previously announced in IAA as A88-51852
(DE88-703000; IC-87/386) Avail: NTIS (US Sales Only) HC A03/MF A01

This paper investigates transient effect on the flow of a thermally radiating and electrically conducting compressible gas in a rotating medium bounded by a vertical flat plate. The transience is provoked by a time dependent perturbation on a constant plate temperature. The problem particularly focusses on an optically thick gas and a gas of arbitrary optical thickness when the difference between the wall and free stream temperatures is small. Analytical results are possible only for limiting values of time and these results are discussed quantitatively. Indeed the assumption of small temperature difference is more appropriate for plates which are opaque rather than transparent. DOE

N89-11168# International Centre for Theoretical Physics, Trieste (Italy).
UNSTEADY HYDROMAGNETIC FREE-CONVECTION FLOW WITH RADIATIVE HEAT TRANSFER IN A ROTATING FLUID. 2: COMPRESSIBLE OPTICALLY THIN FLUID
A. R. Bestman and S. K. Adjepong Nov. 1987 15 p Previously announced in IAA as A88-51851
(DE88-702999; IC-87/385-Pt-2) Avail: NTIS (US Sales Only) HC A03/MF A01

We consider the buoyancy-induced flow of an electrically conducting fluid with radiative heat transfer past a vertical flat plate of infinite length. We assume that the density obeys the simple Boussinesq equation of state while the viscosity and thermal conductivity vary with temperature, that is a compressible fluid. If the temperature of the plate is such that a time dependent component is superimposed on a constant value, the problem is tackled by asymptotic approximation. The results are compared and contrasted with those of incompressible flow. DOE

N89-11169# Little (Arthur D.), Inc., Cambridge, Mass.
EVALUATION OF VAPOR COMPRESSION CYCLES USING NONAZEOTROPIC REFRIGERANT MIXTURES
Richard L. Merriam 1988 12 p Presented at the 2nd DOE/ORNL Heat Pump Conference: Research and Development on the Heat Pump for Space Conditioning Applications, Washington, D.C., 17 Apr. 1988
(Contract DE-AC05-84OR-21400)
(DE88-013225; CONF-8804100-8) Avail: NTIS HC A03/MF A01

A comprehensive investigation is carried out, on a systematic

and consistent basis, to explore a range of advanced heat pump cycle concepts using nonazeotropic refrigerants for COP enhancement and capacity modulation along with the trade-offs associated with refrigerant mixture selection. The objectives of the study were to: identify candidate nonazeotropic mixtures and advanced heat pump cycle concepts with emphasis on their potential for single-speed capacity modulation with mixture composition control; assess the effect of conjunction with nonazeotropic mixture cycles; evaluate the cycles analytically and recommend the most promising cycles and mixtures for further development; and provide recommendations relating to the needs for additional refrigerant property data, experimental studies of basic heat transfer phenomena with mixed refrigerants, development of system components, and/or more detailed modeling of specific components. DOE

N89-11170# Pennsylvania State Univ., University Park. Dept. of Mechanical Engineering.
COMPUTATION OF LOW-SPEED COMPRESSIBLE FLOWS WITH TIME-MARCHING PROCEDURES
Charles L. Merkle and Yun-Ho Choi 1988 40 p Previously announced in IAA as A88-48626
(Grant AF-AFOSR-0196-82; AF Proj. 2308)
(AD-A195800; AFOSR-88-0469TR) Avail: NTIS HC A03/MF A01 CSCL 20D

The extension of time-marching procedures to low Mach number and low Reynolds number conditions is considered. It is shown that the disparate speeds of the acoustic and particle waves prevents convergence at high Reynolds numbers while the requirement that both the Courant and the von Neumann numbers be of order one prevents convergence in very viscous flows. A perturbation expansion is used to introduce pseudo-acoustic waves that propagate at speeds similar to the particle speed at high Reynolds numbers and that allows both the inviscid and viscous time step parameters to be of order one at low Reynolds numbers. The resulting algorithm is shown to give convergence rates that are independent of either Mach number or Reynolds number over a range of five orders of magnitude in both parameters. Results are shown for strong heat addition in low speed flow encompassing this broad range of variables. GRA

N89-11171# West Virginia Univ., Morgantown. Dept. of Civil Engineering.
ON THE CONSTITUTIVE RELATION FOR FRICTIONAL FLOW OF GRANULAR MATERIALS
D. D. Gray and J. M. Stiles Mar. 1988 28 p Prepared in cooperation with EG and G Washington Analytical Services Center, Inc., Morgantown, W. Va.
(Contract DE-AC21-85MC-21353)
(DE88-001089; DOE/MC-21353/2584) Avail: NTIS HC A03

The flow of granular materials is an economically important phenomenon which is poorly understood. Granular materials may flow in several regimes: gas-solid two phase flow, rapid flow, or frictional flow. The purpose of this report is to develop a constitutive relation for the frictional flow regime in which the grains slide or roll over one another. Ultimately this relation will be incorporated into a large computer code which will be able to simulate all aspects of the motion of bed material in fluidized bed combustors. DOE

N89-11172# Tecogen, Inc., Waltham, Mass.
ADVANCED HEAT-PIPE HEAT EXCHANGER AND MICROPROCESSOR-BASED MODULATING BURNER CONTROLS DEVELOPMENT Final Report
A. Lowenstein, B. Cohen, S. Feldman, J. Marsala, M. Spatz, E. Smith, and J. Tandler Feb. 1988 206 p
(Contract GRI-5084-241-1069)
(PB88-217070; GRI-88/0109) Avail: NTIS HC A10/MF A01 CSCL 20D

The work presented includes: (1) the development of a heat-pipe condensing heat exchanger; (2) the development of a nominal 100,000 Btu/hr modulating air/gas valve; (3) the experimental performance studies of a water/copper thermosyphons; (4) the field operation of a six-zone warm-air heating system; (5) the adaptation of a conventional venturi-type burner to modulation; and (6) the results of a one-day workshop for manufacturers of HVAC equipment on heat-pipe heat exchangers. Several of the accomplishments of the project included: An air/gas valve was adapted to furnaces with heat-pipe and drum-type heat exchangers, providing these furnaces with over a 5 to 1 turndown capability. A six-zone warm-air heating system was tested for two winters with the modulating furnaces previously described. A data base for the application of copper/water thermosyphons was started. A ten-tube heat-pipe heat exchanger was incorporated into a conventional heat exchanger with only a small increase in the furnace's dimensions. GRA

N89-11173 City Univ. of New York, N.Y.
TOPOLOGICALLY RELATED QUANTITIES IN TURBULENT FLOWS Ph.D. Thesis
William Alfred Cassidy 1987 156 p
Avail: Univ. Microfilms Order No. DA8801687

The role of changes in the topology of the vortex field in the development of turbulence is studied. Analytical work on helicity and representability in terms of Clebsch variables is presented relating both to the instantaneous topology of the vortex field and to the dynamics of the time development of the fields in the case of incompressible, Newtonian flows. It is found that the topological changes relating to helicity and Clebsch representability are due to only one component of the viscosity term in the Navier-Stokes equation, that component which is parallel to the vorticity at the point. When this component of the viscosity term is subtracted a modified Navier-Stokes equation results which conserves helicity and Clebsch representability. Some analytical properties of the resulting equation are discussed. Dissert. Abstr.

N89-11174# Oak Ridge National Lab., Tenn. Efficiency and Renewables Research Section.
LABORATORY EXAMINATION AND SEASONAL ANALYSES OF THE DYNAMIC LOSSES FOR A CONTINUOUSLY VARIABLE SPEED HEAT PUMP
William A. Miller 1988 30 p Presented at the ASHRAE Annual Meeting, Ottawa, Ontario, 25 Jun. 1988
(Contract DE-AC05-84OR-21400)
(DE88-013207; CONF-880627-3) Avail: NTIS HC A03/MF A01

An air-to-air split-system, continuously variable speed heat pump of nominal, 2-1/2 ton (8.8 kW) cooling capacity was instrumented and tested. The system operating conditions, coefficient of performance, and system capacity were measured during frosting/defrosting tests and during both heating and cooling mode cycling tests. Frosting/defrosting tests were conducted for a range of compressor speeds, outdoor air temperatures, and relative humidities. Cycling tests were conducted for a range of compressor speeds and outdoor temperatures. Dynamic loss algorithms were developed from the data and seasonal analysis simulations were made to estimate the potential energy savings due to compressor and indoor blower modulation. For Ft. Worth (Tex.), Knoxville (Tenn.), and Syracuse (N.Y.), analysis of energy cost savings due to modulation justify a cost premium of $400 for three-year payback. DOE

N89-11175# Argonne National Lab., Ill. Reactor Analysis and Safety Div.
HEAT RELEASE EFFECTS OF REACTING GAS JETS IN LIQUIDS
D. H. Cho, D. R. Armstrong, and L. Bova 1988 9 p Presented at the 25th ASME/Americal Inst. of Chemical Engineers/American Nuclear Society National Heat Transfer Conf., Houston, Tex., 24 Jul. 1988
(Contract W-31-109-eng-38)
(DE88-011971; CONF-880724-21) Avail: NTIS HC A 0

An experimental study of a hydrogen chloride gas jet reacting in an aqueous solution of ammonia was conducted. The profile of the gaseous jet penetration (plume) exhibited a periodic or cyclic change, involving spherical growth, axial expansion, and necking often accompanied by detachment and collapse. Similar periodic

fluctuations were observed in the bath pressure measurements. It is believed that the observed plume mostly consists of ammonia vapor produced due to reaction heat release and that the periodic behavior is caused by the growth and collapse of the ammonia vapor. It was possible to correlate a large amount of plume length data based on the notion that the plume length is determined by the distance required for condensation of the ammonia vapor. The characteristics of pressure fluctuations depended strongly on the bath subcooling, resembling those for vapor jets condensing in liquids. DOE

N89-11176 Council for National Academic Awards (England).
DEVELOPING LAMINAR FLOW AND HEAT TRANSFER IN DUCTS OF ARBITRARY CROSS SECTION Ph.D. Thesis
Richard Stainsby 1987 306 p
Avail: Univ. Microfilms Order No. BRD-80694

A finite element based numerical calculation procedure was developed for the prediction of developing flow and heat transfer in the entrance regions of arbitrary shaped passages. Details of the development of the model are given, as well as its application to a range of duct cross-sectional geometries to yield in some cases original predictions for friction factors and Nusselt numbers. The calculation procedure uses the finite element method to solve parabolic forms of the Navier Stokes equations over a series of axial finite difference steps. This particular combination of finite elements for the cross plane directions and finite differences for the axial direction yields a computationally efficient marching solution which is particularly suitable for implementation of a mini-computer. Simultaneously developing flow and heat transfer predictions were obtained for circular, rectangular, elliptical, isosceles triangular and sine shaped ducts, generally for a Prandtl number of 0.7 and with the (T), (H1) and (H2) thermal boundary conditions. Comparisons are made with available analytical and experimental results. These comparisons show that the method works well over a range of different geometries, and hence inspires confidence in the predictions for geometries such as the sine duct where no other results are available. Dissert. Abstr.

N89-11177# Oak Ridge National Lab., Tenn.
ENTRAINMENT ENHANCEMENT OF A SUPERSONIC JET FOR ADVANCED EJECTORS
Wen-Huei Jou, G. S. Knoke, and Chih-Ming Ho 1988 7 p Presented at the 2nd DOE/ORNL Heat Pump Conference: Research and Development on the Heat Pump for Space Conditioning Applications, Washington, D.C., 17 Apr. 1988
(Contract DE-AC05-84OR-21400)
(DE88-013200; CONF-8804100-11) Avail: NTIS HC A02

Improved ejector performance is required for heat-actuated heat pump applications. Laboratory experiments were conducted to investigate the use of a new rectangular supersonic nozzle configuration for mixing enhancement. Noncircular nozzles were previously found to increase substantially the jet entrainment in subsonic flow. Both flow visualization using schlieren photographs and Pitot measurements in the far field indicate that the improvement in mixing for a supersonic jet is as good as that for a subsonic jet if not better. Mixing enhancement using a rectangular jet provides a technology basis for the development of the desired ejectors for heat pump applications. DOE

N89-11178# Lawrence Livermore National Lab., Calif.
NUMERICAL ESTIMATES OF THE RATE OF CONVERGENCE FOR THE VORTEX SHEET METHOD
E. G. Puckett 25 May 1988 15 p Presented at the 1st National Fluid Dynamics Congress, Cincinnati, Ohio, 24 Jul. 1988
(Contracts W-7405-eng-48; DE-AC03-76SF-00098)
(DE88-013809; UCRL-98639; CONF-880716-7) Avail: NTIS HC A03/MF A01

The vortex sheet method for approximating solutions of the Prandtl equations is demonstrated numerically to the exact solution when it is used to model Blasius flow. This is a random walk method and therefore the error is a random variable. The expected value and the standard deviation of the error as a function of the computational parameters has been estimated. This allows us to estimate the dependence of the error on each parameter and hence to find the relation between the parameters which maximizes accuracy and efficiency. It has been demonstrated that the proper choice parameters leads to a reduced statistical error, thus allowing one to nearly achieve the expected rate of convergence without averaging the solution. DOE

N89-11179# Los Alamos National Lab., N. Mex. Center for Nonlinear Studies and Theoretical Div.
ON 1-D CLOSURE MODELS FOR SLENDER 3-D VISCOELASTIC FREE JETS: VON KARMAN FLOW GEOMETRY AND ELLIPTICAL CROSS SECTION
S. E. Bechtel, M. G. Forest, D. D. Holm, and K. J. Lin (Ohio State Univ., Columbus.) 1988 14 p Presented at the IUTAM Meeting, Cincinnati, Ohio, 1 Jul. 1988
(Contract W-7405-eng-36)
(DE88-014478; LA-UR-88-1742; CONF-880786-1) Avail: NTIS HC A03

In this paper we derive one space dimensional, reduced systems of equations (1-D closure models) for viscoelastic free jets. We begin with the three-dimensional system of conservation laws and a Maxwell-Jeffreys constitutive law for an incompressible viscoelastic fluid. First, we exhibit exact truncations to a finite, closed system of 1-D equations based on classical velocity assumptions of von Karman. Next, we demonstrate that the 3-D free surface boundary conditions overconstrain these truncated systems, so that only a very limited class of solutions exist. We then proceed to derive approximate 1-D closure theories through a slender jet asymptotic scaling, combined with appropriate definitions of velocity, pressure and stress unknowns. Our nonaxisymmetric 1-D slender jet models incorporate the physical effects of inertia, viscoelasticity (viscosity, relaxation and retardation), gravity, surface tension, and properties of the ambient fluid, and include shear stresses and time dependence. Previous special 1-D slender jet models correspond to the lowest order equations in the present asymptotic theory by an a posteriori suppression to leading order of some of these effects, and a reduction to axisymmetry. Solutions of the lowest order system of equations in this asymptotic analysis are presented: For the special cases of elliptical inviscid and Newtonian free jets, subject to the effects of surface tension and gravity, our model predicts oscillation of the major axis of the free surface elliptical cross section between perpendicular directions with distance down the jet, and drawdown of the cross section, in agreement with observed behavior. DOE

N89-11180# Minnesota Univ., Minneapolis.
THE IMPACT OF SEPARATED FLOW ON HEAT AND MASS TRANSFER Progress Report, 1 Sep. 1987 - 30 Apr. 1988
R. J. Goldstein and M. Y. Jabbari 1988 10 p
(Contract DE-FG02-87ER-13800)
(DE88-014653; DOE/ER-13800/T1) Avail: NTIS HC A02/MF A01

The purpose of these studies is to increase our understanding of the key parameters and the fundamental mechanisms in flow and heat transfer under separated flow conditions. Detailed mass transfer studies from a circular cylinder near its base, and from its base plate, have been carried out and reported. In some applications the protruding cylinder may not be circular; therefore, non-symmetrical horseshoe vortices may set up rendering an asymmetrical mass transfer distribution. To learn about this situation a study was initiated to measure the effect of separation on mass transfer from a square cylinder projecting out of a plate. The early results indicate that in the separated region formed ahead of the cylinder vortices are generated which, similar to the case of circular cylinder, cause increased mass transfer both from the cylinder and from the end plate. Sample contours of constant mass transfer coefficient on the end plate and around the cylinder are shown on Figure 1. The angle between the incoming flow and the normal to the upstream facing surface of the cylinder is 20 degrees. Note that near the corners of the cylinder the vortices produce a very high mass transfer coefficient. From this study we conclude that energy separation in the jet will cause significant variation of the recovery temperature near the impingement points

when L/D is small, that adiabatic effectiveness is independent of the jet and ambient temperature difference if the effectiveness is defined using recovery temperatures, and that the heat transfer coefficient also is independent of the entrainment if defined on the basis of the difference between the heated and adiabatic wall temperatures. DOE

N89-11181# City Univ. of New York, N.Y.
PERIODICALLY STRUCTURED MULTIPHASE FLOWS AND HYDRODYNAMIC INSTABILITIES IN NARROW CAPILLARIES Progress Report
Charles Maldarelli Aug. 1988 16 p
(Contract DE-FG02-88ER-13820)
(DE88-015608; DOE/ER-13820/T1) Avail: NTIS HC A03/MF A01

The research program focuses on two multiphase flow regimes in straight circular tubes. The first is the two-phase motion of a train of gas bubbles or liquid segments moving in a continuous liquid which wets the tube wall. The second is the the three-phase motion of an alternating train of gas bubbles or nonwetting liquid segments moving over an annular wetting film of liquid immiscible with the segment fluid. Each of these flows is assumed to be at low Reynolds and capillary numbers. Both experimental and theoretical efforts are involved. DOE

N89-11182# Centre d'Etudes et de Recherches, Toulouse (France). Dept. d'Etudes et de Recherches en Aerothermodynamique.
THREE DIMENSIONAL BOUNDARY LAYERS ON SUBMARINE CONNING TOWERS AND RUDDERS Final Report [COUCHES LIMITES TRIDIMENSIONNELLES SUR MASSIFS ET GOUVERNES DE SOUS-MARINS]
C. Gleyzes Jan. 1988 28 p In FRENCH
(Contract STCAN-780-274)
(CERT-OA-23/5025-AYD; DERAT-23/5025-17; ETN-88-93104)
Avail: NTIS HC A03/MF A01

Solutions for the definition of grids adapted to the calculation of three-dimensional boundary layers on submarine conning towers and on submarine rudders and fins are described. The particular geometry of such bodies (oblique shaped hull, curved fins) required special adaptations. The grids were verified on examples from a test basin. ESA

N89-11183# Centre d'Etudes et de Recherches, Toulouse (France). Dept. d'Etudes et de Recherches en Aerothermodynamique.
BURSTING PHENOMENON IN A FLAT PLATE PULSED BOUNDARY LAYER [PHENOMENE DE BURSTING DANS UNE COUCHE LIMITE PULSEE DE PLAQUE PLANE]
R. Houdeville and A. Corjon Jan. 1988 62 p In FRENCH
(Contract DRET-87-002-20)
(CERT-RSF-OA-69/2259-AYD; DERAT-53/5004-20; ETN-88-93106) Avail: NTIS HC A04/MF A01

Turbulence generation in boundary layers is reviewed, and bursting in the boundary layer of a flat plate subjected to a pulsation from the external flow is analyzed using the VITA and second quadrant methods. Flow measurements in unsteady flow are compared with steady cases corresponding to the time averaged flow. The steady cases enable burst detection methods to be evaluated and arbitrary parameters needed for the techniques to be determined. The VITA method is shown to be reliable for burst detection. At low frequencies, a strong modulation of the probability of burst apparition during pulsation is revealed. No significant difference in the average frequency of burst appearance is noted in the steady case. ESA

N89-11184# Centre d'Etudes et de Recherches, Toulouse (France). Dept. d'Etudes et de Recherches en Aerothermodynamique.
STUDY OF THREE DIMENSIONAL BOUNDARY LAYERS ON THE FRONT OF A FUSELAGE AND AT AN AIR INTAKE [ETUDE DES COUCHES LIMITES TRIDIMENSIONNELLES SUR POINTE AVANT DE FUSELAGE ET SUR ENTREE D'AIR]
C. Gleyzes Dec. 1987 27 p In FRENCH
(Contract Aerospatiale-11-000639)
(CERT-OA-22/5025-AYD; DERAT-22/5025-16; ETN-88-93107)
Avail: NTIS HC A03/MF A01

Solutions adopted to define grids adapted to calculation of the three-dimensional boundary layer on the nose of the fuselage of a civil aircraft at low incidence in order to study laminar flow; and at a subsonic air inlet at incidence, are outlined. Examples corresponding to a nose in cryogenic wind tunnel conditions, and a model inlet at high incidence are presented. ESA

N89-11185# Centre d'Etudes et de Recherches, Toulouse (France). Dept. d'Etudes et de Recherches en Aerothermodynamique.
THEORY OF INSTABILITIES IN THE LAMINAR BOUNDARY LAYER: LITERATURE REVIEW [THEORIE DES INSTABILITES DANS LA COUCHE LIMITE LAMINAIRE: SYNTHESE BIBLIOGRAPHIQUE]
Gregoire Casalis Apr. 1988 66 p In FRENCH
(DERAT-42/5618-28; ETN-88-93112) Avail: NTIS HC A04/MF A01

Stability equations for two and three dimensional flow are recalled. Linear theory is reviewed and mathematical treatments of secondary instabilities and nonlinear aspects of laminar boundary layers are discussed. ESA

N89-11186# Max-Planck-Institut fuer Stroemungsforschung, Goettingen (West Germany).
THE GAS DYNAMICS OF FLUIDS OF HIGH SPECIFIC HEAT
Gerd E. A. Meier and E.-A. Mueller, ed. 1987 76 p In GERMAN; ENGLISH summary
(MPIS-89-1987; ISSN-0374-1257; ETN-88-93207) Avail: NTIS HC A05/MF A01

Effects in the gas dynamics of real fluids other than those in ideal substances are reviewed. Complete adiabatic liquefaction and evaporation are possible for substances whose specific heat exceeds a limit of 20 gas constants. These fluids, consisting of large molecules, have so much internal energy storage capacity in their vibrational degrees of freedom that the heat of evaporation can be supplied or also stored in the case of condensation. Thus liquefaction shock waves, which transform a gas completely or partly into a liquid, are possible. In compression waves and the expansion waves, wave bifurcations which are caused by the splitting of isentropes at the phase boundaries can be observed. In steady flow in nozzles and free jets, Mach number discontinuities arise because of phase transition. The discontinuities are not accompanied by a pressure jump and are characterized by a jump in the sound velocity of the fluid. This is part of the wave bifurcation, which means for steady flow a separation of the waves of different speeds at different locations of the flow nozzle or the jet. In the case of free jets of supersaturated fluids flowing out of a nozzle, the explosion-like disintegration of the jet by propagation of the evaporation wave in three dimensions and the extremely large jet angles are noted. ESA

N89-11187# Centre d'Etudes et de Recherches, Toulouse (France). Dept. d'Etudes et de Recherches en Aerothermodynamique.
BOUNDARY LAYER TRANSITION [TRANSITION DE LA COUCHE LIMITE]
D. Arnal, J. C. Juillen, and F. Vignau Feb. 1988 37 p In FRENCH
(Contract DRET-87-002-018)
(CERT-OA-40/5018-AYD; DERAT-40/5018-24; ETN-88-93320)
Avail: NTIS HC A03/MF A01

A calculation method including the effects of interaction between longitudinal and transversal instabilities on a delta wing is presented. The results of calculations made to qualify the effects of wall cooling on a compressible laminar layer are also presented. The transition processes downstream of a backward facing step with and without wall aspiration are investigated. ESA

N89-11188# Air Force Inst. of Tech., Wright-Patterson AFB, Ohio.
A COMPUTATIONAL STUDY OF COHERENT STRUCTURES IN THE WAKES OF TWO-DIMENSIONAL BLUFF BODIES M.S. Thesis
Jeffrey Alan Pearce Aug. 1988 138 p
(AD-A196820; AFIT/CI/NR-88-99) Avail: NTIS HC A07/MF A01 CSCL 20D

The periodic shedding of vortices from bluff bodies was first recognized in the late 1800's. Currently, there is great interest concerning the effect of vortex shedding on structures and on vehicle stability. In the design of bluff structures which will be exposed to a flow, knowledge of the shedding frequency and the amplitude of the aerodynamic forces is critical. The ability to computationally predict parameters associated with periodic vortex shedding is thus a valuable tool. In this study, the periodic shedding of vortices from several bluff body geometries is predicted. The study is conducted with a two-dimensional finite-difference code employed on various grid sizes. The effects of the grid size and time step on the accuracy of the solution are addressed. Strouhal numbers and aerodynamic force coefficients are computed for all of the bodies considered and compared with previous experimental results. Results indicate that the finite-difference code is capable of predicting periodic vortex shedding for all of the geometries tested. Refinement of the finite-difference grid was found to give little improvement in the prediction; however, the choice of time step size was shown to be critical. Predictions of Strouhal numbers were generally accurate, and the calculated aerodynamic forces generally exhibited behavior consistent with previous studies.
GRA

N89-11189# Pennsylvania State Univ., University Park. Dept. of Mechanical Engineering.
EXPERIMENTAL RESEARCH ON SWEPT SHOCK WAVE/BOUNDARY LAYER INTERACTIONS Annual Report, 1 Apr. 1987 - 31 Mar. 1988
Gary S. Settles 28 Apr. 1988 58 p
(Grant AF-AFOSR-0082-86; AF Proj. 2307)
(AD-A196938; PSU-ME-R-87/88-0031; AFOSR-88-0637TR)
Avail: NTIS HC A04/MF A01 CSCL 20D

This study of swept shock wave interactions with turbulent boundary layers relied entirely on non-intrusive, laser-based optical flow diagnostics. Experiments were carried out to define the flowfield structure of fin-generated interactions over a Mach number range 2.5 to 3.5 using the laser light-screen flow visualization technique. Further experiments resulted in accurate skin friction measurements in fin-generated swept interactions by way of the Laser Interferometer Skin Friction Meter. Techniques were perfected for the assessment of flowfield fluctuation levels using pulsed-laser holographic interferometry. The results of this research have given new insight into the fin-interaction flowfield structure, which involves a supersonic jet produced by shock wave refraction and impinging on the test surface. High skin friction levels were measured in the vicinity of this jet impingement, which compare well with computational predictions carried out by others. Finally, the observed jet impingement structure is shown to be similar to that of leading-edge shock wave impingement on high-speed flight vehicles.
GRA

N89-11190# Naval Postgraduate School, Monterey, Calif.
DEVELOPMENT OF A BOUNDARY LAYER CONTROL DEVICE FOR TIP CLEARANCE EXPERIMENTS IN AN AXIAL COMPRESSOR M.S. Thesis
Muliukur Tarigan Mar. 1988 66 p
(AD-A196968) Avail: NTIS HC A04/MF A01 CSCL 20D

A boundary layer control device was designed to change significantly the case-wall boundary layer thickness entering a large-scale, multistage axial compressor. The device was intended to double the boundary layer thickness in order to evaluate the influence of the inlet boundary layer in controlled tip clearance experiments being conducted on the compressor. The boundary layer characteristics expected to be produced by the control device were predicted empirically and experimental verification was required. Kiel, cobra, and impact probes were used in the experiments and pressures were recorded manually using water manometers. The geometry of the boundary layer control device, an annular array of spires, was derived from shapes developed for simulating the atmospheric boundary layer in large rectangular section wind tunnels. A significantly thicker boundary layer was measured in the compressor than was intended. However, the results were interpreted and recommendations were made for geometry changes necessary to achieve the intended control for the tip clearance investigation.
GRA

N89-11065# Joint Publications Research Service, Arlington, Va.
CASCADE FLOW ANALYSIS BY NAVIER-STOKES EQUATION
Osamu Nozaki *In its* JPRS Report: Science and Technology: Japan 4 Jun. 1987 p 18-20 Transl. into ENGLISH from Kogiken Nyusu (Tokyo, Japan), Aug. 1986 p 7-10 (For primary document see N89-11061 02-31)
Avail: NTIS HC A05/MF A01

N89-11400# Technische Univ., Regensburg (West Germany).
COMPUTATIONAL FLUID DYNAMICS AND SUPERCOMPUTERS, CHAPTER 6
W. Gentzsch *In* AGARD, Computational Fluid Dynamics: Algorithms and Super Computers Mar. 1988 p 141-182 (For primary document see N89-11395 02-60)
Copyright Avail: NTIS HC A09/MF A01

35 INSTRUMENTATION AND PHOTOGRAPHY

Includes remote sensors; measuring instruments and gages; detectors; cameras and photographic supplies; and holography.

For aerial photography see *43 Earth Resources and Remote Sensing*. For related information see also *06 Aircraft Instrumentation*, and *19 Spacecraft Instrumentation*.

N89-11191*# Galileo Electro-Optics Corp., Sturbridge, Mass.
CURVED CHANNEL MCP IMPROVEMENT PROGRAM Final Report
Bruce N. LaPrade and Michael B. Corbett 12 Nov. 1987 65 p
(Contract NAS5-30047)
(NASA-CR-180790; NAS 1.26:180790; Galileo-72132) Avail: NTIS HC A04/MF A01 CSCL 09A

Blowholes and blemishes were determined to start at two stages of manufacturing. Sperical blowholes resulted from trapped gas between the high melting temperature bond glass and the MCP wafer. During thermal processing, the trapped gas expanded and displaced the softened channel glass to form a spherical inclusion. This defect was eliminated by grinding the prefritted bond wafer and channel plate wafer to a flatness which ensured intimate contact prior to fusion. Elliptical blowholes or blemishes were introduced during the fiber draw stage. Contaminants trapped between the core bar and clad tubing volatized providing large quantities of expanding gas. These pockets of gas became elongated to an ellipsoidal shape during fiber draw. Special cleanliness procedures were developed for the grinding, polishing, and acid etching of core bars. Improvements in channel curvature fabrication were implemented. The design of the shearing fixture was evaluated. A new design was developed which eliminated an off-axis moment. The shearing furnace design was evaluated. Steady state thermal conditions instead of thermal transient conditions were determined to reduce curvature nonuniformity.
Author

N89-11192*# General Electric Co., Cincinnati, Ohio. Advanced Technology Operation.
SENSORS FOR CERAMIC COMPONENTS IN ADVANCED PROPULSION SYSTEMS: SUMMARY OF LITERATURE SURVEY AND CONCEPT ANALYSIS, TASK 3 REPORT
W. H. Bennethum and L. T. Sherwood Aug. 1988 108 p

(Contract NAS3-25140)
(NASA-CR-180900; NAS 1.26:180900) Avail: NTIS HC A06/MF A01 CSCL 14B

The results of a literature survey and concept analysis related to sensing techniques for measuring of surface temperature, strain, and heat flux for (non-specific) ceramic materials exposed to elevated temperatures (to 2200 K) are summarized. Concepts capable of functioning in a gas turbine hot section environment are favored but others are reviewed also. Recommendation are made for sensor development in each of the three areas. Author

N89-11193# Aeronautical Research Labs., Melbourne (Australia).
A HYBRID HOT-WIRE DATA ACQUISTION SYSTEM
J. H. Watmuff Nov. 1986 39 p
(ARL-AERO-R-172; AR-004-509) Avail: NTIS HC A03/MF A01

Described are the philosophy, software, hardware and the operation of a hybrid hot-wire signal processing system where unscaled mean and rms quantities are determined by analog circuits whose output voltages are passed to a digital computer for scaling and further processing. The circuits are orchestrated by a compact intelligent microprocessor based data acquisition system which can be supervised by any computer with an RS232C serial interface. Author

N89-11194# Joint Inst. for Nuclear Research, Dubna (USSR). Lab. of Nuclear Problems.
AUTOCOMPENSATION DEVICE FOR ULTRALOW TEMPERATURE MEASUREMENTS
N. L. Gorodishenin, V. A. Evdokimov, S. S. Katushenok, Yu. F. Kiselev, and A. N. Chernikov 1987 7 p In RUSSIAN; ENGLISH summary
(DE88-702900; JINR-13-87-566) Avail: NTIS (US Sales Only) HC A02/MF A01

A noise-protected meter for ultralow temperatures with a thermoresistor symmetrically connected to a low-noise preamplifier at the input and with a driftless digital lock-in detector at the output is described. The negative feedback circuit includes a multiplier of the analogue signal and the digital code. This principle of circuit construction is found to allow a considerable reduction of experimental errors under actual cryogenic conditions. The resistance range being 0.02 to 200 k omega, the operating model of the device provides + or - 0.5 percent accuracy of heart supply below 5x10 to the minus 14 power W. DOE

N89-11195*# Maryland Univ., College Park. Inst. for Physical Science and Technology.
LASER WAVEMETER/SPECTROMETER OPERATING MANUAL Final Report
Leo J. Cotnoir Feb. 1986 49 p
(Contract NAS5-26654)
(NASA-CR-180802; NAS 1.26:180802) Avail: NTIS HC A03/MF A01 CSCL 14B

The Laser Wavemeter/Spectrometer is a compact, rugged instrument using a unique combination of an uncoated (Snyder) wedge interferometer and a coated (Fizeau) wedge interferometer to simultaneously measure the wavelength centroid and spectral characteristics of pulsed or CW lasers. Wavelength centroid measurement accuracies are in the range of 1 part in 1,000,000 using the Snyder stage alone. The Fizeau wedge section is capable of resolving spectral details to 0.002/cm and of locating the position of a fringe to 0.0005/cm. Because the Snyder wedge is uncoated, wavelength centroid measurements are possible over the entire detector range of from about 300 nm to greater than 1.0 micron. The coatings of the Fizeau wedge limit spectral analysis to a 200 nm interval in that range. The instrument is currently configured to operate from 600 nm to 800 nm. Author

N89-11196*# Wyle Labs., Inc., Hampton, Va.
ELECTRICAL NOISE REDUCTION TECHNIQUES CONTRIBUTING TO IMPROVED DATA QUALITY AT THE NATIONAL TRANSONIC FACILITY
J. R. McPhee Nov. 1988 38 p
(Contract NAS1-18304)
(NASA-CR-4193; NAS 1.26:4193) Avail: NTIS HC A03/MF A01 CSCL 09C

In initial use, the high-speed digital data acquisition systems at Langley Research Center's National Transonic Facility produced data containing unacceptably high noise levels. Described is a process whereby the contributing noise sources were identified and eliminated. The effects of 60 Hz power, system grounding, EMI/RFI, and other problems are discussed and the corrective action taken is outlined. The overall effort resulted in an improvement of greater than 5:1 in system performance. Although the report describes a system specifically used for wind tunnel data acquisition, the corrective techniques employed are generally applicable to large scale high-speed data systems where signal resolution in the low microvolts range is important. Author

N89-11197# European Space Agency, Paris (France).
SECURING THE TIME SCALE OF THE NAVEX REFERENCE CLOCK AND RATE DETERMINATIONS BY TIME COMPARISONS WITH THE HELP OF THE GLOBAL POSITIONING SYSTEM (GPS)
Hartmut Nau Aug. 1988 62 p Transl. into ENGLISH of Sicherung des Zeitbezeugesder NAVEX-Hauptuhr und Gandbestimmungen durch Zeitvergleiche mit Hilfe des Global Positioning System (GPS), DFVLR, Oberpfaffenhofen, Federal Republic of Germany Original language document was announced as N88-22879
(ESA-TT-1111; DFVLR-Mitt-87-20; ETN-88-93324) Avail: NTIS HC A04/MF A01; original German version available from DFVLR, VB-PL-DO, 90 60 58, 5000 Cologne, Federal Republic of Germany 22.50 deutsche marks

It is shown that the method of time comparison by GPS is a powerful tool. Experimental results of time comparisons between UTC and an atomic clock are presented. The difference with the method of clock transportations is shown by four examples. The results of syntonization between the reference clock and a clock at Cape Canaveral are summarized. ESA

N89-11198*# National Aeronautics and Space Administration. Lewis Research Center, Cleveland, Ohio.
PARTICLE SIZING BY WEIGHTED MEASUREMENTS OF SCATTERED LIGHT
Donald R. Buchele Oct. 1988 40 p
(NASA-TM-100968; E-4396; NAS 1.15:100968) Avail: NTIS HC A03/MF A01 CSCL 14B

A description is given of a measurement method, applicable to a poly-dispersion of particles, in which the intensity of scattered light at any angle is weighted by a factor proportional to that angle. Determination is then made of four angles at which the weighted intensity is four fractions of the maximum intensity. These yield four characteristic diameters, i.e., the diameters of the volume/area mean (D sub 32 the Sauter mean) and the volume/diameter mean (D sub 31); the diameters at cumulative volume fractions of 0.5 (D sub v0.5 the volume median) and 0.75 (D sub v0.75). They also yield the volume dispersion of diameters. Mie scattering computations show that an average diameter less than three micrometers cannot be accurately measured. The results are relatively insensitive to extraneous background light and to the nature of the diameter distribution. Also described is an experimental method of verifying the conclusions by using two microscopic slides coated with polystyrene microspheres to simulate the particles and the background. Author

36 LASERS AND MASERS

Includes parametric amplifiers.
For related information see also *76 Solid-State Physics*.

N89-11199# Lawrence Livermore National Lab., Calif.
OTHER PROPERTIES OF FREE ELECTRON LASERS: HARMONICS AND OPTICAL GUIDING

T. J. Orzechowski and E. T. Scharlemann 15 Jul. 1988 10 p Presented at the Free Electron Laser Seminar, Beijing, People's Republic of China, 11 Aug. 1988
(Contract W-7405-eng-48)
(DE88-014161; UCRL-99183; CONF-880888-3) Avail: NTIS HC A02/MF A01

Free electron lasers exhibit many interesting phenomena. During the gain process, electrons bunch, and these bunches radiate coherently at harmonics of the fundamental. These bunches can also be responsible for helping to guide the optical signal. We will discuss these topics in this lecture. DOE

N89-11200# Lawrence Livermore National Lab., Calif.
THE ELECTRON LASER FACILITY: MEASUREMENT OF MODES, HARMONICS, PARAMETRIC DEPENDENCE, AND PHASE SHIFT
T. J. Orzechowski 15 Jul. 1988 21 p Presented at the Free Electron Laser Seminar, Beijing, People's Republic of China, 11 Aug. 1988
(Contract W-7405-eng-48)
(DE88-014165; UCRL-99185; CONF-880888-1) Avail: NTIS HC A03/MF A01

The Electron Laser Facility has been used to investigate other phenomena associated with free electron lasers. In particular, we studied the gain in modes other than the fundamental design mode, harmonic generation, paramatic studies (FEL performance versus input power and electron beam current) and phase shift. DOE

N89-11201*# Hampton Inst., Va. Dept. of Physics.
DIRECT SOLAR-PUMPED IODINE LASER AMPLIFIER Semiannual Progress Report, 1 Mar. - 31 Aug. 1988
Kwang S. Han, In H. Hwang, and Larry V. Stock 14 Oct. 1988 50 p
(Grant NAG1-441)
(NASA-CR-183171; NAS 1.26:183171) Avail: NTIS HC A03/MF A01 CSCL 20E

A XeCl laser which was developed earlier for an iodine laser oscillator was modified in order to increase the output pulse energy of XeCl laser so that the iodine laser output energy could be increased. The electrical circuit of the XeCl laser was changed from a simple capacitor discharge circuit of the XeCl laser to a Marx system. Because of this improvement the output energy from the XeCl laser was increased from 60 mj to 80 mj. Subsequently, iodine laser output energy was increased from 100 mj to 3 mj. On the other hand, the energy storage capability and amplification characteristics of the Vortek solar simulator-pumped amplifier was calculated expecting the calculated amplification factor is about 2 and the energy extraction efficiency is 26 percent due to the very low input energy density to the amplifier. As a result of an improved kinetic modeling for the iodine solar simulator pumped power amplifier, it is found that the I-2 along the axis of the tube affects seriously the gain profile. For the gas i-C3F7I at the higher pressures, the gain will decrease due to the I-2 as the pumping intensity increases, and at these higher pressures an increase in flow velocity will increase the gain. Author

N89-11202# Stanford Linear Accelerator Center, Calif.
SIMULATIONS OF THE LASER PHOTOCATHODE INJECTOR
W. Herrmannsfeldt, R. Miller, and H. Hanerfeld Jun. 1988 5 p Presented at the 7th International Conference on High-Power Particle Beams, Karlsruhe, Fed. Republic of Germany, 4 Jul. 1988
(Contract DE-AC03-76SF-00515)
(DE88-015337; SU-SLAC-PUB-4663; CONF-880713-15) Avail: NTIS HC A02/MF A01

New, fully electromagnetic simulations of the beam optics in a laser-photocathode injector have been make using the PIC Code MASK. The recent studies are for the two-cavity design now undergoing tests by R. Sheffield, LANL. Pulses up to 10 nC are simulated, using cavities operating at 1300 MHz with above 1 MeV energy gain per cavity. The work is guided by previous simulation results which show that to achieve good agreement with the best experimental results, it is necessary to use very high RF fields near the cathode and to maintain small beam cross sections, corresponding to very high emission density. DOE

N89-11203*# Desert Research Inst., Reno, Nev. Atmospheric Sciences Center.
AN INERTIAL VELOCITY REFERENCE FOR THE NASA AIRBORNE DOPPLER LIDAR Final Report
Thomas S. Keck and James W. Telford 26 Jul. 1988 11 p
(Contract NAS8-34685)
(NASA-CR-179378; NAS 1.26:179378) Avail: NTIS HC A03/MF A01 CSCL 20E

The following four tasks were studied: (1) modification of the calibration routines to calibrate the Inertial Measurement Unit gyroscope drifts with fixed platform heading; (2) modification of the calibration routines to calibrate the Inertial Measurement Unit accelerometers; (3) checking overall software again for errors; and (4) providing documentation on the above work describing changes to the present software, results of these changes and future operating procedures. Author

N89-11204# Los Alamos National Lab., N. Mex. Materials Science and Technology Div.
LASER PLUME TEMPERATURE MEASUREMENTS IN VARIOUS GASES
Gary K. Lewis, David A. Cremers, and Ray D. Dixon 1988 6 p Presented at the 4th International Symposium on Welding and Melting by Electron and Laser Beams, Cannes, France, 26 Sep. 1988
(Contract W-7405-eng-36)
(DE88-006462; LA-UR-88-540; CONF-880922-2) Avail: NTIS HC A02/MF A01

Nd-YAG laser plume temperatures of 3000--5400 K were measured on 304 stainless steel and 1100 Al in various gases using emission spectroscopy. Temperatures were higher in the reactive gases air, 02, and SF6, compared to inert gases. Ionic spectra were not observed, indicating that the plume primarily consists of hot vapors and does not contain a plasma, in contrast to CO2 laser processing in which plasmas have been observed. The plume temperature remained constant with changes in laser power and with time during the duration of the laser pulse. Light emissions from the plume and from the cooling weld pool after the laser pulse was off were measured and correlated with melt depth. DOE

N89-11205# Joint Inst. for Nuclear Research, Dubna (USSR). Lab. of Theoretical Physics.
COLLECTIVE RESONANCE FLUORESCENCE IN AN INTENSE LASER FIELD WITH PHASE AND AMPLITUDE FLUCTUATIONS
A. S. Shumovskij, R. Tanas, and Tran Quang 1987 19 p Submitted for publication
(DE88-702920; JINR-E-17-87-436) Avail: NTIS (US Sales Only) HC A03/MF A01

The collective resonance fluorescence from a systen of two-level atoms resonantly driven by a strong laser field with the phase and amplitude fluctuations is considered. The effect of the field fluctuations on the spectrum as well as on the degrees of the second-order coherence of the fluorescent field is discussed in detail for the off-resonance case. DOE

N89-11206# Sandia National Labs., Albuquerque, N. Mex.
VACUUM FIZEAU WEDGE WAVEMETER FOR PULSED UV LASERS
Christopher Reiser and Keith R. Lykke Aug. 1988 24 p
(Contract DE-AC04-76DP-00789)
(DE88-015832; SAND-88-1906) Avail: NTIS HC A03/MF A01

We have constructed and tested a vacuum-spaced Fizeau wedge wavemeter that is suitable for measuring the wavelength of pulsed or continuous-wave lasers over the range of 630 nm to 200 nm. A Lasertechnics Model 100 Fizeau wavemeter was modified for ultraviolet operation and demonstrated an accuracy

of 1.6 parts in 10^5 at 248 nm. Extensive computer modeling of the wavemeter has provided optimized design parameters for an improved unit. DOE

N89-11207# Lawrence Livermore National Lab., Calif.
PALADIN: A 10.6-MICRON FREE-ELECTRON LASER AMPLIFIER
T. J. Orzechowski 15 Jul. 1988 20 p Presented at the Free Electron Laser Seminar, Beijing, People's Republic of China, 11 Aug. 1988
(Contract W-7405-eng-48)
(DE88-014164; UCRL-99179; CONF-880888-6) Avail: NTIS HC A03/MF A01

PALADIN is a 10.6-micron free-electron laser amplifier which uses a 45-MeV electron beam produced by a linear induction accelerator. We have measured single pass gain in excess of 25 dB through a 15-micron wiggler and have demonstrated gain guiding. DOE

N89-11208# Lawrence Livermore National Lab., Calif.
AN INTRODUCTION TO THE PHYSICS OF HIGH GAIN FREE ELECTRON LASERS
T. J. Orzechowski, D. Prosnitz, and E. T. Scharlemann 15 Jul. 1988 13 p Presented at the Free Electron Laser Seminar, Beijing, People's Republic of China, 11 Aug. 1988
(Contract W-7405-eng-48)
(DE88-014163; UCRL-99181; CONF-880888-5) Avail: NTIS HC A03/MF A01

Single pass Free Electron Laser Amplifiers using the electron beam generated by Linear Induction Accelerators are being developed at the Lawrence Livermore National Laboratory. The Free Electron Laser models used to describe these systems must account for finite transverse effects such as emittance. The basic equations as well as two-dimensional models are discussed here. DOE

N89-11209# Pacific Northwest Labs., Richland, Wash.
RESONANCE IONIZATION OF Kr METASTABLES USING A SINGLE-FREQUENCY LASER
B. D. Cannon and G. R. Janik Mar. 1988 5 p Presented at the 4th International Symposium on Resonance Ionization Spectroscopy and its Applications, Gaithersburg, Md., 10 Apr. 1988
(Contract DE-AC06-76RL-01830)
(DE88-014757; PNL-SA-15381; CONF-880435-23) Avail: NTIS HC A02/MF A01

A continuous-wave single-frequency dye laser and an argon ion laser were sued to do 1-photon resonant, 2-photon ionization of the metastable 1s(sub 3) and 1s(sub 5) states of krypton to measure iostope shifts and hyperfine splittings for six transitions. Using only the dye laser, we did 2-photon resonant, 3-photon ionization of the 1s metastable state of krypton via the 4d(sub 4)(sup prime) state. We predict resonance ionization with high isotopic selectivity is possible using this state based, on the measured isotope shifts and hyperfine splittings. DOE

N89-11210# Lawrence Livermore National Lab., Calif.
OVERVIEW OF FEL (FREE-ELECTRON LASER) DEVELOPMENT WITH INDUCTION LINACS AT LLNL
Richard J. Briggs 15 Jul. 1988 18 p Presented at the Free Electron Laser Seminar, Beijing, People's Republic of China, 11 Aug. 1988
(Contract W-7405-eng-48)
(DE88-014179; UCRL-99186; CONF-880888-8) Avail: NTIS HC A03/MF A01

The multikiloampere peak currents available from linear induction accelerators make high-gain, free-electron laser amplifier configurations feasible. High extraction efficiencies in a single pass of the electron beam are possible if the wiggler parameters are appropriately tapered, as recently demonstrated at millimeter wavelengths on the 4-MeV ELF facility. Magnetic pulse power systems enable high-repetition-rate operation of the accelerator for high-average-power applications. Key issues involved in extending the technology to shorter wavelengths and higher average powers are described. DOE

N89-11211# Mitre Corp., McLean, Va. JASON Program Office.
LOS ALAMOS XUV FREE ELECTRON LASER PROPOSAL
N. Fortson, D. Hammer, and M. Rosenbluth Mar. 1988 37 p
(Contract DE-AI01-82ER-30024)
(DE88-013485; DOE/ER-30024/T3; JSR-87-301) Avail: NTIS HC A03/MF A01

This report examines a proposed VUX/XUV free electron laser (FEL) facility. Issues examined include accelerator and mirror technology as well as FEL physics in general. As a result of this review specific recommendations are made. DOE

N89-11212# Mound Lab., Miamisburg, Ohio.
HIGH-SPEED PHOTOGRAPHY OF ENERGETIC MATERIALS AND COMPONENTS WITH A COPPER VAPOR LASER
Larry R. Dosser, John W. Reed, and Margaret A. Stark 1988 6 p Presented at the Spring Meeting of the Materials Research Society, Reno, Nev., 4 Apr. 1988
(Contract DE-AC04-76DP-00053)
(DE88-012869; MLM-3491(OP); CONF-880408-32) Avail: NTIS HC A02/MF A01

The evaluation of the properties of energetic materials, such as burn rate and ignition energy, is of primary importance in understanding their reactions and the functioning of devices containing them. One method for recording such information is high-speed photography at rates of up to 20,000 images per second. When a copper vapor laser is synchronized with the camera, laser-illuminated images can be recorded that detail the performance of a material and/or component in a manner never before possible. The laser can also be used for ignition of the energetic material, thus eliminating the need for bridgewires or electric squibs that can interfere with photography. Details of such ignitions are readily observable, and the burn rate of a material can be determined directly from the film. There are indications that information useful for the modeling of pyrotechnic reactions will become available as well. Recent results from high-speed photography of several pyrotechnic materials and devices will be presented. DOE

N89-11213# Stanford Univ., Calif.
GAS-LOADED FREE-ELECTRON LASERS Final Report
1988 9 p
(Contract DE-FG03-84ER-13275)
(DE88-014652; DOE/ER-13275/T1) Avail: NTIS HC A02/MF A01

The goal of this research program is to investigate and develop a gas--loaded free--electron laser (GFEL) as a source of tunable, coherent radiation at wavelengths from the near--infrared to the ultraviolet. DOE

N89-11214# Stanford Univ., Calif.
A GAS-LOADED, FREE-ELECTRON LASER Final Report
1988 9 p
(Contract DE-FG03-84ER-13275)
(DE88-016090; DOE/ER-13275/T2) Avail: NTIS HC A02/MF A01

A gas-loaded free-electron laser (GFEL) was investigated and developed as a source of tunable coherent radiation at wavelengths from the near-infrared to the ultraviolet. DOE

N89-11215# Centre National de la Recherche Scientifique, Toulouse (France). Lab. d'Automatique et d'Analyse des Systemes.
DESIGN AND FABRICATION BY MOLECULAR BEAM EPITAXY OF VISIBLE LIGHT EMITTING RIDGE WAVEGUIDE GaAs-AlGaAs QUANTUM WELL LASERS Ph.D. Thesis - Toulouse Univ.
Francoise Chatenoud 1988 131 p In FRENCH; ENGLISH summary
(LAAS-88-097; ETN-88-93075) Avail: NTIS HC A07/MF A01

A general methodology to determine the threshold parameters of broad-area lasers is developed. The analysis is based on the features associated with quasi two-dimensional effects in quantum wells in order to derive gain-current-wavelength relations; study of propagation and confinement properties in large optical cavities and of oscillation conditions is also included. Single quantum well lasers which operate simultaneously at a minimum threshold current density and with an emission in the range 680 to 750 nm of the visible spectrum are optimized. The geometry of ridge-waveguide index-guided devices is optimized using the study of their lateral confinement. Conditions for the growth of quantum well heterostructures by molecular beam epitaxy are investigated and a reliable stabilized process is established. Precise control of the ridge fabrication is achieved using an in situ characterization technique of the depth etched by reactive ion etching. Infrared and red light emitting devices are fabricated and their results are discussed. At an emission wavelength of 720 nm, broad-area lasers show a threshold current density of 670 A/sq cm, while ridge lasers operate at 20 mA. ESA

N89-11216# Air Force Inst. of Tech., Wright-Patterson AFB, Ohio.
DAMAGE EFFECTS ON THIN ACRYLIC TARGETS CAUSED BY INFRARED RADIATION FROM A PULSED CARBON DIOXIDE LASER M.S. Thesis
Theodore L. Kreifels 7 May 1988 149 p
(AD-A196385; AFIT/CI/NR-88-102) Avail: NTIS HC A07/MF A01 CSCL 09C

The damage on thin acrylic targets caused by focused radiation from a 10 megawatt pulsed carbon dioxide laser was measured as a function of air pressure and target distance from the focal point of the radiation. The laser was fired at targets placed in a test chamber. Target damage and the effects of optical detonations near the target were studied as chamber pressure was reduced from one to 0.01 atmosphere. The first chapter of this major report introduces the fundamental concepts of laser physics. The second chapter discusses the specific characteristics of a carbon dioxide laser. The final chapter presents the equipment, procedures, results, and conclusions of this research. All data is summarized in easy-to-read tables and graphs. Evidence was gathered to conclude that target damage increases as pressure decreases while optical detonations absorb and reflect beam energy. GRA

N89-11217# Medical Coll. of Virginia, Richmond. Dept. of Biomedical Engineering.
BIOLOGICAL APPLICATIONS AND EFFECTS OF OPTICAL MASERS Annual Final Report, Feb. 1962 - Mar. 1982
William T. Ham, Jr., Harold A. Mueller, Ray C. Williams, Walter J. Geeraets, and John J. Ruffolo, Jr. 19 Feb. 1988 29 p
(Contracts DADA17-72-C-2177; DA-49-193-MD-2241)
(AD-A196462) Avail: NTIS HC A03/MF A01 CSCL 06G

Research experiments and projects pertaining to the ocular hazards of lasers and other optical sources are reviewed and discussed in some detail. Early studies to determine threshold retinal damage in the rabbit from ruby and neodymium lasers are described and followed by more elaborate experiments with monkeys using the He;Ne laser. A comparison between threshold retinal lesions in human volunteers, monkeys and rabbits is given. Retinal damage in the rhesus monkey is evaluated in terms of visual acuity. Quantitative data on solar retinitis as determined in the rhesus monkey are provided and the effects of wavelength on light toxicity are evaluated for eight monochromatic laser lines. Experiments performed at Los Alamos to evaluate the ocular effects and hazards of picosecond and nanosecond pulses of radiation from CO2 and HF lasers are described. A list of published papers describing the above research is included. The HF laser effects on the rabbit cornea were very similar to those caused by exposure to the CO2 laser. The energy from the CO2 and HF lasers is completely absorbed in the superficial layers of the cornea, creating a sharp sonic or shock wave which can disrupt the epithelial cells but does not penetrate to the stroma. GRA

N89-11218# Air Force Systems Command, Wright-Patterson AFB, Ohio. Foreign Technology Div.
TWO-DIMENSIONAL SATURATION GAIN AND OUTPUT POWER IN TRANSVERSE FLOW ELECTRICAL DISCHARGE CO2 LASERS
Liyin Chen, Zexiang Chu, and Zhongxiang Wu 24 Jun. 1988 20 p Transl. into ENGLISH from Guangxue Xuebao (China), v. 5, no. 3, Feb. 1985 p 135-141
(AD-A196660; FTD-ID(RS)T-0262-88) Avail: NTIS HC A03/MF A01 CSCL 09C

This article presents the two-dimensional distribution of saturation gain parameters in traverse flow discharge carbon dioxide lasers as well as the laws for their changes along with changes in radiation fields. Use was made of microscopic physical mechanisms to make notes and explanations. We used three types of stability oscillation conditions to respectively calculate the light strength distributions within cavities and output powers. Moreover, this provides a comparison for discussion and offers a type of simple and convenient method for selecting the device with the best design plan. GRA

N89-11219# Arizona Univ., Tucson. Optical Sciences Center.
EFFECT OF THERMAL CYCLING Final Report, Apr. 1985 - Jan. 1987
Stephen F. Jacobs May 1988 49 p
(Contract F29601-85-C-0057)
(AD-A196851; AFWL-TR-87-20) Avail: NTIS HC A03/MF A01 CSCL 20F

The objective of this effort is to evaluate the stability of low expansion Zerodur, developmental Zerodur, ULE, and Cer-Vit as possible substrate materials for high energy laser mirrors. This effort will determine whether there is instability in developmental Zerodur, ULE and Cer-Vit over operating temperatures and coating temperatures (300 to 475 K). Zerodur has already been shown to exhibit instability. Thermal cycling will be investigated as a possible approach to eliminate or reduce hysteresis. The effect of polishing on hysteresis will also be investigated. GRA

N89-11220# Air Force Systems Command, Wright-Patterson AFB, Ohio. Foreign Technology Div.
BASIC RULES OF SATURATED GAIN VARIATION IN A FLOWING LASER CAVITY
Zhongxiang Wu and Haixing Yan 8 Jul. 1988 13 p Transl. into ENGLISH from Jiguang (China), v. 7, no. 3, 1980 p 5-8
(AD-A196861; FTD-ID(RS)T-0260-88) Avail: NTIS HC A03/MF A01 CSCL 09C

From numerical calculation, the basic rules of saturated gain coefficient variation with the field distribution along the flow direction in a Gas Dynamic Laser (GDL) cavity are presented. In connection with variations of vibrational energy and temperature of all modes, these rules are explained with the physical mechanism of relaxation of the active medium. It is pointed out that, for example, there still exists considerable vibrational energy which can be used for Gerry's device with 30 kW monomode output. GRA

N89-11221# National Bureau of Standards, Gaithersburg, Md.
ANALYSIS OF FREE ELECTRON LASER PERFORMANCE UTILIZING THE NATIONAL BUREAU OF STANDARDS' CW MICROTRON Interim Report
Cha-Mei Tang, Phillip Sprangle, Samuel Penner, and Xavier K. Maruyama 19 May 1988 37 p
(Contract N00014-87-F-0066)
(AD-A196928; NRL-MR-6146) Avail: NTIS HC A03/MF A01 CSCL 09C

The CW racetrack microtron (RTM) will be utilized as a driver for a free electron laser (FEL) oscillator. The TRM possesses many exceptional properties of value for the FEL: (1) CW operation, (2) energy from 20 to 185 MeV, (3) small energy spread and emittance, (4) excellent energy stability, and (5) high average power. The 1-D FEL gain formula predicts that the FEL would oscillate at the fundamental approximately from 0.25 to 10 micrometers when up-grading the peak current to greater than or = 2A. This paper presents 3-D self consistent numerical results including several

realistic effects, such as emittance, betatron oscillations, diffraction and refraction. The results indicate that the design value of the transverse emittance is small enough that it does not degrade the FEL performance for intermediate to long wavelengths, and only slightly degrades the performance at the shortest wavelength under consideration. Due to the good emittance, the current density is high enough that focusing, or guiding, begins to manifest itself for wavelengths greater than 2.0 micrometers. GRA

N89-11222# Ohio Wesleyan Univ., Delaware. Dept. of Psychology.
FUNCTIONAL ASSESSMENT OF LASER IRRADIATION Annual Report, Mar. 1983 - Feb. 1984
David O. Robbins Apr. 1988 40 p
(Contract DAMD17-81-C-1065; DA Proj. 3E1-62777-A-878)
(AD-A196930) Avail: NTIS HC A03/MF A01 CSCL 09C

Exposure of the retina to intense spots of coherent light produce immediate and often long term changes in the ability of an animal to perform a visual discrimination task. The size of the initial deficit and the total time for full recovery of visual functioning is related to the energy, position on the retina, and duration of the exposure. GRA

N89-11223# Defense Intelligence Agency, Washington, D.C. Directorate for Scientific and Technical Intelligence.
BIBLIOGRAPHY OF SOVIET LASER DEVELOPMENTS, NUMBER 87, JANUARY - FEBRUARY 1987
29 Dec. 1987 145 p
(AD-A196973; DIA-DST-2700Z-001-88) Avail: NTIS HC A07/MF A01 CSCL 09C

This Soviet Laser Bibliography is no. 87 in a continuing series on Soviet Laser developments. The coverage includes basic research on solid state, liquid, gas, and chemical lasers; components; nonlinear optics; spectroscopy of laser materials; ultrashort pulse generation; theoretical aspects of advanced lasers; and general laser theory. Laser applications are listed under biological effects; communications systems; beam propagation; adaptive optics; computer technology; holography; laser induced chemical reactions; measurement of laser parameters; laser measurement applications; laser-excited optical effects; laser spectroscopy; beam-target interaction; and plasma generation and diagnostics. GRA

N89-11004# Joint Publications Research Service, Arlington, Va.
CHARACTERISTICS OF LASER BEAM FOCUSING WITH SINGLE SPHERICAL MIRRORS DURING LASER TREATMENT Abstract Only
A. G. Borkin, S. V. Drobyazko, G. A. Kosheleva, Yu. V. Pavlovich, Yu. M. Senatorov, V. A. Fromm, and I. V. Kurchatov *In its* JPRS Report: Science and Technology. USSR: Materials Science 4 Apr. 1988 p 8 Transl. into ENGLISH from Avtomaticheskaya Svarka (Kiev, USSR), no. 11, Nov. 1987 p 55-57 (For primary document see N89-11002 02-26)
Avail: NTIS HC A03/MF A01

37 MECHANICAL ENGINEERING

Includes auxiliary systems (nonpower); machine elements and processes; and mechanical equipment.

N89-11224 Durham Univ. (England).
REAL-TIME PATH PLANNING FOR ROBOT ARMS Ph.D. Thesis
Nigel William Balding 1987 222 p
Avail: Univ. Microfilms Order No. BRD-80326

Two new methods are presented for the automatic programming of robots. A model of the robot and its surroundings is held in the computer memory in a form which can be accessed quickly by the path generation algorithm. Information is fed to the computer which defines a task for the robot to perform. The path generation algorithm then calculates the coordinates for the movement of the robot, avoiding obstacles. Finally, the information is downloaded into the robot control computer in its own language. An important feature of the method is the high speed of calculation and data transfer, which is designed for real time operation. The world model is represented as a collection of spheres, some overlapping, and the robot is represented by connected cylinders. This simplified representation is the key to the speed of calculation of the path. Different criteria are used for the optimal path selection, such as minimization of the overall time taken, the distance travelled and the joint rotation. Two path planning methods were developed. These methods provide an on-line, real-time capability for collision free path calculation in a flexible manufacturing environment. Dissert. Abstr.

N89-11225 Stanford Univ., Calif.
KNOWLEDGE-BASED DESIGN OF COMPLEX MECHANICAL SYSTEMS Ph.D. Thesis
Kosuke Ishii 1988 151 p
Avail: Univ. Microfilms Order No. DA8808375

The design of mechanical engineering systems is a complex process that combines creative thinking, experience, intuition, and quantitative analysis. Conventional computer aids for this process have been limited to quantitative aspects of the design process. The recent development of Artificial Intelligence (AI) techniques allows us to incorporate qualitative aspects of design into the computer aids. This thesis presents a framework for applying AI techniques to the design of complex mechanical systems. We use a complex, yet well-understood design example as a vehicle for the effort. We first review how experienced designers use knowledge at various stages of system design. We then propose a knowledge-based model of the design process and develop frameworks for applying knowledge engineering in order to construct a consultation system for the designers. We propose four such frameworks for use at different stages of design: (1) Design Compatibility Analysis (DCA) analyzes the compatibility of the designer's design alternatives with the design specification, (2) Initial Design Suggestion (IDS) provides the designer with reasonable initial estimates of the design variables, (3) Rule-based Sensitivity Analysis (RSA) guides the user through redesign, and (4) Active Constraint Deduction (ACD) identifies the bottlenecks of design by heuristic knowledge. The use of these frameworks eliminates unnecessary iterations and allows the user to obtain a satisfactory solution rapidly. We illustrate the proposed methodology by using as an example the system design of coalfired power generation plants. In addition, we investigate the application of the proposed techniques to other areas of mechanical engineering design. Dissert. Abstr.

N89-11226# Edgerton, Germeshausen and Grier, Inc., Idaho Falls, Idaho.
JOINING OF ADVANCED ALUMINIDES Final Report
D. E. Clark Mar. 1988 47 p
(Contract DE-AC07-76ID-01570)
(DE88-015111; EGG-MS-8000) Avail: NTIS HC A04/MF A01

The weldability of four Ni3/Al-8 percent Cr alloys (IC-221, and two low-Zr modifications) was investigated. Solidification segregation during base metal production decreases weldability by creating low-melting regions susceptible to hot cracking during welding. Extrusion, hot rolling, and annealing procedures were developed to homogenize the base metal microstructure, solving this problem. Weldability was evaluated with the gas tungsten arc welding process and heat-affected zone simulation (Gleeble testing) as a function of Zr content, preheat temperature, and weld travel speed. Weld cracking occurred in the fusion zone; no cracks originated in base material or HAZ. Cracking increased with Zr content at low Zr levels, increased with welding speed, and decreased with preheat. At higher Zr levels, hot cracking was severe, possibly due to a Zr-Ni eutectic. An interdendritic phase present at higher welding speeds, apparently beta prime, is strongly enriched in Ar, and may be associated with weld cracking. Antiphase domains consisting of ordered gamma prime material surrounded by disordered gamma form on rapid cooling and depend in size on welding or simulated welding cooling rates, and can be

expected to affect weld metal properties. The high temperature welding thermal cycle properties of reduced Zr materials are comparable to those of the higher-Zr IC-218 and IC-221. DOE

N89-11227# Academy of Sciences of the Ukrainian SSR, Kharkov. Fiziko-Tekhnicheskij Inst.
THERMAL CALCULATIONS OF NITROGEN-FREE NONMAGNETIC HELIUM CRYOSTATS
A. I. Doroshko, I. S. Zhitomirskij, D. I. Kvasha, V. G. Romanenko, and V. A. Sirenko 1987 16 p In RUSSIAN; ENGLISH summary
(DE88-702807; INIS-SU-19/A) Avail: NTIS (US Sales Only) HC A03/MF A01

Thermal calculations of nitrogen-free helium cryostats are made using a program of hydraulic-thermal calculations for complex cryosystems TEPGIST. A comparison with the experiment is presented, the influence of a number of factors on cryostat resources is studied and an automatic man-machine selection system of optimal design parameters is proposed. DOE

N89-11228 Syracuse Univ., N. Y.
ROBUST CONTROL OF A FLEXIBLE MANIPULATOR ARM Ph.D. Thesis
Victor V. Korolov 1987 200 p
Avail: Univ. Microfilms Order No. DA8806694

The subject is the design and simulation of the end-point controller for a very flexible one-link lightweight manipulator. As a result of this research the robust control for such an arm is designed via a previously developed deterministic approach. The dynamic model for the arm was developed based on the linearized Euler-Bernoulli theory. The nominal system (i.e, the unload arm with corresponding set of the natural frequencies) is supplemented by an uncertain components, which in this case are the possible changes in frequencies of the first and second flexible modes. These changes may be constants or time-dependent functions. The range of frequencies covered is from the natural frequencies of the nominal system to one-fourth of nominal fundamental frequency, which corresponds to a sixteenfold increase in effective mass of the system over the initial effective mass of the arm itself. Two types of control are tested and have shown stable behavior of the system over the whole range of accepted uncertainties. Controllers are synthesized via the use of the Liapunov min-max approach. A Liapunov function of the stable nominal system is employed as a Liapunov function candidate for the actual uncertain system. Dissert. Abstr.

N89-11229# Massachusetts Inst. of Tech., Cambridge. Artificial Intelligence Lab.
UNDERSTANDING BANDWIDTH LIMITATIONS IN ROBOT FORCE CONTROL
Steven D. Eppinger and Warren P. Seering Aug. 1987 20 p Previously announced in IAA as A88-42696
(Contract N00014-86-K-0124)
(AD-A195927; AI-M-948) Avail: NTIS HC A03/MF A01 CSCL 12I

An analytical overview of the dynamics involved in force control is presented. Models are developed which demonstrate, for the one-axis explicit force control case, the effects on system closed-loop bandwidth of: (1) robot system dynamics that are not usually considered in the controller design; (2) drive-train and task nonlinearities; and (3) actuator and controller dynamics. The merits and limitations of conventional solutions are weighed, and some new solutions are proposed. Conclusions are drawn which give insights into the relative of the effects discussed. GRA

N89-11230# Pennsylvania State Univ., University Park. Dept. of Materials Science and Engineering.
EXPERIMENTAL AND THEORETICAL STUDIES ON TRANSPORT PROCESSES IN LASER WELDING Annual Technical Progress Report, 1 Aug. 1987 - 31 Jul. 1988
T. DebRoy 12 Jul. 1988 4 p
(Contract DE-FG02-84ER-45158)
(DE88-013933; DOE/ER-45158/T2) Avail: NTIS HC A02/MF A01

Vaporization of alloying elements is a serious problem in the laser welding of many important engineering alloys. Since the available mass transfer correlations are not applicable for credible assessment of the rates of transport of vaporized species in the gas phase, the role of gas phase mass transfer in the overall vaporization of alloying elements was examined by conducting several critical experiments. The rates of transport of alloying elements in the weld pool were determined from numerically computed fluid flow fields. Since the weld pool is surrounded by plasma during laser welding, the role of plasma in the vaporization of alloying elements was physically modeled by allowing molten copper drops to vaporize isothermally both in the presence and absence of plasma. The transport of alloying elements in both liquid and gas phases was found to be rapid and the overall vaporization rates were controlled by the plasma influenced intrinsic vaporization of alloying elements at the weld pool surface. DOE

N89-11231# Lund Univ. (Sweden). Dept. of Machine Elements.
TRANSACTIONS OF MACHINE ELEMENTS DIVISION: ON THE COMBINED HYDRODYNAMIC AND HYDROSTATIC JOURNAL BEARING
Yong Zhang 1988 112 p
(PB88-214549) Avail: NTIS HC A06/MF A01 CSCL 13I

The oil lubricated combined hydrodynamic and hydrostatic bearing was studied. The variation of oil viscosity with pressure and temperature was considered when solving Reynolds' equation. Perturbation analysis was employed in the investigation of dynamic stability for a linearized equation of motion of the journal center. It was found that without losing its load capacity under heavy load, a combined journal bearing can operate steadily at high speed under zero external load. The ideal pump power loss is normally very small compared to the total power loss. The experiment also show that with 10 percent of the critical speed as a margin, the stability conditions obtained for small oscillations can be applicable for big amplitude vibrations as well. Author

N89-11232# Sunpower, Inc., Athens, Ohio.
PRELIMINARY ASSESSMENT OF A MAGNETICALLY COUPLED FREE-PISTON STIRLING ENGINE HEAT PUMP COMPRESSOR
W. T. Beale and G. Chen 1988 6 p Presented at the 2nd DOE/ORNL Heat Pump Conference: Research and Development on the Heat Pump for Space Conditioning Applications, Washington, D.C., 17 Apr. 1988
(Contract DE-AC05-84OR-21400)
(DE88-013835; CONF-8804100-19) Avail: NTIS HC A02/MF A01

The potential advantages of direct magnetic coupling of a free-piston Stirling engine with a vapor compressor are being investigated experimentally. Results to date indicate no problems with dynamics, mechanical arrangements, efficiency or deterioration. The problems of size and cost remain, but these are determined by the properties of the magnetic material, which are improving rapidly. If the magnet material becomes available at a satisfactory price, the work undertaken here will facilitate a commercially attractive magnet drive system. DOE

N89-11233*# Georgia Inst. of Tech., Atlanta. School of Mechanical Engineering.
EXPERIMENTAL VERIFICATION OF A MODEL OF A TWO-LINK FLEXIBLE, LIGHTWEIGHT MANIPULATOR M.S. Thesis
James David Huggins Jun. 1988 86 p
(Grant NAG1-623)
(NASA-CR-183216; NAS 1.26:183216) Avail: NTIS HC A05/MF A01 CSCL 13I

Experimental verification is presented for an assumed modes model of a large, two link, flexible manipulator design and constructed in the School of Mechanical Engineering at Georgia Institute of Technology. The structure was designed to have typical characteristics of a lightweight manipulator. Author

N89-11234*# Georgia Inst. of Tech., Atlanta. School of Mechanical Engineering.
ON MOTION PLANNING AND CONTROL OF MULTI-LINK LIGHTWEIGHT ROBOTIC MANIPULATORS
Sabri Cetinkunt Nov. 1987 273 p
(Grant NAG1-623)
(NASA-CR-181226; NAS 1.26:181226) Avail: NTIS HC A12/MF A01 CSCL 13I

A general gross and fine motion planning and control strategy is needed for lightweight robotic manipulator applications such as painting, welding, material handling, surface finishing, and spacecraft servicing. The control problem of lightweight manipulators is to perform fast, accurate, and robust motions despite the payload variations, structural flexibility, and other environmental disturbances. Performance of the rigid manipulator model based computed torque and decoupled joint control methods are determined and simulated for the counterpart flexible manipulators. A counterpart flexible manipulator is defined as a manipulator which has structural flexibility, in addition to having the same inertial, geometric, and actuation properties of a given rigid manipulator. An adaptive model following control (AMFC) algorithm is developed to improve the performance in speed, accuracy, and robustness. It is found that the AMFC improves the speed performance by a factor of two over the conventional non-adaptive control methods for given accuracy requirements while proving to be more robust with respect to payload variations. Yet there are clear limitations on the performance of AMFC alone as well, which are imposed by the arm flexibility. In the search to further improve speed performance while providing a desired accuracy and robustness, a combined control strategy is developed. Furthermore, the problem of switching from one control structure to another during the motion and implementation aspects of combined control are discussed. Author

N89-11235# Martin Marietta Energy Systems, Inc., Oak Ridge, Tenn.
MANUAL, VOICE, AND AUTOMATED CONTROL OF A TELEOPERATOR VIEWING SYSTEM
J. V. Draper and J. N. Herndon 1988 18 p Presented at the International Symposium on Teleoperation and Control, Bristol, England, 12 Jul. 1988
(Contract DE-AC05-84OR-21400)
(DE88-011835; CONF-880752-4) Avail: NTIS HC A 03

During teleoperation, manipulator and television camera operation interfere with one another to the detriment of total teleoperator performance. This experiment investigated camera control options which may interfere less with manipulator than conventional manual controls. The experiment evaluated remote task performance with control by computer word recognition (voice input), automation of camera aiming, and manual control using push buttons and joy sticks. Operators worked more slowly with manual control and engaged in control motions for significantly smaller percentages of time than with voice input or automation. There was no difference between manual control and voice control in the number of camera changes made, but the automated tracking system made significantly more changes than the operators did. Camera movements lasted longest when operators used voice control, and changes made by the automated control system lasted longer than changes made with manual control. DOE

N89-11236 Nebraska Univ., Lincoln.
PROBABILISTIC ERROR MODEL OF ROBOT END-EFFECTOR'S DYNAMIC STATE Ph.D. Thesis
Li-Chiin Chang 1987 185 p
Avail: Univ. Microfilms Order No. DA8803743

In most error analysis of robot motion, only kinematics and no forces are considered and it is assumed that the errors of joint variables are independent of each other. Such approach ignores the dynamic coupling effects and assumes zero correlation coefficients among the robot links. A probabilistic method is presented to study the error of robot dynamic state by incorporating the coupling forces among the robot links. The robot's perturbed state vector is first obtained by employing the well developed dynamic equations. Next, by assuming that the probabilistic characteristics of process noise are known, the probabilistic characteristics of robot end-effector's position vector are determined. The error covariance matrix of the robot's perturbed state is found to be infinite due to the fact that robot is an unstable system and therefore a feedback controller for stabilizing the perturbed system is needed. With the assumptions that only joint variables are measurable and that the probabilistic characteristics of measurement noise are known, a Kalman filter is employed to estimate the perturbed state, and a feedback controller designed according to the separation theorem is proposed. The error covariance matrices of estimated perturbed state and residual perturbed state are obtained by application of Kalman filter theory, and then added to find the true perturbed state error covariance. Finally, the error covariance matrix of end-effector's position vector is determined by transforming that of the true perturbed state. The theoretical developments in this error model are first developed for a Two-Link robot and then generalized to an n-link robot.
Dissert. Abstr.

N89-11237*# Jet Propulsion Lab., California Inst. of Tech., Pasadena.
SPACE-BASED MULTIFUNCTIONAL END EFFECTOR SYSTEMS FUNCTIONAL REQUIREMENTS AND PROPOSED DESIGNS
A. H. Mishkin and B. M. Jau 15 Apr. 1988 119 p
(Contract NAS7-918)
(NASA-CR-180390; JPL-Publ-88-16; NAS 1.26:180390) Avail: NTIS HC A06/MF A01 CSCL 13I

The end effector is an essential element of teleoperator and telerobot systems to be employed in space in the next decade. The report defines functional requirements for end effector systems to perform operations that are currently only feasible through Extra-Vehicular Activity (EVA). Specific tasks and functions that the end effectors must be capable of performing are delineated. Required capabilities for forces and torques, clearances, compliance, and sensing are described, using current EVA requirements as guidelines where feasible. The implications of these functional requirements on the elements of potential end effector systems are discussed. The systems issues that must be considered in the design of space-based manipulator systems are identified; including impacts on subsystems tightly coupled to the end effector, i.e., control station, information processing, manipulator arm, tool and equipment stowage. Possible end effector designs are divided into three categories: single degree-of-freedom end effectors, multiple degree of freedom end effectors, and anthropomorphic hands. Specific design alternatives are suggested and analyzed within the individual categories. Two evaluations are performed: the first considers how well the individual end effectors could substitute for EVA; the second compares how manipulator systems composed of the top performers from the first evaluation would improve the space shuttle Remote Manipulator System (RMS) capabilities. The analysis concludes that the anthropomorphic hand is best-suited for EVA tasks. A left- and right-handed anthropomorphic manipulator arm configuration is suggested as appropriate to be affixed to the RMS, but could also be used as part of the Smart Front End for the Orbital Maneuvering Vehicle (OMV). The technical feasibility of the anthropomorphic hand and its control are demonstrated. An evolutionary development approach is proposed and approximate scheduling provided for implementing the suggested manipulator systems in time for space stations operations in the early 1990s.
Author

N89-11238# Edgerton, Germeshausen and Grier, Inc., Idaho Falls, Idaho.
ELECTRIC VEHICLE AUXILIARY POWER SOURCE EVALUATION
F. G. Farmer, A. D. Hill, J. F. Jacobsen, and M. R. Johnson Jun. 1988 50 p
(Contract DE-AC07-76ID-01570)
(DE88-015359; DOE/ID-10205) Avail: NTIS HC A04/MF A01

This report focuses on the electric vehicle auxiliary power

system. This involves a collection of devices needed to operate the vehicle, including headlamps, blowers, instrument panel, entertainment equipment, windshield wipers, horn, turn signals, control electronics, etc. These devices are traditionally connected to a common 12 vdc power bus. In an EV, the traction battery is the prime source of power but this battery is at the wrong voltage level and lacks the regulation required by most auxiliary devices. Hence there is a need for an auxiliary power system. All of the methods for providing auxiliary power that are presently being investigated involve the use of a dc-dc converter whose task is to convert the traction battery voltage to 12 vdc, and to regulate this voltage in the face of traction battery voltage variations. This report addresses three objectives. First, it summarizes the status of currently available dc-dc converters and regulators in terms of the needs and difficulties experienced by in-service electric vehicles. Second, it provides an engineering assessment of these devices to determine whether the technology exists to solve the in-service maintenance and reliability problems. Third, it examines the longer range needs of auxiliary power system design and development. DOE

N89-11239# Foreign Resources Associates, Austin, Tex.
A METHOD FOR IMPROVING THE DEPTH OF PENETRATION AND THE APPEARANCE OF WELDING
Tapani Moisio Jul. 1988 6 p Transl. of Finnish Patent No. 64063 Filed date 26 Jan. 1978 Prepared in cooperation with Rockwell International Corp., Golden, Colo.
(Contract DE-AC04-76DP-03533)
(DE88-012954; RFP-Trans-477) Avail: NTIS HC A02/MF A01

This invention relates to gas-shielded arc welding of high-alloy steel. With this method, the form, surface tension and particularly the depth of penetration and welding speed can be improved. This invention is based on the observation that when welding high-alloy steel, the presence of oxides as a layer of a certain thickness in the area of the welding affects the arc-welding flame. In gas-shielded arc welding, the arc flame is concentrated, and thus its energy flux is aimed at a smaller area, which in turn leads to a deeped penetration. Thus both the depth of fusion and the welding rate improve. This phenomenon is present even more when welding difficult-to-weld batches, but is also clear significant in easily weldable batches. This leads to a leveling out of weldability differences. DOE

N89-11240# Sandia National Labs., Albuquerque, N. Mex.
MICROSOLDERING AND MICROMINIATURE WELDING WITH LASERS
J. L. Jellison and D. M. Keicher 1988 15 p Presented at the Microjoining '88, Cambridge, England, 20 Sep. 1988
(Contract DE-AC04-76DP-00789)
(DE88-013368; SAND-87-2580C; CONF-8809104-1) Avail: NTIS HC A03/MF A01

Miniature welding of electronic and electromechanical components with lasers is a rapidly maturing technology. Extending the use of lasers to microsoldering and microminiature welding applications has also generated moderate interest. Use of lasers for microminiature soldering or welding permits the delivery of accurately controlled amounts of heat to the precise area required. By applying small amounts of heat locally, rework can be accomplished in densely packed circuits without damaging heat sensitive components to conductors. Also, localization of heat obviates the need for using solder alloys of different melting points, which can simplify design. Laser soldering has been applied to conductors ranging from 25 micron dia. wires to coaxial cables in the 0.3 to 1.25 mm range. For the most part, these conductors were soldered to metallized alumina substrates, although in some instances soft substrates were also used. The potential advantages of microminiature welding have also been explored. DOE

N89-11241# Centre National de la Recherche Scientifique, Toulouse (France). Lab. d'Automatique et d'Analyse des Systemes.
GUIDANCE, SENSOR CONTROL AND LOCALIZATION OF A MOBILE AUTONOMOUS ROBOT Ph.D. Thesis - Toulouse Univ.
Ahmed Khoumsi 1988 190 p In FRENCH; ENGLISH summary
(LAAS-88-131; ETN-88-93076) Avail: NTIS HC A09/MF A01

Mobile robot navigation guidance and sensor-based control and localization with respect to the environment are discussed. For the guidance and sensory control system, trajectories, and corresponding movements are studied, and the servocontrol for optimizing these movements in the continuous and discrete cases is outlined. Local obstacle avoidance based on servoing the robot's movement along a circle circumscribing the obstacle and updated with ultrasonic sensors readings, is presented, as well as docking along vertical plane by following a fictive target moving along it. Surveillance monitors are introduced, in order to supervise and control the movement. Localization methods, especially those based on matching a previously acquired geometric environment model with a model built from a local perception are presented. A method based on prediction and verification of segments matching hypotheses in order to find the best transform between the global and the local models, and therefore current robot coordinates (position and orientation) in the plane was developed. The guidance and sensory control, and localization systems were implemented on HILARE and another mobile robot, and simulation and experimental results are given. ESA

N89-11242# European Space Agency, Paris (France).
NONLINEAR CONTROL OF AN H2O2 STEAM REACTOR
Karlheinz Wolfmuller (Deutsche Forschungs- und Versuchsanstalt fuer Luft- und Raumfahrt, Hardthausen, West Germany) Jul. 1988 137 p Trans. into ENGLISH of Nichtlineare Regelung einesH2/O2-Dampfreaktors, DFVLR, Hardthausen/Lampoldshausen, Federal Republic of Germany Original language document was announced as N85-16192
(ESA-TT-902; DFVLR-FB-84-30; ETN-88-93176) Avail: NTIS HC A07/MF A01; original German version available from DFVLR, VB-PL-DO, 90 60 58, 5000 Cologne, Federal Republic of Germany 40 deutsche marks

The dynamic and control aspects of the process of fast steam generation from the combustion of H2 and O2 are investigated. A nonlinear dynamic model is presented. The reduction of the order of the system for synthesis of a controller is achieved by structural assignment and determination of the model parameters. A nonlinear decoupling method is presented and the design of a controller allowing for measured disturbances run through. The aims of the method are verified by numerical simulation. Realization problems are considered. Compliance with the specifications governing the control system and its design method is verified by experimental results from the test rig. ESA

N89-11243# Illinois Univ., Urbana. Decision and Control Lab.
INTEGRAL MANIFOLD IN SYSTEM DESIGN WITH APPLICATION TO FLEXIBLE LINK ROBOT CONTROL Ph.D. Thesis
Huan-Chi C. Tseng Jun. 1988 144 p
(Contract N00014-84-C-0149)
(AD-A197052; UILU-ENG-88-2231; DC-104) Avail: NTIS HC A07/MF A01 CSCL 12I

The integral manifold concept is used in this thesis for controller design in various problems. A definition and the conditions for the existence of the integral manifold are given. Integral manifolds in linear systems are analyzed with special attention given to how the linear system possesses an input dependent manifold. Flexibility in flexible link robots is shown to be a cause for phase delay, which is reduced by a corrective controller based on the integral manifold concept. For a class of nonlinear systems with nonlinear output, a nonlinear PI controller is designed that achieves asymptotic tracking and disturbance rejection of bounded signals which are not only unknown but also slowly varying. Finally, the

existence of a lower order optimal problem is demonstrated which is equivalent to a singularly perturbed optimal problem with initial conditions restricted to a manifold. Throughout this thesis, results obtained from the manifold approach are shown to be consistent with, and sometimes even extend, some established results in singularly perturbed systems. GRA

N89-11244# State Univ. of New York, Stony Brook. Dept. of Mechanical Engineering.
ANALYSIS, SYNTHESIS AND DESIGN OF HIGH-SPEED MECHANISMS Final Report
Ting W. Lee May 1988 106 p
(Grant NSF MSM-85-03576)
(PB88-235106; NSF/ENG-88005) Avail: NTIS HC A06/MF A01 CSCL 13I

Recent advances in kinematics, utilizing fundamental theories of dynamics, coupled with experimental as well as computer graphics techniques in order to develop design methods capable of predicting the performance characteristics of mechanisms subject to various prescribed conditions, including overclosure, manufacturing error and high speed operations are examined. Among the mechanisms selected for the illustration of the design methods are: wobble plate engines, a group of high speed shaft couplings, and several models of robot manipulators. These mechanisms were chosen mainly because they represent a class of mechanisms with realistic complexity and their design methods are either not available or only partially developed. Author

N89-11064# Joint Publications Research Service, Arlington, Va.
GOOD PERFORMANCE OF LE-7 LIQUID OXYGEN TURBOPUMP CONFIRMED
Kenjiro Kamijo *In its* JPRS Report: Science and Technology: Japan 4 Jun. 1987 p 15-17 Transl. into ENGLISH from Kogiken Nyusu (Tokyo, Japan), Aug. 1986 p 5-6 (For primary document see N89-11061 02-31)
Avail: NTIS HC A05/MF A01

38 QUALITY ASSURANCE AND RELIABILITY

Includes product sampling procedures and techniques; and quality control.

N89-11245# Lawrence Livermore National Lab., Calif.
EXPERIMENTS IN THE APPLICATION OF ULTRASOUND DIFFRACTION TOMOGRAPHY FOR NONDESTRUCTIVE TESTING
S. G. Azevedo and J. P. Fitch Jul. 1988 15 p Submitted for publication
(Contract W-7405-eng-48)
(DE88-014694; UCID-21411) Avail: NTIS HC A03/MF A01

We have designed computer programs to simulate ultrasound projection scans and to reconstruct the tomographic planar image. We have also used the reconstruction algorithm on actual test data and have obtained a crude but promising image. DOE

N89-11246 Stanford Univ., Calif.
THE INTERPRETATION OF ELECTROMAGNETIC NONDESTRUCTIVE FLAW DETECTION IN METALS Ph.D. Thesis
Francis Gustav Muennemann 1988 245 p
Avail: Univ. Microfilms Order No. DA8808394

The physics of electromagnetic eddy current flaw detection devices are discussed. Methods of predicting flaw parameters from precision measurements of eddy current probe impedance changes are presented. These methods work for good conductors at relatively high frequencies. The results of experiments which verify the validity of these techniques are also presented. Several subtopics are covered: (1) physics of eddy current devices applied to prediction of flaw signals with various approximations; (2) deduction of crack dimensions from flaw signals (signal inversion); (3) and optimal selection of probes and operating conditions for crack sensitivity and for ease of signal inversion. Dissert. Abstr.

N89-11247# Stanford Linear Accelerator Center, Calif.
QUALITY ASSURANCE MANUAL. VOLUME 2: APPENDICES
Jussi E. Oijala Jun. 1988 398 p
(Contract DE-AC03-76SF-00515)
(DE88-013880; SU-SLAC-TN-88-2-Vol-2) Avail: NTIS HC A17

This paper contains quality assurance information on departments of the Stanford Linear Accelerator Center. Particular quality assurance policies and standards discussed are on: Mechanical Systems; Klystron and Microwave Department; Electronics Department; Plant Engineering; Accelerator Department; Purchasing; and Experimental Facilities Department. DOE

N89-11248 Iowa State Univ. of Science and Technology, Ames.
ULTRASONIC FLAW CLASSIFICATION: AN APPROACH USING MODELING, SIGNAL PROCESSING, AND ADAPTIVE LEARNING Ph.D. Thesis
Lat Sang Koo 1987 199 p
Avail: Univ. Microfilms Order No. DA8805097

In the field of ultrasonic Nondestructive Evaluation (NDE), it is important to be able to classify a flaw as cracklike or volumetric, based on features contained in an ultrasonic scattering response. In the present work, it is demonstrated, based on model studies, that three fundamental features, obtained from the early time response of a flaw, are in principle useful for classification purposes. These features are based on the Kirchhoff approximation for cracks and a new subtracted surface integral formulation of the Born approximation for volumetric flaws. To reliably extract such features from an experimental response, however, it is important to perform both deconvolution and low frequency extrapolation procedures. Here, we show that a new flaw-derived reference deconvolution method and a low frequency extrapolation technique, using the Gerchberg-Papoulis algorithm, can be effective for these purposes. Once these fundamental features are extracted, a simple adaptive learning procedure has been successfully applied for performing the classification. Dissert. Abstr.

39 STRUCTURAL MECHANICS

Includes structural element design and weight analysis; fatigue; and thermal stress.

For applications see *05 Aircraft Design, Testing and Performance* and *18 Spacecraft Design, Testing and Performance.*

N89-11249 Stanford Univ., Calif.
FREE DAMPED VIBRATION OF COMPOSITE PLATES AND SHELLS Ph.D. Thesis
Andrew Sotarios Bicos 1988 157 p
Avail: Univ. Microfilms Order No. DA88-8350

The problem of free damped vibration of laminated fiber-reinforced composite plates and shells was investigated, with the plates and shells either being solid or containing circular cutouts. The equations representing the free damped vibration of these structural members were derived and a finite element was developed for obtaining solutions to these equations. The method includes two steps. First, the undamped natural frequencies and mode shapes are calculated using 4-node elements with selective reduced integration. Second, the damping factors are calculated by means of a damping model, which uses the mode shapes obtained in the first step. A computer code (VIBR8) was written, which can be used to calculate the natural frequencies, mode shapes, and damping factors of rectangular plates, cylinders, and cylindrical panels with free, clamped, or simply supported edges, and with one or two circular cutouts. Tests were also performed measuring the natural frequencies and damping factors of Fiberite T300/934 graphite-epoxy plates. The natural frequencies, mode shapes, and damping factors calculated by the code were compared to the data generated by these tests as well as to

analytical, numerical, and experimental results reported by previous investigators. The results of the computer code agreed closely with the data and the previous results. Using the computer code, parametric studies were performed, which illustrate the information that can be generated by the code. Application of the code to the design of composite panels is discussed. Dissert. Abstr.

N89-11250# Toronto Univ. (Ontario). Inst. for Aerospace Studies.
THE MINI-OSCILLATOR TECHNIQUE: A FINITE ELEMENT METHOD FOR THE MODELING OF LINEAR VISCOELASTIC STRUCTURES Thesis
Donald J. McTavish Mar. 1988 123 p
(UTIAS-323; ISSN-0082-5255) Avail: NTIS HC A06/MF A01

The use of finite elements to model complex structures has been traditionally effective with regard to mass properties and equilibrium elastic stiffness properties. A practical formulation is presented for the analysis of structures whose constituent materials may be classed as linear viscoelastic. Construction of viscoelastic finite element matrices fully compatible with the usual second order equations of motion is demonstrated, given a knowledge of material properties. The viscoelastic material properties are represented in the Laplace domain by the Golla-Hughes-McTavish (GHM) Analytic Model. The Mini-Oscillator Technique is introduced and developed through the consideration of a single modulus finite element for which the mass and elastic stiffness matrices are known. The simplest case of a single degree of freedom finite element is examined in detail to expose a mechanical analogy from which the mini oscillator technique derives its name. The procedure is then extended to the case of a general structural model with many elements. Each finite element may be of a different material with stiffness properties ranging between simple elastic and multi modulus viscoelastic. Author

N89-11251# Sandia National Labs., Albuquerque, N. Mex.
INCIPIENT SPALL, CRACK BRANCHING, AND FRAGMENTATION STATISTICS IN THE SPALL PROCESS
D. E. Grady 1988 9 p Presented at the 2nd International Conference on Mechanical and Physical Behavior of Materials Under Dynamic Loading, Ajaccio, France, 19 Sep. 1988
(Contract DE-AC04-76DP-00789)
(DE88-009587; SAND-88-1194C; CONF-880940-2) Avail: NTIS HC A02/MF A01

Energy based theories of spall fracture and fragmentation are examined. A concept of energy-limited and flaw-limited spall emerges naturally within one of these theories. Conditions favoring incipient spall and crack branching in the spall process are identified. The fragmentation are investigated. DOE

N89-11252# Vibration Inst., Clarendon Hills, Ill.
THE SHOCK AND VIBRATION DIGEST, VOLUME 20, NO. 10 Monthly Report
Judith Nagle-Eshleman, ed. Oct. 1988 80 p
Avail: NTIS HC A05/MF A01

Editorials; articles and reviews; and abstracts from current literature are presented. For individual titles, see N89-11253 through N89-11254.

N89-11253# Missouri Univ., Rolla. Dept.of Mechanical and Aerospace Engineering.
CONTINUUM MODELING OF LATTICED STRUCTURES
S. Abrate *In* Vibration Inst., The Shock and Vibration Digest, Volume 20, No. 10 Oct. 1988 p 3-8 (For primary document see N89-11252 02-39)
Avail: NTIS HC A05/MF A01

Articles concerned with modeling discrete structures by equivalent continua are reviewed. Applications to the dynamic analysis of large space structures or civil engineering structures are of particular interest. This paper is a continuation of an earlier review presented in the Shock and Vibration Digest. Author

N89-11254# National Research Inst., Bankura (India).
THE EFFECTS OF SEISMIC WAVES, PART 2 **c46**
Sasadhar De *In* Vibration Inst., The Shock and Vibration Digest, Volume 20, No. 10 Oct. 1988 p 9-26 (For primary document see N89-11252 02-39)
Avail: NTIS HC A05/MF A01

The literature on the effects of seismic waves on ground motion and structures is reviewed. Mechanisms and predictions of earthquakes are also reviewed and will be published in the October issue. Abnormal animal and plant behavior before earthquakes, and disturbances in the ionosphere will be published as Part 3 in the December issue. Some recent problems in seismology are described. Author

N89-11255# Oak Ridge National Lab., Tenn.
IMPURITY-INDUCED CHANGES IN INTERFACIAL STRENGTH AND THEIR ROLE IN CREEP FRACTURE
E. P. George and D. P. Pope (Pennsylvania Univ., Philadelphia.) 1988 8 p Presented at the Spring Meeting of the Materials Research Society, Reno, Nev., 4 Apr. 1988
(Contract DE-AC05-84OR-21400)
(DE88-013197; CONF-880408-33) Avail: NTIS HC A02/MF A01

Creep cavity nucleation at second phase particles in iron and steel is examined in the light of recent theoretical and experimental results. Theoretical considerations show it to be extremely unlikely that thermal nucleation will occur at Fe3C, FeO or Al2O3 particles, or that athermal nucleation will take place at Fe3C particles. Consistent with this, it is experimentally found that carbides and oxides almost never nucleate cavities in iron and steel, as long as harmful impurities like sulfur are not present. In the presence of segregated impurities like sulfur, oxides do nucleate cavities, but there is insufficient data to determine whether this is because the impurities make thermal or athermal nucleation easier. Finally, sulfides are thought to be nonwetting in iron and steel. As a result, there should be no barrier to thermal nucleation at sulfides, and experiments show that sulfides do nucleate cavities with great ease in iron and steel. DOE

N89-11256 Purdue Univ., West Lafayette, Ind.
A THREE-DIMENSIONAL INVESTIGATION OF STEADY STATE FATIGUE CRACK CLOSURE BEHAVIOR FOR THROUGH-THICKNESS AND PART-THROUGH FLAWS Ph.D. Thesis
Suvendoo Kumar Ray 1987 253 p
Avail: Univ. Microfilms Order No. DA8807664

How through-the-thickness variations in crack tip plasticity affect fatigue crack opening and alter fatigue crack growth in transparent model materials is described. Complete three-dimensional crack opening profiles are measured by the use of optical interferometry for through-thickness, corner, and surface flaws. These crack surface separation data are then used to determine the crack opening load along the three-dimensional flaw perimeter. The point-wise crack opening loads are compared with values obtained from various compliance measurement techniques. In addition, the results obtained from the polymer specimens are examined in context of the closure behavior reported for metal specimens by various investigators. Dissert. Abstr.

N89-11257# Commission of the European Communities (Luxembourg).
BENCHMARK STUDY OF SHEAR BUCKLING OF A CYLINDRICAL VESSEL Final Report
M. Dostal, N. M. Austin, A. Peano, A. Combescure, and R. Bastien 1986 134 p
(PB88-125315; EUR-10592-EN; ISBN-92-825-6368-5) Avail: NTIS HC E06/MF E06; copy not available from STI Facility CSCL 20K

The results of the first phase in a joint European code validation exercise on the static shear buckling behavior of thin, low aspect ratio stainless steel cylinders are reported. Linear and nonlinear finite element analyses were performed by four organizations using three different computer codes. The computed results were compared directly with experimental results. It was discovered that refined finite element models were essential if accurate buckling

loads were to be calculated. Each of the codes appeared to predict reasonably well the final buckled geometry, although the analytical load deflection estimate did not agree exactly with the experiment. Author

N89-11258# Vibration Inst., Clarendon Hills, Ill.
THE SHOCK AND VIBRATION DIGEST, VOLUME 20, NO. 8 Monthly Report
Judith Nagle-Eshleman, ed. Aug. 1988 76 p
Avail: NTIS HC A05/MF A01

The featured article of this volume is entitled: Dynamic Behavior of Foundations in Bilateral and Unilateral Contact. The literature review is on Vibrations and Stability of Mechanical Systems. For individual titles, see N89-11259 through N89-11260.

N89-11259# West Virginia Univ., Morgantown. Coll. of Engineering.
DYNAMIC BEHAVIOR OF FOUNDATIONS IN BILATERAL AND UNILATERAL CONTACT
C. C. Spyrakos *In* Vibration Inst., The Shock and Vibration Digest, Volume 20, No. 8 Aug. 1988 p 3-12 (For primary document see N89-11258 02-39)
Avail: NTIS HC A05/MF A01

Research pertinent to the dynamic response of foundations either attached to the soil interface (bilateral contact) or free to separate from it (unilateral contact) is reviewed. The case of slip is also briefly addressed. The foundations may be subjected to either external forces or seismic excitations with a general time variation. The discussion of references is extensive but by no means exhaustive. Emphasis is placed on presenting the primary features of solution procedures as well as their merits and limitations. Problems that have been either overlooked or need to be further investigated are identified. Author

N89-11260# Waterloo Univ. (Ontario). Dept. of Systems Design Engineering.
VIBRATIONS AND STABILITY OF MECHANICAL SYSTEMS: 4
K. Huseyin *In* Vibration Inst., The Shock and Vibration Digest, Volume 20, No. 8 Aug. 1988 p 13-19 (For primary document see N89-11258 02-39)
Avail: NTIS HC A05/MF A01

The stability instability bifurcation and oscillatory behavior of general mechanical systems is reviewed. Advances that were made since 1983 are described. The review covers both linear and nonlinear theories as well as basic methodology. Author

N89-11261# Vibration Inst., Clarendon Hills, Ill.
THE SHOCK AND VIBRATION DIGEST, VOLUME 20, NO. 6 Monthly Report
Judith Nagle-Eshleman, ed. Jun. 1988 76 p
Avail: NTIS HC A05/MF A01

The feature article of this volume is entitled: A Comparative Overview of Modal Testing and System Identification for Control of Structures. The literature review of this issue is on Nonlinear Random Vibration in Mechanical Systems. For individual titles, see N89-11262 through N89-11263.

N89-11262*# National Aeronautics and Space Administration. Langley Research Center, Hampton, Va.
A COMPARATIVE OVERVIEW OF MODAL TESTING AND SYSTEM IDENTIFICATION FOR CONTROL OF STRUCTURES c63
J.-N. Juang and R. S. Pappa *In* Vibration Inst., The Shock and Vibration Digest, Volume 20, No. 6 Jun. 1988 p 4-15 (For primary document see N89-11261 02-39)
Avail: NTIS HC A05/MF A01

A comparative overview is presented of the disciplines of modal testing used in structural engineering and system identification used in control theory. A list of representative references from both areas is given, and the basic methods are described briefly. Recent progress on the interaction of modal testing and control disciplines is discussed. It is concluded that combined efforts of researchers in both disciplines are required for unification of modal testing and system identification methods for control of flexible structures. Author

N89-11263# Sussex Univ., Brighton (England). School of Engineering and Applied Sciences.
NONLINEAR RANDOM VIBRATION IN MECHANICAL SYSTEMS
J. B. Roberts and J. F. Duanne *In* Vibration Inst., The Shock and Vibration Digest, Volume 20, No. 6 Jun. 1988 p 16-25 (For primary document see N89-11261 02-39)
Avail: NTIS HC A05/MF A01

Various approaches are reviewed to the solution of nonlinear random vibration problems that were published from 1984 to 1986. Emphasis is placed on the applicability of these methods in engineering. Author

N89-11264# Ecole Polytechnique, Montreal (Quebec). Dept. de Genie Mecanique
DYNAMIC ANALYSIS OF SPHERICAL SHELLS: A HYBRID METHOD
Aouni A. Lakis and Quoc Tuy Nguyen Sep. 1988 202 p (EPM/RT-88/23) Avail: NTIS HC A10/MF A01

A new theory is presented for the dynamic analysis of non-uniform thin elastic spherical shells. The theory is a hybrid of classical shell theory and the finite element method. The displacement functions derived from classical shell theory were adapted to a spherical finite element, leading to stiffness and mass matrices for the element. The eigenvalue and eigenvector problem is solved by the standard method. A Fortran V computer program was developed. The free vibration characteristics of spherical shells under different boundary conditions and different circumferential wave numbers were determined. The results allow the conclusion that there is, in most cases, good agreement between the frequencies calculated by the present theory and the results obtained by other authors. Author

N89-11265# Federal Aviation Agency, Atlantic City, N.J.
LONGITUDINAL IMPACT TEST OF A TRANSPORT AIRFRAME SECTION Final Report, Feb. - Oct. 1987
Barry Wade and Richard Johnson (Transportation Research Center of Ohio, East Liberty.) Jul. 1988 286 p
(Contract DTFA03-87-C-00013)
(DOT/FAA/CT-87/26) Avail: NTIS HC A13/MF A01

The results of longitudinally impact testing a 10-foot section of a transport airplane at peak acceleration and corresponding velocity changes of 7.4 g (22.4 ft/sec) and 14.2 g (36 ft/sec), respectively are reported. The purpose of the tests was to measure the responses of the fuselage and floor structure to simulated dynamic crash loads. The airframe test section included a full complement of seats and dummies. Acceleration and load/deflection response measurements were obtained from the instrumented fuselage, floor and seat/dummy installation. Author

N89-11266# Vibration Inst., Clarendon Hills, Ill.
THE SHOCK AND VIBRATION DIGEST, VOLUME 20, NO. 9 Monthly Report
Judith Nagle-Eshleman, ed. Sep. 1988 52 p
Avail: NTIS HC A04/MF A01

The feature article of this volume is entitled: Transverse Flexure of an Elastic Plate Loaded Through a Rigid Inclusion. A literature review is presented of The Effects of Seismic Waves, Part 1. For individual titles, see N89-11267 through N89-11268.

N89-11267# New Jersey Inst. of Tech., Newark. Dept. of Mechanical Engineering.
TRANSVERSE FLEXURE OF AN ELASTIC PLATE LOADED THROUGH A RIGID INCLUSION
Yi-Yuan Yu *In* Vibration Inst., The Shock and Vibration Digest, Volume 20, No. 9 Sep. 1988 p 3-7 (For primary document see N89-11266 02-39)
Avail: NTIS HC A04/MF A01

In the analysis of an elastic plate with a beam connected to it

in a perpendicular direction, the joint between the two may be taken as a rigid inclusion. It will then be important to be able to analyze the tranverse flexure of a plate loaded through the rigid inclusion. For this purpose, information on the stiffness of the plate is needed. An extensive search of literature was conducted to cover both static and dynamic stiffness of plates, the latter in the form of impedances. Author

N89-11268# National Research Inst., Bankura (India).
THE EFFECTS OF SEISMIC WAVES: PART 1 **c46**
Sasadhar De *In* Vibration Inst., The Shock and Vibration Digest, Volume 20, No. 9 Sep. 1988 p 8-18 (For primary document see N89-11266 02-39)
Avail: NTIS HC A04/MF A01

The literature on the effects of seismic waves on ground motion and structures is reviewed. Some recent problems is seismology are described. Author

N89-11269# International Centre for Theoretical Physics, Trieste (Italy).
GEOMETRIC GAUGE THEORY OF METRIC DEFECTS
L. K. Dong, H. Y. Zhang (Academia Sinica, Shenyang, China), and C. W. Lung Aug. 1987 18 p
(DE88-702961; IC-87/244) Avail: NTIS (US Sales Only) HC A03/MF A01

The mechanical behavior of a material manifold with dislocations and disclinations is explored by applying nonriemannian geometry and gauge field theory. A geometric gauge theory of metric defects is introduced by local Lorentz invariance. As a result, we give the connection coefficients with the affine and the gauge connection. Taking the displacement field, the frame field and the gauge field as basic parameters, we obtain the constitutive equations and the governing equations based on a variational principle with respect to the groups of a coordinate transformation and a gauge transformation. DOE

N89-11270 Columbia Univ., New York, N.Y.
RESPONSE OF DISCRETELY STIFFENED STRUCTURES AND TRANSMISSION OF STRUCTURE-BORNE NOISE Ph.D. Thesis
Constantinos Sotirio Lyrintzis 1987 81 p
Avail: Univ. Microfilms Order No. DA8809385

An analytical study is presented to predict the dynamic response and structure-borne noise generation and transmission of complex discretely stiffened and interconnected structures under random loads. The method is based on transfer matrices for the structural response and on modal decomposition for the interior acoustic field. The acoustic enclosure is taken to be rectangular in shape of which a portion of the boundaries is elastic while the remaining surface is acoustically rigid. This formulation can be used for the response and structure-borne noise generation studies in space station and aircraft structures. Numerical results are presented for a variety of acousto-structural problems. It is found that this approach permits easy parametric evaluation and that through proper selection of structural parameters, loading conditions and acoustic characteristics, the vibration response and noise transmission can be reduced. Dissert. Abstr.

N89-11271# National Bureau of Standards, Gaithersburg, Md. Center for Building Technology.
LITERATURE REVIEW OF STRENGTHENING METHODOLOGIES OF EXISTING STRUCTURES
Long T. Phan, H. S. Lew, and Mark K. Johnson Jun. 1988 126 p
(PB88-218219; NBSIR-88/3796) Avail: NTIS HC A07/MF A01 CSCL 20K

The report reviews research studies relevant to structural strengthening of existing reinforced concrete members and frames. The majority of these studies dealt exclusively with restoring and improving seismic resistance of concrete columns and frames. A number of case histories where various strengthening techniques were applied in practice are reviewed. Most studies identified ultimate failure in the strengthened structures as primarily due to failure of the joining elements. Improved load resistance and ductility in concrete structures have been reported in most of these studies. GRA

N89-11272# Associacao Brasileira de Ciencias Mecanicas, Rio de Janeiro.
CONTRIBUTION FOR STRESS ANALYSIS IN BEND ACESSORIES OF PIPING SYSTEMS
F. J. M. Q. deMelo and P. M. S. T. deCastro 1986 15 p In PORTUGUESE; ENGLISH summary Presented at the 4th Brazilian Symposium on Piping and Pressure Vessels, Salvador, Brazil, 28 Oct. 1986
(DE88-701618; INIS-BR-964; CONF-8610317) Avail: NTIS (US Sales Only) HC A03/MF A01

Analytical and numerical studies of the linear elastic behavior of bend pipes, with tangent pipes or flanged ends, such as used in nuclear power plants are presented. Two analytical techniques were developed: one is based on the integration of Euler equation and the other is based on a Fourier analysis. The results obtained using these approaches are compared with results obtained by a finite element code for semiloof shells. DOE

N89-11273# Rensselaer Polytechnic Inst., Troy, N.Y. Mechanics of Materials Lab.
RATCHETTING BEHAVIOR OF TYPE 304 STAINLESS STEEL AT ROOM AND ELEVATED TEMPERATURES
Marina Ruggles and Erhard Krempl 1988 22 p Presented at the International Seminar on the Inelastic Behaviour of Solids: Models and Utilization, Besancon Cedex, France, 30 Aug. 1988
(Contract DE-AC05-84OR-21400)
(DE88-011864; CONF-880877-1) Avail: NTIS HC A03/MF A01

The zero-to-tension ratchetting behavior was investigated under uniaxial loading at room temperature and at 550, 600 and 650 C. In History 1 the maximum stress level of ratchetting was equal to the stress reached in a tensile test at one percent strain. For History 2 the maximum stress level was established as the stress reached after a 2100 s relaxation at one percent strain. Significant ratchetting was observed for History 1 at room temperature but not at the elevated temperatures. The accumulated ratchet strain increases with decreasing stress rate. Independent of the stress rates used insignificant ratchet strain was observed at room temperature for History 2. This observation is explained in the context of the viscoplasticity theory based on overstress by the exhaustion of the viscous contribution to the stress during relaxation. The viscous part of the stress is the driving force for the ratchetting in History 1. Strain aging is presumably responsible for the lack of short-time inelastic deformation resulting in a nearly rate-independent behavior at the elevated temperatures. DOE

N89-11274# Associacao Brasileira de Ciencias Mecanicas, Rio de Janeiro.
DYNAMIC ANALYSIS OF PIPINGS BY MODAL SYNTHESIS
O. B. Augusto and M. MattarNeto 1986 13 p In PORTUGUESE; ENGLISH summary Presented at the 4th Brazilian Symposium on Piping and Pressure Vessels, Salvador, Brazil, 28 Oct. 1986
(DE88-701620; INIS-BR-966; CONF-8610317) Avail: NTIS (US Sales Only) HC A03/MF A01

A Modal Synthesis method, the component modes, and its implementation as a postprocessor of a finite element program is presented. Examples of calculations of stationary and transient vibrations for monitoring pipelines of nuclear power plants are analyzed. DOE

N89-11275 Johns Hopkins Univ., Baltimore, Md.
LASER SPECKLE PHOTOGRAPHY AND DECORRELATION TECHNIQUES IN ELASTIC-PLASTIC FRACTURE STUDIES Ph.D. Thesis
Mark Andrew Richter 1987 82 p
Avail: Univ. Microfilms Order No. DA8807462

In elastic plastic fracture, material behavior is often characterized by the J integral or crack tip opening displacement (CTOD) parameters. To evaluate these parameters accurately, the location of the plastic hinge point, the shape and extent of plastic

deformation ahead of the crack tip, and the value of the plastic rotational factor must be determined. Usually, hinge point location and plastic rotational factor were inferred through crack opening displacement (COD) measurements. The plastic deformation has usually been delineated by macroetching techniques that reveal flow lines. However, it is indicated that laser speckle metrology can be used to analyze directly the hinging phenomenon and delineate the extent of plastic deformation around the crack tip. Using notched 3-point bend bars fabricated from a high strength low alloy steel, a full field map of in-plane displacements was generated over the course of each test. The results indicate the existance of a hinge region, rather than an explicit hinge point. The hinge region appears to contain the computed hinge point location using the range of cited plastic rotational factor values. This indicates that the centroid of the hinge region may be used to calculate CTOD and J integral. Dissert. Abstr.

N89-11276 Georgia Inst. of Tech., Atlanta.
DELAMINATION BUCKLING OF PRESSURE-LOADED, LAMINATED CYLINDRICAL SHELLS AND PANELS Ph.D. Thesis
Zi Qi Chen 1987 143 p
Avail: Univ. Microfilms Order No. DA8803698

Delamination is one of the basic defects inherent in laminar materials. The investigation of the buckling characteristics of delaminated cylindrical shells or panels, when subjected to external pressure, is the topic here. The geometry is such that it covers a wide range of length to radius ratios and radius to thickness ratios as well as panels of different width. The delaminated region is assumed to have constant width and to extend along the entire length of the shell or panel. A model is derived to assess critical loads for quasi-isotropic configurations as well as cross-ply laminated ones with either clamped or simply supported boundary conditions. Moreover, three cases of load behavior during the buckling process have been investigated to establish critical conditions for laterally loaded shells and panels. The emphasis concerns the effect of several factors and parameters on the critical load. These include: length to radius ratio, position of delamination, size of delamination, radius to thickness ratio, cylindrical panel width, and laminate stacking sequence. Furthermore, a postbuckling analysis of a delaminated thin film is carried out in order to better understand the delamination buckling behavior of a pressure-loaded shell-like structure. Dissert. Abstr.

N89-11277# Vibration Inst., Clarendon Hills, Ill.
THE SHOCK AND VIBRATION DIGEST, VOLUME 20, NO. 7 Monthly Report
Judith Nagle-Eshleman, ed. Jul. 1988 57 p
Avail: NTIS HC A04/MF A01

The dynamical behavior of helical springs and the hydrodynamic lift forces acting on a transmission line conductor are discussed. Abstracts of articles on mechanical drives, compressors, electric motors, fans, machine tools, pumps, dynamic structural analysis, aircraft noise, aerodynamics, helicopters, and a number of other topics are included. For individual titles, see N89-11278 through N89-11278.

N89-11278# Aberdeen Univ. (Scotland). Dept. of Engineering.
DYNAMIC BEHAVIOR OF HELICAL SPRINGS
D. Pearson *In* Vibration Inst., The Shock and Vibration Digest, Volume 20, No. 7 Jul. 1988 p 3-9 (For primary document see N89-11277 02-39)
Avail: NTIS HC A04/MF A01

The satisfactory performance of helical springs often depends on their dynamical performance. The widely scattered literature on cylindrical springs of constant helix angle is discussed, treating natural frequencies and normal modes, forced and transient vibration, wave propagation, damping, design and experiments. Other types of helical springs are considered. Author

N89-11279# Associacao Brasileira de Ciencias Mecanicas, Rio de Janeiro.
FATIGUE OF WELDED JOINT IN A STAINLESS STEEL AISI 304 L
N. K. Kuromoto, A. S. Guimaraes, P. E. V. deMiranda, and R. Pascual 1986 16 p In PORTUGUESE; ENGLISH summary Presented at the 4th Brazilian Symposium on Piping and Pressure Vessels, Salvador, Brazil, 28 Oct. 1986
(DE88-701622; INIS-BR-968; CONF-8610317) Avail: NTIS (US Sales Only) HC A03/MF A01

The bending fatigue behavior of the base metal and welded joint of an AISI 304 L stainless steel type, used in the Angra-1 reactor, was determined. An automatic welding process was used with improved procedures in order to ensure better welding metallurgy. Fatigue test samples were taken to permit evaluation of metallurgical variables, especially the role played by delta ferrite. The resulting welded joint showed better fatigue life than the base metal. Delta ferrite was found to play an important role in the initiation and propagation processes of the fatigue cracks. DOE

N89-11280# KMS Fusion, Inc., Ann Arbor, Mich.
MEASUREMENT OF GLASS SHELL BUCKLING STRENGTH USING A PIEZOELECTRIC FILM SENSOR
Roger G. Schneggenburger, Loretta A. Loughrey, David A. Butkiewicz, and Kathlyn A. Bandy 1988 7 p Presented at the 6th Target Fabrication Specialist's Meeting, Los Alamos, N. Mex., 19 Jun. 1988
(Contract DE-AC03-87DP-10560)
(DE88-013016; KMSF-U-1993; CONF-8806170-12) Avail: NTIS HC A02/MF A01

The importance of glass shell strength becomes clear when one attempts to fill 100 carefully characterized, thin wall glass shells with a high pressure of fuel gas. Unless care is exercized in controlling the driving pressure, many of the shells will break, wasting the time and effort of characterization and losing valuable shells. KMS Fusion has pursued shell strength studies for over ten years. We have learned that when glass shells fail from excess stress (both compressive and tensile), they emit a pressure pulse. Filled shells, for example, when removed from the pressurization chamber, can be heard popping from across a room, if filled to a pressure beyond the strength of the glass walls to contain it. This pressure pulse provides a signal for detecting failure during testing. Recently Pennwalt Corporation has advertised a new piezo- and pyro-electric material it calls KYNAR, a thin film made of polyvinylidene fluoride. This material has unusually high piezoelectric response, and seemed a good candidate sensor to detect the buckling collapse of glass shells. DOE

N89-11281 Minnesota Univ., Minneapolis.
FINITE ELEMENT ANALYSIS OF LARGE STRAIN ELASTIC-PLASTIC SOLIDS Ph.D. Thesis
Jen-Huang Chiou 1987 113 p
Avail: Univ. Microfilms Order No. DA8805743

For the formulation of elastic plastic theory at finite strain, Green and Naghdi decomposed the Green-Lagrange strain tensor into the elastic and plastic parts while E. H. Lee decomposed the deformation gradient into a product of the elastic and plastic parts. Through the comparative studies between these two theories, it is felt that E. H. Lee's theory seems more realistic since it is developed from the exact nonlinear kinematics of elastic plastic deformation instead of assuming that the strain rate is the combination of the elastic and plastic strain rates. A general purpose 3-D finite element software package is developed based on E. H. Lee's large strain elastic plastic theory. The simple tension problem and the simple shear problem are solved as examples so that the numerical solutions and the exact analytical solutions can be compared in order to demonstrate the validity of the proposed numerical model. The tensile test of a thin walled Al alloy tube and the compression test of an aluminum ring involving large deformation plasticity are solved and compared with the experimental results. Good agreement is found between the finite element solution and the experimental results. Dissert. Abstr.

N89-11282# Vibration Inst., Clarendon Hills, Ill.
THE SHOCK AND VIBRATION DIGEST, VOLUME 20, NO. 5 Monthly Report
Judith Nagle-Eshleman, ed. May 1988 76 p
Avail: NTIS HC A05/MF A01

Current research on the vibration and stability of axially-moving materials is discussed. Also discussed is recent research in nonlinear plate vibrations and man and machine induced structural vibration. Abstracts are given for articles dealing with such topics in the areas of machines, structures, vehicles, testing techniques, mathematical methods, computational methods, structural components and design methods. For individual titles, see N89-11283 through N89-11283.

N89-11283# California Univ., Berkeley. Dept. of Mechanical Engineering.
CURRENT RESEARCH ON THE VIBRATION AND STABILITY OF AXIALLY-MOVING MATERIALS
J. A. Wickert and C. D. Mote, Jr. *In* Vibration Inst., The Shock and Vibration Digest, Volume 20, No. 5 May 1988 p 3-13 Sponsored by NSF (For primary document see N89-11282 02-39)
Avail: NTIS HC A05/MF A01

Literature on the vibration and dynamic stability of axially-moving materials, such as traveling strings, tapes, cables, beams, and plates, is reviewed. Fundamental modeling issues, research conclusions, and the vibration analyses of such common systems as aerial cable tramways, magnetic tape drives, and band saws are discussed. Some topics for additional research are suggested. Research on the related problem of the vibration of pipes conveying fluids is not discussed. Author

N89-11284 Syracuse Univ., N. Y.
COMPUTER SIMULATION OF THE UNI-AXIAL STRESS-STRAIN BEHAVIOR OF RIBBON-LIKE FIBER NONWOVENS Ph.D. Thesis
Melur Krishnamurthy Ramasubramanian 1987 203 p
Avail: Univ. Microfilms Order No. DA8806702

A micromechanics constitutive model for the overall elastic-plastic behavior of ribbon-like fiber nonwovens, under unit-axial loading, is presented. The basic micro-element of the model consists of a portion of two crossing fibers and the fiber-to-fiber bond between them. The model assumes that the fibers carry only the axial loads and the bond region of the fibers transfer load from one fiber to the contiguous one through the classical shear-lag load transfer mechanism. The constitutive behavior of both the fiber in axial loading and the bond in shear loading are each characterized as an elastic-plastic material. Results from a computer simulation based on the micromechanics model for the uni-axial stress-strain behavior of paper, are presented. Beyond the elastic limit, the model predicts the entire stress-strain curve for the sheet and the variation of lateral contraction ratio, with respect to the applied sheet strain. Comparison with experimental results on the inelastic behavior for a machine-made paper-board are presented. Dissert. Abstr.

N89-11285# Sandia National Labs., Albuquerque, N. Mex.
A STRAIN RATE DEPENDENT BRITTLE FRACTURE MODEL BASED ON CONTINUUM DAMAGE MECHANICS
E. P. Chen 1988 27 p Presented at the Workshop on Dynamic Constitutive/Failure Models for use in Computer Codes, Dayton, Ohio, 9 May 1988
(Contract DE-AC04-76DP-00789)
(DE88-013361; SAND-88-0857C; CONF-8805161-1) Avail: NTIS HC A03/MF A01

Dynamic fracturing in brittle materials is studied in the present investigation using a strain rate dependent continuum damage model. A basic assumption of this model is the existence of a randomly distributed crack network in the material. Under applied tension, these cracks will grow and interact to relieve the stress. This is reflected globally by reducing the stiffness of the material. In compression, the material responds in an elastic, perfectly plastic manner. Explicit strain rate dependence has been included in the model. A brief description of the model is given. Applications of the model to treat engineering scale problems are discussed. DOE

N89-11286# Institut de Mecanique des Fluides de Lille (France). Groupe Mecanique des Structures.
AIRCRAFT CRASHES ON THE RUNWAY: DEVELOPMENT OF A SUPER ELEMENT FOR NONLINEAR ANALYSIS OF A BEAM [CRASH DES AVIONS SUR PISTE: DEVELOPPEMENT D'UN SUPER-ELEMENT POUR L'ANALYSE NON LINEAIRE D'UNE POUTRE]
P. Geoffroy 15 Dec. 1987 35 p In FRENCH
(Contract DRET-85-003)
(Rept-87/56; ETN-88-93101) Avail: NTIS HC A03/MF A01

A thin shell super finite element was developed to study the pre and post elastoplastic buckling behavior of an embedded beam subject to a lateral load. The finite element is derived from a local behavior law analogous in its form to the law of the global behavior of the structure. Analysis results and quasi-static and dynamic tests on reduced scale models of aircraft structures were compared. This element alone cannot be a solution to the response. It is necessary to simultaneously introduce into the finite element model extra degrees of freedom to represent the plastic joints, and to restrain the displacement of the super element nodes to be representative of the real displacements of the structure. By replacing a large part of a structure by a large element, specific to a given behavior, computation time is considerably reduced. ESA

N89-11287*# National Aeronautics and Space Administration. Langley Research Center, Hampton, Va.
THE CSM TESTBED SOFTWARE SYSTEM: A DEVELOPMENT ENVIRONMENT FOR STRUCTURAL ANALYSIS METHODS ON THE NAS CRAY-2
Ronnie E. Gillian and Christine G. Lotts (Planning Research Corp., Hampton, Va.) Sep. 1988 46 p
(NASA-TM-100642; NAS 1.15:100642) Avail: NTIS HC A03/MF A01 CSCL 20K

The Computational Structural Mechanics (CSM) Activity at Langley Research Center is developing methods for structural analysis on modern computers. To facilitate that research effort, an applications development environment has been constructed to insulate the researcher from the many computer operating systems of a widely distributed computer network. The CSM Testbed development system was ported to the Numerical Aerodynamic Simulator (NAS) Cray-2, at the Ames Research Center, to provide a high end computational capability. This paper describes the implementation experiences, the resulting capability, and the future directions for the Testbed on supercomputers. Author

N89-11288# Air Force Inst. of Tech., Wright-Patterson AFB, Ohio.
FINITE ELEMENT ANALYSIS OF SHELL STRUCTURES WITH AN 18-NODE 3-DIMENSIONAL SOLID ELEMENT BASED ON A NEW MIXED FORMULATION M.S. Thesis
Michael F. Ausserer 1988 66 p
(AD-A196698; AFIT/CI/NR-88-71) Avail: NTIS HC A04/MF A01 CSCL 20K

An eighteen node, three dimensional, solid element with 54 degrees of freedom is presented for the finite element analysis of thin plates and shells. The element is based on the Hellinger Reissner principle with independent assumed strain. The independent strain is divided into higher and lower order terms. A modified stress strain relation decoupling inplane and normal strain is used to model thin shell behavior. Numerical results demonstrate that this element is effectively free of locking even for very thin plates and shells. In addition, the element is kinematically stable. In fact, the stiffness matrix associated with the higher order independent strain is a stabilization matrix. GRA

N89-11289# George Washington Univ., Washington, D.C. School of Engineering and Applied Science.
CREEP AND FRACTURE CHARACTERISTICS OF MATERIALS AND STRUCTURES AT ELEVATED TEMPERATURES Final Report
Harold Liebowitz May 1988 353 p
(Contract N00014-84-K-0027)
(AD-A196831) Avail: NTIS HC A16/MF A01 CSCL 11F

The work under this contract was concentrated in three major areas: the effect of mixed mode loading on fracture characteristics, the nature of crack tip stress, strain and energy fields in ductile materials and the nature of crack tip stress strain and energy fields in materials undergoing rate dependent viscoplastic deformation. In each of these areas, new insight was obtained and better understanding of the fundamental physical processes gained. The appendices of this work document the significant research contribution that was made under ONR contract N00014-84-K-0027. GRA

N89-11068# Joint Publications Research Service, Arlington, Va.
NEW TRIAL OF VIBRATION TESTING METHOD
Tetsuhiko Ueda *In its* JPRS Report: Science and Technology: Japan 4 Jun. 1987 p 26-28 Transl. into ENGLISH from Kogiken Nyusu (Toyko, Japan), Sep. 1986 p 3-4 (For primary document see N89-11061 02-31)
Avail: NTIS HC A05/MF A01

42 GEOSCIENCES (GENERAL)

No abstracts in this category.

43 EARTH RESOURCES AND REMOTE SENSING

Includes remote sensing of earth resources by aircraft and spacecraft; photogrammetry; and aerial photography.

For instrumentation see *35 Instrumentation and Photography.*

N89-11290*# Howard Univ., Washington, D. C. Dept. of Geology and Geography.
SNOW COVER, SNOWMELT AND RUNOFF IN THE HIMALAYAN RIVER BASINS Final Technical Report
B. Dey, V. K. Sharma, D. C. Goswami, and P. Subba Rao Jul. 1988 37 p
(Grant NAG5-224)
(NASA-CR-182434; NAS 1.26:182434) Avail: NTIS HC A03/MF A01 CSCL 08H

Not withstanding the seasonal vagaries of both rainfall amount and snowcover extent, the Himalayan rivers retain their basic perennial character. However, it is the component of snowmelt yield that accounts for some 60 to 70 percent of the total annual flow volumes from Hamilayan watersheds. On this large hydropotential predominantly depends the temporal performance of hydropower generation and major irrigation projects. The large scale effects of Himalayan snowcover on the hydrologic responses of a few selected catchments in western Himalayas was studied. The antecedent effects of snowcover area on long and short term meltwater yields can best be analyzed by developing appropriate hydrologic models forecasting the pattern of snowmelt as a function of variations in snowcover area. It is hoped that these models would be of practical value in the management of water resources. The predictability of meltwater for the entire snowmelt season was studied, as was the concurrent flow variation in adjacent watersheds, and their hydrologic significance. And the applicability of the Snowmelt-Runoff Model for real time forecast of daily discharges during the major part of the snowmelt season is examined. Author

N89-11291# Instituto de Pesquisas Espaciais, Sao Jose dos Campos (Brazil).
OBSERVATIONS OF SOUTHERN IRREGULAR VARIABLES
J. E. Steiner, D. Cieslinski, and F. Jablonski May 1988 25 p Presented at the Symposium Commemorative to the 25th Anniversary of the Cerro Tololo Inter-American Observatory, La Serena, Chile
(INPE-4568-PRE/1309) Avail: NTIS HC A03/MF A01

Results of a photometric and spectroscopic survey of Southern Irregular Variables (of types L, I and Is) are summarized. About 400 stars were observed and nearly 20 percent of them were found to be misclassified. Among stars with magnitude fainter than 14, there is an increasing fraction of interesting objects. A total of 12 new Cataclymsic Variables or related objects were identified and a few of them are discussed in some detail. Author

N89-11292*# California Univ., Santa Barbara. Dept. of Geography.
IMPROVEMENT AND EXTENSION OF A RADAR FOREST BACKSCATTERING MODEL Annual Report
David S. Simonett and Yong Wang 20 Sep. 1988 38 p
(Grant NAG5-1010)
(NASA-CR-183259; NAS 1.26:183259) Avail: NTIS HC A03/MF A01 CSCL 02F

Research to-date has focused on modeling development and programming based on model components proposed during the past several months and research progress made by the Simonett team. The model components and programs (in C language under UNIX) finished to date are summarized. These model components may help explain the contributions of various vegetation structural components to the attenuation and backscattering of vegetated surfaces to extract useful data concerning forest stands and their underlying surfaces for both the seawater-on and seawater-off. Author

N89-11293# Pennsylvania State Univ., University Park. Environmental Resources Research Inst.
REMOTE SENSING AND HYDROLOGIC MODELING OF ARID WATERSHEDS: A SCALE ANALYSIS Progress Report
1988 5 p
(Contract DE-FG02-86ER-60472)
(DE88-014625; DOE/ER-60472/02) Avail: NTIS HC A02/MF A01

The ultimate goal of this multiyear research effort is to model long-term (100 to 10,000 yrs), cut and fill cycles in arid region fluvial systems (arroyos). Historic and geologic (late Quaternary) data bases indicate that arid region fluvial systems have oscillated between periods of pronounced aggradation and degradation. This cyclic behavior has affected both water and sediment discharge from arid watersheds as well as ecosystem habitats along hillslopes and valley bottoms. One of the primary causes that has been proposed for this cyclic activity is climatic change for gradual (glacial-interglacial) and catastrophic (volcanic eruptions, el Nino) rates of climatic change on a global scale. The immediate goal of this multiyear research effort is to modify existing numeric hydrologic models (SPUR, KINEROS) which utilize as input multilayered, co-registered remotely sensed data for the prediction of surface hydrology and sediment erosion, transport and deposition in arid region watersheds. It is hypothesized that different types of co-registered, remotely sensed data including digital elevation data sets (DEDS), multispectral scanner (TM, SPOT), and thermal infrared multispectral scanner (TIMS) can be used in conjunction with limited ground truth data to predict values of input parameters for numeric watershed hydrology models and thus to compute watershed hydrologic and sedimentologic characteristics. DOE

N89-11294# Instituto de Pesquisas Espaciais, Sao Jose dos Campos (Brazil).
TECHNIQUE FOR OBTAINING AGRICULTURAL PROPERTY BOUNDARIES THROUGH SATELLITE IMAGERY, CERTIFIED TO CONTROL AND ACCOMPANY AGRICULTURAL ACTIVITY [TECNICA PARA OBTER LIMITES DE PROPRIEDADES AGRICOLAS SOBRE IMAGENS DE SATELITE, VISANDO CONTROLAR E ACOMPANHAR A ATIVIDADE AGRICOLA]
Valdete Duarte Aug. 1988 11 p In PORTUGUESE; ENGLISH summary Presented at the Enserplan-National Meeting of Remote Sensing Applied to Municipal Planning, Campos do Jordao, Oct. 1987
(INPE-4640-PRE/1351) Avail: NTIS HC A03/MF A01

This work is part of a project named Fiscalizacao de Propriedades Agricolas por Satelite (FISATE). The survey of the rural credit for properties with wheat crops in the Assis county in the Sao Paulo State is presented. The following materials were utilized: aerial photographs at the 1:35,000 scale; photomosaic at the 1:100,000; and IBGE topographic charts at the 1:250,000 and 1:50,000 scales. One Banco de Brasil clerk from the Assis agency, was trained on aerial photography handling to be able to make property cadaster from the available photographs. The agricultural properties boundaries outlined on the aerial photographs were transferred to the cartographic maps at the 1:50,000 scale using the KARTOFLEX equipment. From this cartographic map the properties boundaries as well as some features such as rivers, roads, and cities, were extracted to be used as reference points on the satellite data. This information was reduced to 1:100,000 scale map on a transparent film to be compatible to the satellite images. The final product is a transparency in a lithographic film containing the agricultural properties boundaries. This transparency was overlaid on the satellite images and allowed to locate perfectly the agricultural properties. Hence, the wheat plantations were identified and their areal extent evaluated through the satellite images. Author

N89-11295# Instituto de Pesquisas Espaciais, Sao Jose dos Campos (Brazil).
TRAINING ACTIVITIES IN REMOTE SENSING AT THE INSTITUTO DE PESQUISAS ESPACIAIS-INPE/BRAZIL [AS ATIVIDADES DE TREINAMENTO EM SENSORIAMENTO REMOTO NO INSTITUTO DE PESQUISAS ESPACIAIS-INPE/BRASIL]
Tania Maria Sausen and Roberto PereiradaCunha Aug. 1988 21 p In PORTUGUESE; ENGLISH summary Presented at the 2nd Latin American Symposium of Remote Perception, Bogota, Columbia, 16-23 Nov. 1987
(INPE-4686-PRE/1380) Avail: NTIS HC A03/MF A01

The Institute for Space Research (Instituto de Pesquisas Espaciais - INPE) began its research program in remote sensing in 1972, with the launching of the American LANDSAT satellites. Research was developed mainly in the field of natural resources, through the studies of geology, environmental analysis, agriculture and vegetation. In October 1985 the Technical Orientation in Remote Sensing (Coordenadoria de Orientacao Tecnica em Sensoriamento Remoto COT) was created; its main objective is to coordinate the transference of remote sensing technologies and methodologies developed by INPE, to external users. Under the responsibility of COT, there exists a Training Group (Coordenadoria Adjunta de Treinamento), responsible for the realization of national and international training courses for the job training in remote sensing and for the II International Training Course in Remote Sensing. The INPE's Remote Sensing Area has a group of researchers in academic titles of Master of Science in remote sensing and Doctorate in different fields of natural resources, in charge of giving training courses as well as developing researches. This paper explains the remote sensing activities in training courses, realized through the Training Group of COT in the years 1985, 1986 and 1987 and its training policy for the next years. Author

N89-11296*# Michigan Univ., Ann Arbor. Radiation Lab.
EFFECT OF CURVATURE ON THE BACKSCATTERING FROM LEAVES
K. Sarabandi, T. B. A. Senior, and F. T. Ulaby 1988 36 p (Grant NAG5-480)
(NASA-CR-183326; NAS 1.26:183326) Avail: NTIS HC A03/MF A01 CSCL 20F

Using a model previously developed for the backscattering cross section of a planar leaf at X-band frequencies and above, the effect of leaf curvature is examined. For normal incidence on a rectangular section of a leaf curved in one and two dimensions, an integral expression for the backscattered field is evaluated numerically and by a stationary phase approximation, leading to a simple analytical expression for the cross section reduction produced by the curvature. Numerical results based on the two methods are virtually identical, and in excellent agreement with measured data for rectangular sections of coleus leaves applied to the surfaces of styrofoam cylinders and spheres of different radii. Author

N89-11297# Instituto de Pesquisas Espaciais, Sao Jose dos Campos (Brazil).
SPECTRAL STUDIES OF THREE OXISOLS AND A ULTISOL OF BRAZIL
Antonio Roberto Formaggio and Jose Carlos NevesEpiphanio Aug. 1988 24 p In PORTUGUESE; ENGLISH summary Presented at the 2nd Latin American Symposium on Remote Sensors, Bogota, Columbia, 16-20 Nov. 1987
(INPE-4644-PRE/1355) Avail: NTIS HC A03/MF A01

The correlation was verified between spectral behavior of three Oxisols and one Ultisol from Sao Paulo State (Brazil) with their following characteristics: iron oxids and organic matter contents, particle size, colour, surface conditions, cation exchange capacity and parent material. The data was collected in three spectral levels: laboratory, field and satellite. For the first two levels, data were collected between 400 and 1100 mm with a spectroradiometer and a hand held radiometer, respectively. For the satellite level (MSS and TM-LANDSAT) it was used the Multiespectral Imagery Analyser - Image 100 with data from compatible computer tapes (CCTs). The physical and chemical parameters were highly correlated with the spectral behavior of the four soil types. In one of the two study areas, where the parent material is argillic (clay) it was observed a type of spectral discrimination between the soils; and where the parent material originate sandy pedological substrate it was observed another type of discrimination between studied soils. These results show the importance of parent material and soil texture as influencing parameters of the soil spectral behavior. Also, clear indications of the inference potential from soil properties related with iron oxids due strong absorption ocurred mainly at near infrared for the soils originated from eruptive basic rocks. Author

N89-11298# DCS Corp., Alexanderia, Va.
PARAMETRIC ANALYSIS OF MAP DATA Final Report, Sep. 1987 - May 1988
Henry B. Hoyle 31 May 1988 173 p
(Contract DAAB07-87-C-F069)
(AD-A196908; DCS-14020RPT001) Avail: NTIS HC A08/MF A01 CSCL 08B

An approach to using digital map data is needed for future weapons systems. Automatic target recognizers (ATR) need information from digital maps to aid in image interpretation. Digital maps can provide information to help ATRs interpret signatures, to exclude portions of the images from detailed processing, and to put the images in context with the background. Pilots need digital maps to fill in where Forward Looking Infrared (FLIR) sensors are obscured by atmospheric conditions, and to give them the ability to know what to expect over the next hill. This research studied the feasibility of correlating digital maps with FLIR images by doing a parametric error analysis. The concept of an Integrated FLIR/Map System was defined and an approach to further validation of the concept is recommended. GRA

44 ENERGY PRODUCTION AND CONVERSION

Includes specific energy conversion systems, e.g., fuel cells; global sources of energy; geophysical conversion; and windpower.

For related information see also *07 Aircraft Propulsion and Power, 20 Spacecraft Propulsion and Power,* and *28 Propellants and Fuels.*

N89-11299# National Academy of Sciences - National Research Council, Washington, D. C. Commission on Engineering and Technical Systems.
GEOTHERMAL ENERGY TECHNOLOGY: ISSUES, R AND D NEEDS, AND COOPERATIVE ARRANGEMENTS
1987 106 p
(Contract DE-FG01-86CE-31010)
(DE88-011804; DOE/CE-31010/T1) Avail: NTIS HC A06/MF A01

The report addresses four types of geothermal energy: hydrothermal, geopressured, hot dry rock, and magma systems. Hydrothermal systems are the only type that are now economically competitive commercially. Further technology development by the Department of Energy could make the uneconomical hydrothermal resources commercially attractive to the industry. The economics are more uncertain for the longer-term technologies for extracting energy from geopressured, hot dry rock, and magma systems. For some sites, the cost of energy derived from geopressured and hot dry rock systems is projected within a commercially competitive range. The use of magma energy is too far in the future to make reasonable economic calculations. DOE

N89-11300# Sandia National Labs., Albuquerque, N. Mex. Exploratory Batteries Div.
RELIABILITY ANALYSIS OF LITHIUM CELLS
Samuel C. Levy and Per Bro (Southwest Electrochemical Co., Santa Fe, N. Mex.) 1988 16 p Presented at the 4th International Meeting on Lithium Batteries, Vancouver, British Columbia, 23 May 1988
(Contract DE-AC04-76DP-00789)
(DE88-009258; SAND-87-2129C; CONF-880598-2) Avail: NTIS HC A03/MF A01

Fault tree analysis has been used for many years in safety and reliability analyses of nuclear reactors and other large systems. This technique can also be useful in the design of high reliability lithium cells/batteries and in improving the reliability of existing designs. The basic building blocks of a fault tree are discussed and an example, using the lithium-sulfur cell, is given. DOE

N89-11301# Midwest Research Inst., Golden, Colo. Solar Energy Research Inst.
NATIONAL PHOTOVOLTAICS PROGRAM: 1987 PROGRAM REVIEW
Apr. 1988 15 p
(Contract DE-AC02-83CH-10093)
(DE88-001148; DOE/CH-10093/21) Avail: NTIS HC A03/MF A01

A number of photovoltaic systems, components and applications are highlighted under the national program. DOE

N89-11302# Midwest Research Inst., Golden, Colo.
TERNARY ADAMANTINE MATERIALS FOR LOW-COST SOLAR CELLS Final Subcontract Report, 1 Nov. 1984 - 31 Dec. 1986
D. Cahen and G. Hodes Dec. 1987 45 p
(Contract DE-AC02-83CH-10093)
(DE88-001160; SERI/STR-211-3289) Avail: NTIS HC A03/MF A01

Several methods were investigated to prepare CuInSe2, using electroplating techniques near room temperature, to explore them for obtaining photovoltaically active films. No significant photoactivity resulted, unless an annealing step (at greater than or equal to 400 C) was added to the process. Promising PV activity was found only if this anneal was carried out in a Se-containing atmosphere. Therefore, in part of this project, the two steps, metal deposition and chalcogen incorporation, were separated. These experiments showed that chalcogenization is the most critical step in obtaining films that are PV active. The composition of the films obtained after the chalcogenization step can be varied considerably by a chemical, postannealing treatment. PV activity of films was checked in a simple, rapid way by sputtering Cd onto them. Both these junctions, as well as those obtained by ITO deposition, show improved rectification and PV activity, after air anneal of the chalcogenized film, before junction formation. Possible causes for this are discussed. Separate C-V experiments on AlCuInSe2Mo structures, using CuInSe2Mo films, provided direct evidence of the persistence of two types of CuInSe2 layers, distinguishable by their doping concentration. DOE

N89-11303# Mechanical Technology, Inc., Latham, N. Y.
DEVELOPMENT OF A RESIDENTIAL FREE-PISTON STIRLING ENGINE HEAT PUMP
Robert A. Ackermann 1988 8 p Presented at the 2nd DOE/ORNL Heat Pump Conference: Research and Development on the Heat Pump for Space Conditioning Applications, Washington, D.C., 17 Apr. 1988
(Contract DE-AC05-84OR-21400)
(DE88-012917; CONF-8804100-14) Avail: NTIS HC A02/MF A01

After several years of development, the free-piston Stirling engine heat pump (FPSE/HP) has successfully met proof-of-concept targets. The performance targets were achieved during an off-site test and evaluation program conducted at the Lennox Industries Engineering Center. The performance achieved for the module was a cooling thermal coefficient of performance (COP) of 0.91 and a heating thermal COP of 1.62. In addition to its performance achievement, the FPSE/HP module demonstrated good reliability in over 60 days of operation and ran stably and repeatably over a range of ambient conditions from 0 to 105 F. This paper will provide a description of the FPSE/HP module tested at Lennox, describe the developmental history of the FPSE/HP at Mechanical Technology Incorporated (MTI), and present the results of the Lennox tests. This work has been a collaborative effort of MTI, Oak Ridge National Laboratory (ORNL), the Department of Energy (DOE), and the Gas Research Institute (GRI). The financial and technical support provided by ORNL, DOE, and GRI was responsible for the success achieved. DOE

N89-11304# Sandia National Labs., Albuquerque, N. Mex. Wind Energy Research Div.
ROTOR INSTRUMENTATION CIRCUITS FOR THE SANDIA 34-METER VERTICAL AXIS WIND TURBINE
Herbert J. Sutherland and William A. Stephenson Jul. 1988 76 p
(Contract DE-AC04-76DP-00789)
(DE88-014704; SAND-88-1144) Avail: NTIS HC A05/MF A01

Sandia National Laboratories has erected a research oriented, 34-meter diameter, Darrieus vertical axis wind turbine near Bushland, Texas, which has been designated the Sandia 34-m VAWT Test Bed. To meet present and future research needs, the machine was equipped with a large array of sensors. This manuscript details the sensors initially placed on the rotor, their respective instrumentation circuits, and the provisions incorporated into the design of the rotor instrumentation circuits for future research. This manuscript was written as a reference manual for the rotor instrumentation of the Test Bed. DOE

N89-11305# Indal Technologies, Inc., Mississauga (Ontario).
A MODEL FOR THE RESPONSE OF VERTICAL AXIS WIND TURBINES TO TURBULENT FLOW: PARTS 1 AND 2
D. R. Malcolm Jul. 1988 221 p Prepared for Sandia National Labs., Albuquerque, N. Mex.
(Contract DE-AC04-76DP-00789)
(DE88-014708; SAND-88-7021-Pt-1/2) Avail: NTIS HC A10/MF A01

This report describes a project intended to incorporate the

effects of atmospheric turbulence into the structural response of Darrieus rotor, vertical axis wind turbines. The basis of the technique is the generation of a suitable time series of wind velocities, which are passed through a double multiple streamtube aerodynamic representation of the rotor. The aerodynamic loads are decomposed into components of the real eigenvectors of the rotor and subsequently into full-power and cross-spectral densities. These modal spectra are submitted as input to a modified NASTRAN random load analysis and the power spectra of selected responses are obtained. This procedure appears to be successful. Results at zero turbulence agree with alternative solutions, and when turbulence is included, the predicted stress spectra for the Indal 6400 rotor are in good agreement with field data. The model predicts that the effect of turbulence on harmonic frequency peaks and on all lead-lag bending will not be great. However, it appears that only 11 percent turbulence intensity can almost double the rms of cyclic flatwise blade bending. DOE

N89-11306# Sandia National Labs., Albuquerque, N. Mex. Photovoltaic Technology Div.
THE PHOTOVOLTAIC ADVANCED SYSTEMS TEST FACILITY
Jay L. Chamberlin 1988 7 p Presented at the 8th European Photovoltaic Solar Energy Conference, Florence, Italy, 9 May 1988
(Contract DE-AC04-76DP-00789)
(DE88-009589; SAND-87-1769C; CONF-880513-2) Avail: NTIS HC A02/MF A01

Sandia National Laboratories, as part of the United States Department of Energy's (DOE) National Photovoltaics (PV) Program, operates an extensive PV testing laboratory in Albuquerque, New Mexico. The objectives of this laboratory, the Photovoltaic Advanced Systems Test Facility (PASTF), are to assess the performance of PV and balance-of-systems (BOS) hardware and to work with their developers to rectify any performance deficiencies found. The principal resources of the PASTF consist of a materials testing laboratory, a lens and lens/cell testing facility, a module testing facility, an array testing facility, a power conditioner evaluation facility, and specialized test stations for evaluation of BOS hardware. A cell characterization laboratory that is part of the larger Sandia PV effort provides evaluational support in this area. These resources are augmented by Sandia's extensive research and support facilities, principally in the areas of material characterization and environmental testing. The paper describes the resources of the PASTF along with examples of their application to the evaluation of PV hardware. DOE

N89-11307# Argonne National Lab., Ill.
ORGANIC RANKINE-CYCLE POWER SYSTEMS WORKING FLUIDS STUDY: 2-METHYLPYRIDINE/WATER Topical Report No. 3
R. L. Cole, J. C. Demirgian, and J. W. Allen Sep. 1987 284 p
(Contract W-31-109-eng-38)
(DE88-012659; ANL/CNSV-TM-202) Avail: NTIS HC A13/MF A01

A mixture of 35 mole percent (mol percent) 2-methylpyridine and 65 mol percent water was tested at 575, 625, and 675 degree F in a dynamic loop. Samples of the degraded fluid were chemically analyzed to determine the identities of major degradation products and the quantity of degradation. Computed degradation rates were found to be higher than those for Fluorinol 85 or toluene. For this reason (and other reasons, related to fluid handling), other fluids are recommended as the first choice for service in organic Rankine-cycle systems. DOE

N89-11308# Texas A&M Univ., College Station. Dept. of Chemical Engineering.
OXYGEN ELECTRODE IN MOLTEN CARBONATE FUEL CELLS Quarterly Technical Progress Report No. 2
B. Dave, P. K. Adanuvor, R. E. White, M. A. Enayetullah, and A. J. Appleby 31 Jan. 1988 31 p
(Contract DE-FG22-87PC-79931)
(DE88-009628; DOE/PC-79931/1) Avail: NTIS HC A03/MF A01

The following preliminary conclusions can be drawn from the results so far: (1) the effect or the neutralization reaction rate on the steady state polarization curves is the same for both models, (2) changes in the auto-catalytic decomposition rates of O2 sup double bond and O2 sup single bond do not affect the polarization curves significantly, and (3) the fact that the contribution to the overall steady polarization curve can be attributed predominantly to the reduction of O2 sup double bond contradicts the results of Vogel et al., in which the steady state experimental polarization curves were attributed mainly to the reduction of O2 sup single bond species. Therefore, the results of Vogel et al., are at best in closer agreement with Model A than with Model B. DOE

N89-11309# California Univ., Berkeley. Lawrence Berkeley Lab.
FUEL CELLS: A HANDBOOK
K. Kinoshita, F. R. McLarnon, and E. J. Cairns May 1988 168 p
(Contract DE-AC03-76SF-00098)
(DE88-010252; DOE/METC-88-6096) Avail: NTIS HC A08/MF A01

The purpose of this handbook is to present information describing fuel cells that is helpful to scientists, engineers, and technical managers who are not experienced in this technology, as well as to provide an update on the current technical status of the various types of fuel cells. Following the introduction, contents of this handbook are: fuel cell performance variables; phosphoric acid fuel cell; molten carbonate fuel cell; solid oxide fuel cell; alternative fuel cell technologies; fuel cell systems; and concluding remarks. DOE

N89-11310# Pacific Northwest Labs., Richland, Wash.
ADVANCED MATERIALS FOR SOLID OXIDE FUEL CELLS: HAFNIUM-PRASEODYMIUM-INDIUM OXIDE SYSTEM
J. L. Bates, C. W. Griffin, and W. J. Weber Jun. 1988 51 p
(Contract DE-AC06-76RL-01830)
(DE88-015365; PNL-6575) Avail: NTIS HC A04/MF A01

The HfO2-PrO1.83-In2O3 system has been studied at the Pacific Northwest Laboratory to develop alternative, highly electrically conducting oxides as electrode and interconnection materials for solid oxide fuel cells. A coprecipitation process was developed for synthesizing single-phase, mixed oxide powders necessary to fabricate powders and dense oxides. A ternary phase diagram was developed, and the phases and structures were related to electrical transport properties. Two new phases, an orthorhombic PrInO3 and a rhombohedral Hf2In2O7 phase, were identified. The highest electronic conductivity is related to the presence of a bcc, In2O3 solid solution (ss) containing HfO2 and PrO1.83. Compositions containing more than 35 mol percent of the In2O3 ss have electrical conductivities greater than 0.1/(ohm-cm), and the two or three phase structures that contain this phase appear to exhibit mixed electronic-ionic conduction. The high electrical conductivities and structures similar to the Y2O3-stabilized ZrO2(HfO2) electrolyte give these oxides potential for use as cathodes in solid oxide fuel cells. DOE

N89-11311# Chronar Corp., Princeton, N.J.
AMORPHOUS SILICON PHOTOVOLTAIC DEVICES PREPARED BY CHEMICAL AND PHOTOCHEMICAL VAPOR DEPOSITION OF HIGHER ORDER SILANES Annual Subcontract Report, 1 Sep. 1986 - 31 Aug. 1987
A. E. Delahoy and H. E. Schade Jun. 1988 20 p
(Contract DE-AC02-83CH-10093)
(DE88-001189; SERI/STR-211-3363) Avail: NTIS HC A03/MF A01

This report describes results of research on preparing high-efficiency photovoltaic devices by photochemical vapor deposition of higher order silanes. The photostability of these devices was compared to that of devices produced by the glow-discharge technique. Hydrogenated amorphous silicon cell efficiencies of at least 7.5 percent were obtained using p-i-n structures and aluminum back contacts. Using silver contacts increased the efficiency to about 8 percent. After 6 minutes of light soaking, there was no

significant difference between the photostabilities of these cells and those produced by glow discharge. The efficiencies might be increased further if some remaining problems can be addressed, such as by using a different substrate preparation method or a higher pumping speed at the deposition chamber. DOE

N89-11312# Midwest Research Inst., Golden, Colo. Solar Energy Research Inst.
A LIMITED ASSESSMENT AND CHARACTERIZATION OF THE SOLAR RADIATION ENERGY RESOURCES IN THE CARIBBEAN REGION
R. L. Hulstrom Feb. 1988 170 p
(Contract DE-AC02-83CH-10093)
(DE88-001133; SERI/PR-215-3292) Avail: NTIS HC A09/MF A01

The objective is to produce a preliminary assessment and characterization of the Caribbean region (Barbados, Dominican Republic, Guatemala, Jamaica, and Panama) solar radiation energy resources. Such information will be used to estimate the performance of, and identify the most promising applications of, solar heat technologies in the Caribbean region. It is expected that the solar radiation resources in the Caribbean region are very location specific. Sunny areas will have an annual direct-beam resource of about 3,000 kWhm(sup -2) and a global solar radiation resource of about 2,500 kWhm(sup -2). Cloud-covered areas will have annual solar radiation resources of about 1,500 kWhm(sup -2) for both the direct-beam and the global solar radiation. Monthly levels of solar radiation will vary markedly, ranging from an average of 9 to 3 kWhm(sup -2)/day (sup -1) for the direct-beam and from an average of 7 to 4 kWhm(sup -2)/day (sup -1) for the global solar radiation. The Caribbean region is comparable to the Great Plains region of the US, in terms of annual solar radiation resources; however thorough prospecting is required to avoid areas having very low amounts of solar radiation. DOE

N89-11313# Massachusetts Inst. of Tech., Cambridge.
INTEGRATION OF ANALYSIS AND EXPERIMENT FOR STIRLING CYCLE PROCESSES. PART 1: GAS SPRING HYSTERESIS LOSS
A. A. Kornhauser and J. L. Smith, Jr. 1988 7 p Presented at the 2nd DOE/ORNL Heat Pump Conference: Research and Development on the Heat Pump for Space Conditioning Applications, Washington, D.C., 17 Apr. 1988
(Contract DE-AC05-84OR-21400)
(DE88-013202; CONF-8804100-13) Avail: NTIS HC A02

Heat transfer-related hysteresis loss can be an important factor in the performance of Stirling and other reciprocating machines. Analytical predictions of hysteresis loss have been available to designers, but until now they were not experimentally verified. Hysteresis loss was measured in a piston-cylinder gas spring over a range of speeds, pressures, gases, bore/stroke ratios, volume ratios, and internal extended surface geometries. An analysis of a simplified one-dimensional energy equation produced non-dimensional parameters that were used to correlate the experimental data. The loss expression from the analysis was adjusted to fit the correlated data. DOE

N89-11314# Stanford Univ., Calif.
STUDIES IN ADVANCED SILICON SOLAR CELLS
R. M. Swanson Jun. 1988 116 p
(Contract DE-AC04-76DP-00789)
(DE88-013143; SAND-88-7026) Avail: NTIS HC A06/MF A01

This report addresses several issues of interest for the design and fabrication of silicon solar cells. The report begins with a theoretical study concerning the necessity for using more complex mobility models in order to accurately describe the operation of concentrator solar cells. The report then details a modeling and experimental study of recombination under high-level-injection conditions in order to more precisely understand this effect, which will limit cell performance. Becoming more technological, the next section studies the trade-offs between light-trapping and minimization of surface recombination for a variety of texturization schedules. Finally, a study on minimizing surface recombination by optimizing the oxidation parameters is given. The overall utility of the information presented in this document is twofold. First, the mobility, recombination and texturization studies are relevant to improved modeling, prediction, and cell design. Second, the experimental techniques and results are carefully described in order to be useful in the process design and technological optimization of silicon solar cells. DOE

N89-11315*# Lockheed Missiles and Space Co., Sunnyvale, Calif.
PV MODULES FOR GROUND TESTING Final Report
10 Sep. 1986 132 p
(Contract NAS3-24657)
(NASA-CR-179476; NAS 1.26:179476; LMSC/D973480) Avail: NTIS HC A07/MF A01 CSCL 10A

The main objective was to design and build a minimum of three photovoltaic test panels for plasma interaction experiments. These experiments are intended to provide data on the interactions between high-voltage solar arrays and the space plasma environment. Data gathered will significantly contribute to the development of design criteria for the space station solar arrays. Electrical isolation between the solar cell strings and the module mounting plate is required for high-voltage bias. Author

N89-11316# Harvard Univ., Cambridge, Mass. Dept. of Chemistry.
OPTIMIZATION OF TRANSPARENT AND REFLECTING ELECTRODES FOR AMORPHOUS SILICON SOLAR CELLS Final Subcontract Report, 1 Oct. 1986 - 31 Nov. 1987
R. G. Gordon, J. Proscia, K. Gustin, J. Chapple-Sokol, D. Strickler, and R. McCurdy Jun. 1988 72 p
(Contracts DE-AC02-83CH-10093; XB-7-06110-1)
(DE88-001175; SERI/STR-211-3332) Avail: NTIS HC A04

In this research, hydrogenated amorphous silicon (a-Si:H) films were deposited by an inexpensive, thermally induced, atmospheric-pressure chemical vapor deposition (CVD) process. High-quality films were grown at 300 A, more than two orders of magnitude faster than those produced by conventional glow discharge. Sources of uncontrolled oxygen, boron, phosphorus, and carbon contamination were identified and eliminated. The efficiency of a-Si solar cells can be increased by using rough, rather than smooth, tin oxide as the front-surface transparent electrode, because the rough tin oxide-silicon interface increases the absorption of red light (light trapping) and reduces the reflection loss of light across the whole spectrum. We produced, by CVD, rough tin oxide films from tetramethyltin. Cells grown on the rough films have higher efficiencies than those grown on smooth tin oxide. We also used a precursor tin compound (dimethyltin dichloride) that is less costly and less hazardous than others. Rough films can be grown from dimethyltin dichloride more than three times faster than from tetramethyltin. To combine the CVD processes we need a layer that prevents the tin oxide layer from being attacked by the silicon, such as a barrier layer of titanium oxide, which seems to be effective. DOE

N89-11317# Pacific Northwest Labs., Richland, Wash.
ASSESSMENT OF METHANOL ELECTRO-OXIDATION FOR DIRECT METHANOL-AIR FUEL CELLS
S. D. Fritts and R. K. Sen Jul. 1988 43 p
(Contract DE-AC06-76RL-01830)
(DE88-014686; PNL-6077) Avail: NTIS HC A03/MF A01

The Office of Energy Storage and Distribution of the U.S. Department of Energy (DOE) supports the development of a methanol-air fuel cell for transportation application. The approach used at Los Alamos National Laboratory converts the methanol fuel to a hydrogen-rich gas in a reformer, then operates the fuel cell on hydrogen and air. The reformer tends to be bulky (raising vehicle packaging problems), has a long startup period, and is not well suited for the transient operation required in a vehicle. Methanol, however, can be oxidized electrochemically in the fuel cell. If this process can be conducted efficiently, a direct methanol-air fuel cell can be used, which does not require a reformer. The objective of this study is to assess the potential of

developing a suitable catalyst for the direct electrochemical oxidation of methanol. The primary conclusion of this study is that no acceptable catalysts exist that can efficiently oxidize methanol electrochemically and have the desired cost and lifetime for vehicle applications. However, recent progress in understanding the mechanism of methanol oxidation indicates that a predictive base can be developed to search for methanol oxidation catalysts and can be used to methodically develop improved catalysts. DOE

N89-11318# Deutsche Forschungs- und Versuchsanstalt fuer Luft- und Raumfahrt, Stuttgart (West Germany). Inst. for Structural Research and Design Development.

DEVELOPMENT, CONSTRUCTION, AND OPERATION OF A 30/100-kW WIND ENERGY CONVERTER (WEC) Final Report, 31 Mar. 1987

Helmut Boehnisch, Hermann Hald, Christoph Kensche, Alfred Kussmann, Jens-Peter Molly, and Henry Seifert Apr. 1988 220 p In GERMAN; ENGLISH summary
(Contract BMFT-03E-4439A)
(DFVLR-Mitt-88-06; DFVLR-IB-435-87/20; ISSN-0176-7739; ETN-88-93180) Avail: NTIS HC A10/MF A01; DFVLR, VB-PL-DO, 90 60 58, 5000 Cologne, Federal Republic of Germany, 73 deutsche marks

A light weight wind energy converter (WEC) of 25 m rotor diameter which operates in low and medium average wind speed was developed. Built-in self erecting equipment allows assembly of the three bladed WEC at remote areas. Static and dynamic blade tests were performed to qualify the structural blade design. After assembly and erection on the test site, the tower, hydraulic system, and microprocessor controlled operation supervisory system were improved during the test phase. The WEC went into continuous operation for a reference period of 1 yr. The technical availability during that time is higher than 92 pct, the total energy harvest = 104 MWh in an average wind of only 4.2 m/sec. The WEC achieved 6395 hours of grid connected operation, producing a total of 166 MWh electrical energy. ESA

45 ENVIRONMENT POLLUTION

Includes atmospheric, noise, thermal, and water pollution.

N89-11319# Oak Ridge National Lab., Tenn.

MARKERS OF AIR POLLUTION IN FORESTS: NUTRIENT CYCLING

Dale W. Johnson, Helga VanMiegroet, and Wayne T. Swank 1988 12 p Presented at the Workshop on Markers of Air Pollution Effects in Forests, Asheville, N.C., 25 Apr. 1988 Prepared in cooperation with Coweeta Hydrologic Lab., Otto, N.C.
(Contract DE-AC05-84OR-21400)
(DE88-011011; CONF-8804133-2) Avail: NTIS (US Sales Only) HC A03/MF A01

Air pollution may alter either the nutrient content or the flux rates in forest ecosystems, but, with a few exceptions (e.g., SO3(2-) in foliage, Al(3+) or Pb in tree rings), flux measurements provide more sensitive measures of air pollution effects. However, nutrient pools may be significantly affected by air pollution over long periods of time, and the importance of sample archiving as a means of detecting these long-term changes in nutrient pools (e.g., soils) cannot be overemphasized. Acid deposition and or foliar damage by ozone may cause increased foliar leaching, but the degree to which air pollution affects foliar leaching is very difficult to assess in the absence of control sites for comparison. Decomposition may also be altered by increased acid input, trace metal deposition, or gaseous pollution; but, once again, many of these potential changes are very difficult to evaluate for lack of control sites. Acid deposition nearly always influences soil leaching rates to some degree. In the case of SO4(2-), reasonable assumptions about background concentrations often allow an approximate estimate of the degree to which leaching is affected by sulfate deposition. For NO3(-), there is considerably less certainty about exactly what background levels should be. It is therefore more difficult to evaluate the degree to which current NO3(-) leaching rates are affected by atmospheric N deposition without a full analysis of the N cycle of the ecosystem in question. DOE

N89-11320# International Centre for Theoretical Physics, Trieste (Italy).

BASIC THEORY OF DESERTIFICATION

Ernest C. Njau Dec. 1987 18 p Submitted for publication
(DE88-703014; IC-87/413) Avail: NTIS (US Sales Only) HC A03/MF A01

A new theory is developed for explaining the processes that give rise to desertification. This theory is arrived at through analyses of possible influences of Earth's surface albedo modifications upon the general atmospheric circulation patterns with the aid of a recent theory of Sun-Climate/Weather links (Njau, 1985a; 1985b; 1986; 1987a; 1987b). It is shown that surface-albedo modification in a given region will not induce significant changes in the general atmospheric circulation patterns unless the region's size is at least equal to a certain minimum value. DOE

N89-11321# Scripps Institution of Oceanography, San Diego, Calif.

THE FLUX AND RECYCLING OF BIOACTIVE SUBSTANCES IN THE SURFACE SEDIMENTS OF THE DEEP BASINS OFF SOUTHERN CALIFORNIA Progress Report

R. A. Jahnke Jan. 1988 10 p
(Contract DE-FG05-85ER-60334)
(DE88-007999; DOE/ER-60334/T1) Avail: NTIS HC A02/MF A01

Goals of this project are to develop an understanding of the processes that recycling biogenic debris reaching the seafloor and to quantitatively determine the role of seafloor recycling in oceanic biogenic cycles. This includes evaluating the rate at which biogenic elements are released from the sediments due to organic matter decomposition as well as the rate at which certain biogenic elements are consumed in the sediments such as the consumption of O2 by oxic respiration and NO3(-) by denitrification. Benthic fluxes were estimated via the Bottom Lander. Results were combined with results from other West-coast researchers and a preliminary organic carbon budget for Santa Monica Basin was estimated. During the past year, benthic fluxes have been measured by a new in situ benthic chamber instrument and a shipboard incubation method. In addition, sediment cores were recovered from a wider region of the basin's seafloor. Pore waters were extracted from these cores and analyzed for biogenically important elements. Results permit a more accurate estimate of recycling at the seafloor of Santa Monica Basin to be made. Results are described. DOE

N89-11322# Argonne National Lab., Ill.

REVIEW OF ACID RAIN MODELS FOR EUROPE

D. G. Streets 1988 43 p Presented at the Task Force Meeting on Integrated Assessment Modeling Executive Body for the Convention on Long-range Transboundary Air Pollution, Laxenburg, Austria, 13 Apr. 1988
(Contract W-31-109-eng-38)
(DE88-011945; CONF-8804153-1) Avail: NTIS HC A03/MF A01

This report presents the results of a critical review of three European acid rain models: Rains, Bicram, and Acidrain. The Rains model is a PC-based simulation model that can evaluate the effects of acidic deposition on aquatic and terrestrial resources. Emissions and control technology information is sufficient to examine the effects of alternative control strategies. The Rains model could be used now to investigate the cost-effectiveness of alternative control measures in Europe and to give a rough estimate of reduced damage to aquatic and terrestrial resources. The Bicram model is a PC-based, noninteractive model that has similar emissions and cost capability to Rains. It treats ecological damage through an empirical scheme of regional sensitivity measures and critical deposition loadings. Bicram could be used alone to compare alternative control strategies, but is unable to make damage estimates. The somewhat more detailed emissions and control

cost modules of Bicram should be compared with those of Rains. The Acidrain model is a PC-based model designed as a decision aid for policy makers. Its strengths are its interactive, user-friendly software and its rigorous treatment of uncertainty using probability distributions. Before use by the Task Force, it would need to be refined geographically and adapted to the European, rather than U.K, context. DOE

N89-11323# Lamont-Doherty Geological Observatory, Palisades, N.Y.

RECENT CLIMATE CHANGE IN NORTH AMERICA AND CO2: SEARCH IN STRATIFIED DAILY DATA Progress Report, 30 Apr. 1987 - 15 Aug. 1988

George J. Kukla, Joyce E. Gavin, and Thomas R. Karl (National Climatic Center, Asheville, N. C.) Aug. 1988 16 p

(Contract DE-FG02-85ER-60372)

(DE88-014669; DOE/ER-60372/3) Avail: NTIS HC A03

The present report covers the results obtained from April 1987 through August 1988. Our objectives were to identify the CO2 fingerprint using stratified daily weather records, to characterize recent climate fluctuations in North America in terms of the changing frequency and distribution of various daily weather types, to determine empirical relationships of surface air temperature and various meteorological elements (humidity, cloud cover, wind, precipitation, etc.), and to compare these results with that produced by GCM's. DOE

N89-11324# Instituto de Pesquisas Espaciais, Sao Jose dos Campos (Brazil).

CIR AERIAL PHOTOGRAPHY APPLIED TO THE EVALUATION OF THE AIR POLLUTION IMPACT IN A TROPICAL FOREST: THE CASE OF CUBATAO, BRAZIL

Dalton deMorissonValeriano and Flavio Jorge Ponzoni Aug. 1988 11 p

(INPE-4651-PRE/1358) Avail: NTIS HC A03/MF A01

A 1:25,000 color infrared survey was used to map and evaluate the extent of the damage caused by air pollution originated from Cubatao city's industrial plant on the Tropical Forest covering the Serra do Mar mountain range in southeastern Brazilian coast. The survey covered an area of 240 sq km and encompasses a heavily damaged drainage basin and a preserved one. One primary forest and four secondary types were identified in the preserved area by means of their tonal and textural characteristics. Four types of damaged forest covers were discriminated in the polluted valley on the basis of the density and size of the remnant trees. DBH and tree height field measurements of these cover types reveal that the degradation process of the Tropical Forest takes place as a progressive elimination of the larger trees. Although the proliferation of smaller plants follows this process, the impact of the air pollution in the forest favors the occurrence of landslide in the rainy season. Author

N89-11325# Pacific Northwest Labs., Richland, Wash.

ACID PRECIPITATION IN NORTH AMERICA: 1985 ANNUAL AND SEASONAL DATA SUMMARIES FROM ACID DEPOSITION SYSTEM DATA BASE

J. K. Sweeney and A. R. Olsen Nov. 1987 451 p

(Contract DE-AC06-76RL-01830)

(DE88-013563; EPA/600/4-87-035) Avail: NTIS HC A20/MF A01

This report summarizes the 1985 wet deposition precipitation chemistry data collected in North America and available in the Acid Deposition System (ADS) data base. Interpretative statistical analyses are not a focus of this report; however, users of the report will learn about major wet deposition monitoring networks in North America, the extent of their geographic coverage, and general characteristics of wet deposition for 1985. An overview of each network is given. Annual and seasonal statistical summaries for 1985 are provided for pH, hydrogen ion (derived from pH), and the ion species sulfate, nitrate, ammonia, calcium, chloride, sodium, magnesium and potassium. DOE

N89-11326# Duke Univ., Durham, N. C. Dept. of Botany.

INTEGRATION OF KNOWLEDGE ON THE RESPONSE OF VEGETATION TO RISING CO2 Final Technical Report, 8 Aug. 1983 - 31 Mar. 1986

Boyd R. Strain 11 Feb. 1988 17 p

(Contract DE-AS05-83ER-60177)

(DE88-014740; DOE/ER-60177/1) Avail: NTIS HC A03/MF A01

The objective of this project was to review the literature and to publish reviews on the known effects of CO2 enhancement on plants and ecosystems. Assistance was given to Dr. Roger Dahlman, CO2 Project Director, as he prepared the research plan on vegetation response. Following one year of intensive dialog, Dr. Dahlman released the official DOE research plan and a published paper describing the need for the research. We planned, supervised and edited the production of one volume of the six volume State of the Art (SOA) Report released by DOE in December 1985. This monograph summarized relevant research and made recommendations for future needs in the area of plant response to global CO2 increase. It is the most comprehensive treatment to date of the subject. The project required a massive literature review. In 1986 we published a bibliography with abstracts and index. A separate project was accomplished by subcontract to Dr. James Reynolds, first at NC State University and finally at New Mexico State University. Dr. Reynolds conducted a developmental study on the preparation of a generic plant growth model. DOE

N89-11327# National Oceanic and Atmospheric Administration, Silver Spring, Md. Air Resources Lab.

NOAA (NATIONAL OCEANIC AND ATMOSPHERIC ADMINISTRATION) METEOROLOGY DIVISION SUPPORT TO THE ENVIRONMENTAL PROTECTION AGENCY Summary Report, fiscal year 1986

Herbert J. Viebrock, ed. and Evelyn M. Poole-Kober, ed. Feb. 1988 64 p

(PB88-213624; NOAA-TM-ERL-ARL-162) Avail: NTIS HC A04/MF A01 CSCL 13B

The Meteorology Div. provided meteorological research and operational support to the U.S. Environmental Protection Agency. Basic meteorological operational support consisted of the application of dispersion models, and the conduct of dispersion studies and model evaluations. The primary research effort was the development and evaluation of air quality simulation models using numerical and physical techniques supported by field studies. Highlights during FY 1986 included preliminary evaluation of a regional acid deposition model; conduct of a mesoscale acid deposition field study near Philadelphia, PA; completion of the RELMAP user's guide; conduct of terrain studies in the Fluid Modeling Facility; development of a new model for the autocorrelation function of wind components; completion of preparations for the integrated Air Cancer Program field study; and release of UNAMAP Version 6. Author

N89-11328*# Jet Propulsion Lab., California Inst. of Tech., Pasadena.

ENVIRONMENTAL PROJECTS. VOLUME 7: ENVIRONMENTAL RESOURCES DOCUMENT

Len Kushner and Glenn Kroll 15 Sep. 1988 107 p

(Contract NAS7-918)

(NASA-CR-182736; JPL-Publ-87-4-Vol-7; NAS 1.26:182736)

Avail: NTIS HC A06/MF A01 CSCL 13B

The Goldstone Deep Space Communications Complex (GDSCC) in Barstow, California, is part of the NASA Deep Space Network, one of the world's largest and most sensitive scientific telecommunications and radio navigation networks. Goldstone is managed, directed and operated by the Jet Propulsion Laboratory of Pasadena, California. The GDSCC includes five distinct operational sites: Echo, Venus, Mars, Apollo, and Mojave Base. Within each site is a Deep Space Station (DPS), consisting of a large dish antenna and its support facilities. As required by NASA directives concerning the implementation of the National Environmental Policy Act, each NASA field installation is to publish

an Environmental Resources Document describing the current environment at the installation, including any adverse effects that NASA operations may have on the local environment. Author

N89-11329# Instituto de Pesquisas Espaciais, Sao Jose dos Campos (Brazil).
OZONE HOLE OF THE ANTARCTICA: RECENT RESULTS [O BURACO DE OZONIO DA ANTARTICA: RESULTADOS RECENTES]
V. W. J. H. Kirchhoff May 1988 21 p In PORTUGESE Presented at the 1st Seminar on Atmospheric and Space Science of the Brazilian Antarctic Program, INPE, 27-29 Apr. 1988 Sponsored in part by the International Pact CIRM/INPE, Project 9623
(INPE-4518-PRE/1270) Avail: NTIS HC A03/MF A01

The destruction of ozone in the Antarctic region, observed in 1987, is the largest now registered in the last decade. Recent measurements indicate that at least the largest part of the destruction is caused by a chemical reaction of ozone with chlorine. The chlorine reacts catalytically, is not destroyed in the process; the same chlorine atom can destroy thousands of ozone molecules. The chlorine is introduced into the atmosphere in antropogenesis processes, making part of the artificial molecules very stable, the named chlorofluorocarbons, CFCs, which have a long lifetime, and may be transported to the stratosphere. The presence of ultraviolet radiation can liberate the chlorine molecule. Therefore the process of destruction of the ozone can start. Sounding ozone data shows that the total ozone content fell from 300 UD (Dobson units) to 175 UD, during August 13 to September 15, 1987, near Estacao Com. Ferraz. Measurements by the satellite indicate that the hole now dominates all the Antarctic continent. Author

N89-11330# Maryland Univ., College Park. Dept. of Meteorology.
DESIGN AND ANALYSIS OF LARGE-SCALE ATMOSPHERIC DISPERSION EXPERIMENT Annual Progress Report No. 2
Ferdinand Baer and Joshua Holland Jun. 1988 7 p
(Contract DE-FG05-86ER-60468)
(DE88-012911; DOE/ER-60468/2; SR-88-20) Avail: NTIS HC A02/MF A01

The goals of this research are to aid in the design of future large-scale ground-level atmospheric tracer/sampling experiments of the CAPTEX (Cross-Appalachian Tracer Experiment)/ANATEX (Across North America Tracer Experiment) type, to develop probabilistic models of tracer plume concentration/dosage distributions and to use these models to assess the effects of sampling grid design parameters on errors of estimation of experimental tracer plume distribution parameters. DOE

N89-11331# Instituto de Pesquisas Espaciais, Sao Jose dos Campos (Brazil).
CARBON MONOXIDE MEASUREMENTS IN DIFFERENT BRAZILIAN ECOSYSTEMS
E. V. A. Marinho and V. W. J. H. Kirchhoff Aug. 1988 27 p In PORTUGUESE; ENGLISH summary Presented at the 2nd Regional Meeting on Geophysics, Salvador, Brazil, 25-27 Nov. 1987
(Contract FINEP-537/CT)
(INPE-4668-PRE/1368) Avail: NTIS HC A03/MF A01

Carbon monoxide (CO) measurements have been made in Sao Jose dos Campos, an industrial center, and Cachoeira Paulista, both cities in the Vale do Paraiba, at the Dutra Road, in the Horto Florestal of Campos do Joedao (mountain region about 1700 m altitude), in Massaguacu (Coastal Paulista region), Belem and Manaus (equatorial region), and more recently in Natal (northeastern coast) and Cuiaba (central plateau). The purpose of these analyses is to study the behavior of that element in different climatic and regional conditions, polluted and natural environments. In the complex chemistry of the atmosphere, CO is important for being directly related to the ozone chemistry, the hydroxyl radical and methane, among other gases. It has been observed that even remote regions have suffered severe occasional episodes of pollution that can be (and have been) qualitatively identified in the majority of cases. A new phase of ecologic studies is being initiated with quantitative determination of certain gases and a comparison among the various natural ecosystems. The first analyses show that in polluted environments the CO concentrations are three to ten times larger than the concentrations in nonpolluted natural environments. Author

N89-11332# Air Force Inst. of Tech., Wright-Patterson AFB, Ohio.
THE IMPACT OF AN INCREASE IN ATMOSPHERIC METHANE ON THE TEMPERATURE FIELD AND SUBSEQUENT CLIMATIC EFFECTS M.S. Thesis
Jeffrey S. Morrison 1988 65 p
(AD-A196869; AFIT/CI/NR-88-18) Avail: NTIS HC A04/MF A01 CSCL 07C

In this thesis, the direct radiative effects on the temperature field due to the doubling of atmospheric methane are presented, within the context of a globally representative reference atmosphere, and climatic consequences are inferred. Based on the theory of infrared radiative transfer in a plane-parallel atmosphere, this simulation computed the vertical distribution of the change in longwave radiative heating rates that occurs as a result of doubling atmospheric methane. The interaction of methane with other atmospheric constituents which are optically active within the spectral boundaries of the absorption band for CH4 was considered in the analysis of the results. The radiative interaction between water vapor and increased methane was shown to be the dominant reason for a positive change in heating rates in the lower troposphere when methane is doubled. GRA

46 GEOPHYSICS

Includes aeronomy; upper and lower atmosphere studies; ionospheric and magnetospheric physics; and geomagnetism.

For space radiation see *93 Space Radiation.*

N89-11333 York Univ. (England).
A GLOBAL MHD PULSATION EVENT WITH CONJUGATE STUDY AND MODEL OF IONOSPHERIC DAMPING Ph.D. Thesis
Stephen John Davison 1987 238 p
Avail: Univ. Microfilms Order No. BRDX81135

Geomagnetic pulsations are oscillations of the earth's magnetic field which occur in the ultra low frequency (ULF) range. The modes of vibration are found to be directly influenced by the ionospheric boundary conditions at the feet of the oscillating field lines. During equinoctial periods, symmetric conditions are expected at mid to low latitudes. However, at higher latitudes, especially during the solstices, there is the possibility that a single flux tube would experience significantly different boundary conditions. In this thesis an analysis of conjugate data from St. Anthony in Newfoundland and Halley Bay in Antarctica from the 1982 June/July campaign is undertaken. At that time, Halley Bay, which is geographically a high latitude station, was in 24 hours of darkness while St. Anthony underwent a normal diurnal variation in sunlight. A pulsation event is discussed in which it is postulated that these effects are evident. This event is also discussed in terms of its global nature, with reference to reconnection as a possible mode of excitation. Dissert. Abstr.

N89-11334 Virginia Polytechnic Inst. and State Univ., Blacksburg.
VELOCITY AND Q FROM REFLECTION SEISMIC DATA Ph.D. Thesis
Berkan Galip Ecevitoglu 1987 166 p
Avail: Univ. Microfilms Order No. DA8802723

This study has resulted in the discovery of an exact method for the theoretical formulation of the effects of intrinsic damping where the attenuation coefficient, alpha(nu), is an arbitrary function of the frequency nu. Absorption-dispersion pairs are computed using numerical Hilbert transformations; approximate analytical

expressions that require the selection of arbitrary constants and cutoff frequencies are no longer necessary. The inverse problem is also investigated using singular value decomposition (SVD). The sparse matrices encountered in the acquisition of conventional reflection seismology data result in a system of linear equations of the form AX = B, with A the design matrix, X the solution vector, and B the data vector. A technique to improve the sparsity pattern prior to decomposition is described. From an application of the Q = 2 delta tau/pi delta W equation using reference reflections from shallower reflectors, crystalline rocks in South Carolina over the depth interval from about 5 to 10 km yield values of Q in the range Q = 250 to 300. Nonstandard recording geometries and vibroseis recording procedures are suggested to minimize matrix sparseness and increase the useable frequency bandwidth between zero and Nyquist. The direct detection of body wave dispersion by conventional vibroseis techniques may be useful to distinguish between those crustal volumes that are potentially seismogenic and those that are not. Such differences may be due to variations in fracture density and therefore water content in the crust. Dissert. Abstr.

N89-11335# Tokyo Univ. (Japan). Inst. of Space and Astronautical Science.
THE GEOGRAPHICAL DISTRIBUTIONS OF ELECTRONS (0.05-3.2 MeV) AND PROTONS (0.58-35 MeV) AT ALTITUDES OF 350-850 km
K. Nagata, H. Kondo, T. Kohno, H. Murakami, A. Nakamoto, N. Hasebe, J. Kikuchi, and T. Doke (Waseda Univ., Tokyo, Japan) Jan. 1987 22 p
(ISAS-RN-358) Avail: NTIS HC A03/MF A01

The geographical distributions of high energy electrons and protons are shown. OHZORA satellite data, which were acquired with two delta E x E silicon detector telescopes, are used to show particle distributions for altitude intervals of 350 to 500 km, 500 to 600 km, 600 to 700 km, and 700 to 850 km during the period from February 1984 to February 1985. Three energy and particle groups are illustrated: (1) electrons (0.05 to 0.19 MeV) and protons (0.58 to 3.3 MeV), (2) electrons (0.19 to 3.2 MeV), and (3) protons (0.64 to 35 MeV). Special high flux regions are mapped in the South Atlantic magnetic anomaly and in the auroral zones. The low-latitude particle precipitation zones are not identified during quiet time geomagnetic conditions. Author

N89-11336# Los Alamos National Lab., N. Mex.
DEVELOPMENT AND TESTING OF KITES
Tim Murphy Jul. 1988 44 p
(Contract W-7405-eng-36)
(DE88-015057; LA-11329-MS) Avail: NTIS HC A03/MF A01

KITES is a first-principles kinetic theory computer code for modeling the behavior of atmospheric electrons in the presence of strong, short-duration, fast-risetime or high-frequency electromagnetic fields. In this report we describe the development and testing of this code, including a complete description of the kinetic theory model used, the model's range of validity, and the numerical methods used to solve the resulting equations. The model uses only experimentally measured cross sections as input and contains no free parameters. To check the validity of the model, the results of KITES calculations are compared with an analytic model and experimentally measured steady-state electron transport parameters and excellent agreement is found. DOE

N89-11337 Wisconsin Univ., Madison.
A THEORETICAL INVESTIGATION OF THE COLLECTION OF AEROSOL PARTICLES BY FALLING ICE CRYSTALS Ph.D. Thesis
Norman Leslie Miller 1987 235 p
Avail: Univ. Microfilms Order No. DA8800371

A numerical scheme which determines the collection efficiences, kernels and washout rates of aerosol particle (APs) by falling columnar and platelike ice crystals is presented. A theoretical model for the removal of micro-size APs by falling columnar ice which incorporates gravitational, inertial, thermophoretic, diffusiophoretic and electrostatic forcing was formulated. This trajectory model which includes computed velocity, temperature and water vapor density fields, was coupled to a flux model which determines the removal of submicron particles due to Brownian diffusion, thermo and diffusio-phoresis as well as electrostatic forcing. This combined model indicates collection efficiences for APs of radii 0.001 to 10.0 microns for the columnar ice crystal size distribution. An earlier study provides AP collection efficiencies by ice crystal plates for the ice crystal plate size distribution. Dissert. Abstr.

N89-11338 Case Western Reserve Univ., Cleveland, Ohio.
INVESTIGATION OF IONOSPHERIC D REGION AERONOMY USING INCOHERENT SCATTER RADAR AND OPTICAL MEASUREMENTS Ph.D. Thesis
Wen-Ping Ying 1987 308 p
Avail: Univ. Microfilms Order No. DA8802484

The results of complementary radar and optical observations of the lower ionosphere are presented. These studies were accomplished using 430 MHz incoherent scatter radar, tilting filter photometers and 1 m Ebert-Fastie spectrometer. The incoherent scatter radar consists of two operational modes, the total power and ion line power spectrum measurements. When combined together, atmospheric and ionospheric parameters are accessible to varying degrees, as functions of time and height. These include electron concentration, ion neutral collision frequency, neutral atmosphere temperature, pressure and wind, and mean negative and positive ion masses and concentrations. This is made possible by techniques based on the concept of mapping between experimental and theoretical power spectra, combined with electron concentration information from total power measurement, to extract the underlying aeronomical parameters. Dissert. Abstr.

N89-11339 Stanford Univ., Calif.
VELOCITY ANALYSIS BY ITERATIVE PROFILE MIGRATION Ph.D. Thesis
Kamal Mansour Al-Yahya 1987 86 p
Avail: Univ. Microfilms Order No. DA8800895

In conventional seismic processing, the normal movement (NMO) equation is used for velocity analysis. The NMO equation is based on the assumption of flat, horizontal reflectors, so the NMO analysis gives erroneous velocities when the subsurface does not consist of flat and horizontal layers. Imaging by migration is done in a subsequent step using these velocities. Velocity analysis and imaging are combined in one step, since they are complementary processes in the first place. Velocity analysis gives low-wavenumber information about the subsurface while migration gives the high-wavenumber information (the reflectivity). In this scheme, migration itself is used as a velocity indicator. Several schemes can be developed to do velocity analysis using migration. The data is migrated with an initial velocity model and then the velocity error estimated. The initial velocity model is updated next, then the process is repeated until convergence is achieved. The principle that after migration with the correct velocity model, an image in a common-receiver gather (CRG) is aligned horizontally regardless of structure. The deviation from horizontal alignment is therefore a measure of the error in velocity. In relating the curvature to the error in velocity, kinematic arguments which approximate the error estimation are used. The iterative method is applied to a field data set and to a synthetic data set. Dissert. Abstr.

N89-11340# Montana Coll. of Mineral Science and Technology, Butte.
THREE DIMENSIONAL GRAVITY MODELING TECHNIQUES WITH APPLICATION TO THE ENNIS GEOTHERMAL AREA, PART 1 Ph.D. Thesis. Final Report
Dave Semmens Dec. 1987 183 p
(Contract DE-FG07-84ID-12525)
(DE88-014952; DOE/ID-12525/1-Pt-1) Avail: NTIS HC A09/MF A01

Three dimensional gravity modeling was done in the area of the Ennis hot spring in an attempt to determine controlling structure of the Ennis hot spring. The modeling was done in a two-step process where: (1) The topography was modeled by modeling the valley fill from the highest elevation in the modeling area to some

elevation below the lowest station elevation using Talwani and Ewing's (1960) method of modeling with vertically-stacked, horizontal, n-sided polygons. Once the gravity contributions of the valley fill included in this topographic model are calculated, they were removed from the original gravity data; (2) The remaining valley fill was modeled using blocks where the 3-D algorithm for modeling with blocks results from integrating the gravity formula in the X and Z directions and approximating the integration in the Y-direction using a quadrature formula. Finally, an inverse 3-D gravity modeling program was written to automatically adjust the bedrock topography output from this two-step modeling process. The gravity data calculated from the adjusted bedrock topography, output from the inverse modeling program, should match the observed gravity data within the error of the survey. DOE

N89-11341 Ohio State Univ., Columbus.
CONVECTIVE SCALE SELECTION AND THE INITIATION OF DEEP CUMULUS Ph.D. Thesis
Venkatramani Balaji 1987 155 p
Avail: Univ. Microfilms Order No. DA8804011

Studies show that the organized lifting of moist low-level air at horizontal scales on the order of tens of kilometers is closely associated with the formation of severe storms. In the absence of large-scale forcing, the organized lifting at the required scale must be produced by local convection. The linear theory of convection in an isolated boundary layer fails to provide the required scales. The studies of Clark et al. (1986) show that a possible explanation may be found in the excitation of gravity waves in the stable tropospheric layer by boundary layer convection in the presence of vertical wind shear. In the present study, it is shown that the reorganization of the planetary boundary layer subsequent to the development of the deep gravity wave mode leads to the selection of scales appropriate to deep convection. Comparisons between models of convection in the linearized and the full dynamical equations suggest that while the onset of the deep mode may be a linear effect, its enhancement and the subsequent suppression of the shallow boundary layer mode may be significantly modulated by non-linear effects. Several results regarding cloud formation are inferred. The directional shear in the boundary layer appears to a sensitive parameter in selecting spatial organizations of a cloud field. The growth of clouds appears to decouple the boundary layer modes in phase from the stable layer modes, an effect that cyclically enhances and suppresses cloud growth. Finally, the interaction of a moving storm system in its severe stage with the boundary layer modes appear to provide and explanation for the spatial and temporal distribution of new convective cells in a multicellular storm system. Dissert. Abstr.

N89-11342# Los Alamos National Lab., N. Mex.
STUDY OF A SUBSTORM ON MAY 4, 1986
E. W. Hones, J. D. Craven, L. A. Frank, A. B. Galvin, J. S. Murphree, R. D. Elphinstone, and R. C. Elphic (California Univ., Los Angeles.) 1988 16 p Presented at the 27th Plenary Meeting of COSPAR, Espoo, Finland, 18 Jul. 1988
(Contract W-7405-eng-36)
(DE88-014318; LA-UR-88-2222; CONF-880780-1) Avail: NTIS HC A03/MF A01

A substorm on May 4, 1986, midway through the PROMIS campaign of coordinated data acquisition, was uniquely well documented. Both in its aspects at earth and in its magnetotail aspects. The expansive phase onset was imaged by the Viking satellite at 20-second time resolution. Most of the expansive phase was also imaged by DE 1 at 6-minute time resolution. ISEE 1 and 2 were near the tail's axis 18.5 R sub e from earth operating at high data rate and data were recorded by several geosynchronous satellites. This multi-satellite study provides evidence that the active substorm aurora occurs at the feet of field lines that map to a magnetic X-line in the near tail. The longitudinal extension of the aurora during a substorm is associated with cross-rail lengthening of the near-earth neutral line. The concept of the poleward leap of the auroral electrojet (and the auroras) as the culminating feature of the expansive phase finds further support in these data. DOE

N89-11343 Ohio State Univ., Columbus.
ROTATING AND STRATIFIED FLUIDS Ph.D. Thesis
Kiran Babu Chilakamarri 1987 176 p
Avail: Univ. Microfilms Order No. DA8804021

The rotating and linearly and stably stratified fluid flows are considered, in which Coriolis force dominates both the inertial and viscous forces and stratification effects dominate the rotational effects. These flows are important; they occur in the atmosphere and in oceans. Fluid is assumed to be confined between two horizontal parallel planes with obstacles that are not too small fixed to the bottom plane. Both the planes, the obstacle and the fluid rotate with the same angular velocity, the angular velocity vector aligned with the common normal to the planes. Fluid is in uniform motion upstream far from the obstacle. A right circular cylinder, a vertical flat plate parallel to the uniform flow and a body of revolution are considered for objects in the flow, with stratification not too small. The method of matched asymptotic expansions is used throughout. A model for weakly stratified fluid flows over long ridges in a rectangular rotating channel is developed and complete analytic solution of the geostrophic flow is presented. The results of the model compare very well with the experimental observations of the other workers. The fluid turns to the left on the upwind side of the ridge and turns to the right on the leeside of the ridge and the turn is asymmetric (windside vs leeside). A condition for the existence of an eddy in the channel for inviscid flow is discussed. Dissert. Abstr.

N89-11344 Washington Univ., Seattle.
A NONLINEAR WAVE-WAVE INTERACTION THEORY FOR THE GENERATION OF MULTI-SCALE LARGE EDDIES IN A NEUTRAL ATMOSPHERIC BOUNDARY LAYER Ph.D. Thesis
Pierre Doumitt Mourad, III 1987 203 p
Avail: Univ. Microfilms Order No. DA8802306

A re-examination of the current literature shows that there exists at least three classes of two dimensional large eddy states in weakly stratified atmospheric boundary layers. Two of these states contain multiscale large eddies, with horizontal scales on the order of the boundary layer depth, as well as several times this depth. The theory discussed attempts to explain this structure as the result of wave-wave interactions between growing disturbances to a model mean flow, a neutrally stratified Ekman layer. Nonlinear, coupled equations are derived which give the temporal evolution of a set of three isolated disturbances in a general unstable flow. The equations model large eddy/large eddy and large eddy/mean flow interactions. A general theorem shows that the linearly fastest growing disturbances act as a catalyst for the acceleration of the growth of initially slowly growing, or decaying disturbances. In essence, the fastest growing disturbances become unstable as they grow. Dissert. Abstr.

N89-11345# Argonne National Lab., Ill. Biological, Environmental and Medical Research Div.
PARAMETERIZATIONS OF MICROPHYSICAL PROCESSES IN CLOUDS FOR APPLICATION IN MODELS OF REGIONAL ATMOSPHERIC DEPOSITION
In Young Lee 1988 16 p Presented at the International Cloud Physics Conference, Bad Hamburg, Fed. Republic of Germany, 15 Aug. 1988
(Contract W-31-109-eng-39)
(DE88-010017; CONF-880857-1) Avail: NTIS HC A03/MF A01

This report reviews cloud physics parameterizations to examine the theoretical basis and evaluate the applicability to regional models, and to obtain more efficient, improved parameterizations by optimization upon results of a detailed cloud model that incorporates treatments of microphysical processes and cloud dynamics too detailed for routine use in a regional model. DOE

N89-11346# Lawrence Livermore National Lab., Calif. Physics Dept.
ATMOSPHERIC AND GEOPHYSICAL SCIENCES DIVISION Program Report, FY87
May 1988 84 p

(Contract W-7405-eng-48)
(DE88-013780; UCRL-51444-87) Avail: NTIS HC A05/MF A01

In 1988 the Atmospheric and Geophysical Sciences Division began its 15th year as a division. As the Division has grown over the years, its modeling capabilities have expanded to include a broad range of time and space scales ranging from hours to years, and from kilometers to global, respectively. For this report, we have chosen to show a subset of results from several projects to illustrate the breadth, depth, and diversity of the modeling activities that are a major part of the Division's research, development, and application efforts. In addition, the recent reorganization of the Division, including the merger of another group with the Division, is described, and the budget, personnel, models, and publications are reviewed. DOE

N89-11347 Oxford Univ. (England).
TROPOSPHERIC SOUNDING FROM THE TIROS-N SERIES OF SATELLITES Ph.D. Thesis
P. E. Lloyd 1987 145 p
Avail: Univ. Microfilms Order No. BRD-81499

Methods are investigated for using AVHRR (Advanced Very High Resolution Radiometer) data in conjunction with TOVS (TIROS Operational Vertical Sounder) in order to develop a scheme to detect and account for the presence of cloud. TOVS includes the HIRS (High Resolution Infrared Radiation Sounder) and the MSU (Microwave Sounding Unit). To begin with, the AVHRR and HIRS data were collected and their relative calibration studied. The AVHRR data are of much higher resolution than either the HIRS or MSU data and therefore can give much information on the cloud structure within a HIRS field of view. A scheme employing both TOVS and AVHRR data has been developed and is described. Several case studies are presented and their results examined. The performance of the scheme used by the U.K. Meteorological Office for the same purpose but which uses only TOVS data is discussed and the relative performance of the two schemes investigated. The results are encouraging and demonstrate the advantages of using the high resolution AVHRR data together with the TOVS data. Dissert. Abstr.

N89-11348 Kentucky Univ., Lexington.
A NEW DETERMINATION OF EXTINCTION DUE TO ATMOSPHERIC AEROSOLS AND THE RESULTING IMPLICATIONS FOR UPPER STRATOSPHERIC OZONE DEPLETION Ph.D. Thesis
James Ora Manning 1987 307 p
Avail: Univ. Microfilms Order No. DA8806553

A question in the statistical analysis of the vertical distribution of atmospheric ozone centers on the aerosol corrections to these data. To resolve measurement weaknesses, atmospheric extinction coefficients were compiled, standardized, and analyzed. These extinction coefficients provided a means of extracting the extinction and transmission due specifically to atmospheric aerosols. These aerosol transmissions were analyzed for trends, and the wavelength dependence of the aerosol extinction coefficients was characterized to provide the necessary input for corrections to the measurements of atmospheric ozone. Three primary weaknesses of the aerosol corrections to the ozone measurements were addressed. The spatial, temporal, and wavelength dependencies of the atmospheric aerosol transmission which were found, resulted in significant changes in the trend estimates for ozone. In particular, the trend estimates for depletion of upper stratospheric ozone were reduced from 0.08 to 0.05 percent per year for the 1970 to 1980 decade. These new data suggest that the original trend estimates were probably influenced by long term and possible cyclic trends of aerosol transmission. Dissert. Abstr.

N89-11349 Stanford Univ., Calif.
CRUSTAL STRUCTURE OF THE NORTHWESTERN UNITED STATES Ph.D. Thesis
Rufus Douglas Catchings 1987 194 p
Avail: Univ. Microfilms Order No. DA8800911

The region of the northwestern United States between the Rocky Mountains and the Cascade Range, which is about 1000 km in length and is between 400 and 700 km in width was examined. The western edge of the study area occupies a position approximately 250 km east of the subduction zone between the Juan De Fuca and North American lithospheric plate and is immediately east of the active Cascade Range volcanic arc. Four of the first detailed investigations of the crustal structure of the area north of Nevada and west of the Snake River Plain are represented. One of the most important contributions may be that crustal models now exist for the region as a whole which are based on seismic measurement within the region. These crustal models are in agreement with the regional geology and extensional tectonics of the back-arc setting. These data provide an opportunity to examine the deep crustal structure in extensional terranes and provide insights into the processes associated with continental extension and growth. Some of the surprising facts include the discovery of a subvolcanic continental rift between the Columbia Plateau, possibly a second continental rift within northwestern Nevada, and the observation that although the crust has greatly extended beneath much of this area, it remains nearly 40 km thick throughout the area. Dissert. Abstr.

N89-11350# Los Alamos National Lab., N. Mex.
ASSOCIATION OF PLASMA SHEET VARIATIONS WITH AURORAL CHANGES DURING SUBSTORMS
E. W. Hones, Jr., J. D. Craven, L. A. Frank, and G. K. Parks 1988 13 p Presented at the 27th Plenary Meeting of COSPAR, Espoo, Finland, 18 Jul. 1988
(Contract W-7405-eng-36)
(DE88-014319; LA-UR-88-2223; CONF-880780-2) Avail: NTIS HC A03/MF A01

Images of the southern auroral oval taken by the University of Iowa auroral imaging instrumentation on the Dynamics Explorer 1 satellite during an isolated substorm are correlated with plasma measurements made concurrently by the ISEE 1 satellite in the magnetotail. Qualitative magnetic field configuration changes necessary to relate the plasma sheet boundary location to the latitude of the auroras are discussed. Evidence is presented that the longitudinal advances of the auroras after expansive phase onset are mappings of a neutral line lengthening across the near-tail. We observe a rapid poleward auroral surge, occurring about 1 hour after expansive phase onset, to coincide with the peak of the AL index and argue that the total set of observations at that time is consistent with the picture of a poleward leap of the electrojet, marking the beginning of the substorm's recovery. DOE

N89-11351# Instituto de Pesquisas Espaciais, Sao Jose dos Campos (Brazil).
ALGORITHM FOR THE STUDY OF PARTICLE MOVEMENT IN THE INNER MAGNETOSPHERE OF THE EARTH [ALGORITMO PARA O ESTUDO DO MOVIMENTO DE PARTICULAS NA MAGNETOSFERA INTERNA DA TERRA]
O. Mendes, Jr. and O. Pinto, Jr. Aug. 1988 20 p In PORTUGUESE; ENGLISH summary Presented at the 2nd Regional Meeting of Geophysics, Salvador, Brazil, 25-27 November 1987
(Contract FINEP-537/CT)
(INPE-4669-PRE/1369) Avail: NTIS HC A03/MF A01

In the general study of the dynamics of electrically charged particles inside the Earth's inner magnetosphere, it is necessary to determine the trajectories of particles subjected to different electric and magnetic field models. When these fields are not static, and cannot be described in a simple form by scalar potentials, the determination of the trajectories involves a numerical integration of the guiding center-drift velocity equation. This work describes an algorithm for the determination of the trajectories of electrically charged particles inside the inner magnetosphere. The trajectories are obtained by using the guiding center drift-velocity equation, considering an arbitrary pitch angle, and the two first adiabatic invariants of the movement. The parameters involved in these equations as well as their several numerical approaches are described in detail. Such an algorithm can be used in numerical

studies related to the dynamics of the particles inside the inner magnetosphere. Author

N89-11352# Instituto de Pesquisas Espaciais, Sao Jose dos Campos (Brazil).
DEVELOPMENT OF A SEMI-EMPIRICAL MODEL FOR ESTIMATING THE GLOBAL SOLAR RADIATION M.S. Thesis [DESENVOLVIMENTO DE UM MODELO SEMI-EMPIRICO PARA ESTIMATIVA DA RADIACAO SOLAR GLOBAL]
Paulo Roberto PelufoFoster Jul. 1988 107 p In PORTUGUESE; ENGLISH summary
(INPE-4620-TDL/328) Avail: NTIS HC A06/MF A01

The large amount of energy which is continuously received from the sun has led more recently to increased efforts toward a better knowledge of its disposition to satisfy world wide energy demands. There is no unique solution for solar energy utilization, since the local requirements depend on climatological archievements and local availability of materials and technicians. For solving present and future problems strong efforts have to be initiated in collecting and estimating data for availability of solar radiation with high local and temporal resolution. Since the implementation of the Brazilian network of meteorological observing stations the sunshine duration was recorded, by the Campbell-Stokes recorder. The characteristics were analyzed for the 12 different cards, concerning: color, dimension, time of burning and overburning as well as the value of the minimum radiation flux necessary to start burning. At the same time the present study aims at providing a semi-empirical model for the estimation of daily global solar radiation and the components of direct and diffuse radiation. In the model methods of parameterization such as Rayleigh and Mie scattering, absorption due to water vapor, CO2, O3, and oxygen were used. The entries in the model were the meteorological variables observed in the met-station at the surface: atmospheric pressure, air temperature, air moisture, cloud types, and cloudiness. The model was tested for seven places and showed a relative error smaller than the one fiven by the pyranometer (5 percent). Author

N89-11353# Naval Postgraduate School, Monterey, Calif.
STUDIES OF BAROTROPIC FLOW OVER TOPOGRAPHY USING A GALERKIN FINITE ELEMENT MODEL M.S. Thesis
Thomas I. Petoliagis Mar. 1988 200 p
(AD-A196516) Avail: NTIS HC A09/MF A01 CSCL 04B

A finite element shallow-water model is tested with two types of surface topography. The model uses rectangular subdivisions in a vorticity-divergence formulation, and a semi-implicit time discretization. In the first experiment an east-west ridge or valley is placed in a channel with east-west periodic conditions. Linear quasi-geostrophic solutions are derived with the rigid lid assumption. The Rossby waves are successfully simulated in the model with linear solutions as the initial conditions. The model phase speeds are very close to the analytic values when the latter are properly corrected. In the second experiment a ridge is placed across the channel and the Coriolis parameter is set to zero. The initial conditions consist of a uniform flow through the channel and constant free-surface height. The numerical simulations agree with hydraulic jump theory. In the jump cases the model predicts increasing wind speeds and decreasing free surface heights. Higher spatial resolution would be required to properly simulate the details of the hydraulic jump formation. GRA

N89-11354# Air Force Inst. of Tech., Wright-Patterson AFB, Ohio.
A TIME-DEPENDENT MODEL FOR THE LOW-LATITUDE IONOSPHERE M.S. Thesis
Gary D. Wells 1988 112 p
(AD-A196683; AFIT/CI/NR-88-24) Avail: NTIS HC A06/MF A01 CSCL 04A

The theoretical development of a time-dependent, self-consistent model of the low-altitude ionosphere (200 to 3000 km) is presented. This model solves the coupled continuity-momentum and energy equations for an ionosphere composed of two ion species (O+ and H+) and electrons in a quasi-simultaneous manner. Account is taken of effects due to the curvature of the field lines and the inclination of the field line to the vertical. This model allows for electrodynamic plasma drift during the day, effects due to the expansion and contraction of the neutral atmosphere, and ion-neutral drag effects, as well as the transfer of momentum through collisions, conduction parallel to B, frictional heating/cooling due to the relative motion between the ions and the neutrals, and effects due to adiabatic expansion and contraction. Modelling capabilities are improved by including more realistic neutral winds and electric fields. The offset in the geographic and geomagnetic poles is allowed for by mapping the neutral winds and time (both organized in the geographic coordinate system) into the magnetic reference frame. Results from this model are shown to reproduce the important physical processes unique to the low-altitude ionosphere, such as the depletion of plasma at the magnetic equator due to electrodynamic drifts and diffusion, and the seasonal anomaly. GRA

N89-11254# National Research Inst., Bankura (India).
THE EFFECTS OF SEISMIC WAVES, PART 2
Sasadhar De *In* Vibration Inst., The Shock and Vibration Digest, Volume 20, No. 10 Oct. 1988 p 9-26 (For primary document see N89-11252 02-39)
Avail: NTIS HC A05/MF A01

N89-11268# National Research Inst., Bankura (India).
THE EFFECTS OF SEISMIC WAVES: PART 1
Sasadhar De *In* Vibration Inst., The Shock and Vibration Digest, Volume 20, No. 9 Sep. 1988 p 8-18 (For primary document see N89-11266 02-39)
Avail: NTIS HC A04/MF A01

47 METEOROLOGY AND CLIMATOLOGY

Includes weather forecasting and modification.

N89-11355# National Center for Atmospheric Research, Boulder, Colo.
NATIONAL CENTER FOR ATMOSPHERIC RESEARCH Annual Report, fiscal year 1987
May 1988 62 p
(Grant NSF ATM-87-09659)
(PB88-220009; NCAR/AR-87) Avail: NTIS HC A04/MF A01 CSCL 04B

The report describes ongoing research activities and the most significant recent achievements of the National Center for Atmospheric Research, which is operated by the 54-member organization, the University Corporation for Atmospheric Research, under the sponsorship of the National Science Foundation. A section of directories lists the scientific and technical staff, organizational structure, financial statements, visitors and publications. GRA

N89-11356# Federal Aviation Agency, Atlantic City, N.J.
EVALUATION OF ENHANCEMENTS TO THE LOW LEVEL WIND SHEAR ALERT SYSTEM (LLWAS) AT STAPLETON INTERNATIONAL AIRPORT Final Report, Jul. 1987 - Mar. 1988
John D. Barab, Richard D. Page, Bruce L. Rosenburg, Thomas E. Zurinskas, and Glenn R. Smythe (Data Transformation Corp., Silver Spring, Md.) Aug. 1988 164 p
(Contract T12-02Z)
(DOT/FAA/PS-88/14; DOT/FAA/CT-88/6) Avail: NTIS HC A08/MF A01

An operational test and evaluation of enhancements to the 11-station Low Level Wind Shear Alert System (LLWAS) at Stapleton International Airport, Denver, Colorado was conducted during the period August 3 to September 4, 1988. Enhancements included a 12th remote station for gathering wind data, a more sophisticated wind shear microburst detection (WSMD) algorithm, a Digital Equipment Corporation (DEC) PDP 11-73 computer, a DEC VT-240 Cathode Ray Tube (CRT) Display, and an LLWAS message display format, the latter two for local controller use in

the air traffic control (ATC) tower cab. Two sets of objectives were associated with this LLWAS evaluation: meteorological and human factors objectives. The methodology and dual scientific analyses performed were discussed, and detailed results with conclusions and recommendations were provided. Based on the conclusions, it was recommended that the WSMD algorithm remain as an operational constituent of the Denver LLWAS and that human factors considerations be further explored in improving the controller LLWAS interface. Author

N89-11357 Purdue Univ., West Lafayette, Ind.
AN INVESTIGATION OF THE INTERNAL STRUCTURE OF THE THUNDERSTORM OUTFLOW WITH PARTICULAR ATTENTION TO MULTIPLE SURGES Ph.D. Thesis
Diana Lynn Klingle 1987 295 p
Avail: Univ. Microfilms Order No. DA8807629

Thunderstorm outflows and gust fronts have been the focus of much recent research. The motivation was to investigate the role of the gust front in maintaining the parent storm or to identify gust front signatures in Doppler radar data for use in automatic detection algorithms. The features within the outflow known as multiple surges are examined. Concise definitions of multiple and secondary surges are formulated. Data from previously published outflow cases are compiled and some simple statistics are applied in an attempt to characterize multiple surges. Proposed causative mechanisms of multiple surges are also discussed. Three case studies are presented to investigate the causes of multiple surges. The first case study deals with a pulsating downdraft. The second case considers undulations along the top of the outflow boundary and a conceptual model is developed. The growth and dissipation of many cells within a single thunderstorm and the manner in which multiple surges are produced by this mechanism are examined in the third case. It is clearly shown that a variety of mechanisms can produce multiple surges. Some mechanisms are related to the parent storm and some are related to processes such as turbulent mixing. Dissert. Abstr.

N89-11358 Washington Univ., Seattle.
A NUMERICAL MODELING STUDY OF FRONTOGENESIS AND COLD FRONTAL RAINBANDS Ph.D. Thesis
David J. Knight 1987 161 p
Avail: Univ. Microfilms Order No. DA880227

A two dimensional, hydrostatic, primitive equation model is used to investigate the dynamics of frontogenesis in a moist atmosphere. The model includes planetary boundary layer physics and uses an explicit scheme for the prediction of water vapor, cloud water and rain water. The model is initialized with the semi-geostrophic solution to the Eady problem. The initial vertical stability is chosen so that upright convection does not occur. A cold front is forced by shear deformation associated with the nonlinear evolution of the Eady wave. Simulations are performed with 5, 10, 40, and 80 km horizontal resolution and 14 levels in the vertical (4 in the boundary layer). Compared to the dry case, the inclusion of moisture in the model produces a stronger low level jet ahead of the front, a stronger upper level jet, stronger temperature gradients at mid levels, increased vorticity at the front, a stronger ageostrophic circulation across the front and a more concentrated updraft just ahead of the surface front. The first rainband that appears in the numerical simulation forms and intensifies in a region of negative equivalent potential vorticity. Dissert. Abstr.

N89-11359*# Michigan Technological Univ., Houghton. Dept. of Mechanical Engineering.
STRUCTURE OF WIND-SHEAR TURBULENCE
G. Trevino and T. R. Laituri [1988] 29 p Presented at the 26th Aerospace Sciences Meeting, Reno, Nev., Jan. 1988
(Grant NAG1-717)
(NASA-CR-183257; NAS 1.26:183257; AIAA-88-0581) Avail: NTIS HC A03/MF A01 CSCL 04B

The statistical characteristics of wind-shear turbulence are modelled. Isotropic turbulence serves as the basis of comparison for the anisotropic turbulence which exists in wind shear. The question of how turbulence scales in a wind shear is addressed from the perspective of power spectral density. Author

N89-11360# Pacific Northwest Labs., Richland, Wash.
THE PNL SINGLE-TOWER MEASUREMENT MODEL OF ROTATIONALLY SAMPLED TURBULENT WIND, WITH USER'S GUIDE FOR STRS2PC
J. R. Connell, V. R. Morris, D. C. Powell, and G. L. Gower Jun. 1988 96 p
(Contract DE-AC06-76RL-01830)
(DE88-013166; PNL-6580) Avail: NTIS HC A05/MF A01

This report describes a single-tower rotationally sampled wind model, STRS-2, that approximates a set of time series of turbulent wind experienced by individual points rotating in circles in a crosswind plane using measurements from anemometers arrayed vertically along a single line. The purposes of the model are: (1) to use turbulence measurements made economically from conventional single-tower arrays of anemometers, (2) to incorporate measures characteristic of the wind at specific sites under consideration for operation of wind turbines, spanning the height range, and (3) to estimate the unmeasured turbulence characteristics in the crosswind plane that spans the disk of the rotor blades. DOE

N89-11361*# Wisconsin Univ., Madison. Cooperative Inst. for Meteorological Satellite Studies.
THE COOPERATIVE VAS PROGRAM WITH THE MARSHALL SPACE FLIGHT CENTER Final Report, Jul. 1982 - Dec. 1987
George R. Diak and W. Paul Menzel Jul. 1988 80 p
(Contract NAS8-34732)
(NASA-CR-179377; NAS 1.26:179377) Avail: NTIS HC A05/MF A01 CSCL 04B

Work was divided between the analysis/forecast model development and evaluation of the impact of satellite data in mesoscale numerical weather prediction (NWP), development of the Multispectral Atmospheric Mapping Sensor (MAMS), and other related research. The Cooperative Institute for Meteorological Satellite Studies (CIMSS) Synoptic Scale Model (SSM) has progressed from a relatively basic analysis/forecast system to a package which includes such features as nonlinear vertical mode initialization, comprehensive Planetary Boundary Layer (PBL) physics, and the core of a fully four-dimensional data assimilation package. The MAMS effort has produced a calibrated visible and infrared sensor that produces imager at high spatial resolution. The MAMS was developed in order to study small scale atmospheric moisture variability, to monitor and classify clouds, and to investigate the role of surface characteristics in the production of clouds, precipitation, and severe storms. Author

N89-11362*# Utah Univ., Salt Lake City. Dept. of Meteorology.
OPTICAL SCATTERING AND MICROPHYSICAL PROPERTIES OF SUBVISUAL CIRRUS CLOUDS, AND CLIMATIC IMPLICATIONS Final Report, 1 Dec. 1986 - 1 Jun. 1988
Kenneth Sassen, Michael K. Griffin, and Gregory C. Dodd 25 Oct. 1988 25 p
(Grant NAG1-718)
(NASA-CR-183301; NAS 1.26:183301) Avail: NTIS HC A03/MF A01 CSCL 04B

The optical and microphysical properties of subvisual cirrus clouds are derived from ground-based polarization lidar, shortwave radiation flux, and solar corona measurements of two approximately 0.75 km deep cirrus located near the tropopause. The first cloud produced no visual manifestations under excellent viewing conditions, and the second appeared to be a persistent aircraft contrail that was generally visible except in the zenith direction. Average lidar linear depolarization ratios and volume backscatter coefficients for the two clouds were 0.19 and 0.35, and 0.6x10 to the -3 and 1.4x10 to the -3 /km sr, respectively. It is estimated that the zenith-subvisual cirrus contained ice crystals of 25 micron effective diameter at a mean concentration of 25/l and ice mass content of 0.2 mg/cu m. The threshold cloud optical thickness for visual-versus-invisible cirrus, derived from both broadband shortwave flux and 0.694 micrometer lidar data, is found to be

tau sub c approx equal 0.03. Such tau values are comparable to those of 5 to 10 km deep stratospheric aerosol clouds of volcanic origin and polar stratospheric clouds, which are episodic in nature. Hence, we conclude that if these clouds are a fairly common feature of the upper troposphere, as recent SAGE satellite measurements would suggest, then the impact of natural and contrail subvisual cirrus on the planet's radiation balance may be relatively significant. Author

N89-11363# International Centre for Theoretical Physics, Trieste (Italy).
METHOD FOR PREDICTING MONTHLY RAINFALL PATTERNS
Ernest C. Njau Nov. 1987 33 p Submitted for publication
(DE88-703005; IC-87/395) Avail: NTIS (US Sales Only) HC A03/MF A01

A brief survey is made of previous methods that have been used to predict rainfall trends or drought spells in different parts of the earth. The basic methodologies or theoretical strategies used in these methods are compared with contents of a recent theory of Sun-Weather/Climate links (Njau, 1985a; 1985b; 1986; 1987a; 1987b; 1987c) which point towards the possibility of practical climatic predictions. It is shown that not only is the theoretical basis of each of these methodologies or strategies fully incorporated into the above-named theory, but also this theory may be used to develop a technique by which future monthly rainfall patterns can be predicted in further and finer details. We describe the latter technique and then illustrate its workability by means of predictions made on monthly rainfall patterns in some East African meteorological stations. DOE

N89-11364 Minnesota Univ., Minneapolis.
MICROWAVE RADIANCES FROM HORIZONTALLY FINITE, VERTICALLY STRUCTURED PRECIPITATING CLOUDS Ph.D. Thesis
Christian Detlef Kummerow 1987 162 p
Avail: Univ. Microfilms Order No. DA8802405

A model for the transfer of microwave radiances through horizontally finite, vertically structured clouds was developed. Radiances that would be measured from satellite borne radiometers were computed as a function of rainfall rate for finite precipitating clouds that contain liquid as well as frozen hydrometeors. Ice at the top of the precipitating clouds depress brightness temperatures by reflecting radiances emitted by liquid at the lower elevations. Radiation leaking out through the faces of the cloud thus becomes an important finite cloud effect when ice concentrations are high. Recent observations at 37 GHz show a 10 to 15 K difference in the upwelling radiances of the two orthogonally polarized radiances at high rainfall rates. This may be due to the aspherical nature of the ice hydrometeors. The hydrometeors were therefore assumed to be flattened along the axis of fall. A simple regression scheme was used to test the retrievability of the rainfall rate if neither the horizontal size nor shape of the precipitating cloud is known. To simulate real observations, a synthetic data set generated by the aforementioned model with random errors comparable to radiometer noise added to it was used. Dissert. Abstr.

N89-11365# National Oceanographic Data Center, Washington, D. C.
MARINERS WEATHER LOG, VOLUME 32, NUMBER 2, SPRING 1988
R. M. DeAngelis 1988 78 p
(PB88-210828) Avail: NTIS HC A05/MF A01; also available SOD HC $3.50 as 703-029-00014-1 CSCL 04B

The contents of the Mariners Weather Log, volume 32, Number 2, Spring 1988 are as follows: The will to live; Gambling on safety means high stakes; Satellites answer SOS; Eastern north Pacific hurricanes, 1987; Central north Pacific tropical cyclones, 1987; Marine observations program; and Tips to the radio officer. GRA

N89-11366 Washington Univ., Seattle.
A STUDY OF THE DYNAMICS OF MARITIME FRONTS USING REMOTELY SENSED WIND AND STRESS MEASUREMENTS Ph.D. Thesis
Gad Levy 1987 173 p
Avail: Univ. Microfilms Order No. DA8802285

The satellite scatterometer data open unprecedented opportunities to look at maritime storms and fronts. They are combined with observations, modeling efforts, and theory to study 5 cases. These provide the data to investigate frontal behavior in terms of its vorticity and divergence. The appropriate momentum, divergence and vorticity equations are derived and investigated including the inertial and frictional terms. The analysis is used to study frontal dynamics. The results indicate that the large scale horizontal and vertical thermodynamic structure of the boundary layer significantly influence baroclinic waves and frontal structure. These effects promote more efficient mixing and transport of heat, moisture, and westerly momentum in midlatitude storms. Conclusions are presented and discussed. Dissert. Abstr.

N89-11367 California Univ., Los Angeles.
EFFECTS OF DOWNDRAFTS AND MESOSCALE CONVECTIVE ORGANIZATION ON THE HEAT AND MOISTURE BUDGETS OF SQUALL AND NONSQUALL CLOUD CLUSTERS IN THE TROPICS Ph.D. Thesis
Ming-Dean Cheng 1987 244 p
Avail: Univ. Microfilms Order No. DA8803647

A diagnostic cumulus ensemble model is developed to study the effects of downdrafts and mesoscale convective organization on the heat and moisture budgets of squall and nonsquall cloud clusters. The model adopts the spectral representation of a cumulus ensemble and includes the vertical momentum budgets for both convective-scale updrafts and downdrafts. The downdrafts are initiated and maintained by the loading and evaporation cooling effects of rainwater which is generated in the updrafts tilting from the vertical. The diagnostic model is applied to the data taken during Phase 3 of the GARP Atlantic Tropical Experiment (GATE). Convective-scale updrafts tend to warm and dry the cumulus environment, while convective-scale downdrafts tend to cool and moisten the lower cloud layer. It was found that significant downdraft activity is usually associated with organized convection. There is almost no downdraft activity within the analyzed domain when only scattered convection was observed. The intensity of convective-scale downdrafts is related to the tilting angle of the associated updrafts. A remarkable correlation was found between the diagnosed updraft tilting angle and the degree of cloud organization. The horizontal distributions of the updraft tilting angle show local maxima in the regions of organized cumulus convection. The local maxima of the updraft tilting angle are found well before organized precipitation patterns associated with cloud clusters can be identified from the radar echoes. Using the diagnostic cumulus ensemble model the mesoscale effects were isolated from the observed heat and moisture budget residuals. Dissert. Abstr.

N89-11368*# Nebraska Univ., Lincoln. Inst. of Agriculture and Natural Resources.
COMPARISON OF MEASURED AND MODELED RADIATION, HEAT AND WATER VAPOR FLUXES: FIFE PILOT STUDY Final Technical Report, 1 Apr. 1985 - 31 Dec. 1987
Blaine L. Blad, Shashi B. Verma, Kenneth G. Hubbard, Patrick Starks, Cynthia Hays, John M. Norman, and Elizabeth WalterShea Oct. 1988 88 p
(Grant NAG5-561)
(NASA-CR-183304; NAS 1.26:183304; CAMaC-PR-87-7) Avail: NTIS HC A05/MF A01 CSCL 04B

The primary objectives of the 1985 study were to test the feasibility of using radio frequency receivers to collect data from automated weather stations and to evaluate the use of the data collected by the automated weather stations for modeling the fluxes of latent heat, sensible heat, and radiation over wheat. The model Cupid was used to calculate these fluxes which were compared with fluxes of these entities measured using micrometeorological techniques. The primary objectives of the 1986 study were to measure and model reflected and emitted radiation streams at a few locations within the First International Satellite Land-Surface

Climatology Project Field Experiment (FIFE) site and to compare modeled and measured latent heat and sensible heat fluxes from the prairie vegetation. Author

N89-11369# Instituto de Pesquisas Espaciais, Sao Jose dos Campos (Brazil).

A STUDY OF WIND PROFILES UNDER QUASI-NEUTRAL AND INVERSION ATMOSPHERIC CONDITIONS, OVER A TERRA FIRMA FOREST M.S. Thesis

Vicente dePaulaSilvaFilho Sep. 1988 91 p In PORTUGUESE; ENGLISH summary

(INPE-4694-RPE/575) Avail: NTIS HC A05/MF A01

Wind and potential temperature profiles, collected in the Central Amazon under quasi-neutral and inversion atmospheric conditions, are analyzed. The roughness length (z sub o) the zero plane displacement (d), determined using the iterative procedure of Robinson, were 1.38 m and 32.73 m, respectively. Simultaneous measurements of the momentum fluxes and wind profiles allowed the determination of the von-Karman constant (k=0.38). The same similarity was found between wind and temperature profiles under quasi-neutral conditions. The curvature of profiles was analysed using the Deacon numbers. The Bu as a function of Ri shows a very rapid deviation from the neutral profiles for only slightly diabatic cases, corresponding to a fairly large variation of the ratio Kh/Km. The log-linear form remains valid up to quite high degree of stability. Deviations from this form occur from aproximately 41 m height above ground in the Ducke Reserve case. The constant in the log-linear equation is found to have a value of 2.6, implying a critical Ri of 0.38. The Brunt-Vaisala frequency was calculated and the results agreed well with previous experimental values. Author

N89-11370# Air Force Inst. of Tech., Wright-Patterson AFB, Ohio.

TROPICAL 200 mb DIVERGENT CIRCULATIONS AND THEIR RELATION TO OUTGOING LONGWAVE RADIATION M.S. Thesis

Frank Sornatale 1988 78 p

(AD-A196375; AFIT/CI/NR-88-2) Avail: NTIS HC A05/MF A01 CSCL 04B

Annual and interannual variability of the 200 mb level mean meridional circulations (Hadley and Ferrel cells) and 200 mb tropical east-west circulations (Walker circulations) are presented as inferred from the velocity potential field. Also, a relationship is presented between divergence at 200 mb and outgoing longwave radiation (OLR). A major feature of the 200 mb tropical divergent velocity field is the dominance of the western Pacific monsoon region as the source for meridional and zonal overturning motions. Smaller, but significantly similar source regions are found over South and Central America as well as central Africa. Intra-annual variations of the equatorial Hadley cell are dominated by the variations of Asian Monsoon circulations. The seasonal fluctuations in the divergent velocity field in the western Pacific contribute to a strong annual cycle in the inter-annual pattern in the tropics. The results on east-west over-turning motions show that there are three cells associated with the three ascending branches over the Asian monsoon, South and Central America, and Central Africa. The most dominant cell is the Walker cell with its ascending branch over the western Pacific (Asian monsoon) and descending branch in the eastern equatorial Pacific. The intensity and location varies within the year. The inter-annual variability appears to be associated with the El Nino event. The relationship between divergence and the equivalent blackbody temperature index, is significant in the tropical convective region. GRA

N89-11371# Air Force Inst. of Tech., Wright-Patterson AFB, Ohio.

TROPICAL CYCLONE OBSERVATION AND FORECASTING WITH AND WITHOUT AIRCRAFT RECONNAISSANCE M.S. Thesis

Joel D. Martin 1988 123 p

(AD-A196379; AFIT/CI/NR-88-11) Avail: NTIS HC A06/MF A01 CSCL 04B

This thesis attempts to better quantify the contribution of aircraft reconnaissance to the accuracy of Tropical Cyclone (TC) center fix, motion determination, and intensity estimates along with the impact on track forecasts. It analyzes the impact on TC observations and weather forecasts when forecasters must rely only on weather satellites by concentrating on differences in TC position-intensity and track forecasting which occur between periods when aircraft measurements were and were not taken. Over 200 TC cases from the Northwest Pacific between 1979 to 1986, with about 5,000 center position fixes are analyzed. Average and distributions of fix, motion, intensity, and forecast error differences between reconnaissance and non-reconnaissance periods are made. Differences also are examined with respect to satellite type and day-night measurements. Results show that aircraft reconnaissance distinctly improves TC positioning, intensity estimation, and the short range TC forecast. Simultaneous independent satellite measurements of the same TC show that satellite analysts frequently have large differences in their fix estimates but not in their TC intensity estimates. Aircraft reconnaissance does not, on average, appear to improve the TC track forecast beyond 24 hours nor does it affect the conservative current 12-hour motion vector estimate. Recurvature forecasts are improved by having aircraft data, however. GRA

N89-11372# Air Force Inst. of Tech., Wright-Patterson AFB, Ohio.

AN EXAMINATION OF A SIMULATED MICROBURST FLOW AS SENSED BY A SINGLE DOPPLER RADAR M.S. Thesis

Eleanor L. Smith 1988 104 p

(AD-A196381; AFIT/CI/NR-88-90) Avail: NTIS HC A06/MF A01 CSCL 04B

The range and azimuthal limitations of a single Doppler radar in accurately determining velocity-based microburst parameters were studied. A vortex ring model was developed to simulate the microburst flow. The simulated velocities were vertically averaged over the lowest 500 meters of the flow using a Gaussian-squared weighting distribution. Smoothed values of radial shear parameters were examined for microbursts centered less than 30 km from a single Doppler radar; smoothing effects were minimal for azimuths of less than five degrees. Unsmoothed radial shear parameters were also compared as a function of azimuth, range, and arc length for microbursts centered from 15 km to 150 km from a Doppler radar. Detected radial shear decreases with increasing range and azimuth due to beam spreading. For a one-degree beam, the planned NEXRAD sampling rate, the difference in radial shear for a maximum 0.5-degree offset between 15-km and 150-km microbursts is 18 percent, creating non-existent fluctuations. For short arc lengths, the differences in radial shear parameters are small; they increase for longer arc lengths but the shear magnitudes are small. GRA

N89-11373# Air Force Inst. of Tech., Wright-Patterson AFB, Ohio.

ON DERIVING THE 3-DIMENSIONAL KINEMATIC STRUCTURE OF CONVECTIVE STORMS FROM A SINGLE RADAR Ph.D. Thesis

Robert M. Cox May 1988 160 p

(AD-A196405; AFIT/CI/NR-88-30) Avail: NTIS HC A08/MF A01 CSCL 17I

The objectives of this investigation were to determine the feasibility of deriving vertical velocity patterns, the magnitudes of those patterns, and the three-dimensional wind field in severe convective storms. A technique called Tracking Radar Echoes by Correlation (TREC), also called the NEXRAD Transverse Wind algorithm, and data from a single radar were used to determine the internal storm motions. TREC was used to determine the u and v wind components. These components were gridded using a standard objective analysis technique. It has been shown that in weak reflectivity regions random pattern matching can occur, therefore in areas of reflectivity less than 10 dBZ TREC-derived data were viewed with caution. Important results of this study are: (1) there was good agreement in both areal extent and magnitude between the TREC-derived vertical velocities and the dual-Doppler

velocities; (2) for time increments of 5 min or less between radar volume scans, the horizontal wind field derived by TREC agreed with the dual-Doppler wind field during the multicell and transition phases of the storm; and (3) the effects of the generator level motions on the TREC derived wind field were evident only in the supercell phase. GRA

N89-11374# Air Force Inst. of Tech., Wright-Patterson AFB, Ohio.
ACTIVE MODES OF THE PACIFIC INTERTROPICAL CONVERGENCE ZONE (ITCZ) M.S. Thesis
Patrick M. Hayes May 1988 105 p
(AD-A196406; AFIT/CI/NR-88-29) Avail: NTIS HC A06/MF A01 CSCL 04A

Satellite-observed outgoing longwave radiation (OLR) data from eight 6-month cool seasons were examined to find periods of active convection within the Pacific intertropical convergence zone (ITCZ). Descriptive statistics were used to define and describe the time-mean behavior of the Pacific ITCZ. Two seasons (76 to 77 and 82 to 83) showed distinctive El Nino-Southern Oscillation (ENSO) signatures in mean, standard deviation, and frequency distribution of OLR. Four other seasons (74 to 75, 75 to 76, 79 to 80, and 80 to 81) had normal OLR statistics. The remaining seasons preceded and followed the major 82 to 83 event and had intermediate seasonal-mean OLR fields. Time series of an index measuring convective intensity in the ITCZ were analyzed to find active convection periods. Time-longitude diagrams of intensity estimates showed how active modes develop, spread, and propagate across the Pacific. Three types of variability of the active modes were identified. The first type had small spatial scales (less than 4000 km), short temporal scales (10 to 20 day durations), and occurred mostly in the eastern Pacific. The second type had longer spatial scales (5000 to 10,000 km), short temporal scales, and was found throughout. The second type also showed evidence of propagation. The third type had large temporal scales (less than 30 days), medium spatial scales (2000 to 6000 km), and was a fixed feature. GRA

N89-11375# Air Force Inst. of Tech., Wright-Patterson AFB, Ohio.
ESTIMATING EVAPOTRANSPIRATION OF AN IRRIGATED SURFACE FROM UPWIND AND DOWNWIND VERTICAL PROFILES OF TEMPERATURE AND HUMIDITY M.S. Thesis
David F. Zehr 1988 92 p
(AD-A196409; AFIT/CI/NR-88-34) Avail: NTIS HC A05/MF A01 CSCL 04B

Evapotranspiration (ET) and the contribution of horizontal advection of sensible heat were predicted for an irrigated surface in arid regions from upwind and downwind vertical profiles of temperature and humidity. Measurements were made of atmospheric temperature and specific humidity to a height of 70 meters at the upwind and downwind sides of an irrigated alfalfa field with dry upwind conditions. The depth of air whose temperature and humidity profiles were distorted by the irrigated surface defined a control volume. Total ET was estimated via a vapor budget method which essentially calculated the input of water vapor into the control volume. The amount of energy used in ET which was contributed by sensible heat advection was estimated by calculating the amount of internal energy depleted from the control volume. Simultaneous estimates of ET were made with an eddy correlation system, located near the center of the field. The depth of air modified by the irrigated crop averaged 10 for specific humidity and 15 for temperature during the light winds encountered in this study. ET estimates from the vapor budget method compared well with eddy correlation results. Deviation between the two estimates averaged 43 w/sq m (7.2 percent). GRA

N89-11376# Air Force Inst. of Tech., Wright-Patterson AFB, Ohio.
THE USE OF THE Q-VECTOR IN OPERATIONAL METEOROLOGY M.S. Thesis
Charles A. Lemay May 1988 77 p
(AD-A196410; AFIT/CI/NR-88-35) Avail: NTIS HC A05/MF A01 CSCL 04B

Evaluation of atmospheric vertical motion is now possible on widely available and inexpensive microcomputers. Using the Q-vector form of the omega equation, formulated by Hoskins et al. (1978) allows a meteorologist to evaluate vertical motion throughout the atmosphere. Case studies are presented, using an enhanced version of the Barnes (1985) computer program. The first case study deals with a severe weather situation that resulted in tornadic activity through eastern Texas. The second case study covers a two day period in which a Mesoscale Convective Complex (MICC) moved through the Central Plains states. Results of these case studies show that the Q-vector form of the omega equation is a useful tool for evaluating vertical motion and aids in checking the initialization of the prognostic numerical models. The diagnostic charts, from this program, are available one to two hours before other commonly used charts are produced. Program results are best interpreted on meso and synoptic scales; however, the diagnostic results are best used when incorporated with other routinely available charts. A drawback to the program is that nongeostrophic effects such as orographic influences and friction are not included. GRA

N89-11377# Air Force Inst. of Tech., Wright-Patterson AFB, Ohio.
THE ROLE OF A LID IN THE 31 MAY 1985 TORNADO OUTBREAK M.S. Thesis
Robert J. Farrell, Jr. May 1988 173 p
(AD-A196684; AFIT/CI/NR-88-107) Avail: NTIS HC A08/MF A01 CSCL 04B

The Carlson-Ludlam Conceptual Model is useful for predicting severe convective outbreaks. Central to the entire model is the presence of an elevated mixed layer that caps and then helps focus the release of built-up latent instability in a concentrated area. A review of the model's development and a discussion of the concepts involved are presented. The model is very successful at explaining many of the processes which produce severe convection. However, its use is much too time consuming for operational forecasting. Therefore, a computer application is presented that objectively delineates lid involvement. The 31 May 1985 Tornado Outbreak occurred in the NE U.S. Analysis reveals four critical factors in the pre-storm environment responsible for the severity of the outbreak: (1) the presence of a lid and the resulting build-up of a high wet-bulb potential temperature in the boundary layer, (2) readily available soil moisture, (3) underrunning, and (4) forced ascent associated with baroclinic forcing from a migrating short wave. Because vigorous short waves move across the NE U.S. several times each spring and such outbreaks rarely occur, it is concluded that the lid was the most critical factor. GRA

N89-11378# Air Force Inst. of Tech., Wright-Patterson AFB, Ohio.
SYNOPTIC SCALE SENSITIVITY OF TIROS-N MOISTURE CHANNELS IN THE TROPICS M.S. Thesis
Keith G. Blackwell 1988 141 p
(AD-A196686; AFIT/CI/NR-88-21) Avail: NTIS HC A07/MF A01 CSCL 04B

Water vapor radiance data obtained from a satellite borne radiometer were evaluated for synoptic information content and accuracy over the tropical eastern Pacific Ocean. An upper moist layer was defined in terms of precipitable water by integrating sounding data downward from 300 mb. The varying pressure of this upper moist layer was correlated with collocated 6.7 and 7.3 micrometer water vapor brightness temperatures (BT)s. A persistent cluster of elevated BTs was observed over the subtropical Pacific adjacent to the western flank of a series of moisture bursts. Collocated rawinsonde soundings and satellite BTs consistently showed excellent agreement, indicating extreme dryness in the middle and upper troposphere. The anomalous lack of upper tropospheric moisture, the tight clustering of abnormally large BTs, and the close proximity to a large area of active convection suggests these elevated BTs occur only as an occasional

synoptically induced feature. Estimation of the influence of horizontal moisture advection on local BT changes resulted in maximum values of the same order of magnitude as the maximum observed BT changes. However, comparisons at individual grid points showed little similarity. GRA

N89-11379# Air Force Inst. of Tech., Wright-Patterson AFB, Ohio.
MESOSCALE STRUCTURE AND CLIMATOLOGY OF RAIN-SNOW LINES OVER NORTH CAROLINA M.S. Thesis
Kenneth F. Carey 1988 105 p
(AD-A196687; AFIT/CI/NR-88-5) Avail: NTIS HC A06/MF A01 CSCL 04B

The three-dimensional atmospheric structure in the vicinity of the rain-snow line was further explored by means of Barnes-generated fields of divergence. The First Law of Thermodynamics, in a coordinate system following the 0 C isotherm (chosen to represent the rain-snow line), was employed. A 22-year (1986 to 1987) climatology of rain-snow lines in North Carolina was compiled. GRA

48 OCEANOGRAPHY

Includes biological, dynamic, and physical oceanography; and marine resources.

For related information see also *43 Earth Resources and Remote Sensing.*

N89-11380# National Ocean Service, Anchorage, Alaska. Ocean Assessments Div.
BEAUFORT SEA: INFORMATION UPDATE
P. R. Becker Apr. 1988 97 p Sponsored by Minerals Management Service, Anchorage, Alaska
(PB88-208616) Avail: NTIS HC A05/MF A01 CSCL 08C

The report is based on a multi-disciplinary meeting held March 6-7, 1985, as part of preparations for the Beaufort Sea Sale 97. The chapters are based on presentations given: The causeway effect; Modification of nearshore thermal regime resulting from causeways; Summertime sea ice intrusions in the Chukchi Sea; The deepwater limit of ice gouging on the Beaufort Sea Shelf; Distribution, abundance, migration, harvest, and stock identity of Belukha Whales in the Beaufort Sea; Ringed seals in the Beaufort Sea; Beaufort sea socioeconomics; The Baffin Island Oil Spill, (BIOS) Project. GRA

N89-11381*# National Aeronautics and Space Administration. Goddard Inst. for Space Studies, New York, N.Y.
DERIVATION OF REVISED FORMULAE FOR EDDY VISCOUS FORCES USED IN THE OCEAN GENERAL CIRCULATION MODEL
Ru Ling Chou Sep. 1988 14 p
(NASA-TM-4060; GISS-88-182; NAS 1.15:4060) Avail: NTIS HC A03/MF A01 CSCL 08C

Presented is a re-derivation of the eddy viscous dissipation tensor commonly used in present oceanographic general circulation models. When isotropy is imposed, the currently-used form of the tensor fails to return to the laplacian operator. In this paper, the source of this error is identified in a consistent derivation of the tensor in both rectangular and earth spherical coordinates, and the correct form of the eddy viscous tensor is presented. Author

N89-11382# Naval Postgraduate School, Monterey, Calif.
THE CLIMATOLOGICAL SEASONAL RESPONSE OF THE OCEAN MIXED LAYER IN THE EQUATORIAL AND TROPICAL PACIFIC OCEAN M.S. Thesis
Harry J. Ries, Jr. Mar. 1988 97 p
(AD-A196962) Avail: NTIS HC A05/MF A01 CSCL 08C

Seasonal changes of mixed layer depth (MLD) can be related to the forcing by the net surface heating and wind speed. This is shown in this study by comparing the monthly mixed layer depth from temperature profiles in the Bauer-Robinson Numerical Atlas with monthly net surface heating and wind speed obtained from the Weare Marine Climatic Atlas of the Tropical Pacific Ocean. Using a conceptual model based on mixed layer physics, ocean response and atmospheric forcing are examined using the Obukhov mixing length. A pattern in the seasonal variation of upwelling along the Equator is also examined. The model links the atmospheric and oceanic climatologies through the derived MLD (oceanic data) and Obukhov mixing lengths (forcing data). The results show a high degree of pattern similarity between the seasonal response of the ocean and the seasonal changes in atmospheric forcing. The pattern of seasonal influence on MLD at the Equator is very weak in comparison to that of the tropics and sub-tropics. GRA

51 LIFE SCIENCES (GENERAL)

N89-11383# Oak Ridge National Lab., Tenn. Chemical Technology Div.
A COMPOSITE PHOTOBIOELECTRONIC MATERIAL
E. Greenbaum 1988 20 p Presented at the 10th Symposium on Biotechnology for Fuels and Chemicals, Gatlinburg, Tenn., 16 May 1988
(Contract DE-AC05-84OR-21400)
(DE88-012490; CONF-880521-1) Avail: NTIS HC A03/MF A01

The research described presents a method for chemically modifying the surface of green plant photosynthetic membranes in such a way that electrical contact can be made. Colloidal platinum was prepared, precipitated directly onto photosynthetic thylakoid membranes from aqueous solution, and entrapped on fiberglass filter paper. This composition of matter was capable of sustained simultaneous photoevolution of hydrogen and oxygen when irradiated at any wavelength in the chlorophyll absorption spectrum. Experimental data support the interpretation that part of the platinum metal catalyst is precipitated adjacent to the photosystem-I reduction site of photosynthesis and that electron transfer occurs across the interface between photosystem-I and the catalyst. When contacted with metal electrodes, the thylakoid-platinum combination is capable of generating a sustained flow of current through an external load resistor. Procedures for preparing this material and experimental data on its catalytic and electronic properties are presented. DOE

N89-11384*# Houston Univ., Tex. Dept. of Biology.
GROWTH OF PLANT TISSUE CULTURES IN SIMULATED LUNAR SOIL: IMPLICATIONS FOR A LUNAR BASE CELSS (CONTROLLED ECOLOGICAL LIFE SUPPORT SYSTEM) Final Report, 1 Feb. 1987 - 31 Jul. 1988
S. Venketeswaran 1988 65 p
(Grant NAG9-214)
(NASA-CR-183233; NAS 1.26:183233) Avail: NTIS HC A04/MF A01 CSCL 06C

Experiments were carried out on plant tissue cultures, seed germination, seedling development and plants grown on Simulated Lunar Soil to evaluate the potential of future development of lunar based agriculture. The studies done to determine the effect of the placement of SLS on tissue cultures showed no adverse effect of SLS on tissue cultures. Although statistically insignificant, SLS in suspension showed a comparatively higher growth rate. Observations indicate the SLS, itself cannot support calli growth but was able to show a positive effect on growth rate of calli when supplemented with MS salts. This positive effect related to nutritive value of the SLS was found to have improved at high pH levels, than at the recommended low pH levels for standard media. Results from seed germination indicated that there is neither inhibitory, toxicity nor stimulatory effect of SLS, even though SLS contains high amounts of aluminum compounds compared to earth soil. Analysis of seeding development and growth data showed significant reduction in growth rate indicating that, SLS was a poor growth medium for plant life. This was confirmed by the studies done with embryos and direct plant growth on SLS. Further observations attributed this poor quality of SLS is due to it's lack

of essential mineral elements needed for plant growth. By changing the pH of the soil, to more basic conditions, the quality of SLS for plant growth could be improved up to a significant level. Also it was found that the quality of SLS could be improved by almost twice, by external supply of major mineral elements, directly to SLS. Author

52 AEROSPACE MEDICINE

Includes physiological factors; biological effects of radiation; and effects of weightlessness on man and animals.

N89-11385 Joint Publications Research Service, Arlington, Va.
JPRS REPORT: SCIENCE AND TECHNOLOGY. USSR: LIFE SCIENCES
12 Aug. 1987 100 p Transl. into ENGLISH from various Russian articles
(JPRS-ULS-87-010) Copyright Avail: Issuing Activity

Topics addressed include: agricultural science biochemistry; epidemiology; medicine; biophysics; enviroment; laser bioeffects; marine mammals; toxicology; microbiology; pharmacology; virology; physiology; radiation biology; and public health. For individual title, see N89-11386.

N89-11386 Joint Publications Research Service, Arlington, Va.
INDIVIDUAL DIFFERENCES IN ADAPTATION TO HYPOXIA AND COLD BASED ON EMOTIONAL-BEHAVIORAL CRITERION OF BODILY REACTIVITY Abstract Only
V. B. Zagustina, Z. A. Aleksanyan, and N. N. Vasilevskiy *In its* JPRS Report: Science and Technology. USSR: Life Sciences 12 Aug. 1987 p 58 Transl. into ENGLISH from Uspekhi Fiziologicheskikh Nauk (Moscow, USSR), v. 17, no. 4, Oct. - Dec. 1986 p 68-84 Original language document was announced in IAA as A87-24261 (For primary document see N89-11385 02-52)
Copyright Avail: Issuing Activity

Hypoxia is one of the more critical problems in modern medicine. Resistance to hypoxia depends on the level of the development of the nervous system. The most sensitive to oxygen insufficiency are animals with poor higher nerve activity. Those without fear, insensitive to provocational factors and those showing tendency to social domineering are more resistant to acute hypoxia. Data on individual differences to the adaptation to hypoxia are reviewed here. The role of emotional-behavorial reaction is pointed out. Adaptation to cold and hypoxia appears to be based on complex system interaction. This is especially crucial in rapid adaptations and should be considered carefully in optimizing training of alpinists. IAA

N89-11387# Air Force Inst. of Tech., Wright-Patterson AFB, Ohio.
EFFECT OF PHYSICAL FITNESS ON RESPONSE TO ORTHOSTASIS IN HEALTHY YOUNG WOMEN M.S. Thesis
Carolyn K. Gooch 1988 78 p
(AD-A196377; AFIT/CI/NR-88-3) Avail: NTIS HC A05/MF A01 CSCL 06D

The purpose of this study was to examine the relationship between fitness level and cardiovascular response to orthostatic stress in healthy women between the ages of 20 and 35. Subjects were divided into three groups on the basis of VO2max: High-Fit (n = 4; mean VO2max = 57.8 ml/kg/min); Med-Fit (n = 8; mean VO2max = 46.4 ml/kg/min); and Low-Fit (n = 4; mean VO2max = 34.7 ml/kg/min). Subjects were exposed to three trials of 70 deg head up tilt each followed by a ten minute supine rest period. Heart rate and blood pressure were recorded at 1, 3 and 5 minute intervals during head up tilt and at 5 and 10 minute intervals during the supine rest period. The mean heart rate and blood pressure changes from supine to one minute upright were calculated for each group. The change in heart rate per change in systolic blood pressure from supine to 70 deg upright was used as an index of baroreflex responsiveness. There was a strong inverse correlation between fitness level and heart rate both resting and at 1 minute upright (r=.83;r=.84 p less than .001). An analysis of baroreflex indices between groups showed no fitness related differences in heart rate and blood pressure response to orthostasis. GRA

53 BEHAVICRAL SCIENCES

Includes psychological factors; individual and group behavior; crew training and evaluation; and psychiatric research.

N89-11388# Haifa Univ. (Israel). Centre for Study of Psychological Stress.
ENHANCING PERFORMANCE UNDER STRESS BY INFORMATION ABOUT ITS EXPECTED DURATION Interim Report, May - Dec. 1987
Shlomo Breznitz Jun. 1988 33 p
(Contract DAJA45-86-C-0048; DA Proj. 2Q1-61102-B-74-F)
(AD-A196836; ARI-RN-88-53) Avail: NTIS HC A03/MF A01 CSCL 06J

This research note discusses experiments in which four groups of subjects were given two stressful tasks; the Dynamometer test, and the Cold Pressor test. At the same time, the test subjects were given different information about the tests' duration. The information conditions were: no information, exact information, false long (with subsequent encouraging correction), and false short (with subsequent discouraging correction). Endurance was highest with the exact information condition, lowest in the no information condition, and the other two groups produced intermediate results. Timing of the maximal heart rate during the task was systematically related to information, and its role as a potential indicator of psychological breakdown was analyzed. GRA

54 MAN/SYSTEM TECHNOLOGY AND LIFE SUPPORT

Includes human engineering; biotechnology; and space suits and protective clothing.

For related information see also *16 Space Transportation.*

N89-11389# National Highway Traffic Safety Administration, East Liberty, Ohio. Vehicle Research and Test Center.
EVALUATION OF THE PROTOTYPE EUROSID DUMMY AND COMPARISON WITH THE US SID (SIDE IMPACT DUMMIES) Final Report, Nov. 1986 - Mar. 1987
Roger A. Saul Sep. 1987 121 p
(PB88-201934; DOT-HS-807-219) Avail: NTIS HC A06/MF A01 CSCL 05H

As part of their side impact protection programs, the United States and Europe have developed side impact dummies (SID). The dummies differ in many areas including principal thoracic measurement technique. The report describes the National Highway Traffic Safety Administration testing of the EUROSID model to determine its repeatability, durability, biofidelity, and its ability to assess potential injury reduction countermeasures, as contrasted with the U.S. SID. Specific procedures and results of component qualification tests and HYGE sled tests as well as dummy instrumentation procedures are described. GRA

N89-11390 Purdue Univ., West Lafayette, Ind.
CONTROL DESIGN AND PERFORMANCE EVALUATION FOR FLEXIBLE MANIPULATORS Ph.D. Thesis
Kiyoharu Matsuoka 1987 204 p
Avail: Univ. Microfilms Order No. DA8807644

To date, many manipulator designs have been based on rigid body considerations. These designs are often characterized by stiff structures and sluggish responses, while flexible manipulator designs are recognized for such benefits as energy-efficiency and maneuverability. The increasing demands for more accurate modeling of the flexible manipulators result in larger and more

complex nonlinear models with more degrees of freedom. For realistic problems, the required algebra becomes prohibitive and error-prone by paper and pencil. Symbolic processing of nonlinear equations of motion, based on Lagrange formulation and the assumed-modes method, was employed extensively. Since a flexible structure is a distributed-parameter system, any finite-dimensional attempt to control such a system is not free from the ill-effects of intrinsic model errors. A suboptimal gain scheduling scheme with model error accommodation to control flexible manipulators is presented. For the performance evaluation of a control design, a nonlinear closed-loop simulation should be carried out under realistic model error environments. Simplification of such evaluation process by combined use of a simulation language and a properly interfaced symbolic manipulation system is discussed. The effectiveness of both the model-error accommodating control and the performance evaluation process is demonstrated by an example. Dissert. Abstr.

N89-11391 Stanford Univ., Calif.
EXPERIMENTS IN CONTROL OF SATELLITE MANIPULATORS Ph.D. Thesis
Harold Luchsinger Alexander 1988 116 p
Avail: Univ. Microfilms Order No. DA8808343

A new method is presented for space robot control that is based on the operational-space or resolved-acceleration method developed for industrial style manipulators. The new extended version makes allowance for the dynamic reaction of the freely-floating robot body when the manipulator is moved, so that precise specified end-effector accelerations in space may be achieved in spite of the lack of a fixed manipulator base. A mathematical dynamic model is developed for the laboratory robot and the extended control method is experimentally applied to the robot with command of straight-line slews between points fixed in inertial space. Successful trajectory tracking and position regulation are demonstrated independent of the orientation of the command reference frame with respect to the free-floating robot body. The potential of the extended operational space method for non-manipulator control applications is discussed. The extension to three-dimensional space robot control is introduced as well as applications involving multi-manipulator robots and multiple robots. The stability of model-based control methods such as operational space and computed torque is discussed. Dissert. Abstr.

55 SPACE BIOLOGY

Includes exobiology; planetary biology; and extraterrestrial life.

N89-11392# Academy of Sciences of the Ukrainian SSR, Kharkov. Inst. Radiofiziki i Ehlektroniki.
PROBABLE LOCATIONS OF EXTRATERRESTRIAL CIVILIZATIONS
A. V. Arkhipov 1986 14 p In RUSSIAN; ENGLISH summary
(DE88-702605; INIS-SU-25/A) Avail: NTIS (US Sales Only) HC A03/MF A01

The search for extraterrestrial civilizations by monitoring their continuous isotropic radio emissions at frequencies from 100 to 1000 MHz is discussed. Such a possibility has been found at a distance of approximately 20 pc in this frequency range. The search for similar radio sources continues. The discoveries are in the vicinity of four solar-type stars, which would be favorable for the existence intelligent life. The probability of error in this case would be 2 x 10 to the minus 4 power. These four stars are the most promising SETI sources to date. DOE

59 MATHEMATICAL AND COMPUTER SCIENCES (GENERAL)

No abstracts in this category.

60 COMPUTER OPERATIONS AND HARDWARE

Includes hardware for computer graphics, firmware, and data processing.

For components see *33 Electronics and Electrical Engineering.*

N89-11393# Sandia National Labs., Albuquerque, N. Mex.
A PERFORMANCE MODEL FOR MASSIVE PARALLELISM
J. L. Gustafson May 1988 23 p
(Contract DE-AC04-76DP-00789)
(DE88-011763; SAND-88-1281) Avail: NTIS HC A03/MF A01

A popular argument is that vector and parallel architectures should not be carried to extremes because the scalar or serial portion of the code will eventually dominate. Since pipeline stages and extra processors obviously add hardware cost, a corollary to this argument is that the most cost-effective computer is one based on uniprocessor, scalar principles. For architectures that are both parallel and vector, the argument is compounded, making it appear that near-optimal performance on such architectures is a near-impossibility. A new argument is presented that is based on the assumption that program execution time, not problem size, is constant for various amounts of vectorization and parallelism. This has a dramatic effect on Amdahl Law, revealing that one can be much more optimistic about achieving high speedups on massively-parallel and highly-vectorized machines. The revised argument is supported by recent results of over 1000 times speedup on 1024 processors on several practical scientific applications. This document discusses the results and presents a reevaluation of Amdahl's Law. DOE

N89-11394# California Inst. of Tech., Pasadena.
PC-CUBE: A PERSONAL COMPUTER BASED HYPERCUBE
Alex Ho, Geoffrey Fox, David Walker, Scott Snyder, Douglas Chang, Stanley Chen, Matt Breaden, and Terry Cole (Jet Propulsion Lab., California Inst. of Tech., Pasadena.) 1988 6 p
(Contract DE-FG03-85ER-25009)
(DE88-015008; DOE/ER-25009/587) Avail: NTIS HC A02/MF A01

PC-CUBE is an ensemble of IBM PCs or close compatibles connected in the hypercube topology with ordinary computer cables. Communication occurs at the rate of 115.2 K-band via the RS-232 serial links. Available for PC-CUBE is the Crystalline Operating System III (CrOS III), Mercury Operating System, CUBIX and PLOTIX which are parallel I/O and graphics libraries. A CrOS performance monitor was developed to facilitate the measurement of communication and computation time of a program and their effects on performance. Also available are CXLISP, a parallel version of the XLISP interpreter; GRAFIX, some graphics routines for the EGA and CGA; and a general execution profiler for determining execution time spent by program subroutines. PC-CUBE provides a programming environment similar to all hypercube systems running CrOS III, Mercury and CUBIX. In addition, every node (personal computer) has its own graphics display monitor and storage devices. These allow data to be displayed or stored at every processor, which has much instructional value and enables easier debugging of applications. Some application programs which are taken from the book Solving Problems on Concurrent Processors (Fox 88) were implemented with graphics enhancement on PC-CUBE. The applications range

from solving the Mandelbrot set, Laplace equation, wave equation, long range force interaction, to WaTor, an ecological simulation.
DOE

N89-11395# Advisory Group for Aerospace Research and Development, Neuilly-Sur-Seine (France). Fluid Dynamics Panel.
COMPUTATIONAL FLUID DYNAMICS: ALGORITHMS AND SUPERCOMPUTERS
Wolfgang Gentzsch, Ken W. Neves, and H. Yoshihara, ed. (Boeing Military Airplane Development, Seattle, Wash.) Mar. 1988 195 p
(AGARD-AG-311; ISBN-92-835-0448-8) Copyright Avail: NTIS HC A09/MF A01

Cost-effective vectorization of fluid dynamic codes, in particular the Navier/Stokes Code, is covered relative to the supercomputer architecture. Subjects include current supercomputer architecture; minisupercomputers; impact of hardware on computing; software migration issues; benchmarking; guidelines on FORTRAN vectorization at the do-loop level; restructuring of basic linear algebra algorithms; and restructuring guidelines for basic fluid dynamic codes. A glossary of supercomputing terms is given in the Appendix. For individual titles, see N89-11396 through N89-11401.

N89-11396# Boeing Computer Services Co., Seattle, Wash.
HARDWARE ARCHITECTURE, CHAPTER 2
Ken W. Neves *In* AGARD, Computational Fluid Dynamics: Algorithms and Super Computers Mar. 1988 p 11-53 (For primary document see N89-11395 02-60)
Copyright Avail: NTIS HC A09/MF A01

An overview of computer architectures is given. The purpose is not to offer a text book description of the electronics behind computing, but rather an appreciation of the barriers on computer development that have led to the complex design of today's supercomputers. This introductory section will examine: (1) the need for increased computer power as a result of the pressure from new computational processes; (2) the limits and barriers of hardware; (3) a brief history of parallelism; and (4) an overview of parallelism in today's computers. Following this Background section, an indepth look at today's supercomputer architectures and emerging computer products is given. In chapter 3, the impact of new hardware architecture on algorithms will be examined. Like computational fluid dynamics, supercomputing has developed a set of terms, definitions, and ad hoc descriptions of common processes. In this monograph most of these terms will be defined when used. Nevertheless, in an attempt to aid the reader, an informal glossary of supercomputing terms is included in an appendix.
Author

N89-11397# Boeing Computer Services Co., Seattle, Wash.
ALGORITHM AND GENERAL SOFTWARE CONSIDERATIONS **c61**
Ken W. Neves *In* AGARD, Computational Fluid Dynamics: Algorithms and Super Computers Mar. 1988 p 55-98 (For primary document see N89-11395 02-60)
Copyright Avail: NTIS HC A09/MF A01

This chapter of the study examines the relationship between hardware architecture and computational performance. The setting is scientific computation of a generic sense (i.e., application non-specific). In subsequent chapters, the general implications discussed here will be applied to algorithms specific to computational fluid dynamics and to the major computational approaches used in that field. In order to give meaningful appreciation of the concepts discussed, frequent use of examples on specific hardware architectures will be utilized. Quite often several machine types will be included, and several will not. The reasons for this are twofold: (1) it is not always possible to obtain exactly the same benchmark results across machine types, and (2) it is not our intent to give a definitive comparison of machine performance. These reasons may seem superficial at first glance, yet thay are fundamental to the reality of the state-of-the-art of computer metrics.
Author

N89-11398# Technische Univ., Regensburg (West Germany).
VECTORIZATION OF FORTRAN PROGRAMS AT DO-LOOP LEVEL **c61**
W. Gentzsch *In* AGARD, Computational Fluid Dynamics: Algorithms and Super Computers Mar. 1988 p 99-108 (For primary document see N89-11395 02-60)
Copyright Avail: NTIS HC A09/MF A01

In previous chapters the impact of computer hardware on algorithm performance was discusssed. It was made clear that the most effective use of the supercomputers comes from sound understanding of computer architecture and an appropriate computational strategy. In this and subsequent chapters, the focus will by on fluid dynamics applications. Today, and for some years to come, the major interface between the scientist and the computer will continue to be FORTRAN. Some common techniques are presented which are useful in dealing with code optimization within the critical loops of FORTRAN, and in Chapter 5 the important consequences of restructuring the linear algebra algorithms common in CFD applications. Finally, in Chapter 6, major applications will be reviewed from a computational perspective giving a broad-based approach utilizing proper FORTRAN, proper algorithms, and awareness of architectural dependencies. Here we restrict ourselves to discussing some helpful coding techniques, which are easy to understand and to implement. However, it should be emphasized that the selection of an appropriate algorithm is generally far more important than fancy programming techniques (see Chapter 5).
Author

N89-11399# Technische Univ., Regensburg (West Germany).
RESTRUCTURING OF BASIC LINEAR ALGEBRAIC ALGORITHMS, CHAPTER 5 **c61**
W. Gentzsch *In* AGARD, Computational Fliud Dynamics: Algorithms and Super Computers Mar. 1988 p 109-139 (For primary document see N89-11395 02-60)
Copyright Avail: NTIS HC A09/MF A01

In the previous chapter the vectorization of typical do-loops arising in CFD problems was discussed. Until now, we have not considered the algebraic structure of the basic algorithm, by far the most important consideration. Indeed, a good algorithm poorly coded is usually preferable to a poor one optimally coded. For this reason, in the following, we turn our attention to the restructuring of some basic linear algebraic algorithms such as matrix*vector and matrix*matrix operations, linear recursions up to more complex algorithms and iterative methods for the solution of linear algebraic systems of equations with sparse matrices. Problems involving linear algebraic calculations consume large quantities of computer time. If substantial improvements can be made within the arithmetic section, a significant reduction in the overall computation time will be realized.
Author

N89-11400# Technische Univ., Regensburg (West Germany).
COMPUTATIONAL FLUID DYNAMICS AND SUPERCOMPUTERS, CHAPTER 6 **c34**
W. Gentzsch *In* AGARD, Computational Fluid Dynamics: Algorithms and Super Computers Mar. 1988 p 141-182 (For primary document see N89-11395 02-60)
Copyright Avail: NTIS HC A09/MF A01

It is important to optimally adapt codes and algorithms to the vector or parallel computer in use. In addition to faster and larger supercomputers, users must be much better trained than for (scalar) general purpose computers. Details on restructuring typical numerical algorithms to achieve superior performance on vector computers. The focus, of course, is on Computational Fluid Dynamics. During the last two decades CFD gained an important position together with experiments in wind tunnels and analytical methods. The main objective of CFD is to simulate dynamic flow fields through the numerical solution of the governing equations, e.g., the Navier-Stokes equations, using high-speed computers. The simulation of 2-D inviscid and viscous flows on vector computers does not represent any difficulties with respect to memory requirements or computation time. In 3-D, however, one has to compute some 20 to 30 variables per mesh point in a 3-D field per time-step or iteration such as the velocity components,

density, pressure, enthalpy, temperature, concentrations, dissipative fluxes, local time steps, geometry coefficients, dummy arrays, etc. Computations in the case of 3-D are therefore restricted to fairly coarse meshes as well as to solutions which are often not fully converged solutions. The large amount of CPU time involved and the fact that the data cannot be contained in central memory are the main reasons for the long elapsed times for CFD applications. In these cases, the mapping of the problem onto the architecture of the machine and in particular onto special organizations of the memory must be fully considered to take full advantage of the vector computer. Author

N89-11401# Boeing Computer Services Co., Seattle, Wash.
AN INFORMAL GLOSSARY OF TERMS USED IN SUPERCOMPUTING, APPENDIX A **c82**
K. Neves *In* AGARD, Computational Fluid Dynamics: Algorithms and Super Computers Mar. 1988 7 p (For primary document see N89-11395 02-60)
Copyright Avail: NTIS HC A09/MF A01

This informal glossary associated with supercomputers evolved casually. The primary draft was made in 1986 by the IEEE Subcommittee on Supercomputing. In addition, terms have been added and revised. Any rapidly advancing field generates its own new terminology. The new terms arise by applying new meanings to older terms as well as through the coining of new terminology. The process is dynamic and often results in dual meanings of commonly used words and sometimes just plain fuzzy definitions. Nevertheless, it is believed that this tabulation will: (1) help both novices and experts to better communicate, and (2) provide input to more formal dictionary/definition writing processes. Author

N89-11402# Air Force Inst. of Tech., Wright-Patterson AFB, Ohio.
AN INTRODUCTION TO IMPLEMENTING A CAPACITY PLANNING EFFORT IN AN MVS (MULTIPLE VIRTUAL STORAGE) ENVIRONMENT M.S. Thesis
Paul J. Waldowski 1988 58 p
(AD-A196383; AFIT/CI/NR-88-73) Avail: NTIS HC A04/MF A01 CSCL 12E

This thesis describes the development of a new capacity planning methodology to aid computer professionals working on implementing a capacity planning effort in an MVS (Multiple Virtual Storage) environment. The methodology developed utilizes the System Management Facility (SMF), the Resource Measurement Facility (RMF), and the Statistical Analysis System (SAS) in order to bring together many of the past computer performance evaluation ideas and to integrate them with current computer performance evaluation techniques and automated procedures. An automated approach is taken so computer professionals can devote their energies to analyzing and interpreting results, not gathering and calculating input factors. Subsequently, each MVS installation is supplied with the actual usage data to help set accurate user objectives and forecast for tomorrow's data processing needs. GRA

N89-11403# Air Force Inst. of Tech., Wright-Patterson AFB, Ohio.
THE USE OF PORTABLE MICROCOMPUTER AS A DATA COLLECTION TOOL TO SUPPORT INTEGRATED SIMULATION SUPPORT ENVIRONMENTS: A CONCEPT M.S. Thesis
James E. Wilkinson 1988 122 p
(AD-A196414; AFIT/CI/NR-88-76) Avail: NTIS HC A06/MF A01 CSCL 12E

While an integrated simulation environment provides a more organized structure for managing and performing simulation projects, and provides a database management structure for storing, manipulating, and analyzing data, they do not address the actual process of going out and obtaining the data. As a result, many of the common problems associated with poor problem and system definition, and low quality model input data, may still occur. To solve this problem, this study examines the concept of developing a support-support system; a portable microcomputer with software tools designed to support collection of the data, both subjective and objective, required in a simulation study. This data can then be ported into the integrated support system for analysis and model development. In developing this concept, the simulation process is better defined using structured analysis diagrams. Based on this analysis the functions that a support-support system could best accomplish are identified and a conceptual specification developed. An implementation strategy is proposed which is based on the use of readily available software tools, such as dBASE III, an the use of a simple programming language, such as BASIC. To demonstrate how this strategy can be implemented, a BASICA program was developed to support model input data collection. Using a graphic display to define input data requirements and single key inputs, this program should maximize the time an analyst can spend observing the system and minimize the time spent on entering data. GRA

N89-11404# Educational Testing Service, Princeton, N. J.
SCALE DRIFT IN ON-LINE CALIBRATION
Martha L. Stocking May 1988 134 p
(Contract N00014-83-K-0457; Proj. RR0-4204)
(AD-A196439; ETS-RR-88-28-ONR) Avail: NTIS HC A07/MF A01 CSCL 05H

Recent advances in psychometrics and computer technology encourage the development of model-based methods of individualized testing on a microcomputer, where each examines receives short tests and the number of pretest items that can be administered is severely restricted. On-line (i.e., data is collected on operational equipment) methods for calibrating pretest items in this setting face new challenges. In the context of adaptive testing, two LOGIST-based methods of on-line calibration were developed and are described. These two methods are tried out and compared in a simulation study using data for the CAT-ASVAB. GRA

N89-11405# California Univ., Berkeley. Electronics Research Lab.
OPTIMIZATION-BASED DESIGN OF CONTROL SYSTEMS Final Report, 31 Jul. 1986 - 30 Jul. 1987
Elijah Polak 13 Apr. 1988 4 p
(Grant AF-AFOSR-0247-86; AF Proj. 2917)
(AD-A196593; AFOSR-88-0542TR) Avail: NTIS HC A02/MF A01 CSCL 12F

A DEC MicroVax II GPX Color workstation has been acquired for experimentation with the DELIGHT.MIMO interactive software system in the solution of optimal, worst case design of multivariable control systems. A SUN workstation - based system has been expanded for experiments in distributed computing for the optimal, integrated design of flexible structures and their control systems. GRA

N89-10833# Electronique Serge Dassault, St. Cloud (France).
A HIGHLY RELIABLE COMPUTER FOR AIRBORNE APPLICATIONS
Michel Muenier *In* AGARD, Computing Systems Configuration for Highly Integrated Guidance and Control Systems Jun. 1988 17 p (For primary document see N89-10831 02-01)
Copyright Avail: NTIS HC A08/MF A01

N89-10837# Air Force Wright Aeronautical Labs., Wright-Patterson AFB, Ohio. Avionics Lab.
HIGH SPEED PARALLEL PROCESSING NETWORKS FOR ADVANCED ARCHITECTURES
D. Reed Morgan *In* AGARD, Computing Systems Configuration for Highly Integrated Guidance and Control Systems Jun. 1988 17 p (For primary document see N89-10831 02-01)
Copyright Avail: NTIS HC A08/MF A01

61 COMPUTER PROGRAMMING AND SOFTWARE

Includes computer programs, routines, alogorithms, and specific applications, e.g., CAD/CAM.

N89-11406*# Old Dominion Univ., Norfolk, Va. Dept. of Electrical and Computer Engineering.
STRATEGIES FOR CONCURRENT PROCESSING OF COMPLEX ALGORITHMS IN DATA DRIVEN ARCHITECTURES
Progress Report, 16 May 1987 - 15 May 1988
John W. Stoughton and Roland R. Mielke Jun. 1988 126 p
(Grant NAG1-683)
(NASA-CR-181329; NAS 1.26:181329) Avail: NTIS HC A07/MF A01 CSCL 09B

The purpose is to document research to develop strategies for concurrent processing of complex algorithms in data driven architectures. The problem domain consists of decision-free algorithms having large-grained, computationally complex primitive operations. Such are often found in signal processing and control applications. The anticipated multiprocessor environment is a data flow architecture containing between two and twenty computing elements. Each computing element is a processor having local program memory, and which communicates with a common global data memory. A new graph theoretic model called ATAMM which establishes rules for relating a decomposed algorithm to its execution in a data flow architecture is presented. The ATAMM model is used to determine strategies to achieve optimum time performance and to develop a system diagnostic software tool. In addition, preliminary work on a new multiprocessor operating system based on the ATAMM specifications is described. Author

N89-11407*# National Aeronautics and Space Administration. Langley Research Center, Hampton, Va.
OEXP ANALYSIS TOOLS WORKSHOP
L. Bernard Garrett, Robert L. Wright, Deborah Badi, and John T. Findlay (Flight Mechanics and Control, Inc., Hampton, Va.) Aug. 1988 146 p Workshop held in Hampton, Va., 21-22 Jun. 1988 Sponsored by NASA, Washington, D.C.
(NASA-CP-10013; NAS 1.55:10013) Avail: NTIS HC A07/MF A01 CSCL 09B

This publication summarizes the software needs and available analysis tools presented at the OEXP Analysis Tools Workshop held at the NASA Langley Research Center, Hampton, Virginia on June 21 to 22, 1988. The objective of the workshop was to identify available spacecraft system (and subsystem) analysis and engineering design tools, and mission planning and analysis software that could be used for various NASA Office of Exploration (code Z) studies, specifically lunar and Mars missions. Author

N89-11408# California Univ., Berkeley. Computer Science Div.
PRECISION-TIME TRADEOFFS: A PARADIGM FOR PROCESSING STATISTICAL QUERIES ON DATABASES
Jaideep Srivastava and Doron Rotem (California Univ., Berkeley. Lawrence Berkeley Lab.) May 1988 22 p Presented at the 4th International Working Conference on Statistical and Scientific Database Management, Rome, Italy, 21 Jun. 1988
(Contract DE-AC03-76SF-00098)
(DE88-012024; LBL-24767; CONF-8806166-1) Avail: NTIS HC A03/MF A01

Conventional query processing techniques are aimed at queries which access small amounts of data, and require each data item for the answer. In case the database is used for statistical analysis as well as operational purposes, for some types of queries a large part of the database may be required to compute the answer. This may lead to a data access bottleneck, caused by the excessive number of disk assesses needed to get the data into primary memory. An example is computation of statistical parameters, such as count, average, median, and standard deviation, which are useful for statistical analysis of the database. Yet another example that faces this bottleneck is the verification of the truth of a set of predicates (goals), based on the current database state, for the purposes of intelligent decision making. A solution to this problem is to maintain a set of precomputed information about the database in a view or a snapshot. Statistical queries can be processed using the view rather than the real database. A crucial issue is that the precision of the precomputed information in the view deteriorates with time, because of the dynamic nature of the underlying database. Thus the answer provided is approximate, which is acceptable under many circumstances, especially when the error is bounded. DOE

N89-11409 Illinois Univ., Urbana-Champaign.
REPRESENTING HIGH-LEVEL KNOWLEDGE STRUCTURES IN MASSIVELY PARALLEL NETWORKS Ph.D. Thesis
Hon Wai Chun 1987 125 p
Avail: Univ. Microfilms Order No. DA8803002

Traditional artificial intelligence (AI) research has concentrated mostly on modeling high-level thought processes such as problen-solving and planning, and high-level representations such as rule-based heuristics and frame-based knowledge structures. Massively parallel networks were used mainly to model low-level perceptual processes such as vision, speech, associative memory, and learning. Recent research has started to bridge the gap between these disciplines. However, many difficult issues need to be solved before massively parallel techniques can become more applicable and be able to complement traditional AI techniques. These issues include the problem of variable binding, multiple instantiations of knowledge structures, recursion, hierachical abstraction, and temporal constraints. These problems are explored through the presentation of massively parallel models for schema structures, an approach to defining knowledge modules, and a model to represent rules. The massively parallel representational techniques introduced include a representation of constraints which was used to model schemata with temporal sequence constraints, a representation of modular knowledge structures that were used to model adaptive competition as well as interactions among higher-order concepts, a hybrid schema representation which combines connectionist value-passing with marker passing, and a hybrid natural language rule-based system. These techniques were implemented and successfully tested in applications such as speech recognition and natural language understanding.
Dissert. Abstr.

N89-11410# National Aeronautical Lab., Bangalore (India). Systems Engineering Div.
ADAPTIVE FILTERING ALGORITHMS FOR COMMUNICATIONS SIGNAL PROCESSING
J. R. Raol Mar. 1988 15 p
(PD-SE-8808) Avail: NTIS HC A03/MF A01

The effect of eigenvalue spread in the signal is studied. The performances of Least Mean Squares (LMS), Recursive Least Squares (RLS) and Fast Transversal Filter (FTF) algorithms via numerical simulation for channel equalization problem and identification of unknown tap-weights of transversal structure are compared. This exposition, with a touch of tutorial and extensive numerical results would provide valuable insight into the problem of adaptive filtering and application of competitive algorithms to satellite and other communications signal processing problems.
Author

N89-11411# California Univ., Berkeley. Lawrence Berkeley Lab.
PROGRAMMING ABSTRACTIONS FOR RUN-TIME PARTITIONING OF SCIENTIFIC CONTINUUM CALCULATIONS RUNNING ON MULTIPROCESSORS
S. B. Baden Jan. 1988 12 p Presented at the 3rd SIAM Conference on Parallel Processing for Scientific Computing, Los Angeles, Calif., 1 Dec. 1987
(Contract DE-AC03-76SF-00098)
(DE88-007376; LBL-24643; CONF-871251-5) Avail: NTIS HC A03/MF A01

The author discusses a set of software abstractions for implementing various math-physics calculations on a team of processors. He tried out the abstractions on Anderson's Method

of Local Corrections, a type of vortex method for computational fluid dynamics. He ran experiments on 32 processors of the Intel iPSC - a message-passing hypercube architecture - and on 4 processors of a Cray X-MP - a shared-memory vector architecture - and achieved good parallel speedups of 24 and 3.6 respectively. The abstractions should apply to diverse applications, including finite difference methods, and to diverse architectures without requiring that the application be reprogrammed extensively for each new architecture. DOE

N89-11412# National Bureau of Standards, Gaithersburg, Md. Information Systems Engineering Div.
STANDARDS CONFORMANCE TESTING Report, 1980 - 1987
Sharon J. Kemmerer May 1988 61 p
(PB88-215645; NBSIR-88/3768) Avail: NTIS HC A04/MF A01 CSCL 09B

The NBSIR suggests a process to follow when developing a conformance testing program for appropriate NBS/ICST Federal Information Processing Standards (FIPS). These FIPS and the standards they are promoting are implemented into software products by commercial use. A consistent application of testing processes and specific test suites will help align commercial products to conform to these standards. Application of such a testing process will become more critical as Federal agencies begin to request procurement of software implementing these standards. GRA

N89-11413# California Inst. of Tech., Pasadena.
AN O(NlogN) HYPERCUBE N-BODY INTEGRATOR
Mike Warren and John Salmon 1988 5 p
(Contract DE-FG03-85ER-25009)
(DE88-015016; DOE/ER-25009/593) Avail: NTIS HC A02/MF A01

The gravitational N-body algorithm of Barnes and Hut has been successfully implemented on a hypercube concurrent processor. The novel approach of their sequential algorithm has demonstrated itself to be well suited to hypercube architectures. The sequential code achieves O(NlogN) speed by recursively dividing space into subcells, thereby creating a hierarchical grouping of particles. Computing interactions between these groups dramatically reduces the amount of communication between processors, as well as the number of force calculations. Parallelism is achieved through an irregular spatial grid decomposition. Since the decomposition topology is not simple, a general loosely synchronous communication routine has been developed. Operations are simplified if the conventional grey code decomposition is modified so that the bits are taken alternately from each cartesian dimension. A speedup of 180 has been achieved for a 500,000 particle two-dimensional calculation on 256 processors. A speedup of 65 has been obtained for a 64,000 particle three-dimensional calculation on 256 processors. DOE

N89-11414# Groningen Rijksuniversiteit (Netherlands). Dept. of Mathematics and Computing Science.
PARALLEL ALGORITHM FOR A CLASS OF OPTIMIZATION PROBLEMS
Johan J. Lukkien 19 Feb. 1988 14 p
(PB88-209929; CS-8806) Avail: NTIS HC A03/MF A01 CSCL 09B

Many optimization problems consist of searching for an optimal value in the leaves of some kind of a tree. A class of such problems for which a method known as branch and bound is often used is considered. A parallel algorithm is developed which dynamically balances the load on the network on which it runs. A sequential algorithm which is used as the basis for the development of the parallel algorithm is examined. The 0/1 knapsack problem is used as an example, and some experimental results are given. Author

N89-11415 Loughborough Univ. of Technology (England).
FINITE ELEMENTS SOFTWARE AND APPLICATIONS Ph.D. Thesis
Ahmed Sharaf EldinAhmed 1987 655 p
Avail: Univ. Microfilms Order No. BRDX80025

The contents of this thesis are a study of the software for the finite element method. The finite element method is introduced from both the engineering and mathematical points of view. The computer implementation of the method is explained with samples of mainframe, mini- and micro-computer implementations. A solution is presented for the problem of limited stack size for both mini- and microcomputers with stack architectures. Several finite element programs are presented. Special purpose programs to solve problems in structural analysis and groundwater flow are discussed. However, an efficient easy-to-use finite element program for general 2-D problems is presented. Several problems in groundwater flow are considered that include steady, unsteady flows in different types of aquifers. Different cases of sinks and sources in the flow domain are also considered. The performance of finite element methods are also considered. The performance of finite element methods is studied for the chosen problems by comparing the numerical solutions of test problems with analytical solutions (if they exist) or with solutions obtained by other numerical methods. The polynomial refinement of the finite elements is studied for the problems presented in order to offer some evidence as to which finite element simulation is best to use under a variety of circumstances. Dissert. Abstr.

N89-11416# Sandia National Labs., Albuquerque, N. Mex.
TRINITY II: A POST-PROCESSING PROGRAM FOR 2-DIMENSIONAL FINITE ELEMENT ANALYSIS DATA
J. H. Glick and D. K. Gartling May 1988 70 p
(Contract DE-AC04-76DP-00789)
(DE88-010107; SAND-88-0896) Avail: NTIS HC A04/MF A01

TRINITY II is a program for post-processing data from two-dimensional finite element analyses. The program provides graphical display of mesh and solution data as well as data manipulation, file editing and selective printing of data. TRINITY II accepts data from any analysis code that employs the EXODUS file format; post-processing can be done interactively or in batch mode using any graphics device supported by the Sandia Virtual Device Interface. The capabilities and use of the program are described. DOE

N89-11417# Lawrence Livermore National Lab., Calif.
GUIDELINES FOR USING TIPSFD FOR 3D FINITE-DIFFERENCE MESH GENERATION
G. W. Laguna May 1988 41 p
(Contract W-7405-eng-48)
(DE88-012451; UCID-21437) Avail: NTIS HC A03/MF A01

This report presents information to give users of the TIPSFD code a better understanding of how it can be used to generate finite-difference meshes. In particular, this report presents in detail all of the mesh generation parameters and the rationale behind them, in addition to guidelines for creating the initial solid model. This report also presents recently developed features for generating meshes as well as a complete example from solid model creation to mesh generation. DOE

N89-11418# Instituto de Pesquisas Espaciais, Sao Jose dos Campos (Brazil).
COLOR ENHANCEMENT OF REMOTE SENSING IMAGERY USING IHS TRANSFORMATIONS AND DECORRELATION STRETCH METHODS
Luciano VieiraDutra, Paulo Roberto Meneses (Brasilia Univ., Brazil), and Waldir R. Paradella Jun. 1988 11 p
(INPE-4559-PRE/1300) Avail: NTIS HC A03/MF A01

Two digital color image processing methods for providing color contrast stretch and improvement of visual interpretation of remote sensing imagery are presented and compared. The first methodology is based on the transformation of the image represented in RGB coordinates to perception independent IHS (intensity, hue, saturation) coordinates. In IHS space it is possible to process each component independently, therefore achieving better control over the color. Examples of such process include linear operations and hue shifts. After the color enhancement,

high pass filtering operation can be performed to enhance spatial detail. The second methodology is the well known decorrelation method, where a decorrelating spectral rotation is performed, followed by a standard deviation equalization among channels and finally a rotation back to the original coordinate system. Several experiments with LANDSAT TM images were made. The results proved to be valuable and different enhancement procedures were suitable for different observations. Author

N89-11419# Instituto de Pesquisas Espaciais, Sao Jose dos Campos (Brazil).
THE CHECKOUT SYSTEM SOFTWARE FOR THE BRAZILIAN SATELLITE
F. E. C. Viola, D. T. Fernandes, M. J. C. Ciurria, M. C. A. Amorim, and A. R. Benatti May 1988 11 p Prepared for presentation at the 3rd Congresso Latino Americano de Automatica, 3-7 Oct. 1988, Vina del Mal, Chile Submitted for publication
(INPE-4571-PRE/1311) Avail: NTIS HC A03/MF A01

This project was developed in the context of the first Brazilian Space Mission and is part of the Integration and Test Laboratory at INPE-Sao Jose dos Campos. The checkout system software constitutes a tool that, interposed between the test engineer and the electrical and electonric subsystems under test, processes the flow of information and the user commands during the integration and test phases. The digital information received by the computer is properly treated, checked, and translated in a high level graphic form, to be displayed and interpreted by the test engineer. Conceptually, the importance of such a tool is to give a great agility to the integration and test tasks, and its absence would make impossible for a human operator to interpret the great amount of information and interfere in all the real time process. The main user requirements specified to this tool concerns three aspects of a real time system: the automatic checking mechanisms, an interactive programming power and mechanisms to implement data synthesis and high level graphic presentation of the satellite subsystem status during the test activities. In addition, the configuration of this software tool demands some offline capabilities, to generate an operational data base, during the data preparation phase. These data files are accessed by the on line functions. This is the first spacecraft checkout system produced in Brazil, and the applicative software was completely projected and implemented at INPE. Author

N89-11420# California Inst. of Tech., Pasadena.
LATTICE GAUGE THEORY ON THE HYPERCUBE
John Apostolakis, Clive Baillie, Hong-Qiang Ding, and Jon Flower 1988 10 p
(Contract DE-FG03-85ER-25009)
(DE88-015004; DOE/ER-25009/605) Avail: NTIS HC A02/MF A01

Lattice gauge theory, an extremely computationally intensive problem, has been run successfully on hypercubes for a number of years. Herein we give a flavor of this work, discussing both the physics and the computing behind it. DOE

N89-11421# Stanford Univ., Calif. Dept. of Operations Research.
THE FROBENIUS METRIC IN IMAGE REGISTRATION
Karel Zikan and Teresa M. Silberberg (Hughes Aircraft Co., Calabasas, Calif.) Jul. 1988 48 p
(Contracts DE-FG03-87ER-25028; N00014-85-K-0343; NSF DMS-84-20623)
(DE88-016685; SU-SOL-88-13) Avail: NTIS HC A03/MF A01

Image registration involves estimating how one set of n-dimensional points is rotated, scaled, and translated into a second set of n-dimensional points. In practice, n is usually 2 or 3. A Frobenius norm approach is considered in which a point-to-point matching between the sets (if they are of the same cardinalities) and the corresponding transformation are determined. Two strategies are investigated: the pruned tree approach and the parametric linear programming approach. Various versions of tree pruning approach have been investigated by other authors, whereas the parametric programming method is believed to be new. It addresses several inherent problems of the tree pruning method. Both approaches determine the rotation after scale and translation are removed. In the pruned tree approach, possible matchings of 2- or 3-D dimensional points are partially enumerated using a tree search; the tree is pruned according to criteria based on the metric. The parametric approach solves an assignment problem for a number of candidate rotations. Each evaluation results in the point-to-point correspondence; the optimal matching corresponds to the rotation that minimizes the associated cost function. This approach, which has $O(k^3)$ worst case asymptotic complexity, is more tolerant of noise than the pruned tree approach and can be readily extended to the cases where the sets to be registered are of different cardinalities. DOE

N89-11422# Edinburgh Univ. (Scotland). Integrated Systems Group.
ENGEN: AN INTERMEDIATE LANGUAGE TO HILO EXTENSION OF THE FIRST SILICON COMPILER, EXECUTIVE SUMMARY
S. G. Smith, P. B. Denyer, and J. I. Mhar Paris, France ESA 10 Mar. 1988 17 p
(Contract ESTEC-6275/85-NL-PP(SC))
(ESA-CR(P)-2621; ETN-88-93043) Avail: NTIS HC A03/MF A01

The extension of a VLSI silicon compiler (FIRST) to a process-independent form, capable of implementing complex signal processing systems in the CMOS-SOS technology of ESTEC's two primary CMOS-SOS suppliers, and with the potential to incorporate the cell-libraries of other CMOS-SOS vendors, is described. The ENGEN is a FIRST-to-HILO compiler, which directly replaces the physical design subsystem of FIRST. A PRIMITIVE generator library is included in ENGEN, which is sufficiently comprehensive to realize a trial 6-point FIR filter device. Through the structural decomposition of computational elements into universally available logic elements, and the provision of tables for syntax translation between internal representations and vendor's representations of these logic elements, the HILO output of ENGEN is made portable between vendors. An option is included for the user to specify collections of logic elements in more efficient form, using standard-cell library configurations provided by the vendor. A library of such elements, optimized for MEDL CELLSOS, is included in the ENGEN package. ESA

N89-11423# Centre National d'Etudes Spatiales, Toulouse (France).
THE VECTOR FUNCTIONS OF THE MS SYSTEM 570/CX
E. Goddaert and J. C. Berges 21 Jan. 1986 92 p In FRENCH; ENGLISH summary
(CNES-CT/DTI/MS/MN/019; ETN-88-93092) Avail: NTIS HC A05/MF A01

The vector subroutine capabilities provided by a software library on the Matra data system 570/CX are summarized. The functions are microcoded and are accessible to any FORTRAN program. ESA

N89-11424# Centre National d'Etudes Spatiales, Toulouse (France).
PRESENTATION OF RESEARCH AND DEVELOPMENT ACTION 1206: PRELIMINARY STUDY REPORT ON THE CESTAC METHOD
J. C. Berges 7 Mar. 1986 44 p In FRENCH; ENGLISH summary
(CNES-CT/PTI/MS/MN/067; ETN-88-93093) Avail: NTIS HC A03/MF A01

A stochastic method for checking and estimating the rounding off of calculations was developed. The method is proposed for onboard signal processing, and automatic navigation programs, involving fixed point and single precision floating point arithmetic, respectively. ESA

N89-11425# Centre National d'Etudes Spatiales, Toulouse (France).
VECTORIZATION TECHNIQUES ON THE MD SYSTEM 570/CX

E. Goddaert and J. C. Berges 3 Jun. 1986 81 p In FRENCH; ENGLISH summary
(CNES-CT/DTI/MS/MN/147; ETN-88-93095) Avail: NTIS HC A05/MF A01

Vectorization techniques (CPU performances, accuracy) on the extended Kalman filter using the vector functions of the MD system 570/CX are assessed. Tests show that the calculator has vector manipulation primitive capabilities, but cannot be considered as a vector processor, since data are manipulated as scalars. The most efficient use of the machine is to exploit its microprogramming aspects to speed up small parts of critical codes. ESA

N89-11426# Centre National d'Etudes Spatiales, Toulouse (France). Dept. de Mathematiques et Analyse Numerique.
OBJECT ORIENTED SOFTWARE ENGINEERING WITH Ada
F. Laporte 18 Dec. 1986 31 p In FRENCH; ENGLISH summary
(CNES-CT/DTI/MS/MN/326; ETN-88-93097) Avail: NTIS HC A03/MF A01

Software quality and life cycle, and methods to produce good software are reviewed. An object oriented software development methodology is outlined. Ada as an object oriented software development tool, and Ada for artificial intelligence applications are evaluated. An Ada object oriented approach to designing a mini expert system is illustrated. ESA

N89-11427# Instituto de Pesquisas Espaciais, Sao Jose dos Campos (Brazil).
CONCERNING THE USE OF THE MINIMUM MEAN ASYMMETRY AS THE VALIDATION CRITERIA FOR CLUSTERING
Luciano VieiraDutra and Jose Carlos Moreira Aug. 1988 14 p In PORTUGUESE; ENGLISH summary Presented at the 3rd Brazilian Symposium on Remote Sensing, Rio de Janeiro, Brazil, 28-30 Nov. 1984
(INPE-4654-PRE/1361) Avail: NTIS HC A03/MF A01

One of the main problems with the application of clustering algorithm is the evaluation of the results in order to decide if the clusters correspond to real targets (this is known as validity studies). A well-known condition stablish that features describing natural targets follow a Gaussian or at least a symetrical and unimodal distribution is zero. So, by calculating this momentum for all clusters in a given partition, one can determine if this partition is composed of symmetrical distributions. The proposed method consists of partitioning the data in several number of classes using the well-known K-mean algorithm, and choosing the partition that yields the minimum meas asymmetry for all partitions. The method was tested with several groups of data, each one containing a certain number of classes known a priori. Other known validity methods were applied for the same groups of data. The results demonstrate that the mean asymmetry criterion led to partitions that in most cases were near the reality, with a better performance than the other methods that were tested. Author

N89-11428# Grenoble-1 Univ. (France). Lab. de Genie Informatique.
ETIC: A MULTI-USER COMPUTER AIDED DESIGN (CAD) DATABASE MANAGEMENT SYSTEM
Marie-Christine Fauvet May 1988 22 p
(Contract PRC-8/87/BO8200-1980-01-1)
(RR-720-I; ETN-88-93270) Avail: NTIS HC A03/MF A01

A multi-user system for Computer Aided Design (CAD) applications, which offers a formalism and assistance for describing a CAD activity is presented. It allows users to describe and manipulate CAD objects in a project environment. During the project lifetime, it allows definition, checking and merging of project team tasks. The proposed system offers a design environment where it is possible to cooperate and exchange tools, structures, and objects according to initial project rules. The originality of the system consists in the fact that it manages work sharing and task merging. It also offers tools to express object structures, to manipulate objects assuming the dynamic management of links and constraints defined in object structures. ESA

N89-11429# Grenoble-1 Univ. (France). Lab. d'Informatique Fondamentale et d'Intelligence Artificielle.
PARALLELIZING RECURSIVE PROGRAMS
Jean-Michel Hufflen May 1988 14 p Sponsored in part by European Economic Commission ESPRIT project 415 and CNRS, France
(RR-728-I-IMAG-83-LIFIA; ETN-88-93275) Avail: NTIS HC A03/MF A01

A method for transforming recursive functional definitions into parallel programs is proposed. The obtained network presents a diamond and pipelined architecture. The topology of this network is statically fixed; nevertheless, it can simulate an arbitrarily deep recursive stack. The correctness of the transformation is proved. ESA

N89-11430# Washington Univ., Seattle. Dept. of Computer Science.
POKER (4.0): A PROGRAMMER'S REFERENCE GUIDE
Lawrence Snyder Aug. 1987 86 p
(Contract N00014-86-K-0264)
(AD-A196417) Avail: NTIS HC A05/MF A01 CSCL 12E

This document gives a succinct description of the facilities available with the Poker Programming Environment. The emphasis is on what is available rather than how to achieve particular results. Although the sections are self-contained, so that they may be referred to independently, there are a few things you should know: (1) Poker uses interactive graphics. The graphics are described in Section 2; the interaction is described in Section 3; (2) The usual programming language notion of a source program as a monolithic piece of symbolic text has been replaced in Poker by a database. The way to create, view, and change the database is described in Section 4; (3) Object programs (the compiled database) are executed or emulated by Poker and snapshots of the execution can be continuously displayed; (4) Poker supports a variety of CHiP architectures; the current one can be displayed or changed using the CHiP Parameters facility, Section 7; (5) The back page of this document gives a summary of the command; and (6) Other versions of Poker exist; consult Appendix B for your particular system. GRA

N89-11431# Washington Univ., Seattle. Dept. of Computer Science.
POKER (4.1): A PROGRAMMER'S REFERENCE GUIDE
Lawrence Snyder Apr. 1988 97 p
(Contract N00014-86-K-0264; NSF CCR-84-16878)
(AD-A196419; TR-83-03-03) Avail: NTIS HC A05/MF A01 CSCL 12E

This document gives a succinct description of the facilities available with the Poker Parallel Programming Environment. The emphasis is on what is available rather than how to achieve particular results. Although the sections are self-contained, so that they may be referred to independently, there are a few things you should know: (1) Poker uses interactive graphics. The graphics are described in Section 2; the interaction is described in Section 3; (2) The usual programming language notion of a source program as a monolithic piece of symbolic text has been replaced in Poker by a database. The way to create, view, and change the database is described in Section 4; (3) Object programs (the compiled database) are executed or emulated by Poker and snapshots of the execution can be continuously displayed; (4) Poker supports a variety of CHiP architectures; the current one can be displayed or changed using the CHiP Parameters facility; Section 7; (5) The back page of this document gives a summary of the commands; and (6) Other versions of Poker exists; consult Appendix B for your particular system. GRA

N89-11432# Colorado Univ., Boulder. Dept. of Electrical and Computer Engineering.
LATTICE ALGORITHMS FOR COMPUTING QR AND CHOLESKY FACTORS IN THE LEAST SQUARES THEORY OF LINEAR PREDICTION
Cedric J. Demeure and Louis L. Scharf Sep. 1987 40 p

(Contract N00014-85-K-0256)
(AD-A196454; CU/ONR/1) Avail: NTIS HC A03/MF A01 CSCL 12B

This paper poses a sequence of linear prediction problems that are a little different from those previously posed. By solving the sequence of problems we are able to QR factor data matrices of the type usually associated with correlation, pre and post-windowed, and covariance methods of linear prediction. Solutions cover the forward, backward, and forward-backward problems. The QR factor orthogonalizes the data matrix and solves the problem of Cholesky factoring the experimental correlation matrix and its inverse. This means we may use generalized Levinson algorithms to derive generalized QR algorithms, which are then used to derive generalized Schur algorithms. All three algorithms are true lattice algorithms that may be implemented either on a vector machine or on a multi-tier lattice, and all three algorithms generate generalized reflection coefficients that may be used for filtering or classification. GRA

N89-11433# Massachusetts Inst. of Tech., Cambridge. Artificial Intelligence Lab.
AN O(N) ALGORITHM FOR THREE-DIMENSIONAL N-BODY SIMULATIONS M.S. Thesis
Feng Zhao Oct. 1987 74 p
(Contract N00014-86-K-0180)
(AD-A196903; AI-TR-995) Avail: NTIS HC A04/MF A01 CSCL 03C

The author presents an algorithm that computes the gravitational potentials and forces on N point-masses interacting in three-dimensional space. The algorithm, based on analytical techniques developed by Rokhlin and Greengard, runs in order N time. In contrast to other fast N-body methods such as tree codes, which only approximate the interaction potentials and forces, this method is exact; it computes the potentials and forces to within any prespecified tolerance up to machine precision. Presented is an implementation of the algorithm for a sequential machine. The author numerically verifies the algorithm, and compares its speed with that of an O(sq N) direct force computation. He also describes a parallel version of the algorithm that runs on the Connection Machine in order O(log N) time. This document compares experimental results with those of the sequential implementation and discusses how to minimize communication overhead on the parallel machine. GRA

N89-11434# Mitre Corp., Bedford, Mass.
SOFTWARE MANAGEMENT METRICS Final Report
Herman P. Schultz May 1988 52 p
(Contract F19628-86-C-0001)
(AD-A196916; M88-1; ESD-TR-88-001) Avail: NTIS HC A04/MF A01 CSCL 12E

The metrics presented in this document are used to monitor the progress of a software development offer. They provide visibility into developing trends and thereby can be used to forecast potential problems. These metrics are based on Government and industry experiences with a previous set of their use. The term reporting has been changed to management to more precisely describe the metrics' application. This new report includes: a total of 10 metrics instead of 8; 4 new metrics (design progress, design complexity, schedule progress, and requirements volatility); reporting and analysis recommendations; structured descriptions for each metric that include tailoring, interpretation, and behavior discussions; sample Data Item Description (DID) backup sheets for requiring metrics; notes on applications to Ada; and charting and presentation recommendations. GRA

N89-11435# California Univ., San Diego, La Jolla.
THREE-DIMENSIONAL COMPUTER GRAPHICS BRAIN-MAPPING PROJECT Final Report, 10 Mar. - 24 Dec. 1987
Robert B. Livingston 24 Mar. 1988 151 p
(Contract DAMD17-86-C-6093)
(AD-A197053) Avail: NTIS HC A08/MF A01 CSCL 06D

A core group was assembled at UCSD and the Scripps Clinic and Research Foundation, which, together with participating national advisors, could solve problems that stand in the way of engaging computer graphics and database management more effectively in the solution of neurosciences problems. We aimed at improving the interface between neuroanatomy and computer graphics systems so that the groundwork for accurate quantitative morphology will be satisfactory from the neurosciences viewpoint in proceeding to achieve whole brain reconstructions. We have succeeded in developing sound methods for preparing whole brains for sectioning and microscopic analysis, with controls for reducing brain distortions in three dimensions and for correcting the inevitable distortions that accompany slicing brain tissue at microscopic intervals, for combining structure/function data, and for beginning an analysis of whole brain tissue sections at microscopic levels of detail. GRA

N89-11397# Boeing Computer Services Co., Seattle, Wash.
ALGORITHM AND GENERAL SOFTWARE CONSIDERATIONS
Ken W. Neves *In* AGARD, Computational Fluid Dynamics: Algorithms and Super Computers Mar. 1988 p 55-98 (For primary document see N89-11395 02-60)
Copyright Avail: NTIS HC A09/MF A01

N89-11398# Technische Univ., Regensburg (West Germany).
VECTORIZATION OF FORTRAN PROGRAMS AT DO-LOOP LEVEL
W. Gentzsch *In* AGARD, Computational Fluid Dynamics: Algorithms and Super Computers Mar. 1988 p 99-108 (For primary document see N89-11395 02-60)
Copyright Avail: NTIS HC A09/MF A01

N89-11399# Technische Univ., Regensburg (West Germany).
RESTRUCTURING OF BASIC LINEAR ALGEBRAIC ALGORITHMS, CHAPTER 5
W. Gentzsch *In* AGARD, Computational Fliud Dynamics: Algorithms and Super Computers Mar. 1988 p 109-139 (For primary document see N89-11395 02-60)
Copyright Avail: NTIS HC A09/MF A01

62 COMPUTER SYSTEMS

Includes computer networks and special application computer systems.

N89-11436# Michigan State Univ., East Lansing.
MODELS FOR PARALLEL COMPUTATION ON DISTRIBUTED-MEMORY MULTIPROCESSORS
Chung-Ta King and L. M. Ni (Argonne National Lab., Ill.) 1988 25 p Presented at the International Conference on Parallel Processing, University Park, Pa., 15 Aug. 1988 Prepared in cooperation with Argonne National Lab., Ill.
(Contract W-31-109-eng-38)
(DE88-010078; CONF-880856-1) Avail: NTIS HC A03/MF A01

The most severe shortcoming of distributed-memory multiprocessors is the communication overhead. Due to the distributed nature of such systems, data must be moved explicitly among the processors, including the host, so as to carry out a computing job. Efficient algorithm design becomes crucial in fully utilizing the computing power of the multiprocessors. In this paper a model for parallel computation is proposed, which views a computation as consisting of a hierarchy of multiple logical pipelines. The multiprocessor is organized as pipelines to perform the computation, which takes advantage of overlapped communication and computation in the pipelines to reduce the communication overhead in the system. An analytic model is introduced to characterize the effects of partitioning and pipelining on the resulting performance. Through such analyses, important design parameters can be determined and efficient algorithms will result. Three examples are discussed to illustrate the application of the models. Performance analysis through the analytic model shows an almost linear speedup using overlapped and pipelined operations. DOE

N89-11437# Los Alamos National Lab., N. Mex. Computational Physics Group.
PARALLEL PROCESSING A REAL CODE: A CASE HISTORY
David A. Mandell and Harold E. Trease 1988 21 p Presented at the Workshop on Instrumentation for Future Parallel Systems, Santa Fe, N. Mex., 19 May 1988
(Contract W-7405-eng-36)
(DE88-014456; LA-UR-88-1836; CONF-8805169-1) Avail: NTIS HC A03/MF A01

A three-dimensional, time-dependent Free-Lagrange hydrodynamics code has been multitasked and autotasked on a Cray X-MP/416. The multitasking was done by using the Los Alamos Multitasking Control Library, which is a superset of the Cray multitasking library. Autotasking is done by using constructs which are only comment cards if the source code is not run through a preprocessor. The 3-D algorithm has presented a number of problems that simpler algorithms, such as 1-D hydrodynamics, did not exhibit. Problems in converting the serial code, originally written for a Cray 1, to a multitasking code are discussed. Autotasking of a rewritten version of the code is discussed. Timing results for subroutines and hot spots in the serial code are presented and suggestions for additional tools and debugging aids are given. Theoretical speedup results obtained from Amdahl's law and actual speedup results obtained on a dedicated machine are presented. Suggestions for designing large parallel codes are given. DOE

N89-11438# Instituto de Pesquisas Espaciais, Sao Jose dos Campos (Brazil).
SOPMCR: AN OPERATING SYSTEM FOR THE MULTIPROCESSOR FOR COMMUNICATION NETWORKS
Eliane Martins, Ana Maria Ambrosio, and Sergio Katsumi Oshiro Aug. 1988 270 p In PORTUGUESE; ENGLISH summary
(INPE-4675-NTE/284) Avail: NTIS HC A12/MF A01

This work presents a distributed system developed at INPE, designed for the Multiprocessor for Network Communications (MCR). The system supports execution of application processes by request from other processes or external events. These processes communicate with each other by asynchronously exchanging messages; the use of a logical entity called channel permits the interprocess communications, independently of where the processes are being executed. The MCR was designed to be part of a packet-switching communications subnetwork node, among other applications; therefore the system must support the implementation of the lower layers of a communications protocol (layers 2 and 3 in the ISO/OSI architecture). Author

N89-11439# Massachusetts Inst. of Tech., Cambridge. Lab. for Information and Decision Systems.
COMMUNICATION ASPECTS OF PARALLEL PROCESSING
Cueneyt Oezveren 4 Dec. 1988 51 p
(Grant AF-AFOSR-0032-88; AF Proj. 2304)
(AD-A196458; LIDS-P-1721; AFOSR-88-0618TR) Avail: NTIS HC A04/MF A01 CSCL 12D

Parallel processing was motivated by the need to solve very large computational problems, such as the numerical solutions of partial differential equations in the context of computational fluid dynamics, structural mechanics, image processing, etc. This report surveys recent literature on parallel processing algorithms for mainly rings, meshes, and hypercubes. These algorithms include vector, matrix computations, fixed point iterations and linear equation solvers. A group property of above topologies has also been explored in an attempt to develop tools for algorithms and performance analysis. Some special sparsity structure of the iteration dependencies has also been examined. A necessary and sufficient condition for the reducibility of a dependency matrix with sparse, nonzero extended diagonals has been derived. GRA

63 CYBERNETICS

Includes feedback and control theory, artificial intelligence, robotics and expert systems.

For related information see also *54 Man/System Technology and Life Support.*

N89-11440*# University of Central Florida, Orlando. Dept. of Computer Engineering.
AUTOMATED KNOWLEDGE GENERATION Final Report, 1st Year
Harley R. Myler and Avelino J. Gonzalez 28 Sep. 1988 17 p
(Grant NAG10-0042)
(NASA-CR-181317; NAS 1.26:181317) Avail: NTIS HC A03/MF A01 CSCL 09B

The general objectives of the NASA/UCF Automated Knowledge Generation Project were the development of an intelligent software system that could access CAD design data bases, interpret them, and generate a diagnostic knowledge base in the form of a system model. The initial area of concentration is in the diagnosis of the process control system using the Knowledge-based Autonomous Test Engineer (KATE) diagnostic system. A secondary objective was the study of general problems of automated knowledge generation. A prototype was developed, based on object-oriented language (Flavors). Author

N89-11441*# Jet Propulsion Lab., California Inst. of Tech., Pasadena.
KNOWLEDGE-BASED DIAGNOSIS FOR AEROSPACE SYSTEMS
David J. Atkinson 15 Mar. 1988 32 p
(Contract NAS7-918)
(NASA-CR-182641; NAS 1.26:182641; JPL-Publ-88-7) Avail: NTIS HC A03/MF A01 CSCL 09B

The need for automated diagnosis in aerospace systems and the approach of using knowledge-based systems are examined. Research issues in knowledge-based diagnosis which are important for aerospace applications are treated along with a review of recent relevant research developments in Artificial Intelligence. The design and operation of some existing knowledge-based diagnosis systems are described. The systems described and compared include the LES expert system for liquid oxygen loading at NASA Kennedy Space Center, the FAITH diagnosis system developed at the Jet Propulsion Laboratory, the PES procedural expert system developed at SRI International, the CSRL approach developed at Ohio State University, the StarPlan system developed by Ford Aerospace, the IDM integrated diagnostic model, and the DRAPhys diagnostic system developed at NASA Langley Research Center. Author

N89-11442 Purdue Univ., West Lafayette, Ind.
PRACTICAL APPLICATIONS AND LIMITATIONS OF ADAPTIVE CONTROL Ph.D. Thesis
Duane Loren Mattern 1987 348 p
Avail: Univ. Microfilms Order No. DA8807645

The practical application and the limitation of the present methods of adaptive control are investigated. The predictive control of the steam temperature in an electric power plant during start-up is simulated. The model contains two lumped heat exchangers and two stages of water attempering including the spray valve dynamics. A modified temperature ramp yields bounded parameter estimate via persistent excitation. Published methods of adaptive control are revealed to have common structures and adaptation algorithms. The composition of the error signal that drives the parameter estimation scheme is shown to be the limitation of adaptive control in terms of robust stability. The robust stability problem of adaptive control is demonstrated on a second order, weakly nonlinear system (a four cylinder pneumatic engine) with measurement noise and unmodelled dynamics. Persistent excitation is shown to be a means of obtaining robust stability for this system. Dissert. Abstr.

N89-11443# Deutsche Forschungs- und Versuchsanstalt fuer Luft- und Raumfahrt, Oberpfaffenhofen (West Germany). Inst. fuer Dynamik der Flugsysteme.
THE DFVLR MODELS 1 AND 2 OF THE MANUTEC r3 ROBOT
Martin Otter and Stefan Tuerk May 1988 49 p
(DFVLR-Mitt-88-13; ISSN-0176-7739; ETN-88-93181) Avail: NTIS HC A03/MF A01; DFVLR, VB-PL-DO, 90 60 58, 5000 Cologne, Federal Republic of Germany, 20 deutsche marks

A mathematical model of the dynamics of the Manutec r3 robot is described. The model has different degrees of complexity, depending on the effects investigated. Model 1 is a multibody model with 6 degrees of freedom, and model 2 is a model with 3 degrees of freedom. The numerical values of all model parameters are given, and FORTRAN 77 subroutines are documented to numerically evaluate the equations of motion of the 2 models. Most of the model parameters were acquired by measurements in the laboratory. The FORTRAN 77 subroutines are generated symbolically by a multibody program. The mathematical models may be applied for supporting computer-aided control design, dynamic trajectory planning, and dynamic simulations. ESA

N89-11444# Deutsche Forschungs- und Versuchsanstalt fuer Luft- und Raumfahrt, Oberpfaffenhofen (West Germany). Abteilung Automatisierung.
DYNAMIC ROBOT MODELS USING THE MANUTEC r3 AS AN EXAMPLE
Stefan Tuerk Apr. 1988 87 p In GERMAN; ENGLISH summary Report will also be announced as translation (ESA-TT-1132)
(DFVLR-Mitt-88-16; ISSN-0176-7739; ETN-88-93184) Avail: NTIS HC A05/MF A01; DFVLR, VB-PL-DO, 90 60 58, 5000 Cologne, Federal Republic of Germany, 32 deutsche marks

A mathematical, dynamical model for the description of the motions of a robot is outlined. The components of the robot are assumed to be rigid bodies. The movement of the bodies is described by the equations of motion, which include all effects like variable moments of inertia, and centrifugal and Coriolis terms. Elasticity, backlash, and friction in the links are represented by force laws. The inputs of the model are the reference values of the motor's current controllers. These determine the torques in the links via the dynamics of the motors. ESA

N89-11445# Columbia Univ., New York, N.Y. Dept. of Computer Science.
AUTOMATIC CONCEPT FORMATION IN A RICH INPUT DOMAIN Final Report, Mar. 1985 - Mar. 1987
Michael Lebowitz Jun. 1988 49 p
(Contract MDA903-85-K-0103; DA Proj. 2Q1-61102-B-74-F)
(AD-A196719; ARI-RN-88-54) Avail: NTIS HC A03/MF A01 CSCL 12E

Learning by observation involves the creation of categories summarizing experience. In this research note, research during the contact period with UNIMEM is summarized, i.e., it is an Artificial Intelligence system that learns by observation. UNIMEM is a robust computer program that can be run on many domains with real-world problem characteristics, such as uncertainty, incompleteness, and large numbers of examples. We give an overview of the program that illustrates UNIMEM's key elements, including the automatic creation of non-disjoint concept hierarchies that are evaluated over time. We then describe several experiments that we have carried out with UNIMEM, testing it on different domains (universities, Congressional voting records, and terrorist events), and an examination of the effect of varying UNIMEM's parameters on the resulting concept hierarchies. Finally, we discuss future directions for our work with the program. GRA

N89-11446# Air Force Inst. of Tech., Wright-Patterson AFB, Ohio.
ASYNCHRONOUS DIGITAL REGULATORS Ph.D. Thesis
Vernon S. Ritchey 1988 187 p
(AD-A196911; AFIT/CI/NR-88-80) Avail: NTIS HC A09/MF A01 CSCL 12C

A method is presented for designing and analyzing multirate asynchronous digital controls for linear systems. Multirate digital control is a natural approach for systems with widely-spaced natural frequencies. An asynchronous architecture provides a simple approach for assigning control tasks to distributed processors. Previous multirate design methods required either synchronized samplers or high sample rates. Synchronized samplers produce a system that is periodically time varying. Alternatively, high sample rates simulate a continuous controller. In practice, synchronized implementations and implementations with high sample rates may have higher cost, complexity, and weight and lower reliability compared to asynchronous designs. In some cases, an asynchronous implementation with slow sampling will perform as well as a fast, synchronized design. The goal of this research was to develop methods to design and evaluate asynchronous control systems operating at minimal sample rates. The multirate asynchronous design and analysis methods developed in this report use a time-domain approach based on the closed-loop state transition matrix. Design and analysis algorithms (implemented in PC-MATLAB) are included in an Appendix. The analysis is based on a sufficient stability criterion which gives an objective measure of long-term stability and indicates short-term stability. GRA

N89-11447# San Diego State Univ., Calif. Center for Research in Mathematics and Science Education.
ASSESSING SCHEMA KNOWLEDGE Technical Report, 1 Sep. 1986 - 1 Sep. 1987
Sandra P. Marshall 20 May 1988 30 p
(Contract N00014-85-K-0661; Proj. RR0-4206)
(AD-A196933; CRMSE-88-02) Avail: NTIS HC A03/MF A01 CSCL 05H

The purpose of this paper is to explore issues involved in the assessment of cognitive development. The paper is divided into four sections. In the first the author examines the need for new theories of testing and for procedures that go beyond those currently in use. In the second section she proposes an assessment model based upon schema knowledge. In the third she offers data from a computer-based instructional system designed to promote schema development. Finally, in the last section she summarizes my findings and outline some important issues for future research. GRA

N89-11448# Illinois Univ., Urbana. Coordinated Science Lab.
TOWARD INTELLIGENT MACHINE LEARNING ALGORITHMS
Robert E. Stepp, Bradley L. Whitehall, and Lawrence B. Holder May 1988 20 p
(Contracts N00014-82-K-0186; N00014-87-K-0874; NSF IST-85-11170)
(AD-A197049; UILU-ENG-88-2221) Avail: NTIS HC A03/MF A01 CSCL 05H

Machine learning is recognized as a tool for improving the performance of many kinds of systems, yet most machine learning systems themselves are not well equipped to improve their own learning performance. By emphasizing the role of domain knowledge, learning systems can be crafted as knowledge directed systems, and with the addition of a knowledge store for organizing and maintaining knowledge to assist learning, a learning machine learning (L-ML) algorithm is possible. The necessary components of L-ML systems are presented along with several case descriptions of existing machine learning systems that possess limited L-ML capabilities. GRA

N89-11262*# National Aeronautics and Space Administration. Langley Research Center, Hampton, Va.
A COMPARATIVE OVERVIEW OF MODAL TESTING AND SYSTEM IDENTIFICATION FOR CONTROL OF STRUCTURES
J.-N. Juang and R. S. Pappa *In* Vibration Inst., The Shock and Vibration Digest, Volume 20, No. 6 Jun. 1988 p 4-15 (For primary document see N89-11261 02-39)
Avail: NTIS HC A05/MF A01

64 NUMERICAL ANALYSIS

Includes iteration, difference equations, and numerical approximation.

N89-11449# National Aeronautical Lab., Bangalore (India). Systems Engineering Div.
COMPARISON OF RECENT MODEL SELECTION CRITERIA FOR SYSTEM IDENTIFICATION
J. R. Raol Mar. 1988 16 p
(PD-SE-8807) Avail: NTIS HC A03/MF A01

In this paper we study the problem of determination of order of dynamical systems represented by time-series, polynomial and transfer function models. We briefly discuss the merits and demerits of many contemporary and recent criteria. Finally we compare some criteria via numerical simulation and present some interesting observations. Author

N89-11450# International Centre for Theoretical Physics, Trieste (Italy).
GENERAL COMPLEX-ANALYTIC STRUCTURES IN UNIFORM ALGEBRA SPECTRA: A SURVEY
Toma V. Tonev Dec. 1987 22 p Submitted for publication
(DE88-703010; IC-87/408) Avail: NTIS (US Sales Only) HC A03/MF A01

The article is devoted to the development of the theory of complex analytic structure in uniform algebra spectra, more general than one-dimensional ones, to eliminate at the same time the limiting finiteness conditions from the existing classical theory. DOE

N89-11451# General Atomic Co., San Diego, Calif.
THE STEADY STATES OF THE KURAMOTO--SIVASHINSKY EQUATION
J. M. Greene and J. S. Kim Dec. 1987 49 p
(Contract DE-FG03-85ER-13402)
(DE88-011819; GA-A-19031) Avail: NTIS HC A03/MF A01

The Kuramoto--Sivashinsky equation is one of the simple nonlinear partial diffential equations. It represents a system in which the transport of energy through nonlinear mode coupling produces a balance between long wavelength instability and short wavelength dissipation. The steady states and their stabilities give a foundation for understanding the dynamics of the system. They are distinguished according to their energy levels and fall into different branches that are identified by their harmonic content. Various types of solution include laminar states, N-cell states, long wave distorted N-cell states, the giant states, and steady traveling solutions. The linear stability around the steady states gives a guide to the origin of additional steady states through bifurcation and to the identification of each steady state. The index rule is also useful. Conjectured from the numerical observation, the parameter dependence of the steady traveling waves is estimated in the limit of large values of the parameter. In addition, a singular perturbation calculation of traveling waves near bifurcation is carried out. The dynamics of a system can be guided by the systematic study of the bifurcation and stability. DOE

N89-11452# Northrop Services, Inc., Corvallis, Oreg.
CUBIC SPLINE SMOOTHING: A USEFUL TOOL FOR CURVE ESTIMATION
M. S. DeHaan May 1988 10 p
(Contract EPA-68-03-3246)
(PB88-214796; EPA/600/D-88/082) Avail: NTIS HC A02/MF A01 CSCL 12A

Data analysis frequently involves fitting curves to data. Often the investigator has no idea what the underlying functional relationship is and ordinary functions or polynomials fit poorly. This is especially common with experimental data that has a lot of noise and/or measurement error in it. In these cases, spline smoothing can be used to estimate and fit curves with excellent results. Nonparametric cubic spline smoothing is a accurate and widely applicable approach to curve estimation that has been inexplicably underutilized. This tool can be used in the exploratory, descriptive, and predictive stages of bivariate data analysis. Many examples of curve fitting using spline smoothing are given. Smoothing splines are compared to several other common methods of curve fitting. Methods are detailed for implementing spline smoothing on SAS software. Author

N89-11453# Vrije Univ., Amsterdam (Netherlands). Dept. of Mathematics.
HOMOLOGY CLASSES REPRESENTED BY REAL ALGEBRAIC HYPERSURFACES
J. Bochnak and W. Kucharz (New Mexico Univ., Albuquerque.) Sep. 1987 27 p
(Grant NSF DMS-86-02672)
(PB88-202908; Rept-328) Avail: NTIS HC A03/MF A01 CSCL 12A

Let M be a (C sup infinity symbol) manifold. A nonsingular affine real algebraic variety (i.e., up to biregular isomorphism, an algebraic subset of R sup n) diffeomorphism to M is called an algebraic model of M. The celebrated theorem of Tognoli says that each compact (C sup infinity symbol) manifold admits an algebraic model. The problem is studied of constructing, for a given compact (C sup infinity symbol) manifold M of dimension d, an algebraic model X of M whose some homology classes in (H sub (d-1))(X,Z/2) cannot be represented by algebraic hypersurfaces of X. Author

N89-11454# Maryland Univ., College Park. Inst. for Physical Science and Technology.
FUNDAMENTAL RESEARCH IN APPLIED MATHEMATICS Final Report, 1 Mar. 1984 - 31 Dec. 1987
Frank W. J. Olver 25 Feb. 1988 9 p
(Contract DAAG29-84-K-0022)
(AD-A193668; ARO-20606.13-MA) Avail: NTIS HC A02/MF A01 CSCL 12A

The contents of this report on applied mathematics are as follows: Unrestricted computing algorithms for the elementary functions and special functions of mathematical physics; Error analysis of numerical algorithms; New computer arithmetics; Uniform asymptotic solutions of linear differential equations. GRA

N89-11455# National Aeronautical Lab., Bangalore (India). Aerodynamics Div.
AN ITERATIVE SCHEME FOR NUMERICAL SOLUTION OF TRANSONIC SMALL PERTURBATION EQUATION
U. N. Sinha and V. R. Sarasamma Apr. 1988 48 p
(TM-AE-8801) Avail: NTIS HC A03/MF A01

Computational aspects of Transonic Small Perturbation (TSP) equation are studied. The TSP equation is a consistent approximation of comparable Euler Equations with the sole restriction of small perturbation. A new algorithm for solving conservative discretization of TSP equation is presented. Unconditional stability of the scheme was shown and a number of computational experiments were carried out which demonstrate the ruggedness of the scheme. Despite the TSP equation, though not valid near the blunt leading edge, a large number of calculations in the literature have been made for flow past airfoils like NACA 0012 using TSP equation. Handling of boundary condition in the numerical calculation tends to be ad-hoc near the leading edge. It is shown that if the leading edge slope is integrable a satisfactory analysis can be carried out. Numerical calculations confirm the usefullness of the approach. Author

N89-11456# Cornell Univ., Ithaca, N.Y. Lab. of Atomic and Solid State Physics.
THE PAIR POTENTIAL APPROACH FOR INTERFACES: FUNDAMENTAL PROBLEMS AND PRACTICAL SOLUTIONS
A. C. Maggs and N. W. Ashcroft Sep. 1987 7 p Presented at the Conference on Interface Science and Engineering, Lake Placid, N.Y., 12 Jul. 1987
(Contract DE-FG02-85ER-45211)
(DE88-009165; DOE/ER-45211/5; MSC-6356; CONF-870793-6)
Avail: NTIS HC A02/MF A01

A fundamental problem in the use of a central pair-force model

for defect problems is that it omits three-body and higher terms which are necessarily present in real systems. Electronic fluctuation effects are also usually omitted. While these can be small in the simple metals, they are significant in noble and transition metals, as shown by a simple real space argument. To gauge the importance of their effects in interface problems, the structure of a simple sum 5 twist boundary is examined, with the atoms described by both pair- and three-center interactions and as a function of the relative strength of the two. DOE

N89-11457*# Texas Univ., Dallas. Programs in Mathematical Sciences.
UNMODELED DYNAMICS AND NONLINEAR CONTROL: WRAPUP Final Technical Report, Sep. 1987 - Aug. 1988
L. R. Hunt 1988 9 p
(Grant NAG2-366)
(NASA-CR-181524; NAS 1.26:181524) Avail: NTIS HC A02/MF A01 CSCL 12A

Theoretical and applicable results concerning systems of nonlinear ordinary differential equations and control of partial differential equations are examined. Titles and abstracts of recent papers are presented. B.G.

N89-11458# Katholieke Universiteit, Nijmegen (Netherlands). Psychologisch Lab.
ACCESSIBILITY, A CRITERION FOR THE CHOICE OF VISUAL CODING RULES
P. A. vanderHelm and E. L. J. Leeuwenberg 1988 51 p Sponsored by Nederlandse Organisatie voor Zuiver Wetenschappelijk Onderzoek, The Hague
(PB88-209911; Rept-88-NICI-01) Avail: NTIS HC A04/MF A01 CSCL 12A

The concept of accessibility is discussed as a selection criterion, especially for visual kinds of regularity. Accessibility implies an easy extraction of features from a pattern, due to a pattern description in which only features are combined that are indeed compatible in the pattern. The property allows an efficient and largely parallel encoding process, without obstructing a flexible description of regularity and hierarchy in patterns. Accessibility will be specified by holographic regularity and transparent hierarchy, two characteristics which are satisfied by only three kinds of regularity: iteration, symmetry and alternation. Author

N89-11459*# National Aeronautics and Space Administration. Langley Research Center, Hampton, Va.
DOMAIN DECOMPOSITION METHODS FOR THE PARALLEL COMPUTATION OF REACTING FLOWS Final Report
David E. Keyes (Yale Univ., New Haven, Conn.) Sep. 1988 26 p
(Contract NAS1-18107; AF-AFOSR-0117-88)
(NASA-CR-181719; ICASE-88-52; NAS 1.26:181719) Avail: NTIS HC A03/MF A01 CSCL 12A

Domain decomposition is a natural route to parallel computing for partial differential equation solvers. Subdomains of which the original domain of definition is comprised are assigned to independent processors at the price of periodic coordination between processors to compute global parameters and maintain the requisite degree of continuity of the solution at the subdomain interfaces. In the domain-decomposed solution of steady multidimensional systems of PDEs by finite difference methods using a pseudo-transient version of Newton iteration, the only portion of the computation which generally stands in the way of efficient parallelization is the solution of the large, sparse linear systems arising at each Newton step. For some Jacobian matrices drawn from an actual two-dimensional reacting flow problem, comparisons are made between relaxation-based linear solvers and also preconditioned iterative methods of Conjugate Gradient and Chebyshev type, focusing attention on both iteration count and global inner product count. The generalized minimum residual method with block-ILU preconditioning is judged the best serial method among those considered, and parallel numerical experiments on the Encore Multimax demonstrate for it approximately 10-fold speedup on 16 processors. Author

N89-11460# Colorado Univ., Boulder.
PERIODIC SOLUTIONS OF THE HAMILTON-JACOBI EQUATION BY THE SHOOTING METHOD: A TECHNIQUE FOR BEAM DYNAMICS
W. E. Gabella, R. D. Ruth, and R. L. Warnock (Stanford Linear Accelerator Center, Calif.) May 1988 10 p Presented at the 2nd International Committee for Future Accelerators Advanced Beam Dynamics Workshop, Lugano, Switzerland, 11 Apr. 1988
(Contracts DE-AC03-76SF-00515; DE-FG02-86ER-40302)
(DE88-012733; SU-SLAC-PUB-4626; CONF-8804111-3) Avail: NTIS HC A02/MF A01

Periodic solutions of the Hamilton-Jacobi equation determine invariant tori in phase space. The Fourier spectrum of a torus with respect to angular coordinates gives useful information about nonlinear resonances and their potential for causing instabilities. We describe a method to solve the Hamilton-Jacobi equation for an arbitrary accelerator lattice. The method works with Fourier modes of the generating functions, and imposes periodicity in the machine azimuth by a shooting method. We give examples leading to three-dimensional plots in a surface of section. It is expected that the technique will be useful in lattice optimization. DOE

N89-11461# Argonne National Lab., Ill.
PROCEEDINGS OF THE FOCUSED RESEARCH PROGRAM ON SPECTRAL THEORY AND BOUNDARY VALUE PROBLEMS. VOLUME 1: SINGULAR DIFFERENTIAL SYSTEMS
G. W. Pieper Dec. 1987 177 p Program held at Argonne, Ill., 1986-1987
(Contract W-31-109-eng-38)
(DE88-008151; ANL-87-26-Vol-1) Avail: NTIS HC A09/MF A01

This is the first volume of a series of reports containing the proceedings of the Focused Research program on spectral theory and boundary value problems. The topics covered are: M(lambda) theory for singular Hamiltonian systems; M(lambda)-computation for singular differential systems; Levinson's theorem and Titchmarch-Weyl M(lambda) theory for Dirac systems; deficiency indices of powers of Sturm-Liouville expresssions with large leading coefficient; and the Bessel-squared equation in the lim-2, lim-3, and lim-4 cases. DOE

N89-11462# Vrije Univ., Amsterdam (Netherlands). Dept. of Mathematics.
REAL ALGEBRAIC MORPHISMS INTO EVEN-DIMENSIONAL SPHERES
J. Bochnak and W. Kucharz (New Mexico Univ., Albuquerque.) Sep. 1987 30 p
(Grant NSF DMS-86-02672)
(PB88-202916; Rept-330) Avail: NTIS HC A03/MF A01 CSCL 12A

Given affine real algebraic varieties X and Y, the set of regular mappings (real algebraic morphisms) from X into Y, is denoted by R(X,Y). The set R(X,S sup n) of regular mappings from affine nonsingular real algebraic varieties X into S sup n, the unit sphere, is studied. GRA

N89-11463# Rochester Univ., N. Y. Lab. for Laser Energetics.
A CODE FOR THE SOLUTION OF THE VLASOV-FOKKER-PLANCK EQUATION IN ONE OR TWO DIMENSIONS
E. M. Epperlein, G. J. Rickard, and A. R. Bell (Imperial Coll. of Science and Technology, London, England) Jul. 1988 19 p
(Contract DE-FC08-85DP-40200)
(DE88-013288; DOE/DP-40200/73) Avail: NTIS HC A03/MF A01

We describe a code for the solution of the Vlasov-Fokker-Planck (VFP) equation in one or two spatial dimensions using the diffusive approximation in configuration space. The equations are integrated by the Alternating Direction Implicit (ADI) method. We give examples of its application to the simulation of laser-produced plasmas. DOE

N89-11464# California Univ., Berkeley.
SOLUTION METHODS FOR DAMPED LINEAR DYNAMIC SYSTEMS Ph.D. Thesis
Harn-Ching Chen Nov. 1987 120 p Sponsored in part by Lawrence Livermore Lab., Calif.
(Contract W-7405-eng-48)
(DE88-013812; UCRL-21070; UCB/SEMM-87/08) Avail: NTIS HC A06/MF A01

This dissertation considers solution methods for damped linear structural systems which are subjected to transient loading. To accommodate a range of possible applications, the damping is assumed to be non-proportional to mass and stiffness and may also be large and/or lumped. Some important characteristic properties of the damped system are presented. The second-order equations of motion are reduced to a first-order set by doubling the size of the problem to facilitate the subsequent analysis and computation. The Rayleigh-Ritz method is generalized for the matrix pencil associated with a damped system. A projection method is discussed as an alternative. Both provide a basis for computing partial eigensolutions of a large damped dynamic system. The subspace iteration method is modified to extract eigensolutions of a damped dynamic system. The iteration vectors are arranged in such a way that only real arithmetic is required to describe the complex solution vectors. The algorithm is implemented to solve some typical numerical examples. The Lanczos method also is extended to find eigensolutions of a damped dynamic system. The loss of orthogonality between Lanczos vectors is investigated and two schemes are presented to restore the required orthogonality. DOE

N89-11465# International Centre for Theoretical Physics, Trieste (Italy).
INNER PRODUCT FOR A BANACH-ALGEBRA
Noor Mohammad and Alberto Verjovsky Oct. 1987 11 p
(DE88-703156; IC-87/358) Avail: NTIS (US Sales Only) HC A03/MF A01

An intrinsic inner product for a commutative Banach*-algebra is defined. Several conditions for its completeness are established. It is shown that any Banach*-algebra with proper and continuous involution has an auxiliary norm that turns it into an A*-algebra. DOE

N89-11466# International Centre for Theoretical Physics, Trieste (Italy).
QUASI-ADEQUATE SEMIGROUPS
Abdulsalam El-Qallali Nov. 1987 19 p
(DE88-703157; IC-87/359) Avail: NTIS (US Sales Only) HC A03/MF A01

The least fundamental adequate good congruence on an arbitrary type W semigroup S is described as well as the largest superabundant full subsemigroup of S and the largest full subsemigroup of S which is a band of cancellative monoids. Weak type W semigroups are defined by replacing the idempotent-connected property in type W by one of its consequences and a structure theorem is obtained for such semigroups. DOE

N89-11467# International Centre for Theoretical Physics, Trieste (Italy).
SECOND ORDER PARABOLIC EQUATIONS FOR FLOW-DOMAINS
Duong Minh Duc Nov. 1987 14 p
(DE88-703158; IC-87/360) Avail: NTIS (US Sales Only) HC A03/MF A01

Using Poincare weighted inequality we study semigroups corresponding to elliptic operators degenerate in Trudinger's sense. Our results may be applied to the cases in which the domain and coefficient functions are nonsmooth and unbounded. DOE

N89-11468# International Centre for Theoretical Physics, Trieste (Italy).
ON EQUIVARIANT LAGRANGIANS
J. J. Konderak Mar. 1988 12 p
(DE88-703167; IC-88/46) Avail: NTIS (US Sales Only) HC A03/MF A01

Considered here is a functor which with each pair of Riemannian manifolds associates a first order Lagrangian defined on the space of jets of functions from one manifold to the other. With some additional assumptions motivated from the geometry of the manifolds, that factor is called a Riemannian Lagrangian. It is then shown that each Riemannian Lagrangian is induced by elementary symmetric functions and a real valued smooth function. DOE

N89-11469*# National Aeronautics and Space Administration. Lewis Research Center, Cleveland, Ohio.
A NUMERICAL STUDY OF ENO AND TVD SCHEMES FOR SHOCK CAPTURING
Shih-Hung Chang (Cleveland State Univ., Ohio.) and Meng-Sing Liou Sep. 1988 24 p
(NASA-TM-101355; E-4384; ICOMP-88-18; NAS 1.15:101355)
Avail: NTIS HC A03/MF A01 CSCL 12A

The numerical performance of a second-order upwind-based total variation diminishing (TVD) scheme and that of a uniform second-order essentially non-oscillatory (ENO) scheme for shock capturing are compared. The TVD scheme used is a modified version of Liou, using the flux-difference splitting (FDS) of Roe and his superbee function as the limiter. The construction of the basic ENO scheme is based on Harten, Engquist, Osher, and Chakravarthy, and the 2-D extensions are obtained by using a Strang-type of fractional-step time-splitting method. Numerical results presented include both steady and unsteady, 1-D and 2-D calculations. All the chosen test problems have exact solutions so that numerical performance can be measured by comparing the computer results to them. For 1-D calculations, the standard shock-tube problems of Sod and Lax are chosen. A very strong shock-tube problem, with the initial density ratio of 400 to 1 and pressure ratio of 500 to 1, is also used to study the behavior of the two schemes. For 2-D calculations, the shock wave reflection problems are adopted for testing. The cases presented in this report include flows with Mach numbers of 2.9, 5.0, and 10.0. Author

N89-11470# Grenoble-1 Univ. (France). Dept. ARTEMIS.
UNDIRECTED DISTANCES AND THE POSTMAN-STRUCTURE OF GRAPHS
Andreas Sebo Feb. 1988 37 p Revised Sponsored in part by CNRS, France
(RR-714-M; ETN-88-93268) Avail: NTIS HC A03/MF A01

Properties of the distance function and of shortest paths in + or - 1-weighted undirected graphs are presented. These extend basic results on matchings, on the Chinese postman problem, and on plane multicommodity flows. Distances turn out to be efficient tools to generalize the matching-structure of graphs to a structure related to subgraphs having only parity constraints on their degrees, (these are called joins or postman sets). A good characterization (linear in the number of edges), of the minimum weights of paths from a fixed vertex of an undirected graph without negative circuits is obtained. This result contains the well-known minimax theorems on minimum odd joins and maximum packings of odd cuts and strengthens them by constructing a canonical maximum packing of odd cuts with favorable properties. This packing of odd cuts is characteristic for the structure of minimum odd joins. Using these, a Gallai-Edmonds type structural description of minimum odd joins is worked out. ESA

N89-11471# Grenoble-1 Univ. (France). Lab. d'Informatique Fondamentale et d'Intelligence Artificielle.
EQUATIONAL PROBLEMS AND DISUNIFICATION
Hubert Comon and Pierre Lescanne (Centre National de la Recherche Scientifique, Nancy, France) May 1988 41 p
(RR-727-I-IMAG-82-LIFIA; ETN-88-93274) Avail: NTIS HC A03/MF A01

Equational problems i.e., first order formulas whose only predicate symbol is = are considered. Rules for the transformation

of equational problems are proposed, and their correctness and completeness in various models are studied. Completeness results with respect to simple problems called solved forms are given. Such completeness results still hold when adding control which moreover ensures termination. The termination proofs use as little control as possible. In this sense, they are generic since it is possible to find again classical algorithms by strenghtening the control. A by-product of the method is a decision procedure for the validity in the Herbrand Universe of any first order formula with the only predicate symbol =. ESA

N89-11472# Grenoble-1 Univ. (France). Techniques de l'Informatique, des Mathematiques, de la Microelectronique et de la Microscopie Quanti

ON DIFFERENTIAL POLYNOMIALS AND THEIR RESULTANTS

Gouting Chen May 1988 13 p

(RR-723-M; ETN-88-93278) Avail: NTIS HC A03/MF A01

Problems on differential polynomials which contain the normal forms and characteristic polynomial of matrices with coefficients as differential polynomials, differential transformations, and the resultants of differential polynomials, are considered. Pseudo-resultants in the Weyl algebra are analyzed. ESA

N89-11473# Massachusetts Inst. of Tech., Cambridge. Artificial Intelligence Lab.

COMPUTATIONAL STRUCTURE OF THE N-BODY PROBLEM

Jacob Katzenelson Apr. 1988 55 p

(Contract N00014-86-K-0180)

(AD-A196422; AI-M-1042) Avail: NTIS HC A04/MF A01 CSCL 12I

This work considers tree algorithms for the N-body problem where the number of particles is on the order of a million. The main concern of this work is the organization and performance of these computations on parallel computers. The work introduces a formulation of the N-body problem as a set of recursive equations based on a few elementary functions. It is shown that both the algorithm of Barnes-Hut and that of Greengard-Rokhlin satisfy these equations using different elementary functions. The recursive formulation leads directly to a computational structure in the form of a pyramid-like graph, where each vertex is a process, and each arc a communication link. The pyramid is mapped to three different processor configurations: (1) A pyramid of processors corresponding to the processes pyramid graph; (2) An hypercube of processors, e.g., a connection-machine like architecture; and (3) A rather small array, e.g., 2 x 2 x 2, of processors faster then the ones consider in (1) and (2) above. The main conclusion is that simulations of this size can be performed on any of the three architectures in reasonable time. Twenty-four seconds per time step is the estimate for a million equally distributed particles using the Greengard-Rokhlin algorithm on the CM-2 connection machine. The smaller array of processors is quite competitive in performance. GRA

N89-11474# Air Force Wright Aeronautical Labs., Wright-Patterson AFB, Ohio.

DETERMINATION OF COMPLEX EXPONENTIALS, LEAST SQUARES AND PREDICTION METHODS Final Report, Feb. 1985 - Dec. 1987

Charles L. Keller Feb. 1988 47 p

(AD-A196498; AFWAL-TR-88-3042) Avail: NTIS HC A03/MF A01 CSCL 12C

An efficient method for determining a sum of complex exponentials and their complex amplitudes is presented in detail. The principal feature is the application of Lanczos' Progressive Algorithm which eliminates the need for knowing or assuming the number of such quantities in the sum. The method is applicable to appropriate averages of the sampled data also. The algebraic properties of the method of least squares for the linear case are presented and provide the basis for the presentation of the 1-step-ahead prediction for stationary sequences lattice filters and canonical variate analysis. GRA

N89-11475*# Mathematical Analysis Research Corp., Claremont, Calif.

CALCULATING THE CEP (CIRCULAR ERROR PROBABLE) Final Report

25 Aug. 1987 10 p Prepared in cooperation with Jet Propulsion Lab., California Inst. of Tech., Pasadena.

(Contract NAS7-918)

(NASA-CR-182996; NAS 1.26:182996; AD-A196504; JPL-D-4710; ALGO-Pub-0120; TM-31) Avail: NTIS HC A02/MF A01 CSCL 12A

This report compares the probability contained in the Circular Error Probable associated with an Elliptical Error Probable to that of the EEP at a given confidence level. The levels examined are 50 percent and 95 percent. The CEP is found to be both more conservative and less conservative than the associated EEP, depending on the eccentricity of the ellipse. The formulas used are derived in the appendix. GRA

N89-11476# Massachusetts Inst. of Tech., Cambridge. Artificial Intelligence Lab.

ABSTRACTION IN NUMERICAL METHODS

Matthew Halfant and Gerald J. Sussman Oct. 1987 22 p

(Contract N00014-86-K-0180)

(AD-A196990; AI-M-997) Avail: NTIS HC A02/MF A01 CSCL 12E

We illustrate how the liberal use of high-order procedural abstractions and infinite streams helps us to express some of the vocabulary and methods of numerical analysis. We develop a software toolbox encapsulating the technique of Richardson extrapolation, and we apply these tools to the problems of numerical integration and differentiation. By separating the idea of Richardson extrapolation from its use in particular circumstances we indicate how numerical programs can be written that exhibit the structure of the ideas from which they are formed. GRA

65 STATISTICS AND PROBABILITY

Includes data sampling and smoothing; Monte Carlo method; and stochastic processes.

N89-11477# Technische Hogeschool, Delft (Netherlands). Onderafdeling der Wiskunde en Informatica.

PROBLEM ON 0-1 MATRICES

V. deValk 1988 52 p

(PB88-210075; Rept-88-03) Copyright Avail: NTIS HC A04/MF A01 CSCL 12A

The author computes the maximal and the minimal value of the matrix //(M sup 2)// over the class of 0-1 valued NxN matrices M with K entries equal to one for fixed K and N, where //dot// denotes the sum of the entries. This result has applications to graph theory and probability theory. GRA

N89-11478# National Research Inst. for Mathematical Sciences, Pretoria (South Africa).

ROBUST COVARIANCE MATRIX ESTIMATION VIA ROBUST ESTIMATION OF PRINCIPAL COMPONENTS

J. S. Galpin and D. M. Hawkins Aug. 1986 36 p

(PB88-126594; CSIR-TWISK-481) Avail: NTIS HC E05/MF E05; copy not available from STI Facility CSCL 12A

Although the principal component analysis of a covariance matrix is classically performed by using the spectral decomposition of the covariance matrix, this process can be applied in reverse to obtain an estimate of the covariance matrix from the principal components. Several methods of robust estimation of principal components are discussed, and their performance is compared on generated data sets containing data point configurations known to cause problems in covariance matrix estimation. It is shown that several of the proposed methods of robust principal component estimation lead to satisfactory robust covariance matrix estimates, implying that this approach yields a viable method of robustly estimating the covariance matrix. Author

N89-11479# Grenoble-1 Univ. (France). Techniques de l'Informatique, des Mathematiques, de la Microelectronique et de la Microscopie Quanti

PENALIZED LIKELIHOOD ESTIMATION FOR RATES WITH CENSORED SURVIVAL

Anestis Antoniadis and Gerard Gregoire May 1988 32 p
(RR-726-M; ETN-88-93273) Avail: NTIS HC A03/MF A01

A nonparametric procedure for the estimation of the hazard function from censored survival data is proposed. The model is shown to fit into the Aalen multiplicative intensity model for counting processes. The estimator is derived by penalized likelihood methods. The estimate turns out to be a nonnegative hyperbolic smoothing spline function. Standard large sample results for counting processes are used to establish asymptotic properties of the estimator. An example from censored survival analysis theory is presented. ESA

N89-11480# Air Force Inst. of Tech., Wright-Patterson AFB, Ohio.

THE GENERATION OF SCATTEROMETER SURFACE TARGETS WITH SPECIFIED SURFACE STATISTICS M.S. Thesis

James D. Rochier Aug. 1987 129 p
(AD-A196397; AFIT/CI/NR-88-92) Avail: NTIS HC A07/MF A01 CSCL 12C

Many of the models used to study scattering from rough surfaces are based on intuitive concepts and testing of the theories is desired. The generation of physical models based on computer-generated random surfaces with predetermined statistics is investigated. Generation of statistically known surfaces will allow testing of scattering theories by studying the scattering characteristics of the surfaces as their statistics are varied in a known, predetermined manner. This study extends the investigation of generation of random surfaces previously performed for computer simulations and presents interfaces for construction of a physical model. Additionally, a surface so generated is tested to measure conformity to the desired statistics. A portion of a surface with Gaussian statistics was generated and measured and the conclusion reached is that generation of statistically predetermined rough surfaces is feasible. GRA

N89-11481# Air Force Inst. of Tech., Wright-Patterson AFB, Ohio.

GENERAL RESULTS IN OPTIMAL CONTROL OF DISCRETE-TIME NONLINEAR STOCHASTIC SYSTEMS M.S. Thesis

Mark S. Ciancetta 1988 81 p
(AD-A196411; AFIT/CI/NR-88-55) Avail: NTIS HC A05/MF A01 CSCL 12C

This document proposes an approach for the control of a general class of discrete-time nonlinear stochastic systems. The system model incorporates a deterministic linear portion together with a nonlinear function of the state and/or control vectors in combination with a white noise vector, where no Gaussian assumption is made. Under certain conditions imposed on the statistics of the additive nonlinear stochastic term, and assuming perfect state information, the optimal control, which minimizes a quadratic performance index subject to the nonlinear control system constraint, is shown to be a linear function of the state vector. This work also shows that for certain infinite horizon problems, an uncertainty threshold can be found such that the designer can, a priori, put an upper bound on the allowable noise covariance to obtain a bounded optimal constant feedback control. GRA

N89-11482# California Univ., Los Angeles. School of Engineering and Applied Science.

STRONG AND WEAK STABILIZABILITY: LYAPUNOV TYPE APPROACHES Ph.D. Thesis

Wendell M. Miyaji 2 Apr. 1988 80 p
(Grant AF-AFOSR-0132-86; AF Proj. 2304)
(AD-A196431; AFOSR-88-0617TR) Avail: NTIS HC A05/MF A01 CSCL 12D

This theses addresses the problem of determining stabilizing controls for distributed parameter systems. The focus is on controls which provide strong or weak stabilization to the system. One approach to the stabilization of finite dimensional systems and exponential stabilization of infinite dimensional systems has been the use of Lyapunov type functionals. This is one technique which is developed and extended here, to provide new conditions for strong or weak stability. A new functional is presented, and if this functional is strictly positive, a certain semigroup will be strongly stable. This functional suggests an inequality relation which, if satisfied guarantees the weak stability of uniformly bounded semigroups. The relationship between contraction semigroups is examined on a Hilbert space and shift semigroups on a related Hilbert space. In particular, strongly stable semigroups are found to be equivalent in a certain sense to a backward shift semigroup. This provides an alternative view point for strong stability. Since stable semigroups are uniformly bounded and since this condition is important in verifying stability we examine this phenomena. Some new observations are presented to illustrate conditions under which perturbations of uniformly bounded semigroups remain uniformly bounded. GRA

N89-11483# North Carolina Univ., Chapel Hill.

MEASURING THE VAGUE MEANINGS OF PROBABILITY TERMS Interim Report, Feb. 1985 - Feb. 1986

Thomas S. Wallsten, Rami Zwick, Barbara Forsyth, David V. Budescu, and Amnon Rappaport (Florida State Univ., Tallahassee.) Jul. 1988 92 p
(Contract MDA903-83-K-0347; DA Proj. 2Q1-61102-B-747)
(AD-A196944; ARI-RN-88-56) Avail: NTIS HC A05/MF A01 CSCL 12C

A modified air-comparison procedure was employed in two experiments to establish and assess membership functions for numerous probability terms. In both cases, subjects judged: (1) to what degree one probability term better described that probability than another, and (2) to what degree one term rather than another better described a probability. Task 1 data from subjects was analyzed in terms of the axioms of an algebraic-difference structure, and membership function values were obtained for each term according to various ratio and difference scaling models. The axioms were well satisfied, and goodness-of-fit measures for the scaling procedures were quite high. Furthermore, the derived membership functions had interpretable shapes and satisfactorily predicted for each subject the judgements independently obtained in 2. These results support the claims that the scaled values indeed represented the vague meanings of the terms to the subjects in the present context. GRA

N89-11484# Illinois Univ., Urbana. Decision and Control Lab.

BALANCE OF RECURRENCE ORDER IN TIME-INHOMOGENEOUS MARKOV CHAINS WITH APPLICATION TO SIMULATED ANNEALING Ph.D. Thesis

Daniel Patrick Connors Apr. 1988 104 p
(Contracts N00014-84-C-0149; DAAG29-85-K-0094)
(AD-A196980; DC-102; UILU-ENG-88-2222) Avail: NTIS HC A06/MF A01 CSCL 12C

Considered is the class of time inhomogeneous Markov chains whose transition probabilities are proportional to nonnegative powers of a small, time varying parameter. A new notion of order of recurrence is introduced for the states and transitions of such Markov processes. These orders of recurrence provide considerable information about the asymptotic behavior of the process. The orders of recurrence are shown to satisfy a balance equation across every edge cut the graph associated with the Markov chain. This allows for computation of the orders of recurrence. An algorithm for generating all solutions to the order balance equations is given. The method of optimization by simulated annealing falls within the framework of this class of Markov chains. It is shown that if the simulated annealing Markov chain is weakly reversible, then the sum of the order of recurrence of a state and its cost is constant on connected components of recurrent states. In the special case of symmetric neighborhoods, there holds a detailed balance across every edge in the graph of the Markov process. GRA

N89-11485# Purdue Univ., West Lafayette, Ind. Dept. of Statistics.
ON EMPIRICAL BAYES SELECTION RULES FOR NEGATIVE BINOMIAL POPULATIONS
Shanti S. Gupta and TaChen Liang (Wayne State Univ., Detroit, Mich.) May 1988 30 p
(Contract N00014-88-K-0170; NSF DMS-86-06964; NSF DMS-87-02620)
(AD-A196994; TR-88-16C) Avail: NTIS HC A03/MF A01 CSCL 12C

This paper deals with the problem of selecting good negative binomial populations as compared with a standard or a control. The main results are based on the use of the empirical Bayes approach. First the authors derive the monotone empirical Bayes estimators of the concerned parameters. Based on these estimators, they construct monotone empirical Bayes selection rules. Asymptotic optimality properties of the monotone empirical Bayes estimators and the monotone empirical Bayes selection rules are investigated. The respective convergence rates for the estimation problem and for the selection problem are studied, under some conditions. GRA

66 SYSTEMS ANALYSIS

Includes mathematical modeling; network analysis; and operations research.

N89-11486# Lawrence Livermore National Lab., Calif.
ALLOCATING AND LAUNCHING MaRV INTERCEPTORS BASED ON MISS DISTANCE PREDICTIONS
G. C. Corynen Jun. 1988 135 p
(Contract W-7405-eng-48)
(DE88-015370; UCRL-53875) Avail: NTIS HC A07/MF A01

We have developed battle management algorithms for assigning and launching ground-based interceptors to neutralize a threat consisting of multiple decoyed maneuverable reentry vehicles (MaRVs) and ballistic reentry vehicles (BRVs) in their terminal phase. Decisions are based on the minimization of expected leakage risk, and they specifically account for uncertainties and errors in the identity of each threat object, although detailed discrimination issues are not discussed. In contrast to standard probabilistic approaches, the algorithms are physics-based and use kinematic and geometric models for estimating interceptor-MaRV miss distances and probabilities of kill to determine optimal waiting times before launch. Based on a test comparing interceptor and MaRV technologies, the minimax algorithm finds the waiting times for which the minimum probability of kill is a maximum. To avoid a full multidimensional optimization, we use a greedy one-dimensional approach where only the most urgent threat is addressed optimally, conditional to allocating to the remaining threats (dimensions) a nominal quantity of interceptors, determine by previous optimizations. One-on-one engagements are thus emphasized, and the preponderance of the work discussed was directed towards the development of a miss distance prediction algorithm, called the MD Algorithm. DOE

N89-11487# Institute for Defense Analyses, Alexandria, Va.
INTERCEPTOR-TO-TARGET ALLOCATION STRATEGIES FOR STRATEGIC DEFENSE 1: ADAPTIVE STRATEGIES BASED UPON SYSTEM AND THREAT CHARACTERISTICS Final Report, Jan. - Sep. 1987
Maile E. Smith and Thomas S. Paterson Jul. 1988 37 p
(Contract MDA903-84-C-0031)
(AD-A197037; AD-E501004; IDA-P-2058; IDA/HQ-87-32823)
Avail: NTIS HC A03/MF A01 CSCL 15C

This paper examines the topic of interceptor-to-target assignment algorithms and compares the system performance of a strategic defense system (SDS) as a function of the algorithm used. The algorithms range from being similar to some of those being developed under the SDIO's advanced algorithm programs to those used in some of the more popular engagement models. It is shown that the use of less sophisticated algorithms can often lead to RV leakages twice as large compared to cases in which sophisticated algorithms are used. The primary conclusion is that as the defense becomes interceptor-rich and/or the Pk of the interceptor becomes low, the popular one interceptor per target approaches to interceptor allocation, which are typically found in the community-wide engagement models, can perform poorly. When the defense is in either, or both, of these regimes, it can perform significantly better by adopting an approach in which the salvo becomes a credible strategy. Because the salvo strategies have not been implemented in the popular engagement models, the past analyses which have studied these types of architectures have been biased toward providing a lower level of performance. Interceptor allocation strategies for the midcourse and terminal phase are not analyzed in this paper. GRA

N89-11488# Institute for Defense Analyses, Alexandria, Va.
GUIDELINES FOR TAILORING DOD-STD-2167A FOR SDS (STRATEGIC DEFENSE SYSTEM) SOFTWARE DEVELOPMENT Final Report
Robert J. Knapper, Cathy Jo Linn, and John Salasin Feb. 1988 83 p
(Contract MDA903-84-C-0031)
(AD-A197038; AD-E501003; IDA-P-2018; IDA/HQ-87-32194)
Avail: NTIS HC A05/MF A01 CSCL 12H

IDA Paper P-2018 provides the SDIO with guidelines for tailoring of DOD-STD-2167A and related Data Item Descriptions (DIDs) including a suggested interpretation of the review requirements in MIL-STD-1521B for use as guidelines in developing prototype and production software. Although not approved for use, revision A of DOD-STD-2167 was chosen as the subject since it will supersede the current standard in 1987, and because it more adequately addresses modern software technology ideas. The recommendations in this paper are intended to be reflected in Requests for Proposals (RFPs) distributed to vendors proposing to develop SDI software and in contracts left for SDI software acquisition. GRA

67 THEORETICAL MATHEMATICS

Includes topology and number theory.

N89-11489*# Fermi National Accelerator Lab., Batavia, Ill.
ON THE LOCALITY OF THE NO HAIR CONJECTION AND THE MEASURE OF THE UNIVERSE
Tibor Pacher (Heidelberg Univ., West Germany) and Jaime A. Stein-Schabes 16 Aug. 1988 13 p
(NASA-CR-183365; NAS 1.26:183365; FERMILAB-Pub-88/100-A)
Avail: NTIS HC A03/MF A01 CSCL 12A

The reently proposed proof by Jensen and Stein-Schabes of the No Hair Theorem for inhomogeneous spacetimes is analyzed, putting a special emphasis on the asymptotic behavior of the shear and curvature. It is concluded that the theorem only holds locally, and the minimum size a region should be is estimated in order for it to inflate. The assumptions used in the theorem are discussed in detail. The last section speculates about the possible measure of the set of spacetimes that would undergo inflation. Author

70 PHYSICS (GENERAL)

For precision time and time interval (PTTI) see *35 Instrumentation and Photography;* for geophysics, astrophysics or solar physics see *46 Geophysics, 90 Astrophysics,* or *92 Solar Physics.*

N89-11490# Joint Inst. for Nuclear Research, Dubna (USSR). Lab. of Computing Techniques and Automation.
OPTIMIZATION OF THE TWO-DIMENSIONAL MAGNETIC FIELD DISTRIBUTION BASING ON THE INTEGRAL EQUATION METHOD

P. G. Akishin, E. P. Zhidkov, and V. D. Kravtsov 1987 8 p In RUSSIAN; ENGLISH summary
(DE88-702940; JINR-R-11-87-427) Avail: NTIS (US Sales Only) HC A02/MF A01

The problem of optimization of the two-dimensional magnetic field distribution is considered. The integral equation method is used for solving the direct problem. The task is reduced to the minimization of a functional which defines the quality of magnetic field distribution. The code realizing this method is created. The results of numerical experiments are discussed. DOE

N89-11491# Instituto de Pesquisas Espaciais, Sao Jose dos Campos (Brazil).
IMPLEMENTATION OF MAGINT CODE ON THE CDC-CYBER-170/750 SYSTEM
Carlos ShinyaShibata, Joaquin Paulino LeiteNeto, and Antonio Montes Sep. 1988 27 p In PORTUGUESE; ENGLISH summary
(INPE-4663-NTE/282) Avail: NTIS HC A03/MF A01

A magnetic field calculation code, Magint, was implemented on the CDC Cyber-170/750 system of the Institute for Advanced Studies (IEAv/CTA). Presented is a brief description of the code, the commands specifying the conductor configurations, and the data file structures. As an example of application, some calculations are shown referring to a magnetic plasma confinement apparatus under construction at the Plasma Laboratory of the Institute for Space Research (LAP/INPE). Author

71 ACOUSTICS

Includes sound generation, transmission and attenuation. For noise pollution see *45 Environmental Pollution*.

N89-11492 British Broadcasting Corp., Kingswood (England). Research Dept.
THE DEVELOPMENT OF PROTOTYPE ABSORBERS WITH VARIABLE CHARACTERISTICS
E. W. Taylor, K. F. L. Lansdowne, and R. J. Peill Jun. 1988 14 p
(BBC-RD-1988/5) Copyright Avail: BBC, Kingswood Warren, Tadworth, Surrey, United Kingdom

The development of two prototype sound absorbers with controllable absorption characteristics is described. One of these absorbers gives control at predominantly low frequencies (up to 250 Hz), while the other operates at frequencies above this value. The low-frequency absorber is constructed in modular form, while the high-frequency absorber takes the form of a false ceiling to the treated room. Factors which are required to ensure the consistency of the absorption characteristics given by these absorbers are discussed. Author

N89-11493 Lehigh Univ., Bethlehem, Pa.
SPATIAL DISTRIBUTION OF ACOUSTIC INTENSITY IN REVERBERANT FIELDS Ph.D. Thesis
Lung-Hen Henry Chow 1988 194 p
Avail: Univ. Microfilms Order No. DA8806574

Acoustic pressure or acoustic intensity is conventionally used to scale the sound level in dB ref P sub ref or dB ref I sub ref. The acoustic intensity is defined by the product of acoustic pressure p and particle velocity u, but in the literature, an expression like p sup 2/rho C is often quoted. In fact, it is based on planewave approximations which make the pressure and particle velocity being of the same phase all the time such that the use of dB scales in sound pressure and/or intensity as sound level is identical. This case also simplifies acoustic intensity from a vector quantity into a scalar quantity. The acoustic intensity is legitimately calculated by applying the normal mode procedure on pressure and particle velocity since the reverberant field inside an enclosure where an acoustic wave runs against the reflecting walls bring about the boundary condition involving p and u with phase variations. A computer model study of three different shaped enclosures and an experimental study in a model enclosure with cylindrical shape is included. In experiment, a dual channel FFT analyzer is used to make the measurement of the FFT calculated cross-spectrum of pressures between two closely spaced microphones. A good agreement is found between pressure mode shapes of experimental and theoretical scalar pressures. Besides, a three-dimensional flow pattern of vector intensity for three acoustic enclosures is also found here which signifies the directional tendency of intensity flow associated with its intensity magnitude and is different from the pressure mode shape which only shows the magnitude distribution of acoustic pressure. Dissert. Abstr.

N89-10856*# National Aeronautics and Space Administration. Ames Research Center, Moffett Field, Calif.
NOISE OF THE HARRIER IN VERTICAL LANDING AND TAKEOFF
Paul T. Soderman and John D. Foster *In its* The 1987 Ground Vortex Workshop Feb. 1988 p 167-190 (For primary document see N89-10849 02-02)
Avail: NTIS HC A10/MF A01 CSCL 01A

72 ATOMIC AND MOLECULAR PHYSICS

Includes atomic structure, electron properties, and molecular spectra.

N89-11494# Louisiana State Univ., Baton Rouge.
COULOMB STATES IN ATOMS AND SOLIDS Ph.D. Thesis
Darren Mark Ortalano May 1988 133 p
(DE88-013973; LSU-8013973) Avail: NTIS HC A07/MF A01

In this dissertation, an empirical quantum defect approach to describe the valence excitons of the rare gas solids is developed. These Coulomb states are of s-symmetry and form a hydrogen-like series which converges to the bottom of the lowest conduction band. A non-zero quantum defect is found for all of the excitons of neon, argon and xenon. For these systems, then, there exists, in addition to the screened Coulombic component, a non-Coulombic component to the total exciton binding energy. The Wannier formalism is, therefore, inappropriate for the excitons of Ne, Ar and Xe. From the sign of the quantum defect, the non-Coulombic potential is repulsive for Ne and Ar, attractive for Xe, and nearly zero for Kr. This is opposite to that for the Rydberg states of the corresponding rare gas atoms, where the non-Coulombic potential between the electron and the cation is attractive for all of the atoms. The excitons then, are not simply perturbed Rydberg states of the corresponding rare gas atoms (i.e., the excitons do not possess atomic parentage). Interatomic term value/band gap energy correlations and reduced term value/reduced band gap correlations were performed. These correlations were exploited to provide further evidence against both the Wannier formalism and the atomic parentage view point. From these correlations, it was also discovered that the non-Coulombic potential varies smoothly across the valence isoelectronic series of solids, and that it becomes more attractive (or less repulsive) in going from neon to xenon. In order to address the atomic parentage controversy, it was necessary to compare the excitons to the low-n Rydberg states of the rare gas atoms. A review of the quantum defect description of the atomic Rydberg states is, therefore, presented. Also, Rydberg term value/ionization energy correlations are discussed and compared with the analogous exciton correlations. DOE

N89-11495# California Univ., Berkeley. Lawrence Berkeley Lab.
ADVANCES IN METAL ION SOURCES
I. G. Brown May 1988 15 p Presented at the 7th International Conference on Ion Implantation Technology, Kyoto, Japan, 7 Jun. 1988
(Contract DE-AC03-76SF-00098)
(DE88-012020; LBL-24734; CONF-880614-4) Avail: NTIS HC A03/MF A01

Beams of metallic ion species can be produced by the ECR (electron cyclotron resonance) ion source and by the MEVVA (metal

vapor vacuum arc) ion source. Although the ECR source is fundamentally a gaseous ion source, metal ion beams can be produced by introducing metallic feed material into the plasma discharge using a number of techniques. The ion charge states can be very high, which is a significant advantage to most applications. The MEVVA ion source, on the other hand, is specifically a metal ion source. It has produced metallic ion beams from virtually all the solid metallic elements at a current of typically hundreds of milliamperes; the ions produced are in general multiply ionized, but not as highly stripped as those generated in the ECR source. Although the MEVVA source at present operates in a pulsed mode with a low duty cycle (less than or equal to 1 percent), work is in progress to increase the duty cycle significantly. In this paper the operation and performance of the LBL ECR and MEVVA ion sources, with respect to metal ion generation, are described. DOE

N89-11496 Maryland Univ., College Park.
LIE ALGEBRAIC TREATMENT OF SPACE CHARGE Ph.D. Thesis
Robert Douglas Ryne 1987 305 p
Avail: Univ. Microfilms Order No. DA8808600

A major concern in the design and evaluation of charged particle beam transport systems is the accurate computation of single particle trajectories. Calculational tools based on Lie algebraic methods have been extensively developed for this purpose. Computer programs based on Lie algebraic methods require for less storage than conventional programs. Lie algrabraic methods were originally developed to compute the trajectories of charged particles in externally applied electromagnetic fields. However, in the past there has been increased emphasis on the design of beam transport systems that transport high currents. A Lie algebraic treatment of space charge is presented. Specifically, a method is presented for finding approximate solutions of the Vlasov-Poisson equations, treated as an initial value problem. It is shown that the solutions depend on finding certain symplectic mappings, and how to compute these maps is discussed given a beam transport system and initial particle distribution function. Dissert. Abstr.

N89-11497# Argonne National Lab., Ill. Materials Science Div.
BRILLOUIN SCATTERING AT HIGH PRESSURES
M. Grimsditch and A. Polian (Paris VI Univ., France) Feb. 1988 20 p Presented at the NATO Advanced Study Institute on Simple Molecular Systems At Very High Densities, Les Houches, France, 29 Mar. - 5 Apr. 1988
(Contract W-31-109-eng-38)
(DE88-011972; CONF-880372-1) Avail: NTIS HC A03

Technical advances which have made Brillouin scattering a useful tool in high pressure diamond anvil cell (DAC) studies, viz. multipassing and tandem operation of Fabry-Perot interferometers, are reviewed. Experimental aspects, such as allowed scattering geometries, are outlined and the data analysis required to transform Brillouin spectra into sound velocities and elastic constants is presented. Experimental results on H2, N2, Ar, and He are presented, and the close relationship between the Brillouin scattering results and equations of state is highlighted. DOE

N89-11498*# National Aeronautics and Space Administration. Langley Research Center, Hampton, Va.
PSEUDO-SCALAR PI N COUPLING AND RELATIVISTIC PROTON-NUCLEUS SCATTERING
Franz Gross, Khin Maung Maung, J. A. Tjon, L. W. Townsend, and S. J. Wallace (Maryland Univ., College Park.) 1988 12 p Prepared in cooperation with Continuous Electron Beam Accelerator Facility, Newport News, Va.
(Contract DE-AC05-84ER-40150)
(NASA-TM-101199; NAS 1.15:101199; CEBAF-PR-88-010) Avail: NTIS HC A03/MF A01 CSCL 20H

Relativistic p-Ca-40 elastic scattering observables are calculated using relativistic NN amplitudes obtained from the solution of a two-body relativistic equation in which one particle is kept on its mass-shell. Results at 200 MeV are presented for two sets of NN amplitudes, one with pure pseudo-vector coupling for the pion and another with a 25 percent admixture of pseudo-scaling coupling. Both give a very good fit to the positive energy on-shell NN data. Differences between the predictions of these two models (which are shown to be due only to the differences in their corresponding negative energy amplitudes) provide a measure of the uncertainty in contructing Dirac optical potentials from NN amplitudes. Author

N89-11499# Continuous Electron Beam Accelerator Facility, Newport New, Va.
ELECTROPRODUCTION OF BARYON RESONANCES ABOCE THE DELTA(1232)
V. Burkert [1988] 20 p
(Contract DE-AC05-84ER-40150)
(CEBAF-PR-88-012) Avail: NTIS HC A03/MF A01

Results of electroproduction studies of the higher resonances are reviewed and compared to quark model calculations and to predictions from quark counting rules and quantum chromodynamic sum rules. Author

N89-11500*# Fermi National Accelerator Lab., Batavia, Ill.
GAUGED Q-BALLS
Kimyeong Lee, Jaime A. Stein-Schabes, Richard Watkins, and Lawrence M. Widrow (Chicago Univ., Ill.) 30 Sep. 1988 25 p Sponsored in part by NASA, DOE, and NSF
(NASA-CR-183369; NAS 1.26:183369; FERMILAB-Pub-88/139-A)
Avail: NTIS HC A03/MF A01 CSCL 20H

Classical non-topological soliton configurations are considered within the theory of a complex scalar field with a gauged U symmetry. Their existence and stability against dispersion are demonstrated and some of their properties are investigated analytically and numerically. The soliton configuration is such that inside the soliton the local U symmetry is broken, the gauge field becomes massive and for a range of values of the coupling constants the soliton becomes a superconductor pushing the charge to the surface. Furthermore, because of the repulsive Coulomb force, there is a maximum size for these objects, making impossible the existence of Q-matter in bulk form. Also briefly discussed are solitons with fermions in a U gauge theory. Author

N89-11501*# Fermi National Accelerator Lab., Batavia, Ill.
THE DECAY OF HIGHLY EXCITED OPEN STRINGS
D. Mitchell, N. Turok, R. Wilkinson, and P. Jetzer Jun. 1988 37 p Sponsored in part by NASA, DOE, and by Swiss National Science Foundation
(NASA-CR-183364; NAS 1.26:183364; FERMILAB-Pub-88/78-A)
Avail: NTIS HC A03/MF A01 CSCL 20H

The decay rates of leading edge Regge trajectory states are calculated for very high level number in open bosonic string theories, ignoring tachyon final states. The optical theorem simplifies the analysis while enabling identification of the different mass level decay channels. The main result is that (in four dimensions) the greatest single channel is the emission of a single photon and a state of the next mass level down. A simple asymptotic formula for arbitrarily high level number is given for this process. Also calculated is the total decay rate exactly up to N=100. It shows little variation over this range but appears to decrease for larger N. The formalism is checked in examples and the decay rate of the first excited level calculated for open superstring theories. The calculation may also have implications for high spin meson resonances. Author

N89-11502 Max-Planck-Inst. fuer Physik und Astrophysik, Garching (West Germany). Werner-Heisenberg Inst. fuer Physik.
SEARCH FOR NARROW RESONANCE PRODUCTION IN BHABHA SCATTERING AT CENTER-OF-MASS ENERGIES NEAR 1.8 MeV
E. Lorenz, G. Mageras, U. Stiegler, and I. Huszar (Paul Scherrer Inst., Villigen, Switzerland) May 1988 14 p Submitted for publication
(MPE-PAE/Exp-El-190; ETN-88-93191) Copyright Avail:

Fachinformationszentrum Karlsruhe, 7514
Eggenstein-Leopoldshafen 2, Fed. Republic of Germany

Narrow resonances in a fine energy scan of the Bhabha scattering cross section were probed. The statistical sensitivity was 1.6 percent for center-of-mass energies between 1.62 and 1.74 MeV, and 0.8 percent between 1.74 and 1.89 MeV. No significant structure is observed. Upper limits for the intrinsic width of resonances in the above energy range are derived. ESA

N89-11503# Air Force Inst. of Tech., Wright-Patterson AFB, Ohio.
NEUTRON MULTIPLICATION IN BERYLLIUM Ph.D. Thesis
Richard S. Hartley 1988 170 p
(AD-A196877; AFIT/CI/NR-88-59) Avail: NTIS HC A08/MF A01 CSCL 07B

Integral neutron multiplication experiments have been performed using homogeneous spherical shells of beryllium metal of 4.6-, 6.99-, 7.87-, 9.38-, 13.8-, and 19.9-cm thickness. Neutron leakage, produced by Cf-252 and DT neutron sources placed in the center of the shells, were measured with a Bonner sphere spectrometer system. The rate of DT neutron production was normalized using an associated particle system placed inside the target assembly which was inserted into the shells via a re-entrant hole. The neutron fluence was obtained by processing the room-returned and air-scattered corrected count-rate data with a Bonner sphere spectrum unfolding routine and a weighted Bonner sphere technique. The neutron multiplication was obtained directly by comparing the normalized neutron leakage fluence with and without beryllium present. The neutron leakage spectra were calculated for each shell using the discrete ordinates codes ANISN and ONEDANT using ENDF/B-IV and ENDF/B-V respectively. GRA

73 NUCLEAR AND HIGH-ENERGY PHYSICS

Includes elementary and nuclear particles; and reactor theory.

For space radiation see *93 Space Radiation.*

N89-11504# Los Alamos National Lab., N. Mex. Chemistry and Laser Sciences Div.
HIGH ENERGY-INTENSITY ATOMIC OXYGEN BEAM SOURCE FOR LOW EARTH ORBIT MATERIALS DEGRADATION STUDIES
J. B. Cross and N. C. Blais 1988 14 p Presented at the 16th International Symposium on Rarefied Gas Dynamics, Pasadena, Calif., 11 Jul. 1988
(Contract W-7405-eng-36)
(DE88-014316; LA-UR-88-2188; CONF-880781-1) Avail: NTIS HC A03/MF A01

A high intensity (10 to the 19th O-atoms/s-sr) high energy (5 eV) source of oxygen atoms has been developed that produces a total fluence of 10 to the 22d O-atoms/sq cm in less than 100 hours of continuous operation at a distance of 15 cm from the source. The source employs a CW CO2 laser sustained discharge to form a high temperature (15,000 K) plasma in the throat of a 0.3-mm diameter nozzle using 3 to 8 atmospheres of rare gas/O2 mixtures. Visible and infrared photon flux levels of 1 watt/sq cm have been measured 15 cm downstream of the source while vacuum UV (VUV) fluxes are comparable to that measured in low earth orbit. The reactions of atomic oxygen with kapton, Teflon, silver, and various coatings have been studied. The oxidation of kapton (reaction efficiency = 3x10 to the -24 cm + or - 50 percent) has an activation energy of 0.8 Kcal/mole over the temperature range of 25 to 100 C at a beam energy of 1.5 eV and produces low molecular weight gas phase reaction products (H2O, NO, CO2). Teflon reacts with approx 0.1 to 0.2 efficiency to that of kapton at 25 C and both surfaces show a ruglike texture after exposure to the O-atom beam. Angular scattering distribution measurements of O-atoms show a near cosine distribution from reactive surfaces indicating complete accommodation of the translational energy with the surface while a nonreactive surface (nickel oxide) shows specular-like scattering with 50 percent accommodation of the translational energy with the surface. A technique for simple on orbit chemical experiments using resistance measurements of coated silver strips is described. DOE

N89-11505# Los Alamos National Lab., N. Mex.
SPACE NUCLEAR SAFETY PROGRAM Progress Report, Jan. - Mar. 1987
T. C. George, comp. Jul. 1988 15 p
(Contract W-7405-eng-36)
(DE88-015048; LA-11274-PR) Avail: NTIS HC A03/MF A01

This quarterly report describes studies related to the use of PuO2 (of Pu-238) in radioisotope power systems, which were carried out for the Office of Special Nuclear Projects of the U.S. Department of Energy by Los Alamos National Laboratory. Most of the studies discussed are ongoing; the results and conclusions described may change as the work progresses. DOE

N89-11506# Los Alamos National Lab., N. Mex.
POSTANALYSIS OF THE CNPS (COMPACT NUCLEAR POWER SOURCE) CRITICAL EXPERIMENT
R. G. Palmer 1988 13 p Presented at the International Reactor Physics Conference, Jackson Hole, Wyo., 18 Sep. 1988
(Contract W-7405-eng-36)
(DE88-014322; LA-UR-88-2258; CONF-880911-11) Avail: NTIS HC A03

The Compact Nuclear Power Source (CNPS) was designed to produce electric power for remote sites where fuel logistics and costs would justify a remotely sited nuclear power plant. Since the reactor was of novel design with no appropriate benchmarks, a series of critical experiments was carried out at LANL. This paper describes the methodology and reports the results of the postanalysis that was performed on the critical experiments, which included several distinct critical configurations, the measurement of the isothermal temperature coefficient of reactivity and various material worths. Comparisons with measurements indicate that current methods and cross sections are adequate for calculating at least the beginning of life conditions in low enriched U-235-graphite cores. DOE

N89-11507# Los Alamos National Lab., N. Mex.
CRITICAL EXPERIMENTS IN SUPPORT OF THE CNPS (COMPACE NUCLEAR POWER SOURCE) PROGRAM
G. E. Hansen, J. H. Audas, E. R. Martin, R. A. Pederson, G. D. Spriggs, and R. H. White 1988 9 p Presented at the International Reactor Physics Conference, Jackson Hole, Wyo., 18 Sep. 1988
(Contract W-7405-eng-36)
(DE88-014326; LA-UR-88-2272; CONF-880911-12) Avail: NTIS HC A02/MF A01

Zero-power static and kinetic measurements have been made on a mock-up of the Compact Nuclear Power Source (CNPS), a graphite moderated, graphite reflected, U(19.9 pct U-235) fueled reactor design. Critical configurations were tracked from a first clean configuration (184 most central fuel channels filled and all control rod and heat pipe channels empty) to a fully loaded configuration (all 492 fuel channels filled, core-length stainless steel pipe in the twelve heat-pipe channels, and approximately half-core-length boron carbide in the outer 4 control rod channels. Reactor physics data such as material worths and neutron lifetime are presented only for the clean and fully loaded configurations. DOE

N89-11508# Los Alamos National Lab., N. Mex.
ANALYSIS OF SP-100 CRITICAL EXPERIMENTS
J. L. Sapir, D. I. Brandon, P. J. Collins, C. L. Cowan, C. A. Porter, and S. V. Andre (Westinghouse Electric Corp., Madison, Pa.) 1988 15 p Presented at the International Reactor Physics Conference, Jackson Hole, Wyo., 18 Sep. 1988
(Contract W-7405-eng-36)
(DE88-014429; LA-UR-88-2008; CONF-880911-14) Avail: NTIS HC A03/MF A01

In support of the SP-100 space nuclear power source program, preliminary critical benchmark experiments were performed at the

ZPPR facility at ANL-W. These configurations are representative of small, fast-spectrum, BeO-reflected, liquid metal-cooled space reactor designs at a 300-kWe power level. Analyses were performed using MCNP (Monte Carlo) and TWODANT (discrete ordinates) transport codes to calculate system criticality, control worth, and power distribution. Both methods calculated eigenvalues within 0.5 percent of the experimental results. Internal-poison-rod worth was underpredicted and radial reflector worth was overpredicted by both codes by up to 20 percent. MCNP-calculated control drum worths were underestimated by approximately 8 percent. Good agreement with experimental values was observed for U-235 fission and for U-238 fission and capture rates with the best agreement occurring in the fuel region and slightly poorer predictions apparent near BeO moderator. DOE

N89-11509# Austin Research Associates, Inc., Tex.
BEAM HANDLING AND EMITTANCE CONTROL Technical Report, 1 Sep. 1986 - 28 Feb. 1988
J. R. Thompson, M. L. Sloan, B. N. Moore, and J. R. Uglum 15 Jul. 1988 65 p
(Contract N00014-86-C-0568)
(AD-A196789; I-ARA-88-U-24) Avail: NTIS HC A04/MF A01 CSCL 15C

This report reviews the results of calculations which concern techniques of beam handling and emittance control for high current beams in advanced accelerators. Beam quality requirements for acceptable performance of beam driven free electron laser devices for SDI missions are examined. The beam quality achievable in high current, space-charge-limited diodes is reviewed and found to be potentially high. Emittance growth during gas-focused transport due to streaming instabilities between beam electrons and gas ions is briefly examined, and estimated to be modest. The principal threat to beam quality degradation is estimated to occur during the lengthy process of acceleration and transport past protuberances, constrictions, or discontinuities in the waveguide wall, or during beam aperturing. A Hamiltonian-theoretic analysis of emittance growth during high current electron beam transport, coupled with an envelope equation analysis of the induced transverse beam oscillations, is applied to develop scaling laws for the emittance growth suffered during such events as beam acceleration, propagation past irises or constrictions in the waveguide wall, beam aperturing, and axial variation in the magnetic guide filed strength. Criteria area developed for preventing excessive emittance growth by avoiding abrupt axial variations and providing sufficiently strong focusing forces. GRA

74 OPTICS

Includes light phenomena; and optical devices.
For lasers see *36 Lasers and Masers.*

N89-11510# Aeronautical Research Labs., Melbourne (Australia).
IN-PLANE MOIRE OPTICAL PROCESSING AT ARL
K. C. Watters Jul. 1987 42 p
(ARL-Struc-R-428; AR-004-543) Avail: NTIS HC A03/MF A01

The principle and operation of the ARL in-plane moire optical processor are described in detail. The processor uses extensive spatial filtering to produce dual beam interference moire fringes of high contrast. Fringe patterns obtained from a J integral specimen and a cold worked bolt hole specimen are shown. They compare well with displacement contour patterns obtained from a theoretical analysis and strain gage data. Author

N89-11511# Oak Ridge National Lab., Tenn. Solid State Div.
DESIGN OF HIGH-REFLECTIVITY SUPERMIRROR STRUCTURES
John B. Hayter and H. A. Mook 1988 9 p Presented at the 32nd International Technical Symposium on Optical and Opto-electronic Applied Sciences and Engineering, San Diego, Calif., 14 Aug. 1988
(Contract DE-AC05-84OR-21400)
(DE88-015287; CONF-880887-8) Avail: NTIS HC A02/MF A01

A new method is presented of designing supermirrors, based on considering the contribution of each bilayer to the extinction in a given stack of bilayers, and derive and solve the discrete equations governing the choice of layer thicknesses. In the limit of zero layer thickness, the usual continuum result is recovered. The design, which can produce essentially perfect reflectivity over the entire supermirror range, also provides an objective physical mechanism for trading reflectivity to gain angular range. Author

N89-11512# Pacific Northwest Labs., Richland, Wash.
QUANTITATIVE LUMINESCENCE IMAGING SYSTEM DESCRIPTION AND USER'S MANUAL
K. A. Stahl and C. R. Batishko Jun. 1988 54 p
(Contract DE-AC06-76RL-01830)
(DE88-015604; PNL-6592) Avail: NTIS HC A04/MF A01

A Quantitative Luminescence Imaging System (QLIS) was designed and constructed. The system was developed for use in imaging and quantitative analysis of very low light level chemiluminescent phenomena. The luminescent reactions are imaged via microchannel plate image intensifier coupled to a newvicon video camera. The video record of the reaction can be stored on video tape or digitally captured by an image processing system which is integral to a host computer controller. Since the particular experimental conditions for which the QLIS was designed necessitate that the chemiluminescent reaction take place in an rf flux within a waveguide, the system includes a coherent fiber optic image transfer system which allows the video hardware to be mounted externally to the rf waveguide. DOE

N89-11513# Centre d'Essais Aeronautique Toulouse (France).
STATE-OF-THE-ART IN FIBER OPTIC SYSTEMS AT THE AERONAUTIC TEST CENTER, TOULOUSE (FRANCE) [ETAT DE L'ART DANS LE DOMAINE DES SYSTEMES A FIBRES OPTIQUES AU CEAT]
14 Apr. 1988 20 p In FRENCH
(Rept-363300; ETN-88-93103) Avail: NTIS HC A03/MF A01

The advantages of fiber optic communication are reviewed, and the state of the art in light transmission, light reception, optical fibers, and connections is discussed. Aeronautical fiber optic systems (on board and ground) are described. ESA

N89-11514# Air Force Inst. of Tech., Wright-Patterson AFB, Ohio.
A SURVEY OF DIGITAL BEAM FORMING TECHNIQUES AND CURRENT TECHNOLOGY M.S. Thesis
John E. McCord 1988 72 p
(AD-A196376; AFIT/CI/NR-88-81) Avail: NTIS HC A04/MF A01 CSCL 17I

Digital beamforming provides key advantages over analog beamforming in radar applications where proper response to multiple jammers in a rapidly changing environment is required. Ths survey reviews these advantages and various digital methods for attaining them. Disadvantages and limitations are also given. The mathematical basis for beamforming is reviewed. Five experimental digital beamforming systems discussed here reveal the current level of digital implementation. Also covered are current technologies available and future trends for digital beamforming. GRA

N89-11515# Army Lab. Command, Watertown, Mass. Material Technology Lab.
APPLICATIONS OF THE OPTICAL DIFFERENTIAL THERMAL ANALYSIS Final Report
Jaroslav L. Caslavsky May 1988 15 p
(AD-A196706; MTL-TR-88-18) Avail: NTIS HC A03/MF A01 CSCL 20M

ODTA detects temperature contact less, hence, it expands the upper usable temperature limit of DTA up to 3600 C accordingly suitable for studies of systems where enthalpic changes occur at high temperatures. Application of the computer graphics for the evaluation of the ODTA curves is demonstrated on melting of

Y2O3.A12O3 and Ya13-GdA1O3 systems. Measurement errors occurring at temperatures above 1900 C are pointed out and possibilities for their elimination or at least diminution are discussed. GRA

N89-11516# Naval Postgraduate School, Monterey, Calif.
UNIDIRECTIONAL MANCHESTER ENCODED DATA TRANSFER VIA A FIBER OPTIC LINK M.S. Thesis
Robert G. Ragsdale, Jr. Mar. 1988 44 p
(AD-A196961) Avail: NTIS HC A03/MF A01 CSCL 25E

The subject of this thesis is the application of Manchester coding techniques to digital data transfer. Asynchronous receipt of digital data for decoding eliminates many of the technical implementation problems associated with synchronous transmission of data. The thesis goal was to construct the necessary hardware to allow Manchester encoded data transfer over a fiber optic data link. The scope of the project was limited to the transfer of byte size amounts of data from a microcomputer bus through the fiber link back to the computer bus. Successful coding, transmission, and decoding were accomplished as delineated in the hardware design section. GRA

75 PLASMA PHYSICS

Includes magnetohydrodynamics and plasma fusion.
For ionospheric plasmas see *46 Geophysics*. For space plasmas see *90 Astrophysics*.

N89-11517 Wisconsin Univ., Madison.
ALFVEN WAVE STUDIES ON A TOKAMAK Ph.D. Thesis
David Kortbawi 1987 151 p
Avail: Univ. Microfilms Order No. DA8727239

The continuum modes of the shear Alfven resonance are studied on the Tokapole 2 device, a small tokamak operated in a four node poloidal divertor configuration. A variety of antenna designs and the efficiency with which they deliver energy to the resonant layer are discussed. The spatial structure of the driver waves is studied by means of magnetic probes inserted in the current channel. In an attempt to optimize the coupling of energy into the resonance layer, the angle of antenna currents with respect to the equilibrium field, antenna size, and plasma-to-antenna distance are varied. The usefulness of the Faraday shields, particle shields, and local limiters are investigated. Driving antenna currents parallel to the equilibrium field leads to large parasitic loading, due to the wave electric field being heavily attenuated in the edge of the plasma. The wave magnetic fields measure show a spatial resonance, the position of which varies with the value of the equilibrium field and mass density. They are polarized perpendicular to the equilibrium field. A wave propagates radially into the resonant surface where it is converted to the shear Alfven wave. The signal has a short rise time and does not propagate far toroidally. Dissert. Abstr.

N89-11518# College of William and Mary, Williamsburg, Va.
THEORETICAL PLASMA PHYSICS Progress Report, 1 Jan. - 31 Oct. 1988
Allen H. Boozer, George Vahala, and Eugene R. Tracy Jun. 1988 11 p
(Contract DE-FG05-84ER-53176)
(DE88-014285; DOE/ER-53176/4) Avail: NTIS HC A03/MF A01

During the past year we have studied the effect of magnetic islands on transport. Plasma properties near a magnetic separatrix, tokamak current drive, transport in tokamaks with ripple, methods for integrating magnetic field line equations that permit very long integration steps, alpha particle diagnostics that utilize the scattering of light from CO2 laser or millimeter sources, and models of plasma turbulence. These are briefly discussed in this paper. DOE

N89-11519# Massachusetts Inst. of Tech., Cambridge. Plasma Fusion Center.
MASSACHUSETTS INSTITUTE OF TECHNOLOGY PLASMA FUSION CENTER 1987--1988 REPORT TO THE PRESIDENT
Jun. 1988 24 p
(Contract DE-AC02-78ET-51013)
(DE88-014800; DOE/ET-51013/251; PFC/IR-88-4) Avail: NTIS HC A03/MF A01

During the past year, technical progress has been made in all Plasma Fusion Center (PFC) research programs. The Plasma Fusion Center is recognized as one of the leading university research laboratories in the physics and engineering aspects of magnetic confinement fusion. Its research programs have produced significant results on several fronts: the basic physics of high-temperature plasmas (plasmas theory, RF heating, free electron lasers, development of advanced diagnostics, and intermediate-scale experiments on the Versator tokamak and Constance mirror devices), major confinement results on the Alcator C tokamak, including pioneering investigations of the stability, heating, and confinement properties of plasmas at high densities, temperatures and magnetic fields, experiments on the medium-scale TARA tandem mirror, including the development of novel MHD stabilization techniques in axisymmetric geometry, and a broad program of fusion technology and engineering development that addresses problems in several critical subsystem areas (e.g., magnet systems, superconducting materials development, environmental and safety studies, advanced millimeter-wave source development, and system studies of fusion reactor design, operation, and technology requirements. DOE

N89-11520# Nagoya Univ. (Japan). Inst. of Plasma Physics.
THEORY OF HIGH POWER CYCLOTRON RESONANCE HEATING IN NON-UNIFORM MAGNETIC FIELD
Ryo Sugihara and Yuichi Ogawa Jun. 1988 55 p
(IPPJ-875; ISSN-0469-4732) Avail: NTIS HC A04/MF A01

Energy absorption of a plasma due to cyclotron harmonic resonance is evaluated analytically and by a simulation. In the calculation an orbit modification of cyclotron motion of particles is fully taken into account. It is found that the absorption for the fundamental harmonic resonance (m=1) is depressed from that of the conventional linear approximation while the absorptions for m less than or greater than 2 are enhanced, where m is the harmonic number. The enhancement is significant when kp sub t is much less than 1 (K the perpendicular wave number and p sub the gyroradius of a thermal particle) and when the interaction time between the plasma particles and the wave exceeds a critical value that is obtainable analytically. For all m and kp sub t, there appear peaks or saturations in the absorption. The second harmonic ion cyclotron resonance heating experiment in the Princeton Large Tokamak is discussed in terms of this theory. Author

N89-11521 California Univ., Los Angeles.
EXPERIMENTAL STUDY OF TIME-VARYING CURRENT FLOW BETWEEN ELECTRODES IMMERSED IN A LABORATORY MAGNETOPLASMA Ph.D. Thesis
Jose Manuel UrrutiaPaez 1987 144 p
Avail: Univ. Microfilms Order No. DA8802514

The flow of current between electrodes immersed in plasmas is a topic of importance in the operation of plasma probes, plasma confinement research and space based experiments. To date, however, research has been limited to time stationary treatments of the regions immediate to the electrodes themselves. For the case of nonemitting electrodes, positive and negative charge carriers are predicted to flow from the entire plasma into the oppositely charged electrodes, while only one species is involved if one of the electrodes emits charged particles. If the charge carriers are magnetized, the current flow is restricted to flux tubes subtended by the electrodes. A series of experiments designed to explore such concepts are reported for a plasma where the electrons are magnetized and the ions are not. From the careful observation of the magnetic field induced in the plasma by the currents, as well as from detailed measurements of the plasma

parameters and their fluctuations, it is found that currents do not flow as predicted. Ion currents appear to be limited to the vicinity of the negative electrode, while electron currents are seen to flow across magnetic field lines at rates exceeding those allowed by classical diffusion. Dissert. Abstr.

N89-11522# International Centre for Theoretical Physics, Trieste (Italy).
ON HYDROMAGNETIC CHANNEL FLOW INDUCED BY TOOTH PULSES
A. R. Bestman and F. I. Njoku Jan. 1988 12 p Submitted for publication
(DE88-703031; IC-88/10) Avail: NTIS (US Sales Only) HC A03/MF A01

The paper considers unsteady hydromagnetic flow in a channel when the induced magnetic field is not necessarily negligible. The unsteadiness is sustained by velocity tooth pulses applied at one wall of the channel. The skin friction at the wall is compared with the situation when the induced magnetic field is neglected. DOE

N89-11523# Nagoya Univ. (Japan). Inst. of Plasma Physics.
COMPARISON BETWEEN URAMOTO TYPE AND STRAIGHT FILAMENT TYPE SHEET PLASMAS AS A VOLUME PRODUCED H(-) ION SOURCE (I)
Joshin Uramoto Jun. 1988 30 p
(IPPJ-876; ISSN-0469-4732) Avail: NTIS HC A03/MF A01

The Uramoto type sheet plasma (transformed from a cylindrical plasma by two permanent magnets) and a long straight filament cathode type sheet plasma are compared as volume produced H(-) ion sources. For a same discharge power (for example 5A x 100 V = 500 W), a H(-) ion current density (2.5 mA/sq cm) extracted from the Uramoto type sheet plasma, is above 20 times larger that that from the straight filament type (0.125 mA/sq cm). As an essential difference between the two types, it is pointed out that the Uramoto type uses in combination a negative bias voltage on the metallic large vacuum chamber (surrounding the sheet plasma) and a cusp magnetic field produced by the two permanent magnets which are effective on the confinement of electrons and H(-) ions. A pressure gradient discharge of the ordinary Uramoto type is not essential for volume production of H(-) ions, but is very useful to reduce the optimum pressure. Author

N89-11524# KMS Fusion, Inc., Ann Arbor, Mich.
KCl BOUNCE COATING OF GLASS AND POLYMER MICROSHELLS
G. B. DeMaggio, S. R. Murrell, H. K. Lintz, and J. C. Daukas 1988 11 p Presented at the 6th Target Fabrication Specialist's Meeting, Los Alamos, N. Mex., 19 Jun. 1988
(Contract DE-AC08-87DP-10560)
(DE88-013018; KMSF-U-1996; CONF-8806170-9) Avail: NTIS HC A03

The progress that the Inertial Confinement Fusion (ICF) program has seen with increased laser energy and advances in plasma theory has pushed for improvements and advances in both target performance diagnostics and target fabrication. Many advances in target hinge on the ability to prepare implosion pellets with a high degree of sphericity and then overcoat these with thin films of many different materials. The materials desired by the experimenters are quite varied and the requirements for smoothness and uniformity of these coatings are becoming more stringent. This summary describes work being pursued at KMS concerning the preparation of spherical targets with imbedded layers to aid in the evaluation of the implosion process. These layers contain specific elements designed to absorb X-rays and yield an image of the compressed target. In this case, chlorine is the required element; and one chemically stable form in which to include this element is KCl. The complete target requires a thick hydrocarbon (CH) layer on top of the KCl. DOE

N89-11525# Connecticut Univ., Storrs.
ATOMIC PROCESSES IN HIGH TEMPERATURE PLASMAS Progress Report
1988 5 p
(Contract DE-FG02-85ER-53205)
(DE88-013005; DOE/ER-53205/T3) Avail: NTIS HC A02/MF A01

It is proposed to continue the theoretical study of dielectronic recombination (DR) and related resonant processes in electron-ion collisions, with special emphasis on the effect of high temperature plasma environment. The DR work on the B-like ions, improvement of the empirical rate formula, and the static field effect on high Rydberg states will continue. A theoretical procedure will be developed to incorporate the effects of both the static ion microfield and time-dependent electron density of the plasma. In addition, the resonant ionization process will be examined to understand the recent experimental observations. This includes both the cascade Auger decay and simultaneous two-electron emission of the resonant states. Improved electron correlation is needed. DOE

N89-11526# Nagoya Univ. (Japan). Inst. of Plasma Physics.
EXCITATION OF MHD SURFACE WAVES PROPAGATING WITH SHEAR ALFVEN WAVES IN AN INHOMOGENEOUS CYLINDRICAL PLASMA
Y. Amagishi, K. Saeki, and I. J. Donnelly (Australian Nuclear Science and Technology Organisation, Menai.) Jun. 1988 41 p
(IPPJ-872; ISSN-0469-4732) Avail: NTIS HC A03/MF A01

Experimental results are presented which show that the MHD surface waves or fast waves of M = + or - 1 were excited in the range of frequency less than ion cyclotron frequency using a helical antenna in a finite beta and cylindrical plasma. Their dispersion relation and spatial structure were successfully confirmed after the wave signals were separated from those of the local shear Alfven waves that propagated together with the surface waves. In order to obtain the dispersion relations from the signals, we adopted three kinds of methods: (1) conventional cross-power spectrum density using fast Fourier transform, (2) maximum entropy method, and (3) direct estimation of the phase velocity of wave packets. Author

N89-11527# Nagoya Univ. (Japan). Inst. of Plasma Physics.
MODELLING OF THE 2-DIMENSIONAL STRUCTURE AND IMPURITY TRANSPORT FOR A SCRAPE-OFF LAYER WITH A SOLID LIMITER
T. Kawamura, T. Ono, Y. Masuda, and D. Reiter (Kernforschungsanlage, Juelich, West Germany) Jun. 1988 8 p
(IPPJ-873; ISSN-0469-4732) Avail: NTIS HC A02/MF A01

A 2 dimensional modeling of a scrape off layer (SOL) with a solid limiter is presented. After the plasma in a SOL is calculated by a plasma code, SLIM, based on the 2 dimensional fluid equations with source terms due to neutral particles, the neutral transport is calculated by a Monte Carlo code, EIRENE, with the use of the results by SLIM. Then these two calculations are iteratively performed until a nearly self consistent result is obtained. Ionization of neutral impurity particles ejected from the first wall and random diffusion of the charged impurities across the magnetic field lines in the SOL plasma are simulated by a Monte Carlo method. From the statistical analysis on the numerical results the screening efficiency of a SOL, impurity redeposition rate and behavior of impurities in a SOL are analyzed. Author

N89-11528# Wisconsin Univ., Madison. Dept. of Electrical and Computer Engineering.
STELLARATOR THEORY Progress Report
W. N. G. Hitchon Jul. 1988 122 p
(Contract DE-FG02-85ER-53201)
(DE88-014131; DOE/ER-53201/3) Avail: NTIS HC A06/MF A01

This paper discusses progress in the following areas: the propagator method; ripple transport in tokamaks; self-consistent bounce-averaged numerical transport; computations: the bootstrap current; comparisons of stellarator ripple transport calculations; and plasma transport in the Interchangeable module Stellarator (IMS) using a 1D fluid transport code. DOE

N89-11529# Nagoya Univ. (Japan). Inst. of Plasma Physics.
DEVELOPMENT OF THE WORK FUNCTION MONITORING METHOD FOR A CONVERTER OF A NEGATIVE ION SOURCE
Hitoshi Yamaoka, Mamiko Sasao, Motoi Wada, and Henry J. Ramos (University of the Philippines, Quezon City.) Jul. 1988 21 p
(IPPJ-880; ISSN-0469-4732) Avail: NTIS HC A03/MF A01

A method to monitor the change in the work function of the converter surface in a self-extraction negative ion source is developed. The photoelectron emission from the Cs-Mo surface in a plasma is detected by irradiating surface with laser lights. Negative ions produced at the surface shows a strong correlation with the photoelectron current induced by the Ar+ laser is used to detect the change in the cesium coverage, or the work function, while that by the dye laser is found to be suitable to confirm the region of the work function minimum. Author

N89-11530# Sandia National Labs., Albuquerque, N. Mex.
HIGH HEAT FLUX TESTING OF CIT (COMPACT IGNITION TOKAMAK) FIRST WALL TILES
R. D. Watson, C. D. Croessmann, J. G. Watkins, and J. F. Dempsey Mar. 1988 163 p
(Contract DE-AC04-76DP-00789)
(DE88-012241; SAND-87-2452) Avail: NTIS HC A08/MF A01

Sandia National Laboratories' Fusion Technology Divison has performed a series of tests in support of the Compact Ignition Tokamak (CIT) first wall tile design. First, a screening study was done to rank the thermal shock resistance of 25 candidate graphite materials. Intense heat pulses generated by the electron beam test system cracked most of the fine-grained graphites but did not fracture any of the carbon/carbon composite samples. The best performing fine-grained graphites were Union Carbide's TS-1792, TS-1909, and ATJ-S; as well as Fiber Material's type HDG. Next, mechanical tests were performed on prototype first wall tiles made of POCO AXF-5Q, and an FMI 4-D carbon/carbon nut, both designed and fabricated by GA Technologies, Inc. These tests included static tension, compression, and bending loads, as well as dynamic vibration and shock loading. Failure analysis indicates that the carbon/carbon composite nut is the weak link in the design. A resonant frequency of 2000 Hz was measured. The tile assembly survived 3000 transient shock pulses of 350 g acceleration over a 100 ms duration. Finally, ion beam heating tests were performed on prototype tile assemblies. The tile survived peak heat pulses of 1000 W/sq cm for 4 s and 1500 W/sq cm for 3 s without damage. These heat loads exceed design requirements of 850 W/sq cm for 3.2 s. However, a thermal stress crack in the POCO AXF-5Q tile was observed at a power level of 2000 W/sq cm after 2 s. DOE

N89-11531# New York Univ., New York. Inst. of Mathematical Sciences.
ANOMALOUS TRANSPORT ARISING FROM NONLINEAR RESISTIVE PRESSURE-DRIVEN MODES IN A PLASMA
Satoshi Hamaguchi May 1988 106 p
(Contract DE-FG02-86ER-53223)
(DE88-014984; DOE/ER-53223/68; MF-117) Avail: NTIS HC A06/MF A01

Anomalous transport caused by fluctuations of resistive pressure-driven modes is discussed within the framework of magnetohydrodynamics (MHD). The nonlinear reduced equations describing fluctuations localized near a particular magnetic field line are derived for tokamak and reversed-field-pinch (RFP) plasmas, taking into account nonzero viscosity and heat conductivity. Based on the reduced equations, the relationship between the dynamo effect, or the electric field caused by the fluctuations, and the anomalous heat transport is obtained. For an ideally stable but resistively slightly unstable plasma, the anomalous transport is caused particularly by convective motions. The convection is studied as bifurcation from the linearly unstable equilibrium and the expression of the anomalous transport in a tokamak plasma is obtained as a function of the mean pressure gradient near the critical point. In order to evaluate the effects of the convection on the anomalous transport under various conditions, the reduced equations are also solved numerically. It is found that the Nusselt number, that is, the ratio of the total heat conductivity including the anomalous heat transport to the classical collisional heat conductivity, is significantly large under some conditions. This partially explains the large heat losses in controlled thermonuclear fusion devices. DOE

N89-11532# Los Alamos National Lab., N. Mex.
CURRENT NEW APPLICATIONS OF LASER PLASMAS
Allan A. Hauer, David W. Forslund, Colin J. McKinstrie, Justin S. Wark, Philip J. Hargis, Jr., Roy A. Hamil, and Joseph M. Kindel (Mission Research Corp., Los Alamos, N. Mex.) Sep. 1988 39 p
(Contract W-7405-eng-36)
(DE88-015679; LA-11296-MS) Avail: NTIS HC A03/MF A01

Described are several new applications of laser-produced plasmas that have arisen in the last few years. Most of the applications have been an outgrowth of the active research in laser/matter interaction inspired by the pursuit of laser fusion. Unusual characteristics of high-intensity laser/matter interaction, such as intense X-ray and particle emission, were noticed early in the field and are now being employed in a significant variety of applications outside the fusion field. Applications range from biology to materials science to pulsed-power control and particle accelerators. DOE

N89-11533# Etablissement Technique Central de l'Armement, Arcueil (France). Service Physique des Surfaces.
PLASMA SPECTROMETRY APPLIED TO SURFACE TREATMENTS (LASER PVD) Final Report [SPECTROMETRIE DES PLASMAS APPLIQUES AUX TRAITEMENTS DE SURFACE (LASER-PVD)]
D. Degout and G. Farges 29 Mar. 1988 142 p In FRENCH
(Contract DRET-SDR-G3-86-1066)
(ETCA-88-R-036; ETN-88-93108) Avail: NTIS HC A07/MF A01

Processes occurring in plasmas used for surface treatments were defined. The plasma environment in the case of treatment of a metallic surface by a continuous laser beam was analyzed by optical emission spectroscopy, and the main plasma parameters were derived (integrated in time and space). Further understanding of the plasma environment depends on better knowledge of processes linked to species diffusion and to the rate of partial recombination of excited states. The plasma processes involved in deposition of thin layers of titanium nitrate were examined. A special investigation of the cathode zone of the deposit discharge is required in order to understand the elementary reactions observed. ESA

N89-11534# Max-Planck-Inst. fuer Plasmaphysik, Garching (West Germany).
ASDEX CONTRIBUTIONS TO THE DPG FRUEHJAHRSTAGUNG [DPG - FRUEHJAHRSTAGUNG]
Apr. 1988 60 p Conference presented in Duesseldorf, Fed. Republic of Germany, 29 Feb.-4 Mar. 1988
(IPP-III/134; ETN-88-93202) Avail: NTIS HC A04/MF A01

Charge exchange spectroscopy of highly ionized ions in ASDEX; spectroscopic measurement of the ion temperature on ASDEX; measurement of the absolute neutron yield of ASDEX with nuclear emulsion plates; interpretation of neutron rate measurements using the NR code; calculation of neutron propagation for ASDEX; numerical simulation of the response function of a nuclear emulsion plate are some of the topics covered at this conference. Other topics include: measurements of proton and triton spectra in ASDEX discharges; advantages of a helium beam for active charge exchange diagnostics; and simultaneous background measurement in the ASDEX neutral particle diagnostics. For individual titles, see N89-11535 through N89-11543.

N89-11535# Max-Planck-Inst. fuer Plasmaphysik, Garching (West Germany).
CHARGE EXCHANGE SPECTROSCOPY (CXRS) OF HIGHLY IONIZED IONS IN ASDEX
J. V. Hofmann, G. Fussmann, and G. Janeschitz *In its* ASDEX

Contributions to the DPG Fruehjahrstagung Apr. 1988 p 1-7 (For primary document see N89-11534 02-75)
Avail: NTIS HC A04/MF A01

Visible transitions from highly ionized krypton and sulfur were measured and compared with calculations. For H-like oxygen the atomic level population was calculated and the primary charge exchange recombination (CXR) spectroscopy rates and the resulting effective rates were compared. This indicates an exponential decay both for the primary and the effective rates. Lithium-like sulfur and Na-like krypton transitions were measured in the visible range, and a strong decrease of the intensities for higher quantum numbers is observed. To work out effective and primary rate coefficients and to perform a proper comparison to measurements for these systems, more atomic data for 1-resolved CXR into high quantum states and for collision rates between these states for Li- and Na-like systems are needed. ESA

N89-11536# Max-Planck-Inst. fuer Plasmaphysik, Garching (West Germany).
SPECTROSCOPIC MEASUREMENT OF THE ION TEMPERATURE ON ASDEX
P. Lee and R. Nolte (GA Technologies, Inc., San Diego, Calif.) *In its* ASDEX Contributions to the DPG Fruehjahrstagung Apr. 1988 p 8-12 (For primary document see N89-11534 02-75)
Avail: NTIS HC A04/MF A01

On ASDEX a medium size curved crystal spectrometer in Johann mounting was used for SX-ray spectroscopy. The instrument is characterized by: diameter of the rowland circle = 1500 mm, active crystal are = 50 mm x 10 mm, and the detector is a position sensitive proportional counter. Measured ion temperatures are 20 percent lower than results of neutral particle analysis. Deviations are attributed to the influence of line integration over the broad emission profiles. They can be corrected using experimental emission profiles. ESA

N89-11537# Heidelberg Univ. (West Germany). Inst. fuer Angewandte Physik.
MEASUREMENT OF THE ABSOLUTE NEUTRON YIELD OF ASDEX WITH NUCLEAR EMULSION PLATES
R. Klein, J. Hubele, K. Huebner, L. Ingrosso, and B. V. Robouch (European Nuclear Energy Agency, Frascati, Italy) *In* Max-Planck Institut fuer Plasmaphysik, ASDEX Contributions to the DPG Fruehjahrstagung Apr. 1988 p 13-18 (For primary document see N89-11534 02-75)
Avail: NTIS HC A04/MF A01

Nuclear emulsion plates were used to measure the time-integrated neutron fluence at the position of their exposure in ASDEX at neutron rates in the range from 10 to the 11th power to 10 to the 15th power n/sec, depending on the number of discharges available. Ways to determine the observed part of the plasma to scale it to the total plasma volume; to determine the total proton track density in the emulsion from the limited number of tracks to be used when scanning the emulsions; and to take into account the neutron absorption between the plasma and nuclear emulsion and the background of scattered neutrons are discussed. Error analysis is mentioned. ESA

N89-11538# Max-Planck-Inst. fuer Plasmaphysik, Garching (West Germany).
INTERPRETATION OF NEUTRON RATE MEASUREMENTS USING THE NR CODE
K. Huebner, R. Baetzner (Heidelberg Univ., West Germany), B. Bomba, H. Rapp, W. Herrmann, H. Murmann, A. Eberhagen, H.-U. Fahrbach, O. Gehre, and R. Preis et al. *In its* ASDEX Contributions to the DPG Fruehjahrstagung Apr. 1988 p 19-24 (For primary document see N89-11534 02-75)
Avail: NTIS HC A04/MF A01

Neutron rate measurements were used to determine the ion temperature in ohmic discharges to calculate the ion temperature, the nD/nH ratio, the neutron rate, and the neutron emission profile for all kinds of thermonuclear plasmas as well as for D(0) injection in deuterium plasmas; software was developed. Results for thermonuclear plasma with H(0) injection in deuterium are presented. ESA

N89-11539# Heidelberg Univ. (West Germany). Inst. fuer Angewandte Physik.
CALCULATION OF NEUTRON PROPAGATION FOR ASDEX
K. Huebner, R. Baetzner, R. Klein, M. Roos, and B. Wolle *In* Max-Planck Institut fuer Plasmaphysik, ASDEX Contributions to the DPG Fruehjahrstagung Apr. 1988 p 25-34 (For primary document see N89-11534 02-75)
Avail: NTIS HC A04/MF A01

A software package to investigate neutron emission, migration, and scattering in the ASDEX device, and, in particular, to understand the influence of the scattered neutron background on nuclear emulsion measurements was developed. The central part is the VINIA-3DAMC software which follows the propagation of each neutron through the ASDEX device and calculates for each neutron emission and collision the contributions to a desired detector (flux-at-a-point method). The program needs four inputs: nuclear data, neutron source, geometry, and material distribution of the ASDEX structure. ESA

N89-11540# Heidelberg Univ. (West Germany). Inst. fuer Angewandte Physik.
NUMERICAL SIMULATION OF THE RESPONSE FUNCTION OF A NUCLEAR EMULSION PLATE
M. Roos, K. Huebner, B. V. Robouch, and L. Ingrosso (European Nuclear Energy Agency, Frascati, Italy) *In* Max-Planck Institut fuer Plasmaphysik, ASDEX Contributions to the DPG Fruehjahrstagung Apr. 1988 p 35-40 (For primary document see N89-11534 02-75)
Avail: NTIS HC A04/MF A01

The Nuclear Emulsion Plate Monte Carlo (NEPMC) program was designed to simulate proton tracks of neutron-proton collisions by using Monte Carlo algorithms, and to determine the response function of the emulsion, i.e., the measured neutron spectrum for a given spectral neutron fluence arriving at the emulsion. The data base for the NEPMC software needs only the point of emission of the neutron, the weight and energy of the arriving neutron at the plate, and the coordinates of the position where the neutron-proton encounter takes place in the emulsion. The simulation of the proton tracks is done in a Monte Carlo loop. Monoenergetic point sources, and extended neutron sources are considered. ESA

N89-11541# Max-Planck-Inst. fuer Plasmaphysik, Garching (West Germany).
MEASUREMENTS OF PROTON AND TRITON SPECTRA IN ASDEX DISCHARGES
E. Simmet, U. Stroth, H.-S. Bosch, and U. Schumacher *In its* ASDEX Contributions to the DPG Fruehjahrstagung Apr. 1988 p 41-44 (For primary document see N89-11534 02-75)
Avail: NTIS HC A04/MF A01

A diagnostic method was developed on ASDEX to measure the charged fusion products from the d-d-reactions with semiconductor detectors. Protons and tritons can be detected and it is possible to determine the ion temperature Ti from both of the species using the formula Delta E = 91.6 sq rt Ti where Delta E and Ti are the FWHM of the Doppler contribution to the width of the spectrum of protons and tritons and the ion temperature, respectively, both in keV. Spectra could only be obtained for OH-, LH-, and NI(H in D)-heated ASDEX plasmas at low heating power levels. Since the triton spectra suffer more from hard X-ray contributions and energy straggling than the protons, the temperature values deduced from the triton spectra are more uncertain than those from the protons. To improve these points, a shielding box of Pb and Cu mounted around the detector system, thinner foils to lower energy loss and straggling, and a double detector arrangement to substract the magnetic field effects are applied. ESA

N89-11542# Max-Planck-Inst. fuer Plasmaphysik, Garching (West Germany).
ADVANTAGES OF A HELIUM BEAM FOR ACTIVE CHARGE EXCHANGE DIAGNOSTICS
W. Herrmann *In its* ASDEX Contributions to the DPG Fruehjahrstagung Apr. 1988 p 45-53 (For primary document see N89-11534 02-75)
Avail: NTIS HC A04/MF A01

Hydrogen and helium beams are compared for their quality as doping beams for density and temperature profiles expected in ASDEX upgrade with hydrogen and deuterium plasmas. The charge exchange cross-section of helium beams with 20 or 40 keV proves to be larger for a high energy of the analyzed particles than with hydrogen having an energy larger than 15 keV. As helium beams also penetrate better through the plasma, helium beams have distinct advantages for diagnostics of high-density, high-temperature plasmas. Estimates show that helium beams allow measurement of neutral ion temperatures for densities as large as 1.5 times 10 to the 14th power cc. Further advantages of the helium beam are its small halo effect (better space resolution) and the fact that all the beam energy is concentrated in one component. The total beam power is less than for hydrogen beams with the same charge exchange rate. ESA

N89-11543# Max-Planck-Inst. fuer Plasmaphysik, Garching (West Germany).
SIMULTANEOUS BACKGROUND MEASUREMENT IN THE ASDEX NEUTRAL PARTICLE DIAGNOSTICS
H.-U. Fahrbach and H. M. Mayer *In its* ASDEX Contributions to the DPG Furehjahrstagung Apr. 1988 p 54-56 (For primary document see N89-11534 02-75)
Avail: NTIS HC A04/MF A01

A method to determine the background in diagnostics of the energy spectrum of the neutral particle flux leaving the ASDEX plasma was developed. The principle of the method is to chop the signal of all analyzer channels with a period shorter than the desired time resolution. This is done by a square function electric field in a condensor between the stripping cell and detector. During the first half-period the electric force prevents the charged particles from reaching the detectors, and only the background is measured. During the second half-period the field is zero and the sum of the signal and background is detected. The frequency and phase of the electric field are strictly coupled to those of the data acquisition system. Inspection and subtraction of the background are done by software. ESA

N89-11544# Nagoya Univ. (Japan). Inst. of Plasma Physics.
MONTE CARLO STUDY OF ION CYCLOTRON RESONANCE HEATING IN HELICAL SYSTEMS
M. Ohnishi, M. Okamoto, Y. Abe, A. Fukuyama, T. Mutoh, and A. Iiyoshi (Kyoto Univ., Uji, Japan) Aug. 1988 21 p
(IPPJ-884; ISSN-0469-4732) Avail: NTIS HC A03/MF A01

The ion cyclotron resonance heating (ICRH) was studied by the minority scheme in helical systems by a Monte Carlo calculation. For the helical device with the toroidal pitch number of 14, the ratio of the energy deposited to the plasma to the total wave energy absorbed by the minority of protons amounts to 70 percent and the ratio of the energy loss due to the drift loss of the minority ions is only 10 percent. As the toroidal pitch number of the helical magnetic field decreases, the fraction of deposition energy decreases in proportion as the deterioration of the confinement of fast ions. However, since the modulation of helical winding laws and/or the shift of a plasma column can improve the confinement of fast ions, the ICRH can be expected to be na efficient means of plasma heating in helical systems with the medium pitch number (M = 10 to approximately 14) and the appropriate pitch modulation of the helical coils. Author

N89-11545# Nagoya Univ. (Japan). Inst. of Plasma Physics.
TRAPPING AND ACCELERATION OF ELECTRON BY ELLIPTICALLY POLARIZED ELECTROMAGNETIC WAVE PROPAGATING ACROSS STATIC MAGNETIC FIELD
Satoshi Takeuchi Aug. 1988 34 p
(IPPJ-885; ISSN-0469-4732) Avail: NTIS HC A03/MF A01

Suppose that an electromagnetic wave propagating across a magnetic field beta sub 0 polarizes on a plane perpendicular to beta sub 0 and that its phase velocity is a little slower that the light velocity c. It is shown that such wave (EP-wave) can trap a charged particle and accelerate it unlimitedly. The well-known electrostatic and electromagnetic wave trapping accelerations are included as two limiting cases of this acceleration. A brief comment on how to create a slow wave by using a plasma is also presented. Author

N89-11546# Nagoya Univ. (Japan).
OPTIMIZATION OF BOOTSTRAP CURRENT IN A LARGE HELICAL SYSTEM WITH L = 2
N. Nakajima, M. Okamoto, J. Todoroki, Y. Nakamura, and M. Wakatani (Kyoto Univ., Uji, Japan) Aug. 1988 29 p
(IPPJ-889; ISSN-0469-4732) Avail: NTIS HC A03/MF A01

Neoclassical bootstrap currents in the banana and plateau regions are evaluated for an L = 2 large helical system with the major radius of 5 m. Various vacuum magnetic field configurations are invoked to optimize the bootstrap current. In the banana region shifting the magnetic axis and shaping magnetic surfaces have remarkable effects on the bootstrap current and it is clarified that a small outward shift of the magnetic axis and vertically elongated magnetic surfaces are favorable to reduce the bootstrap current. On the contrary, the bootstrap current in the plateau region depends strongly on the toroidal pitch number of helical winding coils but shifting the axis and shaping magnetic surfaces are not effective. The magnitude of bootstrap current is estimated for plasmas in the large helical system predicted by a one dimensional transport code. Author

N89-11547# Nagoya Univ. (Japan). Inst. of Plasma Physics.
POWER ABSORPTION AND CONFINEMENT STUDIES OF ICRF-HEATED PLASMA IN JIPP T-IIU TOKAMAK
K. Ida, Y. Ogawa, K. Toi, K. Kawahata, T. Watari, R. Ando, J. Fujita, Y. Hamada, S. Hirokura, and E. Kako et al. Aug. 1988 22 p Prepared in cooperation with Chubu Inst. of Tech., Kasugai (Japan)
(IPPJ-886; ISSN-0469-4732) Avail: NTIS HC A03/MF A01

The energy confinement characteristics of ICRF-heated tokamak plasmas are studied at high input power density of approximately 2 MW/cu m volume averaged, on the JIPP T-IIU device(R=0.91m/a=0.23m). High electron and ion temperatures were achieved by the operation at a plasma current I sub rho of 280 kA, plasma line-averaged electron density bar n sub e of 7 x 10 to the 13th/cu cm and input power of 2MW, with a suppression of total radiation loss (30 to 40 percent of the total input power) by a carbon coating on the vacuum vessel. The fraction of ICRF power absorbed by the plasma, alpha is determined experimentally from the decay of the stored plasma energy just after the ICRF pulse is terminated. The value of alpha increases slightly with increasing electron density and decreases from 90 to 70 percent as the ICRF power is increased from 1 to 2 MW/cu m volume averaged. The global energy confinement time Tau sub e defined by W sub rho/(P sub OH(+) alpha P sub rf). decreases by a factor of 2 to approximately 3 from that in ohmic plasma as the heating power increases up to 2 MW. It is found that the energy confinement time has a strong line-averaged electron density dependence as Tau sub E infinity bar sub e sup 0.6 which is obtained by the use of the measured absorbed power, while the Kaye-Goldston scaling predicts Tau sub E infinity bar n sub e sup 0.26. Author

N89-11548# Nagoya Univ. (Japan). Inst. of Plasma Physics.
COMPARISON BETWEEN URAMOTO TYPE AND STRAIGHT FILAMENT TYPE SHEET PLASMA AS A VOLUME PRODUCED H(-) ION SOURCE (2)
Joshin Uramoto Aug. 1988 22 p
(IPPJ-887; ISSN-0469-4732) Avail: NTIS HC A03/MF A01

Each dependence of a H(-) ion current of distance (from 3.5 cm to 17 cm) between a sheet plasma center and the first H(-)

extraction electrode, is investigated for a straight filament type or a Uramoto type sheet plasma. For the straight filament type, the H(-) current increases initially with the distance and decreases after a maximum. On the other hand, for the Uramoto type, the H(-) current increases with the distance. Over all the distance, the maximum current of the Uramoto type is about 10 times larger than that of the straight filament type. As a reason for this result, we point out a character that the plasma density and the decay time of negatively charged particles in Uramoto type sheet plasma, hardly decrease even in the long distance which may be necessary for vibrationally excited H2(*) molecules. Author

N89-11549# Nagoya Univ. (Japan). Inst. of Plasma Physics.
SPACE AND TIME RESOLVED MEASUREMENTS OF ION TEMPERATURE WITH THE CVI 5292 A CHARGE EXCHANGE RECOMBINATION LINE AFTER SUBSTRACTING BACKGROUND RADIATION
K. Ida and S. Hidekuma Aug. 1988 22 p
(IPPJ-888; ISSN-0469-4732) Avail: NTIS HC A03/MF A01

An ion temperature profile was obtained with the CVI 5292 A (n = 8 - 7) charge exchange recombination (CXR) line using a space and wave-length resolving visible spectrometer installed on the JIPP TII-U tokamak. Two sets of 50 channels optical fiber arrays: one viewing a fast neutral hydrogen beam (CXR channels) and the other viewing off the neutral beam line (background channels), is arranged on the entrance slit of the spectrometer. This spectrometer is coupled to an image intensifier and CCD detector at the focal plane and provides temperature profile every 1/60 second. An ion temperature is derived from the Doppler broadened line profile after subtracting the simultaneously measured cold component (background channels), which is due to electron-excitation and/or charge exchange recombination in the plasma periphery. An alternative approach to obtain the ion temperature profile without CXR is also demontrated. This method is based on an Abel inversion technique for each wavelength separately. Author

N89-11550# Air Force Inst. of Tech., Wright-Patterson AFB, Ohio.
DETERMINATION OF THE UNSTABLE STATES OF THE SOLID STATE PLASMA IN SEMICONDUCTOR DEVICES Ph.D. Thesis
Mark E. Snyder May 1988 185 p
(AD-A196403; AFIT/CI/NR-88-100) Avail: NTIS HC A09/MF A01 CSCL 20L

When a semiconductor device fails, a complicated set of actions takes place to move the device from a high voltage, low current state to a low voltage, high current state. Accompanying these changes are the collapse of isotropic current flow to a small column or filament of current which rapidly grows and heats the device to the melting point. These actions are collectively called second breakdown. This work reviews past results to show that second breakdown is the formation of a current controlled negative resistance (CCNR) regime which necessarily forces current flow to form a current filament. The current filament is modeled as a solid state plasma column undergoing a self-induced magnetic pinch as a result of the CNNR. The dispersion relation is derived to first order to show that the pinching leads to an unstable equilibrium that could lead to material failure. The minimum set of parameters necessary to the formation of second breakdown are determined to be satisfied by the Bennett pinch criterion. Further application is then made to a bipolar power transistor that has been driven into second breakdown to see how the derived criteria applies to a semiconductor device. GRA

76 SOLID-STATE PHYSICS

Includes superconductivity.

For related information, see also *33 Electronics and Electrical Engineering* and *36 Lasers and Masers.*

N89-11551# Sandia National Labs., Albuquerque, N. Mex.
SMART SEMICONDUCTOR BRIDGE (SCB) IGNITER FOR EXPLOSIVES
R. W. Bickes, Jr. 1988 8 p Presented at the 3rd Canadian Symposium on Mining Automation, Montreal, Quebec, 14 Sep. 1988
(Contract DE-AC04-76DP-00789)
(DE88-012669; SAND-88-1438C; CONF-880986-1) Avail: NTIS HC A02

We have developed a silicon semiconductor bridge (SCB) igniter which, when driven with a low-energy current pulse, produces a plasma discharge that ignites explosive materials pressed against the bridge. Our experiments have demonstrated that SCB explosive devices function in a few tens of microseconds at one-tenth the input energy of hot-wire devices. Despite the low input energies for ignition, tests have revealed SCB devices to be explosively safe, passing electrostatic discharge (ESD) requirements and no-fire current levels. In fact, SCB devices have better no-fire characteristics than hot-wire devices, because of the intimate bridge contact with the underlying thermally conductive substrate. We have tested several different prototype explosive devices including pyrotechnic actuators, secondary explosive deflagration-to-detonation detonators and a primary explosive detonator. In addition, we have tested SCB actuators with breadboarded smart firing sets that will fire the SCB actuators only after transmission of a digital code, after a preset delay, or in a preprogrammed sequence. We have also tested an optical system that requires only a single fiber optic cable connecting the SCB device to a low power laser that both energizes the firing set and transmits a coded firing signal. DOE

N89-11552# Los Alamos National Lab., N. Mex.
ELECTRICAL RESISTIVITY OF U(SUB 1-x)M(SUB x)Be13 UNDER PRESSURE
H. A. Borges, J. D. Thompson, M. C. Aronson, Z. Fisk, and J. L. Smith 1988 9 p Presented at the 6th International Conference on Crystal Field Effects and Heavy Fermion Physics, Frankfurt, Fed. Republic of Germany, 18 Jul. 1988
(Contract W-7405-eng-36)
(DE88-014449; LA-UR-88-1914; CONF-880704-2) Avail: NTIS HC A02/MF A01

Measurements of the electrical resistivity of U(sub 1-x)Th(sub x)Be13 compounds as a function of pressure provide a possible explanation for the unusual behavior of these materials. DOE

N89-11553*# National Aeronautics and Space Administration. Lewis Research Center, Cleveland, Ohio.
USE OF HIGH TEMPERATURE SUPERCONDUCTORS IN MAGNETOPLASMADYNAMIC SYSTEMS
C. B. Reed (Argonne National Lab., Ill.) and J. S. Sovey 1988 7 p Presented at the Conference on Superconductivity and Applications, Buffalo, N.Y., 18 Apr. 1988 Prepared in cooperation with National Aeronautics and Space Administration, Cleveland, Ohio
(Contract W-31-109-eng-38)
(NASA-TM-101219; NAS 1.15:101219; DE88-011954; CONF-880466-5) Avail: NTIS HC A02/MF A01 CSCL 20L

The use of Tesla-class high-temperature superconducting magnets may have an extremely large impact on critical development issues (erosion, heat transfer, and performance) related to magnetoplasmadynamic (MPD) thrusters and also may provide significant benefits in reducing the mass of magnetics used in the power processing system. These potential performance improvements, coupled with additional benefits of high-temperature superconductivity, provide a very strong motivation to develop high-temperature superconductivity (HTS) applied-field MPD thruster propulsion systems. The application of HTS to MPD thruster

propulsion systems may produce an enabling technology for these electric propulsion systems. This paper summarizes the impact that HTS may have upon MPD propulsion systems. DOE

N89-11554# Kernforschungsanlage, Juelich (West Germany).
TI-IMPLANTED OPTICAL WAVEGUIDES IN LINbO3
Ch. Buchal, P. R. Ashley, and D. K. Thomas (Oak Ridge National Lab., Tenn.) 1988 14 p Presented at the European Materials Research Society Meeting, Strasbourg, France, 31 May 1988
(Contract DE-AC05-84OR-21400)
(DE88-015279; CONF-8805147-2) Avail: NTIS HC A03/MF A01

LiNbO3 is the best substrate for modulators and switches for integrated optics. Efficient low loss waveguides are fabricated by introducing Ti into the crystal. The maximum Ti concentration and the corresponding delta n as well as the minimum waveguide dimensions normally are limited by the diffusion characteristics. Ion implantation offers an interesting alternative, especially if infrared applications are intended. During the implantation process an amorphous non-equilibrium phase is generated, and subsequently the crystalline state has to be restored by solid phase epitaxy. This process results in guides with low losses of less than 1 db/cm. Fabrication details and guide characteristics are presented. DOE

N89-11555# Brookhaven National Lab., Upton, N. Y.
SPIN CORRELATIONS IN HIGH T(SUB c) SUPERCONDUCTORS
Gen Shirane 1988 17 p Presented at the International Conference on Magnetism, Paris, France, 25 Jul. 1988
(Contract DE-AC02-76CH-00016)
(DE88-013988; BNL-41441; CONF-880705-3) Avail: NTIS HC A03/MF A01

A review is given of current neutron scattering experiments on La(sub 2)-xSr(sub x)CuO4 and YBa2Cu3O(sub 6+x). Large single crystals have now been successfully grown for both of these high T sub c superconductors and extensive measurements are being carried out on magnetic excitations for wide ranges of temperature and composition. A novel type of two-dimensional spin correlation is found with unusually large J sub 2D approximately = 1000 K. DOE

N89-11556# California Univ., Berkeley. Lawrence Berkeley Lab.
STATE OF THE ART OF NEGATIVE LUMINESCENCE
P. Berdahl, V. Malyutenko, and T. Morimoto (Kyoto Univ., Uji, Japan) Apr. 1988 7 p Presented at the 4th International Conference on Infrared Physics, Zurich, Switzerland, 22 Aug. 1988
(Contract DE-AC03-76SF-00098)
(DE88-010871; LBL-25244; CONF-880870-1) Avail: NTIS HC A02/MF A01

In semiconductors, when the equilibrium carrier concentrations are reduced, either by carrier extraction 6 reversed-biased diode junctions, or by the magnetoconcentration effect, the normal equilibrium process of light emission due to carrier recombination is suppressed. Therefore, semiconductors exhibit negative luminescence. It is most readily observed when the energy gap, E sub g, of the semiconductor is not too large compared to kT; this condition assures that there is some overlap between the blackbody spectrum and the characteristic band-to-band emission spectrum of the semiconductor. DOE

N89-11557# Argonne National Lab., Ill.
MAGNETIC FLUCTUATIONS AND HEAVY ELECTRON SUPERCONDUCTIVITY
M. R. Norman 1988 5 p Presented at the 6th International Conference on Crystal Field Effects and Heavy Fermion Physics, Frankfurt, Federal Republic of Germany, 18 Jul. 1988
(Contract W-31-109-eng-38)
(DE88-011978; CONF-880704-1) Avail: NTIS HC A02/MF A01

A magnetic fluctuation self-energy based on neutron scattering data is used to calculate mass renormalizations, and superconducting critical temperatures and order parameters, for various heavy electron metals. DOE

N89-11558# International Centre for Theoretical Physics, Trieste (Italy).
SIMPLE MODEL FOR THE SUPERCONDUCTING PHASE DIAGRAM NEAR THE METAL-INSULATOR TRANSITION
R. Allub, C. Wiecko, and A. Caro Jan. 1988 20 p
(DE88-703038; IC-88/21) Avail: NTIS (US Sales Only) HC A03/MF A01

We solve a simple model of competing superconductivity and disorder in a mean-field approximation with two order parameters. A phase diagram showing superconducting-normal metal-insulator as well as superconducting-insulator transitions is obtained. Comparison with experiments shows a good qualitative agreement. DOE

N89-11559# Instituto de Pesquisas Espaciais, Sao Jose dos Campos (Brazil).
FLUX METHOD FOR THE FIELD DEPENDENT TRANSPORT THROUGH MULTILAYER DEVICES
Ram Kishore Aug. 1988 41 p Presented at the 3rd Congresso da Sociedade Brasileira de Microeletronica, Sao Paulo, Brazil, 12-14 Jul. 1988 Submitted for publication
(INPE-4647-PRE/1357) Avail: NTIS HC A03/MF A01

A flux method of treating the one dimensional steady state transport problem of excess charged carriers, created by the generating sources, is analyzed for the multilayer devices in the presence of a nonuniform electric field. General analytical expressions for the forward and backward fluxes of excess carriers at any arbitrary boundary of the multilayer device are derived in terms of the reflection and transmission coefficients of the individual layers and boundaries. For an isolated layer, these coefficients are obtained in analytical form in terms of backscattering and absorption probabilities of charged carriers and the layer's thickness. In a multilayer device the reflection and transmission coefficients of any layer or boundary get affected due to the presence of other layers and boundaries. Therefore the effective reflection and transmission coefficients of layers and boundaries are calculated in terms of reflection and transmission coefficients of the isolated layers and boundaries. These effective coefficients are then used to obtain the reflection and transmission coefficients of the entire multilayer device. As an application of this general analysis, a simple example of a multilayer device consisting of only two layers is worked out. The results are shown to reduce to those obtained by other calculations in appropriate limiting cases. Author

N89-11560 Texas Technological Univ., Lubbock.
ELECTRONIC PROPERTIES OF 3-5 SEMICONDUCTOR ALLOYS Ph.D. Thesis
Jeffrey Robert Gregg 1987 286 p
Avail: Univ. Microfilms Order No. DA8806003

The results of two theoretical investigations of the effects of alloy disorder on the electronic properties of some of the technologically important III-V semiconductor alloys are reported. In the first part, the coherent potential approximation (CPA) for calculating the effects of alloy disorder on the electronic structure of alloys is generalized to treat quaternary semiconductor alloys of the form A(sub x)B(sub y)C(sub 1-x-y)D. This generalized formalism is then used, in conjunction with calculated bandstructures for the alloy constituents, to study the effects of alloy disorder on the electronic properties of several III-V quaternary alloys. Results are presented for the state densities, self-energies, band bowling parameters, and bandstructures of these materials. These properties are compared with results obtained in the virtual crystal approximation (VCA). Dissert. Abstr.

N89-11561# International Centre for Theoretical Physics, Trieste (Italy).
POSSIBLE COEXISTENCE OF ANTIFERROMAGNETISM AND SUPERCONDUCTIVITY IN THE HUBBARD MODEL

Zhao-bin Su, Jin-ming Dong, Lu Yu, and Jue-lian Shen (Academia Sinica, Beijing, China) Jan. 1988 9 p Submitted for publication
(DE88-703025; IC-88/3) Avail: NTIS (US Sales Only) HC A02/MF A01

The Hubbard model in the nearly half-filled case was studied in the mean field approximation using the effective Hamiltonian approach. Both antiferromagnetic order parameter and condensation of singlet pairs were considered. In certain parameter ranges the coexistence of antiferromagnetism and superconductivity is energetically favorable. Relevance to the high temperature superconductivity and other theoretical approaches is also discussed. DOE

N89-11562# Joint Inst. for Nuclear Research, Dubna (USSR). Lab. of High Energy.
CURRENT-INDUCED QUANTUM INTERFERENCE IN THE COMPOSITE SUPERCONDUCTOR NbTi-Cu
Eh. Fisher and I. S. Khukhareva 1987 14 p In RUSSIAN; ENGLISH summary
(DE88-703079; JINR-R-8-87-526) Avail: NTIS (US Sales Only) HC A03/MF A01

The I-V-curves for the transversal zero-bias resistance of a NbTi-Cu multifilamentary superconductor have been measured at 1.85 K in the presence of a weak dc-magnetic field (less than or approx. 0.2 Oe) aligned along the NbTi-filaments perpendicular to the current flow. An oscillating dependence of both the critical current and the resistivity behavior from the magnetic field amplitude has been obtained. These oscillations are in excellent agreement with the periodic dependence of the frustration parameter on magnetic flux per unit cell determined by the geometry of the effective two-dimensional structure of the filament lattice. A detailed analysis of the vortex mobility reveals the strong vortex interaction in the critical region of the topological phase transition caused by the annihilation of the thermally activated vortex-pairs. The experimental results demonstrate the complete scaling properties of the obtained non-linear and quantum interference effects. DOE

N89-11563 Texas Technological Univ., Lubbock.
DEFECT MODEL FOR THE ELECTRONIC CONDUCTION AND BREAKDOWN IN DIELECTRIC THIN FILMS Ph.D. Thesis
Tsai-Ku Lin 1987 151 p
Avail: Univ. Microfilms Order No. DA8806011

A stochastic model of defects has been developed to explain the electronic properties of dielectric thin film systems. Consequently, a reaction-diffusion type of equation is obtained. This model considers the dielectric thin film as an open system, in which nonlinearities play an important role for the instabilities of the system. The general experimental observations on the current-voltage characteristics are discussed. The microscopic picture of the conduction are predicted before the destructive breakdown of the films occurs. These conduction stages correspond to the microscopic states of the system and, consequently, are closely related to the defects correlated states. Qualitatively, the microscopic states of the system are correlated with the growth stages of the film. The mechanisms of aging and annealing are also addressed under this reaction-diffusion equation. Dissert. Abstr.

N89-11564# Martin Marietta Energy Systems, Inc., Oak Ridge, Tenn.
ION IMPLANTATION AND THERMAL ANNEALING OF HIGH-T(SSUB c) SINGLE CRYSTALS OF YBa2Cu3O(SUB x)
C. W. White, J. C. McCallum, and L. A. Boatner May 1988 15 p Presented at the European Materials Research Society Meeting, Strasbourg, France, 31 May 1988
(Contract DE-AC05-84OR-21400)
(DE88-012201; CONF-8805147-1) Avail: NTIS HC A03/MF A01

Rutherford backscattering spectrometry (RBS) has been used to study the effects of ion implantation and thermal annealing on single crystals of YBa2Cu3O(sub x). The structural disorder induced by ion implantation results in significant changes in the near-surface composition during subsequent thermal processing. Compositional changes in the near-surface region of the YBa2Cu3O(sub x) single crystals were observed after annealing oxygen- or copper-implanted crystals at temperatures of 500 C or higher in various atmospheres. Unimplanted crystals are not affected by the identical processing conditions. Preliminary results show that sintered polycrystalline ceramic YB2Cu3O(sub x) also undergoes compositional changes as a result of ion implantation and thermal annealing. DOE

N89-11565# Sandia National Labs., Albuquerque, N. Mex.
WHAT IS THE ORIGIN OF GLASSY BEHAVIOR IN THE HIGH-T(SUB c) OXIDES
J. F. Kwak and E. L. Venturini 1988 6 p Presented at the International Conference on Science and Technology of Synthetic Metals, Santa Fe, N. Mex. 26 Jun. 1988
(Contract DE-AC04-76DP-00789)
(DE88-012668; SAND-88-0299C; CONF-880669-3) Avail: NTIS HC A02/MF A01

The anomalous low-field magnetic properties of the high-T(sub c) oxide crystals have been interpreted alternatively in terms of a superconductive glass state or, more recently, giant flux creep. The glass picture as proposed assumes the occurrence of intragranular Josephson junctions on a length scale small compared to the penetration depth, and has been used to explain the properties of both single-crystal and ceramic samples. The flux creep picture deals only with pinning forces and ignores weak links, and thus far has been applied only to single crystals. We show here that neither of these models adequately describes the behavior of ceramic materials. A physically accurate picture of such materials must take into account intergranular Josephson junctions and resultant grain decoupling at low magnetic fields. DOE

N89-11566# International Centre for Theoretical Physics, Trieste (Italy).
EFFECT OF SURFACE STATES ON THE ELECTROCHEMICAL BEHAVIOUR OF SINGLE CRYSTAL n-ZnSe PHOTOELECTRODE
M. S. El-Dessouki Oct. 1987 13 p
(DE88-702726; IC-87/335) Avail: NTIS (US Sales Only) HC A03/MF A01

Surface Photovoltage Spectroscopy (SPS) technique has been used to detect the surface states of ZnSe (110) surfaces. Aqueous electrolyte/ZnSe junction has been electrochemically investigated in dark and under illumination. The effect of surface states on the kinetics of charge transfer through the semiconductor-electrolyte (S/E) junction has been discussed. The low leakage and photocurrents measured by the application of dc bias were attributed to the blocking nature of S/E interface, in which the localized and induced surface states play an important role. DOE

N89-11567# Michigan Technological Univ., Houghton.
THEORY OF DEFECTS IN NON-METALLIC SOLIDS Progress Report, 1 Aug. 1985 - 1 May 1988
1988 27 p
(Contract DE-FG02-85ER-45224)
(DE88-013075; DOE/ER-45224/4) Avail: NTIS HC A03/MF A01

A general method based on ab initio quantum mechanics is being used to study lattice defects in crystalline materials. The model treats the impurity electronic structure and lattice response to the impurity in a self-consistent manner. Simulation of an infinite lattice containing a point defect represented by a cluster may be carried out by minimizing the total energy with respect to parameters that define the lattice configuration, including the defect. States other than ground states may be analyzed by applying symmetry constraints to the calculation. Embedded molecular clusters representing segments of perfect lattice may also be studied. The procedure described above is a practical proposition, and is implemented in a program named ICECAP, for arbitrary host lattice, and for arbitrary point-defect composition and

configuration. Recent applications of ICECAP, incorporating KKLP to color centers and to perfect-lattice clusters show that calculations in which lattice configuration and defect structure are simultaneously self-consistent are possible. Examples are presented. DOE

N89-11568# Wisconsin Univ., Madison. Applied Superconductivity Center.
THE CRITICAL CURRENT DENSITY, THE FABRICATION PROCESS AND THE MICROSTRUCTURE IN SUPERCONDUCTING COMPOSITES OF NBTI FOR HIGH ENERGY PHYSICS Report, 1 Jun. 1985 - 30 Jun. 1988
D. C. Larbalestier 1988 14 p
(Contract DE-AC02-82ER-40077)
(DE88-014241; DOE/ER-40077/4) Avail: NTIS HC A03/MF A01

This paper discusses the transport properties and microstructure of oxide superconductors. In particular, the high critical current density of Nb-Ti alloy is discussed. DOE

N89-11569# Florida Univ., Gainesville. Dept. of Physics.
X-RAY SCATTERING STUDIES OF NON-EQUILIBRIUM ORDERING PROCESSES Progress Report, 1 Nov. 1987 - 31 Oct. 1988
S. E. Nagler Jun. 1988 23 p
(Contract DE-FG05-86ER-45280)
(DE88-012908; DOE/ER-45280/T1) Avail: NTIS HC A03/MF A01

We outline the progress of our project entitled X-ray Scattering Studies of Non-Equilibrium Ordering Processes. The kinetics of the order-disorder transition in Cu sub 3 Au has been carefully examined. Experiments on single crystals have verified that there is anisotropic non-equilibrium scaling in the coarsening regime. Measurements on sputtered films of varying stoichiometry have probed the effects of randomness on kinetics. Investigations on Cu sub 3 Au grown single crystal films have studied the role of dimensionality. Further experiments have begun on the alloy Au 47.5 percent Cd, a super-elastic martensitic system. DOE

N89-11570# Argonne National Lab., Ill. Energy and Environmental Systems Div.
MAGLEV: THE DOUBLE BENEFITS OF HIGH-Tc SUPERCONDUCTORS AND ITS DEVELOPMENT AS AN AEROSPACE TECHNOLOGY
L. R. Johnson and R. F. Giese 1988 13 p Presented at the Conference on Superconductivity and Applications, Buffalo, N.Y., 18 Apr. 1988
(Contract W-31-109-eng-38)
(DE88-012005; CONF-880466-8) Avail: NTIS HC A03

The potential for magnetically levitated (MAGLEV) vehicles is discussed as a means of both inter-city travel and a technology option to relieve the growing problem of air traffic congestion. A brief summary is presented of the two primary MAGLEV concepts: (1) the attractive-force, electromagnetic system (EMS) and (2) the repulsive-force, electrodynamic system (EDS), and continues with a discussion of the advantages, potential for reduced costs and higher reliability, that the newly-discovered, high-temperature superconductors offer for EDS MAGLEV vehicles. A summary of the current status of worldwide MAGLEV research is presented, followed by a discussion of the resurgence of US interest in MAGLEV. An analysis of air-traffic congestion suggests that MAGLEV can substitute for short-to-medium distance air travel. By promoting MAGLEV as an airline technology, airlines can retain their familiar hub-and-spoke systems with MAGLEVs an integral part of the spoke portion. A preliminary analysis suggests that MAGLEV capital costs are likely to be comparable to those of interstate highways, and use of MAGLEVs can delay the need for new airport construction. For each short-to-medium flight diverted to MAGLEV, an airline can substitute a longer flight. The short-haul flights use an inordinate amount of fuel, which is a major component of airline operating costs. MAGLEV energy consumption would be significantly less and would not have the emissions associated with petroleum fuel. Finally, passengers should benefit from MAGLEV technology: travel options will be extended, delays will be reduced, and costs for inter-city travel will be reduced. DOE

N89-11571# Brigham Young Univ., Provo, Utah. Dept. of Mechanical Engineering.
INFLUENCE OF GRAIN BOUNDARY STRUCTURE DISTRIBUTION AND PROCESSING HISTORY ON INTERGRANULAR CREEP CAVITATION Final Report
Brent L. Adams 1988 12 p
(Contract DE-FG02-85ER-45203)
(DE88-015808; DOE/ER-45203/4) Avail: NTIS HC A03/MF A01

A new measure of grain boundary structure in polycrystalline materials has been introduced which overcomes two difficult obstacles in modeling properties. Previous microstructural measures described intercrystalline misorientation and boundary physical orientation separately. The new measure, called the Intercrystalline Structure Distribution Function, successfully combines both of these elements into a single cohesive measure application to a wide class of property models. A method for determining the function from microdiffraction measurements in section planes was developed. DOE

N89-11572# Argonne National Lab., Ill. Materials Sciences Div.
KINETIC PROCESSES OF THE ORTHORHOMBIC TO TETRAGONAL PHASE TRANSITION IN YBa2Cu3O7-DELTA
D. Shi and D. W. Capone, II Feb. 1988 5 p Presented at the Spring Meeting of the Materials Research Society, Reno, Nev., 5-9 Apr. 1988
(Contract W-31-109-eng-38)
(DE88-011993; CONF-880408-31) Avail: NTIS HC A02

The kinetic processes driving the orthorhombic to tetragonal (O-T) phase transition in YBa2Cu3O(7-delta) have been explored to study the formation of the 123 superconducting phases at different temperatures, as well as the oxygen diffusion in the 123 material. An isothermal transformation curve marking the O-T phase transition boundaries has been established over a wide temperature range. These data suggest the existence of two thermodynamically distinct superconducting phases in the 123 material. Magnetization vs. field data are presented for the samples that were isothermally annealed at 400 C. The results indicate that the T-O transformation is a nucleation and growth process which is governed by oxygen diffusion. The growth geometry during the T-O transformation is discussed. DOE

N89-11573# Ohio State Univ., Columbus. Research Foundation.
STRONGLY INTERACTING FERMION SYSTEMS: EMPHASIS ON HEAVY FERMIONS Annual Performance Report
J. W. Wilkins 1988 8 p
(Contract DE-FG02-88ER-45347)
(DE88-014127; DOE/ER-45347/5) Avail: NTIS HC A02/MF A01

The research has been concentrated into three areas: Heavy fermions, exploratory studies of model systems related to high-T(sub c) superconductors and development of new methods for electronic properties. DOE

N89-11574# University of Southern California, Marina del Rey. Inst. of Physics.
DEVELOPMENT OF ADVANCED INTERNAL GAIN RADIATION DETECTOR STRUCTURES BASED ON NEUTRON TRANSMUTATION DOPED SILICON, HIGH T(SUB c) SUPERCONDUCTIVE COMPOUNDS AND THEIR POTENTIAL APPLICATION TO DETECTION OF IONIZING RADIATION Annual Report, 1 Dec. 1986 - 30 Nov. 1987
Gerald C. Huth, Bing-Lin Zhou, Simon Prussin, and Andrzej J. Dabrowski 1987 27 p
(Contract DE-FG03-86ER-60416)
(DE88-012563; DOE/ER-60416/T1) Avail: NTIS HC A03/MF A01

This report covers the period of work from December 1, 1986

through November 30, 1987. The work on mercuric iodide has now entered a new and more developmental phase with support now being obtained from other agencies (NIH, NASA, JPL, the CalTech President's Fund etc.) for specific, directed applications. These include development of arrays of HgI2 X-ray spectrometers for synchrotron radiation application supported by NIH and for long term space mission use supported by NASA. It has been undertaken during the past year (with some work done in the previous year) to re-examine the technology of high field avalanche radiation detector structures which use the controlled surface principle as developed previously under DOE sponsorship. This was undertaken because of the advent of a fundamental advance in silicon single crystal technology - neutron transmutation doped or NTD single crystal. This new material conceptually solves a basic problem that previously halted the development of these potentially useful radiation detection structures. That problem was the non-uniform, (or striated) distribution of donor impurities which adversely affected electric field distribution and thus attainable avalanche gain in these structures. A new effort started late in the year springs from the development of high critical temperature superconducting ceramic compounds. In essence, the phenomenon of superconductivity can now be achieved at temperatures reached by liquid nitrogen rather than expensive and more complicated cryogenic helium. This, in essence, then brings superconductivity into the same temperature range where lithium drifted silicon and intrinsic germanium already operate. The usefulness of superconductivity in detection and spectroscopy of ionizing radiations based on the narrow superconductive band gap is very appealing and theoretical and experimental studies investigating these new materials have begun. DOE

N89-11575# Brookhaven National Lab., Upton, N. Y.
THEORY OF OXYGEN ORDERING AND ABSORPTION IN 1,2,3 HIGH-T(SUB c) SUPERCONDUCTORS
J. P. A. Westerveld, D. M. R. LoCascio, H. Bakker, and D. O. Welch 1988 4 p Presented at the Discussion Meeting on High-T(sub c) Superconductors, Mauterndorf, Austria, 7-11 Feb. 1988 Prepared in cooperation with Amsterdam Univ. (Netherlands) Sponsored in part by Dutch Foundation for Fundamental Research on Matter
(Contract DE-AC02-76CH-00016)
(DE88-007543; BNL-41032; CONF-880207-1) Avail: NTIS HC A02/MF A01

The oxygen content and the oxygen ordering in 1,2,3 high-T(sub c) compounds plays an important role in the superconducting properties of these materials. Experiments show that the absorption and desorption of oxygen mainly occurs in the CuO planes, that are located at maximum distance from the trivalent ion and that the ordering of the oxygen atoms in linear Cu-O-Cu-O-chains in these planes leads to the orthorhombic structure at lower temperatures. Full occupancy of the oxygen positions in these chains along the direction of the b axis leads to 7 oxygen atoms per formula unit. Complete order means that all oxygen positions in the perpendicular direction (along the a axis) are vacant. Disordering in combination with oxygen desorption causes the orthorhombic to tetragonal phase transition at high temperatures. In the tetragonal phase with about 6.5 oxygen atoms per formula unit the oxygen atoms are distributed over the b and a positions in equal amounts. This causes the a and b lattice parameters to be equal and leads to the tetragonal phase. DOE

N89-11576# Los Alamos National Lab., N. Mex.
VORTEX LATTICES IN THEORY AND PRACTICE
Laurence J. Capmbell 1988 11 p Presented at the Workshop on Mathematical Aspects of Vortex Dynamics, Washington, D.C., 25 Apr. 1988
(Contract W-7405-eng-36)
(DE88-014393; LA-UR-88-2429; CONF-8804169-1) Avail: NTIS HC A03/MF A01

The formal simplicity of ideal point vortex systems in two dimensions has long attracted interest in both their exact solutions and in their capacity to simulate physical processes. Attention here is focused on infinite, two-fold periodic vortex arrays, including an expression for the energy density of an arbitrary vortex lattice (i.e., an arbitrary number of vortices with arbitrary strengths in a unit cell parallelogram of arbitrary shape). For the case of two vortices per unit cell, the morphology of stable lattices can be described completely. A non-trivial physical realization of such lattices is a rotating mixture of He-3 and He-4 at temperatures so low that both isotopic components are superfluid. The structure of the expected lattices is quite different from the usual triangular structure. Magnetic flux lines in high-temperature superconductors show a one-parameter family of degenerate ground state of the lattice due to the anisotropy of the vortex-vortex interaction. A final topic, closely related to Josephson-junction arrays, is the case of vortices confined to a grid. That is, the vortices interact pair-wise in the usual manner but are constrained to occupy only locations on an independent periodic grid. By using vortex relaxation methods in the continuum and then imposing the grid it is possible to find low-lying states extremely rapidly compared to previous Monte Carlo calculations. DOE

N89-11577# Lawrence Livermore National Lab., Calif.
THE EFFECT OF VAPOR INCIDENCE ANGLE UPON THIN FILM COLUMNAR GROWTH
A. Mazor, B. G. Bukiet, and D. J. Srolovitz (Michigan Univ., Ann Arbor.) 1988 21 p Presented at the 35th National Vacuum Symposium and 4th International Laser Science Conference, Atlanta, Ga., 2 Oct. 1988 Submitted for publication
(Contract W-7405-eng-36)
(DE88-014396; LA-UR-88-2451; CONF-881002-1) Avail: NTIS HC A03/MF A01

Presented is a generalized theory for the growth of columnar microstructure in vapor deposited thin films under the joint influence of a constant uniform deposition flux coming down with arbitrarily chosen incidence angle, and surface diffusion. The dependences of the Zone 1 to Zone 2 transition temperature, and the characteristic length scales associated with the unstable modes on the deposition angle are predicted. The surface morphology is obtained as a function of vapor incidence angle. For a specific deposition angle, there is a one-parameter family of steady-state surface profiles which corresponds to a range of possible columnar orientation angles, among which only one angle is associated with the tangent rule. These results agree with experimental observations. DOE

N89-11578# EG and G Energy Measurements, Inc., Goleta, Calif.
PREPARATION AND EVALUATION OF MERCURIC IODIDE FOR CRYSTAL GROWTH
N. L. Skinner, C. Ortale, M. M. Schieber, and L. vandenBerg 1988 15 p Presented at the 6th International Workshop on Compound Semiconductors for Room Temperature X-Ray and Nuclear Detectors, Davos, Switzerland, 14 Sep. 1987
(Contract DE-AC08-83NV-10282)
(DE88-014981; EGG-10282-2140; CONF-8709315-4; S-325-TP)
Avail: NTIS HC A03/MF A01

Large quantities, on the order of several hundred, of consistent, high quality mercuric iodide for crystal growth have not been commercially available. The hydrocarbon, anion, and cation impurity levels varied considerably, occasionally preventing crystal growth. This occurred even though the starting materials was from the same vendor and was subjected to the same purification treatment. This paper will describe an aqueous precipitation process of mercuric iodide preparation in batches of 3 kg using Hg(NO sub 3) sub 2, or HgCl and KI. Since these salts are produced in much larger quantities than mercuric iodide, more consistent quality is available. The impurity content of these batched and single crystals are compared. Some of the single crystals grown using the in-house prepared mercuric iodide have yielded a large number of spectroscopy grade nuclear radiation detectors. The influence of the major impurities are discussed. DOE

N89-11579# Argonne National Lab., Ill.
HIGH-POWER RF APPLICATIONS OF HIGH-T(SUB c) SUPERCONDUCTORS

J. R. Delayen and M. T. Lanagan 1988 5 p Presented at the 2nd Annual Conference on Superconductivity and Applications, Buffalo, N.Y., 18-20 Apr. 1988
(Contract W-31-109-eng-38)
(DE88-012055; CONF-880466-6) Avail: NTIS HC A02/MF A01

The RF surface resistance of YBa2Cu3O(sub 7-x) was measured by a half-wave resonant coaxial line technique for bulk ceramic and thick film samples. The surface resistance was found to be dependent upon frequency, temperature, and RF field level. A comparison between design criteria for high power cavities and measured properties was carried out to determine the utility of the YBa2Cu3O(sub 7-x) superconductor. DOE

N89-11580# EG and G Energy Measurements, Inc., Goleta, Calif.
MODIFIED PURIFICATION OF MERCURIC IODIDE FOR CRYSTAL GROWTH
N. L. Skinner, C. Ortale, M. M. Schieber, and L. vandenBerg 1988 24 p Presented at the 2nd Workshop on Purification of Materials for Crystal Growth and Glass Processing, Champion, Pa., 28 Sep. 1987
(Contract DE-AC08-83NV-10282)
(DE88-014960; EGG-10282-2156; CONF-8709309-1) Avail: NTIS HC A03/MF A01

The standard procedure used in our laboratory to purify commercially available mercuric iodide consists of a sequence of steps: (1) repeated sublimation under continous evacuation, followed by (2) melting and recrystallization, and (3) a sublimation process in a closed tube. This paper describes a modification of the standard purification sequence by adding recrystallization of the mercuric iodide in hydrochloric acid. Leaching cation impurities out of mercuric iodide powder with hydrochloric acid has been practiced before by Zaletin, (V.M. Zaletin, I.H. Nozhiua, I.N. Fomin, V.T. Shystov, and N.V. Protasov, Atomic Energy 48, 169 (1980)). Our objective for the hydrochloric acid treatment was to remove nitrates and hydrocarbons which were interfering with the vapor transport during crystal growth. Results of the procedure are presented in terms of total carbon and selected ion content of the treated and untreated material. DOE

N89-11581# Electrotechnical Lab., Sakura (Japan).
MOLECULAR BEAM EPITAXY OF GaP FILMS ON Si SUBSTRATES
H. Kawanami, S. Ishihara, K. Nagai, K. Ishii, and Y. Hayashi 1987 13 p In JAPANESE Submitted for publication
(PB88-131974) Avail: NTIS HC E05/MF E01; as PB88-131933 copy not available from STI Facility CSCL 20L

Molecular beam epitaxy (MBE) of GaP films on Si substrates was developed because this structure has possibilities to realize GaP/Si based on high efficiency (about 35 percent) tandem solar cell and also GaP/Si based optoelectronic IC's. A low temperature Si surface celaning method at a temperature as low as 800 C was established. Single crystalline GaP films were successfully grown on Si (001) substrates in a wide growth temperature range from 300 to 600 C. During the film growth, Sn and Si were doped for n-type dopants and Be was doped for p-type one. Also, Zn-O complexes which act as radiative recombination centers were successfully doped during the growth of GaP films. Process compatibility of Si device process and GaP device process was shown by a fabrication of optoelectronic IC which integrates GaP LED's and Si MOSFET's. Author

N89-11582# California Univ., Berkeley. Lawrence Berkeley Lab. Dept. of Physics.
FAR INFRARED LINEAR RESPONSE AND RADIO FREQUENCY NONLINEAR RESPONSE OF CHARGE DENSITY WAVE CONDUCTORS AND HIGH T(SUB c) SUPERCONDUCTORS Ph.D. Thesis
Mark Stephen Sherwin Jun. 1988 189 p
(Contract DE-AC03-76SF-00098)
(DE88-013595; LBL-25404) Avail: NTIS HC A09/MF A01

The far-ir (FIR) linear response of the charge-density-wave (CDW) conductor (TaSe4)2I and polycrystalline La(sub 1.85)Sr(sub 0.15)CuO4 and La(sub 1.85) Ca(sub 0.15)CuO4 was measured at 8 to 350/cm and 5 to 300K. At low T in (TaSe4)2I, a mode with giant oscillator strength was found at 38/cm. This giant FIR mode lies between the pinned mode and the Peierls gap. It is suggested that a giant FIR mode distinct from the pinned mode is a common feature of CDW conductors. At low T in the high-T sub c superconductors, a reflectance edge was observed near 2.5k sub B T sub c. The BCS-like temperature-dependence of the reflectance edge is suggestive of an energy gap. However, a simple model shows that a BCS-like temperature dependence is also consistent with an interpretation of the reflectance edge as a low-frequency plasmon. It is not yet possible to deduce the energy gap from the FIR spectra. The RF nonlinear response of the CDW conductor NbSe3 was also measured. In combined RF- and dc-electric fields, mode-locking occurs in NbSe3. Complete mode-locking in conventional samples dramatically suppresses sliding CDW conduction fluctuations. Combined RF and dc electric fields on switching NbSe3 induced a large amplitude ac switching noise for RF frequencies greater than 1 MHz, and a period-doubling route to chaos for RF-frequencies less than 1 MHz. The mode-locking behavior of switching and nonswitching NbSe3 is analyzed. A model of CDW elasticity qualitatively reproduces all of the experimental anomalies for dc-, ac- and combined ac- and dc-electric fields. It is suggested that, during mode-locking, the number of degrees of freedom active in CDW transport is reduced. DOE

N89-11583# International Centre for Theoretical Physics, Trieste (Italy).
SUPERCONDUCTIVITY, STRUCTURES, ESR AND SIMS-ANALYSIS OF A HIGH-T(SUB c)Y(SUB 0.33)Ba(SUB 0.67)Cu(SUB 2.33)O(SUB 3.67-SIGMA) COMPOUND
T. Porjesz, J. Bankuti, and T. Karman Oct. 1987 11 p
(DE88-702677; IC-87/273) Avail: NTIS (US Sales Only) HC A03/MF A01

In a new kind of high-T(sub c) Y(sub 0.33)Ba(sub 0.67)Cu(sub 2.33)O(sub 3.67-sigma) compound the superconducting transition comes into being between 92 and 84 K, the value of Meissner state is 68 vol percent, the change in ESR signal provides a possible proof for superconductivity, the main phase has an orthorhombic symmetry and the SIMS analysis offers quite new and valuable information on the material components. DOE

N89-11584# Oak Ridge National Lab., Tenn. Metals and Ceramics Div.
ELECTRON MICROSCOPY OF MODULATED AND ORDERED ALLOYS
J. Bentley 1988 2 p Presented at the MAS/EMSA Microbeam Analysis Conference, Milwaukee, Wis., 7 Aug. 1988
(Contract DE-AC05-84OR-21400)
(DE88-008667; CONF-880841-8; CONF-880841) Avail: NTIS HC A02/MF A01

Modulated and ordered alloys are of interest not only from a basic standpoint but also because they often possess interesting properties or form the basis of commercial materials. Transmission electron microscopy (TEM) provides much unique and valuable information in the study of phase transformations in such alloys but, as this overview of the applicable methods will try to illustrate, the experimental work is often challenging and data interpretation is rarely straightforward. DOE

N89-11585# Los Alamos National Lab., N. Mex.
ELECTRODYNAMICS OF SINGLE-CRYSTAL Eu(SUB 2)CuO(SUB 4): A BOSON EXCITATION SPECTRUM
D. W. Reagor, S. Cheong, S. E. Brown, A. Migliori, Z. Fisk, and J. D. Thompson 1988 12 p Presented at the International Conference on Science and Technology of Synthetic Metals, Santa Fe, N. Mex., 26 Jun. 1988
(Contract W-7405-eng-36)
(DE88-014328; LA-UR-88-2277; CONF-880669-10) Avail: NTIS HC A03/MF A01

Static and microwave measurements of the electronic response of the planar cuprate Eu(sub 2)CuO(sub 4) provide evidence for thermally activated collective excitations. These observations

together with microwave and other measurements on superconductors suggest that paired charge-carrying objects may exist both above and below T sub c in the superconductors. If these objects, which can be related to solitons of a spin density wave ground state, play a role in superconductivity, certain conclusions may be drawn. Discussed here is evidence for such objects and their implications. DOE

N89-11586# Illinois Univ., Urbana. Dept. of Physics and Materials Research Lab.
CONSTRAINTS ON THE GROWTH OF METALLIC SUPERLATTICES
C. P. Flynn 1988 14 p
(Contract DE-AC02-76ER-01198)
(DE88-014633; DOE/ER-01198/T16; MRL-88-0003) Avail: NTIS HC A03/MF A01

It is shown why the epitaxial growth of high quality metallic superlattices generally requires a growth temperature of approximately 3T sub m 8 and two components having similar melting temperatures T sub m. A general observation of oscillations from growing metal surfaces at temperatures of approximately T sub m 8 is also predicted. DOE

N89-11587# Brookhaven National Lab., Upton, N. Y. Dept. of Applied Science.
MICROSTRUCTURAL DEFECTS AND SUPERCONDUCTING CRITICAL CURRENTS IN SUPERCONDUCTORS
M. Suenaga 1988 13 p Presented at the MRS International Meeting on Advanced Materials, Tokyo, Japan, 30 May 1988
(Contract DE-AC02-76CH-00016)
(DE88-013781; BNL-41427; CONF-880529-2) Avail: NTIS HC A03/MF A01

Superconducting critical current density is an extrinsic property of a superconductor and depends primarily on the interaction of crystal-structural defects and magnetic flux lines. The most effective characteristic defect size for the interaction is generally thought to be of an order of the superconducting coherence length. In order to understand critical current densities in the high temperature superconductors, the coherence lengths for some of metallic and oxide superconductors are listed and these are compared with the microstructural defects as observed by transmission electron microscopy. DOE

N89-11588# International Centre for Theoretical Physics, Trieste (Italy).
ELASTIC AND ANELASTIC BEHAVIOUR OF ICOSAHEDRAL QUASICRYSTALS
R. E. Bolmaro and F. Povolo Sep. 1987 14 p
(DE88-702712; IC-87/318) Avail: NTIS (US Sales Only) HC A03/MF A01

A theory is developed, based on theoretical-group analysis, which describes the linear, reversible, time-dependent response of an icosahedral quasicrystal, containing point defects, to stress the field known as anelastic relaxation. We obtain also anelastic relaxation relationships for the practical Young, shear and Poisson moduli. DOE

N89-11589# Oak Ridge National Lab., Tenn.
DYNAMIC INTERACTIONS OF ENERGETIC PROBES WITH CONDENSED MATTER: PROCEEDINGS
Apr. 1988 557 p Proceedings of the 10th Werner Brandt Workshop on Penetration Phenomena held at Alicante, Spain, 7 Jan. 1987
(Contract DE-AC05-84OR-21400)
(DE88-008882; CONF-870155) Avail: NTIS HC A23/MF A01

Individual papers have been indexed separately. Topics addressed include: scanning transmission electron microscopy; inelastic scattering cross sections; calculation of electron beam damage; energy loss; mu-induced wakes; photoemission; tunneling microscopy; exciation of electron-hole pairs; chamical etching effects; electron and positron paths; ions; protons; and cherenkov effect. B.G.

N89-11590 Newcastle-upon-Tyne Univ. (England).
THE ELECTRONIC AND OPTICAL PROPERTIES OF SILICON/GERMANIUM STRAINED LAYER SUPERLATTICES Ph.D. Thesis
Ian Morrison 1987 164 p
Avail: Univ. Microfilms Order No. BRDX80953

An empirical pseudopotential scheme for the calculation of the electronic structure of lattice mismatched semiconductor superlattices is presented. In this method the strain is treated on a microscopic level. A scheme based on the nearly free electron model is used to determine the absolute energies of the constituents. The electronic structure of Si/Ge superlattices with period in the range 10 to 100 A is calculated using this method. The band alignment produced in the calculation is in close agreement with experiment and other calculational procedures. The inclusion of strain is found to be important in predicting the momentum mixing in the superlattice states. The enhancement of the optical transition across the fundamental gap is investigated in a variety of superlattices. The magnitude is found to depend on the confinement of the states and the magnitude of the momentum mixing. The inclusion of strain at a microscopic level is found essential in predicting the magnitude of the transition. Dissert. Abstr.

N89-11591# Northwestern Univ., Evanston, Ill.
SELF-CONSISTENT CHARGE AND SPIN DISTRIBUTIONS IN OXIDE SUPERCONDUCTORS
D. E. Ellis, D. J. Lam, and B. W. Veal (Argonne National Lab., Ill.) Mar. 1988 27 p Presented at the Latin-American Conference on High-Temperature Superconductivity, Rio de Janeiro, Brazil, 5 May 1988 Prepared in cooperation with Centro Brasileiro de Pesquisas Fisicas, Rio de Janeiro
(Contract W-31-109-eng-38)
(DE88-012051; CONF-880522-1) Avail: NTIS HC A03

The self-consistent field local density theory provides a useful first principles theoretical basis for the description of electronic charge and spin distributions in complex materials. The ground state energy levels and charge and spin densities of copper-oxide based superconductors are discussed in terms of both band structure and molecular cluster models. X-ray photoemission and absorption data are considered, along with charge transport properties, to provide essential data necessary to understand basic bonding and excitation mechanisms. An embedded cluster approach is used to represent cluster-host interactions with long-range terms included by Ewald summation. X-ray absorption near-edge spectra (XANES) are calculated for the Cu K-edge and compared with experiment in an effort to identify different valence states assumed to be involved in superconductive electron-pairing in certain models. The effects of probable defects and impurities on the electronic structure, especially those due to transition metals on substitutional sites, are calculated in the cluster scheme. Electric field gradients and isomer shifts are determined at Fe- substituted Cu sites for comparison with Mossbauer data and with the unperturbed host Cu sites. DOE

N89-11592# California Univ., Berkeley. Lawrence Berkeley Lab. Materials and Chemical Sciences Div.
SOME THEORETICAL ASPECTS OF HIGH-T(SUB c) SUPERCONDUCTIVITY
Vladimir Z. Kresin Oct. 1987 6 p Presented at the Low Temperature Electronics and High Temperature Superconductors Symposium, Honolulu, Hawaii, 19 Oct. 1987
(Contract DE-AC03-76SF-00098)
(DE88-013101; LBL-25392; CONF-871072-2) Avail: NTIS HC A02/MF A01

This paper is concerned with properties of new superconducting oxides discovered and with mechanisms of high-(T sub c) superconductivity. At present, there are many experimental data which allow us to conclude that we are dealing with very unusual systems. At the same time, we should stress that the new superconducting oxides display usual, BCS-type superconductivity. This means that: the superconducting state is due to an effective electron-electron attraction caused by some intermediate field; this

attraction leads to Cooper pairing, and the spectrum of excitations possesses an energy gap. However, this state has many peculiar features, such as a small coherence length, non-phonon contribution to the pairing, and a multigap structure. DOE

N89-11593# International Centre for Theoretical Physics, Trieste (Italy).
PAIR POTENTIAL TREND OF ALKALI METALS UNDER EXTERNAL PRESSURE
S. M. Mujibur Rahman Sep. 1987 18 p
(DE88-702973; IC-87/257) Avail: NTIS (US Sales Only) HC A03/MF A01

Structural phase stability of certain alkali metals under external pressure is investigated by looking at their pair potential trend. The effective pair potentials occurring in the real space representation of the band structure contribution relevant to a second-order theory are calculated by using an appropriate dielectric function and a simple empty-core pseudopotential. The relative positions of the neighboring atoms with respect to the minima in the pair potentials uphold a qualitative picture of the phase stability in these systems. DOE

N89-11594# Lawrence Livermore National Lab., Calif.
LOW TEMPERATURE MEASUREMENTS ON UBe13
J. P. Brison, J. C. Lasjaunias, A. Ravex, J. Flouquet, D. Jaccard (Geneva Univ., Switzerland), Z. Fisk, and J. L. Smith 1988 3 p Presented at the International Conference on High Temperature Superconductors and Materials and Mechanisms of Superconductivity, Interlaken, Switzerland, 29 Feb. 1988
(Contract W-7405-eng-36)
(DE88-014446; LA-UR-88-1926; CONF-880206-15) Avail: NTIS HC A02

Transport and specific heat measurements are reported on a new sample of UBe sub 13. Special focuses are given on the zero field specific heat: at low temperature (T less than 150 mK) where the impurity scattering dominates, at intermediate temperature where a quani T (3) law characteristic of an axial state is obeyed and near the critical temperature where critical fluctuations are observed. Correlations are made with magnetoresistivity and thermal conductivity experiments. DOE

N89-11595*# National Bureau of Standards, Gaithersburg, Md.
STRUCTURAL ANOMALIES IN UNDOPED GALLIUM ARSENIDE OBSERVED IN HIGH RESOLUTION DIFFRACTION IMAGING WITH MONOCHROMATIC SYNCHROTRON RADIATION
B. Steiner, M. Kuriyama, R. C. Dobbyn, U. Laor, D. Larson, and M. Brown (Grumman Aerospace Corp., Bethpage, N.Y.) 1988 48 p
(Grant NAGw-976)
(NASA-CR-183268; NAS 1.26:183268) Avail: NTIS HC A03/MF A01 CSCL 20L

Novel, streak-like disruption features restricted to the plane of diffraction have recently been observed in images obtained by synchrotron radiation diffraction from undoped, semi-insulating gallium arsenide crystals. These features were identified as ensembles of very thin platelets or interfaces lying in (110) planes, and a structural model consisting of antiphase domain boundaries was proposed. We report here the other principal features observed in high resolution monochromatic synchrotron radiation diffraction images: (quasi) cellular structure; linear, very low-angle subgrain boundaries in (110) directions, and surface stripes in a (110) direction. In addition, we report systematic differences in the acceptance angle for images involving various diffraction vectors. When these observations are considered together, a unifying picture emerges. The presence of ensembles of thin (110) antiphase platelet regions or boundaries is generally consistent not only with the streak-like diffraction features but with the other features reported here as well. For the formation of such regions we propose two mechanisms, operating in parallel, that appear to be consistent with the various defect features observed by a variety of techniques. Author

N89-11596 Drexel Univ., Philadelphia, Pa.
A THEORY OF SURFACE AND INTERFACE ELECTRONIC PROPERTIES OF CRYSTALLINE SOLIDS: APPLICATIONS TO 2-6 COMPOUNDS Ph.D. Thesis
Joseph Thomas Schick 1987 191 p
Avail: Univ. Microfilms Order No. DA8806516

The surface and interface properties of HgTe and CdTe are studied with the hope of understanding the underlying properties of superlattices as well as the surface characteristics of these compounds. A Green's function (GF) model of the surface and interface systems was employed. The GF of a semi-infinite system is described in terms of the GF derived from the Hamiltonian of the infinite crystal into two semi-infinite crystals in some crystallographic direction. Subsequently the GF of the interface of two crystals is determined by the GF's of the individual semi-infinite systems and the scattering potential describing the coupling between the two crystals. Model calculations of the surface and interface electronic properties of three-dimensional two-band crystals were performed. The bulk states are modified, and under certain conditions localized surface or interface bands are found to occur inside the band gap. The local densities of states of the pure HgTe and CdTe surfaces and interfaces at the important T and J points in the surface Brillouin zone were examined. Numerical calculations were performed for (100) planes where the lattice is composed of alternating layers of anions (TE) and cations (Cd, Hg). The surface or resonance states on the cation terminated (100) surface and CdTe and the anion terminated (100) surface of HgTe were observed even for plain unperturbed surfaces. The energies and strengths of the surface states were found to change under the influence of surface perturbations. Dissert. Abstr.

N89-11597# California Univ., Berkeley. Lawrence Berkeley Lab.
TUNNELING JUNCTIONS AND THE FIELD EFFECT
V. Z. Kresin Aug. 1987 3 p Presented at the International Superconductivity Electronics Conference, Tokyo, Japan, 28 Aug. 1987
(Contract DE-AC03-76SF-00098)
(DE88-013707; LBL-25443; CONF-870880-1) Avail: NTIS HC A02

Tunneling junctions containing a semiconductor film are studied. The key role is played by the proximity effect. A particularly interesting situation arises in the presence of a high T sub c semiconductor. Its presence increases the sharpness of the field effect. The properties of the system Sc-S-N-S are discussed. DOE

N89-11598# Eidgenoessisches Inst. fuer Reaktorforschung, Wuerenlingen (Switzerland).
LATTICE INSTABILITY IN SINGLE-CRYSTAL La(SUB 2-x)Sr(SUB x)/CuO4
P. Boeni, J. D. Axe, G. Shirane, R. J. Birgeneau, D. R. Gabbe, H. P. Jenssen, M. A. Kastner, P. J. Picone, T. R. Thurston, and M. Sato (Institute for Molecular Science, Okazaki, Japan) 1988 13 p Presented at the 4th International Conference on Neutron Scattering (ICNS '88), Grenoble, France, 12 Jul. 1988
(Contract DE-AC02-76CH-00016; NSF DMR-85-01856; NSF DMR-84-18718)
(DE88-013994; BNL-41472; CONF-880715-3) Avail: NTIS HC A03/MF A01

The structural phase transition from the tetragonal to the orthorhombic phase of doped and undoped samples of La(sub 2-x)Sr(sub x)CuO4 has been investigated by using inelastic neutron scattering techniques. The rotational nature of the soft mode leads to moderate electron-phonon coupling and the mode is unlikely to enhance significantly conventional phonon mediated superconductivity. DOE

N89-11599# California Univ., Berkeley. Lawrence Berkeley Lab.
SPIN-ORBIT INTERACTION EFFECTS IN ZINCBLENDE SEMICONDUCTORS: AB INITIO PSEUDOPOTENTIAL CALCULATIONS

Ming-Fu Li (China Scientific and Technical Univ., Beijing.), Michael P. Surh, and Steven G. Louie Jun. 1988 4 p Presented at the 19th International Conference on the Physics of Semiconductors, Warsaw, Poland, 1 Aug. 1988
(Contract DE-AC03-76SF-00098)
(DE88-014663; LBL-25543; CONF-880884-1) Avail: NTIS HC A02/MF A01

Ab initio band structure calculations have been performed for the spin-orbit interaction effects at the top of the valence bands for GaAs and InSb. Relativistic, norm-conserving pseudopotentials are used with no correction made for the gaps from the local density approximation. The spin-orbit splitting at gamma and linear terms in the yields kappa dependence of the splitting are found to be in excellent agreement with existing experiments and previous theoretical results. The effective mass and the cubic splitting terms are also examined. DOE

N89-11600# California Univ., Berkeley. Lawrence Berkeley Lab.
PHONON-PLASMON MECHANISM OF HIGH-T(SUB c) SUPERCONDUCTIVITY
Vladimir Z. Kresin and H. Morawitz (International Business Machines Corp., San Jose, Calif.) May 1988 9 p Presented at the Latin American Conference on High Temperature Superconductivity, Rio de Janeiro, Brazil, 2 May 1988
(Contract DE-AC03-76SF-00098)
(DE88-014869; LBL-25482; CONF-8805158-1) Avail: NTIS HC A02/MF A01

The observed high superconducting transition temperatures are caused, in our view, by the coexistence of strong electron-phonon coupling and the plasmon mechanism. A generalized Eliashberg equation describing the effects of phonons and plasmons on the pairing is presented. The structure of the plasmon bands in conducting, highly anisotropic layered materials are studied. DOE

N89-11601# Sandia National Labs., Albuquerque, N. Mex.
CHEMICAL PREPARATION OF POWDERS AND FILMS FOR HIGH TEMPERATURE SUPERCONDUCTORS
B. C. Bunker, J. A. Voigt, D. L. Lamppa, D. H. Doughty, E. L. Venturini, J. F. Kwak, D. S. Ginley, T. J. Headley, M. S. Harrington, and M. O. Eatough et al. 1988 13 p Presented at the Spring Meeting of the Materials Research Society, Reno, Nev., 4 Apr. 1988
(Contract DE-AC04-76DP-00789)
(DE88-015266; SAND-88-1030C; CONF-880408-35) Avail: NTIS HC A03/MF A01

A precipitation process has been developed to prepare precursor powders which can be calcined and sintered to form high critical temperature superconductors such as YBa(sub 2)Cu(sub 3)O(sub 7-x). Precursor powders are prepared using a continuous precipitation system in which a solution containing highly soluble salts of the desired metal cations is rapidly and completely mixed with a solution containing precipitating anions such as hydroxide and carbonate ions. The resulting amorphous powder can be calcined to form submicron particles of desired superconducting phases which are useful in preparing inks for the ink-jet printing of superconducting interconnects. The powders can be redissolved in organic solvents to form solutions which can be used in spin or dip coating substrates with thin superconducting films. Finally, the powders have been used to prepare bulk ceramics which exhibit the highest reported critical currents of any chem-prep ceramics. Bulk samples prepared from chloride doped precursors exhibit large, oriented grains and extensive flux pinning. DOE

N89-11602# Florida Univ., Gainesville. Dept. of Materials Science and Engineering.
IMPLANTATION STUDIES OF HYDROGEN BY FIELD ION MICROSCOPY AND SPECTROSCOPY Final Report
E. D. Verink, Jr., R. T. DeHoff, and J. J. Hren 1988 3 p
(Contract DE-FG05-84ER-45172)
(DE88-015806; DOE/ER-45172/T1) Avail: NTIS HC A02/MF A01

The depth resolution of the Field Ion Microscope/Imaging Atom Probe (FIM/IAP) is of the order of a crystal d-spacing of the metal under investigations. The current study involved the application if the FIM/IAP to the study of low energy ions (less than 20 keV) implanted into metals to obtain depth profiles. Two ion species of immense technological importance were used, nitrogen and deuterium. Results of this investigation fall into four categories: (1) instrumentation development, (2) development of new experimental techniques, (3) the generation and interpretation of experimental data, and (4) the determination of a number of characteristics of FIM which can influence the interpretation of experimental observations. DOE

N89-11603# International Centre for Theoretical Physics, Trieste (Italy).
NEW QUANTUM INTERFEROMETER EFFECT IN SUPERCONDUCTING OXIDE CERAMICS
J. ChelaFlores and L. N. Shehata Aug. 1987 11 p
(DE88-703152; IC-87/281) Avail: NTIS (US Sales Only) HC A03/MF A01

On the basis of a phenomenological approach to type II high T(sub c) superconductivity, we suggest that in the lanthanum compounds the Mercereau effect for a coupled junction pair should display and ex-dependent shift in the period of modulation of the tunnelling current. DOE

N89-11604*# Fermi National Accelerator Lab., Batavia, Ill.
COSMIC STRINGS AND SUPERCONDUCTING COSMIC STRINGS
Edmund Copeland Aug. 1988 44 p Presented at the 2nd Erice Summer School on Dark Matter, May 1988 Sponsored in part by NASA, and by DOE
(NASA-CR-183361; NAS 1.26:183361; FERMILAB-Pub-88/108-A)
Avail: NTIS HC A03/MF A01 CSCL 20L

The possible consequences of forming cosmic strings and superconducting cosmic strings in the early universe are discussed. Lecture 1 describes the group theoretic reasons for and the field theoretic reasons why cosmic strings can form in spontaneously broken gauge theories. Lecture 2 discusses the accretion of matter onto string loops, emphasizing the scenario with a cold dark matter dominated universe. In lecture 3 superconducting cosmic strings are discussed, as is a mechanism which leads to the formation of structure from such strings. Author

N89-11605# Air Force Inst. of Tech., Wright-Patterson AFB, Ohio.
SURFACE PASSIVATION OF GALLIUM ARSENIDE M.S. Thesis
Robert J. Racicot Apr. 1988 92 p
(AD-A196695; AFIT/CI/NR-88-63) Avail: NTIS HC A05/MF A01 CSCL 07B

The surface passivation of Si doped (100) n-type gallium arsenide (GaAs) by chemical treatment with phosphoric acid (H3P04), phosphorus trichloride (PCl3), and sodium sulfide (Na2S.9H2O) was investigated using room temperature photoluminescence (PL) and a capacitance-voltage (C-V) and current-voltage (I-V) profiler. After passivation, the 300K PL increased for all three treatments. Best results obtained showed improvements of 1.4, 3.5 and 5.3 times greater of PL efficiency for H3PO4, PCl3 and Na2S, respectively, over unpassivated samples that were only cleaned and etched. Samples that were cleaned, etched and washed with de-ionized 18 Mohm, 5 ppm O2 content water showed about the same PL increase as the H3PO4 passivation. Capacitance-voltage and I-V profile curves showed the removal of the surface oxide hysteresis with the PCl3 passivated samples; however, re-oxidation seems to take longer than normal and to be confined to the passivation layer. GRA

N89-11606# Aerospace Corp., El Segundo, Calif. Chemistry and Physics Lab.
FUNDAMENTAL ASPECTS OF THE ELECTRONIC STRUCTURE, MATERIALS PROPERTIES, AND LUBRICATION PERFORMANCE OF SPUTTERED MoS2 FILMS
Paul D. Fleischauer 30 Jun. 1988 39 p

(Contract F04701-85-C-0086)
(AD-A196852; TR-0086A(2945-03)-5; SD-TR-88-61) Avail: NTIS HC A03/MF A01 CSCL 07B

Layered transition metal dichalcogenide (LTMD) compounds constitute a class of materials with unique and unusual properties based on the extreme degree of anisotropy in their layered crystal structures. LTMDs are formed by stacking sandwiches consisting of a layer of transition metal between two layers of chalcogen. There is strong covalent bonding within the sandwiches but weak (van der Waals') bonding between them. Details of the exact crystal type within this general structure vary and result in some LTMDs being very good lubricants and others being poor lubricants or abrasives. Coincidentally, the electrical properties vary greatly also, ranging from insulators to semiconductors, and finally to metals with evidence of superconductivity in some of the class members. GRA

N89-11607# State Univ. of New York, Buffalo. Dept. of Chemistry.
COUPLED EVEN-PARITY SUPERCONDUCTING STATES
D. Sahu, A. Langner, and Thomas F. George Jun. 1988 30 p
(Contract N00014-86-K-0043)
(AD-A196969; UBUFFALO/DC/88/TR-70) Avail: NTIS HC A03/MF A01 CSCL 20C

In situations involving two successive superconducting transitions or in situations in which one superconducting transition induces a secondary superconducting state, the nature of the coupling between the states is of interest. Examples of such coupling include heavy fermion systems and possibly the recently discovered high T sub c superconductors. We use symmetry principles to enumerate the Ginzburg Landau free energies associated with the coupling between s and d wave superconducting states in the square planar, cubic, tetragonal, orthorhombic and hexagonal crystal classes. GRA

77 THERMODYNAMICS AND STATISTICAL PHYSICS

Includes quantum mechanics; theoretical physics; and Bose and Fermi statistics.

For related information see also *25 Inorganic and Physical Chemistry* and *34 Fluid Mechanics and Heat Transfer.*

N89-11608# International Centre for Theoretical Physics, Trieste (Italy).
PLANCK'S ORDERS OF MAGNITUDE AND THE LIMITS OF THE QUANTUM GRAVITY CONCEPTION
H. H. vonBorzeszkowski Feb. 1988 20 p
(DE88-702985; IC-87/321) Avail: NTIS (US Sales Only) HC A03/MF A01

In this paper it is shown how the universal constants h, c and G prevent one from deriving measurable quantum GRT effects for energies near the Planck energy. Planck's units thus screen those GRT regions where difficulties for the quantization procedure occur, from a physically sensible quantum-field (or graviton) interpretation. DOE

N89-11609# International Centre for Theoretical Physics, Trieste (Italy).
QUANTIZATION OF GREEN-SCHWARZ SUPERSTRING
R. E. Kallosh Apr. 1987 17 p
(DE88-702242; IC-87/71) Avail: NTIS (US Sales Only) HC A03/MF A01

The problem of quantization of superstrings is traced back to the nil-potency of gauge generators of the first-generation ghosts. The quantization of such theories is performed. The novel feature of this quantization is the freedom in choosing the number of ghost generations as well as gauge conditions. As an example, we perform quantization of heterotic string in a gauge, which preserves space-time supersymmetry. The equations of motion are those of a free theory. DOE

N89-11610 Texas Univ., Austin.
A FREQUENCY DEPENDENT RAY THEORY Ph.D. Thesis
Terry Lee Foreman 1987 98 p
Avail: Univ. Microfilms Order No. DA8806324

Practical computational procedures for obtaining ray theoretical solutions to the inhomogeneous Helmholtz equation, delta sup 2 psi + kappa sup 2 psi = S(r, omega), may resort to a well known approximation. A computational method is presented which enables one to trace rays without resort to the ray theory approximation providing a solution to the Helmholtz equation is already available. In other words, given a solution to the Helmholtz equation, the exact rays for that case can be computed. The new ray theory therefore serves, not as a computational method, but as a new method of displaying solutions to the Helmholtz equation. Exact ray diagrams are constructed for several cases using this technique. The resulting ray diagrams usually bear little resemblance to the corresponding classical ray diagrams. It is shown that the discrepancy is attributable to the nature of the classical ray theory approximation, which proves in most cases not to be a small perturbation. Some of the properties of the exact rays which distinguish them from their classical counterparts are listed. Dissert. Abstr.

N89-11611 Oxford Univ. (England).
GEOMETRICAL METHODS IN QUANTUM FIELD THEORY: ON THE TOPOLOGY OF SPACES OF HOLOMORPHIC MAPS Ph.D. Thesis
Jens Gravesen 1987 79 p
Avail: Univ. Microfilms Order No. BRD-81527

The space of based holomorphic maps, between a Riemann surface and a generalized flag manifold or a loop group, is compared with the corresponding space of continuous maps. Both spaces have connected components labeled by a (multi-) degree, and if the Riemann surface is the sphere, then it is shown that the two spaces have the same homology in the limit where the degree tends to infinity. The main idea is a generalization of the concept of a principal part of a meromorphic functions to a principal part of a holomorphic map into a flag manifold or a loop group. Then the space of holomorphic maps can be replaced with a configuration space of principal parts, which makes it possible to apply standard techniques in the proofs. Dissert. Abstr.

N89-11612# Brookhaven National Lab., Upton, N. Y. Dept. of Physics.
THE COMPATIBILITY OF GRAVITY AND KAON RESULTS IN THE SEARCH FOR NEW FORCES
Samuel Aronson, Ephraim Fischbach, Daniel Sudarsky, and Carrick Talmadge (Purdue Univ., West Lafayette, Ind.) 1988 10 p Presented at the 22nd Moriond Workshop on Neutrinos and Exotic Phenomena in Particle Physics and Astrophysics, Les Arcs, France, 23 Jan. 1988
(Contract DE-AC02-76CH-00016)
(DE88-013993; BNL-41475; CONF-880173-5) Avail: NTIS HC A02/MF A01

The existing data on energy-dependences of the fundamental parameters of K sup 0 - k sup 0 system, and the limits on the decay K(+) yields pi(+) (invisible neutrals), are used in conjunction with geophysical data to explore the coupling of the putative fifth force to quantities other than baryon number. DOE

N89-11613*# Fermi National Accelerator Lab., Batavia, Ill.
COSMIC STRINGS
David P. Bennett Jul. 1988 15 p Prepared in cooperation with Chicago Univ., Ill. Sponsored in part by NASA, DOE, and NSF
(NASA-CR-183367; NAS 1.26:183367; FERMILAB-Conf-88/85-A)
Avail: NTIS HC A03/MF A01 CSCL 20C

Cosmic strings are linear topological defects which are predicted by some grand unified theories to form during a spontaneous symmetry breaking phase transition in the early universe. They are the basis for the only theories of galaxy formation aside from quantum fluctuations from inflation based on fundamental physics. In contrast to inflation, they can also be observed directly through

gravitational lensing and their characterisitc microwave background anisotropy. It was recently discovered that details of cosmic string evolution are very differnt from the so-called standard model that was assumed in most of the string-induced galaxy formation calculations. Therefore, the details of galaxy formation in the cosmic string models are currently very uncertain. Author

N89-11614*# Fermi National Accelerator Lab., Batavia, Ill.
INFLATION IN A RENORMALIZABLE COSMOLOGICAL MODEL AND THE COSMIC NO HAIR CONJECTURE
Kei-ichi Maeda, Jaime A. Stein-Schabes, and Toshifumi Futamase (Hirosaki Univ., Japan) May 1988 20 p Sponsored in part by NASA, DOE, and by Yamada Science Foundation
(NASA-CR-183363; NAS 1.26:183363; FERMILAB-Pub-88/70-A; UTAP76/88) Avail: NTIS HC A03/MF A01 CSCL 20C

The possibility of having inflation in a renormalizable cosmological model is investigated. The Cosmic No Hair Conjecture is proved to hold for all Bianchi types except Bianchi IX. By the use of a conformal transformation on the metric it is shown that these models are equivalent to the ones described by the Einstein-Hilbert action for gravity minimally coupled to a set of scalar fields with inflationary potentials. Henceforth, it is proven that inflationary solutions behave as attractors in solution space, making it a natural event in the evolution of such models.
Author

N89-11649# Zurich Univ. (Switzerland). Inst. fuer Theoretische Physik.
EXPERIMENTAL TESTS OF RELATIVITY AND GRAVITATION
H. Herold *In* ESA, Space Science and Fundamental Physics May 1988 p 141-149 (For primary document see N89-11638 02-88)
Copyright Avail: NTIS HC A10/MF A01

80 SOCIAL SCIENCES (GENERAL)

Includes educational matters.

No abstracts in this category.

81 ADMINISTRATION AND MANAGEMENT

Includes management planning and research.

No abstracts in this category.

82 DOCUMENTATION AND INFORMATION SCIENCE

Includes information management; information storage and retrieval technology; technical writing; graphic arts; and micrography.

For computer documentation see *61 Computer Programming and Software.*

N89-11615# Stanford Linear Accelerator Center, Calif.
INTEGRATED DATABASE APPROACH FOR GEODETIC APPLICATIONS
Robert Ruland and Detlev Ruland (Wuerzburg Univ., West Germany) Nov. 1987 20 p Presented at the 4th International Working Conference on Statistical and Scientific Database Management, Rome , Italy, 21 Jun. 1988
(Contract DE-AC03-76SF-00515)
(DE88-012726; SU-SLAC-PUB-4474; CONF-8806166-2) Avail: NTIS HC A03/MF A01

Geodetic measurements even of a defined project produce a vast amount of heterogeneous data. The analysis of these data used to be time-and-manpower consuming and only focused on subsets of the data. This paper demonstrates how an integrated database system will provide an immediate standardized and easy access to the entire information support data management, and, consequently, streamline the analysis. DOE

N89-11616 Arizona State Univ., Tempe.
HYPOTHESIS-CONFIRMING INFORMATION SEARCH STRATEGIES AND COMPUTERIZED INFORMATION RETRIEVAL SYSTEMS Ph.D. Thesis
Sheila Maureen Jacobs 1987 175 p
Avail: Univ. Microfilms Order No. DA8802784

A recent trend in information retrieval systems technology is the development of on-line information retrieval systems. An objective of these systems has been to attempt to enhance decision effectiveness by allowing users to preferentially seek information, thereby facilitating the reduction or elimination of information overload. These systems do not necessarily lead to more effective decision making, however. Recent research in information search strategy suggests that when users are seeking information subsequent to forming initial beliefs, they may preferentially seek information to confirm these beliefs. Therefore, decision making effectiveness may be dependent on the accuracy of the decision maker's initial hypothesis of causality. To assess the effect of information retrieval system type on decision effectiveness, a laboratory experiment was conducted. Participants were presented brief work histories describing a job performance problem and suggesting a cause for the problem. They were required to make an initial attribution of causality for the problem, to query either a conventional on-line information retrieval system or a KBDSS. The results are not conclusive. Dissert. Abstr.

N89-11617# Oak Ridge National Lab., Tenn. Information Resources Organization.
INFORMATION STORAGE ALTERNATIVES: AN OVERVIEW OF LASER-BASED OPTICAL TECHNOLOGIES
N. L. Gray and M. C. Mullins Jun. 1988 42 p
(Contract DE-AC05-84OR-21400)
(DE88-013499; ORNL/TM-10525) Avail: NTIS HC A03/MF A01

This report provides a general introduction to laser-based optical data storage for microcomputer-based systems and assesses the current state of the industry. Read Only Memory (ROM) and Write Once, Read Many (WORM) technologies are investigated. The standardization issues facing the industry today are also discussed. Storage and retrieval techniques are presented, with observations regarding their use with massive amounts of data. The outlook for the optical disk market is addressed, and future products and applications are reviewed. Impacts of optical storage on various areas of traditional data storage industries - magnetic, on-line utilities, microfilm, and publishing - are examined. DOE

N89-11618 Union for Experimenting Coll. and Univ., Yellow Springs, Ohio.
A CO-CITATION STUDY OF THE SCIENTIFIC LITERATURE OF TWO INNOVATION RESEARCH TRADITIONS: DIFFUSION OF INNOVATIONS AND TECHNOLOGY TRANSFER Ph.D. Thesis
Charlotte Alice Cottrill 1987 176 p
Avail: Univ. Microfilms Order No. DA8800197

The state of a research field can be studied through the publications produced by its members. The most revealing data from the literature of a field are the references cited by its practioners in their publications. References can be studied with co-citation analysis which is a type of network analysis that identifies the relationship among either cited documents or the combined works of individual scholars. The strength of the relationship is the number of times the pair are cited together by later documents. Co-citation analysis was used to study many research fields and shown to reflect with considerable accuracy the membership of a

specialty and its content and problem orientation. A descriptive structural analysis of the diffusion of innovations and technology transfer literature from 1966 through 1972 is examined. Using samples of the ISI Social Science Citation Index, the documents were reduced to groups of works by authors, and a modified author co-citation analysis was performed to identify the relationships among the works of these scholars. Separate analyses were performed on the diffusion of innovations and technology transfer co-citations and the combined groups of co-citations. Cluster analysis was used to identify groups of highly similar works. Multidimensional scaling was used to generate maps spatially representing the relationships among the subspecialties in subject space. As publications, particularly in journals, constitute the formal communication system of science, the present study is essentially a study of scientific communication. The analyses employed are network methods that were used to investigate communication flows and identify types of relational patterns. Dissert. Abstr.

N89-11619 Utah Univ., Salt Lake City.
DATABASE LOADING BY EXAMPLES: A LEARNING APPROACH TO LOADING INFORMATION RETRIEVAL DATABASES Ph.D. Thesis
Mamdouh H. Ibrahim 1987 148 p
Avail: Univ. Microfilms Order No. DA8804708

Machine learning from examples is a growing research area within the artificial intelligence field where its application to real world problems proves to be very successful. The research in the are of learning from samples and its application to the domains of information retrieval systems is described. The research concentrates on learning concepts presented by the user through examples and the utilization of these concepts to load the document data bases. Loading of document data bases requires reformatting and identifying of key words, phrases, and headers for indexing. A descriptive language and a set of operators were designed and implemented to describe the given examples and the concept definitions. Heuristic rules control the generation and prune the search for the best intermediate description in the space of all possible descriptions. The refinement generalization forms a Maximally Generalized Description (MGD) of the concept by generalizing the last intermediate description based on the application of appropriate generalization operators. The MGD is then used to generate examples and present them to the user. Production rules incorporate the final descriptions along with associated functions to be executed when data from the document match the descriptions. A prototype system is implemented as a C program for the IBM-PC to demonstrate the validity of the discussed approach. Dissert. Abstr.

N89-11620# Northrop Services, Inc., Research Triangle Park, N. C. Environmental Sciences.
REFEREE: BIBLIOGRAPHIC DATABASE MANAGER, DOCUMENTATION
Slate Raymond Oct. 1987 72 p
(Contract EPA-68-02-4198)
(PB88-200787; EPA/600/8-87/052A; EPA/SW/DK-88/047A)
Avail: NTIS HC A04/MF A01 CSCL 05B

The publication is the user's manual for 3.xx releases of REFEREE, a general purpose bibliographic data base management program for IBM compatible microcomputers. The REFEREE software also is available from NTIS. The manual has two main sections: Quick Tour and Reference Guide; and a glossary, three appendixes, and an index. Quick Tour provides information sufficient to enable a new user to install and experiment with the program. Reference Guide provides detailed information about REFEREE databases, records, and fields; the primary command available to the user; and the most common sources of unexpected program behavior. Author

N89-11621# National Bureau of Standards, Gaithersburg, Md. Information Systems Engineering Div.
COMPUTER SCIENCE AND TECHNOLOGY: GUIDE TO DISTRIBUTED DATABASE MANAGEMENT
E. N. Fong and B. K. Rosen Apr. 1988 36 p
(PB88-201561; NBS/SP-500/154) Avail: NTIS HC A03/MF A01 CSCL 05B

Distributed Database Management Systems are exciting and potentially very powerful. However, distributed database management systems often have created increased complexity of database management and controls without providing the expected benefit to the organization's operations. Distributed database management systems may not be desirable for every organization. Their benefits can be realized only with careful planning, and evaluation of alternative strategies. The guide provides an organization's decision makers the appropriate information to make good decisions in evaluating distributed database management technologies for their individual environments. Also, the guide aids in planning for an orderly migration path into a distributed database environment. GRA

N89-11622 East Anglia Univ., Norwich (England).
AN INVESTIGATION OF INFORMATION SYSTEMS PROTOTYPING Ph.D. Thesis
Pamela Jean Mayhew 1987 342 p
Avail: Univ. Microfilms Order No. BRD-80638

This thesis is concerned with the use of prototyping during the development of information systems. Prototyping is a process which involves early practical demonstration of relevant parts of the desired system. This is carried out with a view to improving both the quality and timeliness of the target system. The quality of an information system is largely determined by its adequacy as a tool for human users. Protyping serves to enhance the communication between developers and users, and through this to increase the suitability of the resulting information system. An investigation into the traditional phase oriented approach to systems development reveals that in certain circumstances it can result in incorrect or at best disappointing systems. The prototyping approach is examined as a possible alternative. Particular attention is paid to its use with respect to typical characteristics of information systems. This is followed by an investigation into all aspects of prototyping. Dissert. Abstr.

N89-11623 Lehigh Univ., Bethlehem, Pa.
THE TRANSFORMATIVE COMPRESSION OF COHERENT LANGUAGES Ph.D. Thesis
Stuart Harvey Rubin 1988 156 p
Avail: Univ. Microfilms Order No. DA8806582

One problemn with expert systems is that they do not scale well. This problem, as well as that of expediting the acquisition of knowledge, that of compressing redundancy out of the knowledge base, and that of deriving analogical explanations, can be addressed through the development of appropriate domain-specific languages called Application Languages (ALs). The compiling of ALs through the use of specifically developed Transformation Languages (TLs) is advocated. A TL enables the programmer to utilize previously defined functions for the definition of subsequent functions by knowledge-based analogical means, providing for an extensible AL. The resulting descriptions are more concise and as a consequence, less error-prone, easier to store, explain, debug, and modify. A Seven-Segment Display (SSD) language and a Games Description Language (GDL) are implemented, using specific TLs, in order to demonstrate the utility of the transformative approach. Dissert. Abstr.

N89-11624* National Aeronautics and Space Administration, Washington, D.C.
PATENT ABSTRACTS BIBLIOGRAPHY: A CONTINUING BIBLIOGRAPHY (SUPPLEMENT 33). SECTION 2: INDEXES
Jul. 1988 501 p
(NASA-SP-7039(33); NAS 1.21:7039(33)) Not in stock from SOD CSCL 05B

A subject index is provided for over 4500 patents and patent applications for the period May 1969 through June 1988. Additional indexes list personal authors, corporate authors, contract numbers, NASA case numbers, U.S. patent class numbers, U.S. patent numbers, and NASA accession numbers. Author

N89-11625# Advisory Group for Aerospace Research and Development, Neuilly-Sur-Seine (France). Technical Information Panel.
EVALUATING THE EFFECTIVENESS OF INFORMATION CENTRES AND SERVICES
Sep. 1988 93 p Lecture series held in Luxembourg, 5-6 Sep. 1988, in Athens, Greece, 8-9 Sep. 1988, and in Lisbon, Portugal, 12-13 Sep. 1988
(AGARD-LS-160; ISBN-92-835-0479-8) Copyright Avail: NTIS HC A05/MF A01

The current state-of-the-art of evaluuating information centers and services is presented in both theoretical and practical perspectives. Case studies are used to demonstrate successful evaluation projects from different countries and to focus on specific evaluation methods and measures. In addition to providing a thorough basis for determining the most appropriate evaluation methods and measures for a given situation and potential problems that can arise in using them, the presentations include discussions of what to do once the evaluation is done. Various strategies are proposed for altering the centers and services so that effectiveness is improved. Political, organizational and practical aspects of evaluation projects are covered so that evaluation is seen from a broader context. For individual titles, see N89-11626 through N89-11632.

N89-11626# King Research, Inc., Rockville, Md.
EVALUATING THE EFFECTIVENESS OF INFORMATION USE
Donald W. King and Jose-Marie Griffiths *In* AGARD, Evaluating the Effectiveness of Information Centres and Services Sep. 1988 5 p (For primary document see N89-11625 02-82)
Copyright Avail: NTIS HC A05/MF A01

An approach to evaluating the use, usefulness and value of published/recorded information on the work of its users is described. The reading patterns of professionals and the application of information derived from reading is discussed in detail. Several different indicators of productivity of professionals are developed and correlated with the amount of reading that is done. Finally, several different perspectives on the value of information centers to the professionals they serve are presented. Author

N89-11627# Loughborough Univ. of Technology (England).
MEASURES, METHODS AND MODELS EMPLOYED IN EVALUATING THE EFFECTIVENESS OF INFORMATION CENTERS AND SERVICES
A. J. Meadows *In* AGARD, Evaluating the Effectiveness of Information Centres and Services Sep. 1988 16 p (For primary document see N89-11625 02-82)
Copyright Avail: NTIS HC A05/MF A01

Evaluating the effectiveness of organizations and of the services they offer always depends on assuming some kind of model. The main purpose of modeling is to abstract elements from real-life activities in such a way that these activities can be more readily understood, and so better organised and planned. Models may be used for a variety of purposes; for example, to pinpoint which parts of a system should be sampled to provide an adequate picture of the whole. The drawback of all models is that they reflect only a part of reality, and so can only be used in a limited context. In consequence, models must be explicity formulated and their limitations understood before any evaluation exercise is attempted. The model helps decide what performance measures can usefully be made. For example, a qualitative model may not be appropriate for guiding assessment in terms of quantitative performance measures. Both model and measures therefore have been chosen in the light of the desired outcome from the evaluation. The methodology, is, in turn primarily determined by the model and measures chosen. Author

N89-11628# Polytechnic of Central London (England). Information Research Group.
EUROPEAN EXAMPLES OF EVALUATING THE EFFECTIVENESS OF INFORMATION CENTRES AND SERVICES
John Martyn *In* AGARD, Evaluating the Effectiveness of Information Centres and Services Sep. 1988 15 p (For primary document see N89-11625 02-82)
Copyright Avail: NTIS HC A05/MF A01

There are usually three viewpoints from which an information system, service or product can be evaluated. The first is that of the system or service producers, who will generally be assessing the extent to which their product meets its assigned objectives, and who will be particularly concerned with the improvement of efficiency and effectiveness. Such evaluations do not usually involve comparisons with competing services. The second viewpoint is that of the actual or potential users, whose concern is with the extent to which a system or service meets their perceived needs, and its related cost. This assessment often involves comparisons between services. The third viewpoint, particulary in public-sector operations, is that of the system sponsors, who wish to assess how well a system or service succeeds in meeting policy objectives, some of which may not be explicit. Quantitative evaluative data are often hard to capture, and difficult to interpret. In some European work, a more subjective approach has been taken, using qualitative information supported by such numerical data as may be gathered, to arrive by a judgmental process to an assessment which takes account of the political factors inevitably affecting any evaluation other than the most basic. Author

N89-11629# King Research, Inc., Rockville, Md.
EVALUATING THE PERFORMANCE OF INFORMATION CENTRE STAFF
Jose-Marie Griffiths and Donald W. King *In* AGARD, Evaluating the Effectiveness of Information Centres and Services Sep. 1988 11 p (For primary document see N89-11625 02-82)
Copyright Avail: NTIS HC A05/MF A01

The framework for evaluation described in 'A Framework for Evaluating the Effectiveness of Information Centers and Services' for evaluating staff performance is used. Information center staff are a major resource affecting the overall performance and effectiveness of services provided. Various measures of staff performance are discussed (including quantities, quality and timeliness of staff outputs), and the relationship between staff performance and the effectiveness of services (from a user perspective) is demonstrated. Finally, alternative methods for measuring staff performance are described. Author

N89-11630# King Research, Inc., Rockville, Md.
EVALUATING PERFORMANCE OF INFORMATION CENTRE OPERATIONS AND SERVICES
Jose-Marie Griffiths and Donald W. King *In* AGARD, Evaluating the Effectiveness of Information Centres and Services Sep. 1988 8 p (For primary document see N89-11625 02-82)
Copyright Avail: NTIS HC A05/MF A01

Evaluation of information center resources (e.g, staff, equipment, facilities, etc.) is discussed in terms of input costs, output performance, and productivity. Examples of evaluation of information services (e.g., access to technical reports and other publications, online bibliographic searches, published searches, etc.) are presented in terms of their inout costs and output performance. The linking of resource attributes or charactersitics (e,g., staff competencies, equipment capabilities, facility layout, etc.) to service input costs and output performance (e.g, quality and timeliness of services) is demonstrated. Thus, Center managers can make decisions about resources or allocation of funds involving resources in terms of services involved. A management information system for center management is also described. Author

N89-11631# King Research, Inc., Rockville, Md.
A FRAMEWORK FOR EVALUATING THE EFFECTIVENESS OF INFORMATION CENTRES AND SERVICES
Donald W. King and Jose-Marie Griffiths *In* AGARD, Evaluating the Effectiveness of Information Centres and Services Sep. 1988 14 p (For primary document see N89-11625 02-82)
Copyright Avail: NTIS HC A05/MF A01

Evaluation is a subject of considerable attention at the current time. Three principal aspects of evaluation and information are presented here. The first involves the evaluation of information

workers and services. The second deals with evaluation from the perspective of users served, their organizations and higher levels of aggregation such as to industries, sectors, the entire nation and all nations. The third aspect is how information and information services affect users. Several levels within information service centers are described. One can perform evaluation at each of these levels (i.e, resource components, activities, services and products, functions and information units). That is, at each level one can measure input of resources (i.e, capital, labor, technology, information, etc.) and output quantities produced. Such output divided by input can provide estimates or indicators of productivity. The output of information services is one of several input resources to users. The extent to which this input affects output and productivity is of considerable interest. As shown in Figure 1 on the next page, the input resources (including information) affect user activities, their functions, their organizations, and so on, up to the point that aggregated information use and subsequent productivity affects national goals. Below we attempt to show how these interrelationships work. First, several definitions are given.
Author

N89-11632# Bell Telephone Labs., Inc., Murray Hill, N. J. Libraries and Information Systems.
EVALUATING FOR INFORMATION CENTER PLANNING
W. David Penniman *In* AGARD, Evaluating the Effectiveness of Information Centres and Services Sep. 1988 3 p (For primary document see N89-11625 02-82)
Copyright Avail: NTIS HC A05/MF A01

A business-oriented approach to information center planning and evaluation is presented. The need for output measures a quantitative expression of service value is described and a method of planning incorporating these concepts is provided. Both top-down and bottom-up planning responsibilities are identified and the specific steps involved in a business planning process are given. The competitive nature of information service is emphasized throughout.
Author

N89-11633# Los Alamos National Lab., N. Mex.
COMPUTERIZED CLASSIFIED DOCUMENT ACCOUNTABILITY
Connie B. Norris, ed. and R. Lewin, ed. Aug. 1988 19 p
(Contract W-7405-eng-36)
(DE88-015054; LA-11341) Avail: NTIS HC A03/MF A01

This step-by-step procedure was established as a guideline to be used with the Savvy PC Database Program for the accountability of classified documents. Its purpose is to eventually phase out the use of logbooks for classified document tracking. The program runs on an IBM PC or compatible computer using a Bernoulli Box, a Hewlett Packard 71B Bar Code Reader, an IOMEGA Host Adapter Board for creating mirror images of data for backup purposes, and the Disk Operating System (DOS). The DOS batch files IN and OUT invoke the Savvy Databases for either entering incoming or outgoing documents. The main files are DESTRUCTION, INLOG, OUTLOG, and NAME-NUMBER. The fields in the files are Adding/Changing, Routing, Destroying, Search-Print by document identification, Search/Print Audit by bar code number, Print Holdings of a person, and Print Inventory of an office.
DOE

N89-11634# Instituto de Pesquisas Espaciais, Sao Jose dos Campos (Brazil).
CONCERNING INTERFACES IN NATURAL LANGUAGES
Carlos Alberto deOliveira Aug. 1988 15 p In PORTUGUESE; ENGLISH summary Presented at the 2nd Brazilian Workshop on Simulation, Sao Jose dos Campos, Brazil, 1-2 Sep. 1988
(INPE-4681-PRE/1376) Avail: NTIS HC A03/MF A01

Requirements for natural language interfaces (NLI) are discussed. Also, answers are given to the question what is natural language, and considerations about known NLI are presented. Finally, a man-machine scheme focused on dynamic linguistic knowledge acquisition is suggested.
Author

N89-11401# Boeing Computer Services Co., Seattle, Wash.
AN INFORMAL GLOSSARY OF TERMS USED IN SUPERCOMPUTING, APPENDIX A
K. Neves *In* AGARD, Computational Fluid Dynamics: Algorithms and Super Computers Mar. 1988 7 p (For primary document see N89-11395 02-60)
Copyright Avail: NTIS HC A09/MF A01

83 ECONOMICS AND COST ANALYSIS

Includes cost effectiveness studies.

No abstracts in this category.

84 LAW, POLITICAL SCIENCE AND SPACE POLICY

Includes NASA appropriation hearings; aviation law; space law and policy; international law; international cooperation; and patent policy.

No abstracts in this category.

85 URBAN TECHNOLOGY AND TRANSPORTATION

Includes applications of space technology to urban problems; technology transfer; technology assessment; and surface and mass transportation.

For related information see also *03 Air Transportation and Safety, 16 Space Transportation,* and *44 Energy Production and Conversion.*

N89-11635# Office of Technology Assessment, Washington, D.C.
DEFENSE TECHNOLOGY BASE: INTRODUCTION AND OVERVIEW
Mar. 1988 122 p
(PB88-192562; OTA-ISC-374) Avail: NTIS HC A06/MF A01; also available SOD HC $5.00 as 052-003-01099-2 CSCL 05A

This special report is the first product of the OTA assessment, Maintaining the Defense Technology Base. It provides an overview of the subject, including specific concerns about the health of the defense technology base and the related issues before Congress. Concern centers on the health of those industries both defense-oriented and civilian, that provide the technology that ends up in defense systems, and on the management of the Defense Department's technology base programs and technology facilities.
GRA

N89-11636# Argonne National Lab., Ill.
TECHNOLOGY TRANSFER AT ARGONNE NATIONAL LABORATORY
R. T. Frost and G. J. Besio 1988 7 p Presented at the 1st World Congress on Superconductivity, Houston, Tex., 22 Feb. 1988 Prepared in cooperation with ARCH Development Corp., Argonne, Ill.
(Contract W-31-109-eng-38)
(DE88-012062; CONF-880210-3) Avail: NTIS HC A02/MF A01

The Technology Transfer Center is industry's pathway to Argonne. Through the Center, Argonne has established a number of prototype programs for forging alliances with industry, providing leadership among the national laboratories. Argonne has in place programs for cooperative research and development, industrial

residencies and staff exchanges, post doctoral appointments, contract research, patent licensing and joint ventures through the ARCH Development Corporation, research consortia, and educational outreach initiatives. Each of these programs is described briefly, with examples cited to illustrate implementation. All programs are relevant to the commercialization of superconductor technologies developed at Argonne. DOE

N89-11637*# National Aeronautics and Space Administration. Lewis Research Center, Cleveland, Ohio.
A PERSPECTIVE ON SPACE EXPLORATION TECHNOLOGY CATALYSIS: A RATIONALE FOR INITIATING 21ST CENTURY EXPANSION OF HUMAN CIVILIZATION INTO OUTER SPACE
Gary A. P. Horsham Oct. 1988 10 p
(NASA-TM-101362; E-4395; NAS 1.15:101362) Avail: NTIS HC A02/MF A01 CSCL 12A

The rationale for human exploration of space is examined. Observations of the technocatalytic potential are presented. Transferability to the terrestrial environment of 21st Century Earth is discussed. The many threats to future survival of this planet's sensitive ecosystem are also discussed in relation to the technoecological harmony that might be achievable due to the extreme demands that are naturally imposed on the development of (civilian/human) space technology. The human attempt to inhabit the inner solar system (the Moon, Mars, etc.) is proposed as the ultimate and most appropriate technology driver for the myriad of socioeconomic, ecological, and technological needs that will accompany 21st Century Earth societies. Author

88 SPACE SCIENCES (GENERAL)

N89-11638# European Space Agency, Paris (France).
SPACE SCIENCE AND FUNDAMENTAL PHYSICS
W. R. Burke, comp. May 1988 224 p Alpbach Summer School course held in Alpbach, Austria, 28 Jul.-7 Aug. 1987; sponsored by the Austrian Solar and Space Agency, ESA, CNES, DFVLR, and Schweizerische Naturforschend-Gesellschaft
(ESA-SP-283; ISSN-0379-6566; ETN-88-93157) Copyright Avail: NTIS HC A10/MF A01

Nuclear processes in the early Universe; observations on cosmic abundances of He4 and Li7, and comparison with primordial nucleosynthesis predictions; supernova 1987A in the Large Magellanic Cloud; space observatories for infrared and submillimeter astronomy; galaxy formation; VLBI from ground and space; a far-infrared astronomical observatory in Antarctica; physics and astrophysics of gravitational waves; the detection of gravitational radiation; experimental tests of relativity and gravitation; cosmological puzzles; unified theories and the early Universe; dark matter; proton decay experiment and neutrinos from supernova; fundamental science in ESA's space science program; and the next decades of space astronomy were discussed. For individual titles, see N89-11639 through N89-11655.

N89-11639# Commissariat a l'Energie Atomique, Gif-sur-Yvette (France). Inst. de Physique Fondamentale.
NUCLEAR PROCESSES IN THE EARLY UNIVERSE. PART 1: THE THERMAL HISTORY OF MATTER **c90**
Hubert Reeves *In* ESA, Space Science and Fundamental Physics May 1988 p 1-29 (For primary document see N89-11638 02-88)
Copyright Avail: NTIS HC A10/MF A01

The cosmological constant; cosmic densities; the expansion timescale; reaction timescales; primordial nucleosynthesis; nucleosynthetic yields; testing cosmological models; the Z particle; mass renormalization; and multidimensional models of the Universe are introduced. ESA

N89-11640# Commissariat a l'Energie Atomique, Gif-sur-Yvette (France). Inst. de Physique Fondamentale.
NUCLEAR PROCESSES IN THE EARLY UNIVERSE. PART 2: THE COSMIC QUARK-HADRON PHASE TRANSITION **c90**
Hubert Reeves *In* ESA, Space Science and Fundamental Physics May 1988 p 31-68 (For primary document see N89-11638 02-88)
Copyright Avail: NTIS HC A10/MF A01

The phase diagram for the hadronic (confined) phase of nuclear matter with nucleons and mesons, and the glue (deconfined) phase with quarks and gluons is discussed. Bag models of the nucleon; multidensity Universe; the quark-hadron butterfly, and the Li-7 trench; and the quark-lithium connection are considered. ESA

N89-11641# Observatoire de Paris-Meudon (France).
OBSERVATIONS ON COSMIC ABUNDANCE OF He4 AND Li7, COMPARISON WITH PRIMORDIAL NUCEOSYNTHESIS PREDICTIONS **c89**
Roger Cayrel *In* ESA, Space Science and Fundamental Physics May 1988 p 69-74 (For primary document see N89-11638 02-88)
Copyright Avail: NTIS HC A10/MF A01

Observations of He-4 in metal poor galaxies and of Li-7 in galactic subdwarfs were used to derive constraints on the initial abundances of the elements. An initial abundance of He-4 of 0.23 to 0.24 by mass, and an initial abundance of 10 to the minus 10th power by number of atoms for Li-7, with respect to hydrogen are obtained. These abundances are compatible with a hot big bang having a nucleons/photons ratio of about 2 to 5 times 10 to the minus 10th power, assuming 3 families of particles. ESA

N89-11642# European Southern Observatory, Garching (West Germany).
SUPERNOVA 1987A IN THE LARGE MAGELLANIC CLOUD **c90**
E. J. Wampler *In* ESA, Space Science and Fundamental Physics May 1988 p 75-80 (For primary document see N89-11638 02-88)
Copyright Avail: NTIS HC A10/MF A01

The status of our understanding of Supernova 1987A, the first visual supernova since 1604, is reviewed. Neutrino events, optical observations, and comparisons of theory and observations are discussed. ESA

N89-11643# Max-Planck-Inst. fuer Astronomie, Heidelberg (West Germany).
SPACE OBSERVATIONS FOR INFRARED AND SUBMILLIMETER ASTRONOMY **c89**
Dietrich Lemke *In* ESA, Space Science and Fundamental Physics May 1988 p 81-92 (For primary document see N89-11638 02-88)
Copyright Avail: NTIS HC A10/MF A01

The Infrared Astronomy Satellite, the infrared telescope on Spacelab, cryogenic telescopes, and the Infrared Space Observatory are described. The Cosmic Background Explorer, Hubble Space Telescope, Shuttle Infrared Telescope Facility, the Far Infrared and Submillimeter Telescope, and the Large Deployable Reflector are introduced. ESA

N89-11644# Aquila Univ. (Italy). Dipt. di Fisica.
GALAXY FORMATION: THEORY AND OBSERVATIONAL TESTS **c90**
Nicola Vittorio *In* ESA, Space Science and Fundamental Physics May 1988 p 93-104 (For primary document see N89-11638 02-88)
Copyright Avail: NTIS HC A10/MF A01

Use of observations for testing ideas on galaxy formation is introduced. Observations of the angular structure of the cosmic microwave background, the large scale peculiar velocity field, and large scale matter distribution, and gravitational instability are considered. How these observations can be used to constrain theoretical models is shown. ESA

N89-11645# Max-Planck-Inst. fuer Radioastronomie, Bonn (West Germany).
VERY LONG BASELINE INTERFEROMETRY (VLBI) FROM GROUND AND SPACE **c89**
E. Preuss *In* ESA, Space Science and Fundamental Physics May 1988 p 105-116 (For primary document see N89-11638 02-88)
Copyright Avail: NTIS HC A10/MF A01

Radio astronomy and very long base interferometry (VLBI) are introduced. Temporal and spatial coherence; VLBI imaging; high precision interferometry; areas of scientific impact (extragalactic radio sources, masers, continuum sources associated with stars, Earth rotation, crustal motion); and developments of VLBI are discussed. ESA

N89-11646# Rome Univ. (Italy). Dipt. di Fisica.
A FAR INFRARED ASTRONOMICAL OBSERVATORY IN ANTARCTICA **c89**
G. DallOglio, P. deBernardis, S. Masi, F. Melchiorri, and W. Pecorella *In* ESA, Space Science and Fundamental Physics May 1988 p 117-120 Sponsored by the Programma Nazionale Ricerche, Italy and the Italian Ministry of Public Education (For primary document see N89-11638 02-88)
Copyright Avail: NTIS HC A10/MF A01

The feasibility of a FIR observatory in Antarctica is discussed. The results of measurements of precipitable water vapor, atmospheric transmission and noise in the millimetric windows are given. Very good atmospheric conditions are found and it is concluded that Antarctica provides a unique oportunity for ground-based IR observations. ESA

N89-11647# Max-Planck-Inst. fuer Physik und Astrophysik, Garching (West Germany). Inst. fuer Astrophysik.
PHYSICS AND ASTROPHYSICS OF GRAVITATIONAL WAVES **c90**
Peter Kafka *In* ESA, Space Science and Fundamental Physics May 1988 p 121-130 (For primary document see N89-11638 02-88)
Copyright Avail: NTIS HC A10/MF A01

Quantitative arguments and simple formulas or rules of thumb which any physicist can apply to estimate the emission of gravitational waves from cosmic sources and their effect on detectors are reviewed. Two main antenna principles are sketched: mechanical oscillators, and interference of two beams of electromagnetic radiation. Proposals to use space equipment are mentioned. Two main expected types of signals in the frequency range 0.1 to 10 kHz are discussed: stellar core collapse (supernova) and final coalescence in compact binaries (chirp signal). Estimates of their rates and strength are confronted with the sensitivity of existing antennas and of the km-size laser interferometers being developed. ESA

N89-11648# Max-Planck-Inst. fuer Quantenoptik, Munich (West Germany).
THE DETECTION OF GRAVITATIONAL RADIATION **c90**
W. Winkler *In* ESA, Space Science and Fundamental Physics May 1988 p 131-139 (For primary document see N89-11638 02-88)
Copyright Avail: NTIS HC A10/MF A01

Gravitational wave antennas using bar and beam detectors are discussed. Sensitivity of room temperature bar detectors, and resonance detectors are reviewed. The sensitivity and noise sources of beam detectors are assessed. Antennas based on Doppler tracking of spacecraft are mentioned. ESA

N89-11649# Zurich Univ. (Switzerland). Inst. fuer Theoretische Physik.
EXPERIMENTAL TESTS OF RELATIVITY AND GRAVITATION **c77**
H. Herold *In* ESA, Space Science and Fundamental Physics May 1988 p 141-149 (For primary document see N89-11638 02-88)
Copyright Avail: NTIS HC A10/MF A01

The status of experimental and observational tests of gravitation theories, especially of general relativity, is reviewed. Assessment of tests of the foundations, i.e., special relativity, the constancy of the gravitational constant, and the equivalence principle, suggests that a viable theory of gravitation should be metric. The classical tests of general relativity, i.e., perihelion shift, light deflection, and time delay of light are reviewed within the PPN formalism. Experiments in space to improve results and to measure new effects are mentioned. The binary pulsar as a unique testing ground for gravitation theories is discussed. ESA

N89-11650# Max-Planck-Inst. fuer Physik und Astrophysik, Garching (West Germany).
COSMOLOGICAL PUZZLES **c90**
G. Boerner *In* ESA, Space Science and Fundamental Physics May 1988 p 151-155 (For primary document see N89-11638 02-88)
Copyright Avail: NTIS HC A10/MF A01

Problems with the standard model when confronted with grand unified theories are reviewed. The baryon-antibaryon asymmetry; the horizon problem of the Friedmann-Lemaitre model which would produce too many heavy monopoles, causing recollapse; the flatness problem of the density parameter; and the inflationary universe are discussed. Classical explanations of homogeneity and isotropy are summarized. ESA

N89-11651# Wisconsin Univ., Madison. Dept. of Physics.
UNIFIED THEORIES AND THE EARLY UNIVERSE
D. V. Nanopoulos *In* ESA, Space Science and Fundamental Physics May 1988 p 157-163 (For primary document see N89-11638 02-88)
(Contract DE-AC02-76ER-00881)
Copyright Avail: NTIS HC A10/MF A01

The interface between particle physics and cosmology, particularly inflationary cosmology, is reviewed. Grand unified theories (GUT) and Big Bang Cosmology (BBC) are discussed. The standard model of particle physics was extended to GUTs, super GUTs or possibly superstring theories, while the standard BBC was extended to contain the inflationary era. Inflation predicts omega = 1 and adiabatic, scale invariant energy density perturbations, which will be tested in experiment. Present experimental values are much smaller than one, but it seems that mass is being missed (better light), and there is dark matter that may close the Universe. Particle theory provides a list of candidates, e.g., photino, massive neutrino, axion, for dark matter and particle experimenters are building dark matter detectors to test these ideas. Developments in galaxy formation and observational developments on the large structure of the Universe, may put under severe test the ideas of scale-invariant energy density perturbations. ESA

N89-11652# Kapteyn Astronomical Lab., Groningen (Netherlands).
DARK MATTER **c90**
T. S. vanAlbada *In* ESA, Space Science and Fundamental Physics May 1988 p 165-176 (For primary document see N89-11638 02-88)
Copyright Avail: NTIS HC A10/MF A01

Methods that can be used to determine the total masses of galaxies and systems of galaxies, and of the results obtained are reviewed. Observations show that spiral galaxies are surrounded by invisible material. Dark matter is also present in systems of galaxies of various sizes. Its spatial distribution is related to the distribution of light. On small scales this follows from the symmetry of galaxy rotation curves. On the scale of clusters a relation is implied by the fact that the apex of the flow of galaxies around us lies in the Virgo cluster region. Moreover, the mass excess in the Virgo region deduced from the Virgocentric flow agrees with the mass of the Virgo cluster deduced from the virial theorem. Its density relative to the blue luminosity density increases with the size of the region under consideration. This follows from a comparison of individual galaxies and clusters of galaxies, and also from a comparison of compact groups and loose groups.

However, the density of dark matter relative to the density of all luminous matter does not appear to change markedly from one region to the other. It is not known whether large amounts of dark matter are present in regions where the number density of galaxies is low, in particular the voids. If not, the total density of matter in the Universe is one order of magnitude smaller than the critical density. ESA

N89-11653# Tokyo Univ. (Japan).
PROTON DECAY EXPERIMENT AND NEUTRINOS FROM SUPERNOVA (KAMIOKANDE-2) **c90**
M. Koshiba *In* ESA, Space Science and Fundamental Physics May 1988 p 177-192 (For primary document see N89-11638 02-88)
Copyright Avail: NTIS HC A10/MF A01

A proton decay detector (Kamiokande) consisting of 3000 tonnes of water and a Cerenkov counter was installed 1000 m underground, at 36.42 N, 137.31 E. It detected solar neutrino and supernova 1987A signals. The advantages of the imaging water Cerenkov method and developments of the counter are reviewed. ESA

N89-11654# European Space Agency, Paris (France).
FUNDAMENTAL SCIENCE IN ESA'S SPACE SCIENCE PROGRAM
R. M. Bonnet *In its* Space Science and Fundamental Physics May 1988 p 193-203 (For primary document see N89-11638 02-88)
Copyright Avail: NTIS HC A10/MF A01

European Space Agency missions involving fundamental science are presented. The dark mass problem and the origin of the X-ray background is tackled with the high throughout X-ray spectroscopy mission XMM; the direct measurement of the Hubble constant through the Sunyaev-Zel'dovich effect combining observations from XMM and from the far infrared submillimetric heterodyne spectroscopy mission; an independent check of the existence of massive neutrinos and of the theory of general relativity through helioseismology on board SOHO; and the evolution of our solar system, galaxy, and maybe of the Universe through the analysis of samples of pristine material extracted from the nucleus of a comet. ESA

N89-11655*# Cornell Univ., Ithaca, N.Y.
THE NEXT DECADES OF SPACE ASTRONOMY **c89**
Martin Harwit *In* ESA, Space Science and Fundamental Physics May 1988 p 205-209 Sponsored by NASA Prepared in cooperation with National Air and Space Museum, Washington, D.C. (For primary document see N89-11638 02-88)
Copyright Avail: NTIS HC A10/MF A01

Instrument capabilities, information sources, the history, and epistemology of space astronomy are reviewed. ESA

89 ASTRONOMY

Includes radio, gamma-ray, and infrared astronomy, and astrometry.

N89-11656 Yale Univ., New Haven, Conn.
COLOUR AND SPECTRAL SYNTHESIS OF DISK GALAXIES Ph.D. Thesis
Janet Midori Yamanaka 1987 192 p
Avail: Univ. Microfilms Order No. DA8801674

Models of integrated colors and spectra of disk galaxies are constructed and used to investigate the effect of the star formation history and the initial mass function on the observational properties of galaxies. The models are constructed using evolutionary synthesis techniques. The selection of the components comprising the stellar populations and the parameters of galactic evolution are presented and described. The difficulties and problems of synthesizing composite stellar systems that include very young populations are discussed. Variations of the synthetic broad band colors and line strengths are used to study different star formation scenarios and different forms of the initial mass function. Three different star formation histories are studied: an exponentially decreasing star formation rate, star formation that is cut off or truncated and bursts of star formation superimposed on an old, existing population. Three forms of the initial mass function are used in the models: a power law, a function with a single peak, and a bimodal function. The models are compared to observed nearby galaxies and to galaxies in the distant cluster Cl 1446+2619. Dissert. Abstr.

N89-11657*# National Aeronautics and Space Administration, Washington, D.C.
O STARS AND WOLF-RAYET STARS
Peter S. Conti, Anne B. Underhill, Stuart Jordan, ed., and Richard Thomas, ed. 1988 508 p Prepared in cooperation with Centre National de la Recherche Scientifique, Paris (France) (NASA-SP-497; NAS 1.21:497) Avail: SOD HC $24.00 as 033-000-01021-4; NTIS A01 CSCL 03A

Basic information is given about O and Wolf-Rayet stars indicating how these stars are defined and what their chief observable properties are. Part 2 of the volume discussed four related themes pertaining to the hottest and most luminous stars. Presented are: an observational overview of the spectroscopic classification and extrinsic properties of O and Wolf-Rayet stars; the intrinsic parameters of luminosity, effective temperature, mass, and composition of the stars, and a discussion of their viability; stellar wind properties; and the related issues concerning the efforts of stellar radiation and wind on the immediate interstellar environment are presented. B.G.

N89-11658 Washington Univ., Seattle.
NEW INSIGHTS INTO GLOBULAR CLUSTERS FROM MAIN SEQUENCE PHOTOMETRY Ph.D. Thesis
Michael John Bolte 1987 187 p
Avail: Univ. Microfilms Order No. DA8802193

CCD photometry of main sequence stars is presented for 4 globular clusters, NGC 288, NGC 362, NGC 6752, and NGC 7099. Analysis of B-V color distributions of stars on the main sequences of the clusters indicates a high degree of chemical homogeneity among the stars in a cluster. The most stringent limit is for the cluster NGC 362, for which an upper limit on the standard deviation of the (M/H) distribution of sigma = 0.08 dex is set. The incidence of photometrically detectable binary stars in NGC 362 and NGC 7099 is very low. In NGC 288 there appears to be a second sequence to the redward of the main sequence composed of 14 objects. This sequence is 0.75 mag above the main sequence and may be comprised of equal mass binary systems. Distances were determined to NGC 288, NGC 362, and NGC 7099 by fitting the lower main sequences of these clusters to the local subdwarfs using the recently revised parallax values and Lutz-Kelker corrections. Dissert. Abstr.

N89-11659# Bureau International de l'Heure, Paris (France).
[ACTIVITIES RELEVANT TO BIH ON TIME SCALES OR THE ROTATION OF THE EARTH AND TERRESTRIAL SYSTEMS] Annual Report, 1986
Jun. 1987 190 p Sponsored in part by UNESCO
Avail: NTIS HC A09/MF A01

The Bureau International de l'Heure (BIH) was defined in 1968 by the adoption of astronomical coordinates for a network of 68 optical instruments contributing to earth rotation monitoring. Starting with 1973, the series of Earth Rotation Parameters (ERP) obtained by space geodesy and interferometric techniques were progressively introduced in the maintenance of the direction of the axes of the BIH system. An explanation of the tables is given. B.G.

N89-11660 Harvard Univ., Cambridge, Mass.
LOW MASS X-RAY BINARIES IN GLOBULAR CLUSTERS AND HIERARCHICAL TRIPLE SYSTEMS Ph.D. Thesis
Charles David Bailyn 1987 312 p
Avail: Univ. Microfilms Order No. DA8806063

The relation is examined between low mass X-ray binaries

(LMXRBs) and other stars near them. Part 1 is concerned with LMXRBs in globular clusters. Chapter 1.1 describes the discovery of a candidate for the optical counterpart of the X-ray source in NGC6712, and other uses of the technique of color mapping in globular cluster cores. Chapter 1.2 discusses the formation of LMXRBs in globular clusters by tidal capture, and the subsequent evolution of these systems, and culminates with a detailed evolutionary scenario for both globular cluster LMXRBs (in M15 and NGC 6624) for which orbital periods are known. Chapter 1.3 presents evidence that faint blue horizontal branch stars in globular clusters are centrally concentrated which leads to a suggested formation mechanism for these stars related to that of LXMRBs. Chapter 1.4 forms a link between Parts 1 and 2, discussing the formation of hierarchical triple systems by binary-single star encounters. Part 2 explores the changes in mass transfer rate which would occur in a LMXRB in a hierarchical triple system because of the presence of the third star. Chapters 2.1-3 discuss the short term, long term, and tidally induced changed in the mass transfer rate respectively. Chapter 2.4 applies these considerations to four specific objects. A chapter on methods of numerical integration and stability of hierarchical triple systems is also included. Dissert. Abstr.

N89-11661*# Jet Propulsion Lab., California Inst. of Tech., Pasadena.
THE DEEP SPACE NETWORK: AN INSTRUMENT FOR RADIO ASTRONOMY RESEARCH
N. A. Renzetti, G. S. Levy, T. B. H. Kuiper, P. R. Wolken, and R. C. Chandlee 1 Sep. 1988 75 p
(Contract NAS7-918)
(NASA-CR-182744; JPL-Publ-82-68-Rev-1; NAS 1.26:182744)
Avail: NTIS HC A04/MF A01 CSCL 03A

The NASA Deep Space Network operates and maintains the Earth-based two-way communication link for unmanned spacecraft exploring the solar system. It is NASA's policy to also make the Network's facilities available for radio astronomy research. Three percent of Network time is currently reserved for radio astronomy observations. The Network's microwave communication systems and facilities are being continually upgraded. This revised document, first published in 1982, describes the Network's current radio astronomy capabilities and future capabilities to be made available by the ongoing Network upgrade. The Bibliography, which includes published papers and articles resulting from radio astronomy observations conducted with Network facilities, has been updated to include papers to May 1987. Author

N89-11662 Virginia Polytechnic Inst. and State Univ., Blacksburg.
MULTIPLE POPULATIONS ON THE HORIZONTAL BRANCH Ph.D. Thesis
Deborah Ann Crocker 1987 188 p
Avail: Univ. Microfilms Order No. DA8801157

A number of globular clusters have gaps in the distribution of stars on the horizontal branch. These gaps are not predicted by current theory. It is shown, that through reconstructed mass distributions, that the distribution of stars is clearly bimodal. In other words, that there are multiple populations of stars on the HB. Several theories were tested for their origin by placing the HB stars in the log T sub eff - log g plane. A number of the possible origins for the gap predict that the stars on the blue side of the gap should not lie along the extrapolation of the red sequence of stars. The log T sub eff - log g diagram was used to look for confirmation of the Y-Z anticorrelation hypothesized by Sandage. The gap clusters M15, NGC 288, and M92 were observed. In addition, M3, Mr, M14, and M92 were used to look for the Sandage shift. Between the two clusters which it was felt was better to use to look for the Sandage shift, M5 and M92, it was found that the difference in surface gravity at a given temperature is consistent with a value of zero at about the 1 sigma level. Dissert. Abstr.

N89-11663# Tokyo Univ. (Japan). Inst. of Space and Astronautical Science.
AN OXIDE PASSIVATED AND ION-IMPLANTED Si DETECTOR FOR X-RAY ASTRONOMY
T. Murakami, S. Takano, and M. Matsuoka (Institute of Physical and Chemical Research, Saitama, Japan) Nov. 1986 11 p
(ISAS-RN-353) Avail: NTIS HC A03/MF A01

The characteristics of an oxide passivated and ion-implanted Si detector are studied for applications in low energy X-ray astronomy in space. An energy resolution of 0.34 keV FWHM including amplifier noise was achieved at 5.9 keV using a cooled detector at -40 C with an effective area of 1 sq mm. This detector can be used without a heavy cooling system such as a liquid nitrogen cryostat on a satellite in near earth orbit. Author

N89-11664# Brown Univ., Providence, R. I. Dept. of Physics.
SUPERFLUID HELIUM AS A DARK MATTER DETECTOR
R. E. Lanou, H. J. Maris, and G. M. Seidel 1988 9 p Presented at the 8th Moriond Astrophysics Meeting on Dark Matter, Les Arcs, France, 6 Mar. 1988
(Contract DE-AC02-76ER-03130)
(DE88-012759; DOE/ER-03130/36C; CONF-8803113-6; COO-3130TC-36) Avail: NTIS HC A02/MF A01

The properties of liquid helium-four at temperatures in the vicinity of 100 mK suggest that it might be a suitable medium from which to construct a detector for certain types of dark matter. Among these properties are freedom from contaminants producing background and a high multiplicity of carriers (rotons) produced in energy deposition. It is suggested that there are processes available in helium which may permit discrimination between recoil nuclei and electrons of equal energy deposit. DOE

N89-11641# Observatoire de Paris-Meudon (France).
OBSERVATIONS ON COSMIC ABUNDANCE OF He4 AND LI7, COMPARISON WITH PRIMORDIAL NUCEOSYNTHESIS PREDICTIONS
Roger Cayrel *In* ESA, Space Science and Fundamental Physics May 1988 p 69-74 (For primary document see N89-11638 02-88)
Copyright Avail: NTIS HC A10/MF A01

N89-11643# Max-Planck-Inst. fuer Astronomie, Heidelberg (West Germany).
SPACE OBSERVATIONS FOR INFRARED AND SUBMILLIMETER ASTRONOMY
Dietrich Lemke *In* ESA, Space Science and Fundamental Physics May 1988 p 81-92 (For primary document see N89-11638 02-88)
Copyright Avail: NTIS HC A10/MF A01

N89-11645# Max-Planck-Inst. fuer Radioastronomie, Bonn (West Germany).
VERY LONG BASELINE INTERFEROMETRY (VLBI) FROM GROUND AND SPACE
E. Preuss *In* ESA, Space Science and Fundamental Physics May 1988 p 105-116 (For primary document see N89-11638 02-88)
Copyright Avail: NTIS HC A10/MF A01

N89-11646# Rome Univ. (Italy). Dipt. di Fisica.
A FAR INFRARED ASTRONOMICAL OBSERVATORY IN ANTARCTICA
G. DallOglio, P. deBernardis, S. Masi, F. Melchiorri, and W. Pecorella *In* ESA, Space Science and Fundamental Physics May 1988 p 117-120 Sponsored by the Programma Nazionale Ricerche, Italy and the Italian Ministry of Public Education (For primary document see N89-11638 02-88)
Copyright Avail: NTIS HC A10/MF A01

N89-11655*# Cornell Univ., Ithaca, N.Y.
THE NEXT DECADES OF SPACE ASTRONOMY
Martin Harwit *In* ESA, Space Science and Fundamental Physics May 1988 p 205-209 Sponsored by NASA Prepared

in cooperation with National Air and Space Museum, Washington, D.C. (For primary document see N89-11638 02-88)
Copyright Avail: NTIS HC A10/MF A01

90 ASTROPHYSICS

Includes cosmology; celestial mechanics; space plasmas; and interstellar and interplanetary gases and dust.
For related information see also *75 Plasma Physics.*

N89-11665# Los Alamos National Lab., N. Mex.
POTENTIAL FOAMS AND METAL FOILS FOR COSMIC DUST CAPTURE
Debra A. Wrobleski, Keith H. Abel, A. James Gray, and Joel M. Williams Jul. 1988 44 p
(Contract W-7405-eng-36)
(DE88-012960; LA-11271-MS) Avail: NTIS HC A03/MF A01

The scientific detection of cosmic dust particles will provide information about their astrophysical source and velocity. A suitable capture medium will preserve the particles in such a state (not necessarily the state just before capture) that their intrinsic chemical, mineral, and/or biological information can be determined. Foam and stacked, thin foil arrays provide the best current technology for effecting this capture. This paper presents physical and chemical data about a number of commercial and experimental foams and metal foils that could potentially be used to capture cosmic dust particles. The most promising foams are polystyrene-based: bead, extruded, and emulsion-polymerized. The most promising foils are those made of beryllium, aluminum, or gold. DOE

N89-11666# Brown Univ., Providence, R. I. Dept. of Physics.
INFLATION, COSMIC STRINGS AND GALAXY FORMATION
R. H. Brandenberger Nov. 1987 6 p Presented at the International Conference on Gravitation and Cosmology, Goa, India, 14 Dec. 1987
(Contract DE-AC02-76ER-03130)
(DE88-008629; BROWN/HET-644; CONF-871286-1) Avail: NTIS HC A02

Inflationary universe models and the cosmic string theory provide two district ways to explain the origin of inhomogeneities in the universe on large scales. The two mechanisms for the origin of galaxies and clusters of galaxies are summarized and compared, and some recent results on galaxy formation with hot dark matter and cosmic stings are mentioned. DOE

N89-11667# Tokyo Univ. (Japan). Inst. of Space and Astronautical Science.
INTERPLANETARY MAGNETIC MICROSTRUCTURE OBSERVED BY SAKIGAKE NEAR ITS CLOSEST APPROACH TO COMET HALLEY
Tomoko Nakagawa, Takao Saito, Kiyohumi Yumoto, and Kunio Hirao (Tokai Univ., Kanagawa, Japan) [1986] 19 p
(ISAS-RN-349) Avail: NTIS HC A03/MF A01

Interplanetary magnetic structures at 7 x 10 to the 6th km upstream from Comet Halley were observed by Sakigake on 11 March, 1986. IMF variations associated with multiple crossings of the heliospheric neutral sheet were detected on the same day. Two peculiar regions were found to exist near the neutral sheet, i.e., (1) a region where anomalously many tangential and no discontinuities occurred, and (2) a region where rotational discontinuities occurred predominantly. The field intensity was weak and changed easily in the former region, while it was steady and strong in the latter region. Author

N89-11668# California Univ., Berkeley. Lawrence Berkeley Lab.
ASTROPHYSICAL EVIDENCE ON THE EQUATION OF STATE
N. K. Glendenning 3 Jun. 1988 6 p Presented at the International Conference on Contemporary Topics in Nuclear Structure Physics, Cocoyoc, Mexico, 9 Jun. 1988
(Contract DE-AC03-76SF-00098)
(DE88-011960; LBL-25375; CONF-880639-1) Avail: NTIS HC A02/MF A01

The current situation concerning supernova simulations and the theory of neutron star structure are studied with respect to what they tell about the equation of state. A new mechanism that could help power supernovae is suggested. DOE

N89-11669 Howard Univ., Washington, D. C.
STOCHASTIC THEORY OF FREQUENCY REDISTRIBUTION IN TWO-PHOTON PROCESSES Ph.D. Thesis
Oyekale Oyedeji 1987 101 p
Avail: Univ. Microfilms Order No. DA8807167

The effect of a stochastic microfield on two photon processes is calculated. The redistribution function for an optically active system of two and three levels in interaction with a thermal bath of perturbers is calculated. The external perturbations are treated as random modulations acting on the system in question. This is modeled by using the Model Microfield Method (MMM) as proposed by Brissaud and Frisch. New expressions are obtained for the redistribution function in Raman scattering, fluorescence and two photon absorption which are useful in the analysis of redistribution experiments in dilute gases. The MMM, though phenomenological in nature, allows the physical basis of the effects to be emphasized. Two types of stochastic interactions are considered. First, a simple random mixing of a two state bath is studied in Raman scattering to illustrate the effect of a discrete perturbation. Second, velocity changing collisions in the strong collision model are considered which illustrates the effect of perturbation variables with a continuous range. Dissert. Abstr.

N89-11670 Harvard Univ., Cambridge, Mass.
SHOCKED INTERSTELLAR GAS IN DENSE MOLECULAR CLOUDS Ph.D. Thesis
David Anthony Neufeld 1987 274 p
Avail: Univ. Microfilms Order No. DA8806114

Shock waves are a ubiquitous phenomenon in the interstellar medium which may heat, compress, ionize and dissociate interstellar gas. Following a brief review of previous theoretical work on the interaction of shock waves and dense molecular clouds, a new treatment is presented of the physical and chemical processes that come into play when a fast, dissociative shock wave encounters dense molecular gas. The reformation is followed of molecules in the cooling gas behind such a shock, and how fast molecular shock may be recognized and characterized by the radio and infrared radiation that they emit is discussed. It was found that emission from high J rotational states of SiO and from vibrationally excited states of OH(+) and HeH(+) may prove useful diagnostics of fast shock activity, and a treatment is presented, tailored to astrophysical applications, of the process of electron impact excitation of molecular ion to vibrationally excited states. In comparing line strengths predicted by the dissociative model with existing observations of the shocked gas region in Orion KL, it was found that the presence of a dissociative shock is neither ruled out nor convincingly required by the observations. Dissert. Abstr.

N89-11671*# Smithsonian Astrophysical Observatory, Cambridge, Mass.
MOLECULAR PROCESSES IN COMETS Semiannual Progress Report No. 21, 1 Jan. - 30 Jun. 1988
A. Dalgarno Sep. 1988 9 p
(Grant NsG7-421)
(NASA-CR-182742; NAS 1.26:182742; SAPR-21) Avail: NTIS HC A02/MF A01 CSCL 03B

The transition dipole moments of the c 3 Pi u - a 3 Sigma g +, i 3 Pi g - c 3 Pi u, and i 3 Pi g - b 3 Sigma u + transitions of molecular hydrogen were calculated over a wide range of internuclear distances R. Calculations of the emission spectra are nearing completion. Substantial progress was made in the calculation of the absorption coefficient of a colliding pair of hydrogen atoms in the binary encounter approximation. Detailed calculations were performed on the continuum emission arising

from the excitation of the a 3 sigma g + state of H2 by the impact of electrons of various energies. Each curve is labelled by the electron energy in electron volts. The strong emission near Lyman alpha is interesting in that it is produced by excitation of molecular hydrogen. Author

N89-11672# International Centre for Theoretical Physics, Trieste (Italy).
INHOMOGENEITIES IN A FRIEDMANN UNIVERSE
Gerald E. Tauber Aug. 1987 7 p
(DE88-702981; IC-87/267) Avail: NTIS (US Sales Only) HC A02/MF A01

One of the outstanding problems in cosmology is the growth of inhomogeneities, which are characterized by an anisotropic pressure and density distribution. Following a method developed by McVittie (1967, 1968) it has been possible to find time-dependent spherically symmetric solutions of Einstein's field equations containing an arbitrary pressure and density distribution which connect smoothly to a Friedmann universe for any desired equation of state. DOE

N89-11673*# Fermi National Accelerator Lab., Batavia, Ill.
ON RELATIVE SUPERNOVA RATES AND NUCLEOSYNTHESIS ROLES
W. David Arnett, David N. Schramm, and James W. Truran (Illinois Univ., Chicago.) Aug. 1988 10 p Prepared in cooperation with Arizona Univ., Tucso n Sponsored in part by NASA, NSF and DOE
(NASA-CR-183373; NAS 1.26:183373; FERMILAB-Pub-88/118-A) Avail: NTIS HC A02/MF A01

It is shown that the Ni-56-Fe-56 observed in SN 1987A argues that core collapse supernovae may be responsible for more that 50 percent of the iron in the galaxy. Furthermore it is argued that the time averaged rate of thermonuclear driven Type I supernovae may be at least an order of magnitude lower than the average rate of core collapse supernovae. The present low rate of Type II supernovae (below their time averaged rate of approx. 1/10 yr) is either because the past rate was much higher because many core collapse supernovae are dim like SN 1987A. However, even in this latter case they are only an order of magnitude dimmer that normal Type II's due to the contribution of Ni-56 decay to the light curve. Author

N89-11674*# Fermi National Accelerator Lab., Batavia, Ill.
PHASE TRANSITIONS AS THE ORIGIN OF LARGE SCALE STRUCTURE IN THE UNIVERSE
Neil Turok Aug. 1988 57 p Sponsored in part by NASA, and by DOE
(NASA-CR-183359; NAS 1.26:183359; FERMILAB-Conf-88/116-A) Avail: NTIS HC A04/MF A01 CSCL 03B

A review of the formation of large scale structure through gravitational growth of primordial perturbations is given. This is followed by a discussion of how symmetry breaking phase transitions in the early universe might have produced the required perturbations, in particular through the formation and evolution of a network of cosmic strings. Finally, the statistical mechanics of string networks, for both cosmic and fundamental strings is discussed, leading to some more speculative ideas on the possible role of fundamental strings (superstrings or heterotic strings) in the very early universe. Author

N89-11675*# Fermi National Accelerator Lab., Batavia, Ill.
PHOTOEROSION AND THE ABUNDANCES OF THE LIGHT ELEMENTS
Richard N. Boyd, Gary J. Ferland, and David N. Schramm (Chicago Univ., Ill.) Aug. 1988 15 p Prepared in cooperation with Lawrence Livermore National Lab., Calif.
(Grants NSF PHY-86-00749; NSF AST-85-22213)
(NASA-CR-183372; NAS 1.26:183372; FERMILAB-Pub-88/132-A) Avail: NTIS HC A03/MF A01

The abundances of the rare light elements H-2, He-3, Li-7, and B-11 are shown to be potentially affected by photoerosion. That process, involving the interaction of high energy photons from galactic centers with atomic nuclei, will increase the abundances of H-2, He-3, and B-11 while lowering slightly those of Li-7 and He-4. In some regions of galaxies the effects may be large enough to impact their chemical evolution. In particular this process may have enhanced the H-2 and He-3 abundances near the center of our galaxy over and above those from the big bang, as well as the galactic B-11 abundance over that from cosmic-ray spallation. Author

N89-11676# Air Force Inst. of Tech., Wright-Patterson AFB, Ohio.
THREE PROBABLE STELLAR MASS BLACK HOLES M.S. Thesis
Dale W. Fry 1988 62 p
(AD-A196976; AFIT/CI/NR-88-111) Avail: NTIS HC A04/MF A01 CSCL 03B

According to the theory of general relativity, a spherically symmetric self-gravitating body whose radius/mass ratio in Schwarzchild coordinates decreases to the critical value of 2 must collapse to a point singularity. Such an object is termed a black hole, since out to a characteristic radius known as the event horizon, not even photons can escape its strong gravitational field. It has been postulated that such a field could serve to compress and heat accreting gas, which would then emit soft X-rays, signalling the black hole's presence. One accretion model is that of a black hole in binary orbit with a normal luminous star which is ejecting part of its mass, some of which is captured by the companion black hole and emits X-rays before disappearing inside the event horizon. Objects consisting of degenerate nuclear matter known as neutron stars, and whose existence has been well established, could also serve as the X-ray companion in such a system. One way to distinguish between a neutron star and a black hole is to measure their mass, for if causality is to be preserved, a neutron star cannot exceed about 3 solar masses, while the mass of the black hole is arbitrary. A lower limit on the mass of X-ray emitter in a binary system can be determined if the orbital period, projected orbital velocity, and mass or radius of the luminous companion star can be measured via conventional astronomical methods. GRA

N89-11639# Commissariat a l'Energie Atomique, Gif-sur-Yvette (France). Inst. de Physique Fondamentale.
NUCLEAR PROCESSES IN THE EARLY UNIVERSE. PART 1: THE THERMAL HISTORY OF MATTER
Hubert Reeves *In* ESA, Space Science and Fundamental Physics May 1988 p 1-29 (For primary document see N89-11638 02-88)
Copyright Avail: NTIS HC A10/MF A01

N89-11640# Commissariat a l'Energie Atomique, Gif-sur-Yvette (France). Inst. de Physique Fondamentale.
NUCLEAR PROCESSES IN THE EARLY UNIVERSE. PART 2: THE COSMIC QUARK-HADRON PHASE TRANSITION
Hubert Reeves *In* ESA, Space Science and Fundamental Physics May 1988 p 31-68 (For primary document see N89-11638 02-88)
Copyright Avail: NTIS HC A10/MF A01

N89-11642# European Southern Observatory, Garching (West Germany).
SUPERNOVA 1987A IN THE LARGE MAGELLANIC CLOUD
E. J. Wampler *In* ESA, Space Science and Fundamental Physics May 1988 p 75-80 (For primary document see N89-11638 02-88)
Copyright Avail: NTIS HC A10/MF A01

N89-11644# Aquila Univ. (Italy). Dipt. di Fisica.
GALAXY FORMATION: THEORY AND OBSERVATIONAL TESTS
Nicola Vittorio *In* ESA, Space Science and Fundamental Physics May 1988 p 93-104 (For primary document see N89-11638 02-88)
Copyright Avail: NTIS HC A10/MF A01

N89-11647# Max-Planck-Inst. fuer Physik und Astrophysik, Garching (West Germany). Inst. fuer Astrophysik.
PHYSICS AND ASTROPHYSICS OF GRAVITATIONAL WAVES
Peter Kafka *In* ESA, Space Science and Fundamental Physics May 1988 p 121-130 (For primary document see N89-11638 02-88)
Copyright Avail: NTIS HC A10/MF A01

N89-11648# Max-Planck-Inst. fuer Quantenoptik, Munich (West Germany).
THE DETECTION OF GRAVITATIONAL RADIATION
W. Winkler *In* ESA, Space Science and Fundamental Physics May 1988 p 131-139 (For primary document see N89-11638 02-88)
Copyright Avail: NTIS HC A10/MF A01

N89-11650# Max-Planck-Inst. fuer Physik und Astrophysik, Garching (West Germany).
COSMOLOGICAL PUZZLES
G. Boerner *In* ESA, Space Science and Fundamental Physics May 1988 p 151-155 (For primary document see N89-11638 02-88)
Copyright Avail: NTIS HC A10/MF A01

N89-11652# Kapteyn Astronomical Lab., Groningen (Netherlands).
DARK MATTER
T. S. vanAlbada *In* ESA, Space Science and Fundamental Physics May 1988 p 165-176 (For primary document see N89-11638 02-88)
Copyright Avail: NTIS HC A10/MF A01

N89-11653# Tokyo Univ. (Japan).
PROTON DECAY EXPERIMENT AND NEUTRINOS FROM SUPERNOVA (KAMIOKANDE-2)
M. Koshiba *In* ESA, Space Science and Fundamental Physics May 1988 p 177-192 (For primary document see N89-11638 02-88)
Copyright Avail: NTIS HC A10/MF A01

91 LUNAR AND PLANETARY EXPLORATION

Includes planetology; and manned and unmanned flights. For spacecraft design or space stations see *18 Spacecraft Design, Testing and Performance.*

N89-11677 Arizona State Univ., Tempe.
A COMPARATIVE PLANETOLOGICAL STUDY OF PARTICLE SPEED AND CONCENTRATION DURING AEOLIAN SALTATION Ph.D. Thesis
Steven Hamilton Williams 1987 170 p
Avail: Univ. Microfilms Order No. DA8802798

Aeolian gradation is important on any planetary surface possessing loose particulate material and winds of sufficient strength to initiate motion. The mode of aeolian transport with the greatest potential for geologic alteration is saltation, where sand-sized particle bounce along the surface. The relative contributions of particle concentration and particle speed to saltation flux for a wide range of environmental conditions is determined, the saltation flux predictions of previous investigators to non-terrestrial conditions are extrapolated, the range of environmental conditions over which those predictions remain valid is determined, and the nature and consequences of aeolian activity on other planets is assessed. Flux predictions developed for terrestrial saltation were found to be valid for a narrower range of wind speeds on Mars and Venus than in the terrestrial case.
Dissert. Abstr.

N89-11678*# Iowa Univ., Iowa City. Dept. of Physics and Astronomy.
WAVE-PARTICLE INTERACTIONS IN THE MAGNETOSPHERE OF URANUS
W. S. Kurth, D. A. Gurnett, F. L. Scarf, and F. V. Coroniti (California Univ., Los Angeles.) Jul. 1988 75 p
(Contracts JPL-957723; JPL-957805)
(NASA-CR-183299; NAS 1.26:183299; UI-88-13) Avail: NTIS HC A04/MF A01 CSCL 03B

The Voyager 2 encounter of Uranus has provided observations of plasma waves in and near the magnetosphere. These data, while the first from Uranus, will also be the only direct information on wave-particle interactions at this planet for many years to come. The observations include electrostatic waves upstream of the bow shock, turbulence in the shock, Bernstein emissions and whistler mode waves in the magnetosphere, broadband electrostatic noise in the magnetotail, and a number of the other types of plasma waves which have yet to be clearly identified. Each of these types of waves exist in a plasma environment which both supports the growth of the waves and is modified by interactions with the waves. Wave-particle interactions provide the channels through which the waves can accelerate, scatter, or thermalize the plasmas. The most spectacular example in the case of Uranus is the extremely intense whistler mode activity in the inner magnetosphere which is the source of strong pitch angle diffusion. The resulting electron precipitation is sufficient to produce the auroral emissions observed by Voyager. The strong diffusion, however, presents the problem of supplying electrons in the range of 5 to 40 keV in order to support the losses to the atmosphere.
Author

N89-11679# Academy of Sciences of the Ukrainian SSR, Kharkov.
DECAMETRIC RADIO EMISSION OF JUPITER. PART 3: SOME PHYSICAL CHARACTERISTICS OF S-COMPONENT SOURCES
B. P. Ryabov 1987 48 p In RUSSIAN; ENGLISH summary
(DE88-702812; INIS-SU-35) Avail: NTIS (US Sales Only) HC A03/MF A01

The results of recent observations of Jupiter at 10 to 23 MHz have been used to determine active (with respect to S-bursts) portions in the Northern and Southern trajectories of the Io's tube foot. As has been found, S-bursts are generated by a source inside Io's tube continuously as long as the tube foot remains within the active portions of the trajectory.
DOE

N89-11680 Kent Univ., Canterbury (England).
DUST DETECTION SYSTEMS FOR COMETARY ENCOUNTER Ph.D. Thesis
Graham Cecil Evans 1987 273 p
Avail: Univ. Microfilms Order No. BRDX80034

During its 1986 apparition, Comet Halley was met by five spacecraft from different international agencies. ESA's Giotto probe achieved a 605 km fast flyby of Halley's nucleus on 14 March 1986 at a relative velocity of 68 km/sec; it carried ten scientific experiments to examine the cometary environment. The concept, design to proposal stage, system rationale and development and operation of the Giotto Dust Impact Detection System, DIDSY, is described. It was used during the first exploration of a cometary nucleus and survived the encounter with minimal damage.
Dissert. Abstr.

N89-11681# Los Alamos National Lab., N. Mex.
EXTRACTION OF LIGHT GASSES FROM MARS OR ITS MOONS
David Vaniman 1988 12 p Presented at the SPACE Conference, Albuquerque, N. Mex., 29 Aug. 1988
(Contract W-7405-eng-36)
(DE88-009123; LA-UR-88-1282; CONF-880843-3) Avail: NTIS HC A03/MF A01

The light elements H, C, N, O and S are important for propellant production and life support in space. These light elements occur on Mars, and may occur on the martian moons Phobos and Deimos, in forms that would allow their collection as gasses. The martian north pole apparently contains large amounts (approximately 10

to the 13th MT) of H2O but has not been probed or sampled. The martian atmosphere is relatively well known; a MW-scale plant could produce 1000 MT of O2 per earth-year by dissociation of CO2 from the martian atmosphere. A plant of about 3 MW power might produce 1000 MT of H2 plus O2 per earth-year by extracting and dissociating water from the martian moons (if they are chondritic), but more data and process development are needed before such a plant can be considered with certainty. DOE

N89-11682# Los Alamos National Lab., N. Mex.
PLANETARY SKIN GAMES
D. T. Vaniman and R. C. Reedy 1988 6 p Presented at the GEOTIMES: 19th Lunar and Planetary Science Conference, Houston, Tex., 14 Mar. 1988
(Contract W-7405-eng-36)
(DE88-009161; LA-UR-88-1264; CONF-880391-1) Avail: NTIS HC A02/MF A01

An informal review of techniques for analysis of meteorites and materials from the lunar surface is presented. Attention is given to problems associated with the production rates of cosmogenic nuclides. DOE

92 SOLAR PHYSICS

Includes solar activity, solar flares, solar radiation and sunspots.

For related information see *93 Space Radiation.*

N89-11683# Los Alamos National Lab., N. Mex. Theoretical Div.
PARTICLE PHYSICS CANDIDATES FOR THE COSMION SOLUTION TO THE SOLAR NEUTRINO PROBLEM
Stuart Raby 1988 18 p Presented at the 23rd Rencontre de Moriond Conference: Electroweak Interactions and Unified Theories, Les Arcs, France, 6 Mar. 1988
(Contract W-7405-eng-36)
(DE88-014479; LA-UR-88-1741; CONF-8803109-6) Avail: NTIS HC A03/MF A01

This paper discusses several particle physics candidates for the cosmic solution to the solar neutrino problem. Some of these candidates are: Cold dark matter; No conserved particle number; Conserved particle number but no cosmic asymmetry; and Conserved particle number and a cosmic asymmetry. Also outlined are their properties and methods of detecting them. DOE

N89-11684# Stanford Univ., Calif. Center for Space Science and Astrophysics.
CORONAL MAGNETIC FIELDS PRODUCED BY PHOTOSPHERIC SHEAR
James A. Klimchuk, Peter A. Sturrock, and Wei-Hong Yang (Utah State Univ., Logan.) Apr. 1988 41 p
(Contract N00014-85-K-0111)
(AD-A194591; CSSA-ASTRO-87-17) Avail: NTIS HC A03/MF A01 CSCL 03B

The magneto-frictional method for computing force-free fields examines the evolution of the magnetic field of a line dipole, when there is relative shearing motion between the two polarities. The energy of the sheared field can be arbitrarily large compared with the potential field. It is possible to fit the magnetic energy, as a function of shear amplitude, by a simple functional form. The fit parameters depend only on the distribution of normal field in the photosphere and the form of the shearing displacement. The energy is relatively more enhanced if the shear occurs: (1) where the normal field is strongest; (2) in the inner region of the dipole, near the axis; or (3) over a large fraction of the dipole area. GRA

93 SPACE RADIATION

Includes cosmic radiation; and inner and outer earth's radiation belts.

For biological effects of radiation see *52 Aerospace Medicine.* For theory see *73 Nuclear and High-Energy Physics.*

N89-11685# Los Alamos National Lab., N. Mex.
THE HISTORY OF GAMMA-RAY BURST OBSERVATIONS
R. W. Klebesadel 1988 24 p Presented at the International Symposium on the Physics of Neutron Stars and Black Holes, Tokyo, Japan, 1 Feb. 1988
(Contract W-7405-eng-36)
(DE88-014390; LA-UR-88-2403; CONF-880297-1) Avail: NTIS HC A03/MF A01

Cosmic gamma-ray bursts have been observed for 1-1/2 decades since their fortuitous discovery by nuclear test detection instruments flown on the Vela satellites. Although the volume and detail of data available through these observations has considerably refined our knowledge of the characteristics of these events, there is no confident identification of source objects or reliable model of the processes involved. The observations do suggest, however, that the bursts originate at neutron stars (probably highly-magnetized neutron stars). DOE

N89-11686*# National Aeronautics and Space Administration. Goddard Space Flight Center, Greenbelt, Md.
AN ALL SKY STUDY OF FAST X-RAY TRANSIENTS Ph.D. Thesis
Alanna Connors (Maryland Univ., College Park.) Apr. 1988 322 p
(NASA-TM-89716; Rept-88-014; NAS 1.15:89716) Avail: NTIS HC A14/MF A01 CSCL 03B

In the HEAO 1 A-2 survey of fast X-ray transients, a search of 2 to 20 keV scanning data was made for brief increases in flux, greater than 4 millicrabs, on timescales approximately 1 to 10 to the 4th s above a 12-hour average. The search was divided into two regions, and all-sky survey of the Galaxy, and a survey of the Magellanic Clouds. In the latter, 37 events were found and identified with 4 of the 5 brighest sources in the LMC, plus 2 as flares from a foreground star. Np X-ray bursts, no gamma-ray bursts, and no events from the SMC were found. In the all-sky survey, after excluding well-known variable sources, out of the equivalent of approximately 104 days of data, 15 events were found which falling into 2 broad categories: flares from coronal sources, roughly isotropically distributed, with optically thin thermal spectra; and harder fast transients apparently distributed near the Galactic plane. The first were identified as flares from ubiquitous active cool dwarf stars. It was hypothesized that the second may have been from distant Be-neutron star binaries. However, at least two of the harder, more luminous events remained unidentified. Future research should examine the nature of these rare events, and how they may fit into a hierarchy of hard fast transients from gamma-ray bursts to outbursts from pulsar systems. Author

99 GENERAL

N89-11687# Office of Naval Research Liaison Office, Far East, APO, San Francisco, Calif.
ONR FAR EAST SCIENTIFIC BULLETIN, VOLUME 12, NO. 4, OCTOBER - DECEMBER 1987
George B. Wright and Sandy Kawano, ed. Dec. 1987 101 p Prepared in cooperation with Air Force Office of Scientific Research Liaison Office, Far East, APO and Army Research Office Liaison Office, Far East, APO, San Francisco, Calif.
(AD-A194338; NAVSO-P-3580-Vol-12-No-4; ISSN-0271-7077)
Avail: NTIS HC A06/MF A01

This is a quarterly publication presenting articles covering recent developments in Far Eastern (particularly Japanese) scientific research. It is hoped that these reports (which do not constitute

part of the scientific literature) will prove to be of value to scientists by providing items of interest well in advance of the usual scientific publications. The articles are written primarily by members of the staff of ONR Far East, the Air Force Office of Scientific Research, and the Army Research Office, with certain reports also being contributed by visiting stateside scientists. Occasionally, a regional scientist will be invited to submit an article covering his own work, considered to be of special interest. Author

N89-11688# Max-Planck-Inst. fuer Extraterrestrische Physik, Garching (West Germany). Inst. for Extraterrestrische Physik.
[ACTIVITY REPORT OF THE MAX-PLANCK-INSTITUT FUER PHYSIK UND ASTROPHYSIK] [TAETIGKEITSBERICHT 1986]
Jan. 1987 116 p In FRENCH
(MPE-200; ISSN-0173-699X) Avail: NTIS HC A06/MF A01

The 1986 Progress Report of the Max Planck Institute for Physics and Astrophysics (Intstitute for Extraterrestrial Physics) lists the following four areas of major research: (1) the Galactic Center; (2) the variable neutron star Her-X-1; (3) deterministic chaos and nonlinear dynamics; and (4) source of the cosmic 1.8 MeV gamma line spectra of radioactive Ai-26. This research is being supported by the ROSAT X-ray satellite, two experiments aboard the GRO Cosmic Ray Observatory (NASA), an experiment aboard the ESA Ulysses Mission, and by participation in the activity of the CRRES plasma-wave satellite (NASA). Author

Typical Subject Index Listing

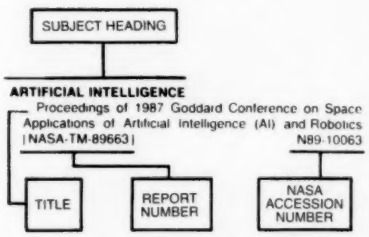

The subject heading is the key to the subject content of the document. Titles, report numbers, and accession numbers of pertinent documents are provided under each subject heading. When the title is insufficiently descriptive of the document content, a title extension has been added, separated from the title by three hyphens. The report number helps to indicate the type of document cited (e.g., NASA report, NASA translation, NASA contractor report). The NASA accession number is the number by which the document abstracts are arranged in this journal and by which the document is sold or requested. The titles, with title extensions if present, are arranged under each subject heading in ascending accession number order. The subject headings have been selected from the latest revision of the *NASA Thesaurus* (NASA SP-7064).

A

A STARS
O stars and Wolf-Rayet stars
[NASA-SP-497] N89-11657

ABRASION
A novel approach to abrasion resistance
[DE88-014180] N89-10949
Influence of martensitic phase in abrasion behaviour of stainless steel 304 L
[DE88-702770] N89-11009

ABRASION RESISTANCE
A novel approach to abrasion resistance
[DE88-014180] N89-10949

ABSORPTION SPECTRA
A differential absorption spectrometer for determining flash X-ray spectra from 10 to 2000 keV
[DE88-014844] N89-10979

ABSORPTIVITY
Development of a semi-empirical model for estimating the global solar radiation
[INPE-4620-TDL/328] N89-11352

ABUNDANCE
Observations on cosmic abundance of He4 and Li7, comparison with primordial nuceosynthesis predictions N89-11641
Photoerosion and the abundances of the light elements
[NASA-CR-183372] N89-11675

ACCELERATED LIFE TESTS
Methodology of flexural fatigue testing composite materials produced by electron-beam evaporation N89-11003

ACCURACY
Accuracy analysis of the semi-analytical method for shape sensitivity analysis N89-10848
Continuous deformation monitoring with GPS
[AD-A196447] N89-10886
Precision-time tradeoffs: A paradigm for processing statistical queries on databases
[DE88-012024] N89-11408

ACID RAIN
Control of environment assisted cracking of Al 7075 using inhibitors
[AD-A196387] N89-11022
Markers of air pollution in forests: Nutrient cycling
[DE88-011011] N89-11319
Review of acid rain models for Europe
[DE88-011945] N89-11322
Acid precipitation in North America: 1985 annual and seasonal data summaries from Acid Deposition System data base
[DE88-013563] N89-11325

ACOUSTIC ATTENUATION
The development of prototype absorbers with variable characteristics
[BBC-RD-1988/5] N89-11492

ACOUSTICS
Thermodynamic improvements for the space thermoacoustic refrigerator (STAR)
[AD-A196958] N89-11071

ACRYLIC RESINS
Damage effects on thin acrylic targets caused by infrared radiation from a pulsed carbon dioxide laser
[AD-A196385] N89-11216

ACRYLONITRILES
Carbon films derived from poly(acrylonitrile): Oxidation, electrical properties, and processing
[DE88-010352] N89-10950

ACTIVATION
Kinetics of boron hydride interconversion reactions
[AD-A196824] N89-10985

ACTIVATION ENERGY
The catalytic, structural, and electronic properties of strained-metal overlayers
[DE88-007932] N89-11013

ADA (PROGRAMMING LANGUAGE)
Object oriented software engineering with Ada
[CNES-CT/DTI/MS/MN/326] N89-11426

ADAPTIVE CONTROL
Bandwidth compression for HDTV broadcasting: Investigation of some adaptive subsampling strategies
[BBC-RD-1988/9] N89-11101
On motion planning and control of multi-link lightweight robotic manipulators
[NASA-CR-181226] N89-11234
Ultrasonic flaw classification: An approach using modeling, signal processing, and adaptive learning N89-11248
Practical applications and limitations of adaptive control N89-11442

ADAPTIVE FILTERS
Adaptive filtering algorithms for communications signal processing
[PD-SE-8808] N89-11410

ADDITIVES
The effect of carbon and boron nitride additions on the fracture toughness of Si3N4
[DE88-013249] N89-11025
Structural anomalies in undoped Gallium Arsenide observed in high resolution diffraction imaging with monochromatic synchrotron radiation
[NASA-CR-183268] N89-11595

ADEQUACY
Quasi-adequate semigroups
[DE88-703157] N89-11466

ADSORPTION
Theory of oxygen ordering and absorption in 1,2,3 high-T(sub c) superconductors
[DE88-007543] N89-11575

ADVECTION
Estimating evapotranspiration of an irrigated surface from upwind and downwind vertical profiles of temperature and humidity
[AD-A196409] N89-11375

AEOLIAN TONES
A comparative planetological study of particle speed and concentration during aeolian saltation N89-11677

AERIAL EXPLOSIONS
Explosion airblast predictions on a personal computer and application to the Henderson, Nevada incident
[DE88-014991] N89-11144

AERIAL PHOTOGRAPHY
CIR aerial photography applied to the evaluation of the air pollution impact in a tropical forest: The case of Cubatao, Brazil
[INPE-4651-PRE/1358] N89-11324

AERIAL RECONNAISSANCE
Tropical cyclone observation and forecasting with and without aircraft reconnaissance
[AD-A196379] N89-11371

AERODYNAMIC CHARACTERISTICS
Aerodynamic design considerations for a free-flying ducted propeller
[DE88-006867] N89-10841
The characteristics of the ground vortex and its effect on the aerodynamics of the STOL configuration N89-10850
Non-linear aerodynamic characteristics obtained from the analysis of flight-data
[AR-004-571] N89-10866
The use of the complex summation method for formulating algorithms for decoupling vertical/horizontal motions of rolling aircraft N89-10889
Investigation of the tumbling phenomenon using computer simulation N89-10896
Numerical simulation of transonic flow around Asuka N89-11067

AERODYNAMIC COEFFICIENTS
Full scale wind tunnel tests on a Ford Escort Mk 3
[TT-8802] N89-10846
Experimental aerodynamic performance of advanced 40 deg-swept 10-blade propeller model at Mach 0.6 to 0.85
[NASA-TM-88969] N89-10865

AERODYNAMIC CONFIGURATIONS
Aeroelasticity and structural optimization of helicopter rotor blades with swept tips N89-10887

AERODYNAMIC FORCES
A computational study of coherent structures in the wakes of two-dimensional bluff bodies
[AD-A196820] N89-11188

AERODYNAMIC INTERFERENCE
Tests on 3 NACA 0012 airfoil models of DFVLR in the NAL 0.3 tunnel: An assessment of 2-D wall interference
[TM-AE-8705] N89-10847

AERODYNAMICS
An approximate, maximum terminal velocity descent to a point
[DE88-000049] N89-10840
Schlieren measurements at the 10,000-foot sled track
[DE88-012748] N89-10899

AEROELASTICITY
Aeroelasticity and structural optimization of helicopter rotor blades with swept tips N89-10887

AERONAUTICAL ENGINEERING
Origin, objectives and activities of the Department of Aerospace Engineering N89-10830
Aviation technology applicable to developing regions
[NASA-TM-89425] N89-10872

AERONOMY
Investigation of ionospheric D region aeronomy using incoherent scatter radar and optical measurements N89-11338

AEROSOLS
A theoretical investigation of the collection of aerosol particles by falling ice crystals N89-11337
A new determination of extinction due to atmospheric aerosols and the resulting implications for upper stratospheric ozone depletion N89-11348

AEROSPACE ENGINEERING
Origin, objectives and activities of the Department of Aerospace Engineering N89-10830

AEROSPACE ENVIRONMENTS
Space-based multifunctional end effector systems functional requirements and proposed designs
[NASA-CR-180390] N89-11237

AEROSPACE SAFETY
STS safety approval process for small self-contained payloads N89-10910

AEROSPACE SYSTEMS
Development of a verification program for deployable truss advanced technology
[NASA-CR-181703] N89-10936
Knowledge-based diagnosis for aerospace systems
[NASA-CR-182641] N89-11441
AEROTHERMODYNAMICS
Flight mechanics and aerothermodynamic software
[CNES-CT/DTI/MS/MN/069] N89-10839
AGING (MATERIALS)
Multistress aging of polymer films
[DE88-008094] N89-11034
AGING (METALLURGY)
The effect of thermal ageing on the stress corrosion cracking of 9Cr1Mo steel in aqueous caustic environments
[NRL-R-1003(R)] N89-10997
AGRICULTURE
Technique for obtaining agricultural property boundaries through satellite imagery, certified to control and accompany agricultural activity
[INPE-4640-PRE/1351] N89-11294
JPRS report: Science and technology. USSR: Life sciences
[JPRS-ULS-87-010] N89-11385
AIR FLOW
Studies of barotropic flow over topography using a galerkin finite element model
[AD-A196516] N89-11353
AIR POLLUTION
Markers of air pollution in forests: Nutrient cycling
[DE88-011011] N89-11319
CIR aerial photography applied to the evaluation of the air pollution impact in a tropical forest: The case of Cubatao, Brazil
[INPE-4651-PRE/1358] N89-11324
NOAA (National Oceanic and Atmospheric Administration) Meteorology Division support to the Environmental Protection Agency
[PB88-213624] N89-11327
Ozone hole of the Antarctica: Recent results
[INPE-4518-PRE/1270] N89-11329
Design and analysis of large-scale atmospheric dispersion experiment
[DE88-012911] N89-11330
Carbon monoxide measurements in different Brazilian ecosystems
[INPE-4668-PRE/1368] N89-11331
The impact of an increase in atmospheric methane on the temperature field and subsequent climatic effects
[AD-A196869] N89-11332
AIR QUALITY
NOAA (National Oceanic and Atmospheric Administration) Meteorology Division support to the Environmental Protection Agency
[PB88-213624] N89-11327
AIR TRAFFIC CONTROL
In-service evaluation of the Traffic Alert and Collision Avoidance System (TCAS) industry prototype
[DOT/FAA/SA-88/2] N89-10885
Evaluation of enhancements to the Low Level Wind Shear Alert System (LLWAS) at Stapleton International Airport
[DOT/FAA/PS-88/14] N89-11356
AIR WATER INTERACTIONS
The climatological seasonal response of the ocean mixed layer in the equatorial and tropical Pacific Ocean
[AD-A196962] N89-11382
AIRBORNE EQUIPMENT
Integrated quartz oscillator for aerospace applications
[ETN-88-93100] N89-11125
An inertial velocity reference for the NASA airborne Doppler lidar
[NASA-CR-179378] N89-11203
AIRBORNE/SPACEBORNE COMPUTERS
A highly reliable computer for airborne applications
N89-10833
Computerized monitoring and control of experiments in space N89-10915
AIRCRAFT ACCIDENT INVESTIGATION
Aircraft accident/incident summary report, Copperhill, Tennessee, February 22, 1986
[PB88-910407] N89-10868
Aircraft accident reports, brief format, US civil and foreign aviation, issue number 2 of 1987 accidents
[PB88-916906] N89-10871
Aircraft accident report: Executive Air Charter, Inc., dba American Eagle, Flight 5452, CASA C-212, N432CA, Mayaguez, Puerto Rico, May 8, 1987
[PB88-910409] N89-10873
AIRCRAFT ACCIDENTS
Aeronautical decision making for air ambulance helicopter pilots: Situational awareness exercises
[DOT/FAA/DS-88/6] N89-10869
Aeronautical decision making for commercial pilots
[DOT/FAA/PM-86/42] N89-10870
Aircraft crashes on the runway: Development of a super element for nonlinear analysis of a beam
[REPT-87/56] N89-11286
AIRCRAFT COMMUNICATION
State-of-the-art in fiber optic systems at the Aeronautic Test Center, Toulouse (France)
[REPT-363300] N89-11513
AIRCRAFT CONTROL
F-15 SMTD low speed jet effects wind tunnel test results N89-10853
AIRCRAFT DESIGN
Origin, objectives and activities of the Department of Aerospace Engineering N89-10830
Advanced avionics architecture pave pillar N89-10834
Aerodynamic design considerations for a free-flying ducted propeller
[DE88-006867] N89-10841
AIRCRAFT LANDING
Investigation of wake vortices of landing aircraft at Frankfurt airport (Federal Republic of Germany)
[DFVLR-MITT-88-15] N89-10862
AIRCRAFT MODELS
An assessment of ground effects determined by static and dynamic testing techniques N89-10854
AIRCRAFT NOISE
Noise of the Harrier in vertical landing and takeoff N89-10856
AIRCRAFT RELIABILITY
Some statistical aspects of attrition studies
[AD-A196665] N89-10891
AIRCRAFT SAFETY
Aircraft accident/incident summary report, Copperhill, Tennessee, February 22, 1986
[PB88-910407] N89-10868
Aircraft accident reports, brief format, US civil and foreign aviation, issue number 2 of 1987 accidents
[PB88-916906] N89-10871
Statistics on aircraft gas turbine engine rotor failures that occurred in US commercial aviation during 1982
[DOT/FAA/CT-88/23] N89-10892
AIRCRAFT STABILITY
F-15 SMTD low speed jet effects wind tunnel test results N89-10853
AIRCRAFT STRUCTURES
Aircraft crashes on the runway: Development of a super element for nonlinear analysis of a beam
[REPT-87/56] N89-11286
AIRCRAFT WAKES
Investigation of wake vortices of landing aircraft at Frankfurt airport (Federal Republic of Germany)
[DFVLR-MITT-88-15] N89-10862
AIRFOILS
Experimental results for the Eppler 387 airfoil at low Reynolds numbers in the Langley low-turbulence pressure tunnel
[NASA-TM-4062] N89-10842
Tests on 3 NACA 0012 airfoil models of DFVLR in the NAL 0.3 tunnel: An assessment of 2-D wall interference
[TM-AE-8705] N89-10847
Effects of a ground vortex on the aerodynamics of an airfoil N89-10855
ALASKA
Beaufort Sea: Information update
[PB88-208616] N89-11380
ALBEDO
Basic theory of desertification
[DE88-703014] N89-11320
ALGEBRA
Restructuring of basic linear algebraic algorithms, chapter 5 N89-11399
General complex-analytic structures in uniform algebra spectra: A survey
[DE88-703010] N89-11450
Homology classes represented by real algebraic hypersurfaces
[PB88-202908] N89-11453
Real algebraic morphisms into even-dimensional spheres
[PB88-202916] N89-11462
Inner product for a Banach-algebra
[DE88-703156] N89-11465
ALGORITHMS
Multicolor pyrometer for materials processing in space
[NASA-CR-183189] N89-11057
A new radar technique for satellite rainfall algorithm development
[NASA-CR-183471] N89-11102
Design definition for a digital beamforming processor
[AD-A196983] N89-11133
Algorithm for the study of particle movement in the inner magnetosphere of the earth
[INPE-4669-PRE/1369] N89-11351
Computational Fluid Dynamics: Algorithms and Supercomputers
[AGARD-AG-311] N89-11395
Algorithm and general software considerations N89-11397
Vectorization of FORTRAN programs at do-loop level N89-11398
Computatinal fluid dynamics and supercomputers, chapter 6 N89-11400
Strategies for concurrent processing of complex algorithms in data driven architectures
[NASA-CR-181329] N89-11406
Adaptive filtering algorithms for communications signal processing
[PD-SE-8808] N89-11410
An O(NlogN) hypercube N-body integrator
[DE88-015016] N89-11413
Parallel algorithm for a class of optimization problems
[PB88-209929] N89-11414
Concerning the use of the minimum mean asymmetry as the validation criteria for clustering
[INPE-4654-PRE/1361] N89-11427
Lattice algorithms for computing QR and Cholesky factors in the least squares theory of linear prediction
[AD-A196454] N89-11432
An O(N) algorithm for three-dimensional N-body simulations
[AD-A196903] N89-11433
Toward intelligent machine learning algorithms
[AD-A197049] N89-11448
Computational structure of the N-body problem
[AD-A196422] N89-11473
ALKALI METALS
Pair potential trend of alkali metals under external pressure
[DE88-702973] N89-11593
ALKALIES
Oxidation reduction potential of the Cu(3)/Cu(2) system in alkaline solutions
[NASA-TT-20309] N89-10963
The effect of thermal ageing on the stress corrosion cracking of 9Cr1Mo steel in aqueous caustic environments
[NRL-R-1003(R)] N89-10997
ALL SKY PHOTOGRAPHY
An all sky study of fast X-ray transients
[NASA-TM-89716] N89-11686
ALLOYING
Calorimetry study of the synthesis of amorphous Ni-Ti alloys by mechanical alloying
[DE88-006468] N89-11010
The catalytic, structural, and electronic properties of strained-metal overlayers
[DE88-007932] N89-11013
ALLOYS
Novel composite materials: Alloys from immiscible components
[AD-A197040] N89-10958
ALTERNATIONS
Accessibility, a criterion for the choice of visual coding rules
[PB88-209911] N89-11458
ALTITUDE
The geographical distributions of electrons (0.05-3.2 MeV) and protons (0.58-35 MeV) at altitudes of 350-850 km
[ISAS-RN-358] N89-11335
ALTITUDE ACCLIMATIZATION
Individual differences in adaptation to hypoxia and cold based on emotional-behavioral criterion of bodily reactivity N89-11386
ALUMINIDES
Joining of advanced aluminides
[DE88-015111] N89-11226
ALUMINUM
Development of an experimental model of self-propagating high temperature oxidation-reduction reactions
[AD-A196978] N89-10987
ALUMINUM ALLOYS
Creep tests for slow and fast fatigue conditions on aluminum alloy specimens
[REPT-M0-535200] N89-11020
Control of environment assisted cracking of Al 7075 using inhibitors
[AD-A196387] N89-11022
ALUMINUM GALLIUM ARSENIDES
Study and fabrication of AlGaAs/GaAs double heterojunction bipolar transistors for integrated injection logic circuits
[LAAS-88-138] N89-11123
ALUMINUM OXIDES
Investigation of a self-lubricating alumina coating formed by anodic spark deposition
[DE88-014947] N89-11035
ALUMINUM SILICATES
Phase transformations in xerogels of mullite composition
[NASA-TM-101349] N89-11038

AMAZON REGION (SOUTH AMERICA)
A study of wind profiles under quasi-neutral and inversion atmospheric conditions, over a terra firma forest
[INPE-4694-RPE/575] N89-11369
AMINES
New non-linear optical polymers
[AD-A196859] N89-11040
AMMONIA
Preliminary design study of hydrogen and ammonia resistojets for prime and auxiliary thrusters
[NASA-CR-182176] N89-10943
AMORPHOUS MATERIALS
Calorimetry study of the synthesis of amorphous Ni-Ti alloys by mechanical alloying
[DE88-006468] N89-11010
AMORPHOUS SILICON
Amorphous silicon photovoltaic devices prepared by chemical and photochemical vapor deposition of higher order silanes
[DE88-001189] N89-11311
Optimization of transparent and reflecting electrodes for amorphous silicon solar cells
[DE88-001175] N89-11316
AMPLIFICATION
Basic rules of saturated gain variation in a flowing laser cavity
[AD-A196861] N89-11220
AMPLIFIERS
Switchable auto gain amplifier
[DE88-012114] N89-11122
Temporal variations in a CW HF MOPA (oscillator/amplifier)
[AD-A196915] N89-11132
Direct solar-pumped iodine laser amplifier
[NASA-CR-183171] N89-11201
Overview of FEL (Free-Electron Laser) development with induction linacs at LLNL
[DE88-014179] N89-11210
AMPLITUDE MODULATION
Digital signal design for meteor-scatter communications
[AD-A196685] N89-11111
AMPLITUDES
Collective resonance fluorescence in an intense laser field with phase and amplitude fluctuations
[DE88-702920] N89-11205
ANALYSIS (MATHEMATICS)
Fundamental research in applied mathematics
[AD-A193668] N89-11454
ANATOMY
Three-dimensional computer graphics brain-mapping project
[AD-A197053] N89-11435
ANELASTICITY
Elastic and anelastic behaviour of icosahedral quasicrystals
[DE88-702712] N89-11588
ANGULAR MOMENTUM
Activities relevant to BIH on time scales or the rotation of the earth and terrestrial systems N89-11659
ANGULAR VELOCITY
Activities relevant to BIH on time scales or the rotation of the earth and terrestrial systems N89-11659
ANIMATION
Television animation store: Control system operation and implementation
[BBC-RD-1988/4] N89-11097
ANISOTROPY
Structure of wind-shear turbulence
[NASA-CR-183257] N89-11359
ANNEALING
Studies of the transpassive nitric acid corrosion of various austenitic CrNi steels in the prolonged Huey test (65 percent HNO3, 120 C, 720 h)
[DE88-010494] N89-10998
Ternary adamantine materials for low-cost solar cells
[DE88-001160] N89-11302
Balance of recurrence order in time-inhomogeneous Markov chains with application to simulated annealing
[AD-A196980] N89-11484
Ion implantation and thermal annealing of high-T(ssub c) single crystals of YBa2Cu3O(sub x)
[DE88-012201] N89-11564
ANNIHILATION REACTIONS
Electronic properties of sigma-conjugated polysilanes
[DE88-012699] N89-11032
ANNUAL VARIATIONS
Laboratory examination and seasonal analyses of the dynamic losses for a continuously variable speed heat pump
[DE88-013207] N89-11174
Acid precipitation in North America: 1985 annual and seasonal data summaries from Acid Deposition System data base
[DE88-013563] N89-11325
Tropical 200 mb divergent circulations and their relation to outgoing longwave radiation
[AD-A196375] N89-11370
Active modes of the Pacific Intertropical Convergence Zone (ITCZ)
[AD-A196406] N89-11374
ANNULAR FLOW
Three component laser anemometer measurements in an annular cascade of core turbine vanes with contoured end wall
[NASA-TP-2846] N89-10844
ANODES
Laser Raman spectroscopy of anodic corrosion and inhibitor films on iron and nickel
[DE88-009958] N89-11008
ANODIZING
Investigation of a self-lubricating alumina coating formed by anodic spark deposition
[DE88-014947] N89-11035
ANTARCTIC REGIONS
Ozone hole of the Antarctica: Recent results
[INPE-4518-PRE/1270] N89-11329
A far infrared astronomical observatory in Antarctica N89-11646
ANTENNA ARRAYS
Array elements for a DBS flat-plate antenna
[BBC-RD-1988/8] N89-11103
A broad-band array of aperture-coupled cavity-backed slot elements
[AD-A196400] N89-11109
ANTENNA DESIGN
Polarisation converters for a DBS flat-plate antenna
[BBC-RD-1988/7] N89-11073
A flat-plate antenna for DBS reception
[BBC-RD-1988/6] N89-11096
Array elements for a DBS flat-plate antenna
[BBC-RD-1988/8] N89-11103
A broad-band array of aperture-coupled cavity-backed slot elements
[AD-A196400] N89-11109
Alfven wave studies on a tokamak N89-11517
The detection of gravitational radiation N89-11648
ANTENNA RADIATION PATTERNS
Determination of characteristic radiation properties of a torus antenna
[ESA-TT-1106] N89-11105
A broad-band array of aperture-coupled cavity-backed slot elements
[AD-A196400] N89-11109
ANTIFERROMAGNETISM
Possible coexistence of antiferromagnetism and superconductivity in the Hubbard model
[DE88-703025] N89-11561
ANTIKNOCK ADDITIVES
A detailed chemical kinetic reaction mechanism for the oxidation of iso-octane and n-heptane over an extended temperature range and its application to analysis of engine knock
[DE88-005370] N89-11053
ANTIMISSILE DEFENSE
Interceptor-to-target allocation strategies for Strategic Defense 1: Adaptive strategies based upon system and threat characteristics
[AD-A197037] N89-11487
APERTURES
A broad-band array of aperture-coupled cavity-backed slot elements
[AD-A196400] N89-11109
APPROXIMATION
A code for the solution of the Vlasov-Fokker-Planck equation in one or two dimensions
[DE88-013288] N89-11463
A frequency dependent ray theory N89-11610
AQUEOUS SOLUTIONS
The effect of thermal ageing on the stress corrosion cracking of 9Cr1Mo steel in aqueous caustic environments
[NRL-R-1003(R)] N89-10997
ARC WELDING
A method for improving the depth of penetration and the appearance of welding
[DE88-012954] N89-11239
ARCHITECTURE
Advanced avionics architecture pave pillar N89-10834
ARCHITECTURE (COMPUTERS)
Computing system configuration for fighter aircraft flight control systems N89-10832
Data and signal processing architectures for future avionics N89-10835
High speed parallel processing networks for advanced architectures N89-10837
Engineering research and development: Thrust area report, FY87
[DE88-013792] N89-11059
A coherent VLSI design environment
[AD-A196428] N89-11130
Vacuum Fizeau wedge wavemeter for pulsed UV lasers
[DE88-015832] N89-11206
A performance model for massive parallelism
[DE88-011763] N89-11393
Hardware architecture, chapter 2 N89-11396
Algorithm and general software considerations N89-11397
Strategies for concurrent processing of complex algorithms in data driven architectures
[NASA-CR-181329] N89-11406
Finite elements software and applications N89-11415
Poker (4.0): A programmer's reference guide
[AD-A196417] N89-11430
Poker (4.1): A programmer's reference guide
[AD-A196419] N89-11431
Models for parallel computation on distributed-memory multiprocessors
[DE88-010078] N89-11436
Computational structure of the N-body problem
[AD-A196422] N89-11473
ARGON
Thermophysical properties of argon. Addendum
[DE88-012722] N89-10986
ARID LANDS
Remote sensing and hydrologic modeling of arid watersheds: A scale analysis
[DE88-014625] N89-11293
Estimating evapotranspiration of an irrigated surface from upwind and downwind vertical profiles of temperature and humidity
[AD-A196409] N89-11375
ARROW WINGS
Experimental investigation of flow near a corner, part 2
[CERT-RT-OA-24/5025-AYD] N89-10861
Three dimensional shear flow. Analysis of the flow in a delta arrow wing with incidence angle
[CERT-RTS-OA-25/5025-AYD] N89-10864
ARTIFICIAL INTELLIGENCE
Representing high-level knowledge structures in massively parallel networks N89-11409
Automated knowledge generation
[NASA-CR-181317] N89-11440
Automatic concept formation in a rich input domain
[AD-A196719] N89-11445
Toward intelligent machine learning algorithms
[AD-A197049] N89-11448
Computational structure of the N-body problem
[AD-A196422] N89-11473
Abstraction in numerical methods
[AD-A196990] N89-11476
Database loading by examples: A learning approach to loading information retrieval databases N89-11619
ARTIFICIAL SATELLITES
Fabricate, calibrate and test a dosimeter for integration into the CRRES (Combined Release and Radiation Effects Satellite) satellite
[AD-A196496] N89-10938
Ion gun operations at high altitudes
[AD-A196965] N89-10939
Experiments in control of satellite manipulators N89-11391
ARTS
The transportation of fine arts materials aboard the space shuttle Columbia. GAS payload No. 481: Vertical horizons N89-10919
ASSESSMENTS
Review of the space shuttle propulsion pressurization system probabilistic risk assessment
[DE88-013163] N89-10928
ASTEROIDS
Outward to the beginning: The CRAF and Cassini Missions of the Mariner Mark 2 program
[NASA-CR-183133] N89-10921
ASTRONOMICAL MODELS
Galaxy formation: Theory and observational tests N89-11644
Cosmological puzzles N89-11650
Unified theories and the early universe N89-11651
Multiple populations on the horizontal branch N89-11662
ASTRONOMICAL OBSERVATORIES
A far infrared astronomical observatory in Antarctica N89-11646
ASTRONOMICAL PHOTOMETRY
New insights into globular clusters from main sequence photometry N89-11658
ASTRONOMICAL SATELLITES
Space observations for infrared and submillimeter astronomy N89-11643

ASTROPHYSICS
Physics and astrophysics of gravitational waves N89-11647
Astrophysical evidence on the equation of state [DE88-011960] N89-11668
Activity report of the Max-Planck-Institut fuer Physik und Astrophysik [MPE-200] N89-11688

ATMOSPHERIC ATTENUATION
Proceedings of the Twelfth NASA Propagation Experimenters Meeting (NAPEX 12) [NASA-CR-182796] N89-11074
Olympus beacon receiver N89-11093

ATMOSPHERIC BOUNDARY LAYER
A nonlinear wave-wave interaction theory for the generation of multi-scale large eddies in a neutral atmospheric boundary layer N89-11344

ATMOSPHERIC CHEMISTRY
Ozone hole of the Antarctica: Recent results [INPE-4518-PRE/1270] N89-11329
Atmospheric and Geophysical Sciences Division [DE88-013780] N89-11346

ATMOSPHERIC CIRCULATION
Basic theory of desertification [DE88-703014] N89-11320
Recent climate change in North America and CO2: Search in stratified daily data [DE88-014669] N89-11323
NOAA (National Oceanic and Atmospheric Administration) Meteorology Division support to the Environmental Protection Agency [PB88-213624] N89-11327
The use of the Q-vector in operational meteorology [AD-A196410] N89-11376

ATMOSPHERIC COMPOSITION
Ozone hole of the Antarctica: Recent results [INPE-4518-PRE/1270] N89-11329
The impact of an increase in atmospheric methane on the temperature field and subsequent climatic effects [AD-A196869] N89-11332
Development and testing of KITES [DE88-015057] N89-11336
A new determination of extinction due to atmospheric aerosols and the resulting implications for upper stratospheric ozone depletion N89-11348

ATMOSPHERIC EFFECTS
Verification of EOSAEL (Electro-Optical Systems Atmospheric Effects Library) snow transmittance predictions [DREV-R-4423/87] N89-11099

ATMOSPHERIC MODELS
The utility of particle precipitation data as an input to thermospheric density models for satellite orbital analysis [AD-A196870] N89-10925
Recent climate change in North America and CO2: Search in stratified daily data [DE88-014669] N89-11323
Parameterizations of microphysical processes in clouds for application in models of regional atmospheric deposition [DE88-010017] N89-11345
A time-dependent model for the low-latitude ionosphere [AD-A196683] N89-11354
Effects of downdrafts and mesoscale convective organization on the heat and moisture budgets of squall and nonsquall cloud clusters in the tropics N89-11367
The climatological seasonal response of the ocean mixed layer in the equatorial and tropical Pacific Ocean [AD-A196962] N89-11382

ATMOSPHERIC PHYSICS
Atmospheric and Geophysical Sciences Division [DE88-013780] N89-11346

ATMOSPHERIC PRESSURE
The thermal resistance of fine powders at atmospheric pressure and under vacuum [DE88-014556] N89-10982

ATMOSPHERIC SOUNDING
Tropospheric sounding from the TIROS-N series of satellites N89-11347
Synoptic scale sensitivity of TIROS-N moisture channels in the tropics [AD-A196686] N89-11378

ATMOSPHERIC TEMPERATURE
Ground-based radiometric observations of emission and attenuation at 20.6, 31.65, and 90.0 GHz N89-11086
Estimating evapotranspiration of an irrigated surface from upwind and downwind vertical profiles of temperature and humidity [AD-A196409] N89-11375

ATMOSPHERICS
Atmospheric and Geophysical Sciences Division [DE88-013780] N89-11346

ATOMIC CLOCKS
Securing the time scale of the NAVEX reference clock and rate determinations by time comparisons with the help of the Global Positioning System (GPS) — Spacelab D1 mission [ESA-TT-1111] N89-11197

ATOMIC PHYSICS
Atomic processes in high temperature plasmas [DE88-013005] N89-11525

ATOMIC STRUCTURE
Atomic probe study of ordering and precipitation in nickel-based alloys N89-10993
Electronic properties of sigma-conjugated polysilanes [DE88-012699] N89-11032
Strongly interacting fermion systems: Emphasis on heavy fermions [DE88-014127] N89-11573

ATTENUATION
Ground-based radiometric observations of emission and attenuation at 20.6, 31.65, and 90.0 GHz N89-11086
Laser communications through the atmosphere N89-11087
ACTS and OLYMPUS propagation experiments N89-11091

AUGER SPECTROSCOPY
Characterization of ceramic films and interfaces by electron microscopic and spectroscopic techniques [DE88-011957] N89-11029

AUGMENTATION
Detailed analysis of the structural consequences of railgun augmentation [DE88-013800] N89-10926
Entrainment enhancement of a supersonic jet for advanced ejectors [DE88-013200] N89-11177

AURORAS
Association of plasma sheet variations with auroral changes during substorms [DE88-014319] N89-11350
Wave-particle interactions in the magnetosphere of Uranus [NASA-CR-183299] N89-11678

AUSTENITIC STAINLESS STEELS
Studies of the transpassive nitric acid corrosion of various austenitic CrNi steels in the prolonged Huey test (65 percent HNO3, 120 C, 720 h) [DE88-010494] N89-10998
Microstructural development of titanium-modified austenitic stainless steel under neutron irradiation in HFIR up to 57 dpa [DE88-013248] N89-10999

AUTOMATIC CONTROL
Olympus beacon receiver N89-11093
Power quality load management for large spacecraft electrical power systems [NASA-TM-100342] N89-11127
Manual, voice, and automated control of a teleoperator viewing system [DE88-011835] N89-11235
Knowledge-based diagnosis for aerospace systems [NASA-CR-182641] N89-11441

AUTOMATIC PILOTS
Flight test results for the Daedalus and Light Eagle human powered aircraft [NASA-CR-183305] N89-10890

AUTOMATIC WEATHER STATIONS
Comparison of measured and modeled radiation, heat and water vapor fluxes: FIFE pilot study [NASA-CR-183304] N89-11368

AUTOMOBILES
Full scale wind tunnel tests on a Ford Escort Mk 3 [TT-8802] N89-10846

AUXILIARY POWER SOURCES
Electric vehicle auxiliary power source evaluation [DE88-015359] N89-11238

AVIONICS
A highly reliable computer for airborne applications N89-10833
Advanced avionics architecture pave pillar N89-10834
Data and signal processing architectures for future avionics N89-10835
Fiber optic buses and networks for advanced avionics architectures N89-10836
In-service evaluation of the Traffic Alert and Collision Avoidance System (TCAS) industry prototype [DOT/FAA/SA-88/2] N89-10885
Acceleration ground test program to verify GAS payload No. 559 structure/support avionics and experiment structural integrity N89-10913

AXIAL FLOW
Experimental investigation of the performance of a supersonic compressor cascade [NASA-TM-100879] N89-10858
Development of a boundary layer control device for tip clearance experiments in an axial compressor [AD-A196968] N89-11190

AXIAL FLOW TURBINES
Rotor instrumentation circuits for the Sandia 34-meter vertical axis wind turbine [DE88-014704] N89-11304

AXIAL LOADS
Transverse flexure of an elastic plate loaded through a rigid inclusion N89-11267

AXISYMMETRIC BODIES
Numerical description of cavitation on axisymmetric bodies [DE88-006826] N89-11147

AZEOTROPES
Evaluation of vapor compression cycles using nonazeotropic refrigerant mixtures [DE88-013225] N89-11169

B

BACKGROUND RADIATION
Simultaneous background measurement in the ASDEX neutral particle diagnostics N89-11543
Space and time resolved measurements of ion temperature with the CVI 5292 A charge exchange recombination line after substracting background radiation [IPPJ-888] N89-11549

BACKSCATTERING
Interference by rain scatter N89-11084
Synthesis of resistive tapers to control scattering patterns of strips [AD-A196402] N89-11110
Modulation of radar backscatter from the ocean by a variable surface current [AD-A196952] N89-11114
Improvement and extension of a radar forest backscattering model [NASA-CR-183259] N89-11292
Effect of curvature on the backscattering from leaves [NASA-CR-183326] N89-11296

BACKWARD FACING STEPS
Investigation on of the flow around a backward facing step with spanwise blowing [CERT-RF-OA-68/2259-AYD] N89-10859

BACKWARD WAVES
Study of optical output couplers for submillimeter wavelength backward-wave oscillators (BWO's) [NASA-TM-101360] N89-11128

BALANCE
Analysis of nonlinear circuits at RF and microwave frequencies by the harmonic balance method [INPE-4693-TDL/342] N89-11126

BALLISTIC MISSILES
Allocating and launching MaRV interceptors based on miss distance predictions [DE88-015370] N89-11486

BANACH SPACE
General complex-analytic structures in uniform algebra spectra: A survey [DE88-703010] N89-11450
Inner product for a Banach-algebra [DE88-703156] N89-11465

BANDWIDTH
Bandwidth compression for HDTV broadcasting: Investigation of some adaptive subsampling strategies [BBC-RD-1988/9] N89-11101
Digital signal design for meteor-scatter communications [AD-A196685] N89-11111

BARIUM OXIDES
Ion implantation and thermal annealing of high-T(ssub c) single crystals of YBa2Cu3O(sub x) [DE88-012201] N89-11564
Superconductivity, structures, ESR and SIMS-analysis of a high-T(sub c)Y(sub 0.33)Ba(sub 0.67)Cu(sub 2.33)O(sub 3.67-sigma) compound [DE88-702677] N89-11583

BAROTROPIC FLOW
Studies of barotropic flow over topography using a galerkin finite element model [AD-A196516] N89-11353

BARYON RESONANCE
Electroproduction of baryon resonances aboce the delta(1232) [CEBAF-PR-88-012] N89-11499

BASE FLOW
Numerical simulation of axisymmetric base flow on tactical missiles with propulsive jet [AD-A196169] N89-11136

BAYES THEOREM
On empirical Bayes selection rules for negative binomial populations [AD-A196994] N89-11485

BEACONS
A digital beacon receiver N89-11092
Olympus beacon receiver N89-11093
BEAMS (RADIATION)
Periodic solutions of the Hamilton-Jacobi equation by the shooting method: A technique for beam dynamics
[DE88-012733] N89-11460
Beam handling and emittance control
[AD-A196789] N89-11509
BEAUFORT SEA (NORTH AMERICA)
Beaufort Sea: Information update
[PB88-208616] N89-11380
BELTS
Current research on the vibration and stability of axially-moving materials N89-11283
BEND TESTS
A mixed-mode bending apparatus for delamination testing
[NASA-TM-100662] N89-10945
BENDING
Contribution for stress analysis in bend acessories of piping systems
[DE88-701618] N89-11272
BERYLLIUM
Neutron multiplication in beryllium
[AD-A196877] N89-11503
BERYLLIUM ALLOYS
Microstructure and properties of rapidly solidified beryllium-transition metal alloys
[DE88-010937] N89-11012
Electrical resistivity of U(sub 1-x)M(sub x)Be13 under pressure
[DE88-014449] N89-11552
BERYLLIUM COMPOUNDS
Low temperature measurements on UBe13
[DE88-014446] N89-11594
BERYLLIUM OXIDES
Analysis of SP-100 critical experiments
[DE88-014429] N89-11508
BIBLIOGRAPHIES
REFEREE: Bibliographic database manager, documentation
[PB88-200787] N89-11620
Patent abstracts bibliography: A continuing bibliography (supplement 33). Section 2: Indexes
[NASA-SP-7039(33)] N89-11624
BIG BANG COSMOLOGY
Galaxy formation: Theory and observational tests N89-11644
Unified theories and the early universe N89-11651
BIMETALS
The catalytic, structural, and electronic properties of strained-metal overlayers
[DE88-007932] N89-11013
BINARY ALLOYS
Atomistic studies of grain boundaries in alloys and compounds
[DE88-011939] N89-11011
BINARY STARS
Low mass X-ray binaries in globular clusters and hierarchical triple systems N89-11660
Three probable stellar mass black holes
[AD-A196976] N89-11676
BINDERS (MATERIALS)
Energetic thermoplastic elastomer synthesis
[AD-A196885] N89-11041
Synthesis of energetic binders
[AD-A196886] N89-11042
BINOMIALS
On empirical Bayes selection rules for negative binomial populations
[AD-A196994] N89-11485
BIOCHEMISTRY
JPRS report: Science and technology. USSR: Life sciences
[JPRS-ULS-87-010] N89-11385
BIOELECTRICITY
A composite photobioelectronic material
[DE88-012490] N89-11383
BIOLOGICAL EFFECTS
Systems report for payload G-652: Project origins N89-10911
GAS-611 firefly in zero gravity N89-10912
Integration of knowledge on the response of vegetation to rising CO2
[DE88-014740] N89-11326
BIOLUMINESCENCE
GAS-611 firefly in zero gravity N89-10912
BIOTECHNOLOGY
Development of Bio-GAS systems N89-10904
BIPOLAR TRANSISTORS
Study and fabrication of AlGaAs/GaAs double heterojunction bipolar transistors for integrated injection logic circuits
[LAAS-88-138] N89-11123
BIT ERROR RATE
Bit-to-bit error dependence in direct-sequence spread-spectrum multiple-access packet radio systems
[AD-A196384] N89-11108
BLACK BODY RADIATION
State of the art of negative luminescence
[DE88-010871] N89-11556
BLACK HOLES (ASTRONOMY)
Three probable stellar mass black holes
[AD-A196976] N89-11676
BLADE TIPS
Development of a boundary layer control device for tip clearance experiments in an axial compressor
[AD-A196968] N89-11190
BLADES
A study of helicopter stability and control including blade dynamics
[NASA-CR-183245] N89-10895
BLAST LOADS
Explosion airblast predictions on a personal computer and application to the Henderson, Nevada incident
[DE88-014991] N89-11144
BLUFF BODIES
A computational study of coherent structures in the wakes of two-dimensional bluff bodies
[AD-A196820] N89-11188
BLUNT BODIES
A computational study of coherent structures in the wakes of two-dimensional bluff bodies
[AD-A196820] N89-11188
BODY-WING CONFIGURATIONS
Experimental investigation of flow near a corner, part 2
[CERT-RT-OA-24/5025-AYD] N89-10861
BOEING 727 AIRCRAFT
In-service evaluation of the Traffic Alert and Collision Avoidance System (TCAS) industry prototype
[DOT/FAA/SA-88/2] N89-10885
BOILERS
Nonlinear control of an H2O2 steam reactor
[ESA-TT-902] N89-11242
BOILING
Future MAUS payload and the TWIN-MAUS configuration N89-10906
Peculiarities of heat transfer at helium boiling in centrifugal force field
[DE88-702809] N89-10974
BOLTZMANN TRANSPORT EQUATION
Flux method for the field dependent transport through multilayer devices
[INPE-4647-PRE/1357] N89-11559
BOOSTER ROCKET ENGINES
Performance of a circular body earth-to-orbit winged transport with various strap-on boosters
[NASA-TM-100603] N89-10929
BORON HYDRIDES
Kinetics of boron hydride interconversion reactions
[AD-A196824] N89-10985
BORON NITRIDES
The effect of carbon and boron nitride additions on the fracture toughness of Si3N4
[DE88-013249] N89-11025
BOUNDARIES
Technique for obtaining agricultural property boundaries through satellite imagery, certified to control and accompany agricultural activity
[INPE-4640-PRE/1351] N89-11294
BOUNDARY LAYER CONTROL
Development of a boundary layer control device for tip clearance experiments in an axial compressor
[AD-A196968] N89-11190
BOUNDARY LAYER FLOW
Investigation on of the flow around a backward facing step with spanwise blowing
[CERT-RF-OA-68/2259-AYD] N89-10859
Study of three dimensional boundary layers on the front of a fuselage and at an air intake
[CERT-OA-22/5025-AYD] N89-11184
BOUNDARY LAYER SEPARATION
Experimental results for the Eppler 387 airfoil at low Reynolds numbers in the Langley low-turbulence pressure tunnel
[NASA-TM-4062] N89-10842
Experimental research on swept shock wave/boundary layer interactions
[AD-A196938] N89-11189
BOUNDARY LAYER STABILITY
Bursting phenomenon in a flat plate pulsed boundary layer
[CERT-RSF-OA-69/2259-AYD] N89-11183
Boundary layer transition
[CERT-OA-40/5018-AYD] N89-11187
The role of a lid in the 31 May 1985 tornado outbreak
[AD-A196684] N89-11377
BOUNDARY LAYER TRANSITION
An experimental study of a laminar wall-jet in the presence of a uniform external flow
[UTIAS-268] N89-11152
BOUNDARY LAYERS
The characteristics of the ground vortex and its effect on the aerodynamics of the STOL configuration N89-10850
Summary of an experimental investigation on the ground vortex N89-10851
BOUNDARY VALUE PROBLEMS
Proceedings of the Focused Research Program on Spectral Theory and Boundary Value Problems. Volume 1: Singular differential systems
[DE88-008151] N89-11461
BOW WAVES
Schlieren measurements at the 10,000-foot sled track
[DE88-012748] N89-10899
BRAIN
Three-dimensional computer graphics brain-mapping project
[AD-A197053] N89-11435
BRAZIL
Training activities in remote sensing at the Instituto de Pesquisas Espaciais-INPE/Brazil
[INPE-4686-PRE/1380] N89-11295
Carbon monoxide measurements in different Brazilian ecosystems
[INPE-4668-PRE/1368] N89-11331
BRAZILIAN SPACE PROGRAM
The checkout system software for the Brazilian satellite
[INPE-4571-PRE/1311] N89-11419
BREADBOARD MODELS
Design definition for a digital beamforming processor
[AD-A196983] N89-11133
BREMSSTRAHLUNG
A differential absorption spectrometer for determining flash X-ray spectra from 10 to 2000 keV
[DE88-014844] N89-10979
BRIDGMAN METHOD
Process modelling for space station experiments
[NASA-CR-183274] N89-10922
BRILLOUIN EFFECT
Brillouin scattering: Its application to the study of damage and amorphization
[DE88-012053] N89-11016
Brillouin scattering at high pressures
[DE88-011972] N89-11497
BRITTLE MATERIALS
A strain rate dependent brittle fracture model based on continuum damage mechanics
[DE88-013361] N89-11285
BRITTLENESS
Low stress brittle fractures in polymers
[DE88-014236] N89-11027
A strain rate dependent brittle fracture model based on continuum damage mechanics
[DE88-013361] N89-11285
BROADBAND
A broad-band array of aperture-coupled cavity-backed slot elements
[AD-A196400] N89-11109
BROADCASTING
OPEX: (Olympus Propagation EXperiment) N89-11090
BUBBLES
Future MAUS payload and the TWIN-MAUS configuration N89-10906
Periodically structured multiphase flows and hydrodynamic instabilities in narrow capillaries
[DE88-015608] N89-11181
BUCKLING
Investigations in the nonlinear domain of composite laminate plates subject to compression loads
[ONERA-RT-17/3542-RY-070-R] N89-10953
Benchmark study of shear buckling of a cylindrical vessel
[PB88-125315] N89-11257
Delamination buckling of pressure-loaded, laminated cylindrical shells and panels N89-11276
Measurement of glass shell buckling strength using a piezoelectric film sensor
[DE88-013016] N89-11280
BURNING RATE
Reaction rates in premixed turbulent flames and their relevance to the turbulent burning speed
[DE88-012021] N89-10960
BURSTS
Bursting phenomenon in a flat plate pulsed boundary layer
[CERT-RSF-OA-69/2259-AYD] N89-11183
The history of gamma-ray burst observations
[DE88-014390] N89-11685

BUS CONDUCTORS
Fiber optic buses and networks for advanced avionics architectures N89-10836

C

CABLES (ROPES)
Current research on the vibration and stability of axially-moving materials N89-11283
CADMIUM TELLURIDES
A theory of surface and interface electronic properties of crystalline solids: Applications to 2-6 compounds N89-11596
CALCULUS OF VARIATIONS
Variational transition state theory
[DE88-013756] N89-10959
CALIBRATING
Fabricate, calibrate and test a dosimeter for integration into the CRRES (Combined Release and Radiation Effects Satellite) satellite
[AD-A196496] N89-10938
Spectrography analysis of stainless steel by the point to point technique
[DE88-702302] N89-10992
Scale drift in on-line calibration
[AD-A196439] N89-11404
CALORIMETERS
Calorimetry study of the synthesis of amorphous Ni-Ti alloys by mechanical alloying
[DE88-006468] N89-11010
CANARD CONFIGURATIONS
Flow around a delta wing with or without a canard (Phi BA = 60 deg). Part 2: Hydrodynamic visualizations in unsteady flow (pitching oscillations)
[ONERA-RT-11/2891-AN-PT-2] N89-10860
CANONICAL FORMS
The Frobenius metric in image registration
[DE88-016685] N89-11421
CARBON
Electrically conductive reticulated carbon composites
[DE88-012856] N89-10948
Carbon films derived from poly(acrylonitrile): Oxidation, electrical properties, and processing
[DE88-010352] N89-10950
The effect of carbon and boron nitride additions on the fracture toughness of Si3N4
[DE88-013249] N89-11025
CARBON DIOXIDE
Recent climate change in North America and CO2: Search in stratified daily data
[DE88-014669] N89-11323
CARBON DIOXIDE CONCENTRATION
Integration of knowledge on the response of vegetation to rising CO2
[DE88-014740] N89-11326
CARBON DIOXIDE LASERS
JPRS Report: Science and Technology. USSR: Materials Science
[JPRS-UMS-88-007] N89-11002
Characteristics of laser beam focusing with single spherical mirrors during laser treatment N89-11004
Glass-ceramic fusion with a CO2 laser
[DE88-012871] N89-11030
Damage effects on thin acrylic targets caused by infrared radiation from a pulsed carbon dioxide laser
[AD-A196385] N89-11216
Two-dimensional saturation gain and output power in transverse flow electrical discharge CO2 lasers
[AD-A196660] N89-11218
CARBON FIBER REINFORCED PLASTICS
Influence of specimen dimension on damage and breaking of composite materials
[REPT-49-062/F] N89-10957
CARBON FIBERS
A novel approach to abrasion resistance
[DE88-014180] N89-10949
Polystyrylpyridine (PSP) resin-based short-fiber composites (injectable compounds)
[REPT-NT-195/87/CRB/GTR.C/NP] N89-10955
CARBON MONOXIDE
Carbon monoxide measurements in different Brazilian ecosystems
[INPE-4668-PRE/1368] N89-11331
CARBORANE
Synthesis of energetic binders
[AD-A196886] N89-11042
CARDIOVASCULAR SYSTEM
Effect of physical fitness on response to orthostasis in healthy young women
[AD-A196377] N89-11387
CARIBBEAN REGION
Aviation technology applicable to developing regions
[NASA-TM-89425] N89-10872
A limited assessment and characterization of the solar radiation energy resources in the Caribbean region
[DE88-001133] N89-11312
CARRIER INJECTION
Study and fabrication of AlGaAs/GaAs double heterojunction bipolar transistors for integrated injection logic circuits
[LAAS-88-138] N89-11123
CASCADE FLOW
Three component laser anemometer measurements in an annular cascade of core turbine vanes with contoured end wall
[NASA-TP-2846] N89-10844
Experimental investigation of the performance of a supersonic compressor cascade
[NASA-TM-100879] N89-10858
JPRS report: Science and technology: Japan
[JPRS-JST-87-018] N89-11061
Cascade flow analysis by Navier-Stokes equation N89-11065
CASSINI MISSION
Outward to the beginning: The CRAF and Cassini Missions of the Mariner Mark 2 program
[NASA-CR-183133] N89-10921
CATACLYSMIC VARIABLES
Observations of southern irregular variables
[INPE-4568-PRE/1309] N89-11291
CATALYSIS
Ligand intermediates in metal catalyzed reactions
[DE88-012123] N89-11007
CATALYSTS
Transition metal mediated transformations of unsaturated molecules
[DE88-013482] N89-10968
The catalytic, structural, and electronic properties of strained-metal overlayers
[DE88-007932] N89-11013
Research on catalyst combustion for gas turbine N89-11063
Assessment of methanol electro-oxidation for direct methanol-air fuel cells
[DE88-014686] N89-11317
CATHODES
Comparison between Uramoto type and straight filament type sheet plasmas as a volume produced H(-) ion source (I)
[IPPJ-876] N89-11523
CAVITATION FLOW
Numerical description of cavitation on axisymmetric bodies
[DE88-006826] N89-11147
Influence of grain boundary structure distribution and processing history on intergranular creep cavitation
[DE88-015808] N89-11571
CAVITIES
A broad-band array of aperture-coupled cavity-backed slot elements
[AD-A196400] N89-11109
CDC CYBER 170 SERIES COMPUTERS
Implementation of MAGINT code cn the CDC-CYBER-170/750 system
[INPE-4663-NTE/282] N89-11491
CELL CATHODES
Lithium secondary batteries: Role of polymer cathode morphology
[AD-A196998] N89-11135
CENSORED DATA (MATHEMATICS)
Penalized likelihood estimation for rates with censored survival
[RR-726-M] N89-11479
CENTRIFUGAL FORCE
Peculiarities of heat transfer at helium boiling in centrifugal force field
[DE88-702809] N89-10974
CERAMIC MATRIX COMPOSITES
Laminate behavior for SiC fiber-reinforced reaction-bonded silicon nitride matrix composites
[NASA-TM-101350] N89-10952
CERAMICS
A novel approach to abrasion resistance
[DE88-014180] N89-10949
Surface structures and reactions of ceramics and metals
[DE88-013752] N89-11028
Characterization of ceramic films and interfaces by electron microscopic and spectroscopic techniques
[DE88-011957] N89-11029
Glass-ceramic fusion with a CO2 laser
[DE88-012871] N89-11030
Phase transformations in xerogels of mullite composition
[NASA-TM-101349] N89-11038
JPRS report: Science and technology: Japan
[JPRS-JST-87-018] N89-11061
Development of transparent zirconia ceramics discussed N89-11062
Sensors for ceramic components in advanced propulsion systems: Summary of literature survey and concept analysis, task 3 report
[NASA-CR-180900] N89-11192
Oxygen electrode in molten carbonate fuel cells
[DE88-009628] N89-11308
New quantum interferometer effect in superconducting oxide ceramics
[DE88-703152] N89-11603
CERENKOV COUNTERS
Proton decay experiment and neutrinos from supernova (Kamiokande-2) N89-11653
CERENKOV RADIATION
Gas-loaded free-electron lasers
[DE88-014652] N89-11213
CHAINS
Current research on the vibration and stability of axially-moving materials N89-11283
CHANNEL FLOW
On hydromagnetic channel flow induced by tooth pulses
[DE88-703031] N89-11522
CHANNELS (DATA TRANSMISSION)
Adaptive filtering algorithms for communications signal processing
[PD-SE-8808] N89-11410
CHARACTERISTICS
The development of prototype absorbers with variable characteristics
[BBC-RD-1988/5] N89-11492
CHARACTERIZATION
Deposition and characterization of ZnS/Si heterojunctions produced by vacuum evaporation
[NASA-TM-101359] N89-11129
CHARGE CARRIERS
Experimental study of time-varying current flow between electrodes immersed in a laboratory magnetoplasma N89-11521
CHARGE DISTRIBUTION
Self-consistent charge and spin distributions in oxide superconductors
[DE88-012051] N89-11591
CHARGE EXCHANGE
Charge exchange spectroscopy (CXRS) of highly ionized ions in ASDEX — tokamak N89-11535
Advantages of a helium beam for active charge exchange diagnostics — ASDEX tokamak N89-11542
CHARGE TRANSFER
Flux method for the field dependent transport through multilayer devices
[INPE-4647-PRE/1357] N89-11559
CHARGED PARTICLES
Ion gun operations at high altitudes
[AD-A196965] N89-10939
Ions generated on or near satellite surfaces
[AD-A196966] N89-10940
The geographical distributions of electrons (0.05-3.2 MeV) and protons (0.58-35 MeV) at altitudes of 350-850 km
[ISAS-RN-358] N89-11335
Algorithm for the study of particle movement in the inner magnetosphere of the earth
[INPE-4669-PRE/1369] N89-11351
CHEMICAL ANALYSIS
Outward to the beginning: The CRAF and Cassini Missions of the Mariner Mark 2 program
[NASA-CR-183133] N89-10921
CHEMICAL BONDS
Transition metal mediated transformations of unsaturated molecules
[DE88-013482] N89-10968
CHEMICAL COMPOSITION
Electrochemical reactions of mixed cobalt/nickel oxide hydroxides in alkaline electrolyte
[ATR-86(9561)-4] N89-10965
Phase transformations in xerogels of mullite composition
[NASA-TM-101349] N89-11038
A detailed chemical kinetic reaction mechanism for the oxidation of iso-octane and n-heptane over an extended temperature range and its application to analysis of engine knock
[DE88-005370] N89-11053
Lithium secondary batteries: Role of polymer cathode morphology
[AD-A196998] N89-11135
Joining of advanced aluminides
[DE88-015111] N89-11226
Spectral studies of three oxisols and a Ultisol of Brazil
[INPE-4644-PRE/1355] N89-11297
CHEMICAL EFFECTS
Integration of knowledge on the response of vegetation to rising CO2
[DE88-014740] N89-11326

CHEMICAL EQUILIBRIUM
The importance of thermodynamics to the modeling of nitrogen combustion chemistry
[DE88-014656] N89-10978
CHEMICAL EVOLUTION
Systems report for payload G-652: Project origins N89-10911
CHEMICAL LASERS
Temporal variations in a CW HF MOPA (oscillator/amplifier)
[AD-A196915] N89-11132
CHEMICAL PROPERTIES
Chemical preparation of powders and films for high temperature superconductors
[DE88-015266] N89-11601
CHEMICAL REACTIONS
Variational transition state theory
[DE88-013756] N89-10959
Electrochemical reactions of mixed cobalt/nickel oxide hydroxides in alkaline electrolyte
[ATR-86(9561)-4] N89-10965
Theoretical studies of chemical reactions: dynamics
[DE88-011994] N89-10970
The importance of thermodynamics to the modeling of nitrogen combustion chemistry
[DE88-014656] N89-10978
The coefficient of first viscosity via three-phonon processes in bulk liquid helium
[AD-A196902] N89-10986
Microscopy and microanalysis of shock-processed materials
[DE88-008471] N89-10990
Experimental studies of the chemistry of metal clusters
[DE88-012034] N89-10994
Surface structures and reactions of ceramics and metals
[DE88-013752] N89-11028
Heat release effects of reacting gas jets in liquids
[DE88-011971] N89-11175
The flux and recycling of bioactive substances in the surface sediments of the deep basins off southern California
[DE88-007999] N89-11321
CHEMILUMINESCENCE
Quantitative Luminescence Imaging System description and user's manual
[DE88-015604] N89-11512
CHINESE SPACE PROGRAM
The first Chinese student space shuttle getaway special program N89-10903
CHIPS (ELECTRONICS)
Design definition for a digital beamforming processor
[AD-A196983] N89-11133
ENGEN: An intermediate language to HILO extension of the FIRST silicon compiler, executive summary
[ESA-CR(P)-2621] N89-11422
CHLOROPLASTS
A composite photobioelectronic material
[DE88-012490] N89-11383
CHOLESKY FACTORIZATION
Lattice algorithms for computing QR and Cholesky factors in the least squares theory of linear prediction
[AD-A196454] N89-11432
CHROMIUM
The effect of thermal ageing on the stress corrosion cracking of 9Cr1Mo steel in aqueous caustic environments
[NRL-R-1003(R)] N89-10997
Studies of the transpassive nitric acid corrosion of various austenitic CrNi steels in the prolonged Huey test (65 percent HNO3, 120 C, 720 h)
[DE88-010494] N89-10998
CIRCUITS
Analysis of nonlinear circuits at RF and microwave frequencies by the harmonic balance method
[INPE-4693-TDL/342] N89-11126
Rotor instrumentation circuits for the Sandia 34-meter vertical axis wind turbine
[DE88-014704] N89-11304
CIRCULAR CYLINDERS
Study of flow past a circular cylinder using a higher order scheme for Navier-Stokes equation
[TM-FM-8806] N89-11142
CIRRUS CLOUDS
Optical scattering and microphysical properties of subvisual cirrus clouds, and climatic implications
[NASA-CR-183301] N89-11362
CLASSIFICATIONS
Ultrasonic flaw classification: An approach using modeling, signal processing, and adaptive learning N89-11248
CLEARANCES
Development of a boundary layer control device for tip clearance experiments in an axial compressor
[AD-A196968] N89-11190
CLEAVAGE
Transition metal mediated transformations of unsaturated molecules
[DE88-013482] N89-10968
CLEBSCH-GORDAN COEFFICIENTS
Topologically related quantities in turbulent flows N89-11173
CLIMATE
Method for predicting monthly rainfall patterns
[DE88-703005] N89-11363
CLIMATE CHANGE
Recent climate change in North America and CO2: Search in stratified daily data
[DE88-014669] N89-11323
CLIMATOLOGY
Development of a semi-empirical model for estimating the global solar radiation
[INPE-4620-TDL/328] N89-11352
Optical scattering and microphysical properties of subvisual cirrus clouds, and climatic implications
[NASA-CR-183301] N89-11362
Mesoscale structure and climatology of rain-snow lines over North Carolina
[AD-A196687] N89-11379
The climatological seasonal response of the ocean mixed layer in the equatorial and tropical Pacific Ocean
[AD-A196962] N89-11382
CLINICAL MEDICINE
JPRS report: Science and technology. USSR: Life sciences
[JPRS-ULS-87-010] N89-11385
CLOSED ECOLOGICAL SYSTEMS
Growth of plant tissue cultures in simulated lunar soil: Implications for a lunar base CELSS (Controlled Ecological Life Support System)
[NASA-CR-183233] N89-11384
CLOSURE LAW
Reynolds stress closure in jet flows using wave models
[NASA-CR-180226] N89-10843
CLOUD PHYSICS
Convective scale selection and the initiation of deep cumulus N89-11341
Parameterizations of microphysical processes in clouds for application in models of regional atmospheric deposition
[DE88-010017] N89-11345
CLOUDS (METEOROLOGY)
Millimeter-wave studies N89-11085
Ground-based radiometric observations of emission and attenuation at 20.6, 31.65, and 90.0 GHz N89-11086
Laser communications through the atmosphere N89-11087
Microwave radiances from horizontally finite, vertically structured precipitating clouds N89-11364
CLUSTER ANALYSIS
Concerning the use of the minimum mean asymmetry as the validation criteria for clustering
[INPE-4654-PRE/1361] N89-11427
CLUSTERS
Experimental studies of the chemistry of metal clusters
[DE88-012034] N89-10994
CLUTTER
Polarimetric clutter modeling: Theory and application
[NASA-CR-183348] N89-11106
COATING
KCl bounce coating of glass and polymer microshells
[DE88-013018] N89-11524
COATINGS
Oxidation reduction potential of the Cu(3)/Cu(2) system in alkaline solutions
[NASA-TT-20309] N89-10963
Methodology of flexural fatigue testing composite materials produced by electron-beam evaporation N89-11003
Investigation of a self-lubricating alumina coating formed by anodic spark deposition
[DE88-014947] N89-11035
Effect of thermal cycling
[AD-A196851] N89-11219
COCKPITS
Design and evaluation of a cockpit display for hovering flight
[NASA-CR-183247] N89-10900
CODING
Workshops and problems for benchmarking eddy current codes
[DE88-009996] N89-11098
Development and testing of KITES
[DE88-015057] N89-11336
Unidirectional Manchester encoded data transfer via a fiber optic link
[AD-A196961] N89-11516
COEFFICIENTS
Coefficients of thermal expansion of common encapsulants
[DE88-015026] N89-10983
The coefficient of first viscosity via three-phonon processes in bulk liquid helium
[AD-A196902] N89-10986
COGNITION
Assessing schema knowledge
[AD-A196933] N89-11447
Measuring the vague meanings of probability terms
[AD-A196944] N89-11483
COHERENT RADIATION
Gas-loaded free-electron lasers
[DE88-014652] N89-11213
COLD ACCLIMATIZATION
Individual differences in adaptation to hypoxia and cold based on emotional-behavioral criterion of bodily reactivity N89-11386
COLD FRONTS
A numerical modeling study of frontogenesis and cold frontal rainbands N89-11358
COLD WORKING
Microstructural development of titanium-modified austenitic stainless steel under neutron irradiation in HFIR up to 57 dpa
[DE88-013248] N89-10999
COLLISION AVOIDANCE
In-service evaluation of the Traffic Alert and Collision Avoidance System (TCAS) industry prototype
[DOT/FAA/SA-88/2] N89-10885
COLOR
Spectral studies of three oxisols and a Ultisol of Brazil
[INPE-4644-PRE/1355] N89-11297
Optimization-based design of control systems
[AD-A196593] N89-11405
COLOR CODING
Color enhancement of remote sensing imagery using IHS transformations and decorrelation stretch methods
[INPE-4559-PRE/1300] N89-11418
COLOR INFRARED PHOTOGRAPHY
CIR aerial photography applied to the evaluation of the air pollution impact in a tropical forest: The case of Cubatao, Brazil
[INPE-4651-PRE/1358] N89-11324
COLUMNS (PROCESS ENGINEERING)
The effect of vapor incidence angle upon thin film columnar growth
[DE88-014396] N89-11577
COMBINATORIAL ANALYSIS
Problem on 0-1 matrices
[PB88-210075] N89-11477
COMBUSTION
Reaction rates in premixed turbulent flames and their relevance to the turbulent burning speed
[DE88-012021] N89-10980
Fluid mechanical properties of flames in enclosures
[DE88-014142] N89-10981
COMBUSTION CHEMISTRY
Combustion of energetic materials
[DE88-011286] N89-10977
The importance of thermodynamics to the modeling of nitrogen combustion chemistry
[DE88-014656] N89-10978
COMBUSTION PHYSICS
Mixing and Demixing Processes in Multiphase Flows With Application to Propulsion Systems
[NASA-CP-3006] N89-11153
Modeling of combustion processes of stick propellants via combined Eulerian-Lagrangian approach N89-11183
COMBUSTION PRODUCTS
Research on catalyst combustion for gas turbine N89-11063
COMETS
Outward to the beginning: The CRAF and Cassini Missions of the Mariner Mark 2 program
[NASA-CR-183133] N89-10921
Molecular processes in comets
[NASA-CR-182742] N89-11671
COMMUNICATION
Through-the-earth communication: Experiment results from Billie Mine and Mississippi Chemical Mine
[DE88-013162] N89-11072
Communication aspects of parallel processing
[AD-A196458] N89-11439
A co-citation study of the scientific literature of two innovation research traditions: Diffusion of innovations and technology transfer N89-11618
COMMUNICATION NETWORKS
SOPMCR: An operating system for the multiprocessor for communication networks
[INPE-4675-NTE/284] N89-11438
COMMUNICATION SATELLITES
PiFEx propagation experiments N89-11075

Results of 1987 MSS helicopter propagation experiment at UHF and L band in Central Maryland N89-11077
LMSS propagation modeling at Virginia Tech N89-11078
ETS-V propagation experiments in Japan N89-11080
Propagation handbook, frequencies above 10 GHz N89-11082
OPEX: (Olympus Propagation EXperiment) N89-11090
ACTS and OLYMPUS propagation experiments N89-11091
A digital beacon receiver N89-11092
Olympus beacon receiver N89-11093

COMPARISON
Workshops and problems for benchmarking eddy current codes
[DE88-009996] N89-11098

COMPATIBILITY
Compatibility and performance of separators in Li/SOCl(sub 2) cells
[DE88-011090] N89-11116

COMPILERS
ENGEN: An intermediate language to HILO extension of the FIRST silicon compiler, executive summary
[ESA-CR(P)-2621] N89-11422

COMPLEX SYSTEMS
Knowledge-based design of complex mechanical systems N89-11225

COMPOSITE MATERIALS
Electrically conductive reticulated carbon composites
[DE88-012856] N89-10948
Novel composite materials: Alloys from immiscible components
[AD-A197040] N89-10958
JPRS Report: Science and Technology. USSR: Materials Science
[JPRS-UMS-88-007] N89-11002
Methodology of flexural fatigue testing composite materials produced by electron-beam evaporation N89-11003
Developments and trends in electrodeposition
[DE88-009822] N89-11014
A composite photobioelectronic material
[DE88-012490] N89-11383
Current-induced quantum interference in the composite superconductor NbTi-Cu
[DE88-703079] N89-11562
The critical current density, the fabrication process and the microstructure in superconducting composites of NbTi for high energy physics
[DE88-014241] N89-11568

COMPOSITE STRUCTURES
Composite structural materials
[NASA-CR-180224] N89-10946
Tension fatigue analysis and life prediction for composite laminates
[NASA-TM-100549] N89-10951
Free damped vibration of composite plates and shells N89-11249

COMPRESSIBLE FLOW
A diagonally inverted LU implicit multigrid scheme for the 3-D Navier-Stokes equations and a two equation model of turbulence
[NASA-CR-182209] N89-10863
Godunov methods and adaptive algorithms for unsteady fluid dynamics
[DE88-013094] N89-11141
Unsteady hydromagnetic free-convection flow with radiative heat transfer in a rotating fluid. 2: Compressible optically thin fluid
[DE88-702999] N89-11168
Computation of low-speed compressible flows with time-marching procedures
[AD-A195800] N89-11170

COMPRESSING
Bandwidth compression for HDTV broadcasting: Investigation of some adaptive subsampling strategies
[BBC-RD-1988/9] N89-11101

COMPRESSION LOADS
Investigations in the nonlinear domain of composite laminate plates subject to compression loads
[ONERA-RT-17/3542-RY-070-R] N89-10953
Nonlinear theories of composite laminates under compression with delamination
[CERT-RT-18/3542-RY-071-R] N89-10954

COMPRESSOR BLADES
Development of a boundary layer control device for tip clearance experiments in an axial compressor
[AD-A196968] N89-11190

COMPRESSORS
Evaluation of vapor compression cycles using nonazeotropic refrigerant mixtures
[DE88-013225] N89-11169
Preliminary assessment of a magnetically coupled free-piston Stirling engine heat pump compressor
[DE88-013835] N89-11232

COMPUTATION
The CSM testbed software system: A development environment for structural analysis methods on the NAS CRAY-2
[NASA-TM-100642] N89-11287
Algorithm and general software considerations N89-11397
An O(N) algorithm for three-dimensional N-body simulations
[AD-A196903] N89-11433

COMPUTATIONAL FLUID DYNAMICS
A diagonally inverted LU implicit multigrid scheme for the 3-D Navier-Stokes equations and a two equation model of turbulence
[NASA-CR-182209] N89-10863
Cascade flow analysis by Navier-Stokes equation N89-11065
Numerical simulation of axisymmetric base flow on tactical missiles with propulsive jet
[AD-A196169] N89-11136
Computation of low-speed compressible flows with time-marching procedures
[AD-A195800] N89-11170
Study of three dimensional boundary layers on the front of a fuselage and at an air intake
[CERT-OA-22/5025-AYD] N39-11184
Boundary layer transition
[CERT-OA-40/5018-AYD] N89-11187
Experimental research on swept shock wave/boundary layer interactions
[AD-A196938] N89-11189
Computational Fluid Dynamics: Algorithms and Supercomputers
[AGARD-AG-311] N89-11395
Vectorization of FORTRAN programs at do-loop level N89-11398
Computatinal fluid dynamics and supercomputers, chapter 6 N89-11400
Communication aspects of parallel processing
[AD-A196458] N89-11439
An iterative scheme for numerical solution of transonic small perturbation equation
[TM-AE-8801] N89-11455

COMPUTATIONAL GRIDS
Study of three dimensional boundary layers on the front of a fuselage and at an air intake
[CERT-OA-22/5025-AYD] N89-11184
Guidelines for using TIPSFD for 3D finite-difference mesh generation
[DE88-012451] N89-11417

COMPUTER AIDED DESIGN
Program of research in structures and dynamics
[NASA-CR-183191] N89-10838
CAD wind tunnel test for half-cut model of Asuka N89-11069
A study of the turn-off behavior of high power gate turn off thyristors (GTO): Computer-aid to design and utilization
[LAAS-88-164] N89-11124
A coherent VLSI design environment
[AD-A196428] N89-11130
Optimization-based design of control systems
[AD-A196593] N89-11405
ETIC: A multi-user Computer Aided Design (CAD) database management system
[RR-720-I] N89-11428
Automated knowledge generation
[NASA-CR-181317] N89-11440

COMPUTER AIDED TOMOGRAPHY
Experiments in the application of ultrasound diffraction tomography for nondestructive testing
[DE88-014694] N89-11245

COMPUTER ASSISTED INSTRUCTION
Assessing schema knowledge
[AD-A196933] N89-11447

COMPUTER GRAPHICS
Analysis, synthesis and design of high-speed mechanisms
[PB88-235106] N89-11244
PC-CUBE: A personal computer based hypercube
[DE88-015008] N89-11394
TRINITY II: A post-processing program for 2-dimensional finite element analysis data
[DE88-010107] N89-11416
The checkout system software for the Brazilian satellite
[INPE-4571-PRE/1311] N89-11419
Three-dimensional computer graphics brain-mapping project
[AD-A197053] N89-11435
Applications of the optical differential thermal analysis
[AD-A196706] N89-11515

COMPUTER INFORMATION SECURITY
Computerized classified document accountability
[DE88-015054] N89-11633

COMPUTER NETWORKS
Fiber optic buses and networks for advanced avionics architectures N89-10836
High speed parallel processing networks for advanced architectures N89-10837
Poker (4.0): A programmer's reference guide
[AD-A196417] N89-11430
Poker (4.1): A programmer's reference guide
[AD-A196419] N89-11431

COMPUTER PROGRAMMING
Real-time path planning for robot arms N89-11224
Improvement and extension of a radar forest backscattering model
[NASA-CR-183259] N89-11292
A model for the response of vertical axis wind turbines to turbulent flow: Parts 1 and 2
[DE88-014708] N89-11305
Three dimensional gravity modeling techniques with application to the Ennis Geothermal Area, part 1
[DE88-014952] N89-11340
Programming abstractions for run-time partitioning of scientific continuum calculations running on multiprocessors
[DE88-007376] N89-11411
Abstraction in numerical methods
[AD-A196990] N89-11476
Guidelines for tailoring DOD-STD-2167A for SDS (Strategic Defense System) software development
[AD-A197038] N89-11488
The transformative compression of coherent languages N89-11623

COMPUTER PROGRAMS
Computing Systems Configuration for Highly Integrated Guidance and Control Systems
[AGARD-LS-158] N89-10831
Computing system configuration for fighter aircraft flight control systems N89-10832
Some statistical aspects of attrition studies
[AD-A196665] N89-10891
Process modelling for space station experiments
[NASA-CR-183274] N89-10922
Tether applications
[NASA-CR-179392] N89-10934
Workshops and problems for benchmarking eddy current codes
[DE88-009996] N89-11098
Verification of EOSAEL (Electro-Optical Systems Atmospheric Effects Library) snow transmittance predictions
[DREV-R-4423/87] N89-11099
Explosion airblast predictions on a personal computer and application to the Henderson, Nevada incident
[DE88-014991] N89-11144
An inertial velocity reference for the NASA airborne Doppler lidar
[NASA-CR-179378] N89-11203
Benchmark study of shear buckling of a cylindrical vessel
[PB88-125315] N89-11257
Development and testing of KITES
[DE88-015057] N89-11336
The use of the Q-vector in operational meteorology
[AD-A196410] N89-11376
Restructuring of basic linear algebraic algorithms, chapter 5 N89-11399
An introduction to implementing a capacity planning effort in an MVS (Multiple Virtual Storage) environment
[AD-A196383] N89-11402
OEXP Analysis Tools Workshop
[NASA-CP-10013] N89-11407
Finite elements software and applications N89-11415
TRINITY II: A post-processing program for 2-dimensional finite element analysis data
[DE88-010107] N89-11416
Guidelines for using TIPSFD for 3D finite-difference mesh generation
[DE88-012451] N89-11417
Parallel processing a real code: A case history
[DE88-014456] N89-11437
Automatic concept formation in a rich input domain
[AD-A196719] N89-11445
Toward intelligent machine learning algorithms
[AD-A197049] N89-11448
Fundamental research in applied mathematics
[AD-A193668] N89-11454
Abstraction in numerical methods
[AD-A196990] N89-11476
Implementation of MAGINT code on the CDC-CYBER-170/750 system
[INPE-4663-NTE/282] N89-11491
Lie algebraic treatment of space charge N89-11496
Numerical simulation of the response function of a nuclear emulsion plate N89-11540

COMPUTER SYSTEMS DESIGN
A hybrid hot-wire data acquisition system
[ARL-AERO-R-172] N89-11193
An investigation of information systems prototyping N89-11622

COMPUTER SYSTEMS PERFORMANCE
An introduction to implementing a capacity planning effort in an MVS (Multiple Virtual Storage) environment
[AD-A196383] N89-11402
Standards conformance testing
[PB88-215645] N89-11412
Vectorization techniques on the MD system 570/CX
[CNES-CT/DTI/MS/MN/147] N89-11425

COMPUTER SYSTEMS PROGRAMS
Flight mechanics and aerothermodynamic software
[CNES-CT/DTI/MS/MN/069] N89-10839
Software management metrics
[AD-A196916] N89-11434

COMPUTER TECHNIQUES
Scale drift in on-line calibration
[AD-A196439] N89-11404
Hypothesis-confirming information search strategies and computerized information retrieval systems N89-11616

COMPUTERIZED SIMULATION
An approximate, maximum terminal velocity descent to a point
[DE88-000349] N89-10840
Investigation of the tumbling phenomenon using computer simulation N89-10896
Sandia National Laboratories flight simulation facilities
[DE88-012108] N89-10898
Atomistic studies of grain boundaries in alloys and compounds
[DE88-011939] N89-11011
Advanced desiccant materials assessment, phase 2
[PB88-217054] N89-11033
Engineering research and development: Thrust area report, FY87
[DE88-013792] N89-11059
A study of the turn-off behavior of high power gate turn off thyristors (GTO): Computer-aid to design and utilization
[LAAS-88-164] N89-11124
A coherent VLSI design environment
[AD-A196428] N89-11130
Optimization of microwave magnetoelastic delay lines
[AD-A196866] N89-11131
Simulations of the laser photocathode injector
[DE88-015337] N89-11202
Experiments in the application of ultrasound diffraction tomography for nondestructive testing
[DE88-014694] N89-11245
Computer simulation of the uni-axial stress-strain behavior of ribbon-like fiber nonwovens N89-11284
The PNL single-tower measurement model of rotationally sampled turbulent wind, with user's guide for STRS2PC
[DE88-013166] N89-11360
The use of portable microcomputer as a data collection tool to support integrated simulation support environments: A concept
[AD-A196414] N89-11403
The DFVLR models 1 and 2 of the Manutec r3 robot
[DFVLR-MITT-88-13] N89-11443
The generation of scatterometer surface targets with specified surface statistics
[AD-A196397] N89-11480
Allocating and launching MaRV interceptors based on miss distance predictions
[DE88-015370] N89-11486
Optimization of the two-dimensional magnetic field distribution basing on the integral equation method
[DE88-702940] N89-11490
Theory of defects in non-metallic solids
[DE88-013075] N89-11567

COMPUTERS
Precision-time tradeoffs: A paradigm for processing statistical queries on databases
[DE88-012024] N89-11408

CONCRETES
Lunar concrete for construction
[NASA-TM-89672] N89-11060
Literature review of strengthening methodologies of existing structures
[PB88-218219] N89-11271

CONCURRENT PROCESSING
An O(NlogN) hypercube N-body integrator
[DE88-015016] N89-11413

CONDENSED MATTER PHYSICS
Dynamic Interactions of Energetic Probes with Condensed Matter: Proceedings
[DE88-008882] N89-11589

CONDENSING
Liquid-vapour phase change between plane liquid surfaces: A continuum analysis to determine real gas effects
[TM-FM-8803] N89-10971

CONFERENCES
The 1987 Ground Vortex Workshop
[NASA-CP-10008] N89-10849
The 1988 Get Away Special Experimenter's Symposium
[NASA-CP-3008] N89-10902
Proceedings of the Twelfth NASA Propagation Experimenters Meeting (NAPEX 12)
[NASA-CR-182796] N89-11074
Mixing and Demixing Processes in Multiphase Flows With Application to Propulsion Systems
[NASA-CP-3006] N89-11153
Proceedings of the Focused Research Program on Spectral Theory and Boundary Value Problems. Volume 1: Singular differential systems
[DE88-008151] N89-11461
Dynamic Interactions of Energetic Probes with Condensed Matter: Proceedings
[DE88-008882] N89-11589
Space science and fundamental physics --- conference
[ESA-SP-283] N89-11638

CONFIDENCE LIMITS
Calculating the CEP (Circular Error Probable)
[NASA-CR-182996] N89-11475

CONFINEMENT
Confined turbulent fluid-particle flow modeling using multiple-realization particle trajectory schemes N89-11157

CONFORMAL MAPPING
Inflation in a renormalizable cosmological model and the cosmic no hair conjecture
[NASA-CR-183363] N89-11614

CONGRUENCES
Quasi-adequate semigroups
[DE88-703157] N89-11466

CONSTITUTIVE EQUATIONS
Finite element analysis of large strain elastic-plastic solids N89-11281

CONSTRUCTION
Lunar concrete for construction
[NASA-TM-89672] N89-11060

CONTACT LOADS
Evaluation of Li/MoS2 secondary battery for load-conditioner. Deep-cycle performance of AA-size cells
[DE88-753437] N89-11118
Dynamic behavior of foundations in bilateral and unilateral contact N89-11259

CONTAMINATION
Development of Bio-GAS systems N89-10904

CONTINENTAL SHELVES
Beaufort Sea: Information update
[PB88-208616] N89-11380

CONTINUOUS RADIATION
Temporal variations in a CW HF MOPA (oscillator/amplifier)
[AD-A196915] N89-11132
Analysis of free electron laser performance utilizing the National Bureau of Standards' CW microtron
[AD-A196928] N89-11221

CONTINUOUS WAVE LASERS
Temporal variations in a CW HF MOPA (oscillator/amplifier)
[AD-A196915] N89-11132
Laser wavemeter/spectrometer operating manual
[NASA-CR-180802] N89-11195

CONTINUUM MECHANICS
Continuum modeling of latticed structures N89-11253

CONTINUUMS
Continuum theories for fluid-particle flows: Some aspects of lift forces and turbulence N89-11155
Programming abstractions for run-time partitioning of scientific continuum calculations running on multiprocessors
[DE88-007376] N89-11411

CONTROL EQUIPMENT
Development of a boundary layer control device for tip clearance experiments in an axial compressor
[AD-A196968] N89-11190

CONTROL SIMULATION
Nonlinear control of an H2O2 steam reactor
[ESA-TT-902] N89-11242

CONTROL STABILITY
Strong and weak stabilizability: Lyapunov type approaches
[AD-A196431] N89-11482

CONTROL SYSTEMS DESIGN
Computing Systems Configuration for Highly Integrated Guidance and Control Systems
[AGARD-LS-158] N89-10831
Computing system configuration for fighter aircraft flight control systems N89-10832
Advanced avionics architecture pave pillar N89-10834
Television animation store: Control system operation and implementation
[BBC-RD-1988/4] N89-11097
Guidance, sensor control and localization of a mobile autonomous robot
[LAAS-88-131] N89-11241
Control design and performance evaluation for flexible manipulators N89-11390
Optimization-based design of control systems
[AD-A196593] N89-11405
Automated knowledge generation
[NASA-CR-181317] N89-11440
Unmodeled dynamics and nonlinear control: Wrapup
[NASA-CR-181524] N89-11457

CONTROL THEORY
On motion planning and control of multi-link lightweight robotic manipulators
[NASA-CR-181226] N89-11234
The Shock and Vibration Digest, Volume 20, No. 6 N89-11261
A comparative overview of modal testing and system identification for control of structures N89-11262
Strong and weak stabilizability: Lyapunov type approaches
[AD-A196431] N89-11482

CONTROLLED FUSION
Massachusetts Institute of Technology Plasma Fusion Center 1987--1988 report to the President
[DE88-014800] N89-11519

CONTROLLERS
Robust control of a flexible manipulator arm N89-11228
Understanding bandwidth limitations in robot force control
[AD-A195927] N89-11229
Experiments in control of satellite manipulators N89-11391

CONVECTION
Measurements and predictions of mixed convection in laminar and turbulent boundary layer flows N89-11164
Convective scale selection and the initiation of deep cumulus N89-11341
Effects of downdrafts and mesoscale convective organization on the heat and moisture budgets of squall and nonsquall cloud clusters in the tropics N89-11367
On deriving the 3-dimensional kinematic structure of convective storms from a single radar
[AD-A196405] N89-11373
Active modes of the Pacific Intertropical Convergence Zone (ITCZ)
[AD-A196406] N89-11374
The use of the Q-vector in operational meteorology
[AD-A196410] N89-11376
The role of a lid in the 31 May 1985 tornado outbreak
[AD-A196684] N89-11377

CONVECTIVE FLOW
Convective scale selection and the initiation of deep cumulus N89-11341

CONVECTIVE HEAT TRANSFER
Unsteady hydromagnetic free-convection flow with radiative heat transfer in a rotating fluid. 1: Incompressible optically thin fluid
[DE88-702998] N89-11140
Unsteady hydromagnetic free-convection flow with radiative heat transfer in a rotating fluid of arbitrary optical thickness
[DE88-703000] N89-11167
Unsteady hydromagnetic free-convection flow with radiative heat transfer in a rotating fluid. 2: Compressible optically thin fluid
[DE88-702999] N89-11168

CONVERGENCE
Numerical estimates of the rate of convergence for the vortex sheet method
[DE88-013809] N89-11178

CONVERTERS
Polarisation converters for a DBS flat-plate antenna
[BBC-RD-1988/7] N89-11073

COORDINATES
Activities relevant to BIH on time scales or the rotation of the earth and terrestrial systems N89-11659

COPOLYMERIZATION
Transition metal mediated transformations of unsaturated molecules
[DE88-013482] N89-10968

COPOLYMERS
Carbon films derived from poly(acrylonitrile): Oxidation, electrical properties, and processing
[DE88-010352] N89-10950
The melting and crystallization kinetics of hydrogenated polybutadiene
[AD-A196988] N89-11045
COPPER
Oxidation reduction potential of the Cu(3)/Cu(2) system in alkaline solutions
[NASA-TT-20309] N89-10963
High-speed photography of energetic materials and components with a copper vapor laser
[DE88-012869] N89-11212
Current-induced quantum interference in the composite superconductor NbTi-Cu
[DE88-703079] N89-11562
Superconductivity, structures, ESR and SIMS-analysis of a high-T(sub c)Y(sub 0.33)Ba(sub 0.67)Cu(sub 2.33)O(sub 3.67-sigma) compound
[DE88-702677] N89-11583
COPPER ALLOYS
Weldability of 2090 Al-Cu-Li alloy
[DE88-011963] N89-11015
COPPER OXIDES
Spin correlations in high T(sub c) superconductors
[DE88-013988] N89-11555
Electrodynamics of single-crystal Eu(sub 2)CuO(sub 4): A boson excitation spectrum
[DE88-014328] N89-11585
Lattice instability in single-crystal La(sub 2-x)Sr(sub x)/CuO4
[DE88-013994] N89-11598
CORNEA
Biological applications and effects of optical masers
[AD-A196462] N89-11217
CORNER FLOW
Experimental investigation of flow near a corner, part 2
[CERT-RT-OA-24/5025-AYD] N89-10861
CORRELATION
Determination of complex exponentials, least squares and prediction methods
[AD-A196498] N89-11474
CORRELATION COEFFICIENTS
The utility of particle precipitation data as an input to thermospheric density models for satellite orbital analysis
[AD-A196870] N89-10925
CORROSION
Experimental and theoretical study of inclusions during initiation of crevice corrosion
[DE88-014635] N89-10989
Studies of the transpassive nitric acid corrosion of various austenitic CrNi steels in the prolonged Huey test (65 percent HNO3, 120 C, 720 h)
[DE88-010494] N89-10998
Methodologies for prediction of metal oxidation-vaporization-erosion
[DE88-013623] N89-11001
Laser Raman spectroscopy of anodic corrosion and inhibitor films on iron and nickel
[DE88-009958] N89-11008
Corrosion phenomena during overcharge in polymer electrolyte cells
[AD-A196997] N89-11134
CORROSION PREVENTION
Laser Raman spectroscopy of anodic corrosion and inhibitor films on iron and nickel
[DE88-009958] N89-11008
Control of environment assisted cracking of Al 7075 using inhibitors
[AD-A196387] N89-11022
State-of-the-art-dehumidification cost-effective corrosion prevention
[AD-A196503] N89-11023
CORROSION RESISTANCE
JPRS Report: Science and Technology. USSR: Materials Science
[JPRS-UMS-88-007] N89-11002
CORROSION TESTS
Studies of the transpassive nitric acid corrosion of various austenitic CrNi steels in the prolonged Huey test (65 percent HNO3, 120 C, 720 h)
[DE88-010494] N89-10998
COSMIC DUST
Microgravity nucleation and particle coagulation experiments support
[NASA-CR-183282] N89-11056
Potential foams and metal foils for cosmic dust capture
[DE88-012960] N89-11565
COSMIC RAY SHOWERS
The history of gamma-ray burst observations
[DE88-014390] N89-11685
COSMIC RAYS
HIEN-LO: An experiment for charge determination of cosmic rays of interplanetary and solar origin
N89-10908
Systems report for payload G-652: Project origins
N89-10911
COSMOCHEMISTRY
Observations on cosmic abundance of He4 and Li7, comparison with primordial nucleosynthesis predictions
N89-11641
COSMOLOGY
On the locality of the no hair conjection and the measure of the universe
[NASA-CR-183365] N89-11489
Cosmic strings
[NASA-CR-183367] N89-11613
Inflation in a renormalizable cosmological model and the cosmic no hair conjecture
[NASA-CR-183363] N89-11614
Space science and fundamental physics -- conference
[ESA-SP-283] N89-11638
Nuclear processes in the early universe. Part 1: The thermal history of matter N89-11639
Nuclear processes in the early universe. Part 2: The cosmic quark-hadron phase transition N89-11640
Cosmological puzzles N89-11650
Fundamental science in ESA's space science program
N89-11654
The next decades of space astronomy N89-11655
Inhomogeneities in a Friedmann universe
[DE88-702981] N89-11672
COST EFFECTIVENESS
State-of-the-art-dehumidification cost-effective corrosion prevention
[AD-A196503] N89-11023
COULOMB POTENTIAL
Coulomb states in atoms and solids
[DE88-013973] N89-11494
COUPLERS
Study of optical output couplers for submillimeter wavelength backward-wave oscillators (BWO's)
[NASA-TM-101360] N89-11128
COUPLING
Pseudo-scalar pi N coupling and relativistic proton-nucleus scattering
[NASA-TM-101199] N89-11498
Phonon-plasmon mechanism of high-T(sub c) superconductivity
[DE88-014869] N89-11600
Coupled even-parity superconducting states
[AD-A196969] N89-11607
COVARIANCE
Robust covariance matrix estimation via robust estimation of principal components
[PB88-126594] N89-11478
General results in optimal control of discrete-time nonlinear stochastic systems
[AD-A196411] N89-11481
CRACK CLOSURE
A three-dimensional investigation of steady state fatigue crack closure behavior for through-thickness and part-through flaws N89-11256
CRACK INITIATION
A three-dimensional investigation of steady state fatigue crack closure behavior for through-thickness and part-through flaws N89-11256
CRACK PROPAGATION
Low stress brittle fractures in polymers
[DE88-014236] N89-11027
A method for obtaining empirical correlations for predicting crack propagation in a burning solid propellant grain
[AD-A196689] N89-11054
Incipient spall, crack branching, and fragmentation statistics in the spall process
[DE88-009587] N89-11251
Impurity-induced changes in interfacial strength and their role in creep fracture
[DE88-013197] N89-11255
A three-dimensional investigation of steady state fatigue crack closure behavior for through-thickness and part-through flaws N89-11256
CRACK TIPS
Creep and fracture characteristics of materials and structures at elevated temperatures
[AD-A196831] N89-11289
CRACKING (FRACTURING)
The role of grain boundary character in the environmentally-assisted intergranular cracking mechanism of nickel-base alloys
[DE88-014130] N89-11018
Joining of advanced aluminides
[DE88-015111] N89-11226
CRACKS
Experimental and theoretical study of inclusions during initiation of crevice corrosion
[DE88-014635] N89-10989
Control of environment assisted cracking of Al 7075 using inhibitors
[AD-A196387] N89-11022
The interpretation of electromagnetic nondestructive flaw detection in metals N89-11246
High heat flux testing of CIT (Compact Ignition Tokamak) first wall tiles
[DE88-012241] N89-11530
CRASH LANDING
Aircraft accident report: Executive Air Charter, Inc., dba American Eagle, Flight 5452, CASA C-212, N432CA, Mayaguez, Puerto Rico, May 8, 1987
[PB88-910409] N89-10873
Aircraft crashes on the runway: Development of a super element for nonlinear analysis of a beam
[REPT-87/56] N89-11286
CRAY COMPUTERS
The CSM testbed software system: A development environment for structural analysis methods on the NAS CRAY-2
[NASA-TM-100642] N89-11287
CREEP PROPERTIES
Multistress aging of polymer films
[DE88-008094] N89-11034
Impurity-induced changes in interfacial strength and their role in creep fracture
[DE88-013197] N89-11255
Creep and fracture characteristics of materials and structures at elevated temperatures
[AD-A196831] N89-11289
What is the origin of glassy behavior in the high-T(sub c) oxides
[DE88-012668] N89-11565
Influence of grain boundary structure distribution and processing history on intergranular creep cavitation
[DE88-015808] N89-11571
CREEP TESTS
Creep tests for slow and fast fatigue conditions on aluminum alloy specimens
[REPT-M0-535200] N89-11020
CRITERIA
Comparison of recent model selection criteria for system identification
[PD-SE-8807] N89-11449
CRITICAL EXPERIMENTS
Analysis of SP-100 critical experiments
[DE88-014429] N89-11508
CRITICAL TEMPERATURE
Near-critical NaCl-H2O: An equation of state and discussion of anomalous properties
[DE88-012029] N89-10969
Electrodynamics of single-crystal Eu(sub 2)CuO(sub 4): A boson excitation spectrum
[DE88-014328] N89-11585
Some theoretical aspects of high-T(sub c) superconductivity
[DE88-013101] N89-11592
CROP GROWTH
Integration of knowledge on the response of vegetation to rising CO2
[DE88-014740] N89-11326
CRUDE OIL
Exploitation and utilization of hydrocarbons
[DE88-012626] N89-11048
CRYOGENIC TEMPERATURE
Autocompensation device for ultralow temperature measurements
[DE88-702900] N89-11194
CRYOGENICS
Good performance of LE-7 liquid oxygen turbopump confirmed N89-11064
CRYOSTATS
Thermal calculations of nitrogen-free nonmagnetic helium cryostats
[DE88-702807] N89-11227
CRYSTAL DEFECTS
Brillouin scattering: Its application to the study of damage and amorphization
[DE88-012053] N89-11016
Theory of defects in non-metallic solids
[DE88-013075] N89-11567
Microstructural defects and superconducting critical currents in superconductors
[DE88-013781] N89-11587
CRYSTAL DISLOCATIONS
Indentation plasticity and fracture in silicon
[NASA-TP-2863] N89-10996
CRYSTAL GROWTH
Low frequency dielectric properties of polyether electrolytes
[AD-A196494] N89-11039

Protein crystal growth in low gravity
[NASA-CR-183183] N89-11055
Preparation and evaluation of mercuric iodide for crystal growth
[DE88-014981] N89-11578
Modified purification of mercuric iodide for crystal growth
[DE88-014960] N89-11580

CRYSTAL LATTICES
Lattice gauge theory on the hypercube
[DE88-015004] N89-11420
Theory of defects in non-metallic solids
[DE88-013075] N89-11567
Kinetic processes of the orthorhombic to tetragonal phase transition in YBa2Cu3O7-Delta
[DE88-011993] N89-11572
Vortex lattices in theory and practice
[DE88-014393] N89-11576
Electron microscopy of modulated and ordered alloys
[DE88-008667] N89-11584
Elastic and anelastic behaviour of icosahedral quasicrystals
[DE88-702712] N89-11588

CRYSTAL OSCILLATORS
Integrated quartz oscillator for aerospace applications
[ETN-88-93100] N89-11125

CRYSTAL STRUCTURE
Kinetic processes of the orthorhombic to tetragonal phase transition in YBa2Cu3O7-Delta
[DE88-011993] N89-11572
Microstructural defects and superconducting critical currents in superconductors
[DE88-013781] N89-11587
A theory of surface and interface electronic properties of crystalline solids: Applications to 2-6 compounds N89-11596
Fundamental aspects of the electronic structure, materials properties, and lubrication performance of sputtered MoS2 films
[AD-A196852] N89-11606

CRYSTAL SURFACES
The pair potential approach for interfaces: Fundamental problems and practical solutions
[DE88-009165] N89-11456

CRYSTALLINITY
Theory of defects in non-metallic solids
[DE88-013075] N89-11567

CRYSTALLIZATION
Crystallization of Zr-Ni metallic glasses
[DE88-007481] N89-11026
The melting and crystallization kinetics of hydrogenated polybutadiene
[AD-A196988] N89-11045
A theoretical investigation of the collection of aerosol particles by falling ice crystals N89-11337

CRYSTALS
The melting and crystallization kinetics of hydrogenated polybutadiene
[AD-A196988] N89-11045

CUBES (MATHEMATICS)
Cubic spline smoothing: A useful tool for curve estimation
[PB88-214796] N89-11452

CULTURE TECHNIQUES
Growth of plant tissue cultures in simulated lunar soil: Implications for a lunar base CELSS (Controlled Ecological Life Support System)
[NASA-CR-183233] N89-11384

CUMULUS CLOUDS
Convective scale selection and the initiation of deep cumulus N89-11341
Effects of downdrafts and mesoscale convective organization on the heat and moisture budgets of squall and nonsquall cloud clusters in the tropics N89-11367

CURING
Coefficients of thermal expansion of common encapsulants
[DE88-015026] N89-10983

CURRENT DENSITY
Synthesis of resistive tapers to control scattering patterns of strips
[AD-A196402] N89-11110
The critical current density, the fabrication process and the microstructure in superconducting composites of NbTi for high energy physics
[DE88-014241] N89-11568
Microstructural defects and superconducting critical currents in superconductors
[DE88-013781] N89-11587

CURRENT SHEETS
Comparison between Uramoto type and straight filament type sheet plasma as a volume produced H(-) ion source (2)
[IPPJ-887] N89-11548

CURVATURE
Effect of curvature on the backscattering from leaves
[NASA-CR-183326] N89-11296

CURVE FITTING
Cubic spline smoothing: A useful tool for curve estimation
[PB88-214796] N89-11452

CURVED PANELS
Curved channel MCP improvement program
[NASA-CR-180790] N89-11191

CYCLES
Evaluation of vapor compression cycles using nonazeotropic refrigerant mixtures
[DE88-013225] N89-11169

CYCLIC LOADS
Effect of protective coatings on life of heat-resistant nickel steel under cyclic heat load N89-11005

CYCLONES
Tropical cyclone observation and forecasting with and without aircraft reconnaissance
[AD-A196379] N89-11371

CYCLOTRON RESONANCE
Advances in metal ion sources
[DE88-012020] N89-11495
Theory of high power cyclotron resonance heating in non-uniform magnetic field
[IPPJ-875] N89-11520

CYLINDRICAL BODIES
Benchmark study of shear buckling of a cylindrical vessel
[PB88-125315] N89-11257

CYLINDRICAL PLASMAS
Comparison between Uramoto type and straight filament type sheet plasmas as a volume produced H(-) ion source (I)
[IPPJ-876] N89-11523
Excitation of MHD surface waves propagating with shear Alfven waves in an inhomogeneous cylindrical plasma
[IPPJ-872] N89-11526

CYLINDRICAL SHELLS
Delamination buckling of pressure-loaded, laminated cylindrical shells and panels N89-11276

D

D REGION
Investigation of ionospheric D region aeronomy using incoherent scatter radar and optical measurements N89-11338

DAMAGE
Plasma exposure tests of a carbon fiber/epoxy composite
[DE88-014724] N89-10947
Explosion airblast predictions on a personal computer and application to the Henderson, Nevada incident
[DE88-014991] N89-11144

DAMAGE ASSESSMENT
Functional assessment of laser irradiation
[AD-A196930] N89-11222

DAMPING
Tether applications
[NASA-CR-179392] N89-10934
Vibrations and stability of mechanical systems: 4 N89-11260
A global MHD pulsation event with conjugate study and model of ionospheric damping N89-11333
Solution methods for damped linear dynamic systems
[DE88-013812] N89-11464

DARK MATTER
Dark matter N89-11652
Superfluid helium as a dark matter detector
[DE88-012759] N89-11664

DATA ACQUISITION
Prototype data acquisition and analysis system for Navy operational flight simulators
[DE88-014557] N89-10901
PiFEx data and archival formats N89-11076
OPEX: (Olympus Propagation EXperiment) N89-11090
A hybrid hot-wire data acquistion system
[ARL-AERO-R-172] N89-11193
Electrical noise reduction techniques contributing to improved data quality at the National Transonic Facility
[NASA-CR-4193] N89-11196
Comparison of measured and modeled radiation, heat and water vapor fluxes: FIFE pilot study
[NASA-CR-183304] N89-11368
An introduction to implementing a capacity planning effort in an MVS (Multiple Virtual Storage) environment
[AD-A196383] N89-11402
The use of portable microcomputer as a data collection tool to support integrated simulation support environments: A concept
[AD-A196414] N89-11403

DATA BASE MANAGEMENT SYSTEMS
The use of portable microcomputer as a data collection tool to support integrated simulation support environments: A concept
[AD-A196414] N89-11403
Precision-time tradeoffs: A paradigm for processing statistical queries on databases
[DE88-012024] N89-11408
ETIC: A multi-user Computer Aided Design (CAD) database management system
[RR-720-I] N89-11428
Three-dimensional computer graphics brain-mapping project
[AD-A197053] N89-11435
REFEREE: Bibliographic database manager, documentation
[PB88-200787] N89-11620
Computer science and technology: Guide to distributed database management
[PB88-201561] N89-11621

DATA BASES
Parametric analysis of map data
[AD-A196908] N89-11298
Precision-time tradeoffs: A paradigm for processing statistical queries on databases
[DE88-012024] N89-11408
Integrated database approach for geodetic applications
[DE88-012726] N89-11615
Database loading by examples: A learning approach to loading information retrieval databases N89-11619
The transformative compression of coherent languages N89-11623

DATA CORRELATION
Association of plasma sheet variations with auroral changes during substorms
[DE88-014319] N89-11350

DATA LINKS
Bit-to-bit error dependence in direct-sequence spread-spectrum multiple-access packet radio systems
[AD-A196384] N89-11108
Unidirectional Manchester encoded data transfer via a fiber optic link
[AD-A196961] N89-11516

DATA PROCESSING
Data and signal processing architectures for future avionics N89-10835
Strategies for concurrent processing of complex algorithms in data driven architectures
[NASA-CR-181329] N89-11406
TRINITY II: A post-processing program for 2-dimensional finite element analysis data
[DE88-010107] N89-11416
Unidirectional Manchester encoded data transfer via a fiber optic link
[AD-A196961] N89-11516
Integrated database approach for geodetic applications
[DE88-012726] N89-11615

DATA RECORDING
Development of Bio-GAS systems N89-10904

DATA REDUCTION
Non-linear aerodynamic characteristics obtained from the analysis of flight-data
[AR-004-571] N89-10866

DATA RETRIEVAL
Hypothesis-confirming information search strategies and computerized information retrieval systems N89-11616
Information storage alternatives: An overview of laser-based optical technologies
[DE88-013499] N89-11617
Database loading by examples: A learning approach to loading information retrieval databases N89-11619

DATA SMOOTHING
Cubic spline smoothing: A useful tool for curve estimation
[PB88-214796] N89-11452

DATA STORAGE
An introduction to implementing a capacity planning effort in an MVS (Multiple Virtual Storage) environment
[AD-A196383] N89-11402

DATA STRUCTURES
The checkout system software for the Brazilian satellite
[INPE-4571-PRE/1311] N89-11419

DATA TRANSMISSION
Proceedings of the Twelfth NASA Propagation Experimenters Meeting (NAPEX 12)
[NASA-CR-182796] N89-11074
ACTS and OLYMPUS propagation experiments N89-11091
A digital beacon receiver N89-11092
Unidirectional Manchester encoded data transfer via a fiber optic link
[AD-A196961] N89-11516

DEBRIS
The first Chinese student space shuttle getaway special program N89-10903
DECAMETRIC WAVES
Decametric radio emission of Jupiter. Part 3: Some physical characteristics of S-component sources [DE88-702812] N89-11679
DECAY RATES
The decay of highly excited open strings [NASA-CR-183364] N89-11501
DECIDUOUS TREES
Results of 1987 MSS helicopter propagation experiment at UHF and L band in Central Maryland N89-11077
DECISION MAKING
Aeronautical decision making for air ambulance helicopter pilots: Situational awareness exercises [DOT/FAA/DS-88/6] N89-10869
Aeronautical decision making for commercial pilots [DOT/FAA/PM-86/42] N89-10870
DECOMPOSITION
Spectrography analysis of stainless steel by the point to point technique [DE88-702302] N89-10992
The flux and recycling of bioactive substances in the surface sediments of the deep basins off southern California [DE88-007999] N89-11321
Velocity and Q from reflection seismic data N89-11334
Domain decomposition methods for the parallel computation of reacting flows [NASA-CR-181719] N89-11459
DECOUPLING
The use of the complex summation method for formulating algorithms for decoupling vertical/horizontal motions of rolling aircraft N89-10889
DEEP SPACE NETWORK
Environmental projects. Volume 7: Environmental resources document [NASA-CR-182736] N89-11328
Activities relevant to BIH on time scales or the rotation of the earth and terrestrial systems N89-11659
The deep space network: An instrument for radio astronomy research [NASA-CR-182744] N89-11661
DEFECTS
Curved channel MCP improvement program [NASA-CR-180790] N89-11191
Ultrasonic flaw classification: An approach using modeling, signal processing, and adaptive learning N89-11248
Geometric gauge theory of metric defects [DE88-702961] N89-11269
Theory of defects in non-metallic solids [DE88-013075] N89-11567
DEFENSE INDUSTRY
Defense technology base: Introduction and overview [PB88-192562] N89-11635
DEFENSE PROGRAM
Interceptor-to-target allocation strategies for Strategic Defense 1: Adaptive strategies based upon system and threat characteristics [AD-A197037] N89-11487
DEFLAGRATION
Role of deflagration in explosive response [DE88-014139] N89-11049
DEFORMATION
Detailed analysis of the structural consequences of railgun augmentation [DE88-013800] N89-10926
Longitudinal impact test of a transport airframe section [DOT/FAA/CT-87/26] N89-11265
In-plane moire optical processing at ARL [ARL-STRUC-R-428] N89-11510
DEGRADATION
High energy-intensity atomic oxygen beam source for low earth orbit materials degradation studies [DE88-014316] N89-11504
DEICING
De-icing of aircraft turbine engine inlets [DOT/FAA/CT-87/37] N89-10894
DELAMINATING
A mixed-mode bending apparatus for delamination testing [NASA-TM-100662] N89-10945
Nonlinear theories of composite laminates under compression with delamination [CERT-RT-18/3542-RY-071-R] N89-10954
Delamination buckling of pressure-loaded, laminated cylindrical shells and panels N89-11276
DELAY LINES
Optimization of microwave magnetoelastic delay lines [AD-A196886] N89-11131
DELTA WINGS
Flow around a delta wing with or without a canard (Phi BA = 60 deg). Part 2: Hydrodynamic visualizations in unsteady flow (pitching oscillations) [ONERA-RT-11/2891-AN-PT-2] N89-10860
Three dimensional shear flow. Analysis of the flow in a delta arrow wing with incidence angle [CERT-RTS-OA-25/5025-AYD] N89-10864
Unsteady low-speed windtunnel test of a straked delta wing, oscillating in pitch. Part 1: General description and discussion of results [AD-A196456] N89-10867
DENSITY (NUMBER/VOLUME)
Far infrared linear response and radio frequency nonlinear response of charge density wave conductors and high T(sub c) superconductors [DE88-013595] N89-11582
DEPLOYMENT
Development of a verification program for deployable truss advanced technology [NASA-CR-181703] N89-10936
DEPOSITION
Characterization of metallic coatings and thin films produced by railgun deposition [AD-A196382] N89-11021
Survivability of coatings: Program review [DE88-009863] N89-11031
Acid precipitation in North America: 1985 annual and seasonal data summaries from Acid Deposition System data base [DE88-013563] N89-11325
DESCENT
An approximate, maximum terminal velocity descent to a point [DE88-000349] N89-10840
An assessment of ground effects determined by static and dynamic testing techniques N89-10854
DESERTIFICATION
Basic theory of desertification [DE88-703014] N89-11320
DESERTS
Basic theory of desertification [DE88-703014] N89-11320
DESICCANTS
Advanced desiccant materials assessment, phase 2 [PB88-217054] N89-11033
DESIGN ANALYSIS
Design and evaluation of a cockpit display for hovering flight [NASA-CR-183247] N89-10900
Design definition for a digital beamforming processor [AD-A196983] N89-11133
Knowledge-based design of complex mechanical systems N89-11225
Robust control of a flexible manipulator arm N89-11228
Space-based multifunctional end effector systems functional requirements and proposed designs [NASA-CR-180390] N89-11237
Analysis, synthesis and design of high-speed mechanisms [PB88-235106] N89-11244
Studies in advanced silicon solar cells [DE88-013143] N89-11314
PV modules for ground testing [NASA-CR-179476] N89-11315
DESORPTION
The Purdue University Get Away Special II (PUGAS II) N89-10918
Theory of oxygen ordering and absorption in 1,2,3 high-T(sub c) superconductors [DE88-007543] N89-11575
DETECTION
Ultrasonic flaw classification: An approach using modeling, signal processing, and adaptive learning N89-11248
Superfluid helium as a dark matter detector [DE88-012759] N89-11664
Dust detection systems for cometary encounter N89-11680
DETECTORS
An oxide passivated and ion-implanted Si detector for X-ray astronomy [ISAS-RN-353] N89-11663
DETONATION
The initiation and detonation of explosives: An alternative concept [DE88-014199] N89-11047
Shock initiation of explosives with a sensitive rate and related topics [DE88-008483] N89-11052
DEVELOPING NATIONS
Aviation technology applicable to developing regions [NASA-TM-89425] N89-10872
DIAGNOSIS
Knowledge-based diagnosis for aerospace systems [NASA-CR-182641] N89-11441
DIAMONDS
IR reflectance and Raman scattering of diamond films [AD-A196899] N89-11043
DICTIONARIES
An informal glossary of terms used in supercomputing, appendix A N89-11401
DIELECTRIC PROPERTIES
Low frequency dielectric properties of polyether electrolytes [AD-A196494] N89-11039
Electron attachment properties of excited dielectric-gas molecules and their possible use for pulse power switching [DE88-009705] N89-11117
DIELECTRICS
Technique for measuring the dielectric constant of thin materials [NASA-CR-183325] N89-10984
Low frequency dielectric properties of polyether electrolytes [AD-A196494] N89-11039
Dielectric millimeter waveguides. Volume 1 [AD-A196844] N89-11112
The propagation of electromagnetic waves in thin dielectric slabs [AD-A196895] N89-11115
Defect model for the electronic conduction and breakdown in dielectric thin films N89-11563
DIFFERENTIAL ANALYZERS
Applications of the optical differential thermal analysis [AD-A196706] N89-11515
DIFFERENTIAL EQUATIONS
Differential operation of NAVSTAR GPS for enhanced accuracy N89-10883
Unmodeled dynamics and nonlinear control: Wrapup [NASA-CR-181524] N89-11457
DIFFRACTION
Experiments in the application of ultrasound diffraction tomography for nondestructive testing [DE88-014694] N89-11245
Structural anomalies in undoped Gallium Arsenide observed in high resolution diffraction imaging with monochromatic synchrotron radiation [NASA-CR-183268] N89-11595
DIFFUSION
Thermophysical properties of argon. Addendum [DE88-012722] N89-10966
Liquid-vapour phase change between plane liquid surfaces: A continuum analysis to determine real gas effects [TM-FM-8803] N89-10971
Mechanisms of gas permeation through polymer membranes [DE88-007761] N89-10980
Migration arising from gradients in shear stress: Particle distributions in Poiseuille flow N89-11159
Nongradient diffusion in premixed turbulent flames N89-11161
Constraints on the growth of metallic superlattices [DE88-014633] N89-11586
DIFFUSION FLAMES
A study of the effect of thermal radiation on laminar flame propagation and ignition, 1981-1987 N89-10967
DIGITAL COMPUTERS
Olympus beacon receiver N89-11093
DIGITAL DATA
Parametric analysis of map data [AD-A196908] N89-11298
DIGITAL FILTERS
The generation of scatterometer surface targets with specified surface statistics [AD-A196397] N89-11480
DIGITAL SIMULATION
Tether applications [NASA-CR-179392] N89-10934
Numerical simulation of transonic flow around Asuka N89-11067
Numerical simulation of the response function of a nuclear emulsion plate N89-11540
DIGITAL SYSTEMS
Digital signal design for meteor-scatter communications [AD-A196685] N89-11111
Design definition for a digital beamforming processor [AD-A196983] N89-11133
Asynchronous digital regulators [AD-A196911] N89-11446
A survey of digital beam forming techniques and current technology [AD-A196376] N89-11514
DIGITAL TECHNIQUES
GPS navigation processing and Kalman filtering N89-10884

A survey of digital beam forming techniques and current technology
[AD-A196376] N89-11514

DIMENSIONS
The Frobenius metric in image registration
[DE88-016685] N89-11421
An O(N) algorithm for three-dimensional N-body simulations
[AD-A196903] N89-11433

DIPOLE MOMENTS
Polarizability and effective permittivity of layered and continuously inhomogeneous dielectric spheres
[PB88-210091] N89-11104
Molecular processes in comets
[NASA-CR-182742] N89-11671

DIRECT BROADCAST SATELLITES
Polarisation converters for a DBS flat-plate antenna
[BBC-RD-1988/7] N89-11073
A flat-plate antenna for DBS reception
[BBC-RD-1988/6] N89-11096
Array elements for a DBS flat-plate antenna
[BBC-RD-1988/8] N89-11103

DIRECT CURRENT
The state-of-the-art of dc power distribution systems/components for space applications
[NASA-CR-182743] N89-10941

DIRECTIONAL SOLIDIFICATION (CRYSTALS)
Process modelling for space station experiments
[NASA-CR-183274] N89-10922

DISCRETE FUNCTIONS
General results in optimal control of discrete-time nonlinear stochastic systems
[AD-A196411] N89-11481

DISK GALAXIES
Colour and spectral synthesis of disk galaxies N89-11656

DISPERSION
Particle dispersion models and drag coefficients for particles in turbulent flows N89-11158

DISPLACEMENT
Laser speckle photography and decorrelation techniques in elastic-plastic fracture studies N89-11275

DISPLAY DEVICES
Design and evaluation of a cockpit display for hovering flight
[NASA-CR-183247] N89-10900

DISSIPATION
Derivation of revised formulae for eddy viscous forces used in the ocean general circulation model
[NASA-TM-4060] N89-11381

DISTANCE
Undirected distances and the postman-structure of graphs
[RR-714-M] N89-11470

DISTRIBUTED PROCESSING
Models for parallel computation on distributed-memory multiprocessors
[DE88-010078] N89-11436
SOPMCR: An operating system for the multiprocessor for communication networks
[INPE-4675-NTE/284] N89-11438
Asynchronous digital regulators
[AD-A196911] N89-11446
Computer science and technology: Guide to distributed database management
[PB88-201561] N89-11621

DISTRIBUTION FUNCTIONS
A code for the solution of the Vlasov-Fokker-Planck equation in one or two dimensions
[DE88-013288] N89-11463

DOCUMENTS
Evaluating the effectiveness of information use N89-11626

DOMAINS
Automatic concept formation in a rich input domain
[AD-A196719] N89-11445
Second order parabolic equations for flow-domains
[DE88-703158] N89-11467

DOPED CRYSTALS
Indentation plasticity and fracture in silicon
[NASA-TP-2863] N89-10996

DOPPLER EFFECT
GPS navigation processing and Kalman filtering N89-10884
Experimental and theoretical studies of vertical annular liquid jets
[DE88-012971] N89-11149
On deriving the 3-dimensional kinematic structure of convective storms from a single radar
[AD-A196405] N89-11373

DOPPLER RADAR
An inertial velocity reference for the NASA airborne Doppler lidar
[NASA-CR-179378] N89-11203
An examination of a simulated microburst flow as sensed by a single Doppler radar
[AD-A196381] N89-11372

DOSAGE
Fabricate, calibrate and test a dosimeter for integration into the CRRES (Combined Release and Radiation Effects Satellite) satellite
[AD-A196496] N89-10938

DOSIMETERS
Fabricate, calibrate and test a dosimeter for integration into the CRRES (Combined Release and Radiation Effects Satellite) satellite
[AD-A196496] N89-10938

DRAG
Continuum theories for fluid-particle flows: Some aspects of lift forces and turbulence N89-11155

DRAG REDUCTION
Turbulent boundary layer drag reduction on an axisymmetric body using circular ring manipulators N89-11145

DROP SIZE
Particle sizing by weighted measurements of scattered light
[NASA-TM-100968] N89-11198

DUCTS
Developing laminar flow and heat transfer in ducts of arbitrary cross section N89-11176

DUST
Dust detection systems for cometary encounter N89-11680

DWARF STARS
Probable locations of extraterrestrial civilizations
[DE88-702605] N89-11392

DYE LASERS
Resonance ionization of Kr metastables using a single-frequency laser
[DE88-014757] N89-11209

DYNAMIC CHARACTERISTICS
SHED: A program for three-dimensional, rigid body, shroud ejection dynamics
[DE88-012410] N89-10927
Theoretical studies of chemical reactions: dynamics
[DE88-011994] N89-10970

DYNAMIC LOADS
Solution methods for damped linear dynamic systems
[DE88-013812] N89-11464

DYNAMIC MODELS
On motion planning and control of multi-link lightweight robotic manipulators
[NASA-CR-181226] N89-11234
Nonlinear control of an H2O2 steam reactor
[ESA-TT-902] N89-11242
Dynamic robot models using the Manutec r3 as an example
[DFVLR-MITT-88-16] N89-11444

DYNAMIC RESPONSE
Dynamic behavior of foundations in bilateral and unilateral contact N89-11259
Response of discretely stiffened structures and transmission of structure-borne noise N89-11270

DYNAMIC STRUCTURAL ANALYSIS
Program of research in structures and dynamics
[NASA-CR-183191] N89-10838
Flight test results for the Daedalus and Light Eagle human powered aircraft
[NASA-CR-183305] N89-10890
Detailed analysis of the structural consequences of railgun augmentation
[DE88-013800] N89-10926
Investigations in the nonlinear domain of composite laminate plates subject to compression loads
[ONERA-RT-17/3542-RY-070-R] N89-10953
The mini-oscillator technique: A finite element method for the modeling of linear viscoelastic structures
[UTIAS-323] N89-11250
Continuum modeling of latticed structures N89-11253
Dynamic analysis of spherical shells: A hybrid method
[EPM/RT-88/23] N89-11264
Response of discretely stiffened structures and transmission of structure-borne noise N89-11270
Dynamic analysis of pipings by modal synthesis
[DE88-701620] N89-11274
The Shock and Vibration Digest, Volume 20, No. 7 N89-11277
Aircraft crashes on the runway: Development of a super element for nonlinear analysis of a beam
[REPT-87/56] N89-11286
The CSM testbed software system: A development environment for structural analysis methods on the NAS CRAY-2
[NASA-TM-100642] N89-11287
Finite element analysis of shell structures with an 18-node 3-dimensional solid element based on a new mixed formulation
[AD-A196698] N89-11288
Solution methods for damped linear dynamic systems
[DE88-013812] N89-11464

DYNAMICS EXPLORER SATELLITES
Association of plasma sheet variations with auroral changes during substorms
[DE88-014319] N89-11350

DYNAMOMETERS
Enhancing performance under stress by information about its expected duration
[AD-A196836] N89-11388

E

EARTH ATMOSPHERE
Ground-based radiometric observations of emission and attenuation at 20.6, 31.65, and 90.0 GHz N89-11086
Laser communications through the atmosphere N89-11087
Design and analysis of large-scale atmospheric dispersion experiment
[DE88-012911] N89-11330
Atmospheric and Geophysical Sciences Division
[DE88-013780] N89-11346
National Center for Atmospheric Research
[PB88-220009] N89-11355

EARTH CRUST
Crustal structure of the northwestern United States N89-11349

EARTH IONOSPHERE
A global MHD pulsation event with conjugate study and model of ionospheric damping N89-11333
The geographical distributions of electrons (0.05-3.2 MeV) and protons (0.58-35 MeV) at altitudes of 350-850 km
[ISAS-RN-358] N89-11335
A time-dependent model for the low-latitude ionosphere
[AD-A196683] N89-11354

EARTH MAGNETOSPHERE
Study of a substorm on May 4, 1986
[DE88-014318] N89-11342
Algorithm for the study of particle movement in the inner magnetosphere of the earth
[INPE-4669-PRE/1369] N89-11351

EARTH MOVEMENTS
The effects of seismic waves: Part 1 N89-11268

EARTH OBSERVATIONS (FROM SPACE)
Very Long Baseline Interferometry (VLBI) from ground and space N89-11645

EARTH ORBITAL ENVIRONMENTS
Verification of single event upset rate estimation methods with on-orbit observations
[AD-A196226] N89-10935
High energy-intensity atomic oxygen beam source for low earth orbit materials degradation studies
[DE88-014316] N89-11504

EARTH ORBITS
Laboratory investigations of low earth orbit environmental effects on spacecraft
[DE88-009135] N89-10932
The determination of the spacecraft contamination environment
[AD-A196435] N89-10937

EARTH RESOURCES
Training activities in remote sensing at the Instituto de Pesquisas Espaciais-INPE/Brazil
[INPE-4686-PRE/1380] N89-11295

EARTH ROTATION
Activities relevant to BIH on time scales or the rotation of the earth and terrestrial systems N89-11659

EARTH TERMINALS
Propagation handbook, frequencies above 10 GHz N89-11082

EARTHQUAKES
The Shock and Vibration Digest, Volume 20, No. 10 N89-11252
The effects of seismic waves, part 2 N89-11254

ECOSYSTEMS
Integration of knowledge on the response of vegetation to rising CO2
[DE88-014740] N89-11326
Carbon monoxide measurements in different Brazilian ecosystems
[INPE-4668-PRE/1368] N89-11331

EDDY CURRENTS
Workshops and problems for benchmarking eddy current codes
[DE88-009996] N89-11098
The interpretation of electromagnetic nondestructive flaw detection in metals N89-11246

EDDY VISCOSITY
Derivation of revised formulae for eddy viscous forces used in the ocean general circulation model
[NASA-TM-4060] N89-11381

EDUCATION
Program of research in structures and dynamics
[NASA-CR-183191] N89-10838
TUBSAT-1, satellite technology for educational purposes N89-10905
Training activities in remote sensing at the Instituto de Pesquisas Espaciais-INPE/Brazil
[INPE-4686-PRE/1380] N89-11295

EFFICIENCY
Experimental aerodynamic performance of advanced 40 deg-swept 10-blade propeller model at Mach 0.6 to 0.85
[NASA-TM-88969] N89-10865
Amorphous silicon photovoltaic devices prepared by chemical and photochemical vapor deposition of higher order silanes
[DE88-001189] N89-11311
PC-CUBE: A personal computer based hypercube
[DE88-015008] N89-11394

EIGENVALUES
New trial of vibration testing method N89-11068
Adaptive filtering algorithms for communications signal processing
[PD-SE-8808] N89-11410
The steady states of the Kuramoto--Sivashinsky equation
[DE88-011819] N89-11451

EINSTEIN EQUATIONS
Inhomogeneities in a Friedmann universe
[DE88-702981] N89-11672

EJECTORS
Entrainment enhancement of a supersonic jet for advanced ejectors
[DE88-013200] N89-11177

EL NINO
Active modes of the Pacific Intertropical Convergence Zone (ITCZ)
[AD-A196406] N89-11374

ELASTIC DEFORMATION
A test methodology for an investigation into heating and cooling phenomena in grossly deformed tensile metallic bars
[AD-A197047] N89-11024
Ratchetting behavior of type 304 stainless steel at room and elevated temperatures
[DE88-011864] N89-11273

ELASTIC PLATES
The Shock and Vibration Digest, volume 20, no. 9 N89-11266
Transverse flexure of an elastic plate loaded through a rigid inclusion N89-11267

ELASTIC PROPERTIES
New trial of vibration testing method N89-11068
Elastic and anelastic behaviour of icosahedral quasicrystals
[DE88-702712] N89-11568

ELASTIC SCATTERING
Brillouin scattering at high pressures
[DE88-011972] N89-11497
Pseudo-scalar pi N coupling and relativistic proton-nucleus scattering
[NASA-TM-101199] N89-11498

ELASTIC SHELLS
Dynamic analysis of spherical shells: A hybrid method
[EPM/RT-88/23] N89-11264

ELASTOMERS
Coefficients of thermal expansion of common encapsulants
[DE88-015026] N89-10983
Energetic thermoplastic elastomer synthesis
[AD-A196885] N89-11041
Development of elastomeric polypeptide biomaterials
[AD-A196900] N89-11044

ELASTOPLASTICITY
Laser speckle photography and decorrelation techniques in elastic-plastic fracture studies N89-11275
Finite element analysis of large strain elastic-plastic solids N89-11281

ELECTRIC BATTERIES
Compatibility and performance of separators in Li/SOCl(sub 2) cells
[DE88-011090] N89-11116
Evaluation of Li/MoS2 secondary battery for load-conditioner. Deep-cycle performance of AA-size cells
[DE88-753437] N89-11118
Magnetic moment test report for the model SAR 8108 battery
[INPE-4574-NTE/280] N89-11121

ELECTRIC BRIDGES
Smart semiconductor bridge (SCB) igniter for explosives
[DE88-012669] N89-11551

ELECTRIC CHARGE
Far infrared linear response and radio frequency nonlinear response of charge density wave conductors and high T(sub c) superconductors
[DE88-013595] N89-11582

ELECTRIC CURRENT
Electronic properties of sigma-conjugated polysilanes
[DE88-012699] N89-11032

ELECTRIC DISCHARGES
Characterization of metallic coatings and thin films produced by railgun deposition
[AD-A196382] N89-11021

ELECTRIC EQUIPMENT TESTS
Magnetic moment test report for the model SAR 8108 battery
[INPE-4574-NTE/280] N89-11121

ELECTRIC FIELDS
Self-consistent charge and spin distributions in oxide superconductors
[DE88-012051] N89-11591

ELECTRIC GENERATORS
Development, construction, and operation of a 30/100-kW Wind Energy Converter (WEC)
[DFVLR-MITT-88-06] N89-11318
Postanalysis of the CNPS (Compact Nuclear Power Source) critical experiment
[DE88-014322] N89-11506

ELECTRIC MOTOR VEHICLES
Electric vehicle auxiliary power source evaluation
[DE88-015359] N89-11238

ELECTRIC PULSES
Electron attachment properties of excited dielectric-gas molecules and their possible use for pulse power switching
[DE88-009705] N89-11117

ELECTRIC ROCKET ENGINES
Use of high temperature superconductors in magnetopiasmadynamic systems
[NASA-TM-101219] N89-11553

ELECTRICAL ENGINEERING
Engineering research and development: Thrust area report, FY87
[DE88-013792] N89-11059

ELECTRICAL PROPERTIES
A composite photobioelectronic material
[DE88-012490] N89-11383

ELECTRICAL RESISTIVITY
Electrically conductive reticulated carbon composites
[DE88-012856] N89-10948
Carbon films derived from poly(acrylonitrile): Oxidation, electrical properties, and processing
[DE88-010352] N89-10950
Conductivity of organic polymers: A nonlinear approach
[DE88-013837] N89-11037
Electrical resistivity of U(sub 1-x)M(sub x)Be13 under pressure
[DE88-014449] N89-11552

ELECTRO-OPTICS
Multicolor pyrometer for materials processing in space
[NASA-CR-183189] N89-11057
Verification of EOSAEL (Electro-Optical Systems Atmospheric Effects Library) snow transmittance predictions
[DREV-R-4423/87] N89-11099
Molecular beam epitaxy of GaP films on Si substrates
[PB88-131974] N89-11581

ELECTROCHEMICAL CELLS
Reliability analysis of lithium cells
[DE88-009258] N89-11300

ELECTROCHEMICAL CORROSION
Control of environment assisted cracking of Al 7075 using inhibitors
[AD-A196387] N89-11022

ELECTROCHEMICAL OXIDATION
Experimental and theoretical study of inclusions during initiation of crevice corrosion
[DE88-014635] N89-10989

ELECTROCHEMISTRY
Electrochemical reactions of mixed cobalt/nickel oxide hydroxides in alkaline electrolyte
[ATR-86(9561)-4] N89-10965
Photoacoustic spectroscopy and the in situ characterization of the electrochemical interface
[DE88-013848] N89-10975
Effect of surface states on the electrochemical behaviour of single crystal n-ZnSe photoelectrode
[DE88-702726] N89-11566

ELECTRODEPOSITION
Developments and trends in electrodeposition
[DE88-009822] N89-11014

ELECTRODES
Research needs in high temperature chemistry
[DE88-012929] N89-10961
Experimental and theoretical study of inclusions during initiation of crevice corrosion
[DE88-014635] N89-10989
Spectrography analysis of stainless steel by the point to point technique
[DE88-702302] N89-10992
Optimization of transparent and reflecting electrodes for amorphous silicon solar cells
[DE88-001175] N89-11316
Experimental study of time-varying current flow between electrodes immersed in a laboratory magnetoplasma N89-11521

ELECTRODYNAMICS
A time-dependent model for the low-latitude ionosphere
[AD-A196683] N89-11354
Electrodynamics of single-crystal Eu(sub 2)CuO(sub 4): A boson excitation spectrum
[DE88-014328] N89-11585

ELECTROJETS
Association of plasma sheet variations with auroral changes during substorms
[DE88-014319] N89-11350

ELECTROLYTES
Research needs in high temperature chemistry
[DE88-012929] N89-10961
Electrochemical reactions of mixed cobalt/nickel oxide hydroxides in alkaline electrolyte
[ATR-86(9561)-4] N89-10965
Low frequency dielectric properties of polyether electrolytes
[AD-A196494] N89-11039
Compatibility and performance of separators in Li/SOCl(sub 2) cells
[DE88-011090] N89-11116

ELECTROLYTIC CELLS
Corrosion phenomena during overcharge in polymer electrolyte cells
[AD-A196997] N89-11134
Lithium secondary batteries: Role of polymer cathode morphology
[AD-A196998] N89-11135

ELECTROMAGNETIC COUPLING
Electroproduction of baryon resonances aboce the delta(1232)
[CEBAF-PR-88-012] N89-11499

ELECTROMAGNETIC FIELDS
A preliminary study on the use of magnetohydrodynamic forces to remove impurities from molten metals
[DE88-013508] N89-10991
Interaction of electromagnetic waves with heterogeneous bodies of arbitrary shape and parameters N89-11095
Development and testing of KITES
[DE88-015057] N89-11336

ELECTROMAGNETIC INTERFERENCE
Manual, voice, and automated control of a teleoperator viewing system
[DE88-011835] N89-11235

ELECTROMAGNETIC RADIATION
Through-the-earth communication: Experiment results from Billie Mine and Mississippi Chemical Mine
[DE88-013162] N89-11072
Synthesis of resistive tapers to control scattering patterns of strips
[AD-A196402] N89-11110
The propagation of electromagnetic waves in thin dielectric slabs
[AD-A196995] N89-11115
The interpretation of electromagnetic nondestructive flaw detection in metals N89-11246
Trapping and acceleration of electron by elliptically polarized electromagnetic wave propagating across static magnetic field
[IPPJ-885] N89-11545

ELECTROMAGNETIC SCATTERING
Polarizability and effective permittivity of layered and continuously inhomogeneous dielectric spheres
[PB88-210091] N89-11104

ELECTROMAGNETIC SHIELDING
Alfven wave studies on a tokamak N89-11517

ELECTROMAGNETIC WAVE TRANSMISSION
The propagation of electromagnetic waves in thin dielectric slabs
[AD-A196995] N89-11115

ELECTROMAGNETS
Optimization of the two-dimensional magnetic field distribution basing on the integral equation method
[DE88-702940] N89-11490

ELECTRON ACCELERATORS
Beam handling and emittance control
[AD-A196789] N89-11509

ELECTRON ATTACHMENT
Electron attachment properties of excited dielectric-gas molecules and their possible use for pulse power switching
[DE88-009705] N89-11117
ELECTRON AVALANCHE
Statistical effects in high-power microwave beam propagation
[DE88-012440] N89-11100
ELECTRON BEAMS
Plasma exposure tests of a carbon fiber/epoxy composite
[DE88-014724] N89-10947
Other properties of free electron lasers: Harmonics and optical guiding
[DE88-014161] N89-11199
Los Alamos XUV free electron laser proposal
[DE88-013485] N89-11211
ELECTRON DIFFRACTION
Constraints on the growth of metallic superlattices
[DE88-014633] N89-11586
ELECTRON DIFFUSION
Defect model for the electronic conduction and breakdown in dielectric thin films N89-11563
ELECTRON MICROSCOPY
Microscopy and microanalysis of shock-processed materials
[DE88-008471] N89-10990
Characterization of ceramic films and interfaces by electron microscopic and spectroscopic techniques
[DE88-011957] N89-11029
Electron microscopy of modulated and ordered alloys
[DE88-008667] N89-11584
Dynamic Interactions of Energetic Probes with Condensed Matter: Proceedings
[DE88-008882] N89-11589
ELECTRON SPECTROSCOPY
Characterization of ceramic films and interfaces by electron microscopic and spectroscopic techniques
[DE88-011957] N89-11029
ELECTRON TRANSFER
A composite photobioelectronic material
[DE88-012490] N89-11383
ELECTRON TUNNELING
Dynamic Interactions of Energetic Probes with Condensed Matter: Proceedings
[DE88-008882] N89-11589
ELECTRON-ION RECOMBINATION
Atomic processes in high temperature plasmas
[DE88-013005] N89-11525
ELECTRONIC COUNTERMEASURES
Synthesis of resistive tapers to control scattering patterns of strips
[AD-A196402] N89-11110
ELECTRONIC EQUIPMENT
Microsoldering and microminiature welding with lasers
[DE88-013368] N89-11240
Quality assurance manual. Volume 2: Appendices
[DE88-013880] N89-11247
ELECTRONIC SPECTRA
Electronic properties of 3-5 semiconductor alloys N89-11560
ELECTRONS
The geographical distributions of electrons (0.05-3.2 MeV) and protons (0.58-35 MeV) at altitudes of 350-850 km
[ISAS-RN-358] N89-11335
Development and testing of KITES
[DE88-015057] N89-11336
Phonon-plasmon mechanism of high-T(sub c) superconductivity
[DE88-014869] N89-11600
ELECTROPLATING
Ternary adamantine materials for low-cost solar cells
[DE88-001160] N89-11302
ELLIPSES
Calculating the CEP (Circular Error Probable)
[NASA-CR-182996] N89-11475
EMISSION SPECTRA
Laser plume temperature measurements in various gases
[DE88-006462] N89-11204
Collective resonance fluorescence in an intense laser field with phase and amplitude fluctuations
[DE88-702920] N89-11205
Measurements of proton and triton spectra in ASDEX discharges — tokamak N89-11541
EMOTIONAL FACTORS
Individual differences in adaptation to hypoxia and cold based on emotional-behavioral criterion of bodily reactivity N89-11386
ENCAPSULATING
Coefficients of thermal expansion of common encapsulants
[DE88-015026] N89-10983
END EFFECTORS
Space-based multifunctional end effector systems functional requirements and proposed designs
[NASA-CR-180390] N89-11237
ENERGY ABSORPTION
Worldwide survey of absorption fluids data
[DE88-013204] N89-10972
ENERGY BUDGETS
A limited assessment and characterization of the solar radiation energy resources in the Caribbean region
[DE88-001133] N89-11312
ENERGY CONSERVATION
Laboratory examination and seasonal analyses of the dynamic losses for a continuously variable speed heat pump
[DE88-013207] N89-11174
Entrainment enhancement of a supersonic jet for advanced ejectors
[DE88-013200] N89-11177
ENERGY CONSUMPTION
Development of a semi-empirical model for estimating the global solar radiation
[INPE-4620-TDL/328] N89-11352
ENERGY DISTRIBUTION
A limited assessment and characterization of the solar radiation energy resources in the Caribbean region
[DE88-001133] N89-11312
ENERGY LEVELS
The compatibility of gravity and kaon results in the search for new forces
[DE88-013993] N89-11612
ENERGY STORAGE
Phase change problem related to thermal energy storage in the manned space station
[DE88-011390] N89-10933
ENERGY TECHNOLOGY
Geothermal energy technology: Issues, R and D needs, and cooperative arrangements
[DE88-011804] N89-11299
ENERGY TRANSFER
Incipient spall, crack branching, and fragmentation statistics in the spall process
[DE88-009587] N89-11251
ENGINE DESIGN
Experimental guidelines for the design of turbine rotor fragment containment rings
[DOT/FAA/CT-88/21] N89-10893
ENGINE FAILURE
Statistics on aircraft gas turbine engine rotor failures that occurred in US commercial aviation during 1962
[DOT/FAA/CT-88/23] N89-10892
ENGINE INLETS
De-icing of aircraft turbine engine inlets
[DOT/FAA/CT-87/37] N89-10894
Study of three dimensional boundary layers on the front of a fuselage and at an air intake
[CERT-OA-22/5025-AYD] N89-11184
ENTRAINMENT
Entrainment enhancement of a supersonic jet for advanced ejectors
[DE88-013200] N89-11177
ENTROPY
Temperature dependence of entropies and specific heats of liquid Na and K
[DE88-702986] N89-10976
ENVIRONMENT EFFECTS
Markers of air pollution in forests: Nutrient cycling
[DE88-011011] N89-11319
Environmental projects. Volume 7: Environmental resources document
[NASA-CR-182736] N89-11328
ENVIRONMENTAL MONITORING
NOAA (National Oceanic and Atmospheric Administration) Meteorology Division support to the Environmental Protection Agency
[PB88-213624] N89-11327
Environmental projects. Volume 7: Environmental resources document
[NASA-CR-182736] N89-11328
Carbon monoxide measurements in different Brazilian ecosystems
[INPE-4668-PRE/1368] N89-11331
EPIDEMIOLOGY
JPRS report: Science and technology. USSR: Life sciences
[JPRS-ULS-87-010] N89-11385
EPITAXY
Constraints on the growth of metallic superlattices
[DE88-014633] N89-11586
EPITHELIUM
Biological applications and effects of optical masers
[AD-A196462] N89-11217
EPOXY MATRIX COMPOSITES
The Purdue University Get Away Special II (PUGAS II) N89-10918
EQUATIONS
Equational problems and disunification
[RR-727-I-IMAG-82-LIFIA] N89-11471
EQUATIONS OF MOTION
Aerodynamic design considerations for a free-flying ducted propeller
[DE88-006867] N89-10841
On 1-D closure models for slender 3-D viscoelastic free jets: von Karman flow geometry and elliptical cross section
[DE88-014478] N89-11179
Experimental verification of a model of a two-link flexible, lightweight manipulator
[NASA-CR-183216] N89-11233
Control design and performance evaluation for flexible manipulators N89-11390
Anomalous transport arising from nonlinear resistive pressure-driven modes in a plasma
[DE88-014984] N89-11531
EQUATIONS OF STATE
Near-critical NaCl-H2O: An equation of state and discussion of anomalous properties
[DE88-012029] N89-10969
Brillouin scattering at high pressures
[DE88-011972] N89-11497
Vortex lattices in theory and practice
[DE88-014393] N89-11576
Astrophysical evidence on the equation of state
[DE88-011960] N89-11668
EQUATORIAL REGIONS
The climatological seasonal response of the ocean mixed layer in the equatorial and tropical Pacific Ocean
[AD-A196962] N89-11382
EQUIPMENT SPECIFICATIONS
User equipment overview N89-10879
Baseline configuration data set: NASA Standard Initiator-2 (NSI-2)
[NASA-CR-172071] N89-11050
Multicolor pyrometer for materials processing in space
[NASA-CR-183189] N89-11057
Vacuum Fizeau wedge wavemeter for pulsed UV lasers
[DE88-015832] N89-11206
The Cooperative VAS Program with the Marshall Space Flight Center
[NASA-CR-179377] N89-11361
EROSION
Ions generated on or near satellite surfaces
[AD-A196966] N89-10940
Methodologies for prediction of metal oxidation-vaporization-erosion
[DE88-013623] N89-11001
Remote sensing and hydrologic modeling of arid watersheds: A scale analysis
[DE88-014625] N89-11293
Photoerosion and the abundances of the light elements
[NASA-CR-183372] N89-11675
ERROR ANALYSIS
The Global Positioning System (GPS) accuracy, system error budget, space and control segment overview N89-10877
GPS/interial navigation system integration for enhanced navigation performance and robustness N89-10880
Probabilistic error model of robot end-effector's dynamic state N89-11236
Parametric analysis of map data
[AD-A196908] N89-11298
Calculating the CEP (Circular Error Probable)
[NASA-CR-182996] N89-11475
ERROR CORRECTING DEVICES
ACTS and OLYMPUS propagation experiments N89-11091
ERRORS
Aeronautical decision making for commercial pilots
[DOT/FAA/PM-86/42] N89-10870
Numerical estimates of the rate of convergence for the vortex sheet method
[DE88-013809] N89-11178
ESTIMATES
Numerical estimates of the rate of convergence for the vortex sheet method
[DE88-013809] N89-11178
Estimating evapotranspiration of an irrigated surface from upwind and downwind vertical profiles of temperature and humidity
[AD-A196409] N89-11375
ESTIMATING
Cubic spline smoothing: A useful tool for curve estimation
[PB88-214796] N89-11452
Robust covariance matrix estimation via robust estimation of principal components
[PB88-126594] N89-11478

ETHERS
New non-linear optical polymers
[AD-A196859] N89-11040
EULER EQUATIONS OF MOTION
High resolution schemes for three-dimensional Euler equations. 1: Estimation of recent TVD schemes
[PB88-214416] N89-10845
An iterative scheme for numerical solution of transonic small perturbation equation
[TM-AE-8801] N89-11455
EULER-LAGRANGE EQUATION
Modeling of combustion processes of stick propellants via combined Eulerian-Lagrangian approach
N89-11163
EUROPE
Review of acid rain models for Europe
[DE88-011945] N89-11322
European examples of evaluating the effectiveness of information centres and services N89-11628
EUROPEAN SPACE PROGRAMS
Fundamental science in ESA's space science program
N89-11654
EUROPIUM
Electrodynamics of single-crystal Eu(sub 2)CuO(sub 4): A boson excitation spectrum
[DE88-014328] N89-11585
EUTECTICS
Microstructure and properties of rapidly solidified beryllium-transition metal alloys
[DE88-010937] N89-11012
EVALUATION
Design and evaluation of a cockpit display for hovering flight
[NASA-CR-183247] N89-10900
Workshops and problems for benchmarking eddy current codes
[DE88-009996] N89-11098
Evaluation of vapor compression cycles using nonazeotropic refrigerant mixtures
[DE88-013225] N89-11169
Measures, methods and models employed in evaluating the effectiveness of information centers and services
N89-11627
Evaluating for information center planning
N89-11632
EVAPORATION
Experiments on liquid-vapour phase change between plane liquid surfaces. Part 1: Experiments with water, freon and mercury
[TM-FM-8804-PT-1] N89-10964
Liquid-vapour phase change between plane liquid surfaces: A continuum analysis to determine real gas effects
[TM-FM-8803] N89-10971
Deposition and characterization of ZnS/Si heterojunctions produced by vacuum evaporation
[NASA-TM-101359] N89-11129
EVAPOTRANSPIRATION
Estimating evapotranspiration of an irrigated surface from upwind and downwind vertical profiles of temperature and humidity
[AD-A196409] N89-11375
EVOLUTION (DEVELOPMENT)
The Global Positioning System (GPS) constellation and coverage N89-10876
EXCIMER LASERS
Near surface chemistry and corrosion behavior of excimer laser surface-melted AISI type 304 stainless steel
[DE88-014440] N89-11019
EXCITATION
The decay of highly excited open strings
[NASA-CR-183364] N89-11501
Phonon-plasmon mechanism of high-T(sub c) superconductivity
[DE88-014869] N89-11600
EXCITONS
Coulomb states in atoms and solids
[DE88-013973] N89-11494
EXHAUST CLOUDS
HCl measurements in space vehicle exhaust clouds
[DE88-013815] N89-10942
EXHAUST GASES
The 1987 Ground Vortex Workshop
[NASA-CP-10008] N89-10849
HCl measurements in space vehicle exhaust clouds
[DE88-013815] N89-10942
EXHAUST NOZZLES
Effects of a ground vortex on the aerodynamics of an airfoil N89-10855
EXPERIMENTATION
PiFEx data and archival formats N89-11076
EXPERT SYSTEMS
Elaboration of specifications for an expert system to aid the choice of analytical methods of orbit extrapolation for satellite localization
[CNES-CT/DTI/MS/MN/160] N89-10924
Automated knowledge generation
[NASA-CR-181317] N89-11440
The transformative compression of coherent languages N89-11623
EXPLOITATION
Exploitation and utilization of hydrocarbons
[DE88-012626] N89-11048
EXPLOSIONS
Experimental and analytical study of vapor explosions in stratified geometries
[DE88-011964] N89-11046
Role of deflagration in explosive response
[DE88-014139] N89-11049
EXPLOSIVES
The initiation and detonation of explosives: An alternative concept
[DE88-014199] N89-11047
Shock initiation of explosives with a sensitive rate and related topics
[DE88-008483] N89-11052
High-speed photography of energetic materials and components with a copper vapor laser
[DE88-012869] N89-11212
Smart semiconductor bridge (SCB) igniter for explosives
[DE88-012669] N89-11551
EXPONENTIAL FUNCTIONS
Determination of complex exponentials, least squares and prediction methods
[AD-A196498] N89-11474
EXPOSURE
Functional assessment of laser irradiation
[AD-A196930] N89-11222
EXTINCTION
A new determination of extinction due to atmospheric aerosols and the resulting implications for upper stratospheric ozone depletion N89-11348
EXTRACTION
Extraction of light gasses from Mars or its moons
[DE88-009123] N89-11681
EXTRAPOLATION
Elaboration of specifications for an expert system to aid the choice of analytical methods of orbit extrapolation for satellite localization
[CNES-CT/DTI/MS/MN/160] N89-10924
Abstraction in numerical methods
[AD-A196990] N89-11476
EXTRATERRESTRIAL LIFE
Probable locations of extraterrestrial civilizations
[DE88-702605] N89-11392
EXTRATERRESTRIAL RADIATION
Systems report for payload G-652: Project origins
N89-10911
Verification of single event upset rate estimation methods with on-orbit observations
[AD-A196226] N89-10935
Fabricate, calibrate and test a dosimeter for integration into the CRRES (Combined Release and Radiation Effects Satellite) satellite
[AD-A196496] N89-10938
EXTREME ULTRAVIOLET RADIATION
Los Alamos XUV free electron laser proposal
[DE88-013485] N89-11211
EXTREMELY LOW RADIO FREQUENCIES
Through-the-earth communication: Experiment results from Billie Mine and Mississippi Chemical Mine
[DE88-013162] N89-11072

F

F-15 AIRCRAFT
F-15 SMTD low speed jet effects wind tunnel test results N89-10853
F-18 AIRCRAFT
Some statistical aspects of attrition studies
[AD-A196665] N89-10891
FABRICATION
Fabricate, calibrate and test a dosimeter for integration into the CRRES (Combined Release and Radiation Effects Satellite) satellite
[AD-A196496] N89-10938
Amorphous silicon photovoltaic devices prepared by chemical and photochemical vapor deposition of higher order silanes
[DE88-001189] N89-11311
Studies in advanced silicon solar cells
[DE88-013143] N89-11314
The critical current density, the fabrication process and the microstructure in superconducting composites of NbTi for high energy physics
[DE88-014241] N89-11568
Preparation and evaluation of mercuric iodide for crystal growth
[DE88-014981] N89-11578
Chemical preparation of powders and films for high temperature superconductors
[DE88-015266] N89-11601
FABRICS
Experimental guidelines for the design of turbine rotor fragment containment rings
[DOT/FAA/CT-88/21] N89-10893
FABRY-PEROT INTERFEROMETERS
Three component laser anemometer measurements in an annular cascade of core turbine vanes with contoured end wall
[NASA-TP-2846] N89-10844
Brillouin scattering at high pressures
[DE88-011972] N89-11497
FAILURE ANALYSIS
Program of research in structures and dynamics
[NASA-CR-183191] N89-10838
Experimental guidelines for the design of turbine rotor fragment containment rings
[DOT/FAA/CT-88/21] N89-10893
Determination of the unstable states of the solid state plasma in semiconductor devices
[AD-A196403] N89-11550
FAILURE MODES
Defect model for the electronic conduction and breakdown in dielectric thin films N89-11563
FAR INFRARED RADIATION
Far infrared linear response and radio frequency nonlinear response of charge density wave conductors and high T(sub c) superconductors
[DE88-013595] N89-11582
FARM CROPS
Estimating evapotranspiration of an irrigated surface from upwind and downwind vertical profiles of temperature and humidity
[AD-A196409] N89-11375
FARMLANDS
Technique for obtaining agricultural property boundaries through satellite imagery, certified to control and accompany agricultural activity
[INPE-4640-PRE/1351] N89-11294
FATIGUE (BIOLOGY)
Enhancing performance under stress by information about its expected duration
[AD-A196836] N89-11388
FATIGUE LIFE
Tension fatigue analysis and life prediction for composite laminates
[NASA-TM-100549] N89-10951
FATIGUE TESTS
JPRS Report: Science and Technology. USSR: Materials Science
[JPRS-UMS-88-007] N89-11002
Methodology of flexural fatigue testing composite materials produced by electron-beam evaporation
N89-11003
Creep tests for slow and fast fatigue conditions on aluminum alloy specimens
[REPT-M0-535200] N89-11020
FAULT TOLERANCE
Risk analysis of earth return options for the Mars rover/sample return mission
[NASA-CR-172081] N89-10923
FAULT TREES
Reliability analysis of lithium cells
[DE88-009258] N89-11300
FEASIBILITY ANALYSIS
MAGLEV: The double benefits of high-Tc superconductors and its development as an aerospace technology
[DE88-012005] N89-11570
FEMALES
Effect of physical fitness on response to orthostasis in healthy young women
[AD-A196377] N89-11387
FERMIONS
Strongly interacting fermion systems: Emphasis on heavy fermions
[DE88-014127] N89-11573
FIBER COMPOSITES
Laminate behavior for SiC fiber-reinforced reaction-bonded silicon nitride matrix composites
[NASA-TM-101350] N89-10952
FIBER OPTICS
Fiber optic buses and networks for advanced avionics architectures N89-10836
State-of-the-art in fiber optic systems at the Aeronautic Test Center, Toulouse (France)
[REPT-363300] N89-11513

Unidirectional Manchester encoded data transfer via a fiber optic link
[AD-A196961] N89-11516

FIBERS
Computer simulation of the uni-axial stress-strain behavior of ribbon-like fiber nonwovens N89-11264

FIELD EFFECT TRANSISTORS
Tunneling junctions and the field effect
[DE88-013707] N89-11597

FIELD THEORY (PHYSICS)
Nongradient diffusion in premixed turbulent flames N89-11161
Geometrical methods in quantum field theory: On the topology of spaces of holomorphic maps N89-11611

FIGHTER AIRCRAFT
Computing system configuration for fighter aircraft flight control systems N89-10832
A highly reliable computer for airborne applications N89-10833

FILAMENT WINDING
Performance of a circular body earth-to-orbit winged transport with various strap-on boosters
[NASA-TM-100603] N89-10929

FILAMENTS
Comparison between Uramoto type and straight filament type sheet plasmas as a volume produced H(-) ion source (I)
[IPPJ-876] N89-11523

FILE MAINTENANCE (COMPUTERS)
Computerized classified document accountability
[DE88-015054] N89-11633

FINITE DIFFERENCE THEORY
A computational study of coherent structures in the wakes of two-dimensional bluff bodies
[AD-A196820] N89-11188
Guidelines for using TIPSFD for 3D finite-difference mesh generation
[DE88-012451] N89-11417

FINITE ELEMENT METHOD
Aeroelasticity and structural optimization of helicopter rotor blades with swept tips N89-10887
Investigations in the nonlinear domain of composite laminate plates subject to compression loads
[ONERA-RT-17/3542-RY-070-R] N89-10953
Mechanics of hydrogen embrittlement N89-11000
Developing laminar flow and heat transfer in ducts of arbitrary cross section N89-11176
Experimental verification of a model of a two-link flexible, lightweight manipulator
[NASA-CR-183216] N89-11233
The mini-oscillator technique: A finite element method for the modeling of linear viscoelastic structures
[UTIAS-323] N89-11250
Benchmark study of shear buckling of a cylindrical vessel
[PB88-125315] N89-11257
Dynamic analysis of spherical shells: A hybrid method
[EPM/RT-88/23] N89-11264
Finite element analysis of large strain elastic-plastic solids N89-11281
Aircraft crashes on the runway: Development of a super element for nonlinear analysis of a beam
[REPT-87/56] N89-11286
Finite element analysis of shell structures with an 18-node 3-dimensional solid element based on a new mixed formulation
[AD-A196698] N89-11288
Finite elements software and applications N89-11415
TRINITY II: A post-processing program for 2-dimensional finite element analysis data
[DE88-010107] N89-11416

FINS
Experimental research on swept shock wave/boundary layer interactions
[AD-A196938] N89-11189

FIRE PREVENTION
Aircraft accident report: Executive Air Charter, Inc., dba American Eagle, Flight 5452, CASA C-212, N432CA, Mayaguez, Puerto Rico, May 8, 1987
[PB88-910409] N89-10873

FIREFLIES
GAS-611 firefly in zero gravity N89-10912

FLAME PROPAGATION
Reaction rates in premixed turbulent flames and their relevance to the turbulent burning speed
[DE88-012021] N89-10960
A study of the effect of thermal radiation on laminar flame propagation and ignition, 1981-1987 N89-10967
Fluid mechanical properties of flames in enclosures
[DE88-014142] N89-10981

FLAME RETARDANTS
Aircraft accident report: Executive Air Charter, Inc., dba American Eagle, Flight 5452, CASA C-212, N432CA, Mayaguez, Puerto Rico, May 8, 1987
[PB88-910409] N89-10873

FLAMES
Modeling of combustion processes of stick propellants via combined Eulerian-Lagrangian approach N89-11163

FLASH BLINDNESS
Functional assessment of laser irradiation
[AD-A196930] N89-11222

FLAT PLATES
Polarisation converters for a DBS flat-plate antenna
[BBC-RD-1988/7] N89-11073
A flat-plate antenna for DBS reception
[BBC-RD-1988/6] N89-11096
Array elements for a DBS flat-plate antenna
[BBC-RD-1988/8] N89-11103
Bursting phenomenon in a flat plate pulsed boundary layer
[CERT-RSF-OA-69/2259-AYD] N89-11183

FLEXIBILITY
Robust control of a flexible manipulator arm N89-11228
Experimental verification of a model of a two-link flexible, lightweight manipulator
[NASA-CR-183216] N89-11233
Control design and performance evaluation for flexible manipulators N89-11390

FLEXIBLE BODIES
A comparative overview of modal testing and system identification for control of structures N89-11262

FLEXING
Methodology of flexural fatigue testing composite materials produced by electron-beam evaporation N89-11003
Transverse flexure of an elastic plate loaded through a rigid inclusion N89-11267

FLIGHT CONTROL
Computing Systems Configuration for Highly Integrated Guidance and Control Systems
[AGARD-LS-158] N89-10831
Computing system configuration for fighter aircraft flight control systems N89-10832
The use of the complex summation method for formulating algorithms for decoupling vertical/horizontal motions of rolling aircraft N89-10889

FLIGHT CREWS
In-service evaluation of the Traffic Alert and Collision Avoidance System (TCAS) industry prototype
[DOT/FAA/SA-88/2] N89-10885

FLIGHT HAZARDS
Investigation of wake vortices of landing aircraft at Frankfurt airport (Federal Republic of Germany)
[DFVLR-MITT-88-15] N89-10862

FLIGHT MECHANICS
Flight mechanics and aerothermodynamic software
[CNES-CT/DTI/MS/MN/069] N89-10839

FLIGHT SAFETY
Aeronautical decision making for air ambulance helicopter pilots: Situational awareness exercises
[DOT/FAA/DS-88/6] N89-10869
Aeronautical decision making for commercial pilots
[DOT/FAA/PM-86/42] N89-10870
Aircraft accident reports, brief format, US civil and foreign aviation, issue number 2 of 1987 accidents
[PB88-916906] N89-10871

FLIGHT SIMULATION
Sandia National Laboratories flight simulation facilities
[DE88-012108] N89-10898
Design and evaluation of a cockpit display for hovering flight
[NASA-CR-183247] N89-10900

FLIGHT SIMULATORS
Prototype data acquisition and analysis system for Navy operational flight simulators
[DE88-014557] N89-10901

FLIGHT TEST VEHICLES
A free-flight experiment of vehicles ranging from high subsonic to high supersonic speeds
[ISAS-RN-362] N89-10888

FLIGHT TESTS
Non-linear aerodynamic characteristics obtained from the analysis of flight-data
[AR-004-571] N89-10866
Sandia National Laboratories flight simulation facilities
[DE88-012108] N89-10898
CAD wind tunnel test for half-cut model of Asuka N89-11069

FLIR DETECTORS
Parametric analysis of map data
[AD-A196908] N89-11298

FLOATING
Experiments in control of satellite manipulators N89-11391

FLOATING POINT ARITHMETIC
Presentation of research and development action 1206: Preliminary study report on the CESTAC method --- calculation check
[CNES-CT/PTI/MS/MN/067] N89-11424

FLOORS
Longitudinal impact test of a transport airframe section
[DOT/FAA/CT-87/26] N89-11265

FLOW COEFFICIENTS
Basic rules of saturated gain variation in a flowing laser cavity
[AD-A196861] N89-11220

FLOW DISTRIBUTION
Summary of an experimental investigation on the ground vortex N89-10851
Ground vortex flow field investigation N89-10852
An assessment of ground effects determined by static and dynamic testing techniques N89-10854
Study of flow past a circular cylinder using a higher order scheme for Navier-Stokes equation
[TM-FM-8806] N89-11142
Turbulence modeling of gas-solid suspension flows N89-11156
Measurements and predictions of mixed convection in laminar and turbulent boundary layer flows N89-11164
Topologically related quantities in turbulent flows N89-11173
Experimental research on swept shock wave/boundary layer interactions
[AD-A196938] N89-11189
Basic rules of saturated gain variation in a flowing laser cavity
[AD-A196861] N89-11220
Experimental and theoretical studies on transport processes in laser welding
[DE88-013933] N89-11230
A nonlinear wave-wave interaction theory for the generation of multi-scale large eddies in a neutral atmospheric boundary layer N89-11344
An investigation of the internal structure of the thunderstorm outflow with particular attention to multiple surges N89-11357

FLOW MEASUREMENT
Three component laser anemometer measurements in an annular cascade of core turbine vanes with contoured end wall
[NASA-TP-2846] N89-10844

FLOW STABILITY
Reynolds stress closure in jet flows using wave models
[NASA-CR-180226] N89-10843
Observations of breakup processes of liquid jets using real-time X-ray radiography N89-11160
Periodically structured multiphase flows and hydrodynamic instabilities in narrow capillaries
[DE88-015608] N89-11181
Theory of instabilities in the laminar boundary layer: Literature review
[DERAT-42/5618-28] N89-11185
Boundary layer transition
[CERT-OA-40/5018-AYD] N89-11187

FLOW THEORY
Theory of instabilities in the laminar boundary layer: Literature review
[DERAT-42/5618-28] N89-11185
Studies of barotropic flow over topography using a galerkin finite element model
[AD-A196516] N89-11353

FLOW VELOCITY
The characteristics of the ground vortex and its effect on the aerodynamics of the STOL configuration N89-10850
Summary of an experimental investigation on the ground vortex N89-10851
Hydrodynamical characteristics of helium two-phase flows at relatively high mass rates
[DE88-702936] N89-11143
On the constitutive relation for frictional flow of granular materials
[DE88-001089] N89-11171

FLOW VISUALIZATION
Ground vortex flow field investigation N89-10852
Flow around a delta wing with or without a canard (Phi BA = 60 deg). Part 2: Hydrodynamic visualizations in unsteady flow (pitching oscillations)
[ONERA-RT-11/2891-AN-PT-2] N89-10860
Unsteady low-speed windtunnel test of a straked delta wing, oscillating in pitch. Part 1: General description and discussion of results
[AD-A196456] N89-10867
Laser/fluorescent dye flow visualization technique developed for system component thermal hydraulic studies
[DE88-012008] N89-11137

FLUID DYNAMICS
Fluid science investigations in microgravity
[PB88-209754] N89-11058
Laser/fluorescent dye flow visualization technique developed for system component thermal hydraulic studies
[DE88-012008] N89-11137

Mixing and Demixing Processes in Multiphase Flows With Application to Propulsion Systems
[NASA-CP-3006] N89-11153
Turbulence modeling of gas-solid suspension flows N89-11156

FLUID FLOW
Oxygen chemistry
[AD-A196989] N89-10988
Friction reduction and heat transfer enhancement in turbulent pipe flow of non-Newtonian liquid-solid mixtures
[DE88-010018] N89-11138
Rotating and stratified fluids N89-11343
Second order parabolic equations for flow-domains
[DE88-703158] N89-11457

FLUID JETS
Observations of breakup processes of liquid jets using real-time X-ray radiography N89-11160

FLUID MANAGEMENT
Development of Bio-GAS systems N89-10904

FLUID MECHANICS
Fluid mechanical properties of flames in enclosures
[DE88-014142] N89-10981

FLUID POWER
Oxygen chemistry
[AD-A196989] N89-10988

FLUTTER ANALYSIS
New trial of vibration testing method N89-11068

FLUX DENSITY
Magnetic moment test report for the model SAR 8108 battery
[INPE-4574-NTE/280] N89-11121
The turbulent heat flux in low Mach number flows with large density variations N89-11162

FLYBY MISSIONS
Outward to the beginning: The CRAF and Cassini Missions of the Mariner Mark 2 program
[NASA-CR-183133] N89-10921
Dust detection systems for cometary encounter N89-11680

FOAMS
Utilization of spray on foam insulation for manned and unmanned spacecraft and structures N89-10914
Microporous polymer foams for biomaterials
[DE88-010578] N89-11036
Potential foams and metal foils for cosmic dust capture
[DE88-012960] N89-11665

FOCUSING
JPRS Report: Science and Technology. USSR: Materials Science
[JPRS-UMS-88-007] N89-11002
Characteristics of laser beam focusing with single spherical mirrors during laser treatment N89-11004
A survey of digital beam forming techniques and current technology
[AD-A196376] N89-11514

FOKKER-PLANCK EQUATION
A code for the solution of the Vlasov-Fokker-Planck equation in one or two dimensions
[DE88-013288] N89-11483

FOLIAGE
Results of 1987 MSS helicopter propagation experiment at UHF and L band in Central Maryland N89-11077

FORCE DISTRIBUTION
Understanding bandwidth limitations in robot force control
[AD-A195927] N89-11229

FORCED CONVECTION
A numerical modeling study of frontogenesis and cold frontal rainbands N89-11358

FORCED VIBRATION
Dynamic behavior of helical springs N89-11278

FORECASTING
Exploitation and utilization of hydrocarbons
[DE88-012626] N89-11048
The role of a lid in the 31 May 1985 tornado outbreak
[AD-A196684] N89-11377

FORESTS
Improvement and extension of a radar forest backscattering model
[NASA-CR-183259] N89-11292
Markers of air pollution in forests: Nutrient cycling
[DE88-011011] N89-11319
CIR aerial photography applied to the evaluation of the air pollution impact in a tropical forest: The case of Cubatao, Brazil
[INPE-4651-PRE/1358] N89-11324

FORMAT
PIFEx data and archival formats N89-11076

FORMING TECHNIQUES
Finite element analysis of large strain elastic-plastic solids N89-11281

FORTRAN
Vectorization of FORTRAN programs at do-loop level N89-11398
Restructuring of basic linear algebraic algorithms, chapter 5 N89-11399

FORWARD SCATTERING
Interference by rain scatter N89-11084

FOUNDATIONS
The Shock and Vibration Digest, Volume 20, No. 8 N89-11258
Dynamic behavior of foundations in bilateral and unilateral contact N89-11259

FOURIER ANALYSIS
The steady states of the Kuramoto–Sivashinsky equation
[DE88-011819] N89-11451
Periodic solutions of the Hamilton-Jacobi equation by the shooting method: A technique for beam dynamics
[DE88-012733] N89-11460

FOURIER TRANSFORMATION
Collective resonance fluorescence in an intense laser field with phase and amplitude fluctuations
[DE88-702920] N89-11205

FRACTURE MECHANICS
Mechanics of hydrogen embrittlement N89-11000
Impurity-induced changes in interfacial strength and their role in creep fracture
[DE88-013197] N89-11255
Laser speckle photography and decorrelation techniques in elastic-plastic fracture studies N89-11275
A strain rate dependent brittle fracture model based on continuum damage mechanics
[DE88-013361] N89-11285
Creep and fracture characteristics of materials and structures at elevated temperatures
[AD-A196831] N89-11289

FRACTURE STRENGTH
Indentation plasticity and fracture in silicon
[NASA-TP-2863] N89-10996
The effect of carbon and boron nitride additions on the fracture toughness of Si3N4
[DE88-013249] N89-11025
Literature review of strengthening methodologies of existing structures
[PB88-218219] N89-11271

FRACTURES (MATERIALS)
Low stress brittle fractures in polymers
[DE88-014236] N89-11027
A strain rate dependent brittle fracture model based on continuum damage mechanics
[DE88-013361] N89-11285

FRAGMENTATION
Incipient spall, crack branching, and fragmentation statistics in the spall process
[DE88-009587] N89-11251

FRAMES
Literature review of strengthening methodologies of existing structures
[PB88-218219] N89-11271

FREE CONVECTION
Unsteady hydromagnetic free-convection flow with radiative heat transfer in a rotating fluid. 1: Incompressible optically thin fluid
[DE88-702998] N89-11140
Unsteady hydromagnetic free-convection flow with radiative heat transfer in a rotating fluid of arbitrary optical thickness
[DE88-703000] N89-11167
Unsteady hydromagnetic free-convection flow with radiative heat transfer in a rotating fluid. 2: Compressible optically thin fluid
[DE88-702999] N89-11168

FREE ELECTRON LASERS
Other properties of free electron lasers: Harmonics and optical guiding
[DE88-014161] N89-11199
The Electron Laser Facility: Measurement of modes, harmonics, parametric dependence, and phase shift
[DE88-014165] N89-11200
PALADIN: A 10.6-micron free-electron laser amplifier
[DE88-014164] N89-11207
An introduction to the physics of high gain free electron lasers
[DE88-014163] N89-11208
Overview of FEL (Free-Electron Laser) development with induction linacs at LLNL
[DE88-014179] N89-11210
Los Alamos XUV free electron laser proposal
[DE88-013485] N89-11211
Gas-loaded free-electron lasers
[DE88-014652] N89-11213
A gas-loaded, free-electron laser
[DE88-016090] N89-11214
Analysis of free electron laser performance utilizing the National Bureau of Standards' CW microtron
[AD-A196928] N89-11221

FREE FLIGHT
A free-flight experiment of vehicles ranging from high subsonic to high supersonic speeds
[ISAS-RN-362] N89-10888

FREE FLOW
The characteristics of the ground vortex and its effect on the aerodynamics of the STOL configuration N89-10850
Summary of an experimental investigation on the ground vortex N89-10851

FREE JETS
On 1-D closure models for slender 3-D viscoelastic free jets: von Karman flow geometry and elliptical cross section
[DE88-014478] N89-11179

FREE-PISTON ENGINES
Development of a residential free-piston Stirling engine heat pump
[DE88-012917] N89-11303

FREQUENCY DISTRIBUTION
Stochastic theory of frequency redistribution in two-photon processes N89-11669

FREQUENCY DIVISION MULTIPLEXING
Study of the multiplexing of image telemetry data from SPOT 4 HRVIR and Vegetation sensors
[CNES-87/229/CT/DRT/TIT/TR] N89-10930

FREQUENCY HOPPING
On the generation of waveforms having comb-shaped spectra
[AD-A196927] N89-11113

FREQUENCY MODULATION
High frequency inverter-cycloconverter system for dc to ac conversion N89-11120

FRICTION
Friction and impact sensitivities of explosives: A comparative study
[DE88-012864] N89-11051

FRICTION FACTOR
On the constitutive relation for frictional flow of granular materials
[DE88-001089] N89-11171

FRICTION REDUCTION
Friction reduction and heat transfer enhancement in turbulent pipe flow of non-Newtonian liquid-solid mixtures
[DE88-010018] N89-11138

FRONTS (METEOROLOGY)
An investigation of the internal structure of the thunderstorm outflow with particular attention to multiple surges N89-11357
A study of the dynamics of maritime fronts using remotely sensed wind and stress measurements N89-11366

FUEL CELLS
Oxygen chemistry
[AD-A196989] N89-10988
Oxygen electrode in molten carbonate fuel cells
[DE88-009628] N89-11308
Advanced materials for solid oxide fuel cells: Hafnium-praseodymium-indium oxide system
[DE88-015365] N89-11310
Assessment of methanol electro-oxidation for direct methanol-air fuel cells
[DE88-014686] N89-11317

FUEL COMBUSTION
Mixing and Demixing Processes in Multiphase Flows With Application to Propulsion Systems
[NASA-CP-3006] N89-11153

FUNCTIONAL DESIGN SPECIFICATIONS
Elaboration of specifications for an expert system to aid the choice of analytical methods of orbit extrapolation for satellite localization
[CNES-CT/DTI/MS/MN/160] N89-10924

FUNCTIONS (MATHEMATICS)
The vector functions of the MS system 570/CX
[CNES-CT/DTI/MS/MN/019] N89-11423

FURNACES
Oxygen electrode in molten carbonate fuel cells
[DE88-009628] N89-11308

FUSELAGES
Longitudinal impact test of a transport airframe section
[DOT/FAA/CT-87/26] N89-11265

G

GALACTIC CLUSTERS
Dark matter N89-11652

GALACTIC EVOLUTION
Cosmic strings
[NASA-CR-183367] N89-11613
Galaxy formation: Theory and observational tests N89-11644
Colour and spectral synthesis of disk galaxies N89-11656
Inflation, cosmic strings and galaxy formation
[DE88-008629] N89-11666

GALACTIC MASS
Dark matter N89-11652
GALAXIES
Dark matter N89-11652
Inflation, cosmic strings and galaxy formation [DE88-008629] N89-11666
GALERKIN METHOD
Studies of barotropic flow over topography using a galerkin finite element model [AD-A196516] N89-11353
GALLIUM ARSENIDES
Design definition for a digital beamforming processor [AD-A196983] N89-11133
Structural anomalies in undoped Gallium Arsenide observed in high resolution diffraction imaging with monochromatic synchrotron radiation [NASA-CR-183268] N89-11595
Spin-orbit interaction effects in zincblende semiconductors: Ab initio pseudopotential calculations [DE88-014863] N89-11599
Surface passivation of Gallium Arsenide [AD-A196695] N89-11605
GALLIUM PHOSPHIDES
Molecular beam epitaxy of GaP films on Si substrates [PB88-131974] N89-11581
GAMMA RAYS
The history of gamma-ray burst observations [DE88-014390] N89-11685
GAS COOLING
Thermodynamic improvements for the space thermoacoustic refrigerator (STAR) [AD-A196958] N89-11071
GAS DYNAMICS
The gas dynamics of fluids of high specific heat [MPIS-89-1987] N89-11186
GAS FLOW
Turbulence modeling of gas-solid suspension flows N89-11156
Particle dispersion models and drag coefficients for particles in turbulent flows N89-11158
Heat release effects of reacting gas jets in liquids [DE88-011971] N89-11175
On hydromagnetic channel flow induced by tooth pulses [DE88-703031] N89-11522
GAS JETS
Heat release effects of reacting gas jets in liquids [DE88-011971] N89-11175
GAS LASERS
A gas-loaded, free-electron laser [DE88-016090] N89-11214
Basic rules of saturated gain variation in a flowing laser cavity [AD-A196861] N89-11220
GAS TRANSPORT
Beam handling and emittance control [AD-A196789] N89-11509
GAS TUNGSTEN ARC WELDING
The potential of a GAS can with payload G-169 N89-10916
Joining of advanced aluminides [DE88-015111] N89-11226
GAS TURBINE ENGINES
Statistics on aircraft gas turbine engine rotor failures that occurred in US commercial aviation during 1982 [DOT/FAA/CT-88/23] N89-10892
GAS TURBINES
Experimental investigation of the performance of a supersonic compressor cascade [NASA-TM-100879] N89-10858
JPRS report: Science and technology: Japan [JPRS-JST-87-018] N89-11061
Research on catalyst combustion for gas turbine N89-11063
GAS-SOLID INTERACTIONS
Turbulence modeling of gas-solid suspension flows N89-11156
GASES
Variational transition state theory [DE88-013756] N89-10959
Mechanisms of gas permeation through polymer membranes [DE88-007761] N89-10980
Kinetics of boron hydride interconversion reactions [AD-A196824] N89-10985
Laser plume temperature measurements in various gases [DE88-006462] N89-11204
Extraction of light gasses from Mars or its moons [DE88-009123] N89-11681
GASOLINE
Exploitation and utilization of hydrocarbons [DE88-012626] N89-11048
GATES (CIRCUITS)
A study of the turn-off behavior of high power gate turn off thyristors (GTO): Computer-aid to design and utilization [LAAS-88-164] N89-11124
GAUGE THEORY
Geometric gauge theory of metric defects [DE88-702961] N89-11269
Lattice gauge theory on the hypercube [DE88-015004] N89-11420
Gauged Q-balls [NASA-CR-183369] N89-11500
Cosmic strings and superconducting cosmic strings [NASA-CR-183361] N89-11604
GELS
Microporous polymer foams for biomaterials [DE88-010578] N89-11036
GEODESY
Integrated database approach for geodetic applications [DE88-012726] N89-11615
GEODETIC SURVEYS
Continuous deformation monitoring with GPS [AD-A196447] N89-10886
Integrated database approach for geodetic applications [DE88-012726] N89-11615
GEOGRAPHY
The geographical distributions of electrons (0.05-3.2 MeV) and protons (0.58-35 MeV) at altitudes of 350-850 km [ISAS-RN-358] N89-11335
GEOLOGICAL FAULTS
Three dimensional gravity modeling techniques with application to the Ennis Geothermal Area, part 1 [DE88-014952] N89-11340
GEOLOGY
Crustal structure of the northwestern United States N89-11349
GEOMAGNETIC PULSATIONS
A global MHD pulsation event with conjugate study and model of ionospheric damping N89-11333
GEOMAGNETIC TAIL
Study of a substorm on May 4, 1986 [DE88-014318] N89-11342
GEOMAGNETISM
A global MHD pulsation event with conjugate study and model of ionospheric damping N89-11333
GEOMETRIC ACCURACY
Geometrical methods in quantum field theory: On the topology of spaces of holomorphic maps N89-11611
GEOMETRIC DILUTION OF PRECISION
The Global Positioning System (GPS) accuracy, system error budget, space and control segment overview N89-10877
GEOMETRY
Continuous deformation monitoring with GPS [AD-A196447] N89-10886
Developing laminar flow and heat transfer in ducts of arbitrary cross section N89-11176
Geometric gauge theory of metric defects [DE88-702961] N89-11269
Optimization of bootstrap current in a large helical system with L = 2 [IPPJ-889] N89-11546
GEOPHYSICS
Atmospheric and Geophysical Sciences Division [DE88-013780] N89-11346
GEOTHERMAL RESOURCES
Geothermal energy technology: Issues, R and D needs, and cooperative arrangements [DE88-011804] N89-11299
Three dimensional gravity modeling techniques with application to the Ennis Geothermal Area, part 1 [DE88-014952] N89-11340
GEOTHERMAL TECHNOLOGY
Geothermal energy technology: Issues, R and D needs, and cooperative arrangements [DE88-011804] N89-11299
GERMANIUM
The electronic and optical properties of silicon/germanium strained layer superlattices N89-11590
GET AWAY SPECIALS (STS)
The 1988 Get Away Special Experimenter's Symposium [NASA-CP-3008] N89-10902
The first Chinese student space shuttle getaway special program N89-10903
Development of Bio-GAS systems N89-10904
TUBSAT-1, satellite technology for educational purposes N89-10905
Future MAUS payload and the TWIN-MAUS configuration N89-10906
Development of experimental systems for material sciences under microgravity N89-10907
HIEN-LO: An experiment for charge determination of cosmic rays of interplanetary and solar origin N89-10908
CSCP: A new Get Away Special (GAS) project N89-10909
STS safety approval process for small self-contained payloads N89-10910
Systems report for payload G-652: Project origins N89-10911
GAS-611 firefly in zero gravity N89-10912
Acceleration ground test program to verify GAS payload No. 559 structure/support avionics and experiment structural integrity N89-10913
Computerized monitoring and control of experiments in space N89-10915
The potential of a GAS can with payload G-169 N89-10916
The Purdue University Get Away Special II (PUGAS II) N89-10918
The transportation of fine arts materials aboard the space shuttle Columbia. GAS payload No. 481: Vertical horizons N89-10919
Inorganic chemical precipitate formation payload design N89-10920
GIOTTO MISSION
Dust detection systems for cometary encounter N89-11680
GLASS
Glass-ceramic fusion with a CO2 laser [DE88-012871] N89-11030
Curved channel MCP improvement program [NASA-CR-180790] N89-11191
Measurement of glass shell buckling strength using a piezoelectric film sensor [DE88-013016] N89-11280
KCl bounce coating of glass and polymer microshells [DE88-013018] N89-11524
What is the origin of glassy behavior in the high-T(sub c) oxides [DE88-012668] N89-11565
GLIDE PATHS
Investigation of wake vortices of landing aircraft at Frankfurt airport (Federal Republic of Germany) [DFVLR-MITT-88-15] N89-10862
GLOBAL POSITIONING SYSTEM
The NAVSTAR GPS System [AGARD-LS-161] N89-10874
The GPS overview and navigation system concept N89-10875
The Global Positioning System (GPS) constellation and coverage N89-10876
The Global Positioning System (GPS) accuracy, system error budget, space and control segment overview N89-10877
GPS signal structure N89-10878
User equipment overview N89-10879
GPS/interial navigation system integration for enhanced navigation performance and robustness N89-10880
Aiding and integration of a GPS receiver N89-10881
Civil and military applications of GPS N89-10882
Differential operation of NAVSTAR GPS for enhanced accuracy N89-10883
GPS navigation processing and Kalman filtering N89-10884
Continuous deformation monitoring with GPS [AD-A196447] N89-10886
Securing the time scale of the NAVEX reference clock and rate determinations by time comparisons with the help of the Global Positioning System (GPS) — Spacelab D1 mission [ESA-TT-1111] N89-11197
GLOBULAR CLUSTERS
New insights into globular clusters from main sequence photometry N89-11658
Low mass X-ray binaries in globular clusters and hierarchical triple systems N89-11660
Multiple populations on the horizontal branch N89-11662
GOALS
Review of aeronautical wind tunnel facilities [NASA-CR-183057] N89-10897
Composite structural materials [NASA-CR-180224] N89-10946
Switchable auto gain amplifier [DE88-012114] N89-11122
GOVERNMENT/INDUSTRY RELATIONS
National Photovoltaics Program: 1987 program review [DE88-001148] N89-11301
National Center for Atmospheric Research [PB88-220009] N89-11355
GRADIENTS
Migration arising from gradients in shear stress: Particle distributions in Poiseuille flow N89-11159

GRAIN BOUNDARIES
Atomistic studies of grain boundaries in alloys and compounds
[DE88-011939] N89-11011
The role of grain boundary character in the environmentally-assisted intergranular cracking mechanism of nickel-base alloys
[DE88-014130] N89-11018
The pair potential approach for interfaces: Fundamental problems and practical solutions
[DE88-009165] N89-11456
Influence of grain boundary structure distribution and processing history on intergranular creep cavitation
[DE88-015808] N89-11571
GRAIN SIZE
Microgravity nucleation and particle coagulation experiments support
[NASA-CR-183282] N89-11056
Spectral studies of three oxisols and a Ultisol of Brazil
[INFE-4644-PRE/1355] N89-11297
GRAND UNIFIED THEORY
Cosmic strings
[NASA-CR-183367] N89-11613
Cosmological puzzles N89-11650
Unified theories and the early universe N89-11651
GRANULAR MATERIALS
On the constitutive relation for frictional flow of granular materials
[DE88-001089] N89-11171
GRAPH THEORY
Undirected distances and the postman-structure of graphs
[RR-714-M] N89-11470
Problem on 0-1 matrices
[PB88-210075] N89-11477
GRAPHITE
Postanalysis of the CNPS (Compact Nuclear Power Source) critical experiment
[DE88-014322] N89-11506
GRAPHITE-EPOXY COMPOSITES
Free damped vibration of composite plates and shells N89-11249
GRAVITATION
Planck's orders of magnitude and the limits of the quantum gravity conception
[DE88-702985] N89-11608
The compatibility of gravity and kaon results in the search for new forces
[DE88-013993] N89-11612
GRAVITATION THEORY
Experimental tests of relativity and gravitation N89-11649
GRAVITATIONAL COLLAPSE
On relative supernova rates and nucleosynthesis roles
[NASA-CR-183373] N89-11673
GRAVITATIONAL CONSTANT
Experimental tests of relativity and gravitation N89-11649
GRAVITATIONAL FIELDS
The compatibility of gravity and kaon results in the search for new forces
[DE88-013993] N89-11612
GRAVITATIONAL WAVE ANTENNAS
Physics and astrophysics of gravitational waves N89-11647
The detection of gravitational radiation N89-11648
GRAVITATIONAL WAVES
Physics and astrophysics of gravitational waves N89-11647
The detection of gravitational radiation N89-11648
GREEN'S FUNCTIONS
A theory of surface and interface electronic properties of crystalline solids: Applications to 2-6 compounds N89-11596
Quantization of Green-Schwarz superstring
[DE88-702242] N89-11609
GREENHOUSE EFFECT
Recent climate change in North America and CO2: Search in stratified daily data
[DE88-014669] N89-11323
GRID GENERATION (MATHEMATICS)
A diagonally inverted LU implicit multigrid scheme for the 3-D Navier-Stokes equations and a two equation model of turbulence
[NASA-CR-182209] N89-10863
Guidelines for using TIPSFD for 3D finite-difference mesh generation
[DE88-012451] N89-11417
GROUND EFFECT (AERODYNAMICS)
The 1987 Ground Vortex Workshop
[NASA-CP-10008] N89-10849
The characteristics of the ground vortex and its effect on the aerodynamics of the STOL configuration N89-10850
Summary of an experimental investigation on the ground vortex N89-10851
Ground vortex flow field investigation N89-10852
An assessment of ground effects determined by static and dynamic testing techniques N89-10854
Effects of a ground vortex on the aerodynamics of an airfoil N89-10855
Numerical investigation of a jet in ground effect using the fortified Navier-Stokes scheme N89-10857
GROUND EFFECT MACHINES
Aerodynamic design considerations for a free-flying ducted propeller
[DE88-006867] N89-10841
GROUND STATE
Self-consistent charge and spin distributions in oxide superconductors
[DE88-012051] N89-11591
GROUND STATIONS
Plan of advanced satellite communications experiment using ETS-VI N89-11089
GROUND TESTS
Acceleration ground test program to verify GAS payload No. 559 structure/support avionics and experiment structural integrity N89-10913
PV modules for ground testing
[NASA-CR-179476] N89-11315
GROUP THEORY
General complex-analytic structures in uniform algebra spectra: A survey
[DE88-703010] N89-11450
Homology classes represented by real algebraic hypersurfaces
[PB88-202908] N89-11453
Real algebraic morphisms into even-dimensional spheres
[PB88-202916] N89-11462
Quasi-adequate semigroups
[DE88-703157] N89-11466
GROWTH
The effect of vapor incidence angle upon thin film columnar growth
[DE88-014396] N89-11577
GUIDANCE (MOTION)
Guidance, sensor control and localization of a mobile autonomous robot
[LAAS-88-131] N89-11241
GUIDANCE SENSORS
Guidance, sensor control and localization of a mobile autonomous robot
[LAAS-88-131] N89-11241
GUN PROPELLANTS
Modeling of combustion processes of stick propellants via combined Eulerian-Lagrangian approach N89-11163
GUSTS
An investigation of the internal structure of the thunderstorm outflow with particular attention to multiple surges N89-11357
GYROSCOPIC STABILITY
The Shock and Vibration Digest, Volume 20, No. 8 N89-11258
Vibrations and stability of mechanical systems: 4 N89-11260

H

HADRONS
Nuclear processes in the early universe. Part 2: The cosmic quark-hadron phase transition N89-11640
HAFNIUM OXIDES
Advanced materials for solid oxide fuel cells: Hafnium-praseodymium-indium oxide system
[DE88-015365] N89-11310
HALLEY'S COMET
Interplanetary magnetic microstructure observed by Sakigake near its closest approach to Comet Halley
[ISAS-RN-349] N89-11667
Dust detection systems for cometary encounter N89-11680
HAMILTON-JACOBI EQUATION
Periodic solutions of the Hamilton-Jacobi equation by the shooting method: A technique for beam dynamics
[DE88-012733] N89-11460
HAMILTONIAN FUNCTIONS
Proceedings of the Focused Research Program on Spectral Theory and Boundary Value Problems. Volume 1: Singular differential systems
[DE88-008151] N89-11461
Possible coexistence of antiferromagnetism and superconductivity in the Hubbard model
[DE88-703025] N89-11561
HANDBOOKS
Propagation handbook, frequencies above 10 GHz N89-11082
HARDNESS
Indentation plasticity and fracture in silicon
[NASA-TP-2863] N89-10996
HARDWARE
Hardware architecture, chapter 2 N89-11396
HARMONIC ANALYSIS
High frequency inverter-cycloconverter system for dc to ac conversion N89-11120
HARMONIC CONTROL
Analysis of nonlinear circuits at RF and microwave frequencies by the harmonic balance method
[INPE-4693-TDL/342] N89-11126
HARMONICS
Other properties of free electron lasers: Harmonics and optical guiding
[DE88-014161] N89-11199
The Electron Laser Facility: Measurement of modes, harmonics, parametric dependence, and phase shift
[DE88-014165] N89-11200
HARRIER AIRCRAFT
Noise of the Harrier in vertical landing and takeoff N89-10856
HEAT
Effects of downdrafts and mesoscale convective organization on the heat and moisture budgets of squall and nonsquall cloud clusters in the tropics N89-11367
HEAT EXCHANGERS
Laser/fluorescent dye flow visualization technique developed for system component thermal hydraulic studies
[DE88-012008] N89-11137
Advanced heat-pipe heat exchanger and microprocessor-based modulating burner controls development
[PB88-217070] N89-11172
HEAT FLUX
The turbulent heat flux in low Mach number flows with large density variations N89-11162
Sensors for ceramic components in advanced propulsion systems: Summary of literature survey and concept analysis, task 3 report
[NASA-CR-180900] N89-11192
Comparison of measured and modeled radiation, heat and water vapor fluxes: FIFE pilot study
[NASA-CR-183304] N89-11368
High heat flux testing of CIT (Compact Ignition Tokamak) first wall tiles
[DE88-012241] N89-11530
HEAT PIPES
Advanced heat-pipe heat exchanger and microprocessor-based modulating burner controls development
[PB88-217070] N89-11172
HEAT PUMPS
Worldwide survey of absorption fluids data
[DE88-013204] N89-10972
An overview of the Stirling engine heat pump program
[DE88-013833] N89-11146
Further investigations on new fluid working systems for absorption heat pumps
[DE88-012622] N89-11151
Engine driven heat pump program overview
[DE88-013240] N89-11165
Laboratory examination and seasonal analyses of the dynamic losses for a continuously variable speed heat pump
[DE88-013207] N89-11174
Entrainment enhancement of a supersonic jet for advanced ejectors
[DE88-013200] N89-11177
Development of a residential free-piston Stirling engine heat pump
[DE88-012917] N89-11303
HEAT RESISTANT ALLOYS
Effect of protective coatings on life of heat-resistant nickel steel under cyclic heat load N89-11005
HEAT STORAGE
Phase change problem related to thermal energy storage in the manned space station
[DE88-011390] N89-10933
HEAT TRANSFER
Worldwide survey of absorption fluids data
[DE88-013204] N89-10972
Peculiarities of heat transfer at helium boiling in centrifugal force field
[DE88-702809] N89-10974
Fluid science investigations in microgravity
[PB88-209754] N89-11058
Friction reduction and heat transfer enhancement in turbulent pipe flow of non-Newtonian liquid-solid mixtures
[DE88-010018] N89-11138
Heat release effects of reacting gas jets in liquids
[DE88-011971] N89-11175
Developing laminar flow and heat transfer in ducts of arbitrary cross section N89-11176
The impact of separated flow on heat and mass transfer
[DE88-014653] N89-11180

Integration of analysis and experiment for Stirling cycle processes. Part 1: Gas spring hysteresis loss
[DE88-013202] N89-11313
Estimating evapotranspiration of an irrigated surface from upwind and downwind vertical profiles of temperature and humidity
[AD-A196409] N89-11375

HEAT TRANSMISSION
The thermal resistance of fine powders at atmospheric pressure and under vacuum
[DE88-014556] N89-10982

HEAT TREATMENT
JPRS Report: Science and Technology. USSR: Materials Science
[JPRS-UMS-88-007] N89-11002
Alloying of metals by teatment with nanosecond laser pulses N89-11006

HEATING
Advanced heat-pipe heat exchanger and microprocessor-based modulating burner controls development
[PB88-217070] N89-11172
Effect of thermal cycling
[AD-A196851] N89-11219
The impact of an increase in atmospheric methane on the temperature field and subsequent climatic effects
[AD-A196869] N89-11332

HEAVY ELEMENTS
Magnetic fluctuations and heavy electron superconductivity
[DE88-011978] N89-11557

HEAVY IONS
HIEN-LO: An experiment for charge determination of cosmic rays of interplanetary and solar origin N89-10908
Search for narrow resonance production in Bhabha scattering at center-of-mass energies near 1.8 MeV
[MPE-PAE/EXP-EL-190] N89-11502

HELICAL FLOW
Monte Carlo study of ion cyclotron resonance heating in helical systems
[IPPJ-884] N89-11544

HELICOPTER CONTROL
A study of helicopter stability and control including blade dynamics
[NASA-CR-183245] N89-10895

HELICOPTER DESIGN
Aeroelasticity and structural optimization of helicopter rotor blades with swept tips N89-10887

HELICOPTERS
Investigation on of the flow around a backward facing step with spanwise blowing
[CERT-RF-OA-68/2259-AYD] N89-10859
Aeronautical decision making for air ambulance helicopter pilots: Situational awareness exercises
[DOT/FAA/DS-88/6] N89-10869
Results of 1987 MSS helicopter propagation experiment at UHF and L band in Central Maryland N89-11077
Preliminary results of MARECS-A measurements in Central Maryland and plans for 1988 MSS experiment in Australia N89-11079
The Shock and Vibration Digest, Volume 20, No. 7 N89-11277

HELIUM
Peculiarities of heat transfer at helium boiling in centrifugal force field
[DE88-702809] N89-10974
Hydrodynamical characteristics of helium two-phase flows at relatively high mass rates
[DE88-702936] N89-11143
Thermal calculations of nitrogen-free nonmagnetic helium cryostats
[DE88-702807] N89-11227

HELIUM IONS
Advantages of a helium beam for active charge exchange diagnostics — ASDEX tokamak N89-11542

HELIUM ISOTOPES
Observations on cosmic abundance of He4 and Li7, comparison with primordial nuceosynthesis predictions N89-11641

HEPTANES
A detailed chemical kinetic reaction mechanism for the oxidation of iso-octane and n-heptane over an extended temperature range and its application to analysis of engine knock
[DE88-005370] N89-11053

HETEROGENEITY
Interaction of electromagnetic waves with heterogeneous bodies of arbitrary shape and parameters N89-11095

HETEROJUNCTION DEVICES
Study and fabrication of AlGaAs/GaAs double heterojunction bipolar transistors for integrated injection logic circuits
[LAAS-88-138] N89-11123

HETEROJUNCTIONS
Deposition and characterization of ZnS/Si heterojunctions produced by vacuum evaporation
[NASA-TM-101359] N89-11129

HF LASERS
Temporal variations in a CW HF MOPA (oscillator/amplifier)
[AD-A196915] N89-11132
Biological applications and effects of optical masers
[AD-A196462] N89-11217

HIGH ALTITUDE
Ion gun operations at high altitudes
[AD-A196965] N89-10939

HIGH ENERGY INTERACTIONS
Search for narrow resonance production in Bhabha scattering at center-of-mass energies near 1.8 MeV
[MPE-PAE/EXP-EL-190] N89-11502

HIGH FLUX ISOTOPE REACTORS
Microstructural development of titanium-modified austenitic stainless steel under neutron irradiation in HFIR up to 57 dpa
[DE88-013248] N89-10999

HIGH FREQUENCIES
High frequency inverter-cycloconverter system for dc to ac conversion N89-11120

HIGH GAIN
An introduction to the physics of high gain free electron lasers
[DE88-014163] N89-11208

HIGH PRESSURE
Brillouin scattering at high pressures
[DE88-011972] N89-11497

HIGH RESOLUTION
High resolution schemes for three-dimensional Euler equations. 1: Estimation of recent TVD schemes
[PB88-214416] N89-10845
Bandwidth compression for HDTV broadcasting: Investigation of some adaptive subsampling strategies
[BBC-RD-1988/9] N89-11101
Structural anomalies in undoped Gallium Arsenide observed in high resolution diffraction imaging with monochromatic synchrotron radiation
[NASA-CR-183268] N89-11595

HIGH SPEED
High speed parallel processing networks for advanced architectures N89-10837

HIGH SPEED PHOTOGRAPHY
High-speed photography of energetic materials and components with a copper vapor laser
[DE88-012869] N89-11212

HIGH TEMPERATURE
Research needs in high temperature chemistry
[DE88-012929] N89-10961
Development of an experimental model of self-propagating high temperature oxidation-reduction reactions
[AD-A196978] N89-10987
Ratchetting behavior of type 304 stainless steel at room and elevated temperatures
[DE88-011864] N89-11273

HIGH TEMPERATURE PLASMAS
Atomic processes in high temperature plasmas
[DE88-013005] N89-11525

HIGH TEMPERATURE SUPERCONDUCTORS
Use of high temperature superconductors in magnetoplasmadynamic systems
[NASA-TM-101219] N89-11553
Spin correlations in high T(sub c) superconductors
[DE88-013988] N89-11555
Far infrared linear response and radio frequency nonlinear response of charge density wave conductors and high T(sub c) superconductors
[DE88-013595] N89-11582
Chemical preparation of powders and films for high temperature superconductors
[DE88-015266] N89-11601

HIGH VACUUM
Lunar concrete for construction
[NASA-TM-89672] N89-11060

HILBERT SPACE
Strong and weak stabilizability: Lyapunov type approaches
[AD-A196431] N89-11482

HISTORIES
The history of gamma-ray burst observations
[DE88-014390] N89-11685

HMX
Friction and impact sensitivities of explosives: A comparative study
[DE88-012864] N89-11051

HOMOGENEITY
Microgravity nucleation and particle coagulation experiments support
[NASA-CR-183282] N89-11056

HOMOLOGY
Homology classes represented by real algebraic hypersurfaces
[PB88-202908] N89-11453

HORIZONTAL ORIENTATION
Synoptic scale sensitivity of TIROS-N moisture channels in the tropics
[AD-A196686] N89-11378

HOVERING
Design and evaluation of a cockpit display for hovering flight
[NASA-CR-183247] N89-10900

HUMAN BEINGS
Biological applications and effects of optical masers
[AD-A196462] N89-11217
Evaluation of the prototype EUROSID dummy and comparison with the US SID (Side Impact Dummies)
[PB88-201934] N89-11389

HUMAN FACTORS ENGINEERING
Evaluation of enhancements to the Low Level Wind Shear Alert System (LLWAS) at Stapleton International Airport
[DOT/FAA/PS-88/14] N89-11356

HUMAN PERFORMANCE
Enhancing performance under stress by information about its expected duration
[AD-A196836] N89-11388

HUMIDITY
Ground-based radiometric observations of emission and attenuation at 20.6, 31.65, and 90.0 GHz N89-11086

HYDRAULIC FLUIDS
Laser/fluorescent dye flow visualization technique developed for system component thermal hydraulic studies
[DE88-012008] N89-11137

HYDROCARBON COMBUSTION
Exploitation and utilization of hydrocarbons
[DE88-012626] N89-11048

HYDROCARBON FUELS
Combustion of energetic materials
[DE88-011286] N89-10977

HYDROCHLORIC ACID
HCl measurements in space vehicle exhaust clouds
[DE88-013815] N89-10942

HYDRODYNAMICS
Modulation of radar backscatter from the ocean by a variable surface current
[AD-A196952] N89-11114
Hydrodynamical characteristics of helium two-phase flows at relatively high mass rates
[DE88-702936] N89-11143
The application of single particle hydrodynamics in continuum models of multiphase flow N89-11154
Periodically structured multiphase flows and hydrodynamic instabilities in narrow capillaries
[DE88-015608] N89-11181
Transactions of machine elements division: On the combined hydrodynamic and hydrostatic journal bearing
[PB88-214549] N89-11231
Parallel processing a real code: A case history
[DE88-014456] N89-11437

HYDROGEN
Preliminary design study of hydrogen and ammonia resistojets for prime and auxiliary thrusters
[NASA-CR-182176] N89-10943
Safety aspects of large-scale handling of hydrogen
[DE88-014422] N89-11070
Molecular processes in comets
[NASA-CR-182742] N89-11671

HYDROGEN EMBRITTLEMENT
Mechanics of hydrogen embrittlement N89-11000

HYDROGEN IONS
Interpretation of neutron rate measurements using the NR code N89-11538
Comparison between Uramoto type and straight filament type sheet plasma as a volume produced H(-) ion source (2)
[IPPJ-887] N89-11548
Implantation studies of hydrogen by field ion microscopy and spectroscopy
[DE88-015806] N89-11602

HYDROGENATION
The melting and crystallization kinetics of hydrogenated polybutadiene
[AD-A196988] N89-11045

HYDROLOGY
Snow cover, snowmelt and runoff in the Himalayan River basins
[NASA-CR-182434] N89-11290

HYDROLOGY MODELS
Remote sensing and hydrologic modeling of arid watersheds: A scale analysis
[DE88-014625] N89-11293

HYDROLYSIS
Research needs in high temperature chemistry
[DE88-012929] N89-10961

HYDROSTATICS
Transactions of machine elements division: On the combined hydrodynamic and hydrostatic journal bearing
[PB88-214549] N89-11231
HYDROTHERMAL SYSTEMS
Geothermal energy technology: Issues, R and D needs, and cooperative arrangements
[DE88-011804] N89-11299
HYDROXIDES
Electrochemical reactions of mixed cobalt/nickel oxide hydroxides in alkaline electrolyte
[ATR-86(9561)-4] N89-10965
HYPERCUBE MULTIPROCESSORS
PC-CUBE: A personal computer based hypercube
[DE88-015008] N89-11394
An O(NlogN) hypercube N-body integrator
[DE88-015016] N89-11413
Lattice gauge theory on the hypercube
[DE88-015004] N89-11420
HYPERFINE STRUCTURE
Resonance ionization of Kr metastables using a single-frequency laser
[DE88-014757] N89-11209
HYPOXIA
Individual differences in adaptation to hypoxia and cold based on emotional-behavioral criterion of bodily reactivity N89-11386
HYSTERESIS
Effect of thermal cycling
[AD-A196851] N89-11219
Integration of analysis and experiment for Stirling cycle processes. Part 1: Gas spring hysteresis loss
[DE88-013202] N89-11313

I

ICE FORMATION
A theoretical investigation of the collection of aerosol particles by falling ice crystals N89-11337
ICE NUCLEI
A theoretical investigation of the collection of aerosol particles by falling ice crystals N89-11337
ICOSAHEDRONS
Elastic and anelastic behaviour of icosahedral quasicrystals
[DE88-702712] N89-11588
IGNITERS
Smart semiconductor bridge (SCB) igniter for explosives
[DE88-012669] N89-11551
IGNITION
A study of the effect of thermal radiation on laminar flame propagation and ignition, 1981-1987 N89-10967
Combustion of energetic materials
[DE88-011286] N89-10977
The initiation and detonation of explosives: An alternative concept
[DE88-014199] N89-11047
Role of deflagration in explosive response
[DE88-014139] N89-11049
Shock initiation of explosives with a sensitive rate and related topics
[DE88-008483] N89-11052
IMAGE PROCESSING
Study of the multiplexing of image telemetry data from SPOT 4 HRVIR and Vegetation sensors
[CNES-87/229/CT/DRT/TIT/TR] N89-10930
Color enhancement of remote sensing imagery using IHS transformations and decorrelation stretch methods
[INPE-4559-PRE/1300] N89-11418
Three-dimensional computer graphics brain-mapping project
[AD-A197053] N89-11435
Communication aspects of parallel processing
[AD-A196458] N89-11439
Quantitative Luminescence Imaging System description and user's manual
[DE88-015604] N89-11512
IMAGERY
The Frobenius metric in image registration
[DE88-016685] N89-11421
Structural anomalies in undoped Gallium Arsenide observed in high resolution diffraction imaging with monochromatic synchrotron radiation
[NASA-CR-183268] N89-11595
IMAGING TECHNIQUES
Multicolor pyrometer for materials processing in space
[NASA-CR-183189] N89-11057
Improvement and extension of a radar forest backscattering model
[NASA-CR-183259] N89-11292
Quantitative Luminescence Imaging System description and user's manual
[DE88-015604] N89-11512
IMIDES
Multistress aging of polymer films
[DE88-008094] N89-11034
IMPACT
Friction and impact sensitivities of explosives: A comparative study
[DE88-012864] N89-11051
IMPACT DAMAGE
Ions generated on or near satellite surfaces
[AD-A196866] N89-10940
Longitudinal impact test of a transport airframe section
[DOT/FAA/CT-87/26] N89-11265
IMPACT STRENGTH
A novel approach to abrasion resistance
[DE88-014180] N89-10949
IMPACT TESTS
Evaluation of the prototype EUROSID dummy and comparison with the US SID (Side Impact Dummies)
[PB88-201934] N89-11389
IMPEDANCE MEASUREMENT
The interpretation of electromagnetic nondestructive flaw detection in metals N89-11246
IMPURITIES
A preliminary study on the use of magnetohydrodynamic forces to remove impurities from molten metals
[DE88-013508] N89-10991
The catalytic, structural, and electronic properties of strained-metal overlayers
[DE88-007932] N89-11013
Modelling of the 2-dimensional structure and impurity transport for a scrape-off layer with a solid limiter
[IPPJ-873] N89-11527
Low temperature measurements on UBe13
[DE88-014446] N89-11594
INCIDENCE
Experimental investigation of flow near a corner, part 2
[CERT-RT-OA-24/5025-AYD] N89-10861
The effect of vapor incidence angle upon thin film columnar growth
[DE88-014396] N89-11577
INCLUSIONS
Experimental and theoretical study of inclusions during initiation of crevice corrosion
[DE88-014635] N89-10989
INCOHERENT SCATTER RADAR
Investigation of ionospheric D region aeronomy using incoherent scatter radar and optical measurements N89-11338
INCOMPRESSIBLE FLOW
Unsteady hydromagnetic free-convection flow with radiative heat transfer in a rotating fluid. 1: Incompressible optically thin fluid
[DE88-702998] N89-11140
Continuum theories for fluid-particle flows: Some aspects of lift forces and turbulence N89-11155
Application of a second-order projection method to the study of shear layers
[DE88-013095] N89-11166
On 1-D closure models for slender 3-D viscoelastic free jets: von Karman flow geometry and elliptical cross section
[DE88-014478] N89-11179
INCONEL (TRADEMARK)
The role of grain boundary character in the environmentally-assisted intergranular cracking mechanism of nickel-base alloys
[DE88-014130] N89-11018
INDIUM COMPOUNDS
Advanced materials for solid oxide fuel cells: Hafnium-praseodymium-indium oxide system
[DE88-015365] N89-11310
Spin-orbit interaction effects in zincblende semiconductors: Ab initio pseudopotential calculations
[DE88-014663] N89-11599
INDUSTRIAL MANAGEMENT
Software management metrics
[AD-A196916] N89-11434
INELASTIC SCATTERING
Lattice instability in single-crystal La(sub 2-x)Sr(sub x)/CuO4
[DE88-013994] N89-11598
INERTIAL CONFINEMENT FUSION
KCl bounce coating of glass and polymer microshells
[DE88-013018] N89-11524
Power absorption and confinement studies of ICRF-heated plasma in JIPP T-IIU tokamak
[IPPJ-886] N89-11547
INERTIAL NAVIGATION
The NAVSTAR GPS System
[AGARD-LS-161] N89-10874
GPS/interial navigation system integration for enhanced navigation performance and robustness N89-10880
An inertial velocity reference for the NASA airborne Doppler lidar
[NASA-CR-179378] N89-11203
INFLATING
On the locality of the no hair conjection and the measure of the universe
[NASA-CR-183385] N89-11489
Inflation, cosmic strings and galaxy formation
[DE88-008629] N89-11666
INFORMATION
Evaluating the Effectiveness of Information Centres and Services
[AGARD-LS-160] N89-11625
Evaluating the effectiveness of information use N89-11626
Measures, methods and models employed in evaluating the effectiveness of information centers and services N89-11627
European examples of evaluating the effectiveness of information centres and services N89-11628
Evaluating the performance of information centre staff N89-11629
Evaluating performance of information centre operations and services N89-11630
A framework for evaluating the effectiveness of information centres and services N89-11631
Evaluating for information center planning N89-11632
INFORMATION DISSEMINATION
Civil and military applications of GPS N89-10882
Evaluating the effectiveness of information use N89-11626
Measures, methods and models employed in evaluating the effectiveness of information centers and services N89-11627
Evaluating the performance of information centre staff N89-11629
Evaluating performance of information centre operations and services N89-11630
INFORMATION MANAGEMENT
Evaluating the Effectiveness of Information Centres and Services
[AGARD-LS-160] N89-11625
Evaluating the effectiveness of information use N89-11626
Measures, methods and models employed in evaluating the effectiveness of information centers and services N89-11627
European examples of evaluating the effectiveness of information centres and services N89-11628
Evaluating the performance of information centre staff N89-11629
Evaluating performance of information centre operations and services N89-11630
A framework for evaluating the effectiveness of information centres and services N89-11631
Evaluating for information center planning N89-11632
INFORMATION RETRIEVAL
Hypothesis-confirming information search strategies and computerized information retrieval systems N89-11616
INFORMATION SYSTEMS
The Propagation Information Center at the University of Colorado N89-11094
Standards conformance testing
[PB88-215645] N89-11412
Hypothesis-confirming information search strategies and computerized information retrieval systems N89-11616
An investigation of information systems prototyping N89-11622
Evaluating the Effectiveness of Information Centres and Services
[AGARD-LS-160] N89-11625
Measures, methods and models employed in evaluating the effectiveness of information centers and services N89-11627
European examples of evaluating the effectiveness of information centres and services N89-11628
INFORMATION THEORY
Assessing schema knowledge
[AD-A196933] N89-11447
Measures, methods and models employed in evaluating the effectiveness of information centers and services N89-11627
INFORMATION TRANSFER
Unidirectional Manchester encoded data transfer via a fiber optic link
[AD-A196961] N89-11516
INFRARED ASTRONOMY
Space observations for infrared and submillimeter astronomy N89-11643
A far infrared astronomical observatory in Antarctica N89-11646
INFRARED RADIATION
Damage effects on thin acrylic targets caused by infrared radiation from a pulsed carbon dioxide laser
[AD-A196385] N89-11216

INFRARED SPECTRA
IR reflectance and Raman scattering of diamond films [AD-A196899] N89-11043
INHIBITORS
Control of environment assisted cracking of Al 7075 using inhibitors [AD-A196387] N89-11022
INHOMOGENEITY
Balance of recurrence order in time-inhomogeneous Markov chains with application to simulated annealing [AD-A196980] N89-11484
Inhomogeneities in a Friedmann universe [DE88-702981] N89-11672
INITIATION
The initiation and detonation of explosives: An alternative concept [DE88-014199] N89-11047
Shock initiation of explosives with a sensitive rate and related topics [DE88-008483] N89-11052
INJECTION MOLDING
Polystyrylpyridine (PSP) resin-based short-fiber composites (injectable compounds) [REPT-NT-195/87/CRB/GTR.C/NP] N89-10955
INJECTORS
Simulations of the laser photocathode injector [DE88-015337] N89-11202
INORGANIC COMPOUNDS
Inorganic chemical precipitate formation payload design N89-10920
INPUT/OUTPUT ROUTINES
The use of portable microcomputer as a data collection tool to support integrated simulation support environments: A concept [AD-A196414] N89-11403
INSOLATION
A limited assessment and characterization of the solar radiation energy resources in the Caribbean region [DE88-001133] N89-11312
INSULATION
Fundamental aspects of the electronic structure, materials properties, and lubrication performance of sputtered MoS2 films [AD-A196852] N89-11606
INSULATORS
Simple model for the superconducting phase diagram near the metal-insulator transition [DE88-703038] N89-11558
INTEGRAL EQUATIONS
Determination of characteristic radiation properties of a torus antenna [ESA-TT-1106] N89-11105
Optimization of the two-dimensional magnetic field distribution basing on the integral equation method [DE88-702940] N89-11490
INTEGRATED CIRCUITS
Design definition for a digital beamforming processor [AD-A196983] N89-11133
Molecular beam epitaxy of GaP films on Si substrates [PB88-131974] N89-11581
INTEGRATORS
An O(NlogN) hypercube N-body integrator [DE88-015016] N89-11413
INTERATOMIC FORCES
Atomistic studies of grain boundaries in alloys and compounds [DE88-011939] N89-11011
INTERCEPTORS
Interceptor-to-target allocation strategies for Strategic Defense 1: Adaptive strategies based upon system and threat characteristics [AD-A197037] N89-11487
INTERFACES
Photoacoustic spectroscopy and the in situ characterization of the electrochemical interface [DE88-013848] N89-10975
Characterization of ceramic films and interfaces by electron microscopic and spectroscopic techniques [DE88-011957] N89-11029
The pair potential approach for interfaces: Fundamental problems and practical solutions [DE88-009165] N89-11456
Concerning interfaces in natural languages [INPE-4681-PRE/1376] N89-11634
INTERFACIAL TENSION
A method for improving the depth of penetration and the appearance of welding [DE88-012954] N89-11239
INTERFERENCE GRATING
In-plane moire optical processing at ARL [ARL-STRUC-R-428] N89-11510
INTERFEROMETERS
New quantum interferometer effect in superconducting oxide ceramics [DE88-703152] N89-11603
INTERIOR BALLISTICS
Modeling of combustion processes of stick propellants via combined Eulerian-Lagrangian approach N89-11163
INTERMETALLICS
Microstructure and properties of rapidly solidified beryllium-transition metal alloys [DE88-010937] N89-11012
Brillouin scattering: Its application to the study of damage and amorphization [DE88-012053] N89-11016
Crystallization of Zr-Ni metallic glasses [DE88-007481] N89-11026
Current-induced quantum interference in the composite superconductor NbTi-Cu [DE88-703079] N89-11562
X-ray scattering studies of non-equilibrium ordering processes [DE88-012908] N89-11569
INTERNAL COMBUSTION ENGINES
A detailed chemical kinetic reaction mechanism for the oxidation of iso-octane and n-heptane over an extended temperature range and its application to analysis of engine knock [DE88-005370] N89-11053
Engine driven heat pump program overview [DE88-013240] N89-11165
INTERNATIONAL COOPERATION
The first Chinese student space shuttle getaway special program N89-10903
INTERNATIONAL SUN EARTH EXPLORERS
Association of plasma sheet variations with auroral changes during substorms [DE88-014319] N89-11350
INTERPLANETARY FLIGHT
Nuclear propulsion: A vital technology for the exploration of Mars and the planets beyond [NASA-TM-101354] N89-10944
INTERPLANETARY MAGNETIC FIELDS
Interplanetary magnetic microstructure observed by Sakigake near its closest approach to Comet Halley [ISAS-RN-349] N89-11667
INTERSTELLAR GAS
Shocked interstellar gas in dense molecular clouds N89-11670
INTERSTELLAR MATTER
Microgravity nucleation and particle coagulation experiments support [NASA-CR-183282] N89-11056
INTERTROPICAL CONVERGENT ZONES
Active modes of the Pacific Intertropical Convergence Zone (ITCZ) [AD-A196406] N89-11374
INVERTED CONVERTERS (DC TO AC)
High frequency inverter-cycloconverter system for dc to ac conversion N89-11120
INVISCID FLOW
Computation of low-speed compressible flows with time-marching procedures [AD-A195800] N89-11170
IODIDES
Preparation and evaluation of mercuric iodide for crystal growth [DE88-014981] N89-11578
Modified purification of mercuric iodide for crystal growth [DE88-014960] N89-11580
IODINE LASERS
Direct solar-pumped iodine laser amplifier [NASA-CR-183171] N89-11201
ION BEAMS
Ion gun operations at high altitudes [AD-A196965] N89-10939
Advances in metal ion sources [DE88-012020] N89-11495
High heat flux testing of CIT (Compact Ignition Tokamak) first wall tiles [DE88-012241] N89-11530
Advantages of a helium beam for active charge exchange diagnostics — ASDEX tokamak N89-11542
ION CHARGE
HIEN-LO: An experiment for charge determination of cosmic rays of interplanetary and solar origin N89-10908
ION CURRENTS
Experimental study of time-varying current flow between electrodes immersed in a laboratory magnetoplasma N89-11521
Comparison between Uramoto type and straight filament type sheet plasma as a volume produced H(-) ion source (2) [IPPJ-887] N89-11548
ION CYCLOTRON RADIATION
Monte Carlo study of ion cyclotron resonance heating in helical systems [IPPJ-884] N89-11544
ION EMISSION
Ion gun operations at high altitudes [AD-A196965] N89-10939
Ions generated on or near satellite surfaces [AD-A196966] N89-10940
ION IMPACT
Ions generated on or near satellite surfaces [AD-A196966] N89-10940
Shocked interstellar gas in dense molecular clouds N89-11670
ION IMPLANTATION
Ti-implanted optical waveguides in LiNbO3 [DE88-015279] N89-11554
Implantation studies of hydrogen by field ion microscopy and spectroscopy [DE88-015806] N89-11602
An oxide passivated and ion-implanted Si detector for X-ray astronomy [ISAS-RN-353] N89-11663
ION RECOMBINATION
Charge exchange spectroscopy (CXRS) of highly ionized ions in ASDEX — tokamak N89-11535
ION SOURCES
Advances in metal ion sources [DE88-012020] N89-11495
Development of the work function monitoring method for a converter of a negative ion source [IPPJ-880] N89-11529
ION TEMPERATURE
Spectroscopic measurement of the ion temperature on ASDEX — tokamak N89-11536
Space and time resolved measurements of ion temperature with the CVI 5292 A charge exchange recombination line after substracting background radiation [IPPJ-888] N89-11549
IONIZATION
Statistical effects in high-power microwave beam propagation [DE88-012440] N89-11100
IONIZATION CHAMBERS
HIEN-LO: An experiment for charge determination of cosmic rays of interplanetary and solar origin N89-10908
IONIZING RADIATION
Development of advanced internal gain radiation detector structures based on neutron transmutation doped silicon, high T(sub c) superconductive compounds and their potential application to detection of ionizing radiation [DE88-012563] N89-11574
IONOSPHERIC COMPOSITION
Investigation of ionospheric D region aeronomy using incoherent scatter radar and optical measurements N89-11338
IRON
Laser Raman spectroscopy of anodic corrosion and inhibitor films on iron and nickel [DE88-009958] N89-11008
IRON ALLOYS
Nitride layer growth in iron and titanium alloys: Studies by electron probe microanalysis [DE88-007207] N89-11017
IRON COMPOUNDS
On relative supernova rates and nucleosynthesis roles [NASA-CR-183373] N89-11673
IRRADIATION
Alloying of metals by teatment with nanosecond laser pulses N89-11006
Functional assessment of laser irradiation [AD-A196930] N89-11222
IRREGULAR VARIABLE STARS
Observations of southern irregular variables [INPE-4568-PRE/1309] N89-11291
IRRIGATION
Estimating evapotranspiration of an irrigated surface from upwind and downwind vertical profiles of temperature and humidity [AD-A196409] N89-11375
ISOMERIZATION
Transition metal mediated transformations of unsaturated molecules [DE88-013482] N89-10968
ISOTROPIC TURBULENCE
Structure of wind-shear turbulence [NASA-CR-183257] N89-11359
ITERATION
Accessibility, a criterion for the choice of visual coding rules [PB88-209911] N89-11458
Periodic solutions of the Hamilton-Jacobi equation by the shooting method: A technique for beam dynamics [DE88-012733] N89-11460
Solution methods for damped linear dynamic systems [DE88-013812] N89-11464

ITERATIVE SOLUTION
Velocity analysis by iterative profile migration N89-11339
An iterative scheme for numerical solution of transonic small perturbation equation
[TM-AE-8801] N89-11455

J

JAMMING
On the generation of waveforms having comb-shaped spectra
[AD-A196927] N89-11113
A survey of digital beam forming techniques and current technology
[AD-A196376] N89-11514
JAPAN
ONR Far East Scientific Bulletin, volume 12, no. 4, October - December 1987
[AD-A194338] N89-11687
JAPANESE SPACE PROGRAM
Interplanetary magnetic microstructure observed by Sakigake near its closest approach to Comet Halley
[ISAS-RN-349] N89-11667
JET EXHAUST
Summary of an experimental investigation on the ground vortex N89-10851
Ground vortex flow field investigation N89-10852
Effects of a ground vortex on the aerodynamics of an airfoil N89-10855
Numerical investigation of a jet in ground effect using the fortified Navier-Stokes scheme N89-10857
JET FLOW
Reynolds stress closure in jet flows using wave models
[NASA-CR-180226] N89-10843
Experimental and theoretical studies of vertical annular liquid jets
[DE88-012971] N89-11149
Confined turbulent fluid-particle flow modeling using multiple-realization particle trajectory schemes N89-11157
Observations of breakup processes of liquid jets using real-time X-ray radiography N89-11160
JET IMPINGEMENT
Noise of the Harrier in vertical landing and takeoff N89-10856
The impact of separated flow on heat and mass transfer
[DE88-014653] N89-11180
Experimental research on swept shock wave/boundary layer interactions
[AD-A196938] N89-11189
JET PROPULSION
Numerical simulation of axisymmetric base flow on tactical missiles with propulsive jet
[AD-A196169] N89-11136
JOINTS (JUNCTIONS)
Transverse flexure of an elastic plate loaded through a rigid inclusion N89-11267
JOSEPHSON JUNCTIONS
What is the origin of glassy behavior in the high-T(sub c) oxides
[DE88-012668] N89-11565
Vortex lattices in theory and practice
[DE88-014393] N89-11576
JOURNAL BEARINGS
Transactions of machine elements division: On the combined hydrodynamic and hydrostatic journal bearing
[PB88-214549] N89-11231
JUPITER (PLANET)
Decametric radio emission of Jupiter. Part 3: Some physical characteristics of S-component sources
[DE88-702812] N89-11679

K

K-EPSILON TURBULENCE MODEL
A diagonally inverted LU implicit multigrid scheme for the 3-D Navier-Stokes equations and a two equation model of turbulence
[NASA-CR-182209] N89-10863
KALMAN FILTERS
GPS navigation processing and Kalman filtering N89-10884
KAONS
The compatibility of gravity and kaon results in the search for new forces
[DE88-013993] N89-11612
KINEMATICS
Probabilistic error model of robot end-effector's dynamic state N89-11236
Analysis, synthesis and design of high-speed mechanisms
[PB88-235106] N89-11244
On deriving the 3-dimensional kinematic structure of convective storms from a single radar
[AD-A196405] N89-11373
KINETIC THEORY
Development and testing of KITES
[DE88-015057] N89-11336
KINETICS
Ligand intermediates in metal catalyzed reactions
[DE88-012123] N89-11007
The melting and crystallization kinetics of hydrogenated polybutadiene
[AD-A196988] N89-11045
KLYSTRONS
Quality assurance manual. Volume 2: Appendices
[DE88-013880] N89-11247
KNOWLEDGE REPRESENTATION
Knowledge-based design of complex mechanical systems N89-11225
Representing high-level knowledge structures in massively parallel networks N89-11409
Knowledge-based diagnosis for aerospace systems
[NASA-CR-182641] N89-11441
KRYPTON
Resonance ionization of Kr metastables using a single-frequency laser
[DE88-014757] N89-11209

L

LAGRANGE MULTIPLIERS
On equivariant Lagrangians
[DE88-703167] N89-11468
LAMINAR BOUNDARY LAYER
Measurements and predictions of mixed convection in laminar and turbulent boundary layer flows N89-11164
Theory of instabilities in the laminar boundary layer: Literature review
[DERAT-42/5618-28] N89-11185
LAMINAR FLOW
A study of the effect of thermal radiation on laminar flame propagation and ignition, 1981-1987 N89-10967
An experimental study of a laminar wall-jet in the presence of a uniform external flow
[UTIAS-268] N89-11152
Mixing and Demixing Processes in Multiphase Flows With Application to Propulsion Systems
[NASA-CP-3006] N89-11153
The application of single particle hydrodynamics in continuum models of multiphase flow N89-11154
Migration arising from gradients in shear stress: Particle distributions in Poiseuille flow N89-11159
Developing laminar flow and heat transfer in ducts of arbitrary cross section N89-11176
LAMINATES
A mixed-mode bending apparatus for delamination testing
[NASA-TM-100662] N89-10945
Tension fatigue analysis and life prediction for composite laminates
[NASA-TM-100549] N89-10951
Laminate behavior for SiC fiber-reinforced reaction-bonded silicon nitride matrix composites
[NASA-TM-101350] N89-10952
Investigations in the nonlinear domain of composite laminate plates subject to compression loads
[ONERA-RT-17/3542-RY-070-R] N89-10953
Nonlinear theories of composite laminates under compression with delamination
[CERT-RT-18/3542-RY-071-R] N89-10954
PRIMEL: A preprocessor for the analysis of laminated composites. Introduction and user's guide (operation system OS/VS2 (MVS))
[DFVLR-MITT-88-14] N89-10956
Delamination buckling of pressure-loaded, laminated cylindrical shells and panels N89-11276
LANDING
Noise of the Harrier in vertical landing and takeoff N89-10856
LANDING GEAR
F-15 SMTD low speed jet effects wind tunnel test results N89-10853
LANDSAT SATELLITES
Training activities in remote sensing at the Instituto de Pesquisas Espaciais-INPE/Brazil
[INPE-4686-PRE/1380] N89-11295
LANTHANUM OXIDES
Spin correlations in high T(sub c) superconductors
[DE88-013988] N89-11555
Lattice instability in single-crystal La(sub 2-x)Sr(sub x)/CuO4
[DE88-013994] N89-11598
LARGE SPACE STRUCTURES
Development of a verification program for deployable truss advanced technology
[NASA-CR-181703] N89-10936
Power quality load management for large spacecraft electrical power systems
[NASA-TM-100342] N89-11127
The Shock and Vibration Digest, Volume 20, No. 10 N89-11252
Continuum modeling of latticed structures N89-11253
LASER ANEMOMETERS
Three component laser anemometer measurements in an annular cascade of core turbine vanes with contoured end wall
[NASA-TP-2846] N89-10844
LASER APPLICATIONS
Laser/fluorescent dye flow visualization technique developed for system component thermal hydraulic studies
[DE88-012008] N89-11137
Bibliography of Soviet laser developments, number 87, January - February 1987
[AD-A196973] N89-11223
Current new applications of laser plasmas
[DE88-015679] N89-11532
LASER CAVITIES
Basic rules of saturated gain variation in a flowing laser cavity
[AD-A196861] N89-11220
LASER DAMAGE
Biological applications and effects of optical masers
[AD-A196462] N89-11217
Functional assessment of laser irradiation
[AD-A196930] N89-11222
LASER FUSION
Current new applications of laser plasmas
[DE88-015679] N89-11532
LASER HEATING
Glass-ceramic fusion with a CO2 laser
[DE88-012871] N89-11030
LASER INTERFEROMETRY
Laser wavemeter/spectrometer operating manual
[NASA-CR-180802] N89-11195
LASER MATERIALS
Bibliography of Soviet laser developments, number 87, January - February 1987
[AD-A196973] N89-11223
LASER OUTPUTS
Characteristics of laser beam focusing with single spherical mirrors during laser treatment N89-11004
Alloying of metals by teatment with nanosecond laser pulses N89-11006
Direct solar-pumped iodine laser amplifier
[NASA-CR-183171] N89-11201
Collective resonance fluorescence in an intense laser field with phase and amplitude fluctuations
[DE88-702920] N89-11205
Biological applications and effects of optical masers
[AD-A196462] N89-11217
Analysis of free electron laser performance utilizing the National Bureau of Standards' CW microtron
[AD-A196928] N89-11221
Bibliography of Soviet laser developments, number 87, January - February 1987
[AD-A196973] N89-11223
Laser speckle photography and decorrelation techniques in elastic-plastic fracture studies N89-11275
A code for the solution of the Vlasov-Fokker-Planck equation in one or two dimensions
[DE88-013288] N89-11463
LASER PLASMA INTERACTIONS
Current new applications of laser plasmas
[DE88-015679] N89-11532
LASER PLASMAS
Current new applications of laser plasmas
[DE88-015679] N89-11532
LASER SPECTROMETERS
Laser wavemeter/spectrometer operating manual
[NASA-CR-180802] N89-11195
Plasma spectrometry applied to surface treatments (laser PVD)
[ETCA-88-R-036] N89-11533
LASER SPECTROSCOPY
Laser Raman spectroscopy of anodic corrosion and inhibitor films on iron and nickel
[DE88-009958] N89-11008
Laser wavemeter/spectrometer operating manual
[NASA-CR-180802] N89-11195
LASER STABILITY
Experimental and theoretical studies of vertical annular liquid jets
[DE88-012971] N89-11149

LASER TARGETS
Damage effects on thin acrylic targets caused by infrared radiation from a pulsed carbon dioxide laser
[AD-A196385] N89-11216
LASER WEAPONS
Beam handling and emittance control
[AD-A196789] N89-11509
LASER WELDING
Experimental and theoretical studies on transport processes in laser welding
[DE88-013933] N89-11230
Microsoldering and microminiature welding with lasers
[DE88-013368] N89-11240
LASERS
Simulations of the laser photocathode injector
[DE88-015337] N89-11202
Effect of thermal cycling
[AD-A196851] N89-11219
LATENT HEAT
Comparison of measured and modeled radiation, heat and water vapor fluxes: FIFE pilot study
[NASA-CR-183304] N89-11368
LAUNCHING
SHED: A program for three-dimensional, rigid body, shroud ejection dynamics
[DE88-012410] N89-10927
HCl measurements in space vehicle exhaust clouds
[DE88-013815] N89-10942
LEACHING
Modified purification of mercuric iodide for crystal growth
[DE88-014960] N89-11580
LEAF AREA INDEX
Effect of curvature on the backscattering from leaves
[NASA-CR-183326] N89-11296
LEARNING
Ultrasonic flaw classification: An approach using modeling, signal processing, and adaptive learning N89-11248
Automatic concept formation in a rich input domain
[AD-A196719] N89-11445
Toward intelligent machine learning algorithms
[AD-A197049] N89-11448
LEAST SQUARES METHOD
Lattice algorithms for computing QR and Cholesky factors in the least squares theory of linear prediction
[AD-A196454] N89-11432
Determination of complex exponentials, least squares and prediction methods
[AD-A196498] N89-11474
LEAVES
Technique for measuring the dielectric constant of thin materials
[NASA-CR-183325] N89-10984
LEVITATION
MAGLEV: The double benefits of high-Tc superconductors and its development as an aerospace technology
[DE88-012005] N89-11570
LIAPUNOV FUNCTIONS
Strong and weak stabilizability: Lyapunov type approaches
[AD-A196431] N89-11482
LIBRARIES
Evaluating the Effectiveness of Information Centres and Services
[AGARD-LS-160] N89-11625
Measures, methods and models employed in evaluating the effectiveness of information centers and services N89-11627
European examples of evaluating the effectiveness of information centres and services N89-11628
Evaluating the performance of information centre staff N89-11629
Evaluating performance of information centre operations and services N89-11630
A framework for evaluating the effectiveness of information centres and services N89-11631
Evaluating for information center planning N89-11632
LIE GROUPS
Lie algebraic treatment of space charge N89-11496
LIFE (DURABILITY)
Composite structural materials
[NASA-CR-180224] N89-10946
State-of-the-art-dehumidification cost-effective corrosion prevention
[AD-A196503] N89-11023
LIFE SUPPORT SYSTEMS
Extraction of light gasses from Mars or its moons
[DE88-009123] N89-11681
LIFT
Continuum theories for fluid-particle flows: Some aspects of lift forces and turbulence N89-11155
The Shock and Vibration Digest, Volume 20, No. 7 N89-11277
LIGANDS
Ligand intermediates in metal catalyzed reactions
[DE88-012123] N89-11007
LIGHT ELEMENTS
Photoerosion and the abundances of the light elements
[NASA-CR-183372] N89-11675
LIGHT EMISSION
Study of optical output couplers for submillimeter wavelength backward-wave oscillators (BWO's)
[NASA-TM-101360] N89-11128
LIGHT SCATTERING
Particle sizing by weighted measurements of scattered light
[NASA-TM-100968] N89-11198
LIMITERS (FUSION REACTORS)
Modelling of the 2-dimensional structure and impurity transport for a scrape-off layer with a solid limiter
[IPPJ-873] N89-11527
LINEAR ACCELERATORS
PALADIN: A 10.6-micron free-electron laser amplifier
[DE88-014164] N89-11207
An introduction to the physics of high gain free electron lasers
[DE88-014163] N89-11208
Overview of FEL (Free-Electron Laser) development with induction linacs at LLNL
[DE88-014179] N89-11210
Quality assurance manual. Volume 2: Appendices
[DE88-013880] N89-11247
LINEAR PREDICTION
Lattice algorithms for computing QR and Cholesky factors in the least squares theory of linear prediction
[AD-A196454] N89-11432
LINEAR SYSTEMS
Integral manifold in system design with application to flexible link robot control
[AD-A197052] N89-11243
Restructuring of basic linear algebraic algorithms, chapter 5 N89-11399
Lattice algorithms for computing QR and Cholesky factors in the least squares theory of linear prediction
[AD-A196454] N89-11432
Solution methods for damped linear dynamic systems
[DE88-013812] N89-11464
LINEAR VIBRATION
Nonlinear random vibration in mechanical systems N89-11263
LINEARITY
Current research on the vibration and stability of axially-moving materials N89-11283
LINEN
The transportation of fine arts materials aboard the space shuttle Columbia. GAS payload No. 481: Vertical horizons N89-10919
LINKAGES
Experimental verification of a model of a two-link flexible, lightweight manipulator
[NASA-CR-183216] N89-11233
LIQUID FLOW
Observations of breakup processes of liquid jets using real-time X-ray radiography N89-11160
LIQUID HELIUM
The coefficient of first viscosity via three-phonon processes in bulk liquid helium
[AD-A196902] N89-10986
Vortex lattices in theory and practice
[DE88-014393] N89-11576
Superfluid helium as a dark matter detector
[DE88-012759] N89-11664
LIQUID HELIUM 2
Superfluid helium as a dark matter detector
[DE88-012759] N89-11664
LIQUID OXYGEN
Good performance of LE-7 liquid oxygen turbopump confirmed N89-11064
LIQUID PHASES
Liquid-vapour phase change between plane liquid surfaces: A continuum analysis to determine real gas effects
[TM-FM-8803] N89-10971
Pair potential trend of alkali metals under external pressure
[DE88-702973] N89-11593
LIQUID POTASSIUM
Temperature dependence of entropies and specific heats of liquid Na and K
[DE88-702986] N89-10976
LIQUID SURFACES
Liquid-vapour phase change between plane liquid surfaces: A continuum analysis to determine real gas effects
[TM-FM-8803] N89-10971
LIQUID-VAPOR INTERFACES
Liquid-vapour phase change between plane liquid surfaces: A continuum analysis to determine real gas effects
[TM-FM-8803] N89-10971
Experiments on liquid-vapor phase change between plane liquid surfaces. Part 2: Observations of large temperature jumps near the interfaces
[TM-FM-8805-PT-2] N89-10973
LIQUIDS
Experiments on liquid-vapour phase change between plane liquid surfaces. Part 1: Experiments with water, freon and mercury
[TM-FM-8804-PT-1] N89-10964
Experimental and theoretical studies of vertical annular liquid jets
[DE88-012971] N89-11149
Heat release effects of reacting gas jets in liquids
[DE88-011971] N89-11175
LITERATURE
A co-citation study of the scientific literature of two innovation research traditions: Diffusion of innovations and technology transfer N89-11618
LITHIUM ALLOYS
Weldability of 2090 Al-Cu-Li alloy
[DE88-011963] N89-11015
LITHIUM ISOTOPES
Observations on cosmic abundance of He4 and Li7, comparison with primordial nuceosynthesis predictions N89-11641
LITHIUM OXIDES
Ti-implanted optical waveguides in LiNbO3
[DE88-015279] N89-11554
LITHIUM SULFUR BATTERIES
Evaluation of Li/MoS2 secondary battery for load-conditioner. Deep-cycle performance of AA-size cells
[DE88-753437] N89-11118
LOAD TESTS
Acceleration ground test program to verify GAS payload No. 559 structure/support avionics and experiment structural integrity N89-10913
A mixed-mode bending apparatus for delamination testing
[NASA-TM-100662] N89-10945
LOADS (FORCES)
Probabilistic error model of robot end-effector's dynamic state N89-11236
LOGIC CIRCUITS
Study and fabrication of AlGaAs/GaAs double heterojunction bipolar transistors for integrated injection logic circuits
[LAAS-88-138] N89-11123
LONG WAVE RADIATION
Tropical 200 mb divergent circulations and their relation to outgoing longwave radiation
[AD-A196375] N89-11370
Active modes of the Pacific Intertropical Convergence Zone (ITCZ)
[AD-A196406] N89-11374
LOSSES
Laboratory examination and seasonal analyses of the dynamic losses for a continuously variable speed heat pump
[DE88-013207] N89-11174
LOW ALTITUDE
A time-dependent model for the low-latitude ionosphere
[AD-A196683] N89-11354
LOW REYNOLDS NUMBER
Experimental results for the Eppler 387 airfoil at low Reynolds numbers in the Langley low-turbulence pressure tunnel
[NASA-TM-4062] N89-10842
LOW SPEED
Unsteady low-speed windtunnel test of a straked delta wing, oscillating in pitch. Part 1: General description and discussion of results
[AD-A196456] N89-10867
LOW TEMPERATURE
Thermal calculations of nitrogen-free nonmagnetic helium cryostats
[DE88-702807] N89-11227
LUBRICANTS
Fundamental aspects of the electronic structure, materials properties, and lubrication performance of sputtered MoS2 films
[AD-A196852] N89-11606
LUBRICATING OILS
Transactions of machine elements division: On the combined hydrodynamic and hydrostatic journal bearing
[PB88-214549] N89-11231
LUBRICATION
Investigation of a self-lubricating alumina coating formed by anodic spark deposition
[DE88-014947] N89-11035

Fundamental aspects of the electronic structure, materials properties, and lubrication performance of sputtered Mo52 films
[AD-A196852] N89-11606
LUMINESCENCE
State of the art of negative luminescence
[DE88-010871] N89-11556
LUNAR BASES
Lunar concrete for construction
[NASA-TM-89672] N89-11060
A perspective on space exploration technology catalysis: A rationale for initiating 21st Century expansion of human civilization into outer space
[NASA-TM-101362] N89-11637
LUNAR EXPLORATION
OEXP Analysis Tools Workshop
[NASA-CP-10013] N89-11407
LUNAR SOIL
Growth of plant tissue cultures in simulated lunar soil: Implications for a lunar base CELSS (Controlled Ecological Life Support System)
[NASA-CR-183233] N89-11384
LUNAR SURFACE
Planetary skin games
[DE88-009161] N89-11682

M

MACH NUMBER
Experimental aerodynamic performance of advanced 40 deg-swept 10-blade propeller model at Mach 0.6 to 0.85
[NASA-TM-88969] N89-10865
The turbulent heat flux in low Mach number flows with large density variations N89-11162
MAGELLANIC CLOUDS
Supernova 1987A in the large magellanic cloud N89-11642
MAGMA
Geothermal energy technology: Issues, R and D needs, and cooperative arrangements
[DE88-011804] N89-11299
MAGNETIC AMPLIFIERS
PALADIN: A 10.6-micron free-electron laser amplifier
[DE88-014164] N89-11207
MAGNETIC FIELD CONFIGURATIONS
Optimization of microwave magnetoelastic delay lines
[AD-A196886] N89-11131
Optimization of the two-dimensional magnetic field distribution basing on the integral equation method
[DE88-702940] N89-11490
Optimization of bootstrap current in a large helical system with L = 2
[IPPJ-889] N89-11546
MAGNETIC FIELDS
Association of plasma sheet variations with auroral changes during substorms
[DE88-014319] N89-11350
Optimization of the two-dimensional magnetic field distribution basing on the integral equation method
[DE88-702940] N89-11490
Implementation of MAGINT code on the CDC-CYBER-170/750 system
[INPE-4663-NTE/282] N89-11491
Theoretical plasma physics
[DE88-014285] N89-11518
Theory of high power cyclotron resonance heating in non-uniform magnetic field
[IPPJ-875] N89-11520
Comparison between Uramoto type and straight filament type sheet plasmas as a volume produced H(-) ion source (I)
[IPPJ-878] N89-11523
Trapping and acceleration of electron by elliptically polarized electromagnetic wave propagating across static magnetic field
[IPPJ-885] N89-11545
Current-induced quantum interference in the composite superconductor NbTi-Cu
[DE88-703079] N89-11562
Decametric radio emission of Jupiter. Part 3: Some physical characteristics of S-component sources
[DE88-702812] N89-11679
MAGNETIC FLUX
Magnetic moment test report for the model SAR 8108 battery
[INPE-4574-NTE/280] N89-11121
MAGNETIC MOMENTS
Magnetic moment test report for the model SAR 8108 battery
[INPE-4574-NTE/280] N89-11121
Magnetic fluctuations and heavy electron superconductivity
[DE88-011978] N89-11557
MAGNETIC PROPERTIES
Thermal calculations of nitrogen-free nonmagnetic helium cryostats
[DE88-702807] N89-11227
What is the origin of glassy behavior in the high-T(sub c) oxides
[DE88-012668] N89-11565
MAGNETIC STORMS
Study of a substorm on May 4, 1986
[DE88-014318] N89-11342
MAGNETIC SUSPENSION
MAGLEV: The double benefits of high-Tc superconductors and its development as an aerospace technology
[DE88-012005] N89-11570
MAGNETIC TAPES
Current research on the vibration and stability of axially-moving materials N89-11283
MAGNETOHYDRODYNAMIC FLOW
Unsteady hydromagnetic free-convection flow with radiative heat transfer in a rotating fluid. 1: Incompressible optically thin fluid
[DE88-702998] N89-11140
Unsteady hydromagnetic free-convection flow with radiative heat transfer in a rotating fluid of arbitrary optical thickness
[DE88-703000] N89-11167
Unsteady hydromagnetic free-convection flow with radiative heat transfer in a rotating fluid. 2: Compressible optically thin fluid
[DE88-702999] N89-11168
On hydromagnetic channel flow induced by tooth pulses
[DE88-703031] N89-11522
MAGNETOHYDRODYNAMIC STABILITY
Anomalous transport arising from nonlinear resistive pressure-driven modes in a plasma
[DE88-014984] N89-11531
MAGNETOHYDRODYNAMIC WAVES
Alfven wave studies on a tokamak N89-11517
Excitation of MHD surface waves propagating with shear Alfven waves in an inhomogeneous cylindrical plasma
[IPPJ-872] N89-11526
MAGNETOHYDRODYNAMICS
Godunov methods and adaptive algorithms for unsteady fluid dynamics
[DE88-013094] N89-11141
A global MHD pulsation event with conjugate study and model of ionospheric damping N89-11333
O stars and Wolf-Rayet stars
[NASA-SP-497] N89-11657
MAGNETOPLASMADYNAMICS
Use of high temperature superconductors in magnetoplasmadynamic systems
[NASA-TM-101219] N89-11553
MAGNITUDE
Planck's orders of magnitude and the limits of the quantum gravity conception
[DE88-702985] N89-11608
MAIN SEQUENCE STARS
New insights into globular clusters from main sequence photometry N89-11658
MAINTENANCE
Review of aeronautical wind tunnel facilities
[NASA-CR-183057] N89-10897
State-of-the-art-dehumidification cost-effective corrosion prevention
[AD-A196503] N89-11023
MAN MACHINE SYSTEMS
Optimization-based design of control systems
[AD-A196593] N89-11405
MAN POWERED AIRCRAFT
Flight test results for the Daedalus and Light Eagle human powered aircraft
[NASA-CR-183305] N89-10890
MANAGEMENT INFORMATION SYSTEMS
Evaluating performance of information centre operations and services N89-11630
MANEUVERABLE REENTRY BODIES
Allocating and launching MaRV interceptors based on miss distance predictions
[DE88-015370] N89-11486
MANIFOLDS (MATHEMATICS)
Integral manifold in system design with application to flexible link robot control
[AD-A197052] N89-11243
Homology classes represented by real algebraic hypersurfaces
[PB88-202908] N89-11453
MANIPULATORS
Real-time path planning for robot arms N89-11224
Robust control of a flexible manipulator arm N89-11228
Experimental verification of a model of a two-link flexible, lightweight manipulator
[NASA-CR-183216] N89-11233
On motion planning and control of multi-link lightweight robotic manipulators
[NASA-CR-181226] N89-11234
Manual, voice, and automated control of a teleoperator viewing system
[DE88-011835] N89-11235
Integral manifold in system design with application to flexible link robot control
[AD-A197052] N89-11243
Control design and performance evaluation for flexible manipulators N89-11390
Experiments in control of satellite manipulators N89-11391
MANNED SPACE FLIGHT
A perspective on space exploration technology catalysis: A rationale for initiating 21st Century expansion of human civilization into outer space
[NASA-TM-101362] N89-11637
MANNED SPACECRAFT
Performance of a circular body earth-to-orbit winged transport with various strap-on boosters
[NASA-TM-100603] N89-10929
MANUAL CONTROL
Manual, voice, and automated control of a teleoperator viewing system
[DE88-011835] N89-11235
MANUALS
Fuel cells: A handbook
[DE88-010252] N89-11309
MANY BODY PROBLEM
An O(NlogN) hypercube N-body integrator
[DE88-015016] N89-11413
An O(N) algorithm for three-dimensional N-body simulations
[AD-A196903] N89-11433
Computational structure of the N-body problem
[AD-A196422] N89-11473
MAPPING
Technique for obtaining agricultural property boundaries through satellite imagery, certified to control and accompany agricultural activity
[INPE-4640-PRE/1351] N89-11294
Parametric analysis of map data
[AD-A196908] N89-11298
MARANGONI CONVECTION
Future MAUS payload and the TWIN-MAUS configuration N89-10906
MARECS MARITIME SATELLITES
Preliminary results of MARECS-A measurements in Central Maryland and plans for 1988 MSS experiment in Australia N89-11079
MARINE METEOROLOGY
Mariners weather log, volume 32, number 2, Spring 1988
[PB88-210828] N89-11365
A study of the dynamics of maritime fronts using remotely sensed wind and stress measurements N89-11366
The climatological seasonal response of the ocean mixed layer in the equatorial and tropical Pacific Ocean
[AD-A196962] N89-11382
MARKETING
Technology transfer at Argonne National Laboratory
[DE88-012062] N89-11636
MARKOV CHAINS
Balance of recurrence order in time-inhomogeneous Markov chains with application to simulated annealing
[AD-A196980] N89-11484
MARS (PLANET)
Extraction of light gasses from Mars or its moons
[DE88-009123] N89-11681
MARS LANDING
OEXP Analysis Tools Workshop
[NASA-CP-10013] N89-11407
MARS SURFACE
Nuclear propulsion: A vital technology for the exploration of Mars and the planets beyond
[NASA-TM-101354] N89-10944
A perspective on space exploration technology catalysis: A rationale for initiating 21st Century expansion of human civilization into outer space
[NASA-TM-101362] N89-11637
MARS SURFACE SAMPLES
Risk analysis of earth return options for the Mars rover/sample return mission
[NASA-CR-172081] N89-10923
MARTENSITE
Influence of martensitic phase in abrasion behaviour of stainless steel 304 L
[DE88-702770] N89-11009
MASERS
Biological applications and effects of optical masers
[AD-A196462] N89-11217
MASS SPECTROMETERS
Spectroscopic measurement of the ion temperature on ASDEX --- tokamak N89-11536

MASS TO LIGHT RATIOS
Dark matter N89-11652
MASS TRANSFER
Fluid science investigations in microgravity
[PB88-209754] N89-11058
The impact of separated flow on heat and mass transfer
[DE88-014653] N89-11180
Experimental and theoretical studies on transport processes in laser welding
[DE88-013933] N89-11230
Low mass X-ray binaries in globular clusters and hierarchical triple systems N89-11660
MATERIALS HANDLING
Safety aspects of large-scale handling of hydrogen
[DE88-014422] N89-11070
MATHEMATICAL MODELS
Program of research in structures and dynamics
[NASA-CR-183191] N89-10838
An approximate, maximum terminal velocity descent to a point
[DE88-000349] N89-10840
Reynolds stress closure in jet flows using wave models
[NASA-CR-180226] N89-10843
Aeroelasticity and structural optimization of helicopter rotor blades with swept tips N89-10887
Process modelling for space station experiments
[NASA-CR-183274] N89-10922
Fluid mechanical properties of flames in enclosures
[DE88-014142] N89-10981
A preliminary study on the use of magnetohydrodynamic forces to remove impurities from molten metals
[DE88-013508] N89-10991
Conductivity of organic polymers: A nonlinear approach
[DE88-013837] N89-11037
Role of deflagration in explosive response
[DE88-014139] N89-11049
LMSS propagation modeling at Virginia Tech N89-11078
Mobile satellite propagation measurements and modeling: A review of results for systems engineers N89-11081
A general analysis for obtaining the viscosity function from viscometric measurements: A case study for the helical screw rheometer
[DE88-006271] N89-11139
Rheology of high concentration polymodal multiphase flow
[DE88-014541] N89-11148
Confined turbulent fluid-particle flow modeling using multiple-realization particle trajectory schemes N89-11157
On 1-D closure models for slender 3-D viscoelastic free jets: von Karman flow geometry and elliptical cross section
[DE88-014478] N89-11179
An introduction to the physics of high gain free electron lasers
[DE88-014163] N89-11208
Experimental verification of a model of a two-link flexible, lightweight manipulator
[NASA-CR-183216] N89-11233
Free damped vibration of composite plates and shells N89-11249
The mini-oscillator technique: A finite element method for the modeling of linear viscoelastic structures
[UTIAS-323] N89-11250
Continuum modeling of latticed structures N89-11253
Finite element analysis of large strain elastic-plastic solids N89-11281
A model for the response of vertical axis wind turbines to turbulent flow: Parts 1 and 2
[DE88-014708] N89-11305
Review of acid rain models for Europe
[DE88-011945] N89-11322
NOAA (National Oceanic and Atmospheric Administration) Meteorology Division support to the Environmental Protection Agency
[PB88-213624] N89-11327
Design and analysis of large-scale atmospheric dispersion experiment
[DE88-012911] N89-11330
Parameterizations of microphysical processes in clouds for application in models of regional atmospheric deposition
[DE88-010017] N89-11345
Development of a semi-empirical model for estimating the global solar radiation
[INPE-4620-TDL/328] N89-11352
A numerical modeling study of frontogenesis and cold frontal rainbands N89-11358
The Cooperative VAS Program with the Marshall Space Flight Center
[NASA-CR-179377] N89-11361
The use of the Q-vector in operational meteorology
[AD-A196410] N89-11376
The DFVLR models 1 and 2 of the Manutec r3 robot
[DFVLR-MITT-88-13] N89-11443
Dynamic robot models using the Manutec r3 as an example
[DFVLR-MITT-88-16] N89-11444
Unmodeled dynamics and nonlinear control: Wrapup
[NASA-CR-181524] N89-11457
Domain decomposition methods for the parallel computation of reacting flows
[NASA-CR-181719] N89-11459
Dynamic Interactions of Energetic Probes with Condensed Matter: Proceedings
[DE88-008882] N89-11589
Measures, methods and models employed in evaluating the effectiveness of information centers and services N89-11627
MATRICES (MATHEMATICS)
The Frobenius metric in image registration
[DE88-016685] N89-11421
On differential polynomials and their resultants
[RR-723-M] N89-11472
Problem on 0-1 matrices
[PB88-210075] N89-11477
Robust covariance matrix estimation via robust estimation of principal components
[PB88-126594] N89-11478
MAXIMUM LIKELIHOOD ESTIMATES
Some statistical aspects of attrition studies
[AD-A196665] N89-10891
Penalized likelihood estimation for rates with censored survival
[RR-726-M] N89-11479
MAXWELL EQUATION
The propagation of electromagnetic waves in thin dielectric slabs
[AD-A196995] N89-11115
MEASUREMENT
Quantization of Green-Schwarz superstring
[DE88-702242] N89-11609
MEASURING INSTRUMENTS
Vacuum Fizeau wedge wavemeter for pulsed UV lasers
[DE88-015832] N89-11206
MECHANICAL ENGINEERING
Knowledge-based design of complex mechanical systems N89-11225
MECHANICAL PROPERTIES
Composite structural materials
[NASA-CR-180224] N89-10946
Fluid mechanical properties of flames in enclosures
[DE88-014142] N89-10981
Experimental research on swept shock wave/boundary layer interactions
[AD-A196938] N89-11189
Two-dimensional saturation gain and output power in transverse flow electrical discharge CO2 lasers
[AD-A196660] N89-11218
Strong and weak stabilizability: Lyapunov type approaches
[AD-A196431] N89-11482
MECHANICAL SHOCK
The Shock and Vibration Digest, Volume 20, No. 10 N89-11252
The Shock and Vibration Digest, Volume 20, No. 7 N89-11277
The Shock and Vibration Digest, volume 20, no. 5 N89-11282
MELTING
Glass-ceramic fusion with a CO2 laser
[DE88-012871] N89-11030
The melting and crystallization kinetics of hydrogenated polybutadiene
[AD-A196988] N89-11045
Modified purification of mercuric iodide for crystal growth
[DE88-014960] N89-11580
MELTS (CRYSTAL GROWTH)
Future MAUS payload and the TWIN-MAUS configuration N89-10906
Process modelling for space station experiments
[NASA-CR-183274] N89-10922
MEMBRANES
Mechanisms of gas permeation through polymer membranes
[DE88-007761] N89-10980
Oxygen chemistry
[AD-A196989] N89-10988
MEMORY
Effects of noise and task loading on a communication task loading on a communication task
[AD-A196378] N89-11107
MEMORY (COMPUTERS)
An introduction to implementing a capacity planning effort in an MVS (Multiple Virtual Storage) environment
[AD-A196383] N89-11402
MERCURY COMPOUNDS
Preparation and evaluation of mercuric iodide for crystal growth
[DE88-014981] N89-11578
Modified purification of mercuric iodide for crystal growth
[DE88-014960] N89-11580
MERCURY TELLURIDES
A theory of surface and interface electronic properties of crystalline solids: Applications to 2-6 compounds N89-11596
MERIDIONAL FLOW
Tropical 200 mb divergent circulations and their relation to outgoing longwave radiation
[AD-A196375] N89-11370
MEROMORPHIC FUNCTIONS
Geometrical methods in quantum field theory: On the topology of spaces of holomorphic maps N89-11611
MESOSCALE PHENOMENA
Effects of downdrafts and mesoscale convective organization on the heat and moisture budgets of squall and nonsquall cloud clusters in the tropics N89-11367
Mesoscale structure and climatology of rain-snow lines over North Carolina
[AD-A196687] N89-11379
MESSAGE PROCESSING
GPS signal structure N89-10878
Digital signal design for meteor-scatter communications
[AD-A196685] N89-11111
METAL COATINGS
Characterization of metallic coatings and thin films produced by railgun deposition
[AD-A196382] N89-11021
METAL FATIGUE
Effect of protective coatings on life of heat-resistant nickel steel under cyclic heat load N89-11005
A three-dimensional investigation of steady state fatigue crack closure behavior for through-thickness and part-through flaws N89-11256
Fatigue of welded joint in a stainless steel AISI 304 L
[DE88-701622] N89-11279
METAL FILMS
Alloying of metals by teatment with nanosecond laser pulses N89-11006
Characterization of metallic coatings and thin films produced by railgun deposition
[AD-A196382] N89-11021
METAL FOAMS
The Purdue University Get Away Special II (PUGAS II) N89-10918
METAL FOILS
Potential foams and metal foils for cosmic dust capture
[DE88-012960] N89-11665
METAL IONS
Advances in metal ion sources
[DE88-012020] N89-11495
METAL PARTICLES
Surface structures and reactions of ceramics and metals
[DE88-013752] N89-11028
METAL SURFACES
Plasma spectrometry applied to surface treatments (laser PVD)
[ETCA-88-R-036] N89-11533
METAL VAPOR LASERS
High-speed photography of energetic materials and components with a copper vapor laser
[DE88-012869] N89-11212
METALLIC GLASSES
Crystallization of Zr-Ni metallic glasses
[DE88-007481] N89-11026
METALS
A preliminary study on the use of magnetohydrodynamic forces to remove impurities from molten metals
[DE88-013508] N89-10991
Experimental studies of the chemistry of metal clusters
[DE88-012034] N89-10994
Methodologies for prediction of metal oxidation-vaporization-erosion
[DE88-013623] N89-11001
A test methodology for an investigation into heating and cooling phenomena in grossly deformed tensile metallic bars
[AD-A197047] N89-11024
Simple model for the superconducting phase diagram near the metal-insulator transition
[DE88-703038] N89-11558
Constraints on the growth of metallic superlattices
[DE88-014633] N89-11586

Implantation studies of hydrogen by field ion microscopy and spectroscopy
[DE88-015806] N89-11602

METASTABLE STATE
Resonance ionization of Kr metastables using a single-frequency laser
[DE88-014757] N89-11209

METEOR TRAILS
Digital signal design for meteor-scatter communications
[AD-A196685] N89-11111

METEORITES
Planetary skin games
[DE88-009161] N89-11682

METEOROID PROTECTION
Utilization of spray on foam insulation for manned and unmanned spacecraft and structures N89-10914

METEOROLOGICAL PARAMETERS
The Cooperative VAS Program with the Marshall Space Flight Center
[NASA-CR-179377] N89-11361

METEOROLOGICAL RADAR
On deriving the 3-dimensional kinematic structure of convective storms from a single radar
[AD-A196405] N89-11373

METEOROLOGICAL SATELLITES
Tropospheric sounding from the TIROS-N series of satellites N89-11347

METEOROLOGY
Atmospheric and Geophysical Sciences Division
[DE88-013780] N89-11346
The use of the Q-vector in operational meteorology
[AD-A196410] N89-11376

METHANE
The impact of an increase in atmospheric methane on the temperature field and subsequent climatic effects
[AD-A196869] N89-11332

METHODOLOGY
Tension fatigue analysis and life prediction for composite laminates
[NASA-TM-100549] N89-10951

METHYL ALCOHOL
Assessment of methanol electro-oxidation for direct methanol-air fuel cells
[DE88-014686] N89-11317

MICROANALYSIS
Microscopy and microanalysis of shock-processed materials
[DE88-008471] N89-10990

MICROBIOLOGY
JPRS report: Science and technology. USSR: Life sciences
[JPRS-ULS-87-010] N89-11385

MICROBURSTS (METEOROLOGY)
Evaluation of enhancements to the Low Level Wind Shear Alert System (LLWAS) at Stapleton International Airport
[DOT/FAA/PS-88/14] N89-11356
An examination of a simulated microburst flow as sensed by a single Doppler radar
[AD-A196381] N89-11372

MICROCHANNEL PLATES
Curved channel MCP improvement program
[NASA-CR-180790] N89-11191

MICROCOMPUTERS
The use of portable microcomputer as a data collection tool to support integrated simulation support environments: A concept
[AD-A196414] N89-11403
Scale drift in on-line calibration
[AD-A196439] N89-11404
Finite elements software and applications N89-11415
Information storage alternatives: An overview of laser-based optical technologies
[DE88-013499] N89-11617

MICROELECTRONICS
Advanced avionics architecture pave pillar N89-10834
The electronic and optical properties of silicon/germanium strained layer superlattices N89-11590

MICROMECHANICS
Computer simulation of the uni-axial stress-strain behavior of ribbon-like fiber nonwovens N89-11284

MICROMINIATURIZATION
Microsoldering and microminiature welding with lasers
[DE88-013368] N89-11240

MICROORGANISMS
The flux and recycling of bioactive substances in the surface sediments of the deep basins off southern California
[DE88-007999] N89-11321

MICROPOROSITY
Microporous polymer foams for biomaterials
[DE88-010578] N89-11036

MICROPROCESSORS
Review of acid rain models for Europe
[DE88-011945] N89-11322

MICROSTRUCTURE
Microscopy and microanalysis of shock-processed materials
[DE88-008471] N89-10990
Microstructural development of titanium-modified austenitic stainless steel under neutron irradiation in HFIR up to 57 dpa
[DE88-013248] N89-10999
Microstructure and properties of rapidly solidified beryllium-transition metal alloys
[DE88-010937] N89-11012
Characterization of ceramic films and interfaces by electron microscopic and spectroscopic techniques
[DE88-011957] N89-11029
Joining of advanced aluminides
[DE88-015111] N89-11226
Ion implantation and thermal annealing of high-T(ssub c) single crystals of YBa2Cu3O(sub x)
[DE88-012201] N89-11564
The critical current density, the fabrication process and the microstructure in superconducting composites of NbTi for high energy physics
[DE88-014241] N89-11568
Influence of grain boundary structure distribution and processing history on intergranular creep cavitation
[DE88-015808] N89-11571
Microstructural defects and superconducting critical currents in superconductors
[DE88-013781] N89-11587
Potential foams and metal foils for cosmic dust capture
[DE88-012960] N89-11665

MICROTRONS
Analysis of free electron laser performance utilizing the National Bureau of Standards' CW microtron
[AD-A196928] N89-11221

MICROWAVE FREQUENCIES
Analysis of nonlinear circuits at RF and microwave frequencies by the harmonic balance method
[INPE-4693-TDL/342] N89-11126
Optimization of microwave magnetoelastic delay lines
[AD-A196866] N89-11131

MICROWAVE RADIOMETERS
Ground-based radiometric observations of emission and attenuation at 20.6, 31.65, and 90.0 GHz N89-11086

MICROWAVE SCATTERING
Synthesis of resistive tapers to control scattering patterns of strips
[AD-A196402] N89-11110

MICROWAVE TRANSMISSION
OPEX: (Olympus Propagation EXperiment) N89-11090

MICROWAVES
A digital beacon receiver N89-11092
Olympus beacon receiver N89-11093
Statistical effects in high-power microwave beam propagation
[DE88-012440] N89-11100
Optimization of microwave magnetoelastic delay lines
[AD-A196866] N89-11131
Microwave radiances from horizontally finite, vertically structured precipitating clouds N89-11364

MIGRATION
Velocity analysis by iterative profile migration N89-11339

MILITARY HELICOPTERS
Design and evaluation of a cockpit display for hovering flight
[NASA-CR-183247] N89-10900

MILITARY OPERATIONS
Beam handling and emittance control
[AD-A196789] N89-11509

MILITARY TECHNOLOGY
Civil and military applications of GPS N89-10882

MILLIMETER WAVES
Millimeter-wave studies N89-11085
Plan of propagation and communication experiments using ETS-VI N89-11088
Dielectric millimeter waveguides. Volume 1
[AD-A196844] N89-11112

MINERALS
Markers of air pollution in forests: Nutrient cycling
[DE88-011011] N89-11319

MINIATURIZATION
Integrated quartz oscillator for aerospace applications
[ETN-88-93100] N89-11125

MINICOMPUTERS
Finite elements software and applications N89-11415

MIRRORS
JPRS Report: Science and Technology. USSR: Materials Science
[JPRS-UMS-88-007] N89-11002
Characteristics of laser beam focusing with single spherical mirrors during laser treatment N89-11004
Effect of thermal cycling
[AD-A196851] N89-11219
Design of high-reflectivity supermirror structures
[DE88-015287] N89-11511

MISCIBILITY GAP
The first Chinese student space shuttle getaway special program N89-10903

MISS DISTANCE
Allocating and launching MaRV interceptors based on miss distance predictions
[DE88-015370] N89-11486

MISSILE CONTROL
Computing Systems Configuration for Highly Integrated Guidance and Control Systems
[AGARD-LS-158] N89-10831

MISSILE DEFENSE
Interceptor-to-target allocation strategies for Strategic Defense 1: Adaptive strategies based upon system and threat characteristics
[AD-A197037] N89-11487

MISSILES
Numerical simulation of axisymmetric base flow on tactical missiles with propulsive jet
[AD-A196169] N89-11136

MISSION PLANNING
OEXP Analysis Tools Workshop
[NASA-CP-10013] N89-11407

MIXED OXIDES
Electrochemical reactions of mixed cobalt/nickel oxide hydroxides in alkaline electrolyte
[ATR-86(9561)-4] N89-10965

MIXING
Experimental and analytical study of vapor explosions in stratified geometries
[DE88-011964] N89-11046
Mixing and Demixing Processes in Multiphase Flows With Application to Propulsion Systems
[NASA-CP-3006] N89-11153
Measurements and predictions of mixed convection in laminar and turbulent boundary layer flows N89-11164

MOBILE COMMUNICATION SYSTEMS
Proceedings of the Twelfth NASA Propagation Experimenters Meeting (NAPEX 12)
[NASA-CR-182796] N89-11074
PiFEx data and archival formats N89-11076
Results of 1987 MSS helicopter propagation experiment at UHF and L band in Central Maryland N89-11077
LMSS propagation modeling at Virginia Tech N89-11078
Preliminary results of MARECS-A measurements in Central Maryland and plans for 1988 MSS experiment in Australia N89-11079
ETS-V propagation experiments in Japan N89-11080
Mobile satellite propagation measurements and modeling: A review of results for systems engineers N89-11081

MODAL RESPONSE
The Shock and Vibration Digest, Volume 20, No. 6 N89-11261
A comparative overview of modal testing and system identification for control of structures N89-11262
Dynamic analysis of pipings by modal synthesis
[DE88-701620] N89-11274

MODELS
Polarimetric clutter modeling: Theory and application
[NASA-CR-183348] N89-11106
Ultrasonic flaw classification: An approach using modeling, signal processing, and adaptive learning N89-11248
Structure of wind-shear turbulence
[NASA-CR-183257] N89-11359
Assessing schema knowledge
[AD-A196933] N89-11447
Comparison of recent model selection criteria for system identification
[PD-SE-8807] N89-11449
Inflation in a renormalizable cosmological model and the cosmic no hair conjecture
[NASA-CR-183363] N89-11614

MODULATION
Modulation of radar backscatter from the ocean by a variable surface current
[AD-A196952] N89-11114

MODULUS OF ELASTICITY
Development of elastomeric polypeptide biomaterials
[AD-A196900] N89-11044

MOIRE FRINGES
In-plane moire optical processing at ARL
[ARL-STRUC-R-428] N89-11510

MOISTURE CONTENT
Effects of downdrafts and mesoscale convective organization on the heat and moisture budgets of squall and nonsquall cloud clusters in the tropics N89-11367

Synoptic scale sensitivity of TIROS-N moisture channels in the tropics
[AD-A196686] N89-11378

MOLECULAR BEAM EPITAXY
Design and fabrication by molecular beam epitaxy of visible light emitting ridge waveguide GaAs-AlGaAs quantum well lasers
[LAAS-88-097] N89-11215
Molecular beam epitaxy of GaP films on Si substrates
[PB88-131974] N89-11581

MOLECULAR CLOUDS
Shocked interstellar gas in dense molecular clouds N89-11670

MOLECULAR GASES
Electron attachment properties of excited dielectric-gas molecules and their possible use for pulse power switching
[DE88-009705] N89-11117

MOLECULAR PHYSICS
Fluid science investigations in microgravity
[PB88-209754] N89-11058

MOLECULAR STRUCTURE
Lattice instability in single-crystal La(sub 2-x)Sr(sub x)/CuO4
[DE88-013994] N89-11598
Molecular processes in comets
[NASA-CR-182742] N89-11671

MOLTEN SALT ELECTROLYTES
Oxygen electrode in molten carbonate fuel cells
[DE88-009628] N89-11308

MOLYBDENUM
The effect of thermal ageing on the stress corrosion cracking of 9Cr1Mo steel in aqueous caustic environments
[NRL-R-1003(R)] N89-10997

MOLYBDENUM DISULFIDES
Evaluation of Li/MoS2 secondary battery for load-conditioner. Deep-cycle performance of AA-size cells
[DE88-753437] N89-11118

MOLYBDENUM SULFIDES
Fundamental aspects of the electronic structure, materials properties, and lubrication performance of sputtered MoS2 films
[AD-A196852] N89-11606

MOMENTUM TRANSFER
Continuum theories for fluid-particle flows: Some aspects of lift forces and turbulence N89-11155

MONKEYS
Functional assessment of laser irradiation
[AD-A196930] N89-11222

MONOCHROMATIC RADIATION
Structural anomalies in undoped Gallium Arsenide observed in high resolution diffraction imaging with monochromatic synchrotron radiation
[NASA-CR-183268] N89-11595

MONOMERS
Synthesis of energetic binders
[AD-A196886] N89-11042

MONTANA
Three dimensional gravity modeling techniques with application to the Ennis Geothermal Area, part 1
[DE88-014952] N89-11340

MONTE CARLO METHOD
Probabilistic error model of robot end-effector's dynamic state N89-11236
Lattice gauge theory on the hypercube
[DE88-015004] N89-11420
Monte Carlo study of ion cyclotron resonance heating in helical systems
[IPPJ-884] N89-11544
Strongly interacting fermion systems: Emphasis on heavy fermions
[DE88-014127] N89-11573

MORPHOLOGY
Microporous polymer foams for biomaterials
[DE88-010578] N89-11036
Lithium secondary batteries: Role of polymer cathode morphology
[AD-A196998] N89-11135
Real algebraic morphisms into even-dimensional spheres
[PB88-202916] N89-11462

MOTION SIMULATORS
Sandia National Laboratories flight simulation facilities
[DE88-012108] N89-10898
Prototype data acquisition and analysis system for Navy operational flight simulators
[DE88-014557] N89-10901

MSAT
PiFEx propagation experiments N89-11075

MULLITES
Phase transformations in xerogels of mullite composition
[NASA-TM-101349] N89-11038

MULTIBEAM ANTENNAS
Plan of propagation and communication experiments using ETS-VI N89-11088

MULTIPATH TRANSMISSION
Results of 1987 MSS helicopter propagation experiment at UHF and L band in Central Maryland N89-11077
LMSS propagation modeling at Virginia Tech N89-11078

MULTIPHASE FLOW
Rheology of high concentration polymodal multiphase flow
[DE88-014541] N89-11148
Mixing and Demixing Processes in Multiphase Flows With Application to Propulsion Systems
[NASA-CP-3006] N89-11153
The application of single particle hydrodynamics in continuum models of multiphase flow N89-11154
Periodically structured multiphase flows and hydrodynamic instabilities in narrow capillaries
[DE88-015608] N89-11181

MULTIPLE ACCESS
Plan of advanced satellite communications experiment using ETS-VI N89-11089
Bit-to-bit error dependence in direct-sequence spread-spectrum multiple-access packet radio systems
[AD-A196384] N89-11108

MULTIPROCESSING (COMPUTERS)
Strategies for concurrent processing of complex algorithms in data driven architectures
[NASA-CR-181329] N89-11406
Programming abstractions for run-time partitioning of scientific continuum calculations running on multiprocessors
[DE88-007376] N89-11411
SOPMCR: An operating system for the multiprocessor for communication networks
[INPE-4675-NTE/284] N89-11438

MULTISPECTRAL BAND SCANNERS
The Cooperative VAS Program with the Marshall Space Flight Center
[NASA-CR-179377] N89-11361

MULTIVARIATE STATISTICAL ANALYSIS
General results in optimal control of discrete-time nonlinear stochastic systems
[AD-A196411] N89-11481

N

N-TYPE SEMICONDUCTORS
Surface passivation of Gallium Arsenide
[AD-A196695] N89-11605

NASA PROGRAMS
Patent abstracts bibliography: A continuing bibliography (supplement 33). Section 2: Indexes
[NASA-SP-7039(33)] N89-11624

NASTRAN
A model for the response of vertical axis wind turbines to turbulent flow: Parts 1 and 2
[DE88-014708] N89-11305

NATURAL GAS
Exploitation and utilization of hydrocarbons
[DE88-012626] N89-11048

NATURAL LANGUAGE (COMPUTERS)
Concerning interfaces in natural languages
[INPE-4681-PRE/1376] N89-11634

NAVIER-STOKES EQUATION
Numerical investigation of a jet in ground effect using the fortified Navier-Stokes scheme N89-10857
A diagonally inverted LU implicit multigrid scheme for the 3-D Navier-Stokes equations and a two equation model of turbulence
[NASA-CR-182209] N89-10863
Cascade flow analysis by Navier-Stokes equation N89-11065
Study of flow past a circular cylinder using a higher order scheme for Navier-Stokes equation
[TM-FM-8806] N89-11142
Experimental and theoretical studies of vertical annular liquid jets
[DE88-012971] N89-11149

NAVIGATION SATELLITES
The NAVSTAR GPS System
[AGARD-LS-161] N89-10874
The GPS overview and navigation system concept N89-10875

NEGATIVE IONS
Development of the work function monitoring method for a converter of a negative ion source
[IPPJ-880] N89-11529

NEGATIVE RESISTANCE CIRCUITS
Determination of the unstable states of the solid state plasma in semiconductor devices
[AD-A196403] N89-11550

NEODYMIUM LASERS
Optimization of microwave magnetoelastic delay lines
[AD-A196866] N89-11131
Laser plume temperature measurements in various gases
[DE88-006462] N89-11204
Biological applications and effects of optical masers
[AD-A196462] N89-11217
Microsoldering and microminiature welding with lasers
[DE88-013368] N89-11240

NETWORK ANALYSIS
A co-citation study of the scientific literature of two innovation research traditions: Diffusion of innovations and technology transfer N89-11618

NETWORK SYNTHESIS
A coherent VLSI design environment
[AD-A196428] N89-11130

NEUROLOGY
Three-dimensional computer graphics brain-mapping project
[AD-A197053] N89-11435

NEUTRAL ATMOSPHERES
A nonlinear wave-wave interaction theory for the generation of multi-scale large eddies in a neutral atmospheric boundary layer N89-11344

NEUTRAL PARTICLES
Simultaneous background measurement in the ASDEX neutral particle diagnostics N89-11543

NEUTRON EMISSION
Measurement of the absolute neutron yield of ASDEX with nuclear emulsion plates — tokamak N89-11537
Interpretation of neutron rate measurements using the NR code N89-11538
Calculation of neutron propagation for ASDEX — tokamak N89-11539

NEUTRON IRRADIATION
Microstructural development of titanium-modified austenitic stainless steel under neutron irradiation in HFIR up to 57 dpa
[DE88-013248] N89-10999

NEUTRON SCATTERING
Calculation of neutron propagation for ASDEX — tokamak N89-11539
Spin correlations in high T(sub c) superconductors
[DE88-013988] N89-11555

NEUTRON SOURCES
Neutron multiplication in beryllium
[AD-A196877] N89-11503

NEUTRON STARS
Astrophysical evidence on the equation of state
[DE88-011960] N89-11668
Three probable stellar mass black holes
[AD-A196976] N89-11676

NEWTONIAN FLUIDS
Microrheological observations of the onset of non-Newtonian behavior in suspensions
[DE88-006198] N89-10962

NICKEL
Studies of the transpassive nitric acid corrosion of various austenitic CrNi steels in the prolonged Huey test (65 percent HNO3, 120 C, 720 h)
[DE88-010494] N89-10998
Effect of protective coatings on life of heat-resistant nickel steel under cyclic heat load N89-11005
Laser Raman spectroscopy of anodic corrosion and inhibitor films on iron and nickel
[DE88-009958] N89-11008

NICKEL ALLOYS
Atomic probe study of ordering and precipitation in nickel-based alloys N89-10993
Calorimetry study of the synthesis of amorphous Ni-Ti alloys by mechanical alloying
[DE88-006468] N89-11010
The role of grain boundary character in the environmentally-assisted intergranular cracking mechanism of nickel-base alloys
[DE88-014130] N89-11018

NIOBIUM ALLOYS
Current-induced quantum interference in the composite superconductor NbTi-Cu
[DE88-703079] N89-11562

NIOBIUM OXIDES
Ti-implanted optical waveguides in LiNbO3
[DE88-015279] N89-11554

NITRIC ACID
Studies of the transpassive nitric acid corrosion of various austenitic CrNi steels in the prolonged Huey test (65 percent HNO3, 120 C, 720 h)
[DE88-010494] N89-10998

NITRIDES
Nitride layer growth in iron and titanium alloys: Studies by electron probe microanalysis
[DE88-007207] N89-11017

NITROGEN IONS
Implantation studies of hydrogen by field ion microscopy and spectroscopy
[DE88-015806] N89-11602
NITROGEN OXIDES
The importance of thermodynamics to the modeling of nitrogen combustion chemistry
[DE88-014656] N89-10978
Research on catalyst combustion for gas turbine N89-11063
The flux and recycling of bioactive substances in the surface sediments of the deep basins off southern California
[DE88-007999] N89-11321
NOISE GENERATORS
Response of discretely stiffened structures and transmission of structure-borne noise N89-11270
NOISE INTENSITY
Effects of noise and task loading on a communication task loading on a communication task
[AD-A196378] N89-11107
NOISE MEASUREMENT
Noise of the Harrier in vertical landing and takeoff N89-10856
NOISE POLLUTION
Effects of noise and task loading on a communication task loading on a communication task
[AD-A196378] N89-11107
NOISE REDUCTION
Electrical noise reduction techniques contributing to improved data quality at the National Transonic Facility
[NASA-CR-4193] N89-11196
Response of discretely stiffened structures and transmission of structure-borne noise N89-11270
NONCONSERVATIVE FORCES
Vibrations and stability of mechanical systems: 4 N89-11260
NONDESTRUCTIVE TESTS
Experiments in the application of ultrasound diffraction tomography for nondestructive testing
[DE88-014694] N89-11245
The interpretation of electromagnetic nondestructive flaw detection in metals N89-11246
Ultrasonic flaw classification: An approach using modeling, signal processing, and adaptive learning N89-11248
NONLINEAR EQUATIONS
The Shock and Vibration Digest, Volume 20, No. 6 N89-11261
Nonlinear random vibration in mechanical systems N89-11263
Control design and performance evaluation for flexible manipulators N89-11390
Unmodeled dynamics and nonlinear control: Wrapup
[NASA-CR-181524] N89-11457
NONLINEAR SYSTEMS
Non-linear aerodynamic characteristics obtained from the analysis of flight-data
[AR-004-571] N89-10866
Analysis of nonlinear circuits at RF and microwave frequencies by the harmonic balance method
[INPE-4693-TDL/342] N89-11126
General results in optimal control of discrete-time nonlinear stochastic systems
[AD-A196411] N89-11481
NONLINEARITY
Nonlinear theories of composite laminates under compression with delamination
[CERT-RT-18/3542-RY-071-R] N89-10954
New non-linear optical polymers
[AD-A196859] N89-11040
NONOSCILLATORY ACTION
A numerical study of ENO and TVD schemes for shock capturing
[NASA-TM-101355] N89-11469
NONUNIFORMITY
Theory of high power cyclotron resonance heating in non-uniform magnetic field
[IPPJ-875] N89-11520
NORMAL DENSITY FUNCTIONS
The generation of scatterometer surface targets with specified surface statistics
[AD-A196397] N89-11480
NORTH AMERICA
Recent climate change in North America and CO2: Search in stratified daily data
[DE88-014669] N89-11323
Acid precipitation in North America: 1985 annual and seasonal data summaries from Acid Deposition System data base
[DE88-013563] N89-11325
NOSES (FOREBODIES)
Study of three dimensional boundary layers on the front of a fuselage and at an air intake
[CERT-OA-22/5025-AYD] N89-11184
NUCLEAR EMULSIONS
Measurement of the absolute neutron yield of ASDEX with nuclear emulsion plates --- tokamak N89-11537
Calculation of neutron propagation for ASDEX --- tokamak N89-11539
Numerical simulation of the response function of a nuclear emulsion plate N89-11540
NUCLEAR ENGINE FOR ROCKET VEHICLES
Nuclear propulsion: A vital technology for the exploration of Mars and the planets beyond
[NASA-TM-101354] N89-10944
NUCLEAR FUEL ELEMENTS
KCl bounce coating of glass and polymer microshells
[DE88-013018] N89-11524
NUCLEAR FUELS
Critical experiments in support of the CNPS (Compace Nuclear Power Source) program
[DE88-014326] N89-11507
NUCLEAR FUSION
ASDEX contributions to the DPG Fruehjahrstagung --- tokamak
[IPP-III/134] N89-11534
Nuclear processes in the early universe. Part 1: The thermal history of matter N89-11639
Observations on cosmic abundance of He4 and Li7, comparison with primordial nucleosynthesis predictions N89-11641
On relative supernova rates and nucleosynthesis roles
[NASA-CR-183373] N89-11673
NUCLEAR PARTICLES
The Purdue University Get Away Special II (PUGAS II) N89-10918
NUCLEAR PHYSICS
Technology transfer at Argonne National Laboratory
[DE88-012062] N89-11636
NUCLEAR POWER PLANTS
Contribution for stress analysis in bend acessories of piping systems
[DE88-701618] N89-11272
Dynamic analysis of pipings by modal synthesis
[DE88-701620] N89-11274
Fatigue of welded joint in a stainless steel AISI 304 L
[DE88-701622] N89-11279
Postanalysis of the CNPS (Compact Nuclear Power Source) critical experiment
[DE88-014322] N89-11506
NUCLEAR PROPULSION
Nuclear propulsion: A vital technology for the exploration of Mars and the planets beyond
[NASA-TM-101354] N89-10944
NUCLEAR REACTIONS
Development of advanced internal gain radiation detector structures based on neutron transmutation doped silicon, high T(sub c) superconductive compounds and their potential application to detection of ionizing radiation
[DE88-012563] N89-11574
NUCLEAR REACTOR CONTROL
Analysis of SP-100 critical experiments
[DE88-014429] N89-11508
NUCLEAR REACTORS
Critical experiments in support of the CNPS (Compace Nuclear Power Source) program
[DE88-014326] N89-11507
NUCLEAR WEAPONS
Engineering research and development: Thrust area report, FY87
[DE88-013792] N89-11059
NUCLEATION
Microgravity nucleation and particle coagulation experiments support
[NASA-CR-183282] N89-11056
Impurity-induced changes in interfacial strength and their role in creep fracture
[DE88-013197] N89-11255
NUMERICAL ANALYSIS
Interaction of electromagnetic waves with heterogeneous bodies of arbitrary shape and parameters N89-11095
Numerical estimates of the rate of convergence for the vortex sheet method
[DE88-013809] N89-11178
Basic rules of saturated gain variation in a flowing laser cavity
[AD-A196861] N89-11220
Communication aspects of parallel processing
[AD-A196458] N89-11439
A numerical study of ENO and TVD schemes for shock capturing
[NASA-TM-101355] N89-11469
NUMERICAL CONTROL
Computerized monitoring and control of experiments in space N89-10915
NUMERICAL INTEGRATION
Abstraction in numerical methods
[AD-A196990] N89-11476
NUMERICAL STABILITY
Advanced desiccant materials assessment, phase 2
[PB88-217054] N89-11033
NUMERICAL WEATHER FORECASTING
The Cooperative VAS Program with the Marshall Space Flight Center
[NASA-CR-179377] N89-11361

O

OBSERVATION
Automatic concept formation in a rich input domain
[AD-A196719] N89-11445
OCEAN CURRENTS
Derivation of revised formulae for eddy viscous forces used in the ocean general circulation model
[NASA-TM-4060] N89-11381
OCEAN DYNAMICS
A study of the dynamics of maritime fronts using remotely sensed wind and stress measurements N89-11366
OCEAN MODELS
Derivation of revised formulae for eddy viscous forces used in the ocean general circulation model
[NASA-TM-4060] N89-11381
The climatological seasonal response of the ocean mixed layer in the equatorial and tropical Pacific Ocean
[AD-A196962] N89-11382
OCEAN SURFACE
Modulation of radar backscatter from the ocean by a variable surface current
[AD-A196952] N89-11114
OCTANES
A detailed chemical kinetic reaction mechanism for the oxidation of iso-octane and n-heptane over an extended temperature range and its application to analysis of engine knock
[DE88-005370] N89-11053
ON-LINE SYSTEMS
Scale drift in on-line calibration
[AD-A196439] N89-11404
ONBOARD DATA PROCESSING
Study of the multiplexing of image telemetry data from SPOT 4 HRVIR and Vegetation sensors
[CNES-87/229/CT/DRT/TIT/TR] N89-10930
Presentation of research and development action 1206: Preliminary study report on the CESTAC method --- calculation check
[CNES-CT/PTI/MS/MN/067] N89-11424
OPERATING SYSTEMS (COMPUTERS)
PC-CUBE: A personal computer based hypercube
[DE88-015008] N89-11394
OPERATIONS RESEARCH
An introduction to implementing a capacity planning effort in an MVS (Multiple Virtual Storage) environment
[AD-A196383] N89-11402
OPERATORS (MATHEMATICS)
Differential operation of NAVSTAR GPS for enhanced accuracy N89-10883
OPTICAL COMMUNICATION
Proceedings of the Twelfth NASA Propagation Experimenters Meeting (NAPEX 12)
[NASA-CR-182796] N89-11074
Laser communications through the atmosphere N89-11087
Bibliography of Soviet laser developments, number 87, January - February 1987
[AD-A196973] N89-11223
State-of-the-art in fiber optic systems at the Aeronautic Test Center, Toulouse (France)
[REPT-363300] N89-11513
OPTICAL DATA PROCESSING
In-plane moire optical processing at ARL
[ARL-STRUC-R-428] N89-11510
Information storage alternatives: An overview of laser-based optical technologies
[DE88-013499] N89-11617
OPTICAL DISKS
Information storage alternatives: An overview of laser-based optical technologies
[DE88-013499] N89-11617
OPTICAL EMISSION SPECTROSCOPY
Plasma spectrometry applied to surface treatments (laser PVD)
[ETCA-88-R-036] N89-11533
OPTICAL FIBERS
State-of-the-art in fiber optic systems at the Aeronautic Test Center, Toulouse (France)
[REPT-363300] N89-11513
OPTICAL PROPERTIES
The determination of the spacecraft contamination environment
[AD-A196435] N89-10937
New non-linear optical polymers
[AD-A196859] N89-11040

Optical scattering and microphysical properties of subvisual cirrus clouds, and climatic implications
[NASA-CR-183301] N89-11362
Applications of the optical differential thermal analysis
[AD-A196706] N89-11515
Ti-implanted optical waveguides in LiNbO3
[DE88-015279] N89-11554
The electronic and optical properties of silicon/germanium strained layer superlattices N89-11590

OPTICAL RADAR
An inertial velocity reference for the NASA airborne Doppler lidar
[NASA-CR-179378] N89-11203

OPTICAL THICKNESS
Unsteady hydromagnetic free-convection flow with radiative heat transfer in a rotating fluid of arbitrary optical thickness
[DE88-703000] N89-11167

OPTICAL WAVEGUIDES
Ti-implanted optical waveguides in LiNbO3
[DE88-015279] N89-11554

OPTIMAL CONTROL
Integral manifold in system design with application to flexible link robot control
[AD-A197052] N89-11243

OPTIMIZATION
Aeroelasticity and structural optimization of helicopter rotor blades with swept tips N89-10887
Optimization of microwave magnetoelastic delay lines
[AD-A196866] N89-11131
Vacuum Fizeau wedge wavemeter for pulsed UV lasers
[DE88-015832] N89-11206
A method for improving the depth of penetration and the appearance of welding
[DE88-012954] N89-11239
Optimization of transparent and reflecting electrodes for amorphous silicon solar cells
[DE88-001175] N89-11316
Parallel algorithm for a class of optimization problems
[PB88-209929] N89-11414
The Frobenius metric in image registration
[DE88-016685] N89-11421
Periodic solutions of the Hamilton-Jacobi equation by the shooting method: A technique for beam dynamics
[DE88-012733] N89-11460
Optimization of the two-dimensional magnetic field distribution basing on the integral equation method
[DE88-702940] N89-11490

ORBIT CALCULATION
Risk analysis of earth return options for the Mars rover/sample return mission
[NASA-CR-172081] N89-10923
Elaboration of specifications for an expert system to aid the choice of analytical methods of orbit extrapolation for satellite localization
[CNES-CT/DTI/MS/MN/160] N89-10924

ORBITAL ASSEMBLY
The potential of a GAS can with payload G-169 N89-10916

ORBITAL MANEUVERS
Payload boomerang technology described N89-11066

ORBITS
The steady states of the Kuramoto--Sivashinsky equation
[DE88-011819] N89-11451

ORDER-DISORDER TRANSFORMATIONS
Atomic probe study of ordering and precipitation in nickel-based alloys N89-10993
Simple model for the superconducting phase diagram near the metal-insulator transition
[DE88-703038] N89-11558
X-ray scattering studies of non-equilibrium ordering processes
[DE88-012908] N89-11569

ORGANIC MATERIALS
Conductivity of organic polymers: A nonlinear approach
[DE88-013637] N89-11037

ORGANOMETALLIC COMPOUNDS
Ligand intermediates in metal catalyzed reactions
[DE88-012123] N89-11007

ORTHOSTATIC TOLERANCE
Effect of physical fitness on response to orthostasis in healthy young women
[AD-A196377] N89-11387

OSCILLATORS
Study of optical output couplers for submillimeter wavelength backward-wave oscillators (BWO's)
[NASA-TM-101360] N89-11128
Temporal variations in a CW HF MOPA (oscillator/amplifier)
[AD-A196915] N89-11132
Analysis of free electron laser performance utilizing the National Bureau of Standards' CW microtron
[AD-A196928] N89-11221

OUTPUT
Study of optical output couplers for submillimeter wavelength backward-wave oscillators (BWO's)
[NASA-TM-101360] N89-11128
Two-dimensional saturation gain and output power in transverse flow electrical discharge CO2 lasers
[AD-A196660] N89-11218

OVERPRESSURE
Explosion airblast predictions on a personal computer and application to the Henderson, Nevada incident
[DE88-014991] N89-11144

OXIDATION
Laboratory investigations of low earth orbit environmental effects on spacecraft
[DE88-009135] N89-10932
Carbon films derived from poly(acrylonitrile): Oxidation, electrical properties, and processing
[DE88-010352] N89-10950
Methodologies for prediction of metal oxidation-vaporization-erosion
[DE88-013623] N89-11001
Surface structures and reactions of ceramics and metals
[DE88-013752] N89-11028
A detailed chemical kinetic reaction mechanism for the oxidation of iso-octane and n-heptane over an extended temperature range and its application to analysis of engine knock
[DE88-005370] N89-11053
A method for improving the depth of penetration and the appearance of welding
[DE88-012954] N89-11239
Assessment of methanol electro-oxidation for direct methanol-air fuel cells
[DE88-014686] N89-11317

OXIDATION-REDUCTION REACTIONS
Oxidation reduction potential of the Cu(3)/Cu(2) system in alkaline solutions
[NASA-TT-20309] N89-10963
Development of an experimental model of self-propagating high temperature oxidation-reduction reactions
[AD-A196978] N89-10987

OXIDE FILMS
Optimization of transparent and reflecting electrodes for amorphous silicon solar cells
[DE88-001175] N89-11316

OXIDES
What is the origin of glassy behavior in the high-T(sub c) oxides
[DE88-012668] N89-11565
Some theoretical aspects of high-T(sub c) superconductivity
[DE88-013101] N89-11592
New quantum interferometer effect in superconducting oxide ceramics
[DE88-703152] N89-11603
An oxide passivated and ion-implanted Si detector for X-ray astronomy
[ISAS-RN-353] N89-11663

OXYGEN
Laboratory investigations of low earth orbit environmental effects on spacecraft
[DE88-009135] N89-10932
Theory of oxygen ordering and absorption in 1,2,3 high-T(sub c) superconductors
[DE88-007543] N89-11575

OXYGEN ATOMS
High energy-intensity atomic oxygen beam source for low earth orbit materials degradation studies
[DE88-014316] N89-11504

OZONE DEPLETION
Ozone hole of the Antarctica: Recent results
[INPE-4518-PRE/1270] N89-11329
A new determination of extinction due to atmospheric aerosols and the resulting implications for upper stratospheric ozone depletion N89-11348

P

PACIFIC OCEAN
Active modes of the Pacific Intertropical Convergence Zone (ITCZ)
[AD-A196406] N89-11374
Synoptic scale sensitivity of TIROS-N moisture channels in the tropics
[AD-A196686] N89-11378
The climatological seasonal response of the ocean mixed layer in the equatorial and tropical Pacific Ocean
[AD-A196962] N89-11382

PACKETS (COMMUNICATION)
Bit-to-bit error dependence in direct-sequence spread-spectrum multiple-access packet radio systems
[AD-A196384] N89-11108

PAINTS
The transportation of fine arts materials aboard the space shuttle Columbia. GAS payload No. 481: Vertical horizons N89-10919

PANELS
Delamination buckling of pressure-loaded, laminated cylindrical shells and panels N89-11276

PARABOLIC DIFFERENTIAL EQUATIONS
Second order parabolic equations for flow-domains
[DE88-703158] N89-11467

PARALLEL COMPUTERS
Computatinal fluid dynamics and supercomputers, chapter 6 N89-11400

PARALLEL PROCESSING (COMPUTERS)
High speed parallel processing networks for advanced architectures N89-10837
A coherent VLSI design environment
[AD-A196428] N89-11130
A performance model for massive parallelism
[DE88-011763] N89-11393
Representing high-level knowledge structures in massively parallel networks N89-11409
An O(NlogN) hypercube N-body integrator
[DE88-015016] N89-11413
An O(N) algorithm for three-dimensional N-body simulations
[AD-A196903] N89-11433
Models for parallel computation on distributed-memory multiprocessors
[DE88-010078] N89-11436
Parallel processing a real code: A case history
[DE88-014456] N89-11437
Communication aspects of parallel processing
[AD-A196458] N89-11439
Domain decomposition methods for the parallel computation of reacting flows
[NASA-CR-181719] N89-11459
Computational structure of the N-body problem
[AD-A196422] N89-11473

PARALLEL PROGRAMMING
Parallel algorithm for a class of optimization problems
[PB88-209929] N89-11414
Parallelizing recursive programs
[RR-728-I-IMAG-83-LIFIA] N89-11429
Poker (4.0): A programmer's reference guide
[AD-A196417] N89-11430
Poker (4.1): A programmer's reference guide
[AD-A196419] N89-11431

PARAMETER IDENTIFICATION
Protein crystal growth in low gravity
[NASA-CR-183183] N89-11055

PARAMETERIZATION
Response of discretely stiffened structures and transmission of structure-borne noise N89-11270
Parametric analysis of map data
[AD-A196908] N89-11298
Parameterizations of microphysical processes in clouds for application in models of regional atmospheric deposition
[DE88-010017] N89-11345
Practical applications and limitations of adaptive control N89-11442

PARITY
Coupled even-parity superconducting states
[AD-A196969] N89-11607

PARTIAL DIFFERENTIAL EQUATIONS
Communication aspects of parallel processing
[AD-A196458] N89-11439
The steady states of the Kuramoto--Sivashinsky equation
[DE88-011819] N89-11451
Domain decomposition methods for the parallel computation of reacting flows
[NASA-CR-181719] N89-11459
Second order parabolic equations for flow-domains
[DE88-703158] N89-11467

PARTICLE ACCELERATORS
Periodic solutions of the Hamilton-Jacobi equation by the shooting method: A technique for beam dynamics
[DE88-012733] N89-11460

PARTICLE BEAMS
Lie algebraic treatment of space charge N89-11496
High energy-intensity atomic oxygen beam source for low earth orbit materials degradation studies
[DE88-014316] N89-11504

PARTICLE COLLISIONS
Numerical simulation of the response function of a nuclear emulsion plate N89-11540

PARTICLE DENSITY (CONCENTRATION)
A comparative planetological study of particle speed and concentration during aeolian saltation N89-11677

PARTICLE EMISSION
The compatibility of gravity and kaon results in the search for new forces
[DE88-013993] N89-11612
PARTICLE INTERACTIONS
Low frequency dielectric properties of polyether electrolytes
[AD-A196494] N89-11039
Stochastic theory of frequency redistribution in two-photon processes N89-11669
PARTICLE PRECIPITATION
The utility of particle precipitation data as an input to thermospheric density models for satellite orbital analysis
[AD-A196870] N89-10925
PARTICLE PRODUCTION
Neutron multiplication in beryllium
[AD-A196877] N89-11503
Interpretation of neutron rate measurements using the NR code N89-11538
PARTICLE SIZE DISTRIBUTION
Rheology of high concentration polymodal multiphase flow
[DE88-014541] N89-11148
Particle sizing by weighted measurements of scattered light
[NASA-TM-100968] N89-11198
A theoretical investigation of the collection of aerosol particles by falling ice crystals N89-11337
PARTICLE THEORY
Particle physics candidates for the cosmion solution to the solar neutrino problem
[DE88-014479] N89-11683
PARTICLE TRAJECTORIES
Algorithm for the study of particle movement in the inner magnetosphere of the earth
[INPE-4669-PRE/1369] N89-11351
Lie algebraic treatment of space charge N89-11496
A comparative planetological study of particle speed and concentration during aeolian saltation N89-11677
PARTICLES
Confined turbulent fluid-particle flow modeling using multiple-realization particle trajectory schemes N89-11157
Particle dispersion models and drag coefficients for particles in turbulent flows N89-11158
Wave-particle interactions in the magnetosphere of Uranus
[NASA-CR-183299] N89-11678
PARTICULATES
The determination of the spacecraft contamination environment
[AD-A196435] N89-10937
Measurements of pressure drop and heat transfer in turbulent pipe flows of particulate slurries
[DE88-013622] N89-11150
PASSIVITY
Surface passivation of Gallium Arsenide
[AD-A196695] N89-11605
An oxide passivated and ion-implanted Si detector for X-ray astronomy
[ISAS-RN-353] N89-11663
PATENT POLICY
Patent abstracts bibliography: A continuing bibliography (supplement 33). Section 2: Indexes
[NASA-SP-7039(33)] N89-11624
PATTERN RECOGNITION
Accessibility, a criterion for the choice of visual coding rules
[PB88-209911] N89-11458
PAYLOAD CONTROL
Hitchhiker capabilities N89-10917
JPRS report: Science and technology: Japan
[JPRS-JST-87-018] N89-11061
Payload boomerang technology described N89-11066
PAYLOAD INTEGRATION
Hitchhiker capabilities N89-10917
PAYLOAD RETRIEVAL (STS)
Payload boomerang technology described N89-11066
PAYLOAD STATIONS
Hitchhiker capabilities N89-10917
PAYLOAD TRANSFER
Payload boomerang technology described N89-11066
PAYLOADS
Space science/space station attached payload pointing accommodation study: Technology assessment white paper
[NASA-CR-182735] N89-10931
OPEX: (Olympus Propagation EXperiment) N89-11090
PELLETS
KCl bounce coating of glass and polymer microshells
[DE88-013018] N89-11524
PENETRATION
A method for improving the depth of penetration and the appearance of welding
[DE88-012954] N89-11239
PERCEPTION
Measuring the vague meanings of probability terms
[AD-A196944] N89-11483
PERFORMANCE PREDICTION
Computing system configuration for fighter aircraft flight control systems N89-10832
A performance model for massive parallelism
[DE88-011763] N89-11393
Algorithm and general software considerations N89-11397
PERFORMANCE TESTS
Fabricate, calibrate and test a dosimeter for integration into the CRRES (Combined Release and Radiation Effects Satellite) satellite
[AD-A196496] N89-10938
Preliminary results of MARECS-A measurements in Central Maryland and plans for 1988 MSS experiment in Australia N89-11079
ETS-V propagation experiments in Japan N89-11080
Plan of advanced satellite communications experiment using ETS-VI N89-11089
ACTS and OLYMPUS propagation experiments N89-11091
Evaluation of Li/MoS2 secondary battery for load-conditioner. Deep-cycle performance of AA-size cells
[DE88-753437] N89-11118
Engine driven heat pump program overview
[DE88-013240] N89-11165
Advanced heat-pipe heat exchanger and microprocessor-based modulating burner controls development
[PB88-217070] N89-11172
Preliminary assessment of a magnetically coupled free-piston Stirling engine heat pump compressor
[DE88-013835] N89-11232
Longitudinal impact test of a transport airframe section
[DOT/FAA/CT-87/26] N89-11265
The photovoltaic advanced systems test facility
[DE88-009589] N89-11306
Fuel cells: A handbook
[DE88-010252] N89-11309
Amorphous silicon photovoltaic devices prepared by chemical and photochemical vapor deposition of higher order silanes
[DE88-001189] N89-11311
Enhancing performance under stress by information about its expected duration
[AD-A196836] N89-11388
Control design and performance evaluation for flexible manipulators N89-11390
PERMANENT MAGNETS
Comparison between Uramoto type and straight filament type sheet plasmas as a volume produced H(-) ion source (I)
[IPPJ-876] N89-11523
PERMEATING
Mechanisms of gas permeation through polymer membranes
[DE88-007761] N89-10980
PERMITTIVITY
Technique for measuring the dielectric constant of thin materials
[NASA-CR-183325] N89-10984
Polarizability and effective permittivity of layered and continuously inhomogeneous dielectric spheres
[PB88-210091] N89-11104
PERSONNEL MANAGEMENT
Evaluating the performance of information centre staff N89-11629
Evaluating performance of information centre operations and services N89-11630
A framework for evaluating the effectiveness of information centres and services N89-11631
PERTURBATION
Integral manifold in system design with application to flexible link robot control
[AD-A197052] N89-11243
Strong and weak stabilizability: Lyapunov type approaches
[AD-A196431] N89-11482
PERTURBATION THEORY
An approximate, maximum terminal velocity descent to a point
[DE88-000349] N89-10840
The steady states of the Kuramoto--Sivashinsky equation
[DE88-011819] N89-11451
Stochastic theory of frequency redistribution in two-photon processes N89-11669
PETN
Friction and impact sensitivities of explosives: A comparative study
[DE88-012664] N89-11051
PH
Spectral studies of three oxisols and a Ultisol of Brazil
[INPE-4644-PRE/1355] N89-11297
PHASE DIAGRAMS
Nitride layer growth in iron and titanium alloys: Studies by electron probe microanalysis
[DE88-007207] N89-11017
Nuclear processes in the early universe. Part 2: The cosmic quark-hadron phase transition N89-11640
PHASE SHIFT
A new radar technique for satellite rainfall algorithm development
[NASA-CR-183471] N89-11102
The Electron Laser Facility: Measurement of modes, harmonics, parametric dependence, and phase shift
[DE88-014165] N89-11200
PHASE TRANSFORMATIONS
Experiments on liquid-vapour phase change between plane liquid surfaces. Part 1: Experiments with water, freon and mercury
[TM-FM-8804-PT-1] N89-10964
Near-critical NaCl-H2O: An equation of state and discussion of anomalous properties
[DE88-012029] N89-10969
Crystallization of Zr-Ni metallic glasses
[DE88-007481] N89-11026
Microporous polymer foams for biomaterials
[DE88-010578] N89-11036
Phase transformations in xerogels of mullite composition
[NASA-TM-101349] N89-11038
Current-induced quantum interference in the composite superconductor NbTi-Cu
[DE88-703079] N89-11562
Kinetic processes of the orthorhombic to tetragonal phase transition in YBa2Cu3O7-Delta
[DE88-011993] N89-11572
Electron microscopy of modulated and ordered alloys
[DE88-008667] N89-11584
Lattice instability in single-crystal La(sub 2-x)Sr(sub x)/CuO4
[DE88-013994] N89-11598
Phase transitions as the origin of large scale structure in the universe
[NASA-CR-183359] N89-11674
PHONONS
The coefficient of first viscosity via three-phonon processes in bulk liquid helium
[AD-A196902] N89-10986
Some theoretical aspects of high-T(sub c) superconductivity
[DE88-013101] N89-11592
Phonon-plasmon mechanism of high-T(sub c) superconductivity
[DE88-014869] N89-11600
PHOSPHORIC ACID
Surface passivation of Gallium Arsenide
[AD-A196695] N89-11605
PHOSPHORIC ACID FUEL CELLS
Fuel cells: A handbook
[DE88-010252] N89-11309
PHOTOACOUSTIC SPECTROSCOPY
Photoacoustic spectroscopy and the in situ characterization of the electrochemical interface
[DE88-013848] N89-10975
PHOTOCATHODES
Simulations of the laser photocathode injector
[DE88-015337] N89-11202
Effect of surface states on the electrochemical behaviour of single crystal n-ZnSe photoelectrode
[DE88-702726] N89-11566
PHOTOCHEMICAL REACTIONS
Novel composite materials: Alloys from immiscible components
[AD-A197040] N89-10958
Amorphous silicon photovoltaic devices prepared by chemical and photochemical vapor deposition of higher order silanes
[DE88-001189] N89-11311
PHOTOCONDUCTIVITY
Multiple pulse photoconductive semiconductor switching
[DE88-011792] N89-11119
PHOTOELECTRIC EMISSION
Electronic properties of sigma-conjugated polysilanes
[DE88-012699] N89-11032
Development of the work function monitoring method for a converter of a negative ion source
[IPPJ-880] N89-11529
Dynamic Interactions of Energetic Probes with Condensed Matter: Proceedings
[DE88-008882] N89-11589

PHOTOINTERPRETATION
CIR aerial photography applied to the evaluation of the air pollution impact in a tropical forest: The case of Cubatao, Brazil
[INPE-4651-PRE/1358] N89-11324
Color enhancement of remote sensing imagery using IHS transformations and decorrelation stretch methods
[INPE-4559-PRE/1300] N89-11418
PHOTOIONIZATION
Resonance ionization of Kr metastables using a single-frequency laser
[DE88-014757] N89-11209
PHOTOLUMINESCENCE
Surface passivation of Gallium Arsenide
[AD-A196695] N89-11605
PHOTOLYSIS
Kinetics of boron hydride interconversion reactions
[AD-A196824] N89-10985
PHOTOMETRY
Investigation of ionospheric D region aeronomy using incoherent scatter radar and optical measurements
N89-11338
PHOTONS
Stochastic theory of frequency redistribution in two-photon processes N89-11669
Photoerosion and the abundances of the light elements
[NASA-CR-183372] N89-11675
PHOTONUCLEAR REACTIONS
Photoerosion and the abundances of the light elements
[NASA-CR-183372] N89-11675
PHOTOSPHERE
Coronal magnetic fields produced by photospheric shear
[AD-A194591] N89-11684
PHOTOSYNTHESIS
A composite photobioelectronic material
[DE88-012490] N89-11383
PHOTOVOLTAIC CELLS
The photovoltaic advanced systems test facility
[DE88-009589] N89-11306
Amorphous silicon photovoltaic devices prepared by chemical and photochemical vapor deposition of higher order silanes
[DE88-001189] N89-11311
PV modules for ground testing
[NASA-CR-179476] N89-11315
PHOTOVOLTAIC CONVERSION
National Photovoltaics Program: 1987 program review
[DE88-001148] N89-11301
PHYSICAL FITNESS
Effect of physical fitness on response to orthostasis in healthy young women
[AD-A196377] N89-11387
PHYSIOLOGICAL RESPONSES
Individual differences in adaptation to hypoxia and cold based on emotional-behavioral criterion of bodily reactivity N89-11386
Effect of physical fitness on response to orthostasis in healthy young women
[AD-A196377] N89-11387
PHYSIOLOGY
JPRS report: Science and technology. USSR: Life sciences
[JPRS-ULS-87-010] N89-11385
PIEZOELECTRICITY
Measurement of glass shell buckling strength using a piezoelectric film sensor
[DE88-013016] N89-11280
PILOT PERFORMANCE
Aeronautical decision making for commercial pilots
[DOT/FAA/PM-86/42] N89-10870
PIPE FLOW
Friction reduction and heat transfer enhancement in turbulent pipe flow of non-Newtonian liquid-solid mixtures
[DE88-010018] N89-11138
Measurements of pressure drop and heat transfer in turbulent pipe flows of particulate slurries
[DE88-013822] N89-11150
Confined turbulent fluid-particle flow modeling using multiple-realization particle trajectory schemes
N89-11157
PIPELINING (COMPUTERS)
Parallelizing recursive programs
[RR-728-I-IMAG-83-LIFIA] N89-11429
Models for parallel computation on distributed-memory multiprocessors
[DE88-010078] N89-11436
PIPES (TUBES)
Low stress brittle fractures in polymers
[DE88-014236] N89-11027
Laser/fluorescent dye flow visualization technique developed for system component thermal hydraulic studies
[DE88-012008] N89-11137
Periodically structured multiphase flows and hydrodynamic instabilities in narrow capillaries
[DE88-015608] N89-11181
Contribution for stress analysis in bend acessories of piping systems
[DE88-701618] N89-11272
Dynamic analysis of pipings by modal synthesis
[DE88-701620] N89-11274
Fatigue of welded joint in a stainless steel AISI 304 L
[DE88-701622] N89-11279
PISTON ENGINES
Preliminary assessment of a magnetically coupled free-piston Stirling engine heat pump compressor
[DE88-013835] N89-11232
PITCHING MOMENTS
Flow around a delta wing with or without a canard (Phi BA = 60 deg). Part 2: Hydrodynamic visualizations in unsteady flow (pitching oscillations)
[ONERA-RT-11/2891-AN-PT-2] N89-10860
PLANAR STRUCTURES
Effect of curvature on the backscattering from leaves
[NASA-CR-183326] N89-11296
PLANCKS CONSTANT
Planck's orders of magnitude and the limits of the quantum gravity conception
[DE88-702985] N89-11608
PLANETARY ATMOSPHERES
Extraction of light gasses from Mars or its moons
[DE88-009123] N89-11681
PLANETARY MAGNETOSPHERES
Wave-particle interactions in the magnetosphere of Uranus
[NASA-CR-183299] N89-11678
PLANETARY SURFACES
A comparative planetological study of particle speed and concentration during aeolian saltation N89-11677
PLANETARY WAVES
Studies of barotropic flow over topography using a galerkin finite element model
[AD-A196516] N89-11353
PLANNING
Evaluating for information center planning
N89-11632
PLANTS (BOTANY)
Growth of plant tissue cultures in simulated lunar soil: Implications for a lunar base CELSS (Controlled Ecological Life Support System)
[NASA-CR-183233] N89-11384
PLASMA CONTROL
Implementation of MAGINT code on the CDC-CYBER-170/750 system
[INPE-4663-NTE/282] N89-11491
Massachusetts Institute of Technology Plasma Fusion Center 1987--1988 report to the President
[DE88-014800] N89-11519
Modelling of the 2-dimensional structure and impurity transport for a scrape-off layer with a solid limiter
[IPPJ-873] N89-11527
PLASMA CURRENTS
Experimental study of time-varying current flow between electrodes immersed in a laboratory magnetoplasma
N89-11521
Optimization of bootstrap current in a large helical system with L = 2
[IPPJ-889] N89-11546
PLASMA DECAY
Comparison between Uramoto type and straight filament type sheet plasma as a volume produced H(-) ion source (2)
[IPPJ-887] N89-11548
PLASMA DENSITY
Comparison between Uramoto type and straight filament type sheet plasma as a volume produced H(-) ion source (2)
[IPPJ-887] N89-11548
PLASMA DIAGNOSTICS
Theoretical plasma physics
[DE88-014285] N89-11518
Massachusetts Institute of Technology Plasma Fusion Center 1987--1988 report to the President
[DE88-014800] N89-11519
Plasma spectrometry applied to surface treatments (laser PVD)
[ETCA-88-R-036] N89-11533
ASDEX contributions to the DPG Fruehjahrstagung --- tokamak
[IPP-III/134] N89-11534
Measurements of proton and triton spectra in ASDEX discharges --- tokamak N89-11541
Advantages of a helium beam for active charge exchange diagnostics --- ASDEX tokamak N89-11542
Simultaneous background measurement in the ASDEX neutral particle diagnostics N89-11543
PLASMA HEATING
Monte Carlo study of ion cyclotron resonance heating in helical systems
[IPPJ-884] N89-11544
Power absorption and confinement studies of ICRF-heated plasma in JIPP T-IIU tokamak
[IPPJ-886] N89-11547
PLASMA INTERACTIONS
Modelling of the 2-dimensional structure and impurity transport for a scrape-off layer with a solid limiter
[IPPJ-873] N89-11527
Plasma spectrometry applied to surface treatments (laser PVD)
[ETCA-88-R-036] N89-11533
PLASMA LAYERS
Association of plasma sheet variations with auroral changes during substorms
[DE88-014319] N89-11350
PLASMA PHYSICS
Theoretical plasma physics
[DE88-014285] N89-11518
PLASMA PINCH
Determination of the unstable states of the solid state plasma in semiconductor devices
[AD-A196403] N89-11550
PLASMA WAVES
Wave-particle interactions in the magnetosphere of Uranus
[NASA-CR-183299] N89-11678
PLASMAS (PHYSICS)
Plasma exposure tests of a carbon fiber/epoxy composite
[DE88-014724] N89-10947
Statistical effects in high-power microwave beam propagation
[DE88-012440] N89-11100
A code for the solution of the Vlasov-Fokker-Planck equation in one or two dimensions
[DE88-013288] N89-11463
Experimental study of time-varying current flow between electrodes immersed in a laboratory magnetoplasma
N89-11521
Stellarator theory
[DE88-014131] N89-11528
Anomalous transport arising from nonlinear resistive pressure-driven modes in a plasma
[DE88-014984] N89-11531
Optimization of bootstrap current in a large helical system with L = 2
[IPPJ-889] N89-11546
Power absorption and confinement studies of ICRF-heated plasma in JIPP T-IIU tokamak
[IPPJ-886] N89-11547
Comparison between Uramoto type and straight filament type sheet plasma as a volume produced H(-) ion source (2)
[IPPJ-887] N89-11548
Determination of the unstable states of the solid state plasma in semiconductor devices
[AD-A196403] N89-11550
PLASMONS
Some theoretical aspects of high-T(sub c) superconductivity
[DE88-013101] N89-11592
PLASTIC PROPERTIES
Indentation plasticity and fracture in silicon
[NASA-TP-2863] N89-10996
A three-dimensional investigation of steady state fatigue crack closure behavior for through-thickness and part-through flaws N89-11256
PLATE THEORY
Transverse flexure of an elastic plate loaded through a rigid inclusion N89-11267
PLATES (STRUCTURAL MEMBERS)
Free damped vibration of composite plates and shells
N89-11249
PLATES (TECTONICS)
Crustal structure of the northwestern United States
N89-11349
PLATING
Developments and trends in electrodeposition
[DE88-009822] N89-11014
PLUMES
Laser plume temperature measurements in various gases
[DE88-006462] N89-11204
Design and analysis of large-scale atmospheric dispersion experiment
[DE88-012911] N89-11330
POINTING CONTROL SYSTEMS
Space science/space station attached payload pointing accommodation study: Technology assessment white paper
[NASA-CR-182735] N89-10931

POLARIMETRY
Polarimetric clutter modeling: Theory and application
[NASA-CR-183348] N89-11106
POLARIZATION (CHARGE SEPARATION)
Trapping and acceleration of electron by elliptically polarized electromagnetic wave propagating across static magnetic field
[IPPJ-885] N89-11545
POLARIZATION (WAVES)
A new radar technique for satellite rainfall algorithm development
[NASA-CR-183471] N89-11102
Polarizability and effective permittivity of layered and continuously inhomogeneous dielectric spheres
[PB88-210091] N89-11104
POLLUTION TRANSPORT
NOAA (National Oceanic and Atmospheric Administration) Meteorology Division support to the Environmental Protection Agency
[PB88-213624] N89-11327
Design and analysis of large-scale atmospheric dispersion experiment
[DE88-012911] N89-11330
Modelling of the 2-dimensional structure and impurity transport for a scrape-off layer with a solid limiter
[IPPJ-873] N89-11527
POLYAMIDE RESINS
New non-linear optical polymers
[AD-A196859] N89-11040
POLYBUTADIENE
The melting and crystallization kinetics of hydrogenated polybutadiene
[AD-A196988] N89-11045
POLYETHER RESINS
Energetic thermoplastic elastomer synthesis
[AD-A196885] N89-11041
POLYETHYLENES
Low stress brittle fractures in polymers
[DE88-014236] N89-11027
Low frequency dielectric properties of polyether electrolytes
[AD-A196494] N89-11039
POLYMER CHEMISTRY
Development of elastomeric polypeptide biomaterials
[AD-A196900] N89-11044
KCl bounce coating of glass and polymer microshells
[DE88-013018] N89-11524
POLYMERIC FILMS
Multistress aging of polymer films
[DE88-008094] N89-11034
POLYMERIZATION
Conductivity of organic polymers: A nonlinear approach
[DE88-013837] N89-11037
POLYNOMIALS
On differential polynomials and their resultants
[RR-723-M] N89-11472
POLYPEPTIDES
Development of elastomeric polypeptide biomaterials
[AD-A196900] N89-11044
POLYURETHANE FOAM
Microporous polymer foams for biomaterials
[DE88-010578] N89-11036
POLYVINYL FLUORIDE
Measurement of glass shell buckling strength using a piezoelectric film sensor
[DE88-013016] N89-11280
POPULATION THEORY
On empirical Bayes selection rules for negative binomial populations
[AD-A196994] N89-11485
POPULATIONS
On empirical Bayes selection rules for negative binomial populations
[AD-A196994] N89-11485
PORTABLE EQUIPMENT
The use of portable microcomputer as a data collection tool to support integrated simulation support environments: A concept
[AD-A196414] N89-11403
POSITION (LOCATION)
The Global Positioning System (GPS) constellation and coverage N89-10876
Probable locations of extraterrestrial civilizations
[DE88-702605] N89-11392
POTASSIUM CHLORIDES
KCl bounce coating of glass and polymer microshells
[DE88-013018] N89-11524
POTENTIAL FIELDS
Coronal magnetic fields produced by photospheric shear
[AD-A194591] N89-11684
POWDER (PARTICLES)
The thermal resistance of fine powders at atmospheric pressure and under vacuum
[DE88-014556] N89-10982
Calorimetry study of the synthesis of amorphous Ni-Ti alloys by mechanical alloying
[DE88-006468] N89-11010
Chemical preparation of powders and films for high temperature superconductors
[DE88-015266] N89-11601
POWER CONDITIONING
The state-of-the-art of dc power distribution systems/components for space applications
[NASA-CR-182743] N89-10941
The photovoltaic advanced systems test facility
[DE88-009589] N89-11306
POWER EFFICIENCY
Thermodynamic improvements for the space thermoacoustic refrigerator (STAR)
[AD-A196958] N89-11071
POWER LINES
The Shock and Vibration Digest, Volume 20, No. 7 N89-11277
POWER TRANSMISSION
Statistical effects in high-power microwave beam propagation
[DE88-012440] N89-11100
PRASEODYMIUM
Advanced materials for solid oxide fuel cells: Hafnium-praseodymium-indium oxide system
[DE88-015365] N89-11310
PREAMPLIFIERS
Switchable auto gain amplifier
[DE88-012114] N89-11122
PRECIPITATES
Inorganic chemical precipitate formation payload design N89-10920
PRECIPITATION (CHEMISTRY)
Inorganic chemical precipitate formation payload design N89-10920
Atomic probe study of ordering and precipitation in nickel-based alloys N89-10993
PREDICTION ANALYSIS TECHNIQUES
Numerical description of cavitation on axisymmetric bodies
[DE88-006826] N89-11147
A computational study of coherent structures in the wakes of two-dimensional bluff bodies
[AD-A196820] N89-11188
Determination of complex exponentials, least squares and prediction methods
[AD-A196498] N89-11474
PREDICTIONS
Tension fatigue analysis and life prediction for composite laminates
[NASA-TM-100549] N89-10951
LMSS propagation modeling at Virginia Tech N89-11078
Measurements and predictions of mixed convection in laminar and turbulent boundary layer flows N89-11164
Developing laminar flow and heat transfer in ducts of arbitrary cross section N89-11176
The effects of seismic waves, part 2 N89-11254
PREMIXED FLAMES
Reaction rates in premixed turbulent flames and their relevance to the turbulent burning speed
[DE88-012021] N89-10960
Nongradient diffusion in premixed turbulent flames N89-11161
PREPROCESSING
PRIMEL: A preprocessor for the analysis of laminated composites. Introduction and user's guide (operation system OS/VS2 (MVS))
[DFVLR-MITT-88-14] N89-10956
PRESSURE
Delamination buckling of pressure-loaded, laminated cylindrical shells and panels N89-11276
Pair potential trend of alkali metals under external pressure
[DE88-702973] N89-11593
PRESSURE DISTRIBUTION
Unsteady low-speed windtunnel test of a straked delta wing, oscillating in pitch. Part 1: General description and discussion of results
[AD-A196456] N89-10867
Numerical description of cavitation on axisymmetric bodies
[DE88-006826] N89-11147
PRESSURE EFFECTS
Role of deflagration in explosive response
[DE88-014139] N89-11049
Electrical resistivity of U(sub 1-x)M(sub x)Be13 under pressure
[DE88-014449] N89-11552
PRESSURE GRADIENTS
The turbulent heat flux in low Mach number flows with large density variations N89-11162
Anomalous transport arising from nonlinear resistive pressure-driven modes in a plasma
[DE88-014984] N89-11531
PRESSURE REDUCTION
Hydrodynamical characteristics of helium two-phase flows at relatively high mass rates
[DE88-702936] N89-11143
Measurements of pressure drop and heat transfer in turbulent pipe flows of particulate slurries
[DE88-013622] N89-11150
PRESSURE VESSELS
Plasma exposure tests of a carbon fiber/epoxy composite
[DE88-014724] N89-10947
PRESSURIZING
Review of the space shuttle propulsion pressurization system probabilistic risk assessment
[DE88-013163] N89-10928
PRINCIPAL COMPONENTS ANALYSIS
Robust covariance matrix estimation via robust estimation of principal components
[PB88-126594] N89-11478
PROBABILITY THEORY
Probabilistic error model of robot end-effector's dynamic state N89-11236
Probable locations of extraterrestrial civilizations
[DE88-702605] N89-11392
Calculating the CEP (Circular Error Probable)
[NASA-CR-182996] N89-11475
Measuring the vague meanings of probability terms
[AD-A196944] N89-11483
PROBLEM SOLVING
Fundamental research in applied mathematics
[AD-A193668] N89-11454
Equational problems and disunification
[RR-727-I-IMAG-82-LIFIA] N89-11471
PROCESS CONTROL (INDUSTRY)
Microstructure and properties of rapidly solidified beryllium-transition metal alloys
[DE88-010937] N89-11012
Chemical preparation of powders and films for high temperature superconductors
[DE88-015266] N89-11601
PRODUCTIVITY
A framework for evaluating the effectiveness of information centres and services N89-11631
PROGRAM VERIFICATION (COMPUTERS)
Verification of EOSAEL (Electro-Optical Systems Atmospheric Effects Library) snow transmittance predictions
[DREV-R-4423/87] N89-11099
PROGRAMMING LANGUAGES
ENGEN: An intermediate language to HILO extension of the FIRST silicon compiler, executive summary
[ESA-CR(P)-2621] N89-11422
Poker (4.0): A programmer's reference guide
[AD-A196417] N89-11430
Poker (4.1): A programmer's reference guide
[AD-A196419] N89-11431
The transformative compression of coherent languages N89-11623
Concerning interfaces in natural languages
[INPE-4681-PRE/1376] N89-11634
PROJECT MANAGEMENT
Technology transfer at Argonne National Laboratory
[DE88-012062] N89-11636
PROJECTILES
Numerical simulation of axisymmetric base flow on tactical missiles with propulsive jet
[AD-A196169] N89-11136
PROPELLANT COMBUSTION
Combustion of energetic materials
[DE88-011286] N89-10977
Modeling of combustion processes of stick propellants via combined Eulerian-Lagrangian approach N89-11163
PROPELLANT GRAINS
A method for obtaining empirical correlations for predicting crack propagation in a burning solid propellant grain
[AD-A196689] N89-11054
Modeling of combustion processes of stick propellants via combined Eulerian-Lagrangian approach N89-11163
PROPELLANTS
Preliminary design study of hydrogen and ammonia resistojets for prime and auxiliary thrusters
[NASA-CR-182176] N89-10943
PROPELLERS
Experimental aerodynamic performance of advanced 40 deg-swept 10-blade propeller model at Mach 0.6 to 0.85
[NASA-TM-88969] N89-10865
PROPULSION
Review of the space shuttle propulsion pressurization system probabilistic risk assessment
[DE88-013163] N89-10928
Mixing and Demixing Processes in Multiphase Flows With Application to Propulsion Systems
[NASA-CP-3006] N89-11153

PROTECTION
Experimental guidelines for the design of turbine rotor fragment containment rings
[DOT/FAA/CT-88/21] N89-10893
PROTECTIVE COATINGS
A novel approach to abrasion resistance
[DE88-014180] N89-10949
JPRS Report: Science and Technology. USSR: Materials Science
[JPRS-UMS-88-007] N89-11002
Effect of protective coatings on life of heat-resistant nickel steel under cyclic heat load N89-11005
Laser Raman spectroscopy of anodic corrosion and inhibitor films on iron and nickel
[DE88-009958] N89-11008
State-of-the-art-dehumidification cost-effective corrosion prevention
[AD-A196503] N89-11023
Survivability of coatings: Program review
[DE88-009863] N89-11031
PROTEINS
Development of elastomeric polypeptide biomaterials
[AD-A196900] N89-11044
Protein crystal growth in low gravity
[NASA-CR-183183] N89-11055
PROTON SCATTERING
Pseudo-scalar pi N coupling and relativistic proton-nucleus scattering
[NASA-TM-101199] N89-11498
PROTONS
The geographical distributions of electrons (0.05-3.2 MeV) and protons (0.58-35 MeV) at altitudes of 350-850 km
[ISAS-RN-358] N89-11335
Measurements of proton and triton spectra in ASDEX discharges --- tokamak N89-11541
Proton decay experiment and neutrinos from supernova (Kamiokande-2) N89-11653
PROTOTYPES
Prototype data acquisition and analysis system for Navy operational flight simulators
[DE88-014557] N89-10901
Evaluation of the prototype EUROSID dummy and comparison with the US SID (Side Impact Dummies)
[PB88-201934] N89-11389
The development of prototype absorbers with variable characteristics
[BBC-RD-1988/5] N89-11492
An investigation of information systems prototyping N89-11622
PSEUDOPOTENTIALS
Spin-orbit interaction effects in zincblende semiconductors: Ab initio pseudopotential calculations
[DE88-014663] N89-11599
PSYCHOMETRICS
Scale drift in on-line calibration
[AD-A196439] N89-11404
PULSE FREQUENCY MODULATION TELEMETRY
Study of the multiplexing of image telemetry data from SPOT 4 HRVIR and Vegetation sensors
[CNES-87/229/CT/DRT/TIT/TR] N89-10930
PULSED LASERS
Laser wavemeter/spectrometer operating manual
[NASA-CR-180802] N89-11195
Damage effects on thin acrylic targets caused by infrared radiation from a pulsed carbon dioxide laser
[AD-A196385] N89-11216
PULSES
Alloying of metals by teatment with nanosecond laser pulses N89-11006
Multiple pulse photoconductive semiconductor switching
[DE88-011792] N89-11119
On hydromagnetic channel flow induced by tooth pulses
[DE88-703031] N89-11522
PURIFICATION
Modified purification of mercuric iodide for crystal growth
[DE88-014960] N89-11580
PURITY
Superfluid helium as a dark matter detector
[DE88-012759] N89-11664
PYRIDINES
Polystyrylpyridine (PSP) resin-based short-fiber composites (injectable compounds)
[REPT-NT-195/87/CRB/GTR.C/NP] N89-10955
PYROLYSIS
Carbon films derived from poly(acrylonitrile): Oxidation, electrical properties, and processing
[DE88-010352] N89-10950
Research needs in high temperature chemistry
[DE88-012929] N89-10961
PYROMETERS
Multicolor pyrometer for materials processing in space
[NASA-CR-183189] N89-11057

Q

QUALITY
Electrical noise reduction techniques contributing to improved data quality at the National Transonic Facility
[NASA-CR-4193] N89-11196
QUANTUM CHROMODYNAMICS
Lattice gauge theory on the hypercube
[DE88-015004] N89-11420
QUANTUM MECHANICS
The initiation and detonation of explosives: An alternative concept
[DE88-014199] N89-11047
QUANTUM THEORY
Planck's orders of magnitude and the limits of the quantum gravity conception
[DE88-702985] N89-11608
Geometrical methods in quantum field theory: On the topology of spaces of holomorphic maps N89-11611
QUANTUM WELLS
Design and fabrication by molecular beam epitaxy of visible light emitting ridge waveguide GaAs-AlGaAs quantum well lasers
[LAAS-88-097] N89-11215
QUARK MODELS
Electroproduction of baryon resonances aboce the delta(1232)
[CEBAF-PR-88-012] N89-11499
QUARKS
Nuclear processes in the early universe. Part 2: The cosmic quark-hadron phase transition N89-11640
QUARTZ CRYSTALS
Integrated quartz oscillator for aerospace applications
[ETN-88-93100] N89-11125
QUATERNARY ALLOYS
Electronic properties of 3-5 semiconductor alloys N89-11560

R

RADAR
On deriving the 3-dimensional kinematic structure of convective storms from a single radar
[AD-A196405] N89-11373
RADAR BEAMS
A survey of digital beam forming techniques and current technology
[AD-A196376] N89-11514
RADAR CROSS SECTIONS
Modulation of radar backscatter from the ocean by a variable surface current
[AD-A196952] N89-11114
RADAR DETECTION
A new radar technique for satellite rainfall algorithm development
[NASA-CR-183471] N89-11102
An examination of a simulated microburst flow as sensed by a single Doppler radar
[AD-A196381] N89-11372
RADAR TARGETS
The generation of scatterometer surface targets with specified surface statistics
[AD-A196397] N89-11480
RADAR TRACKING
On deriving the 3-dimensional kinematic structure of convective storms from a single radar
[AD-A196405] N89-11373
RADIANCE
Microwave radiances from horizontally finite, vertically structured precipitating clouds N89-11364
RADIATION COUNTERS
HIEN-LO: An experiment for charge determination of cosmic rays of interplanetary and solar origin N89-10908
Interpretation of neutron rate measurements using the NR code N89-11538
RADIATION DAMAGE
Survivability of coatings: Program review
[DE88-009863] N89-11031
Damage effects on thin acrylic targets caused by infrared radiation from a pulsed carbon dioxide laser
[AD-A196385] N89-11216
RADIATION DETECTORS
The Purdue University Get Away Special II (PUGAS II) N89-10918
Development of advanced internal gain radiation detector structures based on neutron transmutation doped silicon, high T(sub c) superconductive compounds and their potential application to detection of ionizing radiation
[DE88-012563] N89-11574
RADIATION EFFECTS
Fabricate, calibrate and test a dosimeter for integration into the CRRES (Combined Release and Radiation Effects Satellite) satellite
[AD-A196496] N89-10938
Plasma exposure tests of a carbon fiber/epoxy composite
[DE88-014724] N89-10947
Brillouin scattering: Its application to the study of damage and amorphization
[DE88-012053] N89-11016
Near surface chemistry and corrosion behavior of excimer laser surface-melted AISI type 304 stainless steel
[DE88-014440] N89-11019
Statistical effects in high-power microwave beam propagation
[DE88-012440] N89-11100
The impact of an increase in atmospheric methane on the temperature field and subsequent climatic effects
[AD-A196869] N89-11332
RADIATION HAZARDS
Systems report for payload G-652: Project origins N89-10911
RADIATION MEASUREMENT
Comparison of measured and modeled radiation, heat and water vapor fluxes: FIFE pilot study
[NASA-CR-183304] N89-11368
Simultaneous background measurement in the ASDEX neutral particle diagnostics N89-11543
Development of advanced internal gain radiation detector structures based on neutron transmutation doped silicon, high T(sub c) superconductive compounds and their potential application to detection of ionizing radiation
[DE88-012563] N89-11574
RADIATIVE HEAT TRANSFER
A study of the effect of thermal radiation on laminar flame propagation and ignition, 1981-1987 N89-10967
Unsteady hydromagnetic free-convection flow with radiative heat transfer in a rotating fluid. 1: Incompressible optically thin fluid
[DE88-702998] N89-11140
Unsteady hydromagnetic free-convection flow with radiative heat transfer in a rotating fluid of arbitrary optical thickness
[DE88-703000] N89-11167
Unsteady hydromagnetic free-convection flow with radiative heat transfer in a rotating fluid. 2: Compressible optically thin fluid
[DE88-702999] N89-11168
RADIO ASTRONOMY
Very Long Baseline Interferometry (VLBI) from ground and space N89-11645
RADIO ATTENUATION
Millimeter-wave studies N89-11085
RADIO EMISSION
Decametric radio emission of Jupiter. Part 3: Some physical characteristics of S-component sources
[DE88-702812] N89-11679
RADIO FREQUENCIES
Analysis of nonlinear circuits at RF and microwave frequencies by the harmonic balance method
[INPE-4693-TDL/342] N89-11126
Comparison of measured and modeled radiation, heat and water vapor fluxes: FIFE pilot study
[NASA-CR-183304] N89-11368
High-power RF applications of high-T(sub c) superconductors
[DE88-012055] N89-11579
Far infrared linear response and radio frequency nonlinear response of charge density wave conductors and high T(sub c) superconductors
[DE88-013595] N89-11582
RADIO FREQUENCY INTERFERENCE
Results of APL rain gauge network measurements in mid-Atlantic coast region and comparisons of distributions with CCIR models N89-11083
RADIO METEORS
Digital signal design for meteor-scatter communications
[AD-A196685] N89-11111
RADIO RECEIVERS
Proceedings of the Twelfth NASA Propagation Experimenters Meeting (NAPEX 12)
[NASA-CR-182796] N89-11074
A digital beacon receiver N89-11092
Olympus beacon receiver N89-11093
RADIO SCATTERING
Interference by rain scatter N89-11084
Millimeter-wave studies N89-11085
RADIO TRANSMISSION
Proceedings of the Twelfth NASA Propagation Experimenters Meeting (NAPEX 12)
[NASA-CR-182796] N89-11074
The Propagation Information Center at the University of Colorado N89-11094

Bit-to-bit error dependence in direct-sequence spread-spectrum multiple-access packet radio systems [AD-A196384] N89-11108

RADIOACTIVE DECAY
Proton decay experiment and neutrinos from supernova (Kamiokande-2) N89-11653

RADIOGRAPHY
Observations of breakup processes of liquid jets using real-time X-ray radiography N89-11160

RADIOMETERS
Olympus beacon receiver N89-11093

RADIOSONDES
Ground-based radiometric observations of emission and attenuation at 20.6, 31.65, and 90.0 GHz N89-11086

RAILGUN ACCELERATORS
Detailed analysis of the structural consequences of railgun augmentation [DE88-013800] N89-10926
Characterization of metallic coatings and thin films produced by railgun deposition [AD-A196382] N89-11021

RAIN
Results of APL rain gauge network measurements in mid-Atlantic coast region and comparisons of distributions with CCIR models N89-11083
Interference by rain scatter N89-11084
Millimeter-wave studies N89-11085
A new radar technique for satellite rainfall algorithm development [NASA-CR-183471] N89-11102
Snow cover, snowmelt and runoff in the Himalayan River basins [NASA-CR-182434] N89-11290
A numerical modeling study of frontogenesis and cold frontal rainbands N89-11358
Method for predicting monthly rainfall patterns [DE88-703005] N89-11363
Microwave radiances from horizontally finite, vertically structured precipitating clouds N89-11364
Mesoscale structure and climatology of rain-snow lines over North Carolina [AD-A196687] N89-11379

RAIN GAGES
Results of APL rain gauge network measurements in mid-Atlantic coast region and comparisons of distributions with CCIR models N89-11083

RAMAN SPECTROSCOPY
Laser Raman spectroscopy of anodic corrosion and inhibitor films on iron and nickel [DE88-009958] N89-11008

RANDOM ACCESS MEMORY
Verification of single event upset rate estimation methods with on-orbit observations [AD-A196226] N89-10935

RANDOM LOADS
Response of discretely stiffened structures and transmission of structure-borne noise N89-11270

RANDOM PROCESSES
Polarimetric clutter modeling: Theory and application [NASA-CR-183348] N89-11106

RANDOM VIBRATION
The Shock and Vibration Digest, Volume 20, No. 6 N89-11261
Nonlinear random vibration in mechanical systems N89-11263

RANDOM WALK
Numerical estimates of the rate of convergence for the vortex sheet method [DE88-013809] N89-11178

RANGE FINDERS
The GPS overview and navigation system concept N89-10875

RANKINE CYCLE
Organic Rankine-Cycle Power Systems Working Fluids Study: 2-methylpyridine/water [DE88-012659] N89-11307

RARE GASES
Liquid-vapour phase change between plane liquid surfaces: A continuum analysis to determine real gas effects [TM-FM-8803] N89-10971
Coulomb states in atoms and solids [DE88-013973] N89-11494

RATES (PER TIME)
An assessment of ground effects determined by static and dynamic testing techniques N89-10854

RAY TRACING
Optimization of microwave magnetoelastic delay lines [AD-A196866] N89-11131
A frequency dependent ray theory N89-11610

REACTION BONDING
Laminate behavior for SiC fiber-reinforced reaction-bonded silicon nitride matrix composites [NASA-TM-101350] N89-10952

REACTION KINETICS
Reaction rates in premixed turbulent flames and their relevance to the turbulent burning speed [DE88-012021] N89-10960
Transition metal mediated transformations of unsaturated molecules [DE88-013482] N89-10968
Theoretical studies of chemical reactions: dynamics [DE88-011994] N89-10970
The importance of thermodynamics to the modeling of nitrogen combustion chemistry [DE88-014656] N89-10978
Kinetics of boron hydride interconversion reactions [AD-A196824] N89-10985
The initiation and detonation of explosives: An alternative concept [DE88-014199] N89-11047
A detailed chemical kinetic reaction mechanism for the oxidation of iso-octane and n-heptane over an extended temperature range and its application to analysis of engine knock [DE88-005370] N89-11053
Incipient spall, crack branching, and fragmentation statistics in the spall process [DE88-009587] N89-11251

REACTIVITY
Compatibility and performance of separators in Li/SOCl(sub 2) cells [DE88-011090] N89-11116

REACTOR MATERIALS
Space Nuclear Safety Program [DE88-015048] N89-11505

REACTOR SAFETY
Space Nuclear Safety Program [DE88-015048] N89-11505

REAL GASES
The gas dynamics of fluids of high specific heat [MPIS-89-1987] N89-11186

REAL TIME OPERATION
Real-time path planning for robot arms N89-11224
The checkout system software for the Brazilian satellite [INPE-4571-PRE/1311] N89-11419

REATTACHED FLOW
Experimental results for the Eppler 387 airfoil at low Reynolds numbers in the Langley low-turbulence pressure tunnel [NASA-TM-4062] N89-10842

RECEIVERS
Aiding and integration of a GPS receiver N89-10881

RECIRCULATIVE FLUID FLOW
Investigation on of the flow around a backward facing step with spanwise blowing [CERT-RF-OA-68/2259-AYD] N89-10859

RECOMBINATION REACTIONS
Space and time resolved measurements of ion temperature with the CVI 5292 A charge exchange recombination line after substracting background radiation [IPPJ-888] N89-11549

RECORDING
Computerized classified document accountability [DE88-015054] N89-11633

RECRYSTALLIZATION
Modified purification of mercuric iodide for crystal growth [DE88-014960] N89-11580

RECURSIVE FUNCTIONS
Parallelizing recursive programs [RR-728-I-IMAG-83-LIFIA] N89-11429
Computational structure of the N-body problem [AD-A196422] N89-11473

RECYCLING
Markers of air pollution in forests: Nutrient cycling [DE88-011011] N89-11319
The flux and recycling of bioactive substances in the surface sediments of the deep basins off southern California [DE88-007999] N89-11321

REDUCED GRAVITY
Inorganic chemical precipitate formation payload design N89-10920
Process modelling for space station experiments [NASA-CR-183274] N89-10922
Protein crystal growth in low gravity [NASA-CR-183183] N89-11055
Fluid science investigations in microgravity [PB88-209754] N89-11058

REENTRY VEHICLES
High energy-intensity atomic oxygen beam source for low earth orbit materials degradation studies [DE88-014316] N89-11504

REFLECTANCE
IR reflectance and Raman scattering of diamond films [AD-A196899] N89-11043
Velocity and Q from reflection seismic data N89-11334
Design of high-reflectivity supermirror structures [DE88-015287] N89-11511
Flux method for the field dependent transport through multilayer devices [INPE-4647-PRE/1357] N89-11559

REFLECTION
Optimization of transparent and reflecting electrodes for amorphous silicon solar cells [DE88-001175] N89-11316

REFRIGERANTS
Evaluation of vapor compression cycles using nonazeotropic refrigerant mixtures [DE88-013225] N89-11169

REFRIGERATORS
Thermodynamic improvements for the space thermoacoustic refrigerator (STAR) [AD-A196958] N89-11071

REGULATORS
Asynchronous digital regulators [AD-A196911] N89-11446

RELATIVISTIC PARTICLES
Pseudo-scalar pi N coupling and relativistic proton-nucleus scattering [NASA-TM-101199] N89-11498

RELATIVITY
Experimental tests of relativity and gravitation N89-11649

RELIABILITY
A highly reliable computer for airborne applications N89-10833

RELIABILITY ANALYSIS
Reliability analysis of lithium cells [DE88-009258] N89-11300

RELIABILITY ENGINEERING
Risk analysis of earth return options for the Mars rover/sample return mission [NASA-CR-172081] N89-10923

REMOTE SENSING
Sensors for ceramic components in advanced propulsion systems: Summary of literature survey and concept analysis, task 3 report [NASA-CR-180900] N89-11192
Remote sensing and hydrologic modeling of arid watersheds: A scale analysis [DE88-014625] N89-11293
Training activities in remote sensing at the Instituto de Pesquisas Espaciais-INPE/Brazil [INPE-4686-PRE/1380] N89-11295

REMOTE SENSORS
Synoptic scale sensitivity of TIROS-N moisture channels in the tropics [AD-A196696] N89-11378

REPORTS
Aircraft accident/incident summary report, Copperhill, Tennessee, February 22, 1986 [PB88-910407] N89-10868
Mariners weather log, volume 32, number 2, Spring 1988 [PB88-210628] N89-11365
ONR Far East Scientific Bulletin, volume 12, no. 4, October - December 1987 [AD-A194338] N89-11687
Activity report of the Max-Planck-Institut fuer Physik und Astrophysik [MPE-200] N89-11688

REQUIREMENTS
PV modules for ground testing [NASA-CR-179476] N89-11315

RESEARCH AND DEVELOPMENT
Technology transfer at Argonne National Laboratory [DE88-012062] N89-11636

RESEARCH FACILITIES
Environmental projects. Volume 7: Environmental resources document [NASA-CR-182736] N89-11328
National Center for Atmospheric Research [PB88-220009] N89-11355
Activity report of the Max-Planck-Institut fuer Physik und Astrophysik [MPE-200] N89-11688

RESEARCH MANAGEMENT
National Photovoltaics Program: 1987 program review [DE88-001148] N89-11301
Atmospheric and Geophysical Sciences Division [DE88-013780] N89-11346
National Center for Atmospheric Research [PB88-220009] N89-11355
ONR Far East Scientific Bulletin, volume 12, no. 4, October - December 1987 [AD-A194338] N89-11687

RESIDENTIAL AREAS
Development of a residential free-piston Stirling engine heat pump [DE88-012917] N89-11303

RESIDENTIAL ENERGY
An overview of the Stirling engine heat pump program [DE88-013833] N89-11146
RESISTOJET ENGINES
Preliminary design study of hydrogen and ammonia resistojets for prime and auxiliary thrusters [NASA-CR-182176] N89-10943
RESONANCE FLUORESCENCE
Collective resonance fluorescence in an intense laser field with phase and amplitude fluctuations [DE88-702920] N89-11205
RESONANCE SCATTERING
Search for narrow resonance production in Bhabha scattering at center-of-mass energies near 1.8 MeV [MPE-PAE/EXP-EL-190] N89-11502
RESONANT FREQUENCIES
Dynamic behavior of helical springs N89-11278
RESPONSES
Numerical simulation of the response function of a nuclear emulsion plate N89-11540
RESULTANTS
On differential polynomials and their resultants [RR-723-M] N89-11472
RETINA
Biological applications and effects of optical masers [AD-A196462] N89-11217
Functional assessment of laser irradiation [AD-A196930] N89-11222
REVERBERATION
Spatial distribution of acoustic intensity in reverberant fields N89-11493
REYNOLDS STRESS
Reynolds stress closure in jet flows using wave models [NASA-CR-180226] N89-10843
RHEOLOGY
Microrheological observations of the onset of non-Newtonian behavior in suspensions [DE88-006198] N89-10962
A general analysis for obtaining the viscosity function from viscometric measurements: A case study for the helical screw rheometer [DE88-008271] N89-11139
Rheology of high concentration polymodal multiphase flow [DE88-014541] N89-11148
RIBBONS
Computer simulation of the uni-axial stress-strain behavior of ribbon-like fiber nonwovens N89-11284
RIEMANN MANIFOLD
On equivariant Lagrangians [DE88-703167] N89-11468
RISK
Risk analysis of earth return options for the Mars rover/sample return mission [NASA-CR-172081] N89-10923
Review of the space shuttle propulsion pressurization system probabilistic risk assessment [DE88-013163] N89-10928
RIVERS
Snow cover, snowmelt and runoff in the Himalayan River basins [NASA-CR-182434] N89-11290
ROBOTICS
Experimental verification of a model of a two-link flexible, lightweight manipulator [NASA-CR-183216] N89-11233
On motion planning and control of multi-link lightweight robotic manipulators [NASA-CR-181226] N89-11234
Guidance, sensor control and localization of a mobile autonomous robot [LAAS-88-131] N89-11241
Dynamic robot models using the Manutec r3 as an example [DFVLR-MITT-88-16] N89-11444
ROBOTS
Real-time path planning for robot arms N89-11224
Robust control of a flexible manipulator arm N89-11228
Understanding bandwidth limitations in robot force control [AD-A195927] N89-11229
Probabilistic error model of robot end-effector's dynamic state N89-11236
Integral manifold in system design with application to flexible link robot control [AD-A197052] N89-11243
Analysis, synthesis and design of high-speed mechanisms [PB88-235106] N89-11244
Experiments in control of satellite manipulators N89-11391
The DFVLR models 1 and 2 of the Manutec r3 robot [DFVLR-MITT-88-13] N89-11443
Dynamic robot models using the Manutec r3 as an example [DFVLR-MITT-88-16] N89-11444
ROBUSTNESS (MATHEMATICS)
Robust covariance matrix estimation via robust estimation of principal components [PB88-126594] N89-11478
ROCKET ENGINE CASES
Performance of a circular body earth-to-orbit winged transport with various strap-on boosters [NASA-TM-100603] N89-10929
ROCKET ENGINES
SHED: A program for three-dimensional, rigid body, shroud ejection dynamics [DE88-012410] N89-10927
HCl measurements in space vehicle exhaust clouds [DE88-013815] N89-10942
ROCKY MOUNTAINS (NORTH AMERICA)
Crustal structure of the northwestern United States N89-11349
ROLLING
The use of the complex summation method for formulating algorithms for decoupling vertical/horizontal motions of rolling aircraft N89-10889
ROOM TEMPERATURE
Ratchetting behavior of type 304 stainless steel at room and elevated temperatures [DE88-011864] N89-11273
ROTATING FLUIDS
Unsteady hydromagnetic free-convection flow with radiative heat transfer in a rotating fluid. 1: Incompressible optically thin fluid [DE88-702998] N89-11140
Unsteady hydromagnetic free-convection flow with radiative heat transfer in a rotating fluid of arbitrary optical thickness [DE88-703000] N89-11167
Unsteady hydromagnetic free-convection flow with radiative heat transfer in a rotating fluid. 2: Compressible optically thin fluid [DE88-702999] N89-11168
Rotating and stratified fluids N89-11343
ROTOR AERODYNAMICS
A study of helicopter stability and control including blade dynamics [NASA-CR-183245] N89-10895
A model for the response of vertical axis wind turbines to turbulent flow: Parts 1 and 2 [DE88-014708] N89-11305
ROTOR BLADES
Statistics on aircraft gas turbine engine rotor failures that occurred in US commercial aviation during 1982 [DOT/FAA/CT-88/23] N89-10892
ROTOR BLADES (TURBOMACHINERY)
Experimental guidelines for the design of turbine rotor fragment containment rings [DOT/FAA/CT-88/21] N89-10893
ROTOR BODY INTERACTIONS
Investigation on of the flow around a backward facing step with spanwise blowing [CERT-RF-OA-68/2259-AYD] N89-10859
ROTORS
Rotor instrumentation circuits for the Sandia 34-meter vertical axis wind turbine [DE88-014704] N89-11304
The PNL single-tower measurement model of rotationally sampled turbulent wind, with user's guide for STRS2PC [DE88-013166] N89-11360
RUDDERS
Three dimensional boundary layers on submarine conning towers and rudders [CERT-OA-23/5025-AYD] N89-11182
RUN TIME (COMPUTERS)
Programming abstractions for run-time partitioning of scientific continuum calculations running on multiprocessors [DE88-007376] N89-11411
RYDBERG SERIES
Coulomb states in atoms and solids [DE88-013973] N89-11494

S

S WAVES
Alfven wave studies on a tokamak N89-11517
SAFETY
Safety aspects of large-scale handling of hydrogen [DE88-014422] N89-11070
SAFETY MANAGEMENT
STS safety approval process for small self-contained payloads N89-10910
SAMPLING
Bandwidth compression for HDTV broadcasting: Investigation of some adaptive subsampling strategies [BBC-RD-1988/9] N89-11101
Design and analysis of large-scale atmospheric dispersion experiment [DE88-012911] N89-11330
SANDWICH STRUCTURES
Fundamental aspects of the electronic structure, materials properties, and lubrication performance of sputtered MoS2 films [AD-A196852] N89-11606
SATELLITE ATMOSPHERES
Extraction of light gasses from Mars or its moons [DE88-009123] N89-11681
SATELLITE DESIGN
TUBSAT-1, satellite technology for educational purposes N89-10905
Space observations for infrared and submillimeter astronomy N89-11643
SATELLITE IMAGERY
A new radar technique for satellite rainfall algorithm development [NASA-CR-183471] N89-11102
Technique for obtaining agricultural property boundaries through satellite imagery, certified to control and accompany agricultural activity [INPE-4640-PRE/1351] N89-11294
Color enhancement of remote sensing imagery using IHS transformations and decorrelation stretch methods [INPE-4559-PRE/1300] N89-11418
SATELLITE NETWORKS
The Global Positioning System (GPS) constellation and coverage N89-10876
The Global Positioning System (GPS) accuracy, system error budget, space and control segment overview N89-10877
SATELLITE ORBITS
The utility of particle precipitation data as an input to thermospheric density models for satellite orbital analysis [AD-A196870] N89-10925
SATELLITE SURFACES
Ions generated on or near satellite surfaces [AD-A196966] N89-10940
SATELLITE TRANSMISSION
Propagation handbook, frequencies above 10 GHz N89-11082
SATELLITE-BORNE INSTRUMENTS
An oxide passivated and ion-implanted Si detector for X-ray astronomy [ISAS-RN-353] N89-11663
The history of gamma-ray burst observations [DE88-014390] N89-11685
SATURN (PLANET)
Outward to the beginning: The CRAF and Cassini Missions of the Mariner Mark 2 program [NASA-CR-183133] N89-10921
SCALARS
Pseudo-scalar pi N coupling and relativistic proton-nucleus scattering [NASA-TM-101199] N89-11498
Gauged Q-balls [NASA-CR-183369] N89-11500
SCATTER PROPAGATION
Digital signal design for meteor-scatter communications [AD-A196685] N89-11111
SCATTERING
Laser communications through the atmosphere N89-11087
ACTS and OLYMPUS propagation experiments N89-11091
Development of a semi-empirical model for estimating the global solar radiation [INPE-4620-TDL/328] N89-11352
Optical scattering and microphysical properties of subvisual cirrus clouds, and climatic implications [NASA-CR-183301] N89-11362
The generation of scatterometer surface targets with specified surface statistics [AD-A196397] N89-11480
SCATTERING CROSS SECTIONS
Search for narrow resonance production in Bhabha scattering at center-of-mass energies near 1.8 MeV [MPE-PAE/EXP-EL-190] N89-11502
SCATTEROMETERS
The generation of scatterometer surface targets with specified surface statistics [AD-A196397] N89-11480
SCIENTIFIC SATELLITES
TUBSAT-1, satellite technology for educational purposes N89-10905

SCREWS
Analysis, synthesis and design of high-speed mechanisms
[PB88-235106] N89-11244
SEA WATER
Oxygen chemistry
[AD-A196989] N89-10988
SEARCH PROFILES
Hypothesis-confirming information search strategies and computerized information retrieval systems N89-11616
SEDIMENT TRANSPORT
Remote sensing and hydrologic modeling of arid watersheds: A scale analysis
[DE88-014625] N89-11293
A comparative planetological study of particle speed and concentration during aeolian saltation N89-11677
SEDIMENTS
The flux and recycling of bioactive substances in the surface sediments of the deep basins off southern California
[DE88-007999] N89-11321
SEISMIC WAVES
The Shock and Vibration Digest, Volume 20, No. 10 N89-11252
The effects of seismic waves, part 2 N89-11254
The Shock and Vibration Digest, Volume 20, No. 8 N89-11258
Dynamic behavior of foundations in bilateral and unilateral contact N89-11259
The Shock and Vibration Digest, volume 20, no. 9 N89-11266
The effects of seismic waves: Part 1 N89-11268
Velocity and Q from reflection seismic data N89-11334
Velocity analysis by iterative profile migration N89-11339
SEISMOLOGY
The effects of seismic waves, part 2 N89-11254
The effects of seismic waves: Part 1 N89-11268
SELECTION
Comparison of recent model selection criteria for system identification
[PD-SE-8807] N89-11449
On empirical Bayes selection rules for negative binomial populations
[AD-A196994] N89-11485
SEMICONDUCTOR DEVICES
Determination of the unstable states of the solid state plasma in semiconductor devices
[AD-A196403] N89-11550
Flux method for the field dependent transport through multilayer devices
[INPE-4647-PRE/1357] N89-11559
SEMICONDUCTOR DIODES
State of the art of negative luminescence
[DE88-010871] N89-11556
SEMICONDUCTOR JUNCTIONS
State of the art of negative luminescence
[DE88-010871] N89-11556
SEMICONDUCTORS (MATERIALS)
Multiple pulse photoconductive semiconductor switching
[DE88-011792] N89-11119
Smart semiconductor bridge (SCB) igniter for explosives
[DE88-012669] N89-11551
Electronic properties of 3-5 semiconductor alloys N89-11560
Spin-orbit interaction effects in zincblende semiconductors: Ab initio pseudopotential calculations
[DE88-014663] N89-11599
Fundamental aspects of the electronic structure, materials properties, and lubrication performance of sputtered MoS2 films
[AD-A196852] N89-11606
SENSITIVITY
Accuracy analysis of the semi-analytical method for shape sensitivity analysis N89-10848
Friction and impact sensitivities of explosives: A comparative study
[DE88-012864] N89-11051
Shock initiation of explosives with a sensitive rate and related topics
[DE88-008483] N89-11052
Synoptic scale sensitivity of TIROS-N moisture channels in the tropics
[AD-A196686] N89-11378
SEPARATED FLOW
The impact of separated flow on heat and mass transfer
[DE88-014653] N89-11180
Experimental research on swept shock wave/boundary layer interactions
[AD-A196938] N89-11189
SEPARATORS
Oxygen chemistry
[AD-A196989] N89-10988
A preliminary study on the use of magnetohydrodynamic forces to remove impurities from molten metals
[DE88-013508] N89-10991
Compatibility and performance of separators in Li/SOCl(sub 2) cells
[DE88-011090] N89-11116
SEQUENCING
On the generation of waveforms having comb-shaped spectra
[AD-A196927] N89-11113
SERVOCONTROL
Understanding bandwidth limitations in robot force control
[AD-A195927] N89-11229
SET THEORY
Parallel algorithm for a class of optimization problems
[PB88-209929] N89-11414
SHAPE CONTROL
Beam handling and emittance control
[AD-A196789] N89-11509
SHAPES
Accuracy analysis of the semi-analytical method for shape sensitivity analysis N89-10848
Developing laminar flow and heat transfer in ducts of arbitrary cross section N89-11176
SHEAR FLOW
An examination of a simulated microburst flow as sensed by a single Doppler radar
[AD-A196381] N89-11372
SHEAR LAYERS
Application of a second-order projection method to the study of shear layers
[DE88-013095] N89-11166
SHEAR PROPERTIES
Application of a second-order projection method to the study of shear layers
[DE88-013095] N89-11166
SHEAR STRAIN
Benchmark study of shear buckling of a cylindrical vessel
[PB88-125315] N89-11257
SHEAR STRESS
A general analysis for obtaining the viscosity function from viscometric measurements: A case study for the helical screw rheometer
[DE88-006271] N89-11139
Migration arising from gradients in shear stress: Particle distributions in Poiseuille flow N89-11159
SHEARING
Coronal magnetic fields produced by photospheric shear
[AD-A194591] N89-11684
SHELL THEORY
Dynamic analysis of spherical shells: A hybrid method
[EPM/RT-88/23] N89-11264
SHELLS (STRUCTURAL FORMS)
Free damped vibration of composite plates and shells N89-11249
Finite element analysis of shell structures with an 18-node 3-dimensional solid element based on a new mixed formulation
[AD-A196698] N89-11288
Neutron multiplication in beryllium
[AD-A196877] N89-11503
SHIP HULLS
Three dimensional boundary layers on submarine conning towers and rudders
[CERT-OA-23/5025-AYD] N89-11182
SHOCK WAVE INTERACTION
Experimental research on swept shock wave/boundary layer interactions
[AD-A196938] N89-11189
SHOCK WAVE PROPAGATION
Experimental and analytical study of vapor explosions in stratified geometries
[DE88-011964] N89-11046
SHOCK WAVES
Reynolds stress closure in jet flows using wave models
[NASA-CR-180226] N89-10843
Schlieren measurements at the 10,000-foot sled track
[DE88-012748] N89-10899
Microscopy and microanalysis of shock-processed materials
[DE88-008471] N89-10990
Godunov methods and adaptive algorithms for unsteady fluid dynamics
[DE88-013094] N89-11141
Explosion airblast predictions on a personal computer and application to the Henderson, Nevada incident
[DE88-014991] N89-11144
The Shock and Vibration Digest, volume 20, no. 9 N89-11266
A numerical study of ENO and TVD schemes for shock capturing
[NASA-TM-101355] N89-11469
Shocked interstellar gas in dense molecular clouds N89-11670
SHORT TAKEOFF AIRCRAFT
The 1987 Ground Vortex Workshop
[NASA-CP-10008] N89-10849
The characteristics of the ground vortex and its effect on the aerodynamics of the STOL configuration N89-10850
Ground vortex flow field investigation N89-10852
F-15 SMTD low speed jet effects wind tunnel test results N89-10853
Numerical simulation of transonic flow around Asuka N89-11067
CAD wind tunnel test for half-cut model of Asuka N89-11069
SHROUDED PROPELLERS
Aerodynamic design considerations for a free-flying ducted propeller
[DE88-006867] N89-10841
SIDES
Evaluation of the prototype EUROSID dummy and comparison with the US SID (Side Impact Dummies)
[PB88-201934] N89-11389
SIGNAL FADING
Proceedings of the Twelfth NASA Propagation Experimenters Meeting (NAPEX 12)
[NASA-CR-182796] N89-11074
Results of 1987 MSS helicopter propagation experiment at UHF and L band in Central Maryland N89-11077
LMSS propagation modeling at Virginia Tech N89-11078
Preliminary results of MARECS-A measurements in Central Maryland and plans for 1988 MSS experiment in Australia N89-11079
Laser communications through the atmosphere N89-11087
ACTS and OLYMPUS propagation experiments N89-11091
SIGNAL PROCESSING
Data and signal processing architectures for future avionics N89-10835
GPS signal structure N89-10878
User equipment overview N89-10879
Aiding and integration of a GPS receiver N89-10881
Civil and military applications of GPS N89-10882
Differential operation of NAVSTAR GPS for enhanced accuracy N89-10883
GPS navigation processing and Kalman filtering N89-10884
ACTS and OLYMPUS propagation experiments N89-11091
A digital beacon receiver N89-11092
A hybrid hot-wire data acquistion system
[ARL-AERO-R-172] N89-11193
Ultrasonic flaw classification: An approach using modeling, signal processing, and adaptive learning N89-11248
Velocity analysis by iterative profile migration N89-11339
Adaptive filtering algorithms for communications signal processing
[PD-SE-8808] N89-11410
Excitation of MHD surface waves propagating with shear Alfven waves in an inhomogeneous cylindrical plasma
[IPPJ-872] N89-11526
SILANES
Electronic properties of sigma-conjugated polysilanes
[DE88-012699] N89-11032
SILICON
Indentation plasticity and fracture in silicon
[NASA-TP-2863] N89-10996
Deposition and characterization of ZnS/Si heterojunctions produced by vacuum evaporation
[NASA-TM-101359] N89-11129
Studies in advanced silicon solar cells
[DE88-013143] N89-11314
ENGEN: An intermediate language to HILO extension of the FIRST silicon compiler, executive summary
[ESA-CR(P)-2621] N89-11422
Smart semiconductor bridge (SCB) igniter for explosives
[DE88-012669] N89-11551
The electronic and optical properties of silicon/germanium strained layer superlattices N89-11590
An oxide passivated and ion-implanted Si detector for X-ray astronomy
[ISAS-RN-353] N89-11663
SILICON NITRIDES
Laminate behavior for SiC fiber-reinforced reaction-bonded silicon nitride matrix composites
[NASA-TM-101350] N89-10952

The effect of carbon and boron nitride additions on the fracture toughness of Si3N4
[DE88-013249] N89-11025

SIMULATION
Numerical investigation of a jet in ground effect using the fortified Navier-Stokes scheme N89-10857
Robust control of a flexible manipulator arm N89-11228
An O(N) algorithm for three-dimensional N-body simulations
[AD-A196903] N89-11433
Balance of recurrence order in time-inhomogeneous Markov chains with application to simulated annealing
[AD-A196980] N89-11484

SINGLE CRYSTALS
Indentation plasticity and fracture in silicon
[NASA-TP-2863] N89-10996
Ion implantation and thermal annealing of high-T(ssub c) single crystals of YBa2Cu3O(sub x)
[DE88-012201] N89-11564
Effect of surface states on the electrochemical behaviour of single crystal n-ZnSe photoelectrode
[DE88-702726] N89-11566
X-ray scattering studies of non-equilibrium ordering processes
[DE88-012908] N89-11569
Electrodynamics of single-crystal Eu(sub 2)CuO(sub 4): A boson excitation spectrum
[DE88-014328] N89-11585

SINGLE EVENT UPSETS
Verification of single event upset rate estimation methods with on-orbit observations
[AD-A196226] N89-10935

SINTERING
Chemical preparation of powders and films for high temperature superconductors
[DE88-015266] N89-11601

SITE SELECTION
Laser communications through the atmosphere N89-11087
A far infrared astronomical observatory in Antarctica N89-11646

SKIN FRICTION
Turbulent boundary layer drag reduction on an axisymmetric body using circular ring manipulators N89-11145
Experimental research on swept shock wave/boundary layer interactions
[AD-A196938] N89-11189

SLABS
The propagation of electromagnetic waves in thin dielectric slabs
[AD-A196995] N89-11115

SLEDS
Schlieren measurements at the 10,000-foot sled track
[DE88-012748] N89-10899

SLOT ANTENNAS
A broad-band array of aperture-coupled cavity-backed slot elements
[AD-A196400] N89-11109

SLOTS
A broad-band array of aperture-coupled cavity-backed slot elements
[AD-A196400] N89-11109

SLURRIES
Measurements of pressure drop and heat transfer in turbulent pipe flows of particulate slurries
[DE88-013622] N89-11150

SMALL PERTURBATION FLOW
An iterative scheme for numerical solution of transonic small perturbation equation
[TM-AE-8801] N89-11455

SNOW
Verification of EOSAEL (Electro-Optical Systems Atmospheric Effects Library) snow transmittance predictions
[DREV-R-4423/87] N89-11099
Mesoscale structure and climatology of rain-snow lines over North Carolina
[AD-A196687] N89-11379

SNOW COVER
Snow cover, snowmelt and runoff in the Himalayan River basins
[NASA-CR-182434] N89-11290

SODIUM
Temperature dependence of entropies and specific heats of liquid Na and K
[DE88-702986] N89-10976

SODIUM CHLORIDES
Near-critical NaCl-H2O: An equation of state and discussion of anomalous properties
[DE88-012029] N89-10969

SODIUM HYDROXIDES
Oxidation reduction potential of the Cu(3)/Cu(2) system in alkaline solutions
[NASA-TT-20309] N89-10963

SOFTWARE ENGINEERING
Program of research in structures and dynamics
[NASA-CR-183191] N89-10838
Object oriented software engineering with Ada
[CNES-CT/DTI/MS/MN/326] N89-11426
Software management metrics
[AD-A196916] N89-11434
Automated knowledge generation
[NASA-CR-181317] N89-11440
Guidelines for tailoring DOD-STD-2167A for SDS (Strategic Defense System) software development
[AD-A197038] N89-11488

SOFTWARE TOOLS
The CSM testbed software system: A development environment for structural analysis methods on the NAS CRAY-2
[NASA-TM-100642] N89-11287
Algorithm and general software considerations N89-11397
The use of portable microcomputer as a data collection tool to support integrated simulation support environments: A concept
[AD-A196414] N89-11403
Strategies for concurrent processing of complex algorithms in data driven architectures
[NASA-CR-181329] N89-11406
OEXP Analysis Tools Workshop
[NASA-CP-10013] N89-11407
Finite elements software and applications N89-11415
The checkout system software for the Brazilian satellite
[INPE-4571-PRE/1311] N89-11419
Presentation of research and development action 1206: Preliminary study report on the CESTAC method --- calculation check
[CNES-CT/PTI/MS/MN/067] N89-11424
Object oriented software engineering with Ada
[CNES-CT/DTI/MS/MN/326] N89-11426

SOILS
Spectral studies of three oxisols and a Ultisol of Brazil
[INPE-4644-PRE/1355] N89-11297
Markers of air pollution in forests: Nutrient cycling
[DE88-011011] N89-11319

SOLAR ARRAYS
The photovoltaic advanced systems test facility
[DE88-009589] N89-11306
PV modules for ground testing
[NASA-CR-179476] N89-11315

SOLAR CELLS
Ternary adamantine materials for low-cost solar cells
[DE88-001160] N89-11302
Amorphous silicon photovoltaic devices prepared by chemical and photochemical vapor deposition of higher order silanes
[DE88-001189] N89-11311
Studies in advanced silicon solar cells
[DE88-013143] N89-11314
Molecular beam epitaxy of GaP films on Si substrates
[PB88-131974] N89-11581

SOLAR COLLECTORS
Phase change problem related to thermal energy storage in the manned space station
[DE88-011390] N89-10933

SOLAR CORONA
Coronal magnetic fields produced by photospheric shear
[AD-A194591] N89-11684

SOLAR ENERGY
Direct solar-pumped iodine laser amplifier
[NASA-CR-183171] N89-11201
Development of a semi-empirical model for estimating the global solar radiation
[INPE-4620-TDL/328] N89-11352

SOLAR ENERGY CONVERSION
National Photovoltaics Program: 1987 program review
[DE88-001148] N89-11301

SOLAR FLARES
Verification of single event upset rate estimation methods with on-orbit observations
[AD-A196226] N89-10935

SOLAR NEUTRINOS
Particle physics candidates for the cosmion solution to the solar neutrino problem
[DE88-014479] N89-11683

SOLAR RADIATION
A limited assessment and characterization of the solar radiation energy resources in the Caribbean region
[DE88-001133] N89-11312
Basic theory of desertification
[DE88-703014] N89-11320

SOLAR-PUMPED LASERS
Direct solar-pumped iodine laser amplifier
[NASA-CR-183171] N89-11201

SOLDERED JOINTS
Microsoldering and microminiature welding with lasers
[DE88-013368] N89-11240

SOLID LUBRICANTS
Investigation of a self-lubricating alumina coating formed by anodic spark deposition
[DE88-014947] N89-11035
Fundamental aspects of the electronic structure, materials properties, and lubrication performance of sputtered MoS2 films
[AD-A196852] N89-11606

SOLID MECHANICS
Program of research in structures and dynamics
[NASA-CR-183191] N89-10838

SOLID PROPELLANT COMBUSTION
A method for obtaining empirical correlations for predicting crack propagation in a burning solid propellant grain
[AD-A196689] N89-11054

SOLID PROPELLANT ROCKET ENGINES
A method for obtaining empirical correlations for predicting crack propagation in a burning solid propellant grain
[AD-A196689] N89-11054

SOLID PROPELLANTS
A method for obtaining empirical correlations for predicting crack propagation in a burning solid propellant grain
[AD-A196689] N89-11054
Modeling of combustion processes of stick propellants via combined Eulerian-Lagrangian approach N89-11163

SOLID STATE
Coulomb states in atoms and solids
[DE88-013973] N89-11494

SOLID STATE DEVICES
Determination of the unstable states of the solid state plasma in semiconductor devices
[AD-A196403] N89-11550

SOLIDIFICATION
The first Chinese student space shuttle getaway special program N89-10903
Microstructure and properties of rapidly solidified beryllium-transition metal alloys
[DE88-010937] N89-11012

SOLIDS
Microrheological observations of the onset of non-Newtonian behavior in suspensions
[DE88-006198] N89-10962
A theory of surface and interface electronic properties of crystalline solids: Applications to 2-6 compounds N89-11596

SOLITARY WAVES
Gauged Q-balls
[NASA-CR-183369] N89-11500

SOLUBILITY
Protein crystal growth in low gravity
[NASA-CR-183183] N89-11055
Further investigations on new fluid working systems for absorption heat pumps
[DE88-012622] N89-11151

SOLUTIONS
Oxidation reduction potential of the Cu(3)/Cu(2) system in alkaline solutions
[NASA-TT-20309] N89-10963
Particle physics candidates for the cosmion solution to the solar neutrino problem
[DE88-014479] N89-11683

SOUND FIELDS
Spatial distribution of acoustic intensity in reverberant fields N89-11493

SOUND INTENSITY
Spatial distribution of acoustic intensity in reverberant fields N89-11493

SOUND PRESSURE
Spatial distribution of acoustic intensity in reverberant fields N89-11493

SOUND WAVES
Spatial distribution of acoustic intensity in reverberant fields N89-11493

SOUTHERN HEMISPHERE
Observations of southern irregular variables
[INPE-4568-PRE/1309] N89-11291

SPACE CHARGE
Lie algebraic treatment of space charge N89-11496

SPACE COLONIES
A perspective on space exploration technology catalysis: A rationale for initiating 21st Century expansion of human civilization into outer space
[NASA-TM-101362] N89-11637

SPACE EXPLORATION
A perspective on space exploration technology catalysis: A rationale for initiating 21st Century expansion of human civilization into outer space
[NASA-TM-101362] N89-11637

The deep space network: An instrument for radio astronomy research
[NASA-CR-182744] N89-11661

SPACE FLIGHT
The determination of the spacecraft contamination environment
[AD-A196435] N89-10937
Use of high temperature superconductors in magnetoplasmadynamic systems
[NASA-TM-101219] N89-11553

SPACE OBSERVATIONS (FROM EARTH)
Space science and fundamental physics --- conference
[ESA-SP-283] N89-11638
Galaxy formation: Theory and observational tests N89-11644
Very Long Baseline Interferometry (VLBI) from ground and space N89-11645

SPACE PLASMAS
PV modules for g.ound testing
[NASA-CR-179476] N89-11315

SPACE POWER REACTORS
Space Nuclear Safety Program
[DE88-015048] N89-11505
Analysis of SP-100 critical experiments
[DE88-014429] N89-11508

SPACE PROCESSING
Future MAUS payload and the TWIN-MAUS configuration N89-10906
Development of experimental systems for material sciences under microgravity N89-10907
The Purdue University Get Away Special II (PUGAS II) N89-10918

SPACE SHUTTLE MAIN ENGINE
Performance of a circular body earth-to-orbit winged transport with various strap-on boosters
[NASA-TM-100603] N89-10929

SPACE SHUTTLE PAYLOADS
The 1988 Get Away Special Experimenter's Symposium
[NASA-CP-3008] N89-10902
CSCP: A new Get Away Special (GAS) project N89-10909
Hitchhiker capabilities N89-10917

SPACE SHUTTLES
Review of the space shuttle propulsion pressurization system probabilistic risk assessment
[DE88-013163] N89-10928
The determination of the spacecraft contamination environment
[AD-A196435] N89-10937

SPACE STATIONS
Space science/space station attached payload pointing accommodation study: Technology assessment white paper
[NASA-CR-182735] N89-10931
Phase change problem related to thermal energy storage in the manned space station
[DE88-011390] N89-10933

SPACE WEAPONS
Guidelines for tailoring DOD-STD-2167A for SDS (Strategic Defense System) software development
[AD-A197038] N89-11488

SPACE-TIME FUNCTIONS
On the locality of the no hair conjection and the measure of the universe
[NASA-CR-183365] N89-11489

SPACEBORNE ASTRONOMY
Space science and fundamental physics --- conference
[ESA-SP-283] N89-11638
Very Long Baseline Interferometry (VLBI) from ground and space N89-11645
Fundamental science in ESA's space science program N89-11654

SPACEBORNE EXPERIMENTS
The 1988 Get Away Special Experimenter's Symposium
[NASA-CP-3008] N89-10902
The first Chinese student space shuttle getaway special program N89-10903
Development of Bio-GAS systems N89-10904
Future MAUS payload and the TWIN-MAUS configuration N89-10906
Development of experimental systems for material sciences under microgravity N89-10907
Systems report for payload G-652: Project origins N89-10911
GAS-611 firefly in zero gravity N89-10912
Acceleration ground test program to verify GAS payload No. 559 structure/support avionics and experiment structural integrity N89-10913
Computerized monitoring and control of experiments in space N89-10915
The potential of a GAS can with payload G-169 N89-10916
The Purdue University Get Away Special II (PUGAS II) N89-10918
The transportation of fine arts materials aboard the space shuttle Columbia. GAS payload No. 481: Vertical horizons N89-10919
Inorganic chemical precipitate formation payload design N89-10920

SPACECRAFT COMMUNICATION
Results of APL rain gauge network measurements in mid-Atlantic coast region and comparisons of distributions with CCIR models N89-11083
Millimeter-wave studies N89-11085
Plan of propagation and communication experiments using ETS-VI N89-11088
Plan of advanced satellite communications experiment using ETS-VI N89-11089
The deep space network: An instrument for radio astronomy research
[NASA-CR-182744] N89-11661

SPACECRAFT CONTAMINATION
The determination of the spacecraft contamination environment
[AD-A196435] N89-10937

SPACECRAFT DESIGN
Performance of a circular body earth-to-orbit winged transport with various strap-on boosters
[NASA-TM-100603] N89-10929
Laboratory investigations of low earth orbit environmental effects on spacecraft
[DE88-009135] N89-10932

SPACECRAFT ENVIRONMENTS
The first Chinese student space shuttle getaway special program N89-10903

SPACECRAFT ORBITS
The determination of the spacecraft contamination environment
[AD-A196435] N89-10937

SPACECRAFT POWER SUPPLIES
The state-of-the-art of dc power distribution systems/components for space applications
[NASA-CR-182743] N89-10941
Power quality load management for large spacecraft electrical power systems
[NASA-TM-100342] N89-11127

SPACECRAFT PROPULSION
Preliminary design study of hydrogen and ammonia resistojets for prime and auxiliary thrusters
[NASA-CR-182176] N89-10943

SPACECRAFT REENTRY
Risk analysis of earth return options for the Mars rover/sample return mission
[NASA-CR-172081] N89-10923

SPACECRAFT SHIELDING
Utilization of spray on foam insulation for manned and unmanned spacecraft and structures N89-10914

SPALLATION
Incipient spall, crack branching, and fragmentation statistics in the spall process
[DE88-009587] N89-11251

SPANWISE BLOWING
Investigation on of the flow around a backward facing step with spanwise blowing
[CERT-RF-OA-68/2259-AYD] N89-10859

SPARE PARTS
State-of-the-art-dehumidification cost-effective corrosion prevention
[AD-A196503] N89-11023

SPATIAL DISTRIBUTION
Optimization of the two-dimensional magnetic field distribution basing on the integral equation method
[DE88-702940] N89-11490
Spatial distribution of acoustic intensity in reverberant fields N89-11493

SPATIAL FILTERING
In-plane moire optical processing at ARL
[ARL-STRUC-R-428] N89-11510

SPATIAL RESOLUTION
Space and time resolved measurements of ion temperature with the CVI 5292 A charge exchange recombination line after substracting background radiation
[IPPJ-888] N89-11549

SPECIFIC HEAT
Near-critical NaCl-H2O: An equation of state and discussion of anomalous properties
[DE88-012029] N89-10969
Temperature dependence of entropies and specific heats of liquid Na and K
[DE88-702986] N89-10976
The gas dynamics of fluids of high specific heat
[MPIS-89-1987] N89-11186
Low temperature measurements on UBe13
[DE88-014446] N89-11594

SPECIMEN GEOMETRY
Influence of specimen dimension on damage and breaking of composite materials
[REPT-49-062/F] N89-10957
Creep tests for slow and fast fatigue conditions on aluminum alloy specimens
[REPT-M0-535200] N89-11020

SPECKLE PATTERNS
Laser speckle photography and decorrelation techniques in elastic-plastic fracture studies N89-11275

SPECTRAL RESOLUTION
Color enhancement of remote sensing imagery using IHS transformations and decorrelation stretch methods
[INPE-4559-PRE/1300] N89-11418

SPECTRAL THEORY
Proceedings of the Focused Research Program on Spectral Theory and Boundary Value Problems. Volume 1: Singular differential systems
[DE88-008151] N89-11461

SPECTROMETERS
A differential absorption spectrometer for determining flash X-ray spectra from 10 to 2000 keV
[DE88-014844] N89-10979
Space and time resolved measurements of ion temperature with the CVI 5292 A charge exchange recombination line after substracting background radiation
[IPPJ-888] N89-11549

SPECTROSCOPIC ANALYSIS
Charge exchange spectroscopy (CXRS) of highly ionized ions in ASDEX --- tokamak N89-11535

SPECTRUM ANALYSIS
Multicolor pyrometer for materials processing in space
[NASA-CR-183189] N89-11057
Spectral studies of three oxisols and a Ultisol of Brazil
[INPE-4644-PRE/1355] N89-11297

SPEECH RECOGNITION
Representing high-level knowledge structures in massively parallel networks N89-11409

SPEED REGULATORS
Laboratory examination and seasonal analyses of the dynamic losses for a continuously variable speed heat pump
[DE88-013207] N89-11174

SPHERES
Neutron multiplication in beryllium
[AD-A196877] N89-11503

SPHERICAL SHELLS
Dynamic analysis of spherical shells: A hybrid method
[EPM/RT-88/23] N89-11264

SPIN
Spin correlations in high T(sub c) superconductors
[DE88-013988] N89-11555
Self-consistent charge and spin distributions in oxide superconductors
[DE88-012051] N89-11591

SPIN-ORBIT INTERACTIONS
Spin-orbit interaction effects in zincblende semiconductors: Ab initio pseudopotential calculations
[DE88-014663] N89-11599

SPLINE FUNCTIONS
Cubic spline smoothing: A useful tool for curve estimation
[PB88-214796] N89-11452

SPOT (FRENCH SATELLITE)
Study of the multiplexing of image telemetry data from SPOT 4 HRVIR and Vegetation sensors
[CNES-87/229/CT/DRT/TIT/TR] N89-10930

SPRAYED COATINGS
Utilization of spray on foam insulation for manned and unmanned spacecraft and structures N89-10914

SPREAD SPECTRUM TRANSMISSION
Bit-to-bit error dependence in direct-sequence spread-spectrum multiple-access packet radio systems
[AD-A196384] N89-11108
On the generation of waveforms having comb-shaped spectra
[AD-A196927] N89-11113

SPRINGS (ELASTIC)
The Shock and Vibration Digest, Volume 20, No. 7 N89-11277
Dynamic behavior of helical springs N89-11278
Integration of analysis and experiment for Stirling cycle processes. Part 1: Gas spring hysteresis loss
[DE88-013202] N89-11313

SPUTTERING
Ions generated on or near satellite surfaces
[AD-A196966] N89-10940
Fundamental aspects of the electronic structure, materials properties, and lubrication performance of sputtered MoS2 films
[AD-A196852] N89-11606

STABILITY
A study of helicopter stability and control including blade dynamics
[NASA-CR-183245] N89-10895

Periodically structured multiphase flows and hydrodynamic instabilities in narrow capillaries
[DE88-015608] N89-11181
Pair potential trend of alkali metals under external pressure
[DE88-702973] N89-11593

STABLE OSCILLATIONS
Two-dimensional saturation gain and output power in transverse flow electrical discharge CO2 lasers
[AD-A196660] N89-11218

STACKS
Finite elements software and applications N89-11415

STAINLESS STEELS
Experimental and theoretical study of inclusions during initiation of crevice corrosion
[DE88-014635] N89-10989
Spectrography analysis of stainless steel by the point to point technique
[DE88-702302] N89-10992
The effect of thermal ageing on the stress corrosion cracking of 9Cr1Mo steel in aqueous caustic environments
[NRL-R-1003(R)] N89-10997
Influence of martensitic phase in abrasion behaviour of stainless steel 304 L
[DE88-702770] N89-11009
Near surface chemistry and corrosion behavior of excimer laser surface-melted AISI type 304 stainless steel
[DE88-014440] N89-11019
Ratchetting behavior of type 304 stainless steel at room and elevated temperatures
[DE88-011864] N89-11273
Fatigue of welded joint in a stainless steel AISI 304 L
[DE88-701622] N89-11279

STANDARDS
Spectrography analysis of stainless steel by the point to point technique
[DE88-702302] N89-10992
Standards conformance testing
[PB88-215645] N89-11412

STAR DISTRIBUTION
Multiple populations on the horizontal branch N89-11662

STAR FORMATION
Colour and spectral synthesis of disk galaxies N89-11656

STAR FORMATION RATE
Colour and spectral synthesis of disk galaxies N89-11656

STATISTICAL ANALYSIS
Statistics on aircraft gas turbine engine rotor failures that occurred in US commercial aviation during 1982
[DOT/FAA/CT-88/23] N89-10892
Friction and impact sensitivities of explosives: A comparative study
[DE88-012864] N89-11051
LMSS propagation modeling at Virginia Tech N89-11078
Statistical effects in high-power microwave beam propagation
[DE88-012440] N89-11100
Structure of wind-shear turbulence
[NASA-CR-183257] N89-11359
Concerning the use of the minimum mean asymmetry as the validation criteria for clustering
[INPE-4654-PRE/1361] N89-11427

STATISTICAL DISTRIBUTIONS
Active modes of the Pacific Intertropical Convergence Zone (ITCZ)
[AD-A196406] N89-11374
Concerning the use of the minimum mean asymmetry as the validation criteria for clustering
[INPE-4654-PRE/1361] N89-11427

STATOR BLADES
Three component laser anemometer measurements in an annular cascade of core turbine vanes with contoured end wall
[NASA-TP-2846] N89-10844

STEADY STATE
A three-dimensional investigation of steady state fatigue crack closure behavior for through-thickness and part-through flaws N89-11256

STEAM
Practical applications and limitations of adaptive control N89-11442

STEELS
Effect of protective coatings on life of heat-resistant nickel steel under cyclic heat load N89-11005
Alloying of metals by teatment with nanosecond laser pulses N89-11006
A method for improving the depth of penetration and the appearance of welding
[DE88-012954] N89-11239

STELLAR COLOR
Colour and spectral synthesis of disk galaxies N89-11656
O stars and Wolf-Rayet stars
[NASA-SP-497] N89-11657

STELLAR COMPOSITION
O stars and Wolf-Rayet stars
[NASA-SP-497] N89-11657

STELLAR CORES
On relative supernova rates and nucleosynthesis roles
[NASA-CR-183373] N89-11673

STELLAR EVOLUTION
Supernova 1987A in the large magellanic cloud N89-11642
New insights into globular clusters from main sequence photometry N89-11658

STELLAR LUMINOSITY
O stars and Wolf-Rayet stars
[NASA-SP-497] N89-11657

STELLAR MASS
Three probable stellar mass black holes
[AD-A196976] N89-11676

STELLAR STRUCTURE
Astrophysical evidence on the equation of state
[DE88-011960] N89-11668

STELLARATORS
Stellarator theory
[DE88-014131] N89-11528

STIFFNESS
Continuum modeling of latticed structures N89-11253

STIFFNESS MATRIX
The mini-oscillator technique: A finite element method for the modeling of linear viscoelastic structures
[UTIAS-323] N89-11250

STIRLING CYCLE
Development of a residential free-piston Stirling engine heat pump
[DE88-012917] N89-11303
Integration of analysis and experiment for Stirling cycle processes. Part 1: Gas spring hysteresis loss
[DE88-013202] N89-11313

STIRLING ENGINES
An overview of the Stirling engine heat pump program
[DE88-013833] N89-11146
Preliminary assessment of a magnetically coupled free-piston Stirling engine heat pump compressor
[DE88-013835] N89-11232

STOCHASTIC PROCESSES
Collective resonance fluorescence in an intense laser field with phase and amplitude fluctuations
[DE88-702920] N89-11205
Problem on 0-1 matrices
[PB88-210075] N89-11477
General results in optimal control of discrete-time nonlinear stochastic systems
[AD-A196411] N89-11481
Stochastic theory of frequency redistribution in two-photon processes N89-11669

STORAGE BATTERIES
Evaluation of Li/MoS2 secondary battery for load-conditioner. Deep-cycle performance of AA-size cells
[DE88-753437] N89-11118
Lithium secondary batteries: Role of polymer cathode morphology
[AD-A196998] N89-11135

STORAGE STABILITY
Compatibility and performance of separators in Li/SOCl(sub 2) cells
[DE88-011090] N89-11116

STORM SURGES
An investigation of the internal structure of the thunderstorm outflow with particular attention to multiple surges N89-11357

STORMS
A study of the dynamics of maritime fronts using remotely sensed wind and stress measurements N89-11366

STORMS (METEOROLOGY)
On deriving the 3-dimensional kinematic structure of convective storms from a single radar
[AD-A196405] N89-11373

STRAIN ENERGY RELEASE RATE
A mixed-mode bending apparatus for delamination testing
[NASA-TM-100662] N89-10945

STRAIN GAGES
Rotor instrumentation circuits for the Sandia 34-meter vertical axis wind turbine
[DE88-014704] N89-11304

STRAIN HARDENING
Strain hardening at large strains
[DE88-007909] N89-10995

STRAIN MEASUREMENT
Sensors for ceramic components in advanced propulsion systems: Summary of literature survey and concept analysis, task 3 report
[NASA-CR-180900] N89-11192
The electronic and optical properties of silicon/germanium strained layer superlattices N89-11590

STRAIN RATE
Finite element analysis of large strain elastic-plastic solids N89-11281
A strain rate dependent brittle fracture model based on continuum damage mechanics
[DE88-013361] N89-11285

STRAKES
Unsteady low-speed windtunnel test of a straked delta wing, oscillating in pitch. Part 1: General description and discussion of results
[AD-A196456] N89-10867

STRATEGY
On motion planning and control of multi-link lightweight robotic manipulators
[NASA-CR-181226] N89-11234

STRATIFICATION
Rotating and stratified fluids N89-11343

STRATIFIED FLOW
Rotating and stratified fluids N89-11343

STRATOSPHERE
A new determination of extinction due to atmospheric aerosols and the resulting implications for upper stratospheric ozone depletion N89-11348

STRESS (PHYSIOLOGY)
Effect of physical fitness on response to orthostasis in healthy young women
[AD-A196377] N89-11387

STRESS (PSYCHOLOGY)
Enhancing performance under stress by information about its expected duration
[AD-A196836] N89-11388

STRESS ANALYSIS
A mixed-mode bending apparatus for delamination testing
[NASA-TM-100662] N89-10945
Multistress aging of polymer films
[DE88-008094] N89-11034
The Shock and Vibration Digest, Volume 20, No. 8 N89-11258
Dynamic behavior of foundations in bilateral and unilateral contact N89-11259
Contribution for stress analysis in bend acessories of piping systems
[DE88-701618] N89-11272
Finite element analysis of shell structures with an 18-node 3-dimensional solid element based on a new mixed formulation
[AD-A196698] N89-11288
Rotor instrumentation circuits for the Sandia 34-meter vertical axis wind turbine
[DE88-014704] N89-11304

STRESS CORROSION CRACKING
The effect of thermal ageing on the stress corrosion cracking of 9Cr1Mo steel in aqueous caustic environments
[NRL-R-1003(R)] N89-10997

STRESS-STRAIN RELATIONSHIPS
Computer simulation of the uni-axial stress-strain behavior of ribbon-like fiber nonwovens N89-11284
Creep and fracture characteristics of materials and structures at elevated temperatures
[AD-A196831] N89-11289

STRESSES
Strain hardening at large strains
[DE88-007909] N89-10995
Methodology of flexural fatigue testing composite materials produced by electron-beam evaporation N89-11003
Low stress brittle fractures in polymers
[DE88-014236] N89-11027
Ratchetting behavior of type 304 stainless steel at room and elevated temperatures
[DE88-011864] N89-11273
Measurement of glass shell buckling strength using a piezoelectric film sensor
[DE88-013016] N89-11280

STRING THEORY
The decay of highly excited open strings
[NASA-CR-183364] N89-11501
Cosmic strings and superconducting cosmic strings
[NASA-CR-183361] N89-11604
Quantization of Green-Schwarz superstring
[DE88-702242] N89-11609
Cosmic strings
[NASA-CR-183367] N89-11613
Inflation, cosmic strings and galaxy formation
[DE88-008629] N89-11666

Phase transitions as the origin of large scale structure in the universe
[NASA-CR-183359] N89-11674

STRONTIUM COMPOUNDS
Lattice instability in single-crystal La(sub 2-x)Sr(sub x)/CuO4
[DE88-013994] N89-11598

STRUCTURAL ANALYSIS
Accuracy analysis of the semi-analytical method for shape sensitivity analysis N89-10848
Continuous deformation monitoring with GPS
[AD-A196447] N89-10886
Composite structural materials
[NASA-CR-180224] N89-10946
PRIMEL: A preprocessor for the analysis of laminated composites. Introduction and user's guide (operation system OS/VS2 (MVS))
[DFVLR-MITT-88-14] N89-10956
Experimental research on swept shock wave/boundary layer interactions
[AD-A196938] N89-11189
The Shock and Vibration Digest, Volume 20, No. 10 N89-11252
Longitudinal impact test of a transport airframe section
[DOT/FAA/CT-87/26] N89-11265
Literature review of strengthening methodologies of existing structures
[PB88-218219] N89-11271
Communication aspects of parallel processing
[AD-A196458] N89-11439
Structural anomalies in undoped Gallium Arsenide observed in high resolution diffraction imaging with monochromatic synchrotron radiation
[NASA-CR-183268] N89-11595

STRUCTURAL BASINS
The flux and recycling of bioactive substances in the surface sediments of the deep basins off southern California
[DE88-007999] N89-11321

STRUCTURAL DESIGN
Development of a verification program for deployable truss advanced technology
[NASA-CR-181703] N89-10936
Baseline configuration data set: NASA Standard Initiator-2 (NSI-2)
[NASA-CR-172071] N89-11050
Preliminary assessment of a magnetically coupled free-piston Stirling engine heat pump compressor
[DE88-013835] N89-11232
PV modules for ground testing
[NASA-CR-179476] N89-11315

STRUCTURAL ENGINEERING
Continuous deformation monitoring with GPS
[AD-A196447] N89-10886
A comparative overview of modal testing and system identification for control of structures N89-11262
Communication aspects of parallel processing
[AD-A196458] N89-11439

STRUCTURAL MEMBERS
Literature review of strengthening methodologies of existing structures
[PB88-218219] N89-11271

STRUCTURAL STABILITY
Acceleration ground test program to verify GAS payload No. 559 structure/support avionics and experiment structural integrity N89-10913
Current research on the vibration and stability of axially-moving materials N89-11283
Lattice instability in single-crystal La(sub 2-x)Sr(sub x)/CuO4
[DE88-013994] N89-11598

STRUCTURAL VIBRATION
The Shock and Vibration Digest, volume 20, no. 5 N89-11262

SUBMARINES
Oxygen chemistry
[AD-A196869] N89-10988
Three dimensional boundary layers on submarine conning towers and rudders
[CERT-OA-23/5025-AYD] N89-11182

SUBMILLIMETER WAVES
Study of optical output couplers for submillimeter wavelength backward-wave oscillators (BWO's)
[NASA-TM-101360] N89-11128
Space observations for infrared and submillimeter astronomy N89-11643

SUBROUTINE LIBRARIES (COMPUTERS)
The vector functions of the MS system 570/CX
[CNES-CT/DTI/MS/MN/019] N89-11423

SUBSONIC SPEED
A free-flight experiment of vehicles ranging from high subsonic to high supersonic speeds
[ISAS-RN-362] N89-10888

SUBSTRATES
Deposition and characterization of ZnS/Si heterojunctions produced by vacuum evaporation
[NASA-TM-101359] N89-11129
Effect of thermal cycling
[AD-A196851] N89-11219

SULFATES
Experimental and theoretical study of inclusions during initiation of crevice corrosion
[DE88-014635] N89-10989

SUPERCOMPUTERS
The CSM testbed software system: A development environment for structural analysis methods on the NAS CRAY-2
[NASA-TM-100642] N89-11287
Computational Fluid Dynamics: Algorithms and Supercomputers
[AGARD-AG-311] N89-11395
Hardware architecture, chapter 2 N89-11396
Vectorization of FORTRAN programs at do-loop level N89-11398
Computatinal fluid dynamics and supercomputers, chapter 6 N89-11400
An informal glossary of terms used in supercomputing, appendix A N89-11401

SUPERCONDUCTIVITY
Magnetic fluctuations and heavy electron superconductivity
[DE88-011978] N89-11557
Simple model for the superconducting phase diagram near the metal-insulator transition
[DE88-703038] N89-11558
Possible coexistence of antiferromagnetism and superconductivity in the Hubbard model
[DE88-703025] N89-11561
Current-induced quantum interference in the composite superconductor NbTi-Cu
[DE88-703079] N89-11562
The critical current density, the fabrication process and the microstructure in superconducting composites of NbTi for high energy physics
[DE88-014241] N89-11568
Theory of oxygen ordering and absorption in 1,2,3 high-T(sub c) superconductors
[DE88-007543] N89-11575
Superconductivity, structures, ESR and SIMS-analysis of a high-T(sub c)Y(sub 0.33)Ba(sub 0.67)Cu(sub 2.33)O(sub 3.67-sigma) compound
[DE88-702677] N89-11583
Electrodynamics of single-crystal Eu(sub 2)CuO(sub 4): A boson excitation spectrum
[DE88-014328] N89-11585
Microstructural defects and superconducting critical currents in superconductors
[DE88-013781] N89-11587
Self-consistent charge and spin distributions in oxide superconductors
[DE88-012051] N89-11591
Some theoretical aspects of high-T(sub c) superconductivity
[DE88-013101] N89-11592
Low temperature measurements on UBe13
[DE88-014446] N89-11594
Tunneling junctions and the field effect
[DE88-013707] N89-11597
Lattice instability in single-crystal La(sub 2-x)Sr(sub x)/CuO4
[DE88-013994] N89-11598
Phonon-plasmon mechanism of high-T(sub c) superconductivity
[DE88-014860] N89-11600
Chemical preparation of powders and films for high temperature superconductors
[DE88-015266] N89-11601
New quantum interferometer effect in superconducting oxide ceramics
[DE88-703152] N89-11603
Cosmic strings and superconducting cosmic strings
[NASA-CR-183361] N89-11604
Fundamental aspects of the electronic structure, materials properties, and lubrication performance of sputtered MoS2 films
[AD-A196852] N89-11606
Coupled even-parity superconducting states
[AD-A196969] N89-11607

SUPERCONDUCTORS
Current-induced quantum interference in the composite superconductor NbTi-Cu
[DE88-703079] N89-11562
MAGLEV: The double benefits of high-Tc superconductors and its development as an aerospace technology
[DE88-012005] N89-11570
Strongly interacting fermion systems: Emphasis on heavy fermions
[DE88-014127] N89-11573
Theory of oxygen ordering and absorption in 1,2,3 high-T(sub c) superconductors
[DE88-007543] N89-11575
High-power RF applications of high-T(sub c) superconductors
[DE88-012055] N89-11579
Microstructural defects and superconducting critical currents in superconductors
[DE88-013781] N89-11587
Self-consistent charge and spin distributions in oxide superconductors
[DE88-012051] N89-11591

SUPERFLUIDITY
Superfluid helium as a dark matter detector
[DE88-012759] N89-11664

SUPERHIGH FREQUENCIES
Plan of advanced satellite communications experiment using ETS-VI N89-11089

SUPERLATTICES
Constraints on the growth of metallic superlattices
[DE88-014633] N89-11586
The electronic and optical properties of silicon/germanium strained layer superlattices N89-11590
A theory of surface and interface electronic properties of crystalline solids: Applications to 2-6 compounds N89-11596

SUPERNOVA 1987A
Supernova 1987A in the large magellanic cloud N89-11642
On relative supernova rates and nucleosynthesis roles
[NASA-CR-183373] N89-11673

SUPERNOVAE
Physics and astrophysics of gravitational waves N89-11647
Astrophysical evidence on the equation of state
[DE88-011960] N89-11668

SUPERSONIC FLOW
Experimental investigation of the performance of a supersonic compressor cascade
[NASA-TM-100879] N89-10858
Schlieren measurements at the 10,000-foot sled track
[DE88-012748] N89-10899
Computation of low-speed compressible flows with time-marching procedures
[AD-A195800] N89-11170
Entrainment enhancement of a supersonic jet for advanced ejectors
[DE88-013200] N89-11177

SUPERSONIC SPEED
A free-flight experiment of vehicles ranging from high subsonic to high supersonic speeds
[ISAS-RN-362] N89-10888

SUPERSYMMETRY
Quantization of Green-Schwarz superstring
[DE88-702242] N89-11609

SURFACE FINISHING
Developments and trends in electrodeposition
[DE88-009822] N89-11014
Studies in advanced silicon solar cells
[DE88-013143] N89-11314
Plasma spectrometry applied to surface treatments (laser PVD)
[ETCA-88-R-036] N89-11533

SURFACE IONIZATION
Near surface chemistry and corrosion behavior of excimer laser surface-melted AISI type 304 stainless steel
[DE88-014440] N89-11019

SURFACE PROPERTIES
Experiments on liquid-vapour phase change between plane liquid surfaces. Part 1: Experiments with water, freon and mercury
[TM-FM-8804-PT-1] N89-10964
Nitride layer growth in iron and titanium alloys: Studies by electron probe microanalysis
[DE88-007207] N89-11017
Surface structures and reactions of ceramics and metals
[DE88-013752] N89-11028
Effect of surface states on the electrochemical behaviour of single crystal n-ZnSe photoelectrode
[DE88-702726] N89-11566
The effect of vapor incidence angle upon thin film columnar growth
[DE88-014396] N89-11577
High-power RF applications of high-T(sub c) superconductors
[DE88-012055] N89-11579
Dynamic Interactions of Energetic Probes with Condensed Matter: Proceedings
[DE88-008882] N89-11589
A theory of surface and interface electronic properties of crystalline solids: Applications to 2-6 compounds N89-11596

SURFACE REACTIONS
Laboratory investigations of low earth orbit environmental effects on spacecraft
[DE88-009135] N89-10932
The catalytic, structural, and electronic properties of strained-metal overlayers
[DE88-007932] N89-11013
Near surface chemistry and corrosion behavior of excimer laser surface-melted AISI type 304 stainless steel
[DE88-014440] N89-11019
Corrosion phenomena during overcharge in polymer electrolyte cells
[AD-A196997] N89-11134
Plasma spectrometry applied to surface treatments (laser PVD)
[ETCA-88-R-036] N89-11533
Surface passivation of Gallium Arsenide
[AD-A196695] N89-11605
SURFACE ROUGHNESS
The generation of scatterometer surface targets with specified surface statistics
[AD-A196397] N89-11480
SURFACE STABILITY
Effect of thermal cycling
[AD-A196851] N89-11219
SURFACE TEMPERATURE
Sensors for ceramic components in advanced propulsion systems: Summary of literature survey and concept analysis, task 3 report
[NASA-CR-180900] N89-11192
SURFACE WAVES
Modulation of radar backscatter from the ocean by a variable surface current
[AD-A196952] N89-11114
SURFACTANTS
Control of environment assisted cracking of Al 7075 using inhibitors
[AD-A196367] N89-11022
SURVIVAL
Penalized likelihood estimation for rates with censored survival
[RR-726-M] N89-11479
SUSPENDING (MIXING)
Migration arising from gradients in shear stress: Particle distributions in Poiseuille flow N89-11159
SWITCHING
Multiple pulse photoconductive semiconductor switching
[DE88-011792] N89-11119
SWITCHING CIRCUITS
Electron attachment properties of excited dielectric-gas molecules and their possible use for pulse power switching
[DE88-009705] N89-11117
Switchable auto gain amplifier
[DE88-012114] N89-11122
A study of the turn-off behavior of high power gate turn off thyristors (GTO): Computer-aid to design and utilization
[LAAS-88-164] N89-11124
SYMMETRY
Accessibility, a criterion for the choice of visual coding rules
[PB88-209911] N89-11458
Gauged Q-balls
[NASA-CR-183369] N89-11500
SYNCHRONISM
Asynchronous digital regulators
[AD-A196911] N89-11446
SYNCHRONOUS SATELLITES
Verification of single event upset rate estimation methods with on-orbit observations
[AD-A196226] N89-10935
SYNCHROTRON RADIATION
Structural anomalies in undoped Gallium Arsenide observed in high resolution diffraction imaging with monochromatic synchrotron radiation
[NASA-CR-183268] N89-11595
SYNTHESIS
Dynamic analysis of pipings by modal synthesis
[DE88-701620] N89-11274
SYNTHESIS (CHEMISTRY)
Ligand intermediates in metal catalyzed reactions
[DE88-012123] N89-11007
Calorimetry study of the synthesis of amorphous Ni-Ti alloys by mechanical alloying
[DE88-006468] N89-11010
New non-linear optical polymers
[AD-A196859] N89-11040
Energetic thermoplastic elastomer synthesis
[AD-A196885] N89-11041
Synthesis of energetic binders
[AD-A196886] N89-11042
Development of elastomeric polypeptide biomaterials
[AD-A196900] N89-11044
Ternary adamantine materials for low-cost solar cells
[DE88-001160] N89-11302
Advanced materials for solid oxide fuel cells: Hafnium-praseodymium-indium oxide system
[DE88-015365] N89-11310
Kinetic processes of the orthorhombic to tetragonal phase transition in YBa2Cu3O7-Delta
[DE88-011993] N89-11572
SYNTHETIC RESINS
Polystyrylpyridine (PSP) resin-based short-fiber composites (injectable compounds)
[REPT-NT-195/87/CRB/GTR.C/NP] N89-10955
SYSTEM IDENTIFICATION
A comparative overview of modal testing and system identification for control of structures N89-11262
Comparison of recent model selection criteria for system identification
[PD-SE-8807] N89-11449
SYSTEMS ANALYSIS
Knowledge-based diagnosis for aerospace systems
[NASA-CR-182641] N89-11441
General results in optimal control of discrete-time nonlinear stochastic systems
[AD-A196411] N89-11481
Measures, methods and models employed in evaluating the effectiveness of information centers and services N89-11627
SYSTEMS ENGINEERING
Integral manifold in system design with application to flexible link robot control
[AD-A197052] N89-11243
Quality assurance manual. Volume 2: Appendices
[DE88-013880] N89-11247
Optimization-based design of control systems
[AD-A196593] N89-11405
Software management metrics
[AD-A196916] N89-11434
Guidelines for tailoring DOD-STD-2167A for SDS (Strategic Defense System) software development
[AD-A197038] N89-11488
SYSTEMS INTEGRATION
GPS/interial navigation system integration for enhanced navigation performance and robustness N89-10880
Aiding and integration of a GPS receiver N89-10881
SYSTEMS MANAGEMENT
Software management metrics
[AD-A196916] N89-11434
SYSTEMS SIMULATION
Nonlinear control of an H2O2 steam reactor
[ESA-TT-902] N89-11242
SYSTEMS STABILITY
The Shock and Vibration Digest, Volume 20, No. 8 N89-11258
Vibrations and stability of mechanical systems: 4 N89-11260

T

TACTICS
Numerical simulation of axisymmetric base flow on tactical missiles with propulsive jet
[AD-A196169] N89-11136
TAKEOFF
Noise of the Harrier in vertical landing and takeoff N89-10856
TARGETS
Interceptor-to-target allocation strategies for Strategic Defense 1: Adaptive strategies based upon system and threat characteristics
[AD-A197037] N89-11487
TASK COMPLEXITY
Effects of noise and task loading on a communication task loading on a communication task
[AD-A196378] N89-11107
TASKS
Effects of noise and task loading on a communication task loading on a communication task
[AD-A196378] N89-11107
TATB
Friction and impact sensitivities of explosives: A comparative study
[DE88-012864] N89-11051
TECHNOLOGICAL FORECASTING
Aviation technology applicable to developing regions
[NASA-TM-89425] N89-10872
TECHNOLOGY ASSESSMENT
Space science/space station attached payload pointing accommodation study: Technology assessment white paper
[NASA-CR-182735] N89-10931
Defense technology base: Introduction and overview
[PB88-192562] N89-11635
A perspective on space exploration technology catalysis: A rationale for initiating 21st Century expansion of human civilization into outer space
[NASA-TM-101362] N89-11637
TECHNOLOGY TRANSFER
A co-citation study of the scientific literature of two innovation research traditions: Diffusion of innovations and technology transfer N89-11618
Defense technology base: Introduction and overview
[PB88-192562] N89-11635
Technology transfer at Argonne National Laboratory
[DE88-012062] N89-11636
TELECOMMUNICATION
Effects of noise and task loading on a communication task loading on a communication task
[AD-A196378] N89-11107
TELEMETRY
The checkout system software for the Brazilian satellite
[INPE-4571-PRE/1311] N89-11419
TELEOPERATORS
Manual, voice, and automated control of a teleoperator viewing system
[DE88-011835] N89-11235
TELEVISION CAMERAS
Manual, voice, and automated control of a teleoperator viewing system
[DE88-011835] N89-11235
Quantitative Luminescence Imaging System description and user's manual
[DE88-015604] N89-11512
TELEVISION SYSTEMS
Bandwidth compression for HDTV broadcasting: Investigation of some adaptive subsampling strategies
[BBC-RD-1988/9] N89-11101
TELEVISION TRANSMISSION
Polarisation converters for a DBS flat-plate antenna
[BBC-RD-1988/7] N89-11073
A flat-plate antenna for DBS reception
[BBC-RD-1988/6] N89-11096
Television animation store: Control system operation and implementation
[BBC-RD-1988/4] N89-11097
Array elements for a DBS flat-plate antenna
[BBC-RD-1988/8] N89-11103
TEMPERATURE CONTROL
Development of Bio-GAS systems N89-10904
Practical applications and limitations of adaptive control N89-11442
TEMPERATURE DEPENDENCE
Temperature dependence of entropies and specific heats of liquid Na and K
[DE88-702986] N89-10976
Far infrared linear response and radio frequency nonlinear response of charge density wave conductors and high T(sub c) superconductors
[DE88-013595] N89-11582
TEMPERATURE DISTRIBUTION
Experiments on liquid-vapour phase change between plane liquid surfaces. Part 1: Experiments with water, freon and mercury
[TM-FM-8804-PT-1] N89-10964
Experiments on liquid-vapor phase change between plane liquid surfaces. Part 2: Observations of large temperature jumps near the interfaces
[TM-FM-8805-PT-2] N89-10973
The impact of an increase in atmospheric methane on the temperature field and subsequent climatic effects
[AD-A196869] N89-11332
TEMPERATURE EFFECTS
Further investigations on new fluid working systems for absorption heat pumps
[DE88-012622] N89-11151
TEMPERATURE MEASUREMENT
Sensors for ceramic components in advanced propulsion systems: Summary of literature survey and concept analysis, task 3 report
[NASA-CR-180900] N89-11192
Autocompensation device for ultralow temperature measurements
[DE88-702900] N89-11194
Laser plume temperature measurements in various gases
[DE88-006462] N89-11204
Spectroscopic measurement of the ion temperature on ASDEX --- tokamak N89-11536
Low temperature measurements on UBe13
[DE88-014446] N89-11594
TEMPERATURE PROFILES
A study of wind profiles under quasi-neutral and inversion atmospheric conditions, over a terra firma forest
[INPE-4694-RPE/575] N89-11369

TEMPORAL RESOLUTION
Space and time resolved measurements of ion temperature with the CVI 5292 A charge exchange recombination line after substracting background radiation
[IPPJ-888] N89-11549
TENSILE PROPERTIES
A test methodology for an investigation into heating and cooling phenomena in grossly deformed tensile metallic bars
[AD-A197047] N89-11024
Joining of advanced aluminides
[DE88-015111] N89-11226
Potential foams and metal foils for cosmic dust capture
[DE88-012960] N89-11665
TENSILE STRENGTH
Influence of specimen dimension on damage and breaking of composite materials
[REPT-49-062/F] N89-10957
TENSILE TESTS
Tension fatigue analysis and life prediction for composite laminates
[NASA-TM-100549] N89-10951
TENSION
Tether applications
[NASA-CR-179392] N89-10934
TENSORS
Derivation of revised formulae for eddy viscous forces used in the ocean general circulation model
[NASA-TM-4060] N89-11381
TERMINAL VELOCITY
An approximate, maximum terminal velocity descent to a point
[DE88-000349] N89-10840
TERMINOLOGY
An informal glossary of terms used in supercomputing, appendix A N89-11401
Measuring the vague meanings of probability terms
[AD-A196944] N89-11483
TERRAIN ANALYSIS
Polarimetric clutter modeling: Theory and application
[NASA-CR-183348] N89-11106
TEST FACILITIES
The photovoltaic advanced systems test facility
[DE88-009589] N89-11306
TEST RANGES
A free-flight experiment of vehicles ranging from high subsonic to high supersonic speeds
[ISAS-RN-362] N89-10868
TEST VEHICLES
Full scale wind tunnel tests on a Ford Escort Mk 3
[TT-8802] N89-10846
TETHERLINES
Tether applications
[NASA-CR-179392] N89-10934
THEORETICAL PHYSICS
Theoretical plasma physics
[DE88-014285] N89-11518
THERMAL ANALYSIS
Thermal calculations of nitrogen-free nonmagnetic helium cryostats
[DE88-702807] N89-11227
Applications of the optical differential thermal analysis
[AD-A196706] N89-11515
THERMAL CONDUCTIVITY
Low temperature measurements on UBe13
[DE88-014446] N89-11594
THERMAL CYCLING TESTS
Effect of thermal cycling
[AD-A196851] N89-11219
THERMAL DEGRADATION
The effect of thermal ageing on the stress corrosion cracking of 9Cr1Mo steel in aqueous caustic environments
[NRL-R-1003(R)] N89-10997
Organic Rankine-Cycle Power Systems Working Fluids Study: 2-methylpyridine/water
[DE88-012659] N89-11307
THERMAL EMISSION
Ground-based radiometric observations of emission and attenuation at 20.6, 31.65, and 90.0 GHz N89-11086
THERMAL ENVIRONMENTS
Effect of protective coatings on life of heat-resistant nickel steel under cyclic heat load N89-11005
THERMAL EXPANSION
Coefficients of thermal expansion of common encapsulants
[DE88-015026] N89-10983
Effect of thermal cycling
[AD-A196851] N89-11219
THERMAL INSULATION
Utilization of spray on foam insulation for manned and unmanned spacecraft and structures N89-10914
THERMAL RADIATION
A study of the effect of thermal radiation on laminar flame propagation and ignition, 1981-1987 N89-10967
A test methodology for an investigation into heating and cooling phenomena in grossly deformed tensile metallic bars
[AD-A197047] N89-11024
Two-dimensional saturation gain and output power in transverse flow electrical discharge CO2 lasers
[AD-A196660] N89-11218
THERMAL REACTORS
Massachusetts Institute of Technology Plasma Fusion Center 1987--1988 report to the President
[DE88-014800] N89-11519
THERMAL RESISTANCE
The thermal resistance of fine powders at atmospheric pressure and under vacuum
[DE88-014556] N89-10982
THERMAL SHOCK
High heat flux testing of CIT (Compact Ignition Tokamak) first wall tiles
[DE88-012241] N89-11530
THERMAL STRESSES
Effect of protective coatings on life of heat-resistant nickel steel under cyclic heat load N89-11005
Further investigations on new fluid working systems for absorption heat pumps
[DE88-012622] N89-11151
THERMISTORS
A test methodology for an investigation into heating and cooling phenomena in grossly deformed tensile metallic bars
[AD-A197047] N89-11024
THERMITES
Development of an experimental model of self-propagating high temperature oxidation-reduction reactions
[AD-A196978] N89-10987
THERMODYNAMIC PROPERTIES
Thermophysical properties of argon. Addendum
[DE88-012722] N89-10966
Worldwide survey of absorption fluids data
[DE88-013204] N89-10972
Ligand intermediates in metal catalyzed reactions
[DE88-012123] N89-11007
Fluid science investigations in microgravity
[PB88-209754] N89-11058
THERMODYNAMICS
Research needs in high temperature chemistry
[DE88-012929] N89-10961
The importance of thermodynamics to the modeling of nitrogen combustion chemistry
[DE88-014656] N89-10978
Fluid mechanical properties of flames in enclosures
[DE88-014142] N89-10981
Thermodynamic improvements for the space thermoacoustic refrigerator (STAR)
[AD-A196958] N89-11071
Fuel cells: A handbook
[DE88-010252] N89-11309
Nuclear processes in the early universe. Part 1: The thermal history of matter N89-11639
THERMOMETERS
Autocompensation device for ultralow temperature measurements
[DE88-702900] N89-11194
THERMOPLASTIC RESINS
A test methodology for an investigation into heating and cooling phenomena in grossly deformed tensile metallic bars
[AD-A197047] N89-11024
THERMOPLASTICITY
Energetic thermoplastic elastomer synthesis
[AD-A196885] N89-11041
THERMOSPHERE
The utility of particle precipitation data as an input to thermospheric density models for satellite orbital analysis
[AD-A196870] N89-10925
THIN FILMS
Carbon films derived from poly(acrylonitrile): Oxidation, electrical properties, and processing
[DE88-010352] N89-10950
Brillouin scattering: Its application to the study of damage and amorphization
[DE88-012053] N89-11016
Characterization of metallic coatings and thin films produced by railgun deposition
[AD-A196382] N89-11021
Surface structures and reactions of ceramics and metals
[DE88-013752] N89-11028
Survivability of coatings: Program review
[DE88-009863] N89-11031
IR reflectance and Raman scattering of diamond films
[AD-A196899] N89-11043
Ternary adamantine materials for low-cost solar cells
[DE88-001160] N89-11302
Amorphous silicon photovoltaic devices prepared by chemical and photochemical vapor deposition of higher order silanes
[DE88-001189] N89-11311
Design of high-reflectivity supermirror structures
[DE88-015287] N89-11511
Defect model for the electronic conduction and breakdown in dielectric thin films N89-11563
The effect of vapor incidence angle upon thin film columnar growth
[DE88-014396] N89-11577
Molecular beam epitaxy of GaP films on Si substrates
[PB88-131974] N89-11581
Chemical preparation of powders and films for high temperature superconductors
[DE88-015266] N89-11601
Fundamental aspects of the electronic structure, materials properties, and lubrication performance of sputtered MoS2 films
[AD-A196852] N89-11606
Potential foams and metal foils for cosmic dust capture
[DE88-012960] N89-11665
THIN PLATES
Technique for measuring the dielectric constant of thin materials
[NASA-CR-183325] N89-10984
Finite element analysis of shell structures with an 18-node 3-dimensional solid element based on a new mixed formulation
[AD-A196898] N89-11288
THIN WALLED SHELLS
Measurement of glass shell buckling strength using a piezoelectric film sensor
[DE88-013016] N89-11280
THORIUM ALLOYS
Electrical resistivity of U(sub 1-x)M(sub x)Be13 under pressure
[DE88-014449] N89-11552
THREAT EVALUATION
Interceptor-to-target allocation strategies for Strategic Defense 1: Adaptive strategies based upon system and threat characteristics
[AD-A197037] N89-11487
THREE DIMENSIONAL BOUNDARY LAYER
Three dimensional boundary layers on submarine conning towers and rudders
[CERT-OA-23/5025-AYD] N89-11182
Study of three dimensional boundary layers on the front of a fuselage and at an air intake
[CERT-OA-22/5025-AYD] N89-11184
THREE DIMENSIONAL FLOW
A diagonally inverted LU implicit multigrid scheme for the 3-D Navier-Stokes equations and a two equation model of turbulence
[NASA-CR-182209] N89-10863
Three dimensional shear flow. Analysis of the flow in a delta arrow wing with incidence angle
[CERT-RTS-OA-25/5025-AYD] N89-10864
THREE DIMENSIONAL MODELS
High resolution schemes for three-dimensional Euler equations. 1: Estimation of recent TVD schemes
[PB88-214416] N89-10845
Three dimensional gravity modeling techniques with application to the Ennis Geothermal Area, part 1
[DE88-014952] N89-11340
THRUST REVERSAL
F-15 SMTD low speed jet effects wind tunnel test results N89-10853
An assessment of ground effects determined by static and dynamic testing techniques N89-10854
THUNDERSTORMS
An investigation of the internal structure of the thunderstorm outflow with particular attention to multiple surges N89-11357
THYRISTORS
A study of the turn-off behavior of high power gate turn off thyristors (GTO): Computer-aid to design and utilization
[LAAS-88-164] N89-11124
TILES
High heat flux testing of CIT (Compact Ignition Tokamak) first wall tiles
[DE88-012241] N89-11530
TIME
The Global Positioning System (GPS) constellation and coverage N89-10876
New trial of vibration testing method N89-11068
Balance of recurrence order in time-inhomogeneous Markov chains with application to simulated annealing
[AD-A196980] N89-11484

TIME DEPENDENCE
A time-dependent model for the low-latitude ionosphere
[AD-A196683] N89-11354
TIME FUNCTIONS
General results in optimal control of discrete-time nonlinear stochastic systems
[AD-A196411] N89-11481
TIME LAG
Securing the time scale of the NAVEX reference clock and rate determinations by time comparisons with the help of the Global Positioning System (GPS) --- Spacelab D1 mission
[ESA-TT-1111] N89-11197
TIME MARCHING
Computation of low-speed compressible flows with time-marching procedures
[AD-A195800] N89-11170
TIME MEASUREMENT
Securing the time scale of the NAVEX reference clock and rate determinations by time comparisons with the help of the Global Positioning System (GPS) --- Spacelab D1 mission
[ESA-TT-1111] N89-11197
TIME OPTIMAL CONTROL
General results in optimal control of discrete-time nonlinear stochastic systems
[AD-A196411] N89-11481
TIME SERIES ANALYSIS
Active modes of the Pacific Intertropical Convergence Zone (ITCZ)
[AD-A196406] N89-11374
TIROS N SERIES SATELLITES
Tropospheric sounding from the TIROS-N series of satellites N89-11347
TISSUES (BIOLOGY)
Growth of plant tissue cultures in simulated lunar soil: Implications for a lunar base CELSS (Controlled Ecological Life Support System)
[NASA-CR-183233] N89-11384
TITAN
Outward to the beginning: The CRAF and Cassini Missions of the Mariner Mark 2 program
[NASA-CR-183133] N89-10921
TITANIUM
Microstructural development of titanium-modified austenitic stainless steel under neutron irradiation in HFIR up to 57 dpa
[DE88-013248] N89-10999
Baseline configuration data set: NASA Standard Initiator-2 (NSI-2)
[NASA-CR-172071] N89-11050
Ti-implanted optical waveguides in LiNbO3
[DE88-015279] N89-11554
TITANIUM ALLOYS
Nitride layer growth in iron and titanium alloys: Studies by electron probe microanalysis
[DE88-007207] N89-11017
Current-induced quantum interference in the composite superconductor NbTi-Cu
[DE88-703079] N89-11562
TITANIUM NITRIDES
Characterization of ceramic films and interfaces by electron microscopic and spectroscopic techniques
[DE88-011957] N89-11029
TITANIUM OXIDES
Development of transparent zirconia ceramics discussed N89-11062
TOKAMAK DEVICES
Alfven wave studies on a tokamak N89-11517
Massachusetts Institute of Technology Plasma Fusion Center 1987--1988 report to the President
[DE88-014800] N89-11519
Stellarator theory
[DE88-014131] N89-11528
High heat flux testing of CIT (Compact Ignition Tokamak) first wall tiles
[DE88-012241] N89-11530
ASDEX contributions to the DPG Fruehjahrstagung --- tokamak
[IPP-III/134] N89-11534
Charge exchange spectroscopy (CXRS) of highly ionized ions in ASDEX --- tokamak N89-11535
Spectroscopic measurement of the ion temperature on ASDEX --- tokamak N89-11536
Measurement of the absolute neutron yield of ASDEX with nuclear emulsion plates --- tokamak N89-11537
Calculation of neutron propagation for ASDEX --- tokamak N89-11539
Measurements of proton and triton spectra in ASDEX discharges --- tokamak N89-11541
Advantages of a helium beam for active charge exchange diagnostics --- ASDEX tokamak N89-11542
Simultaneous background measurement in the ASDEX neutral particle diagnostics N89-11543
Power absorption and confinement studies of ICRF-heated plasma in JIPP T-IIU tokamak
[IPPJ-886] N89-11547
Space and time resolved measurements of ion temperature with the CVI 5292 A charge exchange recombination line after substracting background radiation
[IPPJ-888] N89-11549
TOPOGRAPHY
Studies of barotropic flow over topography using a galerkin finite element model
[AD-A196516] N89-11353
TOPOLOGY
Topologically related quantities in turbulent flows N89-11173
Homology classes represented by real algebraic hypersurfaces
[PB88-202908] N89-11453
Real algebraic morphisms into even-dimensional spheres
[PB88-202916] N89-11462
Gauged Q-balls
[NASA-CR-183369] N89-11500
Geometrical methods in quantum field theory: On the topology of spaces of holomorphic maps N89-11611
TORNADOES
The use of the Q-vector in operational meteorology
[AD-A196410] N89-11376
The role of a lid in the 31 May 1985 tornado outbreak
[AD-A196684] N89-11377
TORSION
Strain hardening at large strains
[DE88-007909] N89-10995
TORUSES
Determination of characteristic radiation properties of a torus antenna
[ESA-TT-1106] N89-11105
Periodic solutions of the Hamilton-Jacobi equation by the shooting method: A technique for beam dynamics
[DE88-012733] N89-11460
TOXICOLOGY
JPRS report: Science and technology. USSR: Life sciences
[JPRS-ULS-87-010] N89-11385
TRADEOFFS
Precision-time tradeoffs: A paradigm for processing statistical queries on databases
[DE88-012024] N89-11408
TRAJECTORIES
Confined turbulent fluid-particle flow modeling using multiple-realization particle trajectory schemes N89-11157
TRAJECTORY OPTIMIZATION
An approximate, maximum terminal velocity descent to a point
[DE88-000349] N89-10840
Real-time path planning for robot arms N89-11224
TRANSFORMATIONS (MATHEMATICS)
Velocity and Q from reflection seismic data N89-11334
Equational problems and disunification
[RR-727-I-IMAG-82-LIFIA] N89-11471
On differential polynomials and their resultants
[RR-723-M] N89-11472
TRANSIENT RESPONSE
An all sky study of fast X-ray transients
[NASA-TM-89716] N89-11686
TRANSITION FLOW
An experimental study of a laminar wall-jet in the presence of a uniform external flow
[UTIAS-268] N89-11152
Boundary layer transition
[CERT-OA-40/5018-AYD] N89-11187
TRANSITION METALS
Transition metal mediated transformations of unsaturated molecules
[DE88-013482] N89-10968
The pair potential approach for interfaces: Fundamental problems and practical solutions
[DE88-009165] N89-11456
TRANSITION PROBABILITIES
Balance of recurrence order in time-inhomogeneous Markov chains with application to simulated annealing
[AD-A196980] N89-11484
Phase transitions as the origin of large scale structure in the universe
[NASA-CR-183359] N89-11674
TRANSITION TEMPERATURE
Indentation plasticity and fracture in silicon
[NASA-TP-2863] N89-10996
Superconductivity, structures, ESR and SIMS-analysis of a high-T(sub c)Y(sub 0.33)Ba(sub 0.67)Cu(sub 2.33)O(sub 3.67-sigma) compound
[DE88-702677] N89-11583
TRANSMISSION FLUIDS
Worldwide survey of absorption fluids data
[DE88-013204] N89-10972
TRANSMISSIVITY
Flux method for the field dependent transport through multilayer devices
[INPE-4647-PRE/1357] N89-11559
TRANSMITTANCE
Verification of EOSAEL (Electro-Optical Systems Atmospheric Effects Library) snow transmittance predictions
[DREV-R-4423/87] N89-11099
TRANSONIC FLOW
JPRS report: Science and technology: Japan
[JPRS-JST-87-018] N89-11061
Numerical simulation of transonic flow around Asuka N89-11067
Computation of low-speed compressible flows with time-marching procedures
[AD-A195800] N89-11170
An iterative scheme for numerical solution of transonic small perturbation equation
[TM-AE-8801] N89-11455
TRANSONIC WIND TUNNELS
Electrical noise reduction techniques contributing to improved data quality at the National Transonic Facility
[NASA-CR-4193] N89-11196
TRANSPARENCE
Development of transparent zirconia ceramics discussed N89-11062
Optimization of transparent and reflecting electrodes for amorphous silicon solar cells
[DE88-001175] N89-11316
TRANSPONDERS
OPEX: (Olympus Propagation EXperiment) N89-11090
TRANSPORT PROPERTIES
Experimental and theoretical studies on transport processes in laser welding
[DE88-013933] N89-11230
Anomalous transport arising from nonlinear resistive pressure-driven modes in a plasma
[DE88-014984] N89-11531
TRANSPORT THEORY
Theoretical plasma physics
[DE88-014285] N89-11518
Stellarator theory
[DE88-014131] N89-11528
TRANSVERSE ACCELERATION
Beam handling and emittance control
[AD-A196789] N89-11509
TRAPPED PARTICLES
Trapping and acceleration of electron by elliptically polarized electromagnetic wave propagating across static magnetic field
[IPPJ-885] N89-11545
Potential foams and metal foils for cosmic dust capture
[DE88-012960] N89-11665
TREES (MATHEMATICS)
Parallel algorithm for a class of optimization problems
[PB88-209929] N89-11414
Computational structure of the N-body problem
[AD-A196422] N89-11473
TREES (PLANTS)
LMSS propagation modeling at Virginia Tech N89-11078
TRENDS
Review of aeronautical wind tunnel facilities
[NASA-CR-183057] N89-10897
TRIGGER CIRCUITS
A study of the turn-off behavior of high power gate turn off thyristors (GTO): Computer-aid to design and utilization
[LAAS-88-164] N89-11124
TRITONS
Measurements of proton and triton spectra in ASDEX discharges --- tokamak N89-11541
TROPICAL METEOROLOGY
Tropical 200 mb divergent circulations and their relation to outgoing longwave radiation
[AD-A196375] N89-11370
Tropical cyclone observation and forecasting with and without aircraft reconnaissance
[AD-A196379] N89-11371
TROPICAL REGIONS
Synoptic scale sensitivity of TIROS-N moisture channels in the tropics
[AD-A196686] N89-11378
The climatological seasonal response of the ocean mixed layer in the equatorial and tropical Pacific Ocean
[AD-A196962] N89-11382
TROPICAL STORMS
Tropical cyclone observation and forecasting with and without aircraft reconnaissance
[AD-A196379] N89-11371

TROPOSPHERE
The impact of an increase in atmospheric methane on the temperature field and subsequent climatic effects [AD-A196869] N89-11332
Tropospheric sounding from the TIROS-N series of satellites N89-11347
Synoptic scale sensitivity of TIROS-N moisture channels in the tropics [AD-A196686] N89-11378
TRUSSES
Development of a verification program for deployable truss advanced technology [NASA-CR-181703] N89-10936
TUMBLING MOTION
Investigation of the tumbling phenomenon using computer simulation N89-10896
TUNNEL DIODES
Tunneling junctions and the field effect [DE88-013707] N89-11597
TURBINE BLADES
Aerodynamic design considerations for a free-flying ducted propeller [DE88-006867] N89-10841
Effect of protective coatings on life of heat-resistant nickel steel under cyclic heat load N89-11005
TURBINE PUMPS
JPRS report: Science and technology: Japan [JPRS-JST-87-018] N89-11061
Good performance of LE-7 liquid oxygen turbopump confirmed N89-11064
TURBINE WHEELS
Statistics on aircraft gas turbine engine rotor failures that occurred in US commercial aviation during 1982 [DOT/FAA/CT-86/23] N89-10892
TURBOCOMPRESSORS
Experimental investigation of the performance of a supersonic compressor cascade [NASA-TM-100879] N89-10858
Development of a boundary layer control device for tip clearance experiments in an axial compressor [AD-A196968] N89-11190
TURBOJET ENGINES
De-icing of aircraft turbine engine inlets [DOT/FAA/CT-87/37] N89-10894
TURBOPROP ENGINES
Experimental aerodynamic performance of advanced 40 deg-swept 10-blade propeller model at Mach 0.6 to 0.85 [NASA-TM-88969] N89-10885
TURBULENCE
Reaction rates in premixed turbulent flames and their relevance to the turbulent burning speed [DE88-012021] N89-10960
TURBULENT BOUNDARY LAYER
Turbulent boundary layer drag reduction on an axisymmetric body using circular ring manipulators N89-11145
Measurements and predictions of mixed convection in laminar and turbulent boundary layer flows N89-11164
Experimental research on swept shock wave/boundary layer interactions [AD-A196938] N89-11189
TURBULENT DIFFUSION
Continuum theories for fluid-particle flows: Some aspects of lift forces and turbulence N89-11155
TURBULENT FLOW
Flow around a delta wing with or without a canard (Phi BA = 60 deg). Part 2: Hydrodynamic visualizations in unsteady flow (pitching oscillations) [ONERA-RT-11/2891-AN-PT-2] N89-10860
Friction reduction and heat transfer enhancement in turbulent pipe flow of non-Newtonian liquid-solid mixtures [DE88-010018] N89-11138
Measurements of pressure drop and heat transfer in turbulent pipe flows of particulate slurries [DE88-013622] N89-11150
Mixing and Demixing Processes in Multiphase Flows With Application to Propulsion Systems [NASA-CP-3006] N89-11153
Turbulence modeling of gas-solid suspension flows N89-11156
Confined turbulent fluid-particle flow modeling using multiple-realization particle trajectory schemes N89-11157
Particle dispersion models and drag coefficients for particles in turbulent flows N89-11158
Nongradient diffusion in premixed turbulent flames N89-11161
The turbulent heat flux in low Mach number flows with large density variations N89-11162
Topologically related quantities in turbulent flows N89-11173
Bursting phenomenon in a flat plate pulsed boundary layer [CERT-RSF-OA-69/2259-AYD] N89-11183
The PNL single-tower measurement model of rotationally sampled turbulent wind, with user's guide for STRS2PC [DE88-013166] N89-11360
TURBULENT HEAT TRANSFER
Friction reduction and heat transfer enhancement in turbulent pipe flow of non-Newtonian liquid-solid mixtures [DE88-010018] N89-11138
Measurements of pressure drop and heat transfer in turbulent pipe flows of particulate slurries [DE88-013622] N89-11150
TURBULENT WAKES
Investigation of wake vortices of landing aircraft at Frankfurt airport (Federal Republic of Germany) [DFVLR-MITT-88-15] N89-10862
TWO DIMENSIONAL BODIES
A computational study of coherent structures in the wakes of two-dimensional bluff bodies [AD-A196820] N89-11188
Modelling of the 2-dimensional structure and impurity transport for a scrape-off layer with a solid limiter [IPPJ-873] N89-11527
TWO DIMENSIONAL FLOW
Study of flow past a circular cylinder using a higher order scheme for Navier-Stokes equation [TM-FM-8807] N89-11142
Two-dimensional saturation gain and output power in transverse flow electrical discharge CO2 lasers [AD-A196660] N89-11218
Domain decomposition methods for the parallel computation of reacting flows [NASA-CR-181719] N89-11459
TWO PHASE FLOW
Hydrodynamical characteristics of helium two-phase flows at relatively high mass rates [DE88-702936] N89-11143
Turbulence modeling of gas-solid suspension flows N89-11156
On the constitutive relation for frictional flow of granular materials [DE88-001089] N89-11171

U

U.S.S.R.
JPRS Report: Science and Technology. USSR: Materials Science [JPRS-UMS-88-007] N89-11002
Bibliography of Soviet laser developments, number 87, January - February 1987 [AD-A196973] N89-11223
ULTRAHIGH FREQUENCIES
PiFEx data and archival formats N89-11076
Results of 1987 MSS helicopter propagation experiment at UHF and L band in Central Maryland N89-11077
Preliminary results of MARECS-A measurements in Central Maryland and plans for 1988 MSS experiment in Australia N89-11079
ULTRALIGHT AIRCRAFT
Flight test results for the Daedalus and Light Eagle human powered aircraft [NASA-CR-183305] N89-10890
ULTRASONIC FLAW DETECTION
Experiments in the application of ultrasound diffraction tomography for nondestructive testing [DE88-014694] N89-11245
ULTRAVIOLET RADIATION
Near surface chemistry and corrosion behavior of excimer laser surface-melted AISI type 304 stainless steel [DE88-014440] N89-11019
Los Alamos XUV free electron laser proposal [DE88-013485] N89-11211
UNDERGROUND STRUCTURES
Through-the-earth communication: Experiment results from Billie Mine and Mississippi Chemical Mine [DE88-013162] N89-11072
UNIFORM FLOW
An experimental study of a laminar wall-jet in the presence of a uniform external flow [UTIAS-268] N89-11152
UNITED STATES
National Photovoltaics Program: 1987 program review [DE88-001148] N89-11301
Crustal structure of the northwestern United States N89-11349
UNIVERSAL TIME
Activities relevant to BIH on time scales or the rotation of the earth and terrestrial systems N89-11659
UNIVERSE
On the locality of the no hair conjection and the measure of the universe [NASA-CR-183365] N89-11489
Cosmic strings and superconducting cosmic strings [NASA-CR-183361] N89-11604
Space science and fundamental physics --- conference [ESA-SP-283] N89-11638
Nuclear processes in the early universe. Part 1: The thermal history of matter N89-11639
Nuclear processes in the early universe. Part 2: The cosmic quark-hadron phase transition N89-11640
Unified theories and the early universe N89-11651
The next decades of space astronomy N89-11655
Inhomogeneities in a Friedmann universe [DE88-702981] N89-11672
Phase transitions as the origin of large scale structure in the universe [NASA-CR-183359] N89-11674
UNIVERSITIES
National Center for Atmospheric Research [PB88-220009] N89-11355
UNIX (OPERATING SYSTEM)
Improvement and extension of a radar forest backscattering model [NASA-CR-183259] N89-11292
UNMANNED SPACECRAFT
The deep space network: An instrument for radio astronomy research [NASA-CR-182744] N89-11661
UNSTEADY FLOW
Unsteady hydromagnetic free-convection flow with radiative heat transfer in a rotating fluid. 1: Incompressible optically thin fluid [DE88-702998] N89-11140
Unsteady hydromagnetic free-convection flow with radiative heat transfer in a rotating fluid of arbitrary optical thickness [DE88-703000] N89-11167
Unsteady hydromagnetic free-convection flow with radiative heat transfer in a rotating fluid. 2: Compressible optically thin fluid [DE88-702999] N89-11168
Bursting phenomenon in a flat plate pulsed boundary layer [CERT-RSF-OA-69/2259-AYD] N89-11183
On hydromagnetic channel flow induced by tooth pulses [DE88-703031] N89-11522
UPLINKING
ACTS and OLYMPUS propagation experiments N89-11091
URANIUM ALLOYS
Electrical resistivity of U(sub 1-x)M(sub x)Be13 under pressure [DE88-014449] N89-11552
URANIUM COMPOUNDS
Low temperature measurements on UBe13 [DE88-014446] N89-11594
URANIUM 235
Postanalysis of the CNPS (Compact Nuclear Power Source) critical experiment [DE88-014322] N89-11506
Critical experiments in support of the CNPS (Compace Nuclear Power Source) program [DE88-014326] N89-11507
URANUS (PLANET)
Wave-particle interactions in the magnetosphere of Uranus [NASA-CR-183299] N89-11678
USER MANUALS (COMPUTER PROGRAMS)
Poker (4.0): A programmer's reference guide [AD-A196417] N89-11430
Poker (4.1): A programmer's reference guide [AD-A196419] N89-11431
REFEREE: Bibliographic database manager, documentation [PB88-200787] N89-11620
Computer science and technology: Guide to distributed database management [PB88-201561] N89-11621
USER REQUIREMENTS
The NAVSTAR GPS System [AGARD-LS-161] N89-10874
The GPS overview and navigation system concept N89-10875
The Global Positioning System (GPS) accuracy, system error budget, space and control segment overview N89-10877
User equipment overview N89-10879
Civil and military applications of GPS N89-10882
UTILIZATION
Analysis of free electron laser performance utilizing the National Bureau of Standards' CW microtron [AD-A196928] N89-11221

V

VACUUM
The thermal resistance of fine powders at atmospheric pressure and under vacuum
[DE88-014556] N89-10982
VACUUM DEPOSITION
Deposition and characterization of ZnS/Si heterojunctions produced by vacuum evaporation
[NASA-TM-101359] N89-11129
VAN DER WAAL FORCES
The pair potential approach for interfaces: Fundamental problems and practical solutions
[DE88-009165] N89-11456
VAPOR DEPOSITION
Baseline configuration data set: NASA Standard Initiator-2 (NSI-2)
[NASA-CR-172071] N89-11050
Amorphous silicon photovoltaic devices prepared by chemical and photochemical vapor deposition of higher order silanes
[DE88-001189] N89-11311
The effect of vapor incidence angle upon thin film columnar growth
[DE88-014396] N89-11577
VAPOR PHASES
Experiments on liquid-vapour phase change between plane liquid surfaces. Part 1: Experiments with water, freon and mercury
[TM-FM-8804-PT-1] N89-10964
VAPORIZING
Methodologies for prediction of metal oxidation-vaporization-erosion
[DE88-013623] N89-11001
VAPORS
Experimental and analytical study of vapor explosions in stratified geometries
[DE88-011964] N89-11046
Evaluation of vapor compression cycles using nonazeotropic refrigerant mixtures
[DE88-013225] N89-11169
Laser plume temperature measurements in various gases
[DE88-006462] N89-11204
VARIABILITY
The development of prototype absorbers with variable characteristics
[BBC-RD-1988/5] N89-11492
VARIATIONS
The turbulent heat flux in low Mach number flows with large density variations N89-11162
Collective resonance fluorescence in an intense laser field with phase and amplitude fluctuations
[DE88-702920] N89-11205
Basic rules of saturated gain variation in a flowing laser cavity
[AD-A196861] N89-11220
On equivariant Lagrangians
[DE88-703167] N89-11468
A numerical study of ENO and TVD schemes for shock capturing
[NASA-TM-101355] N89-11469
Magnetic fluctuations and heavy electron superconductivity
[DE88-011978] N89-11557
VATOL AIRCRAFT
The 1987 Ground Vortex Workshop
[NASA-CP-10008] N89-10849
VECTOR ANALYSIS
Vectorization of FORTRAN programs at do-loop level N89-11398
Restructuring of basic linear algebraic algorithms, chapter 5 N89-11399
Computatinal fluid dynamics and supercomputers, chapter 6 N89-11400
VECTOR SPACES
The vector functions of the MS system 570/CX
[CNES-CT/DTI/MS/MN/019] N89-11423
Vectorization techniques on the MD system 570/CX
[CNES-CT/DTI/MS/MN/147] N89-11425
VEGETATION
Technique for measuring the dielectric constant of thin materials
[NASA-CR-183325] N89-10984
VELOCITY
The Global Positioning System (GPS) constellation and coverage N89-10876
Experimental and theoretical studies of vertical annular liquid jets
[DE88-012971] N89-11149
Laboratory examination and seasonal analyses of the dynamic losses for a continuously variable speed heat pump
[DE88-013207] N89-11174
A comparative planetological study of particle speed and concentration during aeolian saltation N89-11677
VELOCITY DISTRIBUTION
Tropical 200 mb divergent circulations and their relation to outgoing longwave radiation
[AD-A196375] N89-11370
VELOCITY MEASUREMENT
Three component laser anemometer measurements in an annular cascade of core turbine vanes with contoured end wall
[NASA-TP-2846] N89-10844
Velocity analysis by iterative profile migration N89-11339
VERTICAL TAKEOFF AIRCRAFT
The 1987 Ground Vortex Workshop
[NASA-CP-10008] N89-10849
Numerical investigation of a jet in ground effect using the fortified Navier-Stokes scheme N89-10857
VERY LARGE SCALE INTEGRATION
A coherent VLSI design environment
[AD-A196428] N89-11130
ENGEN: An intermediate language to HILO extension of the FIRST silicon compiler, executive summary
[ESA-CR(P)-2621] N89-11422
VERY LONG BASE INTERFEROMETRY
Very Long Baseline Interferometry (VLBI) from ground and space N89-11645
VIBRATION
Transactions of machine elements division: On the combined hydrodynamic and hydrostatic journal bearing
[PB88-214549] N89-11231
The Shock and Vibration Digest, Volume 20, No. 10 N89-11252
The Shock and Vibration Digest, Volume 20, No. 8 N89-11258
Vibrations and stability of mechanical systems: 4 N89-11260
The Shock and Vibration Digest, volume 20, no. 9 N89-11266
Current research on the vibration and stability of axially-moving materials N89-11283
VIBRATION DAMPING
Free damped vibration of composite plates and shells N89-11249
The Shock and Vibration Digest, Volume 20, No. 7 N89-11277
The Shock and Vibration Digest, volume 20, no. 5 N89-11282
VIBRATION MEASUREMENT
Dynamic analysis of pipings by modal synthesis
[DE88-701620] N89-11274
VIBRATION TESTS
JPRS report: Science and technology: Japan
[JPRS-JST-87-018] N89-11061
New trial of vibration testing method N89-11068
VIDEO DATA
Quantitative Luminescence Imaging System description and user's manual
[DE88-015604] N89-11512
VISCOELASTICITY
On 1-D closure models for slender 3-D viscoelastic free jets: von Karman flow geometry and elliptical cross section
[DE88-014478] N89-11179
The mini-oscillator technique: A finite element method for the modeling of linear viscoelastic structures
[UTIAS-323] N89-11250
VISCOMETERS
A general analysis for obtaining the viscosity function from viscometric measurements: A case study for the helical screw rheometer
[DE88-006271] N89-11139
VISCOMETRY
Microrheological observations of the onset of non-Newtonian behavior in suspensions
[DE88-006198] N89-10962
VISCOSITY
Microrheological observations of the onset of non-Newtonian behavior in suspensions
[DE88-006198] N89-10962
The coefficient of first viscosity via three-phonon processes in bulk liquid helium
[AD-A196902] N89-10986
Cascade flow analysis by Navier-Stokes equation N89-11065
A general analysis for obtaining the viscosity function from viscometric measurements: A case study for the helical screw rheometer
[DE88-006271] N89-11139
Transactions of machine elements division: On the combined hydrodynamic and hydrostatic journal bearing
[PB88-214549] N89-11231
VISCOUS FLOW
A diagonally inverted LU implicit multigrid scheme for the 3-D Navier-Stokes equations and a two equation model of turbulence
[NASA-CR-182209] N89-10863
Hydrodynamical characteristics of helium two-phase flows at relatively high mass rates
[DE88-702936] N89-11143
VISIBLE SPECTRUM
Design and fabrication by molecular beam epitaxy of visible light emitting ridge waveguide GaAs-AlGaAs quantum well lasers
[LAAS-88-097] N89-11215
VISION
Functional assessment of laser irradiation
[AD-A196930] N89-11222
VISUAL DISCRIMINATION
Accessibility, a criterion for the choice of visual coding rules
[PB88-209911] N89-11458
VISUAL OBSERVATION
Optical scattering and microphysical properties of subvisual cirrus clouds, and climatic implications
[NASA-CR-183301] N89-11362
VOICE CONTROL
Manual, voice, and automated control of a teleoperator viewing system
[DE88-011835] N89-11235
VOLTAGE CONVERTERS (DC TO DC)
Electric vehicle auxiliary power source evaluation
[DE88-015359] N89-11238
VOLTAGE REGULATORS
Electric vehicle auxiliary power source evaluation
[DE88-015359] N89-11238
VORTEX GENERATORS
Investigation of wake vortices of landing aircraft at Frankfurt airport (Federal Republic of Germany)
[DFVLR-MITT-88-15] N89-10862
VORTEX SHEDDING
A computational study of coherent structures in the wakes of two-dimensional bluff bodies
[AD-A196820] N89-11188
VORTEX SHEETS
Numerical estimates of the rate of convergence for the vortex sheet method
[DE88-013809] N89-11178
VORTICES
The 1987 Ground Vortex Workshop
[NASA-CP-10008] N89-10849
The characteristics of the ground vortex and its effect on the aerodynamics of the STOL configuration N89-10850
Summary of an experimental investigation on the ground vortex N89-10851
Ground vortex flow field investigation N89-10852
An assessment of ground effects determined by static and dynamic testing techniques N89-10854
Effects of a ground vortex on the aerodynamics of an airfoil N89-10855
Numerical investigation of a jet in ground effect using the fortified Navier-Stokes scheme N89-10857
A nonlinear wave-wave interaction theory for the generation of multi-scale large eddies in a neutral atmospheric boundary layer N89-11344
Vortex lattices in theory and practice
[DE88-014393] N89-11576
VOYAGER 2 SPACECRAFT
Wave-particle interactions in the magnetosphere of Uranus
[NASA-CR-183299] N89-11678

W

WAFERS
Curved channel MCP improvement program
[NASA-CR-180790] N89-11191
WAKES
A computational study of coherent structures in the wakes of two-dimensional bluff bodies
[AD-A196820] N89-11188
WALL JETS
An experimental study of a laminar wall-jet in the presence of a uniform external flow
[UTIAS-268] N89-11152
WALL PRESSURE
Tests on 3 NACA 0012 airfoil models of DFVLR in the NAL 0.3 tunnel: An assessment of 2-D wall interference
[TM-AE-8705] N89-10847
WALL TEMPERATURE
The impact of separated flow on heat and mass transfer
[DE88-014653] N89-11180

WALLS
High heat flux testing of CIT (Compact Ignition Tokamak) first wall tiles
[DE88-012241] N89-11530
WARFARE
Allocating and launching MaRV interceptors based on miss distance predictions
[DE88-015370] N89-11486
WARNING SYSTEMS
In-service evaluation of the Traffic Alert and Collision Avoidance System (TCAS) industry prototype
[DOT/FAA/SA-88/2] N89-10885
Evaluation of enhancements to the Low Level Wind Shear Alert System (LLWAS) at Stapleton International Airport
[DOT/FAA/PS-88/14] N89-11356
WATER
Near-critical NaCl-H2O: An equation of state and discussion of anomalous properties
[DE88-012029] N89-10969
Organic Rankine-Cycle Power Systems Working Fluids Study: 2-methylpyridine/water
[DE88-012659] N89-11307
Proton decay experiment and neutrinos from supernova (Kamiokande-2) N89-11653
WATER RUNOFF
Snow cover, snowmelt and runoff in the Himalayan River basins
[NASA-CR-182434] N89-11290
WATER TEMPERATURE
Practical applications and limitations of adaptive control N89-11442
WATER TUNNEL TESTS
Numerical description of cavitation on axisymmetric bodies
[DE88-006826] N89-11147
WATER VAPOR
A numerical modeling study of frontogenesis and cold frontal rainbands N89-11358
Synoptic scale sensitivity of TIROS-N moisture channels in the tropics
[AD-A196686] N89-11378
WATERSHEDS
Snow cover, snowmelt and runoff in the Himalayan River basins
[NASA-CR-182434] N89-11290
Remote sensing and hydrologic modeling of arid watersheds: A scale analysis
[DE88-014625] N89-11293
WAVE EQUATIONS
A frequency dependent ray theory N89-11610
WAVE INTERACTION
Interaction of electromagnetic waves with heterogeneous bodies of arbitrary shape and parameters N89-11095
A nonlinear wave-wave interaction theory for the generation of multi-scale large eddies in a neutral atmospheric boundary layer N89-11344
Shocked interstellar gas in dense molecular clouds N89-11670
Wave-particle interactions in the magnetosphere of Uranus
[NASA-CR-183299] N89-11678
WAVE PROPAGATION
Proceedings of the Twelfth NASA Propagation Experimenters Meeting (NAPEX 12)
[NASA-CR-182796] N89-11074
PiFEx propagation experiments N89-11075
PiFEx data and archival formats N89-11076
Results of 1987 MSS helicopter propagation experiment at UHF and L band in Central Maryland N89-11077
LMSS propagation modeling at Virginia Tech N89-11078
Preliminary results of MARECS-A measurements in Central Maryland and plans for 1988 MSS experiment in Australia N89-11079
ETS-V propagation experiments in Japan N89-11080
Mobile satellite propagation measurements and modeling: A review of results for systems engineers N89-11081
Propagation handbook, frequencies above 10 GHz N89-11082
Millimeter-wave studies N89-11085
Plan of propagation and communication experiments using ETS-VI N89-11088
OPEX: (Olympus Propagation EXperiment) N89-11090
ACTS and OLYMPUS propagation experiments N89-11091
A digital beacon receiver N89-11092
The Propagation Information Center at the University of Colorado N89-11094
Statistical effects in high-power microwave beam propagation
[DE88-012440] N89-11100
The propagation of electromagnetic waves in thin dielectric slabs
[AD-A196995] N89-11115
Dynamic behavior of helical springs N89-11278
Alfven wave studies on a tokamak N89-11517
Excitation of MHD surface waves propagating with shear Alfven waves in an inhomogeneous cylindrical plasma
[IPPJ-872] N89-11526
Trapping and acceleration of electron by elliptically polarized electromagnetic wave propagating across static magnetic field
[IPPJ-885] N89-11545
WAVE SCATTERING
Mobile satellite propagation measurements and modeling: A review of results for systems engineers N89-11081
WAVEFORMS
On the generation of waveforms having comb-shaped spectra
[AD-A196927] N89-11113
WAVEGUIDE LASERS
Design and fabrication by molecular beam epitaxy of visible light emitting ridge waveguide GaAs-AlGaAs quantum well lasers
[LAAS-88-097] N89-11215
WAVEGUIDES
Dielectric millimeter waveguides. Volume 1
[AD-A196844] N89-11112
WAVELENGTHS
Laser wavemeter/spectrometer operating manual
[NASA-CR-180802] N89-11195
WEAPON SYSTEMS
Numerical simulation of axisymmetric base flow on tactical missiles with propulsive jet
[AD-A196169] N89-11136
WEAR RESISTANCE
Developments and trends in electrodeposition
[DE88-009822] N89-11014
WEATHER
Method for predicting monthly rainfall patterns
[DE88-703005] N89-11363
Mariners weather log, volume 32, number 2, Spring 1988
[PB88-210828] N89-11365
WEATHER FORECASTING
Method for predicting monthly rainfall patterns
[DE88-703005] N89-11363
Tropical cyclone observation and forecasting with and without aircraft reconnaissance
[AD-A196379] N89-11371
WEATHER STATIONS
Evaluation of enhancements to the Low Level Wind Shear Alert System (LLWAS) at Stapleton International Airport
[DOT/FAA/PS-88/14] N89-11356
WEDGES
Vacuum Fizeau wedge wavemeter for pulsed UV lasers
[DE88-015832] N89-11206
WEIGHTING FUNCTIONS
Particle sizing by weighted measurements of scattered light
[NASA-TM-100968] N89-11198
WEIGHTLESSNESS
GAS-611 firefly in zero gravity N89-10912
WELDABILITY
Weldability of 2090 Al-Cu-Li alloy
[DE88-011963] N89-11015
Joining of advanced aluminides
[DE88-015111] N89-11226
WELDED JOINTS
Weldability of 2090 Al-Cu-Li alloy
[DE88-011963] N89-11015
Joining of advanced aluminides
[DE88-015111] N89-11226
Fatigue of welded joint in a stainless steel AISI 304 L
[DE88-701622] N89-11279
WELDING
JPRS Report: Science and Technology. USSR: Materials Science
[JPRS-UMS-88-007] N89-11002
WEST GERMANY
Activity report of the Max-Planck-Institut fuer Physik und Astrophysik
[MPE-200] N89-11688
WIDEBAND COMMUNICATION
On the generation of waveforms having comb-shaped spectra
[AD-A196927] N89-11113
WIGGLER MAGNETS
Overview of FEL (Free-Electron Laser) development with induction linacs at LLNL
[DE88-014179] N89-11210
WIND EFFECTS
The Shock and Vibration Digest, Volume 20, No. 7 N89-11277
WIND MEASUREMENT
The PNL single-tower measurement model of rotationally sampled turbulent wind, with user's guide for STRS2PC
[DE88-013166] N89-11360
A study of the dynamics of maritime fronts using remotely sensed wind and stress measurements N89-11366
WIND PROFILES
A study of wind profiles under quasi-neutral and inversion atmospheric conditions, over a terra firma forest
[INPE-4694-RPE/575] N89-11369
Estimating evapotranspiration of an irrigated surface from upwind and downwind vertical profiles of temperature and humidity
[AD-A196409] N89-11375
WIND SHEAR
Evaluation of enhancements to the Low Level Wind Shear Alert System (LLWAS) at Stapleton International Airport
[DOT/FAA/PS-88/14] N89-11356
Structure of wind-shear turbulence
[NASA-CR-183257] N89-11359
An examination of a simulated microburst flow as sensed by a single Doppler radar
[AD-A196381] N89-11372
WIND TUNNEL TESTS
Aerodynamic design considerations for a free-flying ducted propeller
[DE88-006867] N89-10841
Experimental results for the Eppler 387 airfoil at low Reynolds numbers in the Langley low-turbulence pressure tunnel
[NASA-TM-4062] N89-10842
Full scale wind tunnel tests on a Ford Escort Mk 3
[TT-8802] N89-10846
Tests on 3 NACA 0012 airfoil models of DFVLR in the NAL 0.3 tunnel: An assessment of 2-D wall interference
[TM-AE-8705] N89-10847
Summary of an experimental investigation on the ground vortex N89-10851
F-15 SMTD low speed jet effects wind tunnel test results N89-10853
Experimental investigation of flow near a corner, part 2
[CERT-RT-OA-24/5025-AYD] N89-10861
Three dimensional shear flow. Analysis of the flow in a delta arrow wing with incidence angle
[CERT-RTS-OA-25/5025-AYD] N89-10864
Unsteady low-speed windtunnel test of a straked delta wing, oscillating in pitch. Part 1: General description and discussion of results
[AD-A196456] N89-10867
Investigation of the tumbling phenomenon using computer simulation N89-10896
Review of aeronautical wind tunnel facilities
[NASA-CR-183057] N89-10897
CAD wind tunnel test for half-cut model of Asuka N89-11069
Electrical noise reduction techniques contributing to improved data quality at the National Transonic Facility
[NASA-CR-4193] N89-11196
WIND TUNNELS
Review of aeronautical wind tunnel facilities
[NASA-CR-183057] N89-10897
WIND TURBINES
Rotor instrumentation circuits for the Sandia 34-meter vertical axis wind turbine
[DE88-014704] N89-11304
A model for the response of vertical axis wind turbines to turbulent flow: Parts 1 and 2
[DE88-014708] N89-11305
Development, construction, and operation of a 30/100-kW Wind Energy Converter (WEC)
[DFVLR-MITT-88-06] N89-11318
The PNL single-tower measurement model of rotationally sampled turbulent wind, with user's guide for STRS2PC
[DE88-013166] N89-11360
WIND VELOCITY
Unsteady low-speed windtunnel test of a straked delta wing, oscillating in pitch. Part 1: General description and discussion of results
[AD-A196456] N89-10867
Studies of barotropic flow over topography using a galerkin finite element model
[AD-A196516] N89-11353
WINDPOWER UTILIZATION
Development, construction, and operation of a 30/100-kW Wind Energy Converter (WEC)
[DFVLR-MITT-88-06] N89-11318
WINDPOWERED GENERATORS
Development, construction, and operation of a 30/100-kW Wind Energy Converter (WEC)
[DFVLR-MITT-88-06] N89-11318

WOLF-RAYET STARS
O stars and Wolf-Rayet stars
[NASA-SP-497] N89-11657
WORK FUNCTIONS
Development of the work function monitoring method for a converter of a negative ion source
[IPPJ-880] N89-11529
WORKING FLUIDS
Further investigations on new fluid working systems for absorption heat pumps
[DE88-012622] N89-11151
Organic Rankine-Cycle Power Systems Working Fluids Study: 2-methylpyridine/water
[DE88-012659] N89-11307

X

X RAY ANALYSIS
Spectrography analysis of stainless steel by the point to point technique
[DE88-702302] N89-10992
X RAY ASTRONOMY
An oxide passivated and ion-implanted Si detector for X-ray astronomy
[ISAS-RN-353] N89-11663
An all sky study of fast X-ray transients
[NASA-TM-89716] N89-11686
X RAY IMAGERY
Observations of breakup processes of liquid jets using real-time X-ray radiography N89-11160
X RAY SCATTERING
X-ray scattering studies of non-equilibrium ordering processes
[DE88-012908] N89-11569
X RAY SOURCES
Low mass X-ray binaries in globular clusters and hierarchical triple systems N89-11660
Three probable stellar mass black holes
[AD-A196976] N89-11676
An all sky study of fast X-ray transients
[NASA-TM-89716] N89-11686
X RAY SPECTRA
A differential absorption spectrometer for determining flash X-ray spectra from 10 to 2000 keV
[DE88-014844] N89-10979
X RAY STARS
Low mass X-ray binaries in globular clusters and hierarchical triple systems N89-11660
X RAYS
Survivability of coatings: Program review
[DE88-009863] N89-11031
Fundamental science in ESA's space science program N89-11654
X-29 AIRCRAFT
Investigation of the tumbling phenomenon using computer simulation N89-10896

Y

YAG LASERS
Optimization of microwave magnetoelastic delay lines
[AD-A196866] N89-11131
YIELD POINT
Influence of specimen dimension on damage and breaking of composite materials
[REPT-49-062/F] N89-10957
YTTRIUM OXIDES
ion implantation and thermal annealing of high-T(ssub c) single crystals of YBa2Cu3O(sub x)
[DE88-012201] N89-11564
Superconductivity, structures, ESR and SIMS-analysis of a high-T(sub c)Y(sub 0.33)Ba(sub 0.67)Cu(sub 2.33)O(sub 3.67-sigma) compound
[DE88-702677] N89-11583
Chemical preparation of powders and films for high temperature superconductors
[DE88-015266] N89-11601

Z

ZERO POWER REACTORS
Analysis of SP-100 critical experiments
[DE88-014429] N89-11508
ZINC SELENIDES
Effect of surface states on the electrochemical behaviour of single crystal n-ZnSe photoelectrode
[DE88-702726] N89-11566
ZINC SULFIDES
Deposition and characterization of ZnS/Si heterojunctions produced by vacuum evaporation
[NASA-TM-101359] N89-11129
ZINCBLENDE
Spin-orbit interaction effects in zincblende semiconductors: Ab initio pseudopotential calculations
[DE88-014663] N89-11599
ZIRCONIUM
Crystallization of Zr-Ni metallic glasses
[DE88-007481] N89-11026
ZIRCONIUM COMPOUNDS
Development of transparent zirconia ceramics discussed N89-11062

Typical Personal Author Index Listing

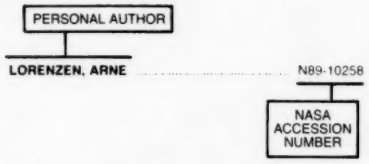

Listings in this index are arranged alphabetically by personal author. The NASA accession number denotes the number by which the citation is identified.

A

ABE, Y. N89-11544
ABEL, KEITH H. N89-11665
ABRATE, S. N89-11253
ACKERMANN, ROBERT A. N89-11303
ADAMS, BRENT L. N89-11571
ADAMS, P. N89-10935
ADAMS, R. J. N89-10869
ADANUVOR, P. K. N89-11308
ADENIJI-FASHOLA, A. A. N89-11157
ADJEPONG, S. K. N89-11140
N89-11167
N89-11168
ADOLF, DOUGLAS B. N89-10983
ADRION, JANEEN N89-10870
AGNESE, J. C. N89-10839
AJIMINE, AKIO N89-10907
AKISHIN, P. G. N89-11490
AL-MOTHAFAR, M. R. D. N89-11120
AL-YAHYA, KAMAL MANSOUR N89-11339
ALAMO, R. G. N89-11045
ALEKSANYAN, Z. A. N89-11386
ALEXANDER, HAROLD LUCHSINGER N89-11391
ALEXANDER, J. IWAN D. N89-10922
ALLEN, J. W. N89-11307
ALLEN, KENNETH C. N89-11085
ALLGOOD, G. O. N89-10901
ALLUB, R. N89-11558
ALTON, LARRY R. N89-10872
ALVAREZ, P. N89-11009
ALVAREZ, R. A. N89-11100
AMAGISHI, Y. N89-11526
AMBROSIO, ANA MARIA N89-11438
AMORIM, M. C. A. N89-11419
ANANDA, MOHAN N89-10875
N89-10876
N89-10877
ANDERSEN, PAUL K. N89-10918
ANDERSON, R. N89-11046
ANDO, R. N89-11547
ANDRE, S. V. N89-11508
ANTONIADIS, ANESTIS N89-11479
APOSTOLAKIS, JOHN N89-11420
APPLEBY, A. J. N89-11308
ARKHIPOV, A. V. N89-11392
ARMSTRONG, D. N89-11046
ARMSTRONG, D. R. N89-11175
ARNAL, D. N89-11187
ARNETT, W. DAVID N89-11673
ARONSON, M. C. N89-11552
ARONSON, SAMUEL N89-11612
ASHCROFT, N. W. N89-11456
ASHLEY, P. R. N89-11554
ATHAVALE, M. M. N89-11163
ATKINSON, DAVID J. N89-11441
AUBERT, J. N89-11036
AUDAS, J. H. N89-11507
AUGUSTO, O. B. N89-11274
AUSSERER, MICHAEL F. N89-11288
AUSTIN, N. M. N89-11257
AXE, J. D. N89-11598
AZEVEDO, S. G. N89-11245

B

BADEN, S. B. N89-11411
BADI, DEBORAH N89-11407
BAER, D. R. N89-11019
BAER, FERDINAND N89-11330
BAETZNER, R. N89-11538
N89-11539
BAILLIE, CLIVE N89-11420
BAILYN, CHARLES DAVID N89-11660
BAKER, KENNETH R. N89-11091
BAKKER, H. N89-11575
BALAJI, VENKATRAMANI N89-11341
BALDING, NIGEL WILLIAM N89-11224
BANDY, KATHLYN A. N89-11280
BANKS, P. N89-10997
BANKUTI, J. N89-11583
BANSAL, NAROTTAM P. N89-11038
BARAB, JOHN D. N89-11356
BARKER, LARRY N89-10943
BARONCINI, DOMINIQUE N89-10955
BARTHELEMY, BRUNO N89-10848
BARTS, R. M. N89-11081
BARTS, R. MICHAEL N89-11078
BASTIEN, R. N89-11257
BATES, J. L. N89-11310
BATISHKO, C. R. N89-11512
BEALE, W. T. N89-11232
BEAULIEU, ROLAND N89-11129
BECHTEL, S. E. N89-11179
BECKER, P. R. N89-11380
BEERMAN, HENRY N89-11057
BELL, A. R. N89-11463
BELL, J. N89-11141
BELL, JOHN B. N89-11166
BELLINA, J. N89-10911
BELO, E. M. N89-10889
BENATTI, A. R. N89-11419
BENNETHUM, W. H. N89-11192
BENNETT, DAVID P. N89-11613
BENTLEY, J. N89-11584
BERDAHL, P. N89-11556
BERGES, J. C. N89-11423
N89-11424
N89-11425
BERNER, JEFF B. N89-11075
N89-11076
BERSTEIN, L. S. N89-10942
BESIO, G. J. N89-11636
BESTMAN, A. R. N89-11140
N89-11167
N89-11168
N89-11522
BHADRA, R. N89-11016
BICKES, R. W., JR. N89-11551
BICOS, ANDREW SOTARIOS N89-11249
BIEN, F. N89-10942
BILLET, MICHAEL L. N89-10851
BIRGENEAU, R. J. N89-11598
BLACK, BRUCE A. N89-11113
BLACKWELL, KEITH G. N89-11378
BLAD, BLAINE L. N89-11368
BLAIS, N. C. N89-11504
BLAKE, J. B. N89-10908
BLAKE, WILLIAM B. N89-10853
BOARDMAN, D. H. N89-11073
BOATNER, L. A. N89-11564
BOCHNAK, J. N89-11453
N89-11462
BOEHNISCH, HELMUT N89-11318
BOENI, P. N89-11598
BOERNER, G. N89-11650
BOLMARO, R. E. N89-11588
BOLSTRIDGE, LOREN D. N89-10885
BOLTE, MICHAEL JOHN N89-11658
BOLTON, P. R. N89-11100
BOMBA, B. N89-11538
BONA, A. N89-10992
BONNET, R. M. N89-11654
BOOZER, ALLEN H. N89-11518
BORGEAUD, M. N89-11106
BORGES, H. A. N89-11552
BORKIN, A. G. N89-11004
BOROWSKI, STANLEY K. N89-10944
BOSCH, H.-S. N89-11541
BOSSAVIT, A. N89-11098
BOSTIAN, C. W. N89-11081
BOSTIAN, CHARLES W. N89-11078
N89-11091
BOTHE, A. N89-11151
BOTTARI, ELIO N89-10879
BOVA, L. N89-11175
BOYD, RICHARD N. N89-11675
BRANDENBERGER, R. H. N89-11666
BRANDON, D. I. N89-11508
BRAUN, A. T. N89-11165
BREADEN, MATT N89-11394
BRENDEL, R. N89-11125
BREZNITZ, SHLOMO N89-11388
BRIGGS, RICHARD J. N89-11210
BRINKMAN, C. R. N89-11034
BRISON, J. P. N89-11594
BRO, PER N89-11300
BROWN, I. G. N89-11495
BROWN, M. N89-11595
BROWN, NANCY N89-10978
BROWN, NORMAN N89-11027
BROWN, S. E. N89-11585
BRUSSAARD, GERT N89-11090
BUCHAL, CH. N89-11554
BUCHELE, DONALD R. N89-11198
BUCKENHAM, N. ROSS N89-10988
BUDESCU, DAVID V. N89-11483
BUETTNER, H. M. N89-11072
BUKIET, B. G. N89-11577
BUKOFZER, D. C. N89-11072
BUNKER, B. C. N89-11601
BURKE, W. R. N89-11638
BURKERT, V. N89-11499
BURNS, JOSEPH M. N89-11109
BUSH, C. N89-10947
BUTKIEWICZ, DAVID A. N89-11280
BUTTERWORTH, J. S. N89-11081

C

CAHEN, D. N89-11302
CAIRNS, E. J. N89-11309
CALEDONIA, G. E. N89-10937
CAMILLONE, N., III N89-11008
CAMPBELL, R. N89-11081
CANNON, B. D. N89-11209
CAPMBELL, LAURENCE J. N89-11576
CAPONE, D. W., II N89-11572
CAPONI, E. A. N89-11114
CAREY, KENNETH F. N89-11379
CARLSON, G. A. N89-10979
CARO, A. N89-11558
CARR, M. J. N89-10990
CARTER, J. G. N89-11117
CASALIS, GREGOIRE N89-11185
CASLAVSKY, JAROSLAV L. N89-11515
CASSANTO, JOHN M. N89-10913
CASSANTO, VALERIE A. N89-10913
CASSIDY, WILLIAM ALFRED N89-11173
CATCHINGS, RUFUS DOUGLAS N89-11349
CAYREL, ROGER N89-11641
CELI, ROBERTO N89-10887
CETINKUNT, SABRI N89-11234
CHAMBERLIN, JAY L. N89-11306
CHANDLEE, R. C. N89-11661
CHANG, DOUGLAS N89-11394
CHANG, LI-CHIIN N89-11236
CHANG, SHIH-HUNG N89-11469
CHAPPLE-SOKOL, J. N89-11316
CHAR, J. M. N89-11160
CHATENOUD, FRANCOISE N89-11215
CHELAFLORES, J. N89-11603
CHEN, C. P. N89-11156
CHEN, E. P. N89-11285
CHEN, F. C. N89-11146
CHEN, G. N89-11232

CHEN, GOUTING N89-11472
CHEN, HARN-CHING N89-11464
CHEN, LIYIN N89-11218
CHEN, STANLEY N89-11394
CHEN, ZI QI N89-11276
CHENETTE, D. L. N89-10935
CHENG, C. C. N89-11029
CHENG, MING-DEAN N89-11367
CHENG, R. K. N89-10960
CHENG, W. N89-10942
CHEONG, S. N89-11585
CHERNIKOV, A. N. N89-11194
CHIGIER, NORMAN N89-11149
CHILAKAMARRI, KIRAN BABU N89-11343
CHILDRESS, CAROLYN N89-10983
CHIOU, JEN-HUANG N89-11281
CHO, D. N89-11046
CHO, D. H. N89-11175
CHOI, U. S. N89-11138
N89-11150
CHOI, YUN-HO N89-11170
CHOU, RU LING N89-11381
CHOW, LUNG-HEN HENRY N89-11493
CHRISTOPHOROU, L. G. N89-11117
CHU, ZEXIANG N89-11218
CHUN, HON WAI N89-11409
CHUNG, J. N. N89-11158
CHURNSIDE, J. H. N89-11087
CIANCETTA, MARK S. N89-11481
CIESLAK, WENDY R. N89-11116
CIESLINSKI, D. N89-11291
CIMBALA, JOHN M. N89-10851
CIURRIA, M. J. C. N89-11419
CLARK, D. E. N89-11226
CLARK, J. N89-10911
CLOUGH, R. L. N89-10948
COHEN, B. N89-11172
COHEN, RAM N89-10938
COLE, R. L. N89-11307
COLE, TERRY N89-11394
COLELLA, P. N89-11141
COLLIER, R. K. N89-11033
COLLINS, LANCE R. N89-11162
COLLINS, P. J. N89-11508
COMBESCURE, A. N89-11257
COMON, HUBERT N89-11471
CONNELL, J. R. N89-11360
CONNORS, ALANNA N89-11686
CONNORS, DANIEL PATRICK N89-11484
CONTI, PETER S. N89-11657
CONTI, R. J. N89-11136
COOK, JERRY D. N89-11128
COPELAND, EDMUND N89-11604
CORBETT, MICHAEL B. N89-11191
CORJON, A. N89-11183
CORONITI, F. V. N89-11678
CORYNEN, G. C. N89-11486
COTNOIR, LEO J. N89-11195
COTTRILL, CHARLOTTE ALICE N89-11618
COWAN, C. L. N89-11508
COWLEY, J. M. N89-11028
COX, ROBERT M. N89-11373
CRANE, ROBERT K. N89-11084
CRAVEN, J. D. N89-11342
N89-11350
CRAWFORD, D. R. N89-11114
CREMERS, DAVID A. N89-11204
CREWS, JOHN H., JR. N89-10945
CRIEL, T. M. N89-10898
CROCKER, ALAN R. N89-10918
CROCKER, DEBORAH ANN N89-11662
CROESSMANN, C. D. N89-11530
CROSS, J. B. N89-11504
CROSS, JON B. N89-10932
CROWE, C. T. N89-11156
CULLINGFORD, HATICE S. N89-11060
CUNNINGHAM, A. M., JR. N89-10867
CURTISS, H. C., JR. N89-10895

D

DABROWSKI, ANDRZEJ J. N89-11574
DALGARNO, A. N89-11671
DALLOGLIO, G. N89-11646
DATSKOS, P. G. N89-11117
DAUKAS, J. C. N89-11524
DAVARIAN, FARAMAZ N89-11074
DAVE, B. N89-11308
DAVEY, K. N89-11098
DAVIS, M. J. N89-10970
DAVISON, STEPHEN JOHN N89-11333
DE, SASADHAR N89-11254
N89-11266
DEANGELIS, R. M. N89-11365
DEBERNARDIS, P. N89-11646
DEBROY, T. N89-11230
DECASTRO, P. M. S. T. N89-11272
DECKER, RAND N89-11153
N89-11154
DEGOUT, D. N89-11533
DEHAAN, M. S. N89-11452
DEHOFF, R. T. N89-11602
DELAHOY, A. E. N89-11311
DELAYEN, J. R. N89-11579
DELBOSCO, E. N89-11121
DELFRATE, JOHN H. N89-10852
DELOACH, STEPHEN R. N89-10886
DELUCA, RUSSELL J. N89-11021
DELUCIA, R. A. N89-10892
DELUCIA, ROBERT A. N89-10893
DEMAGGIO, G. B. N89-11524
DEMELO, F. J. M. Q. N89-11272
DEMEURE, CEDRIC J. N89-11432
DEMIRANDA, P. E. V. N89-11279
DEMIRGIAN, J. C. N89-11307
DEMORISSONVALERIANO, DALTON N89-11324
DEMPSEY, J. F. N89-11530
DENARO, ROBERT P. N89-10880
N89-10883
N89-10884
DENBOER, R. G. N89-10867
DENYER, P. B. N89-11422
DEOLIVEIRA, CARLOS ALBERTO N89-11634
DEPAULASILVAFILHO, VICENTE N89-11369
DESAINT-VICTOR, X. N89-10859
DESHPANDE, M. D. N89-10964
N89-10973
DEVALK, V. N89-11477
DEVORE, LAURI JEAN N89-11030
DEY, B. N89-11290
DIAK, GEORGE R. N89-11361
DIDWALL, E. M. N89-11072
DING, HONG-QIANG N89-11420
DINI, J. W. N89-11014
DIXON, RAY D. N89-11204
DOBBYN, R. C. N89-11595
DODD, GREGORY C. N89-11362
DOEPKENS, J. N89-10906
DOGGER, C. S. N89-10867
DOHERTY, R. D. N89-10995
DOKE, T. N89-11335
DOMINGUE, R. P. N89-10942
DONG, JIN-MING N89-11561
DONG, L. K. N89-11269
DONNELLY, I. J. N89-11526
DOROSHKO, A. I. N89-11227
DOSSER, LARRY R. N89-11212
DOSTAL, M. N89-11257
DOUGHTY, D. H. N89-11601
DRAKE, J. B. N89-10933
DRAPER, J. V. N89-11235
DROBYAZKO, S. V. N89-11004
DUANNE, J. F. N89-11263
DUARTE, VALDETE N89-11294
DUC, DUONG MINH N89-11467
DUCHOVIC, R. J. N89-10970
DUNN, S. N89-11024
DYER, JACK E. N89-10936

E

EASTON, D. S. N89-11026
EATOUGH, M. O. N89-11601
EBERHAGEN, A. N89-11538
ECEVITOGLU, BERKAN GALIP N89-11334
EDESKUTY, F. J. N89-11070
EISLER, G. RICHARD N89-10840
EL-DESSOUKI, M. S. N89-11566
EL-QALLALI, ABDULSALAM N89-11466
ELDINAHMED, AHMED SHARAF N89-11415
ELLIS, D. E. N89-11591
ELPHIC, R. C. N89-11342
ELPHINSTONE, R. D. N89-11342
EMBURY, J. D. N89-10995
EMERIC, DARIO A. N89-11022
EMERSON, RICHARD F. N89-11075
EMSON, C. R. I. N89-11098
ENAYETULLAH, M. A. N89-11308
EPPERLEIN, E. M. N89-11463
EPPINGER, STEVEN D. N89-11229
ERDEMIR, A. N89-11029
ESHLEMAN, JAMES E. N89-10852
EVANS, GRAHAM CECIL N89-11680
EVDOKIMOV, V. A. N89-11194

F

FAHRBACH, H.-U. N89-11538
N89-11543
FALLS, MICHAEL J. N89-11086
FARGES, G. N89-11533
FARMER, F. G. N89-11238
FARRELL, ROBERT J., JR. N89-11377
FAUCHER, B. N89-11048
FAUVET, MARIE-CHRISTINE N89-11428
FEARS, SCOTT POWELL N89-10896
FEIGELSON, ROBERT S. N89-11055
FEIK, R. A. N89-10866
FELDMAN, BRUCE F. N89-11131
FELDMAN, S. N89-11172
FERGUSON, F. T. N89-11056
FERLAND, GARY J. N89-11675
FERNANDES, D. T. N89-11419
FERNANDEZ, H. A. N89-11009
FILIPPOV, YU. P. N89-11143
FINDLAY, JOHN T. N89-11407
FISCHBACH, EPHRAIM N89-11612
FISHER, EH. N89-11562
FISK, Z. N89-11552
N89-11585
N89-11594
FITCH, J. P. N89-11245
FLANERY, R. E. N89-10933
FLEISCHAUER, PAUL D. N89-11606
FLETCHER, R. W. N89-11041
FLOCK, WARREN L. N89-11094
FLOUQUET, J. N89-11594
FLOWER, JON N89-11420
FLYNN, C. P. N89-11586
FOMINSKIY, V. YU. N89-11006
FONG, E. N. N89-11621
FONTANELLA, JOHN J. N89-11039
FOREMAN, TERRY LEE N89-11610
FOREST, M. G. N89-11179
FORMAGGIO, ANTONIO ROBERTO N89-11297
FORSLUND, DAVID W. N89-11532
FORSYTH, BARBARA N89-11483
FORTSON, N. N89-11211
FOSTER, JOHN D. N89-10856
FOX, GEOFFREY N89-11394
FRANK, JONATHAN N89-11057
FRANK, L. A. N89-11342
N89-11350
FRIEDRICH, CRAIG N89-10920
FRISH, MICHAEL N89-11057
FRITTS, S. D. N89-11317
FROMM, V. A. N89-11004
FROST, R. T. N89-11636
FRY, DALE W. N89-11676
FRYDRYCH, D. J. N89-11019
FU, BING-CHEN N89-10903
FUJITA, J. N89-11547
FUJITA, S. N89-10904
FUKUYAMA, A. N89-11544
FUNABIKI, K. N89-10888
FUSSMANN, G. N89-11535
FUTAMASE, TOSHIFUMI N89-11614

G

GABBE, D. R. N89-11598
GABELLA, W. E. N89-11460
GALPIN, J. S. N89-11478
GALVIN, A. B. N89-11342
GAMBARANI, GARY P. N89-10885
GANDY, R. F. N89-10947
GARCIA, DOMINGO N89-11133
GARRETT, L. BERNARD N89-11407
GARTLING, D. K. N89-11416
GARVIS, D. N89-10942
GAVIN, JOYCE E. N89-11323
GEBO, NORMAN N89-11083
GEERAETS, WALTER J. N89-11217
GEHRE, O. N89-11538
GEIER, BODO N89-10956
GEIER, G. JEFFREY N89-10880
GENTZSCH, W. N89-11398
N89-11399
N89-11400
GENTZSCH, WOLFGANG N89-11395
GEOFFROY, P. N89-11286
GEORGE, E. P. N89-11255
GEORGE, T. C. N89-11505
GEORGE, THOMAS F. N89-10986
N89-11607
GESTIDO, G. D. N89-11009
GIESE, R. F. N89-11570
GILETTADESAINTJOSEPH, D. N89-10954
GILLIAN, RONNIE E. N89-11287
GINATI, A. N89-10905
GINLEY, D. S. N89-11601
GIRARD, R. N89-10953
GIVLER, RICHARD C. N89-11155
GLADYSZ, J. A. N89-11007

GLAZ, HARLAND M. N89-11166
GLENDENNING, N. K. N89-11668
GLEYZES, C. N89-11182
N89-11184
GLICK, J. H. N89-11416
GODDAERT, E. N89-11423
N89-11425
GOLDHIRSH, J. N89-11081
GOLDHIRSH, JULIUS N89-11077
N89-11079
N89-11083
GOLDMAN, LOUIS J. N89-10844
GOLDSMITH, THEODORE C. N89-10917
GOLDSTEIN, R. J. N89-11180
GONZALEZ, AVELINO J. N89-11440
GOOCH, CAROLYN K. N89-11387
GOODMAN, D. W. N89-11013
GOPALIENGAR, R. N89-11134
GOPINATH, R. N89-10847
GORDER, PETER JAMES N89-10900
GORDON, R. G. N89-11316
GORIN, A. H. N89-11025
GORODISHENIN, N. L. N89-11194
GOSWAMI, D. C. N89-11290
GOTTLIEB, JACK J. N89-10909
GOTTLIEB, M. N89-10962
GOWER, G. L. N89-11360
GRADY, D. E. N89-11251
GRAHAM, A. L. N89-10962
GRAHAM, R. A. N89-10990
GRAVES, R. S. N89-10982
GRAVESEN, JENS N89-11611
GRAY, A. JAMES N89-11665
GRAY, D. D. N89-11171
GRAY, K. N89-11016
GRAY, N. L. N89-11617
GREEN, B. D. N89-10937
GREENBAUM, E. N89-11383
GREENE, J. M. N89-11451
GREENWOOD, N. N. N89-10985
GREGG, JEFFREY ROBERT N89-11560
GREGOIRE, GERARD N89-11479
GRIFFIN, C. W. N89-11310
GRIFFIN, MICHAEL K. N89-11362
GRIFFITHS, JOSE-MARIE N89-11626
N89-11629
N89-11630
N89-11631
GRIMSDITCH, M. N89-11016
N89-11497
GRONDIN, M. N89-10930
GROSS, FRANZ N89-11498
GROSS, R. J. N89-11147
GUERTS, E. G. N89-10867
GUIMARAES, A. S. N89-11279
GUM, MARY A. N89-10910
GUPTA, SHANTI S. N89-11485
GURNETT, D. A. N89-11678
GUSELLA, EDSON, JR. N89-11126
GUSTAFSON, J. L. N89-11393
GUSTIN, K. N89-11316

H

HAILEY, C. E. N89-11147
HAJIBRAHIM, W. N89-10859
HALD, HERMANN N89-11318
HALFANT, MATTHEW N89-11476
HALL, GENOLA F. N89-11051
HAM, WILLIAM T., JR. N89-11217
HAMADA, S. N89-10999
HAMADA, Y. N89-11547
HAMAGUCHI, SATOSHI N89-11531
HAMIL, R. A. N89-11119
HAMIL, ROY A. N89-11532
HAMMER, D. N89-11211
HAN, KWANG S. N89-11201
HANCOCK, THOMAS M., III N89-10914
HAND, KELLY J. N89-10925
HANERFELD, H. N89-11202
HANSEN, G. E. N89-11507
HANSER, FREDERICK A. N89-10938
HARGIS, PHILIP J., JR. N89-11532
HARRINGTON, M. S. N89-11601
HARRIS, DONOVAN N89-11022
HARTLEY, RICHARD S. N89-11503
HARWIT, MARTIN N89-11655
HASEBE, N. N89-11335
HATAKEYAMA, M. N89-10888
HAUER, ALLAN A. N89-11532
HAUPT, RANDY L. N89-11110
HAWKINS, D. M. N89-11478
HAYASHI, SHIGERU N89-11063
HAYASHI, Y. N89-11581
HAYES, PATRICK M. N89-11374
HAYS, CYNTHIA N89-11368
HAYTER, JOHN B. N89-11511
HEADLEY, T. J. N89-11601
HENDERSON, M. A. N89-10947
HERNDON, J. N. N89-11235
HEROLD, H. N89-11649
HERRMANN, W. N89-11538
N89-11542
HERRMANNSFELDT, W. N89-11202
HESS, RONALD A. N89-10900
HEY, A. N89-11009
HICKOX, C. E. N89-11147
HIDEKUMA, S. N89-11549
HILL, A. D. N89-11238
HILL, R. A. N89-10899
HINMAN, KARL N89-11133
HIRAO, KUNIO N89-11667
HIROKURA, S. N89-11547
HIRSCHFELD, T. B. N89-10949
HISHINUMA, A. N89-10999
HITCHON, W. N. G. N89-11528
HO, ALEX N89-11394
HO, CHIH-MING N89-11177
HO, LORETTA L. G. N89-11075
HOBSON, D. O. N89-10991
HODES, G. N89-11302
HOFMANN, J. V. N89-11535
HOLDER, LAWRENCE B. N89-11448
HOLLAND, JOSHUA N89-11330
HOLM, D. D. N89-11179
HONES, E. W. N89-11342
HONES, E. W., JR. N89-11350
HORSHAM, GARY A. P. N89-11637
HORTON, J. A. N89-11026
HOUDEVILLE, R. N89-11183
HOVESTADT, D. N89-10908
HOYLE, HENRY B. N89-11298
HREN, J. J. N89-11602
HSIEH, K. C. N89-11160
N89-11163
HUBBARD, KENNETH G. N89-11368
HUBELE, J. N89-11537
HUEBNER, K. N89-11537
N89-11538
N89-11539
N89-11540
HUFFLEN, JEAN-MICHEL N89-11429
HUGGINS, JAMES DAVID N89-11233
HUGHES, R. L. N89-10899
HULL, DAVID G. N89-10840
HULSTROM, R. L. N89-11312
HUNT, L. R. N89-11457
HUNTER, ERIC N89-11044
HUNTER, S. R. N89-11117
HURST, P. N89-10997
HUSEYIN, K. N89-11260
HUSZAR, I. N89-11502
HUTH, GERALD C. N89-11574
HUTT, D. N89-11099
HWANG, IN H. N89-11201
HYATT, MARK J. N89-11038

I

IBRAHIM, MAMDOUH H. N89-11619
IDA, K. N89-11547
N89-11549
IDA, N. N89-11098
IIYOSHI, A. N89-11544
INAL, O. T. N89-11017
INGBER, M. S. N89-11147
INGROSSO, L. N89-11537
N89-11540
IPPOLITO, LOUIS J. N89-11082
ISHIGURO, TOMIKO N89-10845
ISHIHARA, KAORU N89-11118
ISHIHARA, S. N89-11581
ISHII, K. N89-11581
ISHII, KOSUKE N89-11225

J

JABBARI, M. Y. N89-11180
JABLONSKI, F. N89-11291
JACCARD, D. N89-11594
JACOBS, SHEILA MAUREEN N89-11616
JACOBS, STEPHEN F. N89-11219
JACOBSEN, J. F. N89-11238
JACOBSMEYER, JAY M. N89-11111
JACOBSON, LOREN A. N89-11012
JAHNKE, R. A. N89-11321
JAMAI, JAMAL N89-11123
JAMESON, ARTHUR R. N89-11102
JANESCHITZ, G. N89-11535
JANIK, G. R. N89-11209
JANISCH, THOMAS V. N89-10915
JAQUES, AL N89-10966
JAU, B. M. N89-11237
JELLISON, J. L. N89-11240
JENKINS, E. G. N89-10846
JENSEN, RICHARD S. N89-10870
JENSSEN, H. P. N89-11598
JERVIS, T. R. N89-11019
JETZER, P. N89-11501
JIN, XUN-SHU N89-10903
JOARDER, R. N. N89-10976
JOHNSON, DALE W. N89-11319
JOHNSON, GARY L. N89-10928
JOHNSON, L. R. N89-11570
JOHNSON, M. R. N89-11238
JOHNSON, MARK K. N89-11271
JOHNSON, RICHARD N89-11265
JOHNSON, V. E. N89-10965
JONCHERE, J. P. N89-11048
JORDAN, STUART N89-11657
JOU, WEN-HUEI N89-11177
JUANG, J.-N. N89-11262
JUILLEN, J. C. N89-11187
JUN, C. W. N89-10986

K

KAFKA, PETER N89-11647
KAHNG, W. H. N89-10986
KAKO, E. N89-11547
KALAFUS, RUDOLPH M. N89-10883
KALLOSH, R. E. N89-11609
KAMEARI, A. N89-11098
KAMEDA, M. N89-10904
KAMIJO, KENJIRO N89-11064
KAMIMIYATA, YOTSUO N89-10907
KAMPWIRTH, R. T. N89-11016
KANE, BRIAN D. N89-10938
KARL, THOMAS R. N89-11323
KARMAN, T. N89-11583
KASTNER, M. A. N89-11598
KASZA, K. E. N89-11137
N89-11150
KATUSHENOK, S. S. N89-11194
KATZENELSON, JACOB N89-11473
KAUL, H. J. N89-10832
KAWAHATA, K. N89-11547
KAWAMURA, T. N89-11527
KAWANAMI, H. N89-11581
KAWANO, SANDY N89-11687
KAWASAKI, Y. N89-10904
KE, SHOU-QUAN N89-10903
KECK, THOMAS S. N89-11203
KEICHER, D. M. N89-11240
KEISNER, KEVIN N89-11133
KELLER, CHARLES L. N89-11474
KELLER, M. DEAN N89-11060
KEMMERER, SHARON J. N89-11412
KEMMERLY, GUY T. N89-10854
KENNEDY, R. N89-10942
KENSCHE, CHRISTOPH N89-11318
KEPLER, R. G. N89-11032
KEYES, DAVID E. N89-11459
KHATIR, ZOUBIR N89-11124
KHOUMSI, AHMED N89-11241
KHUKHAREVA, I. S. N89-11562
KIHM, K. D. N89-11149
KIKUCHI, J. N89-11335
KIM, J. S. N89-11451
KIMURA, T. N89-10904
KINDEL, JOSEPH M. N89-11532
KING, CHUNG-TA N89-11436
KING, DONALD W. N89-11626
N89-11629
N89-11630
N89-11631
KINOSHITA, K. N89-11309
KIOGA, R. N89-10935
KIRBY, D. G. N89-11097
KIRCHHOFF, V. W. J. H. N89-11329
N89-11331
KIRICHENKO, YU. A. N89-10974
KISELEV, YU. F. N89-11194
KISHORE, RAM N89-11559
KITAKOHJI, T. N89-10904
KITAMURA, S. N89-10904
KLEBESADEL, R. W. N89-11685
KLECKER, B. N89-10908
KLEIN, R. N89-11537
N89-11539
KLIMCHUK, JAMES A. N89-11684
KLINGLE, DIANA LYNN N89-11357
KNAPPER, ROBERT J. N89-11468
KNEE, M. J. N89-11101

KNIGHT, DAVID J. N89-11358
KNOKE, G. S. N89-11177
KOCKS, U. F. N89-10995
KOHNO, T. N89-11335
KONDERAK, J. J. N89-11468
KONDO, H. N89-11335
KONG, J. A. N89-11106
KOO, LAT SANG N89-11248
KORNHAUSER, A. A. N89-11313
KOROLOV, VICTOR V. N89-11228
KORTBAWI, DAVID N89-11517
KOSHELEVA, G. A. N89-11004
KOSHIBA, M. N89-11653
KOSHKARIAN, KENT ALLEN N89-11035
KRAFT, R. N89-10998
KRAS, A. N89-11046
KRAUTHAMER, S. N89-10941
KRAVTSOV, V. D. N89-11490
KRAYNIK, ANDREW M. N89-11139
KREIFELS, THEODORE L. N89-11216
KREMPL, ERHARD N89-11273
KRESIN, V. Z. N89-11597
KRESIN, VLADIMIR Z. N89-11592
N89-11600
KROEGER, D. M. N89-11026
KROLL, GLENN N89-11328
KROTHAPALLI, A. N89-10855
KUCHARZ, W. N89-11453
N89-11462
KUHN, RICHARD E. N89-10852
KUIPER, T. B. H. N89-11661
KUKLA, GEORGE J. N89-11323
KULP, T. N89-10942
KUMAI, KAZUMA N89-11118
KUMARI, SANTHA N89-10847
KUMMEROW, CHRISTIAN DETLEF N89-11364
KUNZE, HANS J. N89-10882
KUO, K. K. N89-11160
N89-11163
KURCHATOV, I. V. N89-11004
KURIAT, R. I. N89-11005
KURIYAMA, M. N89-11595
KUROMOTO, N. K. N89-11279
KURTH, W. S. N89-11678
KURTZ, ELLERY N89-10919
KUSHNER, LEN N89-11328
KUSSMANN, ALFRED N89-11318
KVASHA, D. I. N89-11227
KWAK, J. F. N89-11565
N89-11601

L

LAGUNA, G. W. N89-11417
LAITURI, T. R. N89-11359
LAKIS, AOUNI A. N89-11264
LAM, D. J. N89-11591
LAMPPA, D. L. N89-11601
LANAGAN, M. T. N89-11579
LANDIS, GEOFFREY A. N89-11129
LANG, D. N89-10957
LANGNER, A. N89-11607
LANGSTON, J. L. N89-11133
LANOU, R. E. N89-11664
LANSDOWNE, K. F. L. N89-11492
LAOR, U. N89-11595
LAPORTE, F. N89-10924
N89-11426
LAPRADE, BRUCE N. N89-11191
LARBALESTIER, D. C. N89-11568
LARSON, D. N89-11595
LASJAUNIAS, J. C. N89-11594
LASKIN, ROBERT A. N89-10931
LASSITER, EDWARD N89-10875
LAURENT, CRAIG S. N89-11023
LEBOWITZ, MICHAEL N89-11445
LEE, E. L. N89-11049
LEE, IN YOUNG N89-11345
LEE, KIMYEONG N89-11500
LEE, MARK C. N89-10903
LEE, P. N89-11536
LEE, TING W. N89-11244
LEEUWENBERG, E. L. J. N89-11458
LEIDER, H. R. N89-10949
LEIGHTON, D. T., JR. N89-11159
LEISTIKOW, S. N89-10998
LEITENETO, JOAQUIN PAULINO N89-11491
LEMAY, CHARLES A. N89-11376
LEMKE, DIETRICH N89-11643
LEOPOLD, D. N89-10855
LESCANNE, PIERRE N89-11471
LEVY, G. S. N89-11661
LEVY, GAD N89-11366
LEVY, SAMUEL C. N89-11300
LEW, H. S. N89-11271
LEWIN, R. N89-11633
LEWIS, GARY K. N89-11204
LI, MING-FU N89-11599
LIANG, TACHEN N89-11485
LIBBY, PAUL A. N89-11161
LIEBOWITZ, HAROLD N89-11289
LILLELEHT, L. U. N89-11056
LIM, H. H. N89-11106
LIN, F. C. N89-11106
LIN, K. J. N89-11179
LIN, RICHARD Y. N89-10931
LIN, TSAI-KU N89-11563
LINDELL, ISMO V. N89-11104
LINN, CATHY JO N89-11488
LINTZ, H. K. N89-11524
LIOU, MENG-SING N89-11469
LIU, K. V. N89-11138
N89-11150
LIU, Y. Y. N89-11001
LIVINGSTON, ROBERT B. N89-11435
LLOYD, P. E. N89-11347
LOCASCIO, D. M. R. N89-11575
LOEWY, ROBERT G. N89-10946
LOFERSKI, JOSEPH J. N89-11129
LOGAN, K. V. N89-10987
LOLLAR, LOUIS F. N89-11127
LONG, MARIANNA M. N89-11044
LOOMIS, PETER V. W. N89-10884
LORENCE, L. J. N89-10979
LORENZ, E. N89-11502
LOTT, STEPHEN ELDER N89-10989
LOTTS, CHRISTINE G. N89-11287
LOUBRIEL, G. M. N89-11119
LOUGHREY, LORETTA A. N89-11280
LOUIE, STEVEN G. N89-11599
LOUIS, D. N89-10953
LOWENSTEIN, A. N89-11172
LUDWIG, G. O. N89-11121
LUERS, H. N89-10832
LUGOVSKIY, YU. F. N89-11003
LUKKIEN, JOHAN J. N89-11414
LUNG, C. W. N89-11269
LYKKE, KEITH R. N89-11206
LYRINTZIS, CONSTANTINOS SOTIRIOS N89-11270

M

MACCONOCHIE, IAN O. N89-10929
MACRISS, ROBERT A. N89-10972
MADDOCKS, M. C. D. N89-11073
N89-11096
N89-11103
MAEDA, KEI-ICHI N89-11614
MAGERAS, G. N89-11502
MAGGS, A. C. N89-11456
MALASHENKO, I. S. N89-11005
MALCOLM, D. R. N89-11305
MALDARELLI, CHARLES N89-11181
MALYUTENKO, V. N89-11556
MANDELKERN, L. N89-11045
MANDELL, DAVID A. N89-11437
MANN, KENNETH E. N89-10931
MANNING, JAMES ORA N89-11348
MANSER, G. E. N89-11041
N89-11042
MAQUART, JEAN-GABRIEL N89-10955
MARGASON, RICHARD J. N89-10849
MARIANNEAU, G. N89-11125
MARINELLI, W. J. N89-10937
MARINHO, E. V. A. N89-11331
MARIS, H. J. N89-11664
MARKEYEV, A. M. N89-11006
MARSALA, J. N89-11172
MARSHALL, SANDRA P. N89-11447
MARTIN, E. R. N89-11507
MARTIN, JOEL D. N89-11371
MARTIN, RICHARD J. N89-10978
MARTINS, ELIANE N89-11438
MARTYN, JOHN N89-11628
MARUYAMA, XAVIER K. N89-11221
MASI, S. N89-11646
MASON, G. M. N89-10908
MASUDA, Y. N89-11527
MATSUOKA, KIYOHARU N89-11390
MATSUOKA, M. N89-11663
MATTARNETO, M. N89-11274
MATTERN, DUANE LOREN N89-11442
MAUNG, KHIN MAUNG N89-11498
MAYER, H. M. N89-11543
MAYHEW, PAMELA JEAN N89-11622
MAZIASZ, P. J. N89-10999
MAZOR, A. N89-11577
MCCALLUM, J. C. N89-11564
MCCORD, JOHN E. N89-11514
MCCORMICK, LAURIE N89-10918
MCCOY, H. E. N89-11034
MCCURDY, R. N89-11316
MCELROY, D. L. N89-10982
MCGHEE, ROBERT J. N89-10842
MCKAMEY, C. G. N89-11026
MCKENZIE, B. B. N89-11119
MCKINSTRIE, COLIN J. N89-11532
MCLARNON, F. R. N89-11309
MCLEMORE, W. J. N89-10987
MCMILLAN, B. K. N89-10891
MCPHEE, J. R. N89-11196
MCRAE, T. N89-10942
MCTAVISH, DONALD J. N89-11250
MCTIGUE, DAVID F. N89-11155
MEADOWS, A. J. N89-11627
MEIER, GERD E. A. N89-11186
MELCHIORRI, F. N89-11646
MELENDRES, C. A. N89-11008
MENDES, O., JR. N89-11351
MENESES, PAULO ROBERTO N89-11418
MENZEL, W. PAUL N89-11361
MERKLE, CHARLES L. N89-11170
MERRIAM, RICHARD L. N89-11169
MESMER, ROBERT E. N89-10961
METIN, E. N89-11017
MHAR, J. I. N89-11422
MICHAEL, MARK T. N89-10835
MICHL, JOSEF N89-10958
MIELKE, ROLAND R. N89-11406
MIGLIORI, A. N89-11585
MILLARD, BETTY F. N89-10842
MILLER, NORMAN LESLIE N89-11337
MILLER, R. N89-11202
MILLER, WILLIAM A. N89-11174
MISHKIN, A. H. N89-11237
MISYAVICHIOS, A. K. N89-10963
MITCHELL, D. N89-11501
MITCHELL, GLENN A. N89-10865
MIYAJI, WENDELL M. N89-11482
MOHAMMAD, NOOR N89-11465
MOHLER, JONATHAN H. N89-11030
MOHR, P. B. N89-10949
MOISIO, TAPANI N89-11239
MOLENT, L. N89-11024
MOLLY, JENS-PETER N89-11318
MONDY, L. A. N89-10962
MONTES, A. N89-11121
MONTES, ANTONIO N89-11491
MOOK, H. A. N89-11511
MOORE, B. N. N89-11509
MORAWITZ, H. N89-11600
MOREIRA, JOSE CARLOS N89-11427
MOREL, PAUL R. N89-10938
MORGAN, D. REED N89-10837
MORIMOTO, T. N89-11556
MORRIS, J. W., JR. N89-11015
MORRIS, P. J. N89-10843
MORRIS, V. R. N89-11360
MORRISON, IAN N89-11590
MORRISON, JEFFREY S. N89-11332
MORROW, ROBERT K., JR. N89-11108
MOSIER, FRANCES L. N89-10902
MOTE, C. D., JR. N89-11283
MOURAD, PIERRE DOUMITT, III N89-11344
MUCKERHEIDE, M. C. N89-10911
MUELLER, E.-A. N89-11186
MUELLER, HAROLD A. N89-11217
MUENIER, MICHEL N89-10833
MUENNEMANN, FRANCIS GUSTAV N89-11246
MULLER, R. C. N89-10901
MULLINS, M. C. N89-11617
MUNCHI, M. Z. N89-11134
MURAKAMI, H. N89-11335
MURAKAMI, T. N89-11663
MURMANN, H. N89-11538
MURPHREE, J. S. N89-11342
MURPHY, TIM N89-11336
MURRELL, S. R. N89-11524
MUTOH, T. N89-11544
MYLER, HARLEY R. N89-11440

N

NAFTEL, J. CHRIS N89-10929
NAGAI, K. N89-11581
NAGATA, K. N89-11335
NAGLE-ESHLEMAN, JUDITH N89-11252
N89-11258
N89-11261
N89-11266
N89-11277
N89-11282
NAGLER, S. E. N89-11569
NAKAGAWA, TOMOKO N89-11667
NAKAJIMA, H. N89-11546

NAKAMOTO, A. N89-11335
NAKAMURA, Y. N89-11546
NANOPOULOS, D. V. N89-11651
NAOI, KATSUHIKO N89-11135
NARTEN, A. H. N89-11037
NARTEN, M. D. N89-11037
NATESAN, K. N89-11001
NAU, HARTMUT N89-11197
NELEPOVITZ, D. O. N89-10894
NEMOTO, H. N89-10904
NEUFELD, DAVID ANTHONY N89-11670
NEVES, K. N89-11401
NEVES, KEN W. N89-11395
N89-11396
N89-11397
NEVESEPIPHANIO, JOSE CARLOS N89-11297
NEVOLIN, V. N. N89-11006
NGUYEN, QUOC TUY N89-11264
NI, L. M. N89-11436
NICHOLAS, J. N89-10908
NIEUWEJAAR, PER W. N89-10878
N89-10881
NIMIS, JEFFREY A. N89-11054
NJAU, ERNEST C. N89-11320
N89-11363
NJOKU, F. I. N89-11522
NODA, M. N89-10904
NOLTE, R. N89-11536
NORMAN, JOHN M. N89-11368
NORMAN, M. R. N89-11557
NORRIS, CONNIE B. N89-11633
NORWOOD, CHRISTOPHER W. N89-10940
NOVAK, L. M. N89-11106
NOWACZYK, U. N89-11151
NOZAKI, OSAMU N89-11065
NUNZIATO, JACE W. N89-11155

O

OBI, SHINZO N89-10907
OBRIEN, T. K. N89-10951
OEZVEREN, CUENEYT N89-11439
OGAWA, SATORU N89-10845
OGAWA, Y. N89-11547
OGAWA, YUICHI N89-11520
OGUCHI, H. N89-10888
OHMORI, SHINGO N89-11080
N89-11088
OHNISHI, M. N89-11544
OIJALA, JUSSI E. N89-11247
OKAMOTO, M. N89-11544
N89-11546
OKAMOTO, P. N89-11016
OLENSKI, CHRISTOPHER N89-10918
OLSEN, A. R. N89-11325
OLVER, FRANK W. J. N89-11454
OMALLEY, M. W. N89-11119
ONCHI, AKIRA N89-11066
ONO, T. N89-11527
OPPENHEIM, A. K. N89-10981
ORAS, J. J. N89-11137
OROURKE, PETER J. N89-11162
ORRELL, DEAN H., II N89-11107
ORTALANO, DARREN MARK N89-11494
ORTALE, C. N89-11578
N89-11580
ORZECHOWSKI, T. J. N89-11199
N89-11200
N89-11207
N89-11208
OSAKA, TETSUYA N89-11135
OSHIRO, SERGIO KATSUMI N89-11438
OSTERGAARD, JENS N89-11093
OSTGAARD, JOHN C. N89-10834
OTTER, MARTIN N89-11443
OTTO, G. N89-10906
OWENS, B. B. N89-11134
OWENS, BOONE B. N89-11135
OYEDEJI, OYEKALE N89-11669

P

PACHER, TIBOR N89-11489
PAGE, RICHARD D. N89-11356
PAGE, RUSSELL J. N89-10943
PAIGE, ALLAN BRADLEY N89-11152
PAILHAS, GUY N89-10861
N89-10864
PALMER, R. G. N89-11506
PAPPA, R. S. N89-11262
PARADELLA, WALDIR R. N89-11418
PARKS, E. K. N89-10994
PARKS, G. K. N89-11350
PASCUAL, R. N89-11279
PASSMORE, M. A. N89-10846
PATERSON, THOMAS S. N89-11487
PAULSON, JOHN W., JR. N89-10854
PAVLOVICH, YU. V. N89-11004
PEANO, A. N89-11257
PEARCE, JEFFREY ALAN N89-11188
PEARSON, D. N89-11278
PEARSON, J. N89-11016
PECORELLA, W. N89-11646
PEDERSON, R. A. N89-11507
PEILL, R. J. N89-11492
PELUFOFOSTER, PAULO ROBERTO N89-11352
PENFIELD, PAUL, JR. N89-11130
PENNER, SAMUEL N89-11221
PENNIMAN, W. DAVID N89-11632
PEREIRADACUNHA, ROBERTO N89-11295
PERSOON, A. J. N89-10867
PETOLIAGIS, THOMAS I. N89-11353
PETRICH, R. R. N89-11010
PETRY, M. N89-10911
PHAN, LONG T. N89-11271
PHILLIPS, R. E. N89-10952
PHIPPS, G. S. N89-11122
PICONE, P. J. N89-11598
PIEPER, G. W. N89-11461
PINDERA, M. Z. N89-10981
PINNADUWAGE, L. A. N89-11117
PINTO, O., JR. N89-11351
PIROUZ, P. N89-10996
PITZ, WILLIAM J. N89-11053
PITZER, K. S. N89-10969
PODANY, MARK N89-11128
PODDAR, KAMAL N89-11145
POLAK, ELIJAH N89-11405
POLIAN, A. N89-11497
PONZONI, FLAVIO JORGE N89-11324
POOLE-KOBER, EVELYN M. N89-11327
POPE, D. P. N89-11255
POPPLE, R. N89-10947
PORJESZ, T. N89-11583
PORTER, C. A. N89-11508
POTT, E. N89-10998
POVOLO, F. N89-11588
POWELL, D. C. N89-11360
PRASAD, K. U. N89-11044
PREIS, R. N89-11538
PREUSS, E. N89-11645
PRICE, E. W. N89-10987
PRIVON, GEORGE T. N89-11165
PROBSTEIN, R. F. N89-11148
PROSCIA, J. N89-11316
PROSNITZ, D. N89-11208
PRUSSIN, SIMON N89-11574
PUCKETT, E. G. N89-11178

Q

QUANG, TRAN N89-11205

R

RABINOVICH, A. A. N89-11005
RABY, STUART N89-11683
RACICOT, ROBERT J. N89-11605
RAGSDALE, ROBERT G., JR. N89-11516
RAHMAN, S. M. MUJIBUR N89-10976
N89-11593
RAMACHANDRAN, N. N89-11164
RAMASUBRAMANIAN, MELUR KRISHNAMURTHY
N89-11284
RAMOS, HENRY J. N89-11529
RAMOS, J. I. N89-11149
RAND, P. N89-11036
RANSOME, PETER D. N89-11092
RAO, P. SUBBA N89-11290
RAOL, J. R. N89-11410
N89-11449
RAPP, H. N89-11538
RAPPAPORT, AMNON N89-11483
RATHKOPF, J. A. N89-11031
RAUCH, J. N89-10832
RAVEX, A. N89-11594
RAWLINS, W. T. N89-10937
RAY, SUVENDOO KUMAR N89-11256
RAYMOND, SLATE N89-11620
REAGOR, D. W. N89-11585
REED, C. B. N89-11553
REED, JACK W. N89-11144
REED, JOHN W. N89-11212
REEDER, JAMES R. N89-10945
REEDY, R. C. N89-11682
REEVES, HUBERT N89-11639
N89-11640
REHN, L. N89-11016
REISER, CHRISTOPHER N89-11206
REITER, D. N89-11527
REKLIS, R. P. N89-11136
RENKEN, URSULA N89-10956
RENSCHLER, C. L. N89-10950
RENZETTI, N. A. N89-11661
RHATT, R. T. N89-10952
RICHARDSON, SHERRI N89-11012
RICHTER, MARK ANDREW N89-11275
RICHTMEIER, S. C. N89-10942
RICKARD, G. J. N89-11463
RIES, HARRY J., JR. N89-11382
RIGAMONTI, M. N89-10951
RILEY, S. J. N89-10994
RITCHEY, VERNON S. N89-11446
ROBBINS, DAVID O. N89-11222
ROBERTS, J. B. N89-11263
ROBOUCH, B. V. N89-11537
N89-11540
ROCHIER, JAMES D. N89-11480
ROCKHOLT, H. M. N89-10894
RODGER, D. N89-11098
ROLLETT, A. D. N89-10995
ROLOFF, R. R. N89-11136
ROMANENKO, V. G. N89-11227
ROME, J. N89-10947
ROMERO, LOUIS A. N89-11139
ROMIG, A. D., JR. N89-11017
ROOS, M. N89-11539
N89-11540
ROSEN, B. K. N89-11621
ROSENBERGER, FRANZ N89-10922
ROSENBLUTH, M. N89-11211
ROSENBURG, BRUCE L. N89-11356
ROSENTHAL, H. A. N89-10894
ROTEM, DORON N89-11408
ROTMAN, D. A. N89-10981
ROWLAND, JOHN N89-11083
ROZOVSKIY, G. I. N89-10963
RUBIN, STUART HARVEY N89-11623
RUFFOLO, JOHN J., JR. N89-11217
RUGGLES, MARINA N89-11273
RULAND, DETLEV N89-11615
RULAND, ROBERT N89-11615
RUSANOV, K. V. N89-10974
RUSSO, TRACY N89-10893
RUTH, R. D. N89-11460
RUZZANTE, J. N89-11009
RYABOV, B. P. N89-11679
RYBICKI, GEORGE C. N89-10996
RYNE, ROBERT DOUGLAS N89-11496

S

SAEKI, K. N89-11526
SAFFMAN, P. G. N89-11114
SAHU, D. N89-11607
SAINTPE, P. N89-10839
SAITO, TAKAO N89-11667
SALASIN, JOHN N89-11488
SALGADO, L. V. N89-10950
SALMON, JOHN N89-11413
SALVINO, J. T. N89-10892
SALVINO, JAMES T. N89-10893
SANZGIRI, SHASHIKANT N89-11133
SAPIR, J. L. N89-11508
SARABANDI, K. N89-10984
N89-11296
SARASAMMA, V. R. N89-11455
SASAO, MAMIKO N89-11529
SASSEN, KENNETH N89-11362
SATO, M. N89-11598
SATO, S. N89-10888
SAUL, ROGER A. N89-11389
SAUSEN, TANIA MARIA N89-11295
SCARF, F. L. N89-11678
SCHADE, H. E. N89-11311
SCHAEFER, J. P. N89-11122
SCHAFER, CHARLES F. N89-11153
SCHANWALD, L. P. N89-11119
SCHARF, LOUIS L. N89-11432
SCHARLEMANN, E. T. N89-11199
N89-11208
SCHATZ, G. C. N89-10970
SCHICK, JOSEPH THOMAS N89-11596
SCHIEBER, M. M. N89-11578
N89-11580
SCHMIDT, E. L. N89-11151
SCHNEGGENBURGER, ROGER G. N89-11280
SCHNEIDER, T. N89-10947
SCHRAMM, DAVID N. N89-11673
N89-11675
SCHREIBER, H. A. N89-10858
SCHULER, K. W. N89-10926
SCHULTZ, HERMAN P. N89-11434

SCHUMACHER, U. N89-11541
SCHWARZ, R. B. N89-11010
SEASHOLTZ, RICHARD G. N89-10844
SEBO, ANDREAS N89-11470
SEELEY, D. N89-10911
SEERING, WARREN P. N89-11229
SEGALMAN, DANIEL J. N89-10927
SEGURET, J. N89-11048
SEHMER, A. A. N89-10899
SEIDEL, G. M. N89-11664
SEIFERT, HENRY N89-11318
SELLERS, BACH N89-10938
SELVARAJAN, S. N89-11142
SELYUNIN, S. YU. N89-11143
SEMANOV, G. R. N89-11005
SEMARGE, R. E. N89-11017
SEMMENS, DAVE N89-11340
SEN, AYUSMAN N89-10968
SEN, R. K. N89-11317
SENATOROV, YU. M. N89-11004
SENGUPTA, T. K. N89-11142
SENIOR, T. B. A. N89-11296
SENTMAN, L. H. N89-11132
SETTLES, GARY S. N89-11189
SHAIK, KAMRAN N89-11087
SHANKAR, P. N. N89-10964
N89-10971
N89-10973
SHARMA, V. K. N89-11290
SHEHATA, L. N. N89-11603
SHEN, JUE-LIAN N89-11561
SHEPHERD, I. G. N89-10960
SHERWIN, MARK STEPHEN N89-11582
SHERWOOD, L. T. N89-11192
SHI, D. N89-11572
SHIM, R. T. N89-11106
SHINYASHIBATA, CARLOS N89-11491
SHIOMI, TADASHI N89-11089
SHIRANE, G. N89-11596
SHIRANE, GEN N89-11555
SHIRKEY, R. C. N89-11099
SHOGA, M. N89-10935
SHUMOVSKIJ, A. S. N89-11205
SIEGER, G. E. N89-11100
SIHVOLA, ARI N89-11104
SILBERBERG, TERESA M. N89-11421
SIMMET, E. N89-11541
SIMONETT, DAVID S. N89-11292
SINHA, U. N. N89-11455
SIRENKO, V. A. N89-11227
SIRLIN, SAMUEL W. N89-10931
SKINNER, N. L. N89-11578
N89-11580
SLOAN, M. L. N89-11509
SMITH, E. N89-11172
SMITH, E. C. N89-10935
SMITH, ELEANOR L. N89-11372
SMITH, ERNEST K. N89-11094
SMITH, J. L. N89-11552
N89-11594
SMITH, J. L., JR. N89-11313
SMITH, M. D. N89-10942
SMITH, MAILE E. N89-11487
SMITH, S. G. N89-11422
SMYTHE, GLENN R. N89-11356
SNIDER, JACK B. N89-11086
SNYDER, LAWRENCE N89-11430
N89-11431
SNYDER, MARK E. N89-11550
SNYDER, SCOTT N89-11394
SODERMAN, PAUL T. N89-10856
SOFRONIS, PETROS N89-11000
SOLOMON, JAY M. N89-11166
SON, ZUN GAN N89-11143
SORNATALE, FRANK N89-11370
SOVEY, J. S. N89-11553
SPARROW, J. T. N89-10987
SPATZ, M. N89-11172
SPORTIELLO, R. N89-10911
SPRANGLE, PHILLIP N89-11221
SPRECHER, R. N89-10911
SPRIGGS, G. D. N89-11507
SPYRAKOS, C. C. N89-11259
SRIDHARAN, R. N89-10847
SRIVASTAVA, JAIDEEP N89-11408
SROLOVITZ, D. J. N89-11577
STAHL, K. A. N89-11512
STAINSBY, RICHARD N89-11176
STANIEK, S. N89-10906
STANKIEWICZ, NORBERT N89-11128
STARK, MARGARET A. N89-11212
STARKEN, H. N89-10858
STARKS, PATRICK N89-11368
STEAD, MICHAEL R. N89-11115
STECKLER, R. N89-10970
STEELE, W. A. N89-10949
STEGER, JOSEPH L. N89-10857
STEIN-SCHABES, JAIME A. N89-11489
N89-11500
N89-11614
STEINER, B. N89-11595
STEINER, J. E. N89-11291
STEPHENS, J. R. N89-11056
STEPHENSON, WILLIAM A. N89-11304
STEPP, ROBERT E. N89-11448
STERN, S. A. N89-10980
STEWART, D. S. N89-11052
STEWART, VEARLE R. N89-10850
STEWART, W. F. N89-11070
STIEGLER, U. N89-11502
STILES, J. M. N89-11171
STOCK, LARRY V. N89-11201
STOCKING, MARTHA L. N89-11404
STONER, WILLIS A. N89-10943
STOUGHTON, JOHN W. N89-11406
STOUT, M. G. N89-10995
STRAIN, BOYD R. N89-11326
STREETS, D. G. N89-11322
STRICKLER, D. N89-11316
STROTH, U. N89-11541
STUBBINGS, BETH N89-10918
STURROCK, PETER A. N89-11684
STUTZMAN, W. L. N89-11081
STUTZMAN, WARREN L. N89-11078
SU, ZHAO-BIN N89-11561
SUDARSKY, DANIEL N89-11612
SUENAGA, M. N89-11587
SUGIHARA, RYO N89-11520
SULLIVAN, R. BRYAN N89-10890
SUNWOO, A. J. N89-11015
SURH, MICHAEL P. N89-11599
SUSALLA, MICHAEL P. N89-11071
SUSSMAN, GERALD J. N89-11476
SUTHERLAND, HERBERT J. N89-11304
SUZUKI, M. N89-10999
SWANK, WAYNE T. N89-11319
SWANSON, R. M. N89-11314
SWARTZ, A. A. N89-11106
SWEENEY, J. K. N89-11325
SYLWESTER, A. N89-11036
SYLWESTER, A. P. N89-10948
SZYMCZAK, WILLIAM G. N89-11166

T

TAKAKURA, YOKO N89-10845
TAKANASHI, SUSUMU N89-11067
TAKANO, S. N89-11663
TAKAYANAGI, M. N89-10904
TAKEUCHI, SATOSHI N89-11545
TALBOT, L. N89-10960
TALMADGE, CARRICK N89-11612
TAMIR, DAVID N89-10916
TANAKA, M. P. N89-10999
TANAS, R. N89-11205
TANDLER, J. N89-11172
TANG, CHA-MEI N89-11221
TANGER, J. C., IV N89-10969
TANII, JUN N89-10907
TARIGAN, MULIUKUR N89-11190
TAUBER, GERALD E. N89-11672
TAYLOR, E. W. N89-11492
TELFORD, JAMES W. N89-11203
TERADA, NOBUYUKI N89-11118
THEILER, M. N89-10911
THOMAS, D. K. N89-11554
THOMAS, LAWRENCE R. N89-10902
THOMAS, P. D. N89-11136
THOMAS, RICHARD N89-11657
THOMPSON, J. D. N89-11552
N89-11585
THOMPSON, J. L. N89-10869
THOMPSON, J. R. N89-11509
THURSTON, T. R. N89-11598
TILLOTSON, DANIEL H. N89-10885
TIPTON, T. N89-11008
TJON, J. A. N89-11498
TODOROKI, J. N89-11546
TOI, K. N89-11547
TONEV, TOMA V. N89-11450
TOWNSEND, L. W. N89-11498
TRACY, EUGENE R. N89-11518
TRANGENSTEIN, J. N89-11141
TREASE, HAROLD E. N89-11437
TRETYACHENKO, G. N. N89-11005
TREVINO, G. N89-11359
TROUTT, T. R. N89-11158
TRUHLAR, DONALD G. N89-10959
TRURAN, JAMES W. N89-11673
TSENG, HUAN-CHI C. N89-11243
TUERK, STEFAN N89-11443
N89-11444
TURNER, L. R. N89-11098
TUROK, N. N89-11501
TUROK, NEIL N89-11674
TWEEDT, D. L. N89-10858

U

UEDA, TETSUHIKO N89-11068
UGLUM, J. R. N89-11509
UHLHORN, R. W. N89-10836
ULABY, F. T. N89-10984
N89-11296
ULKEN, ROLF N89-10862
UM, C. I. N89-10986
UNDERHILL, ANNE B. N89-11657
URAMOTO, JOSHIN N89-11523
N89-11548
URRUTIAPAEZ, JOSE MANUEL N89-11521
URRY, DAN W. N89-11044

V

VACHEZ, F. N89-11048
VAHALA, GEORGE N89-11518
VAIDYANATHAN, R. N89-10980
VALLET, CATHERINE E. N89-10975
VANALBADA, T. S. N89-11652
VANDALSEM, WILLIAM R. N89-10857
VANDENBERG, L. N89-11578
N89-11580
VANDERHELM, P. A. N89-11458
VANHOY, B. N89-10901
VANIMAN, D. T. N89-11682
VANIMAN, DAVID N89-11681
VANMIEGROET, HELGA N89-11319
VASHCHILO, N. P. N89-11005
VASILEVSKIY, N. N. N89-11386
VEAL, B. W. N89-11591
VENKETESWARAN, S. N89-11384
VENTURINI, E. L. N89-11565
N89-11601
VERINK, E. D., JR. N89-11602
VERJOVSKY, ALBERTO N89-11465
VERMA, SHASHI B. N89-11368
VIEBROCK, HERBERT J. N89-11327
VIEIRADUTRA, LUCIANO N89-11418
N89-11427
VIGNAU, F. N89-11187
VILLALOBOS, G. R. N89-10987
VIOLA, F. E. C. N89-11419
VITEX, V. N89-11011
VITTORIO, NICOLA N89-11644
VOGEL, W. J. N89-11081
VOGEL, WOLFHARD J. N89-11077
N89-11079
VOIGT, J. A. N89-11601
VOIRON, T. N89-10839
VONBORZESZKOWSKI, H. H. N89-11608
VOSEN, J. H. N89-11009
VREEBURG, J. P. B. N89-11058

W

WADA, MOTOI N89-11529
WADE, BARRY N89-11265
WAGNER, A. F. N89-10970
WAKATANI, M. N89-11546
WALDOWSKI, PAUL J. N89-11402
WALKER, BETTY S. N89-10842
WALKER, DAVID N89-11394
WALKER, F. E. N89-11047
WALLACE, S. J. N89-11498
WALLSTEN, THOMAS S. N89-11483
WALRAFEN, GEORGE E. N89-11043
WALTERSHEA, ELIZABETH N89-11368
WAMPLER, E. J. N89-11642
WANG, HUEI N89-11095
WANG, PU SEN N89-11051
WANG, YONG N89-11292
WARK, JUSTIN S. N89-11532
WARNATZ, JUERGEN N89-11053
WARNOCK, R. L. N89-11460
WARREN, MIKE N89-11413
WAS, G. S. N89-11018
WATARI, T. N89-11547
WATKINS, J. G. N89-11530
WATKINS, RICHARD N89-11500
WATMUFF, J. H. N89-11193
WATSON, R. D. N89-11530
WATTERS, K. C. N89-11510
WATTS, H. A. N89-11147
WEAVER, F. J. N89-10982
WEBER, W. J. N89-11310
WEIR, ROBERT J. N89-10841

WELCH, D. O. N89-11575
WELCOME, M. N89-11141
WELLMAN, G. W. N89-10926
WELLS, GARY D. N89-11354
WELLS, JAMES E. N89-10928
WELLS, N. D. N89-11101
WERLE, H. N89-10860
WERNER, PAUL W. N89-10939
WESTBROOK, CHARLES K. N89-11053
WESTERVELD, J. P. A. N89-11575
WESTON, A. M. N89-11049
WESTWATER, ED R. N89-11086
WHITE, C. N89-10937
WHITE, C. W. N89-11564
WHITE, R. E. N89-11308
WHITE, R. H. N89-11507
WHITEHALL, BRADLEY L. N89-11448
WIBERLEY, STEPHEN E. N89-10946
WICKERT, J. A. N89-11283
WIDMAN, FREDERICK W. N89-10929
WIDROW, LAWRENCE M. N89-11500
WIECKO, C. N89-11558
WILKINS, J. W. N89-11573
WILKINSON, JAMES E. N89-11403
WILKINSON, R. N89-11501
WILLIAMS, JOEL M. N89-11665
WILLIAMS, RAY C. N89-11217
WILLIAMS, STEVEN HAMILTON N89-11677
WILLIAMS, TONY N89-10912
WILSON, D. G. N89-10933
WINKLER, W. N89-11648
WINTERSGILL, MARY C. N89-11039
WISHNOW, HOWARD N89-10919
WNEK, GARY E. N89-11040
WOLFE, W. P. N89-11147
WOLFMULLER, KARLHEINZ N89-11242
WOLKEN, P. R. N89-11661
WOLLE, B. N89-11539
WRIGHT, GEORGE B. N89-11687
WRIGHT, ROBERT L. N89-11407
WROBLESKI, DEBRA A. N89-11665
WU, ZHONGXIANG N89-11218
N89-11220
WYATT, F. V. N89-10898

Y

YAKOVCHUK, K. YU. N89-11005
YAMANAKA, JANET MIDORI N89-11656
YAMAOKA, HITOSHI N89-11529
YAN, HAIXING N89-11220
YANG, WEI-HONG N89-11684
YARBROUGH, D. W. N89-10982
YEH, CAVOUR N89-11112
YING, WEN-PING N89-11338
YOKOTA, JEFFREY W. N89-10863
YOSHIHARA, H. N89-11395
YU, LU N89-11561
YU, YI-YUAN N89-11267
YUEH, H. A. N89-11106
YUEN, H. C. N89-11114
YUMOTO, KIYOHUMI N89-11667

Z

ZAGUSTINA, V. B. N89-11386
ZAIKI, Y. N89-10904
ZANOTTI, C. N89-10951
ZAWACKI, THOMAS A. N89-10972
ZEHR, DAVID F. N89-11375
ZERWECKH, SIEGFRIED H. N89-10890
ZHANG, H. Y. N89-11269
ZHANG, YONG N89-11231
ZHAO, FENG N89-11433
ZHAO, XIN N89-10895
ZHIDKOV, E. P. N89-11490
ZHITOMIRSKIJ, I. S. N89-11227
ZHOU, BING-LIN N89-11574
ZHOU, S. N89-10980
ZHU, SHENG-HUA N89-10967
ZIKAN, KAREL N89-11421
ZIMMERMAN, A. H. N89-10965
ZINK, MANFRED N89-11105
ZUK, JOHN N89-10872
ZURINSKAS, THOMAS E. N89-11356
ZUTAVERN, F. J. N89-11119
ZWICK, RAMI N89-11483

Typical Corporate Source Index Listing

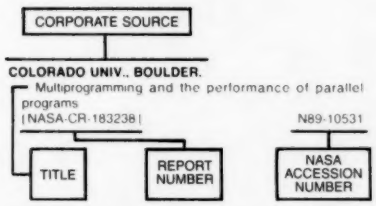

Listings in this index are arranged alphabetically by corporate source. The title of the document provides the user with a brief description of the subject matter. The report number helps to indicate the type of document cited (e.g., NASA report, translation, NASA contractor report). The NASA accession number denotes the number by which the citation is identified. The titles are arranged under each corporate source in ascending accession number order.

A

ABERDEEN UNIV. (SCOTLAND).
Dynamic behavior of helical springs N89-11278

ACADEMY OF SCIENCES OF THE UKRAINIAN SSR, KHARKOV.
Peculiarities of heat transfer at helium boiling in centrifugal force field
[DE88-702809] N89-10974
Thermal calculations of nitrogen-free nonmagnetic helium cryostats
[DE88-702807] N89-11227
Probable locations of extraterrestrial civilizations
[DE88-702605] N89-11392
Decametric radio emission of Jupiter. Part 3: Some physical characteristics of S-component sources
[DE88-702812] N89-11679

ADVISORY GROUP FOR AEROSPACE RESEARCH AND DEVELOPMENT, NEUILLY-SUR-SEINE (FRANCE).
Computing Systems Configuration for Highly Integrated Guidance and Control Systems
[AGARD-LS-158] N89-10831
The NAVSTAR GPS System
[AGARD-LS-161] N89-10874
Computational Fluid Dynamics: Algorithms and Supercomputers
[AGARD-AG-311] N89-11395
Evaluating the Effectiveness of Information Centres and Services
[AGARD-LS-160] N89-11625

AEROJET SOLID PROPULSION CO., SACRAMENTO, CALIF.
Energetic thermoplastic elastomer synthesis
[AD-A196885] N89-11041
Synthesis of energetic binders
[AD-A196886] N89-11042

AERONAUTICAL RESEARCH LABS., MELBOURNE (AUSTRALIA).
Non-linear aerodynamic characteristics obtained from the analysis of flight-data
[AR-004-571] N89-10866
A test methodology for an investigation into heating and cooling phenomena in grossly deformed tensile metallic bars
[AD-A197047] N89-11024
A hybrid hot-wire data acquistion system
[ARL-AERO-R-172] N89-11193
In-plane moire optical processing at ARL
[ARL-STRUC-R-428] N89-11510

AEROSPACE CORP., EL SEGUNDO, CALIF.
The GPS overview and navigation system concept N89-10875
The Global Positioning System (GPS) constellation and coverage N89-10876
The Global Positioning System (GPS) accuracy, system error budget, space and control segment overview N89-10877
Verification of single event upset rate estimation methods with on-orbit observations
[AD-A196226] N89-10935
Electrochemical reactions of mixed cobalt/nickel oxide hydroxides in alkaline electrolyte
[ATR-86(9561)-4] N89-10965
Fundamental aspects of the electronic structure, materials properties, and lubrication performance of sputtered MoS2 films
[AD-A196852] N89-11606

AIR FORCE ENGINEERING AND SERVICES CENTER, TYNDALL AFB, FLA.
HCl measurements in space vehicle exhaust clouds
[DE88-013815] N89-10942

AIR FORCE INST. OF TECH., WRIGHT-PATTERSON AFB, OHIO.
The utility of particle precipitation data as an input to thermospheric density models for satellite orbital analysis
[AD-A196870] N89-10925
Characterization of metallic coatings and thin films produced by railgun deposition
[AD-A196382] N89-11021
A method for obtaining empirical correlations for predicting crack propagation in a burning solid propellant grain
[AD-A196689] N89-11054
Effects of noise and task loading on a communication task loading on a communication task
[AD-A196378] N89-11107
Bit-to-bit error dependence in direct-sequence spread-spectrum multiple-access packet radio systems
[AD-A196384] N89-11108
A broad-band array of aperture-coupled cavity-backed slot elements
[AD-A196400] N89-11109
Synthesis of resistive tapers to control scattering patterns of strips
[AD-A196402] N89-11110
Digital signal design for meteor-scatter communications
[AD-A196685] N89-11111
Optimization of microwave magnetoelastic delay lines
[AD-A196866] N89-11131
A computational study of coherent structures in the wakes of two-dimensional bluff bodies
[AD-A196820] N89-11188
Damage effects on thin acrylic targets caused by infrared radiation from a pulsed carbon dioxide laser
[AD-A196385] N89-11216
Finite element analysis of shell structures with an 18-node 3-dimensional solid element based on a new mixed formulation
[AD-A196698] N89-11288
The impact of an increase in atmospheric methane on the temperature field and subsequent climatic effects
[AD-A196869] N89-11332
A time-dependent model for the low-latitude ionosphere
[AD-A196683] N89-11354
Tropical 200 mb divergent circulations and their relation to outgoing longwave radiation
[AD-A196375] N89-11370
Tropical cyclone observation and forecasting with and without aircraft reconnaissance
[AD-A196379] N89-11371
An examination of a simulated microburst flow as sensed by a single Doppler radar
[AD-A196381] N89-11372
On deriving the 3-dimensional kinematic structure of convective storms from a single radar
[AD-A196405] N89-11373
Active modes of the Pacific Intertropical Convergence Zone (ITCZ)
[AD-A196406] N89-11374
Estimating evapotranspiration of an irrigated surface from upwind and downwind vertical profiles of temperature and humidity
[AD-A196409] N89-11375
The use of the Q-vector in operational meteorology
[AD-A196410] N89-11376
The role of a lid in the 31 May 1985 tornado outbreak
[AD-A196684] N89-11377
Synoptic scale sensitivity of TIROS-N moisture channels in the tropics
[AD-A196686] N89-11378
Mesoscale structure and climatology of rain-snow lines over North Carolina
[AD-A196687] N89-11379
Effect of physical fitness on response to orthostasis in healthy young women
[AD-A196377] N89-11387
An introduction to implementing a capacity planning effort in an MVS (Multiple Virtual Storage) environment
[AD-A196383] N89-11402
The use of portable microcomputer as a data collection tool to support integrated simulation support environments: A concept
[AD-A196414] N89-11403
Asynchronous digital regulators
[AD-A196911] N89-11446
The generation of scatterometer surface targets with specified surface statistics
[AD-A196397] N89-11480
General results in optimal control of discrete-time nonlinear stochastic systems
[AD-A196411] N89-11481
Neutron multiplication in beryllium
[AD-A196877] N89-11503
A survey of digital beam forming techniques and current technology
[AD-A196376] N89-11514
Determination of the unstable states of the solid state plasma in semiconductor devices
[AD-A196403] N89-11550
Surface passivation of Gallium Arsenide
[AD-A196695] N89-11605
Three probable stellar mass black holes
[AD-A196976] N89-11676

AIR FORCE OFFICE OF SCIENTIFIC RESEARCH LIAISON OFFICE, FAR EAST, APO, SAN FRANCISCO, CALIF.
ONR Far East Scientific Bulletin, volume 12, no. 4, October - December 1987
[AD-A194338] N89-11687

AIR FORCE SPACE DIV., LOS ANGELES, CALIF.
User equipment overview N89-10879
Civil and military applications of GPS N89-10882

AIR FORCE SYSTEMS COMMAND, WRIGHT-PATTERSON AFB, OHIO.
Two-dimensional saturation gain and output power in transverse flow electrical discharge CO2 lasers
[AD-A196660] N89-11218
Basic rules of saturated gain variation in a flowing laser cavity
[AD-A196861] N89-11220

AIR FORCE WRIGHT AERONAUTICAL LABS., WRIGHT-PATTERSON AFB, OHIO.
Advanced avionics architecture pave pillar N89-10834
Data and signal processing architectures for future avionics N89-10835
High speed parallel processing networks for advanced architectures N89-10837
F-15 SMTD low speed jet effects wind tunnel test results N89-10853
Determination of complex exponentials, least squares and prediction methods
[AD-A196498] N89-11474

AKRON UNIV., OHIO.
Workshops and problems for benchmarking eddy current codes
[DE88-009996] N89-11098

ALABAMA UNIV., BIRMINGHAM.
Development of elastomeric polypeptide biomaterials
[AD-A196900] N89-11044

ALABAMA UNIV., HUNTSVILLE.
Process modelling for space station experiments
[NASA-CR-183274] N89-10922
Turbulence modeling of gas-solid suspension flows N89-11156

AMSTERDAM UNIV. (NETHERLANDS).
Theory of oxygen ordering and absorption in 1,2,3 high-T(sub c) superconductors
[DE88-007543] N89-11575
APPLIED RESEARCH CORP., LANDOVER, MD.
A new radar technique for satellite rainfall algorithm development
[NASA-CR-183471] N89-11102
AQUANAUTICS CORP., EMERYVILLE, CALIF.
Oxygen chemistry
[AD-A196989] N89-10988
AQUILA UNIV. (ITALY).
Galaxy formation: Theory and observational tests
N89-11644
ARCH DEVELOPMENT CORP., ARGONNE, ILL.
Technology transfer at Argonne National Laboratory
[DE88-012062] N89-11636
ARGONNE NATIONAL LAB., ILL.
Theoretical studies of chemical reactions: dynamics
[DE88-011994] N89-10970
Experimental studies of the chemistry of metal clusters
[DE88-012034] N89-10994
Methodologies for prediction of metal oxidation-vaporization-erosion
[DE88-013623] N89-11001
Laser Raman spectroscopy of anodic corrosion and inhibitor films on iron and nickel
[DE88-009958] N89-11008
Brillouin scattering: Its application to the study of damage and amorphization
[DE88-012053] N89-11016
Characterization of ceramic films and interfaces by electron microscopic and spectroscopic techniques
[DE88-011957] N89-11029
Experimental and analytical study of vapor explosions in stratified geometries
[DE88-011964] N89-11046
Workshops and problems for benchmarking eddy current codes
[DE88-009996] N89-11098
Laser/fluorescent dye flow visualization technique developed for system component thermal hydraulic studies
[DE88-012008] N89-11137
Friction reduction and heat transfer enhancement in turbulent pipe flow of non-Newtonian liquid-solid mixtures
[DE88-010018] N89-11138
Measurements of pressure drop and heat transfer in turbulent pipe flows of particulate slurries
[DE88-013622] N89-11150
Heat release effects of reacting gas jets in liquids
[DE88-011971] N89-11175
Organic Rankine-Cycle Power Systems Working Fluids Study: 2-methylpyridine/water
[DE88-012659] N89-11307
Review of acid rain models for Europe
[DE88-011945] N89-11322
Parameterizations of microphysical processes in clouds for application in models of regional atmospheric deposition
[DE88-010017] N89-11345
Proceedings of the Focused Research Program on Spectral Theory and Boundary Value Problems. Volume 1: Singular differential systems
[DE88-008151] N89-11461
Brillouin scattering at high pressures
[DE88-011972] N89-11497
Magnetic fluctuations and heavy electron superconductivity
[DE88-011978] N89-11557
MAGLEV: The double benefits of high-Tc superconductors and its development as an aerospace technology
[DE88-012005] N89-11570
Kinetic processes of the orthorhombic to tetragonal phase transition in YBa2Cu3O7-Delta
[DE88-011993] N89-11572
High-power RF applications of high-T(sub c) superconductors
[DE88-012055] N89-11579
Technology transfer at Argonne National Laboratory
[DE88-012062] N89-11636
ARINC RESEARCH CORP., ANNAPOLIS, MD.
In-service evaluation of the Traffic Alert and Collision Avoidance System (TCAS) industry prototype
[DOT/FAA/SA-88/2] N89-10885
ARIZONA STATE UNIV., TEMPE.
Surface structures and reactions of ceramics and metals
[DE88-013752] N89-11028
Hypothesis-confirming information search strategies and computerized information retrieval systems N89-11616
A comparative planetological study of particle speed and concentration during aeolian saltation N89-11677
ARIZONA UNIV., TUCSON.
Effect of thermal cycling
[AD-A196851] N89-11219
On relative supernova rates and nucleosynthesis roles
[NASA-CR-183373] N89-11673
ARMY BELVOIR RESEARCH AND DEVELOPMENT CENTER, FORT BELVOIR, VA.
Control of environment assisted cracking of Al 7075 using inhibitors
[AD-A196387] N89-11022
ARMY ENGINEER TOPOGRAPHIC LABS., FORT BELVOIR, VA.
Continuous deformation monitoring with GPS
[AD-A196447] N89-10886
ARMY LAB. COMMAND, WATERTOWN, MASS.
Applications of the optical differential thermal analysis
[AD-A196706] N89-11515
ARMY LAB. COMMAND, WHITE SANDS MISSILE RANGE, N. MEX.
Verification of EOSAEL (Electro-Optical Systems Atmospheric Effects Library) snow transmittance predictions
[DREV-R-4423/87] N89-11099
ARMY RESEARCH OFFICE LIAISON OFFICE, FAR EAST, APO, SAN FRANCISCO, CALIF.
ONR Far East Scientific Bulletin, volume 12, no. 4, October - December 1987
[AD-A194338] N89-11687
ASSOCIACAO BRASILEIRA DE CIENCIAS MECANICAS, RIO DE JANEIRO.
Contribution for stress analysis in bend acessories of piping systems
[DE88-701618] N89-11272
Dynamic analysis of pipings by modal synthesis
[DE88-701620] N89-11274
Fatigue of welded joint in a stainless steel AISI 304 L
[DE88-701622] N89-11279
AUBURN UNIV., ALA.
Plasma exposure tests of a carbon fiber/epoxy composite
[DE88-014724] N89-10947
AUSTIN RESEARCH ASSOCIATES, INC., TEX.
Beam handling and emittance control
[AD-A196789] N89-11509
AVIATION SAFETY COMMISSION, WASHINGTON, D.C.
Aeronautical decision making for commercial pilots
[DOT/FAA/PM-86/42] N89-10870

B

BATH UNIV. (ENGLAND).
High frequency inverter-cycloconverter system for dc to ac conversion N89-11120
BELL TELEPHONE LABS., INC., MURRAY HILL, N. J.
Evaluating for information center planning
N89-11632
BOEING COMPUTER SERVICES CO., SEATTLE, WASH.
Hardware architecture, chapter 2 N89-11396
Algorithm and general software considerations
N89-11397
An informal glossary of terms used in supercomputing, appendix A N89-11401
BRIGHAM YOUNG UNIV., PROVO, UTAH.
Influence of grain boundary structure distribution and processing history on intergranular creep cavitation
[DE88-015808] N89-11571
BRITISH BROADCASTING CORP., KINGSWOOD (ENGLAND).
Polarisation converters for a DBS flat-plate antenna
[BBC-RD-1988/7] N89-11073
A flat-plate antenna for DBS reception
[BBC-RD-1988/6] N89-11096
Television animation store: Control system operation and implementation
[BBC-RD-1988/4] N89-11097
Bandwidth compression for HDTV broadcasting: Investigation of some adaptive subsampling strategies
[BBC-RD-1988/9] N89-11101
Array elements for a DBS flat-plate antenna
[BBC-RD-1988/8] N89-11103
The development of prototype absorbers with variable characteristics
[BBC-RD-1988/5] N89-11492
BROOKHAVEN NATIONAL LAB., UPTON, N. Y.
Spin correlations in high T(sub c) superconductors
[DE88-013988] N89-11555
Theory of oxygen ordering and absorption in 1,2,3 high-T(sub c) superconductors
[DE88-007543] N89-11575
Microstructural defects and superconducting critical currents in superconductors
[DE88-013781] N89-11587
The compatibility of gravity and kaon results in the search for new forces
[DE88-013993] N89-11612
BROWN UNIV., PROVIDENCE, R. I.
Superfluid helium as a dark matter detector
[DE88-012759] N89-11664
Inflation, cosmic strings and galaxy formation
[DE88-008629] N89-11666
BUREAU INTERNATIONAL DE L'HEURE, PARIS (FRANCE).
Activities relevant to BIH on time scales or the rotation of the earth and terrestrial systems N89-11659

C

CALIFORNIA INST. OF TECH., PASADENA.
PC-CUBE: A personal computer based hypercube
[DE88-015008] N89-11394
An O(NlogN) hypercube N-body integrator
[DE88-015016] N89-11413
Lattice gauge theory on the hypercube
[DE88-015004] N89-11420
CALIFORNIA POLYTECHNIC STATE UNIV., SAN LUIS OBISPO.
The potential of a GAS can with payload G-169
N89-10916
CALIFORNIA UNIV., BERKELEY.
Current research on the vibration and stability of axially-moving materials N89-11283
Optimization-based design of control systems
[AD-A196593] N89-11405
Precision-time tradeoffs: A paradigm for processing statistical queries on databases
[DE88-012024] N89-11408
Solution methods for damped linear dynamic systems
[DE88-013812] N89-11464
CALIFORNIA UNIV., BERKELEY. LAWRENCE BERKELEY LAB.
Reaction rates in premixed turbulent flames and their relevance to the turbulent burning speed
[DE88-012021] N89-10960
Near-critical NaCl-H2O: An equation of state and discussion of anomalous properties
[DE88-012029] N89-10969
The importance of thermodynamics to the modeling of nitrogen combustion chemistry
[DE88-014656] N89-10978
Weldability of 2090 Al-Cu-Li alloy
[DE88-011963] N89-11015
Fuel cells: A handbook
[DE88-010252] N89-11309
Programming abstractions for run-time partitioning of scientific continuum calculations running on multiprocessors
[DE88-007376] N89-11411
Advances in metal ion sources
[DE88-012020] N89-11495
State of the art of negative luminescence
[DE88-010871] N89-11556
Far infrared linear response and radio frequency nonlinear response of charge density wave conductors and high T(sub c) superconductors
[DE88-013595] N89-11582
Some theoretical aspects of high-T(sub c) superconductivity
[DE88-013101] N89-11592
Tunneling junctions and the field effect
[DE88-013707] N89-11597
Spin-orbit interaction effects in zincblende semiconductors: Ab initio pseudopotential calculations
[DE88-014663] N89-11599
Phonon-plasmon mechanism of high-T(sub c) superconductivity
[DE88-014869] N89-11600
Astrophysical evidence on the equation of state
[DE88-011960] N89-11668
CALIFORNIA UNIV., DAVIS.
Design and evaluation of a cockpit display for hovering flight
[NASA-CR-183247] N89-10900
CALIFORNIA UNIV., LOS ANGELES.
Aeroelasticity and structural optimization of helicopter rotor blades with swept tips N89-10897
Dielectric millimeter waveguides. Volume 1
[AD-A196844] N89-11112
Effects of downdrafts and mesoscale convective organization on the heat and moisture budgets of squall and nonsquall cloud clusters in the tropics N89-11367
Strong and weak stabilizability: Lyapunov type approaches
[AD-A196431] N89-11482
Experimental study of time-varying current flow between electrodes immersed in a laboratory magnetoplasma
N89-11521
CALIFORNIA UNIV., SAN DIEGO.
Turbulent boundary layer drag reduction on an axisymmetric body using circular ring manipulators
N89-11145

Nongradient diffusion in premixed turbulent flames
N89-11161

CALIFORNIA UNIV., SAN DIEGO, LA JOLLA.
Three-dimensional computer graphics brain-mapping project
[AD-A197053] N89-11435

CALIFORNIA UNIV., SANTA BARBARA.
A study of the effect of thermal radiation on laminar flame propagation and ignition, 1981-1987 N89-10967
Improvement and extension of a radar forest backscattering model
[NASA-CR-183259] N89-11292

CARNEGIE-MELLON UNIV., PITTSBURGH, PA.
Experimental and theoretical studies of vertical annular liquid jets
[DE88-012971] N89-11149

CASE WESTERN RESERVE UNIV., CLEVELAND, OHIO.
Investigation of ionospheric D region aeronomy using incoherent scatter radar and optical measurements
N89-11338

CENTRAL RESEARCH INST. OF ELECTRIC POWER INDUSTRY, TOKYO (JAPAN).
Evaluation of Li/MoS2 secondary battery for load-conditioner. Deep-cycle performance of AA-size cells
[DE88-753437] N89-11118

CENTRE D'ESSAIS AERONAUTIQUE TOULOUSE (FRANCE).
Creep tests for slow and fast fatigue conditions on aluminum alloy specimens
[REPT-M0-535200] N89-11020
State-of-the-art in fiber optic systems at the Aeronautic Test Center, Toulouse (France)
[REPT-363300] N89-11513

CENTRE D'ETUDES ET DE RECHERCHES, TOULOUSE (FRANCE).
Investigation on of the flow around a backward facing step with spanwise blowing
[CERT-RF-OA-68/2259-AYD] N89-10859
Experimental investigation of flow near a corner, part 2
[CERT-RT-OA-24/5025-AYD] N89-10861
Three dimensional shear flow. Analysis of the flow in a delta arrow wing with incidence angle
[CERT-RTS-OA-25/5025-AYD] N89-10864
Three dimensional boundary layers on submarine conning towers and rudders
[CERT-OA-23/5025-AYD] N89-11182
Bursting phenomenon in a flat plate pulsed boundary layer
[CERT-RSF-OA-69/2259-AYD] N89-11183
Study of three dimensional boundary layers on the front of a fuselage and at an air intake
[CERT-OA-22/5025-AYD] N89-11184
Theory of instabilities in the laminar boundary layer: Literature review
[DERAT-42/5618-28] N89-11185
Boundary layer transition
[CERT-OA-40/5018-AYD] N89-11187

CENTRE NATIONAL D'ETUDES SPATIALES, TOULOUSE (FRANCE).
Flight mechanics and aerothermodynamic software
[CNES-CT/DTI/MS/MN/069] N89-10839
Elaboration of specifications for an expert system to aid the choice of analytical methods of orbit extrapolation for satellite localization
[CNES-CT/DTI/MS/MN/160] N89-10924
Study of the multiplexing of image telemetry data from SPOT 4 HRVIR and Vegetation sensors
[CNES-87/229/CT/DRT/TIT/TR] N89-10930
The vector functions of the MS system 570/CX
[CNES-CT/DTI/MS/MN/019] N89-11423
Presentation of research and development action 1206: Preliminary study report on the CESTAC method
[CNES-CT/PTI/MS/MN/067] N89-11424
Vectorization techniques on the MD system 570/CX
[CNES-CT/DTI/MS/MN/147] N89-11425
Object oriented software engineering with Ada
[CNES-CT/DTI/MS/MN/326] N89-11426

CENTRE NATIONAL DE LA RECHERCHE SCIENTIFIQUE, BESANCON (FRANCE).
Integrated quartz oscillator for aerospace applications
[ETN-88-93100] N89-11125

CENTRE NATIONAL DE LA RECHERCHE SCIENTIFIQUE, PARIS (FRANCE).
O stars and Wolf-Rayet stars
[NASA-SP-497] N89-11657

CENTRE NATIONAL DE LA RECHERCHE SCIENTIFIQUE, TOULOUSE (FRANCE).
Study and fabrication of AlGaAs/GaAs double heterojunction bipolar transistors for integrated injection logic circuits
[LAAS-88-138] N89-11123
A study of the turn-off behavior of high power gate turn off thyristors (GTO): Computer-aid to design and utilization
[LAAS-88-164] N89-11124
Design and fabrication by molecular beam epitaxy of visible light emitting ridge waveguide GaAs-AlGaAs quantum well lasers
[LAAS-88-097] N89-11215
Guidance, sensor control and localization of a mobile autonomous robot
[LAAS-88-131] N89-11241

CENTRO BRASILEIRO DE PESQUISAS FISICAS, RIO DE JANEIRO.
Self-consistent charge and spin distributions in oxide superconductors
[DE88-012051] N89-11591

CHICAGO UNIV., ILL.
Cosmic strings
[NASA-CR-183367] N89-11613

CHRONAR CORP., PRINCETON, N.J.
Amorphous silicon photovoltaic devices prepared by chemical and photochemical vapor deposition of higher order silanes
[DE88-001189] N89-11311

CHUBU INST. OF TECH., KASUGAI (JAPAN).
Power absorption and confinement studies of ICRF-heated plasma in JIPP T-IIU tokamak
[IPPJ-886] N89-11547

CITY UNIV. OF NEW YORK, N.Y.
Topologically related quantities in turbulent flows
N89-11173
Periodically structured multiphase flows and hydrodynamic instabilities in narrow capillaries
[DE88-015608] N89-11181

COLLEGE OF WILLIAM AND MARY, WILLIAMSBURG, VA.
Theoretical plasma physics
[DE88-014285] N89-11518

COLORADO UNIV., BOULDER.
The Propagation Information Center at the University of Colorado N89-11094
Lattice algorithms for computing QR and Cholesky factors in the least squares theory of linear prediction
[AD-A196454] N89-11432
Periodic solutions of the Hamilton-Jacobi equation by the shooting method: A technique for beam dynamics
[DE88-012733] N89-11460

COLUMBIA UNIV., NEW YORK, N.Y.
Response of discretely stiffened structures and transmission of structure-borne noise N89-11270
Automatic concept formation in a rich input domain
[AD-A196719] N89-11445

COMISION NACIONAL DE ENERGIA ATOMICA, BUENOS AIRES (ARGENTINA).
Influence of martensitic phase in abrasion behaviour of stainless steel 304 L
[DE88-702770] N89-11009

COMMISSARIAT A L'ENERGIE ATOMIQUE, GIF-SUR-YVETTE (FRANCE).
Nuclear processes in the early universe. Part 1: The thermal history of matter N89-11639
Nuclear processes in the early universe. Part 2: The cosmic quark-hadron phase transition N89-11640

COMMISSION OF THE EUROPEAN COMMUNITIES (LUXEMBOURG).
Exploitation and utilization of hydrocarbons
[DE88-012626] N89-11048
Benchmark study of shear buckling of a cylindrical vessel
[PB88-125315] N89-11257

CONNECTICUT UNIV., STORRS.
Atomic processes in high temperature plasmas
[DE88-013005] N89-11525

CONTINUOUS ELECTRON BEAM ACCELERATOR FACILITY, NEWPORT NEW, VA.
Pseudo-scalar pi N coupling and relativistic proton-nucleus scattering
[NASA-TM-101199] N89-11498
Electroproduction of baryon resonances aboce the delta(1232)
[CEBAF-PR-88-012] N89-11499

CONTROL DYNAMICS CO., HUNTSVILLE, ALA.
Tether applications
[NASA-CR-179392] N89-10934

CORNELL UNIV., ITHACA, N.Y.
The pair potential approach for interfaces: Fundamental problems and practical solutions
[DE88-009165] N89-11456
The next decades of space astronomy N89-11655

COUNCIL FOR NATIONAL ACADEMIC AWARDS (ENGLAND).
Developing laminar flow and heat transfer in ducts of arbitrary cross section N89-11176

COWEETA HYDROLOGIC LAB., OTTO, N.C.
Markers of air pollution in forests: Nutrient cycling
[DE88-011011] N89-11319

D

DANISH RESEARCH CENTER FOR APPLIED ELECTRONICS, HOERSHOLM.
Olympus beacon receiver N89-11093

DARTMOUTH COLL., HANOVER, N.H.
Interference by rain scatter N89-11084

DAYTON UNIV., OHIO.
Dielectric millimeter waveguides. Volume 1
[AD-A196844] N89-11112

DCS CORP., ALEXANDERIA, VA.
Parametric analysis of map data
[AD-A196908] N89-11298

DEFENCE RESEARCH ESTABLISHMENT VALCARTIER (QUEBEC).
Verification of EOSAEL (Electro-Optical Systems Atmospheric Effects Library) snow transmittance predictions
[DREV-R-4423/87] N89-11099

DEFENSE INTELLIGENCE AGENCY, WASHINGTON, D.C.
Bibliography of Soviet laser developments, number 87, January - February 1987
[AD-A196973] N89-11223

DEFENSE LOGISTICS AGENCY, ALEXANDRIA, VA.
State-of-the-art-dehumidification cost-effective corrosion prevention
[AD-A196503] N89-11023

DELTA-T, LEBANON, PA.
GAS-611 firefly in zero gravity N89-10912

DEPARTMENT OF DEFENCE, CANBERRA (AUSTRALIA).
Some statistical aspects of attrition studies
[AD-A196665] N89-10891

DESERT RESEARCH INST., RENO, NEV.
An inertial velocity reference for the NASA airborne Doppler lidar
[NASA-CR-179378] N89-11203

DEUTSCHE FORSCHUNGS- UND VERSUCHSANSTALT FUER LUFT- UND RAUMFAHRT, BRUNSWICK (WEST GERMANY).
Investigation of wake vortices of landing aircraft at Frankfurt airport (Federal Republic of Germany)
[DFVLR-MITT-88-15] N89-10862
PRIMEL: A preprocessor for the analysis of laminated composites. Introduction and user's guide (operation system OS/VS2 (MVS))
[DFVLR-MITT-88-14] N89-10956

DEUTSCHE FORSCHUNGS- UND VERSUCHSANSTALT FUER LUFT- UND RAUMFAHRT, COLOGNE (WEST GERMANY).
Future MAUS payload and the TWIN-MAUS configuration N89-10906

DEUTSCHE FORSCHUNGS- UND VERSUCHSANSTALT FUER LUFT- UND RAUMFAHRT, OBERPFAFFENHOFEN (WEST GERMANY).
The DFVLR models 1 and 2 of the Manutec r3 robot
[DFVLR-MITT-88-13] N89-11443
Dynamic robot models using the Manutec r3 as an example
[DFVLR-MITT-88-16] N89-11444

DEUTSCHE FORSCHUNGS- UND VERSUCHSANSTALT FUER LUFT- UND RAUMFAHRT, STUTTGART (WEST GERMANY).
Development, construction, and operation of a 30/100-kW Wind Energy Converter (WEC)
[DFVLR-MITT-88-06] N89-11318

DIRECTION DES RECHERCHES ETUDES ET TECHNIQUES, PARIS (FRANCE).
Atomic probe study of ordering and precipitation in nickel-based alloys N89-10993

DREXEL UNIV., PHILADELPHIA, PA.
A theory of surface and interface electronic properties of crystalline solids: Applications to 2-6 compounds
N89-11596

DUKE UNIV., DURHAM, N. C.
Integration of knowledge on the response of vegetation to rising CO2
[DE88-014740] N89-11326

DURHAM UNIV. (ENGLAND).
Real-time path planning for robot arms N89-11224

E

EAGLE ENGINEERING, INC., WEBSTER, TEX.
Risk analysis of earth return options for the Mars rover/sample return mission
[NASA-CR-172081] N89-10923

EAST ANGLIA UNIV., NORWICH (ENGLAND).
An investigation of information systems prototyping
N89-11622

ECOLE POLYTECHNIQUE, MONTREAL (QUEBEC).
Dynamic analysis of spherical shells: A hybrid method
[EPM/RT-88/23] N89-11264

EDGERTON, GERMESHAUSEN AND GRIER, INC., IDAHO FALLS, IDAHO.
Joining of advanced aluminides
[DE88-015111] N89-11226
Electric vehicle auxiliary power source evaluation
[DE88-015359] N89-11238
EDINBURGH UNIV. (SCOTLAND).
ENGEN: An intermediate language to HILO extension of the FIRST silicon compiler, executive summary
[ESA-CR(P)-2621] N89-11422
EDUCATIONAL TESTING SERVICE, PRINCETON, N. J.
Scale drift in on-line calibration
[AD-A196439] N89-11404
EG AND G ENERGY MEASUREMENTS, INC., GOLETA, CALIF.
Preparation and evaluation of mercuric iodide for crystal growth
[DE88-014981] N89-11578
Modified purification of mercuric iodide for crystal growth
[DE88-014960] N89-11580
EG AND G WASHINGTON ANALYTICAL SERVICES CENTER, INC., MORGANTOWN, W. VA.
On the constitutive relation for frictional flow of granular materials
[DE88-001089] N89-11171
EIDGENOESSISCHES INST. FUER REAKTORFORSCHUNG, WUERENLINGEN (SWITZERLAND).
Lattice instability in single-crystal La(sub 2-x)Sr(sub x)/CuO4
[DE88-013994] N89-11598
ELECTRICITE DE FRANCE, CLAMART.
Workshops and problems for benchmarking eddy current codes
[DE88-009996] N89-11098
ELECTRONIQUE SERGE DASSAULT, ST. CLOUD (FRANCE).
A highly reliable computer for airborne applications
N89-10833
ELECTROTECHNICAL LAB., SAKURA (JAPAN).
Molecular beam epitaxy of GaP films on Si substrates
[PB88-131974] N89-11581
ENERSCOPE, INC., GLENDALE, ARIZ.
Advanced desiccant materials assessment, phase 2
[PB88-217054] N89-11033
ESSEN UNIV. (WEST GERMANY).
Further investigations on new fluid working systems for absorption heat pumps
[DE88-012622] N89-11151
ETABLISSEMENT TECHNIQUE CENTRAL DE L'ARMEMENT, ARCUEIL (FRANCE).
Plasma spectrometry applied to surface treatments (laser PVD)
[ETCA-88-R-036] N89-11533
EUROPEAN SOUTHERN OBSERVATORY, GARCHING (WEST GERMANY).
Supernova 1987A in the large magellanic cloud
N89-11642
EUROPEAN SPACE AGENCY, PARIS (FRANCE).
Determination of characteristic radiation properties of a torus antenna
[ESA-TT-1106] N89-11105
Securing the time scale of the NAVEX reference clock and rate determinations by time comparisons with the help of the Global Positioning System (GPS)
[ESA-TT-1111] N89-11197
Nonlinear control of an H2O2 steam reactor
[ESA-TT-902] N89-11242
Space science and fundamental physics
[ESA-SP-283] N89-11638
Fundamental science in ESA's space science program
N89-11654
EUROPEAN SPACE AGENCY. EUROPEAN SPACE RESEARCH AND TECHNOLOGY CENTER, ESTEC, NOORDWIJK (NETHERLANDS).
OPEX: (Olympus Propagation EXperiment)
N89-11090

F

FEDERAL AVIATION AGENCY, ATLANTIC CITY, N.J.
Longitudinal impact test of a transport airframe section
[DOT/FAA/CT-87/26] N89-11265
Evaluation of enhancements to the Low Level Wind Shear Alert System (LLWAS) at Stapleton International Airport
[DOT/FAA/PS-88/14] N89-11356
FERMI NATIONAL ACCELERATOR LAB., BATAVIA, ILL.
Thermophysical properties of argon. Addendum
[DE88-012722] N89-10966
On the locality of the no hair conjection and the measure of the universe
[NASA-CR-183365] N89-11489
Gauged Q-balls
[NASA-CR-183369] N89-11500
The decay of highly excited open strings
[NASA-CR-183364] N89-11501
Cosmic strings and superconducting cosmic strings
[NASA-CR-183361] N89-11604
Cosmic strings
[NASA-CR-183367] N89-11613
Inflation in a renormalizable cosmological model and the cosmic no hair conjecture
[NASA-CR-183363] N89-11614
On relative supernova rates and nucleosynthesis roles
[NASA-CR-183373] N89-11673
Phase transitions as the origin of large scale structure in the universe
[NASA-CR-183359] N89-11674
Photoerosion and the abundances of the light elements
[NASA-CR-183372] N89-11675
FLORIDA STATE UNIV., TALLAHASSEE.
Effects of a ground vortex on the aerodynamics of an airfoil N89-10855
The melting and crystallization kinetics of hydrogenated polybutadiene
[AD-A196986] N89-11045
FLORIDA UNIV., GAINESVILLE.
X-ray scattering studies of non-equilibrium ordering processes
[DE88-012908] N89-11569
Implantation studies of hydrogen by field ion microscopy and spectroscopy
[DE88-015806] N89-11602
FOREIGN RESOURCES ASSOCIATES, AUSTIN, TEX.
A method for improving the depth of penetration and the appearance of welding
[DE88-012954] N89-11239
FUJITSU LTD., KAWASAKI (JAPAN).
Development of Bio-GAS systems N89-10904

G

GALILEO ELECTRO-OPTICS CORP., STURBRIDGE, MASS.
Curved channel MCP improvement program
[NASA-CR-180790] N89-11191
GENERAL ATOMIC CO., SAN DIEGO, CALIF.
The steady states of the Kuramoto–Sivashinsky equation
[DE88-011819] N89-11451
GENERAL DYNAMICS CORP., SAN DIEGO, CALIF.
Development of a verification program for deployable truss advanced technology
[NASA-CR-181703] N89-10936
GENERAL DYNAMICS/FORT WORTH, TEX.
Unsteady low-speed windtunnel test of a straked delta wing, oscillating in pitch. Part 1: General description and discussion of results
[AD-A196456] N89-10867
GENERAL ELECTRIC CO., CINCINNATI, OHIO.
Sensors for ceramic components in advanced propulsion systems: Summary of literature survey and concept analysis, task 3 report
[NASA-CR-180900] N89-11192
GEORGE WASHINGTON UNIV., WASHINGTON, D.C.
Investigation of the tumbling phenomenon using computer simulation N89-10896
Creep and fracture characteristics of materials and structures at elevated temperatures
[AD-A196831] N89-11289
GEORGIA INST. OF TECH., ATLANTA.
The effect of carbon and boron nitride additions on the fracture toughness of Si3N4
[DE88-013249] N89-11025
Workshops and problems for benchmarking eddy current codes
[DE88-009996] N89-11098
Experimental verification of a model of a two-link flexible, lightweight manipulator
[NASA-CR-183216] N89-11233
On motion planning and control of multi-link lightweight robotic manipulators
[NASA-CR-181226] N89-11234
Delamination buckling of pressure-loaded, laminated cylindrical shells and panels N89-11276
GEORGIA TECH RESEARCH INST., ATLANTA.
Development of an experimental model of self-propagating high temperature oxidation-reduction reactions
[AD-A196978] N89-10987
GRENOBLE-1 UNIV. (FRANCE).
ETIC: A multi-user Computer Aided Design (CAD) database management system
[RR-720-I] N89-11428
Parallelizing recursive programs
[RR-728-I-IMAG-83-LIFIA] N89-11429
Undirected distances and the postman-structure of graphs
[RR-714-M] N89-11470
Equational problems and disunification
[RR-727-I-IMAG-82-LIFIA] N89-11471
On differential polynomials and their resultants
[RR-723-M] N89-11472
Penalized likelihood estimation for rates with censored survival
[RR-726-M] N89-11479
GRONINGEN RIJKSUNIVERSITEIT (NETHERLANDS).
Parallel algorithm for a class of optimization problems
[PB88-209929] N89-11414

H

HAIFA UNIV. (ISRAEL).
Enhancing performance under stress by information about its expected duration
[AD-A196836] N89-11388
HAMPTON INST., VA.
Direct solar-pumped iodine laser amplifier
[NASA-CR-183171] N89-11201
HARRIS CORP., MELBOURNE, FLA.
Fiber optic buses and networks for advanced avionics architectures N89-10836
HARRY DIAMOND LABS., ADELPHI, MD.
The propagation of electromagnetic waves in thin dielectric slabs
[AD-A196995] N89-11115
HARVARD UNIV., CAMBRIDGE, MASS.
Optimization of transparent and reflecting electrodes for amorphous silicon solar cells
[DE88-001175] N89-11316
Low mass X-ray binaries in globular clusters and hierarchical triple systems N89-11660
Shocked interstellar gas in dense molecular clouds
N89-11670
HEIDELBERG UNIV. (WEST GERMANY).
Measurement of the absolute neutron yield of ASDEX with nuclear emulsion plates N89-11537
Calculation of neutron propagation for ASDEX
N89-11539
Numerical simulation of the response function of a nuclear emulsion plate N89-11540
HELSINKI UNIV. OF TECHNOLOGY, ESPOO (FINLAND).
Polarizability and effective permittivity of layered and continuously inhomogeneous dielectric spheres
[PB88-210091] N89-11104
HOUSTON UNIV., TEX.
Growth of plant tissue cultures in simulated lunar soil: Implications for a lunar base CELSS (Controlled Ecological Life Support System)
[NASA-CR-183233] N89-11384
HOWARD UNIV., WASHINGTON, D. C.
IR reflectance and Raman scattering of diamond films
[AD-A196899] N89-11043
Snow cover, snowmelt and runoff in the Himalayan River basins
[NASA-CR-182434] N89-11290
Stochastic theory of frequency redistribution in two-photon processes N89-11669

I

ILLINOIS UNIV., URBANA.
Experimental and theoretical study of inclusions during initiation of crevice corrosion
[DE88-014635] N89-10989
Investigation of a self-lubricating alumina coating formed by anodic spark deposition
[DE88-014947] N89-11035
Shock initiation of explosives with a sensitive rate and related topics
[DE88-008483] N89-11052
Temporal variations in a CW HF MOPA (oscillator/amplifier)
[AD-A196915] N89-11132
Integral manifold in system design with application to flexible link robot control
[AD-A197052] N89-11243
Toward intelligent machine learning algorithms
[AD-A197049] N89-11448
Balance of recurrence order in time-inhomogeneous Markov chains with application to simulated annealing
[AD-A196980] N89-11484
Constraints on the growth of metallic superlattices
[DE88-014833] N89-11586
ILLINOIS UNIV., URBANA-CHAMPAIGN.
Mechanics of hydrogen embrittlement N89-11000
Representing high-level knowledge structures in massively parallel networks N89-11409

INDAL TECHNOLOGIES, INC., MISSISSAUGA (ONTARIO).
A model for the response of vertical axis wind turbines to turbulent flow: Parts 1 and 2
[DE88-014708] N89-11305
INSTITUT DE MECANIQUE DES FLUIDES DE LILLE (FRANCE).
Aircraft crashes on the runway: Development of a super element for nonlinear analysis of a beam
[REPT-87/56] N89-11286
INSTITUT FRANCAIS DU PETROLE, RUEIL-MALMAISON.
Exploitation and utilization of hydrocarbons
[DE88-012626] N89-11048
INSTITUTE FOR DEFENSE ANALYSES, ALEXANDRIA, VA.
Interceptor-to-target allocation strategies for Strategic Defense 1: Adaptive strategies based upon system and threat characteristics
[AD-A197037] N89-11487
Guidelines for tailoring DOD-STD-2167A for SDS (Strategic Defense System) software development
[AD-A197038] N89-11488
INSTITUTE OF GAS TECHNOLOGY, CHICAGO, ILL.
Worldwide survey of absorption fluids data
[DE88-013204] N89-10972
INSTITUTO DE PESQUISAS ENERGETICAS E NUCLEARES, SAO PAULO (BRAZIL).
Spectrography analysis of stainless steel by the point to point technique
[DE88-702302] N89-10992
INSTITUTO DE PESQUISAS ESPACIAIS, SAO JOSE DOS CAMPOS (BRAZIL).
Magnetic moment test report for the model SAR 8108 battery
[INPE-4574-NTE/280] N89-11121
Analysis of nonlinear circuits at RF and microwave frequencies by the harmonic balance method
[INPE-4693-TDL/342] N89-11126
Observations of southern irregular variables
[INPE-4568-PRE/1309] N89-11291
Technique for obtaining agricultural property boundaries through satellite imagery, certified to control and accompany agricultural activity
[INPE-4640-PRE/1351] N89-11294
Training activities in remote sensing at the Instituto de Pesquisas Espaciais-INPE/Brazil
[INPE-4686-PRE/1380] N89-11295
Spectral studies of three oxisols and a Ultisol of Brazil
[INPE-4644-PRE/1355] N89-11297
CIR aerial photography applied to the evaluation of the air pollution impact in a tropical forest: The case of Cubatao, Brazil
[INPE-4651-PRE/1358] N89-11324
Ozone hole of the Antarctica: Recent results
[INPE-4518-PRE/1270] N89-11329
Carbon monoxide measurements in different Brazilian ecosystems
[INPE-4668-PRE/1368] N89-11331
Algorithm for the study of particle movement in the inner magnetosphere of the earth
[INPE-4669-PRE/1369] N89-11351
Development of a semi-empirical model for estimating the global solar radiation
[INPE-4620-TDL/328] N89-11352
A study of wind profiles under quasi-neutral and inversion atmospheric conditions, over a terra firma forest
[INPE-4694-RPE/575] N89-11369
Color enhancement of remote sensing imagery using IHS transformations and decorrelation stretch methods
[INPE-4559-PRE/1300] N89-11418
The checkout system software for the Brazilian satellite
[INPE-4571-PRE/1311] N89-11419
Concerning the use of the minimum mean asymmetry as the validation criteria for clustering
[INPE-4654-PRE/1361] N89-11427
SOPMCR: An operating system for the multiprocessor for communication networks
[INPE-4675-NTE/284] N89-11438
Implementation of MAGINT code on the CDC-CYBER-170/750 system
[INPE-4663-NTE/282] N89-11491
Flux method for the field dependent transport through multilayer devices
[INPE-4647-PRE/1357] N89-11559
Concerning interfaces in natural languages
[INPE-4681-PRE/1376] N89-11634
INSTRUMENTATION TECHNOLOGY ASSOCIATES, INC., MALVERN, PA.
Acceleration ground test program to verify GAS payload No. 559 structure/support avionics and experiment structural integrity N89-10913
INTERNATIONAL CENTRE FOR THEORETICAL PHYSICS, TRIESTE (ITALY).
Temperature dependence of entropies and specific heats of liquid Na and K
[DE88-702986] N89-10976
Unsteady hydromagnetic free-convection flow with radiative heat transfer in a rotating fluid. 1: Incompressible optically thin fluid
[DE88-702998] N89-11140
Unsteady hydromagnetic free-convection flow with radiative heat transfer in a rotating fluid of arbitrary optical thickness
[DE88-703000] N89-11167
Unsteady hydromagnetic free-convection flow with radiative heat transfer in a rotating fluid. 2: Compressible optically thin fluid
[DE88-702999] N89-11168
Geometric gauge theory of metric defects
[DE88-702961] N89-11269
Basic theory of desertification
[DE88-703014] N89-11320
Method for predicting monthly rainfall patterns
[DE88-703005] N89-11363
General complex-analytic structures in uniform algebra spectra: A survey
[DE88-703010] N89-11450
Inner product for a Banach-algebra
[DE88-703156] N89-11465
Quasi-adequate semigroups
[DE88-703157] N89-11466
Second order parabolic equations for flow-domains
[DE88-703158] N89-11467
On equivariant Lagrangians
[DE88-703167] N89-11468
On hydromagnetic channel flow induced by tooth pulses
[DE88-703031] N89-11522
Simple model for the superconducting phase diagram near the metal-insulator transition
[DE88-703038] N89-11558
Possible coexistence of antiferromagnetism and superconductivity in the Hubbard model
[DE88-703025] N89-11561
Effect of surface states on the electrochemical behaviour of single crystal n-ZnSe photoelectrode
[DE88-702726] N89-11566
Superconductivity, structures, ESR and SIMS-analysis of a high-T(sub c)Y(sub 0.33)Ba(sub 0.67)Cu(sub 2.33)O(sub 3.67-sigma) compound
[DE88-702677] N89-11583
Elastic and anelastic behaviour of icosahedral quasicrystals
[DE88-702712] N89-11588
Pair potential trend of alkali metals under external pressure
[DE88-702973] N89-11593
New quantum interferometer effect in superconducting oxide ceramics
[DE88-703152] N89-11603
Planck's orders of magnitude and the limits of the quantum gravity conception
[DE88-702985] N89-11608
Quantization of Green-Schwarz superstring
[DE88-702242] N89-11609
Inhomogeneities in a Friedmann universe
[DE88-702981] N89-11672
IOWA STATE UNIV. OF SCIENCE AND TECHNOLOGY, AMES.
Ultrasonic flaw classification: An approach using modeling, signal processing, and adaptive learning N89-11248
IOWA UNIV., IOWA CITY.
Wave-particle interactions in the magnetosphere of Uranus
[NASA-CR-183299] N89-11678

J

JET PROPULSION LAB., CALIFORNIA INST. OF TECH., PASADENA.
The first Chinese student space shuttle getaway special program N89-10903
Outward to the beginning: The CRAF and Cassini Missions of the Mariner Mark 2 program
[NASA-CR-183133] N89-10921
Space science/space station attached payload pointing accommodation study: Technology assessment white paper
[NASA-CR-182735] N89-10931
The state-of-the-art of dc power distribution systems/components for space applications
[NASA-CR-182743] N89-10941
Multicolor pyrometer for materials processing in space
[NASA-CR-183189] N89-11057
Proceedings of the Twelfth NASA Propagation Experimenters Meeting (NAPEX 12)
[NASA-CR-182796] N89-11074
PiFEx propagation experiments N89-11075
PiFEx data and archival formats N89-11076
Laser communications through the atmosphere N89-11087
Space-based multifunctional end effector systems functional requirements and proposed designs
[NASA-CR-180390] N89-11237
Environmental projects. Volume 7: Environmental resources document
[NASA-CR-182736] N89-11328
Knowledge-based diagnosis for aerospace systems
[NASA-CR-182641] N89-11441
Calculating the CEP (Circular Error Probable)
[NASA-CR-182996] N89-11475
The deep space network: An instrument for radio astronomy research
[NASA-CR-182744] N89-11661
JOHNS HOPKINS UNIV., BALTIMORE, MD.
Laser speckle photography and decorrelation techniques in elastic-plastic fracture studies N89-11275
JOHNS HOPKINS UNIV., LAUREL, MD.
Results of 1987 MSS helicopter propagation experiment at UHF and L band in Central Maryland N89-11077
Results of APL rain gauge network measurements in mid-Atlantic coast region and comparisons of distributions with CCIR models N89-11083
JOINT INST. FOR ADVANCEMENT OF FLIGHT SCIENCES, WASHINGTON, D. C.
Program of research in structures and dynamics
[NASA-CR-183191] N89-10838
JOINT INST. FOR NUCLEAR RESEARCH, DUBNA (USSR).
Hydrodynamical characteristics of helium two-phase flows at relatively high mass rates
[DE88-702936] N89-11143
Autocompensation device for ultralow temperature measurements
[DE88-702900] N89-11194
Collective resonance fluorescence in an intense laser field with phase and amplitude fluctuations
[DE88-702920] N89-11205
Optimization of the two-dimensional magnetic field distribution basing on the integral equation method
[DE88-702940] N89-11490
Current-induced quantum interference in the composite superconductor NbTi-Cu
[DE88-703079] N89-11562
JOINT PUBLICATIONS RESEARCH SERVICE, ARLINGTON, VA.
JPRS Report: Science and Technology. USSR: Materials Science
[JPRS-UMS-88-007] N89-11002
Methodology of flexural fatigue testing composite materials produced by electron-beam evaporation N89-11003
Characteristics of laser beam focusing with single spherical mirrors during laser treatment N89-11004
Effect of protective coatings on life of heat-resistant nickel steel under cyclic heat load N89-11005
Alloying of metals by teatment with nanosecond laser pulses N89-11006
JPRS report: Science and technology: Japan
[JPRS-JST-87-018] N89-11061
Development of transparent zirconia ceramics discussed N89-11062
Research on catalyst combustion for gas turbine N89-11063
Good performance of LE-7 liquid oxygen turbopump confirmed N89-11064
Cascade flow analysis by Navier-Stokes equation N89-11065
Payload boomerang technology described N89-11066
Numerical simulation of transonic flow around Asuka N89-11067
New trial of vibration testing method N89-11068
CAD wind tunnel test for half-cut model of Asuka N89-11069
JPRS report: Science and technology. USSR: Life sciences
[JPRS-ULS-87-010] N89-11385
Individual differences in adaptation to hypoxia and cold based on emotional-behavioral criterion of bodily reactivity N89-11386

K

KAPTEYN ASTRONOMICAL LAB., GRONINGEN (NETHERLANDS).
Dark matter N89-11652

KATHOLIEKE UNIVERSITEIT, NIJMEGEN (NETHERLANDS).
Accessibility, a criterion for the choice of visual coding rules
[PB86-209911] N89-11458
KENT UNIV., CANTERBURY (ENGLAND).
Dust detection systems for cometary encounter
N89-11680
KENTUCKY UNIV., LEXINGTON.
A new determination of extinction due to atmospheric aerosols and the resulting implications for upper stratospheric ozone depletion N89-11348
KERNFORSCHUNGSANLAGE, JUELICH (WEST GERMANY).
Ti-implanted optical waveguides in LiNbO3
[DE88-015279] N89-11554
KERNFORSCHUNGSZENTRUM, KARLSRUHE (WEST GERMANY).
Studies of the transpassive nitric acid corrosion of various austenitic CrNi steels in the prolonged Huey test (65 percent HNO3, 120 C, 720 h)
[DE88-010494] N89-10998
KING RESEARCH, INC., ROCKVILLE, MD.
Evaluating the effectiveness of information use
N89-11626
Evaluating the performance of information centre staff
N89-11629
Evaluating performance of information centre operations and services N89-11630
A framework for evaluating the effectiveness of information centres and services N89-11631
KMS FUSION, INC., ANN ARBOR, MICH.
Measurement of glass shell buckling strength using a piezoelectric film sensor
[DE88-013016] N89-11280
KCl bounce coating of glass and polymer microshells
[DE88-013018] N89-11524

L

LAMONT-DOHERTY GEOLOGICAL OBSERVATORY, PALISADES, N.Y.
Recent climate change in North America and CO2: Search in stratified daily data
[DE88-014869] N89-11323
LAWRENCE LIVERMORE NATIONAL LAB., CALIF.
Review of the space shuttle propulsion pressurization system probabilistic risk assessment
[DE88-013163] N89-10928
A novel approach to abrasion resistance
[DE88-014180] N89-10949
Fluid mechanical properties of flames in enclosures
[DE88-014142] N89-10981
Developments and trends in electrodeposition
[DE88-009822] N89-11014
Survivability of coatings: Program review
[DE88-009863] N89-11031
The initiation and detonation of explosives: An alternative concept
[DE88-014199] N89-11047
Role of deflagration in explosive response
[DE88-014139] N89-11049
A detailed chemical kinetic reaction mechanism for the oxidation of iso-octane and n-heptane over an extended temperature range and its application to analysis of engine knock
[DE88-005370] N89-11053
Engineering research and development: Thrust area report, FY87
[DE88-013792] N89-11059
Through-the-earth communication: Experiment results from Billie Mine and Mississippi Chemical Mine
[DE88-013162] N89-11072
Statistical effects in high-power microwave beam propagation
[DE88-012440] N89-11100
Godunov methods and adaptive algorithms for unsteady fluid dynamics
[DE88-013094] N89-11141
Application of a second-order projection method to the study of shear layers
[DE88-013095] N89-11166
Numerical estimates of the rate of convergence for the vortex sheet method
[DE88-013809] N89-11178
Other properties of free electron lasers: Harmonics and optical guiding
[DE88-014161] N89-11199
The Electron Laser Facility: Measurement of modes, harmonics, parametric dependence, and phase shift
[DE88-014165] N89-11200
PALADIN: A 10.6-micron free-electron laser amplifier
[DE88-014164] N89-11207
An introduction to the physics of high gain free electron lasers
[DE88-014163] N89-11208
Overview of FEL (Free-Electron Laser) development with induction linacs at LLNL
[DE88-014179] N89-11210
Experiments in the application of ultrasound diffraction tomography for nondestructive testing
[DE88-014694] N89-11245
Atmospheric and Geophysical Sciences Division
[DE88-013780] N89-11346
Guidelines for using TIPSFD for 3D finite-difference mesh generation
[DE88-012451] N89-11417
Allocating and launching MaRV interceptors based on miss distance predictions
[DE88-015370] N89-11486
The effect of vapor incidence angle upon thin film columnar growth
[DE88-014396] N89-11577
Low temperature measurements on UBe13
[DE88-014446] N89-11594
Photoerosion and the abundances of the light elements
[NASA-CR-183372] N89-11675
LEEDS UNIV. (ENGLAND).
Kinetics of boron hydride interconversion reactions
[AD-A196824] N89-10985
LEHIGH UNIV., BETHLEHEM, PA.
Spatial distribution of acoustic intensity in reverberant fields N89-11493
The transformative compression of coherent languages N89-11623
LITTLE (ARTHUR D.), INC., CAMBRIDGE, MASS.
Evaluation of vapor compression cycles using nonazeotropic refrigerant mixtures
[DE88-013225] N89-11169
LOCKHEED MISSILES AND SPACE CO., PALO ALTO, CALIF.
Numerical simulation of axisymmetric base flow on tactical missiles with propulsive jet
[AD-A196169] N89-11136
LOCKHEED MISSILES AND SPACE CO., SUNNYVALE, CALIF.
PV modules for ground testing
[NASA-CR-179476] N89-11315
LOS ALAMOS NATIONAL LAB., N. MEX.
Laboratory investigations of low earth orbit environmental effects on spacecraft
[DE88-009135] N89-10932
Microrheological observations of the onset of non-Newtonian behavior in suspensions
[DE88-006198] N89-10962
Strain hardening at large strains
[DE88-007909] N89-10995
Calorimetry study of the synthesis of amorphous Ni-Ti alloys by mechanical alloying
[DE88-006468] N89-11010
Microstructure and properties of rapidly solidified beryllium-transition metal alloys
[DE88-010937] N89-11012
Shock initiation of explosives with a sensitive rate and related topics
[DE88-008483] N89-11052
Safety aspects of large-scale handling of hydrogen
[DE88-014422] N89-11070
The turbulent heat flux in low Mach number flows with large density variations N89-11162
On 1-D closure models for slender 3-D viscoelastic free jets: von Karman flow geometry and elliptical cross section
[DE88-014478] N89-11179
Laser plume temperature measurements in various gases
[DE88-006482] N89-11204
Development and testing of KITES
[DE88-015057] N89-11336
Study of a substorm on May 4, 1986
[DE88-014318] N89-11342
Association of plasma sheet variations with auroral changes during substorms
[DE88-014319] N89-11350
Parallel processing a real code: A case history
[DE88-014458] N89-11437
High energy-intensity atomic oxygen beam source for low earth orbit materials degradation studies
[DE88-014316] N89-11504
Space Nuclear Safety Program
[DE88-015048] N89-11505
Postanalysis of the CNPS (Compact Nuclear Power Source) critical experiment
[DE88-014322] N89-11506
Critical experiments in support of the CNPS (Compace Nuclear Power Source) program
[DE88-014326] N89-11507
Analysis of SP-100 critical experiments
[DE88-014429] N89-11508
Current new applications of laser plasmas
[DE88-015679] N89-11532
Electrical resistivity of U(sub 1-x)M(sub x)Be13 under pressure
[DE88-014449] N89-11552
Vortex lattices in theory and practice
[DE88-014393] N89-11576
Electrodynamics of single-crystal Eu(sub 2)CuO(sub 4): A boson excitation spectrum
[DE88-014328] N89-11585
Computerized classified document accountability
[DE88-015054] N89-11633
Potential foams and metal foils for cosmic dust capture
[DE88-012960] N89-11665
Extraction of light gasses from Mars or its moons
[DE88-009123] N89-11681
Planetary skin games
[DE88-009161] N89-11682
Particle physics candidates for the cosmion solution to the solar neutrino problem
[DE88-014479] N89-11683
The history of gamma-ray burst observations
[DE88-014390] N89-11685
LOUGHBOROUGH UNIV. OF TECHNOLOGY (ENGLAND).
Full scale wind tunnel tests on a Ford Escort Mk 3
[TT-8802] N89-10846
Finite elements software and applications
N89-11415
Measures, methods and models employed in evaluating the effectiveness of information centers and services
N89-11627
LOUISIANA STATE UNIV., BATON ROUGE.
Coulomb states in atoms and solids
[DE88-013973] N89-11494
LOUISIANA TECH UNIV., RUSTON.
Inorganic chemical precipitate formation payload design N89-10920
LUND UNIV. (SWEDEN).
Transactions of machine elements division: On the combined hydrodynamic and hydrostatic journal bearing
[PB88-214549] N89-11231

M

MARTIN MARIETTA ENERGY SYSTEMS, INC., OAK RIDGE, TENN.
Manual, voice, and automated control of a teleoperator viewing system
[DE88-011835] N89-11235
Ion implantation and thermal annealing of high-T(ssub c) single crystals of YBa2Cu3O(sub x)
[DE88-012201] N89-11564
MARYLAND UNIV., COLLEGE PARK.
Laser wavemeter/spectrometer operating manual
[NASA-CR-180802] N89-11195
Design and analysis of large-scale atmospheric dispersion experiment
[DE88-012911] N89-11330
Fundamental research in applied mathematics
[AD-A193668] N89-11454
Lie algebraic treatment of space charge N89-11496
MASSACHUSETTS INST. OF TECH., CAMBRIDGE.
Flight test results for the Daedalus and Light Eagle human powered aircraft
[NASA-CR-183305] N89-10890
New non-linear optical polymers
[AD-A196859] N89-11040
Polarimetric clutter modeling: Theory and application
[NASA-CR-183348] N89-11106
A coherent VLSI design environment
[AD-A196428] N89-11130
Rheology of high concentration polymodal multiphase flow
[DE88-014541] N89-11148
Understanding bandwidth limitations in robot force control
[AD-A195927] N89-11229
Integration of analysis and experiment for Stirling cycle processes. Part 1: Gas spring hysteresis loss
[DE88-013202] N89-11313
An O(N) algorithm for three-dimensional N-body simulations
[AD-A196903] N89-11433
Communication aspects of parallel processing
[AD-A196458] N89-11439
Computational structure of the N-body problem
[AD-A196422] N89-11473
Abstraction in numerical methods
[AD-A196990] N89-11476

Massachusetts Institute of Technology Plasma Fusion Center 1987--1988 report to the President
[DE88-014800] N89-11519

MATHEMATICAL ANALYSIS RESEARCH CORP., CLAREMONT, CALIF.
Calculating the CEP (Circular Error Probable)
[NASA-CR-182996] N89-11475

MAX-PLANCK-INST. FUER ASTRONOMIE, HEIDELBERG (WEST GERMANY).
Space observations for infrared and submillimeter astronomy N89-11643

MAX-PLANCK-INST. FUER EXTRATERRESTRISCHE PHYSIK, GARCHING (WEST GERMANY).
HIEN-LO: An experiment for charge determination of cosmic rays of interplanetary and solar origin N89-10908
Activity report of the Max-Planck-Institut fuer Physik und Astrophysik
[MPE-200] N89-11688

MAX-PLANCK-INST. FUER PHYSIK UND ASTROPHYSIK, GARCHING (WEST GERMANY).
Search for narrow resonance production in Bhabha scattering at center-of-mass energies near 1.8 MeV
[MPE-PAE/EXP-EL-190] N89-11502
Physics and astrophysics of gravitational waves N89-11647
Cosmological puzzles N89-11650

MAX-PLANCK-INST. FUER PLASMAPHYSIK, GARCHING (WEST GERMANY).
ASDEX contributions to the DPG Fruehjahrstagung
[IPP-III/134] N89-11534
Charge exchange spectroscopy (CXRS) of highly ionized ions in ASDEX N89-11535
Spectroscopic measurement of the ion temperature on ASDEX N89-11536
Interpretation of neutron rate measurements using the NR code N89-11538
Measurements of proton and triton spectra in ASDEX discharges N89-11541
Advantages of a helium beam for active charge exchange diagnostics N89-11542
Simultaneous background measurement in the ASDEX neutral particle diagnostics N89-11543

MAX-PLANCK-INST. FUER QUANTENOPTIK, MUNICH (WEST GERMANY).
The detection of gravitational radiation N89-11648

MAX-PLANCK-INST. FUER RADIOASTRONOMIE, BONN (WEST GERMANY).
Very Long Baseline Interferometry (VLBI) from ground and space N89-11645

MAX-PLANCK-INSTITUT FUER STROEMUNGSFORSCHUNG, GOETTINGEN (WEST GERMANY).
The gas dynamics of fluids of high specific heat
[MPIS-89-1987] N89-11186

MECHANICAL TECHNOLOGY, INC., LATHAM, N. Y.
Development of a residential free-piston Stirling engine heat pump
[DE88-012917] N89-11303

MEDICAL COLL. OF VIRGINIA, RICHMOND.
Biological applications and effects of optical masers
[AD-A196462] N89-11217

MESSERSCHMITT-BOELKOW-BLOHM G.M.B.H., MUNICH (WEST GERMANY).
Computing system configuration for fighter aircraft flight control systems N89-10832

MICHIGAN STATE UNIV., EAST LANSING.
Interaction of electromagnetic waves with heterogeneous bodies of arbitrary shape and parameters N89-11095
Models for parallel computation on distributed-memory multiprocessors
[DE88-010078] N89-11436

MICHIGAN TECHNOLOGICAL UNIV., HOUGHTON.
Structure of wind-shear turbulence
[NASA-CR-183257] N89-11359
Theory of defects in non-metallic solids
[DE88-013075] N89-11567

MICHIGAN UNIV., ANN ARBOR.
Technique for measuring the dielectric constant of thin materials
[NASA-CR-183325] N89-10984
The role of grain boundary character in the environmentally-assisted intergranular cracking mechanism of nickel-base alloys
[DE88-014130] N89-11018
Effect of curvature on the backscattering from leaves
[NASA-CR-183326] N89-11296

MIDWEST RESEARCH INST., GOLDEN, COLO.
National Photovoltaics Program: 1987 program review
[DE88-001148] N89-11301
Ternary adamantine materials for low-cost solar cells
[DE88-001160] N89-11302
A limited assessment and characterization of the solar radiation energy resources in the Caribbean region
[DE88-001133] N89-11312

MINISTRY OF POSTS AND TELECOMMUNICATIONS, KASHIMA (JAPAN).
ETS-V propagation experiments in Japan N89-11080
Plan of propagation and communication experiments using ETS-VI N89-11088

MINISTRY OF POSTS AND TELECOMMUNICATIONS, TOKYO (JAPAN).
Plan of advanced satellite communications experiment using ETS-VI N89-11089

MINNESOTA UNIV., MINNEAPOLIS.
Variational transition state theory
[DE88-013756] N89-10959
Corrosion phenomena during overcharge in polymer electrolyte cells
[AD-A196997] N89-11134
Lithium secondary batteries: Role of polymer cathode morphology
[AD-A196998] N89-11135
The impact of separated flow on heat and mass transfer
[DE88-014653] N89-11180
Finite element analysis of large strain elastic-plastic solids N89-11281
Microwave radiances from horizontally finite, vertically structured precipitating clouds N89-11364

MISSOURI UNIV., ROLLA.
Measurements and predictions of mixed convection in laminar and turbulent boundary layer flows N89-11164
Continuum modeling of latticed structures N89-11253

MITRE CORP., BEDFORD, MASS.
Software management metrics
[AD-A196916] N89-11434

MITRE CORP., MCLEAN, VA.
Los Alamos XUV free electron laser proposal
[DE88-013485] N89-11211

MITSUBISHI ATOMIC POWER INDUSTRIES, INC., TOKYO (JAPAN).
Workshops and problems for benchmarking eddy current codes
[DE88-009996] N89-11098

MONTANA COLL. OF MINERAL SCIENCE AND TECHNOLOGY, BUTTE.
Three dimensional gravity modeling techniques with application to the Ennis Geothermal Area, part 1
[DE88-014952] N89-11340

MOUND LAB., MIAMISBURG, OHIO.
Glass-ceramic fusion with a CO2 laser
[DE88-012871] N89-11030
Friction and impact sensitivities of explosives: A comparative study
[DE88-012864] N89-11051
High-speed photography of energetic materials and components with a copper vapor laser
[DE88-012869] N89-11212

N

NAGOYA UNIV. (JAPAN).
Theory of high power cyclotron resonance heating in non-uniform magnetic field
[IPPJ-875] N89-11520
Comparison between Uramoto type and straight filament type sheet plasmas as a volume produced H(-) ion source (I)
[IPPJ-876] N89-11523
Excitation of MHD surface waves propagating with shear Alfven waves in an inhomogeneous cylindrical plasma
[IPPJ-872] N89-11526
Modelling of the 2-dimensional structure and impurity transport for a scrape-off layer with a solid limiter
[IPPJ-873] N89-11527
Development of the work function monitoring method for a converter of a negative ion source
[IPPJ-880] N89-11529
Monte Carlo study of ion cyclotron resonance heating in helical systems
[IPPJ-884] N89-11544
Trapping and acceleration of electron by elliptically polarized electromagnetic wave propagating across static magnetic field
[IPPJ-885] N89-11545
Optimization of bootstrap current in a large helical system with L = 2
[IPPJ-889] N89-11546
Power absorption and confinement studies of ICRF-heated plasma in JIPP T-IIU tokamak
[IPPJ-886] N89-11547
Comparison between Uramoto type and straight filament type sheet plasma as a volume produced H(-) ion source (2)
[IPPJ-887] N89-11548
Space and time resolved measurements of ion temperature with the CVI 5292 A charge exchange recombination line after substracting background radiation
[IPPJ-888] N89-11549

NATIONAL ACADEMY OF SCIENCES - NATIONAL RESEARCH COUNCIL, WASHINGTON, D. C.
Review of aeronautical wind tunnel facilities
[NASA-CR-183057] N89-10897
Geothermal energy technology: Issues, R and D needs, and cooperative arrangements
[DE88-011804] N89-11299

NATIONAL AERONAUTICAL LAB., BANGALORE (INDIA).
Tests on 3 NACA 0012 airfoil models of DFVLR in the NAL 0.3 tunnel: An assessment of 2-D wall interference
[TM-AE-8705] N89-10847
Experiments on liquid-vapour phase change between plane liquid surfaces. Part 1: Experiments with water, freon and mercury
[TM-FM-8804-PT-1] N89-10964
Liquid-vapour phase change between plane liquid surfaces: A continuum analysis to determine real gas effects
[TM-FM-8803] N89-10971
Experiments on liquid-vapor phase change between plane liquid surfaces. Part 2: Observations of large temperature jumps near the interfaces
[TM-FM-8805-PT-2] N89-10973
Study of flow past a circular cylinder using a higher order scheme for Navier-Stokes equation
[TM-FM-8806] N89-11142
Adaptive filtering algorithms for communications signal processing
[PD-SE-8808] N89-11410
Comparison of recent model selection criteria for system identification
[PD-SE-8807] N89-11449
An iterative scheme for numerical solution of transonic small perturbation equation
[TM-AE-8801] N89-11455

NATIONAL AERONAUTICS AND SPACE ADMINISTRATION, WASHINGTON, D.C.
Oxidation reduction potential of the Cu(3)/Cu(2) system in alkaline solutions
[NASA-TT-20309] N89-10963
Patent abstracts bibliography: A continuing bibliography (supplement 33). Section 2: Indexes
[NASA-SP-7039(33)] N89-11624
O stars and Wolf-Rayet stars
[NASA-SP-497] N89-11657

NATIONAL AERONAUTICS AND SPACE ADMINISTRATION. AMES RESEARCH CENTER, MOFFETT FIELD, CALIF.
The 1987 Ground Vortex Workshop
[NASA-CP-10008] N89-10849
The characteristics of the ground vortex and its effect on the aerodynamics of the STOL configuration N89-10850
Ground vortex flow field investigation N89-10852
Noise of the Harrier in vertical landing and takeoff N89-10856
Numerical investigation of a jet in ground effect using the fortified Navier-Stokes scheme N89-10857
Aviation technology applicable to developing regions
[NASA-TM-89425] N89-10872

NATIONAL AERONAUTICS AND SPACE ADMINISTRATION. GODDARD INST. FOR SPACE STUDIES, NEW YORK, N.Y.
Derivation of revised formulae for eddy viscous forces used in the ocean general circulation model
[NASA-TM-4060] N89-11381

NATIONAL AERONAUTICS AND SPACE ADMINISTRATION. GODDARD SPACE FLIGHT CENTER, GREENBELT, MD.
The 1988 Get Away Special Experimenter's Symposium
[NASA-CP-3008] N89-10902
CSCP: A new Get Away Special (GAS) project N89-10909
STS safety approval process for small self-contained payloads N89-10910
Systems report for payload G-652: Project origins N89-10911
Utilization of spray on foam insulation for manned and unmanned spacecraft and structures N89-10914
Hitchhiker capabilities N89-10917
The transportation of fine arts materials aboard the space shuttle Columbia. GAS payload No. 481: Vertical horizons N89-10919
An all sky study of fast X-ray transients
[NASA-TM-89716] N89-11686

NATIONAL AERONAUTICS AND SPACE ADMINISTRATION. LYNDON B. JOHNSON SPACE CENTER, HOUSTON, TEX.
Lunar concrete for construction
[NASA-TM-89672] N89-11060

NATIONAL AERONAUTICS AND SPACE ADMINISTRATION. LANGLEY RESEARCH CENTER, HAMPTON, VA.
Experimental results for the Eppler 387 airfoil at low Reynolds numbers in the Langley low-turbulence pressure tunnel
[NASA-TM-4062] N89-10842
An assessment of ground effects determined by static and dynamic testing techniques N89-10854
Performance of a circular body earth-to-orbit winged transport with various strap-on boosters
[NASA-TM-100603] N89-10929
A mixed-mode bending apparatus for delamination testing
[NASA-TM-100662] N89-10945
Tension fatigue analysis and life prediction for composite laminates
[NASA-TM-100549] N89-10951
A comparative overview of modal testing and system identification for control of structures N89-11262
The CSM testbed software system: A development environment for structural analysis methods on the NAS CRAY-2
[NASA-TM-100642] N89-11287
OEXP Analysis Tools Workshop
[NASA-CP-10013] N89-11407
Domain decomposition methods for the parallel computation of reacting flows
[NASA-CR-181719] N89-11459
Pseudo-scalar pi N coupling and relativistic proton-nucleus scattering
[NASA-TM-101199] N89-11498

NATIONAL AERONAUTICS AND SPACE ADMINISTRATION. LEWIS RESEARCH CENTER, CLEVELAND, OHIO.
Three component laser anemometer measurements in an annular cascade of core turbine vanes with contoured end wall
[NASA-TP-2846] N89-10844
Experimental investigation of the performance of a supersonic compressor cascade
[NASA-TM-100879] N89-10858
Experimental aerodynamic performance of advanced 40 deg-swept 10-blade propeller model at Mach 0.6 to 0.85
[NASA-TM-88969] N89-10865
Nuclear propulsion: A vital technology for the exploration of Mars and the planets beyond
[NASA-TM-101354] N89-10944
Laminate behavior for SiC fiber-reinforced reaction-bonded silicon nitride matrix composites
[NASA-TM-101350] N89-10952
Indentation plasticity and fracture in silicon
[NASA-TP-2863] N89-10996
Phase transformations in xerogels of mullite composition
[NASA-TM-101349] N89-11038
Study of optical output couplers for submillimeter wavelength backward-wave oscillators (BWO's)
[NASA-TM-101360] N89-11128
Deposition and characterization of ZnS/Si heterojunctions produced by vacuum evaporation
[NASA-TM-101359] N89-11129
Particle sizing by weighted measurements of scattered light
[NASA-TM-100968] N89-11198
A numerical study of ENO and TVD schemes for shock capturing
[NASA-TM-101355] N89-11469
Use of high temperature superconductors in magnetoplasmadynamic systems
[NASA-TM-101219] N89-11553
A perspective on space exploration technology catalysis: A rationale for initiating 21st Century expansion of human civilization into outer space
[NASA-TM-101362] N89-11637

NATIONAL AERONAUTICS AND SPACE ADMINISTRATION. MARSHALL SPACE FLIGHT CENTER, HUNTSVILLE, ALA.
Power quality load management for large spacecraft electrical power systems
[NASA-TM-100342] N89-11127
Mixing and Demixing Processes in Multiphase Flows With Application to Propulsion Systems
[NASA-CP-3006] N89-11153
The application of single particle hydrodynamics in continuum models of multiphase flow N89-11154
Confined turbulent fluid-particle flow modeling using multiple-realization particle trajectory schemes N89-11157

NATIONAL AEROSPACE LAB., AMSTERDAM (NETHERLANDS).
Fluid science investigations in microgravity
[PB88-209754] N89-11058

NATIONAL AEROSPACE LAB., TOKYO (JAPAN).
High resolution schemes for three-dimensional Euler equations. 1: Estimation of recent TVD schemes
[PB88-214416] N89-10845

NATIONAL AIR AND SPACE MUSEUM, WASHINGTON, D.C.
The next decades of space astronomy N89-11655

NATIONAL BUREAU OF STANDARDS, GAITHERSBURG, MD.
Analysis of free electron laser performance utilizing the National Bureau of Standards' CW microtron
[AD-A196928] N89-11221
Literature review of strengthening methodologies of existing structures
[PB88-218219] N89-11271
Standards conformance testing
[PB89-215645] N89-11412
Structural anomalies in undoped Gallium Arsenide observed in high resolution diffraction imaging with monochromatic synchrotron radiation
[NASA-CR-183268] N89-11595
Computer science and technology: Guide to distributed database management
[PB88-201561] N89-11621

NATIONAL CENTER FOR ATMOSPHERIC RESEARCH, BOULDER, COLO.
National Center for Atmospheric Research
[PB88-220009] N89-11355

NATIONAL HIGHWAY TRAFFIC SAFETY ADMINISTRATION, EAST LIBERTY, OHIO.
Evaluation of the prototype EUROSID dummy and comparison with the US SID (Side Impact Dummies)
[PB88-201934] N89-11389

NATIONAL OCEAN SERVICE, ANCHORAGE, ALASKA.
Beaufort Sea: Information update
[PB88-208616] N89-11380

NATIONAL OCEANIC AND ATMOSPHERIC ADMINISTRATION, BOULDER, COLO.
Ground-based radiometric observations of emission and attenuation at 20.6, 31.65, and 90.0 GHz N89-11086

NATIONAL OCEANIC AND ATMOSPHERIC ADMINISTRATION, SILVER SPRING, MD.
NOAA (National Oceanic and Atmospheric Administration) Meteorology Division support to the Environmental Protection Agency
[PB88-213624] N89-11327

NATIONAL OCEANOGRAPHIC DATA CENTER, WASHINGTON, D. C.
Mariners weather log, volume 32, number 2, Spring 1988
[PB88-210828] N89-11365

NATIONAL RESEARCH INST., BANKURA (INDIA).
The effects of seismic waves, part 2 N89-11254
The effects of seismic waves: Part 1 N89-11268

NATIONAL RESEARCH INST. FOR MATHEMATICAL SCIENCES, PRETORIA (SOUTH AFRICA).
Robust covariance matrix estimation via robust estimation of principal components
[PB88-126594] N89-11478

NATIONAL TELECOMMUNICATIONS AND INFORMATION ADMINISTRATION, BOULDER, COLO.
Millimeter-wave studies N89-11085

NATIONAL TRANSPORTATION SAFETY BOARD, WASHINGTON, D. C.
Aircraft accident/incident summary report, Copperhill, Tennessee, February 22, 1986
[PB88-910407] N89-10868
Aircraft accident reports, brief format, US civil and foreign aviation, issue number 2 of 1987 accidents
[PB88-916906] N89-10871
Aircraft accident report: Executive Air Charter, Inc., dba American Eagle, Flight 5452, CASA C-212, N432CA, Mayaguez, Puerto Rico, May 8, 1987
[PB88-910409] N89-10873

NAVAL ACADEMY, ANNAPOLIS, MD.
Low frequency dielectric properties of polyether electrolytes
[AD-A196494] N89-11039

NAVAL AIR PROPULSION TEST CENTER, TRENTON, N.J.
Statistics on aircraft gas turbine engine rotor failures that occurred in US commercial aviation during 1982
[DOT/FAA/CT-88/23] N89-10892
Experimental guidelines for the design of turbine rotor fragment containment rings
[DOT/FAA/CT-88/21] N89-10893

NAVAL MATERIEL COMMAND, HAAKONSVERN (NORWAY).
GPS signal structure N89-10876
Aiding and integration of a GPS receiver N89-10881

NAVAL POSTGRADUATE SCHOOL, MONTEREY, CALIF.
Ion gun operations at high altitudes
[AD-A196965] N89-10939
Ions generated on or near satellite surfaces
[AD-A196966] N89-10940
Thermodynamic improvements for the space thermoacoustic refrigerator (STAR)
[AD-A196958] N89-11071
Development of a boundary layer control device for tip clearance experiments in an axial compressor
[AD-A196968] N89-11190
Studies of barotropic flow over topography using a galerkin finite element model
[AD-A196516] N89-11353
The climatological seasonal response of the ocean mixed layer in the equatorial and tropical Pacific Ocean
[AD-A196962] N89-11382
Unidirectional Manchester encoded data transfer via a fiber optic link
[AD-A196961] N89-11516

NAVAL RESEARCH LAB., WASHINGTON, D.C.
On the generation of waveforms having comb-shaped spectra
[AD-A196927] N89-11113

NEBRASKA UNIV., LINCOLN.
Probabilistic error model of robot end-effector's dynamic state N89-11236
Comparison of measured and modeled radiation, heat and water vapor fluxes: FIFE pilot study
[NASA-CR-183304] N89-11368

NEW JERSEY INST. OF TECH., NEWARK.
Transverse flexure of an elastic plate loaded through a rigid inclusion N89-11267

NEW YORK UNIV., NEW YORK.
Anomalous transport arising from nonlinear resistive pressure-driven modes in a plasma
[DE88-014984] N89-11531

NEWCASTLE-UPON-TYNE UNIV. (ENGLAND).
The electronic and optical properties of silicon/germanium strained layer superlattices N89-11590

NIPPON ELECTRIC CO. LTD., YOKOHAMA (JAPAN).
Development of experimental systems for material sciences under microgravity N89-10907

NORTH CAROLINA UNIV., CHAPEL HILL.
Measuring the vague meanings of probability terms
[AD-A196944] N89-11483

NORTHROP SERVICES, INC., CORVALLIS, OREG.
Cubic spline smoothing: A useful tool for curve estimation
[PB88-214796] N89-11452

NORTHROP SERVICES, INC., RESEARCH TRIANGLE PARK, N. C.
REFEREE: Bibliographic database manager, documentation
[PB88-200787] N89-11620

NORTHWESTERN UNIV., EVANSTON, ILL.
Self-consistent charge and spin distributions in oxide superconductors
[DE88-012051] N89-11591

NOTRE DAME UNIV., IND.
Migration arising from gradients in shear stress: Particle distributions in Poiseuille flow N89-11159

O

OAK RIDGE NATIONAL LAB., TENN.
Prototype data acquisition and analysis system for Navy operational flight simulators
[DE88-014557] N89-10901
Phase change problem related to thermal energy storage in the manned space station
[DE88-011390] N89-10933
Research needs in high temperature chemistry
[DE88-012929] N89-10961
Photoacoustic spectroscopy and the in situ characterization of the electrochemical interface
[DE88-013848] N89-10975
The thermal resistance of fine powders at atmospheric pressure and under vacuum
[DE88-014556] N89-10982
A preliminary study on the use of magnetohydrodynamic forces to remove impurities from molten metals
[DE88-013508] N89-10991
Microstructural development of titanium-modified austenitic stainless steel under neutron irradiation in HFIR up to 57 dpa
[DE88-013248] N89-10999
Crystallization of Zr-Ni metallic glasses
[DE88-007481] N89-11026
Multistress aging of polymer films
[DE88-008094] N89-11034

Electron attachment properties of excited dielectric-gas molecules and their possible use for pulse power switching
[DE88-009705] N89-11117
An overview of the Stirling engine heat pump program
[DE88-013833] N89-11146
Engine driven heat pump program overview
[DE88-013240] N89-11165
Laboratory examination and seasonal analyses of the dynamic losses for a continuously variable speed heat pump
[DE88-013207] N89-11174
Entrainment enhancement of a supersonic jet for advanced ejectors
[DE88-013200] N89-11177
Impurity-induced changes in interfacial strength and their role in creep fracture
[DE88-013197] N89-11255
Markers of air pollution in forests: Nutrient cycling
[DE88-011011] N89-11319
A composite photobioelectronic material
[DE88-012490] N89-11383
Design of high-reflectivity supermirror structures
[DE88-015287] N89-11511
Electron microscopy of modulated and ordered alloys
[DE88-008667] N89-11584
Dynamic Interactions of Energetic Probes with Condensed Matter: Proceedings
[DE88-008882] N89-11589
Information storage alternatives: An overview of laser-based optical technologies
[DE88-013499] N89-11617

OBSERVATOIRE DE PARIS-MEUDON (FRANCE).
Observations on cosmic abundance of He4 and Li7, comparison with primordial nucleosynthesis predictions N89-11641

OFFICE NATIONAL D'ETUDES ET DE RECHERCHES AEROSPATIALES, PARIS (FRANCE).
Flow around a delta wing with or without a canard (Phi BA = 60 deg). Part 2: Hydrodynamic visualizations in unsteady flow (pitching oscillations)
[ONERA-RT-11/2891-AN-PT-2] N89-10860
Investigations in the nonlinear domain of composite laminate plates subject to compression loads
[ONERA-RT-17/3542-RY-070-R] N89-10953
Nonlinear theories of composite laminates under compression with delamination
[CERT-RT-18/3542-RY-071-R] N89-10954

OFFICE OF NAVAL RESEARCH LIAISON OFFICE, FAR EAST, APO, SAN FRANCISCO, CALIF.
ONR Far East Scientific Bulletin, volume 12, no. 4, October - December 1987
[AD-A194338] N89-11687

OFFICE OF TECHNOLOGY ASSESSMENT, WASHINGTON, D.C.
Defense technology base: Introduction and overview
[PB88-192562] N89-11635

OHIO STATE UNIV., COLUMBUS.
Convective scale selection and the initiation of deep cumulus N89-11341
Rotating and stratified fluids N89-11343
Strongly interacting fermion systems: Emphasis on heavy fermions
[DE88-014127] N89-11573

OHIO WESLEYAN UNIV., DELAWARE.
Functional assessment of laser irradiation
[AD-A196930] N89-11222

OLD DOMINION UNIV., NORFOLK, VA.
Strategies for concurrent processing of complex algorithms in data driven architectures
[NASA-CR-181329] N89-11406

OXFORD UNIV. (ENGLAND).
Tropospheric sounding from the TIROS-N series of satellites N89-11347
Geometrical methods in quantum field theory: On the topology of spaces of holomorphic maps N89-11611

P

PACIFIC NORTHWEST LABS., RICHLAND, WASH.
Near surface chemistry and corrosion behavior of excimer laser surface-melted AISI type 304 stainless steel
[DE88-014440] N89-11019
Resonance ionization of Kr metastables using a single-frequency laser
[DE88-014757] N89-11209
Advanced materials for solid oxide fuel cells: Hafnium-praseodymium-indium oxide system
[DE88-015365] N89-11310
Assessment of methanol electro-oxidation for direct methanol-air fuel cells
[DE88-014686] N89-11317
Acid precipitation in North America: 1985 annual and seasonal data summaries from Acid Deposition System data base
[DE88-013563] N89-11325
The PNL single-tower measurement model of rotationally sampled turbulent wind, with user's guide for STRS2PC
[DE88-013166] N89-11360
Quantitative Luminescence Imaging System description and user's manual
[DE88-015604] N89-11512

PAGE (R. J.) CO., SANTA ANA, CALIF.
Preliminary design study of hydrogen and ammonia resistojets for prime and auxiliary thrusters
[NASA-CR-182176] N89-10943

PANAMETRICS, INC., WALTHAM, MASS.
Fabricate, calibrate and test a dosimeter for integration into the CRRES (Combined Release and Radiation Effects Satellite) satellite
[AD-A196496] N89-10938

PENNSYLVANIA STATE UNIV., STATE COLLEGE.
Summary of an experimental investigation on the ground vortex N89-10851

PENNSYLVANIA STATE UNIV., UNIVERSITY PARK.
Reynolds stress closure in jet flows using wave models
[NASA-CR-180226] N89-10843
Transition metal mediated transformations of unsaturated molecules
[DE88-013482] N89-10968
Observations of breakup processes of liquid jets using real-time X-ray radiography N89-11160
Modeling of combustion processes of stick propellants via combined Eulerian-Lagrangian approach N89-11163
Computation of low-speed compressible flows with time-marching procedures
[AD-A195800] N89-11170
Experimental research on swept shock wave/boundary layer interactions
[AD-A196938] N89-11189
Experimental and theoretical studies on transport processes in laser welding
[DE88-013933] N89-11230
Remote sensing and hydrologic modeling of arid watersheds: A scale analysis
[DE88-014625] N89-11293

PENNSYLVANIA UNIV., PHILADELPHIA.
Atomistic studies of grain boundaries in alloys and compounds
[DE88-011939] N89-11011
Low stress brittle fractures in polymers
[DE88-014236] N89-11027

PHYSICAL SCIENCES, INC., ANDOVER, MASS.
The determination of the spacecraft contamination environment
[AD-A196435] N89-10937
Multicolor pyrometer for materials processing in space
[NASA-CR-183189] N89-11057

POLITECNICO DI TORINO (ITALY).
Origin, objectives and activities of the Department of Aerospace Engineering N89-10830

POLYTECHNIC OF CENTRAL LONDON (ENGLAND).
European examples of evaluating the effectiveness of information centres and services N89-11628

PRINCETON UNIV., N. J.
A study of helicopter stability and control including blade dynamics
[NASA-CR-183245] N89-10895

PURDUE UNIV., WEST LAFAYETTE, IND.
The Purdue University Get Away Special II (PUGAS II) N89-10918
A three-dimensional investigation of steady state fatigue crack closure behavior for through-thickness and part-through flaws N89-11256
An investigation of the internal structure of the thunderstorm outflow with particular attention to multiple surges N89-11357
Control design and performance evaluation for flexible manipulators N89-11390
Practical applications and limitations of adaptive control N89-11442
On empirical Bayes selection rules for negative binomial . populations
[AD-A196994] N89-11485

R

RENSSELAER POLYTECHNIC INST., TROY, N.Y.
Composite structural materials
[NASA-CR-180224] N89-10946
Ratchetting behavior of type 304 stainless steel at room and elevated temperatures
[DE88-011864] N89-11273

ROBERTS RESEARCH LAB., TORRANCE, CALIF.
Baseline configuration data set: NASA Standard Initiator-2 (NSI-2)
[NASA-CR-172071] N89-11050

ROCHESTER UNIV., N. Y.
A code for the solution of the Vlasov-Fokker-Planck equation in one or two dimensions
[DE88-013288] N89-11463

ROCKWELL INTERNATIONAL CORP., GOLDEN, COLO.
A method for improving the depth of penetration and the appearance of welding
[DE88-012954] N89-11239

ROHR INDUSTRIES, INC., CHULA VISTA, CALIF.
De-icing of aircraft turbine engine inlets
[DOT/FAA/CT-87/37] N89-10894

ROME UNIV. (ITALY).
A far infrared astronomical observatory in Antarctica N89-11646

S

SAN DIEGO STATE UNIV., CALIF.
Assessing schema knowledge
[AD-A196933] N89-11447

SANDIA NATIONAL LABS., ALBUQUERQUE, N. MEX.
An approximate, maximum terminal velocity descent to a point
[DE88-000349] N89-10840
Aerodynamic design considerations for a free-flying ducted propeller
[DE88-006867] N89-10841
Sandia National Laboratories flight simulation facilities
[DE88-012108] N89-10898
Schlieren measurements at the 10,000-foot sled track
[DE88-012748] N89-10899
Detailed analysis of the structural consequences of railgun augmentation
[DE88-013800] N89-10926
SHED: A program for three-dimensional, rigid body, shroud ejection dynamics
[DE88-012410] N89-10927
Electrically conductive reticulated carbon composites
[DE88-012856] N89-10948
Carbon films derived from poly(acrylonitrile): Oxidation, electrical properties, and processing
[DE88-010352] N89-10950
Microrheological observations of the onset of non-Newtonian behavior in suspensions
[DE88-006198] N89-10962
A differential absorption spectrometer for determining flash X-ray spectra from 10 to 2000 keV
[DE88-014844] N89-10979
Coefficients of thermal expansion of common encapsulants
[DE88-015026] N89-10983
Microscopy and microanalysis of shock-processed materials
[DE88-008471] N89-10990
The catalytic, structural, and electronic properties of strained-metal overlayers
[DE88-007932] N89-11013
Nitride layer growth in iron and titanium alloys: Studies by electron probe microanalysis
[DE88-007207] N89-11017
Electronic properties of sigma-conjugated polysilanes
[DE88-012699] N89-11032
Microporous polymer foams for biomaterials
[DE88-010578] N89-11036
Compatibility and performance of separators in Li/SOCl(sub 2) cells
[DE88-011090] N89-11116
Multiple pulse photoconductive semiconductor switching
[DE88-011792] N89-11119
Switchable auto gain amplifier
[DE88-012114] N89-11122
A general analysis for obtaining the viscosity function from viscometric measurements: A case study for the helical screw rheometer
[DE88-006271] N89-11139
Explosion airblast predictions on a personal computer and application to the Henderson, Nevada incident
[DE88-014991] N89-11144
Numerical description of cavitation on axisymmetric bodies
[DE88-006826] N89-11147
Continuum theories for fluid-particle flows: Some aspects of lift forces and turbulence N89-11155
Vacuum Fizeau wedge wavemeter for pulsed UV lasers
[DE88-015832] N89-11206
Microsoldering and microminiature welding with lasers
[DE88-013368] N89-11240

Incipient spall, crack branching, and fragmentation statistics in the spall process
[DE88-009587] N89-11251

A strain rate dependent brittle fracture model based on continuum damage mechanics
[DE88-013361] N89-11285

Reliability analysis of lithium cells
[DE88-009258] N89-11300

Rotor instrumentation circuits for the Sandia 34-meter vertical axis wind turbine
[DE88-014704] N89-11304

A model for the response of vertical axis wind turbines to turbulent flow: Parts 1 and 2
[DE88-014708] N89-11305

The photovoltaic advanced systems test facility
[DE88-009589] N89-11306

A performance model for massive parallelism
[DE88-011763] N89-11393

TRINITY II: A post-processing program for 2-dimensional finite element analysis data
[DE88-010107] N89-11416

High heat flux testing of CIT (Compact Ignition Tokamak) first wall tiles
[DE88-012241] N89-11530

Smart semiconductor bridge (SCB) igniter for explosives
[DE88-012669] N89-11551

What is the origin of glassy behavior in the high-T(sub c) oxides
[DE88-012668] N89-11565

Chemical preparation of powders and films for high temperature superconductors
[DE88-015266] N89-11601

SANDIA NATIONAL LABS., LIVERMORE, CALIF.

Combustion of energetic materials
[DE88-011286] N89-10977

SCIENCE RESEARCH COUNCIL, CHILTON (ENGLAND).

Workshops and problems for benchmarking eddy current codes
[DE88-009996] N89-11098

SCRIPPS INSTITUTION OF OCEANOGRAPHY, SAN DIEGO, CALIF.

The flux and recycling of bioactive substances in the surface sediments of the deep basins off southern California
[DE88-007999] N89-11321

SIGNAL PROCESSORS LTD., CAMBRIDGE (ENGLAND).

A digital beacon receiver N89-11092

SMITHSONIAN ASTROPHYSICAL OBSERVATORY, CAMBRIDGE, MASS.

Molecular processes in comets
[NASA-CR-182742] N89-11671

SOCIETE NATIONALE DES POUDRES ET EXPLOSIFS, VERT-LE-PETIT (FRANCE).

Polystyrylpyridine (PSP) resin-based short-fiber composites (injectable compounds)
[REPT-NT-195/87/CRB/GTR.C/NP] N89-10955

SOCIETE NATIONALE INDUSTRIELLE AEROSPATIALE, SURESNES (FRANCE).

Influence of specimen dimension on damage and breaking of composite materials
[REPT-49-062/F] N89-10957

SOUTHAMPTON UNIV. (ENGLAND).

The use of the complex summation method for formulating algorithms for decoupling vertical/horizontal motions of rolling aircraft N89-10889

STANFORD LINEAR ACCELERATOR CENTER, CALIF.

Simulations of the laser photocathode injector
[DE88-015337] N89-11202

Quality assurance manual. Volume 2: Appendices
[DE88-013880] N89-11247

Integrated database approach for geodetic applications
[DE88-012726] N89-11615

STANFORD UNIV., CALIF.

Protein crystal growth in low gravity
[NASA-CR-183183] N89-11055

Gas-loaded free-electron lasers
[DE88-014652] N89-11213

A gas-loaded, free-electron laser
[DE88-016090] N89-11214

Knowledge-based design of complex mechanical systems N89-11225

The interpretation of electromagnetic nondestructive flaw detection in metals N89-11246

Free damped vibration of composite plates and shells N89-11249

Studies in advanced silicon solar cells
[DE88-013143] N89-11314

Velocity analysis by iterative profile migration N89-11339

Crustal structure of the northwestern United States N89-11349

Experiments in control of satellite manipulators N89-11391

The Frobenius metric in image registration
[DE88-016685] N89-11421

Coronal magnetic fields produced by photospheric shear
[AD-A194591] N89-11684

STATE UNIV. COLL. OF NEW YORK, BUFFALO.

The coefficient of first viscosity via three-phonon processes in bulk liquid helium
[AD-A196902] N89-10986

STATE UNIV. OF NEW YORK, BUFFALO.

Coupled even-parity superconducting states
[AD-A196969] N89-11607

STATE UNIV. OF NEW YORK, STONY BROOK.

Analysis, synthesis and design of high-speed mechanisms
[PB88-235106] N89-11244

SUNPOWER, INC., ATHENS, OHIO.

Preliminary assessment of a magnetically coupled free-piston Stirling engine heat pump compressor
[DE88-013835] N89-11232

SUSSEX UNIV., BRIGHTON (ENGLAND).

Nonlinear random vibration in mechanical systems N89-11253

SVERDRUP TECHNOLOGY, INC., CLEVELAND, OHIO.

A diagonally inverted LU implicit multigrid scheme for the 3-D Navier-Stokes equations and a two equation model of turbulence
[NASA-CR-182209] N89-10863

SYRACUSE UNIV., N. Y.

Mechanisms of gas permeation through polymer membranes
[DE88-007761] N89-10980

Robust control of a flexible manipulator arm N89-11228

Computer simulation of the uni-axial stress-strain behavior of ribbon-like fiber nonwovens N89-11284

SYSTEMS CONTROL TECHNOLOGY, INC., ARLINGTON, VA.

Aeronautical decision making for air ambulance helicopter pilots: Situational awareness exercises
[DOT/FAA/DS-88/6] N89-10869

Aeronautical decision making for commercial pilots
[DOT/FAA/PM-86/42] N89-10870

T

TAU CORP., LOS GATOS, CALIF.

GPS/interial navigation system integration for enhanced navigation performance and robustness N89-10880

Differential operation of NAVSTAR GPS for enhanced accuracy N89-10883

GPS navigation processing and Kalman filtering N89-10884

TECHNISCHE HOGESCHOOL, DELFT (NETHERLANDS).

Problem on 0-1 matrices
[PB88-210075] N89-11477

TECHNISCHE UNIV., BERLIN (WEST GERMANY).

TUBSAT-1, satellite technology for educational purposes N89-10905

TECHNISCHE UNIV., REGENSBURG (WEST GERMANY).

Vectorization of FORTRAN programs at do-loop level N89-11398

Restructuring of basic linear algebraic algorithms, chapter 5 N89-11399

Computatinal fluid dynamics and supercomputers, chapter 6 N89-11400

TECOGEN, INC., WALTHAM, MASS.

Advanced heat-pipe heat exchanger and microprocessor-based modulating burner controls development
[PB88-217070] N89-11172

TENNESSEE UNIV., KNOXVILLE.

Conductivity of organic polymers: A nonlinear approach
[DE88-013837] N89-11037

TEXAS A&M UNIV., COLLEGE STATION.

Oxygen electrode in molten carbonate fuel cells
[DE88-009628] N89-11308

TEXAS INSTRUMENTS, INC., DALLAS.

Design definition for a digital beamforming processor
[AD-A196983] N89-11133

TEXAS TECHNOLOGICAL UNIV., LUBBOCK.

Electronic properties of 3-5 semiconductor alloys N89-11560

Defect model for the electronic conduction and breakdown in dielectric thin films N89-11563

TEXAS UNIV., AUSTIN.

Novel composite materials: Alloys from immiscible components
[AD-A197040] N89-10958

Preliminary results of MARECS-A measurements in Central Maryland and plans for 1988 MSS experiment in Australia N89-11079

A frequency dependent ray theory N89-11610

TEXAS UNIV., DALLAS.

Unmodeled dynamics and nonlinear control: Wrapup
[NASA-CR-181524] N89-11457

TOKYO UNIV. (JAPAN).

A free-flight experiment of vehicles ranging from high subsonic to high supersonic speeds
[ISAS-RN-362] N89-10888

The geographical distributions of electrons (0.05-3.2 MeV) and protons (0.58-35 MeV) at altitudes of 350-850 km
[ISAS-RN-358] N89-11335

Proton decay experiment and neutrinos from supernova (Kamiokande-2) N89-11653

An oxide passivated and ion-implanted Si detector for X-ray astronomy
[ISAS-RN-353] N89-11663

Interplanetary magnetic microstructure observed by Sakigake near its closest approach to Comet Halley
[ISAS-RN-349] N89-11667

TORONTO UNIV. (ONTARIO).

An experimental study of a laminar wall-jet in the presence of a uniform external flow
[UTIAS-268] N89-11152

The mini-oscillator technique: A finite element method for the modeling of linear viscoelastic structures
[UTIAS-323] N89-11250

TRW SPACE TECHNOLOGY LABS., REDONDO BEACH, CALIF.

Modulation of radar backscatter from the ocean by a variable surface current
[AD-A196952] N89-11114

U

UNION FOR EXPERIMENTING COLL. AND UNIV., YELLOW SPRINGS, OHIO.

A co-citation study of the scientific literature of two innovation research traditions: Diffusion of innovations and technology transfer N89-11618

UNITED KINGDOM ATOMIC ENERGY AUTHORITY, RISLEY (ENGLAND).

The effect of thermal ageing on the stress corrosion cracking of 9Cr1Mo steel in aqueous caustic environments
[NRL-R-1003(R)] N89-10997

UNIVERSITY OF CENTRAL FLORIDA, ORLANDO.

Automated knowledge generation
[NASA-CR-181317] N89-11440

UNIVERSITY OF SOUTHERN CALIFORNIA, MARINA DEL REY.

Development of advanced internal gain radiation detector structures based on neutron transmutation doped silicon, high T(sub c) superconductive compounds and their potential application to detection of ionizing radiation
[DE88-012563] N89-11574

UTAH UNIV., SALT LAKE CITY.

Ligand intermediates in metal catalyzed reactions
[DE88-012123] N89-11007

Optical scattering and microphysical properties of subvisual cirrus clouds, and climatic implications
[NASA-CR-183301] N89-11362

Database loading by examples: A learning approach to loading information retrieval databases N89-11619

V

VIBRATION INST., CLARENDON HILLS, ILL.

The Shock and Vibration Digest, Volume 20, No. 10 N89-11252

The Shock and Vibration Digest, Volume 20, No. 8 N89-11258

The Shock and Vibration Digest, Volume 20, No. 6 N89-11261

The Shock and Vibration Digest, volume 20, no. 9 N89-11266

The Shock and Vibration Digest, Volume 20, No. 7 N89-11277

The Shock and Vibration Digest, volume 20, no. 5 N89-11282

VILLANOVA UNIV., PA.

Computerized monitoring and control of experiments in space N89-10915

VIRGINIA POLYTECHNIC INST. AND STATE UNIV., BLACKSBURG.

Accuracy analysis of the semi-analytical method for shape sensitivity analysis N89-10848

LMSS propagation modeling at Virginia Tech N89-11078

Mobile satellite propagation measurements and modeling: A review of results for systems engineers N89-11081

ACTS and OLYMPUS propagation experiments N89-11091

Velocity and Q from reflection seismic data
N89-11334
Multiple populations on the horizontal branch
N89-11662

VIRGINIA UNIV., CHARLOTTESVILLE.
Microgravity nucleation and particle coagulation experiments support
[NASA-CR-183282] N89-11056

VRIJE UNIV., AMSTERDAM (NETHERLANDS).
Homology classes represented by real algebraic hypersurfaces
[PB88-202908] N89-11453
Real algebraic morphisms into even-dimensional spheres
[PB88-202916] N89-11462

W

WASHINGTON STATE UNIV., PULLMAN.
Particle dispersion models and drag coefficients for particles in turbulent flows N89-11158

WASHINGTON UNIV., SEATTLE.
A nonlinear wave-wave interaction theory for the generation of multi-scale large eddies in a neutral atmospheric boundary layer N89-11344
A numerical modeling study of frontogenesis and cold frontal rainbands N89-11358
A study of the dynamics of maritime fronts using remotely sensed wind and stress measurements N89-11366
Poker (4.0): A programmer's reference guide
[AD-A196417] N89-11430
Poker (4.1): A programmer's reference guide
[AD-A196419] N89-11431
New insights into globular clusters from main sequence photometry N89-11658

WATERLOO UNIV. (ONTARIO).
Vibrations and stability of mechanical systems: 4
N89-11260

WEST VIRGINIA UNIV., MORGANTOWN.
On the constitutive relation for frictional flow of granular materials
[DE88-001089] N89-11171
Dynamic behavior of foundations in bilateral and unilateral contact N89-11259

WESTINGHOUSE DEFENSE AND ELECTRONIC SYSTEMS CENTER, BALTIMORE, MD.
Propagation handbook, frequencies above 10 GHz
N89-11082

WISCONSIN UNIV., MADISON.
A theoretical investigation of the collection of aerosol particles by falling ice crystals N89-11337
The Cooperative VAS Program with the Marshall Space Flight Center
[NASA-CR-179377] N89-11361
Alfven wave studies on a tokamak N89-11517
Stellarator theory
[DE88-014131] N89-11528
The critical current density, the fabrication process and the microstructure in superconducting composites of NbTi for high energy physics
[DE88-014241] N89-11568
Unified theories and the early universe N89-11651

WYLE LABS., INC., HAMPTON, VA.
Electrical noise reduction techniques contributing to improved data quality at the National Transonic Facility
[NASA-CR-4193] N89-11196

Y

YALE UNIV., NEW HAVEN, CONN.
Colour and spectral synthesis of disk galaxies
N89-11656

YORK UNIV. (ENGLAND).
A global MHD pulsation event with conjugate study and model of ionospheric damping N89-11333

Z

ZURICH UNIV. (SWITZERLAND).
Experimental tests of relativity and gravitation
N89-11649

Typical Contract Number Index Listing

Listings in this index are arranged alphanumerically by contract number. Under each contract number the NASA accession numbers denoting documents that have been produced as a result of research done under that contract are arranged in ascending order. The NASA accession number denotes the number by which the citation is identified.

AEROSPATIALE-11-000639 ..... N89-11184
AEROSPATIALE-21-003395 ..... N89-10859
AF PROJ. 2304 ..... N89-11439
N89-11482
AF PROJ. 2307 ..... N89-11189
AF PROJ. 2308 ..... N89-11170
AF PROJ. 2917 ..... N89-11405
AF-AFOSR-0032-88 ..... N89-11439
AF-AFOSR-0082-86 ..... N89-11189
AF-AFOSR-0117-88 ..... N89-11459
AF-AFOSR-0132-86 ..... N89-11482
AF-AFOSR-0196-82 ..... N89-11170
AF-AFOSR-0247-86 ..... N89-11405
ARPA ORDER 4696 ..... N89-10988
BC-85-302-21 ..... N89-10955
BMFT-03E-4439A N89-11318
DA PROJ. 2Q1-61102-B-74-F N89-11388
N89-11445
DA PROJ. 2Q1-61102-B-747 ..... N89-11483
DA PROJ. 3E1-62777-A-878 ..... N89-11222
DA-49-193-MD-2241 ..... N89-11217
DAAB07-87-C-F069 ..... N89-11298
DAAG29-83-K-0081 ..... N89-11163
DAAG29-84-K-0022 ..... N89-11454
DAAG29-85-K-0094 ..... N89-11484
DAAG29-85-K-0125 ..... N89-10987
DAAH01-82-C-0519 ..... N89-11136
DAAL03-87-K-0055 ..... N89-10958
DADA17-72-C-2177 ..... N89-11217
DAJA45-86-C-0019 ..... N89-10985
DAJA45-86-C-0048 ..... N89-11388
DAMD17-81-C-1065 ..... N89-11222
DAMD17-86-C-6093 ..... N89-11435
DE-AC02-76CH-00016 ..... N89-11555
N89-11575
N89-11587
N89-11598
N89-11612
DE-AC02-76CH-03000 ..... N89-10966
DE-AC02-76ER-00881 ..... N89-11651
DE-AC02-76ER-01198 ..... N89-10989
N89-11035
N89-11586
DE-AC02-76ER-03130 ..... N89-11664
N89-11666
DE-AC02-78ET-51013 ..... N89-11519
DE-AC02-82ER-40077 ..... N89-11568
DE-AC02-83CH-10093 ..... N89-11301
N89-11302
N89-11311
N89-11312
N89-11316
DE-AC03-76SF-00098 ..... N89-10960
N89-10969
N89-10978
N89-10981
N89-11015
N89-11178
N89-11309
N89-11408
N89-11411
N89-11495
N89-11556
N89-11582
N89-11592
N89-11597
N89-11599
N89-11600
N89-11668
DE-AC03-76SF-00515 ..... N89-11202
N89-11247
N89-11460
N89-11615
DE-AC03-87DP-10560 ..... N89-11280
DE-AC04-76DP-00053 ..... N89-11030
N89-11051
N89-11212
DE-AC04-76DP-00789 ..... N89-10840
N89-10841
N89-10898
N89-10899
N89-10926
N89-10927
N89-10948
N89-10950
N89-10962
N89-10977
N89-10979
N89-10983
N89-10990
N89-11013
N89-11017
N89-11032
N89-11036
N89-11116
N89-11119
N89-11122
N89-11139
N89-11144
N89-11147
N89-11155
N89-11206
N89-11240
N89-11251
N89-11285
N89-11300
N89-11304
N89-11305
N89-11306
N89-11314
N89-11393
N89-11416
N89-11530
N89-11551
N89-11565
N89-11601
DE-AC04-76DP-03533 ..... N89-11239
DE-AC05-84ER-40150 ..... N89-11498
N89-11499
DE-AC05-84OR-21400 ..... N89-10901
N89-10933
N89-10947
N89-10961
N89-10972
N89-10975
N89-10982
N89-10991
N89-10999
N89-11026
N89-11034
N89-11037
N89-11117
N89-11146
N89-11165
N89-11169
N89-11174
N89-11177
N89-11232
N89-11235
N89-11255
N89-11273
N89-11303
N89-11313
N89-11319
N89-11383
N89-11511
N89-11554
N89-11564
N89-11584
N89-11589
N89-11617
DE-AC05-84OS-21400 ..... N89-11025
DE-AC06-76RL-01830 ..... N89-11019
N89-11209
N89-11310
N89-11317
N89-11325
N89-11360
N89-11512
DE-AC07-76ID-01570 ..... N89-11226
N89-11238
DE-AC08-83NV-10282 ..... N89-11578
N89-11580
DE-AC08-87DP-10560 ..... N89-11524
DE-AC09-76SR-00001 ..... N89-10998
DE-AC21-85MC-21353 ..... N89-11171
DE-AI01-82ER-30024 ..... N89-11211
DE-AS05-83ER-60177 ..... N89-11326
DE-FC08-85DP-40200 ..... N89-11463
DE-FG01-86CE-31010 ..... N89-11299
DE-FG02-84ER-13295 ..... N89-10968
DE-FG02-84ER-45158 ..... N89-11230
DE-FG02-84ER-45161 ..... N89-11027
DE-FG02-85ER-13411 ..... N89-11007
DE-FG02-85ER-45184 ..... N89-11018
DE-FG02-85ER-45203 ..... N89-11571
DE-FG02-85ER-45211 ..... N89-11456
DE-FG02-85ER-45224 ..... N89-11567
DE-FG02-85ER-53201 ..... N89-11528
DE-FG02-85ER-53205 ..... N89-11525
DE-FG02-85ER-60372 ..... N89-11323
DE-FG02-86ER-13579 ..... N89-10959
DE-FG02-86ER-13597 ..... N89-11149
DE-FG02-86ER-40302 ..... N89-11460
DE-FG02-86ER-45228 ..... N89-11028
DE-FG02-86ER-53223 ..... N89-11531
DE-FG02-86ER-60472 ..... N89-11293
DE-FG02-87ER-13649 ..... N89-10980
DE-FG02-87ER-13800 ..... N89-11180
DE-FG02-87ER-45295 ..... N89-11011
DE-FG02-88ER-13820 ..... N89-11181
DE-FG02-88ER-45347 ..... N89-11573
DE-FG03-84ER-13275 ..... N89-11213
N89-11214
DE-FG03-85ER-13402 ..... N89-11451
DE-FG03-85ER-25009 ..... N89-11394
N89-11413
N89-11420
DE-FG03-86ER-13527 ..... N89-11161
DE-FG03-86ER-60416 ..... N89-11574
DE-FG03-87ER-25028 ..... N89-11421
DE-FG05-84ER-45172 ..... N89-11602
DE-FG05-84ER-53176 ..... N89-11518
DE-FG05-85ER-53192 ..... N89-10947
DE-FG05-85ER-60334 ..... N89-11321
DE-FG05-86ER-45280 ..... N89-11569
DE-FG05-86ER-60468 ..... N89-11330
DE-FG07-84ID-12525 ..... N89-11340
DE-FG22-86PC-90960 ..... N89-11148
DE-FG22-87PC-79931 ..... N89-11308
DE-F60686-ER-13567 ..... N89-11158
DOT-FA71NA-AP-98 ..... N89-10892
N89-10893
DRET-SDR-G3-86-1066 ..... N89-11533
DRET-84-34-001 ..... N89-10954
DRET-84-34-302 ..... N89-10955
DRET-85-003 ..... N89-11286
DRET-86-044 ..... N89-11125
DRET-87-34-001 ..... N89-10953
DRET-87-002-20 ..... N89-11183
DRET-87-002-018 ..... N89-11187
DTFA01-80-C-10080 ..... N89-10870
DTFA01-80-C-10093 ..... N89-10885
DTFA01-87-C-00014 ..... N89-10869
DTFA03-86-C-0050 ..... N89-10894
DTFA03-87-C-00013 ..... N89-11265
EPA-68-02-4198 ..... N89-11620

EPA-68-03-3246 ..... N89-11452
ESTEC-6275/85-NL-PP(SC) N89-11422
FINEP-537/CT N89-11331
N89-11351
F04701-85-C-0086 ..... N89-10935
N89-11606
F19628-78-C-0247 ..... N89-10938
F19628-79-C-0175 ..... N89-10938
F19628-82-C-0090 ..... N89-10938
F19628-83-C-0139 ..... N89-10937
F19628-86-C-0001 ..... N89-11434
F19628-87-C-0016 ..... N89-11133
F29601-85-C-0057 ..... N89-11219
F30602-81-C-0206 ..... N89-11112
F33615-85-C-3013 ..... N89-10867
F49620-85-C-0151 ..... N89-11040
GRI-5084-241-1089 ..... N89-11172
GRI-5084-243-1089 ..... N89-11033
JPL-957723 ..... N89-11678
JPL-957805 ..... N89-11678
MDA903-83-K-0347 ..... N89-11483
MDA903-84-C-0031 ..... N89-11487
N89-11488
MDA903-85-K-0103 ..... N89-11445
NAGW-976 ..... N89-11595
NAG1-441 ..... N89-11201
NAG1-623 ..... N89-11233
N89-11234
NAG1-657 ..... N89-10843
NAG1-683 ..... N89-11406
NAG1-717 ..... N89-11359
NAG1-718 ..... N89-11362
NAG1-836 ..... N89-10890
NAG2-111 ..... N89-10855
NAG2-198 ..... N89-10855
NAG2-244 ..... N89-10895
NAG2-366 ..... N89-11457
NAG5-224 ..... N89-11290
NAG5-270 ..... N89-11106
NAG5-480 ..... N89-10984
N89-11296
NAG5-561 ..... N89-11368
NAG5-865 ..... N89-11056
NAG5-1010 ..... N89-11292
NAG8-489 ..... N89-11055
NAG8-684 ..... N89-10922
NAG9-214 ..... N89-11384
NAG10-0042 ..... N89-11440
NASW-4003 ..... N89-10897
NASW-4307 ..... N89-10963
NAS1-18107 ..... N89-11459
NAS1-18274 ..... N89-10936
NAS1-18304 ..... N89-11196
NAS3-23337 ..... N89-10943
NAS3-24657 ..... N89-11315
NAS3-25140 ..... N89-11192
NAS3-25266 ..... N89-10883
NAS5-26654 ..... N89-11195
NAS5-30041 ..... N89-11102
NAS5-30047 ..... N89-11191
NAS7-918 ..... N89-10931
N89-10941
N89-11074
N89-11237
N89-11328
N89-11441
N89-11475
N89-11661
NAS7-1002 ..... N89-11057
NAS8-34685 ..... N89-11203
NAS8-34732 ..... N89-11361
NAS8-35835 ..... N89-10934
NAS8-36718 ..... N89-11156
NAS9-17249 ..... N89-11050
NAS9-17878 ..... N89-10923
NCC2-383 ..... N89-10900
NGL-33-018-003 ..... N89-10946
NGR-09-010-078 ..... N89-10838
NSF AST-85-22213 ..... N89-11675
NSF ATM-87-09659 ..... N89-11355
NSF CCR-84-16878 ..... N89-11431
NSF DMR-84-18718 ..... N89-11598
NSF DMR-85-01856 ..... N89-11598
NSF DMS-84-20623 ..... N89-11421
NSF DMS-86-02672 ..... N89-11453
N89-11462
NSF DMS-86-06964 ..... N89-11485
NSF DMS-87-02820 ..... N89-11485
NSF IST-85-11170 ..... N89-11448
NSF MSM-85-03576 ..... N89-11244
NSF PHY-86-00749 ..... N89-11675
NSG7-421 ..... N89-11671
N00014-07-G-0185 ..... N89-11045
N00014-80-C-0622 ..... N89-11130
N00014-82-K-0186 ..... N89-11448
N00014-83-K-0457 ..... N89-11404
N00014-84-C-0149 ..... N89-11243
N89-11484
N00014-84-K-0027 ..... N89-11289
N00014-85-K-0111 ..... N89-11684
N00014-85-K-0258 ..... N89-11432
N00014-85-K-0326 ..... N89-11132
N00014-85-K-0343 ..... N89-11421
N00014-85-K-0661 ..... N89-11447
N00014-85-1588 ..... N89-11134
N89-11135
N00014-86-C-0111 ..... N89-11114
N00014-86-C-0164 ..... N89-11042
N00014-86-C-0568 ..... N89-11509
N00014-86-K-0043 ..... N89-10986
N89-11607
N00014-86-K-0124 ..... N89-11229
N00014-86-K-0180 ..... N89-11433
N89-11473
N89-11476
N00014-86-K-0264 ..... N89-11430
N89-11431
N00014-86-K-0402 ..... N89-11044
N00014-87-C-0098 ..... N89-11041
N00014-87-C-0334 ..... N89-10988
N00014-87-F-0066 ..... N89-11221
N00014-87-K-0109 ..... N89-11043
N00014-87-K-0874 ..... N89-11448
N00014-88-K-0170 ..... N89-11485
PRC-8/87/BO8200-1980-01-1 ..... N89-11428
PROJ. RR0-4106 ..... N89-11044
PROJ. RR0-4204 ..... N89-11404
PROJ. RR0-4206 ..... N89-11447
STCAN-780-274 ..... N89-11182
STPA-85-95-004 ..... N89-10861
N89-10864
STPA-86-96-015-00-471-75-86 ..... N89-10957
STPA-437103/79 ..... N89-11020
T12-02Z N89-11356
W-31-109-ENG-38 ..... N89-10970
N89-10994
N89-11001
N89-11008
N89-11016
N89-11029
N89-11046
N89-11098
N89-11137
N89-11138
N89-11150
N89-11175
N89-11307
N89-11322
N89-11436
N89-11461
N89-11497
N89-11553
N89-11557
N89-11570
N89-11572
N89-11579
N89-11591
N89-11636
W-31-109-ENG-39 ..... N89-11345
W-7405-ENG-36 ..... N89-10932
N89-10962
N89-10995
N89-11010
N89-11012
N89-11019
N89-11052
N89-11060
N89-11070
N89-11162
N89-11179
N89-11204
N89-11336
N89-11342
N89-11350
N89-11437
N89-11504
N89-11505
N89-11506
N89-11507
N89-11508
N89-11532
N89-11552
N89-11576
N89-11577
N89-11585
N89-11594
N89-11633
N89-11665
N89-11681
N89-11682
N89-11683
N89-11685
W-7405-ENG-48 ..... N89-10928
N89-10942
N89-10949
N89-10981
N89-11014
N89-11031
N89-11047
N89-11049
N89-11053
N89-11059
N89-11072
N89-11100
N89-11141
N89-11166
N89-11178
N89-11199
N89-11200
N89-11207
N89-11208
N89-11210
N89-11245
N89-11346
N89-11417
N89-11464
N89-11486
XB-7-06110-1 ..... N89-11316
506-49-31-01 ..... N89-10936
186-02-04-02 ..... N89-10931
314-40-31-30-21 ..... N89-11328
476-30-40-11 ..... N89-10941
505-01-51 ..... N89-10872
505-60-21-01 ..... N89-10842
505-61-01-01 ..... N89-11196
505-61-71 ..... N89-10849
505-62-01 ..... N89-11198
505-62-21 ..... N89-10844
N89-10863
N89-11469
505-62-61 ..... N89-10858
505-63-1A N89-10996
505-63-01-05 ..... N89-10945
N89-10951
505-63-01-10 ..... N89-11287
505-63-81 ..... N89-10952
505-90-21-01 ..... N89-11459
506-41-11 ..... N89-11129
506-49-11-01 ..... N89-10929
535-03-01 ..... N89-10865
549-03-21-01 ..... N89-11441
584-01-21 ..... N89-11128
643-10-03-04 ..... N89-11074
906-85-01-03 ..... N89-11407
906-85-44 ..... N89-10944
N89-11637

Typical Report Number Index Listing

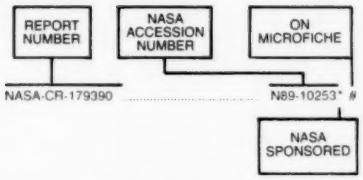

Listings in this index are arranged alphanumerically by report number. The NASA accession number denotes the number by which the citation is identified. An asterisk (*) indicates that the item is a NASA report. A pound sign (#) indicates that the item is available on microfiche.

A-87093 ..... N89-10872* #
A-88008 ..... N89-10849* #

AAE-88-5 ..... N89-11132 #

AD-A193668 ..... N89-11454 #
AD-A194338 ..... N89-11687 #
AD-A194591 ..... N89-11684 #
AD-A195800 ..... N89-11170 #
AD-A195927 ..... N89-11229 #
AD-A196169 ..... N89-11136 #
AD-A196226 ..... N89-10935 #
AD-A196375 ..... N89-11370 #
AD-A196376 ..... N89-11514 #
AD-A196377 ..... N89-11387 #
AD-A196378 ..... N89-11107 #
AD-A196379 ..... N89-11371 #
AD-A196381 ..... N89-11372 #
AD-A196382 ..... N89-11021 #
AD-A196383 ..... N89-11402 #
AD-A196384 ..... N89-11108 #
AD-A196385 ..... N89-11216 #
AD-A196387 ..... N89-11022 #
AD-A196397 ..... N89-11480 #
AD-A196400 ..... N89-11109 #
AD-A196402 ..... N89-11110 #
AD-A196403 ..... N89-11550 #
AD-A196405 ..... N89-11373 #
AD-A196406 ..... N89-11374 #
AD-A196409 ..... N89-11375 #
AD-A196410 ..... N89-11376 #
AD-A196411 ..... N89-11481 #
AD-A196414 ..... N89-11403 #
AD-A196417 ..... N89-11430 #
AD-A196419 ..... N89-11431 #
AD-A196422 ..... N89-11473 #
AD-A196428 ..... N89-11130 #
AD-A196431 ..... N89-11482 #
AD-A196435 ..... N89-10937 #
AD-A196439 ..... N89-11404 #
AD-A196447 ..... N89-10886 #
AD-A196454 ..... N89-11432 #
AD-A196456 ..... N89-10867 #
AD-A196458 ..... N89-11439 #
AD-A196462 ..... N89-11217 #
AD-A196494 ..... N89-11039 #
AD-A196496 ..... N89-10938 #
AD-A196498 ..... N89-11474 #
AD-A196503 ..... N89-11023 #
AD-A196504 ..... N89-11475* #
AD-A196516 ..... N89-11353 #
AD-A196593 ..... N89-11405 #
AD-A196660 ..... N89-11218 #
AD-A196665 ..... N89-10891 #
AD-A196683 ..... N89-11354 #
AD-A196684 ..... N89-11377 #
AD-A196685 ..... N89-11111 #
AD-A196686 ..... N89-11378 #
AD-A196687 ..... N89-11379 #
AD-A196689 ..... N89-11054 #
AD-A196695 ..... N89-11605 #
AD-A196698 ..... N89-11288 #
AD-A196706 ..... N89-11515 #
AD-A196719 ..... N89-11445 #
AD-A196789 ..... N89-11509 #
AD-A196820 ..... N89-11188 #
AD-A196824 ..... N89-10985 #
AD-A196831 ..... N89-11289 #
AD-A196836 ..... N89-11388 #
AD-A196844 ..... N89-11112 #
AD-A196851 ..... N89-11219 #
AD-A196852 ..... N89-11606 #
AD-A196859 ..... N89-11040 #
AD-A196861 ..... N89-11220 #
AD-A196866 ..... N89-11131 #
AD-A196869 ..... N89-11332 #
AD-A196870 ..... N89-10925 #
AD-A196877 ..... N89-11503 #
AD-A196885 ..... N89-11041 #
AD-A196886 ..... N89-11042 #
AD-A196899 ..... N89-11043 #
AD-A196900 ..... N89-11044 #
AD-A196902 ..... N89-10986 #
AD-A196903 ..... N89-11433 #
AD-A196908 ..... N89-11298 #
AD-A196911 ..... N89-11446 #
AD-A196915 ..... N89-11132 #
AD-A196916 ..... N89-11434 #
AD-A196927 ..... N89-11113 #
AD-A196928 ..... N89-11221 #
AD-A196930 ..... N89-11222 #
AD-A196933 ..... N89-11447 #
AD-A196938 ..... N89-11189 #
AD-A196944 ..... N89-11483 #
AD-A196952 ..... N89-11114 #
AD-A196958 ..... N89-11071 #
AD-A196961 ..... N89-11516 #
AD-A196962 ..... N89-11382 #
AD-A196965 ..... N89-10939 #
AD-A196966 ..... N89-10940 #
AD-A196968 ..... N89-11190 #
AD-A196969 ..... N89-11607 #
AD-A196973 ..... N89-11223 #
AD-A196976 ..... N89-11676 #
AD-A196978 ..... N89-10987 #
AD-A196980 ..... N89-11484 #
AD-A196983 ..... N89-11133 #
AD-A196988 ..... N89-11045 #
AD-A196989 ..... N89-10988 #
AD-A196990 ..... N89-11476 #
AD-A196994 ..... N89-11485 #
AD-A196995 ..... N89-11115 #
AD-A196997 ..... N89-11134 #
AD-A196998 ..... N89-11135 #
AD-A197037 ..... N89-11487 #
AD-A197038 ..... N89-11488 #
AD-A197040 ..... N89-10958 #
AD-A197047 ..... N89-11024 #
AD-A197049 ..... N89-11448 #
AD-A197052 ..... N89-11243 #
AD-A197053 ..... N89-11435 #

AD-E501003 ..... N89-11488 #
AD-E501004 ..... N89-11487 #
AD-E951147 ..... N89-11136 #

AFGL-TR-87-0303 ..... N89-10937 #
AFGL-TR-88-0066 ..... N89-10938 #

AFIT/CI/NR-88-2 ..... N89-11370 #
AFIT/CI/NR-88-3 ..... N89-11387 #
AFIT/CI/NR-88-5 ..... N89-11379 #
AFIT/CI/NR-88-11 ..... N89-11371 #
AFIT/CI/NR-88-18 ..... N89-11332 #
AFIT/CI/NR-88-21 ..... N89-11378 #
AFIT/CI/NR-88-24 ..... N89-11354 #
AFIT/CI/NR-88-29 ..... N89-11374 #
AFIT/CI/NR-88-30 ..... N89-11373 #
AFIT/CI/NR-88-34 ..... N89-11375 #
AFIT/CI/NR-88-35 ..... N89-11376 #
AFIT/CI/NR-88-50 ..... N89-11107 #
AFIT/CI/NR-88-55 ..... N89-11481 #
AFIT/CI/NR-88-56 ..... N89-11111 #
AFIT/CI/NR-88-59 ..... N89-11503 #
AFIT/CI/NR-88-62 ..... N89-11131 #
AFIT/CI/NR-88-63 ..... N89-11605 #
AFIT/CI/NR-88-69 ..... N89-10925 #
AFIT/CI/NR-88-71 ..... N89-11288 #
AFIT/CI/NR-88-73 ..... N89-11402 #
AFIT/CI/NR-88-76 ..... N89-11403 #
AFIT/CI/NR-88-77 ..... N89-11021 #
AFIT/CI/NR-88-80 ..... N89-11446 #
AFIT/CI/NR-88-81 ..... N89-11514 #
AFIT/CI/NR-88-85 ..... N89-11054 #
AFIT/CI/NR-88-90 ..... N89-11372 #
AFIT/CI/NR-88-92 ..... N89-11480 #
AFIT/CI/NR-88-99 ..... N89-11188 #
AFIT/CI/NR-88-100 ..... N89-11550 #
AFIT/CI/NR-88-102 ..... N89-11216 #
AFIT/CI/NR-88-107 ..... N89-11377 #
AFIT/CI/NR-88-110 ..... N89-11109 #
AFIT/CI/NR-88-111 ..... N89-10988 #
AFIT/CI/NR-88-111 ..... N89-11676 #
AFIT/CI/NR-88-131 ..... N89-11110 #
AFIT/CI/NR-88-160 ..... N89-11108 #

AFOSR-88-0469TR ..... N89-11170 #
AFOSR-88-0542TR ..... N89-11405 #
AFOSR-88-0617TR ..... N89-11482 #
AFOSR-88-0618TR ..... N89-11439 #
AFOSR-88-0637TR ..... N89-11189 #
AFOSR-88-0688TR ..... N89-11040 #

AFWAL-TR-87-3098-PT-1 ..... N89-10867 #
AFWAL-TR-88-3042 ..... N89-11474 #

AFWL-TR-87-20 ..... N89-11219 #

AGARD-AG-311 ..... N89-11395 #

AGARD-LS-158 ..... N89-10831 #
AGARD-LS-160 ..... N89-11625 #
AGARD-LS-161 ..... N89-10874 #

AI-M-948 ..... N89-11229 #
AI-M-997 ..... N89-11476 #
AI-M-1042 ..... N89-11473 #

AI-TR-995 ..... N89-11433 #

AIAA-88-0467 ..... N89-10863* #
AIAA-88-0581 ..... N89-11359* #

ALGO-PUB-0120 ..... N89-11475* #

AMSMI-RD-CR-85-9 ..... N89-11136 #

ANL-87-26-VOL-1 ..... N89-11461 #
ANL-88-15 ..... N89-11150 #

ANL/CNSV-TM-202 ..... N89-11307 #

ANL/FE-88-2 ..... N89-11001 #

AR-004-509 ..... N89-11193 #
AR-004-543 ..... N89-11510 #
AR-004-571 ..... N89-10866 #

ARC-R87-157 ..... N89-11102* #

ARI-RN-88-53 ..... N89-11388 #
ARI-RN-88-54 ..... N89-11445 #
ARI-RN-88-56 ..... N89-11483 #

ARL-AERO-R-172 ..... N89-11193 #

ARL-AERO-TM-390 ..... N89-10866 #

ARL-STRUC-R-428 ..... N89-11510 #

ARL-STRUC-TM-482 ..... N89-11024 #

ARO-20606.13-MA ..... N89-11454 #
ARO-22530.3-MS ..... N89-10987 #
ARO-24449.4-CH ..... N89-10958 #

ATR-86(9561)-4 ..... N89-10965 #

AVSCOM-TM-88-B-015 N89-10951* #
AVSCOM-TR-88-C-30 N89-10952* #
BBC-RD-1988/4 N89-11097
BBC-RD-1988/5 N89-11492
BBC-RD-1988/6 N89-11096
BBC-RD-1988/7 N89-11073
BBC-RD-1988/8 N89-11103
BBC-RD-1988/9 N89-11101
BNL-41032 N89-11575 #
BNL-41427 N89-11587 #
BNL-41441 N89-11555 #
BNL-41472 N89-11598 #
BNL-41475 N89-11612 #
BRDEC-2464 N89-11022 #
BROWN/HET-644 N89-11666 #
CAMAC-PR-87-7 N89-11368* #
CEBAF-PR-88-010 N89-11498* #
CEBAF-PR-88-012 N89-11499 #
CERT-OA-22/5025-AYD N89-11184 #
CERT-OA-23/5025-AYD N89-11182 #
CERT-OA-40/5018-AYD N89-11187 #
CERT-RF-OA-68/2250-AYD N89-10859 #
CERT-RSF-OA-69/2259-AYD N89-11183 #
CERT-RT-OA-24/5025-AYD N89-10861 #
CERT-RT-18/3542-RY-071-R N89-10954 #
CERT-RTS-OA-25/5025-AYD N89-10864 #
CMR-88-9 N89-11055* #
CNES-CT/DTI/MS/MN/019 N89-11423 #
CNES-CT/DTI/MS/MN/069 N89-10839 #
CNES-CT/DTI/MS/MN/147 N89-11425 #
CNES-CT/DTI/MS/MN/160 N89-10924 #
CNES-CT/DTI/MS/MN/326 N89-11426 #
CNES-CT/PTI/MS/MN/067 N89-11424 #
CNES-DLA/SDT/ED/SA N89-10839 #
CNES-87/229/CT/DRT/TIT/TR N89-10930 #
CONF-870155 N89-11589 #
CONF-870793-6 N89-11456 #
CONF-870880-1 N89-11597 #
CONF-871072-2 N89-11592 #
CONF-871203-5 N89-10982 #
CONF-871251-5 N89-11411 #
CONF-871286-1 N89-11666 #
CONF-871298 N89-11031 #
CONF-880173-5 N89-11612 #
CONF-880206-15 N89-11594 #
CONF-880207-1 N89-11575 #
CONF-880210-3 N89-11636 #
CONF-880282-1 N89-10933 #
CONF-880297-1 N89-11685 #
CONF-880372-1 N89-11497 #
CONF-880391-1 N89-11682 #
CONF-880408-31 N89-11572 #
CONF-880408-32 N89-11212 #
CONF-880408-33 N89-11255 #
CONF-880408-35 N89-11601 #
CONF-880432-1 N89-11016 #
CONF-880435-23 N89-11209 #
CONF-880466-5 N89-11553* #
CONF-880466-6 N89-11579 #
CONF-880466-8 N89-11570 #
CONF-880473-8 N89-11051 #
CONF-880513-2 N89-11306 #
CONF-880521-1 N89-11383 #
CONF-880522-1 N89-11591 #
CONF-880529-2 N89-11587 #
CONF-880543-1 N89-10970 #
CONF-880598-2 N89-11300 #
CONF-880606-2 N89-10969 #
CONF-880613-15 N89-10999 #
CONF-880614-4 N89-11495 #
CONF-880625-1 N89-11034 #
CONF-880627-3 N89-11174 #
CONF-880639-1 N89-11668 #
CONF-880665-1 N89-11116 #
CONF-880669-3 N89-11565 #
CONF-880669-4 N89-10948 #
CONF-880669-5 N89-11032 #
CONF-880669-7 N89-11037 #
CONF-880669-10 N89-11585 #
CONF-880693-4 N89-11049 #
CONF-880699-7 N89-11119 #
CONF-880704-1 N89-11557 #
CONF-880704-2 N89-11552 #
CONF-880705-3 N89-11555 #
CONF-880713-15 N89-11202 #
CONF-880715-3 N89-11598 #
CONF-880716-7 N89-11178 #
CONF-880724-20 N89-11046 #
CONF-880724-21 N89-11175 #
CONF-880730-8 N89-10979 #
CONF-880732-1 N89-10975 #
CONF-880740-1 N89-11147 #
CONF-880752-4 N89-11235 #
CONF-880772-1 N89-11137 #
CONF-880780-1 N89-11342 #
CONF-880780-2 N89-11350 #
CONF-880781-1 N89-11504 #
CONF-880786-1 N89-11179 #
CONF-880802-2 N89-11053 #
CONF-880802-8 N89-10960 #
CONF-880802-9 N89-10978 #
CONF-880818-2 N89-10840 #
CONF-880827-2 N89-11139 #
CONF-880827-3 N89-10962 #
CONF-880836-1 N89-10841 #
CONF-880837-1 N89-11010 #
CONF-880841 N89-11584 #
CONF-880841-4 N89-11017 #
CONF-880841-5 N89-11026 #
CONF-880841-7 N89-10990 #
CONF-880841-8 N89-11584 #
CONF-880843-3 N89-11681 #
CONF-880844-1 N89-10995 #
CONF-880855-1 N89-11014 #
CONF-880855-2 N89-11012 #
CONF-880856-1 N89-11436 #
CONF-880857-1 N89-11345 #
CONF-880858-1 N89-11138 #
CONF-880870-1 N89-11556 #
CONF-880877-1 N89-11273 #
CONF-880884-1 N89-11599 #
CONF-880885-2 N89-10949 #
CONF-880887-8 N89-11511 #
CONF-880888-1 N89-11200 #
CONF-880888-3 N89-11199 #
CONF-880888-5 N89-11208 #
CONF-880888-6 N89-11207 #
CONF-880888-8 N89-11210 #
CONF-880889-1 N89-10981 #
CONF-880891-2 N89-11144 #
CONF-880911-11 N89-11506 #
CONF-880911-12 N89-11507 #
CONF-880911-14 N89-11508 #
CONF-880912-4 N89-10950 #
CONF-880912-5 N89-11036 #
CONF-880922-2 N89-11204 #
CONF-880925-1 N89-11070 #
CONF-880939-1 N89-11013 #
CONF-880940-2 N89-11251 #
CONF-880943-2 N89-10932 #
CONF-880948-1 N89-11117 #
CONF-880950-1 N89-11008 #
CONF-880986-1 N89-11551 #
CONF-881002-1 N89-11577 #
CONF-8810317 N89-11272 #
CONF-8810317 N89-11274 #
CONF-8810317 N89-11279 #
CONF-8811238 N89-11009 #
CONF-8708178-3 N89-10961 #
CONF-8709309-1 N89-11580 #
CONF-8709315-4 N89-11578 #
CONF-8803109-6 N89-11683 #
CONF-8803113-6 N89-11664 #
CONF-8804100-6 N89-11165 #
CONF-8804100-8 N89-11169 #
CONF-8804100-10 N89-10972 #
CONF-8804100-11 N89-11177 #
CONF-8804100-13 N89-11313 #
CONF-8804100-14 N89-11303 #
CONF-8804100-19 N89-11232 #
CONF-8804100-21 N89-11146 #
CONF-8804104-3 N89-11060* #
CONF-8804111-3 N89-11460 #
CONF-8804133-2 N89-11319 #
CONF-8804142-2 N89-11015 #
CONF-8804153-1 N89-11322 #
CONF-8804159-1 N89-11030 #
CONF-8804169-1 N89-11576 #
CONF-8805132-11 N89-11100 #
CONF-8805147-1 N89-11564 #
CONF-8805147-2 N89-11554 #
CONF-8805152-1 N89-11029 #
CONF-8805158-1 N89-11600 #
CONF-8805161-1 N89-11285 #
CONF-8805169-1 N89-11437 #
CONF-8805173-1 N89-10942 #
CONF-8806121-1 N89-11098 #
CONF-8806125-2 N89-11166 #
CONF-8806125-3 N89-11141 #
CONF-8806161-1 N89-10994 #
CONF-8806166-1 N89-11408 #
CONF-8806166-2 N89-11615 #
CONF-8806170-9 N89-11524 #
CONF-8806170-12 N89-11280 #
CONF-8809104-1 N89-11240 #
CONF-8809107-1 N89-11019 #
CONF-8809108-1 N89-10901 #
COO-3130TC-36 N89-11664 #
CRIE-T-86088 N89-11118 #
CRMSE-88-02 N89-11447 #
CS-8806 N89-11414 #
CSB-MEMO-3 N89-10891 #
CSIR-TWISK-481 N89-11478 #
CSSA-ASTRO-87-17 N89-11684 #
CU/ONR/1 N89-11432 #
DC-102 N89-11484 #
DC-104 N89-11243 #
DCS-14020RPT001 N89-11298 #
DERAT-22/5025-16 N89-11184 #
DERAT-23/5025-17 N89-11182 #
DERAT-24/5025-14 N89-10861 #
DERAT-25/5025-14 N89-10864 #
DERAT-40/5018-24 N89-11187 #
DERAT-42/5618-28 N89-11185 #
DERAT-52/5004-23 N89-10859 #
DERAT-53/5004-20 N89-11183 #
DE88-000349 N89-10840 #
DE88-001089 N89-11171 #
DE88-001133 N89-11312 #
DE88-001148 N89-11301 #
DE88-001160 N89-11302 #
DE88-001175 N89-11316 #
DE88-001189 N89-11311 #
DE88-005370 N89-11053 #
DE88-006198 N89-10962 #
DE88-006271 N89-11139 #
DE88-006462 N89-11204 #
DE88-006468 N89-11010 #
DE88-006826 N89-11147 #
DE88-006867 N89-10841 #
DE88-007207 N89-11017 #
DE88-007376 N89-11411 #
DE88-007481 N89-11026 #
DE88-007543 N89-11575 #
DE88-007761 N89-10980 #
DE88-007909 N89-10995 #
DE88-007932 N89-11013 #
DE88-007999 N89-11321 #
DE88-008094 N89-11034 #
DE88-008151 N89-11461 #
DE88-008471 N89-10990 #
DE88-008483 N89-11052 #
DE88-008629 N89-11666 #
DE88-008667 N89-11584 #
DE88-008882 N89-11589 #
DE88-009123 N89-11681 #
DE88-009135 N89-10932 #
DE88-009161 N89-11682 #
DE88-009165 N89-11456 #
DE88-009258 N89-11300 #
DE88-009587 N89-11251 #
DE88-009589 N89-11306 #
DE88-009628 N89-11308 #
DE88-009705 N89-11117 #
DE88-009822 N89-11014 #
DE88-009863 N89-11031 #
DE88-009958 N89-11008 #
DE88-009996 N89-11098 #
DE88-010017 N89-11345 #
DE88-010018 N89-11138 #
DE88-010078 N89-11436 #
DE88-010107 N89-11416 #
DE88-010252 N89-11309 #
DE88-010352 N89-10950 #
DE88-010494 N89-10998 #
DE88-010578 N89-11036 #
DE88-010671 N89-11556 #

DE88-010937 ..... N89-11012 #
DE88-011011 ..... N89-11319 #
DE88-011090 ..... N89-11116 #
DE88-011286 ..... N89-10977 #
DE88-011390 ..... N89-10933 #
DE88-011783 ..... N89-11393 #
DE88-011792 ..... N89-11119 #
DE88-011804 ..... N89-11299 #
DE88-011819 ..... N89-11451 #
DE88-011835 ..... N89-11235 #
DE88-011864 ..... N89-11273 #
DE88-011939 ..... N89-11011 #
DE88-011945 ..... N89-11322 #
DE88-011954 ..... N89-11553* #
DE88-011957 ..... N89-11029 #
DE88-011960 ..... N89-11668 #
DE88-011963 ..... N89-11015 #
DE88-011964 ..... N89-11046 #
DE88-011971 ..... N89-11175 #
DE88-011972 ..... N89-11497 #
DE88-011978 ..... N89-11557 #
DE88-011993 ..... N89-11572 #
DE88-011994 ..... N89-10970 #
DE88-012005 ..... N89-11570 #
DE88-012008 ..... N89-11137 #
DE88-012020 ..... N89-11495 #
DE88-012021 ..... N89-10960 #
DE88-012024 ..... N89-11408 #
DE88-012029 ..... N89-10989 #
DE88-012034 ..... N89-10994 #
DE88-012051 ..... N89-11591 #
DE88-012053 ..... N89-11016 #
DE88-012055 ..... N89-11579 #
DE88-012062 ..... N89-11636 #
DE88-012108 ..... N89-10898 #
DE88-012114 ..... N89-11122 #
DE88-012123 ..... N89-11007 #
DE88-012201 ..... N89-11564 #
DE88-012241 ..... N89-11530 #
DE88-012410 ..... N89-10927 #
DE88-012440 ..... N89-11100 #
DE88-012451 ..... N89-11417 #
DE88-012490 ..... N89-11383 #
DE88-012563 ..... N89-11574 #
DE88-012622 ..... N89-11151 #
DE88-012626 ..... N89-11048 #
DE88-012659 ..... N89-11307 #
DE88-012668 ..... N89-11565 #
DE88-012669 ..... N89-11551 #
DE88-012699 ..... N89-11032 #
DE88-012722 ..... N89-10966 #
DE88-012726 ..... N89-11615 #
DE88-012733 ..... N89-11460 #
DE88-012748 ..... N89-10899 #
DE88-012759 ..... N89-11664 #
DE88-012856 ..... N89-10948 #
DE88-012864 ..... N89-11051 #
DE88-012869 ..... N89-11212 #
DE88-012871 ..... N89-11030 #
DE88-012908 ..... N89-11569 #
DE88-012911 ..... N89-11330 #
DE88-012917 ..... N89-11303 #
DE88-012929 ..... N89-10961 #
DE88-012954 ..... N89-11239 #
DE88-012960 ..... N89-11685 #
DE88-012971 ..... N89-11149 #
DE88-013005 ..... N89-11525 #
DE88-013016 ..... N89-11280 #
DE88-013018 ..... N89-11524 #
DE88-013075 ..... N89-11567 #
DE88-013094 ..... N89-11141 #
DE88-013095 ..... N89-11166 #
DE88-013101 ..... N89-11592 #
DE88-013143 ..... N89-11314 #
DE88-013162 ..... N89-11072 #
DE88-013163 ..... N89-10928 #
DE88-013166 ..... N89-11360 #
DE88-013197 ..... N89-11255 #
DE88-013200 ..... N89-11177 #
DE88-013202 ..... N89-11313 #
DE88-013204 ..... N89-10972 #
DE88-013207 ..... N89-11174 #
DE88-013225 ..... N89-11169 #
DE88-013240 ..... N89-11165 #
DE88-013248 ..... N89-10999 #
DE88-013249 ..... N89-11025 #
DE88-013288 ..... N89-11463 #
DE88-013361 ..... N89-11285 #
DE88-013368 ..... N89-11240 #
DE88-013482 ..... N89-10968 #
DE88-013485 ..... N89-11211 #
DE88-013499 ..... N89-11617 #
DE88-013508 ..... N89-10991 #
DE88-013563 ..... N89-11325 #
DE88-013595 ..... N89-11582 #
DE88-013622 ..... N89-11150 #
DE88-013623 ..... N89-11001 #
DE88-013707 ..... N89-11597 #
DE88-013752 ..... N89-11028 #
DE88-013756 ..... N89-10959 #
DE88-013780 ..... N89-11346 #
DE88-013781 ..... N89-11587 #
DE88-013792 ..... N89-11059 #
DE88-013800 ..... N89-10926 #
DE88-013809 ..... N89-11178 #
DE88-013812 ..... N89-11464 #
DE88-013815 ..... N89-10942 #
DE88-013833 ..... N89-11146 #
DE88-013835 ..... N89-11232 #
DE88-013837 ..... N89-11037 #
DE88-013848 ..... N89-10975 #
DE88-013880 ..... N89-11247 #
DE88-013933 ..... N89-11230 #
DE88-013973 ..... N89-11494 #
DE88-013988 ..... N89-11555 #
DE88-013993 ..... N89-11612 #
DE88-013994 ..... N89-11598 #
DE88-014127 ..... N89-11573 #
DE88-014130 ..... N89-11018 #
DE88-014131 ..... N89-11528 #
DE88-014139 ..... N89-11049 #
DE88-014142 ..... N89-10981 #
DE88-014161 ..... N89-11199 #
DE88-014163 ..... N89-11208 #
DE88-014164 ..... N89-11207 #
DE88-014165 ..... N89-11200 #
DE88-014179 ..... N89-11210 #
DE88-014180 ..... N89-10949 #
DE88-014199 ..... N89-11047 #
DE88-014236 ..... N89-11027 #
DE88-014241 ..... N89-11568 #
DE88-014285 ..... N89-11518 #
DE88-014316 ..... N89-11504 #
DE88-014318 ..... N89-11342 #
DE88-014319 ..... N89-11350 #
DE88-014322 ..... N89-11506 #
DE88-014326 ..... N89-11507 #
DE88-014328 ..... N89-11585 #
DE88-014390 ..... N89-11685 #
DE88-014391 ..... N89-11060* #
DE88-014393 ..... N89-11576 #
DE88-014396 ..... N89-11577 #
DE88-014422 ..... N89-11070 #
DE88-014429 ..... N89-11508 #
DE88-014440 ..... N89-11019 #
DE88-014446 ..... N89-11594 #
DE88-014449 ..... N89-11552 #
DE88-014456 ..... N89-11437 #
DE88-014478 ..... N89-11179 #
DE88-014479 ..... N89-11683 #
DE88-014541 ..... N89-11148 #
DE88-014556 ..... N89-10982 #
DE88-014557 ..... N89-10901 #
DE88-014625 ..... N89-11293 #
DE88-014633 ..... N89-11586 #
DE88-014635 ..... N89-10989 #
DE88-014652 ..... N89-11213 #
DE88-014653 ..... N89-11180 #
DE88-014656 ..... N89-10978 #
DE88-014683 ..... N89-11599 #
DE88-014689 ..... N89-11323 #
DE88-014686 ..... N89-11317 #
DE88-014694 ..... N89-11245 #
DE88-014704 ..... N89-11304 #
DE88-014708 ..... N89-11305 #
DE88-014724 ..... N89-10947 #
DE88-014740 ..... N89-11326 #
DE88-014757 ..... N89-11209 #
DE88-014800 ..... N89-11519 #
DE88-014844 ..... N89-10979 #
DE88-014869 ..... N89-11600 #
DE88-014947 ..... N89-11095 #
DE88-014952 ..... N89-11340 #
DE88-014960 ..... N89-11580 #
DE88-014981 ..... N89-11578 #
DE88-014984 ..... N89-11531 #
DE88-014991 ..... N89-11144 #
DE88-015004 ..... N89-11420 #
DE88-015008 ..... N89-11394 #
DE88-015016 ..... N89-11413 #
DE88-015026 ..... N89-10983 #
DE88-015048 ..... N89-11505 #
DE88-015054 ..... N89-11633 #
DE88-015057 ..... N89-11336 #
DE88-015111 ..... N89-11226 #
DE88-015266 ..... N89-11601 #
DE88-015279 ..... N89-11554 #
DE88-015287 ..... N89-11511 #
DE88-015337 ..... N89-11202 #
DE88-015359 ..... N89-11238 #
DE88-015365 ..... N89-11310 #
DE88-015370 ..... N89-11486 #
DE88-015604 ..... N89-11512 #
DE88-015608 ..... N89-11181 #
DE88-015679 ..... N89-11532 #
DE88-015806 ..... N89-11602 #
DE88-015808 ..... N89-11571 #
DE88-015832 ..... N89-11206 #
DE88-016090 ..... N89-11214 #
DE88-016885 ..... N89-11421 #
DE88-701618 ..... N89-11272 #
DE88-701620 ..... N89-11274 #
DE88-701622 ..... N89-11279 #
DE88-702242 ..... N89-11609 #
DE88-702302 ..... N89-10992 #
DE88-702605 ..... N89-11392 #
DE88-702677 ..... N89-11583 #
DE88-702712 ..... N89-11588 #
DE88-702726 ..... N89-11586 #
DE88-702770 ..... N89-11009 #
DE88-702807 ..... N89-11227 #
DE88-702809 ..... N89-10974 #
DE88-702812 ..... N89-11679 #
DE88-702900 ..... N89-11194 #
DE88-702920 ..... N89-11205 #
DE88-702936 ..... N89-11143 #
DE88-702940 ..... N89-11490 #
DE88-702961 ..... N89-11269 #
DE88-702973 ..... N89-11593 #
DE88-702981 ..... N89-11672 #
DE88-702985 ..... N89-11606 #
DE88-702986 ..... N89-10976 #
DE88-702998 ..... N89-11140 #
DE88-702999 ..... N89-11168 #
DE88-703000 ..... N89-11167 #
DE88-703005 ..... N89-11383 #
DE88-703010 ..... N89-11450 #
DE88-703014 ..... N89-11320 #
DE88-703025 ..... N89-11561 #
DE88-703031 ..... N89-11522 #
DE88-703038 ..... N89-11558 #
DE88-703079 ..... N89-11562 #
DE88-703152 ..... N89-11603 #
DE88-703156 ..... N89-11485 #
DE88-703157 ..... N89-11466 #
DE88-703158 ..... N89-11467 #
DE88-703167 ..... N89-11468 #
DE88-753437 ..... N89-11118 #

DFVLR-FB-84-30 ..... N89-11242 #
DFVLR-FB-87-46 ..... N89-11105 #

DFVLR-IB-435-87/20 ..... N89-11318 #

DFVLR-MITT-87-20 ..... N89-11197 #
DFVLR-MITT-88-06 ..... N89-11318 #
DFVLR-MITT-88-13 ..... N89-11443 #
DFVLR-MITT-88-14 ..... N89-10956 #
DFVLR-MITT-88-15 ..... N89-10882 #
DFVLR-MITT-88-16 ..... N89-11444 #

DIA-DST-2700Z-001-88 ..... N89-11223 #

DODA-AR-004-595 ..... N89-11024 #
DODA-AR-005-257 ..... N89-10891 #

DOE/CE-31010/T1 ..... N89-11299 #

DOE/CH-10093/21 ..... N89-11301 #

DOE/DP-40200/73 ..... N89-11463 #

DOE/ER-01198/T16 ..... N89-11586 #
DOE/ER-01198/T21 ..... N89-10989 #
DOE/ER-01198/T25 ..... N89-11035 #
DOE/ER-03130/36C ..... N89-11664 #
DOE/ER-13275/T1 ..... N89-11213 #
DOE/ER-13275/T2 ..... N89-11214 #
DOE/ER-13295/2 ..... N89-10988 #
DOE/ER-13411/3 ..... N89-11007 #
DOE/ER-13579/20 ..... N89-10959 #
DOE/ER-13597/T1 ..... N89-11149 #
DOE/ER-13649/1 ..... N89-10980 #
DOE/ER-13800/T1 ..... N89-11180 #
DOE/ER-13820/T1 ..... N89-11181 #
DOE/ER-25009/587 ..... N89-11394 #
DOE/ER-25009/593 ..... N89-11413 #
DOE/ER-25009/605 ..... N89-11420 #
DOE/ER-30024/T3 ..... N89-11211 #
DOE/ER-40077/4 ..... N89-11568 #
DOE/ER-45158/T2 ..... N89-11230 #
DOE/ER-45161/T1 ..... N89-11027 #
DOE/ER-45172/T1 ..... N89-11602 #
DOE/ER-45184/4 ..... N89-11018 #
DOE/ER-45203/4 ..... N89-11571 #
DOE/ER-45211/5 ..... N89-11456 #
DOE/ER-45224/4 ..... N89-11567 #
DOE/ER-45228/37 ..... N89-11028 #

DOE/ER-45280/T1 ..... N89-11569 #
DOE/ER-45295/1 ..... N89-11011 #
DOE/ER-45347/5 ..... N89-11573 #
DOE/ER-53176/4 ..... N89-11518 #
DOE/ER-53192/T3 ..... N89-10947 #
DOE/ER-53201/3 ..... N89-11528 #
DOE/ER-53205/T3 ..... N89-11525 #
DOE/ER-53223/68 ..... N89-11531 #
DOE/ER-60177/1 ..... N89-11326 #
DOE/ER-60334/T1 ..... N89-11321 #
DOE/ER-60372/3 ..... N89-11323 #
DOE/ER-60416/T1 ..... N89-11574 #
DOE/ER-60468/2 ..... N89-11330 #
DOE/ER-60472/02 ..... N89-11293 #

DOE/ET-51013/251 ..... N89-11519 #

DOE/ID-10205 ..... N89-11238 #
DOE/ID-12525/1-PT-1 ..... N89-11340 #

DOE/MC-21353/2584 ..... N89-11171 #

DOE/METC-88-6096 ..... N89-11309 #

DOE/PC-79931/1 ..... N89-11308 #
DOE/PC-90960/8 ..... N89-11148 #

DOT-HS-807-219 ..... N89-11389 #

DOT/FAA/CT-87/26 ..... N89-11265 #
DOT/FAA/CT-87/37 ..... N89-10894 #
DOT/FAA/CT-88/6 ..... N89-11356 #
DOT/FAA/CT-88/21 ..... N89-10893 #
DOT/FAA/CT-88/23 ..... N89-10892 #

DOT/FAA/DS-88/6 ..... N89-10869 #

DOT/FAA/PM-86/42 ..... N89-10870 #

DOT/FAA/PS-88/14 ..... N89-11356 #

DOT/FAA/SA-88/2 ..... N89-10885 #

DP-TR-106 ..... N89-10998 #

DREV-R-4423/87 ..... N89-11099

E-3437 ..... N89-10885* #
E-4113 ..... N89-10858* #
E-4183 ..... N89-10844* #
E-4184 ..... N89-10996* #
E-4332 ..... N89-11038* #
E-4335 ..... N89-11128* #
E-4369 ..... N89-10944* #
E-4377 ..... N89-10952* #
E-4384 ..... N89-11469* #
E-4389 ..... N89-11129* #
E-4395 ..... N89-11637* #
E-4396 ..... N89-11198* #
E-4412 ..... N89-10863* #

EE-88-183 ..... N89-10923* #

EGG-MS-8000 ..... N89-11226 #

EGG-10282-2140 ..... N89-11578 #
EGG-10282-2156 ..... N89-11580 #

EPA/SW/DK-88/047A ..... N89-11620 #

EPA/600/D-88/082 ..... N89-11452 #
EPA/600/4-87-035 ..... N89-11325 #
EPA/600/8-87/052A ..... N89-11620 #

EPM/RT-88/23 ..... N89-11264 #

ESA-CR(P)-2621 ..... N89-11422 #

ESA-SP-283 ..... N89-11638 #

ESA-TT-902 ..... N89-11242 #
ESA-TT-1106 ..... N89-11105 #
ESA-TT-1111 ..... N89-11197 #

ESD-TR-88-001 ..... N89-11434 #

ETCA-88-R-036 ..... N89-11533 #

ETL-R-138 ..... N89-10886 #

ETN-88-93043 ..... N89-11422 #
ETN-88-93075 ..... N89-11215 #
ETN-88-93078 ..... N89-11241 #
ETN-88-93077 ..... N89-11123 #
ETN-88-93076 ..... N89-11124 #
ETN-88-93091 ..... N89-10930 #
ETN-88-93092 ..... N89-11423 #
ETN-88-93093 ..... N89-11424 #
ETN-88-93094 ..... N89-10839 #
ETN-88-93095 ..... N89-11425 #
ETN-88-93096 ..... N89-10924 #
ETN-88-93097 ..... N89-11426 #
ETN-88-93098 ..... N89-10953 #
ETN-88-93099 ..... N89-10954 #
ETN-88-93100 ..... N89-11125 #
ETN-88-93101 ..... N89-11286 #
ETN-88-93102 ..... N89-10955 #
ETN-88-93103 ..... N89-11513 #
ETN-88-93104 ..... N89-11182 #
ETN-88-93105 ..... N89-10859 #
ETN-88-93106 ..... N89-11183 #
ETN-88-93107 ..... N89-11184 #
ETN-88-93108 ..... N89-11533 #
ETN-88-93111 ..... N89-10860 #
ETN-88-93112 ..... N89-11185 #
ETN-88-93113 ..... N89-10861 #
ETN-88-93157 ..... N89-11638 #
ETN-88-93176 ..... N89-11242 #
ETN-88-93180 ..... N89-11318 #
ETN-88-93181 ..... N89-11443 #
ETN-88-93182 ..... N89-10956 #
ETN-88-93183 ..... N89-10862 #
ETN-88-93184 ..... N89-11444 #
ETN-88-93191 ..... N89-11502 #
ETN-88-93202 ..... N89-11534 #
ETN-88-93207 ..... N89-11186 #
ETN-88-93268 ..... N89-11470 #
ETN-88-93270 ..... N89-11428 #
ETN-88-93273 ..... N89-11479 #
ETN-88-93274 ..... N89-11471 #
ETN-88-93275 ..... N89-11429 #
ETN-88-93278 ..... N89-11472 #
ETN-88-93317 ..... N89-10957 #
ETN-88-93319 ..... N89-10864 #
ETN-88-93320 ..... N89-11187 #
ETN-88-93321 ..... N89-11020 #
ETN-88-93323 ..... N89-11105 #
ETN-88-93324 ..... N89-11197 #

ETS-RR-88-28-ONR ..... N89-11404 #

EUR-10592-EN ..... N89-11257 #
EUR-11328 ..... N89-11151 #
EUR-11360 ..... N89-11048 #

FERMILAB-CONF-88/85-A ..... N89-11613* #
FERMILAB-CONF-88/116-A ..... N89-11674* #

FERMILAB-PUB-88/70-A ..... N89-11614* #
FERMILAB-PUB-88/78-A ..... N89-11501* #
FERMILAB-PUB-88/100-A ..... N89-11489* #
FERMILAB-PUB-88/108-A ..... N89-11604* #
FERMILAB-PUB-88/118-A ..... N89-11673* #
FERMILAB-PUB-88/132-A ..... N89-11675* #
FERMILAB-PUB-88/139-A ..... N89-11500* #

FNAL-TM-1517-A-ADD ..... N89-10966 #

FTD-ID(RS)T-0260-88 ..... N89-11220 #
FTD-ID(RS)T-0262-88 ..... N89-11218 #

GA-A-19031 ..... N89-11451 #

GALILEO-72132 ..... N89-11191* #

GISS-88-182 ..... N89-11381* #

GRI-88/0109 ..... N89-11172 #
GRI-88/0125 ..... N89-11033 #

HDL-TR-2145 ..... N89-11115 #

I-ARA-88-U-24 ..... N89-11509 #

IC-87/71 ..... N89-11609 #
IC-87/244 ..... N89-11269 #
IC-87/257 ..... N89-11593 #
IC-87/267 ..... N89-11672 #
IC-87/273 ..... N89-11583 #
IC-87/281 ..... N89-11603 #
IC-87/318 ..... N89-11588 #
IC-87/321 ..... N89-11608 #
IC-87/335 ..... N89-11566 #
IC-87/358 ..... N89-11465 #
IC-87/359 ..... N89-11466 #
IC-87/360 ..... N89-11467 #
IC-87/365 ..... N89-10976 #
IC-87/384-PT-1 ..... N89-11140 #
IC-87/385-PT-2 ..... N89-11168 #
IC-87/386 ..... N89-11167 #
IC-87/395 ..... N89-11363 #
IC-87/408 ..... N89-11450 #
IC-87/413 ..... N89-11320 #
IC-88/3 ..... N89-11561 #
IC-88/10 ..... N89-11522 #
IC-88/21 ..... N89-11558 #
IC-88/46 ..... N89-11468 #

ICASE-88-52 ..... N89-11459* #

ICOMP-88-18 ..... N89-11469* #

IDA-P-2018 ..... N89-11488 #
IDA-P-2058 ..... N89-11487 #

IDA/HQ-87-32194 ..... N89-11488 #
IDA/HQ-87-32823 ..... N89-11487 #

INIS-BR-964 ..... N89-11272 #
INIS-BR-966 ..... N89-11274 #
INIS-BR-968 ..... N89-11279 #
INIS-BR-1038 ..... N89-10992 #
INIS-BR-1072 ..... N89-11009 #

INIS-SU-19/A ..... N89-11227 #
INIS-SU-21 ..... N89-10974 #
INIS-SU-25/A ..... N89-11392 #
INIS-SU-35 ..... N89-11679 #

INPE-4518-PRE/1270 ..... N89-11329 #
INPE-4559-PRE/1300 ..... N89-11418 #
INPE-4568-PRE/1309 ..... N89-11291 #
INPE-4571-PRE/1311 ..... N89-11419 #
INPE-4574-NTE/280 ..... N89-11121 #
INPE-4620-TDL/328 ..... N89-11352 #
INPE-4640-PRE/1351 ..... N89-11294 #
INPE-4644-PRE/1355 ..... N89-11297 #
INPE-4647-PRE/1357 ..... N89-11559 #
INPE-4651-PRE/1358 ..... N89-11324 #
INPE-4654-PRE/1361 ..... N89-11427 #
INPE-4663-NTE/282 ..... N89-11491 #
INPE-4668-PRE/1368 ..... N89-11331 #
INPE-4669-PRE/1369 ..... N89-11351 #
INPE-4675-NTE/284 ..... N89-11438 #
INPE-4681-PRE/1376 ..... N89-11634 #
INPE-4686-PRE/1380 ..... N89-11295 #
INPE-4693-TDL/342 ..... N89-11126 #
INPE-4694-RPE/575 ..... N89-11369 #

IPP-III/134 ..... N89-11534 #

IPPJ-872 ..... N89-11526 #
IPPJ-873 ..... N89-11527 #
IPPJ-875 ..... N89-11520 #
IPPJ-876 ..... N89-11523 #
IPPJ-880 ..... N89-11529 #
IPPJ-884 ..... N89-11544 #
IPPJ-885 ..... N89-11545 #
IPPJ-886 ..... N89-11547 #
IPPJ-887 ..... N89-11548 #
IPPJ-888 ..... N89-11549 #
IPPJ-889 ..... N89-11546 #

ISAS-RN-349 ..... N89-11667 #
ISAS-RN-353 ..... N89-11663 #
ISAS-RN-358 ..... N89-11335 #
ISAS-RN-362 ..... N89-10888 #

ISBN-0-90-4947-07-6 ..... N89-10846
ISBN-92-825-6368-5 ..... N89-11257 #
ISBN-92-835-0448-8 ..... N89-11395 #
ISBN-92-835-0464-X ..... N89-10831 #
ISBN-92-835-0477-1 ..... N89-10874 #
ISBN-92-835-0479-8 ..... N89-11625 #
ISBN-951-754-449-9 ..... N89-11104 #

ISSN-0082-5255 ..... N89-11250 #
ISSN-0082-5263 ..... N89-11152 #
ISSN-0173-699X ..... N89-11688 #
ISSN-0176-7739 ..... N89-10862 #
ISSN-0176-7739 ..... N89-10956 #
ISSN-0176-7739 ..... N89-11318 #
ISSN-0176-7739 ..... N89-11443 #
ISSN-0176-7739 ..... N89-11444 #
ISSN-0271-7077 ..... N89-11687 #
ISSN-0374-1257 ..... N89-11186 #
ISSN-0379-6566 ..... N89-11638 #
ISSN-0469-4732 ..... N89-11520 #
ISSN-0469-4732 ..... N89-11523 #
ISSN-0469-4732 ..... N89-11526 #
ISSN-0469-4732 ..... N89-11527 #
ISSN-0469-4732 ..... N89-11529 #
ISSN-0469-4732 ..... N89-11544 #
ISSN-0469-4732 ..... N89-11545 #
ISSN-0469-4732 ..... N89-11546 #
ISSN-0469-4732 ..... N89-11547 #
ISSN-0469-4732 ..... N89-11548 #
ISSN-0469-4732 ..... N89-11549 #

JINR-E-17-87-436 N89-11205 #

JINR-R-8-87-446 N89-11143 #
JINR-R-8-87-526 N89-11562 #
JINR-R-11-87-427 N89-11490 #

JINR-13-87-566 N89-11194 #

JPL-D-4710 N89-11475* #

JPL-PUBL-82-68-REV-1 N89-11661* #
JPL-PUBL-87-4-VOL-7 N89-11328* #
JPL-PUBL-87-43 N89-10931* #
JPL-PUBL-88-7 N89-11441* #
JPL-PUBL-88-16 N89-11237* #
JPL-PUBL-88-22 N89-11074* #
JPL-PUBL-88-26 N89-10941* #

JPL-400/341 N89-10921* #

JPRS-JST-87-018 N89-11061 #

JPRS-ULS-87-010 N89-11385

JPRS-UMS-88-007 N89-11002 #

JSR-87-301 N89-11211 #

KMSF-U-1993 N89-11280 #
KMSF-U-1996 N89-11524 #

L-16430 N89-10842* #

LA-SUB-651-2C-1 N89-11052 #

LA-UR-88-427 N89-11010 #
LA-UR-88-540 N89-11204 #
LA-UR-88-582 N89-10962 #
LA-UR-88-674 N89-10995 #
LA-UR-88-1229 N89-10932 #
LA-UR-88-1264 N89-11682 #
LA-UR-88-1282 N89-11681 #
LA-UR-88-1586 N89-11012 #
LA-UR-88-1741 N89-11683 #
LA-UR-88-1742 N89-11179 #
LA-UR-88-1836 N89-11437 #
LA-UR-88-1914 N89-11552 #
LA-UR-88-1926 N89-11594 #
LA-UR-88-1960 N89-11019 #
LA-UR-88-2008 N89-11508 #
LA-UR-88-2045 N89-11070 #
LA-UR-88-2188 N89-11504 #
LA-UR-88-2222 N89-11342 #
LA-UR-88-2223 N89-11350 #
LA-UR-88-2258 N89-11506 #
LA-UR-88-2272 N89-11507 #
LA-UR-88-2277 N89-11585 #
LA-UR-88-2403 N89-11685 #
LA-UR-88-2405 N89-11060* #
LA-UR-88-2429 N89-11576 #
LA-UR-88-2451 N89-11577 #

LA-11271-MS N89-11665 #
LA-11274-PR N89-11505 #
LA-11296-MS N89-11532 #
LA-11329-MS N89-11336 #
LA-11341 N89-11633 #

LAAS-88-097 N89-11215 #
LAAS-88-131 N89-11241 #
LAAS-88-138 N89-11123 #
LAAS-88-164 N89-11124 #

LBL-24643 N89-11411 #
LBL-24687 N89-10978 #
LBL-24734 N89-11495 #
LBL-24767 N89-11408 #
LBL-25022 N89-11015 #
LBL-25230 N89-10960 #
LBL-25244 N89-11556 #
LBL-25330 N89-10969 #
LBL-25375 N89-11668 #
LBL-25392 N89-11592 #
LBL-25404 N89-11582 #
LBL-25443 N89-11597 #
LBL-25482 N89-11600 #
LBL-25543 N89-11599 #

LBS-88-7271 N89-11060* #

LIDS-P-1721 N89-11439 #

LMSC/D878344 N89-11136 #
LMSC/D973480 N89-11315* #

LSU-8013973 N89-11494 #

M-591 N89-11153* #

MF-117 N89-11531 #

MLM-3491(OP) N89-11212 #
MLM-3497(OP) N89-11030 #
MLM-3504(OP) N89-11051 #

MPE-PAE/EXP-EL-190 N89-11502

MPE-200 N89-11688 #

MPIS-89-1987 N89-11186 #

MRL-88-0003 N89-11586 #

MSC-6356 N89-11456 #

MTL-TR-88-18 N89-11515 #

M88-1 N89-11434 #

NAL/TR-950T N89-10845 #

NAPC-PE-144 N89-10893 #

NAS 1.15:4060 N89-11381* #
NAS 1.15:4062 N89-10842* #
NAS 1.15:88969 N89-10865* #
NAS 1.15:89425 N89-10872* #
NAS 1.15:89672 N89-11060* #
NAS 1.15:89716 N89-11686* #
NAS 1.15:100342 N89-11127* #
NAS 1.15:100549 N89-10951* #
NAS 1.15:100603 N89-10929* #
NAS 1.15:100642 N89-11287* #
NAS 1.15:100662 N89-10945* #
NAS 1.15:100879 N89-10858* #
NAS 1.15:100968 N89-11198* #
NAS 1.15:101199 N89-11498* #
NAS 1.15:101219 N89-11553* #
NAS 1.15:101349 N89-11038* #
NAS 1.15:101350 N89-10952* #
NAS 1.15:101354 N89-10944* #
NAS 1.15:101355 N89-11469* #
NAS 1.15:101359 N89-11129* #
NAS 1.15:101360 N89-11128* #
NAS 1.15:101362 N89-11637* #
NAS 1.21:497 N89-11657* #
NAS 1.21:7039(33) N89-11624*
NAS 1.26:4193 N89-11196* #
NAS 1.26:172071 N89-11050* #
NAS 1.26:172081 N89-10923* #
NAS 1.26:179377 N89-11361* #
NAS 1.26:179378 N89-11203* #
NAS 1.26:179392 N89-10934* #
NAS 1.26:179476 N89-11315* #
NAS 1.26:180224 N89-10946* #
NAS 1.26:180226 N89-10843* #
NAS 1.26:180390 N89-11237* #
NAS 1.26:180790 N89-11191* #
NAS 1.26:180802 N89-11195* #
NAS 1.26:180900 N89-11192* #
NAS 1.26:181226 N89-11234* #
NAS 1.26:181317 N89-11440* #
NAS 1.26:181329 N89-11406* #
NAS 1.26:181524 N89-11457* #
NAS 1.26:181703 N89-10936* #
NAS 1.26:181719 N89-11459* #
NAS 1.26:182176 N89-10943* #
NAS 1.26:182209 N89-10863* #
NAS 1.26:182434 N89-11290* #
NAS 1.26:182641 N89-11441* #
NAS 1.26:182735 N89-10931* #
NAS 1.26:182736 N89-11328* #
NAS 1.26:182742 N89-11671* #
NAS 1.26:182743 N89-10941* #
NAS 1.26:182744 N89-11661* #
NAS 1.26:182796 N89-11074* #
NAS 1.26:182996 N89-11475* #
NAS 1.26:183057 N89-10897* #
NAS 1.26:183133 N89-10921* #
NAS 1.26:183171 N89-11201* #
NAS 1.26:183183 N89-11055* #
NAS 1.26:183189 N89-11057* #
NAS 1.26:183191 N89-10838* #
NAS 1.26:183216 N89-11233* #
NAS 1.26:183233 N89-11384* #
NAS 1.26:183245 N89-10895* #
NAS 1.26:183247 N89-10900* #
NAS 1.26:183257 N89-11359* #
NAS 1.26:183259 N89-11292* #
NAS 1.26:183268 N89-11595* #
NAS 1.26:183274 N89-10922* #
NAS 1.26:183282 N89-11056* #
NAS 1.26:183299 N89-11678* #

NAS 1.26:183301 N89-11362* #
NAS 1.26:183304 N89-11368* #
NAS 1.26:183305 N89-10890* #
NAS 1.26:183325 N89-10984* #
NAS 1.26:183326 N89-11296* #
NAS 1.26:183348 N89-11106* #
NAS 1.26:183359 N89-11674* #
NAS 1.26:183361 N89-11604* #
NAS 1.26:183363 N89-11614* #
NAS 1.26:183364 N89-11501* #
NAS 1.26:183365 N89-11489* #
NAS 1.26:183367 N89-11613* #
NAS 1.26:183369 N89-11500* #
NAS 1.26:183372 N89-11675* #
NAS 1.26:183373 N89-11673* #
NAS 1.26:183471 N89-11102* #
NAS 1.55:3006 N89-11153* #
NAS 1.55:3008 N89-10902* #
NAS 1.55:10008 N89-10849* #
NAS 1.55:10013 N89-11407* #
NAS 1.60:2846 N89-10844* #
NAS 1.60:2863 N89-10996* #
NAS 1.77:20309 N89-10963* #

NASA-CP-3006 N89-11153* #
NASA-CP-3008 N89-10902* #
NASA-CP-10008 N89-10849* #
NASA-CP-10013 N89-11407* #

NASA-CR-4193 N89-11196* #
NASA-CR-172071 N89-11050* #
NASA-CR-172081 N89-10923* #
NASA-CR-179377 N89-11361* #
NASA-CR-179378 N89-11203* #
NASA-CR-179392 N89-10934* #
NASA-CR-179476 N89-11315* #
NASA-CR-180224 N89-10946* #
NASA-CR-180226 N89-10843* #
NASA-CR-180390 N89-11237* #
NASA-CR-180790 N89-11191* #
NASA-CR-180802 N89-11195* #
NASA-CR-180900 N89-11192* #
NASA-CR-181226 N89-11234* #
NASA-CR-181317 N89-11440* #
NASA-CR-181329 N89-11406* #
NASA-CR-181524 N89-11457* #
NASA-CR-181703 N89-10936* #
NASA-CR-181719 N89-11459* #
NASA-CR-182176 N89-10943* #
NASA-CR-182209 N89-10863* #
NASA-CR-182434 N89-11290* #
NASA-CR-182641 N89-11441* #
NASA-CR-182735 N89-10931* #
NASA-CR-182736 N89-11328* #
NASA-CR-182742 N89-11671* #
NASA-CR-182743 N89-10941* #
NASA-CR-182744 N89-11661* #
NASA-CR-182796 N89-11074* #
NASA-CR-182996 N89-11475* #
NASA-CR-183057 N89-10897* #
NASA-CR-183133 N89-10921* #
NASA-CR-183171 N89-11201* #
NASA-CR-183183 N89-11055* #
NASA-CR-183189 N89-11057* #
NASA-CR-183191 N89-10838* #
NASA-CR-183216 N89-11233* #
NASA-CR-183233 N89-11384* #
NASA-CR-183245 N89-10895* #
NASA-CR-183247 N89-10900* #
NASA-CR-183257 N89-11359* #
NASA-CR-183259 N89-11292* #
NASA-CR-183268 N89-11595* #
NASA-CR-183274 N89-10922* #
NASA-CR-183282 N89-11056* #
NASA-CR-183299 N89-11678* #
NASA-CR-183301 N89-11362* #
NASA-CR-183304 N89-11368* #
NASA-CR-183305 N89-10890* #
NASA-CR-183325 N89-10984* #
NASA-CR-183326 N89-11296* #
NASA-CR-183348 N89-11106* #
NASA-CR-183359 N89-11674* #
NASA-CR-183361 N89-11604* #
NASA-CR-183363 N89-11614* #
NASA-CR-183364 N89-11501* #
NASA-CR-183365 N89-11489* #
NASA-CR-183367 N89-11613* #
NASA-CR-183369 N89-11500* #
NASA-CR-183372 N89-11675* #
NASA-CR-183373 N89-11673* #
NASA-CR-183471 N89-11102* #

NASA-SP-497 N89-11657* #
NASA-SP-7039(33) N89-11624*

NASA-TM-4060 N89-11381* #

NASA-TM-4062 ..... N89-10842* #
NASA-TM-88969 ..... N89-10865* #
NASA-TM-89425 ..... N89-10872* #
NASA-TM-89672 ..... N89-11060* #
NASA-TM-89716 ..... N89-11686* #
NASA-TM-100342 ..... N89-11127* #
NASA-TM-100549 ..... N89-10951* #
NASA-TM-100603 ..... N89-10929* #
NASA-TM-100642 ..... N89-11287* #
NASA-TM-100662 ..... N89-10945* #
NASA-TM-100879 ..... N89-10858* #
NASA-TM-100968 ..... N89-11198* #
NASA-TM-101199 ..... N89-11498* #
NASA-TM-101219 ..... N89-11553* #
NASA-TM-101349 ..... N89-11038* #
NASA-TM-101350 ..... N89-10952* #
NASA-TM-101354 ..... N89-10944* #
NASA-TM-101355 ..... N89-11469* #
NASA-TM-101359 ..... N89-11129* #
NASA-TM-101360 ..... N89-11128* #
NASA-TM-101362 ..... N89-11637* #

NASA-TP-2846 ..... N89-10844* #
NASA-TP-2863 ..... N89-10996* #

NASA-TT-20309 ..... N89-10963* #

NAVSO-P-3580-VOL-12-NO-4 ..... N89-11687 #

NBS/SP-500/154 ..... N89-11621 #

NBSIR-88/3768 ..... N89-11412 #
NBSIR-88/3796 ..... N89-11271 #

NCAR/AR-87 ..... N89-11355 #

NLR-MP-87023-U ..... N89-11058 #

NOAA-TM-ERL-ARL-162 ..... N89-11327 #

NRL-MR-6146 ..... N89-11221 #
NRL-MR-6190 ..... N89-11113 #

NRL-R-1003(R) N89-10997

NSF/ENG-88005 ..... N89-11244 #

NTSB/AAB-88/06 ..... N89-10871 #

NTSB/AAR-88/02-SUMM ..... N89-10868 #
NTSB/AAR-88/07 ..... N89-10873 #

ONERA-RT-11/2891-AN-PT-2 ..... N89-10860 #
ONERA-RT-17/3542-RY-070-R ..... N89-10953 #

ORNL/TM-10525 ..... N89-11617 #
ORNL/TM-10747 ..... N89-10991 #

OTA-ISC-374 ..... N89-11635 #

PB88-125315 ..... N89-11257 #
PB88-126594 ..... N89-11478 #
PB88-131974 ..... N89-11581 #
PB88-192562 ..... N89-11635 #
PB88-200787 ..... N89-11620 #
PB88-201561 ..... N89-11621 #
PB88-201934 ..... N89-11389 #
PB88-202908 ..... N89-11453 #
PB88-202916 ..... N89-11462 #
PB88-208616 ..... N89-11380 #
PB88-209754 ..... N89-11058 #
PB88-209911 ..... N89-11458 #
PB88-209929 ..... N89-11414 #
PB88-210075 ..... N89-11477 #
PB88-210091 ..... N89-11104 #
PB88-210828 ..... N89-11365 #
PB88-213624 ..... N89-11327 #
PB88-214416 ..... N89-10845 #
PB88-214549 ..... N89-11231 #
PB88-214796 ..... N89-11452 #
PB88-215645 ..... N89-11412 #
PB88-217054 ..... N89-11033 #
PB88-217070 ..... N89-11172 #
PB88-218219 ..... N89-11271 #
PB88-220009 ..... N89-11355 #
PB88-235106 ..... N89-11244 #
PB88-910407 ..... N89-10868 #
PB88-910409 ..... N89-10873 #
PB88-916906 ..... N89-10871 #

PD-SE-8807 ..... N89-11449 #
PD-SE-8806 ..... N89-11410 #

PFC/IR-88-4 ..... N89-11519 #

PNL-SA-15381 ..... N89-11209 #

PNL-6077 ..... N89-11317 #
PNL-6575 ..... N89-11310 #
PNL-6580 ..... N89-11360 #
PNL-6592 ..... N89-11512 #

PSI-1038/TR-862 ..... N89-11057* #
PSI-9139/TR-728 ..... N89-10937 #

PSU-ME-R-87/88-0031 ..... N89-11189 #

RADC-TR-88-32-VOL-1 ..... N89-11112 #
RADC-TR-88-86 ..... N89-11133 #

REPT-M0-535200 ..... N89-11020 #

REPT-NT-195/87/CRB/GTR.C/NP ..... N89-10955 #

REPT-26 ..... N89-11104 #
REPT-49-062/F ..... N89-10957 #
REPT-87/56 ..... N89-11286 #
REPT-88-NICI-01 ..... N89-11458 #
REPT-88-03 ..... N89-11477 #
REPT-88-014 ..... N89-11686* #
REPT-88-158 ..... N89-10902* #
REPT-328 ..... N89-11453 #
REPT-330 ..... N89-11462 #
REPT-3011-01-03-4675 ..... N89-10885 #
REPT-4761-6002-UT-00 ..... N89-11114 #
REPT-363300 ..... N89-11513 #
REPT-437103/79 ..... N89-11020 #

RFP-TRANS-477 ..... N89-11239 #

RR-714-M ..... N89-11470 #
RR-720-I ..... N89-11428 #
RR-723-M ..... N89-11472 #
RR-726-M ..... N89-11479 #
RR-727-I-IMAG-82-LIFIA ..... N89-11471 #
RR-728-I-IMAG-83-LIFIA ..... N89-11429 #

S-325-TP ..... N89-11578 #

SAND-87-1432 ..... N89-10927 #
SAND-87-1769C ..... N89-11306 #
SAND-87-2034 ..... N89-10898 #
SAND-87-2052C ..... N89-11139 #
SAND-87-2054C ..... N89-10962 #
SAND-87-2129C ..... N89-11300 #
SAND-87-2396C ..... N89-11116 #
SAND-87-2452 ..... N89-11530 #
SAND-87-2580C ..... N89-11240 #
SAND-87-3011C ..... N89-10840 #
SAND-88-0021C ..... N89-10841 #
SAND-88-0079 ..... N89-11122 #
SAND-88-0184C ..... N89-11147 #
SAND-88-0230C ..... N89-10979 #
SAND-88-0270C ..... N89-11032 #
SAND-88-0299C ..... N89-11565 #
SAND-88-0334C ..... N89-11119 #
SAND-88-0497 ..... N89-10899 #
SAND-88-0617 ..... N89-10926 #
SAND-88-0662C ..... N89-11017 #
SAND-88-0681C ..... N89-11144 #
SAND-88-0750C ..... N89-11013 #
SAND-88-0777 ..... N89-10983 #
SAND-88-0857C ..... N89-11285 #
SAND-88-0896 ..... N89-11416 #
SAND-88-0956C ..... N89-10990 #
SAND-88-1030C ..... N89-11601 #
SAND-88-1121C ..... N89-11036 #
SAND-88-1144 ..... N89-11304 #
SAND-88-1194C ..... N89-11251 #
SAND-88-1281 ..... N89-11393 #
SAND-88-1347C ..... N89-10950 #
SAND-88-1438C ..... N89-11551 #
SAND-88-1784C ..... N89-10948 #
SAND-88-1906 ..... N89-11206 #
SAND-88-7021-PT-1/2 ..... N89-11305 #
SAND-88-7026 ..... N89-11314 #
SAND-88-8001 ..... N89-10977 #

SAPR-21 ..... N89-11671* #

SD-TR-88-61 ..... N89-11606 #
SD-TR-88-68 ..... N89-10935 #

SERI/PR-215-3292 ..... N89-11312 #

SERI/STR-211-3289 ..... N89-11302 #
SERI/STR-211-3332 ..... N89-11316 #
SERI/STR-211-3363 ..... N89-11311 #

SR-5 ..... N89-10938 #
SR-88-20 ..... N89-11330 #

SU-SLAC-PUB-4474 ..... N89-11615 #

SU-SLAC-PUB-4626 ..... N89-11460 #
SU-SLAC-PUB-4663 ..... N89-11202 #

SU-SLAC-TN-88-2-VOL-2 ..... N89-11247 #

SU-SOL-88-13 ..... N89-11421 #

SU-SPO-1018 ..... N89-11055* #

TM-AE-8705 ..... N89-10847 #
TM-AE-8801 ..... N89-11455 #

TM-FM-8803 ..... N89-10971 #
TM-FM-8804-PT-1 ..... N89-10964 #
TM-FM-8805-PT-2 ..... N89-10973 #
TM-FM-8806 ..... N89-11142 #

TM-31 ..... N89-11475* #

TR-33 ..... N89-11039 #
TR-83-03-03 ..... N89-11431 #
TR-88-16C ..... N89-11485 #
TR-0086A(2940-05)-7 ..... N89-10935 #
TR-0086A(2945-03)-5 ..... N89-11606 #

TT-8802 ..... N89-10846

UBUFFALO/DC/88/TR-70 ..... N89-11607 #
UBUFFALO/DC/88/TR-71 ..... N89-10986 #

UCB/SEMM-87/08 ..... N89-11464 #

UCID-21384 ..... N89-11031 #
UCID-21411 ..... N89-11245 #
UCID-21436 ..... N89-11072 #
UCID-21437 ..... N89-11417 #
UCID-21443 ..... N89-10928 #

UCRL-21070 ..... N89-11464 #
UCRL-51444-87 ..... N89-11346 #
UCRL-53860 ..... N89-11047 #
UCRL-53868-87 ..... N89-11059 #
UCRL-53875 ..... N89-11486 #
UCRL-97328 ..... N89-11014 #
UCRL-97832 ..... N89-11100 #
UCRL-97861 ..... N89-11049 #
UCRL-98040 ..... N89-11053 #
UCRL-98343 ..... N89-10949 #
UCRL-98639 ..... N89-11178 #
UCRL-98693 ..... N89-10942 #
UCRL-98976 ..... N89-11141 #
UCRL-98977 ..... N89-11166 #
UCRL-99056 ..... N89-10981 #
UCRL-99179 ..... N89-11207 #
UCRL-99181 ..... N89-11208 #
UCRL-99183 ..... N89-11199 #
UCRL-99185 ..... N89-11200 #
UCRL-99186 ..... N89-11210 #

UI-88-13 ..... N89-11678* #

UILU-ENG-88-0505 ..... N89-11132 #
UILU-ENG-88-2221 ..... N89-11448 #
UILU-ENG-88-2222 ..... N89-11484 #
UILU-ENG-88-2231 ..... N89-11243 #

UTAP76/88 ..... N89-11614* #

UTIAS-268 ..... N89-11152 #
UTIAS-323 ..... N89-11250 #

UVA/528260/CHE89/103 ..... N89-11056* #

Y/DV-724 ..... N89-11025 #

☆ U.S. GOVERNMENT PRINTING OFFICE: 1988— 241-445/80024

FEDERAL REGIONAL DEPOSITORY LIBRARIES

ALABAMA

AUBURN UNIV. AT MONTGOMERY LIBRARY
Documents Department
Montgomery, AL 36193
(205) 271-9650

UNIV. OF ALABAMA LIBRARY
Documents Dept.-Box S
University, AL 35486
(205) 348-6046

ARIZONA

DEPT. OF LIBRARY, ARCHIVES AND PUBLIC RECORDS
Third Floor—State Cap.
1700 West Washington
Phoenix, AZ 85007
(602) 255-4121

UNIVERSITY OF ARIZONA LIB.
Government Documents Dept.
Tucson, AZ 85721
(602) 621-6433

ARKANSAS

ARKANSAS STATE LIBRARY
One Capitol Mall
Little Rock, AR 72201
(501) 371-2326

CALIFORNIA

CALIFORNIA STATE LIBRARY
Govt. Publications Section
P.O. Box 2037
Sacramento, CA 95809
(916) 324-4863

COLORADO

UNIV OF COLORADO LIB.
Government Pub. Division
Campus Box 184
Boulder, CO 80309
(303) 492-8834

DENVER PUBLIC LIBRARY
Govt. Pub. Department
1357 Broadway
Denver, CO 80203
(303) 571-2131

CONNECTICUT

CONNECTICUT STATE LIBRARY
Government Documents Unit
231 Capitol Avenue
Hartford, CT 06106
(203) 566-7029

FLORIDA

UNIV. OF FLORIDA LIBRARIES
Library West
Documents Department
Gainesville, FL 32611
(904) 392-0367

GEORGIA

UNIV. OF GEORGIA LIBRARIES
Government Reference Dept.
Athens, GA 30602
(404) 542-8949

HAWAII

UNIV. OF HAWAII LIBRARY
Govt. Documents Collection
2550 The Mall
Honolulu, HI 96822
(808) 948-8230

IDAHO

UNIV. OF IDAHO LIBRARY
Documents Section
Moscow, ID 83843
(208) 885-6344

ILLINOIS

ILLINOIS STATE LIBRARY
Information Services Branch
Centennial Building
Springfield, IL 62756
(217) 782-5185

INDIANA

INDIANA STATE LIBRARY
Serials Documents Section
140 North Senate Avenue
Indianapolis, IN 46204
(317) 232-3686

IOWA

UNIV. OF IOWA LIBRARIES
Govt. Documents Department
Iowa City, IA 52242
(319) 353-3318

KANSAS

UNIVERSITY OF KANSAS
Doc. Collect—Spencer Lib.
Lawrence, KS 66045-2800
(913) 864-4662

KENTUCKY

UNIV. OF KENTUCKY LIBRARIES
Govt. Pub. Department
Lexington, KY 40506-0039
(606) 257-3139

LOUISIANA

LOUISIANA STATE UNIVERSITY
Middleton Library
Govt. Docs. Dept.
Baton Rouge, LA 70803
(504) 388-2570

LOUISIANA TECHNICAL UNIV. LIBRARY
Documents Department
Ruston, LA 71272-0046
(318) 257-4962

MAINE

UNIVERSITY OF MAINE
Raymond H. Fogler Library
Tri-State Regional Documents Depository
Orono, ME 04469
(207) 581-1680

MARYLAND

UNIVERSITY OF MARYLAND
McKeldin Lib.—Doc. Div.
College Park, MD 20742
(301) 454-3034

MASSACHUSETTS

BOSTON PUBLIC LIBRARY
Government Docs. Dept.
Boston, MA 02117
(617) 536-5400 ext.226

MICHIGAN

DETROIT PUBLIC LIBRARY
Sociology Department
5201 Woodward Avenue
Detroit, MI 48202-4093
(313) 833-1409

MICHIGAN STATE LIBRARY
P.O. Box 30007
Lansing, MI 48909
(517) 373-1593

MINNESOTA

UNIVERSITY OF MINNESOTA
Government Pubs. Division
409 Wilson Library
309 19th Avenue South
Minneapolis, MN 55455
(612) 373-7870

MISSISSIPPI

UNIV. OF MISSISSIPPI LIB.
Documents Department
University, MS 38677
(601) 232-5857

MONTANA

UNIV. OF MONTANA
Mansfield Library
Documents Division
Missoula, MT 59812
(406) 243-6700

NEBRASKA

UNIVERSITY OF NEBRASKA - LINCOLN
Love Library
Documents Department
Lincoln, NE 68588-0410
(402) 472-2562

NEVADA

UNIVERSITY OF NEVADA LIB.
Govt. Pub. Department
Reno, NV 89557-0044
(702) 784-6579

NEW JERSEY

NEWARK PUBLIC LIBRARY
5 Washington Street
Newark, NJ 07101-0630
(201) 733-7812

NEW MEXICO

UNIVERSITY OF NEW MEXICO
Zimmerman Library
Government Pub. Dept.
Albuquerque, NM 87131
(505) 277-5441

NEW MEXICO STATE LIBRARY
Reference Department
325 Don Gaspar Avenue
Santa Fe, NM 87503
(505) 827-3826

NEW YORK

NEW YORK STATE LIBRARY
Empire State Plaza
Albany, NY 12230
(518) 474-5563

NORTH CAROLINA

UNIVERSITY OF NORTH CAROLINA AT CHAPEL HILL
Davis Library
BA/SS Documents Division
Chapel Hill, NC 27515
(919) 962-1151

NORTH DAKOTA

UNIVERSITY OF NORTH DAKOTA
Chester Fritz Library
Documents Department
Grand Forks, ND 58202
(701) 777-4629
In cooperation with North Dakota State Univ. Library

OHIO

STATE LIBRARY OF OHIO
Documents Department
65 South Front Street
Columbus, OH 43266-0334
(614) 462-7051

OKLAHOMA

OKLAHOMA DEPT. OF LIB.
Government Documents
200 NE 18th Street
Oklahoma City, OK 73105
(405) 521-2502, ext. 252

OKLAHOMA STATE UNIV. LIB.
Documents Department
Stillwater, OK 74078
(405) 624-6546

OREGON

PORTLAND STATE UNIV. LIB.
Documents Department
P.O. Box 1151
Portland, OR 97207
(503) 229-3673

PENNSYLVANIA

STATE LIBRARY OF PENN.
Government Pub. Section
P.O. Box 1601
Harrisburg, PA 17105
(717) 787-3752

TEXAS

TEXAS STATE LIBRARY
Public Services Department
P.O. Box 12927—Cap. Sta.
Austin, TX 78711
(512) 475-2996

TEXAS TECH. UNIV. LIBRARY
Govt. Documents Department
Lubbock, TX 79409
(806) 742-2268

UTAH

UTAH STATE UNIVERSITY
Merrill Library, U.M.C. 30
Logan, UT 84322
(801) 750-2682

VIRGINIA

UNIVERSITY OF VIRGINIA
Alderman Lib.—Public Doc.
Charlottesville, VA 22903-2498
(804) 924-3133

WASHINGTON

WASHINGTON STATE LIBRARY
Documents Section
Olympia, WA 98504
(206) 753-4027

WEST VIRGINIA

WEST VIRGINIA UNIV. LIB.
Documents Department
Morgantown, WV 26506-6069
(304) 293-3640

WISCONSIN

MILWAUKEE PUBLIC LIBRARY
814 West Wisconsin Avenue
Milwaukee, WI 53233
(414) 278-3065

ST. HIST LIB. OF WISCONSIN
Government Pub. Section
816 State Street
Madison, WI 53706
(608) 262-4347

WYOMING

WYOMING STATE LIBRARY
Supreme Ct. & Library Bld.
Cheyenne, WY 82002
(307) 777-5919

National Aeronautics and
Space Administration
Code NTT-4
Washington, D.C.
20546
Official Business
Penalty for Private Use, $300

SPECIAL FOURTH-CLASS RATE
POSTAGE & FEES PAID
NASA
PERMIT No. G 27

NASA

POSTMASTER: If Undeliverable (Section 158
Postal Manual) Do Not Return